

LINES
LECTURE NOTES IN EARTH SCIENCES

104

Robert Hack
Rafiq Azzam · Robert Charlier
Editors

Engineering Geology for Infrastructure Planning in Europe

A European Perspective



Springer

Lecture Notes in Earth Sciences

104

Editors:

S. Bhattacharji, Brooklyn

H. J. Neugebauer, Bonn

J. Reitner, Göttingen

K. Stüwe, Graz

Founding Editors:

G. M. Friedman, Brooklyn and Troy

A. Seilacher, Tübingen and Yale

Springer

Berlin

Heidelberg

New York

Hong Kong

London

Milan

Paris

Tokyo

Robert Hack
Rafiq Azzam
Robert Charlier (Eds.)

Engineering Geology for Infrastructure Planning in Europe

A European Perspective



Springer

Editors

Dr. Robert Hack
Engineering Geology
Int. Inst. for Geo-Information Sciences and Earth Observation
Mijnbouwstraat 120
2628 RX Delft
The Netherlands

Univ.-Prof. Dr. Rafiq Azzam
Lehrstuhl für Ingenieurgeologie und Hydrogeologie
RWTH Aachen
Lochnerstrasse 4–20
52064 Aachen
Germany

Dr. Robert Charlier
Institut de Mécanique et de Génie Civil (bât. B52)
Université de Liège
Chemin de Chevreuils 1
4000 Liège 1
Belgium

Library of Congress Control Number: 2004103475

“For all Lecture Notes in Earth Sciences published till now please see final pages of the book“

ISSN 0930-0317
ISBN 3-540-21075-X Springer-Verlag Berlin Heidelberg New York

This work is subject to copyright. All rights are reserved, whether the whole or part of the material is concerned, specifically the rights of translation, reprinting, re-use of illustrations, recitation, broadcasting, reproduction on microfilms or in any other way, and storage in data banks. Duplication of this publication or parts thereof is permitted only under the provisions of the German Copyright Law of September 9, 1965, in its current version, and permission for use must always be obtained from Springer-Verlag. Violations are liable for prosecution under the German Copyright Law.

Springer-Verlag is a part of Springer Science+Business Media
springeronline.com

© Springer-Verlag Berlin Heidelberg 2004
Printed in Germany

The use of general descriptive names, registered names, trademarks, etc. in this publication does not imply, even in the absence of a specific statement, that such names are exempt from the relevant protective laws and regulations and therefore free for general use.

Cover design: Erich Kirchner, Heidelberg
Typesetting: Camera ready by author
Printed on acid-free paper 32/3142/du - 5 4 3 2 1 0

Introduction

This book focuses on the contribution of Engineering Geology to modern geotechnical design methods that are used to build safe and durable structures.

Recently, in Europe many large ground engineering structures were designed and constructed to improve the infrastructure such as high-speed and underground railways, inner-city light rails, roads, harbours, coastal protection and waterways. Also for the exploitation of natural resources and building materials, many European countries are engaged in major mining projects. It was clearly recognized that, in many projects, the uncertainties related to the subsurface and the associated risk significantly contributed to major budget over runs and to problems during and after construction. Such experience suggests that there is an urgent need for a better assessment of the subsurface conditions and an improved risk analysis as part of the numerical modelling of soil and rock structures. The majority of papers within this book is concerned with these issues.

A significant number of papers give information on professional topics which are of steadily increasing importance in Europe. Examples are the current and future status of co-operation between engineering geologist and geotechnical engineers, the standardization of the geotechnical description of soil and rock, and educational requirements in connection with the "Bologna Process".

The papers in this volume continue the series of "*Lecture notes in Earth Sciences*". They were presented during the *First European Regional Conference* of the *International Association of Engineering Geology and the Environment* (IAEG) held in 2004 in Liège. This inaugural *EurEnGeo* conference was hosted by the University of Liège and was jointly organized by the national IAEG groups from Belgium, the Netherlands, and Germany.

The Organising Committee expresses its acknowledgement for the commitment of all authors who contributed, the editors and the committee members.

On behalf of the Organising Committee *EurEnGeo2004*, Christian Trève, *Chairman*, Richard Rijkers, *Secretary*, Helmut Bock, *Treasurer*

Conference Organisation

Honorary Committee

Edelgard Bulmahn	<i>Federal minister of Science and Research (Germany)</i>
Philippe Busquin	<i>E.C. commissioner - European Research Area</i>
Willy Legros	<i>Rector University of Liège</i>
Ed de Mulder	<i>President I.U.G.S.</i>
Ricardo Oliveira	<i>Past President I.A.E.G.</i>
Niek Rengers	<i>President I.A.E.G.</i>
Friedrich - W. Wellmer	<i>President of the DGG and BGR</i>

Organising Committee

Christian Trève - <i>president</i>	CFE, Brussels	BELGIUM
Richard Rijkers - <i>secretary</i>	TNO-NITG, Utrecht	NETHERLANDS
Helmut Bock - <i>treasurer</i>	Q+S, Bad Bentheim	GERMANY
Robert Charlier	ULg, Liège	BELGIUM
Robert Hack	ITC, Delft	NETHERLANDS
Robin Koster	Van Oord, Rotterdam	NETHERLANDS
Kurt Schetelig	RWTH, Aachen	GERMANY
Joost van der Schrier	Royal Haskoning, Nijmegen	NETHERLANDS
Christian Schroeder	ULg, Liège	BELGIUM
Jean-Francois Thimus	UCL, Louvain-la-Neuve	BELGIUM

Advisory Committee

Marcel Arnould	Paris	FRANCE
Rafiq Azzam	Aachen	GERMANY
Johan Bosch	Delft	NETHERLANDS
Rodney Chartres	Purley	UNITED KINGDOM
Antonio Gomes Coelho	Lisbon	PORTUGAL
Michael De Freitas	London	UNITED KINGDOM
Michel Deveughele	Paris	FRANCE
Antonio Gens	Barcelona	SPAIN
Rolf Katzenbach	Darmstadt	GERMANY
Frans Molenkamp	Delft	NETHERLANDS
Alberic Monjoie	Liège	BELGIUM
Victor Osipov	Moscow	RUSSIA
Lars Persson	Stockholm	SWEDEN
Hans Ziegler	Bern	SWITZERLAND

Scientific Committee

Alain van Cotthem	Brussels	BELGIUM
Peter Fookes	Winchester	UNITED KINGDOM
Robert Hack	Delft	NETHERLANDS
Lucien Halleux	Liège	BELGIUM
Patric Jacobs	Gent	BELGIUM
Christoph Lempp	Halle / Saale	GERMANY
Jan Nieuwenhuis	Delft	NETHERLANDS
Mike Rosenbaum	Nottingham	UNITED KINGDOM
Volker Schenk	Schrozberg	GERMANY
Luis Ribeiro e Sousa	Lisbon	PORTUGAL
Martin van Staveren	Delft	NETHERLANDS
Dieter Wenner	Stuttgart	GERMANY

Preface

Dear Reader,

The material in this volume ranges over a wide spectrum of expertises related to engineering geology but concentrates on infrastructure in Europe. Part of the volume has a scientific character reporting on theoretical and applied research that one day may be useful in the actual practice of day-to-day engineering geology projects while other contributions concentrate on education or organisational aspects of projects or describe interesting case histories and real-life projects. For those involved in infrastructure and engineering geology, this volume will likely be a source of ideas for research, handling projects and it provides an overview over the developments in infrastructure and engineering geology in Europe in the last decade.

It is obvious that just the editors do not have all the expertise required to do a thorough review over such a wide range of topics as included in this volume. Many experts have been contacted to do the tedious job of reviewing. Probably the review spoiled part of their winter holiday and we are sorry for that, but they can be ascertained that their valuable input has been highly appreciated. They were: from Germany: *Christof Lempp, Kurt Schetelig, and Dieter Wenner*; from Belgium: *Lucien Halleux, Patric Jacobs, Christian Schroeder, and Christian Trève*; from the Netherlands: *Gerard Arends, Laurent Gareau, Marco Huisman, Harry Kolk, Robin Koster, Michiel Maurenbrecher, Jan Nieuwenhuis, Derk van Ree, Niek Rengers, Richard Rijkers, Joost van der Schrier, Siefko Slob, and Cees van Westen*, from Switzerland, *Simon Löv*, and last but certainly not least *Marcel Arnould* from France.

May 2004

The editors, Robert Hack, Rafiq Azzam and Robert Charlier

Table of Contents

Professional Practices

Cooperation between (Engineering) Geologist and Geotechnical Engineers

The Joint European Working Group of the ISSMGE, ISRM and IAEG for the Definition of Professional Tasks, Responsibilities and Co-operation in Ground Engineering	1
<i>Helmut Bock, E. Broch, R. Chartres, M. Gambin, J. Maertens, L. Maertens, D. Norbury, P. Pinto, W. Schubert, and H. Stille</i>	
Some Basic Considerations about the Necessities and Possibilities of Cooperation between Civil Engineers and Engineering Geologists	9
<i>Rolf Katzenbach and Gregor Bachmann</i>	
Current Issues Relating to the Professional Practice of Engineering Geology in Europe	15
<i>David Norbury</i>	
Feasibility Studies and Design of High-Speed Railway (TGV) Projects in Portugal	31
<i>Ricardo Oliveira and Rui Abreu</i>	
Austrian Guideline for Geomechanical Design of Tunnels – Necessity for Cooperation between Geologists, Geotechnical and Civil Engineers	39
<i>Ludwig Schwarz, Stefan Eder, Bruno Mattle, and Helmut Hammer</i>	
Soil Investigations Requirements from the Construction Industry	47
<i>Christian Treve</i>	

Common Educational Requirements

The Necessity of Combining Geologists and Engineers for Fieldwork in the Practice of Geotechnics	54
<i>Michael H. de Freitas</i>	
Contribution of On-Line Tools on Internet for the Teaching of Slopes and Tunnels Stability	59
<i>René-Michel Faure and Jean-François Thimus</i>	

German Higher Education in the Framework of the Bologna Process 69
Roland Richter

**International Standardisation of Geotechnical Description
of Soil/Rock and Testing Practices (ISO, CEN);
Geotechnical Exchange Format (GEF)**

International Standardisation of Ground Investigation and Testing Methods . . . 74
Volker Eitner and Ferdinand Stölben

Towards Quality Assurance and an Adequate Risk Management
in Geotechnical Engineering – Application of Eurocode 7 and DIN 4020
in Engineering Geology 86
*Kurt Schetelig, Michael Heitfeld, Paul von Soos, Manfred Stocker,
and Mark Mainz*

Aggregate Research in Support of European Standardisation 94
Björn Schouenborg and Urban Åkesson

Standardised Methods for Sampling by Drilling and Excavation
and for Groundwater Measurements 101
Ferdinand Stölben and Volker Eitner

Engineering Geological Methods

Methods of (Digital) Characterisation of the Surface

Interpretation of SCPT Data Using Cross-over
and Cross-Correlation Methods 110
Lou Areias and William Van Impe

Evaluation Concept and Testing Method
for Heavy Metal Contaminant Transport in the Underground 117
Rafiq Azzam and Mouad Lambarki

Geo-engineering Evaluation with Prime Consideration
to Liquefaction Potential for Eskisehir City (Turkey) 125
N. Pinar Koyuncu and Resat Ulusay

Engineering Geology Property Parameters for the Tertiary
in The Netherlands 133
P. Michiel Maurenbrecher and Dominique Ngan-Tillard

Various Assessments of the Characteristic Values of Soil Cohesion
and Friction Angle: Application to New Caledonian Laterite 144
Véronique Merrien-Soukatchoff, Kamel Omraci, and Le Nickel-SLN

Numerical Analysis of a Tunnel in an Anisotropy Rock Mass. Envalira Tunnel (Principality of Andorra)	153
<i>Dídac Plana, Carlos López, Josep Cornelles, and Pere Muñoz</i>	
Engineering-Geological Properties of Carbonate Rocks in Relation to Weathering Intensity	162
<i>Davor Pollak</i>	
Engineering Geocryological Mapping for Construction in the Permafrost Regions	172
<i>Felix Rivkin, Irina Kuznetsova, Nadezhda Ivanova, and Sergey Suhodolsky</i>	
3D Terrestrial Laser Scanning as a New Field Measurement and Monitoring Technique	179
<i>Siefko Slob and Robert Hack</i>	
Engineering Geology in International Dredging and Infrastructure	190
<i>Willem J. Vlasblom</i>	
Prediction of the Uniaxial Compressive Strength of a Greywacke by Fuzzy Inference System	203
<i>Kivanc Zorlu, Candan Gokceoglu, and Harun Sonmez</i>	

New Development in Site Investigation

Self-healing of Fractures around Radioactive Waste Disposal in Clay Formations	211
<i>Bjorn Debecker, André Vervoort, Jan Verstraelen, and Martine Wevers</i>	
Hydrogeological Investigations in Deep Wells at the Meuse/Haute Marne Underground Research Laboratory	219
<i>Jacques Delay and Marc Distinguin</i>	
Java Tomography System (JaTS), a Seismic Tomography Software Using Fresnel Volumes, a Fast Marching Eikonal Solver and a Probabilistic Reconstruction Method: Conclusive Synthetic Test Cases	226
<i>Sandrine Sage, Gilles Grandjean, and Jacques Verly</i>	
Using the Complete Nano Engineering Geological Spectrum to Assess the Performance of Clay Barriers	236
<i>Robrecht M. Schmitz, Christian Schroeder, Jacques Thorez, and Robert Charlier</i>	

Modelling of Soil and Rock Behaviour

- Rock Splitting in the Surrounds of Underground Openings:
An Experimental Approach Using Triaxial Extension Tests 244
Enrico Bauch and Christof Lempp
- A Constitutive Model for Chemically Sensitive Clays 255
Nathalie Boukpeti, Robert Charlier, Tomasz Hueckel, and Zejia Liu
- Relocation of a Problematic Segment of a Natural Gas Pipeline
Using GIS-Based Landslide Susceptibility Mapping, Hendek (Turkey) 265
Engin Cevik and Tamer Topal
- Micro-structure and Swelling Behaviour of Compacted Clayey Soils:
A Quantitative Approach 275
Valéry Ferber, Jean-Claude Auriol, and Jean-Pierre David
- Physical and Numerical Modelling of a Two-Well Tracer Test
at the Laboratory Scale 285
*Christophe Fripiat, Benoît Wauters, Vincent Feller, Patrick Conde,
Mohammed Talbaoui, and Alain Holeyman*
- Soil Investigation Aspects of a Complex Metro Project in Amsterdam 294
Jurgen Herbschleb
- Effects of the Determination of Characteristic Values of Soil Parameters 304
Britta Kruse
- Basic Soil Properties of a Number of Artificial Clay –
Sand Mixtures Determined as a Function of Sand Content 308
Beata Łuczak-Wilamowska
- The Effect of Sand on Strength of Mixtures of Bentonite-Sand 316
Mohammad C. Pakbaz and Navid Khayat
- Nonconventional and Simple View of the Soil-Structure Interaction Problem . . 321
J. Paul Smith-Pardo, Mete A. Sozen, and Julio A. Ramirez
- Effect of Pore Fluid Salinity on Compressibility
and Shear Strength Development of Clayey Soils 327
Leon A. van Paassen and Laurent F. Gareau

New Geotechnical In-situ Testing and Sampling Techniques

- Hydraulic Monitoring of Low-Permeability Argillite
at the Meuse/Haute Marne Underground Research Laboratory 341
Jacques Delay and Martin Cruchaudet

Hydrogeologic Exploration during Excavation of the Lötshberg Base Tunnel (AlpTransit Switzerland)	347
<i>Marc Pesendorfer and Simon Loew</i>	
Coring Performance to Characterise the Geology in the “Cran aux Iguanodons” of Bernissart (Belgium)	359
<i>Jean-Pierre Tshibangu, Fabrice Dagrain, Hughes Legrain, and Benoît Deschamps</i>	
ConsoliTest – Using Surface Waves for Estimating Shear-Wave Velocities in the Dutch Subsurface	368
<i>Rogier Westerhoff, Vincent van Hoegaerden, Jan Brouwer, and Richard Rijkers</i>	

Geo-monitoring and Special Field Measurements or Techniques

Multi-level Groundwater Pressure Monitoring at the Meuse/Haute-Marne Underground Research Laboratory, France	377
<i>Jacques Delouvrier and Jacques Delay</i>	
Application of Borehole Radar for Monitoring Steam-Enhanced Remediation of a Contaminated Site in Fractured Limestone, Maine, USA	385
<i>Colette Grégoire, John W. Lane, Jr., and Peter K. Joesten</i>	
Site Investigation for Abandoned Lignite Mines in Urban Environment	393
<i>Paul Marinos, Harry Aroglou, Mark Novack, Maria Benissi, and Vassilis Marinos</i>	
Behaviour of the Weak Rock Cut Slopes and Their Characterization Using the Results of the Slake Durability Test	405
<i>Joan Martinez-Bofill, Jordi Corominas, and Albert Soler</i>	
Determination of the Failure Surface Geometry in Quick Slides Using Balanced Cross Section Techniques – Application to Aznalcóllar Tailings Dam Failure	414
<i>José Moya</i>	

Case Studies of Infrastructure Projects

Inner-City Projects (Ground Improvement, Bored Tunnels, Deep Shafts)

Obstacle Investigation RandstadRail in Rotterdam, The Netherlands	422
<i>Robert Berkelaar and Melinda van den Bosch</i>	
Tunnelling in Urbanised Areas – Geotechnical Case Studies at Different Project Stages	435
<i>Stefan Eder, Gerhard Poscher, and Bernhard Kohl</i>	

Geotechnical Characterization and Stability of a Slope in the Marnoso-Arenacea Formation for the Realization of an Underground Car Park in Urbino (Italy) . . . 444
Umberto Gori, Ennio Polidori, Gianluigi Tonelli, and Francesco Veneri

Cross Connections at Pannerdensch Canal Tunnel –
 Freezing Soil Mass Design and Execution Comparison 455
Hans Mortier and Léon L.T.C. Tuunter

Effects of Lime Stabilization on Engineering Properties
 of Expansive Ankara Clay 466
M. Celal Tonož, Resat Ulusay, and Candan Gokceoglu

**European Traffic Routes (High-Speed Lines, Alpine Base Tunnels,
 Oil-Gas Pipeline Routes, Channel Crossings, etc.)**

The Belgian High-Speed Railway Soumagne Tunnel Project 475
Iwan Couchard, Alain Van Cotthem, and Servais Hick

High Speed Lines in Belgium: Various Engineering Geological
 and Geotechnical Aspects 485
Bernard Dethy and Saâd Bouhenni

An Overview of the Geological and Geotechnical Aspects
 of the New Railway Line in the Lower Inn Valley 504
Stefan Eder, Gerhard Poscher, and Christoph Sedlacek

Stability and Serviceability of a Gas Pipeline
 at the Base of a Steep Creeping Slope 513
Rolf Katzenbach, Matthias Seip, and Johannes Giere

Investigation of Karst Cavities and Earth Subsidence with Combined Application
 of Boring and Geophysics in the Progress of High-Speed Railway Routes 521
Bodo Lehmann, Rudolf Pöttler, Alexander Radinger, and Manfred Kühne

Engineering Geological Considerations in Tunnelling through Major Tectonic
 Thrust Zones – Cases along the Egnatia Motorway, Northern Greece 527
Vassilios P. Marinos, Georgios Aggistalis, and Nikolaos Kazilis

Tunnelling Problems in Older Sand Formations 538
Jan Dirk Nieuwenhuis and Arnold Verruijt

Engineering Geological Model of the Contact between Two Petrographic
 and Stratigraphic Units along the Zagreb-Split Highway, Croatia 549
Tomislav Novosel, Željko Mlinar, and Damir Grgec

Overconsolidated, Early-Pleistocene Clays in Relation to Foundation Design and Construction of HSLSouth, Province of Brabant, The Netherlands	555
<i>Floris Schokking</i>	

Mininig Projects and Natural Resources

Location of Buried Mineshafts and Adits Using Reconnaissance Geophysical Methods	565
<i>Martin Culshaw, Laurance Donnelly, and David McCann</i>	

Geological-Technical and Geo-engineering Aspects of Dimensional Stone Underground Quarrying	574
<i>Mauro Fornaro and Enrico Lovera</i>	

Leibis/Lichte Dam in Germany	585
<i>Markus Kühnel</i>	

Creep Behaviour of Alpine Salt Rock and the Influence of Insoluble Residues in Solution Mining	593
<i>Gerhard Pittino and Johann Golser</i>	

Assessment of Rock Slope Stability in Limestone Quarries in the Tournai's Region (Belgium) Using Structural Data	604
<i>Jean-Pierre Tshibangu, K. Pierre-Alexandre Deloge, Benoît Deschamps, and Christophe Coudyzer</i>	

Studying Underground Motions in the Ramioul's Cave – Belgium	614
<i>Jean-Pierre Tshibangu, Michel Van Ruymbeke, Sara Vanduycke, Yves Quinif, and Thierry Camelbeeck</i>	

Regional Planning and Surfaces Characteristics, Redevelopment and Reclamation of Land

Drying-Up of a Natural Spring for Ensuring Stability of an Artificial Slope: Is It Sustainable Development?	624
<i>Marie Dachy, Sandrine Sage, and Alain Dassargues</i>	

Suitability Maps of Underground Construction in the Province of South-Holland	631
<i>Jurgen Herbschleb, Brecht B.T. Wassing, and Henk J.T. Weerts</i>	

Liquefied Natural Gas Terminal Siting in a Highly Seismic Region on the Mexican Pacific Coast	641
<i>Yannick Zaczek and Nicolas Lambert</i>	

Hazard and Risk in Engineering Geology

Hazardous Geological Processes in Civil Engineering

- National Environmental Monitoring of the Slovak Republic –
Part Geological Hazards 650
Alena Klukanová and Pavel Liscak
- Stability and Subsidence Assessment over Shallow Abandoned Room
and Pillar Limestone Mines 657
Roland F. Bekendam
- Numerical Modelling of Seismic Slope Stability 671
*Céline Bourdeau, Hans-Balder Havenith, Jean-Alain Fleurisson,
and Gilles Grandjean*
- A Multidisciplinary Approach for the Evaluation
of the “Bottegone” Subsidence (Grosseto, Italy) 685
Otello Del Greco, Elena Garbarino, and Claudio Oggeri
- Influence of Underground Coal Mining on the Environment
in Horna Nitra Deposits in Slovakia 694
Jozef Malgot and Frantisek Baliak
- Sustainable Passive and Active Remedial Measures of Creeping Bedrock Slopes:
Two Case Studies from Austria 701
Michael Moser and Stefan Weidner

New Developments in Risk Evaluation

- Problems in Defining the Criteria for an Earthquake Hazard Map –
A Case Study: The City of Haifa, Northern Israel 708
Ram Ben-David
- Some Positive and Negative Aspects of Mine Abandonment
and Their Implications on Infrastructure 719
Laurance Donnelly, Fred Bell, and Martin Culshaw
- Seismic and Flood Risk Evaluation in Spain from Historical Data 727
*Mercedes Ferrer, Luis González de Vallejo, J. Carlos García,
Angel Rodríguez, and Hugo Estévez*
- Landslide Risk Assessment in Italy:
A Case Study in the Umbria-Marche Apennines 738
Mario Floris and Francesco Veneri

Modelling of Landslide-Triggering Factors – A Case Study in the Northern Apennines, Italy	745
<i>Mario Floris, Milena Mari, Roberto W. Romeo, and Umberto Gori</i>	
Management of Combined Natural Risks – A New Approach	754
<i>Jörg Hanisch</i>	
Technique of Quantitative Assessment of Karst Risk on the Local and Regional Levels	760
<i>Alexei Ragozin and Vladimir Yolkin</i>	
Cut-and-Cover Tunnel below Boulevard River Meuse, Maastricht, The Netherlands	767
<i>Joost S. van der Schrier and Rijk H. Gerritsen</i>	
The Geotechnical Baseline Report as Risk Allocation Tool	777
<i>Martin Th. van Staveren and Johan G. Knoeff</i>	
Matching Monitoring, Risk Allocation and Geotechnical Baseline Reports . . .	786
<i>Martin Th. van Staveren and Ton J.M. Peters</i>	
Smart Site Investigations Save Money!	792
<i>Martin Th. Van Staveren and Adriaan J. van Seters</i>	
Author Index	801

The Joint European Working Group of the ISSMGE, ISRM and IAEG for the Definition of Professional Tasks, Responsibilities and Co-operation in Ground Engineering

Helmut Bock et al.*

Q+S Consult, Stoltenkampstr. 1, D-48455 Bad Bentheim, Germany
QS-Consult@t-online.de
Tel: +49 5922 2700
Fax: +49 5922 2799

Abstract. In July 2002, a Joint European Working Group on the professional competencies of engineering geologists and geotechnical engineers was established formally by the Presidents of the three international learned societies which are relevant in the field of ground engineering; ISSMGE, ISRM and IAEG. The European Federation of Geologists (EFG) is represented in the Working Group as observer at present.

In addition, the establishment of the Working Group forms an important part in the effort to foster a mutual understanding between the three societies.

The Working Group identified the need for two reports, namely:

A document specifically for the three international learned societies on the professional competencies of engineering geologists and geotechnical engineers, including a specification of the interfaces and areas of co-operation between them, and

A document with relevant recommendations for an input to EU Directives. This contribution gives a brief account on the background of the Working Group, its Terms of Reference and the current state of deliberations. With regard to the first document, work has progressed to a point that, during 2004, a proposal can be expected to be submitted to the Presidents of the three societies for further consideration and adoption by the respective Boards and Councils.

Keywords: European union, legislation, registration, professionalism, ground engineering relationship, ISSMGE, ISRM, IAEG.

1 Background

The need for a joint working group of the major international ground engineering societies to define the professional fields of engineering geology and geotechnical engineering was identified in a meeting of representatives of the European national groups of the IAEG in Helsinki in August 2001. In this meeting a draft report

* Co-authors of this article are: Broch, E. (Norway); Chartres, R. (U. K.); Gambin, M. (France); Maertens, J. (Belgium); Maertens, L. (Belgium); Norbury, D. (U. K.); Pinto, P. (Portugal); Schubert, W. (Austria) and Stille, H. (Sweden).

“*Engineering Geology in Europe*” that had been produced by the European Federation of Geologists (EFG) (Suárez and Regueiro 2000) was discussed intensively. The Helsinki meeting concluded that the issue is of importance for most European countries. In many countries this relationship is focused also on the division of responsibilities between geologists and engineers in the civil engineering construction process. The meeting was unanimous in its decision that the EFG document was not acceptable for this purpose. The meeting furthermore decided to seek co-operation with the International Society of Soil Mechanics and Geotechnical Engineering (ISSMGE) and the International Society for Rock Mechanics (ISRM) to work out proper definitions of the fields of engineering geology and geotechnical engineering within the European ground engineering context.

The proposal to form a joint working group was made in March 2002 by the then President designate of the IAEG, Niek Rengers, to William van Impe (President of the ISSMGE) and Marc Panet, the then President of the ISRM. The new working group was tasked to prepare a draft to be discussed by the three societies at the European level. This could lead to a common position of the three societies at the European level on this important issue. That position could then be presented to the European authorities in discussions on issues of professional affiliation and accreditation at the European and national levels. The definition of tasks and responsibilities of geotechnical engineers and engineering geologists should also consider the influence of differing educational backgrounds as well as on a definition of the training and practical experience that is to be considered as minimum requirement to fulfil a position in these professional fields in Europe. As such, it is linked with an important and urgent issue to be approached at the European level, namely, what should be the content of university educational programmes in engineering geology and geotechnical engineering at the Bachelor and Masters levels? These issues should be resolved by a follow-up working group to be formed by ISSMGE, ISRM and IAEG.

The proposal was enthusiastically agreed by the Presidents of the ISSMGE and ISRM. Each president nominated three members from his society as follows:

ISSMGE:	Mike Gambin (France)	ISSMGE Board Member
	Pedro Sêco e Pinto (Portugal)	ISSMGE Vice-President For Europe
	Luc Maertens (Belgium)	ISSMGE Member of TC 20 “Professional Practice”
ISRM:	Einar Broch (Norway)	ISRM and Past-President of ITA
	Wulf Schubert (Austria)	ISRM Board Member
	Håkan Stille (Sweden)	
IAEG:	Helmut Bock (Germany)	Chairman of the Joint Working Group
	Rodney Chartres (U.K.)	Secretary of the Joint Working Group
	Jan Maertens (Belgium)	
EFG:	David Norbury (U.K.)	Secretary General

The Joint European Working Group was formally established in July 2002. It held its inaugural meeting in March 2003 in Brussels and, in November 2003, a second meeting in Graz, Austria.

2 Terms of Reference

In his proposal, Niek Rengers suggested to the Working Group its first task should be to define the professional practice of engineering geologists and geotechnical engineers as a basis for use in Europe (in a geographical sense). This should be illustrated with a definition of the tasks and responsibilities that are assigned to the different types of professionals on the one hand and the educational background and professional experience on the other. Given the fact that the situation of professional definitions and accreditation is different in most European countries, a first step would be to make an inventory of the situation in each country, to be followed by a suggestion for a uniform approach to be submitted to the European Union and to those European countries that are not yet member of the European Union.

At the inaugural meeting in Brussels in March 2003, the Joint Working Group agreed its Terms of Reference, as follows:

1. Prepare an inventory of current professional regulations in the field of ground engineering for the EU member and future member countries.
2. Describe and illustrate categories of projects for which the professional input of geotechnical engineers and engineering geologists is required.
3. Specify the individual contributions of geotechnical engineers and engineering geologists in solving ground engineering problems. Detail the respective contributions with regard to competent persons and the methods employed, training, experience, tasks and responsibilities required.
4. Make recommendations for regulations / input to EU Directives in the field of ground engineering.
5. Prepare, for a new joint Working Group, recommendations for European model curricula in higher education, including post-graduate training and professional experience.

The result of the deliberations of the Joint Working Group will be presented to the three Societies / Associations, which each will decide how they will take decisions on its acceptance within their own organisation.

3 Current State

Since its inaugural meeting in March 2003, the Joint Working Group concentrated on Points 2 and 3 of the Terms of Reference in order to produce, as quickly as possible, the document for the three sister societies. It developed a draft that was submitted on 16th July, 2003 to the Presidents of the ISSMGE, ISRM and IAEG. During their meeting on 22nd August, 2003 in Prague, the Presidents agreed that the draft gave a good introduction to the competencies of the sister societies. Moreover, ISSMGE President W. van Impe suggested that the draft report would be useful for the work of ISSMGE Technical Committee (TC) 20 on “Professional Practice” and probably would be integrated into the final report of that TC.

At its meeting of November 2003 in Graz, the Joint Working Group reviewed all aspects of the draft and agreed on the structure and content of the final document. Currently, it is in the process of finalising the document with the objective of submitting it to the Presidents by mid 2004.

The main points and further explanations, where appropriate, of the draft document of July 2003 are presented. Although the final version will be similar to the draft, there will be some changes and modifications in the final document. Quite properly, these cannot be published prior to submission of the final version to the Presidents.

4 Principal Aspects of the Draft Document of July 2003

In specifying the professional tasks, responsibilities and co-operation of engineering geologists and geotechnical engineers, the Working Group followed the basic idea put forward by Sir John Knill (2002). Figure 4.1 illustrates his view on the relationship between engineering geology and geotechnical engineering.

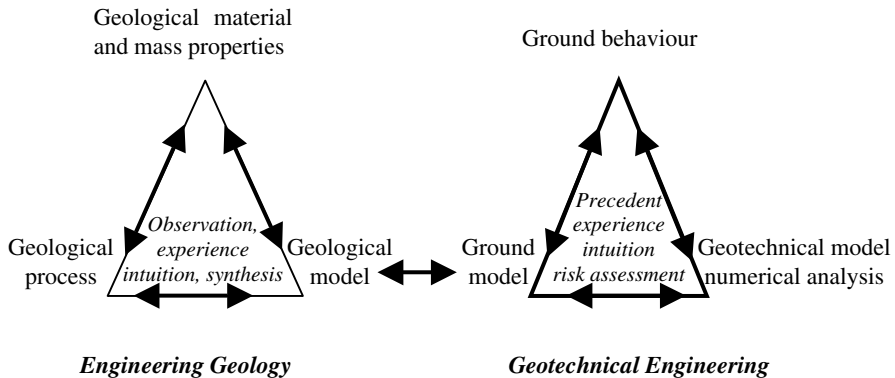


Fig. 4.1. The relationship between engineering geology and geotechnical engineering (after Knill 2002).

The grouping of the main aspects of each of the disciplines in the form of triangles originally relates to Burland, who, in 1999, defined a “soil mechanics triangle” to visualise the main aspects which define that discipline (Fig. 4.2). The interactive character of the various aspects is also indicated in this figure “*The geotechnical method is not serial, but instead involves feedback between data acquisition, material and model idealization, technical evaluation, judgement and risk management*” (Morgenstern 2000: p. 2). All aspects must be kept in balance and no aspect should be omitted.

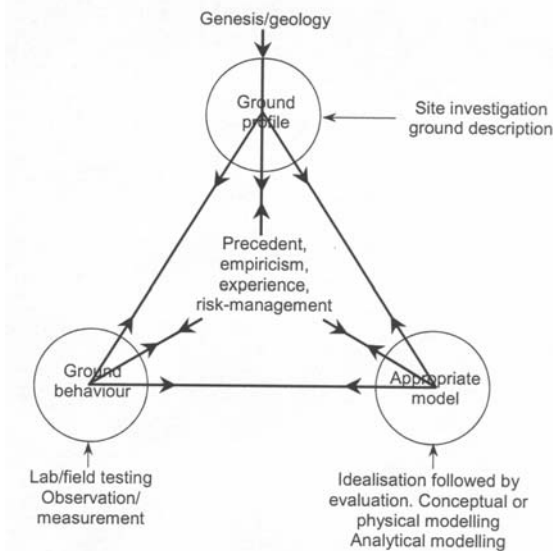


Fig. 4.2. Burland's soil mechanics (more correctly: geotechnical engineering) triangle (Morgenstern 2000).

Knill (2002) argued that with minor changes of terminology Burland's soil mechanics triangle can be adapted to represent the scopes of rock mechanics, geotechnical engineering and also of engineering geology (ref. Fig. 4.1, left triangle).

In the attempt for a synopsis of all of the principal aspects mentioned above, the Working Group developed the diagram of Fig. 4.3. Both soil and rock mechanics are understood as disciplines within the wider spectrum of geomechanics. Geomechanics itself can be represented by a triangle with the three poles "solid mechanics", "fluid mechanics" and "mechanics of discontinua". Within the "Triangle of Geomechanics", the relative positions of soil and rock mechanics can be located as shown in Fig. 4.3. Soil mechanics is the discipline that is characterised by the mechanical interaction between solids and fluids, whilst rock mechanics has a strong adherence towards the mechanics of discontinua with major influences from solid and fluid mechanics.

Critical is the transition from the geological model (the output from the engineering geology triangle; left of Figs. 4.1 and 4.3) to the ground model (the input to the geotechnical engineering triangle; right of Figs. 4.1 and 4.3). The ground model is a modified geological model with embedded engineering parameter and material properties (input from the geomechanics triangle; Fig. 4.3, top). The transition between the two models and the associated specification of the characteristic soil and rock parameters is a highly interactive process and central in ground engineering.

From Fig. 4.3, it can be depicted that there is a gradual transition from the more geologically-oriented tasks (left) to the more engineering-oriented tasks (right). As all tasks are highly interdependent, there are no clear boundaries identifiable within the spectrum of aspects shown in Fig. 4.3. However, there are definite

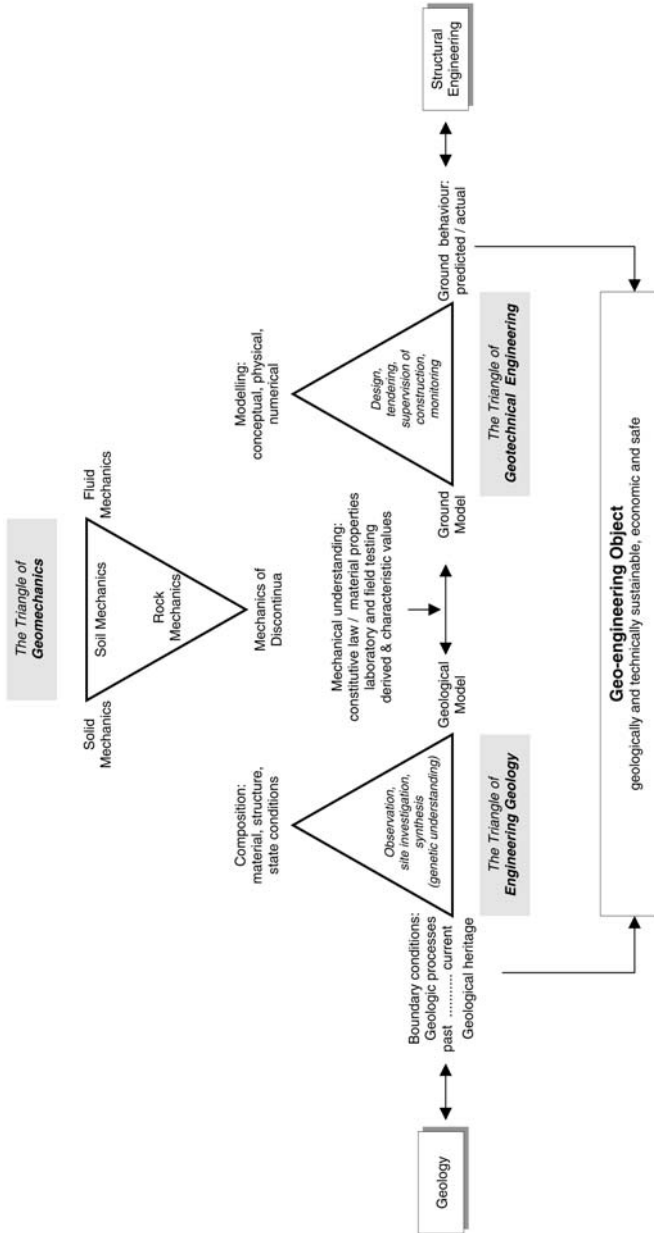


Fig. 4.3. The position of engineering geology and geotechnical engineering.

preferences for engineering geologists and geotechnical engineers in carrying out specific tasks and to accept professional responsibility. For the engineering geologist these are described in detail in the following section.

5 Professional Competencies of Engineering Geologists (Draft of July 2003)

In ground engineering, the key competency of engineering geologists is the delineation of the site geology and its transfer into appropriate and scientifically valid ground models. Such models are fundamental for any geotechnical design. The creation of geological models requires the assembly, interpretation and synthesis of diverse and often highly-fragmented geological and technical data. Ground models are converted geological models with embedded parameters required for engineering analysis and are usually established in co-operation with geotechnical engineers.

Acquaintance with geological processes and awareness of the natural environment through fieldwork give engineering geologists key competencies in geological hazard prevention and on geo-environmental issues. An example is the assessment of the compatibility of engineering structures with the geological environment. These competencies are of growing importance in urban and regional planning.

Uncertainty and risks are fundamental concerns for engineering geologists. Geological observation will always remain partial because most soils and rocks can never be fully exposed, and are either buried or otherwise obscured. Uncertainty in ground conditions, whatever the origin, contributes to the risk that a project will not meet budget or programme targets, or could fail. Engineering geologists contribute through formal procedures to risk assessment and management that are also of considerable concern to the insurance industry and in litigation.

In general, engineering geologists are familiar with the pertinent geo-scientific methodologies. They understand the physical, mechanical and chemical behaviour of geological materials and are able to identify and interpret geological events and processes, including those that may affect the project during its lifetime. They are knowledgeable of the basic engineering terminology and methods for communicating with geotechnical engineers and for understanding the engineering requirements for the design and construction of geo-engineered structures. Beyond this, engineering geologists are versatile with specialised methods, in particular:

Synthesis of Fragmentary Data Based on Genetic Understanding

The delineation of comprehensive geological models requires the synthesis of diverse, highly fragmentary data from geological and geomorphological evidence and from geotechnical and geophysical site investigations. Such synthesis is best carried out against the background of a genetic understanding of the site geology. Engineering geologists, like other geologists, are familiar with the genesis of geological materials, structures, processes and landforms.

Training for Site-Related Work

Engineering geologists are specially trained in fieldwork. From inspection of the landscape and natural and artificial exposures they are able to identify geological features and processes that are important in ground engineering. Examples are extensional fractures at the crest and compression structures at the toe of slopes that are indicative of large-scale instabilities, or morphological depressions and dry valleys that may be indicators of karstic terrain.

Versatility in Handling of Cartographic Documents, Maps and Geo Information Systems

Engineering geologists, like other geologists, are versatile in presenting complex information in space and time in cartographic documents. They have a leading edge in the handling and interpretation of 3-D and 4-D geotechnical data through information technology and a wide range of state-of-the-art ground investigation techniques (e.g. instrumented drilling, 3-D seismic data, satellite images). Engineering geological maps, data banks and geo information systems (GIS) are indispensable for a highly developed infrastructure.

Observation and Analysis of Geological Data as Keys in Contractual Disputes

Contractual disputes, in particular involving unforeseen ground conditions, are increasingly common in today's ground engineering. The costs of arbitration and litigation, and the consequential financial risks, are considerable. This situation places increased demands for proper recording and the documenting of information and for its careful interpretation. Engineering geologists are trained to observe, identify, describe and classify geological and technical phenomena in the field and on the construction site and to then apply analyses and syntheses to the data that has been collected.

Familiarity with Fractured and Ageing Materials

Rocks and over-consolidated soils constitute materials which are intrinsically fractured. Such fractures are indicators of past and current geological processes, e.g. jointing, faulting and ageing (weathering). They have significant effects on the mechanical behaviour of soils and rocks. Engineering geologists have developed methods in the evaluation, classification, description and data presentation of fracture planes (e. g. hemispherical projection technique). Furthermore, they have developed tools for the mechanical analysis and design of fractured systems (e.g. "key block" and rock fall analyses).

Preconditions for developing the competencies of engineering geologists are a study at tertiary level and several years' of practical on-site professional experience. Engineering geologists are best trained through a first degree in geology or a specialist degree in the subject followed by a post-graduate vocational course that provides the foundation to the geo-environment, hazards, hydrogeology, soil and rock mechanics, foundation engineering and underground construction.

References

- Knill Sir J (2002) Core values: The First Hans Cloos Lecture. Proceedings of the 9th Congress of IAEG, Durban, pp. 1-45.
- Morgenstern NR (2000) Common ground. Int. Conf. Geotech. Geol. Eng., Melbourne, Vol. 1: 1-30.
- Suárez L, Regueiro M (2000) Engineering Geology in Europe. Draft dossier. EFG, pp. 1-36.

Some Basic Considerations about the Necessities and Possibilities of Cooperation between Civil Engineers and Engineering Geologists

Rolf Katzenbach and Gregor Bachmann

Technische Universität Darmstadt
Institute and Laboratory of Geotechnics
Petersenstraße 13 - 64287 Darmstadt
katzenbach@geotechnik.tu-darmstadt.de
Tel: +49 61 51 16 21 49
Fax: +49 61 51 16 66 83

Abstract. The education of civil engineers and engineering geologists is different. While civil engineers are commonly educated and trained in mathematical and mechanical based sciences as statics, geotechnics, structural engineering etc. the education of engineering geologists is mainly based on natural science, added with some engineering courses. Nevertheless, the careers of both have in spite of their different priorities and capabilities – which all are necessary in complex building projects – several points of contact. Especially during the construction of tunnels, the cooperation of civil engineers and engineering geologists is important. For example the inhomogeneous rock and groundwater conditions have decisive importance for the bearing and deformation behaviour of those constructions. Therefore a detailed investigation program and a qualified geotechnical and geological interpretation and modelling is necessary. The typical field of a civil engineer is the examination of the structural stability (Ultimate Limit State - ULS) and the serviceability (Serviceability Limit State - SLS) of the construction due to Euro-Code (especially EC 1 and EC 7) and the corresponding national technical standards (codes, recommendations, guidelines etc.). A main activity of an engineering geologist is the assessment of the natural circumstances. The cooperation of both professions is settled in the valuation of the subsoil conditions before and during the construction process. The cooperation of engineering geologists and geotechnical engineers lies in the assessment of the subsoil conditions before and during the construction process of ambitious projects with special regard to the bearing and deformation behaviour which is highly influenced by the inhomogeneity and the variance of the subsoil conditions.

Keywords: cooperation, civil, ULS, ultimate, limit, state, serviceability, SLS, assessment, subsoil, modelling, risk, stochastic.

Introduction

The cooperation between civil engineers and engineering geologists is necessary, especially during difficult construction projects with special regard to the bearing and deformation behaviour that is highly influenced by the inhomogeneity and the variance of the subsoil conditions. For example:

- Tunnel constructions
- Slope reinforcements
- Subsoil modelling
- Environmental geotechnics

Especially during the construction of tunnels, the inhomogeneous rock and groundwater conditions have decisive importance for the bearing and deformation behaviour of those constructions and therefore a detailed investigation of the conditions is necessary. To minimize the risk during the construction process the right knowledge and assessment of the subsoil conditions has essential significance.

Procedure of the Planning and the Construction Process in Geotechnics

Figure 1 derives a schematic overview of the planning and construction process in Geotechnics. During the first step of a project – the selection of the site respectively the route of a track – the following procedures are performed:

- Examination of the geological conditions and specialities at a basic level (including tectonics, pseudotectonics, earthquake risks, caverns etc.).
- Design, tender, realization and soil mechanical and geological estimation and assessment of the first, preliminary soil investigation to prepare a first concept of the possibilities of the available construction methods.
- General decision of the lateral position of the line respectively of the gradient and a conceptual pre-decision of the construction design.

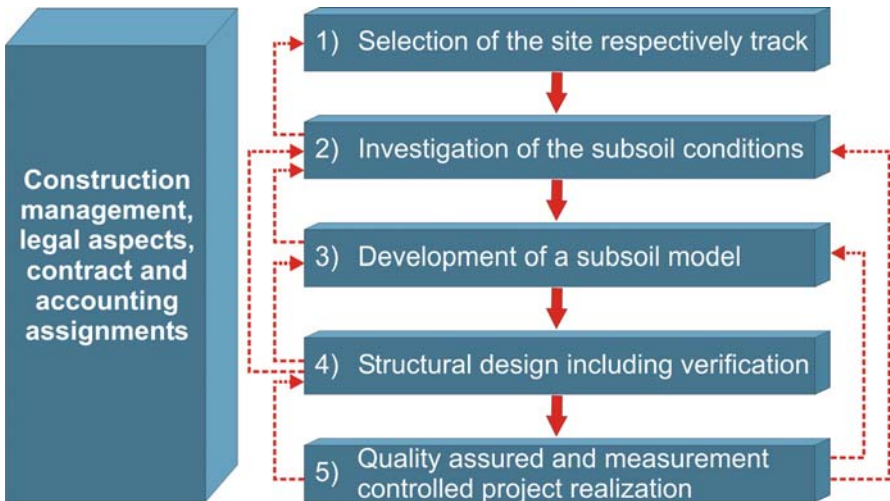


Fig. 1. Planning and construction process in Geotechnics.

The second step of a project – the main soil investigation – deals with the following procedure:

- Design, tender, realization, estimation and assessment of the design investigations of the subsoil and groundwater conditions including the choice of the investigation technique for the accurate analysis of the natural circumstances:
 - examination of the drilling core including site investigation
 - soil mechanical field- and laboratory testing
 - (engineering) geological investigations (stratigraphy, tectonics, sedimentology, mineralogy/petrography and hydrology)
 - geophysical measurements

In the third step – the development of a geotechnical soil model – the following steps are carried out:

- Volumetric estimation of the random direct soil investigation with use of the results of plain and volumetric geophysical measurements.
- Determination of the characteristic soil parameters with the use of deterministic and probabilistic estimation methods including “engineering judgement”.
- Summarization of the geotechnical soil modelling (three-dimensional, chronological, characteristic calculation values including standard deviation).

In this step a major problem arises. In consequence of the random testing significance of direct soil investigations an unavoidable remaining risk, the so called subsoil risk is a major problem during geotechnical soil modelling.

During the fourth step – the structural design including its verification (“four-eye-check” by the proof engineer) – the following steps are performed:

- Structural static design of the structure.
- Structural static modelling of the structural system (two-dimensional, three-dimensional, time-varying) with respect of the effects of soil-structure interaction (Katzenbach et al. 1998, Paul 1998)
- Preparation and verification of the structural stability (ULS – Ultimate Limit State) in consideration of the high-grade static indefinite system consisting of the subsoil and the structure (soil-structure-interaction). For example:
 - Sliding
 - Tilting
 - Bearing capacity failure
 - Slope stability failure
 - Dimensioning of structures
- Creation and verification of the proof of the structural serviceability (SLS – Serviceability Limit State). For example:
 - Settlements und differential settlements
 - Horizontal displacements

In the fifth step of the planning and construction process in Geotechnics – the quality assurance and the measurement controlled construction – the following steps are performed due to the EC-based philosophy of the “Observational Method” (Katzenbach and Gutwald 2003)

- Documentation, evaluation and assessment of the in-situ conditions by the use of geotechnical methods for the “conservation of evidence” at the site:
 - Mapping of the excavation and the heading face.
 - Monitoring of measurements (geotechnical and geodetic measurement program).
- Permanent checking and extrapolation
 - of the geotechnical modelling and
 - of the structural design and the verification of the stability and the serviceability of the structure.

Definition of the Subsoil Risk

The subsoil risk is an unavoidable remaining risk which can lead to unpredictable effects and difficulties during the use of the subsoil respectively the use of the present contents of the subsoil – groundwater, contamination etc. (Englert 1995, Katzenbach 1995). The subsoil risk exists although

- the person, who provides the subsoil, has done everything for the complete investigation and characterization of the subsoil and groundwater conditions with respect to the current, updated standards and laws,
- and although the contractor had fulfilled the demands of his examination and notice duty.

The Reason of the Subsoil Risk

The reason of the subsoil risk (unavoidable remaining risk) lies in the limited information of the geotechnical investigation and the complex, nature predetermined material subsoil (including its ingredients) which can only be approximately characterized with technical modelling. The geotechnical investigations of the subsoil are assessed as random tests. The use of stochastic methods for the assessment of the subsoil conditions in the tested area – concerning the natural material soil – has only a representative character and is not approved. The spreading of a stochastic analysis – for example the Kriging-analysis (figure 2) – depends on the use of different covariance-functions which lead to diverging results (Kolymbas 1998).

Possibilities of Cooperations between Engineering Geologists and Geotechnical Engineers

The cooperation of engineering geologists and geotechnical engineers lies in the assessment of the subsoil conditions before and during the construction process of ambitious projects with special regard to the bearing and deformation behaviour which is highly influenced by the inhomogeneity and the variance of the subsoil conditions.

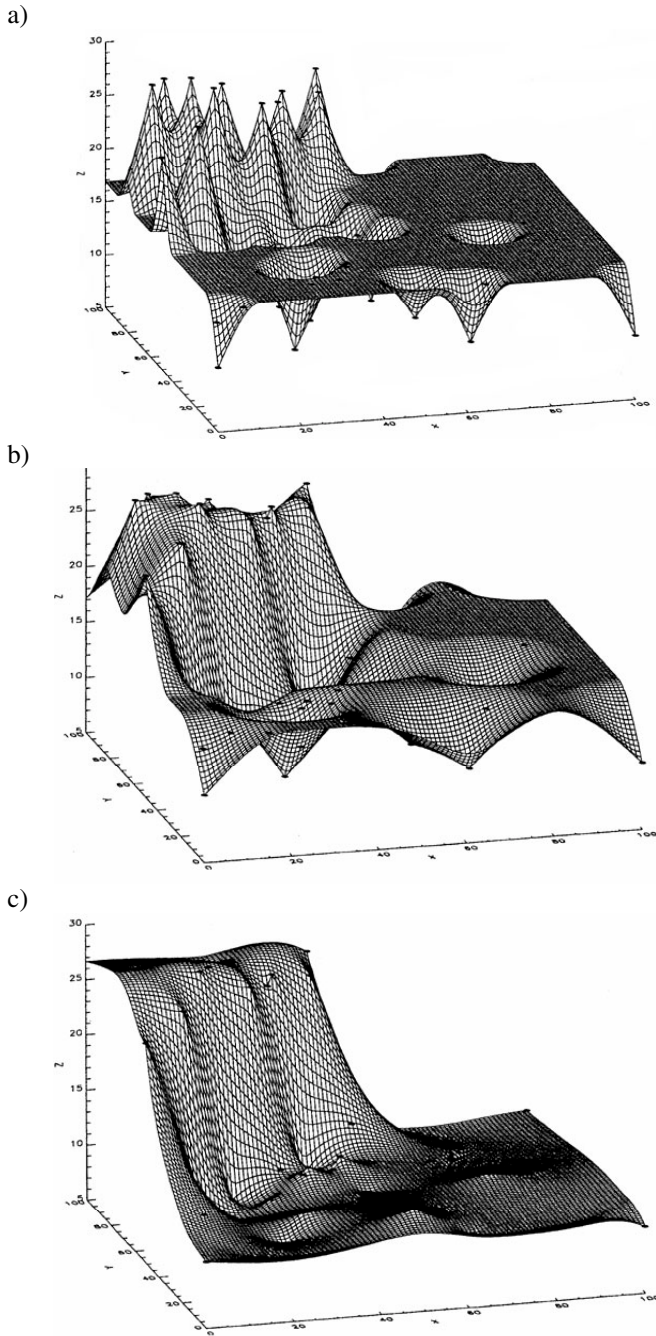


Fig. 2. Kriging-faces with different covariance-functions (Kolymbas 1998): a) with small range, b) with medium range, c) with large range.

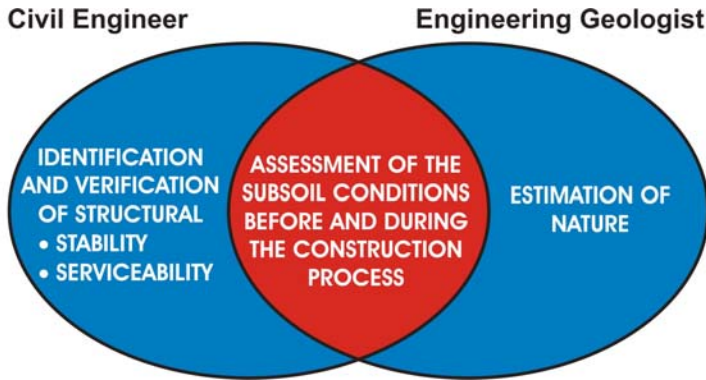


Fig. 3. Cooperation between civil engineers and engineering geologists.

References

- DGGT-/HVBI-/BDBBohr-/DIN-Gemeinschaftstagung 'Bemessung und Erkundung in der Geotechnik – Neue Entwicklungen im Zuge der Neuauflage der DIN 1054 und DIN 4020 sowie der europäischen Normung - 4.-5.2.2003 - Heidelberg, 8-1 – 8-24.
- Englert K (1995) Das Baugrundrisiko – ein oft falsch verstandener Begriff. Tiefbau, Heft 6, 464-465.
- Katzenbach R (1995) Baugrundrisiko – Wer ist in welchen Fällen verantwortlich? Mitteilungen des Institutes und der Versuchsanstalt für Geotechnik der Technischen Hochschule Darmstadt, Heft Nr. 34, 147-156.
- Katzenbach R, Festag G & Annette R (1998) Soil-structure interaction influenced by shallow tunnelling in urban areas International Conference on Soil-Structure Interaction in Urban Civil Engineering. 8./9. October.
- Katzenbach R & Gutwald J (2003) Interaktion in der Geotechnik – Baugrunderkundung, Bemessung, Bauausführung und Beobachtungsmethode.
- Kolymbas D (1998) Geotechnik – Bodenmechanik und Grundbau. Berlin: Springer.
- Paul T (1998) Soil-Structure Interaction in Urban Environments: Some Issues for Planners. International Conference on Soil-Structure Interaction in Urban Civil Engineering. 8./9. October 1998.

Current Issues Relating to the Professional Practice of Engineering Geology in Europe

David Norbury

Secretary General, European Federation of Geologists
and Associate Director, CL Associates, UK
david.norbury@mesg.co.uk
Tel: +44 118 932 8888
Fax: +44 118 932 8383

Abstract. The continuing internationalisation of the construction industry in which Engineering Geologists work has resulted in significant changes in the way we work, in the way we demonstrate to others our ability to do the work, and the environment in which we carry out our work. The pace of these changes is increasing and, shortly, few of us will be able to recall the relatively relaxed and informal ways in which we worked, even as recently as the beginning of the 1990s.

The formalisation of engineering geologists' work and reporting has come about through increasing codification of technical activities, in description of soils and rocks, in field and laboratory testing. This codification has also seen the introduction of minimum qualifications for practitioners, and this links with moves towards the international recognition of professional qualifications. The Directives on recognition have been around for comment since about 2001, and are likely to appear in European Law towards the end of 2004. This then begs the question of the need for Registration, and whether such a step would offer sufficient advantages to be of overall benefit.

This paper seeks to outline some of these recent changes, suggest how they might affect professional practice, and to try to look forward to implications for the future.

Keywords: Registration, competent person, codes of practice, standards, professional practice.

Introduction

Over recent years there has been a major shift in attitudes towards more transparent professionalism, in particular in the areas of competence and responsibility. There is an increasing need for professionals delivering to the public (sensu lato) to set, measure and demonstrate attainment of acceptable standards. Development of the necessary levels of competence and responsibility has been enshrined in national professional qualifications. The maintenance of these levels has been rather more informally attained through life long learning, generally termed CPD (Continuous or Continuing Professional Development). Increasingly there is also now a need to demonstrate that the required competence has been achieved and is being maintained. These trends are occurring at national level but are also appearing in proposals emanating from the European Parliament in Brussels.

Engineering Geologists belong to the profession of Ground Engineering that practices engineering with, on or in geological materials. Ground engineering is of considerable economic importance and benefits society in providing the means of efficient structures and sustainable use of resources and space. This is frequently not appreciated by the general public as most geo-engineered solutions are hidden in the ground. Nevertheless, ground-engineered structures are testament to substantial technological and intellectual achievements.

This fundamental input to the welfare and protection of society includes:

- the safety of residential, commercial and industrial structures,
- the essential supply of energy and mineral resources,
- the mitigation of geological hazards,
- the alleviation of human-induced hazards,
- the efficient functioning of the engineering infra-structure, and
- the contribution towards a sustainable environment.

Ground Engineering is based on the professional input of geologists and engineers, and specifically includes the scientific disciplines of engineering geology, soil mechanics, rock mechanics, hydrogeology and mining geomechanics. The execution of such projects requires the input of a range of scientific and engineering specialities, and these specialists have to be able to communicate between themselves in order to agree on theoretical models, and parameters within the models. In addition, and perhaps even more important is the need to communicate with other interested parties, not least the owner of the project.

Thus, the practice of Engineering Geology requires the communication of observations, test results and a ground model. This communication has to be unambiguous and clearly understood if the works are to proceed smoothly. In these days of engineering projects becoming increasingly international this clear communication also needs to take place between practitioners from different countries using a common international language. National codification of description terminology and field and laboratory test procedures has been appearing over the last thirty years, but the next step forward is for these national standards to be overridden by international standards. This process is reaching fruition in the first decade of the 21st century.

As with other professionals, Engineering Geologists need to demonstrate that they have obtained sufficient and suitable training and experience to act as competent professionals. The ultimate demand for such recognition is from clients and the society as a whole, but the recognition of such attainment levels comes from peer review within the profession. Peer reviewed titles have been available through national institutions in a number of countries for several years. Although the titles may be similar, it is not easy for others such as clients in one country to appreciate a qualification from another country. These practical difficulties limit mobility and international professional practice, and it has long been an aspiration to have some form of international qualification or professional passport. This concept is being brought forward by the European Parliament with the upcoming Directive on Mutual Recognition of Professional Qualifications. This Directive defines the Common Platform concept of professional competence, with the intention of achieving genuine mobility of professionals.

The History of Codification

Engineering Geology as a professional practice has been in existence for some 70 years, although others may argue that the practice has been around as long as man has been carrying out engineering works in and on the ground. In the early days the few practitioners readily communicated amongst themselves in terms of standard procedures and meanings of words and results, but this became increasingly difficult as the industry grew.

From the early days when there was no published guidance, there has been an increasing range of publications offering the opportunity for standardisation of practice in two distinct areas. Many of the procedures to be used in the field and in the laboratory became standardised, if informally at an early stage. Most such guidance has been prepared at a national level, but there has historically been limited co-ordination of these standards between countries. However, the description of soils and rocks, which is arguably the basis of all engineering geological studies and investigations, did not achieve the same early progress in this sense. Most guidance has been advisory rather than compulsory, possibly because geologists have tended to be independently minded practitioners.

As construction projects and engineering geology have become increasingly international, the need for common procedures and practices increases. Over the last 25 years so, in committee rooms around the world, work has been going on at an accelerating pace to prepare international standards. The Standards bodies responsible for co-ordinating and delivering this work are the Comité Européen de Normalisation (CEN) and the International Standards Organisation (ISO).

The intention by ISO and CEN in preparing international standards is to help raise levels of quality, safety, reliability, efficiency, compatibility and communication, and to provide these benefits at an economical cost. They contribute to making the development, manufacturing and supply of products and services more efficient, safer and cleaner. They make trade between countries easier and fairer and safeguard consumers, and users in general, of products and services.

Why Codify Engineering Geology?

The geologist has to collate and interpret the geological information and to compile a realistic geological model, and to include realistic assessments of the degree of uncertainty within the model. The key aspect of the Engineering Geologists' role then comes into play – the communication of all aspects of this model to other members of the design team and the project owner / client and, increasingly, the public.

This communication of information using normal geological nomenclature in a qualitative sense has often left listeners confused. As even standard geological nomenclature is usually qualitatively, rather than quantitatively, defined, even other geologists can be left uncertain as to the meaning intended. Over the years, a language of better defined terms has grown up which should enable the geologists

better to communicate, not least because there is now a core of standard terminology with which the listeners will be familiar. It is the derivation and definition of this standard terminology which is one of the main reasons for recent advances in the drafting and implementation of codes in Engineering Geology.

The history of the development of codes in the practice of Engineering Geology is outlined here, largely by reference to publications in the United Kingdom, being the author's base of experience. This is not to ignore the many significant developments in other countries but, as the developments have been along similar lines at similar times, by way of illustration in one country. Examples of Standards from other countries are included in the References. Nationalist attitudes are now superseded, and we are in a profession where the guidance has become international and normative.

Codification of Description

Before about 1970, there was no standard terminology allowing communication of descriptions of geological materials or their properties. This limitation was not too severe initially as the small number of practitioners were all known one to the other, and the early pace of life allowed and the embryonic nature of the science required much closer co-operation than is possible in these increasingly hectic times of international practice. Through the initial decades, most of the practitioner's efforts were directed at establishing systems of recording field data, storing samples, designing and building testing machines, and evaluating methods of foundation analysis. There was little time left to worry about preparing Codes of Practice.

Nevertheless, the first Code of Practice (CP 2001) was published in the UK in 1957. This Code laid down key underlying precepts for the description of soils in that soils should be described in accordance with their likely engineering behaviour but little in the way of defined terminology.

The use of undefined terminology caused confusion and ambiguity in communication and, as a result frequent contractual arguments and claims based on unexpected ground conditions. This can hardly be surprising as, if the terminology is variable and undefined, there will always be someone who could misread the ground conditions being predicted. For instance, terms such as highly fissured, or moderately jointed were not defined and therefore meant different things to different readers. This situation was untenable, and the nettle was grasped by the Engineering Group of the Geological Society of London who published, in the early 1970's, Working Party Reports on Core Logging and on Preparation of Maps and Plans (Anon 1970, 1972). These Reports formed the basis of UK practice and, as it turned out, international practice in many regards. Similar activities on the international scene resulted in a number of publications by 1981 on field investigation, geological mapping and soil and rock description, Anon (1977), IAEG (1981) and ISRM (1978). At the same time, in the UK this decade of guidance culminated in BS 5930 (1981), the seminal National Standard in site investigation and engineering geological activities. It is important to note however, that even at this stage

this British Standard was designated as a Code of Practice, meaning that the guidance was advisory rather than normative (compulsory). This designation was maintained through to the update in BS 5930 (1999). However, the Codes are referenced in contract specification documents, and so become binding, and in legal arguments about claims or failures, the courts will expect the national guidance to have been followed. Therefore the practice, at least by default, is that the Codes of Practice are Standards.

Despite the codification in various countries proceeding separately, there has been a good deal of inclusion of practices from one country into that of another country. For this reason, the preparation of international codes has not been as difficult as might have been anticipated, at least as far as the description of soils and rocks is concerned (ISO 2003 a, b, c). However, the historic development of local codes has tended to reflect and emphasise local geological conditions, and the classifications were rather more difficult to bring together into an international standard. This proved particularly difficult in the classification of soils, and resulted in the need for a simple and separate ISO Standard on this topic (ISO 2003 b).

For example, the Scandinavian countries have different soils (coarse glacial deposits and quick clays) and Japan (volcanic soils, silts and sands liable to liquefaction) which, national practice has, for sound technical reasons, needed to incorporate (SGS, 1981; JGS, 2000). Other National Standards on the description and classification of soil include ASTM D2487(1993), D3282(1993), DIN 4022 (1987) and DIN 18196 (1988). Guidance on the description and classification of rocks for use in engineering applications include Anon (1995), ASTM D5878(1995) and D4879(1989).

Codification of Field and Laboratory Testing

Just as important as the codification of the primary communicator – the description – is the standardisation of field and laboratory procedures. This includes all aspects relating to forming the hole or exposure, the execution of field tests and the recovery of samples as well as the carrying out of laboratory tests. If the results of any of these activities are to be applicable and relevant in the minds of others, the procedures used need to be clearly identifiable and standard.

The codification of laboratory testing on soils was started at an early stage of the industry. By the late 1940's, the early practitioners and young specialist companies were formulating procedures and practice from scratch. The procedures required included everything from how to drill a borehole, to the basic field tests, to the taking and description of samples, their storage and transport and laboratory testing. In fact, even the design of the testing machines needed to be evolved along with the test procedures. Methods of field investigation vary from country to country (influenced in part by geology) but, with the basic principles having become common over the years, standardisation is possible.

In laboratory testing, however, national practices became well advanced before the concept of formal international standardisation were recognised. As a result

there are differences between countries. Although most of the differences are not great, the time taken to work all differences through in international committee would have delayed the achievement of the Eurocodes particularly as a change in test method now would require reconsideration of historically measured properties and correlations. The ISO and CEN work under way at the time of writing is therefore to prepare Technical Specifications which will not be normative.

The testing of rocks in commercial practice on the other hand started slightly later, by which time the potential need for international co-operation was better appreciated. In the meantime, national practices had not developed in the same way as for soils. It was therefore possible for the rock testing procedures to be better organised with the International Society of Rock Mechanics taking the lead by producing a series of Suggested Methods (ISRM, 1978). As there were no precedent procedures in place, these were rapidly taken up by the professional community and became internationally recognised without the involvement of national standards bodies. It would therefore be comparatively straightforward, but not necessarily easy, to prepare normative international standards for most rock tests.

Codification of Qualifications

A further aspect of codification that applies in any subject is the identification of qualifications and experience necessary for those who plan, execute and interpret ground investigations. The guidance documents and codes prepared up to the end of the 1980's did not try to lay down rules on the qualifications and experience needed from those working as specialists in engineering geology. In the very early days, this was felt to be unnecessary, after all everybody knew everybody else and their capabilities and limitations. This has been increasingly not the case, and it is now necessary to define the roles and the allowable practitioners. It is interesting to consider who benefits most from such codification. Is it the client, who can feel better protected with proper professional advisors, is it the insurers who feel they have lower exposure, is it the individual practitioners who feel this improves their status in society, is it the employers who can recognise a qualified practitioner, or is it the companies who can see a market with fair competition? The truth is probably a bit of all of these. The position taken by the Standards institutions is based on the latter views, and Standards documents currently in preparation include definitions of specialist practitioners. These definitions will therefore become normative requirements in the practice of Ground Engineering.

The Future of Codification

After 25 years in preparation, the suite of Eurocodes is, in late 2003, becoming a reality. These Eurocodes bring together codes of practice for building and civil engineering structures, and provide a world class standard for all aspects of con-

struction. Included with Eurocode 7 : Geotechnical Design are elements of codes on the description and classification of soils and rocks, field investigation methods, field and laboratory testing, assessment of engineering parameters and design procedures. For the first time, engineering geologists throughout Europe will be talking a common language in reporting the findings of their work. The improvement of the position is even more widespread than Europe as, in accordance with the Vienna agreement, the standards drawn up by CEN and ISO undergo parallel voting procedures for common adoption. Thus, for example, the proposals for the description of soils and rocks, prepared by ISO (2003a, b, c), will be incorporated also into Eurocode 7. Thus, it will now be the case that Engineering Geologists around the world will be able to pass on their geological information, without misunderstanding and ambiguity. The brown sandy clay of the Japanese will be the same as the brown sandy clay of the Swedish geologist. Similarly, the results of field or laboratory testing will be transferable around the world. Major exceptions to this rule are China and the USA, who are not members of either of these Standards bodies, and who have had no input to the drafting of the Codes.

A Schedule of the Codes and Specifications being prepared by ISO and CEN in engineering geological investigation areas is given in Table 1. A Technical Committee of ISO prepared the Codes on the description and classification of soils and rocks. The reason this work item was proposed initially was, in accordance with the ISO mission, to encourage and allow international communication in applied science, and therefore to allow more and fairer competition for international trade. This enshrines therefore the concept of engineering geologists the world over all having a single reading of a ground model, and therefore competing for contracts and co-operating in design briefs on an equal footing.

The Eurocodes do not however, completely subsume national practices built up over the years. This is right and proper given that variations in engineering geological practice have a base in the different geological conditions in different countries. For instance the geological conditions in Scandinavia, with extensive shield rocks and quick clays, vary widely from the liquefaction prone sediments of the Pacific rim, and the deep weathering profiles of the tropics. These conditions require different approaches to investigation and testing. The description of the materials can however be based on a single standard approach.

The national differences in approach required can be incorporated into National Annexes, which allow key safety and technical issues to remain a national responsibility, and allow geological and climatic variations to be taken into account. However, these National Annexes are enhancements of, rather than local rewrites of, the overarching international codes.

The Professional Profile of a Geologist

Much of today's geological practice affects the health, safety and welfare of the public, the environment, and the economy and feasibility of engineered works. Mining, quarrying, construction, geotechnics, development of water resources, waste disposal and flood avoidance measures are just a few examples of activities

Table 1. Codes in preparation by CEN/TC 341 and ISO/TC 182/SC 1 on Geotechnical investigation and testing.

ISO Reference Number	Title	Publication as EN / ISO standard
14688-1	Identification of soil	2002-06
14688-2	Classification of soil	2002-12
14689	Identification of rock	2002-12
22475-1	Sampling methods	2006-06
22475-2	Sampling – Qualification criteria	2006-06
22476-1	Cone Penetration tests	2006-06
22476-2	Dynamic Probing	2004-12
22476-3	Standard Penetration test	2004-12
22476-4	Menard Pressuremeter test	2006-06
22476-5	Flexible Dilatometer test	2006-06
22476-6	Self-boring Pressuremeter test	2006-06
22476-7	Borehole Jack test	2006-06
22476-8	Full Displacement Pressuremeter	2006-06
22476-9	Field Vane test	2006-06
22476-10	Weight Sounding test	2002-12
22476-11	Flat Dilatometer test	2002-12
22477-1	Testing of piles	2006-06
22477-2	Testing of anchorages	2006-06
22477-3	Testing of shallow foundations	2006-06
22477-4	Testing of nailing	2006-06
22477-5	Testing of reinforced fill	2006-06
17892-1	Water Content	2003-06
17892-2	Density of fine grained soils	2003-06
17892-3	Density of solid particles	2003-06
17892-4	Particle Size distribution	2003-06
17892-5	Oedometer test	2003-06
17892-6	Fall Cone test	2003-06
17892-7	Compression test	2003-06
17892-8	Unconsolidated Triaxial test	2003-06
17892-9	Consolidated Triaxial test	2003-06
17892-10	Direct Shear test	2003-06
17892-11	Permeability test	2003-06
17892-12	Atterberg Limits	2003-06

that may significantly change the landscape and the quality of life of local inhabitants. It is essential in fulfilling these roles that the professional work of the geologist is always of the highest possible standard.

During the 19th and 20th century much of the world was explored, mapped, surveyed and its resources identified by geologists who qualified in European universities. Although this trend continues today, our industry is becoming increasingly international. Technical and financial assistance comes from a range of sources, training and research facilities are available in all countries, and consultants from across the world fly in to provide advice to clients and funders. In addition, many modern infrastructure projects traverse national boundaries, e.g.

modern infrastructure projects traverse national boundaries, e.g. Channel Tunnel, Storabelt Link, Rhinebraun Coal and its dewatering effects.

This globalisation requires professionals of equal training, experience and status to meet and deal with the technical and professional issues on an equal footing. Thus, it essential that some form of international technical passport is recognised, that will allow practice in a range of jurisdictions.

Recent developments internationally within the natural resource and finance sector increasingly require that technical reports, particularly those reporting on a company's mineral resource assets, must be signed off by a "qualified person". The Canadian Securities Administrators specify (Toronto Stock Exchange, 1999, National Instrument 43, 2001) that a qualified person:

- must be a geologist or engineer;
- must be an individual, not a firm;
- must have at least five years of experience relevant to the particular project; and
- must belong to a self-regulatory organisation with disciplinary powers that is recognised by statute (a "professional association").

Similar requirements are insisted upon by the Australian Stock Exchange and by various government bodies responsible for the licensing and regulation of mineral exploration and development.

These institutions have published lists of professional titles that they recognise. In many jurisdictions the EurGeol and EurIng titles are so recognised, subject to the individual having the relevant experience. Certain national organisations are similarly recognised

The Reporting Code (2001) set new and specific definitions for Competent Persons, as follows.

DEFINITION OF A COMPETENT PERSON

A Competent Person is a corporate member of a recognised professional body relevant to the activity being undertaken, and with enforceable Rules of Conduct. A Competent Person should have a minimum of five years experience relevant to the style of mineralisation and type of deposit under consideration. If the Competent Person is estimating or supervising the estimation of Mineral Resources or Mineral Reserves, the relevant experience must be in the estimation, evaluation and assessment of Mineral Resources or Mineral Reserves respectively.

In addition to the normally understood academic training followed by professional and technical training, the experience required from the signatory to a report has to be in a field directly relevant to the report being signed off. The implication of this precedent is that all professionals signing off reports will have to examine their competence to do so. A reasonable test might be whether the signatory would feel comfortable justifying their competence to their peers or under cross examination by an aggressive lawyer.

Access to employment in another Member State is a fundamental aspect of the free movement of persons within the European Union. The European Union policy objectives are:

- increasing the community's workers' chances of finding work and adding to their professional experience;
- encouraging the mobility of workers, as a way of stimulating the human resource response to the requirements of the employment market;
- developing contacts between workers throughout the member states as a way of promoting mutual understanding, creating a community social fabric and hence "an ever closer union among the peoples of Europe,

Regrettably, this policy is still largely an aspiration. This was recognised by the Commission in the Veil Report (European Commission, 1996) which concluded that "free movement is not yet a daily reality for Europe's citizens", and noted that, in the case of the non-regulated professions, "the reality and size of the problem of the recognition of qualifications have been underestimated" (European Commission, 1997):

The profession of geology is regulated in only two countries within the European Union, namely Italy and Spain. Where Member States do regulate, each one does so by reference to the diplomas and other qualifications obtained in its national system of education and training. The situation in a selection of countries is summarised in Table 2. In Greece the situation is more serious as, although these problems do not arise, geological reports are only accepted by the statutory authorities when engineers sign them. It is difficult to reconcile this requirement with the Competent Person concept outlined above.

In an attempt to overcome, or at least to minimise, these problems the European Commission has encouraged national professional organisations to co-operate at the European level (European Directives 89/48/EEC and 92/51/EEC). For example, the Commission has welcomed the contribution that Common platforms and initiatives taken by the private sector can make to genuine mobility of professionals. It has also been noted that such initiatives might be particularly valuable in the field of non-regulated professions, which includes both geology and engineering.

The European Professional Titles in Practice

The development of defined professional roles is closely linked with development of Directives in the European Union. In order to facilitate mobility of workers, the availability of internationally recognised qualifications is essential. The Directive on this subject is being amended in 2003 and will probably be enacted within a year or two thereafter. The position for practitioners to be able to practice, at least for limited periods, in any EU country, is the holding of a recognised qualification. This qualification is likely to be the Common Platform of the European Federation titles of European Engineer (EurIng) awarded by the European Federation of Engineers (FEANI) and European Geologist (EurGeol) awarded by the European Federation of Geologist (EFG). These titles show that the bearer has undertaken

Table 2. Summary of the regulatory position in a selection of European countries.

Italy	<ul style="list-style-type: none"> • each region has its own Order of Geologists who administer the system • geologists must be a member of the Order to legally practice • foreign academic qualifications have no legal validity 	It is virtually impossible for qualified professional geologists from other EU States to practice in Italy
Spain	<ul style="list-style-type: none"> • there are two systems for a EU citizen to legally practice • one is to obtain recognition of academic title by the Ministry of Education, Culture and Sports • second is governed by the terms of the free movement directive and operated by the Ministry of Science and Technology 	On receipt of official authorisation, the Official Association of Spanish Geologists (ICOG), registers all geologists. In order to practise the professional must register in the association. Persons holding the EurGeol title are recognised by ICOG as national geologists
United Kingdom	<ul style="list-style-type: none"> • the regulated title “Chartered Geologist” is conferred by The Geological Society of London • application for this title can be made from a migrant who is a national of a Member State 	Market forces reign, and no qualifications are required to practice
Ireland	<ul style="list-style-type: none"> • A “qualified person” has a recognised geoscience degree • at least 5 years experience in the relevant field, and • is a member of a relevant recognised “professional association” that admits members on the basis of academic qualifications and experience, requires compliance with professional codes of ethics, and has disciplinary powers 	Reports submitted to government under the requirements of the Mining Act and to the Environmental Protection Agency will only be accepted if signed off by a suitably “qualified person”.
Other	<ul style="list-style-type: none"> • market forces govern the situation • anybody can call himself a geologist and practice as such without professional qualifications • Where qualified employment is involved however, non-nationals may come up against the problem of the <i>de facto</i> recognition of their qualifications and diplomas 	Problems have arisen in Belgium, Germany and Denmark where qualifications from other countries have not been recognised for minor reasons, and with no allowance being made for professional experience

appropriate tertiary level study, carried out appropriate training and gained sufficient experience, all over a combined minimum total of eight years, to be able to act as a professional engineer or geologist, and that this record has been submitted to his or her peers for validation. The holder of such a title agrees to work within the Code of Conduct operated by the awarding Federation and will be able to work

in any European country, at least for limited periods, without the need to qualify separately in that country. These are major developments in providing commonality of professional standards, and represent development exactly as hoped for by ISO and CEN, but driven forward by the European Commission.

The European Commission recognises the value of such titles in facilitating the free movement of geologists within the Community. To guarantee wider international recognition the Federations have entered into reciprocal recognition agreements with kindred professional associations outside Europe.

The titles of EurIng and EurGeol currently have no legal status and confer no rights to work in any country. However, it is increasingly clear that possession of the title will speed the Engineering Geologist's application to work outside their home base. The national member geological associations of the European Federations have agreed that any professional holding the title will be automatically given the same rights and privileges as a national geologist, up to the legal and competency limits that each National Association might have. In those cases where the National Association is the office in charge of the recognition of foreign titles, the recognition will be automatic. In those where its role is assisting a statutory registration authority, its recommendation will be favourable to the recognition, mentioning explicitly that the applicant bears the title of European Geologist.

The EU Directive on Recognition of Professional Qualifications is likely to be implemented shortly. The European Federations are already preparing to apply for recognition as the Competent Authority and for their awarded titles to be accepted within as the Common Platform within the Competent Person concept.

It is for these reasons that a Joint European Working Group on the professional competencies of engineering geologists and geotechnical engineers was formally established in 2002 by the Presidents of the ISRM, ISSMGE and the IAEG. Over recent years, and across several European countries, there has been an ongoing debate on the particular contribution and responsibilities of engineering geologists and geotechnical engineers in solving problems in ground engineering. The interactive elements of this debate are the triangles of engineering geology, geotechnical engineering proposed by Knill (2002) and the triangle of geomechanics. This need is also underlined by differing professional definitions and accreditation rules that exist for geologists and engineers within different European countries, and by the growing demand for geologically and technically sustainable, cost effective and safe geo-engineering solutions. Internally, the Joint Working Group is seen as a means of strengthening the co-operation across the three international societies and to identify common ground. The output from the Working Group and related discussions are covered by other papers in the opening session of this conference.

Registration

There is still uncertainty as to what Registration, or Licensing, is, and what it might mean to professional practitioners. Not least of the uncertainties is whether it is the professional practice that should be regulated, or whether it is simply another form of protectionism towards the title Engineer or Geologist. One of the

most common justifications in favour of registration is on the basis of enhancement of status. This appears spurious, as status comes from performance, not from imposition of title, and probably reflects the long term downward trend in numbers of engineering graduates in the industry, and moving towards chartered status. Licensing exists in various forms (for example Canada, USA and parts of Australia), but there is little evidence that this introduces any financial benefits to the professions.

A recent meeting considered the difference between statutory title and voluntary regulation (Davies, 2003). As most governments are anti-regulation, legislators are unlikely to be persuaded of the benefits of statutory imposition, unless on grounds of public safety, value for public money or national wealth. Imposition will certainly not be introduced just to possibly enhance the salaries of practitioners.

The current arrangement of self policing, by competent nominated authorities (such as the EFG or FEANI) provides little or no regulation. Members are required to practice in accordance with the Code of Ethics, but this will only be challenged when a complaint is made or in the courts. The European Federation of Geologists has put in place a system of mandatory CPD, with the records of individual members being audited on a regular basis (annual or triennial). A higher level of regulation, on the other hand, would require a bureaucracy to police the industry, and individuals would have to provide any required self-justification to that policing body. One logical suggestion is that this could be the existing professional Federations, but there is a view in government circles that this should be removed from self control and transferred to civil servants. Although this would remove the direct cost from the institutions (but not from the individual members), most professionals would view this possibility with some alarm. In fact, the cost implications mean that this scenario is unlikely to arrive. This leaves the current institutions with the need to consider how they might operate Registration if the need arises.

The potential impact of Regulation on the industry could be very substantial, but it is less certain that it would benefit the industry. The key questions to ask include who should pay for Registration, and by whom and how would it be operated? In the UK the Science and Engineering Councils currently control the professions of geology and engineering respectively, providing umbrella control above the national title awarding bodies. The level of Regulation remains low however, and the focus of specialisation is broad. To increase the level of regulation would probably require narrower focus, and there is therefore a possibility of geology and engineering becoming rather more fragmented across the disciplines than is currently the case.

At present, an individual will carry the title Chartered / Professional / European Geologist or Engineer as appropriate, and would be required to operate within his or her competence as discussed above. One possibility would be for there to be a proliferation of titles such as Chartered Geophysicist, European Hydrogeologist and so on. There are those who might favour such moves, but the secretariat necessary to manage this will be expensive. The most important point however is the dilution of the impact and importance of the current titles. We can sell the compe-

tence and relevance of geology or engineering to the public without having to explain the subtle difference between different types of practitioners. The experience of other professions can readily illustrate the right approach. For instance barristers' rights of audience cover every practice area, but for an admiralty lawyer to appear in a murder prosecution could be breaching the code of ethics, and therefore this would not happen. There is absolutely no reason why ground engineers could not similarly be relied upon to work within their competence, so that each specialist would restrict themselves to the areas in which they demonstrably have the requisite experience.

Recent correspondence on the subject in the UK has tended towards the greater use of titles to show the public that they are dealing with a competent professional. Thus, all work would need to be signed off as suitable in terms of the core design and safety requirements by a titled Engineer or Geologist. These professionals would need to meet the requirements of a Competent Person. This is similar to the requirements that already exist in the UK for dams and nuclear structures, so this could be readily extended to encompass the signing off of ground engineering aspects of projects. It is not clear why this is not routinely required already. This also comes close to the requirements of those countries, such as Italy and Spain, in which the industry is currently regulated.

Concluding Remarks

Over a remarkably short span, engineering geology has gone from the early professionals who managed without codes, to today's world where we are being increasingly controlled by codes. The codes coming into place in the 2000's define how we drill holes, take and test samples, describe soils and rocks. Perhaps the biggest change however is reserved for the fact that we will have to carry internationally recognised qualifications if we want to be able to practice wherever we want, and that this will be possible.

Acknowledgements

I would like to thank the many people with whom I have held discussions with, sat in meetings with and generally evolved the ideas presented in this paper. In particular, I would identify fellow members of the EFG Board, John Clifford particularly, and Helmut Bock and Rodney Chartres from the Joint Working Group. The ideas presented in this paper are mine, and do not necessarily represent the views of either the EFG or my employer, both of whom I thank for permission to publish this paper.

References

- Anon (1970). The logging of rock cores for engineering purposes. Geological Society Engineering Group Working Party Report of the Engineering Group of the Geological Society of London. *Quarterly Journal of Engineering Geology*, **3**(1), 1-25.
- Anon (1972). The preparation of Maps and Plans in terms of Engineering Geology. Working Party Report of the Engineering Group of the Geological Society of London. *Quarterly Journal of Engineering Geology*, **5**, 297-367.
- Anon (1977) The description of rock masses for engineering purposes. Working party report of the Engineering Group of the Geological Society of London. *Quarterly Journal of Engineering Geology*, 1977, **10**, 355-388.
- Anon (1995). Description and classification of weathered rocks for engineering purposes. Working Party Report of the Engineering Group of the Geological Society of London *Quarterly Journal of Engineering Geology*, **28**(3), 207-242.
- ASTM : D2487-93 (1993). Classification of Soils for Engineering Purposes (Unified Soil Classification System). ASTM, PA, USA.
- ASTM : D3282-93 (1993). Standard Classifications of soils and soil aggregate mixtures for highway construction purposes. ASTM, PA, USA.
- ASTM : D5878-95 (1995). Standard Guide ofr using Rock Mass Classification Systems for Civil Engineering Purposes. ASTM, PA, USA.
- ASTM : D 4879-89 (1989). Standard Guide for Geotechnical Mapping of Large Underground Openings in Rock.
- BS CP 2001 (1957) Site Investigation. BSI, London.
- BS 5930 (1981) Code of Practice for Site Investigations. BSI, London.
- BS 5930 (1999) Code of Practice for Site Investigations. BSI, London
- Davies, Sir David (2003) Note summarising Discussion on Engineering Registration. Engineering and Technology Board. June 2003.
- DIN 4022 (1987) Classification and Description of soil and rock. DIN 4022, Part 1.
- DIN 18196 (1988). Soil Classification for civil engineering purposes. Deutsche Norm.
- European Commission (1997): Report of High Level Panel on Free Movement of Persons, Chaired by Mrs. Simone Veil, presented to the Commission on 18 March 1997.
- European Commission Press Release (1997): Free movement of people: Commission outlines follow-up measures to High Level Panel report.
- European Directive 89/48/EEC (1989): publ OJ L 9.24.1.1989, p.16.
- European Directive 92/51/EEC (1992): publ OJ L 209.24.7.1992, p.25.
- IAEG (1981) Rock and soil description and Classification for Engineering Geological Mapping. Report by IAEG Commission on Engineering Geological Mapping. *Bulletin IAEG Vol 24, pp 235 – 274*.
- ISO (2003a). Geotechnical Engineering – Identification and classification of soil – Part 1 Identification and Description. *EN 14688 – 1. ISO/TC 182/SC 1*.
- ISO (2003b). Geotechnical Engineering – Identification and classification of soil – Part 2 Classification. *EN 14688 – 2. ISO/TC 182/SC 1*.
- ISO (2003c). Geotechnical Engineering – Identification and classification of rock. *EN 14689. ISO/TC 182/SC 1*.
- ISRM (1978). Rock Characterisation, Testing and Monitoring. ISRM Suggested Methods Editor E T Brown. Pergamon Press, Oxford.
- JGS (2000). Method of classification of geomaterials for engineering purposes. Japanese Geotechnical Society 0051-2000.
- Knill, Sir John (2002). Core Values: The First Hans Cloos Lecture. – Proceed. 9th Congress, IAEG, Durban, 16 – 20 Sep. 2002.
- National Instrument 43-101 (2001): Canadian Securities Administrators.

- The Reporting Code (2001): The Code for the Reporting of Mineral Exploration Results, Mineral Resources and Minerals Reserves. Publ. by European Federation of Geologists, Institution of Mining and Metallurgy, Institute of Geologists of Ireland, and The Geological Society of London.
- SGS, Swedish Geotechnical Society (1981) Soil Classification and Identification D8:81. Laboratory Committee of Swedish Geotechnical Society. SGF Laboratory Manual, Part 2. Byggeforskringsrådet.
- Toronto Stock Exchange (1999): Setting New Standards – Final Report by the Mining Standards Task Force.

Feasibility Studies and Design of High-Speed Railway (TGV) Projects in Portugal

Ricardo Oliveira^{1,2} and Rui Abreu²

¹New University of Lisbon, Lisbon, Portugal

coba@coba.pt

Tel: +351 217925024

Fax: +351 217970348

²COBA, Environmental and Engineering Consultants, Lisbon, Portugal

coba@coba.pt

Tel: +351 217925000

Fax: +351 217970348

Abstract. Portugal is starting a large program of high-speed train routes connecting the main cities in the country and these cities to central Europe throughout Spain. The country has a very wide range of lithological types and the main routes cross some important hilly zones. These facts, together with the severe geometric restrictions associated with the High-Speed Trains, attach an important role to Engineering Geology both at the Feasibility stage and at the Design stage of the projects. The paper illustrates this important role with examples of studies currently under way in Portugal.

Keywords: high speed trains; railway, TGV, Lisbon, Badajoz, standards, feasibility study, Lisbon, Porto, Madrid.

1 Introduction

The development of the railway programme in Portugal includes some high-speed connections linking the main cities inside the country and some of those cities to Spain and central Europe. Many discussions about possible alternatives and political arrangements with Spain concerning the connecting points at the border of both countries took place while studies assessing the feasibility of alternatives were carried out (traffic, economic, technical, environmental, etc). The major issue related to this subject concerns the connection of the two most important Portuguese cities (Lisbon and Oporto) to the Spanish high-speed train network, this being the main scope of the feasibility study put for tender by RAVE (the Portuguese railway company responsible for the high-speed train projects). The study consists of the assessment of technical and environmental conditions of the three transversal corridors crossing three different regions of the country (North-D, Center-B and South-A), as shown in Fig. 1.1.

After some general considerations about the main geological and geomorphological conditions prevailing in the three corridors, the paper illustrates the



Fig. 1.1. Location of the alternative corridors.

basic studies carried out for the connection Lisbon-Badajoz (connecting point in Spain, towards Madrid) and the main geotechnical issues related to the design of such line (excavation, embankments, structure foundations and construction materials), highlighting the role of Engineering Geology in the technical evaluation of the alternatives.

2 General Geological and Morphological Description of the Alternative Corridors

The Lisboa/Porto–Madrid High-Speed Railway Line considered three geographically spaced corridors, with different geological and geomorphological characteristics. This situation produced great concerns of different geotechnical nature, which were identified during the Feasibility Study (Coba/Eurostudios, 2003a, 2003b).

Corridor A starts at a hilly zone, at the right bank of the Tagus River, which is associated with Jurassic formations (clays, marls, sandstones, conglomerates and limestones). Then it crosses the Tagus alluvial valley, filled with tens of meters

thick sandy mud formations and geomorphology flattened over a length of 14 km, followed by an extensive zone with smooth morphology, with small hills, that is associated to the Mio-Pliocene and Plistocene sediment deposits and terrace alluvia (sandstones, conglomerates, cobbles and sands with clayey beds). Then, the ground level increases gradually, associated with intrusive formations (granites, gneisses, diorites, gabbros and quartzdiorites) and metamorphic formations (schists, greywackes, lidites, quartzites and amphibolites), occurring a sharper relief, moderately hilly, characterised by considerable steep slopes and round tops, sometimes with V-shaped deep valleys.

Corridor B is constrained by the existence of a significant extension of alluvial deposits in the initial section of the line, associated with the crossing of the Tagus and Almonda rivers alluvial plain. An extensive zone follows with smooth morphology, with small hills, associated with Mio-Pliocene and Plistocene sedimentary deposits and terrace alluvia (sandstones, conglomerates, cobbles and sands and clayey beds). In the last 50 km of this corridor, in the S. Mamede mountain, the relief becomes sharper, moderately hilly, characterised by steep slopes and round tops, sometimes with V-shaped deep valleys. This zone is associated with granite intrusive rocks and Paleozoic schist-greywacke formations.

Corridor D starts in a low and flattened zone that is associated with the Cretacic clayey-sand sedimentary formations, mostly covered by extensive Plio-Plistocene beach deposits arranged in successive levels facing the sea. Continuing eastwards, cloritic schist and interbedded schist and greywacke formations from the PreCambrian and Cambrian are found, that afterwards cross a wide granite region that extends up to the border. This section corresponds to a mountain area, cut off by a wide central depression in the region of Viseu. From km 110 onwards, the mountain area evolves towards a peneplain that lengthens up to the Spanish border, abruptly cut off by the valleys with various streams, affluent of the Douro river.

Given the work scale (1/25000) and the goals of the Feasibility Study, the different geological formations identified on the geological maps, based on stratigraphic and petrological criteria, were assembled in large geotechnical units with similar behaviour and problems.

3 Main Engineering Geological Issues

The main purpose of the geological and geotechnical studies was the preliminary characterisation of the area crossed by the different alternative corridors in order to identify the major geotechnical constraints inherent to the alternatives, in view of the technico-economic optimization of the design. The studies covered the most complex geological sections, namely large excavations, embankments over compressive alluvial plains, tunnel sections and sites for the special structures, including bridges and viaducts. The analysis of the geological and geotechnical data allowed:

- the geological characterisation of the corridors formations;
- the analysis of the geological risk associated with eventual occupation of the area;
- the identification of the existing main aquifers in the area;
- the study of the large excavations and embankments, including the preliminary definition of the conditions for the re-use of the excavated materials in the embankments, the adopted geometry in the excavation and embankment slopes and the conditions of the embankment foundation;
- the preliminary definition of the track foundation;
- the characterization of the local conditions of the sections in tunnel;
- the preliminary definition of the foundation conditions for the construction of the special structures, namely bridges and viaducts;
- the location of the potential borrow and material deposit areas.

The geological and geotechnical study is illustrated in a number of plans and longitudinal section, at horizontal scale of 1/25.000 and vertical scale of 1/2.500, where a summary of the collected information is shown. The engineering geological studies were very important for the multi-criteria analysis, including the comparison of the layout alternatives of each corridor, and have influenced the selection of the most advantageous alternatives under the technical, economic and environmental points of view. The geological and geotechnical constraints have influenced various criteria, viz:

- *Economic Criteria* – in the earthworks quantities and in the types and depths of the bridges and viaducts foundations;
- *Maintenance Criteria* – in the estimation of the length of the large excavation and embankment of slopes with eventual need of maintenance during the project exploitation;
- *Construction Criteria* – associated with the need of using blasting for quarrying in rock sections, with consequences on the costs and delays.

4 Detailed Engineering Geology Characteristics Related to the Connection Lisbon-Badajoz (Corridor A)

4.1 Design Considerations

4.1.1 General

Meanwhile it has been decided that the connection between Lisbon and Madrid would be via Badajoz in Spain, since the line Badajoz-Madrid is already under design. The following considerations result from the feasibility studies that have been conducted in this corridor.

4.1.2 Excavations

Given the geomorphological conditions of the project area and the geometric constraints of the lay-out, an analysis of the alternative alignments in this corridor was

made and those that presented detrimental geotechnical constraints with immediate consequences on the costs and delays of the works have been disregarded. The definition of the longitudinal section of the chosen alignments led to the occurrence of excavations in general with reduced dimensions, however in some cases exceeding 12 m high, and in sporadic situations reaching a maximum height of 35 m to the axis. The definition of the slope inclinations took into account: the height, the geomechanical characteristics of the concerned formations, the landscaping and the characteristics inherent to the lay-out, namely cut/fill volume ratios. For its definition, it was very important the field observation and the experience of the authors with similar ground. From the above and bearing in mind the shortage of available geological information in this stage, the slope excavation geometries shown on Table 4.1 have been adopted for quantities estimation. The total volume of excavation of the selected alternative is about 20.000.000 to 33.000.000 m³, which corresponds to an average of 110.000 to 165.000 m³/km. Considering the inexistence of geotechnical investigations to quantify the mechanical excavation/blasting ratio, those values were based on the data from the surface reconnaissance and on the experience in similar geological formations. On the basis of this criterion, the total excavated volume to be blasted is estimated from 9 to 16%, corresponding to some 2.000.000 to 4.300.000 m³. Corridor A is characterised by a high heterogeneous lithology, being composed of formations of variable ages (PreCambrian to the Quaternary) and different natures (sedimentary, metamorphic and intrusive). However, as expected, the largest excavations occur in the metamorphic and intrusive formations. The surface reconnaissance allows anticipating that most of the excavated soil and rock materials along the line (after stripping of topsoil) can be used in the construction of embankments. Anyway, precautions must be taken, namely concerning their distribution, compactness and drainage and in the selection of the poorest materials to be placed in the core of the embankments. Given the shortage of construction materials in some sections of the alignment, it can be necessary to use borrow areas to be selected not far from the zones where the embankments are to be executed.

Table 4.1. Excavation Slope Geometry.

Geological Formations		Weathering Degree	Slope Inclination (v/h)	Bench Spacing (m)
Sedimentary	Soil	-	1/2 a 1/1,5	6
	Rocks	Very weathered	1/1,5	6 to 8
		Slightly weathered	1/1 a 1,5/1	8
Intrusive	Very weathered	1/1,5	8	
	Slightly weathered	1/1 a 1,5/1	8 to 10	
Metamorphic	Very weathered	1/1,5	8	
	Slightly weathered	1/1	8 to 10	

4.1.3 Embankments

The embankments have also a height, in general, lower than 12 m, however, some have heights from 12 to 25 m, and in punctual situations can reach a maximum of 30-35 m to the axis. As a result of the topographic and hydrological characteristics of the project area and the assumed environmental and landscape options, it was necessary to consider a significant number of viaducts with a total extension of some 24 to 36 km (about 13 to 18% of the lay-out). As a direct consequence of this, the volume of fill (about 18.000.000 to 30.000.000 m³) is lower than the volume of excavations. The available geological information allows anticipating that the ground conditions, after removing the surface materials (stripping of top-soil), are in general adequate to the foundation of the embankments. However some particular situations require a careful attention at the level of the embankment foundation. These situations are in general associated with thick dimension embankments in hilly areas (particularly embankments at mid-slope) and the embankments founded on materials with insufficient load bearing conditions. This is specially the case of embankments on the crossing of the river Tagus alluvial valley, composed of sandy mud soils with significant thickness and poor geotechnical characteristics. Based on the characteristics of the materials to be used in the embankments, on the soil occupation constraints, on the embankment thicknesses, on the availability of suitable material and the landscaping aspects, a 1/3 to 1/1,5 (V/H) inclination was considered for the embankment slopes. Table 4.2 presents the criterion adopted in the definition of the embankment slopes. The adopted inclinations represent a commitment between the need of assuring the stability of the embankments and the requirement to optimise the cut/fill ratio, and had also into account the environmental and landscaping constraints.

Table 4.2. Embankment Slope Geometry.

Geological Formations	Fill Materials	Foundation Conditions	Slope Inclinations (v/h)
Sedimentary	soil fill	Weak	1/3
		Adequate	1/2 a 1/1,5
	soil-rock fill	Adequate	1/1,5
Intrusive	soil and soil-rock fill	Adequate	1/1,5
	Rock fill	Adequate	1/1,5 a 1/1,3
Metamorphic	soil and soil-rock fill	Adequate	1/1,5
	Rock fill	Adequate	1/1,5 a 1/1,3

4.1.4 Track Foundation

The identified soils are in general within classes QS1 to QS3 (Classification UIC 719-R, 1994) and Type 1 to 3 (Classification GIF, 2001). The reduced geological and geotechnical information implied the adoption of a simplified criterion in the definition of the characteristics of the capping layer. Table 4.3 presents the suggested thicknesses of the capping layer, depending on the nature of materials. With regard to the materials to be applied in the capping layer, it has been as-

sumed that there were not enough quantities of appropriate re-usable materials in some sections of the layout. Thus, it has been considered that, in the next stage of the studies, the use of cement and/or lime treated soils and borrow areas should be analysed as well as the excavation of appropriate borrow areas. This situation occurs essentially in the sedimentary and metamorphic formations. The adopted thickness of the capping layer had into account a P3 ($E_f > 80$ MPa) track foundation, composed of class QS3 materials (classification UIC) founded on a ground pertaining essentially to classes QS1 and QS2 (Classification UIC).

Table 4.3. Track Foundation Conditions.

Geologic Formations	Classification UIC-719-R (1994)		Classification GIF (2001)	
	Subgrade Materials	Capping Layer (m)	Subgrade Materials	Capping Layer (m)
Sedimentary deposits (sandstone, conglomerates, cobbles, sands, clays, marls)	QS1	0,50 m of QS3 materials	Type 1	0,60 m of Type3 materials
Metamorphic formations (schists, greywacks, lidites, quartzites and anfibolites)	QS2	0,35 m of QS3 materials	Type 2	0,40 m of Type3 materials
Intrusive formations (granites, gneisses, diorites, quartzites and amphibolites).	QS2 a QS3	0 a 0,35 m of QS3 materials	Type 2 a 3	0 a 0,40 m of Type3 materials 3

4.1.5 Viaducts and Bridges Foundations

During the feasibility study, no specific geotechnical investigations were carried out for the evaluation of the foundation of the engineering structures. Therefore, just general geotechnical considerations were made, as there is not available information to estimate the geotechnical parameters of the ground and the foundation conditions of the special structures. It has been estimated that, in general, a considerable number of bridges and viaducts will be founded on shallow foundations, in association with essentially metamorphic and intrusive formations. However, some structures founded on deep foundations were identified, in general associated with less compact/consistent sedimentary formations that can require piles about 10-12 m deep. An exception is made with regard to the crossing (bridge and viaducts) of the Tagus alluvial valley where piles can reach over 40 m deep.

4.2 Bridge over the Tagus River

Either analysed solutions for corridor A will imply the crossing of the Tagus alluvial valley, composed of compressive soils with poor geotechnical characteristics that extend over some 12 km. In this stage of the studies, it has been assumed that

the crossing of the mentioned alluvial valley will be made by means of a bridge, in the areas of the stream, and in viaduct at the banks, in order to overcome eventual foundation difficulties (reduced shear strength and high deformability of the foundation), increased by the important seismic action in this region. This scenario leads to the construction of a special engineering structure with a length of about 13-14 kilometers, founded on deep foundations, composed of piles with some 30 to 40 m and even more. The estimation of the piles depth is based on the experience of the authors in similar projects in the vicinity of this crossing, namely the studies concerning the crossing over the Tagus in the Motorway A10, at Carregado, and the Vasco da Gama bridge, immediately upstream of Lisbon. In this paper it is not mentioned a new alternative for the river Tagus crossing, now under study, located in Lisbon, connecting Chelas (in the North bank) and Barreiro (in the South bank), that requires about 70 m deep piles. The results of the study of such an alternative will be discussed in future papers.

5 Final Considerations

The development of this long railway infrastructure crossing formations with very diversified geotechnical characteristics require that the criteria to be followed in the definition of the major geological and geotechnical constraints is approached on the basis of the occurring lithologies, weathering degrees and morphologies. Having into account the working scale (1/25000) and the available geological and geotechnical information at this stage of the studies, the simplification of criteria was fundamental for an easy and coherent application. This way it was possible to make a comparative analysis of solutions, under the geological and geotechnical point of view, having contributed in such a way to a multi-criteria analysis and, therefore, to the final decision as to the selection of the alignment to be further studied.

References

- COBA/EUROESTUDIOS (2003a). Estudo de Viabilidade dos Corredores Transversais da Ligação Ferroviária de Alta Velocidade entre Lisboa/Porto e Madrid. Lote 1. Nota Técnica n.º 4 – Critérios Geológicos e Geotécnicos.
- COBA/EUROESTUDIOS (2003b). Ligações Ferroviárias de Alta Velocidade Lisboa/Porto-Madrid. Lote 1. Estudo de Viabilidade dos Corredores Transversais da Ligação Ferroviária de Alta Velocidade entre Lisboa/Porto e Madrid – 1ª Fase. Volume 2. Estudos de Traçado e da Infra-estrutura. Tomo 2.2 – Geologia e Geotecnia.

Austrian Guideline for Geomechanical Design of Tunnels - Necessity for Cooperation between Geologists, Geotechnical and Civil Engineers

Ludwig Schwarz¹, Stefan Eder¹, Bruno Mattle¹, and Helmut Hammer²

¹ILF Consulting Engineers, Framsweg 16, A-6020 Innsbruck

ludwig.schwarz@ibk.ilf.com

Tel: +43 512 2412-275

Fax: +43 512 2412-200

²Büro für Geotechnik Dr. Hammer, Bahnhofstraße 1, A-6175 Kematen i. Tirol

gth@geotechnik-hammer.com

Tel: +43 5232 3980

Fax: +43 5232 3984

Abstract. Rising competitive pressure in the construction business, ever tighter schedules being set up by the clients and ongoing disputes between engineering geologists and civil engineers about the role of geotechnical engineers have – in the last few years – led to increasing discussions between engineers and geologists about the allocation of competences during the design process of underground structures. In the course of this debate, which is often polemic and anything but objective, important information is quite frequently lost – a development which may not only be to the disadvantage of the client but which may also do damage to the reputation of the professions involved. The design procedure of the new Austrian guideline for the “*geomechanical design of underground structures*” requires a close collaboration of geologists, geotechnical and civil engineers, yet without allocating competences. While preparing the tender documents for the first construction lot of the Northern feeder line of the Brenner base tunnel, the necessity of a close cooperation of the involved professions became apparent due to the complex geological situation encountered in the project area and the enormous amount of data available. Despite these difficult boundary conditions, the successful application of the guideline was last but not least the result of the joint efforts of the multidisciplinary design team.

Keywords: Austria, geomechanical tunnel design, cooperation, underground structures.

Introduction

The tight budget situation of the public construction sector is one of the main reasons for the increasing competitive pressure affecting the civil engineering industry and all related professions (designers, consultants, etc.). Other reasons are ever-tighter time schedules for the design of underground structures drawn up by the client. And last but not least there is the ongoing dispute about the role of geotechnical engineers in the area of conflict between engineering geology and

civil engineering that intensifies this discussion amongst the individual professions. As a consequence, more and more discussions about the allocation of competences during the individual design steps can be observed. In the wake of these, at times, rather heated discussions, the sight for the actual goal is sometimes lost. In general, there is a broad consensus about the necessity for teamwork between geologists, geotechnical and civil engineers, but in reality the opposite is often the case. The recent example of a tender design for an approx. 7.9 km long tunnel in an area, which is characterized by very complex geological and geotechnical conditions, showed that despite such discussions, a productive cooperation is not only possible but also imperative for the successful implementation of the design concept.

Guideline for the Geomechanical Design of Tunnels

The geomechanical design of tunnels is - to a certain extent - still based on experience, on simple empirical calculations and on standardized rock mass classifications (RMR, Q-system, etc.). Yet, in order to make the design of underground structures more comprehensible and consistent the “*guideline for the geomechanical design of underground structures using sequential excavation methods*” was developed (ÖGG 2001, Schubert et al. 2001, Schubert et al. 2003). This new design approach, which was introduced to experts in Autumn 2001, proposes a step-by-step procedure, starting with the determination of rock mass types and the allocation of rock mass behaviour types. In the next step, based on this rock mass classification, the combined behaviour of rock mass and support (= system behaviour) of the planned structure is ascertained and the tunnel construction method is determined. The guideline outlines the minimum requirements for the individual design steps without specifying the design methods to be adopted. It rather proposes the use of a methodology in line with the respective design stage. As a technical guideline, the *geomechanical guideline* intentionally abstains from discussing questions of risk and responsibility sharing including the resulting assignment of tasks and competences (ÖGG 2001). Due to the time pressure experienced with many projects, it has become common practice to implement design steps, like the definition of rock mass types and the determination of excavation and support measures, almost contemporaneously. It is not just for this reason, but for the sake of the design concept in general that a successful implementation requires teamwork of geologists, geotechnical and civil engineers. This article concentrates on step one of the design procedure, the “*determination of rock mass types*”. This first step influences all following design steps and is thus decisive for the quality of the entire design process. The project in question demanded an intensive collaboration of all design team professions involved to guarantee a comprehensible data evaluation and a reliable rock mass classification. Detailed information about the design procedure in compliance with the “*geomechanical guideline*” can be found in (ÖGG 2001, Schubert et al. 2001, Schubert et al. 2003).

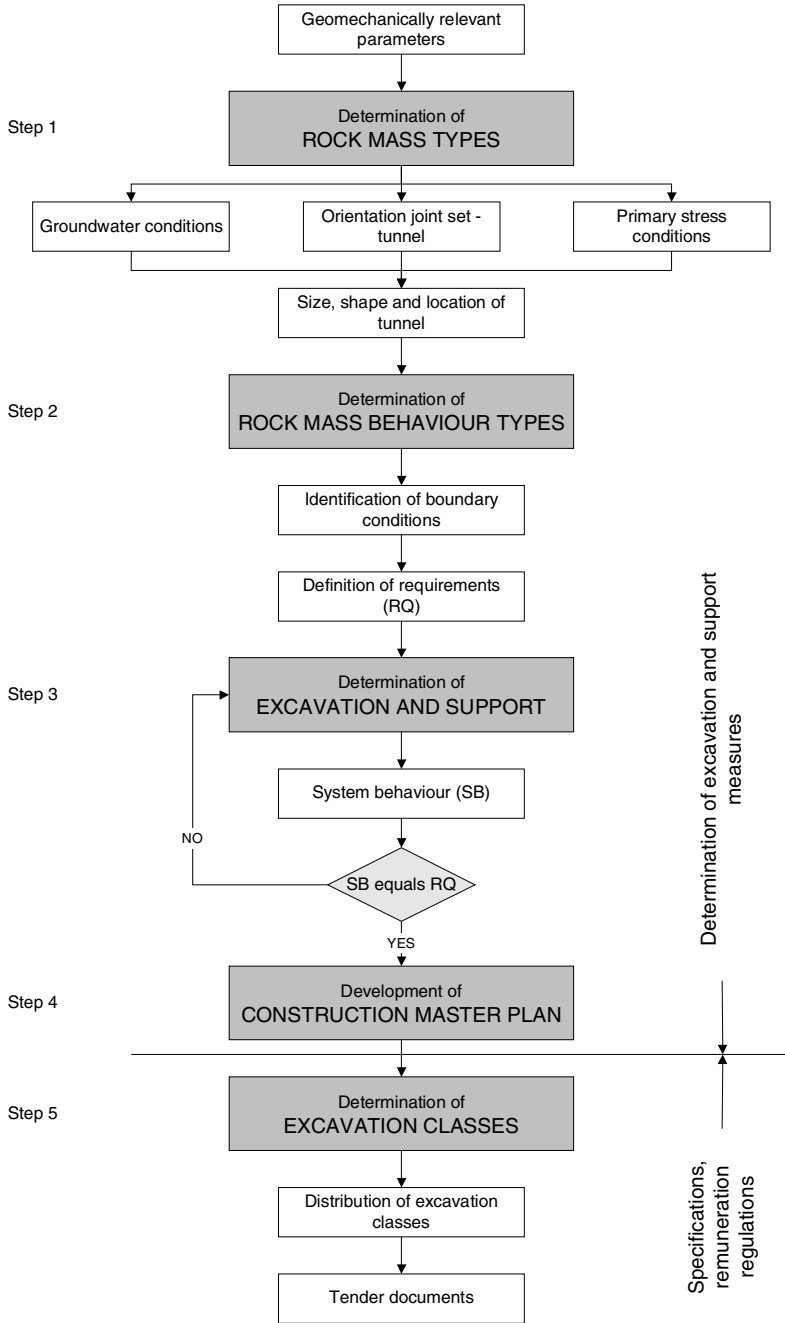


Fig. 1. Flow chart of geomechanical design procedure according to (ÖGG 2001).

Case Study: Tender Design “Lower Inn Valley Railway Tunnels”

Project Description

As part of the future Munich-Verona high-speed railway axis, the approx. 43 km long Feeder Line North, 80 % of which will be running underground, will be constructed in the Lower Inn Valley, Tyrol, Austria (Figure 2). After extensive geological and geotechnical reconnaissance works, the approx. 7.9 km long Stans / Terfens tunnel section, referred to as construction lot H5 (consisting of a 3.6 km stretch of hard rock and a 4.3 km stretch of soft rock) reached the construction stage in 2002. This construction lot was one of the first large tunnel projects in Austria that was designed and put up for tender according to the 2001 “*geomechanical guideline*”. When starting this job, the new design approach was only a few months old and none of the team members had any experience with its implementation. It was a challenge to prove its practical suitability for a project of such dimensions in as complex a geological situation as in the Lower Inn Valley, and with regard to the cooperation of the individual design team professions.

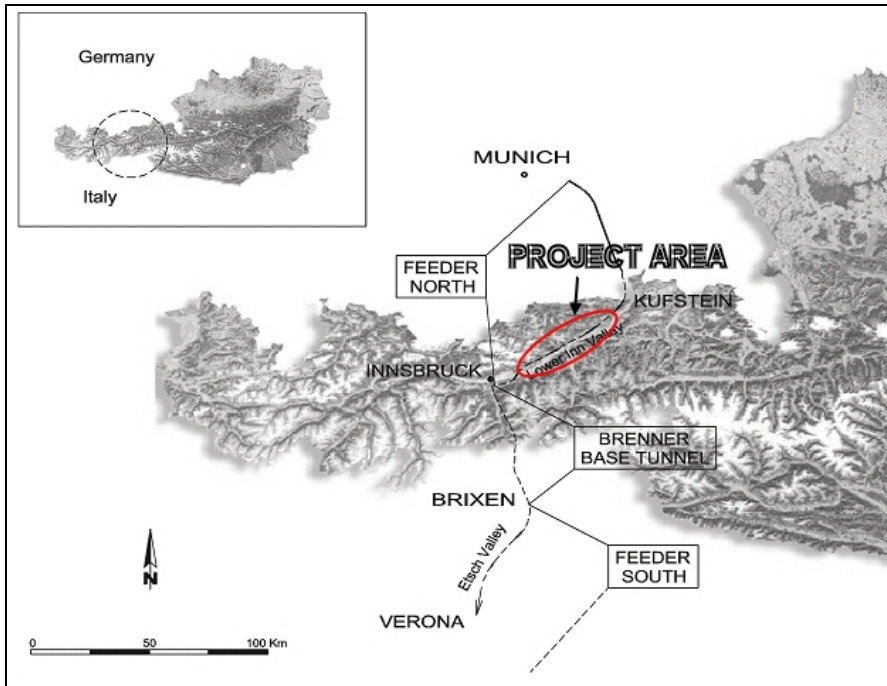


Fig. 2. Map of project area through the Lower Inn Valley (Western Austria).

Data Inquiry, Data Processing

The project area of lot H5 is situated along a geologically very complex zone at the southern boundary of the Northern Calcareous Alps. Apart from hard rock, the subsoil along the proposed tunnel alignment is mainly composed of soils of glacio-fluviatile nature (for details on the geological situation, see (Bartl and Köhler 2000, Eder et al. 2003a, Eder et al. 2003b, Schwarz et al. 2003). To clarify geological and hydrogeological questions, which are of project-strategic and project-relevant significance on the one hand and to compile the database needed for the tunnel design and the tender document preparation on the other hand, an extensive geological and geotechnical reconnaissance program was carried out. The program comprised a wide range of methods to fulfil the required tasks. The applied methodology covered the whole state-of-the-art investigation repertoire including: geological mapping (at a 1:10,000 and 1:5,000 scale), exploratory boreholes with borehole tests, hydrogeological groundwater monitoring including hydraulic testing and groundwater modelling, laboratory tests, geophysical investigations, and pilot tunnels. The extent of the applied investigations is summarized in table 1. More details on the reconnaissance program can be found in (Bartl and Köhler 2000, Eder et al. 2003a, Schwarz et al. 2003).

Already at this stage of the project, the wide range of reconnaissance methods required joint efforts of geologists, and geotechnical and civil engineers in order to coordinate the individual investigations to reap the maximum benefit. Once the tender phase was reached, the data collected so far were transferred into a rock mass classification according to the new guideline to compile the necessary documents.

Determination of Rock Mass Types – A Flexible Approach to Rock Mass Classification

The term “rock mass type” stands for a geotechnically relevant rock volume including discontinuities and tectonic structures, which is homogeneous with respect to its geological and geotechnical properties. In contrast to other previously applied classification schemes, key parameters may flexibly be chosen depending on the geological situation and may furthermore be updated and expanded as the knowledge increases. In other words, the number of rock mass types elaborated as well as the number and type of key parameters describing a rock mass type are determined by the project-specific geological situation and the respective project stage (Fasching 2001, ÖGG 2001, Schubert et al. 2001, Schubert et al. 2003). Each rock mass type is defined by the basic geological architecture and by geotechnically relevant key parameters. Determining the rock mass types, a multi-methodological approach was adopted to get the optimum benefit of all the information available and to guarantee a reliable rock mass classification. The methods applied ranged from simple statistical calculations to sophisticated FE simulations. The geological architecture was described based upon the data derived from several sources including: geological mapping, exploratory boreholes, and first and

Table 1. Reconnaissance works for construction lot H5 (supplemented after (Bartl and Köhler 2000, Schwarz et al. 2003).

Type of investigations	Number of investigations	Length [m]	Comments
Geological mapping			entire area 1:10,000, certain parts of the project area 1:5,000
Exploratory core drillings	57 drilling with continuous coring		50 boreholes were equipped with standpipes, 7 boreholes with inclinometers, in all boreholes in-situ tests were carried out to gain information on the physical and hydraulic properties of the rock mass
Hydrogeological investigations	97 monitoring wells 76 springs and fountains 16 streams		groundwater level and discharge were measured at least every 4 weeks, at sensitive sites every 2 weeks, hydro-chemical and isotopechemical samples were examined twice a year, at sensitive sites every 4 weeks
Laboratory tests	approx. 310 soil tests approx. 730 rock tests		including hydrochemical, isotope-chemical groundwater tests, as well as tests aimed at exploring the physical rock and soil properties
Geophysical investigations	7 seismic profiles	6.200	
Pilot tunnels	3 tunnels	5.653	in total approx. 2,100 tunnel face recordings

foremost the advance of the exploratory tunnels. The characteristic rock mass parameters were also derived from several sources and methods including: laboratory tests, in-situ tests carried out in boreholes and in the exploratory tunnels, back-calculations of deformations of the exploratory tunnels, and back-calculations of the unsupported height of the tunnel face in the exploratory tunnels and of the slopes in the project area. Figure 3 shows the procedure and methodology applied to determine the rock mass types.

The derivation and allocation of characteristic rock mass parameters turned out to be much more difficult than anticipated - due to the extensive database and the complex methodology. On several occasions, discrepancies between the back-calculation results and the exploratory tunnel observations on the one hand and the parameters derived from laboratory and in-situ tests on the other hand were observed. In addition, in some cases neither plausible rock testing data were

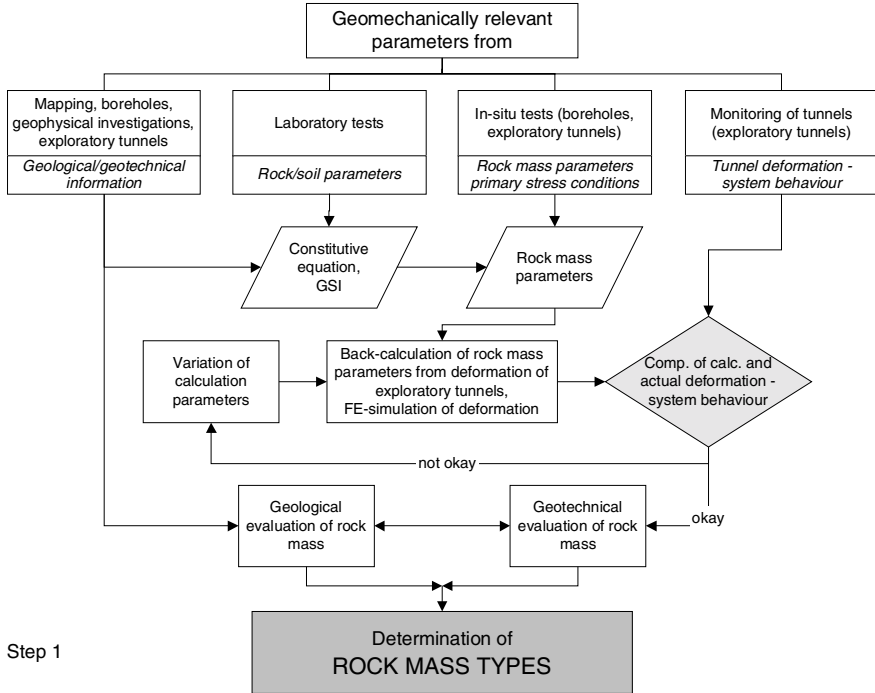


Fig. 1. Procedure applied for definition of rock mass types.

available nor back-calculations were possible. In most cases, these discrepancies occurred in fault zones or fracture zones where the heterogeneous structure and the intensive fracturing of the rock mass made it impossible to recover suitable samples for laboratory testing or to define representative borehole sections for in-situ testing. Although this rock mass is confined to relatively short zones along the planned tunnel alignment, these zones still constitute technically relevant sections of considerable economic risk (see also (Püstow et al. 2001, Riedmüller et al. 2001)). In all these cases, intensive discussions of the geological model, of the rock mass behaviour observed in the exploratory tunnels and of the back-calculation results, as well as laboratory and in-situ tests, which demanded the input of all design team professions involved (geologists, geotechnical and civil engineers including the tunnel designer), were imperative to determine the reasons for these discrepancies and plausible key parameters. The involvement of the tunnel designer was of prime importance as he was not only able to assess the relevance and consequence of individual parameters for the tunnel design, but was furthermore able to qualify the significance of discussions or to focus these discussions on the decisive parameters.

Conclusion

Despite a few points, which remain to be clarified – a revision is currently under preparation (Schubert et al. 2003) – the *geomechanical guideline* has proven its suitability for the design of underground structures. This statement has to be qualified by adding that the full benefit of this flexible classification procedure can only be gained if a close collaboration of geologists, as well as geotechnical and civil engineers is ensured. The geomechanical guideline understands itself as a technical guideline, which intentionally abstains from discussing questions of risk and responsibility distribution, including the resulting assignment of tasks and competences (ÖGG 2001). To achieve a productive and successful cooperation of the professions involved, the project management is to distribute the tasks according to professional competence. In addition, it is finally to be guaranteed that the ensuing responsibilities and risks are accepted by the respective professions.

References

- Bartl, M., Köhler, M. (2000): Munich-Verona Rail Link, Investigations for the northern approach in Austria and for the Brenner Base Tunnel. In: Felsbau 18, No. 4, pp. 7-13. Essen.
- Eder, S., Poscher, G. & Schwarz, L. (2003a): Baugrundmodelle und hydrogeologische Modelle für Tunnelvortriebe in quartären Sedimenten am Beispiel der Zulaufstrecke Nord der Eisenbahnachse Brenner. 14. Tagung für Ingenieurgeologie, pp. 77-82. Kiel.
- Eder, S., Schwarz, L. & Hammer, H. (2003b): Geotechnik quartärer Sedimente am Beispiel der geomechanischen Planung des Tunnels Stans/Terfens der Zulaufstrecke Nord der Eisenbahnachse Brenner. 14. Tagung für Ingenieurgeologie, pp. 369-370. Kiel.
- Fasching, A. (2001): Rock Mass Characterization in an Early Stage of a Tunnel Project. In: Felsbau 19, No. 4, pp. 43-48. Essen.
- ÖGG (Österreichische Gesellschaft für Geomechanik) (2001): Richtlinie für die Geomechanische Planung von Untertagebauwerken mit zyklischem Vortrieb. Salzburg.
- Püstow H., Riedmüller, G. & Schubert, W. (2001): Tunnelling in a Tectonic Melange of High Structural Complexity. In: Felsbau 19, No. 4, pp. 34-42. Essen.
- Riedmüller, G., Brosch, F.J., Klima, K. & Medley, E.W. (2001): Engineering Geological Characterization of Brittle Faults and Classification of Fault Rocks. In: Felsbau 19, No. 4, pp. 13-19. Essen.
- Schubert, W., Goricki, A., Button, E.A., Riedmüller, G., Pölser, P., Steindorfer, A.F. & Vanek, R. (2001): Consistent Excavation and Support Determination for the Design and Construction of Tunnels. In: Felsbau 19, No. 5, pp. 85-92. Essen.
- Schubert, W., Goricki, A., Riedmüller, G. (2003): Guideline for the Geomechanical Design of Underground Structures with Conventional Excavation. In: Felsbau 21, No. 4, pp. 13-18. Essen.
- Schwarz, L., Eder, S., Hammer, H. & Sedlacek, C. (2003): Interpretationsmöglichkeiten bei Erkundungsstollen am Beispiel des Ausbaus der Unterinntaltrasse. 4. Österreichische Geotechniktagung, pp. 343-361. Wien.

Soil Investigations Requirements from the Construction Industry

Christian Treve

CFE, Design Department, Herrmann-Debroux avenue 42, B-1160 Brussels, Belgium
ctreve@cfe.be
Tel: + 32 2 661 12 25
Fax: + 32 2 661 14 03

Abstract. When the majority of soil investigation methods concentrate on the characterization of the soil in terms of soil-structure interactions or structural risk evaluation, too little attention is paid to the engineering geological factors influencing the choice of the construction methods. Typical cases are presented to illustrate this point. These are selected in fields such as dewatering and temporary slopes stability.

Keywords: Groundwater model, compressive layers, soil suction.

1 Preliminary

Before the construction of a major project, a site investigation is - or should be - quite common. Mostly, this site investigation is initiated by the designer and therefore conducted with the purpose of providing the designer with the data necessary for the conception, the design, and in some cases for the risk assessment evaluation of the final project. In a typical case, a contractor is requested to submit a tender price in a few days or weeks. To assess the soil conditions, he has practically no other alternative than to refer to the existing site investigation report. Unfortunately, more often than not, this study has not been oriented to answer the specific requirements of the contractor. As a result, he will derive his construction methods, and make an estimate of the costs, based on very few geotechnical elements. By doing so, he takes major financial risks. To cover those risks some form of financial premium must be added in his tender price. As a consequence of the dramatic reduction of the time allowed for the construction phase, those tender assumptions are often used in practise with little opportunities for additional geological studies. At this stage, an error in the assessment of the soil conditions can lead to an unacceptable risk for the workers' safety. The purpose of this paper is to draw the attention of the geological and geotechnical community to some special requirements of the construction industry. With case histories, it will be shown how a better documentation of the subsoil conditions can generate a dramatic improvement in the safety of the works, pay for itself and can even generate significant savings for the owner.

2 Some Typical Requirements

2.1 Comprehensive Groundwater Model

Short term and long-term impact of the project on the watertable is too often disregarded. Collection of hydrogeological data on the subsoil in the vicinity of the project is most important. Data about the level of the water table and most of all, about the natural variations of the water table with the seasons should always be available. Piezometers and regular monitoring of the water head long before the construction starts and, when possible, as soon as the project is contemplated, is of premium importance. Permeability and the relations between the various water bearing layers must be clarified. Too often, the permeability of the water bearing layers is only estimated based on laboratory tests. With some experience, hydrogeologists do know that those figures are at best, only indicative because only the most clayey samples can be taken and tested conveniently. Hydrogeological data must be collected using in-situ pumping tests with wells and piezometers implemented in all the water-bearing layers. This is, however, not enough. Factual data should also be implemented in a global hydrogeological model allowing not only a correct estimate of the short-term impact of the project on the ground water flow (during the construction), but also of the long-term influence.

Case History

In Brussels, the storm buffer reservoir of the Place Flagey is located at a low point where three valleys meet. Those valleys cut into the sandy hills of the Brusselian (Eocene) surrounding the place and are partially filled with quaternary sandy colluviums and alluviums including very soft clayey materials and peat layers. At the bottom of the quaternary deposits, a thin layer of sandy gravel drains the ground water to the north. The walls of the reservoir cut deep through the alluvial deposits and reach into the Ypresian sands and clays basement what was expected to be a watertight clay layer laying under the Brusselian sands. Hydrogeologically, the situation is quite complex as the new reservoir forms some sort of underground barrage through the main valley and disturbs the natural underground flow, which has to find its way around the basin into the sandy colluviums laying at the foot of the lateral slopes. During the design period, the disturbing effects of the basin on the water table were not considered in detail. As a result, the effects of the construction are discovered – and handled – on a day-by-day basis. One of the first effects appears during the construction of the first diaphragm walls. For organisation reasons, the downstream wall was first constructed from a working surface lying 2 m above the water table. As the construction of the wall proceeded, its effect on the water table was immediately recorded by the piezometers. The water table rose upstream and sank downstream (figure 1). As a result, the original bentonite head of 2 m for the upstream walls was reduced under the safety level with major risks for the stability of the excavations and the final water-tightness of the reservoir. Considering this, it is now obvious that an extensive hydrogeological

study of the site and of the effects of all the construction phases on the watertable would have allowed a better management of the underground water flow by excavating the upstream wall ahead of the downstream wall (figure 2).

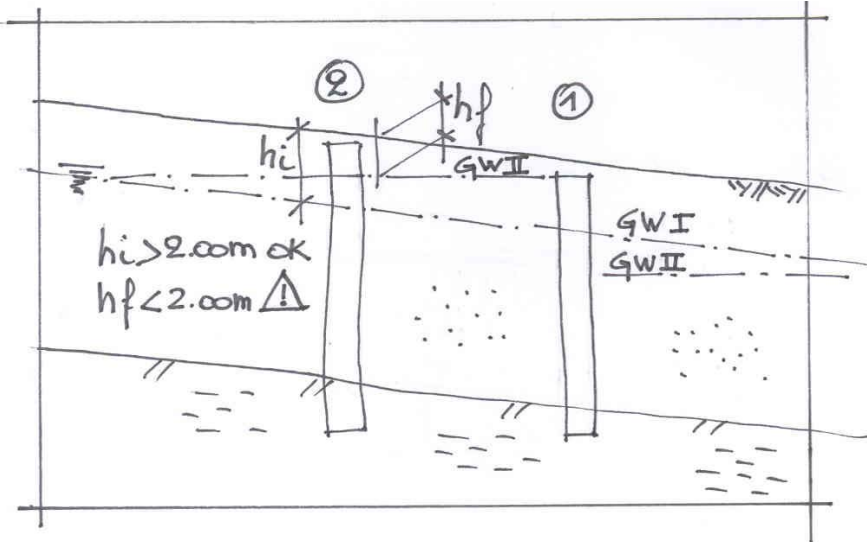


Fig. 1. Impact of the construction of a watertight screen on flowing groundwater.

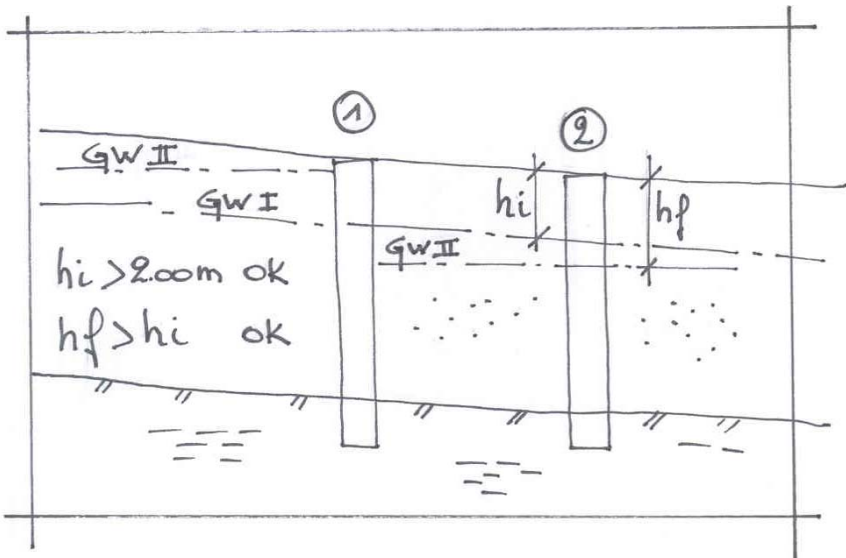


Fig. 2. Permanent disturbance of the water table after completion of an underground structure.

Later, after completion of the slurry walls and the start of the dewatering, it was observed that the influence of the works beyond the walls and under the clay layer was much more important than anticipated. Additional site investigation indicated that the watertight layer was locally eroded in the past and that through this gap the excavation was in connection with the outside world. To fix this problem, the client ordered a second bentonite-cement wall along the internal side of the first slurry wall and cutting all the layers down to the clayey basement. The construction of the reservoir can also have a long-term effect on the water table. The effect of this is still unclear but potentially dangerous as many peat layers are located in areas where a lowering of the water table is now anticipated. The conclusion of this experience is that an extensive hydrogeological investigation of the site completed with a comprehensive hydrological model of the area should have allowed a better management of the underground water flows and would have permitted substantial savings.

2.2 Effect of the Dewatering of the Water Table - Recharge Wells

It is common practise for the Engineer to prescribe that the construction of a project has to be carried out in perfectly dry conditions. Doing so, he implicitly prescribes some form of dewatering. Impact of the dewatering on the water table is then a direct consequence of the prescribed construction method and should be properly appreciated at the preliminary design stage. Where and when recharge wells are necessary should be described and be included in tender program. To prescribe, as very often happens, that the impact of the dewatering outside the limits of the construction site is not allowed, is just not technically acceptable (figure 3). If a recharge well is located close to the construction pit, the recharge water flow necessary to maintain the original water level rises exponentially if the distance to the pit decreases. To be effective, the recharge wells must be located at some distance from the pit.

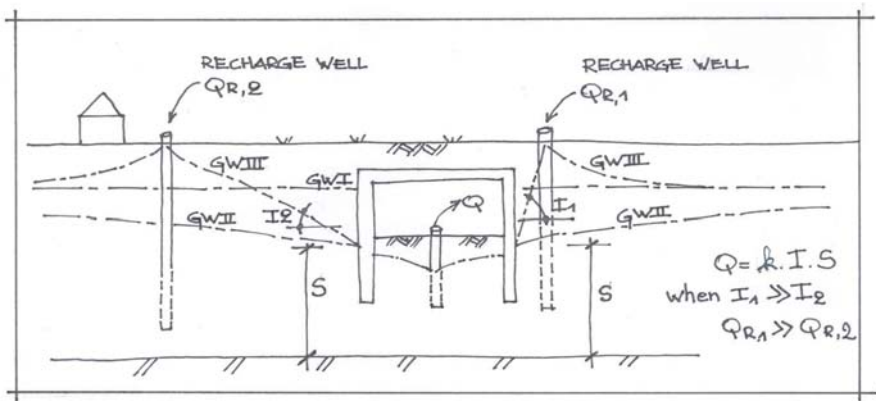


Fig. 3. Correlation between the return yield and the distance to the recharge wells.

2.3 Long Term Impact on the Water Table

If a project intersects the ground water flow, a barrier effect is bound to occur. This effect should be properly anticipated so that variations of the water table upstream and downstream can be correctly forecast and if necessary controlled.

2.4 Investigation for Compressive Layers in the Area

If some form of dewatering is necessary or even compulsory, the contractor should be provided with an extensive survey of the location of the potentially compressible layers (peat, soft organic clays, etc.) in the expected radius of influence of the dewatering. Such a survey is time consuming and can only be done during the preliminary study period. Based on the conclusions of this investigation, restriction on the dewatering can be implemented – if necessary - into the tender documents. The alternative, and the easy way out for the Engineer, is to transfer the responsibility contractually to the contractor for the consequences of the prescribed dewatering. This is of course the most common approach, but the client should be aware that the additional risk surely will be converted into a higher price of the project during tender. Moreover, in case of a major influence on the neighbourhood, the responsibility of the owner will certainly be engaged for at least one part of the damages.

Case History

The consequence of the dewatering of the Zeebrugge sea lock is a textbook example in Belgium. The lock was constructed in an open pit excavated in sands after an extensive lowering of the water table. Due to the nature of the underground, no damage was anticipated or even observed in the immediate surrounding area. Unfortunately, after a few weeks of pumping, major damage was reported in many houses of the old village of Zeebrugge, located more than 700 m from the construction site. After additional geological investigations, it was discovered that the village was built partially on a backfilled marine ditch containing thick layers of peat and that the actual influence of the dewatering extended well beyond the village (figure 4).

2.5 Effect of Suction in the Soil

Geotechnical engineers are able to estimate accurately most soil - structure interactions. However, one field seems practically out of reach: the accurate slope stability estimate in unsaturated soils. Practically, most temporary slopes and many permanent slopes are designed using soil parameters derived from the observational method and/or experiences. The slopes are calculated taking into account some form of apparent cohesion or suction into the soil. But soil suction,

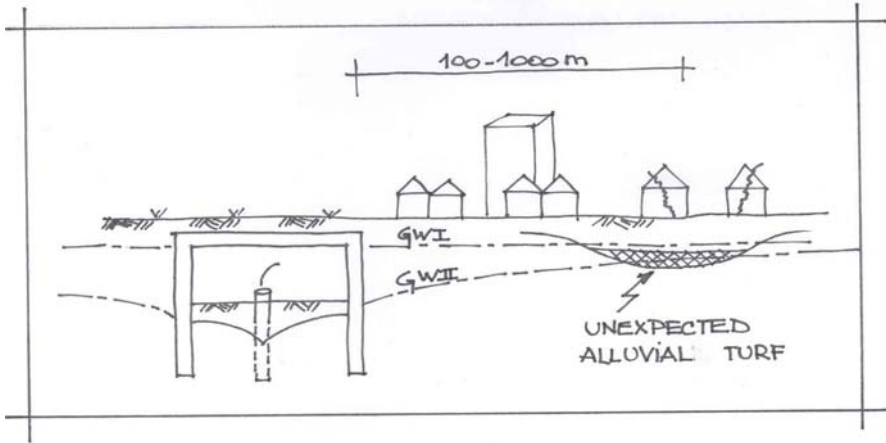


Fig. 4. Impact of the dewatering of the water table on unexpected buried turf layers in Zeebrugge (Belgium).

which depends on many factors, still cannot be efficiently estimated on site and has to be back calculated from previous slopes. We certainly need far more research in this field to be able to forecast accurately soil suction considering such factors as the water content, the grain size distribution, the relative density, and time effects (Figure 5). We really cannot allow most modern slopes to be designed in 2004 the same way these were 100 or more years ago.

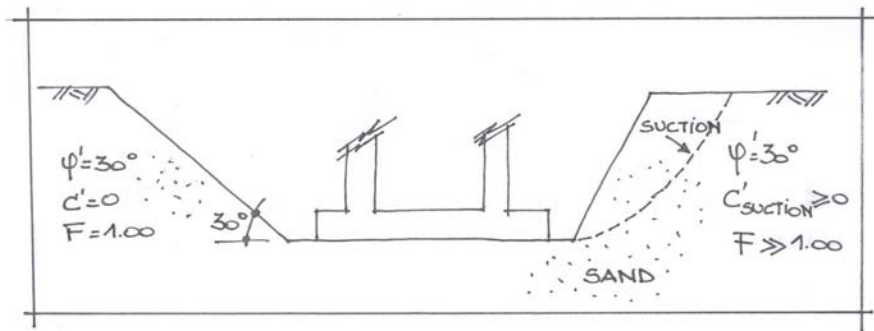


Fig. 5. Stability of temporary slopes needs to consider soil suction.

Case History

The embankments of the Paependorpsebrug, in Utrecht (The Netherlands) were built using washed sea sands with a very low fine content. The slopes of one of the embankments were designed using an estimate of the additional cohesion resulting of the suction. At the client's request, a complementary soil investigation was

carried out with the purpose to check the effective apparent cohesion of those sands. Unsaturated triaxial tests were carried out on disturbed samples previously compacted at the same water content of the embankment. The results indicate that the apparent cohesion of remoulded sands can be measured (figure 6). Nevertheless, more research remains to be done to identify the elements actually relevant to the development of this cohesion.

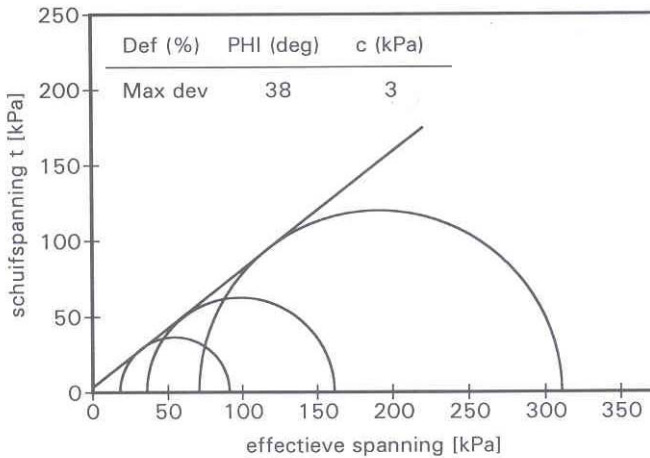


Fig. 6. Actual unsaturated triaxial test on freshly constructed washed sea-sand embankment.

3 Conclusions

Those few examples illustrate the need for more comprehensive research in the fields of Soil Mechanics and Engineering Geology. The Construction Industry has an urgent need for directly applicable knowledge, recommendations, and practices. The geological environment of each individual project should be investigated in detail prior to the construction phase because it is generally impossible to allow for enough time for a detailed investigation during the construction phase itself. Anticipating those geological hazards and taking the required steps to reduce the construction risk should be the first aim of any designer. Doing so, he will not only preserve the economical interests of his client and of the community but he will also positively contribute to the future of the industry.

The Necessity of Combining Geologists and Engineers for Fieldwork in the Practice of Geotechnics

Michael H. de Freitas

Reader in Engineering Geology,
Department of Civil and Environmental Engineering
Imperial College, London, SW7 2AZ
m.defreitas@imperial.ac.uk
Tel: +44 20 7594 6023
Fax: +44 20 7594

Abstract. This paper reviews the post-graduate training that can only be accomplished by having engineers and geologists working together in the field. It describes how meaningful communication and mutual appreciation of fundamental issues concerning a definition of ground and a prediction of how it will respond to engineering, and environmental, change may be established. Fieldwork suitable for achieving this and an awareness of fundamental misconceptions is also described.

Keywords: Field training, engineering geologists, geotechnical engineers.

Background

This paper records experiences gained teaching post-graduate (in this case Master's) students of geotechnics at Imperial College, London. These students usually have a first degree in either engineering or geology. Their first degree has taught them the nature of their subject and how it may be used in practice. Now, as post-graduate students, their task is to learn how they are to use the subject in the practice of geotechnics. The difference between their first degree (which can be thought of as "knowing-about") and their Master's degree (which is "knowing how-to") is therefore profound and this difference should be reflected in the nature of the taught MSc course. That is the main reason why good Master's courses are not the equivalent of a 4th year of first-degree teaching. To teach post-graduates how to use their subject in practice it is necessary to broaden their knowledge because no subject can be used in practice without interfacing with other subjects; it is also necessary to raise their understanding of subjects to a level where their knowledge can be used both safely and competently in practice. Some of this can only be achieved in the field.

Starting Position

Tutors must remember that most graduates have been taught with the aid of simplified and idealised exercises. These were designed to illustrate basic but complex theories, which in themselves often simplified much more complex natural processes and mechanisms. Geologists, and nowadays “Earth Scientists” (for whom geology *per se* may have represented no more than 50% of their course), are particularly vulnerable to such simplifications, especially in the subjects of mineralogy, petrology, petrography, geological structures and stratigraphy. Civil engineers are also vulnerable if they have graduated from a course where too much time has been given to the teaching of current Codes of Practice at the expense of fundamentals needed for engineering design and analyses, and education in issues which can be loosely described as “managerial” and “environmental”. In addition to this, current graduates in both engineering and geology now often lack the practical skills formerly gained from laboratory and fieldwork as these activities have been sacrificed by colleges in their attempt to economise on the cost of the course. Given this background, it is not surprising to find that the first and fundamental problem encountered by students on post-graduate courses is appreciating that nature is not simple. The second fundamental problem for these students follows from the first, *i.e.* that those who wish to work with nature, as must be done in geotechnics, have to abandon many of the preconceptions acquired from oversimplification during their first degree.

Four Fundamental Problems

1. Communication. When engineers and geologists meet to work together, neither realise that their greatest barrier to successful collaboration is communication. With luck they will at least know what they are saying to each other but that is no guarantee they will know what the other is talking about. There has to be a substantial degree of commonality for communication to be effective and for geotechnical students that commonality is the ground. Geologists and engineers will never communicate effectively if they are not taken *together* to study the ground. Further, it is not just the ground they need to see but the ground “in action” *i.e.* in its dynamic mode, as when failed or failing, or conducting fluids and consolidating. No teachers of Life Sciences would deny their students the opportunity of studying their subjects in the living form – and so it should be with geotechnics. Soil and rock masses are not static if either the mechanical or chemical forces within them are not in equilibrium, and this aspect of their behaviour should be seen.

2. Fundamental Issues. The two most common questions to answer in geotechnics are “What is there?” and “How will it respond to change?” Students should be shown the nature of the data they require and the ways in which it needs to be used to answer those questions. Just taking students to exposures of soil and

rock, on a geological tour, is not sufficient; they need to see the response of these materials to a lack of equilibrium, as can be seen in weathered profiles and the processes of mechanical failure, so that the reaction of the mass to chemical change, to load and to deformation can be illustrated and explained. Only in this way will students appreciate that the criteria we use to describe “What is there?” usually bear little or no direct relationship to “How will it respond?” That link is normally made by indirect association – usually empirical and involving other data such as tests of shear strength, stiffness, and conductivity.

Almost all other problems encountered in the commercial practice of geotechnics may be placed beneath problems 1 and 2 described above, *e.g.* problems associated with description, anisotropy, scale, time and the quest for the “correct” answer – as if a unique answer is available for each and every question and situation

3. Fundamental Misconceptions. The two most damaging misconceptions are that engineers believe there is an answer to all their questions on geology and geologists believe all ground problems can be quantified and analysed with the aid of idealization and simplification. This fallacy is most clearly demonstrated in the field but it takes time for it to be appreciated. Students who fail to obtain a satisfactory answer from a fellow student will suspect they are unlucky in asking someone who does not know. Naturally, there is advantage in asking the tutor for the tutor should know better than they, although the tutor may not know the answer either. In working practice, they may have to ask colleagues whose experience is no greater than their own! Here it is important for students to appreciate that success is most readily obtained by being able to recognize what is known from what is not known and from what needs to be known. Common parlance describes this as “class-centred” learning, which cynics recognise as a common disguise for over-large, under-resourced and under-supervised classes. However, in the field, “class-centred” learning is essential but is only productive if its *purpose* is explained. More than one field trip is required to achieve this; our experience at Imperial suggests that five field days of positive activity are required before meaningful dialogue between equals begins to take effect. The implication of this is that MSc’s in geotechnics require more than five days of supervised *joint* fieldwork and our experience at Imperial is that 12 to 15 days are needed.

4. The Reluctant Fieldworker. It is common to encounter young geotechnical engineers who believe they can pursue a meaningful career in the subject without ever going into the field: these are usually students from an engineering background. It is possible for such a career to be followed but it is rare. Many of the students who hold these views will return to companies and organisations where they may be either the *only* geotechnical person or the most highly qualified geotechnician on the staff. They will not realize, whilst at college, that under these circumstances their employer will look to them to answer any and all geotechnical problems that it receives, regardless of their training (soil and rock mechanics, engineering geology or seismology). It is vital for these students to place their current point of view into perspective, appreciate the complexity of the ground, even of ground with “simple” geology, and experience the dialogue required to at

least engage a geologist who can help resolve their problems. This cannot be done in the classroom – it must be done in the field with geologists. Our experience is that such students do change their views and become much better engineers as a result.

5. Numerical Modelling. Many of today's students of geotechnical engineering will use numerical modelling as their primary source of analyses. Geologists will be valued if they can provide data that will enable these analyses to be used appropriately; however both the engineer and the geologist must realise that the ground has to be "idealized" for this to happen, and appreciate what that means in practice. There are four basic tasks where geologists and engineers need to clearly understand how each comes to a decision. *Defining the geometry of the problem:*- This is simple to illustrate in the classroom (sand on clay, clay on bedrock, etc.). It is therefore crucial that students study vertical profiles and their lateral extensions, in both soils and rocks. Only in the field can the questions associated with defining a boundary be adequately addressed, e.g. to what extent should colour, grain size, grain shape, composition, bounding, fabric, structure, porosity, consistency, strength, deformability, etc. etc. control the position of a boundary when defining the geometry of a problem?

Selecting Parameter Values. Here the relevance of scale and time can only be resolved by reference to the ground in-situ. Many engineers and geologists will have to come to these decisions during their working life using only cores – or possibly just the logs of cores. It is therefore essential that they appreciate the importance of seeing ground in-situ and thus the caution that should be exercised on issues of scale when it is *not* seen in-situ. Time is important for two reasons. To set the initial stresses it is necessary to recreate the relevant geological history. For example, does the geologist appreciate the mechanical significance, in terms of loading and unloading, of an unconformity, of erosion of a valley, of a weathering profile and of joints? Would the engineer recognise these in the field (or from borehole logs) and have any understanding of their relative positions in the local geological history and of their influence within the mass? The time over which an analysis is supposed to apply is also relevant: for example, students need to see ground at different liquidity indices if it is sensitive to water (as most soft ground is).

Defining the Form of Analysis. This should reflect how the ground will respond to the changes to be simulated. For this, a knowledge of the products of processes is required, e.g. the presence or absence of rigid body movements and, if present, the form of displacements to be expected, e.g. rotation or translation. To answer these questions, geologists and engineers need to study the ground together, the former to identify what has happened during a response of the ground to change (e.g. consolidation and settlement) and the latter to attribute the appropriate mechanics to the movements, including the relevant boundary conditions.

Interpretation of Results. Predictions once made should be compared with reality and for this field analogues are needed. These could be engineering structures

exhibiting deformation, landscapes recording failure and case histories of ground response. All of this is field-based and involves both geology and engineering.

Fieldwork

Of the many activities that can be pursued in the field the three most relevant to this aspect of education are observation, recording, and interpretation. Sections, exposures, landscapes, failures, and circumstances (e.g. damage to buildings) should be observed and recorded to scale as annotated sketches. Sketches require a mental distillation of facts and oblige the observer to consider either the subject or the scene to be recorded. Photos do not demand this intellectual involvement and are no substitute for sketches although they can provide valuable support for them. These sketches should then be interpreted because it is the products of processes that have been sketched, (e.g. landslides, failures etc) and the purpose of doing that is to appreciate the processes that formed them, and may still be operating. The sequence of stages that constitute a “process” should also be illustrated, if only as cartoons, so that a conceptual model of products and processes can begin to be formed. With such field work students are well placed to mature to good quality practitioners of geotechnics.

Conclusions

Geologists and engineers need to feed off each other to succeed in geotechnology. They are unlikely to do this in practice if, during their education and training, they are not shown both the need for it and the ways it can be achieved. Fieldwork is an irreplaceable component of this, made most effective when geologists and engineers are obliged to study the ground together and arrive at joint conclusions that they can justify by reference to the reality of what they see in the ground around them.

References

Much interesting and relevant insight to the problems and proposed solutions in the education required for Civil and Structural engineering can be obtained from:

Allen, H. G. (Editor) 2000. Civil and Structural Engineering Education in the 21st Century. Proceedings of a Conference 26th –28th April 2000 at the University of Southampton
Vols 1 and 2. ISBN 0854327177

Contribution of On-Line Tools on Internet for the Teaching of Slopes and Tunnels Stability

René-Michel Faure¹ and Jean-François Thimus²

¹ Centre d'Etudes des Tunnels, 69500 Bron, France
rene-michel.faure@equipement.gouv.fr
Tel: +33 4 72143481
Fax: +33 4 72143490

² Université catholique de Louvain, 1348 Louvain-la-Neuve, Belgium
thimus@gce.ucl.ac.be
Tel: +32 1 0472122
Fax: +32 1 0472179

Abstract. We present there, the co-operative works done since several years, for building e-learning tools for slope stability and underground works. The aim of these tools is continued teaching, that is to say, that we don't deal with elementary theories, such as continuum mechanics or soil mechanics, but we suppose a sufficient background for the reader, and so we can speak immediately of ground works. With this concept, the main difficulty is the numerical illustration of methods for the immediate identification by the reader of the main parameter among all parameters used by the method. These e-learning tools, called DIDACTU for tunnels and DIDACPENTE for slopes, will evolve in a next future by completing the missing scopes as the chapters Investigations and Materials that will be written. A larger co-operation is welcome. DIDACTU and DIDACPENTE are reachable at: www.solem.ch or <http://lita/gce.ucl.ac.be/~kbt>.

Keywords: e-learning, tunnel, slope stability.

1 Introduction

e-learning is the use of networks for teaching, methods, theories and sometimes practise as we can explain selected images of works. From discussions with others colleagues, all through the world, e-learning is sometime frightening some teachers that believe that the face to face with student is now vanishing. On an other hand, e-learning is available at any time and appears as a solution for crowded courses, and mainly it gives also the possibility of illustrating theories trough calculus managed by the reader. Also one powerful possibility of e-learning is the world wide accessibility, and it is a challenge for countries in which the educational system must be improved.

In TC 18 (learning) of ITA, we look carefully at the evolution of teaching methods for underground works, and in the past TC 11 of ISSMFE, the first trials of using networks was done through the WASSS project (World Area Slope Stability Server), a data base of instability cases for teaching slope stability. (Faure et al, 1998)

2 First Trials for Sharing a Data Base of Cases

After the project XPENT for an expert system (Faure et al, 1988, Faure et al, 1992), the works were devoted to the building of a database of cases, as the typical reasoning of an expert is based on the similarity of cases, which is called case based reasoning (CBR). It was not a large database, as we required only cases with

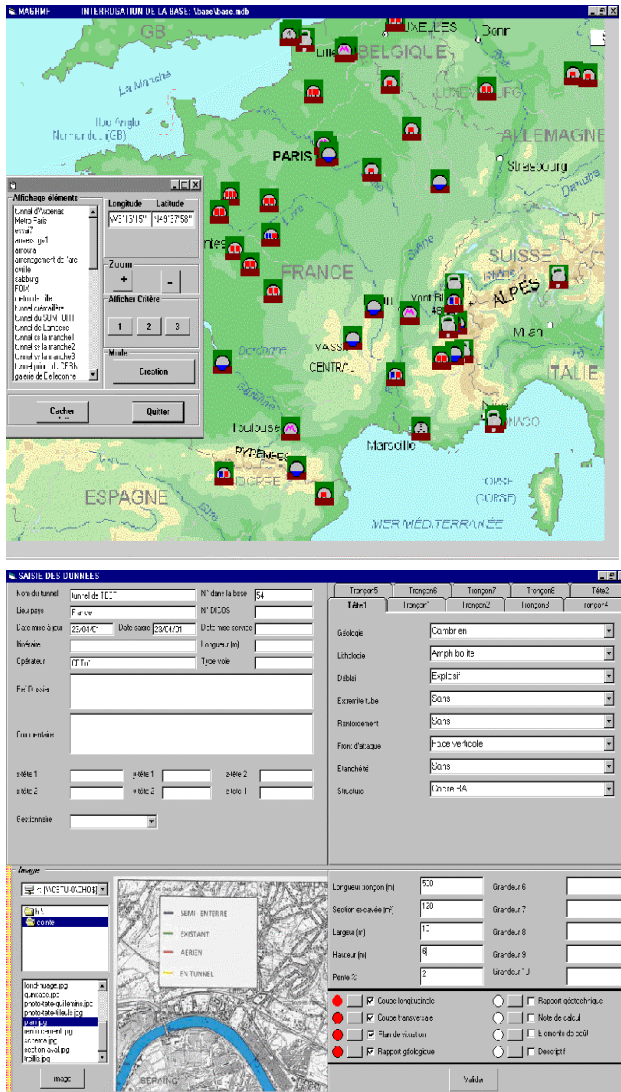


Fig. 1. This figure shows above the query of the data base from a map, and below the only screen for the meta data.

an interest for teaching. The main objection was about the property of data, and the difficulties were in a general framework for the description of one case. These two difficulties were over passed with the concept of data and meta data, that allows a very simple format for a small amount of data, the meta data that are only the spatial definition of the case and the existence of detailed data, these second being described in a free manner in an HTML page. This distinction between meta data and data allows also the half confidentiality of data, only the meta data are shown to every one, the owner of the detailed data, that are announced in the meta data, keeping the decision of showing them only on request. This approach was used both for tunnels (Faure & Hémond, 2001) and for slopes (Faure, 1999).

3 On-Line Codes

As to perform calculations for students works, some codes were translated within the PHP language, and shared on a web site. The difficulty of this operation is in a clever definition of the front-end. Effectively, the exchanges between the user and the computer have to be redefined, causing the ergonomics to become less good, and many trials are necessary for an acceptable result. The following figure shows the data sheet and the drawing of the Nixes et Trolls code for the calculation of retaining walls made with blocks and reinforced by geo-synthetics.

4 e-Learning Tools

The next step is the mixing of on line codes, base of cases and text, building so an e-learning tool. At this time two e-learning tools are under development, one for slopes called DIDACTPENTE, including also retaining walls, the second about tunnels called DIDACTU. In the following chapter we present DIDACTU.

5 The Chapters of Didactu

DIDACTU share the site of the world of tunnels with a data base called KBT, (Faure & Hémond, 2001) which is a data base of interesting cases of tunnels. (see fig 3).

When asking DIDACTU, its structure appears immediately in a rule at the top of the screen where we can find the titles of the six chapters that are:

- Project (Projet)
- Investigations (Reconnaissances)
- Design (Dimensionnement)
- Digging (Creusement)
- Materials (Matériaux)
- Tunnel life (Maintenance)

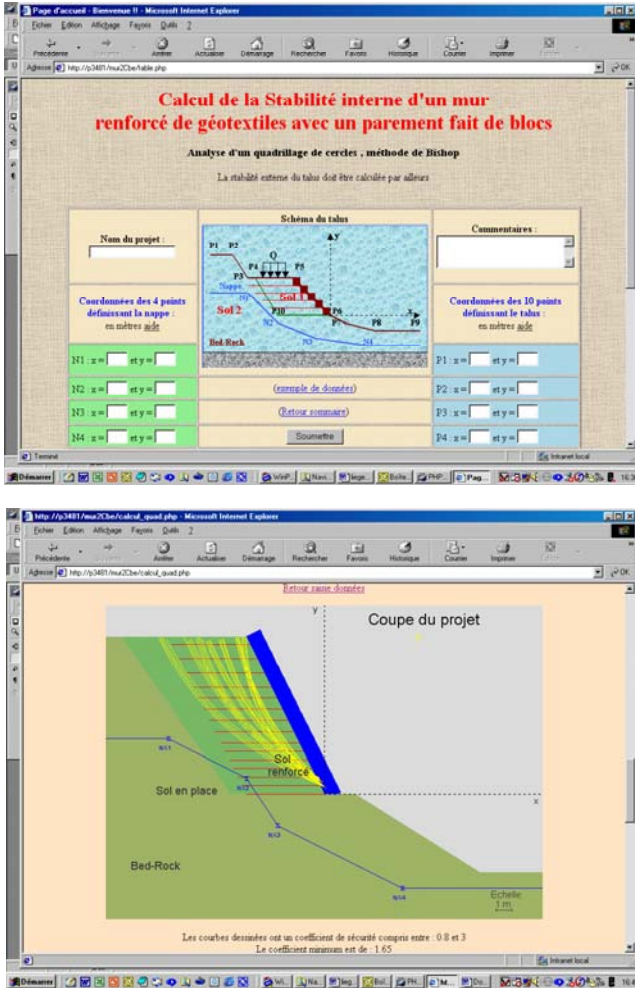


Fig. 2. A part of an input screen and the display of the calculus.

The usual approach for e-learning is the one coming from the lecture of a book. We shall use this navigation, page following page, for the presentation of the actual DIDACTU.

5.1 Project

This short part tries to give some philosophy for the designer. Underground works are not similar to usual structure works, as the soil and the structure are closely embedded. We have also to take in account the finality of the works and also all safety features that new rules induced now.

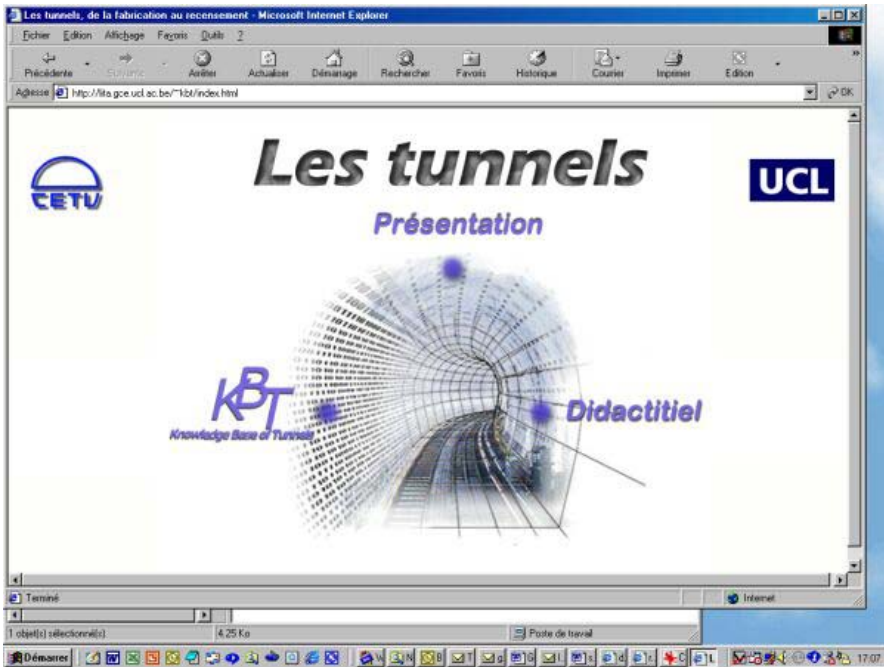


Fig. 3. This first page of the site gives the way to DIDACTU and KBT.

5.2 Investigation

This part, not yet available, will explain all the kinds of investigations we can do when building a tunnel. This chapter will be a description of methods of investigation.

5.3 Design

This chapter is the most developed, and includes on lines codes for calculations. We have the following sub sections:

5.3.1 Introduction

This introduction presents the methods that are used for the definition of the lining of the tunnel and the main parameters that we find in all methods. For each method presented an "identity card" of it can be popped up and gives to the user the hypothesis used by the method. A classification of methods is presented, from the less complex method for circular tunnel in homogenous and elastic material, to a horseshoe tunnel computed with finite elements method.

5.3.2 Empirical Methods

In this chapter we find the methods developed by Therzaghi, Barton, Bieniawski (see fig 4), Hoek, Kaiser et Bawden and the AFTES method, this last one is generally used in France, Switzerland and Belgium. (Dossier Pilote des Tunnels, 1998).

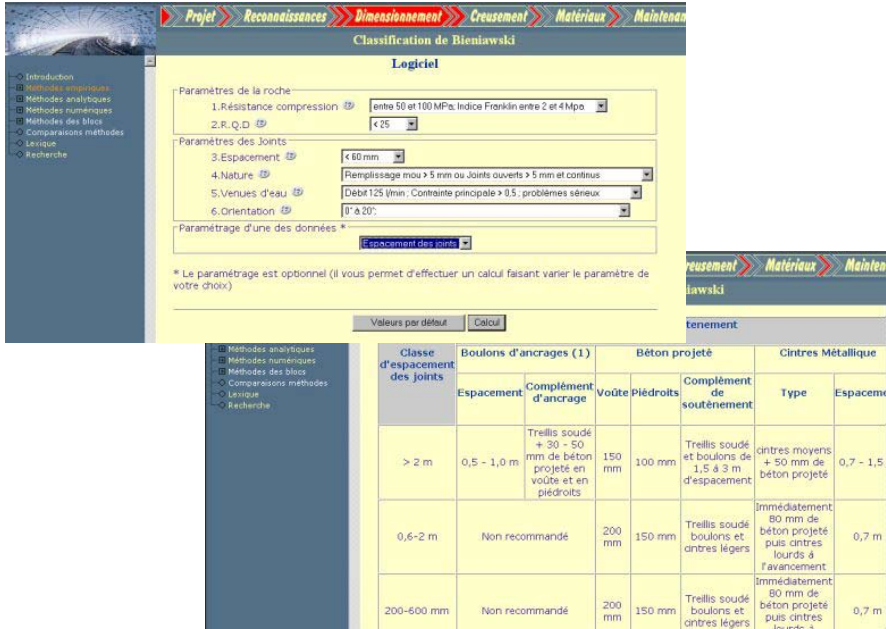


Fig. 4. This two screens show the input and a part of the results of the Beniawski Method.

For the AFTES method that recommends the kind of support, the input of data needs two screens, but all along the input the user is aided by the display of definition and the range of each parameters, and the results are presented in a graphic manner. (see fig 5 and fig 6) (AFTES, 1993)

An interesting capability of the codes is the automatic calculus for an unknown parameter, giving to it several values for making a curve which shows the influence of the selected parameter.

5.3.3 Analytical Methods

The analytical methods developed in DIDACTU are the methods of Lamé, Kirsch, Einstein-Schwartz for elastic media. For elasto-plastic media we can find the method of Panet completed by the extend proposed by Detournay for a media with an anisotropic pre-existing stress field. (Fairhurst and Detournay, 1987) (Schwartz and Einstein, 1979) (Fairhurst and Carranza-Torres, 2000)

Limit analysis is also represented by the methods of Caquot, Atkinson and Potts, and Mühlhaus and these three methods are presented together as we have the same data.

5.3.4 Numerical Methods

Finite elements method and boundary elements methods are presented. With FEM, pre-defined cases can be computed by only a presentation of BEM is done, at this time. (Lousberg and Thimus, 1985)

All the codes presented in DIDACTU are, either re-written in PHP language, either modified to be run with files (data and results), these files being managed by PHP commands. PHP is chosen because it is an easy to learn language that can be use in its own computer for debugging before setting the code in a server. PHP allows also the building of easy to use interfaces, with pop windows for giving, in context, explanations to the user. For simple algorithms the code was directly written, but for finite elements method, as data are very numerous, we have to find how to reduce them. For demonstration and teaching use, as it is done in DI-DICTU, we choose some pre-defined cases with a small number of parameters, and the mesh is predefined and chosen from a sketch. (see fig 7)

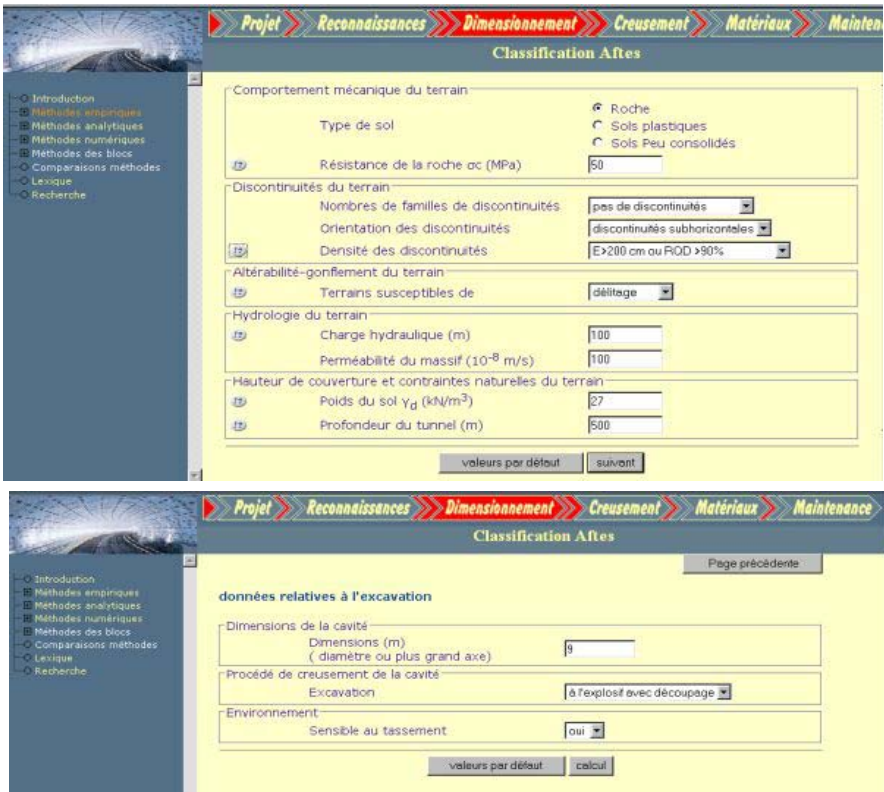


Fig. 5. The two input screens for the AFTES method.



Fig. 6. The output of the AFTES method in a graphical manner.



Fig. 7. The choice of a mesh is done by clicking on the chosen mesh.

5.4 Boring

This chapter is for the description of machines and all methods that are used for boring a tunnel.

5.5 Materials

With the development of new materials, especially concrete that is now used for different purposes, it is compulsory to describe accurately the benefits or the dis-

agreements we can find with a good or a bad use of this material. A special part will be devoted to the behaviour of concrete under a fire load using all the data from the Mont Blanc tunnel fire. (Faure et al, 2002) (Faure & Hémond , 2001).

5.6 Life of a Tunnel

As all works, a tunnel must be inspected to prevent repairs. In this part of DIDACTU we present the different operations that tunnel operators use to do for the benefit of the users.

6 Comparisons

With DIDACTU, it is very easy to compute the same case with several methods and to discover the change in the result following the hypothesis hidden in each method. This approach is very useful when teaching, as it supports the comprehension of the theories.

7 As a Conclusion, Next Improvements

The whole world of tunnel is not yet in DIDACTU and certainly will never be. But we can improve it, by improvements of that is already coded and by addition of new topics. During the coming year we have to set chapters Investigations and Materials. We hope that we can find help from students but also from companies that have lot of pictures and interesting references. We think also to develop a new navigational system based on case design, as for example, when we design a tunnel in soil, it would be helpful to hide all information about rocks and give access to information dealing with soil.

References

- AFTES: Groupe de travail n°7. (1993) Les méthodes usuelles de calcul du revêtement. Tunnel et Ouvrage Souterrains, n° 117, pp 139-163.
- AFTES: Groupe de travail n°7. (1993) Soutènement. Tunnel et Ouvrage Souterrains, n° 117, pp 61-71. Fairhurst C. Carranza-Torres C. (2000) Some comments on design procedures for tunnel support in rocks. In Closing the Circle.
- Fairhurst C & Detournay E (1987) Two dimensional elastoplastic analysis of a long, cylindrical cavity under non hydrostatic loading. Int. J. Rock Mech. Vol 24 n°4 pp 197-211.
- Faure RM, Mascarelli D, Vaunat J, Leroueil S & Tavenas F (1992) Present state and development of Xpent, expert system for slopes stability problems. Proc. 6th Int. Symposium. on Landslides, Bell ed., Christchurch.

- Faure RM, Leroueil S, Rajot JP, Laroche P, Seve G & Tavenas F (1988) Xpent, système expert en stabilité des pentes. Proc 5th Int. Symposium. on Landslides, Bonnard ed., Lausanne.
- Faure RM (1999) Databases and the management of landslides. Int. Symposium. on landslides. Shikoku (Japan).
- Faure RM, Thimus JF, & Hémond G (2004) DIDACTU, an e-learning tool for underground works. Proc ITA, Singapore.
- Faure RM & Hémond G (2001) Reconnaissance de l'état du béton du tunnel du Mont Blanc après l'incendie de Mars 1999, Proc ITA 2000, Milan, p.
- Faure RM, Pozzi V, Trasino C & Hémond G (2002) Colour and speed drill measurement for risk mitigation of a lining after a fire. The experience of Mont Blanc tunnel. Proc. ITA symposium, Sydney.
- Faure RM, Pairault T, Hama M & Turcott-Rios E (1998) The 4th release of WASSS. 8th Int. Symposium of Geology Engineering, Vancouver.
- Dossier pilote des tunnels (1998) CETu, Ministère de l'Équipement et des transports.
- Lousberg E & Thimus JF (1985), Cours de Mécanique des Roches, Université de Louvain la Neuve.
- Schwartz CW & Einstein H (1979) Simplified analysis for tunnel supports. J. of the geotechnical engineering division.

German Higher Education in the Framework of the Bologna Process

Roland Richter

Wissenschaftliches Sekretariat für die Studienreform im Land Nordrhein-Westfalen,
44780 Bochum, Germany
roland.richter@wss.nrw.de
Tel: +49.234.32-11925
Fax: +49.234.32-14269

Abstract. In 1997/98, the 16 German Länder tentatively agreed on the establishment of a new degree structure for German higher education in the form of Bachelor's and Master's programmes. Moreover, the German government passed federal legislation that officially adopted accreditation as a new steering instrument to approve these newly established Bachelor's and Master's programmes. Thus, since 1998 almost all universities, Fachhochschulen (FH), faculties, and especially the engineering departments have been busy designing new Bachelor's and Master's degree programmes. On the other hand, accreditation of programmes as a means of quality assurance has become the new pre-requisite for state recognition, which is operated by an overarching national Accreditation Board that on its turn recognises agencies that accredit particular degree programmes. All these changes will be a challenge and are likely to change the overall structure of the traditional German higher education system severely.

Keywords: Germany, Higher Education, Bologna Process, Two-Tier-Programme Structure, Quality Assessment, Accreditation, Recognition.

1 German Higher Education in Transition

In 1997/98, the 16 German Länder tentatively agreed on the establishment of a new degree structure for German higher education in the form of Bachelor's and Master's programmes. Moreover, the German government passed federal legislation that officially adopted accreditation as a new steering instrument to approve these newly established Bachelor's and Master's programmes. These decisions ended long-standing discussions about restructuring traditional courses. They also did much to address the concerns about the international competitiveness of German students and the attractiveness of Germany to foreign students. Until the mid 1980s, these discussions were characterised by two main goals. The first was to modernise the curricular content by attempting to meet the changing societal needs. The second goal was to shorten the extremely long duration of studies by placing programmes in a tighter time scheme. Several national advisory bodies put forth proposals that called for the reduction of the content and material offered in first year programmes, shifting more specialized material to later phases of study. In this context, the question arose: "What are the reasons that students study so

long?" Of course, part of the answer could be explained by the inadequate abilities of students to learn the material or by social problems that prevent them from participating. But, what was more important to HE policy makers was the assumption that the long-lasting duration of studies might have been caused by the lack of quality teachers and teaching skills, not to mention the poor quality of management by the faculties and departments. So began the debate on teaching quality and assessment in Germany, albeit later than most other countries in Europe. As a result, institutions have had to evaluate their performance and to demonstrate that the large amount of money spent for these institutions had been spent for good reasons. Despite these changes in Germany, it was not until the mid 1990s when the first agencies for evaluation of study programmes were set up - and there are, still, some Länder and institutions that are of the opinion that the introduction of regional or national schemes of quality assessment of teaching procedures is not necessary.

At the same time, politicians and academics noticed that the number of foreign students from certain countries such as the US, UK, had decreased substantially and saw the international competitiveness of Germany at risk. A number of reports with many recommendations to improve the situation were issued. The first attempts were aimed at convincing people outside Germany of the high quality of German higher education by means of public relations activities. However, in light of international trends in higher education, it soon became clear that there was no way to address this issue except to take over and introduce an international model of study programmes most foreign students are familiar with, i.e., the Bachelor-Master structure. Thus, very early, before the Sorbonne Declaration was issued in 1998, the German Rector's Conference, the Conference of Ministers of Education and the Science Council took decisions on the introduction of Bachelor's and Master's programmes. As stated above, these changes were written into law in amendments to the Federal Framework Law on Higher Education providing opportunities to the institutions to design new two-cycle programmes. It was planned that, at first, the new two-cycle system should co-exist next to the traditional German study programmes (Magister, Diplom, Staatsexamen) for a trial period of five years. In the meantime, before the trial period was over and without any serious evaluation of this new structure, the Minister's Conference took the decision to abolish the old system of German degrees by 2010. (Berner and Richter 2001)

2 The European Higher Education Framework

These initiatives have been supported very effectively by the Bologna Declaration of the 29 European education ministers signed in 1999 and the so-called Bologna process, which addresses the enhancement of the cross-border collaboration to align the different European higher education systems to one another and to improve student mobility and international exchange up to the year 2010. According to the agenda of the declaration, there are four out of six fields of action which each signatory state has to deal with: the adoption of a system of easily readable and comparable degrees, the adoption of a system essentially based on two main cycles, undergraduate and graduate, the establishment of a system of credits - such

as the ECTS - and the promotion of European co-operation in quality assurance. (Reichert and Tauch 2003) In Germany, since 1998 almost all universities, Fachhochschulen (FH), faculties, and especially the engineering departments have been busy designing new Bachelor's and Master's degree programmes. But, up until now, in addition to approximately 9,000 traditional German study programmes still being offered by the institutions, only some 1,900 new programmes have gained recognition from the respective Ministries of Education in the Länder. This means that the new programmes have not gathered more than about 3 – 5 percent of the total number of students enrolled. Moreover, analyses of these programmes have made it obvious that there is still a long way to go, not only in promoting the new two-cycle system as such, but also in respect of the re-shaping of concept and content of the programmes themselves. Thus, the introduction of the two-cycle system, credit points, and modules is not only a matter of a formal adjustment of the system. It is also an issue of intense debate regarding the goals, content, and means necessary to bring about a framework for qualifications to be met by all graduates throughout Europe for Bachelor's and Master's degrees.

3 Quality Assessment, Accreditation, Recognition

Since the mid-1990s, nearly all Länder governments have amended their higher education laws to implement obligatory internal quality assessment procedures into the quality management of the institutions. At the moment there are, in total, 12 agencies, networks or institutes on the Länder or the national level offering different quality assessment models for permanent or contractual evaluation. Nevertheless, we have to state that there is still no deeply rooted culture of assessment and evaluation in German higher education management and that there are, in total, only a few attempts to further the implementation on a broad scale and to convince the institutions that they will benefit from introducing quality assessment procedures. The implementation of the new programmes brought on a new problem: "How the recognition procedures should be organised?" It became clear very quickly that, for reasons of competitiveness, the old model of designing and re-designing national subject-oriented framework syllabi, which usually took much time (app. 8 years) for negotiations and consensus between all of the 16 Länder, would have been of no help for rapid implementation of the new programmes. Thus, the solution has been the introduction of a unique accreditation model in 1998/99, which reflects the federal structure of Germany. This new approach to quality assurance is operated by a national Accreditation Board that recognises agencies that accredit particular degree programmes. Thus, accreditation by one of the six currently existing agencies has become a prerequisite in the framework of state recognition of programmes. (Akkreditierungsrat 2003).

4 Drafting Bachelor's and Master's Structures

The requirements that have to be met by faculties introducing new Bachelor's and Master's programmes in order to receive accreditation are, for instance, the design

of goals, qualifications, competencies, modules and credit points. These requirements will be a challenge and are likely to change the overall structure of the traditional German higher education system severely. In Germany, both types of institutions, Fachhochschulen (FH) and universities, are allowed to design Bachelor's and Master's programmes. It is assumed that FHs will offer more praxis-oriented programmes and universities more research-oriented ones, even though FHs will be allowed to offer more university-style courses and vice versa. Theoretically, in the end there might be a merging of FHs and universities. However practically speaking, it will take a long time. As a matter of fact, in 2002, the Conference of Ministers for Interior Affairs responsible for personnel and salary issues within the civil service at large has taken three decisions: first, Bachelor's degrees of FHs and universities equally will lead to positions within the middle management of the civil service comparable with the status of former FH graduates; second, university Master's degrees will automatically lead to positions within the upper salary groups; third, concerning the FH Master's programmes and degrees, the accreditation agency has to investigate if the FH Master's programme really meets the requirements university Master's programmes are required to meet. If not, graduates from the FH Master's programme will be treated like graduates from ordinary Bachelor's programmes. (Akkreditierungsrat 2003)

There is an obvious need for a fundamental re-drafting of programmes when one takes into consideration the details involved in establishing the Bachelor's and Master's programmes, especially in context of the four key actions of Bologna process that aim to create more mobility and sustainable employability of graduates. In order to provide graduates with everything necessary to enter the labour market and to be successful, the reforms call for a shift from a focus on content to competencies, from teaching to learning, and from availability to demand. Thus, students and learning outcomes become the centre of all activities instead of teachers and learning input. The fact that graduates will have to demonstrate at the point of examinations knowledge and qualifications in respect to academic and societal needs makes it necessary for teachers to think not only about their own research but about the role their own subject plays in a given programme and with their colleagues. They will also have to consider what is needed to train successful graduates who will be able to find their place in the related marketplace. Here, fortunately, we do not have to re-invent the wheel. In the EU framework, on the basis of the National Framework Qualifications of the Quality Assurance Agency of England (QAA), some basic qualifications for graduates with Bachelor's and Master's degrees have been developed and defined within the so-called Dublin Descriptors of the Joint Initiative initiated by Flanders and the Netherlands.

Furthermore, speaking of mobility of students, the modularisation of the content of studies and the development of a common credit point system are regarded as proper means to support mutual recognition of student's records and degrees Europe-wide. Again, this is very demanding for the German academic because German professors in the Humboldtian tradition usually think of themselves as individual researchers, who will now be forced to engage in teamwork and cooperation to bring about a coherent and well-organised curriculum and the appropriate distribution of related credit points. Fortunately, the "Tuning Project", fi-

nanced by the EU, has tried to find solutions to the related questions in a European framework through cooperation of some 100 faculties in seven different subjects (history, geology, economics etc.), by trying to create a common understanding of what, for example, a Bachelor's programme in history or economics should be (what are the qualifications aimed at, what should be the content, what constitutes a module and a credit point?). The accrediting agencies have to watch out that the submitted programmes are not old wine in new bottles.

5 Outlook

As an outline into the future it can be concluded that under the umbrella of the Bologna process, it is pretty certain that all national systems of higher education, including the German system will not undergo a transition into a single European model. Instead, the renewed national systems will draw from both the historically rooted specifics of the individual higher education systems and the need of common ideas of a European higher education area into account for supporting further exchange, mobility, and employability of students and teachers. In 1998, the European ministers of education decided that the implementation of the new system was supposed to take place within 10 years time (2010). Thus, more and more regional politicians and academics realise that they have to take part in the game and that it will change the culture of higher education in all European countries tremendously. Furthermore, the transformation of the different traditional European degree systems into the new structure is not only a problem for the higher education systems but also one for the related societies and the European Union at large. All stakeholders involved, institutions, politicians and industry/commerce, should deal with the concerns of students and others who fear that there might be problems concerning the acceptance of the new degrees in the national labour markets. Overall, the situation seems a bit paradoxical because the industry at first was asking for a new, competitive structure, and now they seem to be afraid to hire graduates with new degrees because it is not quiet clear to them what these graduates are able to do. Thus, all stakeholders in- and outside the higher education institutions have to work together to make the new model competitive and supportive of the targets the Bologna process is aiming at: Mobility and employability of graduates within the single European market.

References

- AKKREDITIERUNGSRAT, 2003: Accrediting Accreditation Agencies and Accrediting Degree Programmes leading to Bakkalaureus/Bachelor's and Magister/Master's Degrees - Basic Standards and Criteria. <http://www.accreditation-council.de>.
- BERNER, H. & RICHTER, R. (2001) Accreditation of Degree Programmes in Germany, in: *Quality in Higher Education*, 7 (3), pp. 247-257.
- REICHERT, S & TAUCH, Ch. (2003): Bologna four years after: Steps toward sustainable reform of higher education in Europe. Report prepared for the Graz and Berlin Conferences of May/ September 2003 (Trends in Learning Structures in European Higher Education III).

International Standardisation of Ground Investigation and Testing Methods

Volker Eitner¹ and Ferdinand Stölben²

¹ DIN Deutsches Institut für Normung e.V., Normenausschuss Bauwesen (NABau),
Burggrafenstr. 6, 10787 Berlin, Germany
volker.eitner@din.de

Tel.: +49 30 2601 2526
Fax: +49 30 2601 42526

² Stölben Bohrunternehmen GmbH, Barlstr. 42, 56856 Zell/Mosel, Germany
stoelben@stoelbenbohr.de

Tel.: +49 6542 93660
Fax: +49 6542 936699

Abstract. Three committees of the International Organisation for Standardisation (ISO) and European Committee for Standardisation (CEN) prepare common standards on equipment and methods used for soil and rock identification, drilling, sampling, field and laboratory testing of rock and soil as well as groundwater measurements as part of the ground and site investigation services. These standards for investigation and testing are important for the safety of infrastructures, e. g. such as roads, bridges, canals, railways, airfields, harbours, tunnels, sewer and communication lines and other structures, e.g. buildings dams. They also facilitate the development of a common global market for the free trade of services and equipment for geotechnical investigation and testing. The standardisation in this field also leads to an apparent cost reduction in the building market.

Keywords: Geotechnical engineering, standardisation, ground investigation, testing.

Introduction

The world is getting smaller since the continuous progress of technical and economical globalisation, which is also present in the building and construction business. Therefore standards are necessary to solve problems due to communication difficulties or technical differences among clients, consultants, contractors etc. that often lead to a reduction of safety and serviceability. Standards on identification and classification, sampling, field and laboratory testing for geotechnical purposes are currently prepared by the European Committee for Standardisation (CEN) and the International Organisation for Standardisation (ISO) according to the Vienna Agreement.

The World Trade Organisation (WTO) is the international organisation dealing with the global rules of trade between nations. Its main function is to ensure that trade flows as smoothly, predictably and freely as possible. ISO (International Organisation for Standardisation) has built a strategic partnership with WTO. The

political agreements reached within the framework of WTO require underpinning by technical agreements. ISO has the complementary scopes, the framework, the expertise and the experience to provide this technical support for the growth of the global market.

The Agreement on Technical Barriers to Trade (TBT) – sometimes referred to as the Standards Code – aims to reduce impediments to trade resulting from differences between national regulations and standards. As far as international consensus-based standards are concerned, the Agreement invites the signatory governments to ensure that the standardising bodies in their countries accept and comply with a “Code of good practice for the preparation, adoption and application of standards”.

The TBT Agreement recognises the important contribution that international standards and conformity assessment systems can make to improving efficiency of production and facilitating international trade. Where international standards exist or their completion is imminent, therefore, the Code of Good Practice says that standardising bodies should use them, or the relevant parts of them, as a basis for standards they develop. It also aims at the harmonisation of standards on as wide a basis as possible, encouraging all standardising bodies to play as full a part as resources allow in the preparation of international standards by the relevant international body, including the ISO.

1 Technical Committees for Standardisation in Geotechnical Investigation and Testing

1.1 General

The standardisation in the field of geotechnical investigation and testing is done in three committees of ISO International Organisation for Standardisation and CEN European Committee for Standardisation, partly according to the Vienna Agreement that stipulates the general exchange of information at Central Secretariat level, the co-operation on standards drafting between ISO and CEN, the adoption of existing International standards as European standards and the parallel approval of standards (see Figure 1):

- ISO/TC 182/SC 1 “Geotechnical Investigation and Testing”;
- CEN/TC 250/SC 7 “Geotechnical Design”;
- CEN/TC 341 “Geotechnical Investigation and Testing”.

1.2 ISO/TC 182/SC 1 Geotechnical Investigation and Testing

ISO/TC 182/SC 1 was established together with its parent technical committee ISO/TC 182 “Geotechnics” in 1982. It was named “Classification and Presentation” according to its scope including all matters facilitating the communication with the aid of documents in the geotechnical field, such as

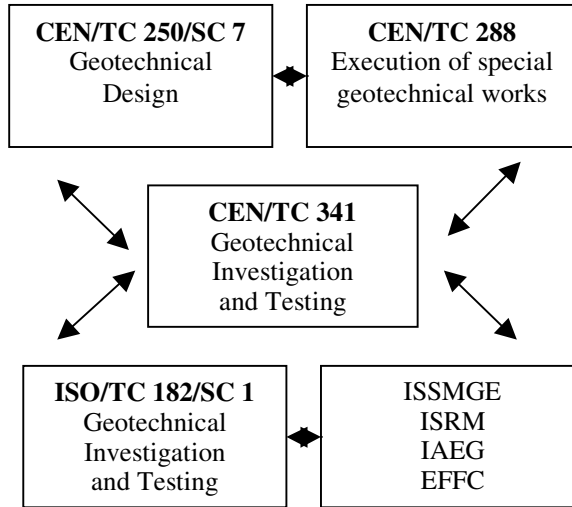


Fig. 1. Technical committees on geotechnical engineering (from Eitner et al. 2002).

- classification of soil and rock;
- terminology, both standardisation of terms and definitions not treated in connection with specific standards of other subcommittees, and in connection with specific standards of other subcommittees, and the co-ordination of the terminology the other subcommittees;
- symbols to be used in calculations;
- symbols to be used on drawings and graphs, expressing, data on soil and rock.

The secretariat and the chairmanship were held by Sweden (SIS) but changed to Germany (DIN) in 1988.

ISO/TC 182/SC 1 prepares standards on identification, description and classification of soil and rock. It is also the international mirror committee of CEN/TC 341. Currently, ISO/TC 182/SC 1 has: 14 participating members: The standards organisations of Austria, China, Czech Rep., Finland, France, Germany, Italy, Japan, Korea (Rep. of), Luxembourg, Netherlands, Norway, Sweden and UK and 10 observers (O-members): Argentina, Australia, Belgium, Iceland, India, Ireland, Israel, Portugal, South Africa, Turkey. There are several liaisons with other committees and organisations such as ISO/TC 82 “Mining”, CEN/TC 341, CEN/TC 288, ISRM, ISSMGE and IAEG.

In 2001 the committee resolved to add some new work items to its working program and to change its name and scope due to the formation of the new CEN/TC 341 “Geotechnical Investigation and Testing”. Name, scope and working program are identical now. There is a very close co-operation between both committees according to the “Vienna Agreement”.

1.3 CEN/TC 341 Geotechnical Investigation and Testing

The scope of CEN/TC 341 comprises standardisation in the field of geotechnical investigation and testing pertaining to equipment and methods used for drilling, sampling, field and laboratory testing of rock and soil as well as groundwater measurements as part of the ground and site investigation services.

The goal of this standardisation work is to harmonise the quality requirements for equipment and to achieve comparable results whenever standardised equipment is used and standardised methods are applied. Manufacturers and users of equipment and methods of geotechnical investigation and testing should find European standards valuable for common use as they enable comparable results to be obtained and reduce the variability of the results of geotechnical data which are the basis for the geotechnical design. European standards for investigation and testing are important for the safety of infrastructures, e. g. such as roads, bridges, canals, railways, airfields, harbours, tunnels, sewer and communication lines and other structures, e. g. buildings dams. These European standards also facilitate the development of a common European market for the trade of services and equipment for geotechnical investigation and testing. The standardisation in the field of geotechnical investigation and testing will also lead to an apparent cost reduction in the building market. Currently CEN/TC 341 has five working groups (see Table 1).

Other working groups on field and laboratory testing are planned for the future.

Table 1. Working groups of CEN/TC 341 Geotechnical investigation and testing.

WG	Title	Convenor/ Secretariat
1	Drilling and sampling methods and groundwater measurements	Germany (DIN)
2	Cone and piezocone penetration Tests	Netherlands (NEN)
3	Dynamic probing and standard Penetration test;	Germany (DIN)
4	Testing of geotechnical structures	France (AFNOR)
5	Borehole expansion tests	France (AFNOR)

1.4 CEN/TC 250/SC 7 Geotechnical Design

Since the mid-seventies, working groups have prepared European harmonised technical specifications for the design of buildings on behalf of the European Commission. These documents - also called "Eurocodes" - should be available for different construction types and building type-independent problems, foundations and permissible loading of building. After the Council of the European Community agreed upon a new concept concerning technical harmonisation and standardisation, the Eurocodes were given to CEN for further preparation and publication as European standards or pre-standards.

Table 2. Subcommittees of CEN/TC 250 Structural Eurocodes.

SC	Title
1	Basis of design and actions on structures
2	Design of concrete structures
3	Design of steel structures
4	Design of composite steel and concrete structures
5	Design of timber structures
6	Design of masonry structures
7	Geotechnical design
8	Design provisions for earth quake resistance
9	Design of aluminium structures

Every Eurocode consists of more than one part. Altogether there are more than 50 parts.

The Eurocodes are a series of standards for the design of buildings, geotechnical structures and earth quake resistance. They are prepared by CEN/TC 250 “Structural Eurocodes” which has 9 subcommittees (see Table 2).

Eurocode 7, prepared by CEN/TC 250/SC 7, is the basic code for the geotechnical design having two parts finally Part 1 on general rules and Part 2 on ground investigation and testing.

Eurocode 7 Part 1 was finalised and available as ENV 1997-1 (European pre-standard) in November 1994. After two years all CEN members were asked to comment and to decide about its future development. Eurocode 7 Part 1 was revised and will be soon available as EN after formal vote. Then all CEN members are required to give this European standard the status of a national standard without any alteration beside a National Annex with the safety values and further detailed specifications.

CEN/TC 250/SC 7 created two further project teams PT 2 and PT 3 in autumn of 1994 to prepare two standards on design assisted by laboratory and field-testing. After finalisation in summer 1997 they were available as ENV 1997-2 and ENV 1997-3. In March 2001 CEN started the 2-year enquiry asking for comments. During revision both parts were merged to one standard (EN 1997-2 “Eurocode 7: Geotechnical design – Part 2: Ground investigation and testing”); hereby all specifications on test equipment and test execution were deleted and transferred to the work program of CEN/TC 341. Only design related matters such as interpretation and evaluation of test results and the planning of geotechnical investigation and testing were left.

2 Standardisation Projects

2.1 Identification and Classification of Soil and Rock

ISO/TC 182/SC 1 has finalised two standards which were published by CEN and ISO in 2002: ISO 14688-1 “Geotechnical investigation and testing – Identification and classification of soil – Part 1: Identification and description” and ISO 14689-1

“Geotechnical investigation and testing – Identification and classification of rock – Part 1: Identification and description” in 2003.

A second final draft of ISO 14688-2 “Geotechnical investigation and testing – Identification and classification of soil – Part 2: Classification principles” was prepared for a second parallel formal vote due to severe comments on the first draft.

Two new work items resulting in Technical Specifications (TS) were accepted in 2002:

- ISO/TS 14688-3 “Geotechnical investigation and testing – Identification and classification of soil – Part 3: Electronic exchange of data of identification and description of soil”;
- ISO/TS 14689-2 “Geotechnical investigation and testing – Identification and classification of rock – Part 2: Electronic exchange of data of identification and description of rock”.

ISO 14688-1 and ISO 14688-2 establish the basic principles for the identification and a classification of soils on the basis of those material and mass characteristics most commonly used for soils for engineering purposes.

The general identification and description specified by ISO 14688-1 of soils is based on a flexible system for immediate (field) use by suitably experienced persons covering both material and mass characteristics by visual and manual techniques. Details are given of the individual characteristics for identifying soils and the descriptive terms in regular use, including those related to the results of tests from the field. The field of application of this standard is natural soils in-situ and similar man-made materials in-situ and soils redeposited by man. It generally permits soil to be identified with adequate accuracy for general or preliminary characterisation more accurate identification and classification based on grading, plasticity or organic content often require laboratory tests that are not covered. In addition to identifying soils, the condition in which a soil is encountered, any particular secondary constituents, other features of a soil, such as carbonate content, particle shape, surface roughness of particles, odour, any common names and the geological classification should all be indicated. ISO 14688-1 specifies several methods for the determination of these soil characteristics. It uses for example particle size as the fundamental basis for designating mineral soils.

The principles for a soil classification according to ISO 14688-2 support the soil grouping into classes of similar composition and geotechnical properties. Soils shall be therefore classified into soil groups on the basis of their nature that is the composition only, irrespective of their water content or compactness, taking into account the following characteristics:

- particle size distribution (grading),
- plasticity,
- organic content.

The most common approach in classification is to divide the soils on the basis of particle size grading and plasticity. The division is made on the relative size fractions present for the coarser soil fractions, determined on the whole sample, and on the plasticity of the finer fractions. It is important to notice that ISO

14688-2 does not cover the soil classification because ISO/TC 182/SC 1 was not able to reach a compromise on such a classification. This part of ISO 14688 does not replace any existing national or regional soil classification.

ISO 14689-1 is based on international practice (IAEG 1981, ISRM 1977a, 1977b, 1978, 1980, 1984, ISSMGE 1994) and relates to the identification and the description of rock material and mass on the basis of mineralogical composition, predominant grain size, genetic groups, discontinuities, structure and other components. The standard also provides rules for the description of other characteristics as well as for their designation and applies to the description of rock for geotechnical engineering. The description is carried out on cores and other samples of natural rock and on rock masses.

ISO 14688-1 and ISO 14689-1 both recommend to use the symbols of ISO 710 series to represent soils on borehole legends or on engineering geological maps.

ISO/TS 14688-3 and ISO/TS 14689-2 will cover requirements for the electronic exchange of data on identification and description of soil and rock. They will provide a data exchange format (XML) that facilitates the data exchange independently from a certain hardware or software system.

CEN will also vote on these standards according to the Vienna Agreement and adopt them as European standards, if the majority of CEN members agrees.

2.2 Drilling and Sampling Methods and Groundwater Measurements

CEN/TC 341 is preparing standards dealing with the investigation of soil, rock and groundwater measurements for use as subsoil and construction materials as part of the geotechnical investigation services. It defines concepts and specifies requirements relating to exploration by excavation, drilling, sampling and groundwater measurements. More information in detail is given in Stölben & Eitner (2004). ISO will also vote on this standard according to the Vienna Agreement and adopt them as an International standard, if the majority of p-members of ISO/TC 182/SC 1 agree.

2.3 Field Testing

CEN/TC 341 prepares in co-operation with ISO/TC 182/SC 1 several standards specifying the requirements for indirect ground investigations of soil and rock by field tests. These standards will be published under the common title “ISO 22476 Geotechnical investigation and testing – Field testing”:

- Part 1: Electrical cone and piezocone penetration tests;
- Part 2: Dynamic probing;
- Part 3: Standard penetration test;
- Part 4: Menard pressuremeter test;
- Part 5: Flexible dilatometer test;
- Part 6: Self-boring pressuremeter test;
- Part 7: Borehole jack test;

- Part 8: Full displacement pressuremeter test;
- Part 9: Field vane test;
- Part 10: Weight sounding test (TS);
- Part 11: Flat dilatometer test (TS);
- Part 12: Permeability tests;
- Part 13: Water pressure tests;
- Part 14: Pumping tests;
- Part 15: Mechanical cone penetration test;
- Part 16: Plate loading tests.

The common purpose of these standards is to eliminate as far as possible erroneous assessments of subsoil conditions as well as to limit scatter when repeating tests and improve reproducibility when undertaking field testing.

ISO 22476-1 and ISO 22476-15 deal with the execution and reporting on cone penetration tests. These tests are performed with a cylindrical penetrometer with conical tip, or cone and if applied, the friction sleeve, are measured. The results from a cone penetration test can in principle be used to evaluate soil stratification, soil type, soil density and in situ stress conditions and mechanical soil properties.

ISO 22476-2 on dynamic probing will be published in 2004. It covers the determination of the resistance of soils and soft rocks in-situ to the dynamic penetration of a cone. A hammer of a given mass and given falling height is used to drive the cone. The penetration resistance is defined as the number of blows required driving the penetrometer over a defined distance. A continuous record is provided with respect to depth but no samples are recovered.

Four procedures are included, covering a wide range of specific work per blow:

- Dynamic probing light (DPL): test representing the lower end of the mass range of dynamic equipment;
- Dynamic probing medium (DPM): test representing the medium mass range of dynamic equipment;
- Dynamic probing heavy (DPH): test representing the medium to very heavy mass range of dynamic equipment;
- Dynamic probing super-heavy (DPSH): test representing the upper end of the mass range of dynamic equipment.

The test results of this standard are specially suited for the qualitative determination of a soil profile together with direct explorations (e.g. drilling) or as a relative comparison of other in-situ tests. They may also be used for the determination of the strength and deformation properties of soils, generally of the cohesionless type but also possibly in fine-grained soils, through appropriate correlations. The results can also be used to determine the depth to very dense ground layers indicating the length of end bearing piles.

ISO 22476-3 on the "Standard Penetration Test" will be also published in 2004. It covers the determination of the resistance of soils at the base of a borehole to the dynamic penetration of a split barrel sampler and the obtaining of disturbed samples for identification purposes. The standard penetration test is used mainly for the determination of the strength and deformation properties of cohesionless soils, but some valuable data may also be obtained in other types of soils. The

basis of the test consists in driving a sampler by dropping a hammer of 63,5 kg mass on to an anvil or drive head from a height of 760 mm. The number of blows (N) necessary to achieve a penetration of the sampler of 300 mm (after its penetration under gravity and below a seating drive) is the penetration resistance.

EN ISO 22476-4 describes the procedure for conducting a Ménard pressuremeter test in natural soils and treated or untreated fills, and in very hard soils or soft rocks, either on land or off-shore. The Ménard pressuremeter test is performed by the radial expansion of a tricell probe placed in the ground. During the injection of the liquid volume in the probe, the inflation of the three cells first brings the outer cover of the probe into contact with the borehole walls and then presses on them resulting in a soil displacement. Pressure applied to, and the associated volume expansion of the probe are measured and recorded so as to obtain the stress-strain relationship of the soil as tested.

EN ISO 22476-5 describes the procedure for conducting a test with the flexible dilatometer in natural soils and treated or untreated fills, and in very hard soils, soft or hard rocks, either on land or off-shore. The test with the flexible dilatometer is performed by the expanding of a flexible dilatometer membrane placed in the ground. The pressure applied to, and the associated expansion of the probe are measured and recorded so as to obtain a stress-displacement relationship for the soil as tested.

EN ISO 22475-6 describes the procedure for conducting a self-boring pressuremeter test in natural fine soils, either on land or off-shore. The self-boring pressuremeter test is performed by the radial expansion of a tri-cell or mono-cell probe placed in the ground by means attached to it. Pressure applied to, and the associated volume expansion of the probe are measured and recorded so as to obtain the stress-strain relationship of the soil as tested. During boring and pressuremeter test, data is recorded automatically.

EN ISO 22476-7 describes the procedure for conducting a borehole jacking test in natural soils and treated or untreated fills, and in very hard soils or soft rocks, ($E_B < 1000$ MPa) either on land or off-shore. The borehole jacking test is performed by the diametrical opening of two cylindrical steel loading plates placed in the ground. Pressure applied to, and associated opening of the probe are measured and recorded so as to obtain a stress-displacement relationship of the ground as tested in the range of the expected design stresses.

The weight sounding test according to CEN ISO/TS 22476-10 is primarily used to give a continuous soil profile and an indication of the layer sequence. The penetrability in even stiff clays and dense sands is good. The weight sounding test is also used to estimate the density of cohesionless soils and to estimate the undrained shear strength of cohesive soils. The weight sounding penetrometer consists of a screw-shaped point, rods, weights or other loading system and a handle or a rotating device. The weight sounding test is made as a static sounding in soft soils when the penetration resistance is less than 1 kN. When the resistance exceeds 1 kN the penetrometer is rotated, manually or mechanically, and the number of half turns for a given depth of penetration is recorded.

The flat dilatometer test according to CEN ISO/TS 22476-11 covers the determination of the in situ strength and deformation properties of fine grained

soils using a blade shaped probe having a thin circular steel membrane mounted flush on one face. Results of flat dilatometer tests are mostly to obtain information on soil stratigraphy, in situ state of stress, deformation properties and shear strength. The basis of the test consists of inserting vertically into the soil a blade-shaped steel probe with a thin expandable circular steel membrane mounted flush on one face and determining, at selected depths or in a semi-continuous manner, the contact pressure exerted by the soil against the membrane when the membrane is flush with the blade and subsequently the pressure exerted when the central displacement of the membrane reaches 1,10 mm. The flat dilatometer test is most appropriate in clays, silts and sands where particles are small compared to the size of the membrane.

2.4 Testing of Geotechnical Structures

CEN/TC 341 started to prepare a set of standards for testing geotechnical structures (ISO 22477) such as

- Pile load tests;
- testing of anchorages;
- testing of soil nailing;
- testing of reinforced fills

to eliminate as far as possible erroneous assessments of these geotechnical structures and the uncertainties of design methods as well as to limit scatter when repeating tests and improve reproducibility when testing geotechnical structures.

2.5 Laboratory Testing

Based on international recommendations for laboratory testing (DIN, ISSMGE ed. 1998) a set of Technical Specifications were prepared under the common title ISO/TS 17892 “Geotechnical investigation and testing – Laboratory testing”

- Part 1: Determination of water content;
- Part 2: Determination of density of fine grained soils;
- Part 3: Determination of density of solid particles;
- Part 4: Particle size distribution;
- Part 5: Oedometer test;
- Part 6: Fall cone test;
- Part 7: Compression test;
- Part 8: Unconsolidated triaxial test;
- Part 9: Consolidated triaxial test;
- Part 10: Direct shear test;
- Part 11: Permeability test;
- Part 12: Determination of Atterberg limits.

These Technical Specifications will be available in 2004.

2.6 Design Assisted by Field and Laboratory Testing (Geotechnical Investigation)

As already mentioned CEN/TC 250/SC 7 revises ENV 1997-2 and ENV 1997-3 in order to convert them into European standards (EN). Both standards merged to a single part (EN 1997-2) defining the concepts and specifying requirements relating to planning of geotechnical investigations and testing and evaluation of test results in order to provide the geotechnical data necessary for the design of buildings and civil engineering works, the aim being to prevent damage to the new structures and to maximise cost-effectiveness during the planning and construction stages.

3 Conclusions

Figure 2 illustrates the links of the standards prepared by the different Technical committee on geotechnical design, investigation and testing.

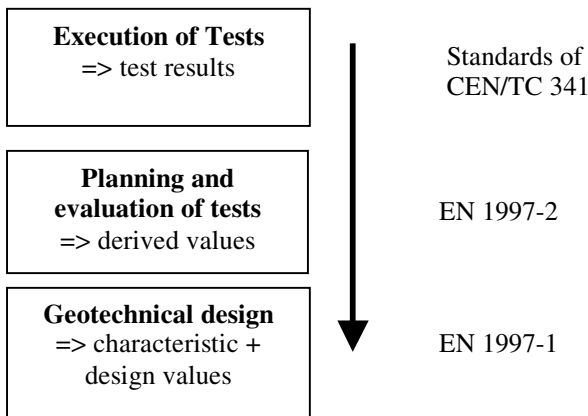


Fig. 2. Standardisation in geotechnical engineering (from Eitner et al. 2002).

The standards of CEN/TC 341 specify the test equipment and the correct test procedure leading to comparable test results. These test results are used by Eurocode 7 Part 2 (EN 1997-1) for evaluation and interpretation leading to derived values. Eurocode 7 Part 1 (EN 1997-1) uses these values for the determination of characteristic values and design values.

Together with standards for the execution of special geotechnical works, an almost complete set of geotechnical standards are currently in preparation.

This set of standards will facilitate trade, exchange and technology transfer through:

- enhanced product and service quality and reliability at a reasonable price;
- improved health, safety and environmental protection;
- greater compatibility and interoperability of goods and services;
- simplification for improved usability;
- reduction in the number of models and procedures, and thus reduction in costs;
- increased distribution efficiency, and ease of maintenance.
- Users will have more confidence in geotechnical products and services that conform to International Standards.

References

- DIN (ed.) (2000). Economic benefits of standardisation - Summary of results. Final report and practical examples (Executive Summary). Beuth Verlag, Berlin (in German, English and Spanish, www.din.de).
- DIN, ISSMGE (eds.) (1998). Recommendations of the ISSMGE for Geotechnical Laboratory Testing. Beuth Verlag, Berlin (in English, French and German).
- Eitner, V., Katzenbach, R. & Stölben, F. (2002): Geotechnical investigation and testing - An outlook on European and international standardisation. - In: Honjo, Y. et al. (eds.) (2002): Foundation design codes and soil investigation in view of international harmonisation and performance based design. - Proceed. International Workshop IWS Kamakura, Japan, 10-12 April 2002, pp. 211-215, Rotterdam (Balkema).
- IAEG (1981). Rock and Soil Description and Classification for Engineering Geological Mapping, Bulletin of the International Association of Engineering Geology, No.24, pp.235-274.
- ISRM (1977 a). Suggested Method for Petrographic Description of Rocks, Int. J. Rock Mech. Min. Sci. & Geomech. Abstr. Vol.15, pp.41-45.
- ISRM (1977 b). Suggested Methods for the Quantitative Description of Discontinuities in Rock Masses, Int. J. Rock Mech. Min. Sci. & Geomech. Abstr. Vol.15, pp.319-368.
- ISRM (1978). Suggested Methods for Determining the Uniaxial Compressive Strength and Deformability of Rock Materials, Int. J. Rock Mech. Min. Sci. & Geomech. Abstr. Vol.16, pp.135-140.
- ISRM (1980). Basic Geotechnical Description of Rock Masses, Int. J. Rock Mech. Min. Sci. & Geomech. Abstr. Vol.18, pp.85-110.
- ISRM (1984). Suggested Method for Determining Point Load Strength, Int. J. Rock Mech. Min. Sci. & Geomech. Abstr. Vol.22, No.2, pp.51-60.
- ISSMGE (1994). Testing Method of Indurated Soils and Soft Rocks - Suggestions and Recommendations, ISSMFE Technical committee on Indurated Soils and Soft Rocks, pp.65-69.
- Stölben, F., & Eitner, V. (2004). Standardised methods for sampling by drilling and excavations and for groundwater measurements. Proc. EurEnGeo, Liege.

Towards Quality Assurance and an Adequate Risk Management in Geotechnical Engineering – Application of Eurocode 7 and DIN 4020 in Engineering Geology

Kurt Schetelig¹, Michael Heitfeld¹, Paul von Soos²,
Manfred Stocker³, and Mark Mainz¹

¹ Ingenieurbüro Heitfeld-Schetelig GmbH (IHS), D - 52074 Aachen, Preusweg 74
info@ihs-online.de
Phone +49 241 705160
Fax +49 241 7051620

² Reußweg 30, D - 81247 München
Phone +49 89 882738
Fax +49 89 8205255

³ Bauer Spezialtiefbau GmbH, Wittelsbacher Straße 5, D - 86529 Schrobenhausen
manfred.stocker@bauer.de
Phone +49 8252 971200
Fax +49 82 52 971031

Abstract. A key issue of engineering geology is the extreme variety of soil and rock, their heterogeneity and at places anisotropy, the fabric of rockmasses, the influence of water, the primary stresses and their change into a secondary stress field by loading or unloading. Changeable properties of some kinds of soil and rock, the effect of different scales of laboratory tests, field tests and the size of the structure create further questions. Considering the difficulties of investigation of the underground, size and complexity of the structure and its construction procedure Eurocode 7 and DIN 4020 have introduced geotechnical categories. The design concept in geotechnical category 3 is mostly combined with the observational method. This requires the establishment of an adequate monitoring system and a permanent comparison of the design assumptions (pre-calculated displacements or stresses) with the recorded values. The goals and handling of Eurocode 7 and DIN 4020 are demonstrated by means of site examples.

Keywords: Eurocode 7, DIN 4020, risk management, quality assurance, scaling effect, observational method, monitoring, collapse feature.

1 Fundamentals of Eurocode 7 and DIN 4020

General aim of Eurocode 7, Chapter 4 “Geotechnical Investigations” and the German DIN 4020 “Geotechnische Untersuchungen für bautechnische Zwecke” is the introduction of unified European geotechnical standards for the investigation of the subsoil, planning and construction of geotechnical structures and accompa-

nying investigations during construction and/or operation. This may include a monitoring system to measure the reaction of the subsoil on the structure and the preceding construction work as well as all impacts of the structure and its construction procedure on surrounding buildings or the environment. Important objects of these standards are the determination of essential tasks and responsibilities to be taken by the owner, the engineer or the contractor, from the preparatory phase until the usage of a structure. Both, Eurocode 7 and DIN 4020, distinguish “geotechnical categories” 1, 2 and 3 in relation to the geotechnical difficulties to be expected or mastered, the size and importance of the structure for the public as well as the risks for public health and infrastructure of public services in case of any malfunctioning or failure. An essential of DIN 4020 is the introduction of the “Expert in Geotechnical Engineering” with specific experiences in disciplines being involved, e.g. soil or rock mechanics, engineering geology, grouting etc.. The “Expert in Geotechnical Engineering” can either be an individual or a board of consultants. Eurocode 7 has already been approved by the European Union and will be introduced by the member states in accordance with specific regulations for the transition phase from national to european standards. A further goal of these two standards, particularly of DIN 4020, is to reduce the damages in civil engineering which are caused by inadequate investigation of soil and rock and their specific mechanical or hydraulic behaviour. Therefore, insurance companies have favoured the elaboration of the standards. Moreover, they aim at a reasonable and adequate distribution of risks, duties and responsibilities between the owner of a structure, the engineer, the contractor and the expert in geotechnical engineering. This will be obtained by a detailed description of geotechnical investigations and measures to be taken into account or to be applied. Therefore, for each investigation a geotechnical report is required which contains purpose and extent of the investigations being executed, listing, evaluation and interpretation of all laboratory and field tests and measurements as well as advices for the engineer and the contractor. This geotechnical report should also include remarks on geotechnical questions which cannot be answered at the time being. Further investigations, mostly large scale tests or an adequate design concept then have to be adapted to that situation. Technical standards or regulations cannot determine the relation between owner and contractor. They are free to agree upon any contract. But, a certain improvement of the relations between owner and contractor and a contribution to open-minded relations between all partners as well as to fair tender documents and contracts could be a great success of DIN 4020.

2 Special Properties and Behaviour of Soil and Rock

Contrary to most artificial materials like concrete or steel, soil and rock are characterized by extreme variety and general inhomogeneity originating from stratification in soil or discontinuities in rockmasses. Some soils and rocks also show anisotropy. This leads to complex stress-strain behaviour and difficulties in determining the mechanical parameters. Changeable properties of some kinds of soil and rock, e.g. overconsolidated clays or shales, cause additional problems in case

of drying or access of water (shrinkage or swelling) or in case of changes in the stressfield. A special problem of geotechnical engineering is the scaling effect. The extreme difference between the size of tested samples and the scale of inhomogeneities as well as the size of the structure and the underground being involved, demand a thorough evaluation and interpretation for each individual project and each investigation programme. Laboratory tests usually are being carried out with samples of some cm^3 up to a few dm^3 . In field tests, a soil or rock volume of about 0.1 to 0.3 m^3 is activated. This is 10 to 100 times the volume of a laboratory test. Some inhomogeneities with regular distribution may be encountered by field tests. Nevertheless, conventional field tests only can examine volumes being about 3 to 5 magnitudes smaller than the ground volume finally being affected by the structure. That means, that the influence of widely spaced discontinuity systems, faults or larger inhomogeneities, can only be encountered using the observational method. For this method a monitoring system with permanent recording, evaluation and interpretation of all measured values and the constant comparison with the design assumptions is essential. An integration of all geological and geotechnical features into a comprehensive concept is necessary and that is especially true for all structures of geotechnical category 3 (Katzenbach u. Strüber 2003). Developing a model demands the definition of the purpose, the availability, reliability, variation and extreme values of data to be integrated and the results being expected. DIN 4020 recommends calculation models, being adapted to specific tasks, e.g. investigation of stability, settlements, seepage or other problems. Usually the models contain:

- geometrical data, i.e. the simplification of the true dimensions to a model which eases calculations
- geological data, mostly simulated by homogeneous zones, occasionally with a separate simulation of discrete zones, e.g. faults
- geotechnical data being derived from laboratory tests, field tests and measurements in the field (observational method).

3 Examples

3.1 Construction Pit EBV-Carré in Aachen close to Thermal Springs

The EBV-Carré in the centre of Aachen was constructed in 2002 - 2003, including a 4 star Novotel hotel, top-class offices and a shopping mile. The construction pit was excavated in Devonian shales (Famenne formation) with some sandstone intercalations, a variable lime content and some limestone intercalations (fig. 1).

The main difficulty of the project was its location adjacent to the Aachen fault ("faulle du midi" in Belgium) along which middle Devonian shales and limestones are overthrust upon Carboniferous siltstones. Limestones are embedded along this fault and form the path for thermal waters with temperatures exceeding 70°C (Langguth u. Pommerening 1992, Pommerening 1993).

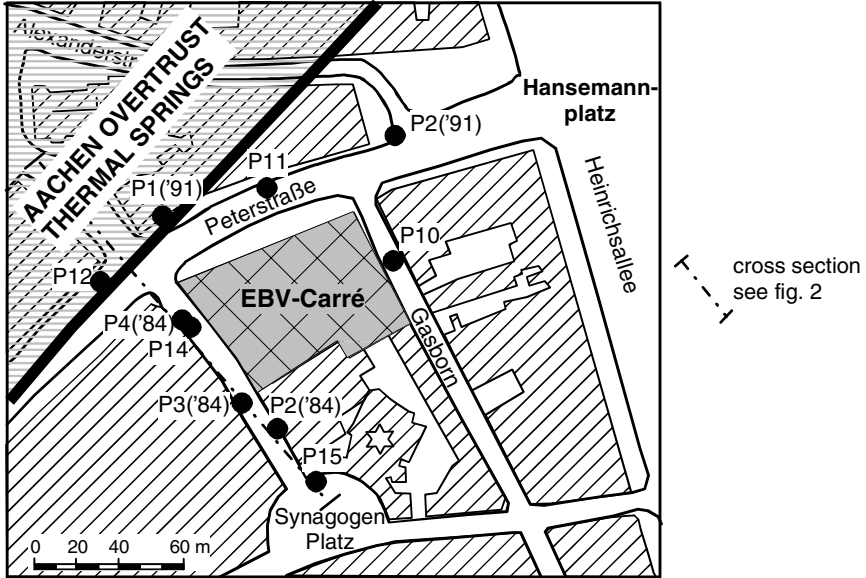


Fig. 1. EBV-Carré Aachen. Construction Site Adjacent to the Thermal Springs.

A prerequisite for the construction was to eliminate all risks of any impact on quality and quantity of the thermal waters. Due to strong karstification, the springs react extremely sensitive on any lowering of the thermal water level. Since the EBV-Carré is located immediately south of the thermal spring area, the depth of the construction pit and the construction of its enclosure had to be planned carefully with respect to the adjacent thermal springs (fig. 2). A 16 m deep construction pit was wished to enable a maximum parking capacity. A minimum capacity for the hotel, the business tract and the shopping mile could be offered by a 3-storey parking house allowing for an excavation of only 11 m depth. After a detailed study of all available information on local stratigraphy and tectonics, an investigation programme was elaborated, mainly based on 14 core borings in which groundwater gauges were installed and water pressure tests were carried out during the drilling. The results clearly demonstrated that an optimized alternative with a 13 m deep construction pit with a 4-storey parking house could be recommended. This solution then was agreed upon. A confirmation of the design assumptions was obtained by a thorough and detailed geological documentation and a permanent recording of the groundwater gauges as well as the chemical composition of the encountered groundwater flow. In a worst case scenario supplementary grouting was prepared, but these measures did not become necessary.

An essential of the success of this project was the very early formation of a work group comprising the owner (EBV Aktiengesellschaft), the city of Aachen (Lord Major, environment authority), the authorities of Northrhine-Westfalia, the engineer (architect) and a board of consultants, consisting of engineers for geotechnical engineering (Prof. Dieler), engineering geology (IHS) and hydrogeology (HIS u. Prof. Langguth).

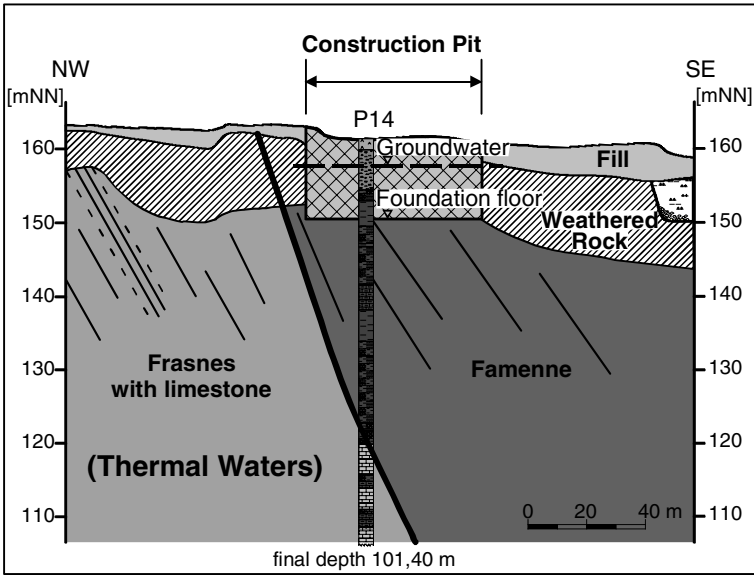


Fig. 2. EBV-Carré Aachen. Geological Cross Section.

3.2 Re-use of Mining Sites after Closing of Hard Coal Mines

In many mining areas for ore, schist or hard coal there are numerous problems due to abandoned mine workings. These mainly result from shafts, subsidences and collapse features due to failure of mining spaces at shallow depths. Problems arise from uncertainties about the locations of documented, assumed or unknown subterranean spaces and their stability conditions. Mostly, they have collapsed meanwhile or are in a borderline equilibrium and slight impacts like changes of the stressfields (induced by near excavation or any change in saturation) can lead to failure. Under favourable geological conditions and due to a limited load by the overlying rock some openings even still can be present. The risks resulting from rising groundwater level after mining cessation were evaluated based upon the well studied examples of the abandoned Aachen hard coal fields. Due to the rising groundwater the uplift forces increase and hence the effective stresses around the openings decrease. This is a positive effect. Simultaneously, the intensive saturation, induced by the groundwater recharge, leads to a reduction in friction along the discontinuity planes or at rock-to-rock contacts, respectively. Consequently, the shear strength of the rockmass is reduced. Both tendencies may compensate each other partly, but the true stability conditions cannot be predicted reliably up to now (fig. 3).

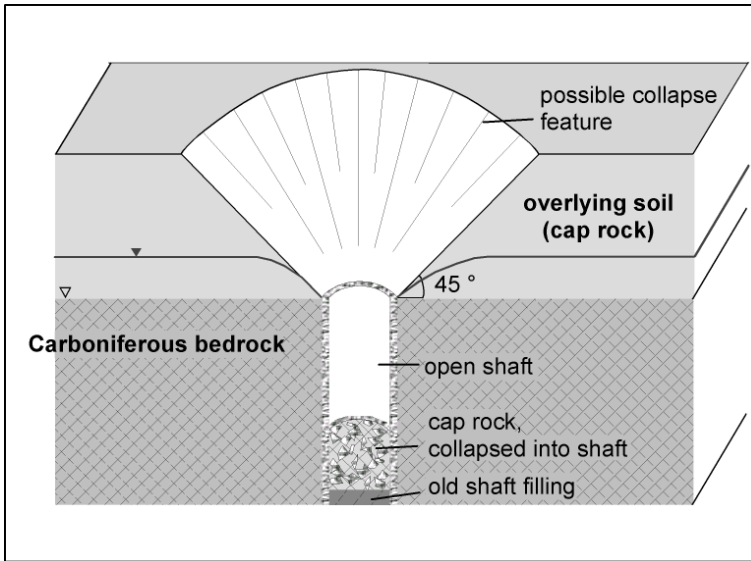


Fig. 3. Old Hard Coal Mine Shaft. Risk of Failure.

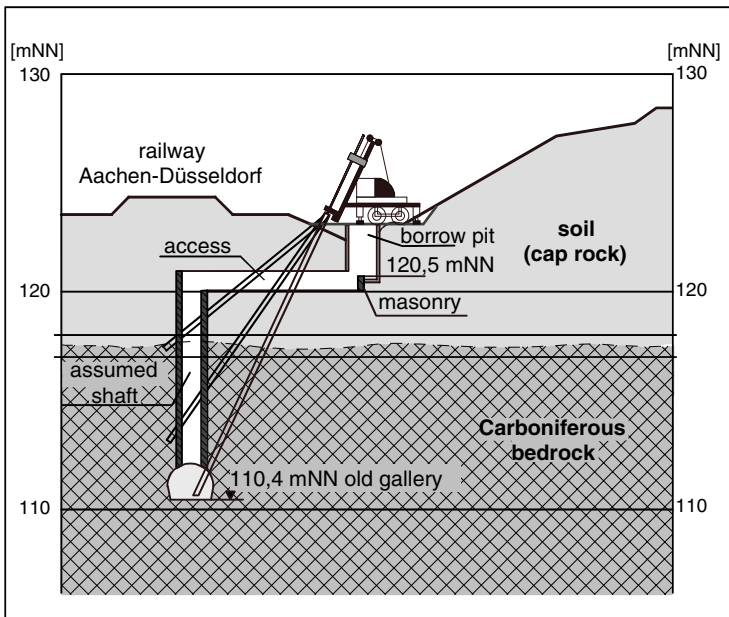


Fig. 4. Search for Old Shafts.

The location of many old shafts and exploitation areas which endanger existing or planned structures, were identified by studying historical maps, documents and other information sources. The exact location then was determined by inclined core borings (fig. 4). Details of the general concept and the remedial measures are dealt with in Heitfeld et al. 2002a and 2002b.

MAINZ studies the stability conditions of surfacenear mining hollows based on observations from well investigated case studies and collapse features. Due to their large sizes, laboratory simulation is difficult and using observations from true dimension objects, as favoured in Eurocode 7 and DIN 4020, promise the most realistic results. Moreover, high quality core samples of the overlying strata have been recovered. Laboratory and field tests yield information on the general classification of the soils being involved, their shear strength and stress-strain behaviour. MAINZ intends to develop mathematical models for representative load cases. The calculations are meant to yield information about the stability conditions of surfacenear spaces and will support the reliability of any failure prediction. Main object is a tool to support evaluation and consultancy services for any re-use of former mining sites by the Authorities or private agencies.

4 Conclusions

The examples described are projects with complicated underground conditions which can be investigated using conventional soil and rock mechanical testing up to a limited degree. An integrated approach, comprising the antropogenic history of the site as well as information from several disciplines, mainly engineering geology and hydrogeology, obtained from former projects, is of major importance. Another aspect is the specific mechanical behaviour of various soils and rocks which often only can be recognized during construction work, e.g. disintegration of rock due to stress release, swelling and stress-strain behaviour of overconsolidated soils. A thorough interpretation was and is necessary in all projects and the transferability of former experiences has to be validated by a project-specific comparison of the geotechnical conditions and the design concept for the object. A fair cooperation of all project participants from the owner to the contractor as well as the integration of specific experts, e.g. for geotechnical engineering and engineering geology, from first planning to operation of the structure accompanied by a permanent exchange with the Authorities and the board of consultants (“Prüfingenieure”) are essential for the successful realization of all projects in geotechnical category 3. Finally, it has to be pointed out, that a comprehensive documentation of the subsoil conditions exposed during the construction phase, equipment, installation and results of the monitoring system next to an integrated evaluation and interpretation of all measurements and experiences are prerequisites for a successful realization of the design and safety concept. Many soil and rock properties can only be determined by such documentations and experiences. They cannot be derived from individual laboratory tests, boreholes or field tests. Therefore, the value of good documentations of well designed and executed projects for future projects cannot be overestimated.

References

- DIN 4020 (09.2003): Geotechnische Untersuchungen für bautechnische Zwecke.
- EUROCODE 7: Entwurf, Berechnung und Bemessung in der Geotechnik.
- HEITFELD, K.-H., HEITFELD, M., ROSNER, P., SAHL, H. & SCHEDELIG, K. (2002a): Mine Water Recovery in the Coal Mining District of Aachen - Impacts and Measures to Control Potential Risks.- International Conference Uranium Mining and Hydrogeology III; p. 1012 - 1020, 6 fig.; Freiberg.
- HEITFELD, M., ROSNER, P., KLÜNKER, J., SAHL, H. & WELZ, A. (2002b): Bewertung des Gefährdungspotentials und Sicherungsmaßnahmen in Altbergbaubereichen des Aachener Steinkohlenreviers.- 2. Altbergbaukolloquium, p. 317 - 335, 5 fig.; Clausthal-Zellerfeld.
- KATZENBACH, R. & STRÜBER, S. (2003): Schwierige Tunnelvortriebe im Locker- und Festgestein - Anforderungen an Erkundung, Planung und Ausführung.- Geotechnik 2003/4, p. 224 - 229, 11 fig.; Essen.
- LANGGUTH, H.R. & POMMERENING, J. (1992): Untersuchungen zur natürlichen Hydrodynamik einer Thermalquelle in Aachen.- In Mineralne in termalne vode v gospodarstvu in znanosti Slovenije. Mineral and Thermal Waters in Economy and Science in Slovenia. II Postvet meeting, p. 33 - 41, 4 fig.; Ljubljana/Slovenien.
- POMMERENING, J. (1993): Hydrogeologie, Hydrogeochemie und Genese der Aachener Thermalquellen.- Mitt. Ingenieurgeol. u. Hydrogeol. RWTH Aachen, H. 50, 168 p., 60 fig., 16 tab.; Aachen.

Aggregate Research in Support of European Standardisation

Björn Schouenborg and Urban Åkesson

SP Swedish National Testing and Research Institute, Box 857, S-501 15 BORÅS, Sweden
Bjorn.schouenborg@sp.se
Tel: +4633165433
Fax: +4633134516

Abstract. The first generation of harmonized European standards for aggregates is almost complete. Product standards and test methods exist for all areas defined in the mandate from the European Commission. This package of standards is mandatory from June 2004. However, much work remains to implement the standards in all countries, gather information from their use and finally to improve them in the second generation. Today, aggregates are usually tested as such, as if they were only to be used as unbound materials. Bridging the gap between different standardisation committees is therefore necessary. Introduction of more advanced technologies in the field of aggregate testing, e.g. image analysis of size and shape in the quarry, in the production and in the laboratory can enhance the productivity and quality. Databases with experience of the use in each country should be compiled through networking. This can help understanding the different usage due to climatic, geological and cultural differences. Working towards a package of standards that are more related to the functioning of the aggregates in the construction is another challenge.

Keywords: aggregates, pre-normative research, European standards, testing, image analysis, recycled aggregates, frost resistance, harmful fines.

1 Introduction

Aggregates are the most important mining industry materials in terms of production and volume produced in Europe and second in value only to energy mineral resources such as fossil fuels. On average, the annual consumption is about 10 tons per capita. The increasing consumption and flow of aggregates across country borders in combination with the introduction of new alternative materials and environmental legislations raise the requirements of a renewed standardisation organisation. In order to enhance the development in this area, new techniques and knowledge need to be introduced. This paper introduces the present work of harmonizing European standards and presents some recent research work and ideas for research in support of the standardisation.

2 European Standardisation of Aggregates

2.1 Short Background

A major trend in the European aggregate industry is the increased flow of aggregates between different countries. This flow of products is encouraged by the European Community (EC). One consequence of the increased trade is that the major European standardisation body, CEN (Comité Européen de Normalisation), has been given the commission to develop harmonized product standards and standardised test methods in this area. The work was actually started well before the European Commission gave CEN a mandate. The Technical Committee (TC) that is responsible for developing the standards is denoted "TC 154 Aggregates". The work of TC 154 started in 1987 and spans over the following areas: *Aggregates for concrete and mortar -- Aggregates for unbound and bound purposes -- Aggregates for bituminous mixtures -- Light-weight aggregates -- Railway track ballast -- Armour stones.*

The first generation of standards will be mandatory in mid 2004. All EC- and affiliated countries are required to use them. Several other TCs, indirectly, deal with aggregate materials, such as TC 104 Concrete and related products, TC 125 Masonry, TC 227 Road Materials, TC 229 Precast concrete products, TC 250 Structural Eurocodes; Geotechnical design and TC 292 Characterization of waste. These standards depend on each other and make cross references to each other.

However, the standardisation work is not finished! Every 5 years, the standards are revised and, if necessary, changed. New standards may be needed and are developed and assessed by TC 154. It is of crucial importance that all information from the use of the existing standards is gathered in a systematic way in order to have a real improvement of the second generation standards, especially the product standards! Documented experience from the use of the standards is the most efficient way to improve them. *We also need further research in order to accomplish any real development in this area!*

2.2 Standardised Tests for Alternative Materials

A major trend, not only for aggregates, is the ever increasing awareness of our nature's sensitivity and demands. Some countries have been forced to act due to the simple fact that there is a shortage in natural aggregate resources. In other cases, the demands from society require a change towards a more sustainable production and consumption. Legislation by significantly increased deposition taxes work in the same way; "everything shall be re-used" when possible. Alternative aggregate materials and a more "efficient" use of existing deposits are some important solutions (see Arm 2000 for a comprehensive list of references).

An ad hoc group was formed under TC 154 to deal with Recycled Aggregates. The outcome of which was a technical report giving guidance on the most suitable properties to verify. However, it only makes reference to standardized test methods. It is not until the second generation of product standards that we may have

separate standards for alternative aggregates (recycled aggregates and aggregates from secondary sources). Meanwhile, such products have to undergo the same testing procedure as natural aggregates. For several reasons this is not a good solution. It has been shown that the properties of alternative aggregates, in many cases, need to be assessed with modified standard test methods or completely new methods (Ewerthsson et al. 2000, Schouenborg et al. 1997, Schouenborg et al. 2003). The test results are often erroneous when “aggregate methods” are used. One such example is presented in figure 2.1 where it can be seen that determining the particle size distribution by traditional sieving, using a mechanical shaker in 10 minutes, clearly changes the properties of the tested material (Stenberg et al. 1997). This may indeed endanger the function and service life of the construction.

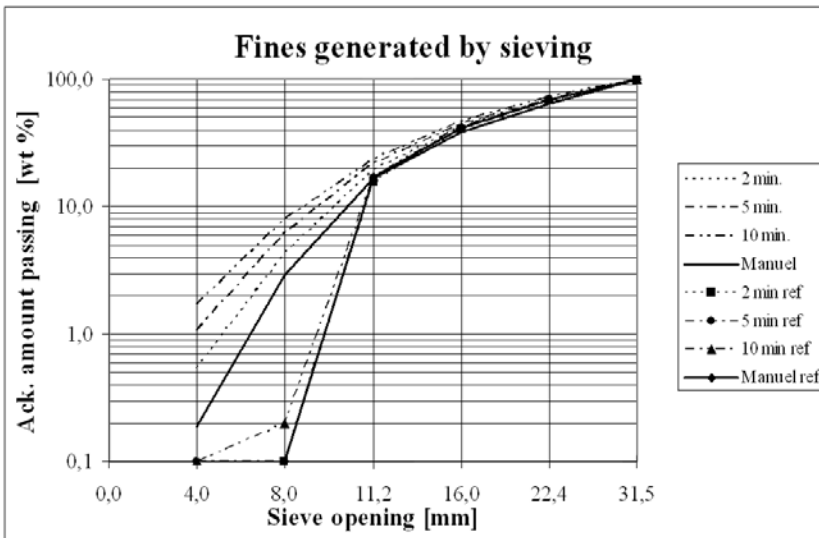


Fig. 2.1. Sieving of crushed concrete in a mechanical shaker generates extra amounts of fine aggregates.

3 Research on a European Level

In the past 10 years, many European R&D projects have been carried out in support of standardisation and to enhance the use of alternative materials. During the long time of standardisation, several needs for research have been identified. The objectives of a few such projects are outlined below.

The project, *Testing of Industrial Products - Aggregates for Construction*, consisted of three parts. (1) A bibliographic study of mechanical tests on aggregates. (2) A cross-testing programme, carried out from 1993 to 97, included 20 test procedures on 21 different properties of aggregates with up to 50 or more European laboratories undertaking each test. (3) Research on sampling examined the sam-

pling variation due to product variation and sampling under different conditions. Twenty one part reports have been issued on the findings (Ballman et al. 1999). One national co-ordinator was appointed for each European country. See also the homepage of the project: <http://projects.bre.co.uk/aggregate/index.htm>.

A wide variety of aggregate types in common use across Europe, particularly those with a siliceous composition may be vulnerable to attack by the alkaline pore fluid in concrete. This attack, in wet conditions, can produce cracking and disruption of the concrete (figure 3.1). The deterioration mechanism for siliceous aggregates is termed Alkali Silica Reaction (ASR). The objective of the *PARTNER* project is to provide the basis for a unified European testing methodology to evaluate and classify the alkali reactivity of aggregates in concrete. This will enable TC 154 to respond to Mandate 125 by standardizing methods and requirements in future CEN Standards. To achieve this by evaluating the tests developed by RILEM TC 106, and some regional tests, for their suitability for use with the wide variety of aggregate and geological types found across Europe. To calibrate the results of these accelerated tests against behaviour in concrete in real structures and in field sites. To produce an "Atlas of the geology and petrography of European aggregates". To educate European petrographers and organizations in the effective use of these methods. For further information please visit our home page: www.partner.eu.com.

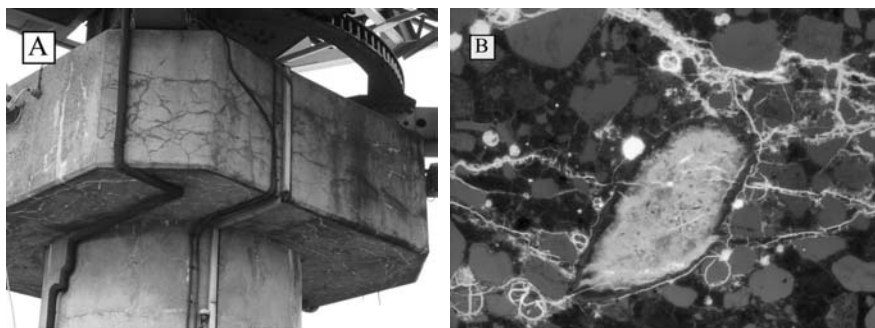


Fig. 3.1. A, Bridge damaged by Alkali Silica reaction (ASR). B, Fluorescent microscopic image of ASR damage in concrete. The photos have kindly been provided by Dr Ted Sibbick, BRE, UK and Bent Grelk, RAMBOLL, DK.

The current status of freeze/thaw testing of aggregates (EN 1367-1) in the European Union is only sufficient to enable continued use of aggregates on a regional basis. Freeze/thaw testing in pure water doesn't correspond to the performance of the aggregates in some harsh climates. The project *Frost resistance test on aggregates with salt (FRAS)* was therefore formed in 2002 to respond to the needs of TC 154. The project includes testing in pure and salt water, in air and in water. Fifteen European laboratories participate in the precision trials. The tests were completed in the autumn of 2003. For further information please contact the author or the project co-ordinator petursson.p@rabygg.is.

4 The Demand for Pre-normative Research

The necessity for research in support of standardisation is still large. Several demands have been identified during the process of standardisation, directly from the industry and also through the research projects. Some of them are discussed below.

Because aggregates are often tested as unbound materials the real performance in a construction is not clear. Bridging the gap between different standardisation committees is therefore necessary. Frost resistance of an aggregate in a Concrete (TC 104) or Asphalt (TC 227) is not the same as in the unbound state (TC 154). Alkali reactive aggregates behave very different in different climates and in different concrete mixes due to several factors. A few examples are synergistic effects between frost and ASR, the initial alkali content of the concrete, the types of alkali, added alkali by de-icing salt and pessimum effects. Test methods for aggregates will be assessed and improved in the PARTNER project. However, the demand for more research in this area is to assist the concrete designers with tools for proper concrete mixes in different climates and types of constructions.

The results from testing harmful fines in accordance with the Methylene Blue Value (EN 933-9) do not always correspond to the performance in the construction and vary greatly depending on the rock type and grading. Without proper knowledge this test tends to be used for several purposes originally not intended followed by erroneous results and consequences. The durability of aggregates containing certain amounts of swelling clays should be assessed by testing in the laboratory and in the field. This test method needs to be validated by further investigations.

As described above, there is a need to develop new test methods for alternative materials, tests that correlate to their performance in the construction. In addition, there is probably also the need to have methods to assess their performance when mixed with natural aggregates since the logistics doesn't always permit the entire construction to be built with such materials.

Alternative materials and, in cases, natural aggregates may contain harmful components, e.g. metals. The present method for leaching of aggregates in TC 154 is only suitable for production control. There is therefore a need to develop relevant leaching tests that correspond to the leaching in different types of constructions and environments and to define requirements accordingly. What is allowed in the short and long run?

There is a need to develop and correlate on-line systems for process control with standardised laboratory tests, e.g. different types of computer aided image analysis of particle shape and size (Wang 1997 and refs. therein). Several systems exist today, but the results from them do not always correlate with each other. A similar problem arises when the size distribution of filler and fines are determined by X-ray sedigraph, laser granulometer, air jet sieving or hydrometer.

Screening tests could be used more often and "legalised" through standardisation. One example is the correlation of rock microstructure with mechanical properties (e.g. Åkesson et al., 2003; Helgason and Fuxén, 2002). Screening tests may also be used when assessing the bedrock quality and suitability for different end

uses. Different concepts of bedrock classification in infrastructurally very active regions have therefore been developed (Persson, L. & Schouenborg., B. 1996). Such classification maps provide information for an efficient use of the materials extracted where big infrastructure projects are planned.

5 Concluding Remark

As can be seen from the above, there is no need for geological scientists to despair. There is a big demand for future research in support of standardisation. The first generation of aggregate standards has been developed on the basis that every European country should be able to use them and most laboratories. The first generation of European standards therefore contains many “old” test methods. However, when new techniques are developed within the industry to support more cost efficient production and usage in more advanced applications, the price and requirements will rise. New standardised methods have then to be developed.

The present knowledge and R&D structure in this field is strongly fragmented both on a European and national level and it is adapted to the situation before European harmonisation and the formation of an open European market. The creation of an inter-active virtual network, recurrent seminars and education/training courses can greatly improve this situation. The Network could provide a forum for exchange of research results and identification of future research priorities. This will have large beneficial economical and environmental consequences. Such a network has been proposed in the Expression of Interest for the 6th R&D Framework Programme of the EC: AGREED (Sustainable Development, Economy, Environment and Properties of Aggregates in Europe).

References

- Åkesson U, Stigh J, Lindqvist JE & Göransson M (2003) The influence of foliation on fragility of granitic rocks, image analysis and quantitative microscopy. *Engineering Geology* 68, 275-288.
- Arm M (2000) Properties of alternative aggregates (in Swedish). Licentiate thesis. Royal Institute of Technology, Stockholm, Sweden.
- Ballmann P, Collins R, Delalande G, Elshout JP, Mishellany A & Sym R (1999) Testing of aggregates for construction. EC internal reports of project no. MAT 1 - CT 93 – 0040.
- EN 933-9. Tests for geometrical properties of aggregates. Part 9. Assessment of fines – Methylene Blue test.
- EN 1367-1. Tests for thermal and weathering properties. Part 1 - Determination of resistance to freezing and thawing.
- Evertsson CM (2002) Cone Crusher Performance. Doctoral Thesis. Department of Machine and Vehicle System, Chalmers University of Technology, Sweden.
- Ewertsson C, Schouenborg B & Aurstad J (2000) Test methods adapted to alternative materials, part 2- Resistance towards fragmentation (in Swedish) *Nordtest Technical Report 440*.

- Helgason T.S & Fuxén S (2002) Testing and conformity assessment of construction aggregates using the PM techmodel software. 9th Nordic Aggregate Research Conference, 12-14 September 2002, Reykjavik, Iceland.
- Persson L & Schouenborg B (1996) Quality classification of rock in Sweden. European Aggregates. Vol 2-3, 32 – 37.
- Schouenborg B, Andersson H, Carling M & Arm M (1997) Test methods for alternative materials for road sub bases. Swedish Road Administration Publication BY 20° 97:10295 (in Swedish).
- Schouenborg B, Petursson P, Aurstad J, Hagnestål L & Winblad J (2003) Test methods adapted for alternative and recycled porous aggregate materials, part 3 – Water absorption NORDTEST Project No 1531-01.
- Stenberg F & Schouenborg B (1997) Test methods adapted to alternative materials, part 2 - Particle size distribution. (in Swedish) SP RAPPORT 1997:08
- Wang W (1997) Computer Vision for Rock Aggregates. Doctoral Thesis. Royal Institute of Technology, Stockholm, Sweden.

Standardised Methods for Sampling by Drilling and Excavation and for Groundwater Measurements

Ferdinand Stölben¹ and Volker Eitner²

¹ Stölben Bohrunternehmen GmbH, Barlstr. 42, 56856 Zell/Mosel, Germany
stoelben@stoelbenbohr.de

Tel.: +49 6542 93660

Fax: +49 6542 936699

² DIN Deutsches Institut für Normung e.V., Burggrafenstr. 6, 10787 Berlin, Germany
volker.eitner@din.de

Tel.: +49 30 2601 2526

Fax: +49 30 2601 42526

Abstract. The Technical Committees of the European Committee for Standardisation (CEN) and the International Organisation for Standardisation (ISO) on geotechnical investigation and testing prepare among others several common standards that deal with the direct investigation of soil, rock and groundwater as subsoil and construction materials as part of the geotechnical investigation services. EN ISO 22475-1 defines concepts and specifies requirements relating to exploration by excavation, drilling and sampling as well as groundwater measurements. EN ISO 22475-2 specifies the technical qualification criteria for an enterprise and personnel performing drilling and sampling services in order that both have the appropriate experience, knowledge and qualifications as well as the correct drilling and sampling equipment for the task to be carried out according to EN ISO 22475-2. EN ISO 22475-3 applies for the conformity assessment of enterprises and personnel for ground investigation drilling and sampling and groundwater measurements according to EN ISO 22475-1 that comply with the technical qualification criteria according to EN ISO 22475-3.

Keywords: drilling, sampling, groundwater measurements, standardisation, geotechnical investigation.

1 Introduction

The Technical Committee of the European Committee for Standardization CEN/TC 341 "Geotechnical investigation and testing" prepares a set of standards in cooperation with the ISO/TC 182/SC 1 according to the Vienna Agreement. The aim is to prepare identical European and international standards (EN ISO). One of these standards – EN ISO 22475 "Geotechnical investigation and testing - Sampling by drilling and excavation methods and groundwater measurements" – deals with principles of the direct investigation of soil, rock and groundwater as subsoil and construction materials as part of the geotechnical investigation services. This standard consists of the following parts: Part 1: Technical principles for execution, Part 2: Technical qualification criteria for enterprises and personnel,

and Part 3: Conformity assessment of enterprise and personnel, and defines concepts and specifies requirements relating to sampling by drilling and excavation and groundwater measurements. The aims of such explorations are:

- to recover soil and rock samples of a quality sufficient to assess the general suitability of a site for geotechnical engineering purposes and to determine the required soil and rock characteristics in the laboratory
- to obtain information on the sequence, thickness and orientation of strata;
- to establish the type, composition and condition of strata and joint system and faults;
- to obtain information on groundwater conditions and recover water samples for assessment of the interaction of groundwater, soil, rock and construction material;
- to allow in-situ testing to be carried out.

EN ISO 22475 does not cover soil sampling for the purposes of agricultural and environmental soil investigation and water sampling for the purposes of quality control, quality characterization, and identification of sources of pollution of water, including bottom deposits and sludges. Separate standards cover different geodyraulic test such as permeability tests, water pressure tests, pump tests etc.

2 Technical Principles of Execution

2.1 Equipment

The drilling and sampling equipment selected shall be of the appropriate size and type to produce the required quality of a sample. If applicable, the drilling and sampling equipment shall be in accordance with ISO 3351-1, ISO 3352-1 and ISO 10097-1. Drilling rigs with appropriate stability, power and equipment such as drill rods, casing, core barrels and bits shall be selected in order that the required sampling and borehole tests may be carried out to the required depth of the borehole and sampling categories. A selection of equipment which is currently used is given in an informative annex. The drilling rig and equipment shall allow all drilling functions to be adjusted accurately. Where appropriate, the following drilling data should be measured and recorded against depth:

- Drill head rotational torque;
- drill head rotational speed;
- feed thrust and pulling force;
- penetration rate;
- depth of hammering intervals;
- topographical depth;
- direction when inclined drilling;
- drilled length when inclined drilling;
- flushing medium pressure at the output of the pump;
- flushing medium circulation rate (input);
- flushing medium recovery rate.

2.2 Soil Sampling

Techniques for obtaining soil samples can be generally divided in the following groups: sampling by drilling, sampling using samplers, and block sampling. Combinations of these sampling methods are possible and sometimes required due to the geological conditions and the purpose of the investigation. There are three categories A, B and C of sampling methods. For given ground conditions, they are related to the best obtainable laboratory quality class of soil samples (defined in EN 1997-2) as shown in Tab. 1:

- category A sampling methods: samples of quality class 1 to 5 can be obtained;
- category B sampling methods: samples of quality class 3 to 5 can be obtained;
- category C sampling methods: only samples of quality class 5.

Samples of quality class 1 or 2 can only be obtained by using category A sampling methods. The intention is to obtain samples in which no or only slight disturbance of the soil structure has occurred during the sampling procedure or in handling of the samples. The water content and the void ratio of the soil correspond to that in-situ. No change in constituents or in chemical composition of the soil has occurred. Certain unforeseen circumstances such as varying of geological strata may lead to lower sample quality classes being obtained. By using category B sampling methods, this will preclude achieving sampling quality class better than 3. The intention is to obtain samples containing all the constituents of the in-situ soil in their original proportions and the soil has retained its natural water content. The general arrangement of the different soil layers or components can be identified. The structure of the soil has been disturbed. Certain unforeseen circumstances such as varying of geological strata may lead to lower sample quality classes being obtained.

Table 1. Quality classes of soil samples for laboratory testing and sampling categories to be used (from EN 1997-2).

Soil properties / quality class	1	2	3	4	5
<u>Unchanged soil properties</u>					
particle size, particle size distribution	*	*	*	*	
water content	*	*	*		
density, density index , permeability	*	*			
compressibility, shear strength	*				
<u>Properties that can be determined</u>					
sequence of layers	*	*	*	*	*
boundaries of strata – broad	*	*	*	*	
boundaries of strata – fine	*	*			
Atterberg limits, particle density, organic content	*	*			
water content	*	*	*	*	
density, density index, porosity, permeability	*		*		
compressibility, shear strength			*		
Sampling category to be used	A				
			B		
					C

By using category C sampling methods, this will preclude achieving sampling quality class better than 5. The soil's structure in the sample has been totally changed. The general arrangement of the different soil layers or components has been changed so that the in-situ layers cannot be identified accurately. The water content of the sample may not represent the natural water content of the soil layer sampled.

2.3 Rock Sampling

Techniques for obtaining rock samples can be divided in the following groups: sampling by drilling, sampling from trial pits, headings, shafts and from borehole bottom, and integral sampling. Combinations of these sampling methods are possible and sometimes required due to the geological conditions. Rock samples are of the following types: cores (complete and incomplete), cuttings and retained returns, and block sampling. The quality of the rock recovery is achieved by applying the following three parameters: total core recovery, TCR, rock quality designation, RQD, and solid core recovery, SCR. After recovery of the core barrels to the surface the rock recovery shall be assessed. In case the samples are extruded from the sampler and placed in a core box the sample shall be carefully logged. Core losses shall be filled with a dummy. There are three categories of rock sampling methods depending on the best obtainable quality of rock samples under given ground conditions: category A sampling methods, category B sampling methods, and category C sampling methods. By using category A sampling methods it is intended to obtain samples in which no or only slight disturbance of the rock structure has occurred during the sampling procedure of the samples. The strength and deformation properties, water content, density, porosity and the permeability of the rock sample correspond to the in-situ values. No change in constituents or in chemical composition of the rock mass has occurred. Certain unforeseen circumstances such as varying of geological conditions may lead to lower sample quality being obtained. By using category B sampling methods it is intended to obtain samples that contain all the constituents of the in-situ rock mass in their original proportions and the rock pieces have retained their strength and deformation properties, water content, density and porosity. By using category B sampling the general arrangement of discontinuities in the rock mass may be identified. The structure of the rock mass has been disturbed and thereby the strength and deformation properties, water content, density, porosity and permeability for the rock mass itself. Certain unforeseen circumstances such as varying of geological conditions may lead to lower sample quality being obtained. By using category C sampling methods the structure of the rock mass and its discontinuities has been totally changed. The rock material may have been crushed. Some changes in constituents or in chemical composition of the rock material may occur. The rock type and its matrix, texture and fabric may be identified.

2.4 Sampling of Groundwater for Construction Purposes

Groundwater sample methods shall be selected according to need. The quality of a groundwater sample is characterized by the extent to which it contains original constituents, such as suspended matter, dissolved gases and salts, or to which they have been contaminated during drilling. Groundwater can be sampled for the following purposes:

- to determine its aggressiveness to concrete;
- to determine its corrosive nature;
- to establish any risk to subsurface drainage systems and filters due to clogging and similar effects;
- to identify changes in groundwater quality or flow rate resulting from construction work;
- to determine its suitability as mixing water for construction material.

The number and location of collection points shall be specified in advance on the basis of the engineering problems involved and the local geological and hydrological conditions (see EN 1997-2). If a group of aquifers is encountered, it may be necessary to collect separate samples from each aquifer. If it is intended to take water samples for chemical analysis, only air and clean water may be used as flushing medium.

2.5 Groundwater Measurements

In order to obtain data on the magnitude, variation and distribution of the heads of groundwater or pore pressures in the ground, appropriate groundwater measuring stations shall be installed. The type and arrangement of groundwater measurements shall be specified in accordance with EN 1997-2. If drilling for piezometers, flushing additives should be avoided. When flushing additives are used the effects on the filter and the ground shall be considered and if necessary special measures shall be taken. Open or closed systems can be used to conduct groundwater measurements. The choice between open or closed systems should be made depending on the permeability of the ground, the rate of change in pore water pressure and the required precision and duration of the measurements. In both systems a filter should be installed in the ground at the location at which the head of groundwater or the pore pressure shall be measured. The filter shall prevent ingress of soil particles into the measuring system. In both systems a filter should be installed in the ground at the location at which the head of groundwater or the pore pressure shall be measured. The filter shall prevent ingress of soil particles into the measuring system. All components and equipment intended for installation in the ground shall be sufficiently resistant to mechanical loading and chemical attack by constituents in the groundwater. Any reactions between the materials used and the ground, in particular the formation of galvanic effects, shall be prevented. Groundwater measuring stations shall be positioned and secured in such a way that third parties are not at risk. Appropriate measures shall be taken to avoid any

risk to the groundwater measuring station due to contamination, flooding, traffic or frost. Open systems can be divided in three groups as follows (see Fig. 1): a) observation borehole, b) open pipe, and c) open pipe with inner hose.

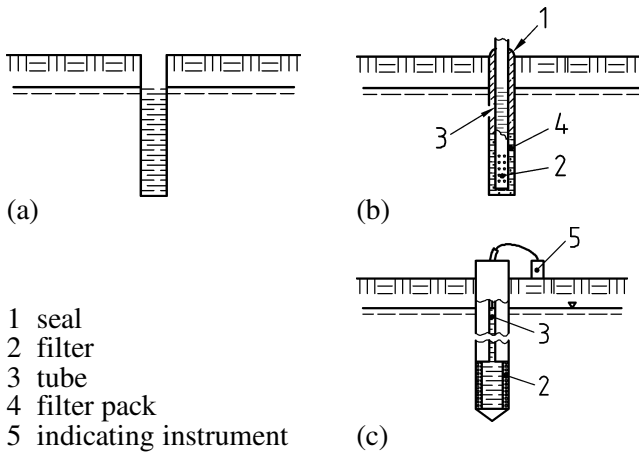


Fig. 1. Examples of open systems according to EN ISO 22475-1.

The piezometer in closed systems shall consist of a robust casing which is installed in the ground with a filter at the lower end (filter tip) and a water-filled chamber behind from where the water pressure is transmitted to the measuring device. Filters with sufficiently high air entry values shall be used. The pressure measurements can be performed as illustrated by Fig. 2: a) hydraulic measuring systems, b) pneumatic measuring systems, and c) electrical measuring systems.

All measuring systems used shall be calibrated prior to commissioning the groundwater measuring station. This applies to both new and reused equipment. All parts of the measuring system that affect the accuracy of the measurements shall be calibrated. The calibration results shall be documented in a report which, in addition to a description of the calibration procedure, shall include all information required to evaluate the measurements. Measurements shall be checked if they represent effects of installation, time lag or groundwater fluctuations. The results of the measurements shall be documented in a report which shall enable the values measured to be related to a particular stratum and interpreted unambiguously.

2.6 Handling, Transport and Storage of Samples

The conditions of soil and rock samples that were present after sampling according to sampling category A, B, or C, have to be preserved. National laws or regulations have to be considered when transporting samples known or suspected to contain hazardous material. A separate traceability record shall accompany each

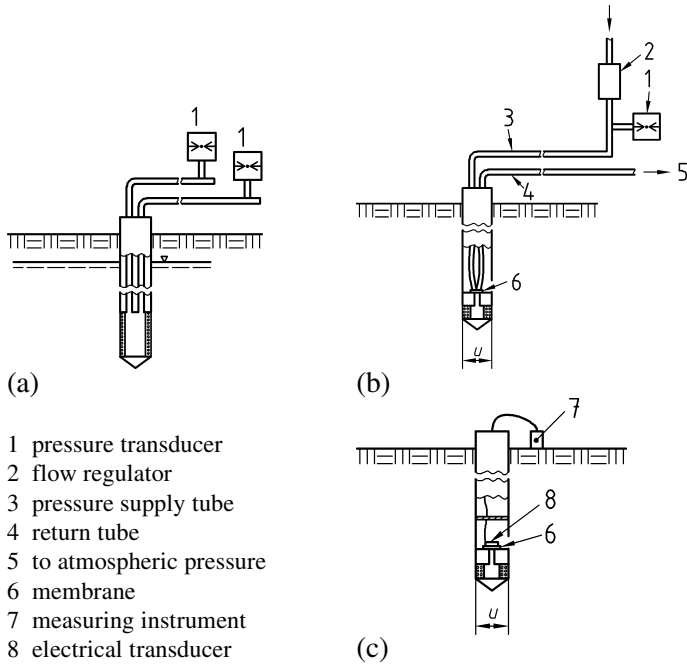


Fig. 2. Examples of closed systems according to EN ISO 22475-1.

shipment so that the possession of the sample is traceable from collection to shipment to laboratory disposition. When transferring the possession of samples the persons(s) relinquishing and receiving the samples shall sign, date, record the time and check completely the traceability record. Every soil and rock sample has to be protected any time from direct sun light, heat, frost and rain.

2.7 Reporting

At the project site, a "Field Report" of sampling by drilling and excavation and groundwater measurements shall be completed which shall consist of the following, if applicable:

- (a) summary log;
- (b) drilling record;
- (c) sampling record;
- (d) back-filling record;
- (e) record of identification and description of soil and rock;
- (f) record of the installation of piezometers;
- (g) record of groundwater measurements.

All field investigations shall be recorded and reported such that third persons are able to check and understand the results. Additionally, a "Report of the Results" shall be completed which shall include the following essential information, if applicable:

- (a) the field report (in original and/or computerised form);
- (b) a graphical presentation of the record of the identification and description of soil and rock;
- (c) a graphical presentation of the back-filling;
- (d) a graphical presentation of the piezometer;
- (e) a graphical presentation of the results of the groundwater measurements.

3 Technical Qualification Criteria

EN ISO 22475-2 specifies the technical qualification criteria for an enterprise and personnel performing sampling by drilling and excavations methods and groundwater measurement services so that both have the appropriate experience, knowledge and qualifications as well as the correct equipment for sampling by drilling and excavation methods and groundwater measurements for the task to be carried out according to EN ISO 22475-1.

4 Conformity Assessment

EN ISO 22475-3 applies for the conformity assessment of enterprises and personnel performing sampling by drilling and excavation methods and groundwater measurements according to EN ISO 22475-1 that comply with the technical qualification criteria according to EN ISO 22475-2. This part specifies the eligibility for conformity assessment, the application and assessment procedure as well as the re-assessment. The assessment report is given in an informative annex.

5 Conclusions

EN ISO 22475 will harmonize drilling and sampling methods and groundwater measurements for geotechnical engineering purposes and will allow to compare these geotechnical services on common basis. This will lead to a fairer competition. They were also prepared to increase the quality world-wide on this field in geotechnical engineering. Part 1 specifies the general principles of execution and Part 2 the technical qualification criteria for enterprises and personnel that perform sampling and groundwater measurements according to Part 1. If an enterprise or personnel fulfils these technical qualification criteria of Part 2, they can prove their conformity by: 1) a declaration of conformity by a contractor (first party control), 2) a declaration of conformity by a client (second party control), and 3) a declaration of conformity by a conformity assessment body (third party control).

Every enterprise or personnel may decide individually, if they want to declare its conformity with Part 2 by first, second or third party control because none of these three documents requires such a declaration (see Fig. 3). A declaration of conformity may only be required by contract. If an enterprise or personnel performing sampling and groundwater measurements according to Part 1 want to achieve a declaration of conformity by a conformity assessment body, the conformity assessment body is advised to use Part 3 which covers the conformity assessment of enterprises and personnel.

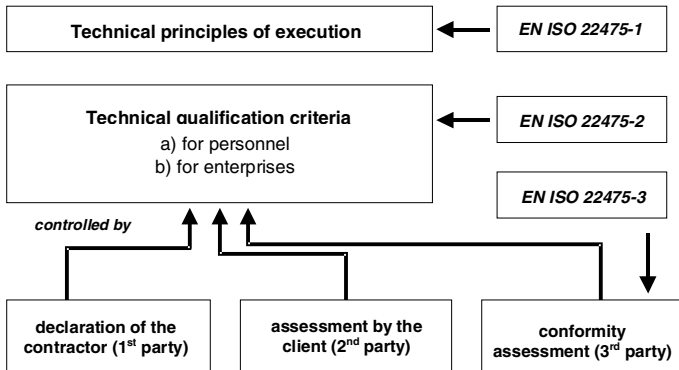


Fig. 3. Conformity assessment (after Stölben & Eitner, 2003).

This standard can be used for all geotechnical investigation purposes and geoclastic conditions which have led to two different strategies described in EN 1997-2: a) Drilling aimed at recovering the complete soil column, with samples obtained by the drilling tools along the borehole and by special samplers at selected depths at the borehole bottom, and b) Drilling to recover samples only at specific elevations, previously defined, e.g. by separately conducted penetration tests.

References

- EN 791, Drilling rigs — Safety.
 EN 1997-1, Eurocode 7: Geotechnical design — Part 1: General Rules.
 EN 1997-2, Eurocode 7: Geotechnical design — Part 2: Ground investigation and testing.
 ISO 3551-1, Rotary core diamond drilling equipment — System A — Part 1: metric units.
 ISO 3552-1, Rotary core diamond drilling equipment — System B — Part 1: metric units.
 ISO 5667 (all parts), Water quality — Sampling.
 ISO 10097-1, Wireline diamond core drilling equipment — System A — Part 1: Metric units.
 Stölben F & Eitner V (2003) Aufschluss- und Probenentnahmeverfahren und Grundwassermessungen im Rahmen von geotechnischen Erkundungen – Technische Grundlagen der Ausführungen, Qualifikationskriterien und Konformitätsbewertung. – Berichte von der 14. Tagung für Ingenieurgeologie, 26. bis 29. März 2003, Kiel; pp. 233 – 238.

Interpretation of SCPT Data Using Cross-over and Cross-Correlation Methods

Lou Areias and William Van Impe

Department of Civil Engineering - Laboratory of Soil Mechanics
University of Ghent, Technologiepark 905, B-9052 Ghent, Belgium
Lou.Areias@UGent.be
Tel: +32 (0)9 264 5722
Fax: +32 (0)9 264 5849

Abstract. A common method of determining arrival times of polarized shear (S) waves in the seismic cone penetration (SCPT) test is the cross-over method. This method relies on personal judgment to pick first arrivals and is difficult to automate. A better approach is to use cross-correlation methods, which rely less on operator judgment and can be automated to increase both efficiency and reliability of analysis. This paper uses a case study to illustrate the use of both the cross-over and cross-correlation methods to calculate shear wave velocity (V_s) in the SCPT test method.

Keywords: seismic cone penetration test, shear waves, cross-over, cross-correlation

Introduction

The SCPT test is an enhancement of the cone penetration (CPT) test widely used in soil investigations to determine soil stratigraphy and geotechnical design parameters (Robertson et al., 1986). The test is performed using standard CPT equipment and comprises geophones or accelerometers fitted in the cone penetrometer. A seismic source commonly consisting of a hammer-trigger system is used to generate seismic signals from the surface. The test can measure both S and compression (P) waves. The most common parameter measured with the SCPT test is the dynamic shear modulus (G_o). Accurate measurement of S wave arrival times is crucial in determining S wave velocity (V_s) in the SCPT test method. This is because G_o is related to the bulk density (ρ) of the material and V_s by:

$$G_o = \rho V_s^2 \quad [1]$$

A small error in V_s , therefore, results in a relative large error in G_o . Arrival times in SCPT tests are commonly picked from time-domain traces using direct methods. Some examples include picking the first peak or trough of a trace and the cross-over method. They consist of visually selecting arrival times from traces by noting their shape or other key features. A major disadvantage of these methods is their dependence on operator judgment and limited potential for automation. Other

methods of measuring arrival times are available, which are based on indirect techniques. Two of these methods are the cross-correlation and cross-spectrum methods. They rely less on operator judgment than direct methods, and can be built-in the SCPT test method to pick arrival times automatically. The cross-over and cross-correlation methods are further illustrated in this paper using a case study.

Cross-over Method

Reverse polarity is a unique property of S waves and is used as a key parameter in the cross-over method to identify the first arrival of S waves in the SCPT test. Polarized S signals are generated by striking opposite ends of a shear-wave source. The shear source commonly consists of a steel or wooden beam and is placed at the surface. Hitting the beam in the horizontal direction with a hammer generates predominantly S waves. An example of negative and positive polarized S waves is shown in Figs. 1&2. The signals shown were obtained from a depth of 5 m at a site in Limelette, Belgium. The cross-over method consists of superimposing time domain records containing pairs of polarized S waves and observing their cross-over points. The first cross-over point defines the S arrival time from which V_s is calculated. Only a single point of the trace record is therefore used to identify the first arrival. With this method, potentially useful information contained in the rest of the trace is not used. This method can provide reliable results when good quality signals are available. However, poor or shifted signals are difficult to analyze with this technique. A further drawback with this and other direct methods is the difficulty in comparing test data because of their inherent operator biasness.

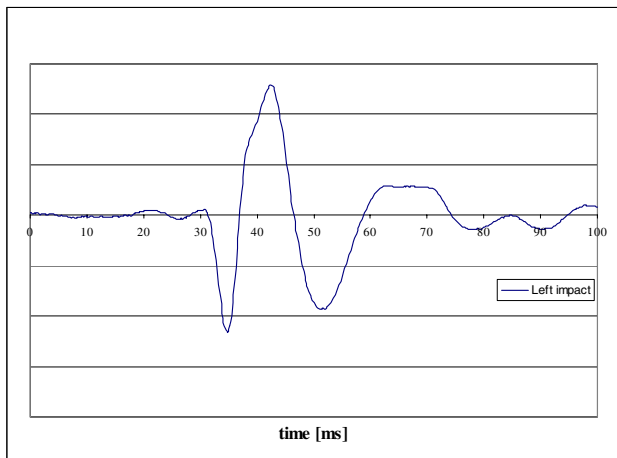


Fig. 1. Negative polarized signal from depth 5 m generated with mechanical hammer (left impact).

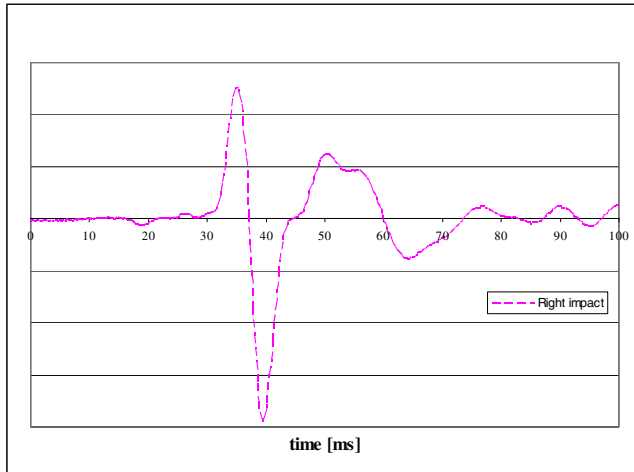


Fig. 2. Positive polarized signal from depth 5 m generated with sledge hammer (right impact).

Cross-Correlation Method

This method consists of measuring the similarity between two signals. One signal is displaced varying amounts relative to the other and corresponding values of the two signals are multiplied together and the products summed to give the value of cross-correlation. Whenever the two signals are nearly the same, the cross-correlation is large; whenever the two signals are unlike, the cross-correlation is small. The cross-correlation (Φ_{xy}) of two signals x_t and y_t is expressed as:

$$\phi_{xy}(\tau) = \sum_k x_k y_{(k + \tau)} \quad [2]$$

where τ is the displacement of y_t relative to x_t . This technique can be used to determine the time shift between two signals x_t and y_t , which can then be used to calculate V_s profiles from SCPT test data. Because it uses the complete signal trace, this method of analysis is more reliable and consistent than direct methods such as the cross-over method. In addition, this technique can also be used to calculate compression (P) wave velocity (V_p) in the same test. Finally, this method can easily be automated, which further increases efficiency and cuts down in analysis and processing time.

Case Study

SCPT data from the Limelette site were analyzed using the cross-over and cross-correlation methods to illustrate the use of these methods. The analyzed data

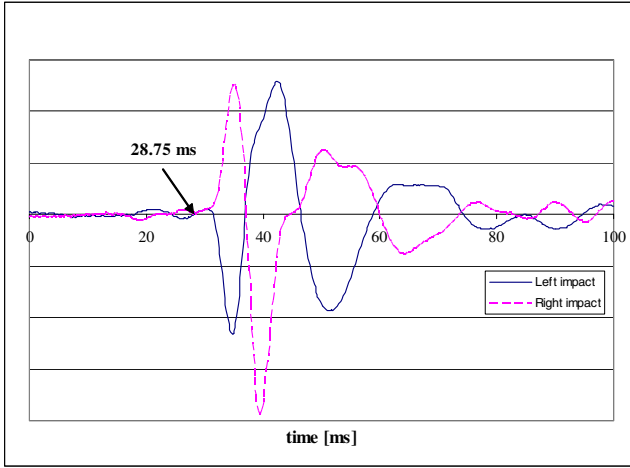


Fig. 3. Cross-over method showing superimposed polarized signals from depth 5 m.

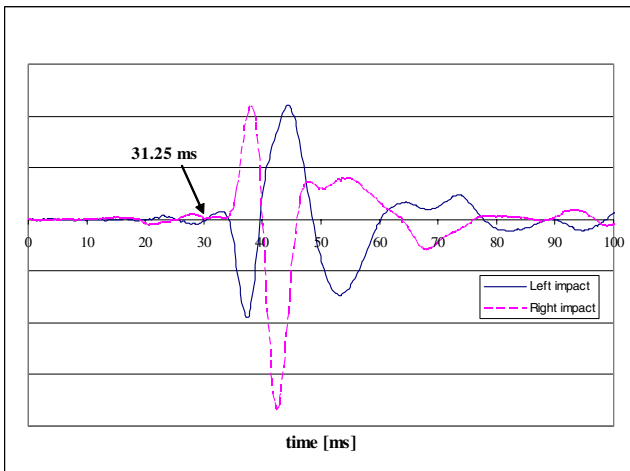


Fig. 4. Cross-over method showing superimposed polarized signals from depth 6 m.

were obtained from depths of 5 and 6 m in a typical SCPT test. The signals were generated using an adjustable mechanical hammer on one side of a steel impact beam and a sledge hammer on the opposite side. The mechanical hammer generated negative polarized S signals and was regulated to provide consistent energy impacts between tests (Areias et al. 1999). The impacts produced with the sledge hammer to obtain positive polarized S lead to higher impact energy variability than the mechanical hammer. This can negatively influence signal quality as Fig. 2 suggests. The procedure describing the cross-over method is represented in Figs. 3&4, which show two pairs of superimposed polarized S waves from depths

5 and 6 m, respectively. An approximate travel time difference of 2.50 ms was measured between the two signals giving V_s of 160.0 m/s for a travel path of 0.4 m. Picking arrival times in the cross-over method is not always easy as can be appreciated from examining Figs 3&4. Determining the correct cross-over point unavoidably requires personal judgment and experience. The cross-correlation analysis uses only one signal from each test depth. Either negative or positive polarity signals may be used but they must have the same polarity. The results of this analysis are given for both polarities for comparison. Using the negative polarity signals, a time shift of 2.50 ms was calculated, as shown in Fig. 5. Using the positive polarized signals, a time shift of 2.75 ms was determined, as given in Fig. 6. The respective V_s are then 160.0 and 145.5 m/s. Good agreement was found between the cross-over and the negative polarized cross-correlation methods. The slightly different time shift found for the positive polarized signal is probably due to the lower quality signals generated by the sledge hammer, as mentioned. Other factors can, however, influence V_s measurement. A full description of these factors is beyond the scope of this paper. However, in addition to signal quality, research currently ongoing by the main author suggests that V_s is influenced by the type of seismic source used, the method of calculating V_s and by inherent trigger-induced signal measurement variability produced by the test.

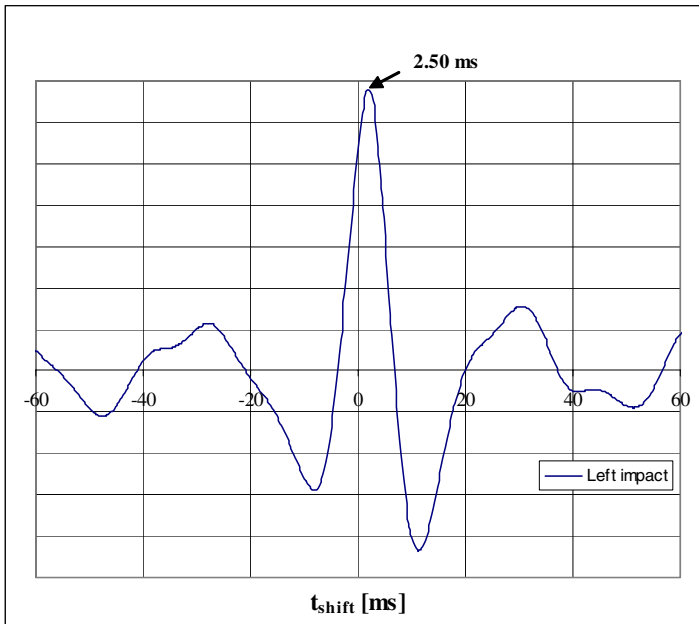


Fig. 5. Cross-correlation of negative polarized signals from depths 5 and 6 m.

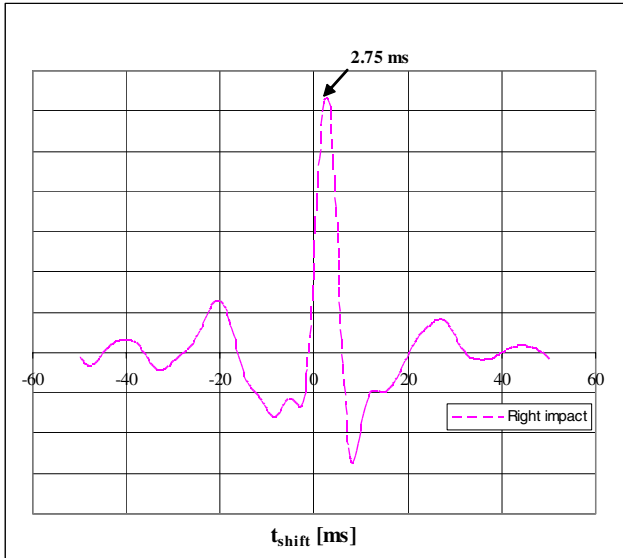


Fig. 6. Cross-correlation of positive polarized signals from depths 5 and 6 m.

Automatic Picking

Arrival time (or other events) can be picked automatically using coherence measures as criteria. A number of such methods exist and are well documented in the literature (Paulson and Merdler, 1968; Garotta, 1971; Sheriff and Geldart, 1995). Whenever coherence exceeds a predefined threshold value, arrival times can be picked. A grade can be assigned based on coherence values and reported together with the results. The cross-correlation method is relatively easy to program to pick interval times corresponding to maximum values of coherence. This is more difficult with the cross-spectrum method, for example, which requires specifying criteria for determining which frequencies should be selected to calculate V_s . For this reason, the cross-correlation method is recommended for integration in the SCPT test method.

Conclusions

The cross-correlation method is relatively easy to program to pick interval times corresponding to maximum values of coherence in the SCPT test method. Unlike the cross-over method, which relies on operator judgment for interpretation, this method can be integrated in the SCPT test method to provide consistent results. Finally, this technique can also be used to calculate V_p , which further increases efficiency and cuts costs by reducing analysis and processing time.

References

- Areias L, Van Impe WF and Haegeman W (1999) Variation of shear wave energy with coupling stress in the SCPT method. *European Journal of Environmental and Engineering Geophysics*, Volume 4, 87-95.
- Garotta R. (1971) Selection of seismic picking based upon the dip moveout and amplitude of each event. *Geophys. Prosp.*, 19: 357-70.
- Paulson K.V. and Merdler S.C. (1968) Automatic seismic reflection picking. *Geophysics*, 33: 431-40.
- Robertson P.K., Campanella R.G., Gillespie D. and Rice A. (1986) Seismic CPT to measure in situ shear wave velocity. *ASCE, Journal of Geotechnical Engineering*, Vol. 112, No. 8, 791-803.
- Sheriff R.E. and Geldart L.P. (1995) *Exploration seismology*, 2nd ed.. Cambridge University Press.

Evaluation Concept and Testing Method for Heavy Metal Contaminant Transport in the Underground

Rafiq Azzam and Mouad Lambarki

Department of Engineering Geology and Hydrogeology, RWTH-Aachen University,
Lochner Str. 4-20, 52064 Aachen, Germany
{azzam,m.lambarki}@lih.rwth-aachen.de
Tel: +49 241 8095740
Fax: +49 241 8092280

Abstract. The evaluation of the contaminant transport is dictated by the Federal Soil Protection Regulation (BBodSchV, 1999) for sites that are suspected to endanger the groundwater. A prognosis for contaminant transport by infiltrated water must therefore be carried out. Within the framework of a research project supported by the BMBF (Federal Ministry for Education and Research), a new investigation concept for the prediction of contamination input into the groundwater was developed.

This concept considers the estimation of the emission (**E**) of the contaminants i.e. the amount and concentration of the leachate of the contamination source in correlation with the time. The amount of leachate can be estimated by the infiltration of the groundwater recharge for every hydrological year using hydrological parameters. The expected concentration can be obtained from elution tests. In a second step, the transmission (**T**) i.e. the pollutant transport through the unsaturated zone into the groundwater is evaluated. This evaluation considers the transport mechanisms advection, diffusion and the retardation potential of the transmission zone. As a result, the immission (**I**) into the groundwater, the amount and concentration of the contaminants input can be estimated. Finally, it is important to evaluate the sensitivity of the system by classifying the groundwater according to the source value. This evaluation technique comprises the characterization of the site and the estimation of the contamination potential by conducting laboratory and in-situ tests and numerical simulation modelling involving iteration for a contaminant mass balance.

In this paper, a new testing method for the determination of the characteristic parameters for the transport mechanisms including the retardation potential is described. This method is carried out in a diffusion cell. An evaluation concept for the contaminant transport based on the testing results is presented and discussed.

Keywords: Contaminant transport, Prognosis, Heavy metal, Diffusion, Advection, Sorption, Emission, Transmission, Immission, contaminant transport.

1 Introduction

According to the new Federal Soil Protection Law (BBodSchG, 1998) a prognosis of contaminant transport is required in order to evaluate the potential danger arising from dump sites, low hazardous earth fills and suspicious surfaces. In accor-

dance with the current version of the Federal Soil Protection Regulation (BBodSchV, 1999) a "seepage water prognosis" is defined as an estimation of the contaminant input into the groundwater (the transition area between the unsaturated and saturated zones) via infiltrated water at a specific site. Since a common methodology for the prognosis does not exist, it can be performed in three ways: by back calculations from groundwater analyses downstream the contamination, by in-situ sampling, and by laboratory tests.

However, the BMBF has set up a research project to develop a scientifically based methodology and practical procedures for such a prognosis. In the scope of this research project the authors developed a prognosis method for heavy metals contaminant transport comprising, a so-called ETI concept (Figure 1). This concept considers the estimation of the emission (**E**) of the contaminants, i.e. the time dependant amount and concentration of the leachate of the contamination source. The amount of leachate can be estimated by the infiltration of the groundwater recharge for every hydrological year using hydrological parameters. The expected concentration can be obtained from elution tests. In a second step, the transmission (**T**) i.e. the pollutant transport through the unsaturated zone into the groundwater is evaluated. This evaluation considers the transport mechanisms advection, diffusion and the retardation potential of the transmission zone. As a result, the immission (**I**) into the groundwater, the amount and concentration of the contaminants input can be estimated.

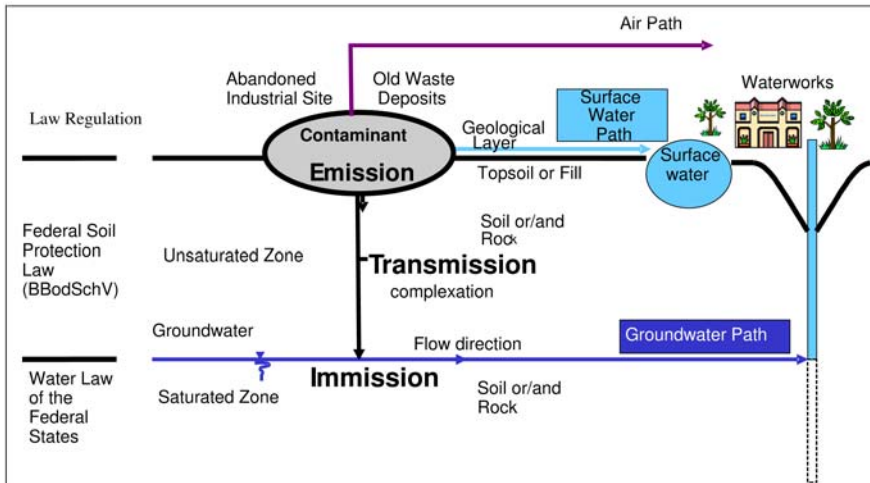


Fig. 1. The ETI-Concept.

2 Heavy Metals Contamination

Soil and groundwater are very important natural resources. Due to increasing demand on them, their limited quantities, and the difficulties of remediation once contaminated, their protection has become increasingly important. The problem of

groundwater contamination by heavy metals has received much attention in recent years. Lead, in particular is a heavy metal of serious environmental concern. One of the physiological effects of lead is that it is detrimental to the neurological development of children, reduction in their IQ, and other health effects as approved by several case studies (Nedunuri et al. 1995). Some of the sources of lead are gasoline, paints, additives to fuel, pigments and stack emissions from some metal industries. Major sources of lead in groundwater are the smelter sites and areas where significant mining activities took place. Seepage water from mine tailings can contaminate surface water, irrigated soils, and groundwater, causing harm to human beings and animals. Contaminant transport in the vadose zone and its interaction with the soil minerals is important to understand. The types of reactions that are likely to control the distribution of metals in soils are mineral precipitation and dissolution, ion exchange, diffusion, adsorption and desorption, aqueous complexation, and biological immobilization and mobilization.

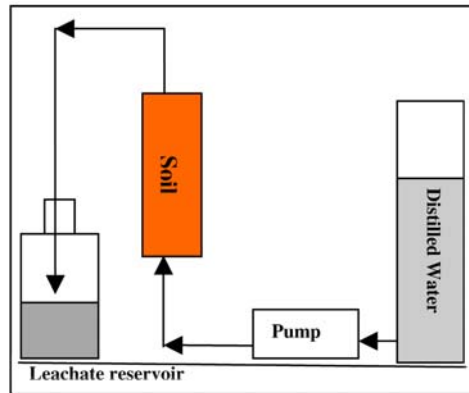


Fig. 2. Column test.

3 Testing Methods

3.1 Quantification of the Emission

The first step to be taken regarding the prognosis of pollutant transport is the estimation of the Emission. For the characterization, evaluation and quantification of the Emission from a contaminated landfill it is necessary to perform elution and column tests on the contaminated soil (Figure 2). The aim of the tests is to determine the potential of the contamination source as well as the concentration of the leachate as a function of time. Since the contamination is related to the infiltration of water as a solvent, it is important to determine the physical properties of the topsoil such as the permeability, and hydrological data of the site e.g. precipitation and infiltration quantity. As a result of the investigation, the amount and concentration of the contaminant can be obtained for every hydrological year using hy-

drological parameters. Figure 3 shows the amount of contaminant in [mg/l] for every hydrological year until the pollutant source is exhausted.

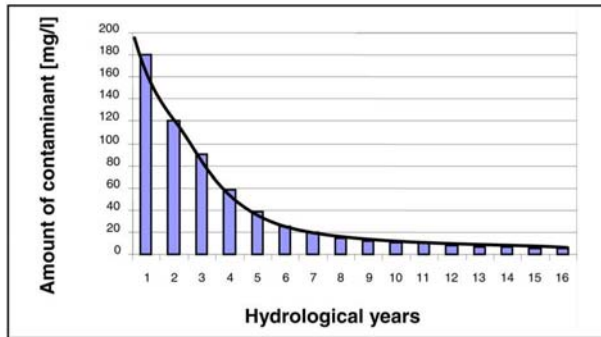


Fig. 3. Emission for certain a Water/Pore relationship.

Since the contamination intensity vary depending on the pH- and EH-values in the soil or in the regarded deposit, sequential extraction and batch methods are accomplished in addition to the validation of the column tests. The goal is to determine the potential source strength and to obtain the kinetic data (desorption characteristics as well as their dependence on time and physical conditions).

3.2 Transmission through the Unsaturated Zone

Risk assessment of the soil-groundwater transmission based on the German federal soil protection law deals with the mobile contaminants and their concentration in seepage water. Area of interest is the transition between the saturated and unsaturated zones. If this area cannot be investigated directly, a seepage water prognosis has to be worked out. In this project, a new developed laboratory test (diffusion-advection cell) was used for the evaluation of the Transmission. This evaluation test simulates the transport processes in the unsaturated zone considering advection, diffusion, and retardation (Figure 4). The aim of the test is to determine the advective and diffusive mass flow, leaching behaviour and sorption characteristics of the top soil.

The new developed diffusion-advection tests was conducted using a soil specimen 1 cm thick, a hydraulic gradient of $i=1$ and a concentration gradient, which corresponds to the source strength of the first hydrological year. A description of the test set-up and an explanation of the basic principle of this method are given as follows: a soil specimen is placed between two reservoirs: a top reservoir containing a heavy metal solution ($C_L > 0$) and a bottom reservoir containing distilled water ($C_0 = 0$). During the test, solution samples from both reservoirs were collected. The solution samples were analyzed for heavy metal concentration. The test procedure satisfies the conditions of stationary state method. The initial concentration is kept constant during the test.

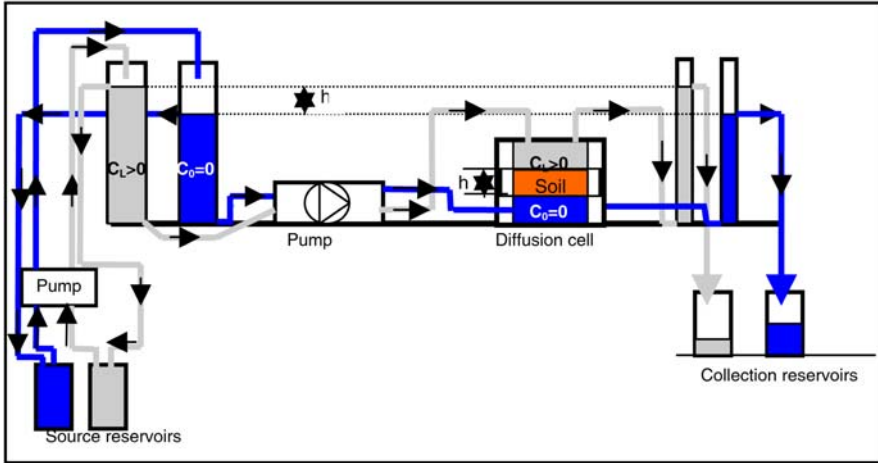


Fig. 4. Diffusion-Advection Cell.

The advantages of the applied test procedure are particularly the similarity with natural conditions as well as the simple determination of the diffusion coefficient and the total sorption capacity of the soil after reaching the stationary condition. The sorption parameters can be determined by solving the partial differential equation (Figure 5). The disadvantage, however, is the very long duration of test. Therefore, in this project the sample thickness was kept small (1cm) to keep the test duration as short as possible.

The observed mass flux versus elapsed time, in upper and lower reservoirs, is shown in Figure 6. By means of this test, the transport characteristics (permeability, diffusion coefficient, retardation and sorption) of the unsaturated zone were determined under real conditions. The difference between the input mass flux and the output mass flux represents the adsorption capacity of a certain soil layer.

3.3 Immission

From the results of diffusion-advection tests conducted on the top soil, the input and output mass fluxes are determined. Therefore, to implement this evaluation concept, the unsaturated zone is divided into several layers with equal thicknesses, whereby the output mass flux of the upper layer is equal to the input mass flux of the underlying soil layer (Figure 7). Similar calculations are repeated by iteration for all soil layers in the unsaturated zone. The balance of this mass flux allows the quantification of the mass input into the groundwater (Figure 8).

For the estimation of the endangerment potential, i.e. whether the test value specified in BBSchG is exceeded at the place of study, it is important to compare the contaminant concentrations at the transition between saturated and unsaturated zone with the test values. Important parameters for the immission are the rate of contaminant input (discharge rate) in the groundwater per time as well as the duration, until the pollutant capacity is exhausted.

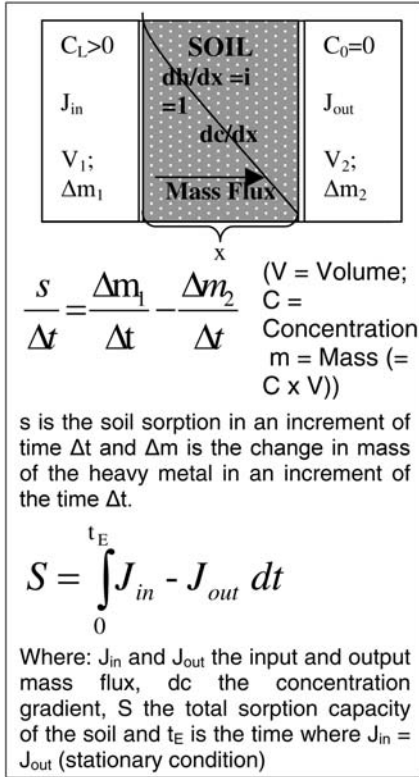


Fig. 5. Concentration profiles in soil samples.

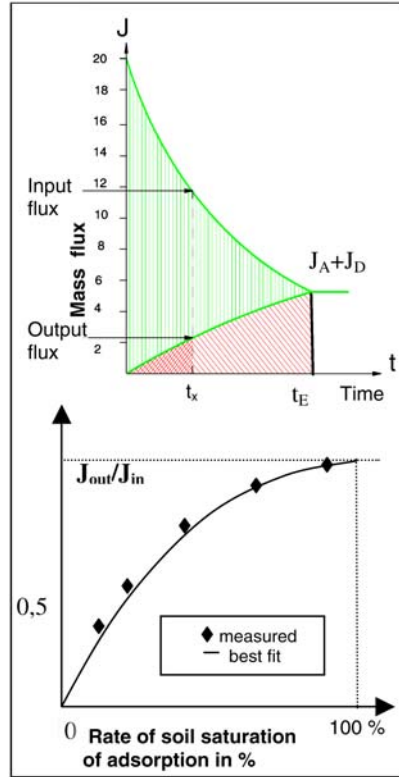


Fig. 6. Results of the diffusion and advection test.

4 Summary and Conclusions

A new investigation concept for the prediction of the contaminant input into the groundwater was developed. This concept, which is called **ETI**-concept, considers the estimation of the emission (**E**) from the contaminants using column tests. The evaluation of the transmission (**T**) is based on the results of tests carried out on natural soil in the new developed device diffusion-advection cell. This evaluation considers the transport mechanisms advection, diffusion and retardation potential of the unsaturated zone. The discharge rate from the tested soil layer is determined. As a result, the immission (**I**) into the groundwater, the amount and concentration of the contaminants input as well as the duration until the pollutant capacity is exhausted, can be estimated. The immission is a result of a balance of mass flux in the unsaturated zone until reaching the groundwater.

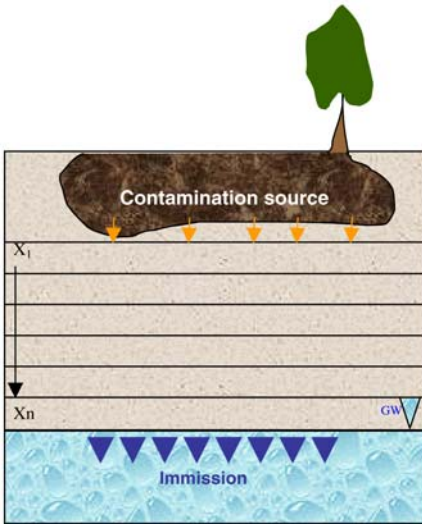


Fig. 7. Dividing of unsaturated zone in layers with equal height.

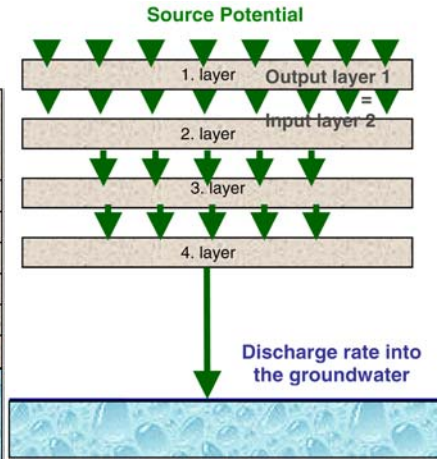


Fig. 8. Balance of mass flux and input into the groundwater.

The results of the preliminary investigations regarding the suitability of the developed diffusion-advection tests for a prognosis of groundwater endanger are very satisfactory. Generally, the developed technique compared to other investigation methods simulates the natural conditions in a laboratory dimension. In consideration of real conditions in landfills, the retention of natural soil in the unsaturated zone is controlled by the soil properties, the pollutant type and concentration and by the transport process it self and can be acquired just by diffusion-advection tests. The retention can be determined by comparison of the permeation rates in and out of the specimen. Sorption determined by Batch or shaking tests in a suspension is not eligible to describe physical-chemical process and quantity of retarded pollutants by natural soils in the transmission zone.

References

- Azzam R, Lambarki M & Syhre B (2003): Evaluation Method for Heavy Metal Contaminant Transport and it's Input into the Groundwater Considering the ETI-Concept. Con-Soil 2003, Gent, Belgium.
- Azzam R (1993): Stofftransportprozesse in natürlichen Dichtungsstoffen unter Berücksichtigung der Verdichtbarkeit sowie des Einflusses strukturverändernder Chemikalien auf die Materialeigenschaften. Mitteilung zur Ing.- u. Hydrogeologie, 49, 199 S., Aachen 1993.
- BBodSchG (1998): Gesetz zum Schutz des Bodens vom 17. März 1998. Bundesgesetzblatt Jahrgang 1998, Teil I, Nr.16. S. 505-510.

- BBodSchV (1999): Bundes-Bodenschutz- und Altlastenverordnung vom 16. Juli 1999, Bundesblatt Jahrgang 1999, Teil1, Nr. 36. S. 1554-1682.
- Lambarki M, Azzam, R & Syhre B (2003): Entwicklung eines Säulenversuches für die Sickerwasserprognose. 14.Nationale Tagung für Ingenieurgeologie, Kiel. ISBN 3-00-011203-0. S. 33-39.
- Nedunuri KV, Govindaraju RS, Erickson LE & Schwab AP (1995): Modelling of heavy metal movement in vegetated, unsaturated soils with emphasis on geochemistry. Proceedings of the 10th Annual Conference on Hazardous Waste Research, 57- 66, Kansas, 1995.

Geo-engineering Evaluation with Prime Consideration to Liquefaction Potential for Eskisehir City (Turkey)

N. Pinar Koyuncu¹ and Resat Ulusay²

¹ General Directorate of Mineral Research and Exploration, Feasibility Studies Department, Ankara, Turkey

pinar@mta.gov.tr

Tel: +90 312 2873430/2180

²Hacettepe University, Geological Engineering Department,

06532 Beytepe, Ankara, Turkey

resat@hacettepe.edu.tr

Tel: +90 312 2977767

Fax: +90 312 2992034

Abstract In Turkey, cities are growing in importance and urban areas are expanding rapidly. Eskisehir is one of the highly urbanized and industrialized cities of Turkey. In this study, the city is selected for geo-engineering assessments to be considered in future urban planning due to its ground and seismotectonic conditions. Seismic hazard analyses indicated that magnitude of a probable earthquake and PGA associated with the closest fault may be about 6.4 and 300 gal, respectively. Liquefaction assessments suggest that shallow-seated sand layers, particularly near to the meanders of a river flowing through the city have moderate-to-high liquefaction susceptibility. In addition, GIS-aided engineering geological map of the city center are constructed and some recommendations are presented.

Keywords: engineering geological map, Eskisehir, liquefaction, seismic, hazard.

1 Introduction

In Turkey, cities are growing in importance, and urban areas are expanding rapidly, because the population of the nation is increasing and proportionally more people are congregating in urban areas. This situation results in new problems for urban planning and redevelopment of the country. In addition to municipal problems, other problems include the mitigation of natural hazards, which are to a certain degree caused, or at least enhanced, by human activities. Eskisehir, one of the ten biggest settlements in Turkey, is an industry and university city, and located in NW Central Anatolia (Figure 1). An important part of the metropolitan area is founded on an alluvial plane consisting of loose sediments and is very close to the active faults. However, any detailed engineering-geological assessment for the city has not been carried out. In this study, therefore, an area of 34 km² at the central and northern parts of the city, where new districts have been permitted for

settlement, is selected for geo-engineering evaluations to be considered in future urban planning. This evaluation incorporated topography, surface and bedrock geology, seismotectonics, groundwater conditions and geological hazards with prime consideration to liquefaction. In addition to geological mapping, data from about 200 geotechnical boreholes and laboratory tests are evaluated. Finally GIS-aided liquefaction susceptibility and engineering geological maps are constructed, and some recommendations are presented.

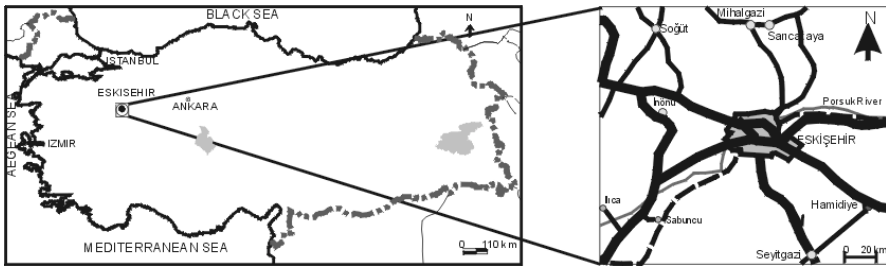


Fig. 1. Location map of Eskisehir city.

2 Study Area

2.1 Description of the Study Area

Historically, urban population growth in Eskisehir has been confined primarily to upslope surrounding the city from its south. However, particularly in the last two decades, development has spread rapidly to the lowlands formed by the alluvial deposits carried by Porsuk River, which cuts the city. The southern part of the city is bounded by gentle slopes with inclinations between 5° and 17° . The population of the city reached to about one million following rapid industrialization and the opening of two universities.

2.2 Lithological Units

The bedrock cropping out in the study area and its vicinity comprises Mesozoic gabbro and marble, Eocene conglomerate member of the Mamuca formation, and Miocene conglomerate, conglomerate-sandstone, claystone-marl-tuffite and limestone (Gözler et al., 1996). The Quarternary deposits covering large areas are represented by the recent and old alluvial sequences (Figure 2). Eocene conglomerates, mainly consisting of pebbles embedded in plastic clay, behave like a stiff soil rather than a rock. The uppermost levels of the Miocene units are heavily weathered and soft, except the limestone, which are partly silicified, and highly strong. The old alluvial sequence, cropping out at topographically higher elevations when compared to the recent alluvium, is considerably stiff, and occasionally

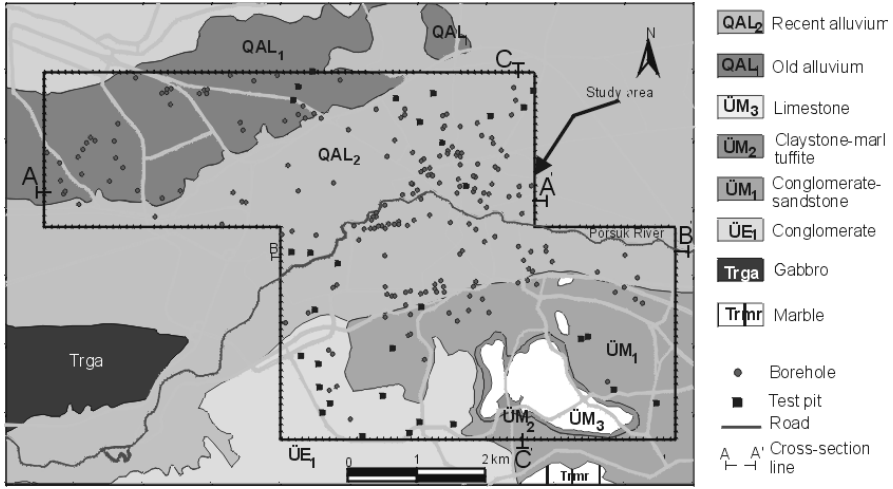


Fig. 2. Geological map and locations of boreholes and test pits.

involves carbonate-cemented conglomerate layers. The recent alluvium generally consists of loose sediments and its thickness is about 30-40 m, and 90m at the margins and central part of the plain, respectively.

2.3 Seismotectonics and Seismic Hazard Assessment

The faults in the Eskisehir region are NW-SE trending and exhibit normal faulting characteristics with slight lateral components (Figure 3). They form the Eskisehir plain and have inclinations between 60° and 80° (Gözler et al.,1996). The most important fault zone called as Eskisehir-Inonu Fault Zone (EIFZ) (Saroğlu et al.,

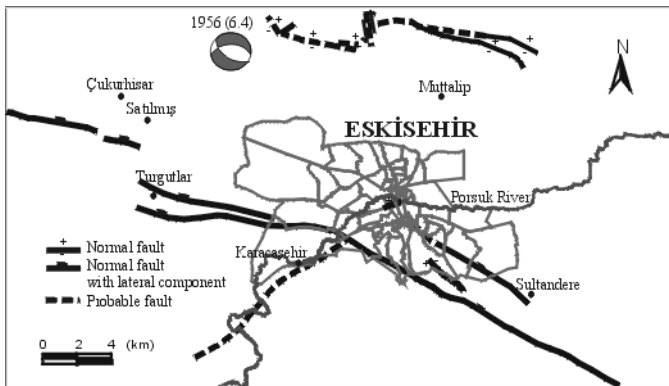


Fig. 3. Main tectonic elements in the vicinity of Eskisehir (modified from Altunel and Barka, 1998).

1992; Altunel and Barka, 1998) consists of several segments and extends as a zone of 1- 4 km wide, and dips towards north. Morphological evidence, position of the ophiolitic rocks and distribution of the earthquake epicenters along this zone suggest that it is an active fault and the most important earthquake source for the city. The Eskisehir region is situated in the second order earthquake zone of Turkey. The most devastating strong earthquake with a magnitude of 6.4 in the region occurred in 1956. Its epicenter was about 10 km away from the city center (Figure 3). It resulted in two deaths and heavy damages particularly at the western part of the city. Although limited data is available, Altunel and Barka (1998) suggest that the Oklubal-Turgutlar segment of the EIFZ might be the probable causative fault and the focal depth was greater than 10 km. In addition, the most recent earthquakes ($M > 4$) indicate the activity of the Sultandere segment of the EIFZ passing near the south of the city (Figure 3). To estimate the peak ground acceleration (PGA) for use in liquefaction assessments, deterministic seismic hazard approach (Abrahamson, 2000) was employed. For the purpose, epicenters of three destructive earthquakes, which were also felt in Eskisehir, and two faults close to the city were considered as point and line earthquake sources, respectively (Table 2.1). Based on magnitude-length of surface rupture relationship based on data from Turkish earthquakes (Aydan, 1997), expected magnitudes of the faults as line sources were estimated, and, except line sources 2, the closest distances from these sources to the city center were considered (Table 2.1). By using the attenuation relationship based on M_s and distance to focus and suggested for Turkey by Aydan et al. (1996) PGA values were estimated. Table 2.1 suggests that the city can be considerably affected by the line source 2 and PGA values between 200 and 320 gal are expected due to a probable earthquake associated with the EIFZ. Seismic hazard analysis by Gulkan et al. (1993) also shows that the potential PGA with a 10% probability of exceedence over a period of 100 years is between 200 and 300 gal for this area.

Table 2.1. Results of deterministic seismic hazard analysis

Source no. and name	L (km)	R (km)	M_s	PGA (gal)
Point 1: 1999 Kocaeli earthquake	98	99	7.4	181
Point 2: 1999 Duzce earthquake	101	101.6	7.2	141
Point 3: 1967 Mudurnu earthquake	74	81	7.2	238
Line 1: Kütahya fault	53	56	5.9	137
Line 2: Eskisehir-Inonu Fault Zone	3.4	40	6.4	323

L: closest distance to the city; R: distance from focus; M_s : surface magnitude; Epicentral distances are considered for point sources.

3 Geo-engineering Assessments

3.1 Subsurface Ground Conditions and Natural Slopes

The data from 203 shallow-seated (3-13 m) geotechnical boreholes and 154 water wells in conjunction with observations in test pits (Figure 2) were evaluated. The SPT-N values obtained from the old alluvium range between 20 and 50, and increase with depth. This sequence consists of a mixture of very stiff fine and hard coarse-grained sediments. The uppermost 3 m of the recent alluvial sequence is composed of sandy clayey silts (SPT- N= 3-40) and occasionally underline by loose silty sand layers and/or lenses (SPT-N= 10-12), particularly near the meanders of Porsuk River. These layers overlay gravelly sands and sandy gravels (SPT-N = 10-50) (Figure 4). The Eocene conglomerates with SPT-N values of 20-50 behave like a stiff soil. The uppermost portion (0-4 m) of the Miocene conglomerate – sandstone is characterized by clayey-sandy silts (SPT-N= 4-50) and can be easily excavated. The limestones and sandstones at the southern part of the site yielded Schmidt rebound numbers of 35-50 and 25-37, respectively. The laboratory test results indicated that the recent alluvium involves GW-GP, SW-SP and SM group soils, while the old alluvium consists of GW, GP, SP and SM groups. Fine grained fraction of the alluvial sequence, weathered portion of the conglomerate-sandstone and matrix of the Eocene conglomerates, on which buildings have been founded, consist of soils with medium-to-low swelling potential. Based on the evaluations of groundwater data (Kacaroglu, 1991), the depth of the groundwater table in the Eskisehir Plain generally lies between 0.5 m and 7.5 m in April and May, and between 2 and 13 m in summer season. Seasonal fluctuation in groundwater table in the metropolitan area is between 0.1-0.5m and the water table is shallower in the recent alluvium when compared to that in the old alluvium. The flow direction of the water table is generally from west to east, and the water table is recharged by the Porsuk River. No natural slope instability has been reported in the study site. Gentle topography, and nearly horizontal strata, and shallow weathering depth in rock units play a positive role in the stability of natural slopes.

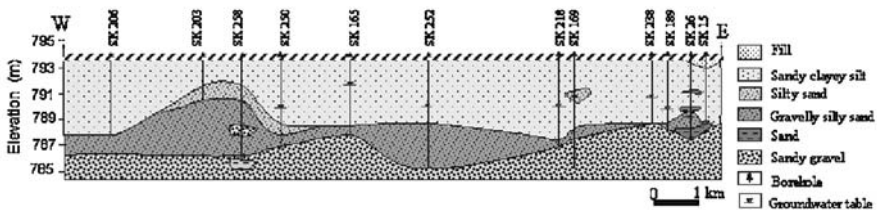


Fig. 4. Ground condition in the alluvial sequence (section A-A').

3.2 Liquefaction Potential

Liquefaction potential assessments were based on field SPT performance data (Youd and Idriss, 2001) for 200, 300 and 400 gal to evaluate the effect of the PGA on the factor of safety against liquefaction (F_L). In addition, severity of liquefaction was quantified by liquefaction potential index (I_L) suggested by Iwasaki et al. (1982), and microzones for the study area based on I_L were constructed for three PGA values. An engineering geological map of the site in Figure 5 suggests that in the case of PGA= 300 gal, the northern banks of the Porsuk River, particularly its meandering parts, seem to be more susceptible areas to liquefaction. It is also noted that if the PGA increases to 400 gal, extent of liquefaction- susceptible areas will expand towards south and east. Possible ground surface disruption due to liquefaction was also evaluated using the empirical method by Ishihara (1985) for three PGA values. The data plot in Figure 6 indicates that surface disruption may be more evident when a PGA value of 400 gal affects the site. In such a case, if the positions of the boreholes employed in the assessments are considered, a surface disruption zone along a NE-SW trending zone passing from mid of the city seems to be probable.

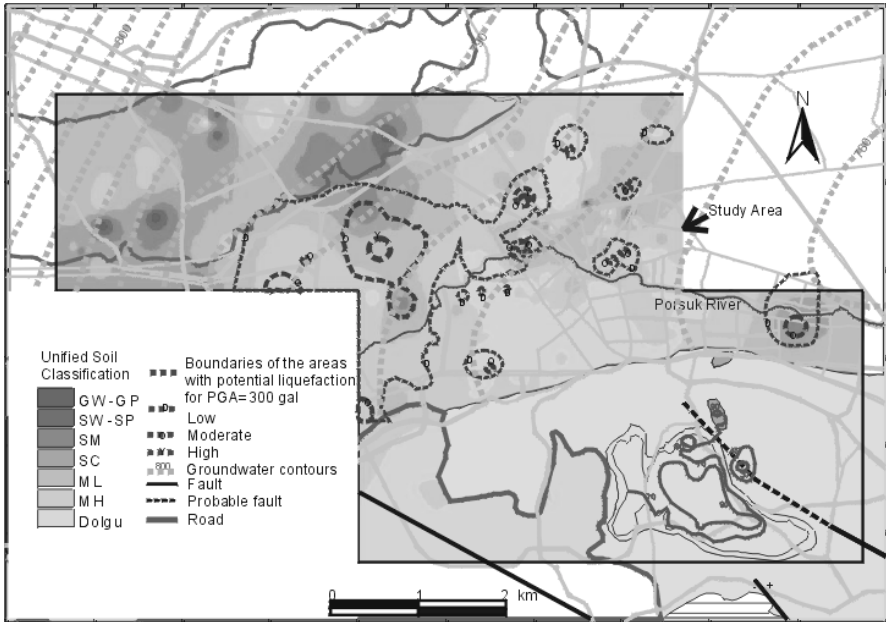


Fig. 5. Engineering geological map of the study area.

3.3 Engineering Geological Mapping

An engineering geological map of the city was constructed using GIS methodology and the available data. This map includes soil and rock classes in engineering

sense, groundwater table and liquefaction potential. It is evident from the map in Figure 5 that the districts having liquefaction potential coincide with sandy soils, and the old alluvial sequence seems not to be liquefaction- susceptible due to its considerably dense nature.

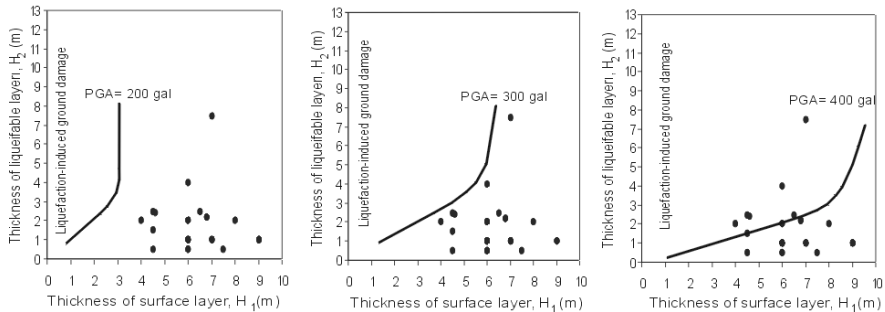


Fig. 6. Estimated surface effects of the liquefaction based on different PGA values.

4 Concluding Remarks

In this study, geo-engineering assessments for the central part of Eskisehir metropolitan area is presented and a GIS-aided engineering geological map of the study site is constructed. The most important earthquake source in the close vicinity of the city is the Eskisehir-Inonu Fault Zone (EIFZ), which may produce earthquakes with magnitudes of about 6, and a probable earthquake may cause a PGA of 300 gal. The presence of a shallow-seated groundwater table and silty sand layers, particularly near the meanders of Porsuk River, may result in moderate-to-high liquefaction susceptibility. However, depending in increase of the PGA, the areal extent of liquefaction phenomena may expand. The assessments also revealed that swelling problems due to soil heave and instabilities in natural slopes are not expected due to soil properties and suitable orientation between discontinuities and natural slopes. Detailed studies on activity and seismic conditions, particularly along the EIFZ and dynamic properties of the grounds of the city with prime consideration to amplification phenomena, and establishment of a strong motion station in the city are strongly recommended for future urban planning and for mitigation of probable natural hazards.

Acknowledgements

The authors express their sincere thanks to Prof. Dr. Can Ayday of Anadolu University in Eskisehir and to the staff from his institute for their kind interest and help during data collection, site investigations and providing the GIS programs.

References

- Abrahamson NA (2000) State of the practice of seismic hazard evaluation. Conference on Geotechnical and Geological Engineering, Melbourne, Australia (on CD).
- Altunel E, Barka A (1998) Eskişehir fay zonunun Inonu-Sultandere arasında neotektonik aktivitesi. Türkiye Jeoloji Bülteni, 41 (2): 41-52 (in Turkish).
- Aydan Ö (1997) The seismic characteristics and the occurrence pattern of Turkish Earthquakes. Turkish Earthquake Foundation Report, TDV/TR 97-007, 41p.
- Aydan Ö, Sezaki M, Yazar R (1996) The seismic characteristic of Turkish Earthquakes. 11th Worth Conference on Earthquake Engineering, Accapulco, Mexico, CD-2, Paper No. 1025.
- Gözler Z, Cevher F, Ergül E, Asutay HJ (1996) Orta Sakarya ve güneyinin jeolojisi. MTA Report No. 9973, 87 p (unpublished, in Turkish).
- Gülkan P, Kocyiğit A, Yücemem MS, Doyuran V, Başöz N (1993) En son verilere göre hazırlanan Türkiye deprem bölgeleri haritası. Middle East Technical University, Civil Engineering Department Report No. 93-01, 156 p (in Turkish).
- Ishihara K, (1985) Stability of natural deposits during earthquakes. Proc. 11th Int. Conf. on Soil Mech. and Found. Eng., AA Balkema, Rotterdam, Vol 1, pp 321-376.
- Iwasaki T, Tokida K, Tatsuoka F, Watanabe S, Yasuda S, Sato H (1982) Microzonation for soil liquefaction potential using simplified methods. Proceedings 3rd International Earthquake Microzonation Conference, Vol.3, pp 1319-1331.
- Kacaroglu F (1991) Eskişehir Ovası yeraltısuyu kirliliği incelemesi. PhD Thesis, Hacettepe University, 340p (unpublished, in Turkish).
- Saroglu F, Emre Ö, Boray A (1992) 1:1 000 000 scaled active fault map of Turkey. MTA, Ankara.
- Youd TL, Idriss IM (2001) Liquefaction resistance of soils: Summary report from the 1996 NCEER and 1998 NCEER/NSE workshops on evaluation of liquefaction resistance of soils. Journal of Geotechnical and Geoenvironmental Engineering 127(4): 297-313.

Engineering Geology Property Parameters for the Tertiary in The Netherlands

P. Michiel Maurenbrecher and Dominique Ngan-Tillard

Geoengineering CiTG, TU Delft, POBox 5028, 2600 GA Delft, The Netherlands
p.m.maurenbrecher@citg.tudelft.nl
Tel: +31 15-2785192
Fax: +31 15 2784103

Abstract. As engineering geologists we are measuring in the field and in the laboratory a large array of geological, geotechnical, geophysical and geomechanical parameters for an equally diverse amount of objectives for civil engineering structures, for mining, for assessing natural hazards, etc. As new geotechnical models are devised to investigate, for example the performance of underground spaces in deep soils both the availability of data for parameters become less and the few conventional tests on deep samples provide unexpected values. This paper compiles a record of the geotechnical parameters of the main clay formations found in the Netherlands Tertiary as well as briefly states the context in which these parameters are used to study the performance of the deeper sediments in relation to gravitational settlement and underground space studies. The clays are studied at unusually deep depths for geotechnical purposes, which require caution when using geotechnical values from similar formations at shallower depths in Belgium and the UK. The relatively sparse data and the strange properties appear to result in more questions than answers.

Keywords: Tertiary clay, Netherlands, Belgium, UK, Boom clay, Ieper clay, geotechnical properties

Introduction

Tertiary clays in the Netherlands receive little attention in that they are located at depths from about 40m to 1500 m with few exposures. Only recently, studies have been performed requiring geotechnical parameters of these deeper Tertiary clays. These mainly concern settlement analyses in the northern Netherlands prior to natural gas extraction, Hoefnagels et al.(1995), and Cheung et al. (2000), natural long term settlement, Kooi, (2000), analyses for repositories for hazardous waste (Wildenborg et al. 2000 , Voncken 1999, Voncken and Maurenbrecher, to be published), and for tunnelling (Rijkers 2002). The Tertiary deposits could also be of interest in seismic hazard analysis: they may be too shallow and plastic to act as a source but may influence the attenuation of seismic waves as they pass through these deposits to the surface. The data on Tertiary clays from the Netherlands remains incidental and sporadic. Recent exploratory boreholes have been made by TNO-NITG to study the clays. They indicate that their thicknesses are greater than was expected.

legend figure 4) of the Palaeocene/Eocene, Oligocene and Miocene/Pliocene indicate the depositional basin of the Tertiary deposits. The maps are similar to that presented by Fookes (1966) but indicate further the lithological variation expected throughout the basin. Irrespective of which map is chosen they all indicate care must be exercised when dealing with, say, the London/Ieper Clay formation as they can vary lithologically depending on the geographical location within the basin. Figure 1 shows sandy-clayey deposits in the UK section of the basin whereas in the Netherlands the deposits are more sandy in the southeast becoming clayey in the north west.

The sediments of the basins have been subject to upwarping along the London-Brabant massif “Artois Axis” whereas the sediments in the central and northern Netherlands have been subjected to rifting subsidence (Ziegler, 1982). As a result of uplift and subsidence and erosional/depositional processes associated with upwarping and subsidence the Ieper Clay in the Netherlands would be situated at depths ranging from 100 to 1500 m compared to London Clays and Ieper Clays in the UK and Belgium which outcrop or are found at shallow depths.

For the younger Oligocene Boom Clay from the Rupel Formation the same principles apply in comparing shallow depth parameters for the Boom clay and the deeper formations both in Belgium and the Netherlands as with the Ieper/London clay formations. The Boom clay has been extensively tested in Belgium in connection with the underground experimental storage facility at Mol (see for example Barnichon, 2002). The clay has also been examined for numerous projects in and around Antwerpen for both foundations and tunnels. Among others, (Schittkat 1983) proposed for example a geotechnical subdivision of the Boom clay for the construction of the Scheldt Surge Barrier. The clay also outcrops extensively and forms a commercial source deposit for the brickwork and ceramics industry around Antwerpen (Vandenbergh 2002).

In addition the clay is examined for its jointing which consistently showed preferred orientation at different quarries located several tens of kilometres apart (Vandenbergh 2002). Towards the centre of the Oligocene basin, figure 2, (Ziegler 1982), the Boom clay would be subjected to ongoing faulting activity of the Roer Graben system during deposition and subsequently probably inducing different stress fields and hence jointing pattern than those present in the Boom clay deposited at the edge of the basin and subjected to the Brabant-London Massif uplift. Similar differences were found in the London clay jointing patterns (Chandler et al. 1998, Skempton et al. 1969). The Boom and London clay jointing are induced by flexure shearing. Little is known what the situation is with regard to joints in the deeper clays of the Netherlands. Yet as figures 1, 2 and 3 indicate, throughout the Cenozoicum faulting was active in the depositional basins so that shear induced preferential fissures in the clay can be expected.

Younger still are the Tertiary clays of the Miocene and Pliocene. The distribution of these clays occurs over much the same area as the Oligocene (see Figure 3 from Ziegler, 1982). The clays are not well documented and one is restricted, for the Netherlands, to Fagnoul (1966). The Miocene/Pliocene outcrops in the south-eastern part of the Netherlands and the clay from the upper Pliocene, Brunsummer Klei, have been commercially used in the ceramics and brick-making industry

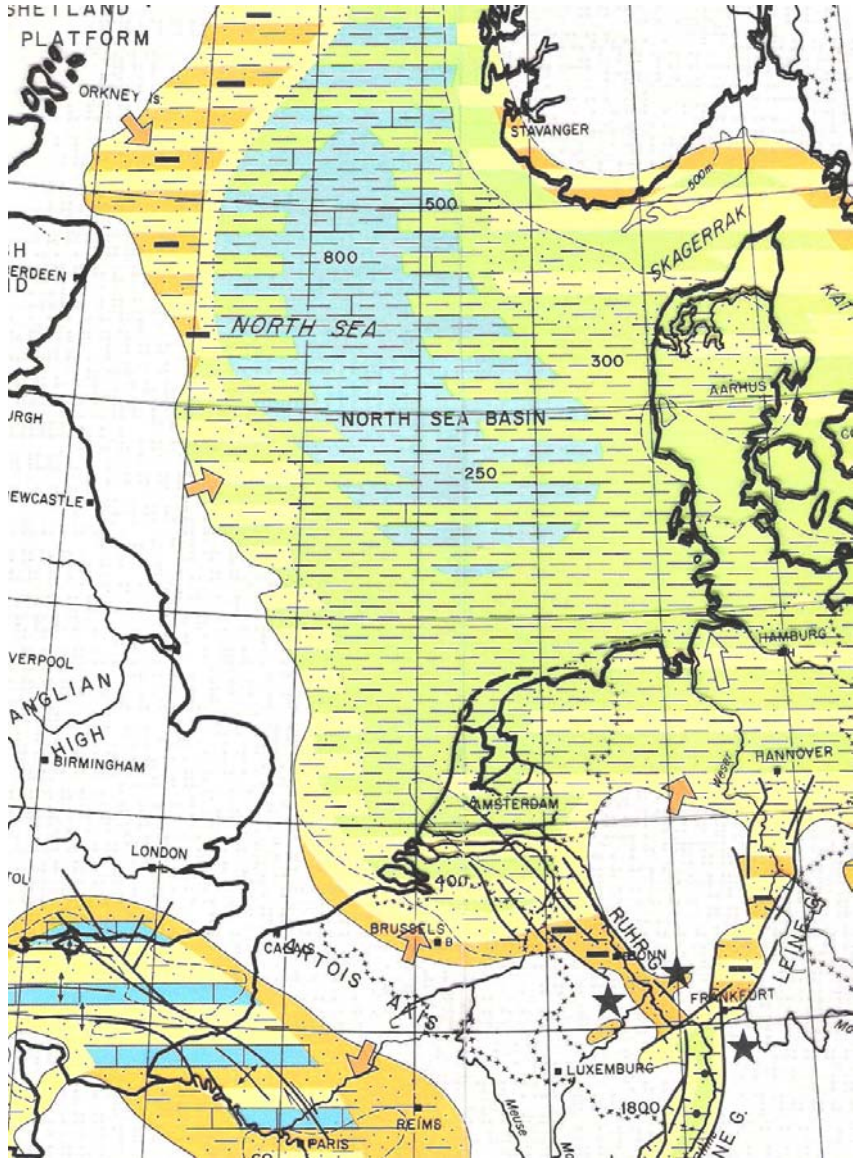


Fig. 2. Palaeogeographic Map of the Oligocene indicating extend of Boom/Ruppel Clay deposition, see figure 4 for legend (from Ziegler, 1982).

(Schins and Nelissen 1989). Kooi (2000) states in his study on natural settlement in the Netherlands that “permeability data for clay and shale in the subsurface is virtually absent” with respect to modelling subsidence by consolidation of clays. In this instance, he would also refer to all the Tertiary and the deeper Quaternary

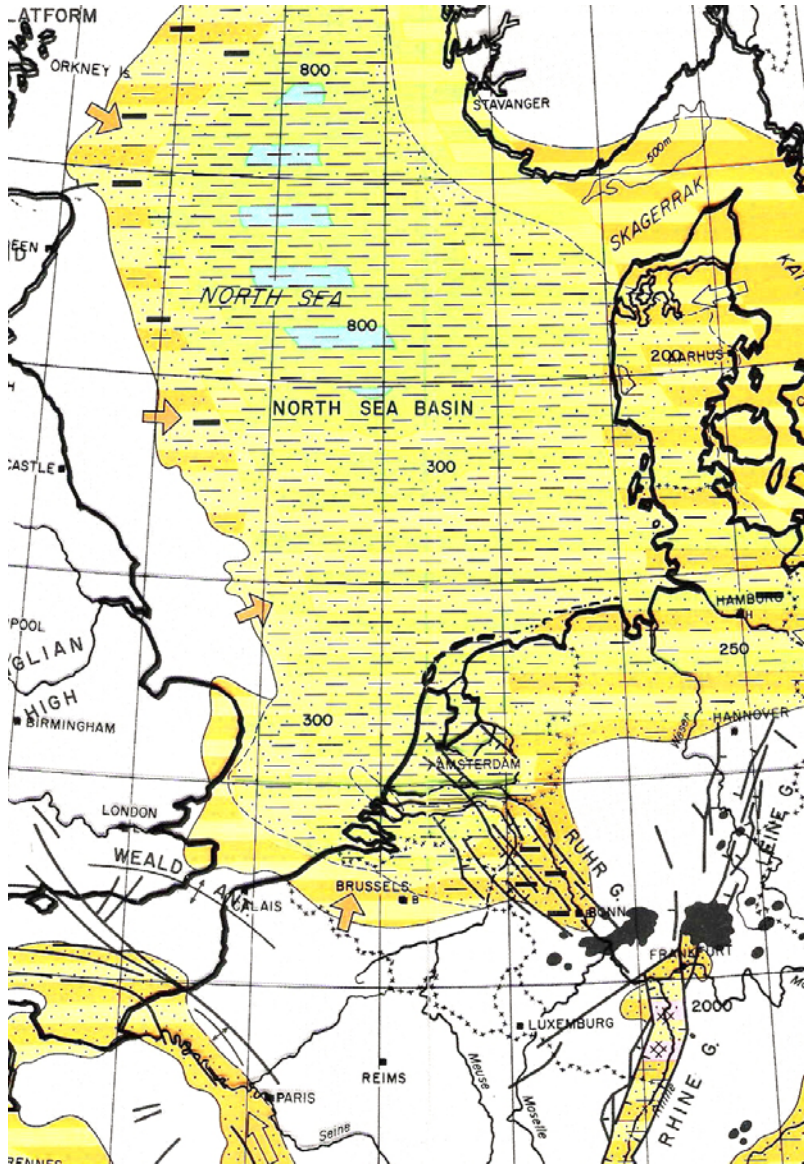



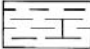
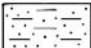
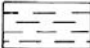
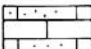
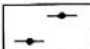
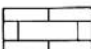
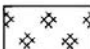


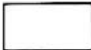


Fig. 3. Palaeogeographic Map of the Miocene-Pliocene indicating extend of younger Tertiary clays such as the Brunssum Clay see legend Figure 4 (from Ziegler, 1982).

clays. Wildenborg et al. (2000) also states that, despite having obtained deep Boom Clay samples at Blija (Friesland) further characterization is necessary as well as studying other deeper horizons of the Asse and Ieper clays of the Eocene.



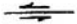




LITHOLOGICAL SYMBOLS

	Sand and conglomerate		Carbonate and shale
	Sand		Shale, some carbonate
	Sand and shale		Shale
	Carbonate and sand		Organic shale
	Carbonate		Halite

DEPOSITIONAL ENVIRONMENTS

	Areas of non-deposition		Deltaic, coastal and shallow-marine clastics
	Uninterpreted areas		Shallow-marine shale
	Continental, lacustrine		Deeper-marine shale

TECTONIC SYMBOLS

	Normal fault		Fold axis
	Transcurrent fault		Continental slope
	Steep reverse and thrust faults, active deformation front of fold belt		Sea mount
			Sea floor spreading axis

SPECIAL SYMBOLS ON PALAEOGEOGRAPHIC MAPS

	Direction of clastic influx		Direction of intra-basinal clastic transport
	Direction of marine incursion		

Fig. 4. Legend for palaeogeographic maps in figures 1, 2 and 3 (from Ziegler, 1982).

Properties of the Tertiary Clays in The Netherlands

Tables 1a, 1b and 1c present a summary of the geotechnical properties that were found on basis of a literature review and is predominantly based on the report by Wildenborg et al. (2000).

Table 1. Compilation of geotechnical properties Tertiary Clays of The Netherlands.

Table 1a. Hydraulic conductivity/porosity and thicknesses of Tertiary formations.

	Formation	Lithology	Thickness		Porosity		Hydraulic conductivity	
			m		%		m/s	
Pliocene	Oosterhout	sand/clay	50	400	35		2.1×10^{-4}	1×10^{-9}
Miocene	Breda zand	sand/clay	50		27		1.9×10^{-6}	2×10^{-5}
	Breda Klei	sand/clay		300		30	1×10^{-9}	
Oligocene	Veldhoven (Clay)	clay	0	75	40	50	8×10^{-6}	2.1×10^{-7}
	Veldhoven Voort (Sand)	sand	0	75			1×10^{-5}	1×10^{-6}
	Rupel (Boom) Western Scheldt	clay	50		33	39	k_h 1×10^{-11}	k_v 4×10^{-8}
	Rupel (Boom) Blija (NL) deep							
	Rupel (Boom) Mol/Weelde (B) deep			200			k_h 1.3×10^{-12}	k_v 3.4×10^{-12}
Eocene	Asse	clay	0	100				
	Brussel	sand	0	100	30	35	2×10^{-6}	5×10^{-7}
	Ieper (London)	clay	50	300	40	50	2×10^{-8}	
Palaeocene	Landen	clay	50	100	15	17	$< 1 \times 10^{-8}$	

Note: The younger values of hydraulic conductivity range are based on sample and insitu determinations where as the deeper formations on sample and down-hole logging interpretation. These values are from Wildenborg et al. (2000) and were obtained from numerous reports.

Table 1b. Identification, index and undrained shear strength test values.

Rupel (Boom) Formation	Depth range samples	Clay fraction % < 2µm	m/c %	Liquid Limit LL %	Plastic Limit PL %	Wet density kN/m ³	Undrained		
							Strength MPa	E MPa	ν Poisson ratio
Western Scheldt	25-40	81-62	25.3-23.8	91-76	30-25	19.4-19.3	0.2-0.45		
Blija (NL) deep	200-700	66-55	23.5-27.3	104-105	31-33	19.2-20.2	0.8-2.6	180-600	
Mol/Weelde (B) deep				75-93	28-30	20.1	2-2.2	200-400	0.4-0.45

The results indicate the range of test results summarized from Wildenborg et al. (2000).

Table 1c. Drained shear strength and compressibility results from triaxial and oedometer tests.

Formation: First three Rupel (Boom)	Depth range samples					Critical State Parameters		
		c' kPa	ϕ' degrees	E MPa	ν Poissons ratio	λ compression index	κ swelling index	p_c MPa precon- solidation stress
Western Scheldt	25-40							
Blija (NL) deep	200-700	90-720	8.1-13.1			0.14-0.24	0.06-0.07	6-8
Mol/Weelede (B) deep					0.125-0.2			
Asse		1800	2					
Ieper (London)		see text	see text					

The results indicate the range of drained triaxial test results summarized from Wildenborg et al. (2000).

Examination of the literature and several discussions with the geological survey in the Netherlands (TNO-NITG) indicate that only recently more knowledge is being gained on the geotechnical properties of some of the clay horizons of the Tertiary. Often studies rely on extensive testing and site investigation work done on the London Clay for which its equivalent in the Netherlands and Belgium, the Ieper (or Ypre) Clay has been investigated only to a limited extent in Belgium. The only published example that could be found was by Raedeschelders (1955). The Delft Cell test was used to determine the shear strength of the clay for a proposed excavation of a canal cutting in Belgium. It was agreed earlier (DeBeer 1950) that the cell test shear strength results in a lower value than obtained from a triaxial test. De Beer (loc cit.) provides a table of test results including index tests of clays at various locations in Belgium. In addition to Boom clay tested at Duffel two other clays were tested again at Duffel and at Oudenaarden. The latter has very similar plasticity values as the clay from Duffel. The tests by Raedemaker (1955) give similar cell test values for the Ieper Clay as does the De Beer (loc cit.) for the clay at Oudenaarde (friction of 25 to 27° and cohesion of 2 to 5 kPa). The values are not unlike those obtained by the triaxial test for London Clay. This may, on the basis of arguments presented by Bishop (in paper by De Beer) be coincidental as the triaxial test owing to larger strain capability should give a higher value.

The properties of the younger Asse clay (Eocene) appear to be restricted to one test result presented in Wildenborg et al. (2000). Of the Tertiary clays tested in the Netherlands it was taken at the greatest depth of 561 m. The shear strength values are described aptly by the report as “extreme” with an effective friction angle of 2° and an effective cohesion of about 1.8 MPa.

The Boom clay has received recently in the Netherlands increased attention, both in the relatively shallow depths for the Westerschelde Tunnel (Geodelft 1998 and Wiebens 2000) and, as with the Asse Clay, from much greater depths at Blija in the north of the Netherlands (northern extremity of the Province of Friesland). Again the triaxial tests for the deep Blija and deep samples taken at Weelde (Belgium) (from Wildenborg et al. loc. cit.) reveal at high cell pressures low angles of shear with surprisingly high effective cohesion intercept values.

Kooi (2000) in his land subsidence study compares densities derived from down-hole sonic logging. The logging penetrates through the full depth of the Tertiary sediments and shows little indication of density increase with depth in both the southern and northern half of the Netherlands. Furthermore there was also no increase in density of the Tertiary deposits in the northern half of the Netherlands despite this half having been subjected to ice loading of the Saalien. The number of logs is relatively few so more analyses would be required to confirm such trends. For settlement analysis, consolidation parameters typically obtained for Boom and London clays were used from existing literature.

The clays of the Miocene-Pliocene can be found to outcrop (as well as some older clays) in southern Limburg. The only publication that could be found on these clays was from a clay derived from Brunssum. The geology map (Felder and Bosch, 1984) shows that such a clay could have been obtained from the Kiezeloooliet Brunssum Klei Formation of the Lower Pliocene. The map also shows up to three clay pits in this formation though none of these pits listed on the map is associated with the name Kéramo' as stated in Fagnoul's (1966) paper. The paper is restricted to clay fraction determination using ultra-sonic vibrations to separate the clay particles at the University of Liège. The clay fraction increases from 4% to 26% as a result of ultra-sonic treatment. Atterberg tests showed for non-treated soils a liquid limit of 44%, a plastic limit of 19%, and a clay fraction of 15%. The mineralogy consists predominantly of kaolinite with illite and chlorite. Schins and Nelissen (1989) state that the Brunssumer Clay was used during the war though tests for use in ceramics had shown the clay not to be suitable for manufacturing basic ceramic products in the Sphinx factories, Maastricht. The clay was used previously for manufacture of bricks and clay pipes together with deposits of the Quaternary Tegelen clay.

Conclusions

A preliminary survey on Tertiary clay properties in the Netherlands reveals a scarcity of information and some perplexing results from recent investigations. Sediment densities were found to remain relatively constant to large depths yet triaxial tests gave very high effective cohesion values with very low effective internal friction values. Both results are based on relatively few measurements and tests so that as the authors of these studies advise further investigation is required. What often is missing from the publications examined except for the earliest by De Beer (1950) and the recent work performed on the Boom clay of the Westerscheldt tunnel, is supporting suite of geotechnical index tests such as plasticity, insitu

moisture content and clay fraction/ particle size distribution. Comparisons between strength and consolidation tests are usually difficult to make as these tests are not only dependent on the type of test used but also on their loading programme and (usually not discussed) the sample handling.

References

- Barnichon, J.D. (2002) Contribution of the bounding surface plasticity to the simulation of gallery excavation in plastic clays, *Engineering Geology*, Elsevier, 64 217–231.
- Chandler, R. J., Willis, M. R., Hamilton, P. S. & Andreou, I. (1998). Tectonic shear zones in the London Clay Formation *Géotechnique* 48, 2, pp.257-270.
- Chandler, R. J. & Hamilton, P. S. (1999). On the measurement of the undrained strength of discontinuities in the direct shear box *Géotechnique* 49, 5, 615-620.
- Cheung, G., M.A. Alvarez Grima, P.M. Maurenbrecher and F. Schokking, (2000) Statistical analysis of benchmark stability prior to natural gas extraction in a Holocene clay and peat area, province of Friesland, The Netherlands, Proceedings of the 6th International symposium on Land Subsidence, Ravenna, Italia, 24-29 September 2000. Eds. Carbo- gnan, L., G. Gambolati, A.I. Johnson, Padova Italy, ISBN 88-87222 06-1 pp 237-254.
- De Beer, E.E. (1950) The Cell Test, *Géotechnique*, 2, 2 pp.162-172.
- Raedeschelders, H. (1955) Etude de la stabilité d'une tranchée dans une argile Tertiaire, *Géotechnique*, 5 1 pp79-85.
- Fagnoul, (1966) Granulométrie et plasticité de sols argileux soumis a des traitements par ultrasons. *Géotechnique*, 16 2 pp149-161.
- Felder, W.M. and P.W.Bosch (1984) Geologische kaart van Zuid Limburg en omgeving; Pré-Kwartair, Rijks Geologisch Dienst, Haarlem (Now TNO-NITG, Utrecht).
- Fookes, P.G. (1966) London Basin Tertiary Sediments, in "Correspondence", *Géotechnique*, 16 3 pp260-263.
- Geodelft (1998) Database Westerschelde Oeververbinding.
- Hoefnagels A.A.J.V., Maurenbrecher, P.M. and S. Schokking, (1995), Long-term movements on benchmarks in the Groningen area preceding hydro carbon extraction, Land Subsidence Natural Causes, Measuring Techniques Proceedings 5th Int. Symp. On Land Subsidence, (Editors: Barends, F.B.J., F.J.J. Brouwer, F.H. Schröder) The Hague AA Balkema, pp3132-324.
- Kooi, H. (1999) Land subsidence due to compaction in the coastal area of The Netherlands: the role of lateral fluid flow and constraints from well-log data, *Global and Planetary Change* 27 2000 pp207–222.
- Raedeschelders, H. (1955), Etude de la stabilité d'une tranchée dans une argile Tertiaire, *Géotechnique*, 5, 1 pp.79-87.
- Rijkers, R. (2002), Aanleg dwarsverbindingen Westerscheldetunnel middles grondbe- vriezing, Informatie Editie groundwater en bodem, Nederlands Instituut voor Toegepaste Geowetenschappen TNO, Nr. 12 december, pp1-8.
- Schins, W.J.H. and R.G.W.J. Nelissen (1989) Het gebruik van Limburgse delfstoffen bij de N.V. Koninklijke Sphinx in de loop van haar geschiedenis, in *Delfstoffen in Limburg*, (The use of Limburg minerals at the Royal Sphinx in the course of her history, in *Minerals of Limburg*) Afdeling Limburg der Nederlandse Geologische Vereniging pp167-295.
- Schittekat, J., Henriët, J., Vandenberghé, N. (1983) Geology and Geotechnique of the Scheldt Surge Barrier, Characteristics of an Overconsolidated Clay. 8th International Harbour Congress, Antwerp, pp1.121-1.135.

- Skempton, A. W., Schuster, R. L. & Petley, D. J. (1969). Joints and Fissures in the London Clay at Wraybury and Edgware. *Géotechnique* 19, pp205-217.
- Vandenberghe, N. (2002) Excursion guide Ingeokring (Netherlands section of the IAEG) field visit to Belgium September 2002.
- Voncken, F.J.J. (1999) Retrievable underground disposal of hazardous waste in The Netherlands, Report prepared for Interfacultaire werkgroep Gebruik Ondergrondse Ruimte GOR- Interfaculty workgroup Use of Underground Space, TA/IG/98-029, Delft University of Technology, Department of Applied Earth Sciences, Faculty of Civil Engineering and Earth Sciences 167p.
- Voncken, F.J.J. and P.M. Maurenbrecher, (to be published), Overview of feasibility study to store hazardous waste in The Netherlands, in *Geo-Engineering of hazardous and radioactive waste disposal*, Newcastle Upon Tyne, The Engineering Group of the Geological Society (to be published in Geological Society Special Publication).
- Wiebens, H.G.P. (2000), Modelling of the Boom clay of the Westerschelde tunnel based on statistics and data clustering, *Memoirs of the Centre of Engineering Geology in the Netherlands*, No. 195 112p.
- Wildenborg, A.F.B., B. Orlic, G. de Lange, C.S. de Leeuw, W. Zijl, F. van Weert, E.J.M. Veling, S. de Cock, J.F. Thimus, C. Lehnen- de Rooij and E.J. den Haan, (2000), Transport of radionuclides disposed of in clay of tertiary origin, (TRACTOR), TNO-report NITG 00-223-B 171p.
- Ziegler, P.A. (1982) *Geological Atlas of Western and Central Europe*, Shell International Petroleum Maatschappij BV/ Elsevier Scientific Publishing Company, Amsterdam pp130.

Various Assessments of the Characteristic Values of Soil Cohesion and Friction Angle: Application to New Caledonian Laterite

Véronique Merrien-Soukatchoff¹ and Kamel Omraci², and Le Nickel-SLN³

¹ Laboratoire Environnement Géomécanique Ouvrages, Ecole des Mines, Nancy, France
Veronique.Merrien@mines.inpl-nancy.fr

Tel: (33) 3 83 58 42 92

Fax: (33) 3 83 53 38 49

² Ecole Polytechnique, Département de Génie Minier, Avenue Hassan Badi, Belfort El Harrach, Algiers, Algeria

³ Le Nickel-SLN, Pointe Doniambo, BPE5, 98848 Nouméa Cedex, Nouvelle Calédonie

Abstract. *In situ* measurements, as well as laboratory tests, yield varied information on ground material. In order to carry out computations, it is necessary to reduce the scattered and uncertain information to a characteristic value. The approach used to derive this characteristic value is seldom explained in the literature. Yet, this data-simplification methodology may influence results by virtue of both the choices adopted for data collation and the computation methodology. Studies conducted on the properties of New Caledonian lateritic materials, for the purpose of guiding the design of open pits and dumpsites, have led to collecting result on a variety of triaxial tests. A number of different collation and statistical interpretation techniques for these tests have been attempted and have led to significantly distinct average cohesion and friction angle values. This paper underscores, in the specific case of New Caledonian laterite, the variability of results due to the way in which data are interpreted and the impracticality of justifying one methodology over another. It shows either the importance of taking great caution when defining practical rules and design for these constructions.

Keywords: Laterite, cohesion, friction angle, scattering, characteristic values, mean, median, variability

1 Introduction

In situ measurements, as well as laboratory tests, yield varied information on ground material due to the effects of natural scattering and uncertainty (Einstein, 2003). In order to carry out computations, it is necessary to select a set of characteristic values, even for the simplest cases. This concept of characteristic value however is not a universal one, and it is required for example to produce a design in accordance with Eurocode 7. Along the same lines, the development of computational codes has led to generating efficient models for studying the stability of works, yet one of the current challenges in the field of geotechnical engineering

consists of having enough data available for model input, especially when using stochastic computational codes. Over the past few years, stochastic models have in fact been experiencing widespread development. Each parameter and each variable in these models is to be characterized by its variability, in order to run stochastic computational codes. Until now, the need has been felt to be able to estimate at least a mean and a standard deviation for each factor included as a computation function. To highlight the difficulty involved in distilling the information available and to underscore the equivocal nature of this task, our paper will present the various analyses conducted while studying the lateritic material at New Caledonian dumpsites. Between 1990 and 1999, the LAEGO research group, in collaboration with the Nickel SLN Company, studied the properties of New Caledonian lateritic materials in order to direct the design of open pits and dumpsites associated with the mining of nickel ore (Omraci 1992, Omraci 1996, Merrien-Soukatchoff and Omraci 2000, Omraci et al. 2003). These studies have led to compiling the results of different triaxial tests. We then studied in greater detail the results from two mechanical probes drilled into a specific waste site. After briefly describing the lateritic material investigated in the following section, we will demonstrate how the computational method utilized, along with the data collocation choices, have led to significantly different values of both the cohesion and friction angle.

2 The New Caledonian Lateritic Material and Basic Data

The nickel ore, in New Caledonia is quarried in open-pit mines, within peridotite rocks covered with lateritic soil. The sterile ground is stored in specially-prepared sites. A typical cross section in the middle of a dumpsite is presented in Figure 1. Within one of the dumps, two mechanical cores (80 m in depth, 100 mm in diameter and placed 5 m apart) were drilled in order to learn more about the physical and mechanical behaviour of this kind of soil. Physical, as well as both short-term and long-term triaxial tests were performed. In this paper, we will pay special attention to drained properties. Let us start by noting that drilling was carried out,

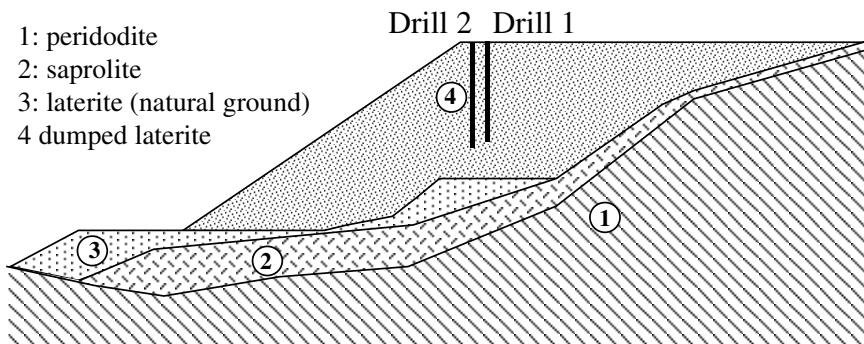


Fig. 1. Geological cross-section of the studied dumpsite.

to the extent possible, by use of a punching method (with the sample then being packed in a metallic sheath and labeled “undisturbed”). In some instances however, it was necessary to resort to a wet drilling technique, which implies that the extracted material did not contain its natural water content for testing purpose and was thus labelled “disturbed”.

We will subsequently use the term “sample” to denote a section of intact drilled core, approximately 50 cm long, from which 3 of 4 experimental cores were extracted for triaxial testing. Triaxial compression tests CU and CD have made it possible to determine the stress couples (σ'_3, σ'_1) considered to be characteristic of the limit strength of the material (which corresponds to a peak, or 10% strain). We will not discuss herein the relevance of determining that way the σ'_1 limit for a given σ'_3 value. It is important however to observe that from one of the tests we were able to extract a stress couple (σ'_3, σ'_1) (which we called a triaxial point) considered to be relevant for a subsequent slope stability study. By taking both core-drilling operations into account, we obtained 47 value couples for drained properties (see Table 1); these corresponded to 3 depths for the CD tests (10 points or value couples) and 11 depths for the CU tests (37 points for value couples). On the basis of these value couples several questions may be raised regarding the determination of cohesion and friction angle values from this data, i.e.:

- Which “characteristic” value is relevant: the mean, median or mode?
- Is it possible to use a linear regression for this determination? And if so, which one?
- How are the test results to be collated in order to obtain a characteristic value for c and ϕ ?

Table 1. Different tests corresponding to 3 CD samples (10 triaxial points) and 11 CU samples (37 triaxial points).

Drill number	Depth (m)	Type of test	Number of triaxial points	σ'_3 values for the tests (kPa)			
1	5,00÷5,30	CD	3	100	200	600	
1	10,50÷10,90	CD	4	100	200	400	600
1	16,00÷16,40	CD	3	100	200	600	
10							
2	33,00÷33,65	CU	4	200	400	600	800
1	35,00÷35,50	CU	3	200	400	600	
1	38,00÷38,40	CU	4	200	400	600	800
2	41,40÷41,75	CU	4	50	100	200	400
2	41,75÷41,90	CU	3	200	400	600	
2	45,60÷46,10	CU	3	200	400	600	
2	46,10÷46,40	CU	3	400	600	800	
1	52,00÷52,40	CU	4	50	100	200	400
2	52,00÷52,40	CU	3	200	400	800	
1	55,30÷55,70	CU	4	200	400	600	800
2	61,50÷61,75	CU	2	200	400		
37							

Beginning with the unprocessed result, several clustering techniques may be considered:

- evaluating the data one sample at a time and then computing an average for the cohesion and friction angle values,
- recombining all of the points, or
- taking the data from one depth interval to the next.

A variance analysis has allowed concluding that the sampling (and therefore the depth) exerted no influence on the cohesion and friction angle.

3 The Various Computational Methods

In order to systematically process the data statistically, we decided to compute the cohesion and friction angle according to the two following methods:

- by examining the triaxial points two by two, and
- using linear regression techniques.

Although the first method is seldom used (except among economists apparently), we took the triaxial items two at a time. For any two points, the determination of c and φ yields a unique result. This method leads to a most surprising value for each couple, yet the combination of couples proves to be quite realistic. For the second method, in the presence of several stress couples (σ'_3, σ'_1), different regressions may be used depending on the way the Mohr-Coulomb criterion has been written. Two different expressions were used:

$$\sigma'_1 - \sigma'_3 \operatorname{tg}^2\left(\frac{\pi}{4} + \frac{\varphi'}{2}\right) - 2c' \operatorname{tg}\left(\frac{\pi}{4} + \frac{\varphi'}{2}\right) = 0 \tag{1}$$

and:
$$t = c' \cos \varphi' + s \sin \varphi' \tag{2}$$

with:
$$s = \frac{\sigma'_1 + \sigma'_3}{2} \text{ and } t = \frac{\sigma'_1 - \sigma'_3}{2}$$

which leads to four possible linear regressions:

- σ'_1 versus σ'_3 ,
- σ'_3 versus σ'_1 ,
- t versus s , and
- s versus t .

Each of these “blind” regressions can then lead to a negative value of cohesion, which is physically unacceptable. For this reason, constraint-based regressions (i.e. imposing a non-negative cohesion) were also performed. Let us point out that eliminating potential negative values of cohesion does comply with standard geotechnical practice; constraint-based regressions however lead to a greater mean cohesion value (22 kPa, as opposed to an average value near 0 for the CU tests, see Table 3) and to a slightly lower friction angle (38°, as opposed to 40° for the

CU tests). Moreover, when distilling the data to just a single value, is difficult to justify to impose a zero cohesion when the automatic processing tends to a negative value and to keep the value as it is positive. Even though a negative cohesion value may seem physically infeasible, if the problem consists of determining whether the stability is attained or not, a line segment with a negative intercept, within a given stress range, can be relevant. The various methods tested have provided nine different ways for computing cohesion and friction angle values (see Table 2).

Table 2. The nine methods for computing the target cohesion and friction angle (independently of any subsequent data collation).

Method number	Method
1	Taking triaxial points two at a time
2	σ'_1 versus σ'_3 regression
3	σ'_3 versus σ'_1 regression
4	t versus s regression
5	s versus t regression
6	σ'_1 versus σ'_3 regression, imposing a cohesion ≥ 0
7	σ'_3 versus σ'_1 regression, imposing a cohesion ≥ 0
8	t versus s regression, imposing a cohesion ≥ 0
9	s versus t regression, imposing a cohesion ≥ 0

4 Various Clustering Techniques

A number of different techniques are always available for compiling the results of triaxial tests. The “traditional” technique is to compute the characteristic values sample by sample (14 samples in our case) taking the 3 or 4 triaxial test results corresponding to each sample. Yet since no sampling influence was detected (see the end of Section 2 above), we can consider each triaxial test as a single soil test and then collate all tests in order to determine the cohesion and friction angle values. For both clustering possibilities, we have tested the various computational methods; for some of them, we deduced a mean or median cohesion and friction angle. When required to choose just one characteristic value to carry out a stability analysis, it is difficult to justify which value is the most relevant: mean, median or mode? In the following discussion, we will focus on mean values and, in some instances, on the median since it has been impossible to explore all possible combinations and the mean is generally handy to compute in any event. Choosing the mean however is not really justifiable, given that the median is a more robust estimator than the mean (Mosteller et al., 1973). We always work on the CU and CD triaxial tests separately and, for additional information, have also combined them. Results of the various clustering techniques are presented in Table 3. Whenever possible, both the mean and median of the cohesion and friction angle have been computed.

Table 3. Results of the various clustering techniques (entries in italics represent computation of the median, whereas bold characters represent the minima and maxima).

Sample clustering	CU		CD		All points (CU+CD)		Mean CU +CD	
	c' in kPa	φ'	c' in kPa	φ'	c' in kPa	φ'	c' in kPa	φ'
(σ ₁ , σ ₃) or (s, t) taking triaxial points two at a time, computing c' et φ' sample by sample, then the sample mean	15.9	38.0	26.3	35.0	18.1	37.3	21.1	36.5
(σ ₁ , σ ₃) or (s, t) taking triaxial points two at a time, computing c' et φ' sample by sample, then the sample median	20.2	38.7	46.6	35.7	22.0	37.6	33.4	37.2
s vs. t regression sample by sample and mean of c et φ	-1.4	40.4	25.7	34.2	4.9	39.0	12.2	37.3
<i>s vs. t regression sample by sample and median of c et φ</i>	12.1	39.3	28.4	36.4	12.1	38.0	20.3	37.8
t vs. s regression sample by sample and mean of c et φ	-8.2	40.9	24.6	34.3	-0.6	39.4	8.2	37.6
<i>t vs. s regression sample by sample and median of c et φ</i>	5.7	39.4	26.5	36.5	7.3	38.3	16.1	37.9
s vs. t regression, sample by sample imposing a cohesion ≥ 0 and mean of c et φ	22	34.2	35	30.2	25	33.3		
<i>s vs. t regression, sample by sample imposing a cohesion ≥ 0 and median of c et φ</i>	12	38	28	29.3	12	37.3		
σ ₁ vs. σ ₃ regression sample by sample and mean of c et φ	-4.2	40.6	25.3	34.2	2.6	39.1	10.6	37.4
<i>σ₁ vs. σ₃ regression sample by sample and median of c et φ</i>	9.6	39.4	27.7	36.4	10.2	38.1	18.6	37.9
σ ₃ vs. σ ₁ regression sample by sample and mean of c et φ	15.8	39.2	27.2	34.1	18.4	38.0	21.5	36.7
<i>σ₃ vs. σ₁ regression sample by sample and median of c et φ</i>	22.7	38.2	31.4	36.4	25.1	37.6	27.0	37.3
Combining all points								
(σ ₁ , σ ₃) or (s, t) taking triaxial points two by two, and meaned	3.5	38.5	31.4	35.1	9.6	37.8	17.4	36.8
<i>(σ₁, σ₃) or (s, t) taking triaxial points two by two, and then taking the median</i>	11.8	37.9	27.3	36.1	16.1	37.5	19.6	37.0
c' and φ' compute from a regression (σ ₃ , σ ₁) on all points	13.5	39.2	12.3	35.7	19.1	37.9	16.3	38.5
c' and φ' compute from a regression (σ ₁ , σ ₃) on all points	25.9	38.2	26.3	34.7	37.4	36.4	31.6	37.3
c' and φ' compute from a regression (t,s) on all points	15.8	39.0	15.3	35.5	22.7	37.6	19.2	38.3
c' and φ' compute from a regression (s,t) on all points	9.7	39.5	7.2	36.1	13.1	38.4	11.4	38.9

Table 4. Summary of test results for the mean.

	CU		CD		All points (CU+CD)		Mean CU +CD	
	c' in kPa	ϕ'	c' in kPa	ϕ'	c' in kPa	ϕ'	c' in kPa	ϕ'
Minimum positive mean values compute independently for cohesion and friction angle	3.5	34.2	7.2	30.2	2.6	33.3	8.2	36.5
Mean positive mean values compute independently for cohesion and friction angle	9.9	38.9	23.3	34.5	15.5	37.7	17.0	37.5
Maximum positive mean values compute independently for cohesion and friction angle	25.9	40.9	35.0	36.1	37.4	39.4	31.6	38.9
Difference between minimum and maximum positive mean values compute independently for cohesion and friction angle	22.4	6.7	27.8	5.9	34.7	6.1	23.4	2.4

In order to enhance the contrast in results, the minimum and maximum values for the mean computation have been collated in collated in Table 4. In this table the maximum and minimum have been extracted independently for the cohesion and friction angle although their variations are dependent.

As seen in both Table 3 and collated in Table 4, results are quite scattered. Several findings can be highlighted:

- The way in which the regression is performed has a significant impact on the result. If we compare for example the two rows from Table 3 i.e. σ'_1 versus σ'_3 and σ'_3 versus σ'_1 , computed when grouping all the points (3rd and 4th line from the end of the table), a difference of 12 kPa is found in evaluating the cohesion and a difference of 1° for the friction angle. Due to this outcome, it would be better to carry out an orthogonal regression, which does not bias either of the two variables.
- The possible variation, in this case, due to the method of computation and the way the tests are gathered lead to a variation of around 30 kPa for the cohesion and 3° for the friction angle,
- We did not indicate any preference within the different means since it would be impossible to justify such preference,
- For this case, the median cohesion is systematically greater than the mean, while the median friction angle is generally lower than the mean except for the case where we took triaxial tests results two at a time.

Let us point out that our study concerns only one third of the data now available and that the increase of data can have an influence on the scattering.

5 Influence on the Slope Stability Computation

In order to assess the influence of scattering results on slope stability, Table 5 lists the safety factors for a 90-m high slope. The first row of the table recalls the parameters adopted for the standard computation (Omraci et al., 2003): the c' and ϕ' values are those computed from a regression (t,s) on all points and for all triaxial tests (CU+CD). The other rows in Table 5 display an assessment of the safety factor (as deduced from abacuses) for the values shown in Table 4.

If we set Case 2 as the reference, the variation in the safety factors range between -11% and -4% for Cases 3 and 4 and tend to worsen the result. The mean slope adopted in the dumpsites studied herein is 27° . Since the negative impact of the various computational methods and distinct combinations is limited to less than -7% for this slope, these results exert no influence on the construction practices and design of laterite dumps; in addition, the selected safety factor (greater than 1.5) takes these possible variations into account. Moreover, for practical purposes, *in situ* feedback (monitoring and evaluation of the dumpsites) for over 10 years has made it possible to calibrate and reinforce the modelling approach. Let us point out, that we have computed as an indicator of an inappropriate use of these results the factor of safety using both the minimum value of c' corresponding to all of the data collations and, independently, the minimum value of ϕ' , even though these parameters cannot be independently computed. Since this approach has led to greatly undervaluing stability and proves to be unrealistic, we do not present it in Table 5.

Table 5. Safety factors for a 90-m high slope with different slope angle β ($\gamma=18 \text{ KN/m}^3$).

Case		c' (in kPa)	ϕ'	F for $\beta = 40^\circ$	F for $\beta = 35^\circ$	F for $\beta = 30^\circ$	F for $\beta = 27^\circ$
1	Values adopted for the computation	23	38.0	1.2	1.4	1.6	1.8
2	Mean positive mean value for each parameter (CD tests) - Reference case	23.3	34.5	1.1	1.3	1.5	1.6
3	c' and ϕ' corresponding to the minimum mean ϕ' (CD tests)	7.2	36.1	1.0 (-11%)	1.1 (-11%)	1.4 (-8%)	1.5 (-6%)
4	c' and ϕ' corresponding to the minimum mean c' (CD tests)	35	30.2	1.1 (-4%)	1.2 (-5%)	1.4 (-6%)	1.5 (-7%)

6 Conclusion

This paper has discussed, for the specific case of New Caledonian laterite, variability due to the type of data interpretation when assessing the characteristic limit values for a soil. Even when estimating a mean for both the cohesion and friction

angle, different computational methods and techniques for collating test data are available. The various computational methods and data collation techniques have led, in this case, to computing a mean cohesion of $\pm 25\text{kPa}$ and mean friction angle of $\pm 3^\circ$. Yet, these variations are not independent and lead, in the worst case, to a 10% decrease in the safety factor when computing slope stability. For the specific case of the dumpsites investigated herein, these results exert no influence on construction practices and design, owing to the precautionary measures taken into account when setting up the dumpsites (high safety factor, monitoring, weak slope adapted to the situation). As a consequence of the difficulty involved in computing a mean, we have elected not to explore the various ways that a standard deviation could have been calculated in order to provide input for stochastic computational codes. This study suggests extreme prudence when introducing input variability in models.

References

- Einstein HH (2003) Uncertainty in rock mechanics and rock engineering - Then and now. ISRM 2003 – Technology roadmap for rock mechanics. 8-12 September 2003. Johannesburg, South Africa. pp. 603-608.
- Merrien-Soukatchoff V & Omraci K (2000) Détermination des conditions aux limites pour un calcul de stabilité de talus. *Revue Française de Géotechnique*. No. 92. pp. 31-39.
- Mosteller F & Rourke R (1973) *Sturdy Statistics*. Addison-Wesley Publishing Company. Reading, Massachusetts, USA. 395 pp.
- Omraci K (1992) *Comportement mécanique des latérites. Application à l'étude de la stabilité de la décharge Mont-Jardin (Nouvelle Calédonie)*. DEA degree thesis. Ecole des Mines de Nancy. France.
- Omraci K (1996) *Etude de la stabilité des décharges de latérites de la Nouvelle Calédonie. Application au cas de la décharge Mont-Jardin*. Ph.D. dissertation. INP Lorraine - Ecole des Mines de Nancy, France.
- Omraci K, Merrien-Soukatchoff V, Tisot JP, Piguet JP, Le Nickel-SLN (2003) Stability analysis of lateritic waste deposit. *Engineering Geology*, Volume 68, Issues 3-4. March 2003. pp. 189-199.

Numerical Analysis of a Tunnel in an Anisotropy Rock Mass. Envalira Tunnel (Principality of Andorra)

Dídac Plana, Carlos López, Josep Cornelles, and Pere Muñoz

Department of Tunnels, Eurogeotècnica SA: Av. Corts Catalanes, nº 5-7, 2on,
08190 Sant Cugat del Vallès, Barcelona, Spain
didac.plana@eurogeotecnica.com
Tel: +34 935 830 480
Fax: +34 935 836 960

Abstract. The Envalira Tunnel (Principality of Andorra) passes through a rock mass of phyllite and quartzite, and its construction had some parts with great difficulties due to the different mylonite zones and fractured strips that generate a weak plane orientation. In those zones, great deformations were measured concentrated in one side of the section, showing a strong asymmetric behaviour. There were some sections of the tunnel that had many instrumental implementations to control its behaviour. With all these data, it has been possible to build a numeric model of finite element method that reproduces the tensional and deformational behaviour of the tunnel in order to compare the results obtained with the measured data. The interest of this case was how to model the anisotropy of the rock mass and to get as a result the asymmetry behaviour in tensions and deformations. For that purpose, it was thought to work with a “jointed rock model” that is available in the commercial program Plaxis. The results of the numerical model seems to have a good setting with the real behaviour of the tunnel, reproducing quite well the asymmetric problems on deformation and tension distribution onto the support.

Keywords: Anisotropy, tunnel, rock mechanics, numerical model, instrumentation, backup analysis

Introduction

The Envalira Tunnel route connects Andorra and France, passing beneath the 2400 metre high pass of Envalira. The length of the route is 4.192 meters, from which 2.805 meters are properly in tunnel with an area of 61.35 m². The construction of the Envalira Tunnel started in 1999 and was open to the traffic in December 2002. The Tunnel passes through the axial Pyrenees Mountains constituted by a rock mass of Cambrian – Ordovician phyllite and quartzite. Some parts of the tunnel had great difficulties due to different mylonite zones and fractured strips that generate a weak plane orientation because of one predominant joint family almost parallel to the tunnel track and apparent dip angle of 40°-45°. In those zones, great deformations were measured concentrated in the north crown side of the tunnel cross section, showing a strong asymmetric behaviour. There were some sections

of the tunnel that had many instruments installed to monitor its behaviour: two borehole extensometers of three rods 2.5 m, 6 m and 12 m length in radial direction placed in the both tunnel crown sides; tangential and radial pressure cells in the rock surface placed in the both tunnel crown sides, strain gauges in the tunnel support, four studs for convergence measurements and topographic points on both sidewalls. Beside the instrumentation a systematic characterization of the tunnel front was made. With all these data, it has been possible to build a numeric model of the finite element method that reproduces the stress and deformation behaviour of the tunnel. In order to compare the results obtained. The interest of this case was how to model the anisotropy of the rock mass and to get as a result the asymmetry behaviour in stress and deformation.

Main Characteristics of the Studied Section

One cross section (called S-27) has been analysed as this has full instrument implementation. The section is situated 282 m below surface in a rock mass consisting of phyllite and quartz-phyllite. The rock mass has a Bieniawski quality index RMR between 26 and 31.. The global rock mass stiffness modulus is estimated to be $1.35 \cdot 10^6$ kPa, based on correlations with the RMR index. Moreover, data measurements indicate that deformations were very high in the orthogonal direction to the main joint family, obtaining equivalent stiffness values of around $5.04 \cdot 10^4$ kPa. These stiffness differences depend on the joint orientations and explain the asymmetric deformation behaviour of the studied tunnel cross section. The tunnel support is made by a shotcrete seal 7 cm thick and a shotcrete layer 18 cm thick with wire mesh 150 mm x 150 mm x D6 mm and TH 29 steel sets spaced at 0.75 m intervals. In addition, 4 m length grouted rock bolts were inserted on a grid interval of 0.75 m x 1.0 m pattern. The lining was completed with a coat of shotcrete 5 cm thick and wire mesh. The construction process has followed the NATM (New Austrian Tunnelling Method) in two steps. Firstly, this is done by excavating the top heading 2 m in advance and progressively constructing the support lining. Then the excavation and support of the bench is done in advances of 4 to 5 m long and a gap of 9 to 11 m between north and south sidewalls. The distress observed in this cross section are an important fracture in the north crown side and some clamps that fix the steel sets onto the rock by means of bolts were broken in the north sidewall. Figures 1 and 2 illustrate examples of the type of damage that occurred. The localisation of these distress and damage occurrences together with the instrumentation data can be used to validate the results obtained with the numerical model.

Model of Anisotropy Behaviour

The interest of this study was to model the anisotropy of the rock mass and to obtain as a result the asymmetric behaviour in stress and deformation. For that



Fig. 1. Detail of some clamps of steel sets broken.



Fig. 2. Detail of the support fractured in the north crown side in the top heading advance section.

purpose, it was thought to work with a “jointed rock model” that is available in the commercial program Plaxis. This model uses the standard and the most common parameters for the rock, and it has the possibility to define different values for some of them depending on the direction considered. In that particular case, the stiffness modulus in the radial direction from the north crown side is about 25 times smaller than the global rock mass value. The model gives the possibility to introduce this deformational anisotropy in the rock mass defining the weak orien-

tation. The breaking criterion used in the model is Mohr-Coulomb criterion, introducing the minor resistant parameters that will correspond with the joint family properties. In table 1 the parameter values are listed.

The in situ filed stresses in the tunnel track are obtained by applying a pressure equal to the earth weight onto the model surface, with a horizontal stress of 0.8 times the vertical stress. In figures 3 and 4 are shown the deformed shape in the top heading excavation advance stage and in the final stage, obtained with the anisotropic model. It can be seen that maximum displacements are in the north crown side. These are around half as small as in the south crown side. The maximum radial displacement obtained with the model is around 16 cm, against the 14 cm measured in this section. The temporal evolution of the radial displacement has a good qualitative fitting between measured and calculated values, as can be seen in figure 5. It is reasonable that the displacement values obtained with the model were larger than the measured ones. This is because it is not possible to measure the displacements before the instruments were implemented.

Table 1. Parameters used in the anisotropy model, with 1: rock mass, 2: joint direction).

Material	E_1 (kPa)	ν_1	E_2 (kPa)	G_2 (kPa)	ν_2	c'_{ref} (kPa)	ϕ' (°)	ψ (°)	γ_{sat} (kN/m ³)
Quartz phyllite	$1.35 \cdot 10^6$	0.3	$5.04 \cdot 10^4$	$2.65 \cdot 10^4$	0.1	150	28	0	27

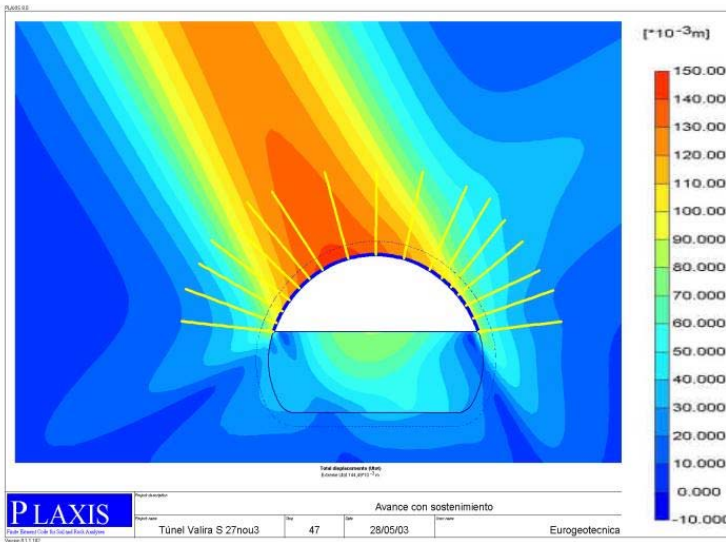


Fig. 3. Contour shadings of displacements at the end of construction of the top heading advance.

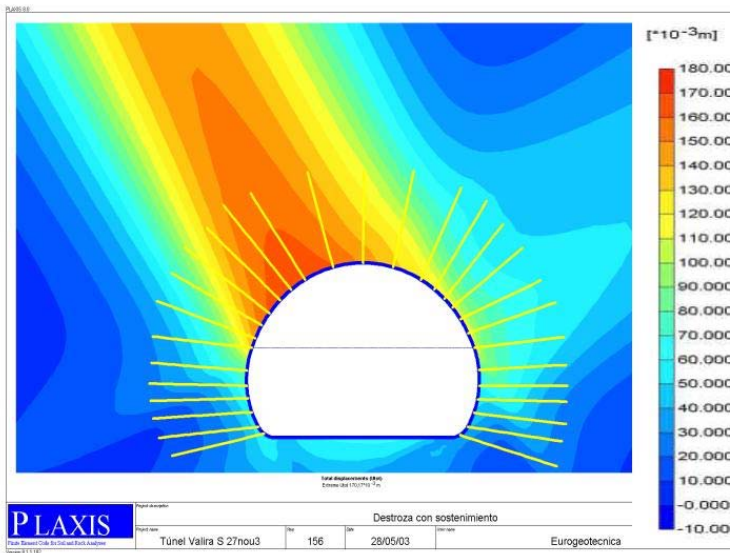


Fig. 4. Contour shadings of displacements at the end of the tunnel construction.

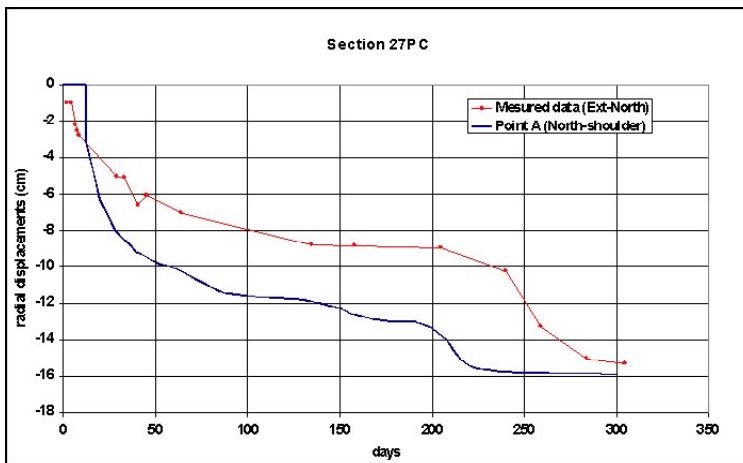


Fig. 5. Plot of radial displacements obtained in the numerical analysis (blue line) and measured (read line), of a point placed in the north crown side of the tunnel section., during the tunnel construction process.

It can be seen that the deformation of the calculated sections fits quite well in both qualitatively and quantitatively with the measured values. Main characteristics are the large deformations in the north crown side and large vertical displacements in the base of the sidewalls. That can be seen by comparing figures 6, 7, 8 and 9 where radial displacements are shown.

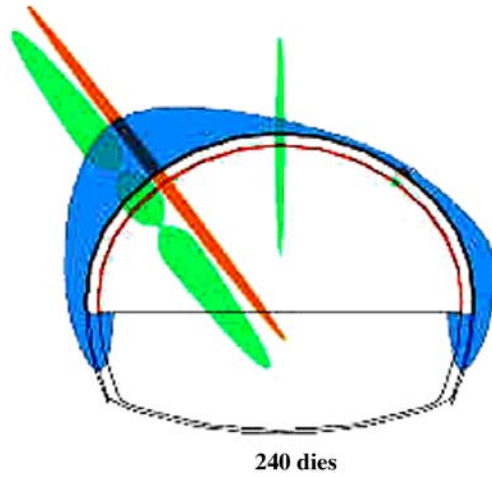


Fig. 6. In blue colour is shown the measured radial deformation at the end of the top heading advance (240 days). The orange ellipses represent the rock pressure measured with pressure cells, and the green ellipses represent the strain state measured with strain gauges.

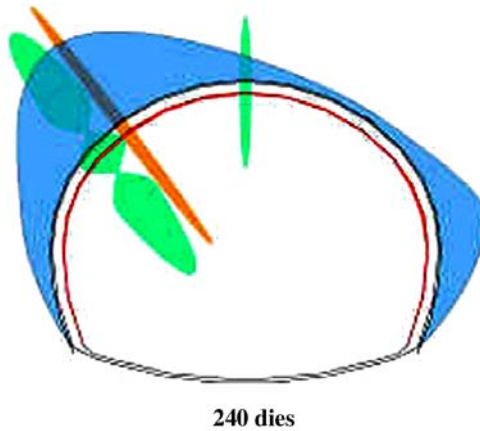


Fig. 7. In blue colour is shown the measured radial deformation when the whole section is excavated (280 days). The orange ellipses represent the rock pressure measured with pressure cells, and the green ellipses represent the strain state measured with strain gauges.

It should be mentioned that these bands where tangential deformations and stresses concentrates, are placed in the areas where most of distress and damage has been observed.

The tangential strains distribution presented in figures 10 and 11 show that deformations and stresses have developed on particular bands that represent the ground progressive failure zones.

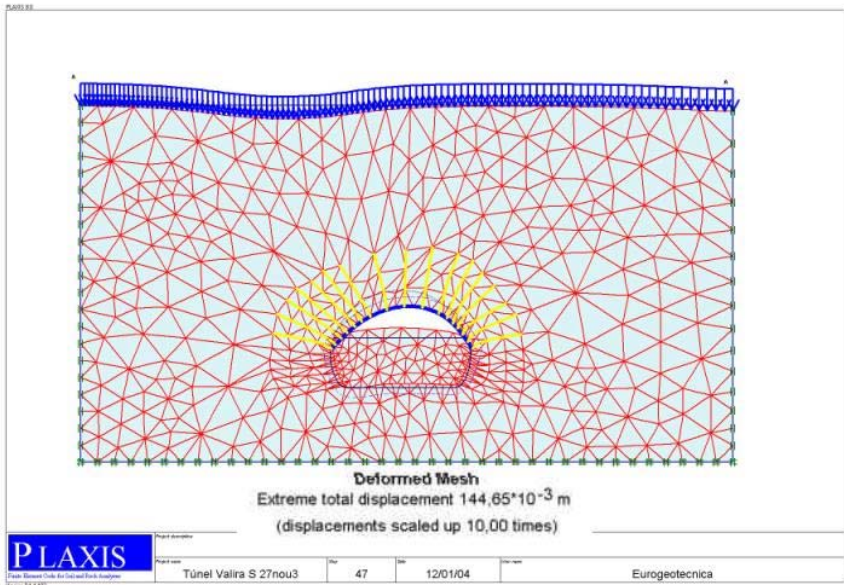


Fig. 8. Displacements obtained with the numerical analysis, at the end of the top heading advance.

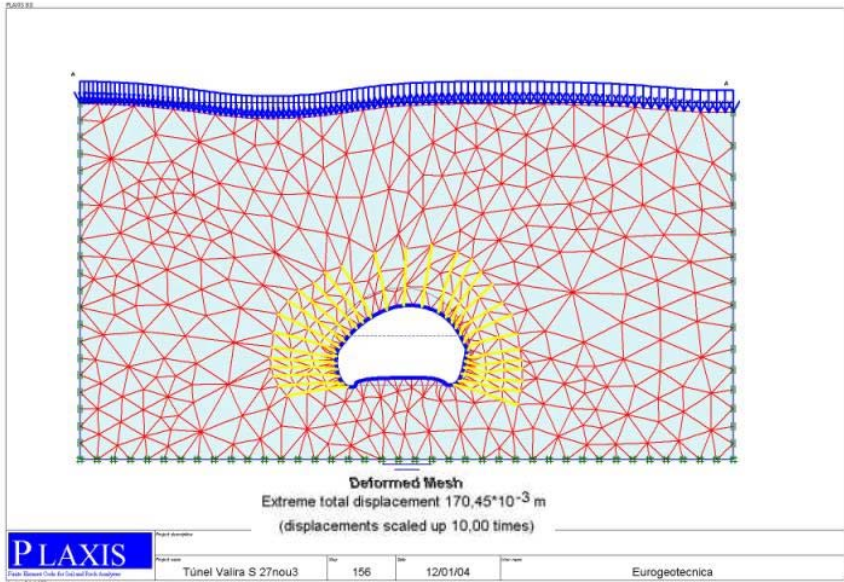


Fig. 9. Displacements obtained with the numerical analysis, when excavation of the bench is done.

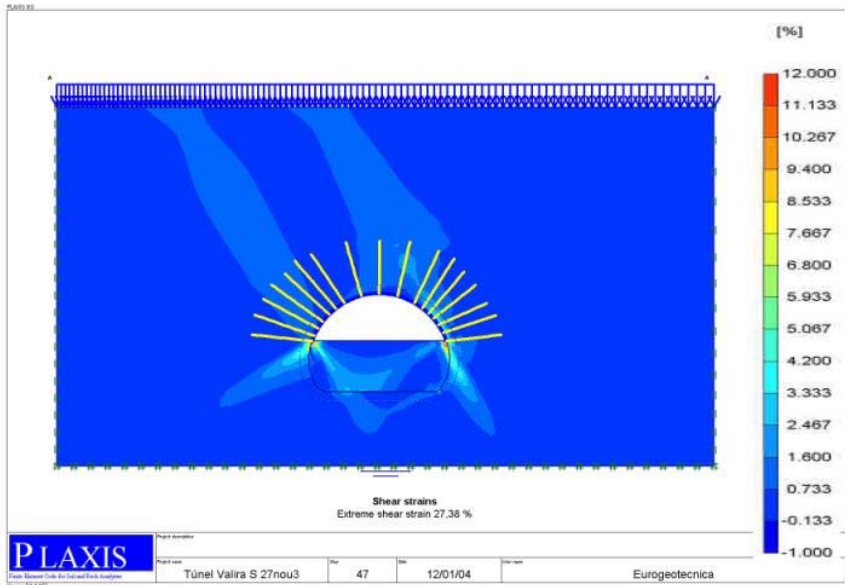


Fig. 10. Tangential deformations obtained with the numerical analysis, in the top heading advance.

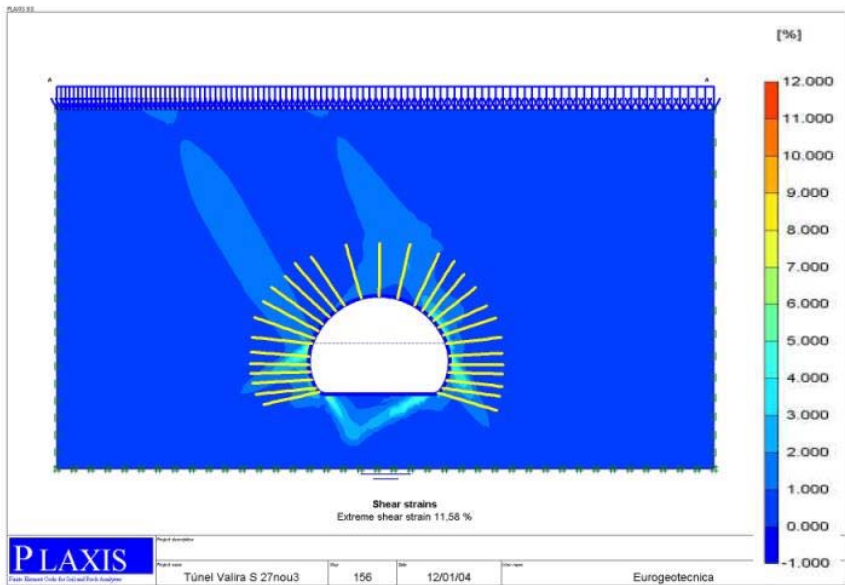


Fig. 11. Tangential deformations obtained with the numerical analysis, when excavation of the bench is done.

Conclusions

A numerical analysis of the Envalira Tunnel construction, in the Principality of Andorra, has been carried out successfully using commercial finite element method package. The particular interest was to model the anisotropic characteristics of the rock mass, due an intensive and penetrative jointed rock in some shear and faults zones in the rock mass through which the tunnel passes. Modelling has shown why substantial asymmetry in the tunnel structural behaviour developed. The results obtained are compared with the data measured as the tunnel construction progressed in the sections that were extensively instrumented. The problem has been analysed using the “Jointed Rock Model”, from the finite element compute program Plaxis. In this model are added different stiffness properties in two different directions, so an elastic anisotropy is defined. In addition, the anisotropy in plastic behaviour is possible by introducing a maximum of three directions with its own strength parameters and where local Mohr-Coulomb criterion is applied. In the case studied, only one weak direction is defined, corresponding to the joint plane family of a shear band zone. The results of the numerical model give a promising simulation of the real behaviour of the tunnel in the cross section studied. It reproduces quite well the asymmetric problems on deformation and stress distribution onto the tunnel support. It appears that this kind of methodology can be a good tool for the analysis of tunnels in an anisotropic rock mass. Such situations are quite common, for example, in highly fractured areas or rock with stratification. The anisotropic rock mass properties produce asymmetric strains and stresses distributions onto the rock support that had to be taken into account for its design. These numerical analyses can be used at an earlier design or project feasibility stage. Subsequently, during construction, the method can be used to assess designed support structure in relation to unexpected changes in the rock properties. This would allow for timely changes for alternative or revised support tunnel lining.

References

- Comas E (2000) Túnel d’Envalira i accessos. SOBB: Catalanian Civil Works Technicians Association Review, number 24, June 2002, XII, pp 24-27.

Engineering-Geological Properties of Carbonate Rocks in Relation to Weathering Intensity

Davor Pollak

Institute of Geology, Sachsova 2, HR-10000 Zagreb, Croatia
pollak@igi.hr
Tel: +38516160812
Fax: +38516144713

Abstract. For most of the purposes engineering-geological explorations are done on the surface. Afterwards the surface data get correlated with other exploration results in order to produce rock mass quality model. The modelling of subsurface and deeper zones in karst areas in Croatia is usually a difficult task because of a complex geology. The evaluation of rock mass quality in those zones is even more demanding mainly because of the specific weathering processes of carbonate rocks. Since karstification significantly changes engineering-geological properties of carbonate rocks, it is of vital importance to determine the degree of weathering in surface and subsurface zones. Engineering-geological properties of carbonate rocks in the surface zone, subsurface and deeper zones are compared and discussed in the paper. Facts and examples are taken from recent highway projects in Croatia. From those data it has been recognized, that depending on the basic block size, two basic weathering models can be established. Each of the models has its specific engineering-geological properties.

Keywords: carbonate rocks, porosity, uniaxial compressive strength, classification of karstified limestone, block size.

Introduction

An engineering geological model of the underground, which is made for the purpose of determining the rock mass quality, is a complex work that requires multi-disciplinary approach. In the regions built of carbonate rocks, the rock mass quality assessment is more difficult, within other things, because of the fact that they are weathered in a specific way. Great part of Croatia is built of carbonate rocks that are intensively karstified. According to engineering classification by Waltham and Fookes (2003), the area mostly belongs to mature (kIII) and complex (kIV) karst. Most carbonate sediments in this region were formed by shallow water sedimentation on the carbonate platform during Mesozoic age. After that period the climate was changing and today moderate continental and Mediterranean climate prevails. As opposed to various karst regions formed in different geological and climate conditions (Amin and Bankher 1997; Tang 2002), Croatian karst region presented in this paper is characteristic for frequent appearance of pits, sink-

holes and well developed dolinas and karst poljes. Besides that, numerous areas are intensively tectonized (Herak 1991).

Weathering Influence on the Intact Rock Properties

For the understanding of the engineering geological properties of any terrain in hard carbonate rocks, it is very important to determine physical and mechanical properties of the intact rock. In many areas of Croatia carbonate rocks are surely “touched” by secondary and diagenetic processes and disturbances. It has been observed that, under the effects of various tectonic phases, many samples are fractured, recrystallized, dolomitized, dedolomitized and karstified and such are the true representatives of the material that builds the terrain. Because of that, the ‘intact’ rock samples in many areas of Croatia show the significant deviations of physical and mechanical properties from the ideal equivalents that were not influenced by the tectonic disturbances and diagenetic processes (Pollak and Braun 1998).

Porosity

Primary porosity eases and enables the accelerated weathering of the intact carbonate rock. In that way, more porous rocks differentiate from carbonate rocks of lower porosity with the appearance of the outcrops. Among others, it is known that increasing porosity of rocks generally results in the decrease of their strength. According to previous tests Tomašić and Ženko (1993), it is obvious that, depending on structure (but on texture and diagenetic properties as well) of the carbonate rocks, primary porosity can be significant (even up to 15%) and in that way it can influence the engineering geological properties of carbonate rocks.

Uniaxial Compressive Strength

Putting into relation the uniaxial compressive strength and the weathering zone where the sample was taken from, it can be seen to which extent the sample is weathered. Such thing is predictable for granite and sandstone (Beavis 1985). However, greater amount of the carbonate rocks with small porosity represents the exception. Based on the available data from several areas and lithostratigraphic units, mainly limestones with low porosity, it is obvious that the carbonate rocks in the surface zone don't have lower strength values of intact samples from those collected from greater depths (Figure 1). Based on past experience and numerous data of strength testing of carbonate rocks with low porosity, the intact sample strength depends much more on fracturing, structure (Figure 2) and texture of sediments and of diagenetic processes than on weathering processes.

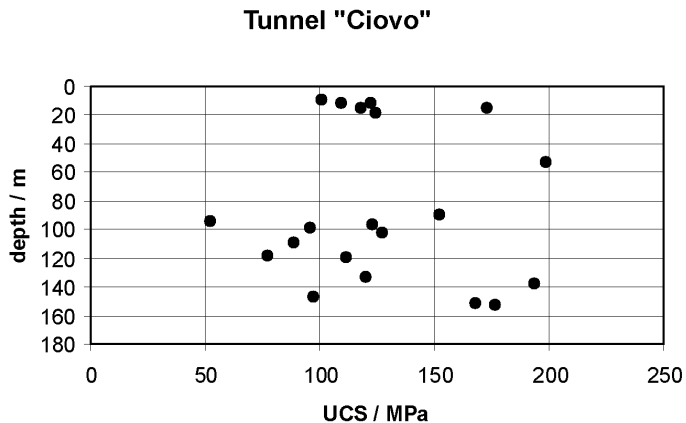


Fig. 1. Dependence of uniaxial compressive strength of intact samples on depth. Upper Cretaceous (Turonian, Senonian) limestones in the "Ciovo" tunnel.

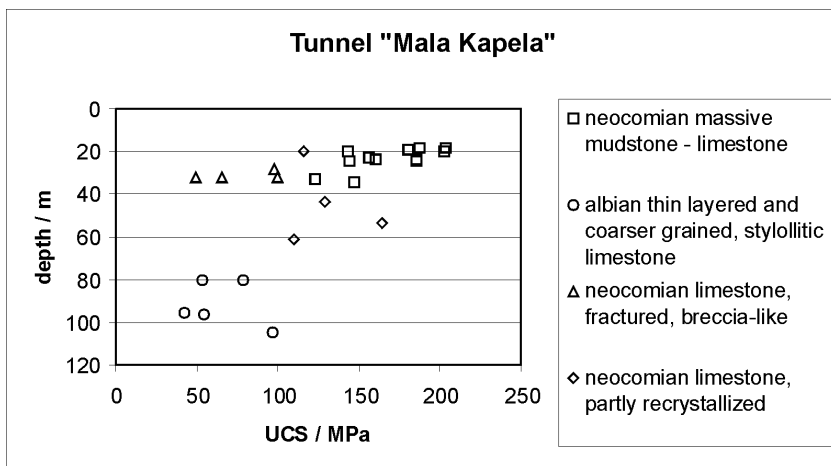


Fig. 2. Dependence of uniaxial compressive strength of intact samples on depth and structure. Tunnel "Mala Kapela".

Weathering Influence on Rock Mass Properties

In many areas, even the first overview of the terrain can determine that almost every lithostratigraphic unit is weathered in a specific way. Such fact is hard to determine by surface investigations, but it can very often be presumed because of the thickness and the properties of cover, of the number and morphology of karst phenomena, of the appearance and intensity of karstified surfaces and similar. The differences in ways of weathering, and consequently in morphologic phenomena

that are characteristic for individual units in the same weathering conditions, are primarily defined by petrologic composition, structure, texture and diagenetic processes which the rocks have passed through (Tišljár and Velić, 1991). The distribution or exchange of lithofacies in space is also important, as well as the tectonic activity of the region.

Weathering Zones

It is hard and unreliable to compare the karstification intensity of lithostratigraphic units and to establish weathering zones only by survey of the terrain. The data gathered by geological and engineering-geological mapping, geophysical measuring, core drilling and laboratory testing are most commonly used for that purpose. Depending on all the properties of investigated area, weathering zones in karst have very different characteristics, spreading and mutual relations. Because of the specific weathering of the carbonate rocks the zones in the extremely karstified areas are mostly very irregular. Regardless of the fact that using the expression “weathering zone” clearly determined regular zoning is presumed, which is not very often the fact in the karst regions. It is very often the case that the separated environments mutually interlace and irregularly exchange vertically and laterally. Irregular “zoning” appears on the large faults or in tectonically fractured areas, where borders with other geotechnical units could be even vertical.

Properties of Discontinuities

The weathering in karst areas takes place mostly along the preferred directions, i.e. cracks, joints, faults, bedding discontinuities and so on. Therefore, one of the most important steps for the assessment and determination of weathering zones, but for the assessment of rock mass category as well, is the determination of all discontinuity properties on the surface and in the deeper weathering zones. High variability in almost every property of discontinuity can be seen very quickly in the regions built of carbonate rocks. Aperture, gouge and roughness of discontinuity in carbonate rocks can often vary in high ranges. In any case, that significantly hardens any assessment or prognosis. Because the mechanical properties of discontinuities depend mostly on these properties (Rongqiang et al. 1993), their determination is of primary importance for rock mass classifications.

Weathering Zones and Engineering Geological Characteristics

Regardless of the fact that the weathering in carbonate rocks is conditioned with numerous factors and their engineering geological characteristics vary in wide range, the regularities that can be shown on simplified and idealized model have been noticed. Taking into consideration all the particularities of weathering in carbonate rocks in highly developed karst and in moderate continental-mediterran-

ean climate of Croatia, two totally different and opposite theoretical models can be schematically presented. The models are defined by the characteristics of intact rock and by the size of the basic block, i.e. the block that is physically separated with discontinuities. The cover influence has not been considered. On one side there are thick bedded, almost massive carbonate rocks with rare but highly distinguished discontinuities and almost undisturbed intact rock (Figure 3, model A). On the other side there are thin bedded or laminated, fractured or massive carbonate rocks with dense distribution of numerous discontinuities with low persistency and in great extent with disturbed 'intact' rock (Figure 3, model B).

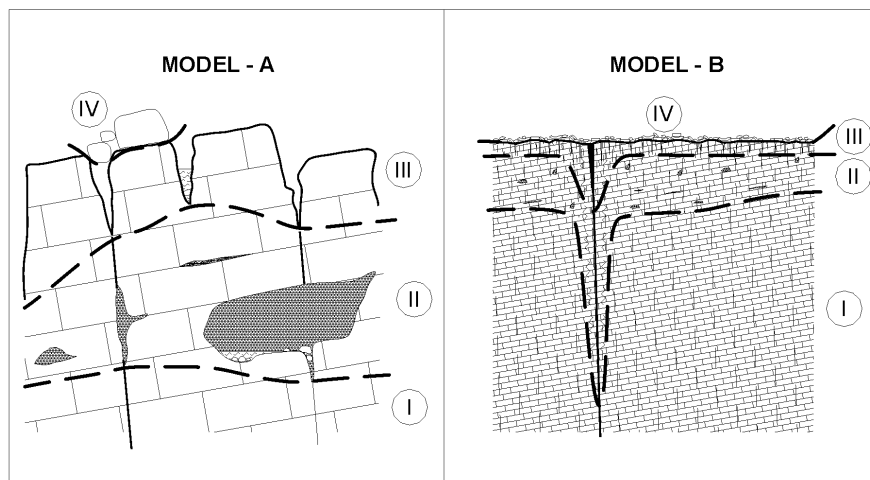


Fig. 3. Schematic display of model of weathering in carbonate rocks of developed and mature karst in Croatia.

Model A

Intact rock is represented by carbonate rocks of various structures, low porosity, homogeneous or quasi-homogeneous and isotropic one. They are completely lithified rocks that have not been weakened by recrystallization or other post-diagenetic processes. In the laboratory sample without cracks and joints show maximal mechanic properties for intact rocks, which are almost the same in all the separated zones. The layer thicknesses are high (for example the reef and fore-reef development of Senonian deposits, Croatia) or the rock has no distinguished layer discontinuities (for example massive mudstone / limestones of Neocomian age or non bedded, massive limestone Jelar breccias, Croatia – Vlahović et al. 1999).

Zone I

Rock mass is massive or consists of great blocks limited by discontinuities with high persistency with no traces of karstification. Walls of discontinuities are fresh,

closed or with aperture of max. 1 cm, mostly filled with calcite. Bedding discontinuities are closed. The media is anisotropic or isotropic. The depth of this zone is variable, but it can reach the surface very rarely and locally.

Zone II

Basic rock mass from the zone I with the appearances of karstification along the most expressed discontinuities. By means of karstification, some discontinuities are widened up to aperture of several centimetres, often covered with the layer of crystalline calcite and partially filled with clay. Layer discontinuities are still mostly closed or with the aperture of less than 1 cm. Caverns, pits and caves of various dimensions are frequent.

Zone III

Surface karstification zone with huge blocks on the outcrops, which are separated by joints with even metric aperture and without gouge. Bedding discontinuities are also often highly karstified, with aperture up to several centimetres, very often without gouge (Figure 4a). Walls of the majority of discontinuities have become rough-undulating or smooth-undulating because of the weathering. Joints with large aperture connected to the surface, as well as the thickness of this zone can reach up to dozen meters in depth. Open joints correspond to over 10% of total rock volume. Such rocks on the surface often build steep slopes or cliffs (Figure 4b) and the openings of caves or pits with greater dimensions can be found. Sink-holes of various dimensions are frequent.

Zone IV

Unbounded blocks of huge dimensions. Cover depends on climate. It is often missing or it fills the depressions.

Model B

Opposite to model A, which is built mostly of undisturbed rock, the other extreme is represented by model B. That means, the intact rock of model B is exceptionally heterogenous due to: structure and texture of the rock (lamination, thin layers - figure 5a, stromatolites - figure 5b, numerous stylolites and so on), tectonic fracturing (cracks, veins, joints) or it is homogeneous but significantly weakened by the activities of various processes (recrystallization, dolomitization - figure 5b or dedolomitization). Opposite to intact rock of the model A, the weathering influence on physical and mechanical properties can often be seen on these samples.

Zone I

Thin bedded, laminated or massive rock with numerous discontinuities of various genesis. Discontinuities are so frequent, but poorly distinguished, with no aperture, that the media can be taken as quasi-isotropic. There is no aperture on the discontinuities and, if there is gouge, it is exclusively carbonate. There are no traces of karstification.

a)



b)



Fig. 4. Surface weathering: a) of metric blocks of very well bedded limestones of Senonian age (Bisko, Croatia); b) of huge and massive blocks of carbonate “Jelar” breccias of Upper Eocene - Lower Oligocene (Tulove grede, Velebit Mt., Croatia).

a)



b)



Fig. 5. Surface weathering: a) platy limestones of Turonian age (Stupi, Vranjica, Croatia); b) exchange of early diagenetic and stromatolite late diagenetic 'hauptdolomite' (Gorski Kotar, Croatia).

Zone II

Rock mass properties are the same as in zone I, but on more expressed discontinuities the weathering processes are visible and smaller caverns are also possible. Aperture of discontinuities almost does not exist. Besides the numerous cracks and joints the diagenetic changes are visible (recrystallization, dolomitization, etc.). The intact rock is locally porous, and the separation of blocks along the bedding planes is possible.

Zone III

Only some secondary discontinuities are filled with clay, max. up to several centimetres thick. Many of them are planar or stepped, very clearly expressed. Only in some places, the wider discontinuities (over 10 cm) connected with surface, filled with clay or cover material are possible. The rock is often cavernous, porous. Bedding planes are highly expressed and in places the interlayer joints are opened. Unbounded material that fills open joints represents over 10 % of total rock mass volume.

Zone IV

In the areas with no cover, rock debris and fragments are exposed at the surface (figure 5a). The areas with cover are often overgrown by vegetation and below the humus layer there is a mixture of fragments, debris and cover material in various ratios (figure 5b). The areas built of rocks shown in this model are often flattened or with mild slopes, almost without sinkholes, or they are very shallow with mild brims.

The thickness of all the mentioned zones on both models depends on local conditions and varies within wide range. Depending on geological, morphologic or climatic conditions, some zones can be completely missing or even have the inverse order.

Conclusion

Development of an engineering geological model of the underground is a complex task that includes numerous investigations and requires interdisciplinary approach. The facies type of rocks and their structure and texture determine the way and the intensity of weathering of the carbonate rocks. Because of that, for the determination of weathering characteristics of carbonate rocks it is very important to study the microfacies characteristics. Unique way of weathering of carbonate rocks is mostly connected to relatively good solubility of minerals that build them, so they are weathered along the preferred directions. Because of that, studying of all discontinuity properties in surface and subsurface weathering zones is of exceptional importance. It is obvious that the variations of weathering ways are very wide, depending on the structure and texture of the rocks, fracturing intensity, morphology of area and climatic conditions. Nevertheless, depending on the basic block size, two basic weathering models can be separated. On one side, there are thick

layered, almost massive carbonate rocks with rare, but highly distinguished discontinuities and almost undisturbed intact rock (model A). On the other side, there are thin layered or laminated, fractured or massive carbonate rocks with dense distribution of numerous discontinuities with low persistency (model B). It is important to mention that in nature, frequent changes in sedimentation conditions, the activity of various diagenetic and post diagenetic processes and tectonic activity, can produce mixing and various combinations of weathering models.

References

- Amin AA, Bankher KA (1997) Karst Hazard Assessment of Eastern Saudi Arabia. *Natural Hazards* 15: 21-30.
- Beavis FC (1985) *Engineering Geology*. Blackwell Scientific Publications, Geoscience Texts, Vol 5, 231 p.
- Herak M (1991) Dinaridi: Mobilistički osvrt na genezu i strukturu. *Acta geologica* 21/2: 35-117.
- Pollak D, Braun K (1998) Sedimentology in the service of engineering geology: Study of some results of the explorations for highway construction and tunneling in Croatia. 8th International IAEG Congress, Balkema, Rotterdam, pp 195-199.
- Rongqiang L, Hongxin C, Defang K (1993) Research on the effect of gouge thickness on the mechanical properties of joints. *The Engineering Geology of Weak Rock*, Cripps et al. (eds). Balkema, Rotterdam.
- Tang T (2002) Surface sediment characteristics and tower karst dissolution, Guilin, southern China. *Geomorphology* 49: 231-254.
- Tišljar J, Velić I (1991) Carbonate facies and depositional environments of the Jurassic and Lower Cretaceous of the coastal Dinarides (Croatia). *Geološki vjesnik* 44: 215-234.
- Tomašić I, Ženko T (1993) Utjecaj strukturalno tekturnih značajki i dijagenetskih procesa na poroznost arhitektonskog kamena. *Rudarsko-geološko-naftni zbornik* 5: 165-172.
- Vlahović I, Velić I, Tišljar J and Matičec D (1999) Lithology and origin of Tertiary Jelar breccia within the framework of Tectogenesis of Dinarides. *Harold Reading's IAS Lecture Tour '99; Field trip guide book: Some carbonate and clastic successions of the external Dinarides, Croatia; Institute of Geology; Zagreb*, 23-25.
- Waltham AC, Fookes PG (2003) Engineering classification of carst ground conditions. *Quarterly Journal of Engineering Geology and Hydrogeology* 36: 101-118.

Engineering Geocryological Mapping for Construction in the Permafrost Regions

Felix Rivkin, Irina Kuznetsova, Nadezhda Ivanova, and Sergey Suhodolsky

Industrial and Research Institute of Engineering Survey for Construction, Okruzhnoi ps. 18,
Moscow, Russia, 105187
f-rivkin@narod.ru
Tel: +7 95 3662576
Fax: +7 95 3662576

Abstract. Results of compiling a digital engineering geological and engineering geocryological maps at all stages of a geotechnical survey for construction are presented. The technique has been used for the engineering survey along the main pipelines in the northern regions of European Russia and Western Siberia and in the mountain regions of Transbaikalia, Eastern Siberia, and the Far East.

Keywords: permafrost, engineering-geocryological mapping and zoning, matrix legend, Siberia, Russia, Transbaikalia

1 Introduction

Geological mapping is the main link in the system of geotechnical survey for construction in the permafrost region. Using GIS technologies, interrelating maps and digital databases, makes it possible to consider GIS information models of the territory. Such maps include and demonstrate characteristics of a studied site in a form convenient for further use of engineering geocryological information. During development of a site, engineering geocryological maps are used to optimize the location of engineering facilities, to assess the potential environmental impact, to estimate environmental stability, as well as for the purpose of environmental engineering. Oil and gas facilities - pipelines, terminals, roads, etc. have been intensely constructed for the last years in the northern regions of Russia, especially in its European part and Western Siberia. A stepwise system of engineering survey for construction has been traditionally used in Russia. The scale of mapping changes depending on the stage of the survey, thereby maintaining a necessary degree of detail for the survey (Shamanova et al. 2001). An analysis of the conditions of realization of numerous projects that have been performed for the last years indicated a new trend; very often, the survey is realized at one stage rather than in several steps. After the first stage of the survey, which is performed without field studies and is used to develop tender proposals and design assumptions, the remaining (detailed) survey is factually conducted in one-step and in a very short space of time. We should note that the engineering geocryological field studies in

the permafrost region are seasonal. In such a situation the requirements to the technique of different-scale geocryological mapping, complexity of studies, and methods of processing engineering geocryological data and presentation of survey results become substantially higher. In this case engineering geocryological maps should include information necessary and sufficient for selecting routes of linear structures, design solutions, and construction methods. Long-term complex engineering geocryological surveys for construction, performed in the region of perennially frozen rocks (in plain and mountain areas), made it possible to develop and realize the technique of geocryological zoning and mapping. The technique is based on a complex analysis of engineering geocryological conditions of the territory (Rivkin et al. 2000).

2 Methods and Research Area

The technique of compiling digitized engineering geological and engineering geocryological maps for all stages of geotechnical survey for construction is based on detailed methods of engineering geocryological zoning. This technique has been realized during the engineering survey, performed in the northern regions of European Russia and Western Siberia (Yamal Peninsula) and in the mountain regions of Transbaikalia for the main pipelines designed for transporting oil and gas to the states of the Pacific region (with a total length of about 5000 km) and to other states. The compiled maps are small-scale (1:2500000 and 1:500000), medium-scale (1:200000 and 1:25000), and detailed (1:5000 and 1:2000). The maps of such scales are compiled for the preliminary, investment justification, and design stages of a survey, respectively. The key link of mapping is the development of matrix explications, the application of which (in contrast of hierarchic legends) makes it possible to use more completely the possibilities of GIS technologies. The matrix explication is not only the method for analyzing, organizing, and generalizing information but also a legend to a map. As a result, mapped information is complete and is read simply. The matrix of engineering geocryological conditions of a territory reflects the structure of interrelation between the main natural factors, used to compile a map, and the structure of the thematic digitized layers of this map. This method proposes to combine the techniques for compiling two main types of engineering geological maps: maps of zoning and maps of conditions.

3 Results and Discussion

Geological, structural-geomorphological, and landscape-geocryological principles are used to construct matrix legends depending on the scale of maps and the region of the study. Used were the regional regularities of interaction between the main environmental components: genesis, composition and thickness of surface sediments; vegetation, geocryological, engineering geological, and hydrogeologi-

cal conditions, and the character and intensity of exogenous geological processes. This makes it possible to synthesize information about natural conditions in the study region. The composition of a matrix table is variable and depends on the map type and scale, regional natural conditions, and aim of survey. A matrix includes (with regard to scale and regional geological conditions) the main factors responsible for the natural conditions. The engineering geological and engineering geocryological maps can then be used for constructing main pipelines and developing oil and gas fields in different regions of Russia.

3.1 Engineering Geocryological Maps for Substantiating Construction of Main Pipelines in Mountain Regions of Eastern Siberia and Far East

3.1.1 Engineering Geocryological Map of Eastern Siberia and Far East of Scale 1:2500000

The engineering geocryological map of Eastern Siberia and Far East of scale 1:2500000 covers the region with routes of designed pipelines as well as the regions with perspective oil- and -gas fields and possible ways of oil-and-gas transportation (Ivanova et al. 2003) (Fig. 3.1). The purpose of the map is to give a general knowledge of zonal and regional features of engineering geocryological conditions in order to preliminarily assess the conditions for construction. The colour shows the bedrock formations and Quaternary geological-genetic complexes (in the areas where their thickness exceeds 5 m). Areas with different geocryological conditions are differently shaded depending on the distribution, thickness, and average annual temperature of perennially frozen rocks (PFRs). Contour lines show regions with different seismicity. According to the morphological and structural principle, 46 engineering geological regions with similar geomorphological and structural-tectonic features have been distinguished on the map for four large geological structures (Siberian Platform and Baikal-Stanovoi, Mongol-Okhot, and Sikhote Alin folded zones) (Table 3.1). Figure 1 shows the schematic map (black-and-white version) of regional zoning and the planned pipelines routes location.

3.1.2 Engineering Geological and Geocryological Maps of Eastern Siberia and Far East of Scale 1:200000

The engineering geological and geocryological maps of Eastern Siberia and Far East of scale 1:200000 reflect the engineering geological conditions of the territory with regard to the specific features of the designed structure; an oil pipeline laid in the 2-3 m deep trench. The maps have been compiled on the structural-geomorphological basis, which makes it possible to reflect the paragenetic relations between topographic features and geological-genetic complexes of Quaternary sediments (in the surface horizon) composing these complexes. Using the matrix legend in order to analyze natural conditions makes it possible to map the entire diversity of combinations of bedrock formations and depths of their occurrence with the composition and genesis of eluvial-slope Quaternary sediments. Only Quaternary complexes with a thickness of more than 10 m are shown on

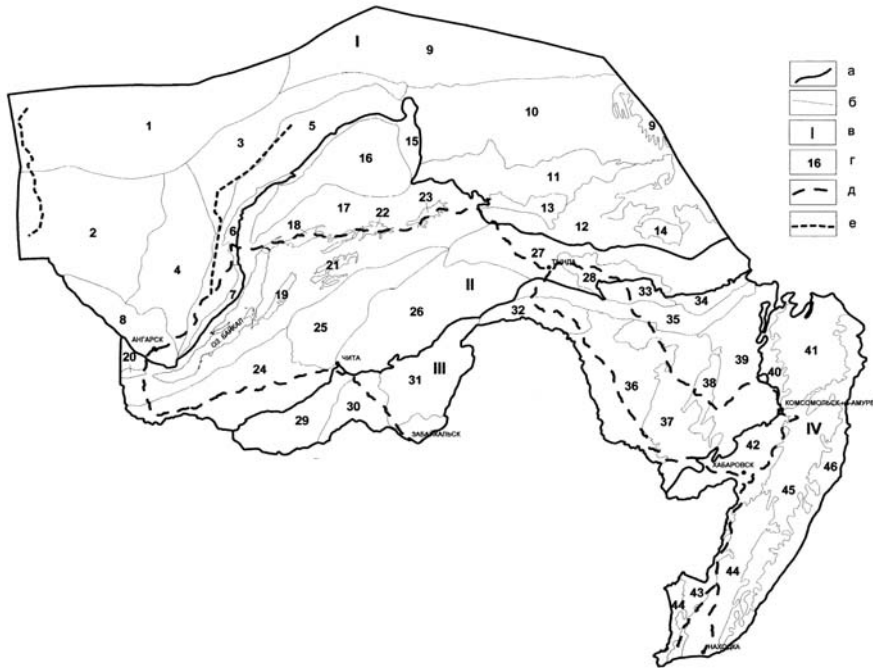


Fig. 3.1. The schematic map (black-and-white version) of engineering-geological zoning and the planned pipelines routes location. 1 - geological structure (tectonic) regions boundaries; 2 - engineering-geological regions boundaries; 3 - number of a geological structure; 4 - number of a engineering-geological regions; 5 - projectile pipelines routes; 6 - prospective pipelines routes.

Table 3.1. Geological structures and Engineering-geocryological regions of Eastern Siberia and Far East.

Geological structure (tectonic)			
I. Sibirskaia platforma	II. Baikalo-Stanovaia skladchataia zona	III. Mongolo-Okhotskaia skladchataia zona:	IV. Sikhote-Alinskaia skladchataia zona
Engineering-geological regions			
1 - Tungusskii	15 - Chuiskii i Zhuia-Patomskii	29 - Khentei-Chikoiskii	40 - Tuguro-Chukchagiroyoronskii
2 - Taseevskii	16 - Vitimo-Patomskii	30 - Aginskii	41 - Nizhne-Amurskii,
3 - Leno-Katangskii	17 - Baikalskii	31 - Shilko-Argunskii	42 - Sredne-Amurskii
4 - Angaro-Lenskii	18 - Verkhne-Angarskii	32 - Verkhne-Amurskii,	43 - Prihankaiskii
5 - Predbaikalskii	19 - Barguzinskii	33 - Verkhne-Zeiskii	44 - Arsen'evskii
6 - Kirengskii	20 - Tunkinskii	34 - Udskii	45 - Sikhote-Alinskii
7 - Onotskii	21 - Tsipinskii i Tsipikanskii	35 - Tukuringra-Dzhagdinskii	46 - Vostochno-Sikhote-Alinskii
8 - Irkutsko-Cheremkhovskii	22 - Muiskii	36 - Amuro-Zeiskii	
9 - Viliuiskii	23 - Charskii	37 - Khingano-Bureinskii	
10 - Prialdanskii	24 - Selenginskii	38 - Bureinskii	
11 - Aldanskii	25 - Vitimskii	39 - Bureino-Badzhalskii	
12 - Timp-ton-Uchurskii	26 - Olekminskii		
13 - Chul'manskii	27 - Stanovoi		
14 - Tokinskii	28 - Zeiskii		

accumulative levels. Based on the established latitudinal-zonal regularities of formation of frozen rocks, we have distinguished six types of geocryological conditions with respect to the combination of the permafrost distribution, average annual temperature, and thickness. Typical intervals of depths of seasonal thawing and freezing, ice content of rocks, and exogenous geological processes are mapped.

3.2 Engineering Geocryological Maps for Constructing Main Pipelines on Coastal Plains in Western Siberia and Northern European Russia

Special medium-scale and detailed engineering geocryological maps (at scales of 1:100 000 to 1:200000) were compiled in order to economically substantiate construction and designing of main oil pipelines and development of oil-and-gas fields on coastal plains of Western Siberia and northern European Russia.

3.2.1 Engineering Geocryological Maps for Substantiating Construction of Main Pipelines of Scale 1:200000

The Engineering geocryological maps for substantiating construction of main pipelines of scale 1:200000 has been compiled on the geological-geomorphological and landscape basis. This makes it possible to reflect paragenetic relations between landscapes and geological-genetic complexes of Quaternary sediments occurring within landscapes, taking into account lithology, ice content, depth of seasonal thawing and freezing, and temperature of these sediments. Landscapes and geological-geomorphological and lithological characteristics are located in different parts of the matrix. This makes it possible to reflect the entire diversity of combinations of surface and geological-geocryological conditions (genesis, lithology, properties, temperature, ice content of soils, etc.) in the pipeline route. This is one of the important elements of mapping since the relation between the surface (landscapes) and engineering geocryological conditions is stable in the given region. Information has been mapped to a depth of 15 m. Figure 3.2 shows the structure of the matrix table used to compile the map. The map demonstrates the geological-geomorphological conditions, genesis, composition and properties of soils (including ice content, salinity, etc.), and geocryological conditions (distribution and temperature of frozen and thawed soils, depth of seasonal thawing and freezing, and hazardous geocryological processes and formations).

3.2.2 Detailed Engineering Geocryological Maps (Scales of 1:25000 to 1:2000) for Designing a Main Pipeline

The detailed engineering geocryological maps (scales of 1:25000 to 1:2000) for designing a main pipeline are compiled based on results of complex field studies. However, the scheme for constructing matrix tables in order to analyze and classify engineering geocryological conditions is similar to the scheme shown in Fig. 3.2. The only difference is that this matrix is more detailed. According to the

Geological - genetics complexes of a grounds Landscape and surface characteristic		Geomorphological levels																								
		Genesis & sediments age																								
		Cryolitology charavteristic of the grounds																								
		# of a Engineering - Geocryological region																								
Landscape characteristic The Surface angle, degree. Ground temperature, °C Indexes of a landscapes		1	2	3	4	5	6	7	8	9	10	11	12	13	14	15	16	17	18	19	20	21	22	23	24	
	a																									
	b																									
	c																									
	d																									
	e																									
	f																									
	g																									
	h																									
	i																									
	j																									
	k																									
	l																									
	m																									
	n																									
	o																									
	q																									
	p																									
	r																									
	s																									
	t																									
	u																									
	v																									
	w																									

Fig. 3.2. The Matrix form legend for Engineering geocryological map for pipeline construction. (Yamal Peninsula, Russia). The black cells demonstrate engineering-geological regions identified in a research area.

mapping scale, landscape (surface) conditions and lithological and geocryological characteristics of soils composing the upper section are shown in detail on the large-scale maps. It is obvious that the size of the matrix tables substantially increases in this case. However, this disadvantage is compensated by the fact that it is convenient to use the compiled maps and matrix tables as bases for geocryological prediction, assessment of environmental impact, designing of pipelines, and unification of construction methods (Chekhina and Rivkin 2003, Rivkin et al. 2000).

4 Conclusion

Using a matrix analysis of engineering geocryological conditions makes it possible to create rapidly special maps for construction. Such maps allow not only solving traditional problems of engineering survey, but these form the basis for making geocryological prediction (using GIS methods), assessing occurrence and development of natural and technogenic hazards, and estimating potential environmental impact and engineering geological risks of construction and operation of different facilities.

References

- Chekhina IV, Rivkin FM (2003) Natural Risk Evaluation of Geocryological Hazards (the Varandey Peninsula Coast of the Barents Sea), Proc. Extend. Abstracts. 8th Permafrost Conf., Zurich, July 20-25, Zurich 2003, pp. 15-16.
- Ivanova NV, Kuznetsova IL, Rivkin FM, Suhodolsky SE, Chekhina IV (2003) Engineering Geological Support of the Technical and Economic Justification of Construction of Transcontinental Oil Pipelines - (in press) (in Russian).
- Rivkin FM, Koreisha MM, Popova AA, Levantovskaya NP, Chekhina IV (2000) Application of GIS Technologies during Engineering Survey, Engineering Geological Survey in the Cryolithozone: Theory, Methodology, and Practice, St. Petersburg, pp.230-235 (in Russian).
- Shamanova II, Rivkin FM, Popova AA (2001) Engineering Geocryological Mapping for Designing Main Pipelines in Northern Plain Regions, Proc. 2nd Conference of Russian Geocryologists, June 6-8, vol. 4, pp. 309-315 (in Russian).

3D Terrestrial Laser Scanning as a New Field Measurement and Monitoring Technique

Siefko Slob and Robert Hack

ITC, Mijnbouwstraat 120, Delft, The Netherlands

{slob,hack}@itc.nl

Tel: +31 15 2789673, +31 15 2789671

Tel: +31 15 2789676

Abstract. 3D terrestrial laser scanning is a relatively new, but already revolutionary, surveying technique. The survey yield a digital data set, which is essentially a dense “point cloud”, where each point is represented by a coordinate in 3D space. The most important advantage of the method is that a very high point density can be achieved, in the order of 5 to 10 mm resolution. In order to analyse the character and shape of the scanned surfaces it is necessary to convert the irregularly distributed point data into 3D surface information using surface reconstruction. The reconstructed surface can subsequently be visualized using a variety of 3D visualization techniques. From the reconstructed 3D surfaces, it is also possible to generate 2D profiles or elevation contour lines for use in regular GIS or CAD packages. A number of applications are described in this paper, which may illustrate the possible benefits of using laser scanning as a technique in engineering geological practice and research: volume analysis and monitoring, detailed and large-scale topographic mapping, tunnelling, rock face surveying, and digital outcrop mapping.

Keywords: 3D Laser scanning, surface reconstruction, survey, monitoring, digital outcrop mapping, volume analysis, tunnelling, rock face

Introduction

3D terrestrial laser scanning is a relatively new, but already revolutionary, surveying technique. Different laser scanning systems exist, but the technique used outdoors for geodetic surveying or for measuring large civil engineering structures is the “time-of-flight” or “laser range finding” technique. The “time-of-flight” or “ranging” scanners have a laser diode that sends a pulsed laser beam to the scanned object. The pulsed laser beam moves through a rapidly changing elevation and azimuth angle of a mirror inside the instrument. The pulse is diffusely reflected by the surface of the scene or object and part of the light returns to the receiver. The time that light needs to travel from the laser diode to the object surface and return is very precisely measured. Knowing the speed of light, the distance from the scanner to the object and the azimuth and angle of the beam, the position of each point where the beam is reflected can be calculated. The survey yields a digital data set, which is essentially a dense “point cloud”, where each point is represented by a coordinate in 3D space (X, Y and Z, relative to the scan-

ner's position) and the reflected intensity (I) of the laser beam. With this data, the 3D shape of any object or environment can be determined and analysed. A new generation of ranging laser scanners also yields for each point the passive colour (i.e.: red, green, and blue reflection values). Very large and complex objects can also be scanned from different positions. Most software used to capture the survey data allow to merge different surveys into a single point cloud. In this way, the "shadow" areas of surveys can be complemented with scans where the previously hidden areas can be "seen" by the laser beam. The most important advantage of the method is that a very high point density can be achieved, in the order of 5 to 10 mm resolution. Therefore, the shape of the surveyed object or scene can be modelled at a very high detail and accuracy in three dimensions. The method can measure objects and scenes at a distance of nearly 200 meters under ideal conditions. In real-world situations however, 50-100 meters is more usual. The method is also rapid: a full 360° scan can be carried out with the latest models in less than 4 minutes. The laser scanner fits on a regular surveying tripod and has a normal laptop attached to operate the scanner and to store the survey data. Most of the software used to operate the scanner also allow the user to instantly georeference the scanned (X,Y,Z) data to a local or global reference grid. Currently, a number of 3D laser scanning devices are on the market that use the ranging principle, from different manufacturers (E.g. Leica-Cyrax, Riegl, Trimble-Mensi) (Figure 1). The underlying principles of the different laser scanners are essentially the same, but the quality of the generated data (for instance: resolution, accuracy, precision, scanning speed, and laser beam divergence) may vary between manufacturers and models.



Fig. 1. Three current models from different manufacturers, from left to right: Mensi GS200, Leica (Cyrax) HDS3000, Riegl LMS Z210.

Surface Reconstruction Techniques

The mere visualisation of the point cloud gives the user already a very good 3D perspective of the scanned scene or object. Some end-users actually prefer to use

the georeferenced or raw point cloud data “as is” and to integrate it into existing 3D modelling programs and databases such as AutoCad. However, in order to analyse the character and shape of the scanned surfaces it is necessary to convert the irregularly distributed point data into 3D surface information. Particularly for the design industry and the medical imaging industry, 3D prototyping and visualization software has been developed that make use of advanced 3D surface reconstruction techniques and algorithms. In 3D geological modelling, surface reconstruction techniques are also being used (Cowan et al., 2002). However, the objective here is to reconstruct large (small-scale) 3D geological shapes (volumes) based on mostly very limited borehole data and geophysical profiles. In surface reconstruction of point cloud data, however, the objective is to reconstruct relatively small (large-scale) 3D surfaces based on very dense data. Surface reconstruction algorithms can roughly be divided into Polygonal and Parametric. An example of polygonal techniques is 3D Delaunay triangulation, which creates irregular, triangular patches based on simple linear interpolation between the points in 3D space. Examples of parametric techniques are NURBS (Non-Uniform Rational B-Splines) or Fast RBF (Radial Basis Functions), which use parametric functions to define surface patches. Parametric techniques create more “natural-looking” surfaces and more accurate representations, particularly for areas where data are missing, but it requires more computing power and time than polygonal interpolation techniques. A comparison of the two interpolation techniques is given in figure 2.

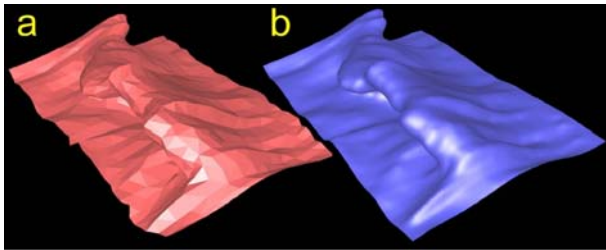


Fig. 2. Comparison of 3D triangulation (a) and a parametric surface (b) of a geological shape after digital rendering (from: Cowan et al., 2002).

Visualisation and Analysis

The reconstructed surface can subsequently be visualized using a variety of 3D visualization techniques. The main purpose is to allow the user to interactively view objects or scenes from different angles and directions. Different lighting techniques may for example be used to highlight shapes and surface characteristics, such as roughness. In practice, however, it is not sufficient to merely view the surfaces. Mostly the end-user wants to integrate and analyse the data in existing software packages. From the reconstructed 3D surfaces, it is possible to generate 2D profiles or elevation contour lines (Figure 4). This derived information can

subsequently be used in regular GIS or CAD systems for further analysis integration with existing information. A number of applications are described in the remainder of this paper, which may illustrate the possible benefits of using laser scanning as a technique in engineering geological practice and research.

Applications

Volume Analysis and Monitoring

An obvious first applications that comes to mind in which advantages in terms of survey speed and precision are achieved, is surveying and monitoring volumes of earth fill or spoil heaps. If a previous base level is known, the amount of earth fill can be computed by surveying the new topographic surface and subtracting its base level. For example, monitoring the size of spoil heaps during quarrying or mining operations has always been a very elaborate process. Through regular surveying with a 3D laser scanner, this can be done much faster and more accurate compared to traditional geodetic surveying techniques. An example is given in figure 3.

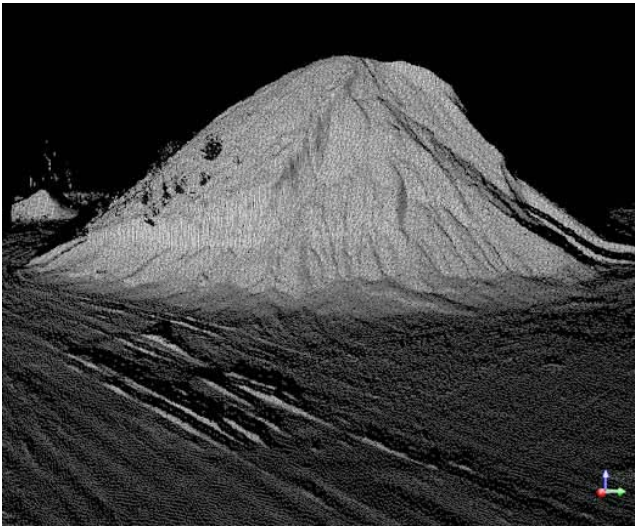


Fig. 3. Example of a 3D laser scan survey (point cloud with reflected intensity) of a sand pile. (From: Mensi, 2003).

Detailed and Large-Scale Topographic Mapping

Another application is for detailed topographic mapping of a specific site. Particularly for large building construction sites, in quarries or areas affected by mass

movement or subsidence, this technique can be very useful. A detailed topographic survey can be done very rapidly, without having to access the (hazardous or busy) site. This obviously gives many advantages. A good example where laser scanning proved its benefit was after the dike collapse of August 2003 in Wilnis, The Netherlands (see figure 4). The terrain affected by the dike failure was very complex and chaotic, but through a laser scan survey a detailed digital terrain model could be made without having to access the site (Anonymous, 2003).

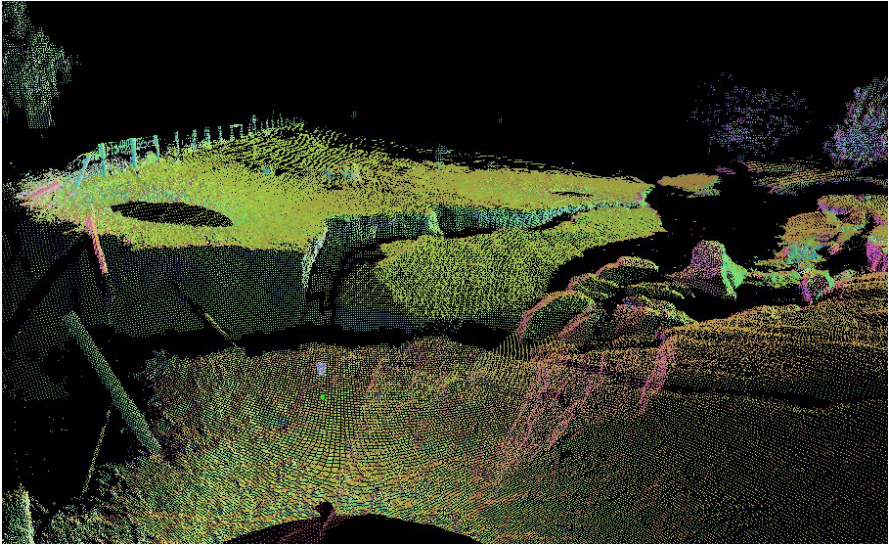


Fig. 4. 3D laser scan point cloud of the dike burst in Wilnis, August 2003. The colour indicates reflected colour intensity (Picture courtesy: Jan Berends, Geometius).

Tunnelling

Specialised laser scanners have been developed to measure the geometry of tunnel alignments. For this purpose a different type of laser scanner can be used that measures differences in phase of the emitted and reflected laser beam, rather than the difference in time. This type can measure (only for short ranges) the geometry with a higher detail, accuracy, and speed than the ranging scanners. Mounted on a small vehicle or carriage along rails allows for rapid surveying of tunnel alignments. For instance, the thickness of the applied shotcrete can be monitored and control on the final geometry of the tunnel can be done with this method. Since the internal geometry can be captured at a very high precision, it may also be suitable to monitor deformation with this phase-based scanner. An example is given in the figure below (Figure 5).

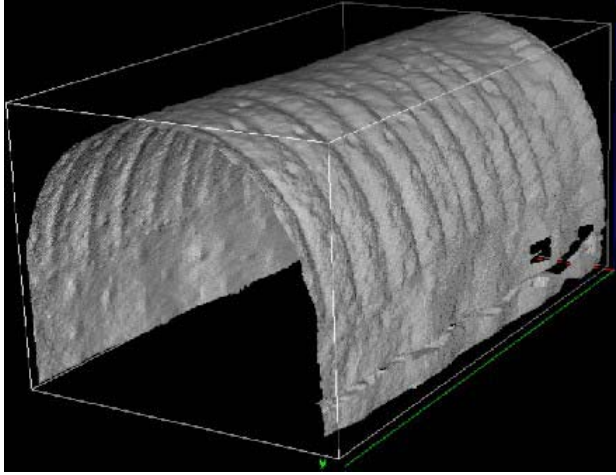


Fig. 5. Laser scan survey of the Plabutsch road tunnel near Graz, Austria. (From: Riegl, 2003).

Rock Face Surveying

Another practical example where 3D terrestrial laser scanning may prove its benefit is in digital outcrop mapping and rock face surveying. Obviously, with this technique rock faces, for example, along highways, can be surveyed without having to be near to the actual rock face and without disturbing or endangering the traffic. In addition, rock faces that are difficult to access can be measured without complicated and expensive installations such as scaffolding. The survey data may be used through 3D visualisation techniques and the creation of 2D profiles to assess the stability of slopes, to determine the location of potential loose blocks, and in order to determine optimal stability measures. Two examples of laser scan surveys of rock faces are given below in Figure 6 and 7.

Digital Outcrop Mapping

Digital outcrop mapping using laser scanning is an identified topic for research. The focus is on determination of rock and soil mass parameters, particularly discontinuity information, using laser scan surveys of discontinuous rock or soil masses. Research is currently under way at ITC (Slob et al., 2002) and the University of Arizona (Monte et al., 2003). This research is aiming to extract more information from the 3D point cloud data than merely the geometrical aspects. Through connecting point clouds using surface reconstruction techniques, the shape of scanned rock or soil surfaces can be reconstructed in a vector format (Figures 8 and 9).

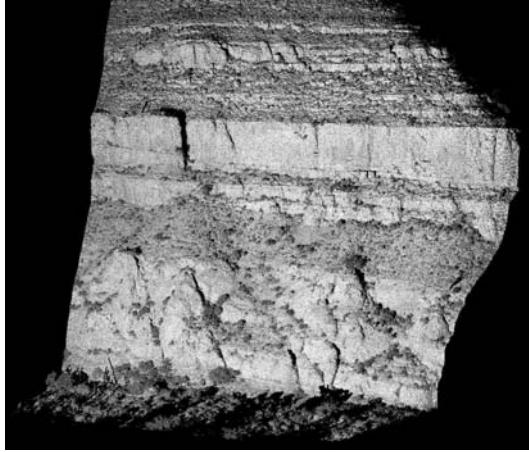


Fig. 6. 3D digital rendering of a point cloud of a high rock face made with an Optech Ilris laser scanner. The intensity of the reflected laser beam (brightness) gives an almost photo-realistic image. (From: Optech, 2003).



Fig. 7. 3D digital rendering of a point cloud of a limestone cliff along the westcoast of France made using a Riegler LMS-Z420i system. Each individual point in the “cloud” is coloured using a high-resolution digital camera. (Data: Riegler).

The reconstructed digital rock or soil surface is composed of a very large number of small triangles or facets. The shape of many exposed rock or soil surfaces (the angularity) is determined completely or for a large part by the discontinuities inherent to the rock or soil mass. The digital facets are then part of a discontinuity surface. Because of the high data density of the laser data, it is possible to have for a single rock outcrop thousands to millions of facets. Consequently, this allows a similar amount of orientation calculations, which will provide a very solid basis to

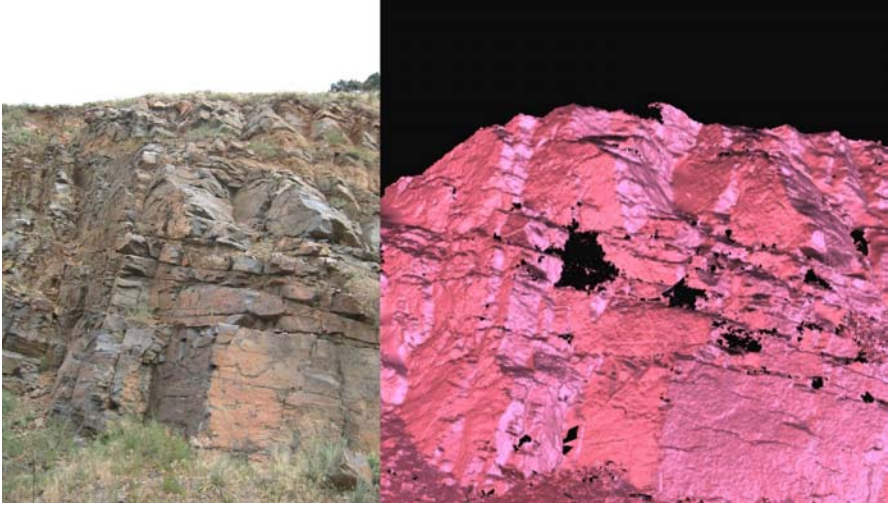


Fig. 8. Reconstructed rock surface on the basis of a laser scan survey using the first generation Cyrax laser scanner. On the left is the actual rock face. (Data: 3D Scan LLC, USA).

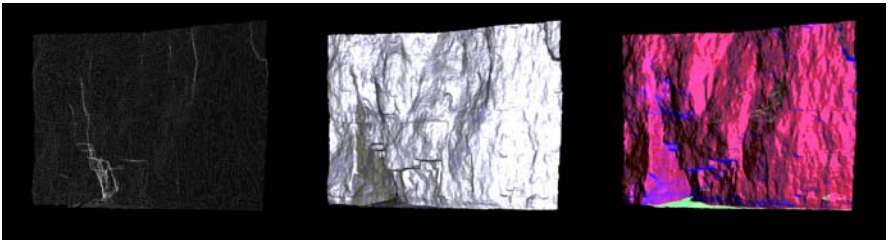


Fig. 9. From a 3D point cloud (left) to a reconstructed 3D surface, visualised using different digital rendering techniques on the right. (Data: Riegl, Austria).

statistically analyse the discontinuity information of any exposed rock mass. The orientation of each individual facet can be calculated it is possible using simple geometrical rules, to determine the orientation of each individual triangle. This is done through the calculation of the normal vector (pole), which is the cross product of any two of the three vectors that represent the sides of each triangle (see Figure 11). By statistical analysis, such as multivariate clustering analysis (Zhou and Maerz, 2001) or by plotting of the orientations of all the facets in a stereo net, the different discontinuity sets and their average orientations can be determined (Figures 10, 11 and 12).

Not only orientation, but also discontinuity spacing distributions, surface roughness (Figure 13), waviness, and other important rock or soil mass properties could theoretically be inferred. The reflected laser intensity (Figure 6), but also colour (Figure 7) can subsequently be used as additional data to classify the scanned rock or soil mass into homogeneous units.

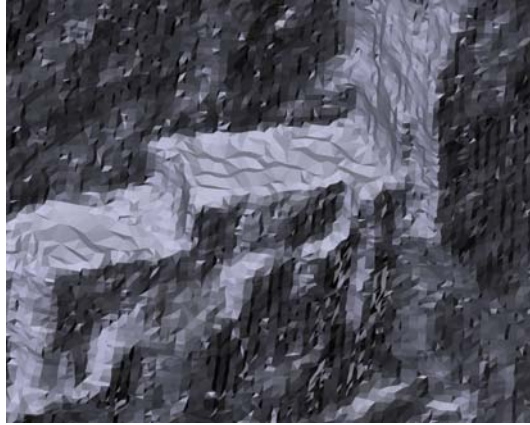


Fig. 10. A small section of the limestone rock outcrop (shown in figure 7), triangulated and rendered. This is analysed to identify possible discontinuity sets (see figure 11 below). Dimensions: approximately. 1.5 x 1.5 m.

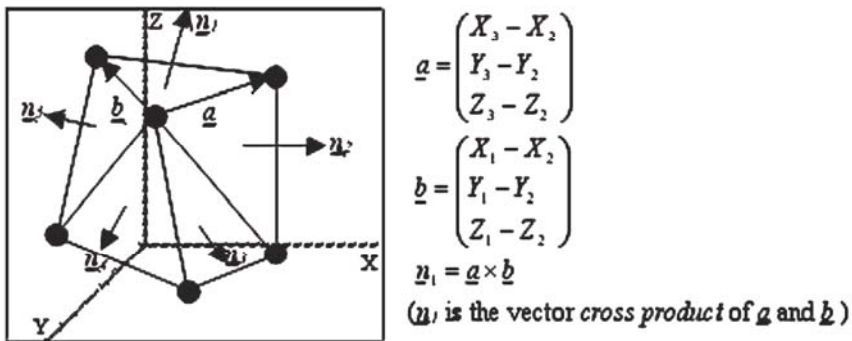


Fig. 11. Determination of normal vector of individual triangles using basic geometrical rules. The normal vector is used to calculate the orientation of each triangle (in terms of strike and dip).

Acknowledgements

The following persons are thanked for their kind assistance and contribution:

- Jürgen Nussbaum (Riegl, Austria) for supplying the limestone cliff data set from France (figure 7 and 9).
- Roger Moore (3D Scan LLC, USA) for supplying the Mt. Vernon data set from Colorado, USA (figure 8).
- Jan Berends (Geometius, The Netherlands) for supplying the image of the Wilnis dike burst (figure 4).

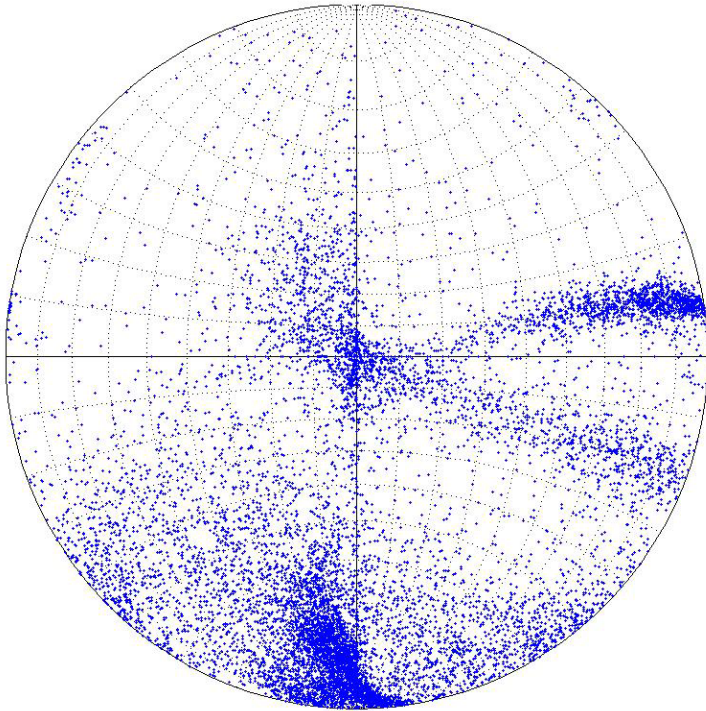


Fig. 12. A polar plot of all individual facets (about 10.000) composing the small rock outcrop from figure 10. It is evident that several discontinuity sets can be distinguished.

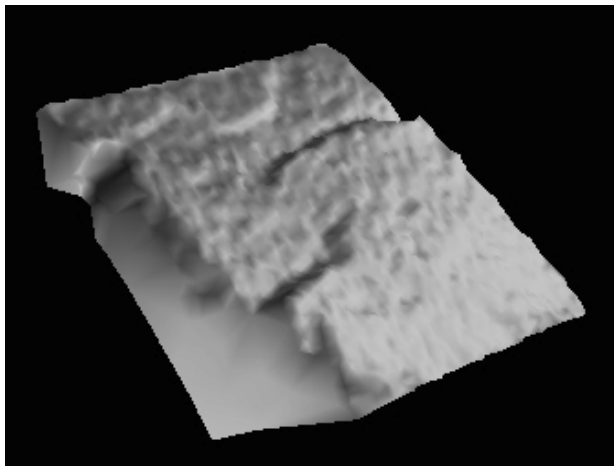


Fig. 13. Detail of a rock face scan (Mt Vernon data set), where surface roughness can easily be observed.

References

- Anonymous (2003) 3D Model van dijk in Wilnis. VI Matrix oktober 2003.
- Cowan EJ et. al. (2002). Rapid geological modeling. Applied Structural Geology for Mineral Exploration and Mining, International Symposium, Australian Institute of Geologists, International Structural Conference, Kalgoorlie, WA, Australia, 23-25 September 2002.
- Leica (Cyra) (2003) Cyra Technologies - 3D Laser Scanning. <http://www.cyra.com>
- Mensi (2003) MENSİ - 3D laser scanner / 3D scanners for surveying applications. <http://www.mensi.com>.
- Monte J, Kemeny J and Nasrallah J (2003) Using laser scanning and photogrammetry to collect rock discontinuity data for slope stability analysis. AEG News, Program with abstracts. 2003 Annual Meeting, Vail, USA.
- Optech (2003) Manufacturer of Laser-Based Ranging, Mapping and Detection Systems. <http://www.optech.on.ca>.
- Riegl (2003) Laser Measurement Systems. <http://www.riegl.co.at>.
- Slob S, Hack HRGK and Turner AK (2002). An approach to automate discontinuity measurements of rock faces using laser scanning techniques. ISRM International Symposium on Rock Engineering for Mountainous Regions. Eurock 2002 Funchal, Portugal.
- Zhou, W. and Maerz, N.H. Rock Mechanics and Explosives Research Center, University of Missouri-Rolla. Multivariate Clustering Analysis of Discontinuity Data: Implementation and Applications Rock Mechanics in the National Interest; Proceedings of the 38th U.S. Rock Mechanics Symposium, Washington, D.C., July 7-10, 2001, pp 861-868.

Engineering Geology in International Dredging and Infrastructure

Keynote

Willem. J. Vlasblom

Delft University of Technology, Faculty of Mechanical Engineering and Maritime Technology, section Dredging Engineering, Delft, The Netherlands
W. J. Vlasblom@wbmt.tudelft.nl
Tel: +31 15 2783973
Fax: +31 15 2782492

Abstract. Engineering geology supports the execution of dredging works in all stages. An industry that takes the full profit of his knowledge is the international dredging contractor. Based on own experiences the importance of his work is emphasised in a number of cases. Finally, a number of future developments in which he shall play an important role are highlighted.

Keywords: dredging, quality, volume, control, transparent, soil, rock, wear

Introduction

From start of the steam engine in the late 19th century up to Second World War, the mechanical engineer dominated the dredging possibilities. Strength and wear dominated the output of the dredgers. After the world war and in the Netherlands after the big flood in 1953 knowledge of the dredging processes took over the importance of mechanical engineering and it was the civil engineer who became more and more important. Geological knowledge was important only on jobs outside areas with experimental knowledge about the shallow sub-surface geology. Today international dredging contractors are working all over the world and the Engineering Geologist makes it possible to build infrastructures without big problems with production and wear of the dredgers. Nowadays, Engineering Geologists are involved from the tender stage until completion of large infrastructure jobs as:

- The New International Hong Kong Airport (Figure 1)
For which 950 ha of land was reclaimed. Preceding to the reclamation, 70 Mm³ of unsuitable material was removed to reach the alluvial layers with sufficient bearing capacity. The reclamation required 75 Mm³ from marine and 35 Mm³ from land sources. To extract the marine sand dredgers removed another 120 Mm³ of unsuitable material.



Fig. 1. The New Hong Kong International Airport under construction.

- The extensions of the industrial area's in Singapore (Figure 2)
A number of large reclamation projects are carried out and still under construction in Singapore. The total reclaimed volume in the last 4 years is more than 700 Mm³. To fulfil these volume requirements a part of the sand had to be extracted from borrow areas from which some were more than 100 km away from Singapore.
- The Betuwe Route in The Netherlands (Figure 3).
The Betuwe Route is a 160 km long, two tracks railway, from the North Sea to the German border. The route includes 5 tunnels, of which 3 are bored in soft soil. It required 16 Mm³ sand, mainly and inland sources. To reduce the sound hindrance, 60 km acoustic screens are placed.

All examples of large infra structural works require good insight in the local geology besides the geo-technical properties of the soil. For the (Engineering) geologist and for the dredging people this has always been obvious, but in the past, this was certainly not the case for the designers of infrastructure works. In the sixties and seventies of the last century it was quite normal when a contractor had to bid for dredging of a harbour that had only boreholes available on places where quay walls, sheet piles or buildings had to be constructed. So his bid for dredging the harbour was based on the assumption that the soil in the dredging area was in dredgeability comparable with the soil outside the dredging area. Consequently, this resulted in claims frequently. Although, it still happens today it is certainly an exception and not common any more.



Fig. 2. Reclamation work at Singapore.



Fig. 3. The Basement for Betuwe Route.

The Engineering Geologist

In the dredging world, the Engineering geologist has come to a stay. As said, he is involved in all steps from pre-tendering to the execution of the dredging jobs. Due to his geological knowledge, he reduces the (financial) risks related to the interpretation of the soil for dredging purposes.

Pre-tender Stage

The engineering geologist has to be involved in the pre-tender stage, particular in the soil investigation for the construction and foundation of infrastructure works. This includes also the sand-borrow areas necessary to construct the structures. Important in this stage is to give dredging contractors the opportunity to attend the soil investigation and to ask for the requirements. The engineering geologist can give the necessary geological description of the soil or rock mass in the dredging areas and he needs to check whether the laboratory test are executed according to the classifications.

Tender Stage

In this stage, a number of things can go wrong at the contractor's side, such as:

- Interpretation of soil or rock mass information is not correct.
- Frequently, data is averaged over geological areas with a different history. This may result in great differences between estimated and realised productions.
- Overlooking possible differences between several soil and rock investigation programs due to better drilling and test methods
- Overlooking the importance of the minerals in the soil or rock mass for wear (rock) (Verhoef, 1997) or adhesion problems (clay)

Some Examples

In many cases the productions of cutter suction dredgers is determined by the available power on the cutter head of the dredger used. Therefore the ratio of used (not installed) power over the production, called Specific Energy (SPE in $\text{Watts/m}^3/\text{s}$ or Joule/m^3), is an important parameter for the production estimator. As long as the relation between specific energy and a geo-technical parameter is linear, it is allowed to calculate the productions by transformation of the mean value of the geo-technical parameter to a mean specific energy value. However, one should not forget the additional condition that the cutting process does not change within the range of the geo-technical parameter. For instance to estimate the production of a cutter suction dredger dredging rock, the estimator needs information about the strength (compressive and tensile), the fracturing and the minerals in the rock. The ratio compressive strength over tensile strength deter-

mines how the rock fails, brittle or ductile. Ductile failure requires much more specific energy than brittle failure and results therefore in less production. Besides, ductile failure leads to high temperature wear with much higher wear rates. The fracturing is important whether to know if the strength is important at all. If the rock is much fractured (spacing smaller than the depth of the cutting tool) the strength of the rock is not decisive for the production and if the rock is intact, the strength is very important.

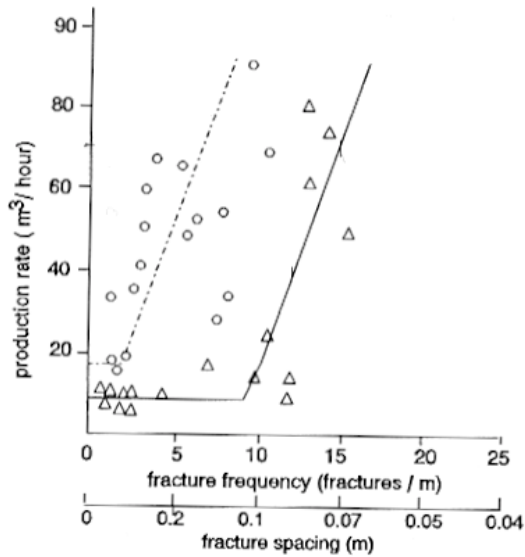


Fig. 4. Relation between production and fracture spacing (Data from Fowell & Johnson, 1991).

The minerals in the soil or rock mass determine the wear rate of the cutting tools and thus the downtime of the dredger to change cutting teeth and/or the cutter head. An increase of quartz contents may give an exponential increase in wear. Adhesion is important when the clay sticks to the cutting tools. Frequently, the strength and fracturing vary widely in the dredging area without any relation to the place or space. Therefore, the estimator uses mean values to arrive to the dredging parameter SPE. To do this he can step into “trap-falls”:

1. Taking the mean of the geo-technical parameter is allowed only when the soil or rock mass is from the same origin and has the same degree of weathering. Different soils or rock types with a different origin may change the failure mode and so the required energy necessary for failure. The present internal texture of the soil or rock is a result of weathering and sea level changes in the past; so different units can have different degrees of weathering. Weathering and/or fracture spacing has more influence on the production than the intact rock strength.

2. Different rock investigation programs.

In recent years, the quality of the rock investigations offshore is much improved. The influence of, for example, movement of the bore string by wave impact has been reduced and consequently the core may be less broken than in the past. Resulting in a higher mean strength and a higher RQD value or lower fracture index of the rock mass than in older investigations. If the relation between the geo-technical parameters to specific energy is based on the older data, it is obvious that productions estimates may be erroneous.

It is certainly true that the engineer geologist is more aware of these problems than the production estimator is.

Pre-execution

Its role in the pre-execution of dredging projects is to minimise the risks or to optimise the operations related to the soil or rock mass information. During the execution of the site preparation contract for the New Hong Kong International Airport the sand for the reclamation came from different indicated borrow areas (Plant et al. 1998). After having studied the soil information the geologist was not sure whether a marine clay layer overlaid the sand. An additional investigation showed a thick alluvial clay layer to be present. Before extracting the sand from this pit, the execution method could be changed in time.

For optimising reasons an additional soil investigation was executed in borrow area Po Toi too. The additional information was a reason to change the executing method, which resulted in a higher production of the hopper dredgers and more sand extracted from the pits.

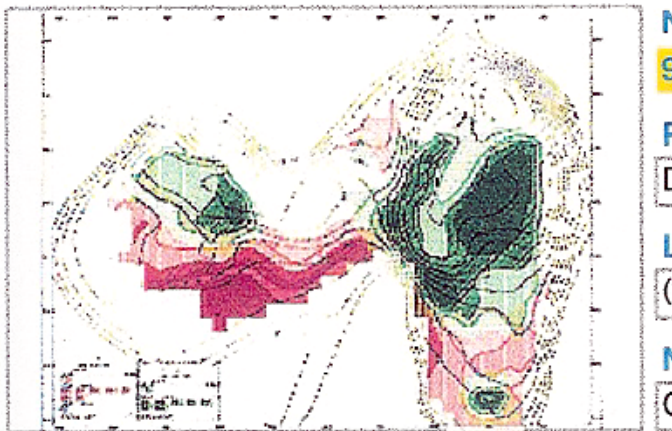


Fig. 5. The clay layer (green) in borrow area East Sha Chau.

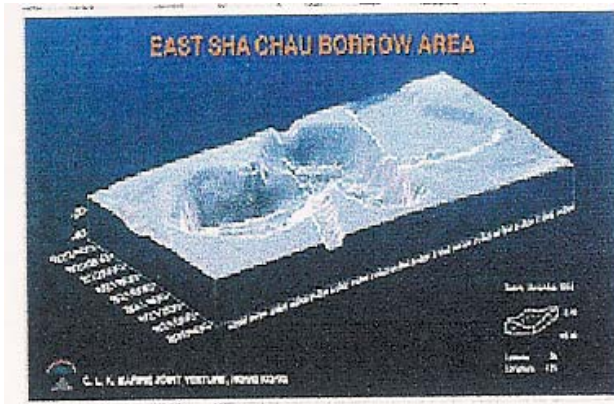


Fig. 6. Borrow area East Sha Chau during extraction.

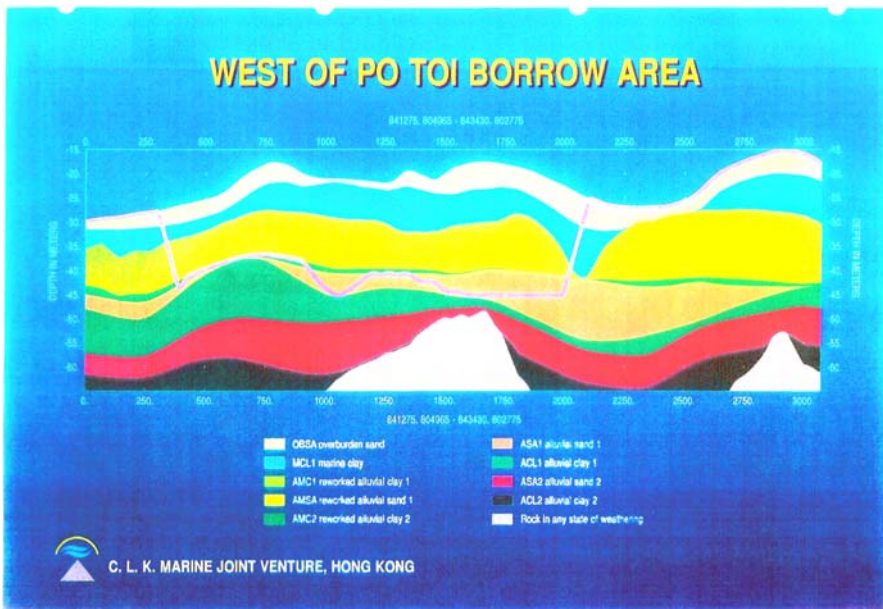


Fig. 7. Geological profile over Borrow area West of Po Toi.

During Execution

Besides the soil or rock mass information for the dredgers, the engineering geologist can play an important role in Volume and Quality Control. To explain this more in detail data from the case Chek Lap Kok Hong Kong is used again (Vlasblom 1999).

Volume Control

Control of the dredged volumes and levels was reached by using the geo-statistical visualisation software package BLUEPACK (Best Linear Unbiased Estimator), developed by the Centre de Geostatistique at Fontainebleau France. This software package was used extensively on this project. In the tender phase much work was done already with this package, so it was evident to continue with the models created with this software from the platform area as well as from the borrow pits. In the platform BLUEPACK was used to calculate the so-called 500 kPa levels (Base of unsuitable material) using CPT data. The Client provided this CPT data in the tender phase as levels picked from some 3500 CPT tests. These levels were used to krig (a statistical interpolation) a regular grid and were accepted by the Client. This grid combined with grids derived from land and marine surveys as well as the supplied formation levels gave the needed quantity information. (Figure 8).

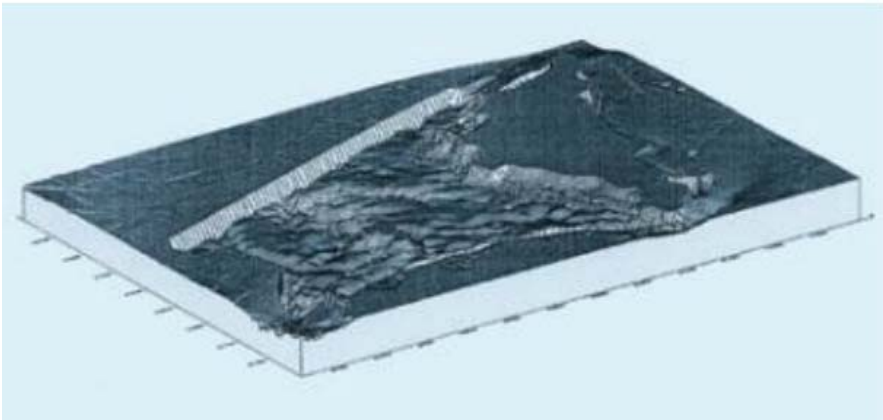


Fig. 8. Dredge levels of the Airport Platform Area.

Quality Control

The sampling of the marine fill in the reclamation area was originally planned to consist of continuous vibrocores down to dredge levels in a 50 m grid. This would mean that many thousands of vibrocores (land and marine- !) would be needed. All cores had to be tested (sieve analysis) and kept for further reference. This would have resulted in severe logistical difficulties with several rigs on site, onsite logging, sample storage, and analysis and management of test results. Cone penetration Tests (CPTs) can provide the same information (and more) in a faster, cleaner and more manageable way. Cone resistance, friction ratio and pore pressure give adequate information on the nature, density, and fines content of the fill material. Although the contractor was aware that he had to reinforce his attention to the fill quality, the switch over from vibrocores to CPTs giving the reduction of

the logistical problems was more important. In order to convince the Client, a trial area was chosen (BI/3) where 14 vibrocores and CPTs were carried out at the same location. The results showed that CPTs can be used and are even preferable, as CPTs have no ambiguity because of core losses and bad recovery as vibrocores can have. To approve the fill material however, the contract requirements had to be changed. The requirement applicable to vibrocore samples was a fine content of less than 20 %. This requirement had to be translated to CPT-values. The following agreement was made on required cone and sleeve resistance and pore pressure to approve the fill. The fill material complied with the Specifications if:

- The friction ratio was less than 0.45 %,
- The deviation between pore pressure and hydrostatic pressure was no more than 0.2 bar, or
- The cone resistance was not less than 4 MPa, or
- The fines content in the gradings were less than 20%, when vibrocore samples were taken.

Non - compliance of any test was based on a continuous length of 1.00 m or 10 % of the total test length, should more than one non-complying interval of less than one metre have occurred. These Specifications were applied to every CPT. If a CPT appeared to be out of those specifications, a vibrocore could be taken and if the samples did not meet the requirements, the extent of the non-complying area had to be determined by additional CPTs. The CPT testing grid had a 100 m spacing and the marine CPTs in the seawall areas had a 75 m spacing. It was also agreed to carry out a limited number of vibrocores on land in a grid with 200 m spacing to supply additional samples to the Client. This also provided a means of continuously comparing the CPT results with physical samples obtained from the vibrocores, because the vibrocores were taken at the same location as the CPT tests. This resulted in more than 600 CPT tests and more than 40 vibrocores. Figure 9 shows a map of these CPT locations as used on site. The contractor's attention on forehand for the quality of the fill, during the design of the borrow pits paid off: none of these tests failed!

The Airport Authority obtained important and relevant geo-technical information regarding the quality of the sand fill from the extensive series of CPTs too. CPT results can be fed directly into many geo-technical calculations like settlements, bearing capacity, liquefaction potential, and relative density. A direct correlation to these parameters is never possible by a visual interpretation of the vibrocores. In new contracts, it is advisable to express the quality requirements of the fill directly in CPT results and not in SPT blow count or Proctor density.

In Situ Density Testing

According to the contract, the upper 4 m of the platform should be compacted to a Proctor Density of more than 95 %. The fill material had to be tested for every 50 cm layer. Because the Type C material (marine sand) was placed hydraulically, the material could only be tested at the surface. It was agreed that Test 15B of BS

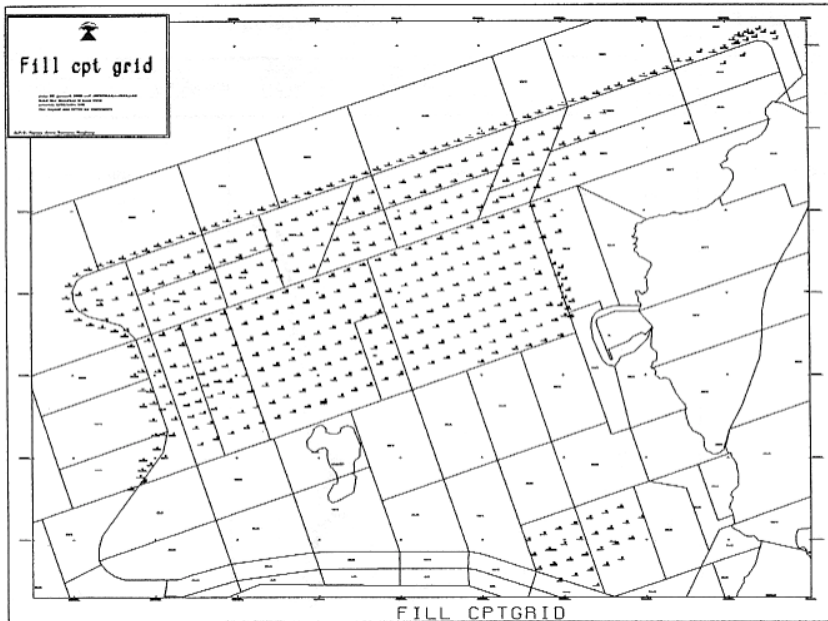


Fig. 9. CPT grid for quality control of the reclamation.

1377 (sand replacement method with large pouring cylinder) would be used to determine the density at the surface in the areas where only capping was carried out with marine sand. More than 50 of these tests were carried out in the capping layer. All tests showed Proctor Densities of more than 95%. It is important, however, that the surface of the test area is not disturbed and that the test is carried out with great care. In areas where sand was placed in a much thicker layer this in situ test was not sufficient. It was suggested to use the CPT results from the quality control programme to determine whether the required density was obtained. Before this proposal was accepted, it was necessary to prove the suitability of CPTs and to determine a criterion applicable to CPTs to replace the 95 % Proctor Density criterion. This resulted in some extensive testing (22 CPTs & 27 sand replacement tests) in a trial area. Figure 11 shows that the 95 % Proctor Density corresponds with 53 % Relative Density. This is in accordance with literature values.

Future Developments

1. Transparent soil or updating soil information while dredging.

Dredging is the best soil investigation, but how to use machine data to update the soil info?

Existing soil investigation by boreholes, seismic, CPTs, etc. is in most cases

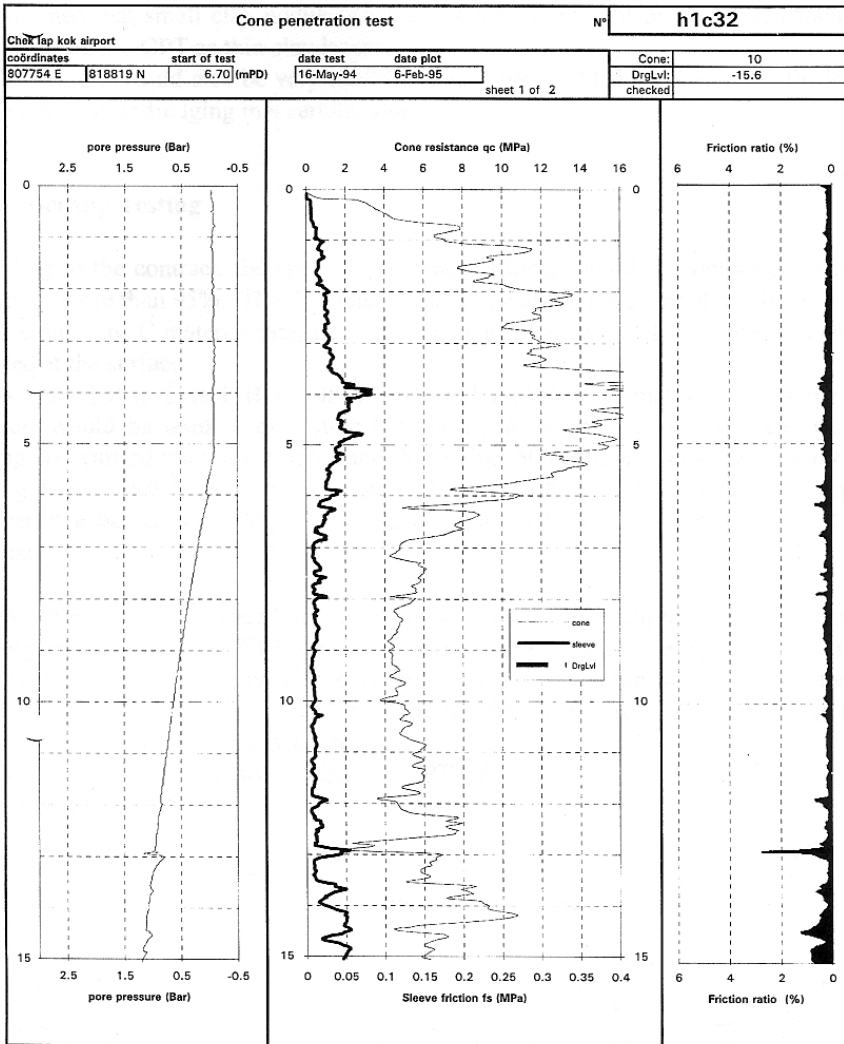


Fig. 10. CPT test showing over the fill.

insufficient to get an accurate 3D picture of the soil. This can result in differences in local engineering properties of the soil than measured or expected that induces more risk in dredger productions, but also in more risk for constructions such as quay walls, jetties, slopes, etc. Finally, differences result in bases for claims. The production of a dredger is estimated with the use of geotechnical data. When inverting this process, geo-technical data may be estimated from the production by measuring the decisive dredgability factors. Such a development is not only of interest in the field of dredging but also for tunnelling pur-

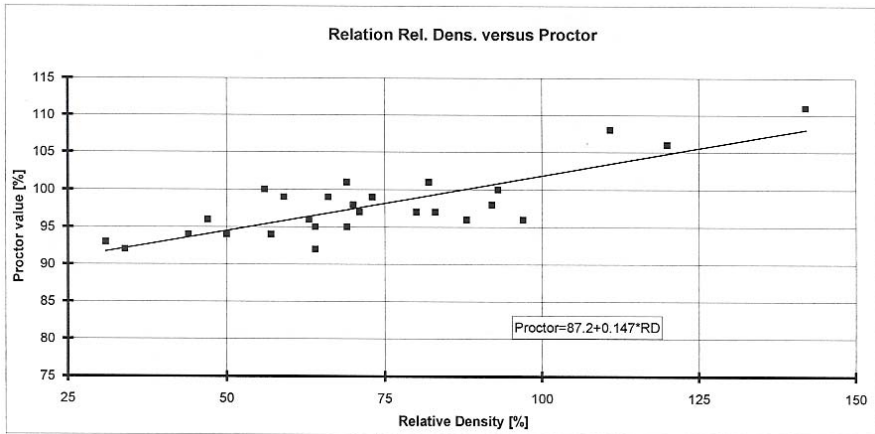


Fig. 11. Relative density versus measured proctor density.

poses. (Integral Tunnelling Control System). Preliminary studies to such systems have been done by Siezen (1996), Orlic (1997) and Brugman et al. (1999), and showed that such systems could be very beneficially for the industry.

2. Wear.

New developments in measuring wear and calculation techniques (Discrete Elements Methods) can improve the wear models considerable. Now it is possible to measure the thickness of pipelines in several micrometers. With the aid of discrete element methods, it is possible to estimate the forces of sand particles exerted on the pipe wall. These to developments open the way to new and more accurate wear models.

Conclusions

The conclusion is very simple and short; the engineer geologist in indispensable employee for an international dredging contractor. His profession fills the gabs in the relation between the geology and the geo-technical parameters important for the production and wear of the dredging equipment.

References

- Brugman MHA, Hack HRGK & Dirks WG (1999) A three-dimensional system for estimation of dredging production in rock (Een drie-dimensionaal systeem voor de raming van baggerproducties in rots). *Geotechniek*, april. pp. 22-26. (in Dutch).

- Fowell RJ & Johnson ST (1991) Cuttability assessment applied to drag tool tunnelling machines. Proc. ISRM International congress on Rock Mechanics, Aachen, Germany, Vol. 2: pp 985-990. Balkema Rotterdam.
- Orlic B (1997) Predicting subsurface conditions for geotechnical modelling. PhD thesis Technical University Delft, ISBN 90-6164-140-3 (ITC Publication ; 55) (ITC Dissertation ; 46). Pp.192 pp.
- Plant GW, Covil CS & Hughes RA (1998) Site preparation for the new Hong Kong International Airport, Thomas Telford, ISBN 0-7277-2696-X.
- Siezen MR (1996) A 3D Dredgeability Classification system, Master thesis Faculty of Applied Earth Sciences. Memoir of the Centre for Engineering Geology in the Netherlands, No 140.
- Verhoef PNW (1997) Wear of rock cutting tools, A.A, Balkema/Rotterdam/Brookfiels, ISDN 90 5410 434 1 t.
- Vlasblom WJ (1999) Production and quality control aspects during excavation of reclamation works at Chek Lap Kok. Terra at Aqua No. 74, March 74, pp. 21-27, ISSN 0376-6411.

Prediction of the Uniaxial Compressive Strength of a Greywacke by Fuzzy Inference System

Kıvanc Zorlu¹, Candan Gokceoglu², and Harun Sonmez²

¹ Mersin University, Department of Geological Engineering, 33342 Ciftlikkoy Mersin Turkey

² Hacettepe University, Department of Geological Engineering, Applied Geology Division 06532 Beytepe Ankara Turkey
cgokce@hacettepe.edu.tr
Tel: +90 312 297 77 35
Fax: +90 312 299 20 34

Abstract. Rock engineering projects require the uniaxial compressive strength of intact rock. High quality core samples are needed for the application of uniaxial compressive strength in laboratory. In this study, to establish some predictive models taking into consideration multiple regression techniques and fuzzy inference system is aimed. Ankara greywackes is selected as the material, because of its highly problematic nature as mentioned by many previous researchers. For this purpose, a series of rock mechanics tests were carried out, and uniaxial compressive strength, point load index, block punch index, unit weight, apparent porosity, water absorption by weight, P-wave velocity, Schmidt hardness and tensile strength of greywacke were obtained. Using the obtained results, two prediction models were constructed to predict the uniaxial compressive strength of selected greywacke. The values account for and root mean square error indices were calculated as 41.49% and 15.62 the multiple regression model; 81.24% and 13.06 for the fuzzy inference system. As a result, these indices revealed that the prediction performances of the fuzzy model are higher than that of multiple regression equations.

Keywords: empirical relationships, fuzzy inference system, multiple regression, prediction, uniaxial compressive strength

1 Introduction

Indirect estimation of the mechanical parameters of thinly bedded and highly fractured rocks is one of the major study areas of the engineering geologists and rock engineers. The highly fractured greywackes crop out Ankara, capital city of Turkey. A dense urbanisation occurs and population rapidly grows in Ankara. For this reason, many engineering projects are planned and constructed, and the geomechanical properties of the greywackes are increasingly needed. Due to its problematic nature, the core samples required for the uniaxial compressive strength can not extracted easily. The purpose of the present study is to establish regression and fuzzy models for predicting the uniaxial compressive strength of the Ankara greywackes, using some simple index tests such as point load, block punch index etc., because these tests require relatively small samples.

2 Sampling and Test Results

A reliable prediction model requires sufficient number and high quality data. In this study, an extensive field study was performed to select the blocks to be used in the standard core preparation workings in laboratory. Although approximately 200 blocks were collected from the field, only 82 sample sets for the rock mechanics tests were obtained in accordance with the procedures given by ISRM (1981), ISRM (1985) and Ulusay et al. (2001). Each data set includes uniaxial compressive strength, point load index, block punch index, unit weight, and apparent porosity, water absorption by weight, P-wave velocity, Schmidt hardness, and tensile strength.

3 Prediction Models

To predict the uniaxial compressive strength (UCS) of the Ankara greywacke, some prediction models were established based on multiple regressions and fuzzy inference system.

3.1 Regression Analyses

The simple regression analyses were performed to define type of the relation between dependent and independent parameters by considering linear, power, logarithmic, exponential functions. The relations were given in Table 2 with their

Table 1. The summary of the test results (number of data=82).

Statistical Parameter	Unit Weight	Water Absorption by Weight	Apparent Porosity	P-Wave Velocity	Schmidt Hardness	Block Punch Index	Point Load Index	Tensile Strength	Uniaxial Compressive Strength
Minimum	23.6 kN/m ³	0.2%	0.57%	2463.1m/s	29	4.0MPa	0.46 MPa	2.8 MPa	17.5 MPa
Maximum	27.6 kN/m ³	3.3%	7.96%	5800 m/s	53	32.7 MPa	6.34 MPa	13.7 MPa	156.0 MPa
Average	25.4 kN/m ³	1.03%	2.60%	4321.1 m/s	40	16.5 MPa	3.12 MPa	6.7 MPa	58.5 MPa
St.Deviation	0.92	0.67	1.61	1.61	6.63	6.93	1.46	1.46	26.5

Table 2. Correlation coefficients of the simple regressions between the uniaxial compressive strength and the other parameters.

Independent Variable	Uniaxial Compressive strength, UCS			
	Number of data: 82			
	Type of function			
	Linear	Logarithmic	Power	Exponential
Unit Weight	0.26	0.26	0.27	0.27
Water Absorption by Weight	-0.42	-0.37	-0.44	-0.49
Apparent Porosity	-0.42	-0.37	-0.44	-0.49
P-Wave Velocity	0.52	0.52	0.56	0.56
Schmidt Hardness	0.50	0.51	0.52	0.51
Block Punch Index	0.71 [*]	0.67 [*]	0.71 [*]	0.71 [*]
Point Load Index	0.64 [*]	0.57	0.58	0.63 [*]
Tensile Strength	0.65 [*]	0.62 [*]	0.62 [*]	0.62 [*]

^{*}Statistically significant at P=0.05 level

correlation of coefficients. The UCS values exhibit much more meaningful relations with block punch index (BPI), point load ($Is_{(50)}$) and tensile strength (σ_t) than the other parameters. In addition, the relationships between the uniaxial compressive strength and unit weight, P-wave velocity, Schmidt hardness are not meaningful, although many previous researchers (Sachpazis, 1990; Grasso et al., 1992; Gokceoglu, 1996) determined the relationships with high correlation coefficients. Rock type is an important consideration for the empirical relation between the Schmidt hammer rebound number and compressive strength values (Cargill and Shakoor, 1990). The P-wave velocity (V_p) was also used in the multiple regression analyses by considering slightly higher correlation coefficient among the other parameters. A multiple regression analysis was performed between dependent parameter (UCS) and independent parameters (V_p , BPI, $Is_{(50)}$ and σ_t). Consequently, the following relation was obtained:

$$UCS = 0.0065 V_p + 1.468 BPI + 4.094 Is_{(50)} + 2.418 \sigma_t - 225 \quad (r=0.80) \quad (3.1)$$

The crosscheck between the measured and the predicted values was illustrated in Figure 1. As can be seen in Figure 1, the multiple prediction model is more reliable than the simple regression equations. In addition, the determination of P-wave velocity, block punch index, tensile strength, and point load index requires relatively small samples when compared with the uniaxial compressive tests. For this reason, this predictive model based on multiple regression can be used in practical engineering purposes.

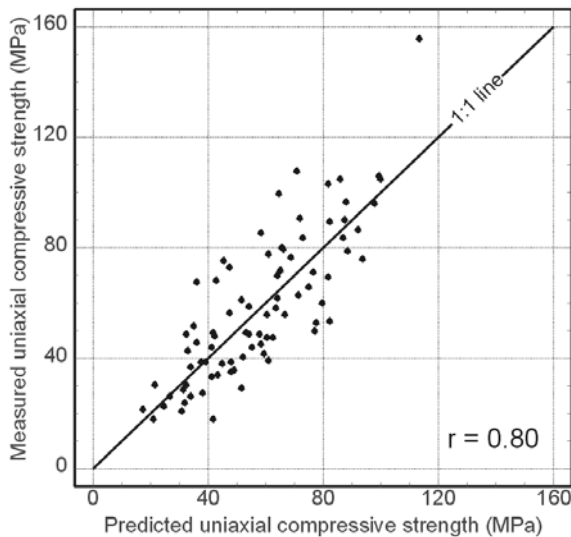


Fig. 1. The cross-check between the measured and the predicted uniaxial compressive strength values predicted from the multiple regression (Eq. 3.1).

4 Fuzzy Inference System

In the last years, the fuzzy inference systems began to be used in the areas of rock mechanics and engineering geology (e.g. Alvares Grima and Babuska, 1999; Finol et al., 2001; Gokceoglu, 2002; Sonmez et al., 2003 etc.). In this study, the Mamdani fuzzy inference system was employed to construct a prediction model for the uniaxial compressive strength of the Ankara greywackes. The model includes four inputs (P-wave velocity, block punch index, point load index, tensile strength) and one output (uniaxial compressive strength) (Figure 2). In this study, the fuzzy sets of the membership functions were obtained from the relationships between the inputs and the output. The graphical illustrations of the membership function are given in Figure 3 for the input parameters and Figure 4 for the output parameter. As shown in both Figure 3 and Figure 4, inputs and output parameters are normalized considering the highest values of them. Therefore, the range of both inputs and output vary between zero and one. The other component of a fuzzy inference system is the “if-then” rules. Total number of the linguistic rules of the fuzzy inference system constructed in this study is 53. Due to the calculation simplicity, the centroid method is considered for the defuzzification process. A typical example of the constructed fuzzy model with used if-then rules for given input values is illustrated in Figure 5. In other words, 5 of 53 if-then rules are used for the input values given in the example. The cross-correlations between predicted and measured data were applied (Figure 6) and the strong coefficient of correlation of 0.82 was obtained.

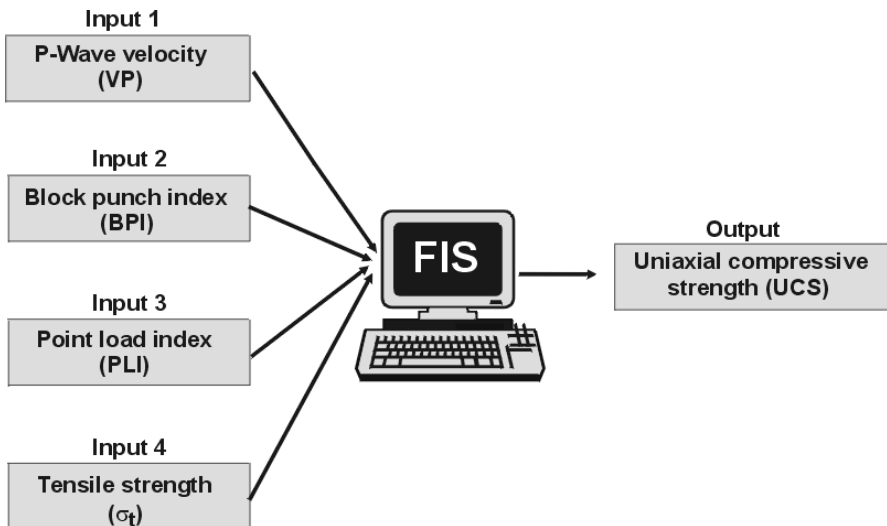


Fig. 2. The schematic illustration of the fuzzy inference model.

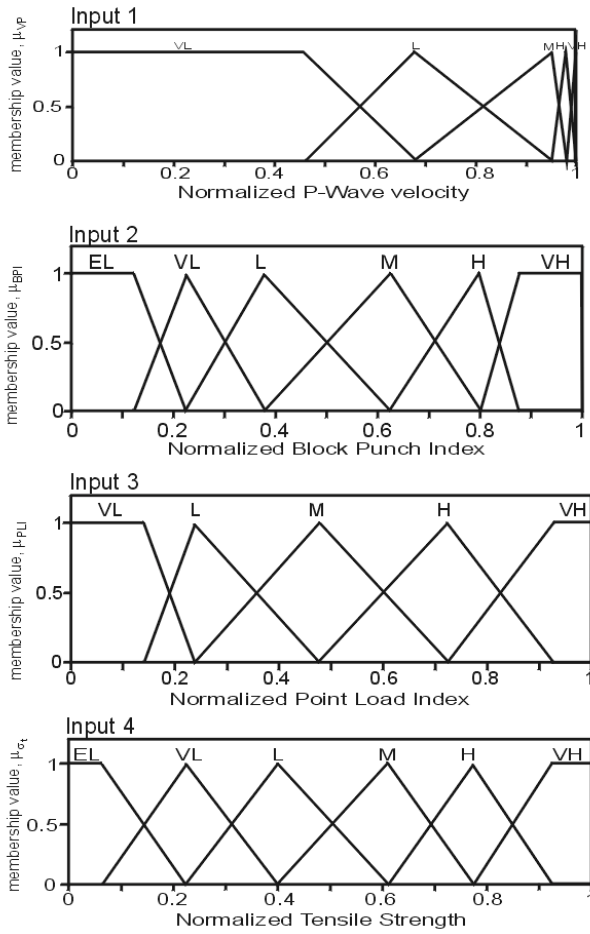


Fig. 3. The membership functions of the normalized input parameters.

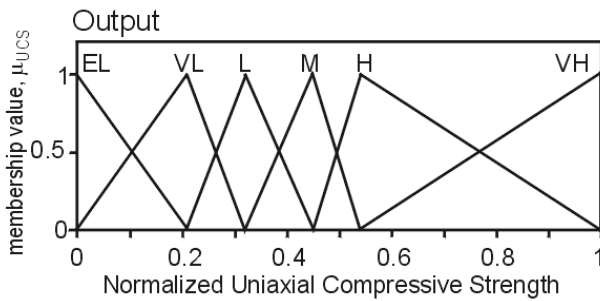


Fig. 4. The membership functions of the normalized output parameter.

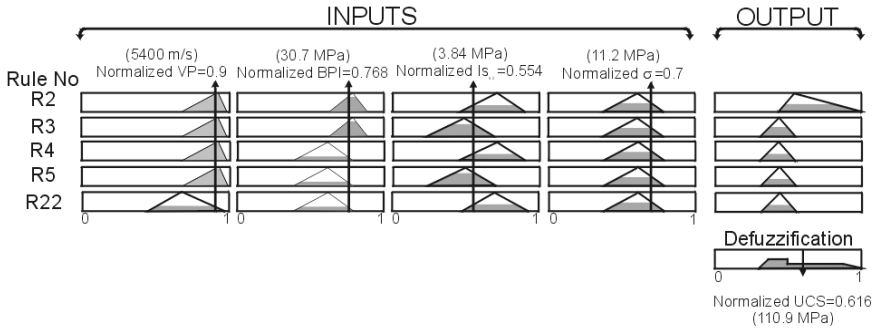


Fig. 5. An example calculation for the fuzzy inference model.

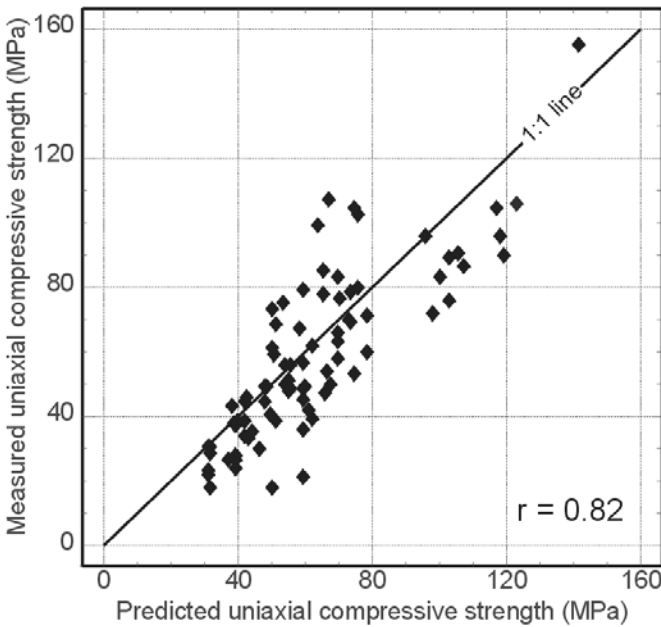


Fig. 6. The relation between the measured and the predicted uniaxial compressive strength values from the fuzzy inference system.

5 Assessment of the Prediction Performance

The variance account for (VAF) and the root mean square error (RMSE) indices were calculated to assess the prediction performance of the models developed in the study as employed by Alvarez Grima and Babuška (1999), Finol et al. (2001), Gokceoglu (2002) and Nefeslioglu et al. (2003). The calculated indices are given

in Table 3. If the VAF is 100 and RMSE is 0, the model will be excellent. When making a comparison between fuzzy model and multiple regression equation, the prediction performance of the fuzzy model is higher than that of the multiple regression model, taking into consideration the performance indices (see Table 3).

Table 3. The values account for (VAF) and the root mean square error (RMSE) indices of the prediction models.

Model	VAF (%)	RMSE
Multiple Regression	41.49	15.62
Fuzzy Inference System	81.24	13.06

6 Results and Conclusions

In this study, a multiple regression equation for the prediction of the uniaxial compressive strength were developed. In addition, a fuzzy inference system having four inputs, one output and 53 linguistic rules was developed for the same purpose. To assess the prediction capacities of the developed models, the values account for (VAF) and the root mean square error (RMSE) indices were obtained as 41.49% and 15.62 the multiple regression model; 81.24% and 13.06 for the fuzzy inference system. The fuzzy based model exhibited the most reliable predictions when compared with the simple and multiple regression models. The developed models have a sufficient capacity to use in practical purposes.

References

- Alvarez Grima M, Babuška R (1999) Fuzzy model for the prediction of unconfined compressive strength of rock samples. *International Journal of Rock Mechanics and Mining Science* 36, pp 339-349
- Cargill JS, Shakoor A (1990) Evaluation of emperical methods for measuring the uniaxial compressive strength of rock. *International Journal of Rock Mechanics, Mining Science and Geomechanical Abstracts* vol 27 (6), pp 495-503.
- Finol J, Guo YK, Jing XD (2001) A rule based fuzzy model for the prediction of petro-physical rock parameters. *Journal of Petroleum Science and Engineering* vol 29, pp 97-113.
- Gokceoglu C (1996) Schmidt sertlik çekici kullanılarak tahmin edilen tek eksenli sıkışma dayanımı verilerinin güvenilirliği üzerine bir değerlendirme. *Journal of Geological Engineering* vol 48, pp 78-81 (in Turkish).
- Gokceoglu C (2002) A fuzzy triangular chart to predict the uniaxial compressive strength of Ankara agglomerates from their petrographic composition. *Engineering Geology* vol 66, pp 39-51.
- Grasso P, Xu S, Mahtab A (1992) Problems and promises of index testing of rock. In: Tillerson and Waversik (eds.), *Rock Mechanics*. Balkema, Rotterdam, pp.879-888.
- ISRM (Internatinal Society for Rock Mechanics) (1981) *Rock Characterization, Testing and Monitoring: ISRM Suggested Methods*. E.T. Borwn (ed.), Pergamon Press, 211 pp.

- ISRM (International Society for Rock Mechanics) (1985) Suggested method for determining point load strength. *Int. J. Rock Mech. Min. Sci. Geomech. Abstr.*, vol 22(2), pp 51-60.
- Nefeslioglu HA, Gokceoglu C, Sonmez H (2003) A mamdani model to predict the weighed joint density. Palade V., Howlett R.J., and Jain L.C.: KES 2003, LNAI vol 2773, pp 1052-1057.
- Sachpazis CI (1990) Correlating schmidt hardness with compressive strength and Young's modulus of carbonate rocks. *Bulletin of the International Association of Engineering Geology* vol 42, pp 75-83.
- Sonmez H, Gokceoglu C, Ulusay R (2003) An application of fuzzy sets to the Geological Strength Index (GSI) system used in rock engineering. *Engineering Applications of Artificial Intelligence*, vol 16/3, pp 251-269.
- Ulusay R, Gokceoglu C, Sulukcu S (2001) Draft ISRM suggested method for determining block punch strength index (BPI). *Int. J. Rock Mech. Min. Sci.*, vol 38 (8), pp 1113-1119.

Self-healing of Fractures around Radioactive Waste Disposal in Clay Formations

Bjorn Debecker^{1,2}, André Vervoort^{1,2}, Jan Verstraelen^{1,2}, and Martine Wevers^{1,2}

¹ Research Unit Mining, KULeuven, Kasteelpark Arenberg 40, B-3001 Leuven, Belgium

² Department of Metallurgy and Materials Engineering, KULeuven

bjorn.debecker@bwk.kuleuven.ac.be

Tel: +32 16 321774

Fax: +32 16 321988

Abstract. The feasibility of storing radioactive waste in low permeable clays is studied extensively nowadays. Fracturing and healing of fractures is of great importance as they determine to a large extent the buffering properties for the transport of radionuclides. The research presented studies micro-fracturing and healing by recording acoustic emission in triaxial loading laboratory tests. The results show that increasing time delays between two successive loading cycles has an increasing effect on the recorded acoustic pattern. Future simulations with a boundary element code might enable to link the results closer to the mechanisms of micro-fracturing and self-healing.

Keywords: Self-healing of fractures, clay, acoustic emission, Kaiser-effect.

1 Introduction

Clay is one of the possible host rock formations for the underground geological disposal of radioactive waste. At several research sites in Europe, the feasibility of clay as a natural barrier for this type of storage is investigated. Around an excavation at least locally, stresses are redistributed resulting in possible fracturing at different scales (Mertens et al. 2002). The deterioration in permeability and strength due to these induced fractures imply the overall performance to decrease. However, under a triaxial stress state, these fractures might close over time and possibly be healed again. It is important that these mechanisms linked to fracturing and healing are well understood in order to predict the transport of radionuclides accurately over long time periods. At the KULeuven, the occurrence and possible healing of micro-cracks is studied by means of acoustic emission (AE) during laboratory tests. This research is done within the framework of the EU-SELFRAC project and examines the former phenomena in particular in Boom Clay from the Mol research site (B) and Opalinus Clay from the Mont Terri research site (CH). Other research groups within this project examine the evolution of porosity and permeability. The tertiary Boom clay is primarily a mixture of illite, smectite and kaolinite with some pyrite inclusions (Wouters and Vandenberghe, 1994). The laboratory samples are excavated at a depth of around 200m during the recent construction of the extension of the underground laboratory. The

Opalinus clay is a Mesozoic argillaceous formation consisting of ca. 55% clay minerals, 20% quartz and 25% carbonates (Mazurek et al. 2002). The samples for this study were excavated at a depth of around 300m.

2 Methodology

The laboratory experiments presented here are cyclic triaxial loading tests. During the entire testing, acoustic activity in the sample is measured. A constant external pore pressure is applied via the upper piston. When a rock is loaded, deformation energy accumulates in the rock. If the deviatoric load becomes sufficiently large, micro-cracks originate and energy is released. This energy release causes an elastic wave propagation, which can be recorded and is called a ‘hit’ (Lavrov et al. 2002). Recording of the hits allows quantifying the acoustic activity within the sample. The acoustic measurement is done by two sensors, attached to the upper and lower loading piston. The sensors measure all acoustic activity within a range of 100 – 2000 kHz. A threshold amplitude and amplification can be set in order to allow maximal resolution and filter the most apparent noise. Noise can be produced among other sources, by deformation of the loading frame or by friction between the pistons and platelets at the end of the sample. It is believed that most of this noise can be recognized on the acoustic data and be filtered as well. (Vanbrabant et al., 2002). Comparing absolute numbers of hits is only recommended within the same test. This is because the number of recordings does not only depend on acoustic emission, but also on the attachment of the acoustic sensor to the loading cell or sample. On the other hand, under a constant set-up, the stresses at which acoustic activity appears can be compared for different tests.

If a sample is uniaxially loaded until a given maximum load level, then unloaded and reloaded again to a higher load level, it is observed that in this second loading cycle acoustic activity starts at the previous maximum load level. This phenomenon is called the Kaiser effect and the ratio of the load at which AE starts over the previous maximum load, is called the Felicity ratio (Fr) (Figure 1). The Felicity ratio is thus a means of quantifying the Kaiser effect and a perfect Kaiser effect corresponds to a Fr of one (Holcomb 1993). The mechanism behind the Kaiser effect is that new micro-cracks only originate after the previous maximum load at which the rock was subjected, is exceeded. Before that, only existing mi-

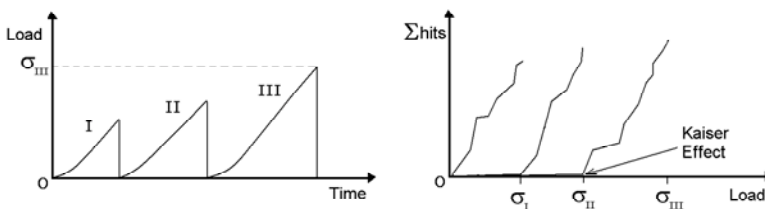


Fig. 1. (Theoretical) Kaiser effect in a cyclic loading test (left) as it is observed on a cumulative hits vs. load graph (right).

cro-cracks are reactivated, allowing limited energy release without any significant acoustic activity. The Kaiser effect thus serves as stress memory of the rock, however it is observed that this memory seems to deteriorate with time varying from several months to years (Korner and Lord 1989).

Under a triaxial stress state, the Kaiser effect depends not only on the maximal principal stress σ_1 , but also on σ_2 and σ_3 . For triaxial tests with $\sigma_3 = \sigma_2$, Lavrov (2003) determined the following relation:

$$\sigma_{IKE}^{II} - (k+1)\sigma_3^{II} = \sigma_{IMAX}^I - (k+1)\sigma_3^I \quad [1]$$

where I and II denotes respectively the first and second loading cycle and k is a rock-dependent dimensionless coefficient. However, if during the entire test the confining pressure $\sigma_3 = \sigma_2 = \sigma_{ISO}$ is kept constant, than this relation is reduced to $\sigma_{IKE}^{II} = \sigma_{IMAX}^I$, which is the same as for uniaxial tests. Note that Lavrov's discussion does not involve pore pressure, and thus the total stresses are equal to the effective stresses. The influence of the pore pressure on these relations are, as far as the authors know, not studied so far. The effect of applying a pore pressure on acoustic emission is double. On the one hand, flow through pores linked to an increase in pore pressure generates acoustic emissions. On the other hand, an increasing pore pressure decreases the effective stresses, which are responsible for the crushing in the solid. The net influence of pore pressure on acoustic phenomena is thus complex and yet not fully understood. Therefore, only total stresses are discussed further in the continuation of this text, as these are known with certainty throughout the tests.

It is believed that if micro-cracks close or possibly heal after a loading cycle, the acoustic behaviour is altered in the next loading cycle. If the sample is loaded a second time, new micro-cracks originate or closed ones reopen at a lower load level than the previous maximum load level. As a consequence, acoustic activity should appear earlier than in tests without healing. This is measured by decreasing Felicity ratio values. The applied loading procedure in this research starts with a triaxial isotropic loading ($\sigma_1 = \sigma_2 = \sigma_3 = \sigma_{ISO} = 5\text{MPa}$) during minimum 48 hours. An external pore pressure of 0.5 MPa is applied which remains constant during the entire test. This isotropic loading period is necessary because consolidation and saturation processes can generate initially much AE, but the hit rate (recorded hits per time) due to these processes becomes constant and low after such time periods. However, this does not imply that the samples are completely consolidated or saturated after these time periods. Afterwards, there is a first loading cycle whereby the confining stress and external pore pressure remain constant at respectively 5 MPa and 0.5 MPa, and the axial load is increased. Hereafter the axial load is decreased to the initial isotropic stress state ($\sigma_1 = \sigma_2 = \sigma_3 = 5\text{MPa}$), and after a given time delay a second loading cycle is applied. Often, a third loading cycle is applied immediately after the second one (Figure 2). Given the high loading rate (around 0.1 mm/min) and the low permeability of the clay, the loading cycles are considered to be rather undrained than drained. The tests examine if increasing time delays would generate decreasing Fr values.

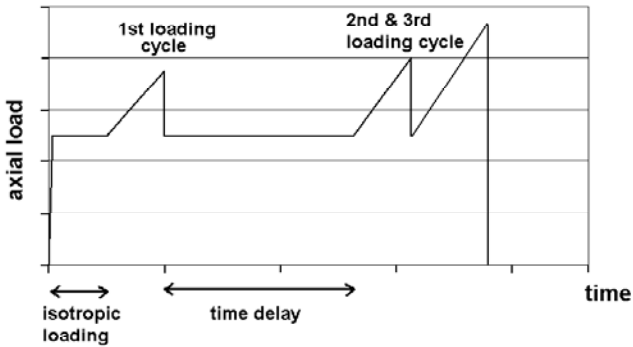


Fig. 2. Example of general cyclic loading scheme.

3 Discussion of Results of an Opalinus Clay Sample with a Time Delay of 22 Days

In this paragraph, one test on a Opalinus clay sample is discussed in detail, while in the following paragraph all tests so far on Opalinus and Boom clay are summarized. Figure 3 shows an overall view of the cumulative number of hits versus time during the entire test. The test consists of 3 days of isotropic loading, a first loading cycle, 22 days time delay and finally a second and third loading cycle. The hit rate during isotropic loading stabilises almost from the start at around 6 hits per hour. In the tests with Boom clay much initial consolidation noise was recorded during this isotropic loading (Debecker et al. 2003). An average hit rate of 6 hits per hour is also observed during the time delay between first and second loading cycle. The number of AE hits recorded during the loading cycles is relatively small in comparison to the total number of hits.

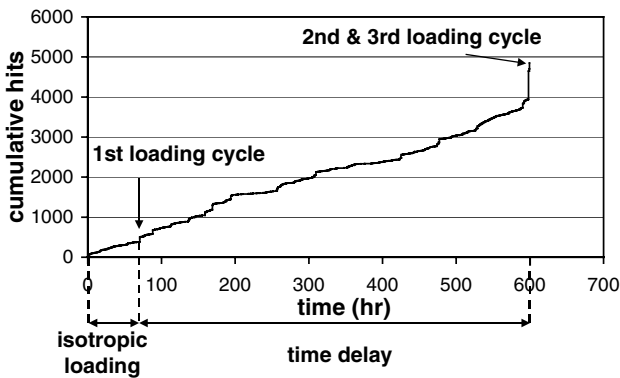


Fig. 3. Test on Opalinus clay sample: cumulative hits vs. time.

Figure 4 represents the three loading cycles and the corresponding acoustic measurements. In the first loading cycle (Figure 4a), the axial load was increased from the isotropic load value of 5 MPa up to 11 MPa and a total number of 118 hits were recorded (Figure 4b). A significant increase of acoustic activity started around 6 MPa. The hit rate in this first loading cycle is more or less constant at 2 hits per second (compared to 6 hits per hour during isotropic loading). After 22 days of isotropic loading at 5MPa, a second loading cycle up to 15 MPa was performed. A third loading cycle up to 17 MPa followed nearly immediately after the second one (Figure 4c). There were 78 hits recorded in the second loading cycle, and 40 in the third loading cycle (Figure 4d).

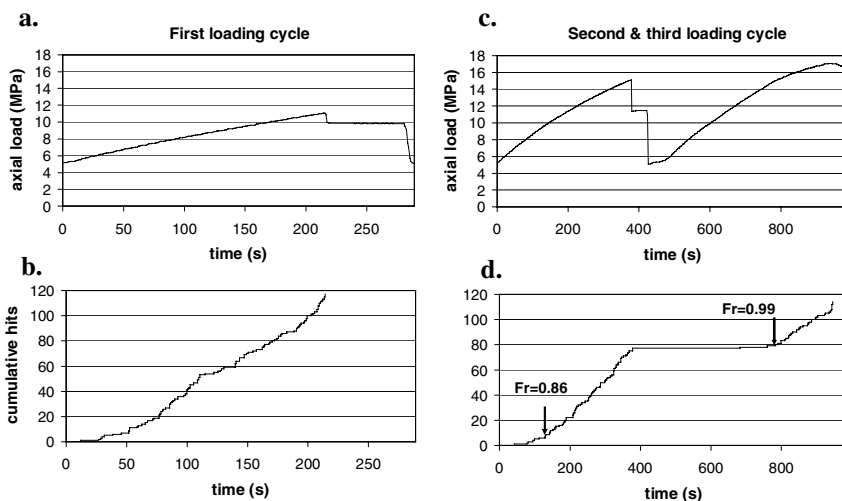


Fig. 4. Test on Opalinus clay sample: axial load vs. time (a,c) and cumulative hits vs. time (b,d) during respectively the first and the second-third loading cycles.

On the cumulative number of hits versus axial load curve, the Kaiser effect could be determined for both loading cycles, together with the corresponding Fr values (Figure 5). The Fr is calculated as 0.86 in the second loading cycle, while it is 0.99 for the third loading cycle. In this test, there is a clear difference in Fr for the load cycle with time delay and the one without. Note that the calculated Fr value also depends on the method of determining the Kaiser effect. In this study, the Kaiser effect is always determined by the intersection point of two straight lines that can be fitted through the hit curve. This is a conservative approach, while other methods can give different results (Shen 1995). In order to compare different tests qualitatively, it is important to use always the same method.

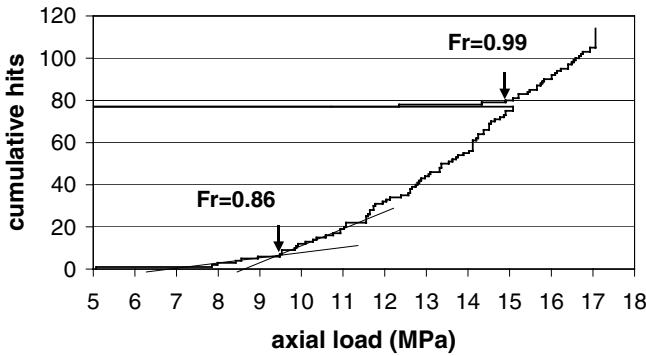


Fig. 5. Test on Opalinus clay sample: cumulative hits vs. axial load.

4 Overview of All Tests Conducted

Table 1 summarises all the calculated values for Fr , determined on the cumulative hits vs. time curve, from all tests performed, both on Boom clay and Opalinus clay samples. The values corresponding to (almost) no time delay were determined at the end of a test, between the second and the third loading cycle. For all tests with a time delay longer than 3 days, the Fr in the loading cycle after the time delay was always lower in comparison to the loading cycle with no time delay, for both types of clay. In addition to this, it seems that increasing time delays correspond to decreasing Fr values. On first sight, the absolute differences in Fr value might seem rather small for making any final conclusion. However, one has to consider

that Fr is defined as $Fr = \frac{\sigma_{I_{KE}}^{II}}{\sigma_{I_{MAX}}^I}$ and that tests only start from the isotropic

stress of 5.0 MPa. Hence, the theoretical minimal limit for the Fr is $5 \text{ MPa} / (\text{max. loading cycle I}) \cong 5/11 = 0.45$ for the Opalinus clay and $5/7 = 0.7$ for the Boom Clay. Therefore, it is considered that it might be better to define a ratio based on deviatoric stresses instead of absolute stresses. This allows enlarging the range of values down to 0 on the lower side, providing a better resolution. The Deviatoric

Stress Ratio (DSR) is defined as $DSR = \frac{(\sigma_1 - \sigma_{ISO})_{KE}^{II}}{(\sigma_1 - \sigma_{ISO})_{max}^I}$ where σ_{iso} is the iso-

tropic stress value present during the time delay between cycles. It also corresponds to the confining pressure ($\sigma_2 = \sigma_3$) during the entire test. By doing this, the trends discussed above become more distinct and thus confirmed (see also Table 1). It would be too premature to try to compare the rate of healing from both types of clays, but it is a good sign that the acoustic pattern evolves in the same way with time for both clays.

Table 1. Calculated average values for Fr and DSR for all tests performed.

Delay between cycles	Boom clay		Opalinus clay	
	Fr	DSR	Fr	DSR
no delay	0.98	0.98	0.98	0.98
1-3 days	0.98	0.91	1.00	1.00
9 days	0.94	0.80	0.88	0.74
14 days	0.97	0.86	0.91	0.85
21-22 days	0.94	0.72	0.86	0.74

5 Conclusions and Future Research

The results of the experimental part of this research seem to confirm that increasing time delay between two successive loading cycles causes the Felicity ratio to decrease. This behaviour is observed for Boom clay and for Opalinus clay. It remains yet the question if this decrease of Fr is due to self-healing during the time delay or due to other phenomena. In the simulation part of the research, the boundary element code DIGS is used to simulate the response of micro-fracturing behaviour in a laboratory sample when crack properties are altered (in order to simulate healing). It is hoped that this can demonstrate that the experimental results are at least partially due to self-healing.

Acknowledgements

The research presented in this paper was conducted as part of the project Selfrac, co-funded by the European Commission and performed within the fifth EURATOM framework programme, key action Nuclear Fission (1998-2002). The authors acknowledge the financial support.

References

- Debecker B, Vervoort A, Wevers M (2003) Disposal of Radioactive Waste in Clay Formation: Effect of Cyclic Loading on Clay Behavior. In: Proceedings of Int. Symposium on Rock Stress, Kumamoto (J), November 4-6, 2003. AA Balkema Publishers, pp 261-265.
- Holcomb DJ (1993) General Theory of the Kaiser Effect. In: Int J Rock Mech Min Sci & Geomech Abstr, 30 (7), pp 929-935.
- Korner RM, Lord AE (1989) AE Detection of Prestress in Soil and Rock, In: Fourth Conference on Acoustic Emission/Microseismic Activity in Geologic Structures and Materials - The Pennsylvania State University, October 22-24, 1985, Hardy, HR Jr (ed), Trans Tech Publications, Clausthal-Zellerfeld, Germany, pp 73-86.

- Lavrov A, Vervoort A, Filimonov Y, Wevers M, Mertens J (2002) Acoustic emission in host rocks material for radioactive waste disposal: comparison between clay and rock salt. In: *Bul. of Eng Geol and Env* 61, pp 379-387.
- Lavrov A (2003) The Kaiser effect in rocks: principles and stress estimation techniques. In: *Int J Rock Mech & Min Sci*, 40 (2003), pp 151-171.
- Mazurek M, Elie M, Hurford A, Leu W, Gautschi A (2002) Burial history of Opalinus clay. In: *Proceedings of the Int. meeting on Clays in natural and engineered barriers for radioactive waste confinement*, Reims, December 9-12, 2002. pp 101-102.
- Mertens J, Bastiaens W, Dehandschutter B (2002) Characterisation of induced discontinuities in the Boom clay around the underground excavations. In: *Proceedings of the Int. meeting on Clays in natural and engineered barriers for radioactive waste confinement*, Reims, December 9-12, 2002. pp 43-44.
- Shen HW (1995) Objective Kaiser stress evaluation in rock. In: *Proceedings of the fifth conference on AE/MA in geologic structures and materials*. Clausthal-Zellerfeld, Trans Tech Publications, 1995. pp197-204.
- Vanbrabant Y, Vervoort A, Wevers M (2002) Self-healing processes in clay-dominant rocks using acoustic emission technique: First results of laboratory experiments. In: *Proceedings of the Int. meeting on Clays in natural and engineered barriers for radioactive waste confinement*, Reims, December 9-12, 2002. pp 45-46.
- Wouters L, Vandenberghe N (1994) *Geologie van de Kempen. Een synthese*. NIROND, Brussel.

Hydrogeological Investigations in Deep Wells at the Meuse/Haute Marne Underground Research Laboratory

Jacques Delay and Marc Distinguin

Agence Nationale pour la Gestion de Déchets Radioactifs (ANDRA), Laboratoire de Recherche Souterrain de Meuse/Haute-Marne, RD 960, F-55290 Bure, France
jacques.delay@andra.fr
Tel: +33 3 29 75 53 52, +33 3 29 75 53 43
Fax: +33 3 29 75 53 89

Abstract. ANDRA (Agence Nationale pour la Gestion de Déchets Radioactifs) has developed an integrated approach to characterizing the hydrogeology of the carbonate strata that encase the Callovo-Oxfordian argillite at the Meuse/Haute-Marne Laboratory site. The argillites are difficult to characterize due to their low permeability. The barrier properties of the argillites can be inferred from the flow and chemistry properties of the encasing Oxfordian and Dogger carbonates. Andra's deep hole approach uses reverse air circulation drilling, geophysical logging, flow meter logging, geochemical sampling, and analyses of the pumping responses during sampling. The data support numerical simulations that evaluate the argillite's hydraulic behaviour.

Keywords: ANDRA, radioactive waste, underground laboratory, argillite, drilling, flow logging, geophysical logging, hydrogeologic testing, water sampling.

1 Introduction

Since 1991 ANDRA (Agence Nationale pour la Gestion de Déchets Radioactifs) has been performing research on geologic disposal of radioactive waste in France. In 1999 ANDRA began constructing an underground research laboratory approximately 300 km east of Paris on the boundary of the Meuse and Haute-Marne departments. The laboratory investigates the Callovo-Oxfordian argillite, a 130-m thick middle Jurassic stratum, at a depth about 420 meters below the surface. Argillite is a clay-rich sedimentary rock with low permeability and a capacity for radionuclide retention. The use of deep boreholes to characterize the strata above and below the argillite is the focus of this paper. These methods have evolved considerably since the beginning of ANDRA's site investigation programs (Delay and Aranyossy, 1994). The argillite's encasing units are Jurassic carbonates with some marls. The hydrogeology of the encasing units provides information on the properties of the argillite. It is difficult to characterize argillites directly, because standard well tests take a long time and only affect small rock volumes. However, groundwater flow in the encasing units reflects the barrier properties of the argil-

lite. For example, studies of groundwater isotopes in similar strata below the Callovo-Oxfordian (Marty et al., 2003) show geochemical evidence for hydrogeologic isolation over geologic time scales.

2 Geological and Hydrogeological Context of the Meuse/Haute Marne Site

The main selection criteria for the site were the depth of argillite between 400 and 600 meters and the avoidance of tectonic faults. The site selection used literature surveys, seismic reflection studies, and confirmatory drilling. The laboratory's main stratigraphic units (Figure 1) are (1) Kimmeridgian limestones and marls (surface to 150 m), (2) Oxfordian limestones (150 m to 422 m), (3) the Callovo-Oxfordian argillite (422 m to 569 m) and (4) Dogger limestones and dolostones (559 m to 786 m). These strata gently dip west toward the center of the Paris Basin. The lower conductivity Kimmeridgian ($\sim 10^{-9} \text{ m s}^{-1}$) supports a head difference of tens of meters between the surficial materials and the Oxfordian. The Oxfordian is a porous medium where flow occurs in oolites and calcarenites. The hydraulic conductivities of single strata of the Oxfordian lie largely between 10^{-9} m s^{-1} and 10^{-7} m s^{-1} with some locally more permeable horizons. The higher flows generally are associated with specific strata at recognizable stratigraphic horizons that are laterally persistent. The Callovo-Oxfordian argillite is a layer with a very low hydraulic conductivity of about $10^{-12} \text{ m s}^{-1}$ or possibly lower. The Dogger consists of limestones and dolomites with some thin clay-rich marl layers. In the vicinity of the laboratory site, the Dogger has lower hydraulic conductivities (10^{-12} - 10^{-8} m s^{-1}) than in the same strata in other parts of France. The heads in the Oxfordian and Dogger generally differ across the Callovo-Oxfordian by a few meters to tens of meters. This gradient is downwards at the laboratory, though it can be upwards elsewhere in the region. The Callovo-Oxfordian itself has a head that is higher

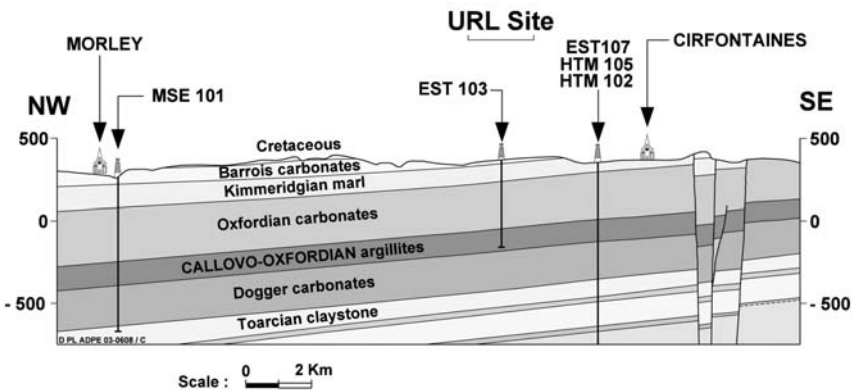


Fig. 1. Stratigraphic units and geologic cross section of the Meuse/Haute-Marne laboratory region.

than either of the two encasing carbonate units. This anomalous head may be the result of chemical potential gradients driven by salinity differences between the Oxfordian and the Callovo-Oxfordian as discussed further in Delay and Cruchaudet (2004).

ANDRA has undertaken three drilling and testing campaigns at the Meuse/Haute-Marne site. The first three deep holes were drilled and tested between 1994 and 1996 to locate the laboratory site. Six more holes were drilled in 2000 as monitoring holes for shaft construction. The most recent drilling phase (2003) produced seven holes up to 20 km from the laboratory (four Oxfordian, and three Dogger) to better understand the regional hydrogeology.

3 Drilling Techniques Adopted by Andra

The preferred drilling technique for deep holes at the laboratory site is percussion drilling with reverse air circulation. The method uses a double-walled drill rod, where the downward circulation of air moves in the annulus between the two walls of the drill rod, and the returned air with cuttings travels up the inner tube. Reverse air circulation avoids several common drilling problems such as disturbances to the hydrochemistry, reduction of the hydraulic conductivity near the borehole (skin), and destabilization of clays due to water contact. Percussion drilling methods are much faster than coring, but they only allow examination of cuttings rather than core. Among percussion drilling methods, however, reverse-air circulation is attractive because it reduces the mixing of materials from different depths thus enhancing the value of the extracted cuttings and fluids. Reverse air circulation works best if the water inflow rates are relatively low, as the airflow and pressure requirements are more severe when the borehole encounters a zone with significant water flow. Since 2000, the drilling systems have been adapted to monitor continuously the rate of progress, rotation, torque, and mudflow and pressure, if used.

4 Geophysical Logging

Wireline geophysical logging for ANDRA's deep wells includes sonic logs, gamma logs, and porosity logs. The sonic logs measure the dynamic mechanical properties of the rock, and gamma logs measure natural radioactivity that is strongly associated with clay content. Schlumberger's Combinable Magnetic Resonance (CMR) tool has been adapted to measure porosity due to concerns that neutron-based tools might affect ^{14}C contents that are used for groundwater age dating. The CMR tool also measures both total and free water porosity (Kenyon and Straley, 1989, Howard and Kenyon, 1990).

5 Hydrogeologic Testing Techniques

5.1 Overview of Testing Methods

When ANDRA began its work, a common approach for detailed hydrogeologic testing of rock involved packer testing of entire boreholes often with packer spacings of 2 meters or less. In newer approaches, flow logs provide a detailed picture of the heterogeneity of hydraulic properties. Packer tests or more detailed pumping tests are reserved for specific conducting features identified by the flow logging. Additional information on hydraulic heads and larger scale hydraulic properties then come from permanent multi-packer installations that monitor responses to shaft excavation and other laboratory or repository operations.

5.2 Flow Logging

The flow logging methods include spinner, electrical conductivity, and heat-pulse flow meter logging.

Spinner logging measures the velocity of the water moving along the borehole using an impeller. The method can resolve velocities down to a few millimetres per second, which for a 4-inch (10-cm) borehole is a flow of about 1 L min^{-1} (Delouvier and Seguin, 2003). For the pumping conditions of the laboratory's wells in the carbonates, spinner logging identifies only the most conductive features of the borehole, that is, those with transmissivities greater than about $3 \times 10^{-7} \text{ m}^2 \text{ s}^{-1}$.

Fluid conductivity logging (Tsang et al., 1990) is significant technology advancement from radioactive waste research programs starting in Switzerland. The fluid conductivity method replaces the water of the borehole with water having a contrasting electrical conductivity. The method monitors the inflow of natural waters to the hole using repeated electrical conductivity logs. For a 300-m borehole, these logs typically run over a period of a few days. The electrical conductivity logs show spikes at the water inflow points. These peaks broaden and move along the hole depending on their inflow rate. The analysis uses a numerical inversion simulation to obtain the inflow locations and rates. Fluid conductivity flow logging has been successfully applied in Meuse/Haute-Marne laboratory boreholes for transmissivities between $10^{-9} \text{ m}^2 \text{ s}^{-1}$ and $10^{-5} \text{ m}^2 \text{ s}^{-1}$.

The *heat pulse flow meter* (Paillet et al., 1996, Öhberg and Rouhiainen, 2000) measures flow using either the travel time of the thermal pulse or the dilution of temperature from a continuous heat source. A Finnish adaptation of the method, the Posiva log, characterizes detailed heterogeneity over a wide range of flow rates from about 0.2 mL min^{-1} to over 1.0 L min^{-1} . The main adaptation of the Posiva log is the use of flexible rubber cups that press against the borehole wall to isolate a 1-m section of the borehole. There is no pressure across the rubber cups because water flowing outside the measurement section is bypassed through the flow meter with no pressure loss. The process is entirely automated and can log a hole at about 15 m h^{-1} in 0.1 m increments. The Posiva flow logs show strong correlations with porosity logs (Figure 2). If this correlation can be established,

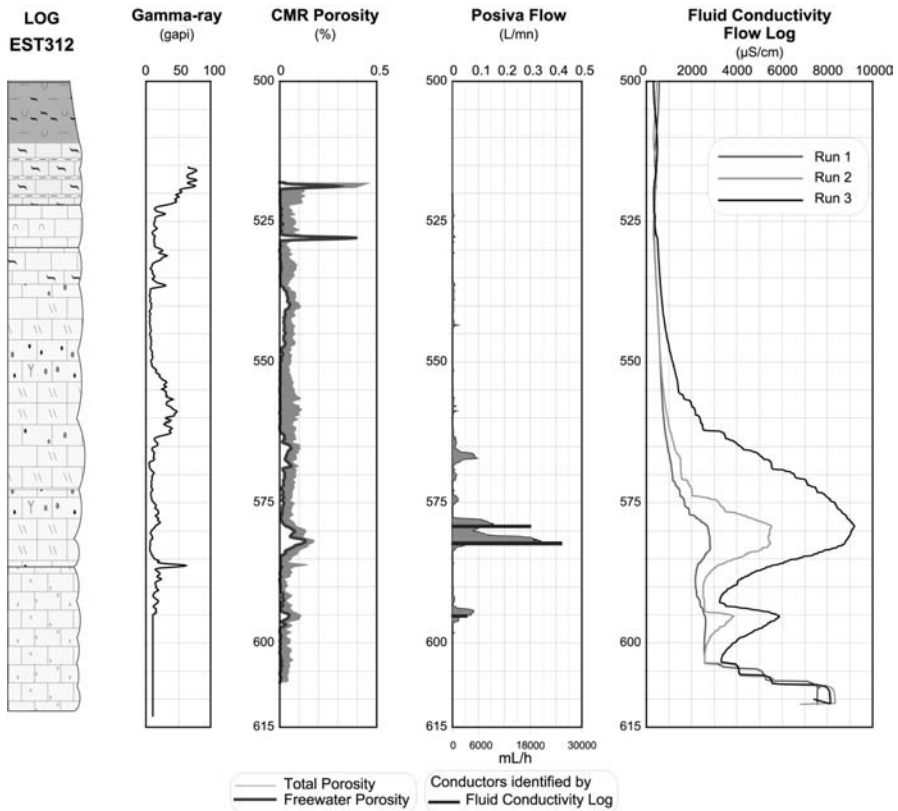


Fig. 2. Summary of testing and logging results from borehole EST 312.

then permeability may be inferred from porosity logs using calibrations developed at boreholes where both logs have been run.

5.3 Pump, Packer, and Tracer Testing

Flow logging measures hydraulic properties near the well. Transient-flow analyses adapted from the petroleum industry (Horne, 1995) measure properties that represent scales of hundreds of meters during month-long chemical sampling campaigns. The advantage of the transient flow methods is ability to identify skin effects, which are local variations of transmissivity near the borehole. Transmissivity analyses from flow logs assume steady flow, which is strongly influenced by skin, and thus are vulnerable to underestimating the hydraulic conductivity. Although skin is normally associated with the effects of drilling, skin can arise also from natural heterogeneities of the rock, particularly if the borehole penetrates a conducting feature in a locally less permeable location. Petroleum approaches also identify the geometries of the conducting features indicating if they

are extensive or if they are finite. Most of the pumping tests are performed over the entire open section of the boreholes. As such, their properties reflect the most significant conductor or conductors in hole. The flow logs show where these conductors are. If necessary, packer tests can be employed to isolate specific conducting features for hydraulic testing or geochemical sampling, and the analysis methods for the tests will use the same petroleum-based approaches as the open hole tests. During the 2003 drilling program, an additional well was added to make a well pair intersecting a conductive zone at about 120-m depth in the Oxfordian. The second well was drilled 12 m from the first, and it provided a base for tracer testing to obtain effective porosity and pressure interference testing for storativity. The tests used a dipole injection method where saline tracer was injected in one well and recovered in the other well while it was being pumped at four times the injection rate. The use of packers to isolate the injection interval optimized the tracer control and helped to assure nearly complete recovery of the tracer.

5.4 Interference Testing from Shaft Construction

Four wells at the laboratory site have been equipped with multi-packer monitoring systems (Delouvrier and Delay, 2004). These use the Westbay casing system that allows isolation of large number of intervals in a single hole. The shaft construction produces responses in the monitoring network when it intersects conducting features. Analyses of these responses provide additional measures of hydraulic diffusivity, transmissivity, and storativity.

6 Hydrochemical Measurements

The successful water sampling of deep fluids requires careful attention to all aspects of the drilling operation to avoid contamination and to allow corrections for drilling effects (Klopmann et al., 2001, Matray et al., 2001). Major constituents are sampled using month-long pumping on major conducting zones. For the volatile constituents that require pressurization, ANDRA uses wireline samplers that retrieve preserve the water under in situ pressure conditions. Andra maintains a field laboratory at the drill site where fluid parameters (Eh, pH, T, etc.) are measured immediately after sampling. The Dogger at the laboratory site carries water with relatively high salinities (5000 mg L^{-1} similar to the Callovo-Oxfordian) as compared with the Oxfordian (500 mg L^{-1}). Isotopic data will further define the distributions of groundwater chemical types.

7 Conclusions

ANDRA has undertaken a detailed characterization program for two carbonate stratigraphic units, the Oxfordian and the Dogger. The data provide a detailed picture of hydraulic head variations, water chemistry, and hydraulic conductivity.

These data will support future analyses both to define the role of the Callovo-Oxfordian argillite as a flow barrier and to understand the groundwater flow system in these carbonate units.

Acknowledgements

The authors gratefully acknowledge the contributions of his Andra colleagues, in particular Thomas Doe, who assisted with preparation of the manuscript.

References

- Delay J and Aranyosy JF (1994) Les mesures hydrogéologiques dans les forages de reconnaissance des sites potentiels pour le stockage des déchets radioactifs, *Hydrogéologie* 4:53-62.
- Delay J and Cruchaudet M (2004) Hydraulic monitoring of low permeability argillite at the Meuse/Haute-Marne Underground Research Laboratory. *Proceedings EurEngGeo, Liège*, this volume.
- Delouvrier J and Delay J (2004) Implementation of a multi-level monitoring system around the ANDRA underground research laboratory, *Proceedings EurEnGeo, Liège*, this volume.
- Delouvrier J and Seguin M (2003) Use of combined logging and testing operations in the water well management industry - 5th Cannes Water Symposium, pp 23-27.
- Horne R (1995) *Modern well test analysis, a computer-aided approach*, Petroway Publishing, Palo Alto California, USA.
- Howard JJ and Kenyon WE (1990) Proton magnetic resonance and pore size variations in reservoir sandstones -, 65th Society of Petroleum Engineers Annual Technical Conference and Exhibition, New Orleans, Louisiana USA, Paper SPE 20600.
- Kenyon WE and Straley C (1989) Poresize distributions and NMR in Microporous Cherty Sandstone. *Transactions of the SPWLA 30th Annual Logging Symposium*, Denver, Colorado, USA, Paper LL.
- Kloppmann W, Matray JM and Aranyosy JF (2001) Contamination of deep formation waters by drilling fluids: correction of the chemical and isotopic composition and evaluation of errors. *Applied Geochemistry*: 16, 1083-1096.
- Marty B, Dewonck S, France-Lanord C (2003) Geochemical evidence for efficient aquifer isolation over geological timeframes. *Nature* 425:55 – 58.
- Matray JM, Kloppmann W, Vinsot A, Aranyosy JF (2001) – Caractérisation géochimique des eaux des formations profondes : correction de la contamination induite avec calcul des incertitudes. *Hydrogéologie* 2:69-81.
- Öhberg A and Rouhiainen P (2000) Posiva groundwater flow measuring techniques. *Posiva Oy Report 2000-12*, Olkiluoto, Finland.
- Paillet FL, Crowder RE and Hess AE (1996) High-resolution flowmeter logging applications with the heat-pulse flowmeter. *Journal of Environmental Engineering Geophysics*, 1:1-11.
- Tsang CF, Hufschmied H and Hale FV (1990) Determination of fracture inflow parameters with a borehole fluid conductivity logging method. *Water Resources Research*, 26:561-578.

Java Tomography System (JaTS), a Seismic Tomography Software Using Fresnel Volumes, a Fast Marching Eikonal Solver and a Probabilistic Reconstruction Method: Conclusive Synthetic Test Cases

Sandrine Sage¹, Gilles Grandjean², and Jacques Verly³

¹ GeomaC, University of Liège, Bât. B52/3, Chemin des Chevreuils 1, 4000 Liège 1, Belgium

S.Sage@ulg.ac.be

Tel: +32.4.366.9625,

Fax: +32.4.366.9520

² BRGM, BP 6009, 45060 Orléans, France

G.Grandjean@brgm.fr

³ Montefiore, University of Liège, Belgium

Jacques.Verly@ulg.ac.be

Abstract. Problems related to landscape management, natural hazards and civil engineering involve subsurface structures that can be delineated by geophysical imaging. Seismic tomography can accurately characterize a medium according to its velocity variations. Traditional seismic travel time tomography based on ray-tracing methods assumes that the waves' frequency is infinite. Therefore, only the medium located along the ray path has an impact on the wave propagation. In subsurface tomography, the infinite frequency assumption does not hold, as targets have about the same size as the wavelength. The seismic waves' propagation is affected not only by the medium along the shortest travel time path but also by the medium located in its vicinity. In this study, Fresnel volumes are used to determine the medium affecting the wave propagation given the seismic waves' frequency. The choice of the travel time computation and reconstruction methods determines the overall efficiency and soundness of the tomography process. In this research, a second order Fast Marching eikonal solver is used for computing travel times. The Fast Marching Method is an original approach that propagates a monotonously expanding wave front in a medium. It is fast, reliable and easy to implement in both 2D and 3D. An innovative probabilistic approach enables the iterative reconstruction process based upon Fresnel volumes. This study compares the performances of JaTS, our java Fresnel volume tomography software to those of Sardine, a ray-tracing tomography software, over an unfavourable synthetic case.

Keywords: seismic tomography, Fresnel volumes, probabilistic approach.

1 Introduction

Most of the problems related to environmental geophysics, landscape management, natural hazards, or civil engineering involve subsurface structures and proc-

esses. Mapping contaminated areas, characterization of abandoned exploitations, void and cavity detection are as many examples showing the usefulness of geophysical imaging. Nowadays, tomographic techniques are increasingly used because of the development of high-technology equipments. Tomography principles can thus be invoked to compute the velocity field and to characterize the medium according to this physical parameter's variations. Tomography techniques offer the advantage of estimating the velocity field with a relatively good accuracy, provided enough data is available. Because these techniques can consider either borehole data or surface data, they can be used to address a wide range of environmental problems and they will probably be subject to future developments in geophysical imaging.

Velocity tomography is a nonlinear problem whose solution can generally be approximated by iterative algorithms updating an initial wave propagation model until the observed travel times fit the calculated ones (Tarantola, 1987). A first difficulty lies in the choice of the wave propagation model. In order to avoid problems inherent to ray-tracing in heterogeneous media (Vidale, 1988), we first opted for an eikonal solver based on finite differences as defined by Podvin and Lecomte (1991), Vidale (1988) or Zhao (1996). This algorithm is based on plane-wave propagation that handles large velocity contrasts: transmission, diffraction and refraction are considered for both outward and reverse wave propagation so that causality is honored. Nevertheless, this modelling scheme has a high computing cost that would have jeopardized the efficiency of our iterative reconstruction. We thus implemented a second order Fast Marching Method (FMM; Sethian and Popovici, 1999) to solve the eikonal equation. Adapted from the propagating wave fronts theory (Sethian, 1996a-c), this original level set method has the advantage of being optimal for first-arrival travel time computation. Once that the travel times are computed, wave paths from sources to receivers can be determined straightforwardly. We chose to materialize wavepaths by fat wavepaths (Hagedoorn, 1954), i.e. Fresnel volumes (Cerveny and Soares, 1992; Vasco et al., 1995), rather than by conventional rays. This makes it possible to consider the interactions between the wave and local heterogeneities. Depending on the source nominal frequency, these Fresnel wavepaths constitute the basis of the reconstruction technique inspired by Husen and Kissling (2001) or Watanabe et al. (1999), leading to the inverted velocity field.

JaTS, the Java Tomography Software, implements the above-mentioned 2D algorithms (Grandjean and Sage, 2003). This pure Java code (J2SE 1995-2003) ensures full portability across multiple platforms. JaTS can be used either on a laptop, on a desktop or on a workstation. Sardine (Demanet, 2000) is a C++ tomography software running with Windows NT/95/98. It implements a finite difference eikonal solver (Vidale, 1988) for travel time computation. Rays are defined as the steepest gradient of the travel time field and a classic SIRT (Dines et al., 1979) approach is used for reconstructing the velocity model. JaTS and Sardine are compared over a synthetic case study for borehole data.

2 JaTS Algorithmic Scheme

JaTS is fully portable, user-friendly, Java 2D seismic tomography software. It represents a tightly integrated tool suite that supports the entire process of importing the SG2 field records, first-break picking, forward modelling, and velocity-field computing across multiple platforms. JaTS implements original algorithms achieving optimal accuracy with reasonable computing costs. A second order Fast Marching Method (FMM) is used for solving the eikonal equation, therefore enabling a fast and robust computation of seismic traveltimes between sources and receivers. The wavepaths are materialized by Fresnel volumes rather than by conventional rays. This approach accounts for complex velocity models and has the advantage of considering the effects of the wave frequency on the velocity model resolution. The model is computed by a Simultaneous Iterative Reconstruction Technique (SIRT) that has been reformulated to integrate Fresnel wavepaths by using a probabilistic approach. The JaTS core is mainly based on two algorithms respectively dedicated to the travel times computation and to the velocity field reconstruction. Our approach consists in using Fresnel volumes to determine the wavepaths. The wave frequency thus determines the final resolution of the inverted model (Husen and Kissling, 2001). The velocity field reconstruction is based on a simultaneous iterative reconstruction technique (SIRT) described by Dines and Lytle (1979).

2.1 Traveltime Calculation Using the FMM

Solving the eikonal equation on a discrete lattice by a fast tracking scheme was presented by Cao and Greenhalgh (1994). The FMM proposed by Sethian and Popovici (1999) uses an upwind scheme for resolving the following eikonal equation:

$$|\nabla t(x,y,z)| = s(x,y,z) \quad (1)$$

where t is the travel time field and s is the slowness function. Applying the upwind approximation to the gradient, the computing of the travel times in (1) requires the solution of the equation:

$$\begin{aligned} & \max(D_{ijk}^{-x}t, 0)^2 + \min(D_{ijk}^{+x}t, 0)^2 + \\ & \max(D_{ijk}^{-y}t, 0)^2 + \min(D_{ijk}^{+y}t, 0)^2 + \\ & \max(D_{ijk}^{-z}t, 0)^2 + \min(D_{ijk}^{+z}t, 0)^2 = s_{ijk}^2 \end{aligned} \quad (2)$$

where $D_{ijk}^{-x}t$ can be expressed as a backward x difference operator at cell i, j, k and s_{ijk} is the slowness at the cell i, j, k . This scheme actually mimics a propagating wave front. We achieved second-order accuracy by choosing a three-point finite-difference operator. In order to reduce the propagation plane-wave assumption errors near the source, we decided to compute analytically two rings of voxels around the source so that the FMM algorithm could be used straight from the start (Grandjean and Sage, 2003).

2.2 The Fresnel Wavpath Approach

Cerveny and Soares (1992) used a “araxial ray theory” to define Fresnel volumes. In a medium between source S and receiver R, the Fresnel volume is defined by the set of points P, where the waves are delayed after the shortest travelttime t_{SR} by less than half a period

$$\Delta t = t_{SP} + t_{RP} - t_{SR} < 1/(2f) \quad (3)$$

where f is the frequency of the source signal. These waves can thus be added constructively to form the first arrival of the wave. This approach considers the source wave frequency in the analysis, thus enabling the evaluation of the tomography resolution and reducing the sparseness of ray distribution. Band-limited waves propagated in the ground are thus affected not only by structures along the ray-path, as assumed by the ray theory, but also by structures located in the vicinity of the ray path. Watanabe et al. (1999) proposed a numerical definition of Fresnel volumes, characterized by a weighting function that depends linearly on the delay expressed in (3):

$$\omega = 1 - 2f \Delta t, \quad (0 < \Delta t < 1/(2f)) \quad (4)$$

$$0, \quad (1/(2f) < \Delta t)$$

As a demonstration, figure 1 shows a synthetic acoustic model (a) on which a wave front is propagated using the FMM (b). Two Fresnel wavpaths are shown for frequencies of 300 Hz (c) and 50 Hz (d). These examples illustrate how the wave frequency determines the medium affecting the wave propagation. In the first case, the wave is purely refracted by the acoustic heterogeneity, whilst in the second case, the wave is partially refracted, the other part being propagated directly from the source to the receiver. If ray-tracing techniques are used for reconstructing data collected over the latter case, this phenomenon will not be accounted for and the reconstruction will be biased.

2.3 Reconstruction Algorithm: SIRT Revisited

The fundamentals of the proposed SIRT state that a slowness (S) perturbation in cell j generates a travel time (t) perturbation according to:

$$\frac{\Delta S_j}{S_j} = \frac{t^o - t^c}{t^c} = \frac{\Delta t}{t^c} \quad (5)$$

$$\Delta S_j = S_j \frac{\Delta t}{t^c}$$

where superscripts O and C refer respectively to observed and calculated quantities. We now state that the Fresnel weights defined in (4) represent the probability that a cell delays the wave propagating from a source to a receiver by Δt . The

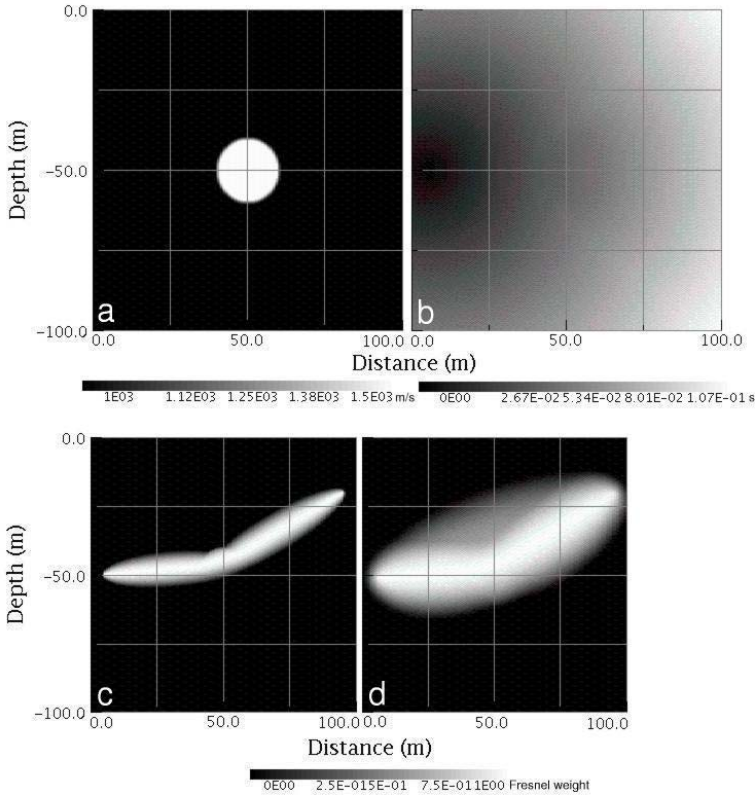


Fig. 1. Velocity model (a), travel time panel (b) and two Fresnel wavepaths, computed with a frequency of 300 Hz (c) and 50 Hz (d). The source and receiver are respectively located at (x=5 m, y=-50 m) and (x=95 m, y=-20 m).

probability that a travel time difference Δt between the observed and the calculated travel times is generated by the cell j crossed by a Fresnel wavepath i is thus:

$$P_{ij}^{\Delta} = \frac{\omega_{ij}}{\sum_{j=1}^M \omega_{ij}} \tag{6}$$

where M represents the number of grid cells. An expansion of (5) given (6) yields:

$$S_j^{k+1} = S_j^k \left(1 + \frac{1}{N} \sum_{i=1}^N \frac{\Delta t_i}{t_i^c} \frac{\omega_{ij}}{\sum_{j=1}^M \omega_{ij}} \right) \tag{7}$$

at iteration $k+1$, k being an iteration index.

A tapering filter option helps reducing undesired artifacts close to the sources and receivers position. In these particular zones the reconstruction may yield unfavourable results, essentially because of a combination of poor azimuthal coverage and of the presence of high-weight sectors further from the immediate location of the sources or receivers. Other artifacts appear within reconstructions when there is not enough data available compared to the number of slowness cells to update. In that case, some particular zones of the model, i.e., the most covered by Fresnel wavepaths, are over-corrected compared to others. In order to force the model to be adjusted in a more homogeneous way, a macro-grid may be used for smoothing the evaluated slowness values (Kissling et al., 2001). The success of the inversion is determined by the degree of resemblance between the observed travel times and the computed travel times. A likelihood function is used to compute the resemblance criterion. This quantity represents the misfit between the observed and calculated travel times in the L2 norm and is classically defined by:

$$L = \exp\left(\frac{-\sum_R \left(\frac{t^c - t^o}{\sigma}\right)^2}{2}\right) \quad (8)$$

where σ is the uncertainty on the observed travel times and R represents the number of data. Ideally, the solution is completed when the likelihood function reaches one. However, in order to avoid divergence in case of erroneous data or to limit the number of iterations, the end-user has complete control over the likelihood threshold that must be achieved.

3 JaTS over Synthetic Borehole Case-Studies

JaTS was run on a model with 3 different acquisition devices in order to evaluate its sensitivity to azimuthal covering and geometry variations. A 25 m x 25 m, 1 000 m/s constant-velocity background is hosting an L-shaped 1 500 m/s velocity anomaly located in the top right corner of the grid, a rectangular 1 500 m/s velocity anomaly centred on the grid and a rectangular 1 900 m/s velocity anomaly located in the bottom right corner of the grid (fig. 2a). The wavefront frequency is 400 Hz. Devices of 48 sources and receivers were tested. The sources and receivers were located on each side of the grid for simulating a crosshole tomographic survey (fig. 3a), on successive sides of the grid, simulating a “shooting-a-well” survey (fig. 3b), or spread around the entire grid, simulating ideal angular covering (fig. 3c). The reconstructed velocity models are represented with a RGBa colour system. Models need to contain some information about their reliability. Classically, the inverted velocity distribution is presented along with the ray density distribution in order to know where the model is well constrained, and where it is not. In order to simplify the result analysis, these two kind of information are represented on the same plot by using a RGBa colour system: the velocity distribution is mapped using a RGB colour map, while the averaged weighting function is taken into account by the saturation parameter α . This way, the plotted colours

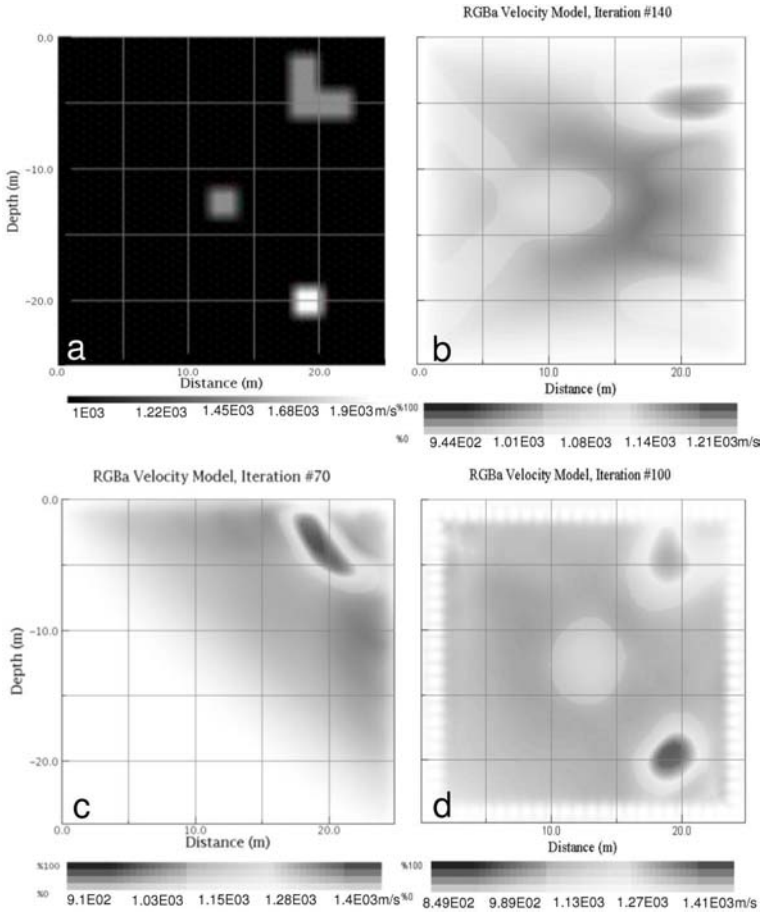


Fig. 2. A constant velocity background hosts an L-shaped anomaly and two smaller rectangular anomalies (a). Reconstructions are computed using the crosshole configuration (b), the shooting-a-well configuration (c) and the ideal angular-covering configuration (d).

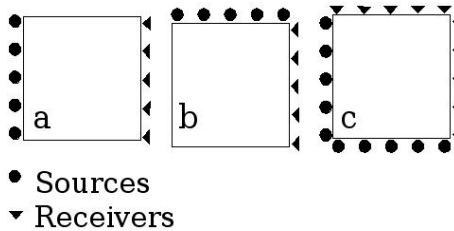


Fig. 3. Possible device configurations around the grid. Crosshole configuration (a), shooting-a-well configuration (b) and ideal angular-covering configuration (c).

represent the velocity grades according to a given colour map, and higher the reliability, higher the colour saturation. Locations where no Fresnel wave has travelled are plotted in white. The velocity reconstructions are successful in locating the anomalies in the areas of significance (saturated colouring). An exception thereof is for the shooting-a-well configuration, which only detects the upper-right anomaly (fig 2c). The crosshole configuration reconstruction has generated artefacts along the diagonals (fig 2b) because of the unfavourable positioning of the anomalies (fig 2a). The anomalies are also smeared along the horizontal direction. The ideal angular-covering configuration reconstruction yields the most resembling model (fig 2d).

4 Comparison of JaTS and Sardine over an Unfavorable Synthetic Case

JaTS and Sardine reconstructions are compared after running the two programs on an unfavourable model. A 50 m x 50 m, layered medium is hosting a rectangular 1 700 m/s velocity anomaly located in the bottom left corner of the grid. The top-most layer has a 1 000 m/s velocity and the bottommost layer has a 1 500 m/s velocity (fig 4a). The wavefront frequency is 50 Hz. Devices of 27 sources and receivers were tested. The sources and receivers were located on each side of the grid for simulating a crosshole tomographic survey. The JaTS velocity reconstruction delineates the rectangular anomaly (fig 4b) while the Sardine reconstruction only detects the bottommost layer and fails to locate the rectangular anomaly (fig 4c and d). It should be noted that Sardine also offers a fat-ray option that could overcome this case's difficulty. This option was not used, as the purpose of the actual comparison is showing that classic ray-tracing techniques face severe limitations in the interpretation of unfavourable cases, where anomalies are comparable in size to the dominant wavelength.

5 Conclusion

JaTS is a fully-portable, tightly integrated, seismic tool suite dedicated to invert seismic velocity fields. The algorithms used for travel time computation are based on a second order Fast Marching Method that appears to be fast and accurate enough for computing the Fresnel volumes of each source-receiver pairs. A probabilistic Simultaneous Iterative Reconstruction Technique is used to compute the velocity field. JaTS can be used profitably for the reconstruction of subsurface applications, where the infinite frequency assumption often does not hold. It has been shown that classic ray-tracing techniques can face severe limitations in the interpretation of such unfavourable cases. Further development is currently under way for reducing the JaTS execution time. An attenuation tomography module should be integrated to JaTS shortly. Automatic first-break picking, 3D process-

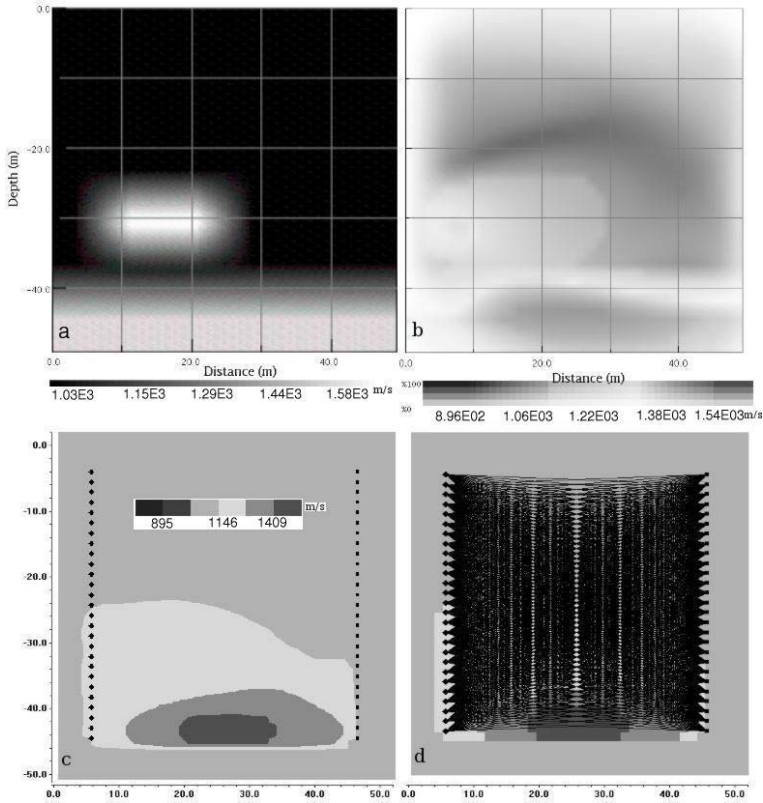


Fig. 4. A layered medium hosts a rectangular anomaly (a). Reconstructions are computed using JaTS (b) and Sardine (c). The Sardine ray covering information is presented separately (d).

ing, and initial model estimation are issues that remain to be considered. A JaTS demo is freely available on JaTS website at:

http://www.ulg.ac.be/geomac/publications/JaTS_SSage_GGrandjean/Home.html

References

- Cao, S., and Greenhalgh, S. 1994. Finite-difference solution of the eikonal equation using an efficient, first-arrival, wavefront tracking scheme, *Geophysics*, 59 4, 632-643.
- Cerveny, V. and Soares, J.E.P., 1992. Fresnel volume tay-tracing. *Geophysics*, 57, 7, 902-915.
- Demagnet, D. Tomographies en 2D et 3D à partir de mesures géophysiques en surface et en forage, Ph.D. diss., University of Liège, 2000.

- Dines, K.A., and Lytle R.J., 1979. Computerized geophysical tomography. *Proc. IEEE*, 67, 7, 1065-1073.
- Grandjean G. and Sage S. JaTS: a fully portable seismic tomography software based on Fresnel wavepaths and a probabilistic reconstruction approach. Submitted for review, *Computers&Geosciences*, July 2003, 16 pp.
- Hagedoorn, J.G., 1954. A process of seismic reflection interpretation . *Geophys. Prosp.*, 2, 85-127.
- Husen, S. and Kissling, E., 2001. Local Earthquake tomography between rays and waves: fat ray tomography. *Phys. Earth Planet. Int.*, 123, 129-149.
- Kissling E; Husen S. and Haslinger, F., 2001. Model parametrization in seismic tomography: a choice of consequence for the solution quality. *Phys. Earth Planet. Int.*, 123, 89-101.
- Podvin, P. and Lecomte I., 1991. Finite difference computation of traveltimes in very contrasted velocity models: a massively parallel approach and its associated tools. *Geophys. J. Int.*, 105, 271-284.
- Sethian, J.A., 1996a. A fast marching level set method for mototonically advancing fronts. *Proc. Nat. Acad. Sci.*, 93, 1591-1595.
- Sethian, J.A., 1996b. Theory, algorithms and applications of level set methods for propagating interfaces. *Acta Numerica*, 5, 309-395.
- Sethian, J.A., 1996c. Level set methods. Cambridge Univ. Press.
- Sethian, J.A. and Popovici, A.M., 1999. 3-D travelttime computation using the fast marching method. *Geophysics*, 64, 2, 516-523.
- Tarantola, A. 1987. Inverse problem theory. Methods of data fitting and model parameter estimation. Elsevier Publishing Company.
- Vasco, D.W., Peterson, J.E. Jr., and Majer E.R., 1995. Beyond ray-tomography:wavepaths and Fresnel volumes. *Geophysics*, 60, 1790-1804.
- Vidale, J.E., 1988. Finite-Difference calculation of traveltimes. *Bull. Seis. Soc. Am.*, 78, 2062-2076.
- Watanabe, T., Matsuoka, T., and Ashida, Y., 1999. Seismic travelttime tomography using Fresnel volume approach. 69th Proc. S.E.G.
- Zhao, P., 1996. An efficient computer program for wavefront calculation by the finite-difference method. *Computers and Geosciences*, 22, 3, 239-251.

Using the Complete Nano Engineering Geological Spectrum to Assess the Performance of Clay Barriers

Robrecht M. Schmitz^{1,3}, Christian Schroeder¹, Jacques Thorez²,
and Robert Charlier²

¹ GéomaC - Géomécanique et Géologie de l'Ingénieur, Chemin des Chevreuils 1 - B52/3, Université de Liège, B-4000 Liège, Belgium

² Geology Department - Université de Liège, Belgium

³ National Scientific Research Fund (F.N.R.S.), Belgium

RM.Schmitz@ulg.ac.be

Tel: +32 4 366 9215

Fax: +32 4 366 9326

Abstract. Clays are geomaterials used in various (over 100) applications in our society. The more common geotechnical applications are clay barriers to contain waste, slurry walls etc. But even if clays are not used as construction material, the engineering geologist encounters them frequently during construction of e.g. foundations and tunnels. As clays are end products of the weathering of silicate geomaterials they are stable as such, but within this group of clay minerals, geotechnical properties vary enormously. Some of these variations are due to chemo-plasticity e.g. reflected in the effect of the composition of the pore fluid on the mechanical properties of clay. One approach to deal with these chemo plastic effects is to separate them according to the scale or level on which they are acting. In clays one can discern the level of the clay silicate sheets (TOT or TO), the clay interlayer level and the clay particles level. This contribution aims to show how an analysis of the processes on these three levels can help to assess the geotechnical properties of clays in contact with various fluids.

Keywords: clay barrier, hydraulic conductivity, scale effects, interlayer level, particle level, tetrahedral-octahedral level.

Introduction: How Can a Fluid Influence the Mechanical Behaviour of Clay?

Depending on the scale, different alteration processes are important. Therefore a three-scale approach is followed: on scale 1, tetrahedral - octahedral sheets are concerned; on scale 2, the interlayers; and on scale 3 the clay particles.

Tetrahedral – Octahedral Level

This is the smallest level at which clay minerals are analysed. The general opinion found in literature dealing with clay barriers and landfill leachates is that the layer silicates remain intact (e.g. an Illite remains an Illite, and a Kaolinite remains a

Table 1. The three different scales on which a nano engineering geology analysis should be based.

Level	Tetrahedral – Octahedral sheets	Interlayers	Particles
Time needed for alteration in nature	Several years to centuries	Diffusion (lab sample) months	Flow (lab sample) weeks
Scale	Ångströms	nanometers	micrometers

Kaolinite) see Kohler (1988) and the literature overview by Prinz (1997) and recently by Schmitz (et al. 2001, 2002a and 2003b). An example of a process in which layer silicate damage occurs is the ripping of a Tetrahedral sheet during kaolonitisation by transformation.

Interlayer Level

In geotechnical terms the main difference between clay minerals is related to differences in interlayer space whatever its origin (Schmitz et al. 2004). Clay mineralogists study this interlayer space in order to classify clay minerals by X-ray diffraction analysis. The appropriate way to introduce clay mineralogy to geotechnics is to analyse changes in EBS, equivalent basal spacings (Schmitz et al. 2002b, 2003a and 2004).

Particle Level

Long-term tests have shown that dissolution of calcite, reduction of the swelling capacity of smectites, decrease of plasticity, increase of size of clay particles due to aggregation take place (Prinz 1997). Chemicals can dissolve cementing agents between clay particles. As a result clay particles become free and the colloidal behaviour is changed (Komodromos and Göttner 1988). The following interactions between the particles are generally analysed as a function of fluid composition:

- The thickness of the double layer
- The type and size of elementary aggregates
- The inter-particle forces (di Maio and Fenelli 1994), including cementation

Summary

With the differentiation of processes related to the three levels: TOT and TO sheet level, interlayer level and clay particle level, one can assess the influence of various fluids on the geotechnical properties of clays by analysing the processes at each level separately (see figure 1).

To illustrate this approach several examples will be presented in which the distance between clay particles is related to change in the diffuse double layer thickness; the interlayer changes to XRD analysis and changes in TOT or TO sheets by referring to clay mineral literature.

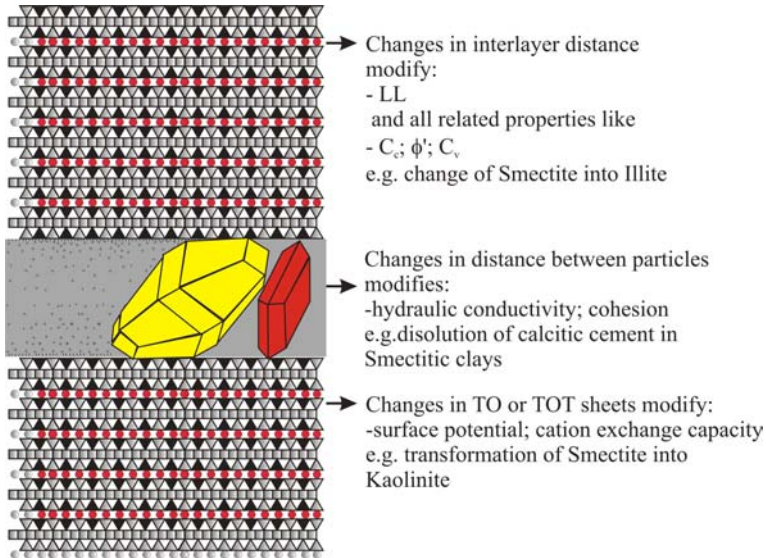


Fig. 1. The three-scale model. The influence of fluids on the geotechnical properties of clays can be studied by differentiating the effect of these fluids at the different scales of a clay material. See figure 2 for an explanation of the symbols.

Clay Mixed with Brines: Interlayer Level (Level 2)

If salt solutions are mixed with clays, the thickness of the double layer decreases up to the concentration where it is completely lost; cations are absorbed to the surface, or crystallise to salt. Thereby the clay particles can approach each other. Upon rehydration the double layers will be reactivated. The repulsion between the clay particles will redevelop although some interlayers will not be rehydrated. This process can occur during e.g. artificial or natural illitisation of a smectite (figure 2).

Illitisation is accompanied by an increase in grainsize (figure 2), especially if the clay is (unavoidably) dried during the test. In geotechnical terms this is reflected by an increase of permeability, a decrease of the compression coefficient, a decrease of the Atterberg limits, etc. These changes have been confirmed (Schmitz and van Paassen 2003, Delvaux 2003) by measurements of Belgian Tertiary clays (see figure 3).

Clay Percolated by Brines: Particle Level (Level 1)

Contrary to the tests described in the previous section; in this section a clay, initially prepared with water, then permeated by brines in an oedometer, is con-

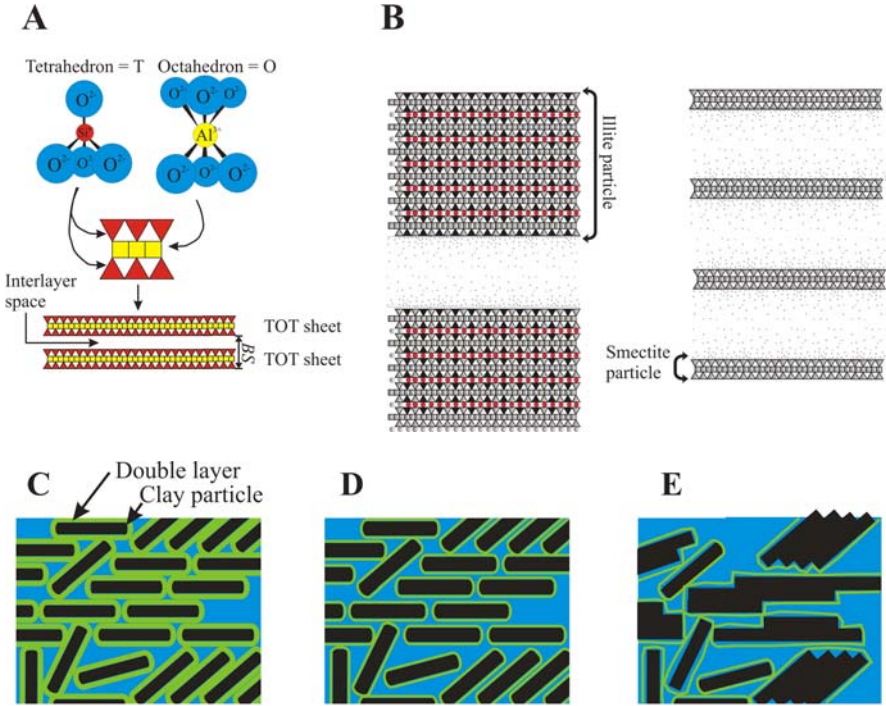


Fig. 2. A: Definitions B: Difference in geotechnical properties between an open illite and a smectite is predominantly related to the differences of the interlayer space. C-E particle size increases if a clay is exposed to an ever increasing salt concentration.

sidered. In this case one analyses differences in structure, in contrast to changes affecting remoulded soils as discussed above. Why using an oedometer? Because the stress conditions (plane strains) are identical to those encountered in a landfill liner. The distance between two clay particles is governed by the repulsion that can be described with the double layer model (Fam and Dusseault 1999). Results of such tests (Delvaux 2003) show that the permeation of salts cause a settlement of the clay. If clay particles approach each other there is less space for a liquid to flow. Consequently the same percolation that causes a settlement of the clay barrier should cause a reduction of the hydraulic conductivity. To test this, a repulsive law based on the double layer theory was introduced into a numerical code in order to test several clay to clay particle arrangements. The different assemblages are shown in figure 4.

Using the cubic law the decrease in distance between clay particles is related to a decrease in hydraulic conductivity. In figure 4d results of the numerical simulations are compared to those of the lab tests. Both numerical and experiment results showed that if a clay, with an initial low concentration of cations, is permeated with an ever increasing concentration of these cations then the hydraulic conductivity decreases but not much more than a factor 10.

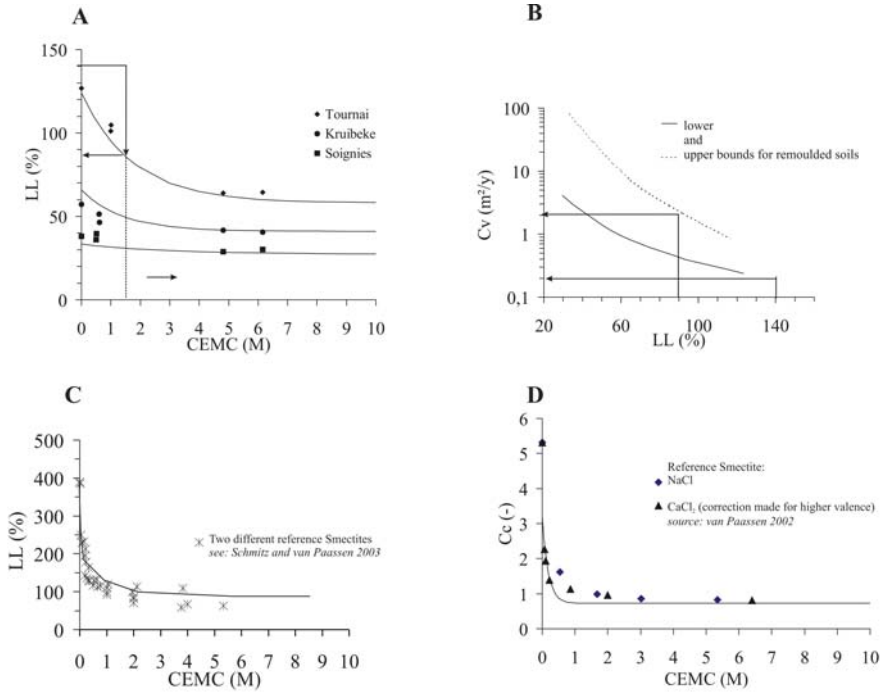


Fig. 3. A: The LL of Belgian Tertiary clays decreases with increasing salt concentration. B: This decrease induces an increase in permeability (C_v) (Bardet 1997). Quantitatively this was also confirmed by Delvaux (2003). C: Decrease of the LL of two commercial Bentonites (reference smectite) with an increasing salt concentration (Schmitz and van Paassen 2003) can be related with the correlation by Terzaghi and Peck (1967) to the C_c as is confirmed in D.

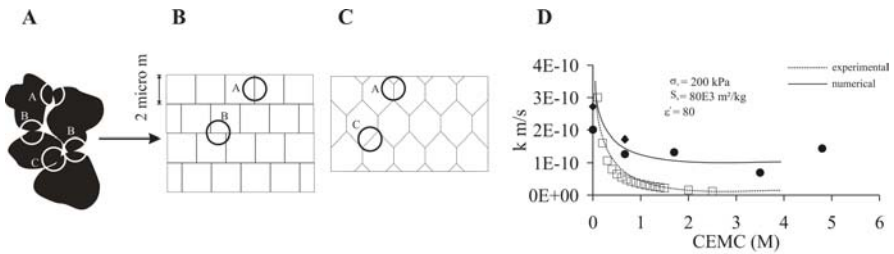


Fig. 4. A: Flow takes place around clay particles. Several hypothetic orientations (meshes for numeric simulations shown in B and C). D: Results of the numerical simulation compared to lab test results.

Podzolisation: TOT Level (Level 3)

In the third example an alteration on level 3, affecting the TOT or TO sheets, is discussed. Clay barriers must isolate waste during a life span that exceeds a scientist's life. To predict the behaviour of a barrier on a long term a new method needed to be developed. Natural Belgian Tertiary clays have been percolated by genuine landfill leachates. After percolation during several months the clay mineralogy has been analysed by XRD and microscopic analyses of thin sections. The results are a partial, artificially induced "chloritisation" and "illitisation" affecting the original swelling (montmorillonite) component; a slight alteration of illite; appearance of an amorphous phase. These clay mineral alteration trends find some similarities with a downward pedogenetic alteration, and mimics in fact the first stages of leaching and destructuration as occurring during podzolization. This means that if during the leaching phase, this alteration path known from nature is followed to the end, the clay mineral alteration would cause changes in the TOT structure of the original clay minerals and produce kaolinite with a TO-sheet structure. This will also induce changes of geotechnical properties ($>\phi'$; $<$ Cation exchange capacity) especially if the original material does not contain kaolinite (Schmitz et al. 2003a).

Discussion

With the three level approach an engineering geological assessment can be made (a kind of nano-RMR). Even if the clay has not been in contact with the fluid during laboratory tests, the behaviour of the clay-leachate combination can be predicted. As an example the permeated of a clay barrier by ethanol is discussed:

- Tetrahedral – Octahedral Level

In the clay mineral literature no interactions have been reported.

- Interlayer Level:

Organic liquids can enter the interlayer spaces depending on type of organic fluid and clay mineral. Because the reactions, known from literature are complex, some tests on remoulded samples were conducted. The XRD results showed that the interlayers were only slightly affected (no complete collapse known from smectites with salts). Furthermore the processes were completely reversible when reexposed to water.

- Clay particle level:

If it is assumed that the interaction between clay particles can be described with the double layer theory, the percolation of ethanol (relative dielectric constant is smaller than that of the pore water of Belgian Tertiary clays) will cause a decrease of double layer thickness.

To summarise the results: percolation of ethanol through a clay barrier (e.g. Belgian Tertiary clays) will cause a "move together" of clay particles, depending on the orientation of the clay particles with respect to the principle stress; this will cause a slight decrease of permeability (Delvaux 2003) or a large increase of permeability (Wienberg 1990). No other reactions will happen during the next cen-

tury than those observed within months in the laboratory. In this case the orientation of the clay particles plays an important role and the engineering geologist has to direct his geotechnical analysis towards this aspect in the laboratory.

Conclusion

In literature quite contradicting results can be found: addition of salt causes both increase and decrease of the hydraulic permeability. As the analysis of this problem in terms of the three scales approach has shown, this apparent contradiction is related to the scale at which the processes take place and this depends on the instant when the clay is contacted by the salt (Boac = Before or after consolidation). This seems trivial but these facts are often overlooked in many research projects. Many examples of the application of the three-scale analysis are given in Schmitz (2004) stretching from the heating of clay to addition of hydrous lime, where this simple concept can be used to explain complex processes. It is advised that the reader tries himself to reread some literature with the three-scale concept in mind.

Symbols

BS	Basal spacing (Å)
CEMC	concentration equivalent monovalent cations (M = mol/l)
Cc	compression index (-)
Cv	consolidation coefficient (m ² /y)
EBS	Equivalent basal spacing (Å)
k	hydraulic conductivity (m/s)
LL	liquid limit (% fluid content)
RMR	rock mass rating
Sa	specific surface (kg/m ²)
TO	tetrahedral – octahedral sheets
TOT	tetrahedral – octahedral – tetrahedral sheets
XRD	X-ray diffraction
ε'	relative dielectric constant (-)
φ'	effective friction angle (°)
σ _v	vertical stress (kPa)

References

- Bardet JD (1997) *Experimental Soil Mechanics*. Prentice Hall.
- Delvaux B (2003) *Analyse géotechnique d'argiles belges en fonction de la nature du fluide interstitiel*. Travail de fin d'études. Faculté des Sciences Appliquées. Université de Liège, Liège.
- Fam MA, Dusseault MB (1999) Determination of the reactivity of clay-fluid systems using liquid limit data. *Canadian Geotechnical Journal*, Volume 36, pp. 161-165.

- Kohler E (1988) Beständigkeit mineralischer Dichtstoffe gegenüber organischen Prüfflüssigkeiten. *Abfallwirtschaft in Forschung und Praxis*, vol. 30, pp. 117-124.
- Komodromos A, Göttner JJ (1988) Beeinflussung von Tonen durch Chemikalien, Teil II Gefüge- und Festigkeitsuntersuchungen. *Müll und Abfall*, Vol. 12, pp. 552-562.
- Maio di C, Fenelli GB (1994) Residual strength of Kaolin and Bentonite: the influence of their constituent pore fluid. *Géotechnique*, Vol. 44, No. 4, pp. 217-226.
- Paassen van LA (2002) The influence of pore fluid salinity on the consolidation behaviour and undrained shear strength development of clayey soils. *Memoirs of the Centre of Engineering Geology in the Netherlands*, No. 216, TU-Delft, Delft.
- Prinz H (1997) *Abriß der Ingenieurgeologie*. Ferdinand Enke Verlag, Stuttgart.
- Schmitz RM (2004) Experimental and numerical modelling of the hydromechanical behaviour of clay barriers exposed to leachates. Dr. Thesis in Preparation. Université de Liège, Liège.
- Schmitz RM, Schroeder Ch, Charlier R (2004) Chemo-mechanical interactions in clay: A correlation between clay mineralogy and Atterberg limits. Accepted for publication in *Applied Clay Sciences*.
- Schmitz RM, Schroeder Ch, Bolle A, Thorez J, Charlier R (2003b) Änderung der geotechnischen und mineralogischen Eigenschaften natürlicher Tone durch Einwirkung von Deponiesickerwasser. *Müll und Abfall*, Vol. 35, N° 12, pp. 635-639.
- Schmitz RM, Schroeder Ch, Charlier R (2003a) Microstructure of clays and their influence on their geotechnical properties. *Weimar Conference Unsaturated Soils 2003*. Accepted for publication.
- Schmitz RM, van Paassen LA (2003) The decay of the liquid limit of clays with increasing salt concentration. *Dutch association of Engineering geology, Delft, Ingeokring Newsletter* Vol. 9, N°. 1, pp. 10-14.
- Schmitz RM, Schroeder Ch, Charlier R (2002b) A correlation between clay mineralogy and Atterberg limits. In: de Gennaro V, Delage P (eds) *Proceedings International Workshop of Young Doctors in Geomechanics*. Presse de l'École Nationale des Ponts et Chaussées, Paris, pp 27-30.
- Schmitz RM, Ourth AS, Dosquet D, Illing P, Schroeder C, Verbrugge JC, Bolle A, Charlier R, Thorez J (2002a) The suitability of some Belgian Tertiary clays as construction material for landfill seals: Interaction with domestic landfill leachates. *Aardkundige Mededelingen* Vol. 12, pp. 261-264.
- Schmitz RM, Dosquet D, Illing P, Rodriguez C, Ourth AS, Verbrugge JC, Hilligsmann S, Schroeder C, Bolle A, Thorez J, Charlier R (2001) Clay – leachate interaction: a first insight. In: Delage P (ed) *6th KIWIR International Workshop on Key Issues in Waste Isolation Research*, Presse de l'École Nationale des Ponts et Chaussées, Paris, pp. 245-269.
- Terzaghi K., Peck R.B. (1967) *Soil Mechanics in Engineering Practice*. Second edition. John Wiley & Sons Inc. New York.
- Wienberg, R. (1990) Zum Einfluß organischer Schadstoffe auf Deponietone - Teil 1: Unspezifische Interaktionen. *Abfallwirtschaftsjournal*, Vol. 2, N°. 4, pp. 222-230.

Rock Splitting in the Surrounds of Underground Openings: An Experimental Approach Using Triaxial Extension Tests

Enrico Bauch and Christof Lempp

Department of Geoscience – Engineering Geology
Martin-Luther-Universität Halle-Wittenberg, D-06099 Halle/Saale, Germany
{bauch,lempp}@geologie.uni-halle.de
Tel: +49 345 5526090
Fax: +49 345 5527582

Abstract. The phenomenon of rock splitting, i. e. the tensile crack formation under general pressure conditions, may be explained by different theoretical approaches such as critical stress conditions and critical strain based on the theory of elasticity, or critical angle of dilatation based on the theory of plasticity. Nevertheless, there are only rare attempts to simulate the rock splitting process in systematic rock mechanical experiments. In this paper we demonstrate results of experiments performed at different modes of extensional conditions in triaxial tests using three different boundary conditions and modifying pore pressure conditions as well as strain rates and stress rates. Our results partly confirm theoretical assumptions, nevertheless, they support the experience that tensile cracks in the triaxial extensional tests do not occur simply dependent from stress- or strain conditions. Additionally their occurrence depends on time, i.e. the velocities of changes of stress and strain as well as, presumably, on the scale of the observed space. Otherwise, the experimental results in decimetre dimensions do not sufficiently coincide with observations from several underground galleries with rock splitting and rock shell formation at their walls in meter to tens of meters dimension.

Keywords: triaxial extension test, splitting, core-disking, tensile fracture, red beds

1 Introduction

Splitting of hard rocks in the neighbourhood of underground openings at distinct depths may be a common phenomenon (Fairhurst & Cook 1966). Its explanation, however, is insufficient due to the lack of understanding of some causal interdependencies: The tensional crack generation shows sub-parallel orientation to the underground contours, there is an absence of shear traces on the crack surfaces despite overburden pressure conditions, and there is mostly a sudden appearance of the splitting cracks with a time delay after the underground opening operation. Time dependent stress concentration as well as stress release as a function of hol-

low space generation and geometry, must play a role. Additionally, the splitting cracks occur both on relatively small scales, for example at the walls of deep boreholes or at their bases (where it is called core dinking), and also on larger scales, for example around shafts, tunnels or caverns, forming shells at their margins. The phenomenon of splitting crack formation is not restricted to brittle hard rocks, it is also related to comparable ductile rock salt.

There are different attempts to find theoretical explanations for the rock splitting phenomenon: Stacey (1981, 1982) developed a theory of triaxial extensional strain based on the extended Hooke's law of elasticity. Following Stacey (1982) and the effective tensile stress σ_3' assumed by Brown & Trollope (1967) we find his explanation of core dinking to be a critical extensional strain ε_c with

$$\varepsilon_c = \varepsilon_3 = \varepsilon_{axial} = \frac{\sigma_3 - \nu(\sigma_1 + \sigma_2)}{E} \quad (1.1)$$

where ε_3 becomes negative in case of positive compressive stress, if

$$\sigma_3' \equiv \sigma_3 - \nu(\sigma_1 + \sigma_2) < 0 \quad (1.2)$$

Stacey (1982) notes that critical extensional strain may occur in a drilling core at generally external compressive stress conditions (Roedel 1996). Mühlhaus & Vardoulakis (1986) offer another theoretical explanation for the splitting phenomenon, which is based on the theory of plasticity (Lempp & Mühlhaus 1985). Consequently, splitting or dinking in the neighbourhood of a free surface will occur depending on the amount of the angle of dilatation β before reaching the peak stress. The critical dilatant plastic volume change, expressed as angle of dilatation:

$$\beta = \frac{\Delta\varepsilon_p}{\Delta\gamma_p} = \frac{\sqrt{3}(\Delta\varepsilon_l + 2\Delta\varepsilon_q)}{2(\Delta\varepsilon_q - \Delta\varepsilon_l)} \quad (1.3)$$

where ε_l = the axial strain; ε_q = the radial strain; $\gamma_p = \frac{2}{\sqrt{3}} (\varepsilon_q - \varepsilon_l)$

is lower in the extensional stress regime than in the compression stress regime (40.8° compared to 60°). Thus, the dilatation angle in the extensional field forms a failure criterion in terms of the plasticity theory given by:

$$\frac{\sqrt{3}}{2} < \beta < \sqrt{3} \quad (1.4)$$

Both theoretical approaches to the splitting process are worthwhile to be proofed by experimental element tests using rock samples at compression as well as extensional triaxial stress conditions. Nevertheless, the required experimental investigations seem to be rare. Apart from the famous "pinching-off test", also known as "Bridgeman's experiment" (Jaeger & Cook 1979), there are only a few

and incomplete published data available about extensional splitting of hard rock materials under laboratory test conditions. The pinching-off test represents a special condition of a triaxial extension test. However, it does not coincide with a controlled triaxial extension test with failure under triaxial pressure conditions (Fig. 2.1). The aim of this study is the presentation of several results of extensional triaxial experiments compared with compression triaxial experiments, both carried out with two types of clastic rocks. The different triaxial stress conditions, as well as the different loading paths in the experiments, were chosen in order to find out possible or relevant failure criteria characterized by tensional crack propagation at a pressure that is effective in the three principal stress directions.

2 Simulation of Rock Splitting

Cylindrical specimens with diameter of 70 mm and a length/diameter ratio of 2:1 can be tested in the triaxial cell used and there can be applied two separately controlled principle stresses as well as the pore-fluid pressure. One principle stress in the radial orientation is applied as confining pressure on the jacketed specimen. The other principle stress is applied by a loading piston in the axial direction. Pore-fluid pressure needs to be kept lower than the amount of axial and radial stresses. The maximum cell pressure is 100MPa. Loading can be either stress or strain controlled with possible changes during the tests.

2.1 Sample Sets Used

Two distinct types of clastic rocks (red beds) from the Permocarboneous infill of the north-eastern German Basin were investigated. These red beds are geologically well studied and a wide range of structural data is available (Katzung & Ehmke 1993, Lützner 1988, 1987, Schwab 1977). In the past the geotechnical studies were mainly concerned with porosity and permeability of the hydrocarbon-bearing reservoir rocks (Bärle 1993, Farquhar et al. 1993, Kleditsch & Kurze 1993) as well as hydraulic-fracturing-behaviour in the case of less permeable rock formations (Guyatt & Allen 1996). Both selected lithotypes were tested for their particular different petrophysical and geomechanical properties (Hecht et al. (in review); Table 2.1) in order to differentiate possible influences on rock splitting.

2.2 Modes of Triaxial Tests (Compression and Extension)

The triaxial compression test, as a rule, starts from a state of isostatic load ($\sigma_1 = \sigma_2 = \sigma_3$), and then the axial load (σ_1) is increased up to shear failure keeping the confining pressure at a constant lower level ($\sigma_1 > \sigma_2 = \sigma_3$). In contrast, during

Table 2.1. Sample sets used – petrographical and petrophysical properties.

sample set	rock description	grain size	sorting	cementation	density [g·m ⁻³]	connective porosity [%]	ultrasonic wave velocity [m·s ⁻¹]	uniaxial compressive strength [MPa]	tensile strength [MPa]
Lithotype 1	fluvial Sandstone, feldspars bearing cross bedding	medium to coarse sand	moderately	calcit	2.35	3.82	3127	54	3.9
Lithotype 2	aeolian Sandstone, laminated bedding	very fine to medium sand	very well	calcit	2.42	2.85	3454	88	4.9

the triaxial extension test the axial load (σ_3) decreases under the level of the confining pressure that stays at a fixed level ($\sigma_1 = \sigma_2 > \sigma_3$). Consequently, one generally starts at isostatic pressure conditions and then either axial stress increases (compression) or decreases (extension) at constant radial stress. The changing axial stress is controlled with a set of rate specific stress or strain rate conditions until failure. In the study presented here, the triaxial extension test is carried out with two additional, especially modified procedures. Thus, one uses the following three modes to simulate rock splitting under extensional triaxial stress (Fig. 2.1):

- a) rate-controlled mode;
- b) abrupt mode;
- c) modified pinching-off mode (Bridgeman's experiment).

2.2.1 Rate-Controlled Mode

In the rate-controlled mode the axial stress is reduced monotonically and slowly ("quasi-static") until rock splitting of the cylindrical specimen occurs about perpendicular to the sample axis. Confining and pore-fluid pressure remain constant during axial unloading. Such rate-controlled mode extension tests never reached any extensional fracturing of the specimen, despite a wide variety of applied settings such as:

- various confining pressures ($\sigma_1 = \sigma_2$: 10-80MPa);
- various rates of changing stress or strain (0.1-15MPa/min; 0.001-0.02mm/min);
- dry or water-saturated specimens (w : 0.5-4%); and
- various pore-fluid pressures (p_{fl} : 0-80MPa).

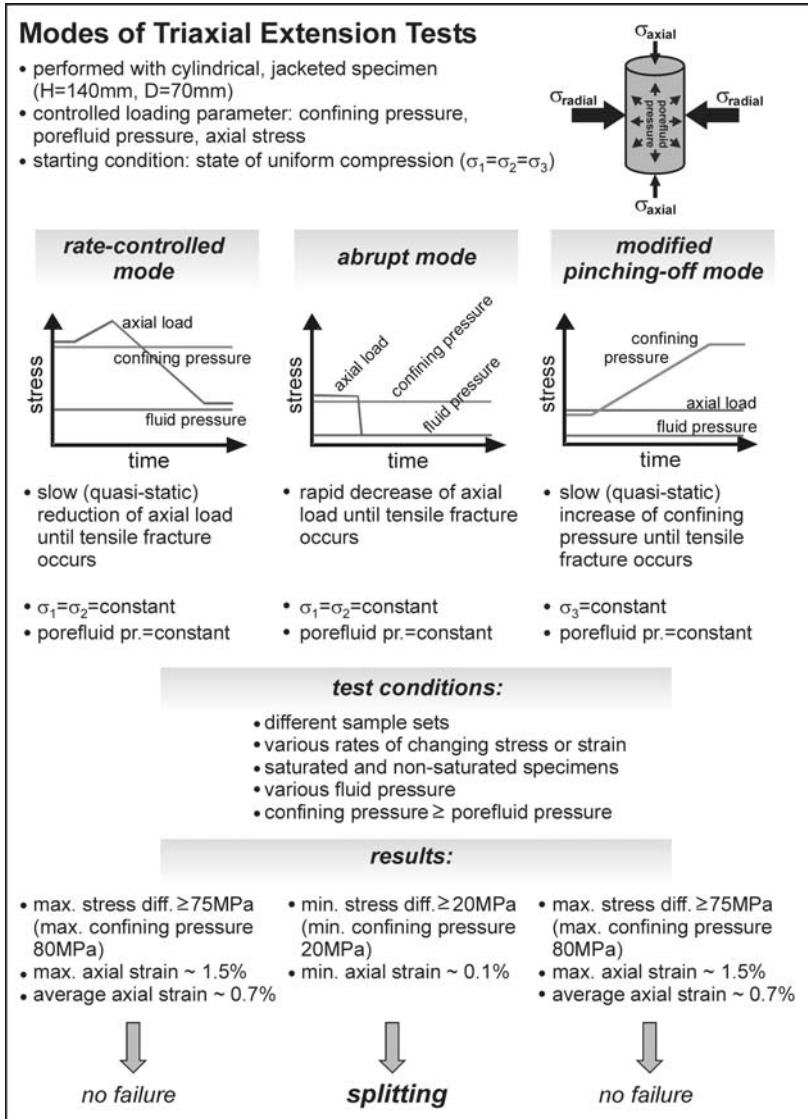


Fig. 2.1. Modes of triaxial extension tests.

Each sample persists at the maximum applied stress difference of 75MPa during extension. Average axial strain of the specimen during extensional loading was 0.7%, maximum values reach up to axial elongations of 1.5% without cracking. In addition, a substantial increase of the velocity of the controlled axial unloading (up to 15MPa/min) had no visible influence and generated no fracturing.

2.2.2 Abrupt Mode

Extensional tests in abrupt mode are performed by rapid and nearly uncontrolled decrease of axial load (σ_3). Confining and pore-fluid pressures ($\sigma_1 = \sigma_2$; p_{fl}) remain constant for each test at specific and always elevated levels. The difference to the controlled mode consists in the axial unloading performance that is comparably high. The axial re-deformation becomes suddenly effective; the stored energy is released like in an explosion. In this case, the confining pressure in the radial direction ($\sigma_1 = \sigma_2$) and the zero-stress in the axial direction (σ_3) represent the maximum stress difference, which becomes effective within a very short time. Under these conditions rock splitting could be simulated and experimentally generated at comparably low confining pressures (respectively stress differences of >20 MPa for Lithotype 1 and >25 MPa for Lithotype 2). Actual measurement of strain or of changing length of specimen is technically difficult using the triaxial cell and one creates questionable results due to the indeterminate time of stress release. Usually the values for the strain are overestimated. Occasionally, a strain of 0.1% was already sufficient to cause fracturing. In other tests, however, higher amounts of strain changes were observed. An influence of pore water saturation and of pore-fluid pressure on fracture generation could not be determined in this abrupt extensional test mode. Usually, only one tensional fracture subnormal to the axis of the specimen was formed, preferably near one of its ends. Multiple fractures distributed over the specimen length also occurred (Fig. 2.2). An additional and comparable method to generate tensile fractures in the triaxial loading cell is the abrupt stress reduction simultaneously in axial and radial directions. Amounts ($\sigma_1 = \sigma_2$ and σ_3), as well as differences of stress components ($\sigma_1 - \sigma_3$), that are necessary for tensile fracture generation approximately range in the same order as in cases of abrupt axial unloading. Overall abrupt stress reduction generates tensile fractures that in most cases occur near the middle of the specimen (half length of the $l/d = 2/1$ specimens, Fig. 2.2). Again, pore fluid pressure and degree of pore saturation appear not to influence the tensile fracture generation.

2.2.3 Modified Pinching-Off Mode (Bridgeman's Experiment)

In this mode the confining pressure ($\sigma_1 = \sigma_2$) is continuously increased up to failure while axial load (σ_3) stays constant at a relatively low level. In Bridgeman's pinching-off experiment zero axial load ($\sigma_3 = 0$) is effective and the confining pressure ($\sigma_1 = \sigma_2$) exclusively is applied to a central section of the radial surface of a long cylindrical, either unjacketed or jacketed, specimen. In our modified pinching-off experiment the stresses affect the entire jacketed specimen under controlled stress and strain conditions, especially, however, the axial load remains at low levels. Both axial and radial stress components, as well as pore-fluid pressure, can be set independently. These triaxial test conditions again did not achieve the aim to generate rock splitting or tensile fractures. Applied stresses and the related

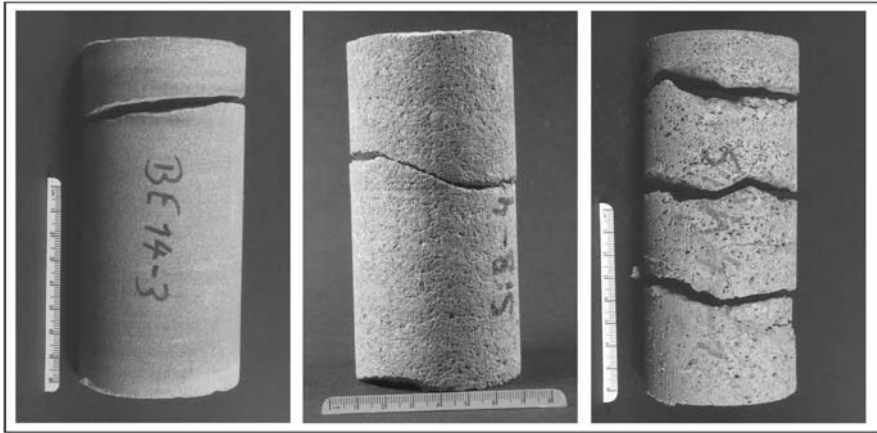


Fig. 2.2. Examples of tensile fractures due to splitting in triaxial extension test (abrupt mode).

spatial deformations of the specimens are nearly identical with those of the rate-controlled test mode. This is why this modified pinching-off test may be only a special case of a rate-controlled triaxial extension test.

3 Discussion

The results so far of these triaxial extension tests, performed with clastic sedimentary rocks, demonstrate that tensile fractures at overall pressure conditions could only be simulated in the so called abrupt mode with a rapid decrease of the axial stress component, which unloads a compressed cylindrical specimen. Comparing this mode with the other triaxial extension testing modes, i.e. with a rate controlled reduction of axial stress (rate-controlled mode) and with a continuous increase of the confining pressure (modified pinching-off mode), apparently the short time axial de-loading results in relatively low driving forces due to stress difference or change of axial strain that regularly and successfully lead to rock splitting, visible as tensile fractures. The magnitudes of stresses and stress differences causing rock splitting or core dinking with tensile fracture patterns usually range between tensile strength and uniaxial compressive strength (cf. Jaeger & Cook 1979). In the abrupt mode of extensional testing, this is also confirmed for both lithotypes investigated in this study (Table 3.1). It should be noted that Lithotype 2, which shows higher compressive as well as tensile strengths compared with Lithotype 1, again shows higher resistance to extensional fracturing.

Table 3.1. Comparison of results: compression and extension tests.

sample set	stress difference extension test [MPa]	uniaxial compressive strength [MPa]	tensile strength [MPa]
Lithotype 1	20	54	3.9
Lithotype 2	25	88	4.9

Following Obert & Stephenson (1965) splitting occurs in the core-disking experiment when

$$\sigma_{\text{radial}} > 3,400 + 2S_0 + 0.7\sigma_{\text{axial}} \quad (3.1)$$

where S_0 = the inherent shear strength (equivalent to cohesion).

Confining pressure, that produces extension fractures in the abrupt mode, i.e. if $\sigma_1 = \sigma_2 = \sigma_{\text{radial}}$ is in the same range but lower in comparison to calculated values according to equation (3-1). This application of equation (3-1), including transformation in MPa-dimension, is valid for $S_0 \sim 5\text{-}10\text{MPa}$, which is nearly equivalent to cohesion or tensile strength of the evaluated rocks, and is valid with the abrupt decrease of $\sigma_3 = \sigma_{\text{axial}}$ to zero. Using the abrupt extensional mode, the relevant stress difference (radial minus axial) at failure is 20 MPa to 25 MPa; the calculated values come to 30-40MPa. In controlled extensional testing modes all specimens sustained essentially higher stress differences without failure. The stress differences exceed those in compression tests (Fig. 3.1). Equation (3-1) then informs that any stress difference decreases with an increase of the total stress. Furthermore, based on the strain criterion according to equations (1-1) and (1-2), some experimental results support the theoretical considerations. For example, the triaxial extension experiments performed in the abrupt mode with Lithotype 1 result in amounts of critical extension strain of 0.1% in the axial direction. This critical value is valid for this rock with elastic parameters $E=12,000\text{ MPa}$ and $\nu=0.25$, and it was effective only in the abrupt extension experiments at $\sigma_1 = \sigma_{\text{radial}} = 25\text{ MPa}$ and $\sigma_3 = \sigma_{\text{axial}}$ at zero. However, in the other extension experiments with controlled modes, higher amounts of axial strain clearly took place without any tensile crack formation. Consequently, neither measured stress differences, nor achievable axial stretching may be proper indications for extensional fracturing, if they are used as single parameters.

The stress ranges for both lithotypes, defined by means of maximum and minimum principle (effective) stress at failure, have their relations lower under triaxial extensional conditions (abrupt mode) than under triaxial compression conditions (Fig. 3.1). However, this is in contrast to the rock failure conditions in the continuously controlled extension tests, where the stress difference is higher

under extension (without reaching the tensile failure state) than under compression the shear failure state was reached. Additionally, lower changes of axial strain are clearly observed at failure due to extension before reaching the failure state in the controlled mode, than at shear failure due to compression loading.

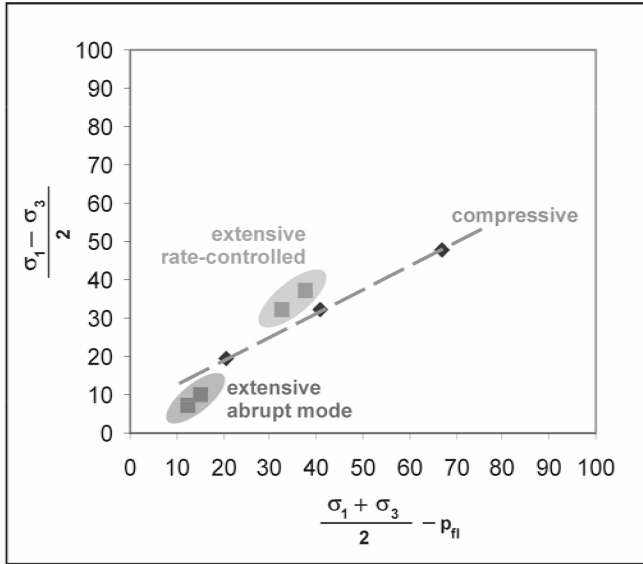


Fig. 3.1. Failure states in triaxial extension and triaxial compression tests.

Unfortunately, it is an unsolved technical problem to determine the plastic volume change, and the related angle of dilatation of the specimens before reaching the splitting failure in the abrupt extensional testing mode. This is why the theoretical determination of the rock splitting phenomenon as it is offered by the theory of plasticity (see equations (1-3) and (1-4)), is necessary and may be possible to proof in the future.

4 Conclusion

The results of the triaxial extension tests in all three described modes show that neither the values of applied stresses or stress differences, nor the enforced deformation or amounts of axial strain alone explain the splitting process. Fracturing with a tensile character, the so called splitting, happens exclusively in the defined abrupt mode in a triaxial extension test at comparable low stresses, stress differences and axial strains. This suggests a time dependent fracturing behaviour. Further research needs to be done to quantify this assumed time dependency of the formation of extension fractures. Even the fastest rates of change of axial unload-

ing or radial loading, applied as controlled rates that are still technically measurable in the available apparatus, were also investigated in this study and they did not lead to any extensional failure. These experimental findings may correspond with observations in situ, where extensional fracturing in the surrounds of underground openings, visible as shells around the hollow space, do occur as a rule, with some time delay after opening a cavern or tunnel in a rock mass. Nevertheless, the velocity of de-loading under experimental triaxial test conditions is some orders higher than is often the case of splitting failure generation that takes place in situ. Using the abrupt mode in triaxial testing, the fracture forms within some seconds; in the case of the excavation of an underground hollow space, the shell generation takes more time (minutes, hours, days). This difference of velocity is supposed to correlate with the observed scale: a specimen of decimetre scale as compared with a structure of meter to tens of meters dimension. In application of the present findings, even a weak support of an underground wall with expected splitting risk, implemented as soon as possible after excavation, may retard the splitting process as well as hinder the already known strength reduction effect of the rock mass. The further weakening of the rock mass will be diminished due to the changing stress distribution, if the abrupt splitting is suppressed by light support as early as technically possible. This may be not an usual procedure in hard rock formations, that do actually not need any support, but tend to have rock splitting failure.

References

- Bärle C (1993) Porenraumuntersuchungen ausgewählter Rotliegend Sandsteinproben Norddeutschlands unter besonderer Berücksichtigung der Porengeometrie. *Forschungsergebnisse aus dem Bereich Hydrogeologie und Umwelt* 11: 160.
- Brown ET & Trollope DH (1967) The failure of linear brittle materials under effective tensile stress. *Felsmechanik* 1: 229-241.
- Fairhurst & Cook (1966) 1st Int. Congr. ISRM, 3.75, Lisboa, pp 687-692.
- Farquhar RA, Smart BGD, Todd AC, Tomkins DE & Tweedie AJ (1993) Stress sensitivity of low petroleum sandstones from the 'Rotliegendes' sandstone. *Proc. Soc. Petroleum Engineers Annual Technical Conference and Exhibition* 5: 851-861.
- Guyatt RCP & Allen JP (1996) Application of horizontal wells to a tight-gas reservoir: a case history. *J. Soc. Petroleum Engineers* 11/3: 203-209.
- Hecht C, Bönsch C & Bauch E (in review) Relations of rock structure and composition to petrophysical and geomechanical rock properties: examples from permocarboniferous red beds. *Rock Mech. and Rock Eng.*
- Jaeger JC & Cook NGW (1979) *Fundamentals of Rock Mechanics*. Halsted, New York.
- Katzung G & Ehmke G (1993) *Das Prätertiär in Ostdeutschland*. Verlag Sven von Loga, Köln.

- Kleditsch O & Kurze M (1993) Ergebnisse petrografischer Untersuchungen an Sandsteinen des tieferen Oberrotliegenden im Raum Altmark/ Westmecklenburg. Geologisches Jahrbuch A 131: 141-178.
- Lempp Ch & Mühlhaus HB (1985) Splitting and core dinking in deep boreholes. 2nd Int. Symposium on Observation of the Continental Crust through Drilling: 94.
- Lütznert H (1987) Sedimentary and volcanic Rotliegendes of the Saale Depression. Excursion guide symposium on Rotliegendes in central Europe, Central Institute for Physics of the Earth, Academy of Sciences of the GDR: 1-197.
- Lütznert H (1988) Sedimentology and basin development of intramontane Rotliegend basins in central Europe. Zeitsch. Geol. Wiss. 16: 845-863.
- Mühlhaus HB & Vardoulakis I (1986) Axially-symmetric buckling of the surface with bending stiffness. Mechanics of materials, Vol. 5: 109-120.
- Obert L & Stephenson DE (1965) Stress conditions under which core discing occurs. Soc. Min. Eng. Trans., 232: 227-235.
- Roeckel Th (1996) Der Spannungszustand in der Erdkruste am Beispiel der Tiefbohrungen des KTB-Programms. In: Gudehus G, Nataf, O (eds) Veröffentlichungen des Institutes für Bodenmechanik und Felsmechanik der Universität Fridericiana, Karlsruhe.
- Schwab M (1977) Zur Paläotektonischen Entwicklung des Halleschen Permosilesgebietes (Nordöstlicher Saaletrog). Hallesches Jahrbuch für Geowiss. 1: 69-84.
- Stacey TR (1981) A simple extension strain criterion for fracture of brittle rock. Int. J. Rock Mech. Min. Sci. & Geomech. Abstr. 18: 469-474.
- Stacey TR (1982) Contribution to the mechanism of core dinking. J. South. Afr. Min. Metall 18: 269-274.

A Constitutive Model for Chemically Sensitive Clays

Nathalie Boukpeti¹, Robert Charlier¹, Tomasz Hueckel², and Zejia Liu³

¹Department GeomaC, University of Liege, Belgium

Nathalie.Boukpeti@ulg.ac.be

Tel: +32-4 366 91 43

Fax: +32-4 366 95 20

²Department of Civil and Environmental Engineering, Duke University, USA

³The State key Laboratory for Structural Analysis of Industrial Equipment,
Dalian University of Technology, China

Abstract. This paper deals with a chemo-hydro-mechanical (CHM) model for unsaturated clays. The chemo-mechanical effects are described within an elasto-plastic model using the concept of chemical softening proposed by Hueckel (1997). The constitutive behaviour of partially saturated clays is modelled following Alonso-Gens' formulation. The equilibrium equations with the chemo-hydro-mechanical constitutive relations are combined with the governing equations for liquid transfer and contaminant transport, and are solved numerically using finite elements. Numerical examples are presented to analyse the chemical effects upon the response during wetting of a clay specimen, and during an excavation.

Keywords: constitutive model, unsaturated clay, plastic mechanisms.

1 Introduction

It has been recognized that the presence of certain chemicals in the pore fluid of clayey soils affects their hydro-mechanical behaviour. Understanding of the chemical effects is essential for the design of clay barriers or the assessment of borehole or tunnel stability. Both expansive and contractive strain have been measured on clay specimens permeated with organic liquids, depending on the chemical concentration and the stress level (Fernandez and Quigley 1991). Compaction of clay specimens upon exposure to salt solutions has also been observed and is explained by the osmotic effect (Di Maio 1996). It was shown that part of this compaction is irreversible. The chemo-mechanical behaviour of clay has been described by means of models based on the micro-structure (e.g., Guimaraes et al. 2001). The macroscopic behaviour can also be represented in a phenomenological manner using the framework of plasticity. Within this framework, the concept of chemical softening was proposed by Hueckel (1997) to describe strains occurring in clay under constant stresses due to the presence of a single chemical. It is assumed that the yield surface shrinks as the contaminant mass concentration increases. In order to predict adequately the chemical expansion observed during permeation of clay with organic liquids (ethanol and dioxane) at low external

stress, Hueckel (1997) formulated a chemo-elastic strain of expansion as a function of concentration. Similar concepts were used in the model presented by Boukpeti (2003). To represent the behavior of unsaturated soils, various approaches have been considered (e.g., Matyas and Radhakrishna 1968). The model presented in this paper follows the ‘Alonso-Gens’ formulation (Alonso et al. 1990), which considers the effects of suction (difference between air and water pressure) on the compression coefficient, on the pre-consolidation pressure, and on the cohesion. The model presented in this paper is based on the constitutive equations proposed by Collin (2003) and Collin et al. (2002) for unsaturated soils, applicable in particular to chalk. The yield surface is composed of an elliptical cap, a frictional line and a traction limit. The effects of suction and chemical concentration are incorporated into the model. The chemo-hydro-mechanical model results in the coupling of the governing equations for equilibrium (including the constitutive equations), flow and mass transport. The fluid flow model takes into account unsaturated conditions and is described by Collin (2003). For the chemical mass transport, only the advective and diffusive effects are considered in this paper. A complete description of the mass transport model is given by Radu et al. (1994) and Li et al. (1999). In the following section, the constitutive equations for the chemo-hydro-mechanical behaviour of unsaturated clays are presented. Next, two numerical examples are discussed; wetting of a clay specimen with a chemical, and an excavation in chemically sensitive clay. The numerical simulations were performed using the finite elements program LAGAMINE.

2 Constitutive Model

2.1 General Formulation

The constitutive equations, expressed in rate form, relate the strain tensor ε_{ij} to the stress tensor σ_{ij} , the suction s , and the chemical mass concentration c . A positive strain corresponds to compaction. The suction is defined by the difference between the air and water pressure ($s \geq 0$). The mass concentration is the ratio of mass of chemical to the total mass of fluid ($c \leq 1$). In the formulation given below, the stress tensor designates alternatively the net stress (difference between total stress and air pressure), in the case of unsaturated conditions, or the effective stress in the case of full saturation. The strain rate is decomposed into an elastic (reversible) part and a plastic (irreversible) part. The elastic part can also be decomposed into mechanical, suction, and chemical contributions, namely:

$$\dot{\varepsilon}_{ij} = \dot{\varepsilon}_{ij}^e + \dot{\varepsilon}_{ij}^p = \dot{\varepsilon}_{ij}^{e,m} + \dot{\varepsilon}_{ij}^{e,s} + \dot{\varepsilon}_{ij}^{e,c} + \dot{\varepsilon}_{ij}^p \quad (2.1-1)$$

The plastic deformation occurs when the yield condition on stresses is verified. However, this plastic strain rate can be generated by variations in suction or concentration at constant stress state. The mechanical elastic stress-strain law is given by:

$$\dot{\sigma}_{kl} = C_{kl ij}^e \dot{\epsilon}_{ij}^{m,e} \tag{2.1-2}$$

with the compliance elastic tensor $C_{kl ij}^e$ defined as:

$$C_{kl ij}^e = 2G \delta_{ik} \delta_{jl} + \left[\frac{(1+e)}{3\kappa} \sigma_{mm} - \frac{2}{3}G \right] \delta_{ij} \delta_{kl} \tag{2.1-3}$$

where G is the elastic shear modulus, e is the void ratio and κ is the elastic volumetric coefficient. The elastic deformation induced by suction is given by:

$$\dot{\epsilon}_{ij}^{s,e} = \frac{1}{3} \frac{\kappa_s}{(1+e)} \frac{\dot{s}}{(s+p_{at})} \delta_{ij} = h_{ij}^e \dot{s} \tag{2.1-4}$$

where e is the void ratio, p_{at} is the atmospheric pressure and κ_s is the elastic stiffness parameter for changes in suction defined in the Alonso-Gens' model. This isotropic deformation is contractive for an increase in suction s (drying) and expansive for a decrease of s (wetting). The reversible chemical strain is also isotropic:

$$\dot{\epsilon}_{ij}^{c,e} = -\frac{1}{3} \beta \dot{c} \delta_{ij} = l_{ij}^e \dot{c} \tag{2.1-5}$$

The coefficient β is the chemical expansion coefficient defined by Hueckel as:

$$\beta = -F_0 \beta_0 \exp[\beta_0 (1 - c + \ln c)] \left(\frac{1}{c} - 1 \right) \tag{2.1-6}$$

where F_0 and β_0 are material constants dependent on the soil and the chemical. The plastic deformation is described within the framework of strain-hardening/softening plasticity. The yield criterion reads:

$$f(\sigma_{ij}, \theta) \leq 0 \tag{2.1-7}$$

where θ is an internal variable depending on plastic strain, suction and chemical concentration. During plastic loading, the yield function f verifies the consistency condition:

$$\dot{f} = \frac{\partial f}{\partial \sigma_{ij}} \dot{\sigma}_{ij} + \frac{\partial f}{\partial \theta} \dot{\theta} = 0 \tag{2.1-8}$$

The evolution of the internal variable θ is described by the general hardening law:

$$\dot{\theta} = \frac{\partial \theta}{\partial \epsilon^p} \dot{\epsilon}^p + \frac{\partial \theta}{\partial s} \dot{s} + \frac{\partial \theta}{\partial c} \dot{c} \tag{2.1-9}$$

In the particular plastic models described in the next section, either the volumetric or the shear component of the plastic strain rate is considered in the hardening law. The plastic strain vector is defined by the non-associated flow rule:

$$\dot{\epsilon}_{ij}^p = \dot{\Lambda}^p \frac{\partial g}{\partial \sigma_{ij}} \tag{2.1-10}$$

where g is the plastic potential and $\dot{\Lambda}^p$ is the plastic multiplier.

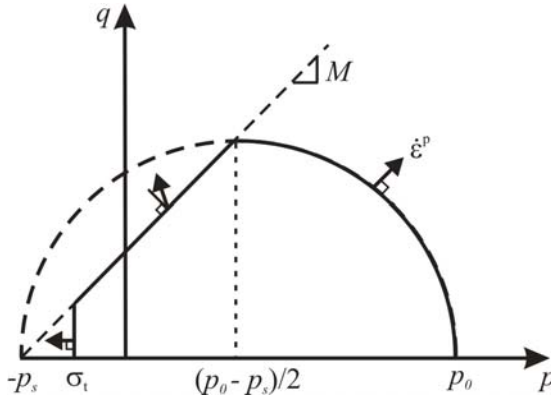


Fig. 2.1. Yield surface in the stress plane (q, p) .

2.2 Plastic Behaviour

Three plastic mechanisms are considered: pore collapse or plastic volumetric compaction, frictional failure with possible dilation, and tensile failure. These three mechanisms are represented by three plastic models with the following yield criteria:

$$f_1 = q^2 + M^2(\beta)(p + p_s)(p - p_0) = 0 ; \quad p > (p_0 - p_s)/2 \tag{2.2-1}$$

$$f_2 = q - M(\beta)(p + p_s) = 0 ; \quad \sigma_t < p < (p_0 - p_s)/2 \tag{2.2-2}$$

$$f_3 = p + \sigma_t = 0 \tag{2.2-3}$$

where p_0 is the pre-consolidation pressure, p_s is a measure of the cohesion ($p_s \geq 0$), σ_t is the tensile strength, and $M(\beta)$ is a parameter related to the friction angle and function of the Lode angle as defined by Van Eekelen (1980). The stress invariants p and q are defined as: $p = \sigma_{kk} / 3$ and $q = \sqrt{3/2 s_{ij} s_{ij}}$, where s_{ij} is the deviatoric part of the stress tensor. In the stress plane (q, p) f_1 is represented by an

ellipse with intercepts on the p -axis $-p_s$ and p_0 (see Fig. 2.1). The yield function f_2 is plotted as a friction line of slope M and intercept on the p -axis $-p_s$. The tensile failure criterion $f_3 = 0$ is represented as a vertical line in Figure 1. In this case, an associated flow rule is used with no hardening. The description of the pore collapse model and the frictional failure model is completed below.

2.2.1 Pore Collapse Model

The pore collapse model is based on the Cam clay model; the yield surface f_1 is elliptical, the flow rule is associated, and the internal variable p_0 evolves with the volumetric component of the plastic strain. The effects of suction and chemical concentration on the internal variable p_0 is described by:

$$p_0(s, c) = p_c S(c) \left(\frac{p_0^*}{p_c} \right)^{\frac{\lambda(0) - \kappa}{\lambda(s) - \kappa}} \tag{2.2-4}$$

where p_c is a reference pressure, p_0^* is the pre-consolidation pressure for $s = 0$ and $c = 0$, and $\lambda(0)$ is the compression coefficient at zero suction. The compression coefficient $\lambda(s)$ is a decreasing function of s :

$$\lambda(s) = \lambda(0) \left[(1 - r) \exp(-\beta' s) + r \right] \tag{2.2-5}$$

where r is a constant representing the maximum stiffness of the clay (at large suction) and β' is a constant controlling the stiffness increase with suction increase, as defined in the Alonso-Gens' model. For a vanishing value of concentration, equation (2.2-5) defines the Loading Collapse line (LC) represented in Fig. 2.2a. The chemical softening function $S(c)$ is of the form proposed by Hueckel:

$$S(c) = \exp(-ac) \tag{2.2-6}$$

where a is a constant representing the strength of chemical softening. The chemical softening line (CHS) is depicted in Fig. 2.2b. The evolution of p_0^* follows the volumetric hardening law:

$$\dot{p}_0^* = \frac{1 + e}{\lambda - \kappa} p_0^* \dot{\epsilon}_v^p \tag{2.2-7}$$

2.2.2 Frictional Failure Model

Frictional failure takes place when the state of stress verifies the yield criterion f_2 . Plastic strain obey a non-associated flow rule with the plastic potential:

$$g_2 = q - M'(p + p_r) = 0 \tag{2.2-8}$$

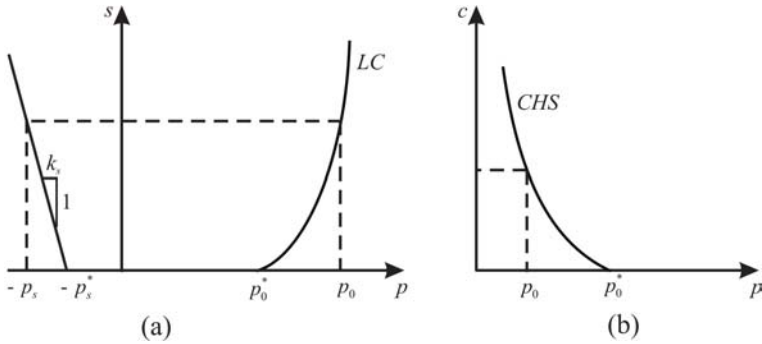


Fig. 2.2. Yield surface; a) in the plane (s, p) , b) in the plane (c, p) .

where $M'(\beta)$ is related to the dilatancy angle and a function of the Lode angle, and p_r is determined from the requirement that the stress point lies on g_2 . The internal variable p_s evolves as a linear function of suction:

$$p_s = p_s^* + k_s s \tag{2.2-9}$$

where k_s is a constant, and p_s^* is the value of the variable p_s for saturated conditions. This type of hardening law for the effect of suction was proposed in the Alonso-Gens' model and is illustrated in Fig. 2.2a.

3 Numerical Examples

3.1 Wetting of Clay with Organic Liquid

In this example, we analyse the chemical effect of an organic contaminant on the behaviour of a partially saturated clay specimen during wetting. The cylindrical specimen of 2 cm thickness and 5.38 cm diameter is in oedometric conditions (uniaxial deformation). Initially, an external vertical load of 133 kPa is applied on the specimen, and the coefficient $K_0 = 0.625$. The air pressure is at atmospheric pressure, $p_a = 100$ kPa, and is assumed constant during the test. The initial pore pressure is $p_w = -78.5$ MPa, which corresponds to a suction $s = 78.6$ MPa, and a saturation degree $S_r = 0.49$. The initial chemical concentration is zero. The chemo-hydraulic boundary conditions consist of a fixed value of chemical concentration at the top boundary, $c = 0.6$, and fixed values of suction at the top and bottom boundary, $s = -28.6$ MPa at the top, and s is equal to its initial value at the bottom. The parameters of the CHM system are listed in Table 1. Values of the mechanical and transport coefficients ($k_{w,int}$ is the intrinsic permeability and d_m is the molecular diffusion coefficient) are typical for clay; the chemical parameters are chosen

within the range of values given by Hueckel (1997) for clay and organic liquids. Figure 3.1 depicts the evolution of suction and chemical concentration along the specimen with time. Equilibrium of flow is reached much faster than chemical equilibrium. The volumetric deformation of the specimen due to wetting with water and with an organic liquid is represented in Fig. 3.2, with a positive strain representing expansion. In the absence of chemical effects, swelling occurs as a result of a decrease of suction, which is governed by the parameter κ_s . Chemical effects are of two types. In the case of a highly over consolidated clay (large value of p_0), the model predicts expansive strain controlled by the parameters F_0 and β_0 . On the contrary, if the clay is slightly over consolidated or normally consolidated, additional chemical compaction is predicted, which is governed by the plastic yield criterion ($f_l = 0$) and the parameter α . It is apparent in Fig. 3.2 that the chemical plastic compaction is larger at the top of the specimen than at the bottom. This is correlated with smaller value of suction, and therefore smaller pre-consolidation pressure p_0 , at the top than at the bottom of the clay specimen.

Table 1. Model parameters typical for clay and water solution of organic liquid.

Mechanical	κ	λ	κ_s	e	G	M	p_s	p_0^1	p_0^2
	0.02	0.1	0.11	0.66	10 MPa	1.2	2.078 MPa	2000 MPa	0.2 MPa
Chemical	F_0	β_0	a						
	-0.04	1.32	3.45						
Transport	$k_{w,int}$	d_m							
	m^2 $4.7 \cdot 10^{-18}$	m^2/s 10^{-9}							

¹ highly overconsolidated clay; ² slightly over consolidated clay

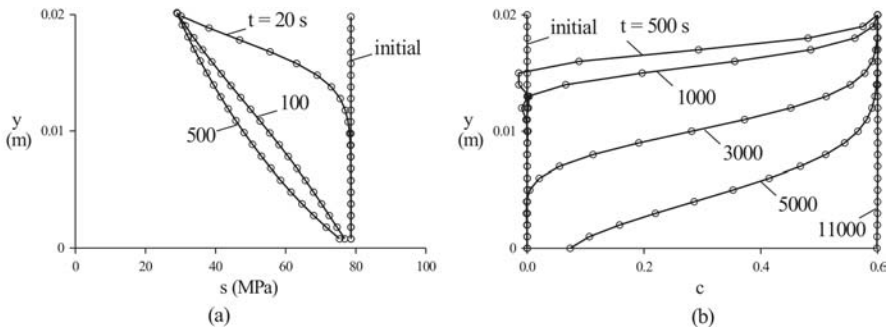


Fig. 3.1. Wetting of clay with organic liquid: (a) suction, (b) chemical concentration.

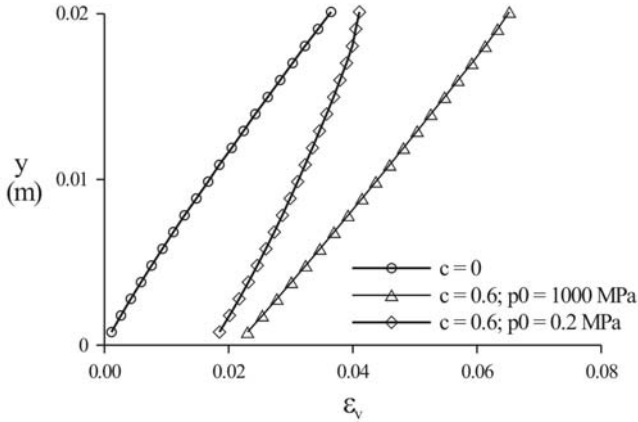


Fig. 3.2. Volumetric response to wetting with organic liquid; p_0^1 is for a highly over consolidated clay, p_0^2 is for a slightly consolidated clay.

3.2 Excavation in Chemically Sensitive Clay

The perturbations caused by an excavation may lead to chemical reactions occurring around the opening, e.g. oxidation to air, or significant swelling due to water circulation. In this section, we consider the problem of an excavation in hard clay soil in unsaturated conditions, with the presence of a contaminant diffusing in the soil from the tunnel boundary. The tunnel is circular with 5 m diameter and is located 220 m deep. The geometry, initial and boundary conditions are depicted in Fig. 3.3. Assuming a soil unit weight of 21 kN/m^3 , the initial state of stress at the tunnel's depth is 4.6 MPa, and is assumed to be isotropic. The initial pore pressure distribution is in equilibrium under gravity, with $p_w = -78.5 \text{ MPa}$ at the top boundary of the model. The air pressure is $p_a = 100 \text{ kPa}$ and is assumed to remain fixed. The excavation is modelled by reducing the stress applied to the tunnel's face from its initial value to zero. Simultaneously, the chemical concentration is increased from $c = 0$ to $c = 0.6$. The model parameters are similar to those listed in Table 1 except for: $G = 200 \text{ MPa}$, $p_s = 72.75 \text{ MPa}$, $p_0^1 = 2500 \text{ MPa}$, $p_0^2 = 10 \text{ MPa}$, $k_{w,int} = 4.7 \cdot 10^{-14} \text{ m}^2$, $d_m = 3 \cdot 10^{-8} \text{ m}^2/\text{s}$. Figure 3.4a shows the concentration distribution along the horizontal line passing through the tunnel centre as a function of the distance to the tunnel face after 2300 days. It is apparent that the chemical has diffused into the soil over a distance of approximately 10 m. The volumetric strain distribution is depicted in Fig. 3.4b. The volumetric changes in the absence of chemical are close to zero. Chemical effects induce an expansion of about 2.5% close to the tunnel's face, in the case of a highly over consolidated clay ($p_0 = 2500 \text{ MPa}$). In the case of a soil with a smaller pre-consolidation pressure, some chemical compaction occurs in addition to the expansion. However, with the value of $p_0 = 10 \text{ MPa}$ chosen here, the plastic chemical compaction is not significant.

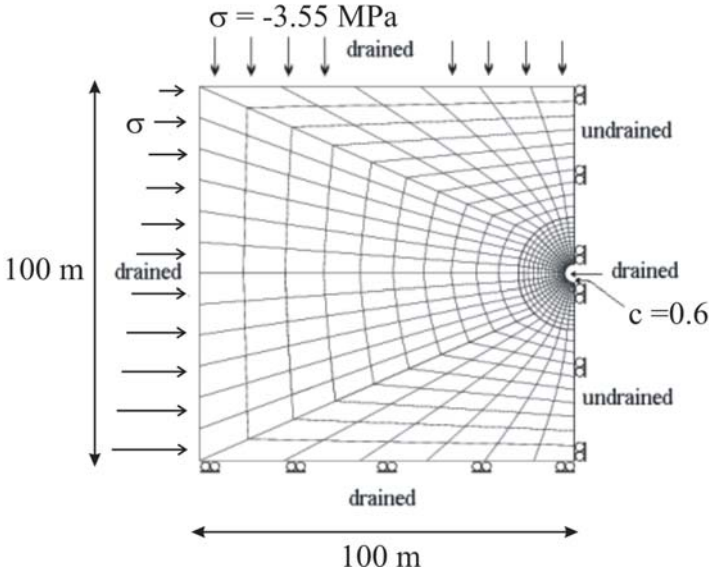


Fig. 3.3. Geometry of the tunnel, initial and boundary conditions.

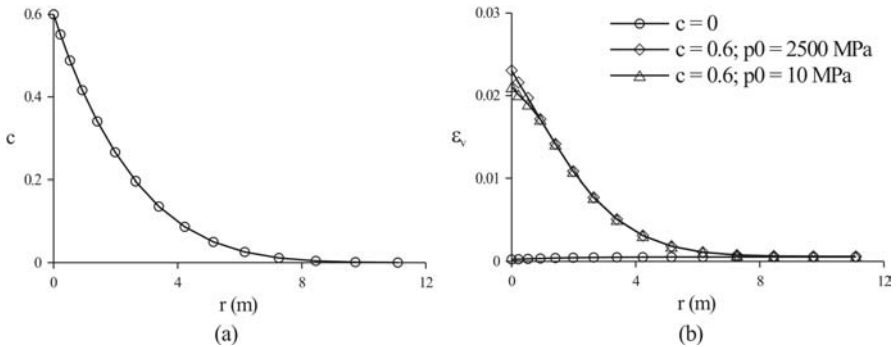


Fig. 3.4. (a) chemical concentration distribution; (b) volumetric strain distribution.

4 Concluding Remarks

A constitutive model for the chemo-hydro-mechanical(CHM) behavior of unsaturated soil has been presented. The chemical effects are described using the concepts of chemical softening and elastic expansive strain as proposed by Hueckel (1997). The formulation uses the framework set by Alonso et al. (1990) to describe the behavior of unsaturated soil. The model has been implemented into the finite elements code LAGAMINE and applied to two numerical examples. It was shown that the predicted chemical strain depend on the value of the pre-consoli-

ation pressure, and therefore on the suction level (or saturation degree). This type of results suggests to investigate experimentally the chemical effects on the mechanical behavior of clay in various saturation conditions.

Acknowledgements

This work is sponsored by Ministry of Education of Belgium under the international joint research project “Qualité et durabilité de la protection des nappes aquifères sous sites d'enfouissement technique avec barrières argileuses d'étanchéité” and The National Natural Science Foundation of China under the project No. 59878009. The support is greatly acknowledged.

References

- Alonso EE, Gens A, Josa A (1990) A constitutive model for partially saturated soils. *Geotechnique* 40(3): 405-430.
- Boukpeti N, Charlier R, Hueckel T (2003) Modelling contamination of clays, VII International conference on Computational Plasticity (COMPLAS 2003), Barcelona.
- Collin F (2003) Couplages thermo-hydro-mécaniques dans les sols et les roches tendres partiellement saturés. Thèse de doctorat de l'Université de Liège.
- Collin F, Cui YJ, Schroeder C, Charlier R (2002) Mechanical Behavior of Lixhe chalk partly saturated by oil and water: experiment and modelling. *International Journal of Numerical and Analytical. Methods in Geomechanics* 26: 897-924.
- Di Maio C (1996) Exposure of bentonite to salt solution: osmotic and mechanical effects. *Géotechnique* 46(4): 695-707.
- Hueckel T (1997) Chemo-plasticity of clays subjected to stress and flow of a single contaminant. *International journal for numerical and analytical methods in geomechanics*, 21: 43-72.
- Fernandez F and Quigley RM (1991) Controlling the destructive effect of clay-organic liquid interactions by application of effective stresses. *Canadian Geotechnical Journal* 28: 388-398.
- Guimaraes L do N, Gens A, Sanchez M, Olivella S (2001) Chemo-mechanical modelling of expansive clays. 6th International Workshop on Key Issues on Waste Isolation Research, Paris.
- Li X, Cescotto S, Thomas HR (1999) Finite element method for contaminant transport in unsaturated soils, *ASCE Journal of Hydrologic engineering*, 4(3): 265-274.
- Matyas E L, Radhakrishna H S (1968) Volume change characteristics of partially saturated soils. *Géotechnique* 18 : 432-448.
- Radu JP, Biver P, Charlier R, Cescotto S (1994) 2 and 3D finite element modelling of miscible pollutant transport in groundwater, below the unsaturated zone. International Conference on Hydrodynamics, Wuxi, China.
- Van Eekelen H A M (1980) Isotropic yield surfaces in three dimensions for use in soil mechanics. *International Journal for Numerical and Analytical Methods in Geomechanics* 4: 98-101.

Relocation of a Problematic Segment of a Natural Gas Pipeline Using GIS-Based Landslide Susceptibility Mapping, Hendek (Turkey)

Engin Cevik and Tamer Topal

Dept. of Geological Engineering, METU, 06531, Ankara, Turkey
topal@metu.edu.tr
Tel:+90 312 210 26 90
Fax:+90 312 210 12 63

Abstract. A segment of natural gas pipeline constructed in 1997 to supply natural gas to a steel factory was broken due to a landslide with fire near Hendek, Turkey. Re-routing of the pipeline is planned but it requires preparation of landslide susceptibility map of the corresponding segment. In this study, statistical methods namely statistical index (Wi) and weighting factor (WF) have been used with geographic information systems (GIS) by analyzing several intrinsic factors controlling the landslides to prepare landslide susceptibility map of the problematic segment of the pipeline. For this purpose, thematic layers including landslide inventory, lithology, slope, aspect, elevation, land use/land cover, distance to stream, and drainage density were used. In the study area, landslides mainly occur in the unconsolidated to semi-consolidated clayey unit and regolith. Lithology, land use/land cover, elevation, slope, and distance to stream are found to be the important parameters for the study area whereas aspect is not. Nevertheless, the drainage density has a very low contribution. Based on the findings obtained in this study, an alternative route to be studied for detailed engineering geological investigations is proposed.

Keywords: GIS, Hendek, Landslide, Statistical methods, Susceptibility mapping, gas, pipeline, Turkey.

1 Introduction

Among various natural hazards, landslides are the most widespread and damaging. They cause loss of life and property, damage to natural resources (e.g. vegetation, land and soil) and hamper developmental projects such as roads, bridges and communication lines (Saha et al. 2002). Therefore, potential landslide-prone areas should be identified in advance in order to reduce such damage. In this respect, landslide susceptibility assessment can provide valuable information essential for hazard mitigation through proper project planning and implementation (Carrara et al. 1995; Gökçeoğlu and Aksoy 1996; Soeters and Van Westen 1996; Aleotti and Chowdhury 1999; Pistocchi et al. 2002; Donati and Turini 2002). A pipeline was constructed in 1997 in order to supply natural gas to Ereğli Steel Factory in Turkey. However, an accident (landslide) occurred near Hendek (Fig. 1.1). A section

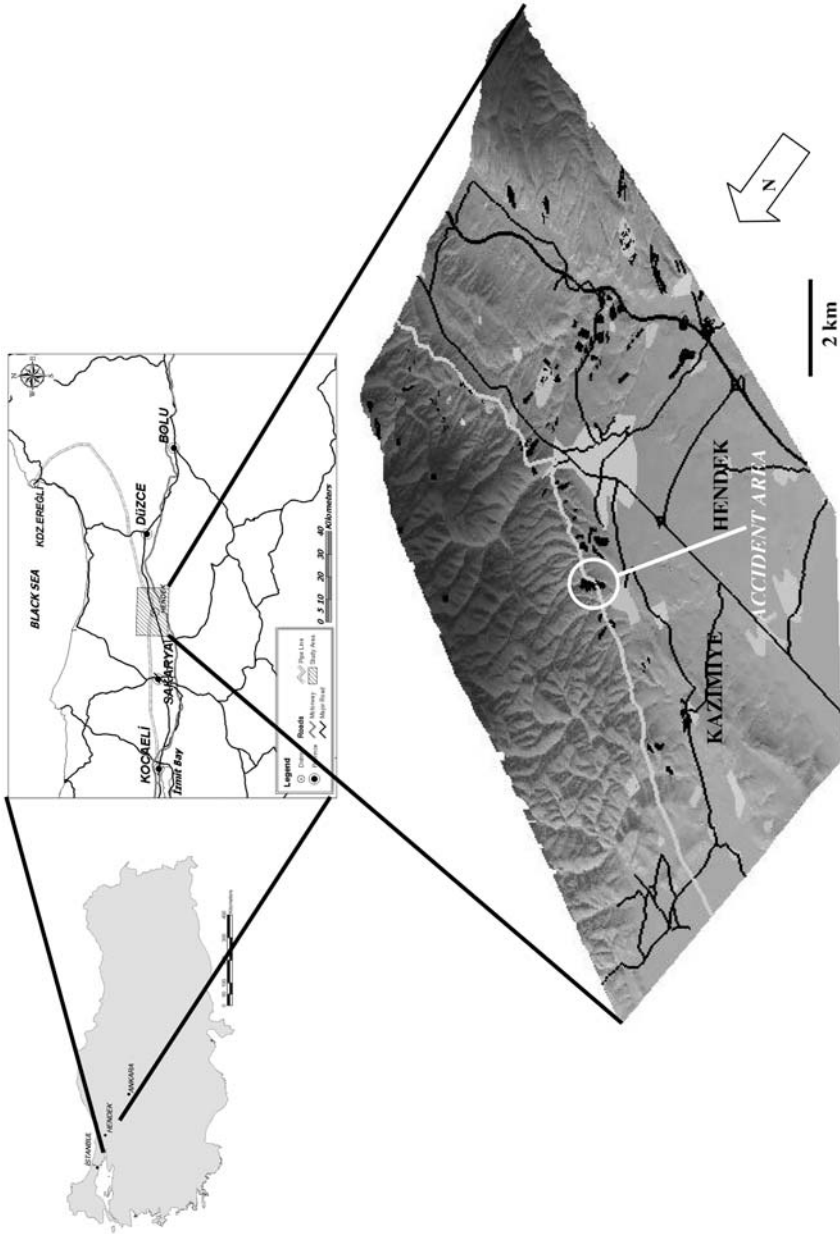


Fig. 1.1. Location map of the study area.

of the pipeline was broken due to the landslide with a fire. The fire was extinguished after 3 days. Re-routing of the problematic section of the pipeline is still under discussion, but it requires preparation of landslide susceptibility map of the corresponding segment. The purpose of this study is to prepare landslide suscepti-

bility maps using two different statistical methods, namely statistical index (W_i) and weighting factor (W_f) for the problematic segment (from 60 km to 83 km) of the natural gas pipeline by analyzing several intrinsic factors controlling the landslides. It is also intended to evaluate the maps for the purpose of their applicability for possible re-routing of the pipeline in the future. Study area covers about 290 km². Climatic characteristics of the region resemble the characteristics of both Marmara and Black Sea regions. In winter season weather condition is generally rainy and mild, and in summer it is hot. Relative humidity level is high for every season.

2 Route Geology

In the study area, sedimentary rocks are observed. Hendek formation (Ordovician), Aydos formation (Ordovician), Ereğli formation (Ordovician-Lower Devonian), Yemişliçay formation (Turonian-Campanian), Akveren formation (Upper Cretaceous- Paleocene), Çaycuma formation (Lower-Middle Eocene), Örencik formation (Pliocene-Pleistocene) and alluvium (Quaternary) constitute the main lithological units exposed in the study area (Fig. 2.1). About 40% and 21% of the pipeline were constructed in Hendek and Örencik formations, respectively. Rest of the pipeline passes through various other units with a percentage less than about 19%. The lithological description and landslide characteristics of the units are

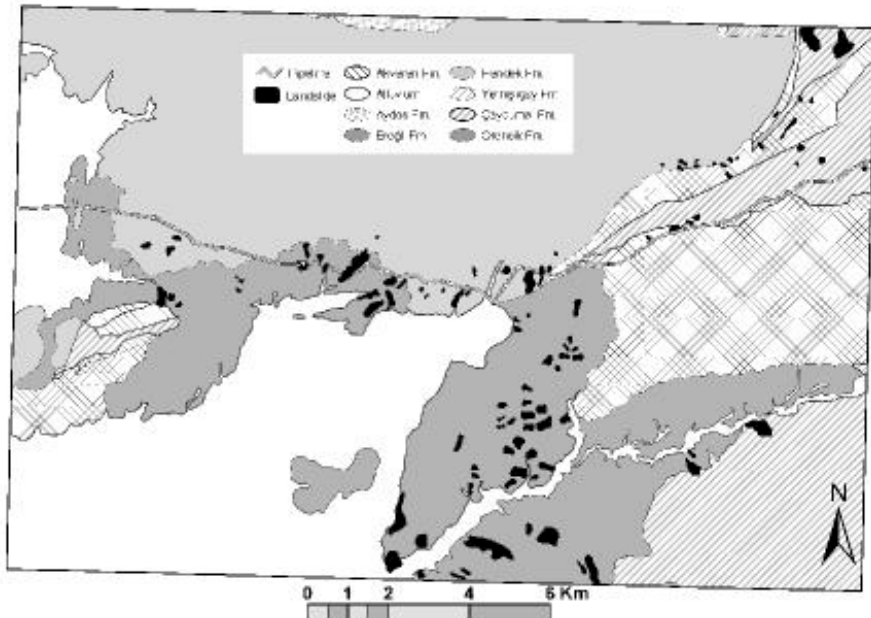


Fig. 2.1. Geological map of the study area (After Emre and others, 1999).

Table 2.1. Lithological description and landslide characteristics of the units.

Formation Name (Age)	Description	Type of Failure
Alluvium (Holocene)	unconsolidated clay, silt, sand, and gravel	-
Örencik (Pliocene- Pleistocene)	unconsolidated to semiconsolidated claystone and mudstone with sandstone and conglomerate; this unit is characterized by erosional valleys with several landslides developed mainly adjacent to the valleys	Mainly rotational, rarely rotational to flow
Çaycuma (Lower- Middle Eocene)	thin to medium bedded marl, sandstone with mudstone alternations and conglomerate. Local small landslides exist in this unit	Translational to rotational
Akveren (Campanian- Lower Paleocene)	thin to thick bedded claystone, clayey limestone-marl with siltstone and karstic reefal limestone. No landslide exists in the study area.	-
Yemişliçay (Cretaceous)	thin to medium bedded volcanic sandstone with rarely claystone, agglomerate, tuff, tuffite, limestone, andesite and basalt. Some local and small landslides exist in the study area	Translational to rotational
Ereğli (Ordovician- Lower Devonian)	thin to medium bedded shale-sandstone alternations with limestone interbedding. No landslide exists in this unit	-
Aydos (Ordovician)	medium to thick bedded, strong to very strong, massive sandstone and conglomerate. No landslide exists in the study area	-
Hendek (Ordovician)	thin to medium bedded, medium strong, shale with sandstone interbedding. Landslides are rarely observed in this unit	Translational to flow

summarized in Table 2.1. Most of the landslides observed in the study area are located within unconsolidated to semi-consolidated clay dominant Örencik formation. Landslides developed in the Örencik formation are shallow to very deep, whereas they are surficial to shallow in other formations. The study area and its close vicinity are significantly affected from Neotectonic activity of the region. Structural and geomorphological features related to right-lateral strike slip fault (a strand of the North Anatolian Fault Zone), can be seen in the region. Therefore, earthquakes may trigger landslides in the future. Considering the fact that the study area is small, seismicity is expected to have uniform effect all over the area. Therefore, seismicity is not used in the landslide susceptibility analyses.

3 Methodology

In this study, maps relevant to landslide susceptibility analysis were constructed using GIS software Arc Map 8 in UTM (Zone 36N) projection system. First, a digital elevation model of the study area was prepared from topographical map. This model was used to prepare slope, aspect, distance to stream, drainage density and elevation maps. Geology and landslide maps were compiled from published reports and checked in the field. Lithology and distance to fault maps were derived from a 1:25,000 scale geology map. The landslide map previously prepared for a very large area by Emre et al. (1999) and Duman et al. (2001) was checked in the field and the map was digitized to produce a landslide inventory map. The land use/land cover map prepared by General Directorate of Rural Services of Turkey was also used in this study. Finally, overlay analyses were carried out using both statistical index (W_i) and weighting factor (W_f) methods.

4 Susceptibility Analyses

In this study, landslide susceptibility analyses were performed using statistical bivariate methods, namely, statistical index (W_i) method of Van Westen (1997) and weighting factor (W_f) method. For this purpose, landslide inventory, lithology, slope, aspect, elevation, land use/land cover, distance to stream, and drainage density layers were used. Seismicity and precipitation data were not included in the susceptibility analyses because they have uniform effects on landslide triggering mechanism due to the spatial limitations of the study area. Distance to fault data layer was also not included in the analyses due to the existence of inverse relationship between landslide distribution and distance to fault.

4.1 Statistical Index (W_i) Method

In the first phase of the landslide susceptibility analysis, the statistical index method proposed by Van Westen (1997) was employed under a GIS environment. In this method, a weight value for a parameter class is defined as the natural logarithm of the landslide density class, divided by the landslide density in the entire map (Van Westen 1997; Rautela and Lakhera 2000). The formula given below forms the basis of the approach:

$$W_i = \ln \frac{\text{Densclass}}{\text{Densmap}} = \ln \frac{\frac{N_{pix}(S_i)}{N_{pix}(N_i)}}{\frac{SN_{pix}(S_i)}{SN_{pix}(N_i)}} \quad (4.1)$$

where W_i = the weight given to a certain parameter class, Densclass = landslide density within the parameter class, Densmap = landslide density within the entire map, $N_{pix}(S_i)$ = number of pixels that contain landslides in a certain parameter class, and $N_{pix}(N_i)$ = total number of pixels in a certain parameter class.

The W_i method is based on statistical correlation of the landslide inventory map with attributes of different parameter maps. In this study, every parameter map was crossed with the landslide inventory map, and density of the landslide in each class was calculated. Correlation results were stored in resultant rasters and the density of the landslides per parameter class was calculated. Then, W_i value of each attribute was calculated (Table 4.1). Finally, all layers were summed up and resultant susceptibility map was obtained. Final susceptibility map (Fig. 4.1) was divided into 5 classes according to 20 % equal class of total number of elements. The classes are very low susceptibility, low susceptibility, moderate susceptibility, high susceptibility, and very high susceptibility.

4.2 Weighting Factor (W_f) Method

Assigning weighting factor for various attributes is a common method used frequently. The weighting factor values may be selected either arbitrarily mainly on the basis of expert opinion (Anbalagan 1992; Turrini and Visintainer 1998) or through some intermediate processes (Rautela and Lakhera 2000; Lee and Min 2001; Dai et al. 2001). The weighting factor (W_f) method used in this study is a modification of W_i method. In W_f method, the weighting factor values were found by using a procedure which considers W_i values of every attribute. To do this, firstly, landslide inventory map was rasterized (15 m pixel size). The rasterized landslide inventory map was crossed with all other rasterized parameter maps. In each layer, W_i values for each pixel of the landslide area were found. Then, all pixel values belonging to each layer were summed up. By using the maximum and minimum of all layers, the results were stretched. Finally, the weighting factor ranging between 1 and 100 for each layer was determined by utilizing the following formula:

$$W_f = \frac{(Twi_value) - (Min_TWi_value)}{(Max_TWi_value) - (Min_TWi_value)} \times 100 \quad (4.2)$$

where W_f = weighting factor calculated for each layer, TW_i_value = total weighting index value of cells within landslide bodies for each layer, $Min_TW_i_value$ = minimum total weighting index value within selected layers, and $Max_TW_i_value$ = maximum total weighting index value within selected layers. The weighting factor (W_f) value of each layer is given in Table 4.1. In this study, W_f value for each layer was multiplied by W_i value of each attribute, and all the pixels for every layer were summed up. Resultant map was reclassified by dividing the total number of elements into equal 20 % classes. Landslide susceptibility map produced by using W_f method is given in Fig. 4.2.

5 Discussion and Conclusion

Based on the landslide susceptibility analyses of the study area, lithology, land use/land cover, elevation, slope, and distance to stream are found to be the important parameters for the study area whereas aspect is not. Nevertheless, the drainage

Table 4.1. Distribution of landslides for various data layers and rating system adopted in this study.

Data Layers	Classes	Landslide area (%)	Wi	Wf
Lithology	Akveren fm.	0.7	0.122	100.00
	Hendek fm.	11.7	2.967	
	Alluvium	2.6	2.364	
	Çaycuma fm.	14.8	3.266	
	Örencik fm.	66.1	4.680	
	Yemişliçay fm.	4.1	1.857	
	Aydos fm.	0	0.000	
	Ereğli fm.	0	0.000	
Slope Angle (Degree)	0-10	48.9	3.312	56.38
	10-20	36.9	3.053	
	20-30	12.3	2.032	
	30-40	1.9	0.392	
	40-50	0	0.000	
	50-60	0	0.000	
	>60	0	0.000	
Aspect	N	11.2	2.409	1.00
	NE	7.5	1.361	
	E	10.2	1.688	
	SE	12.9	1.862	
	S	11.5	1.797	
	SW	11.1	1.820	
	W	11.6	1.789	
	NW	14.2	2.038	
	FLAT	9.8	1.605	
Elevation	10-150 m	63.1	3.466	57.71
	150-300 m	24.6	3.025	
	300-400 m	7	0.903	
	400-500 m	4.2	0.897	
	500-600 m	1.1	0.174	
	>600 m	0	0.000	
Land use \ Land cover	Bushes	1.1	0.100	71.73
	Pasture Area	1.5	0.399	
	Agricultural Area	48.5	3.885	
	Forest	10.7	1.887	
	Walnut	38.2	3.641	
Distance to Stream	0-100 m	23.1	3.011	41.21
	100-200 m	31.5	2.890	
	200-300 m	24.2	2.559	
	300-400 m	12.9	2.030	
	>400 m	8.3	1.671	
Drainage Density	A	18	2.467	8.84
	B	1	0.851	
	C	20	1.868	
	D	5.6	1.269	
	E	43.8	2.513	
	F	4.4	1.643	
	G	6.6	2.991	
	H	0.6	0.311	
Distance to Fault	0-100 m	4.9	0.280	39.84
	100-250 m	8	0.598	
	250-500 m	10	0.553	
	500-1000 m	14	0.303	
	>1000 m	63.1	-0.184	

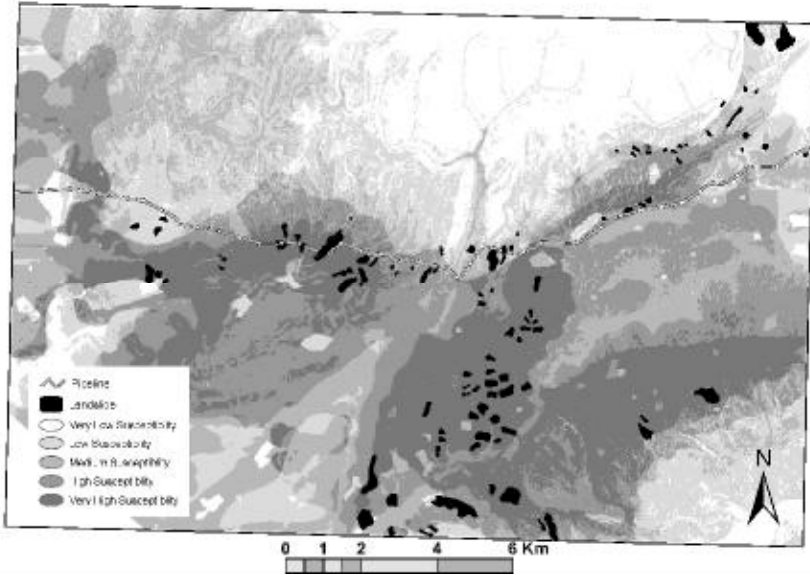


Fig. 4.1. Landslide susceptibility map produced by the Wi method.

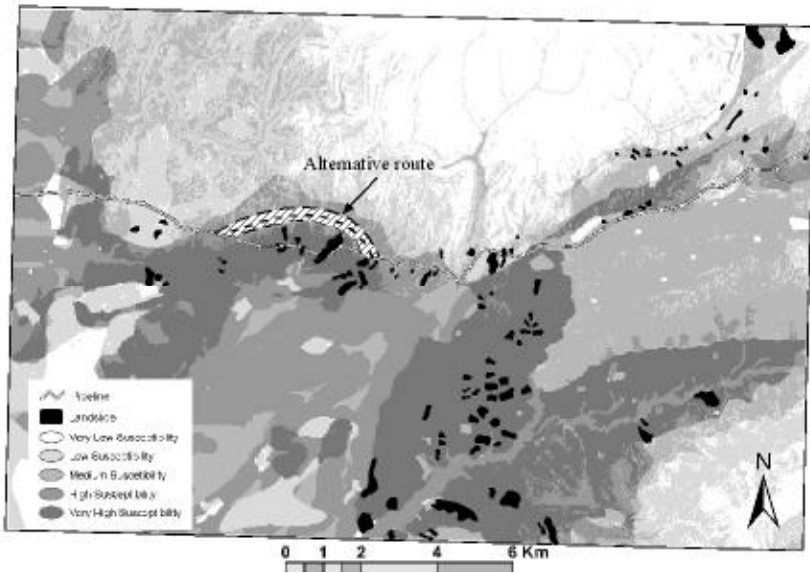


Fig. 4.2. Landslide susceptibility map produced by the Wf method.

density has a very low contribution. The ratings (%) of the layers found on the basis of Wf values indicate that the geology has the highest rating value (100%). Thus, it is the most important parameter for the study area. In fact, this is in good

agreement with the field observations. The field studies reveal that the landslides are mainly formed within the unconsolidated to semi-consolidated Örencik formation. Other high rating percentages attained in slope and elevation layers may also be attributed to the effect of the Örencik formation. In other words, this formation controls both the slope and elevation. In addition to this, the agricultural activities significantly promote landslides. Distance to stream is also an important parameter. Many large landslides including the one which had broken the pipeline are next to the streams. Both W_i and W_f methods used in this study yield quite identical landslide susceptibility maps. Very high susceptibility zones by W_i and W_f methods contain 48.15% and 57.88% of landslide area, respectively. High susceptibility zones by W_i and W_f methods, however, include 22.60% and 13.62% of landslide area, respectively. The other zones contain landslide area less than 20%. Although relatively low percentages found for very high susceptibility zones indicate that both methods seem to underestimate the reality by a factor of two, the evaluation of very high and high susceptibility zones together yields significantly higher percentages (70.75% and 71.50% for W_i and W_f methods, respectively). This is attributed to the subdivision of the susceptibility zones using five uniform 20% classes of the total number of elements, rather than inconvenience of the methods. Based on these findings, it can be stated that a very high susceptibility zone identified by W_f method predicts higher percentages of landslide area. In addition to this, the landslide susceptibility zones by the W_f method are much more distinct and homogeneous than that of the W_i method. Therefore, W_f method may be preferred for practical applications in the project area. It can also be seen that very high susceptibility zones in both methods perfectly match with the Örencik formation. Therefore, the Örencik formation may be considered a unit susceptible to landslides and this formation should be avoided during re-routing of the pipeline.

Field studies performed in the study area also reveal that gully erosion is very active especially in the Örencik formation. Sloping barren areas where pipeline excavation and agricultural activities exist are seriously affected from the erosion. The erosion may even create gullies as deep as 0.8 m. Such deep gullies alter the stability of the slopes by removal of some slope materials and by permitting significant amount of groundwater infiltration into the slope forming material. Therefore, backfilling material of the pipeline should be compacted and a suitable granular material must be put on the slopes of the barren land along the pipeline in order to prevent such erosion. Agricultural activities should not be allowed in the close vicinity of the pipeline. Alluvium should be avoided during re-routing since agricultural activities and settlement are concentrated within this unit.

The Hendek formation is another important lithology in which about 40% of the pipeline is located. This unit has also some landslides, but they are mainly surficial where thin regolith occurs over the formation. Installation of the pipeline below thin regolith may be quite safe against landslides. Therefore, re-routing of the pipeline along the Hendek formation where thin regolith cover exists may be considered during practical applications.

Based on the landslide susceptibility map and the field observations, an alternative route where a large failed landslide occurred is suggested (Fig. 4.2). The route

is mainly located in the Hendek formation. It passes from the northern part of the large landslide so that the very high susceptibility zone is excluded. Nevertheless, detailed engineering geological investigations are required for fine adjustment of the route.

References

- Aleotti P, Chowdhury R (1999) Landslide hazard assessment: summary review and new perspectives. *Bull Eng Geol Env* 58: 21-44.
- Anbalagan R (1992) Landslide hazard evaluation and zonation mapping in mountainous terrain. *Engineering Geology* 32: 269-277.
- Carrara A, Cardinali M, Guzzetti F, Reichenbach P (1995) GIS technology in mapping landslide hazard. In: Carrara A, Guzzetti F (eds) *Geographical information systems in assessing natural hazards*, Kluwer, Dordrecht, pp.135-175.
- Dai FC, Lee CF, Li J, Xu ZW (2001) Assessment of landslide susceptibility on the natural terrain of Lantau Island, Hong Kong. *Environmental Geology* 40: 381-391.
- Donati L, Turrini MC (2002) An objective method to rank the importance of the factors predisposing to landslides with the GIS methodology: application to an area of the Apennines (Valneria; Perugia, Italy). *Engineering Geology* 63: 277-289.
- Duman TY, Emre Ö, Çan T, Ateş Ş, Keçer M, Erkal T, Durmaz S, Doğan A, Çörekçioğlu E, Göktepe A, Cicioğlu E, Karakaya F (2001) Turkish landslide inventory mapping project: Methodology and results on Zonguldak quadrangle (1/500 000). *Fourth Int. Turkish Geology Symposium*, p.160.
- Emre Ö, Ateş Ş, Keçer M, Erkal T, Yılmaz T, Durmaz S (1999) Pazarcık-KDZ Ereğli doğalgaz ana iletim hattı Paşaköy (Adapazarı) – KDZ Ereğli arasının heyelan etüdü. MTA Report No. 10187 (in Turkish).
- Gökçeoğlu C, Aksoy H (1996) Landslide susceptibility mapping of the slopes in the residual soils of the Mengen region (Turkey) by deterministic stability analyses and image processing techniques. *Engineering Geology* 44: 147-161.
- Lee S, Min K (2001) Statistical analysis of landslide susceptibility at Yongin, Korea. *Environmental Geology* 40: 1095-1113.
- Pistocchi A, Luzi L, Napolitano P (2002) The use of predictive modeling techniques for optimal exploitation of spatial databases: a case study in landslide hazard mapping with expert system-like methods. *Environmental Geology* 41: 765-775.
- Rautela P, Lakhera RC (2000) Landslide risk analysis between Giri and Tons rivers in Himachal Himalaya (India). *International Journal of Applied Earth Observation and Geoinformation* 2: 153-160.
- Saha AK, Gupta RP, Arora MK (2002) GIS-based landslide hazard zonation in the Bhagirathi (Ganga) valley, Himalayas. *International Journal of Remote Sensing* 23: 357-369.
- Soeters R, Van Westen CJ (1996) Slope instability recognition analysis and zonation. In: Turner KT, Schuster RL (eds) *Landslide: investigation and mitigation* Transportation Research Board National Research Council, Special Report no: 247, Washington D.C., pp.129-177.
- Turrini MC, Visintainer P (1998) Proposal of a method to define areas of landslide hazard and application to an area of the Dolomites, Italy. *Engineering Geology* 50: 255-265.
- Van Westen CJ (1997) Statistical landslide hazard analysis. ILWIS 2.1 for Windows Application guide. ITC Publication, Enschede, pp.73-84.

Micro-structure and Swelling Behaviour of Compacted Clayey Soils: A Quantitative Approach

Valéry Ferber, Jean-Claude Auriol, and Jean-Pierre David

French Public Works Research Laboratory (Laboratoire Central des Ponts et Chaussées)
route de Bouaye, BP 4129, 44341 Bouguenais Cédex, France
valery.ferber@lcpcc.fr
Tel: +33 2 40 84 57 85
Fax: +33 2 40 84 59 97

Abstract. In this paper, the clay aggregate volume and inter-aggregate volume in compacted clayey soils are quantified, on the basis of simple hypothesis, using only their water content and dry density. Swelling tests on a highly plastic clay are then interpreted by describing the influence of the inter-aggregate volume before swelling on the total volume of samples after swelling. This approach leads to a linear relation between these latter parameters. Based on these results, a description of the evolution of the microstructure due to imbibition can be proposed. Moreover, this approach enables a general quantification of the influence of initial water content and dry density on the swelling behaviour of compacted clayey soils.

Keywords: compacted clay, microstructure, aggregates, swelling behaviour.

1 Introduction

The swelling behaviour of clayey soils is a recurrent subject in geotechnical engineering. The last decades researches on this problem have revealed that this phenomenon depends on numerous parameters which can be classified in the three following families :

- *Internal intrinsic parameters* of the soil, like clay content (Seed *et al.*, 1962a and 1962b, Holtz and Gibbs, 1956), specific surface (Shiming, 1984), cation exchange capacity, its index properties (Tadanier and Nguyen, 1984, Fleureau *et al.*, 1993) or grain size distribution (Day, 1991);
- *Internal non intrinsic parameters* of the soil, like water content and dry density *before swelling* (Seed *et al.*, 1962a, Holtz *et al.*, 1956, Cox, 1978) or microstructure (Gens *et al.*, 1995) ;
- *External parameters*, like stress (Seed *et al.*, 1962a, Cox, 1978) or chemistry of the water added (Seed *et al.*, 1962b).

In earthworks engineering, water content and dry density of compacted soils are commonly measured in the field, but their influence on the long-term behaviour of embankment materials is not well understood so far. For this reason, the

goal of the research presented in this paper was to determine a method for the study of the influence of water content and dry density on the swelling behaviour of compacted soils. It appears that only a micro-structural approach enables a thorough interpretation of swelling tests. These considerations are synthesized in this paper in a micro-structural model: the “aggregate model”. The basic hypothesis and the main formulation of this model will be presented first. Then, the results of swelling tests on compacted clay will be interpreted according to this framework and the contribution of this approach on the understanding of the phenomenon will be discussed. Finally, an application of this method will be presented.

2 Microstructure of Compacted Clays: The “Aggregate Model”

2.1 Basic Hypothesis

The model we propose is founded on four basic hypothesis, illustrated in Figure 1, which can be summarized as follows:

1. clay particles gather together to form aggregates (Tessier, 1984, Mitchell, 1993, Navarro and Alonso, 2001) ;
2. due to the strong affinity between clay particles and water, all the water of the soil is located in the clay aggregates ;
3. all the air included in the soil is located out of the aggregates. This hypothesis implies that aggregates are saturated and then that the density of the aggregates depends only on their water content ;
4. consequently, the volume between aggregates, generally called “inter-aggregate volume” (Navarro *et al*, 2001), is equal to the air volume. Then, the dry density of the soil and its inter-aggregate volume are directly linked, which is consistent with mercury intrusion porosimetry tests (Wan *et al*, 1995).

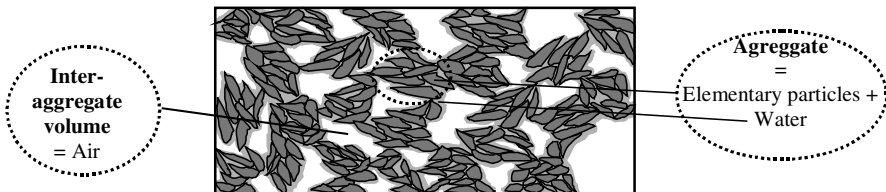


Fig. 1. Schematic representation of the microstructure of a clayey soil.

2.2 Quantification of Micro-structural Parameters

Based on this four hypothesis, two micro-structural parameters can be determined and linked to current geotechnical parameters. In order to ensure a relevant com-

parison between samples, all the parameters are divided by the dry mass of soil, noted m_s . These parameters are:

- the aggregate volume, noted V_{ag}/m_s :

$$\frac{V_{ag}}{m_s} = \frac{1}{\rho_s} + \frac{W}{\rho_w} \tag{2.1}$$

where ρ_s is the specific density of the particles, W the water content and ρ_w the density of water (equal to 1 g.cm^{-3} in this paper).

- the inter-aggregate volume, noted V_{inter}/m_s :

$$\frac{V_{inter}}{m_s} = \frac{1}{\rho_d} - \frac{1}{\rho_s} - \frac{W}{\rho_w} = \frac{V_t}{m_s} - \frac{1}{\rho_s} - \frac{W}{\rho_w} \tag{2.2}$$

where ρ_d is the dry density of the sample.

It can be noted that the sum of V_{ag}/m_s and V_{inter}/m_s is the total volume of the sample divided by the dry mass of soil, V_t/m_s , *i.e.* the inverse of the dry density.

3 Swelling Tests

3.1 Materials and Procedure

The swelling tests were performed in conventional oedometric cells on a very plastic clay from the Ardennes (France). This clay is characterized by a liquid limit of 98 %, a plasticity index of 61 %, a methylene blue absorption value of 10.66 g/100g and a specific density of the particles of 2.72 g.cm^{-3} . It contains approximately 66 % of particles smaller than $2 \mu\text{m}$ and 99 % of particles smaller than $80 \mu\text{m}$. The optimum standard Proctor dry density is 1.44 g.cm^{-3} and the optimum water content 28 %. The clay was first air-dried and then hydrated in order to obtain six different values of water content between 20 and 32 %. The characteristics of all samples tested are presented in Table 1. For each value of water content, six samples were compacted in the oedometric mould by a dynamic compaction device at various compaction energies (noted Comp.En. in Table 1), leading to six different values of dry density. The swelling was generated by filling the

Table 1. Water content, compaction energy and dry density (in g.cm^{-3}) of compacted samples.

Water content	Comp.En. 14 blows	Comp.En. 28 blows	Comp.En. 35 blows	Comp.En. 42 blows	Comp.En. 49 blows	Comp.En. 56 blows
W~20 %	1.201	1.324	1.363	1.394	1.418	1.44
W~22 %	1.163	1.272	1.302	1.367	1.367	1.441
W~24.5 %	1.176	1.322	1.359	1.397	1.426	1.457
W~27 %	1.154	1.318	1.366	1.403	1.421	1.476
W~29 %	1.181	1.337	1.394	1.412	1.437	1.479
W~32 %	1.233	1.385	1.408	1.414	1.425	1.426

oedometric cell with de-ionised water under a vertical stress of 3 kPa. The deformation caused by the imbibition was measured regularly until it reached an asymptotic value.

3.2 Results

A new interpretation of swelling tests is proposed hereafter, in order to describe the evolution of microstructure during swelling. It consists in representing the total volume of samples V_t/m_s before and after swelling versus the inter-aggregate volume V_{inter}/m_s before swelling. The swelling tests results of samples compacted at a water content of 29 % are presented in Figure 2 with this method. In this representation, it must be noted that V_t/m_s before swelling is mathematically related to V_{inter}/m_s before swelling by equation (2.2), conducting to equation (3.1). The slope of this relation is 1 and, for a given soil, its origin ordinate, equal to $1/\rho_s + W/\rho_w$, depends only on the water content before swelling.

$$\frac{V_t}{m_s} = \frac{V_{inter}}{m_s} + \frac{1}{\rho_s} + \frac{W}{\rho_w} \tag{3.1}$$

The dotted line in Figure 2 represents the sample volume before swelling and squares represent the total sample volume after swelling. This representation reveals a linear relation between inter-aggregate volume before swelling and total sample volume after swelling, with slope α and origin ordinate β , which can easily be estimated by a linear regression.

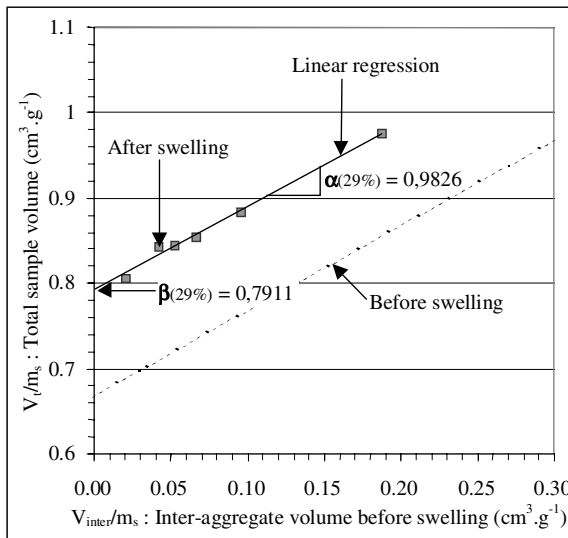


Fig. 2. Experimental results for a water content before swelling of 29 %.

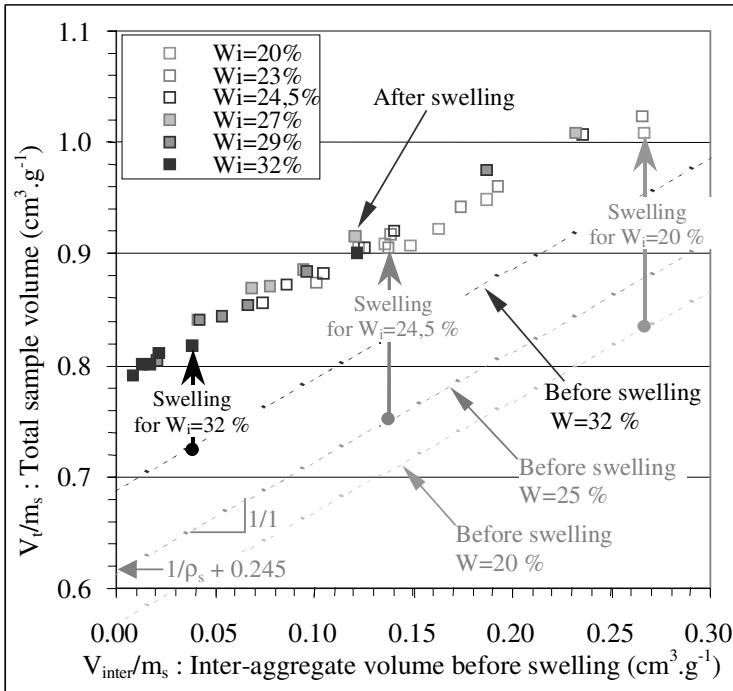


Fig. 3. Interpretation of all swelling tests with micro-structural parameters.

In order to evaluate the influence of water content *before swelling* on swelling behaviour, all the series of swelling tests were interpreted with the same method (Figure 3). In Figure 3, squares represent total sample volume *after swelling*. Dotted lines represent the total sample volume *before swelling* for three different values of water content. It appears that the volume *after swelling* chiefly depends on the inter-aggregate volume *before swelling*.

The slope α and origin ordinate β , as defined above (*cf* Figure 2), were calculated for each series of tests, *i.e.* for each value of water content *before swelling*. These two parameters are plotted versus water content *before swelling* in Figure 4. It appears that the water content *before swelling* has a non-negligible influence on the slope of the regression line. The results show that the higher the water content *before swelling*, the steeper the slope α . The origin ordinate β remains almost constant, at approximately $0.793 \text{ cm}^3 \cdot \text{g}^{-1}$.

3.3 Micro-structural Interpretation

These experimental results show two main points for the “aggregate model”:

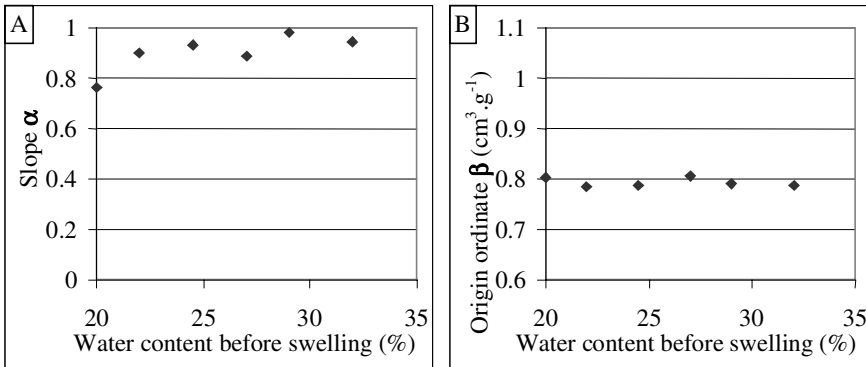


Fig. 4. Influence of water content *before swelling* on the linear behaviour.

- 1-The origin ordinate β calculated by linear regression on V_l/m_s *after swelling* represents the volume of a sample with no inter-aggregate volume, i.e. a sample only constituted of aggregates. Then, V_l/m_s *after swelling* for $V_{inter}/m_s = 0$ characterizes the aggregates swelling behaviour, independently from their initial organization. Thus, if aggregates are assumed to be saturated *after swelling*, their final water content can be calculated by equation (2.1) from calculated values of β (cf figure 4-B). According to these experiments, this final water content of aggregates is comprised between 41.7 and 43.7 %, with an average value of 42.6 %. This value could probably be considered as an intrinsic parameter, characterizing the attraction of water by this clay;
- 2-Since the slope α of the relation between V_l/m_s and V_{inter}/m_s is equal to 1 *before swelling*, it can be said that if the inter-aggregate volume kept constant during swelling, this slope would still be equal to 1 *after swelling*. This is almost the case for samples compacted at the optimum Procor water content. On the other hand, for lower water contents, the slopes are always lower than 1 (cf figure 4-A) suggesting that the inter-aggregate volume decreased during swelling. Moreover, it appears that this decrease is more important when the water content *before swelling* is low. For example, for a water content of 20 % *before swelling*, the slope *after swelling* is 0.76, indicating a loss of inter-aggregate volume of 24 %. Thus, in a dry soil, swelling is accompanied by significant microscopic re-organizations which conduct to a partial loss of volume.

This linear relation between inter-aggregate volume *before swelling* and total volume *after swelling* is an interesting new result. Even if it is easily understandable that a high inter-aggregate volume *before swelling* leads to a high total sample volume *after swelling*, the authors identified no reason why this relation is linear. Further investigations on microstructure will probably be necessary to explain this experimental observation.

Thus, it seems that the swelling behaviour of a compacted soil can be considered as the result of a “competition” between:

- a decrease of volume due to aggregates re-organizations ;
- an increase of volume due to the expansion of the aggregates by adsorption of water.

A schematic illustration of these phenomena is given in Figure 5 for both dry and optimum Proctor water contents. Thus, according to the authors, the water content *before swelling* controls not only the initial volume of aggregates, but also the potential loss of inter-aggregate volume caused by their re-organization during imbibition. This structure modification could be the consequence of a loss of mechanical strength of both the aggregates and the structure they form, caused by the adsorption of water.

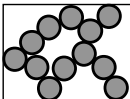
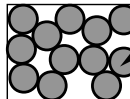
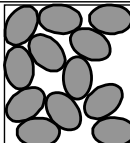
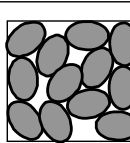
	1. Dry	2. Optimum Proctor water content	<i>Aggregate = particles + water</i>
Before swelling			$m_s(1) = m_s(2)$ $V_t(1) = V_t(2)$ $V_{ag}(1) < V_{ag}(2)$ $V_{inter}(1) > V_{inter}(2)$
After swelling			$V_{ag}(1) \sim V_{ag}(2)$ $V_t(1) > V_t(2)$

Fig. 5. Schematic interpretation of microstructure influence on swelling.

4 Application

The linear relations observed in the swelling behaviour (*cf* Figures 2 and 3) give the opportunity to quantify in a very simple manner the volume of samples *after swelling*, noted $V_{t,f}/m_s$:

$$\frac{V_{t,f}}{m_s} = \alpha(W_i) \cdot \left(\frac{1}{\rho_{d,i}} - \frac{1}{\rho_s} - \frac{W_i}{\rho_w} \right) + \beta(W_i) \tag{4.1}$$

where $\rho_{d,i}$ and W_i are respectively the dry density and the water content *before swelling*, $\alpha(W_i)$ and $\beta(W_i)$ the slope and the origin ordinate given by swelling tests for a given water content *before swelling* W_i (*cf* Figures 2, 3 and 4). Since the total sample volume *before swelling* is the inverse of $\rho_{d,i}$, the deformation caused by imbibition can be predicted for any water content and dry density *before swelling*, on the basis of the experimental results presented in this paper:

$$\varepsilon = \rho_{d,i} \cdot \left[\alpha(W_i) \cdot \left(\frac{1}{\rho_{d,i}} - \frac{1}{\rho_s} - \frac{W_i}{\rho_w} \right) + \beta(W_i) - \frac{1}{\rho_{d,i}} \right] \tag{4.2}$$

where ε is the swell deformation.

The validity of this expression is limited to the range of water contents and dry densities tested in these experimentations. In these ranges, theoretical iso-swelling curves can be calculated to illustrate quantitatively the influence of initial state in the Proctor diagram (*cf* Figure 6). This kind of representation was first proposed by Holtz and Gibbs (1956) and could have an interesting potential for practical applications. A linear regression was adopted in order to describe the evolution of α with the water content *before swelling* and the mean value of β was adopted (*cf* Figure 4). In order to evaluate the consequence of such calculation simplifications and of experimental uncertainties, calculated and measured deformations are plotted in Figure 7. Their differences are reported as a histogram in Figure 8. The standard deviation indicates that the difference between measured and calculated deformations is of 1.52 points of deformation for a confidence range of 90 % ($= 1.66.\sigma$). Thus, it can be seen that linear regressions and experimental uncertainties lead to a reasonable error in the calculation, regarding the high swell deformations measured for this clay.

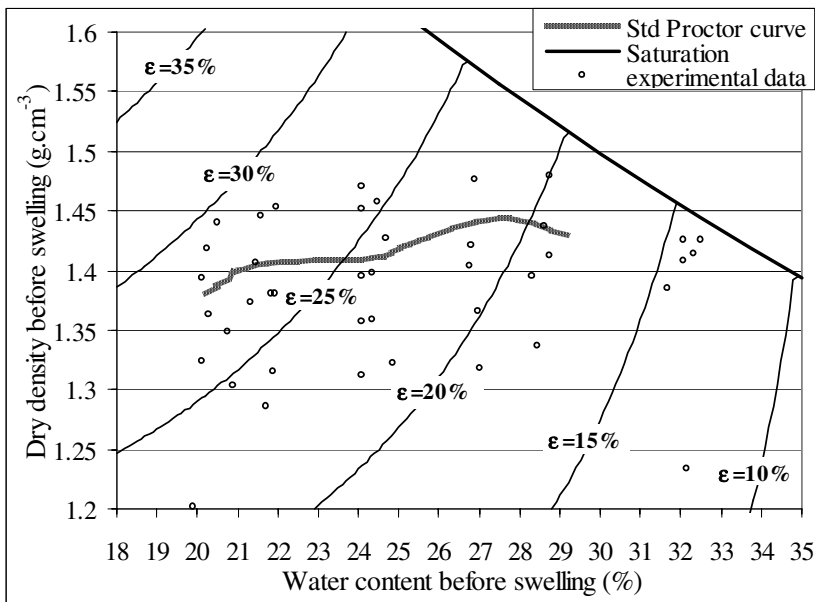


Fig. 6. Iso-swelling curves in the Proctor diagram.

5 Conclusion

This paper shows that the influence of initial water content and dry density on the swelling behaviour of compacted clays is quite complex, but can be explained and quantified by microstructural considerations and simple experiments. According to the authors, two fundamental facts should be underlined:

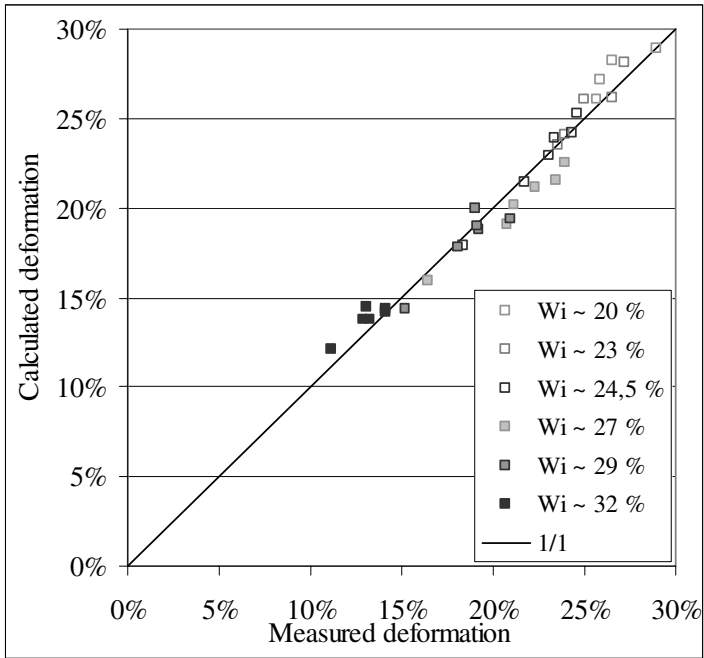


Fig. 7. Calculated deformation vs measured deformation.

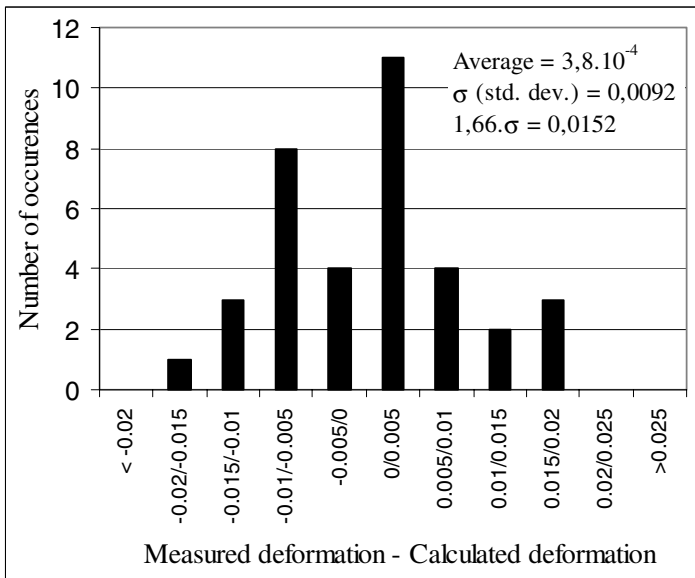


Fig. 8. Difference between measured and calculated deformation.

- the coupled influence of water content and dry density on the swelling behaviour ;
- the complicated influence of water content which controls the swelling potential of aggregates but also the stability of the structure they form.

It must be said that similar results were obtained on several other clayey and silty soils. In particular, the linear relation between inter-aggregate volume *before swelling* and the total sample volume *after swelling* was observed in all cases.

The experimental procedure and the interpretation proposed here could also be used in order to study the influence of other parameters as the vertical stress or the chemical characteristics of the water added. Finally, the study of a large group of soils with this method could give the opportunity to correlate the potential adsorption of water with current identification tests, in order to predict the swelling behaviour in a simple but quite objective manner.

References

- Cox DW (1978) Volume change of compacted clay fill. In : Clay fills, Proceedings of the conference held at the institution of Civil Engineers, 14-15 nov 1978, London, pp 79-86.
- Day RW (1991) Expansion of compacted gravelly clay. *Journal of geotechnical engineering* 117 n°6 : 968-972.
- Fleureau JM, Kheirbek-Saoud S, Soemitro R, Taibi S (1993) Behaviour of clayey soils on drying-wetting paths, *Can Geotech J* 30 n°2 : 287-296.
- Gens A, Alonso EE, Surlol J (1995), Effect of structure on the volumetric behaviour of a compacted soil. In : Alonso et Delage (eds), UNSAT'95, Balkema - Presses de l'ENPC, Paris, pp 83-88.
- Holtz WG , Gibbs HJ (1956) Engineering properties of expansive clays. *Trans. ASCE*, vol 121 : 641-663.
- Mitchell JK (1993) *Fundamentals of soil behavior* 2nd edition. Univ. of California, Berkeley, John Wiley & Sons Inc.
- Navarro V, Alonso EE (2001) Secondary compression of clays as a local dehydration process. *Geotechnique* 51 n°10 : 859-869.
- Seed HB, Woodward RJ, Lundgreen R (1962a) Prediction of swelling potential for compacted clays. *Journal of the soil mechanics and foundation division, ASCE, SM3*, 3169 : 53-87.
- Seed HB, Mitchell JK, Chan CK (1962b) Studies of swell and swell pressure characteristics of compacted clays. *Bull. of the Highway research board, Washington*, vol 313 : 12-39.
- Shiming H (1984) Identification of expansive soils by specific surface area values. In : Fifth International Conf on Expansive Soils, Adelaide, South Australia, pp 1-3.
- Tadanier R, Nguyen VU (1984) Index properties of expansive soils in New South Wales. In : Fifth International Conf on Expansive Soils, Adelaide, South Australia, pp 321-326.
- Tessier D (1984) Etude expérimentale de l'organisation des matériaux argileux. INRA. Thèse Univ Paris VII, UER des sciences physiques de la terre, 361 p.
- Wan AWL, Gray MN, Graham J (1995), On the relations of suction, moisture content and soils structure in compacted clays. In : Alonso et Delage (eds), UNSAT'95, Balkema - Presses de l'ENPC, Paris, pp 215-222.

Physical and Numerical Modelling of a Two-Well Tracer Test at the Laboratory Scale

Christophe Frippiat, Benoît Wauters, Vincent Feller, Patrick Conde,
Mohammed Talbaoui, and Alain Holeyman

Civil and Environmental Engineering, Catholic University of Louvain, Place du Levant, 1,
1348 Louvain-la-Neuve
holeyman@gce.ucl.ac.be
Tel: +32 10 47 21 12
Fax: +32 10 47 21 79

Abstract. Two-well tracer tests were performed at the laboratory scale on a large hand-compacted Bruxellian sand sample (about 2 m³), using electrical sensors buried in the soil and placed in piezometers to monitor solute concentrations. First, heterogeneity within the soil was investigated using simple one-dimensional transport experiments. Deduced permeability values showed some non-negligible variations, that had to be taken into account when interpreting two-dimensional experiments. A numerical model was then developed under Modflow®, in order to simulate two-well tracer test recovery curves under heterogeneous soil conditions. Comparison of numerical results and experimental data highlighted the need for a sufficiently refined measurement grid, as phenomena occurring in zones where fewer sensors were installed were not well simulated.

Keywords: two-well tracer test, large-scale laboratory sample, soil heterogeneity

1 Introduction

Field tracer tests are often difficult to analyse because subsurface conditions are never completely mastered and other effects, such as well bore mixing or flow field distortion near the well, are poorly controlled (Brouyère 2003). Theoretical work in order to better understand influence of these effects has been developed during the past years (Brouyère 2003, Novakowski 1992, Zlotnik and Logan 1996). But still very few laboratory investigations on large soil samples were performed in order to assess these effects under controlled conditions. This study represents a first step in this direction and shows how, given a certain soil characterization, it is possible to predict solute transport between an injection well and a recovery well.

2 Materials and Methods

2.1 Physical Model and Measurement Device

The laboratory tests were performed within an experimental device designed for transport experiments at an intermediate scale between classical laboratory col-

umn tests (about 20 centimetres) and in situ tests (from a few metres to several kilometres). The physical model consisted in a two cubic meters box (2 metres long with a 0.8 metres wide and 1.2 metres high cross-section) flanked by two water reservoirs used to impose upstream and downstream water conditions to the flow system (Fripiat et al. 2003a). The sample of Bruxellian sand was manually compacted in ten successive layers, in order to obtain a relatively homogeneous soil with about 40% total porosity. The measuring system consisted of 14 electrical sensors allowing local concentration measurements in the soil as well as in free solution (Fripiat et al. 2003b). A general linear calibration equation, compatible with Ohm's law, was used to relate electrical conductivity of the liquid phase C (expressed in μScm^{-1}) to electrical voltage drop V (in Volts) measured between the sensor electrodes

$$C = \frac{A}{V} + B \quad (1)$$

where A and B are calibration parameters. As those parameters depend on soil properties between the electrodes, they have to be determined once the sensors are in place. The tracer was a weakly concentrated salt solution (NaCl diluted in tap water). In such conditions, solution electrical conductivity is linearly related to solute concentration (at least at a constant temperature). In the next part of this paper solute concentration will be directly expressed in terms of solution electrical conductivity.

Table 1. Sensor and piezometer positions.

		C0	C1	C2	C3	C4	C5	C6	C7	C8	C9	C10	C13	Inj	Rec	P4	P5
x	M	0	2.00	2.00	0.30	0.30	0.50	0.50	0.75	1.25	1.50	1.50	1.00	0.40	1.60	1.00	1.00
y	M	-	-	-	0.25	0.55	0.55	0.25	0.4	0.4	0.25	0.55	1.00	0.40	0.40	0.20	0.60
z	M	-	-	-	0.22	0.56	0.21	0.55	0.40	0.35	0.32	0.32	-	-	-	-	-

Sensor positions as well as piezometers and wells positions in the model are summarized in Table 1. x is the distance from the model inlet, y is the distance from the left side of the sample (looking towards flow direction) and z is the elevation from sample bottom. Sensor C0 was placed in the upstream water tank, sensors C1 and C2 were placed in the downstream one, and sensor C13 recorded flux concentration in a piezometer.

2.2 Methods

Two kinds of tracer tests were performed. First, one-dimensional experiments were used to calibrate conductivity sensors and to characterize heterogeneity in the soil sample. Then, a two-well injection-recovery test was performed and analysed using data from the first experimental phase. In this section, it is proposed to briefly review the methods used to generate and to process experimental results. After having saturated the physical model with a solution at a background conductivity of $1000 \mu\text{Scm}^{-1}$ (measured at 18°C), three instantaneous stepwise variations in conductivity were successively performed: to $1300 \mu\text{Scm}^{-1}$, to $1500 \mu\text{Scm}^{-1}$ and

then back to $1000 \mu\text{Scm}^{-1}$, in order to reveal possible hysteresis effects. It can be shown that an approximate analytical solution to this problem is given by

$$\frac{C - C_0}{C_f - C_0} = \frac{1/V - 1/V_0}{1/V_f - 1/V_0} = \frac{1}{2} \left[\operatorname{erfc} \left(\frac{x - vt}{2\sqrt{\alpha_L vt}} \right) + \exp \left(\frac{x}{\alpha_L} \right) \operatorname{erfc} \left(\frac{x + vt}{2\sqrt{\alpha_L vt}} \right) \right] \quad (2)$$

where Equation 1 has been incorporated and calibration parameters dropped out. C is the conductivity [μScm^{-1}], V is the measured electrical tension [V], erfc is the complementary error function, x is the longitudinal position [m], v is the mean velocity along the travelled path [ms^{-1}], t is the time [s] and α_L is the longitudinal dispersivity [m]. Subscript 0 relates to background values and subscript f relates to stabilized final values. First, the three steps in conductivity were analysed separately. Local soil hydrodispersive parameters were deduced by least-square fitting of Equation 2 with relative measurements collected with each sensor. In a second step, experimental values recorded between breakthrough (i.e. at a theoretically constant conductivity) were used to deduce values for the calibration parameters. Then, the whole flow domain was numerically modelled and partitioned in zones of constant permeability. The flow parameters (the permeability values in the different zones) were then adjusted to produce the best fit between measurements and computed breakthrough curve. Dispersivities were kept constant and equal to the numerical grid, as calculating new values would have drastically increased the numerical difficulty of the optimisation procedure without bringing a huge improvement to solute transport modelling. The second type of tracer test involved two-dimensional effects in flow and transport and required numerical modelling to analyse concentration measurements. A background flow was created through the sample, tracer solution was injected during a short time in one well, and a constant pumping rate at the other well allowed recovery of the injected tracer 1.2 m farther.

3 One-Dimensional Tracer Test

The aim of this experimental phase is to obtain a set of calibration parameters for each sensor and to derive a description of soil macroscopic heterogeneity, in order to be able to correctly interpret any further experiment conducted within this soil sample. Fixed-head upstream and downstream conditions were respectively 0.92 m and 0.52 m, so that an average gradient of 0.2 was created in the sand sample. This high value was adopted in order to decrease experiment duration. Mean measured flow was about $8.3 \cdot 10^{-6} \text{ m}^3\text{s}^{-1}$, leading to an estimated bulk permeability of about $7.6 \cdot 10^{-5} \text{ ms}^{-1}$.

Table 2. Results of 1D-experiments and calibration procedure.

		C1	C2	C3	C4	C5	C6	C7	C8	C9	C10	C13
Step 1	v 10^{-5} ms^{-1}	4.48	4.62	2.58	2.20	3.05	1.86	3.41	2.63	2.51	2.91	3.24
	α_L cm	9.6	7.3	0.6	0.7	1.0	1.1	1.9	2.1	4.1	4.0	0.9
Step 2	v 10^{-5} ms^{-1}	4.76	4.00	2.74	2.35	3.16	1.82	3.62	2.63	2.56	2.46	3.39
	α_L cm	10.7	17.8*	0.6	0.9	2.2*	23.4*	2.4	3.7*	8.1*	9.5*	1.4
Step 3	v 10^{-5} ms^{-1}	3.18	4.02	2.82	2.28	3.21	2.028	3.89	2.81	2.86	3.06	4.01
	α_L cm	6.9	7.2	0.9	1.0	1.3	1.1	1.9	1.7	3.1	2.6	1.9
Mean	v 10^{-5} ms^{-1}	4.62	4.21	2.61	2.28	3.14	1.90	3.64	2.69	2.54	2.81	3.55
	α_L cm	8.0	7.0	0.7	0.8	1.1	1.1	2.0	2.2	3.5	4.0	1.5
Calib.	A $\text{V } \mu\text{Scm}^{-1}$	692	737	5001	3717	3714	3569	4366	3778	3686	3572	820
	B μScm^{-1}	81.4	85.6	-344	-360	-300	-317	-325	-264	-311	-269	-63

* Denoted values were not taken into account when computing mean parameters

3.1 Analytical Modelling and Sensor Calibration

Local soil hydrodispersive parameters deduced by inverse modelling are shown in Table 2. Sensors placed in the soil showed an hysteresis effect, background electrical tension values at the end of the experiment being higher than values measured before the first step. This deviation was probably due to a temperature effect, the thermal inertia of soil grains being higher than that of the flowing solution. This effect can be roughly approximated using a linear relationship

$$C_{\text{cor}} = C_{\text{meas}} (1 + K t) \quad (3)$$

where C_{cor} is the corrected conductivity, C_{meas} is the measured one and t is the time. Coefficient K was found constant for each sensor and corresponded to an increase of about 2°C of the flowing solution after the whole experiment, which agreed with temperature measurements.

Finally, conductivity levels were simulated for each sensor, using the complete injection curve. As an example, measured and theoretical breakthrough curves of sensor C7 are shown in Figure 1. Local cyclic deviations between curves could be explained via small cyclic temperature variations at the model inlet.

3.2 Numerical Modelling

A 2D numerical model of the laboratory set-up was prepared using Modflow® and MT3D®. It was composed of 200×80 cells of $1 \text{ cm} \times 1 \text{ cm}$. The flow was assumed unconfined but the effect of the unsaturated zone was not taken into account (no capillary fringe and no mass transfer above the water table). Local longitudinal dispersivity was assumed equal to the numerical grid size (1 cm). This numerical model was first used to characterize soil heterogeneity. Velocity measurements obtained from one-dimensional inverse modelling (summarized in Table 2) were used to deduce permeability values in the numerical model. The

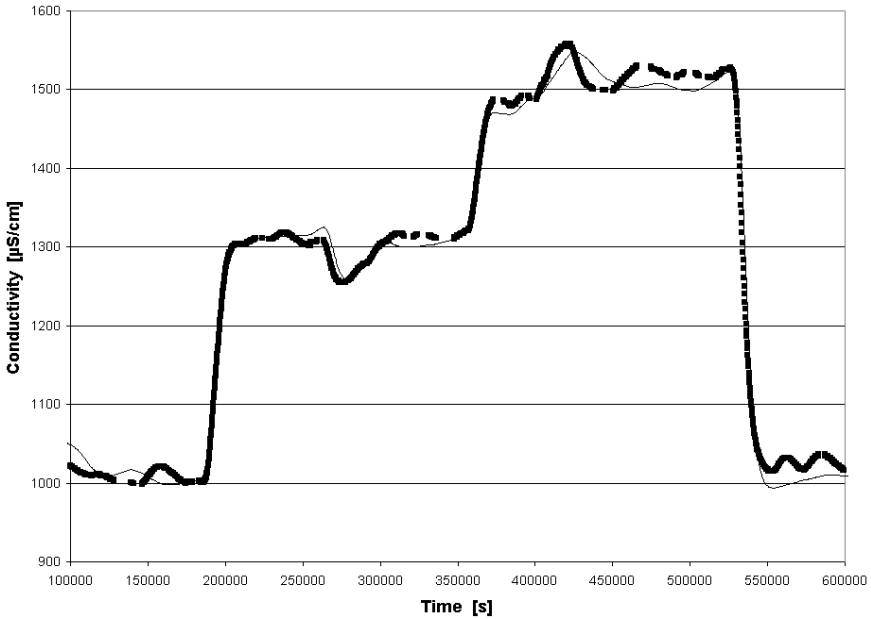


Fig. 1. Breakthrough curve at sensor C7 during 1D experimental phase. Black dots are experimental measurements and solid line is the theoretical breakthrough curve.

first step was to delineate zones within the model where permeability could be assumed constant. A reasonable, although arbitrary, choice was to take rectangular zones, each corresponding to one sensor, and placed before the sensor. Another choice could be to take zones centred on sensors. Those two delineation choices are illustrated on Figure 2.

Then, an iterative optimisation procedure was performed under Matlab®, in order to find permeability values that allowed to optimally simulate each velocity found from 1D experiment. Results in terms of estimated permeability k are shown on Table 3, as well as discrepancy between numerical simulation of the velocity v_{mod} and experimental velocity measurements v_{meas} .

In delineation case I as well as in delineation case II, one obtained a mean error on migration velocity of about 15 %, but the variance of this error seemed higher in case II.

4 Two-Well Tracer Test

4.1 Experimental Results

Fixed-head boundary conditions were kept identical as in one-dimensional experiments and the same soil sample was tested. Pumping in the recovery well was

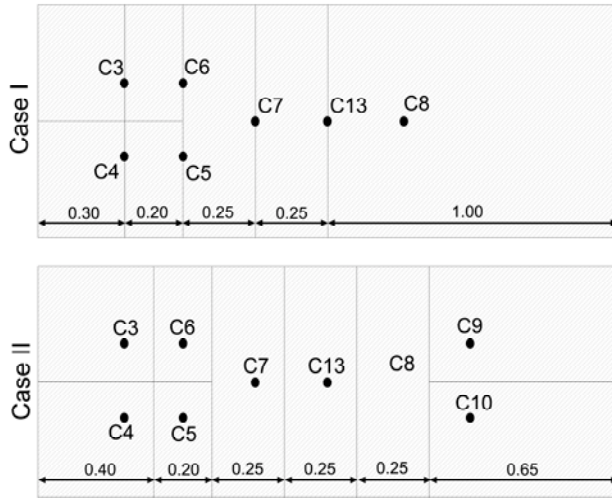


Fig. 2. Delineation of zones of constant permeability. Length measurements are in m.

Table 3. Permeability values from optimization procedure.

			C3	C4	C5	C6	C7	C13	C8	C9	C10
Case I	K	10^{-5} ms^{-1}	6.93	6.42	7.40	3.25	9.46	9.75	6.22	-	-
	v_{meas}	10^{-5} ms^{-1}	2.61	2.28	3.14	1.90	3.64	3.55	2.69	-	-
	v_{mod}	10^{-5} ms^{-1}	2.35	2.79	3.00	2.34	3.05	3.07	3.11	-	-
	Discr.	10^{-5} ms^{-1}	0.26	-0.51	0.14	-0.44	0.59	0.48	-0.42	-	-
Case II	K	10^{-5} ms^{-1}	6.20	6.31	7.17	4.66	8.37	7.81	6.43	5.66	6.54
	v_{meas}	10^{-5} ms^{-1}	2.61	2.28	3.14	1.90	3.64	3.55	2.69	2.54	2.81
	v_{mod}	10^{-5} ms^{-1}	2.41	2.62	2.77	2.47	2.81	2.87	2.92	2.84	3.11
	Discr.	10^{-5} ms^{-1}	0.20	-0.34	0.37	-0.57	0.73	0.68	-0.23	-0.30	-0.30

performed during the whole experiment at a constant rate of $1.5 \cdot 10^{-6} \text{ m}^3\text{s}^{-1}$, while injection at $1500 \mu\text{Scm}^{-1}$ was performed during 2000 s at a constant rate of $2.0 \cdot 10^{-6} \text{ m}^3\text{s}^{-1}$. As some sensors were first intended to characterize soil heterogeneity, they did not record any quantifiable information during two-well tracer test. Measurements from sensors placed upstream the injection well, as well as sensors not placed on the main flow axis, were not analysed, as it was not possible to clearly distinguish between response of the two-well system and background variations due to slight modification at the model inlet. In the next part of the text, only bell-shaped curves recorded at sensors C7, C13, C8 and at the recovery well will be analysed. In a first step, equivalent macroscopic values for permeability k_{eq} and dispersivity α_{Leq} were calculated using Modflow and are shown in Table 4. Those results are in general accordance with values deduced from 1D experiments shown on Table 2.

Table 4. 2D tracer test results.

		C7		C13			C8		Recovery				
		Exp.	I	II	Exp.	I	II	Exp.	I	II	Exp.	I	II
k_{eq}	10^{-5} ms^{-1}	7.33	-	-	7.99	-	-	5.11	-	-	7.59	-	-
α_{Leq}	cm	<1	-	-	2.5	-	-	1.2	-	-	2.5	-	-
t_{fa}	10^3 s	3.96	4.16	4.16	8.95	9.36	9.36	18.40	14.56	14.56	16.08	19.24	19.76
t_p	10^3 s	9.20	10.36	10.92	15.06	16.64	17.68	29.32	22.88	23.40	26.52	29.12	29.64
C_{max}	$\mu\text{S cm}^{-1}$	1421	1407	1419	1245	1325	1350	1283	1279	1308	1096	1115	1118

4.2 Numerical Modelling

Figure 3 shows the experimental curve at the recovery well, as well as corresponding theoretical curves in permeability cases I and II. The results were analysed considering first-arrival time t_{fa} , peak time t_p , and maximum concentration C_{max} , and are shown in Table 4. With a mean error of about 5%, maximum conductivity levels are generally well simulated, as well as arrival and peak times for sensors C7 and C13. This might mean that errors on velocities and dispersivities compensate to produce right dispersion coefficients. But C8 and recovery well shows greater differences (up to 20%) in characteristic times, which might reflect increased uncertainty on estimated permeability, due to the reduced number of sensors in this zone (as sensors C1 and C2 were not taken into account in the inverse modelling process). Moreover, adjusting dispersivity values should improve the

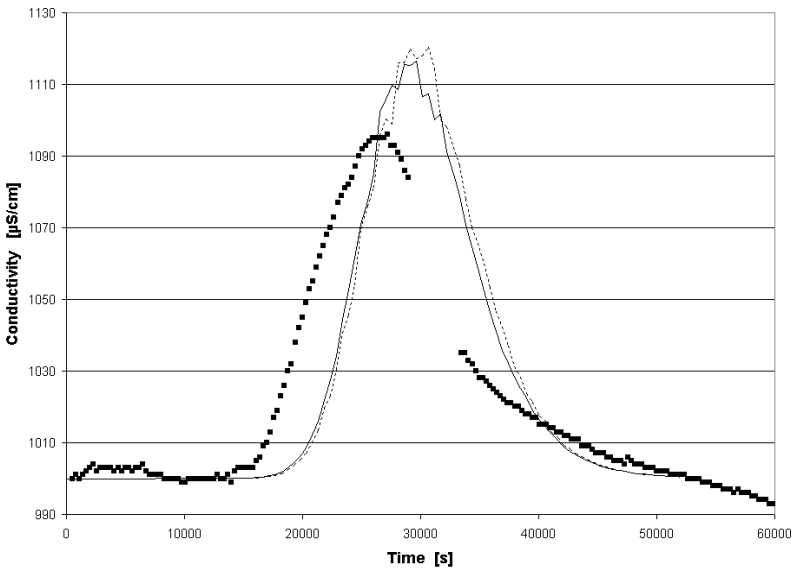


Fig. 3. Breakthrough curve at the recovery well. Black dots are experimental values, solid line corresponds to simulation I and dashed line corresponds to simulation in case II.

numerical simulation. It should also be noted at this point that no mixing effect in the injection well was included in the modelling. It is however well known that such effects may produce time delay and increased apparent dispersion (Brouyère, 2003). However, delay between first-arrival time and peak time remains relatively the same when comparing experimental data and modelling results. This might be due to the fact that estimated dispersivities in Table 4 are comparable to the local constant value used in the numerical model. Finally, numerical modelling predicted a recovery of about 97% of the solute mass injected, and integration of the experimental curve on Figure 3 provides a recovery of about 92% of the injected mass.

5 Conclusion

Results presented in this paper are only a first insight into tracer test modelling at a medium scale in the laboratory. The basic deterministic approach used here to simulate heterogeneity showed however relatively satisfactory results, at least for sensors placed in well-characterized zones, with errors between numerical modelling and measured parameters of about 5%. However, measurements near the pumping well were simulated with more difficulty, as less sensors were available in this zone. This raises the issue of correctly designing the measurement points distribution, as the electrical sensors used in the laboratory only allow one to perform local measurements. There must be a sufficient number of sensors to derive mean values that are representative of the mean behaviour of the flow system. Otherwise one has to find other characterizing tools. Future work will consist in taking permeability measurements in the physical model, so that a geostatistical characterization of soil heterogeneity can be used in a stochastic simulation of the permeability field (Gelhar and Axness 1983). This simulation will be conditioned by direct and indirect permeability measurements (Rentier et al. 2001), by head measurements and by concentration measurement.

Acknowledgements

The authors wish to thank the Laboratory of Civil Engineering of Louvain-la-Neuve, which provided helpful advice when performing physical experiments. They also would like to thank the Belgian National Fund for Scientific Research, which granted Christophe Fripiat a Research Fellowship (Ref : FC 64914).

References

- Brouyère S (2003) Modeling tracer injection and well-aquifer interactions : A new mathematical and numerical approach. *Water Resources Research* 39(3).
- Fripiat C, Servais T, Conde P, Talbaoui M, Holeyman A (2003a) Medium-scale laboratory model to assess soil contaminant dispersivity. In: *Proceedings of the 13th European Conference on Soil Mechanics and Geotechnical Engineering, August 25-28, 2003, Praha, Czech Republic.*

- Frippiat C, Renard A, Holeyman A (2003b) Development of a new electric conductivity sensor in order to characterize soil solute concentration. In: Proceedings of the 9th European Meeting of Environmental and Engineering Geophysics, August 31 - September 4, 2003, Praha, Czech Republic.
- Gelhar L W, Axness C L (1983) Three-dimensional stochastic analysis of macrodispersion in aquifers. *Water Resources Research* 19(1):161-180.
- Novakowski K S (1992) An evaluation of boundary conditions for one-dimensional solute transport. I. Mathematical development. *Water Resources Research* 28(9):2399-2410.
- Rentier C, Brouyère S, Dassargues A (2001) Integrating geophysical and tracer data for accurate solute transport modelling in heterogeneous porous media. In: Proceedings of "Groundwater Quality 2001", Sheffield (U.-K.), pp 115-118.
- Zlotnik V A, Logan J D (1996) Boundary conditions for convergent radial tracer tests and effect of well bore mixing volume. *Water Resources Research* 32(7):2323-2328.

Soil Investigation Aspects of a Complex Metro Project in Amsterdam

Jurgen Herbschleb

Adviesbureau Noord/Zuidlijn/Royal Haskoning Amsterdam, The Netherlands
j.herbschleb@royalhaskoning.com
Tel: +31 20 5697 700
Fax: +31 20 5697 756

Abstract. The municipality of Amsterdam wishes to reduce the level of car traffic within the City Centre. As a consequence the public transport is to be extended by a new (bored) North/South Metro line. The excavation depths for the stations will exceed 30 m and will be constructed in difficult soft soil conditions. A further significant aspect is that the building pits are very near (3 to 5 m) to buildings of historical importance. The design philosophy of the station boxes was to determine an acceptable balance between the safety requirements and construction costs. The guidelines for the design, both for the building pits and the bored tunnel, are the predicted deformations of the adjacent building foundations. One of the more important geotechnical risks for this project is incorrect determination of the deformations arising from the building processes alongside the route of the metro. As such it should be realised that advanced finite element programs with second order material models require different geotechnical parameters than analytical models. The careful selection of calculation (soil) models, the level of safety (risk analysis), and site investigation is the start of the determination of the geotechnical parameters. This paper will focus on the interpretation of the site investigation for this complex project and will concentrate on the process followed, the problems encountered with the interpretation, the obtained results, and the used tools for geotechnical risk management.

Keywords: risk management, classification, homogeneous zones, unloading stiffness, soil investigation, metro, underground railway, Amsterdam, Netherlands.

1 Introduction

The Amsterdam North/South metro line will connect the North, Centre, and South districts of Amsterdam. The total length of the metro is 9 km, of which 4 km will be constructed underground. The following two major restrictions were imposed for this project: 1) No significant damage to historic buildings, and 2) Disruption of city life should be limited. To minimise the effects of the construction to adjacent historical buildings a bored tunnel will be adopted for the underground sections in the city centre. The tunnel follows the street pattern as closely as possible (Figure 1) and descends to a great depth. Consequently, the metro stations are at a great depth as well. A building pit will be constructed for the stations, having braced diaphragm walls to a level of over 40 m below street level. The excavation will be carried out to a depth of over 30 m in soft soil conditions with high ground

water levels. The influence of construction on historic buildings was a significant design issue since the distance to the stations is local only 3 m. Much design effort was required and special test procedures were carried out to investigate the effects of underground construction in the Amsterdam City.



Fig. 1. Aerial view with alignment.

2 Geology

The subsurface of Amsterdam is composed of sediments, up to depths varying between 800 to 1000 m below ground level. The sediments (sands, silts, clays, and peat) have originated from marine-, glacial-, eolian, and river environments. In the upper 350 m of sediments two main geological important units are distinguished the Holocene (10.000 years to present) and the Pleistocene (10.000 - 2.5 million before present) deposits, see Figure 2 for a general geological profile of North-Holland. The oldest and deepest Pleistocene deposits are marine clays and fine-grained sands, which extend down to a level of 250- 350 m below ground level. During its maximum extension, the Saalian ice cap reached into Amsterdam, where glacier tongues excavated a deep basin in the unconsolidated Pleistocene deposits (de Gans, 2000). During this period mainly glacial and melt water deposits were formed within the basin. After melting of the ice cap, the Amsterdam Basin was flooded with the sea and partially filled with marine sands and clays (Eemclay). During the last ice age (100.000 - 10.000 years ago), the Netherlands experienced a tundra climate. The Amsterdam Basin was filled mainly with sand. These sand layers are very important for foundation practice in Amsterdam and mark the end of the Pleistocene. The Holocene deposits (mainly peat and clay) were mainly formed under the influence of the sea.

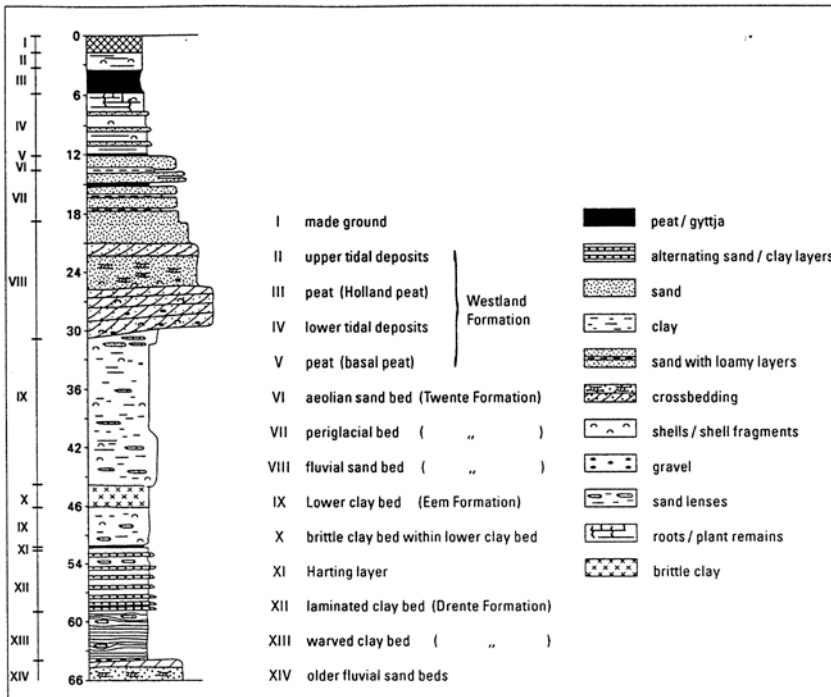


Fig. 2. Geological profile of Amsterdam (Gans 2000).

3 Site Investigation

3.1 Introduction

Along the route of the North/South line a comprehensive soil investigation has been performed. This soil investigation consisted of a total of 125 boreholes and about 400 CPT's each up to a depth of 70 m. As well as these borings and CPT's, special tests like Cone Pressure Meters (CPM) were also carried out. In the laboratory the samples of the borings were classified and tested. The laboratory tests were used mainly to determine the strength and stiffness parameters of the soils, specially the Pleistocene Marine Eemclay. The determination of geotechnical parameters cannot be seen apart from boundary conditions like: 1) calculations models, and 2) the required safety. The calculation models and design of the building pit determine the type of geotechnical parameters. Advanced finite element programs with second order material models require different geotechnical parameters than analytical models. The careful selection of the calculation (soil) models, the level of safety (risk analysis), and site investigation is the start of the determination of the geotechnical parameters. Part of this determination is to access the reliability of the (geotechnical) data.

Table 1. Sources of Uncertainty (Mann 1993).

Type I Uncertainty (errors, bias and imprecision)	
Errors in measurement	Inadequate sampling
Bias in measurement process	Physical limitation to sampling
Imprecision of measurement process	Inability to know true accuracy
Type II Uncertainty (stochastically)	
Inherent natural variation	Heterogeneity in materials
Anisotropy in materials	Noise in computational systems
Physical inability to sample adequately	Practical need to use average values rather than distribution functions
Type III Uncertainty (Ignorance)	
Lack of Knowledge	Incomplete knowledge
Erroneous knowledge	Imperfect concepts
Ambiguity in concepts, data, models	Need for generalisations
Need for simplifications	Computational inaccuracies
Use of incorrect models (conceptual or mathematical)	

3.2 Site Investigation Plan

The goal of the site investigation is to obtain a consistent “image” of the sub-surface that is the basis of a sound safe design. The “image” of the sub-surface in case of this project is acquired by distinguishing the different soil layers to a depth of 70 m below ground level, determination of the variation in (geotechnical) properties of the soil layers, defining the geohydrology, and knowledge on obstacles. The investigated geotechnical parameters were selected by analysing the design steps required, for example, the following is at least required for the building pits of the deep stations: the strength and stiffness properties of the soil on short (undrained) and long (drained, creep) term, volumetric weight as a function of the depth to calculate the vertical equilibrium of the soil, water pressure, and the geohydrology.

3.3 Geological Uncertainties

In general, three major types of uncertainties are recognised because each type has a different source and is treated differently (Mann 1993). Type 1 uncertainty arises through error, bias and imprecision of measurement processes. A second type of uncertainty (Type II) arises from inherent variation in natural parameters. And the third type of uncertainty is due to lack of knowledge, or scientific ignorance (Type III) (Table 1). Morgenstern (2000) recently emphasised that uncertainty is chronic in geotechnical practice and therefore geotechnical risk must be managed. An

essential component of assuring geotechnical performance, over the wide range of deliverables, requires that the geotechnical engineer maintains an on-going awareness of factors that contribute to unsuccessful performance and introduce this awareness into comprehensive risk management tools.

3.3.1 Type I Uncertainty

The setup of the site investigation for the Amsterdam North/South line has been such that the type I uncertainty is minimised to a very low level. This is done by using several contractors both for lab- and field testing, cross checking of lab tests, independent quality assurance, and expert opinions and independent quality control. The variance as found in the resulting values of a geotechnical parameter in this project is a function of: a) complexity of the site investigation, b) natural variance of the soil, c) sensitivity of laboratory tests to sample disturbance, d) stress dependency of parameter, e) type of investigation, f) (geological) history of soil sample, and g) differences between laboratory and in-situ tests. With simple laboratory tests, like volumetric weight the variance is caused only by the natural variance. In the case of complex site investigation like triaxial tests, the variance is caused by all of the above.

3.3.2 Type II Uncertainty

The type II uncertainty relates to the interpretation of the site investigation. Within this project, the main uncertainties have been defining “homogeneous” layers and deriving “average” values. In this project, a soil layer is defined homogenous when the variance of the volumetric weight samples is less than 5%. In addition, a statistical analysis was made on the CPT data to define more accurately certain soil layers.

3.3.3 Type III Uncertainty

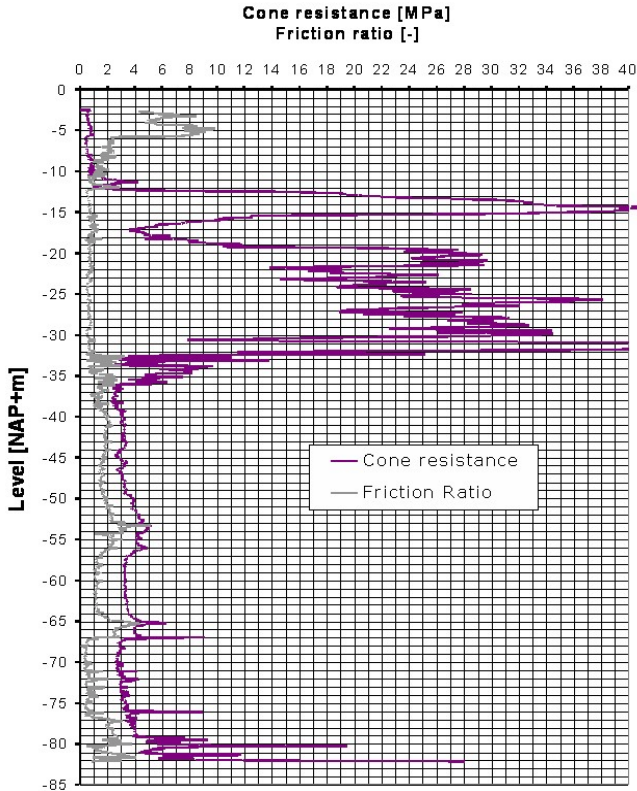
The type III uncertainty (lack of knowledge) has been overcome by executing several real-scale in-situ tests (de Wit, 1999). Also specialist knowledge was sought at research institutes, universities and special consultants both in and outside the Netherlands. Furthermore, research was made to define the correct finite element model for each type of calculation; also, comparison was made with analytical models where possible. However despite the research the (geotechnical) risks have to be managed, for this reason it has been decided to adopt the so-called Observational Method as part of the design of the stations and bored tunnel (Herbschleb, 2001).

3.4 Laboratory Investigation

Soil investigation in the laboratory consisted of classification test, Atterberg limits, torque vane, permeability, triaxial test, relative density, oedometer test, particule size distribution (psd), see table 2.

Table 2. Amount of lab. tests (Herbschleb, 2001).

Classification	Psd	Triaxial	Oedometer
2730	802	344	236

**Fig. 3.** Typical CPT of Amsterdam (Herbschleb 2002).

3.5 Interpretation of Site Investigation Data

With the interpretation of the site investigation data and derivation of the design values, the following aspects are considered: 1) goal of calculation (stability, deformation, etc), 2) type of calculation (analytical, finite element, etc), and 3) available data, standard deviation and range of values. The goal of the calculation is important, in the case of deformation predictions the goal is to simulate the behaviour as close as possible. In the case of stability calculations, the goal is to obtain a required safety margin against failure. This means that for both cases different values of the same parameter is required. A Finite Element model uses (complex) mathematical soil models, with specific boundary conditions to the value of the geotechnical parameters. This means that the type of calculation is important also,

as each type requires its own parameters. The variation in the data is a function of the complexity of the soil tests, natural variance of the soil, the sensitivity of the sample to disturbance, type of site investigation (laboratory or in-situ), and dependence of the parameter for instance on in-situ stress or strain. For simple laboratory tests, like volumetric weight, the variance is only a function of the natural variance of the soil. In the case of complex test like triaxial test the variance is a function of all mentioned elements.

Another important aspect in the determination of the design value is the expected outcome of a calculation. When only small deformations are expected in the design then also the parameters should be determined at small strain levels. Due to the possible variance and range found in the interpretation it is necessary to define upper and lower boundaries of parameter. In case of this project, the upper and lower boundaries were derived using the following two options (Herbschleb 2001): a) Characteristic value. This represents the statistical lower and upper boundary of the average value of a parameter with an accuracy of 90%. This value was derived for the simple laboratory test, and b) Representative choice. Statistics can only be applied to non-biased data. Such data are in this case the stiffness properties and angle of internal friction.

3.5.1 Unloading Stiffness (E_{ur})

The unloading stiffness is an important soil property to the design of the bored tunnel and deep stations, because excavation of the soil causes unloading. For this reason, the unloading stiffness is derived from the following tests: Oedometer with unloading step, Triaxial test (loading and unloading), and Cone Pressio Meter (CPM), in-situ tests. A value of E_{ur} is calculated from an Oedometer test with unloading step equally to the way an E_{oed} value is calculated from a loading step. From this test, a correlation between the void ratio and E_{ur} is derived, to be able to calculate the E_{ur} at other soil samples. Also from the triaxial tests the unloading stiffness could be derived. Within this site investigation, the (un)loading behaviour was simulated in the lab by triaxial test using different stress paths. The E_{ur} is calculated from an triaxial unloading test using the so-called E_0 instead of an E_{50} value from a “standard” triaxial test, see figure 4. A Cone Pressio Meter test is similar to a Self Boring Pressuremeter test, except that in this case the load-cell is pushed into the soil using a CPT. By loading and unloading the soil at different depths the unloading stiffness can be calculated. See figure 5 for a representation of the several tests, as can be seen from the graph the range of values for this specific parameter (E_{ur}) is rather large, namely between 10 and 90 MPa. Standard statistical procedures to derive an average value, lower an upper boundary of a range of values does not apply in this case. The main reasons are that the data set is a combination of several data sets (Oedeometer, etc). In addition, stiffness is a function of the followed stress path and strains. In this case the values are normalised to a value of 100 kPa, both the dependency to strains remains. For this reason the average, lower and upper boundaries are chosen values. The values are chosen using the following arguments: the upper boundary value is taken at a small strain

(unloading) stiffness ($\pm 10^{-4}$) as present within the CPM test, the lower boundary value is taken a relative large strains ($\pm 10^{-2}$), which results from loading a sample in an Oedometer test, and the average value is than taken in between the results of the Triaxial (unloading) test and the CPM test results.

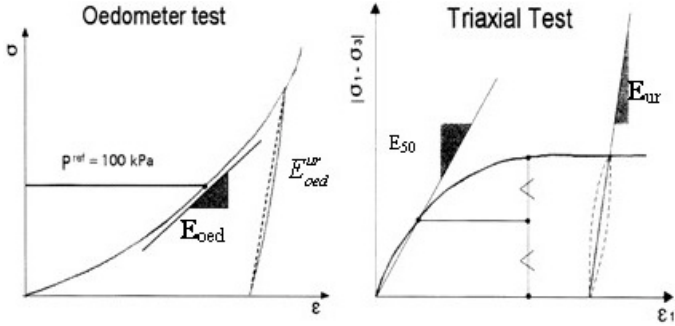


Fig. 4. Definition of Stiffness (Plaxis Manual).

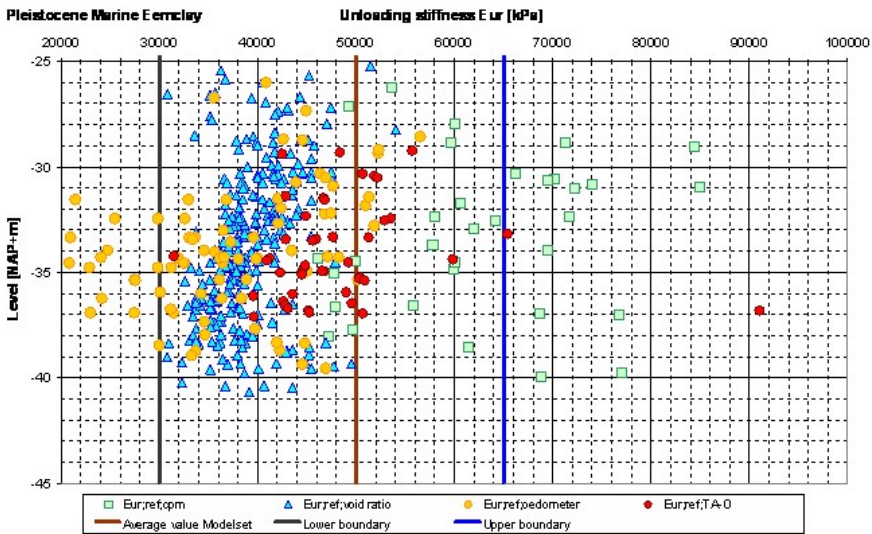


Fig. 5. Overview of unloading stiffness (Herbschleb, 2001).

4 Geotechnical Risk Management Tools

4.1 Introduction

Underground projects involving subsurface excavation, present many risks, all of which must be assumed by either the owner or the contractor. The greatest risks

are usually associated with the materials encountered and their behaviour during excavation and installation of support. To manage these risks at the North/South-line project a so-called Geotechnical Baseline Report (GBR) has been used. Furthermore, the Observational Method is used in combination with extensive monitoring during the complete project.

4.2 Geotechnical Baseline Report

A GBR establishes a contractual understanding of the subsurface site conditions, referred to as baseline. Risks associated with conditions consistent with or less adverse than the baseline are allocated to the contractor, and those significantly more adverse than the baseline are accepted by the owner. The latter conclusion derives from the philosophy that the owner owns the ground (ASCE 1997). The concept of a GBR was developed in the USA and guidelines have been published by the American Society of Civil Engineers (ASCE 1997). Within the USA, a GBR is since 1997 common practice and is applied on projects like the Seattle Monorail Project and Toronto's Rapid Expansion Program (Westland 1998). Also in Europe a GBR has been used on occasions (Öresund-tunnel link). The above-described concept of a GBR was introduced in the Netherlands at the North/South-line project and has been used since then also on other projects.

4.3 Monitoring Plan

To anticipate ground movement and damage to buildings during construction and to enable timely and appropriate actions, an effective monitoring concept has been designed. Buildings will be monitored using a fully automatic system of total stations and sensors. This on-line system will provide direct data for interpretation in the design office (validation of models!). A system of partly automatic and partly manual monitoring (vertical and horizontal subsurface deformation, strut forces, etc) will be carried out during the construction activities for the stations and bored tunnel. An area of about 70 m around the building pit will be monitored. The monitoring information is analysed and processed in such a way that during the construction period changes to the design/process if required can be made (Observational Method). Possible design/process adjustments are developed in advance as back up measures. Some of the monitoring activities will start in advance of the actual construction activities to be able to investigate the "natural" behaviour of the buildings.

5 Conclusions

Few criteria (standards, guidelines, etc) describe the amount of site investigation data necessary for complex projects. At this project, the site investigation plan was based on prior knowledge of the geology. One of the assumptions has been that

the soil layers are (nearly) horizontal. At locations where erosion has taken place and at locations where differing conditions were found, an additional site investigation was made. The interpretation of the geotechnical properties has been a complex process due to the different boundary conditions (stress paths) assumed in the parameters for each model, dependency to strain, etc. This means that statistics could not be applied to all geotechnical parameters. On basis of this research, the upper and lower boundaries were set. Extensive parametric studies were carried out taking into account the upper and lower bound values of both geotechnical parameters as well as material properties of the concrete structure. In a complex project, like the excavation of a building pit (dimensions: $l \times h \times w = 120 \text{ m} \times 30 \text{ m} \times 20 \text{ m}$), in a busy city very close ($<5 \text{ m}$.) to existing vulnerable houses all elements (geo-technical parameters, calculation models, and structural design) are linked in a complex way. With the aid of an extensive site investigation program and analysis of the geotechnical parameters, research in FE models a sturdy design has been developed. Nevertheless small uncertainties still exist. To manage these small uncertainties, risk management tools like a GBR and Observational Method are used. Currently the (major) construction works at the North-Southline have started. The interpretation of the site investigation will be validated against the obtained monitoring data to have a better understanding of the soil-structure interaction in this project.

References

- ASCE (American Society of Civil Engineers) (1997) Geotechnical Baseline Reports for Underground Construction. Guidelines and Practices. The Technical Committee on Geotechnical Reports of the Underground Technology Research Council.
- Gans W de, Beets DJ & Centineo MC (2000). Late Saalian and Eemian deposits in the Amsterdam Glacial Basin. *Netherlands Journal of GeoSciences* 79 147-160.
- Herbschleb J & de Wit JCWM (2000) Design of Deep Underground stations in soft soil conditions. *Proceedings GeoEng2000*, Melbourne, Australia.
- Herbschleb J, de Wit JCWM (2001) The observational method, an aid in difficult soft soil conditions, *Proceedings XVIII ISMGE Congress*, Istanbul, Turkey.
- Herbschleb J (2001) Case grondonderzoek: de Noord/Zuidlijn te Amsterdam. PAO -cursus, Delft.
- Herbschleb J (2002) Site investigation lecture. TU-Delft, faculty Technical Earth-Sciences.
- de Wit JCWM, Roelands JCS & de Kant M (1999) Full scale test on environmental impact of diaphragm wall trench excavation in Amsterdam, *Proceedings: Geotechnical Aspects of Underground Construction in Soft Ground*, Japan.
- Mann CJ (1993) *Uncertainty in Geology. Computers in Geology - 25 years of Progress*. Oxford University Press.
- Morgenstern NR (2000) Common Ground. *Proceedings GeoEng2000*, Melbourne, Australia.
- Thurner R & Schweiger HF (2000) Reliability analysis for geotechnical problems via Finite Elements, a practical application. *Proceedings GeoEng2000*, Melbourne, Australia.
- Westland J, Busbridge JR & Ball JG (1998) Managing Subsurface Risk for Toronto's Rapid Transit Expansion Program. *Proceedings North-American Tunneling*, Balkema.

Effects of the Determination of Characteristic Values of Soil Parameters

Britta Kruse

Technical University Berlin - Engineering Geology - Sekr. ACK 8
Ackerstrasse 76, 13355 Berlin, Germany
Dirk.Siewert@stump.de
Tel: +30 53011068
Fax: +30 53011068

Abstract. In April 1996 the German version of the Eurocode EC 7 “Geotechnical design - General rules” was published as a “pre-standard”, entitled V ENV 1997-1. It regulates stability analyses under the partial safety concept. Both the preface of V ENV 1997-1 and the National Application Document (NAD) for Germany refer to the package of standards “100” which is also required for calculations under the partial safety concept, since the data in the V ENV 1997-1 alone do not suffice for this purpose. Irrespective of the above, it was decided to switch over all German standards governing constructional engineering, including geotechnical engineering, to the partial safety concept. In this context the DIN V 1054-100 was transformed from the “100” package of standards into the new DIN 1054 “Stability analyses in earthwork and foundation engineering”. This article is intended to focus the reader’s attention on the special function performed by the determination of characteristic values of soil parameters in stability analyses under the partial safety concept. The above situation will be illustrated with the help of the calculation of slope failure.

Keywords: partial safety concept, characteristic values of soil parameters.

1 Introduction

Determining the characteristic values of soil parameters is of central importance for stability analyses under the partial safety concept in geotechnical engineering. The characteristic values of soil parameters have a great impact on the dimensions of buildings to be calculated. It should, however, be noted in this context that information on this topic is held in rather general terms in the Eurocode 7 (V ENV 1997-1) and in DIN 1054, 2003 with the result that the determination of the characteristic values of soil parameters becomes an empirical undertaking, i.e. it largely lies within the user’s discretion. As is demonstrated in the first part of this article using the example of the calculation of slope failure, the subjective determination of the characteristic values of soil parameters leads to different allowable angles of slope, and, as a result, to varying safety levels. The second part of this article shows that the range of allowable angles of slope and thus that the range of safety levels can be reduced by applying statistical methods aimed at determining the characteristic values of soil parameters.

2 Slope Design

2.1 General

To illustrate the differences between subjective and statistical determination of characteristic values of shear parameters, the allowable angle of slope will be determined for an arbitrary model slope. The aim underlying this calculation is purely illustrative. For the sake of simplicity it is assumed that the slope consists of boulder clay and is exposed neither to water in any form nor to any type of loading. Based on these assumptions the results are not relevant in any practical terms, but only for illustration of the problem of determining characteristic values for shear parameters. The system and boundary conditions are illustrated in Figure 2.1.

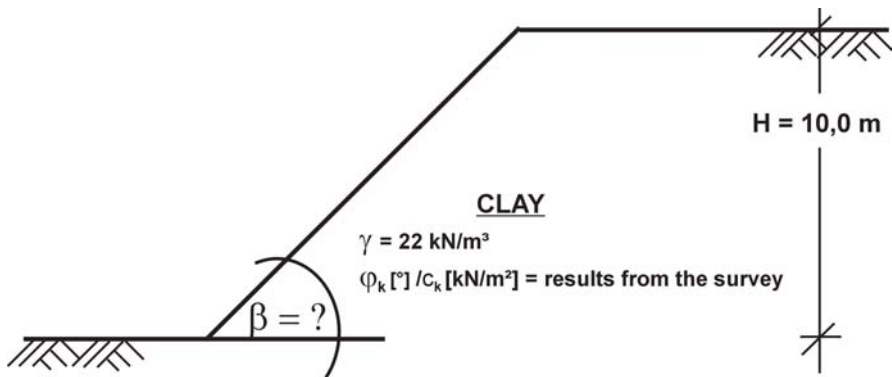


Fig. 2.1. System and boundary conditions for slope design.

The allowable angle of slope is calculated according to Simmer (1980). According to Item 6.4.2 of DIN 1054, 2003 the characteristic values of shear strength must be converted with the partial safety factors γ_ϕ and γ_c for resistance forces into the design values for shear strength. The unit weight of the soil is assumed to be constant.

2.2 Calculation with Subjectively Determined Characteristic Values

2.2.1 Determination of Characteristic Values by Geotechnical Engineers

To illustrate the problem of determining shear parameters, the author conducted a survey with geotechnical engineers at a workshop. The intention was that each geotechnical engineer determined the characteristic values of the angle of friction and cohesion as defined by the specifications of DIN 1054, 2003, based on the results of five shear tests (Table 2.1).

Table 2.1. Results of shear tests.

Sample	1	2	3	4	5
φ'_k [°]	29,8	35,4	33,5	34,8	35,7
c'_k [kNm ⁻²]	42,1	12,2	31,2	13,6	16,7

The results of the survey are as follow. The range of the characteristic values determined by the geotechnical engineers for the angle of friction is from a minimum value of $\varphi'_k = 29.5^\circ$ to a maximum value of $\varphi'_k = 35.0^\circ$. The characteristic values of cohesion range from a minimum of $c'_k = 2.0$ kNm⁻² up to a maximum of $c'_k = 20.0$ kNm⁻².

2.2.2 Results Based on the Characteristic Values as Derived from the Survey

Since the geotechnical engineers provided pairs of values for the characteristic parameters of angle of friction φ'_k and cohesion c'_k , the calculations of the allowable slope inclinations for the model slope are made for these combinations. The resulting range of calculated allowable slope inclinations is from a minimum value of $\beta = 35^\circ$ to a maximum value of $\beta = 63^\circ$. Clearly, such a wide range cannot be satisfactory. An alternative approach is to apply statistical procedures for the calculation of the characteristic values of shear parameters.

2.3 Calculation with Statistically Determined Characteristic Values

2.3.1 Determination of characteristic values by statistical methods

The characteristic value as estimated value of the mean value (Table 2.2) is calculated according to Bauduin (2001).

Table 2.2. Characteristic value estimated by statistical methods.

Estimation of the range of mean values following statistical methods			
ND (normal distribution)		LND (logarithmic normal distribution)	
φ'_k [°]	c'_k [kNm ⁻²]	φ'_k [°]	c'_k [kNm ⁻²]
31,5	10,8	31,5	12,1

For values with a linear trend, the confidence interval of a linear regression curve can be calculated. The lower limit of the calculated confidence interval is to provide the characteristic value as an estimated mean value in this process (Bauduin, 2001). This method results in the largest estimate of the mean value for the angle of friction of $\varphi'_k = 34.2^\circ$ which is slightly larger than the mean value of the random sample. For the cohesion the value becomes $c'_k = 13.2$ kNm⁻² which is larger than the minimum value of the random sample.

2.3.2 Results Based on the Characteristic Values Estimated by Statistical Methods

The results of the calculations of the allowable slope inclinations with the characteristic values estimated by statistical methods are from a minimum $\beta = 51^\circ$ up to a maximum $\beta = 59^\circ$.

3 Concluding Remark

For the example described it is obvious that using statistical methods for the determination of characteristic values for shear parameters results in a marked reduction in the range of allowable slope inclinations compared to the results of subjective determination. Therefore, statistical methods are likely an appropriate tool for the determination of characteristic values of shear parameters.

References

- Bauduin Ch (2001): Ermittlung charakteristischer Werte. in: Ulrich Smolctzyk (ed). Grundbautaschenbuch, Teil 1: Geotechnische Grundlagen. Kapitel 1.2. Ernst & Sohn Verlag für Architektur und technische Wissenschaften GmbH. Berlin 2001.
- Simmer E (1970): Grundbau Teil 1: Bodenmechanik und erdstatische Berechnungen, Kapitel 6.5.5: "Standsicherheitsuntersuchungen in besonderen Fällen.", 17., neubearbeitete und erweiterte Auflage, Verlag B.G. Teubner, Stuttgart 1980.
- STANDARDS
- V ENV 1997 – 1: Eurocode 7 – Entwurf, Berechnung und Bemessung in der Geotechnik – Teil 1 : Allgemeine Regeln – Deutsche Fassung ENV 1997 – 1: 1994. Ausgabe 04.96. Aus: DIN, Deutsches Institut für Normung e.V. (ed.). Geotechnik: Eurocode Teil 7-1, DIN V ENV 1997 – 1; Normen. 1. Aufl., Beuth Verlag. Berlin, Wien, Zürich 1996.
- DIN 1054 (2003): Baugrund – Sicherheitsnachweise im Erd- und Grundbau. Normenausschuss Bauwesen (NABau) im DIN Deutsches Institut für Normung e.V., Berlin 01/2003.

Basic Soil Properties of a Number of Artificial Clay – Sand Mixtures Determined as a Function of Sand Content

Beata Łuczak-Wilamowska

Faculty of Geology, Warsaw University
Żwirki i Wigury 93, 02-089 Warszawa, Poland
b.luczakw@uw.edu.pl
Tel: +48 22 554-06-06
Fax: +48 22 554-00-01

Abstract. Soil mixtures were composed from the Polish Neogene clays occurring on the Polish Lowland and the fine-grained dune sand in weight proportions of the dried components. As the products of mixing, new soils were obtained, having modified physical, mechanical and screening properties as a function of their different granular and mineral composition. The granular composition varies from the soils which are similar to clays, through the clay loam, sandy clay loam up to sandy loam. With comparison to the untreated clay, soil mixtures by far compact better and achieve lower values of porosity index n and void ratio e (n 27–22%; e 0.37–0.29; raw clay n 43%, e 0.76), and therefore they achieve lower values of coefficient of permeability (k $1.83 \cdot 10^{-9}$ to $2 \cdot 10^{-11}$ m/s) by maximum compaction. The soil mixtures show lower values of free swelling and linear shrinkage (FS_{HG} 40–20%; L_S 10.6–7.4%; raw clay: FS_{HG} 70%; L_S 14.7%). The mentioned features are crucial while selecting the mineral component of the lining system of burdensome objects such as landfills. Moreover, shear parameters of clay mixtures are improved as compared to the raw clay: starting from the angle of internal friction ϕ 6.2° and cohesion c 46.6 kPa by raw clay, to ϕ 33.5° and c 43.5 kPa by the soil mixture showing the highest sand content among the modeled soils. The values of the mentioned parameters are fundamental by selecting of mineral lining, and in course of construction of earth objects.

Keywords: soil mixture, clay, dune sand, permeability

1 Introduction

Modelling of physical, mechanical, and screening properties was carried out on soil mixtures composed of the Polish Neogene clays occurring on the Polish Lowland and the fine-grained dune sand. The formation of Neogene clays covers almost half of the State area (Wichrowski 1981). It constitutes a clayey barrier, truly existing in nature, protecting ground water from negative impact of human activity. Being readily available over a considerable area, the clays are most often used as a ceramic raw material. Due to absorptive capacity and low hydraulic conductivity, the clays are prospective as a sealing material applicable to construction of

mineral seal in the waste landfills containing moderately toxic substances, and to reclamation layers as well. The studies were carried out on clay samples from the delf in Budy Mszczonowskie representing the main clay type – the brown clay. The main component of the particles of clay fraction is smectite, prevailing over illite and kaolinite. In this size fraction quartz is present subordinately. Macroscopically distinguished types of clay do not differ significantly with respect to mineral composition. Additional components modify colour of clayey sediments: goethite – brown, organic matter – grey and black (Łuczak-Wilamowska 2002). The clays from Budy Mszczonowskie do not differ significantly from Neogene clays occurring in the other regions of Poland with respect to mineral and chemical composition (Łuczak-Wilamowska 1997). In order to modify properties of the clays, a more coarse-grained soil should be used as an admixture. It would become a load-bearing framework of a soil mixture, whereas the clay would constitute the filling of an inter-granular space. Easily accessible and homogeneous quartz dune-sand was selected as the component of soil mixtures. In order to homogenize, the soil mixtures were saturated with water over the liquid limit (Table 2.1). Symbols were used to describe relative proportions of these raw materials in soil mixtures: for example, M20s denotes the mixture composed of 20 % of sand (first soil) and 80 % of clay (second soil), recalculated to dry compounds. One should be aware that the granulometric composition of the brown clay itself (the second soil from the example above) shows the presence of up to 10 % of the grains of sandy fraction. Therefore, the actual sandy fraction content of M20s is about 27 % as can be read out from the Feret's diagram (Fig. 1.1).

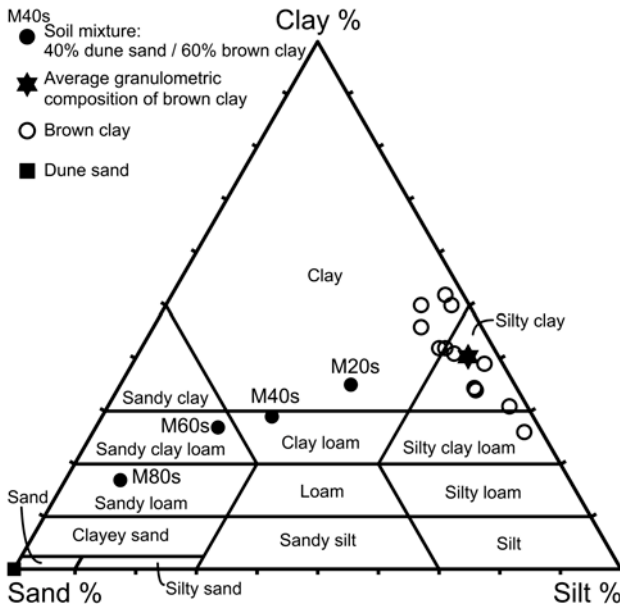


Fig. 1.1. Projection of granulation of the analysed soils on the Feret's diagram (modified from Łuczak-Wilamowska 2002).

2 Physical Properties of Soil Mixtures

Values of the fundamental physical parameters: plasticity, compactibility, maximum dry bulk density ρ_{dmax} , porosity n , void ratio e , angle of internal friction φ and cohesion c were measured according to the Polish Standard PN-88/B-04481. Liquid limit was determined using the method of the Vasilyev cone. The initial moisture content was determined after careful homogenization of soil mixtures. The parameters of plasticity of soil mixtures and brown clay samples are presented in Table 2.1. The values of consistency limits and plasticity index decrease along with the increasing content of sand in a soil.

Table 2.1. Parameters of plasticity of soil mixtures and brown clay.

Soil	Mixing moisture [%]	Plasticity limit PL [%]	Liquid limit LL [%]	Plasticity index I_p [%]	Symbols (Unified Soil Classification System)
Brown clay	71	21.3	48.6	27.3	CL-CH
M20s	52	20.3	36.3	16.0	CL
M40s	47	17.8	29.6	11.8	CL
M60s	40	16.9	25.6	8.7	CL
M80s	32	18.6*	20.6	2.0*	MH

* low accuracy owing to difficulty in determination of plasticity limit; less cohesive soil.

According to the Unified Soil Classification System (Das 1994), the brown clay was classified as CL-CH, the soil mixtures M20s, M40s and M60s were classified as CL, and the soil mixture showing the highest sand content, M80s, was classified as MH (Table 2.1). All the soil mixtures show a rectilinear correlation of plasticity index and liquid limit in the plasticity chart. It should be mentioned that the Vasilyev cone was used instead of the recommended Casagrand's apparatus for the determination of liquid limit. Comparing results obtained by these two different methods may, however, introduce some additional error, especially due to thixotropy processes occurring in Casagrand's apparatus in soil samples with high content of clay minerals. Porosity n and void ratio e achieved minimal values by maximum dry bulk density ρ_{dmax} . Parameters n and e indirectly influence the magnitude of infiltration, and the value of dry bulk density, ρ_d , is one of the parameters that effects the value of strength parameters. Values of ρ_{dmax} obtained experimentally in the Standard Proctor Density test (i.e. by attainment of the optimum moisture content) increase along with the increasing content of sand in soil mixtures, and reach a maximum for M80s. However, an attempt to obtain values of ρ_{dmax} and of the optimum moisture content in brown clay failed because in the regime of low moisture content this soil did not undergo homogenization and contained macropores. In turn, with high moisture content, the clay was highly adhesive and it stuck to the punner. Moreover, along with the water addition, the soil imbibed it unequally, and the achievement of unique moisture content of the entire sample was impossible (Table 2.2). In soil mixtures, values of minimum

porosity, n_{min} and void ratio in the densest state, e_{min} , decrease along with the increasing content of sand, and in case of M80s achieve minimum values of 22 % and 0.29, respectively (Table 2.2). It is worth to notice that the porosity and void ratio of the brown clay having an undisturbed structure are $n=43$ % and $e=0.76$, respectively. The experiments show that the addition of sand to clay improves the compactibility of the resulting soil, i.e. the soil mixture achieves higher values of dry bulk density. Similarly, such treatment also causes a decrease in the values of n_{min} and e_{min} in the densest state, and as a result, it can cause diminishing in the values of effective porosity and coefficient of permeability. Compared to soil mixtures, the dune-sand and the brown clay do not compact well (Table 2.2).

Table 2.2. Table 2.2. Values of optimum moisture content, maximum dry bulk density, particle density, porosity and void ratio of soil mixtures and their components.

	Optimum moisture content [%]	Maximum dry bulk density ρ_{dmax} [Mg·m ⁻³]	Particle density ρ_s [Mg·m ⁻³]	Porosity n [%]	Void ratio e [-]
Brown clay	-	1.85	2.70	43	0.76
M20s	17.0	1.983	2.69	27	0.37
M40s	13.1	1.989	2.68	26	0.35
M60s	12.9	1.998	2.67	25	0.34
M80s	11.1	2.057	2.66	22	0.29
Sand	9.8	1.79	2.63	32	0.47

3 Free Swell and Linear Shrinkage

According to recommendation of Head (1992), the free swell FS_{HG} was established by the method of Holtz and Gibbs (1956). It achieves medium values in soil mixtures. Accordingly, the volume of soil mixtures could increase when exposed to water under a small load. Free swell decreases along with the increasing content of sand; linear shrinkage measured according to the British Standard (BS1377: Part 2: 1990: 6.5) shows similar variability as the values of the free swell (Table 3.1). Parameters of swelling, which describe behaviour of a soil when exposed to water, were established using the diagrams of Van der Merwe (1964) and Seed

Table 3.1. Free swell and linear shrinkage of tested soils.

Soil	Free swell FS_{HG} [%]	Linear shrinkage L_S \pm std.dev. [%]	Activity [-]	Swelling potential [%]	Potential expansiveness	Degree of expansion
Brown clay	70	14.7 \pm 0.21	0.5÷1.5	25÷1.5	very high ÷ medium	high ÷ medium
M20s	40	10.6 \pm 0.49	0.5	<1.5	low	low
M40s	35	9.1 \pm 0.07	0.5	<1.5	low	low
M60s	30	8.1 \pm 0.28	0.4	<1.5	low	low
M80s	20	7.4 \pm 0.42	0.2	<1.5	low	low
Sand	0	-	-	-	-	-

et al. (1962). All the soil mixtures are characterized by low potential expansiveness and low degree of expansion, by swelling potential not higher than 1.5 % and by activity not higher than 0.5 (Table 3.1). The above-mentioned parameters of soil mixtures have lower values as compared to the brown clay. Therefore, the process of interaction: soil mixture – water does not exhibit pronounced magnitudes of disadvantageous phenomena such as swelling or shrinkage which is important for earth constructions.

4 Strength and Filtration Properties of Soil Mixtures

4.1 Shearing Resistance

The shearing resistance of the soil mixtures was determined in a series of shear box tests. The test conditions and assumed criterions of cutting were described in Łuczak-Wilamowska (2002). As the value of shearing resistance, the maximum value of the shear stress in the sample was assumed. The initial moisture content of the soil samples was slightly higher than the optimum moisture content, and the dry bulk density was near to the maximum dry bulk density ρ_{dmax} (Tables 2.2, 4.1). In a general way, by higher values of normal stress ($\sigma_n > \sim 150$ kPa), the shearing resistance increases along with the increasing content of sand in soil mixtures (Fig. 4.1).

Table 4.1. Shearing resistance of soil mixtures and their components. Tests in a box shear apparatus.

Soil	Initial moisture content [%]	Bulk density ρ [Mg·m ⁻³]	Final moisture content [%]	Angle of internal friction $\phi \pm$ std.dev. [°]	Cohesion c [kG·cm ⁻²]; $10^2 \pm$ std.dev. [kPa]
Brown clay	26.8	2.09	23.3	6.2 ± 1.5	0.466 ± 0.075
M20s	17.7	2.32	16.8	6.7 ± 1.4	0.844 ± 0.072
M40s	15.2	2.25	13.1	17.5 ± 1.6	0.927 ± 0.088
M60s	13.4	2.27	12.9	19.5 ± 0.9	0.683 ± 0.050
M80s	11.8	2.30	10.4	33.5 ± 1.0	0.435 ± 0.068
Sand	10.0	1.97	9.2	39.2 ± 0.8	0

4.2 Compressibility and Permeability

Compressibility and coefficient of permeability of soil mixtures and their components were analysed in the consolidometer in a regime of steadily increasing load by measuring the pressure of pore water and the sample height. The compressibility of mineral soils, i.e. ability of mutual displacement of the structural elements of the spatial system of grains and soil particles, is the main factor controlling the deformability of soils exposed to the load. The methods of consolidation tests and

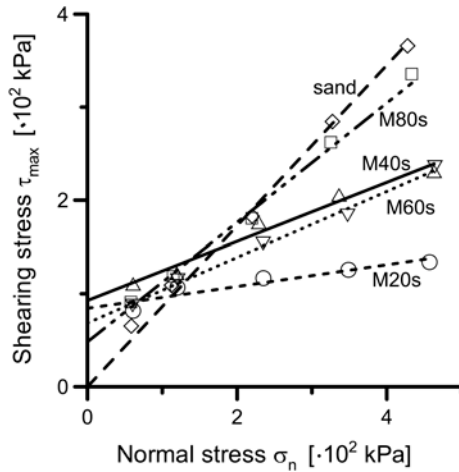


Fig. 4.1. Relationship of shearing stress versus normal stress for soil mixtures and dune-sand (modified from Łuczak-Wilamowska 2002).

of the determination of the coefficient of permeability were described in Łuczak-Wilamowska (2002); some data are recalled here. The relationship between the coefficient of permeability and the void ratio in the steady stage of the test in the consolidometer is shown in Figure 4.2, according to the method of Al-Tabbaa and Wood (1987). When exposed to a consolidating load, soil mixtures show variable values of the coefficient of permeability. Gradients of straight lines approximating relationship $k(e)$ increase along with the increasing content of sand in soil mixtures (R^2 in the range 0.76 – 0.94). During the experiment in the consolidometer, the samples of soil mixtures did not achieve maximum compacting, i.e. e_{min} , according to the Proctor compaction test. That is why the rectilinear relationships $k(e)$ were extrapolated to the values of e_{min} (Fig. 4.2), and corresponding values of k were read out. The clear relationship between the obtained values of k by e_{min} and the content of sand in soil mixtures cannot be observed (Table 4.2). In soil mixtures, k is in the range $2 \cdot 10^{-11}$ – $1.83 \cdot 10^{-9}$ $\text{m} \cdot \text{s}^{-1}$ by minimum values of e (e_{min}), i.e. by degree of compaction = 1. Nevertheless, the soil mixtures and the raw clay show values k of the order of magnitude 10^{-9} $\text{m} \cdot \text{s}^{-1}$ over the whole range of degree of compaction in consolidometric tests, starting from 0.72 and 0.83 for raw clay

Table 4.2. Extrapolated values of coefficient of permeability k by void ratio in densest state.

Soil	Void ratio in densest state e [-]	Coefficient of permeability k [$\text{m} \cdot \text{s}^{-1}$]
M20s	0.37	$1.83 \cdot 10^{-9}$
M40s	0.35	$3.80 \cdot 10^{-10}$
M60s	0.34	$1.03 \cdot 10^{-9}$
M80s	0.29	$2.00 \cdot 10^{-11}$

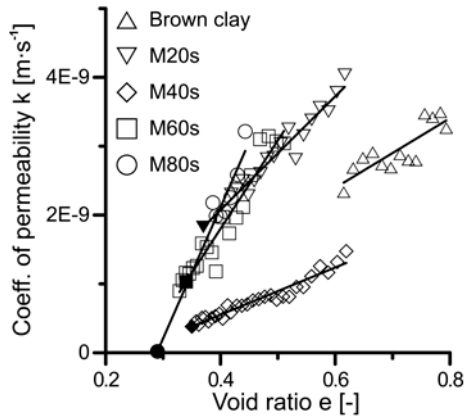


Fig. 4.2. Relationship of coefficient of permeability versus void ratio (modified from Luczak-Wilamowska 2002). Solid symbols denote values of permeability extrapolated to maximum values of compaction (i.e. degree of compaction = 1) in the Standard Proctor Density test.

and M80s as end-members, respectively. Permeability of each sample can be observed in the Fig. 4.2. All analysed soil mixtures match the condition of suitability of soils as mineral liners for landfills (Rowe et al. 1995) as they have $k < 10^{-9} \text{ m}\cdot\text{s}^{-1}$ by maximum compacting. It is difficult to state, however, if raw clays would fulfil this condition when their structure would be disturbed. Nevertheless, good homogenisation of soil mixtures eliminates macropores, occurring in clays with disturbed structure.

5 Conclusions

The research resulted in the following conclusions:

- Values of parameters of plasticity, swelling, and shrinkage decrease along with the increasing content of sand in soil mixtures.
- Compared to raw clay, soil mixtures show lesser susceptibility to water: lower activity, potential expansiveness and swelling potential. Lowering of swelling and shrinkage is advantageous, enabling the preservation of continuity of mineral sealing beds.
- For the values of normal stress equal to 150 kPa and more, shearing resistance increases along with the increasing sand content in soil mixtures.
- Values of the coefficient of permeability of soil mixtures by maximum compacting, determined consolidometrically and graphically, are within the range $1.83 \cdot 10^{-9} - 2 \cdot 10^{-11} \text{ m}\cdot\text{s}^{-1}$. Accordingly, all the studied soil mixtures fulfil the general condition of suitability as mineral liners for landfills, and the variability of this parameter is not critical for the valuation of sealing properties. The lowest permeability exhibits M80s, the soil mixture showing the best compactibility (lowest porosity and highest dry bulk density).

- Very low value of the coefficient of permeability ($2 \cdot 10^{-11}$ m/s) and high values of strength parameters (angle of internal friction, void ratio and maximum dry bulk density), which exhibits the soil mixture M80s, incline towards considering the usage of small quantities of clay for sealing sandy basements of landfills.

References

- Al-Tabbaa A, Wood DM (1987) Some measurements of the permeability of kaolin. *Geotechnique* 37, 4: 499-503.
- Das BM (1994) *Principles of Geotechnical Engineering*. PWS Publishing, Boston.
- Head KH (1992) *Manual of Soil Laboratory Testing, Volume 1: Soil Classification and Compaction Tests*, Pentech Press Limited, London.
- Holtz WG, Gibbs HJ (1956) Engineering properties of expansive clays. *ASCE Transactions* 121, Paper 2814 (with discussions): 641-663.
- Łuczak-Wilamowska B (1997) Pliocene clays of the Polish Lowland: The perspective insulating material of waste deposits. In: Marinos PG, Koukis GC, Tsiambaos GC, Stournaras GC (eds) *Proceedings International Symposium on Engineering Geology and the Environment*, organized by the Greek National Group of IAEG, Athens, Greece, 23-27 June. Balkema, Rotterdam, pp 1983-1988.
- Łuczak-Wilamowska B (2002) Neogene clays from Poland as mineral sealing barriers for landfills: experimental study. *Applied Clay Science* 21: 33-43.
- Rowe RK, Quigley RM, Booker JR (1995) *Clayey Barrier Systems for Waste Disposal Facilities*. Chapter 3: Clayey barriers: compaction, hydraulic conductivity and clay mineralogy. E & FN Spon, London, pp 82-119.
- Seed H, Woodward R, Lundgren R (1962) Prediction of swelling potential for compacted clays. *Journ. Soil Mech. Found. Div. SM*. 3: 53-87.
- Van der Merwe DH (1964) The prediction of heave from the Plasticity Index and percentage of clay fraction of soils. *Trans. S. Afr. Instn. Civ. Engrs.* 6: 103-107.
- Wichrowski Z (1981) Mineralogical studies of clays of the Poznań series. *Archiwum Mineralogiczne* 37, 2: 93-196 (in Polish, with English summary).

The Effect of Sand on Strength of Mixtures of Bentonite-Sand

Mohammad C. Pakbaz and Navid Khayat

Shahid Chamran Univ. Ahwaz, Iran
{mpakbaz, navid606}@yahoo.com
Tel: +98 611 333-7010
Fax: +98 611 333-7010

Abstract. The main purpose of this research is to evaluate the effect of sand on strength of compacted samples of bentonite sand mixtures. Samples of bentonite with 10,30,50,70, and 80 percent by weight of sand at standard proctor optimum water content were compacted and tested to measure confined and unconfined strength. Unconfined strength of mixtures increased with percentage of sand until 50 percent and then it decreased thereafter. On the other hand, the confined strength of mixtures tested in triaxial UU increased with percentage of sand.

Keywords: Bentonite, Sand, Shear strength, Triaxial, Unconfined.

Introduction

Because of its low permeability, bentonite has been recommended to be used in clay – liner and cut off trench systems. For this, hydraulic properties of bentonite – sand mixtures have been studied by many researchers before (e.g. D'Appolonia, 1980; Edil and Ertickson, 1985). Also, the use of sand for improving shrinkage crack characteristics of bentonite in clay – liners has been studied and recommended (Salehi, 2001). Data regarding strength characteristics of bentonite – sand mixtures are lacking in literature (Khayat, 2003). In this regard a research program is being conducted at the Civil Engineering department of Shahid Chamran University. Part of the results of testing is presented in the following sections.

Materials

The bentonite used is commercially available bentonite commonly applied in oil well operation in Ahwaz and the sand is local sand used in concrete. The portion of the sand used in this research passing sieve No. 10 is well graded.

Procedures

Bentonite–sand mixtures characteristics and index properties are given in Table 1 and 2. Data regarding standard proctor tests (ASTM D69870) performed on each

mixtures are given in Table 3. In order to prepare test specimens, each sample is thoroughly mixed with the amount of water required (ω_{opt}). To make sure that the moisture is distributed uniformly through the samples, each sample is kept in a sealed plastic bag for 24 hours before compaction. The unconfined strength test specimens are formed in a modified mold with 70 mm diameter and 140 mm height, by compacting to standard proctor criteria. In order to achieve this, each sample is placed in the mold in two layers and each layer is compacted 7 times with a 5-kg. Hammer from a height of 45 cm. Triaxial specimens were extracted with a 37.8mm diameter tube sampler from a compacted sample in standard proctor mold and then jacked out. From the jacked sample then a specimen with a height of 76.2mm was cut with the use of a wire saw and a surgical blade. The unconfined compression tests were performed according to ASTM D2166-66. The UU triaxial tests were performed on each sample at cell pressures of 75, 150, 300 kPa according to ASTM.

Table 1. Proportions of sand and bentonite used in samples tested.

Mixture name	Percentage of sand	Percentage of bentonite
B	0	100
B90 S10	10	90
B70 S30	30	70
B50 S50	50	50
B30 S70	70	30

Table 2. Index properties of sand – bentonite mixtures tested.

Index properties Mixture name	LL (%)	PL (%)	PI (%)	CF (%)	A_c	G_s
B	107.8	47.7	60.1	92.7	0.65	2.7
B90 S10	85.5	45.7	39.8	80.2	0.5	2.7
B70 S30	69.1	40	29.1	60.9	0.48	2.69
B50 S50	63.8	38.8	23	44.3	0.5	2.68
B30 S70	39.8	26.3	13.5	31.7	0.43	2.67

Table 3. Standard compaction test data for sand – bentonite mixtures.

Mixture name	ω_{opt} (%)	γ_{wet} (KN/m^3)	γ_d (KN/m^3)
B	24.3	16.21	13.05
B90 S10	23.48	18.22	14.75
B70 S30	20.73	19.47	16.13
B50 S50	15.43	20.7	17.93
B30 S70	14.33	19.6	17.14

Results

In Fig. 1 stress – strain relationships for samples tested in unconfined compression is shown and in Fig.2 the unconfined strength is plotted against the percentage of sand for these samples. As it is shown, the unconfined strength of samples is increased with the increase in the percentage of sand until 50 percent and then it is decreased thereafter. In Figs. 3, 4, and 5 the effect of percentage of sand on shear strength of samples tested in UU for cell pressures of 75, 150, and 300 kPa is shown respectively. With the increase in percentage of sand the strength of mixtures is increased and this effect is more for higher confining pressure.

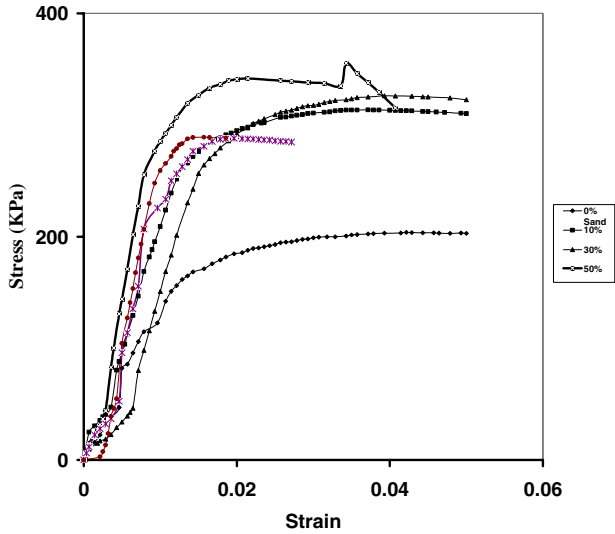


Fig. 1. Stress - strain relationship for samples tested in unconfined compression.

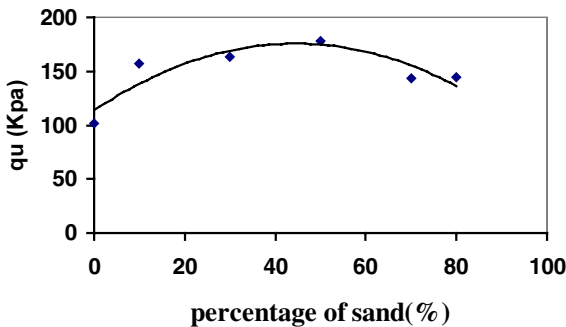


Fig. 2. Unconfined compression strength against percentage of sand.

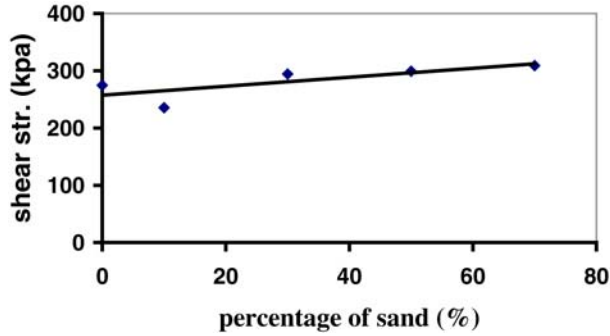


Fig. 3. Shear strength against percentage of sand for confining pressure of 75 Kpa.

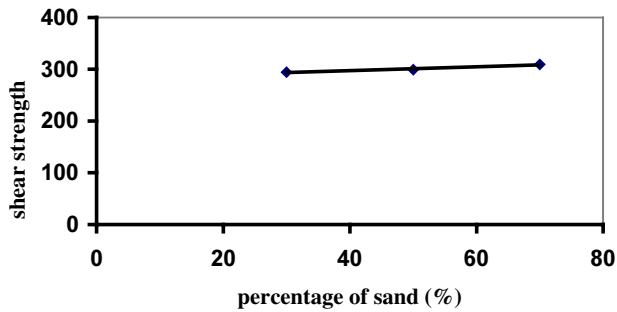


Fig. 4. Shear strength against percentage of sand for confining pressure of 150 Kpa.

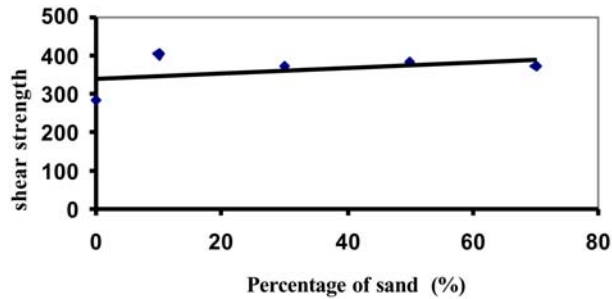


Fig. 5. Shear strength against percentage of sand for confining pressure of 300 Kpa.

Discussion

The decrease in unconfined compression strength of bentonite–sand mixtures after 50 percent of sand can be because with the increase in the percentage of sand, the lack of confinement of specimen together with a lower cohesiveness between soil

particles make the specimens show a lower strength. In triaxial UU tests, since the specimens were not fully saturated, the application of cell pressure in undrained condition could have actually caused an increase in effective stress on specimens as a result of compression of air. Therefore, an increase in strength for a higher cell pressure was observed. In this case the increase in percentage of sand would increase the frictional resistance upon the increase in effective stress.

Conclusions

According to the limited test results presented, the following conclusions are drawn: (1) The unconfined compression of mixtures of bentonite – sand increased with percent sand until 50 percent and decreased after that, and (2) The confined strength of mixtures of bentonite – sand in UU increased with the percentage of sand and with cell pressure.

References

- D'Appolonia, D.J., (1980). "Soil bentonite slurry trench cutoffs". *J. of Geotechnical Engineering*, ASCE, Vol. 106, No. 4. PP 399-417.
- Edil, T.B, and Erickson, A.E. (1985). "Procenure and equipment factors affecting permeability testing of a bentonite-sand liner material". In *hydraulic barriers in soil and rock*. Edited by A. I. Johnson, R. K. Frobels, N. J. Cavalli and C. B. Petterson. ASTM special technical publication No. 874, pp: 155-170.
- Khayat, N. (2003). "Evaluation of shear strength characteristics of bentonite-sand mixtures", M.S. Thesis, Shahid Chamran University, Ahwaz, Iran.
- Salehi, S. (2001). "Laboratory Evaluation of plasticity, hydraulic conductivity, compressibility and shrinkage potential properties of Bentonite-sand mixtures" M.S. Thesis, Shahid Chamran University, Ahwaz, Iran.

Nonconventional and Simple View of the Soil-Structure Interaction Problem

J. Paul Smith-Pardo¹, Mete A. Sozen², and Julio A. Ramirez³

¹ General Electric Faculty for the Future Graduate Student Fellow (Gefff)
1284 School of Civil Engineering, Purdue University, West Lafayette, IN 47907, USA
jpsmith@purdue.edu

Tel: +1 765 494-2234

Fax: +1 765 496-1105

² Kettelhut Distinguished Professor of Civil Engineering,
1284 School of Civil Engineering, Purdue University, West Lafayette, IN 47907, USA
sozen@ecn.purdue.edu

Tel: +1 765 494-2187

Fax: +1 765 496-2378

³ School of Civil Engineering, Purdue University, West Lafayette, IN 47907, USA
ramirez@ecn.purdue.edu

Tel: +1 765 4942716

Fax: +1 765 496-1105

Abstract. A mathematical model is proposed for the calculation of settlement and rotation of shallow foundations under combined vertical load and bending moment. The main advantage of the suggested approach is the consideration of both: (i) the nonlinear nature of the problem and, (ii) the interaction effect between vertical load and bending moment and the corresponding displacement and rotation. The formulation provides physical insight and could be generalized for the analysis of soil-shallow-foundation-structure systems under any type of loading. Using the proposed approach, the calculated vertical force-displacement relationships for eccentrically loaded shallow foundations on sand compare very well with the experimental results from previous studies. An experimental program, currently underway, to calibrate the suggested model for the analysis of foundations under loading conditions corresponding to seismic excitation of frame buildings will also be discussed.

Keywords: Soil-Structure Interaction, Foundation Rocking and Settlement, Nonlinear Analysis, Soil-Foundation Modeling.

Introduction

Code provisions (Fema 273 1997) for the rehabilitation of buildings establish that for reinforced concrete frames in medium to high seismic risk zones, the interaction between the supporting soil and the structure must be taken into account. Soil-Structure Interaction (SSI) problems should include explicit modeling of each foundation under combined loads according to FEMA 273 (Fema 273 1997).

Solutions for the vibrations of foundations on soil are based on the work by Horace Lamb (Lamb 1904) on the propagation of elastic waves induced by the application of a point load on the surface of an elastic semi-infinite media. To date, general formulas and charts for the calculation of impedances (dynamic stiffness and damping) of surface or embedded foundations of any shape (Gazetas 1991) are readily available and included in code design provisions (Fema 273 1997). However, these formulas/derivations are based on the assumption of a linear response of the soil-foundation substructure. Few studies exist that consider the nonlinear nature of the response of the soil-foundation subsystem and such studies are based on complex finite element (F.E) analyses used to represent the stress-strain relationship for the soil (Noorzai et al. 1994). A mathematical model is proposed in this paper for the calculation of settlement and rotation of shallow foundations under combined vertical load and overturning moment. The formulation provides a clear physical insight of the phenomenon and includes the nonlinear response of the soil.

Modeling of the Soil-Foundation Subsystem

The response of foundations under combined vertical load and overturning moment is proposed to be determined completely on the basis of the results from a simple plate load test on the bearing soil. It is assumed that the relationship between the vertical displacement at the center of the plate normalized with respect to the plate diameter (or plate side, if square) and the average vertical stress is a material property of a given soil. The slope of that curve is considered a soil material property and is equal to the subgrade modulus multiplied by the width of the plate (assumed square). The experimental results of footings on medium density sand (Briaud et al. 1994) and on low plasticity clay (Consoli et al. 1998) shown in Figure 1 support this basic assumption. Consider a rigid rectangular foundation of dimensions $B \times L$ (B in the direction of bending) under combined axial load and overturning moment. Given the midpoint displacement, δ , and the rotation, θ , (foundation slippage is neglected), the subgrade modulus $K_s(x)$ at any abscise x along the width, B , of the plate can be calculated based on the result of a plate load test (see Figure 2) as:

$$K_s(x) = \frac{(K_s B)_{plate}}{B} \quad (1)$$

The corresponding stiffness matrix K relating the applied vertical load, P , and the overturning moment, M , with δ and θ is given by:

$$K = \begin{bmatrix} K_\delta & K_{\delta\theta} \\ K_{\theta\delta} & K_\theta \end{bmatrix} \quad (2)$$

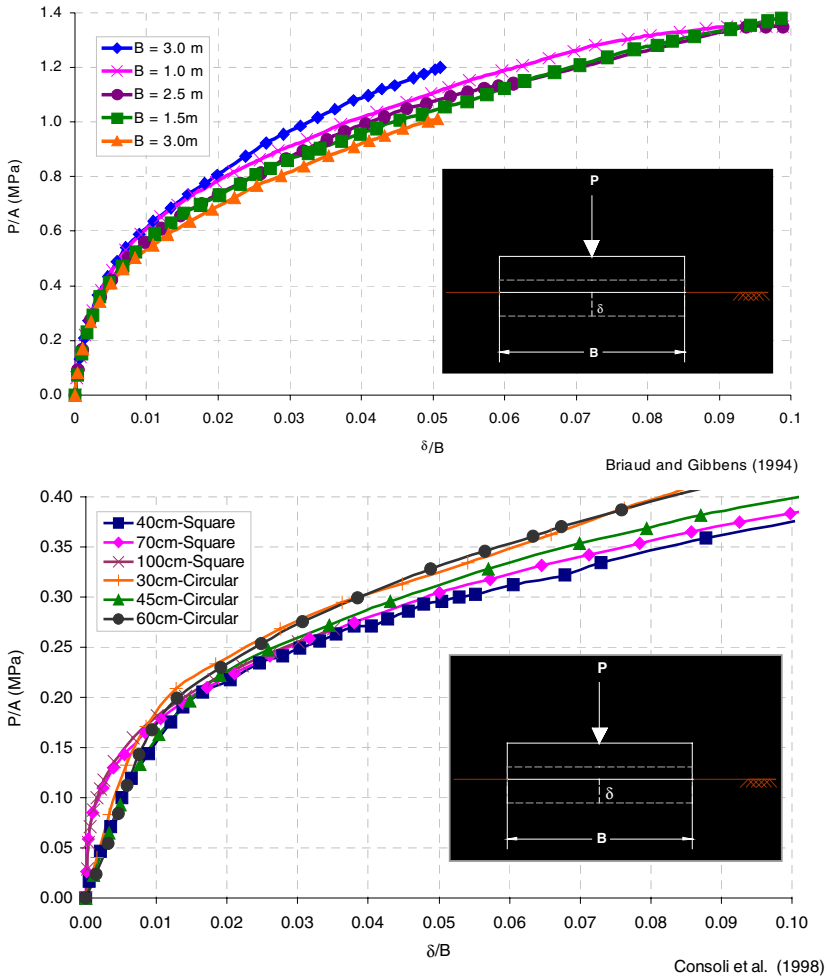


Fig. 1. Pressure-Normalized Settlement for Concentrically Loaded Foundations: top: Footings on Medium Density Sand (Briaud and Gibbens 1994), bottom: Footings on Low Plasticity Clay (Consoli et al. 1998).

where:

$$\begin{aligned}
 K_{\delta} &= \int_0^B K_S(x)Ldx, \\
 K_{\theta} &= \int_0^B K_S(x)L(x - B/2)^2 dx, \\
 \text{and } K_{\delta\theta} &= K_{\theta\delta} = \int_0^B K_S(x)L(x - B/2)dx
 \end{aligned}
 \tag{3}$$

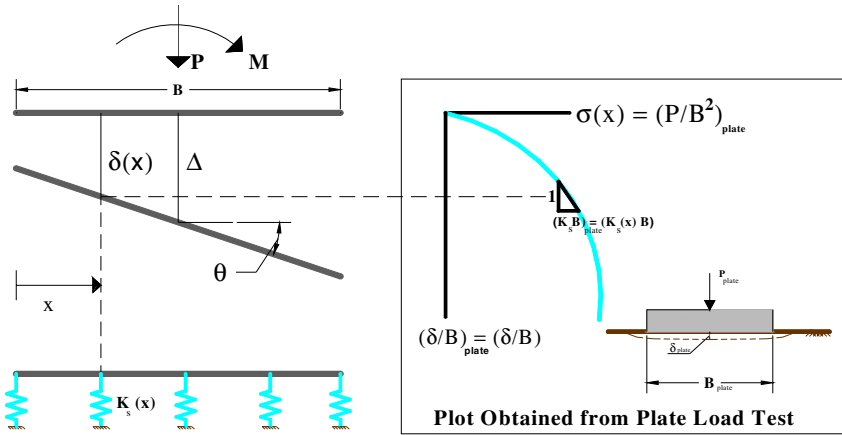


Fig. 2. Proposed Mathematical Model.

The nonlinear nature of the problem is evident: (i) the terms of the stiffness matrix K (Eq. 3) depend on δ and θ , and (ii) P and M are coupled. Notice also that the case $K_s(x) = \text{constant}$ correspond to the classical Winkler formulation (thus, linear behavior of the bearing soil and not interaction of P and M , i.e., $K_{\sigma\delta} = 0$). Solution of this problem requires considering the equilibrium equation in differential form:

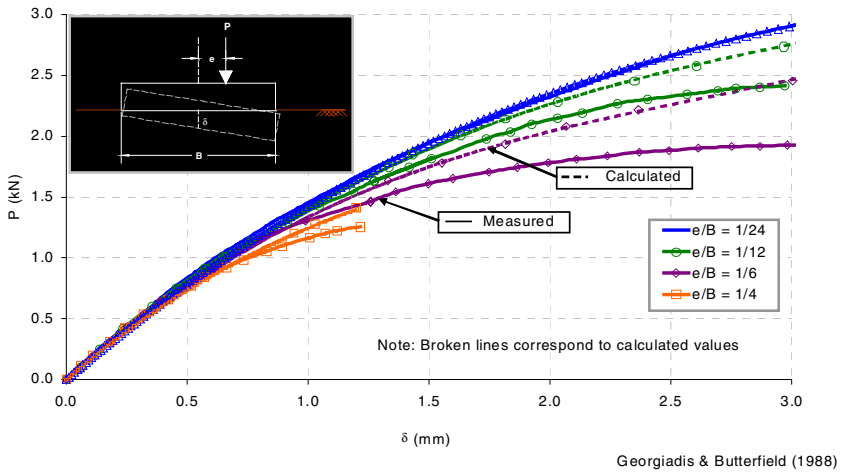
$$\begin{Bmatrix} dP \\ dM \end{Bmatrix} = K \begin{Bmatrix} d\delta \\ d\theta \end{Bmatrix} \tag{4}$$

Georgiadis and Butterfield (Georgiadis and Butterfield 1988), and Montrasio and Nova (Montrasio and Nova 1997) reported results for the vertical displacement at the center of eccentrically loaded foundations on sand. The footings used by Georgiadis and Butterfield were steel plates 50mm wide (direction of bending) by 400mm long.

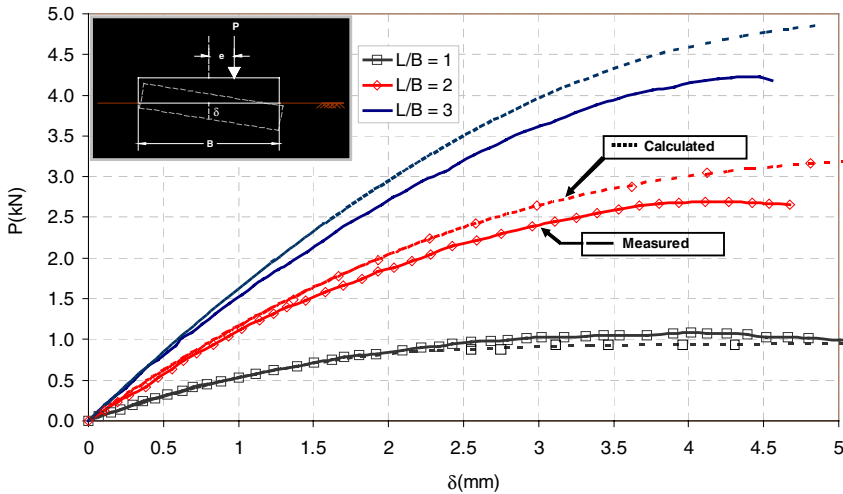
Footings tested by Montrasio and Nova were 100mm-side square steel plates. Calculated vertical force-displacement (at the center of the plate) for the footings tested by these researchers are shown in Figure 3 with dashed lines. Experimental values are indicated in the same figures with continuous lines. The similarity in the results encourages the use of the proposed methodology for the calculation of the response of foundations under combined vertical force and overturning moment.

Extension of the Model and Experimental Program

A study is being undertaken that considers the application of the proposed mathematical model in the calculation of the response under lateral loads of low-



Georgiadis & Butterfield (1988)



Montrasio and Nova (1997)

Fig. 3. Experimental/Calculated Response of Eccentrically Loaded Foundations: top: Test Results by Georgiadis and Butterfield (1988), bottom: Test Results by Montrasio and Nova (1997).

to-medium rise (residential) R/C structures. The loading conditions for the foundations of laterally loaded buildings consist of an approximately constant vertical load (corresponding to gravity load) and an increasing overturning moment (as the applied lateral load, simulating earthquake excitation, increases). The condition of approximately constant axial load is approached as the number of bays in the structure becomes larger. An experimental program is being conducted at Purdue

University to calibrate the proposed model for foundations subjected to constant axial load and varying overturning moment. Previous tests consisted of varying both the axial load and the overturning moment (constant eccentricity).

Summary and Conclusions

A simple formulation for the calculation of settlement and rotation of foundations under combined vertical load and overturning moment has been presented. Using the proposed approach, the calculated vertical force versus center displacement relationships for eccentrically loaded shallow foundations on sand compare very well with the experimental results from previous studies. Extension of the suggested mathematical model to foundations subjected to constant axial load and varying overturning moment is currently underway, to better represent the loading of foundations of buildings under lateral forces.

References

- Briaud JL, and Guibbens RM (1994), Predicted and Measured Behavior of Five Spread Footings on Sand, Settlement '94 ASCE conference at Texas A&M University, June 16-18, 1994 ; Jean-Louis Briaud and Robert M. Gibbens eds.
- Consoli NC, Schnaid F, and Milititsky J (1998), Interpretation of Plate Load Tests on Residual Soil Site, ASCE Journal of Geotechnical and Environmental Engineering, Vol. 124, No.9, pp. 857-867.
- FEMA 273 (1997), Federal Emergency Management Agency (FEMA), Seismic Rehabilitation Guidelines, Chapter 3: Modeling and Analysis (Systematic Rehabilitation) Section 3.2.6: Soil Structure Interaction.
- Gazetas G (1991), Formulas and Charts for Impedances of Surface and Embedded Foundations, ASCE Journal of Geotechnical Engineering, Vol. 117, No. 9, pp. 1363-1381.
- Georgiadis M, and Butterfield R (1988), Displacements of Footings on Sand under Eccentric and Inclined Loads, Canadian Geotechnical Journal, Vol. 25, pp. 199-211.
- Lamb H (1904), On the Propagation of Tremors over the Surface of Elastic Solid, Philosophical Transactions of the Royal Society of London, Vol. 203, pp. 1-42.
- Montrasio L, and Nova R (1997), Settlement of Shallow Foundations on Sand: Geometrical Effects, Geotechnique, Vol. 47, No. 1, pp. 46-60.
- Noorzaei J, Viladkar MN, and Godble PN (1994), Nonlinear Soil Structure Interaction in Plane Frames, Engineering Computations, Vol. 11, 303-316.

Effect of Pore Fluid Salinity on Compressibility and Shear Strength Development of Clayey Soils

Leon A. van Paassen¹ and Laurent F. Gareau²

¹ GeoDelft, P.O.Box 69, 2600 AB Delft, NL

L.A.vanPaassen@GeoDelft.nl

Tel: +31 15 269 38 13

Fax: +31 15 261 08 21

² Technical University Delft, dep. of Civil Engineering and Geosciences

Engineering Geology, Mijnbouwstraat 120, 2628 RX, Delft, NL

L.Gareau@CiTG.tudelft.nl

Tel: +31 15 278 89 69

Fax: +31 15 278 28 36

Abstract. Investigations of shear strength, compressibility and moisture content of a recent marine clay in the Caspian Sea showed soil profiles with a lower shear strength and higher moisture content, than expected for a normally consolidated soil. Further, measured preconsolidation pressures were lower than the calculated in-situ effective stress, suggesting that the deposit was underconsolidated. The pore fluid salinity was also measured and showed an increase with depth up to saturation concentration. A research project was carried out to study the effect of pore fluid salinity on shear strength and compressibility of remoulded clays. Results of this study showed that increasing pore fluid salinity caused a decrease of the moisture content for a normally consolidated clayey soil of high plasticity. The remoulded shear strength corresponded with the measured moisture contents. The observed compressive behaviour of these clays is explained using the modified effective stress concept, which considers not only (excess) pore pressure and effective pressure, but also the electrochemical repulsive and attractive forces between the clay particles. The laboratory tests on remoulded clays show opposite results to the measurements on the natural soils. The effects of soil structure are used to explain the differences for the measurements of moisture content, undrained shear strength and preconsolidation pressure. The oedometer test procedure was reviewed and additional tests were performed on natural clay samples from this site. Results showed that the measured pre-consolidation pressure depends largely on the salinity of the permeating fluid used in the oedometer apparatus and suggest that when testing marine clays with very high pore fluid salinity, using a brine solution that closely resembles the pore fluid chemistry yields a measured preconsolidation pressure closer to the known geological stress history.

Keywords: salinity, undrained shear strength, compressibility, correlations, modified effective stress, soil fabric, oedometer test procedure.

Introduction

Compressibility and shear strength are two mechanical parameters of soils, which are essential for the design of large infrastructure projects in near- and off-shore environments. Accurate predictions of the compressibility of soft soil layers and

the consolidation time are needed to optimise the construction process and to minimise maintenance costs during and after construction. The shear strength (cohesion and friction) of the soil is an important factor to determine the stability of the foundation. The classical approach to determine the compressibility and shear strength is based on the concept of effective stresses. In this classical approach the pore fluid and solid particles are both assumed to be chemically inert, so no chemical interaction takes place between the different phases. In reality, however, neither the pore fluid nor the solid particles are chemically inert, especially when clay minerals are present in the solid phase. On micro-scale interactive forces are present between solid particles, dissolved material and water molecules. Although a lot of soils in near- and offshore environments are saturated with brines or brackish groundwater and contain clay minerals, the influence of pore fluid salinity on the compressibility and shear strength is often neglected. Firstly the presence of a dissolved phase in the soil may result in errors in the determination of the basic soil parameters. In wet state the salt ions are dissolved and part of the fluid phase, while in dry state the salt ions are crystallized and part of the solid phase. Due to this phase change all results of laboratory tests which involve drying of the soil, need to be corrected (Imai *e.a.*, 1978; Van Paassen, 2002). These include moisture content, dry unit weight, fluid unit weight, particle density and atterberg limits and indirectly oedometer results.

Secondly the presence of salt ions in the pore fluid can change the mechanical behaviour of a clayey soil fundamentally. Most clay minerals have a net negative charge on the particle surface. Due to this charge electro-chemical forces exist between the solid, liquid and dissolved phase. To take these electro-chemical forces into account the classic approach based on effective stresses needs to be adapted.

Theoretical Model

Classical Effective Stress Theory

The procedure, which is most widely used, to predict the settlement of a soil mass involves dividing up the soil mass in layers. For each layer the compression and recompression indices and the pre-consolidation pressure have to be determined. The standard method to determine the compressibility parameters is with an oedometer test. However, this can be a time-consuming (expensive) method and in a lot of cases the compressibility parameters are estimated or derived from experience. If a soil is normally consolidated - the pre-consolidation pressure is equal to the existing vertical effective stress at present time - a continuous profile of the shear strength and the void ratio can be obtained using an iterative procedure and some useful correlations.

For homogeneous clayey soils the effective stress (σ_v') at a particular depth (z) is equal to the bulk unit weight of the overburden (γ_b) times the total layer thickness minus the hydrostatic pore pressure (u):

$$\sigma'_v = \sigma_t - u = z(\gamma_b - \gamma_f) \quad (1)$$

The bulk unit weight is a function of the weight of the solid particles (γ_s), the fluid weight (γ_f) and the void ratio (e):

$$\gamma_b = \frac{\gamma_s + e\gamma_f}{1 + e} \quad (2)$$

The void ratio, according to the one-dimensional consolidation theory (Terzaghi and Peck, 1948), is negatively proportional to the logarithm of the effective stress:

$$e = e_0 - C_c \log_{10} \left(\frac{\sigma'_v}{\sigma'_{v0}} \right) \quad (3)$$

If the compression index (C_c) is known and constant and an initial void ratio (e_0) and effective stress (σ'_{v0}) are assumed, equations 1,2 and 3 result iteratively in a gradually increasing pressure gradient. The shear strength can be calculated from the effective stress, if the effective cohesion and friction are known.

For inhomogeneous clayey soils the compression index is not constant but can be correlated with the moisture content and the plasticity boundaries. The moisture content (w) of a clayey soil at a given depth depends largely on the plasticity boundaries. To account for variations in liquid limit (LL) and plastic limit (PL) with depth, the liquidity index (LI) is calculated:

$$LI = \frac{w - PL}{LL - PL} = \frac{w - PL}{PI} \quad (4)$$

The liquidity index shows a moderately narrow band when plotted versus strength or stress on a semi-logarithmic scale, instead of the varying pattern of the moisture content (Skempton, 1970). Assuming that the undrained shear strength at liquid limit is fairly constant at approximately 1.7 kN/m² (Youssef et al., 1965) and that the undrained shear strength at plastic limit is 100 times greater than the shear strength at liquid limit, approximately 170 kN/m² (Skempton and Northey, 1952), the undrained shear strength (c_u) can be related to the liquidity index:

$$LI = 0.5(\log(170) - \log(c_u)) \quad (5)$$

Based on these assumptions and further assuming that the effective overburden pressure at the liquid limit is approximately 6.3 kN/m², the compression index can be calculated from empirical relations with the plasticity boundaries. (Wroth, 1979; Wroth and Wood, 1978; Pandian and Nagaraj, 1990; Sridharan and Nagaraj, 2000; Carter and Bentley, 1991). Wroth (1979) relates the compression index for remoulded clayey soils with the plasticity index (PI):

$$C_c = 0.5PI \frac{\gamma_s}{\gamma_f} \quad (6)$$

Using these correlations and the iterative procedure (eq. 1, 2 and 3) a fairly continuous vertical profile of compressibility and undrained shear strength can be obtained for both homogeneous and inhomogeneous normally consolidated remoulded soils based on measurement of moisture content, unit weight and plasticity boundaries at regular intervals. The obtained profile is called the normal consolidation line (NCL).

Modified Effective Stress Theory

The procedure mentioned above is based on effective stress only and does not account for the interparticle electro-chemical forces, which are present between the solid, liquid and dissolved phase. Two interparticle forces are distinguished: short-range forces and long-range forces. The short-range forces are the forces acting between the particles at the contact points, which include Born repulsion, surface and ion hydration, primary valence bonding and cementation (Mitchell, 1993). The long-range forces are divided in attraction forces and repulsion forces. Although the long-range forces are negligibly small compared to short-range forces in coarse-grained soils, they can play a dominant role in fine-grained soils. Secondly the influence is more important in soils with a high moisture content, where mechanical forces like interparticle friction are relatively less abundant (Sridharan and Prakash, 1999).

The long-range attractive forces (A) are due to Coulombic attraction and London-Van der Waals forces. The long-range repulsive forces (R) between particles are dominated by electrostatic repulsion of equally charged particles. Ideally clay particles are electrically neutral. However, most clay minerals in natural soils have a net charge, which is mostly negative. Isomorphous substitution, replacement of high valence cations by low valence cations in the molecular structure of the clay particle, is the most important factor, and causes a net negative charge at the clay surfaces (Lambe and Whitman, 1969). The total surface charge of a particle depends on charge density and the surface area. The specific surface, in square meters per gram, is inversely related to the clay particle size. The smaller the clay particle, the larger the specific surface and often the larger the total surface charge.

The net negative charge is compensated by adsorption of dissolved cations or polar water molecules from the pore fluid. The Cation Exchange Capacity (CEC), which is the amount of adsorbed milli-equivalents per gram of soil, is often used as a measure of the total surface charge of clay. The charged particle surface together with the charge distribution in the pore fluid adjacent to the surface is termed the diffuse double layer (DDL). The dissolved cations in the DDL are exchangeable. The pore fluid chemistry, including the amount and type of cations, also affects the long-range repulsive forces. The thickness of the DDL – which is a measure to indicate the decrease of surface potential with distance from the clay particle surface and can be visualised by the volume of adsorbed water – is inversely proportional to the cation valence and to the squareroot of the electrolyte concentration (i.e. an increase in pore fluid salinity or cation valence causes a decrease of DDL thickness and consequently a decrease of long-range repulsive forces).

Integration of both short- and long-range forces gives a total net repulsive force, $(R-A)$. To account for these interparticle electro-chemical forces the net repulsive force should be included in a modified effective stress concept (Sridharan and Prakash, 1999):

$$\sigma_v' = \sigma_t - u - (R - A) \quad (7)$$

The effective stress is now determined by two factors, the traditional effective stress, $(\sigma_t - u)$, and the net repulsive stress, $(R-A)$. The long-range repulsive force decreases the effective stress. The influence of R on the effective stress is high for particles with a large specific surface (or small particle size) and high charge density and for pore fluids with low salinity. The use of this modified effective stress theory would be useful in the prediction of soil engineering properties, particularly for marine situations. It is very difficult to measure the net repulsive stresses $(R-A)$ and consequently it is rarely included in practice. An example is presented herein where interpretation of geotechnical test results could be improved by considering the role of repulsive stresses.

Investigation of Natural Clays from the Caspian Sea

In 1996 a site investigation was carried out by Fugro Engineers BV in which boreholes were drilled down to a maximum depth of 180 m below the seabed in the Caspian Sea. At regular depth intervals samples of approximately 1 m length were taken using a 72 mm diameter piston sampler. The samples were used for different geotechnical laboratory tests, including: moisture content, bulk and dry unit weight, particle density, liquid and plastic limit, grain size distribution, undrained shear strength, oedometer tests for compressibility, pre-consolidation pressure and consolidation rate, SEM analysis, mineral composition and pore fluid salinity. From these test results a fairly continuous vertical profile of the clay deposit at this site is obtained. As the Caspian Sea is an active sedimentary basin with continuous sedimentation during the whole Quaternary and part of the Tertiary period, a normally consolidated soil profile was expected. However the test results on the drilled samples did not correspond with the theoretical normal consolidation line (NCL) and seemed to suggest otherwise.

The soil profiles showed strata of high to extremely high plasticity clay. The in-situ moisture content was measured according to BS1377:Part2:1990 and compared to the measured liquid and plastic limit and to the NCL. (Figure 1a). The pre-consolidation pressure was determined in the oedometer test (BS1377:Part 2:1990) and compared to the calculated overburden pressure from measured moisture content, average bulk unit weight (used in the oedometer test) and the NCL. (Figure 1b). The undrained shear strength is measured in the field using the fall cone test (ETC5; Eurocode 7) on both the undisturbed and the remoulded sample and compared to the undrained shear strength calculated from the measured liquidity index (eq. 5) and to the NCL (Figure 1c). The clays appeared to have very high moisture contents with depth and preconsolidation pressures less than the effective overburden stress. These data, considered in isolation might lead to

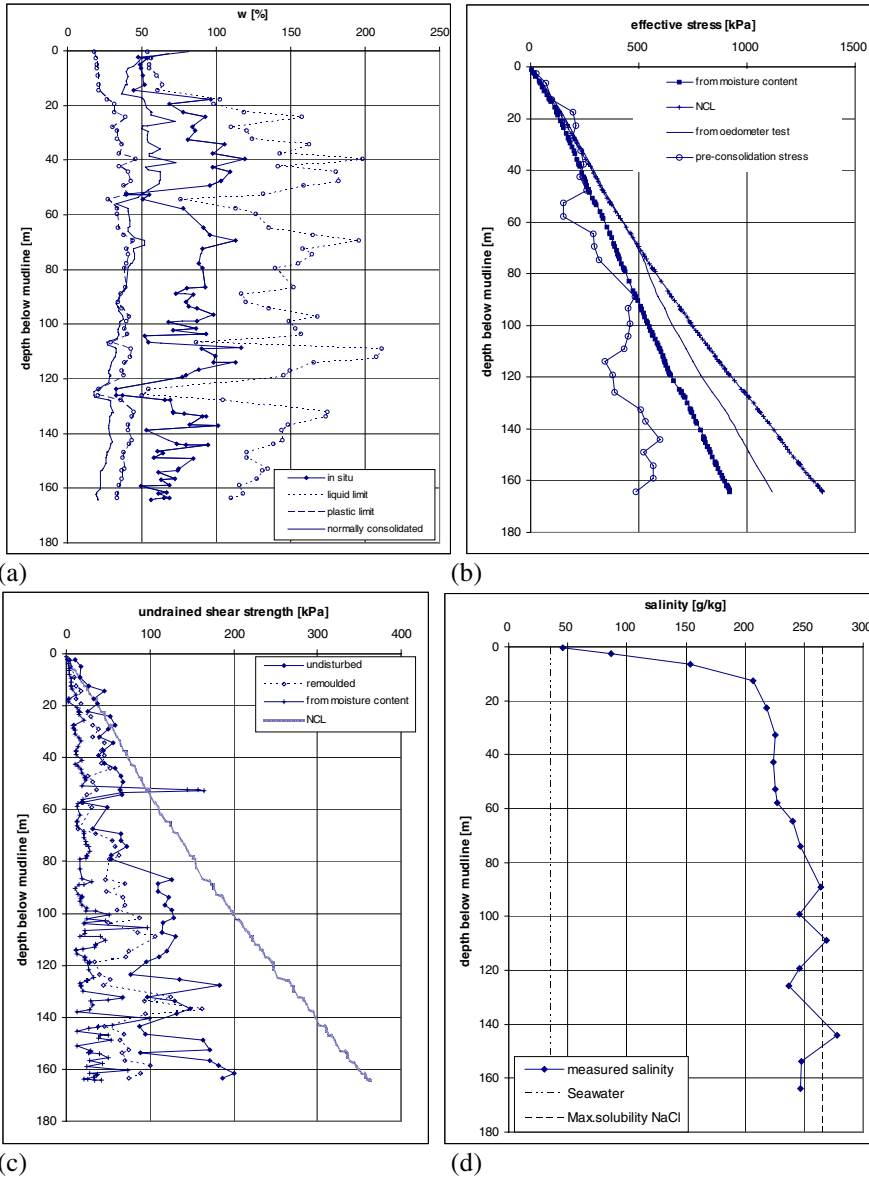


Fig. 1. Soil profiles from the Caspian Sea: a) moisture content; b) pre-consolidation pressure; c) undrained shear strength and d) pore fluid salinity.

effective overburden stress. These data, considered in isolation might lead to the conclusion that the deposit was not completely consolidated. There was no evidence of geologic conditions, such as rapid sedimentation or presence of shallow gas that would result in underconsolidation at this site. At the same time, Fig-

ure 1.c shows that undrained shear strengths were lower than expected for normally consolidation conditions, but relatively higher than would be expected for the high moisture contents measured if c_u is calculated according to Equation 5. High undrained shear strengths seem to contradict the conclusion that this deposit was underconsolidated. Figure 1.d shows that pore fluid salinity increased with depth up to a saturation concentration below about 90 metres depth. These high liquidity values and high pore fluid salinities gave reason to suggest that the pore fluid salinity caused this apparently underconsolidated soil condition.

Investigation of Influence of Pore Fluid Salinity on Remoulded Clays

In 2000, a laboratory test program was set up at TUDelft to investigate the influence of pore fluid salinity on consolidation behaviour and undrained shear strength on artificially prepared remoulded clay samples. Two industrial dry clay powders were used:

- Colclay A90, mainly consisting of Na-Montmorillonite;
- Speswhite, mainly consisting of Kaolinite.

Three different salt types were used (NaCl, KCl and CaCl₂) and the pore fluid salinity was varied. Samples were prepared by dissolving the salts in distilled water and mixing the solutions with dry clay powder into a homogeneous slurry. Different tests were performed, using different types of equipment: atterberg limit tests according to BS1377:Part 2:1990, undrained shear strength tests using the fallcone method (ETC5; Eurocode 7) and one-dimensional consolidation tests, measuring consolidation rate, compressibility and salinity change with increasing pressure. Some results are shown in figures 2, 3 and 4.

The results of the tests showed that the influence of pore fluid salinity on the compressibility and undrained shear strength development of clayey soils depends on the plasticity (or actually the specific surface and cation exchange capacity), the moisture content and the salinity itself. Soils with a high plasticity (Colclay A90), with moisture contents above the plastic limit and with a salinity around or below the salinity of seawater are influenced by the pore fluid salinity. Soils with low plasticity (Speswhite), with moisture contents above the plastic limit or with very high pore fluid salinities are hardly influenced by changes in pore fluid salinity. An increase of the pore fluid salinity causes a decrease of the moisture content, decrease of the liquid limit (Figure 2), compressibility (Figure 4) and undrained shear strength (Figure 3). The undrained shear strength showed comparable results to the compression curves (Figure 3), which supports a correlation between undrained shear strength and effective stress. The undrained shear strength curves are concave and between liquid and plastic limit a bit lower than the suggested correlation (eq. 5), but they correspond with other correlations suggested by Skempton (1970) and Burland (1990). The results support the use of the iterative procedure (eq. 1, 2 and 3) and the use of correlations to describe a nor

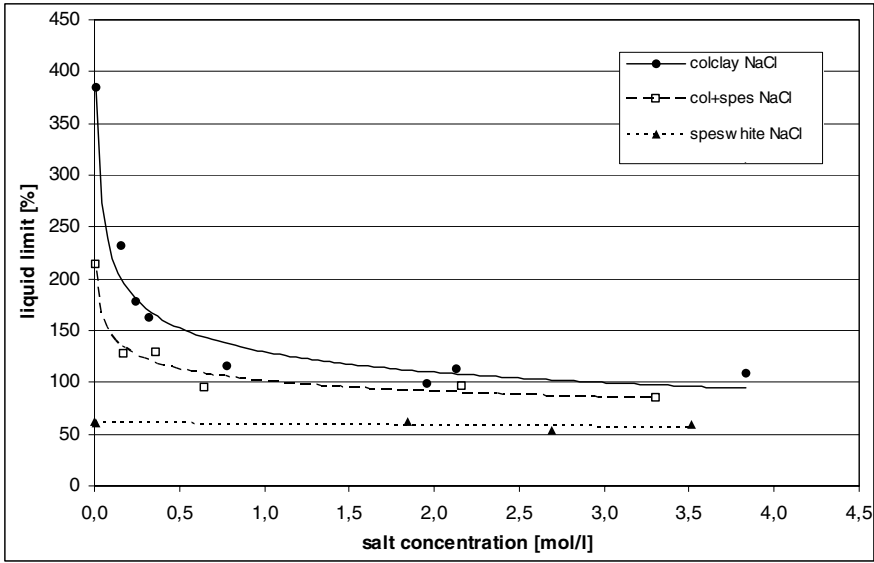


Fig. 2. Liquid limit versus pore fluid salinity for Colclay, Speswhite and a 50/50 mixture of Colclay and Speswhite and dissolved sodium chloride.

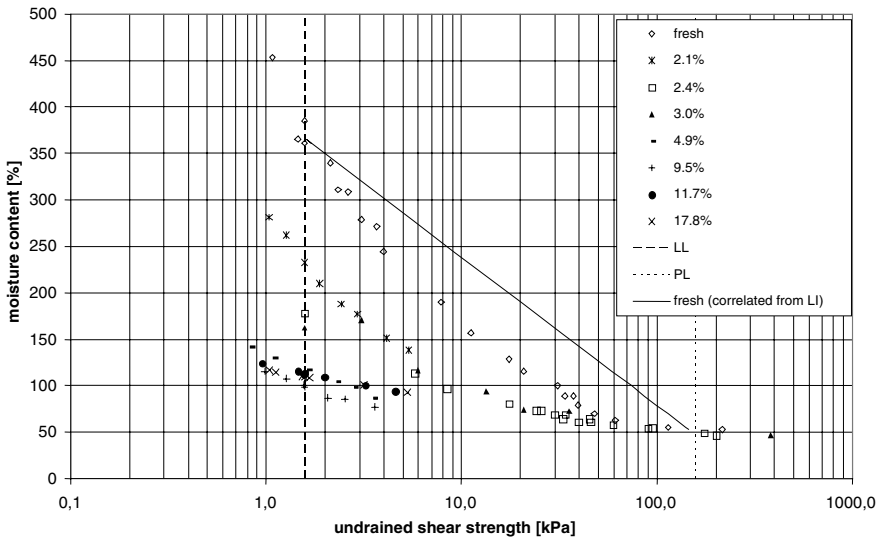


Fig. 3. Undrained shear strength versus moisture content for Colclay A90 with different sodium chloride solutions (with variable salt/solid ratio).

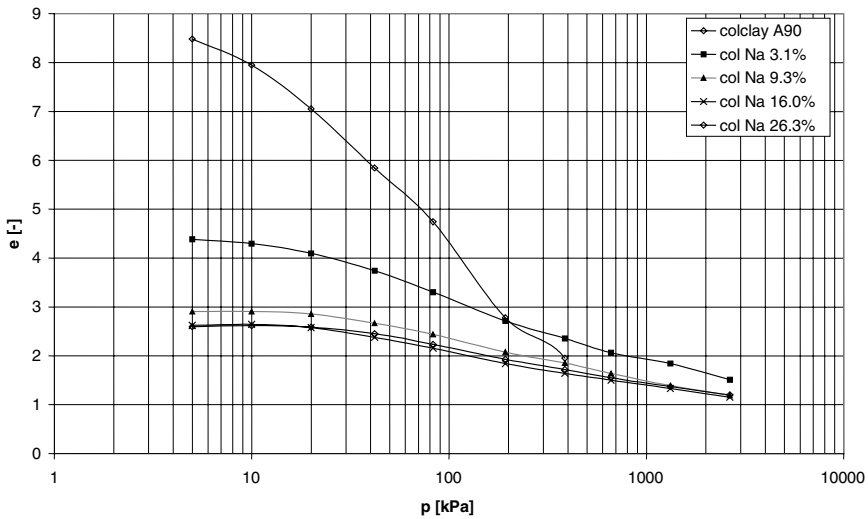


Fig. 4. Void ratio versus pressure for Colclay A90 with different sodium chloride solutions (with variable salt/solid ratio).

mally consolidated clayey soil. Secondly the influence of pore fluid salinity corresponds to the modified effective stress theory. Increase of pore fluid salinity causes a decrease of net repulsive forces, $(R-A)$, and a consequent increase of modified effective stress, resulting in a decrease of moisture content. Electrochemical forces become more important at higher moisture contents and for finer grained soils with high surface charge, like Colclay A90. However, these results do not explain the soil profiles observed in the Caspian Sea.

Discussion

It is apparent that remoulded high plasticity clays behave differently than the samples from the Caspian Sea. The remoulded clays showed a decrease of moisture content with increasing pore fluid salinity at a given confining pressure. In terms of liquidity index, undrained shear strength and stress development, the remoulded soils showed generally no distinct deviation from the normally consolidated condition if, regardless of salinity. Still the classical effective stress theory can be used to describe the soil behaviour. A change in salinity caused a decrease in moisture content, liquid limit, compressibility and undrained shear strength. These effects correspond to the modified effective stress theory. The undisturbed samples, however, showed no decrease of moisture content or liquid limit with increasing salinity. The soil profiles (Figure 1) did not correspond to the NCL, but suggested the soil was underconsolidated. Still the modified effective stress theory can be used to explain the observations in the Caspian Sea if the role of fabric, its' stability and disturbance or soil structure effects are considered. The role of soil structure is

acknowledged and discussed by many authors (Terzaghi and Peck, 1948; Bjerrum, 1967; Skempton, 1970; Mitchell, 1993; Burland, 1990; Pandian and Nagaraj, 1990; Barbour, 1990). SEM images of the high plasticity clays observed in the Caspian Sea show that even at 112 m depth an edge-to-face flocculated fabric exists between clay particles and aggregates of clay particles. This suggests these particles are deposited in an open fabric, which remains relatively stable during burial. Due to the stability of the fabric an increase in pore fluid salinity does not result in a significant decrease of the liquidity index (that is, it does not result in significant volume reduction due to compaction) with increasing overburden pressure. In addition the high void ratios cause a lower bulk unit weight and consequently the overburden pressure increases with a lower gradient than would be expected for a normally consolidated remoulded soil, resulting in even higher void ratios than already caused by the stable fabric. The high void ratio or liquidity index is consistent with the field observations by Fugro, and may suggest that the observed conditions are simply a result of the edge-to-face fabric of the natural Caspian Sea soils. However, the high undrained shear strength compared to the measured moisture content and the low pre-consolidation pressure are not yet explained. According to the modified effective stress theory, the increase of pore fluid salinity causes a decrease of the net repulsive stress between the clay particles and consequently an increase of the effective stress. This increase of effective stress does not cause a significant decrease of the moisture content as the volume reduction is restricted due to the stability of the fabric. However, due to the decrease in DDL-thickness the clay particles still want to compact. The decrease of repulsive stress works in fact as a negative pore pressure at particle level and as a result the effective stress at the particle contacts increases. If during sampling the overburden stress is removed and the sample disturbance is minimal, the soil sample still has an internal effective stress, due to the increased salinity. Consequently, the measured undrained shear strength may be higher than calculated from the measured liquidity index. This is consistent with the field observations by Fugro. The remoulded undrained shear strength shows also higher values than calculated. Probably remoulding the soil does not remove the internal effective stress completely at microscale, but only disturbs the clay-aggregates on macroscale. The scale of remoulding and shear can be studied, using microscopic techniques. The low pre-consolidation pressure can also be explained using the modified effective stress theory including the effects of sample disturbance in the test procedure. During sedimentation the total stress increases due to the weight of overlying sediment. The increase of salinity causes an extra increase of effective pressure, ($R-A$), at the particle and/or aggregate contacts. After sampling the overburden pressure on top of the sample is removed, however, the internal effective stress in the soil due to the salinity increase is still present. If the sample is undisturbed, the measured pre-consolidation pressure during reloading will be equal to the calculated effective overburden pressure. Although the true effective stress is not measured, the soil appears normally consolidated ($OCR = 1$) (figure 5a).

In both the laboratory tests and the tests on the undisturbed samples of Fugro, fresh water was used as surrounding fluid in the oedometer cell. Due to the concentration difference, leaching in the oedometer cell causes the ($R-A$) to increase,

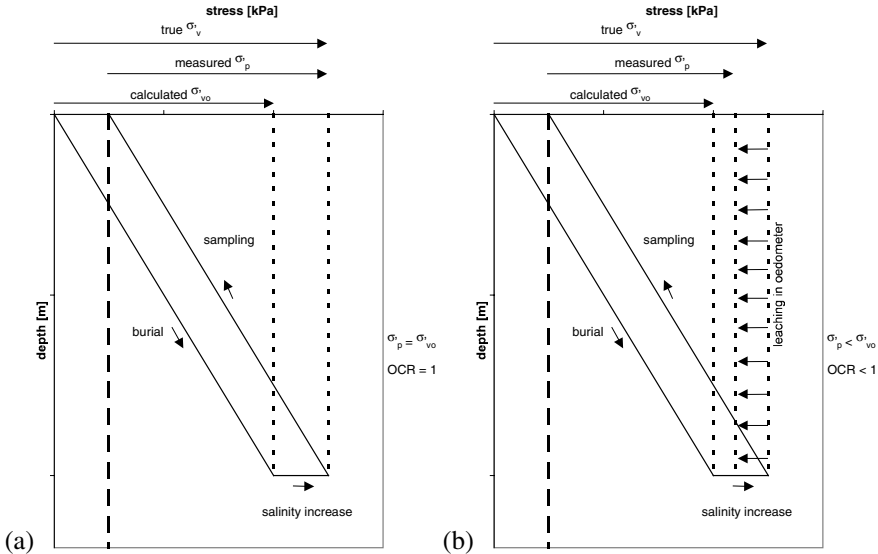


Fig. 5. Differences between measured, calculated and true pre-consolidation pressure for undisturbed (a) and disturbed (b) soil.

resulting in a decrease of the internal effective stress. Consequently the measured pre-consolidation pressure will be lower than the calculated effective overburden pressure, resulting in an *OCR* smaller than 1, and an apparent underconsolidated condition (figure 5b). To prove this hypothesis two original samples from the Caspian Sea, number 35 and number 37, from respectively 92 and 97 m depth, were reloaded with different fluid salinities in the oedometer cell. The initial void ratios were calculated from the measured in situ moisture content and were corrected for pore fluid salinity. Figure 6 shows the resulting compression curves.

The compression curves of both samples show that the measured pre-consolidation pressure is influenced by the permeant water salinity. It is clearly shown that with fresh water in the oedometer cell a lower pre-consolidation pressure is measured than with salt water. The pre-consolidation pressure is determined according to BS:1377:Part2:1990 and compared to the expected pre-consolidation pressure for a normally consolidated soil based on average effective unit weight and from the originally measured in situ moisture content. The results are presented in table 1.

When the oedometer tests were carried out with the same fluid salinity in the oedometer cell as in the sample, the measured pre-consolidation pressure approaches the present day overburden pressure, but is still lower than expected from the measured moisture content. To explain this the role of fabric stability and the disturbing effect of leaching in the oedometer cell is used. Pandian and Nagaraj (1990) indicate that a soil with a stable fabric shows little deformation or decrease of void ratio at the first part of the compression curve and can have an apparent pre-consolidation pressure, which is much higher than expected based on measured liquidity of the remoulded sample. The observed pre-consolidation pres-

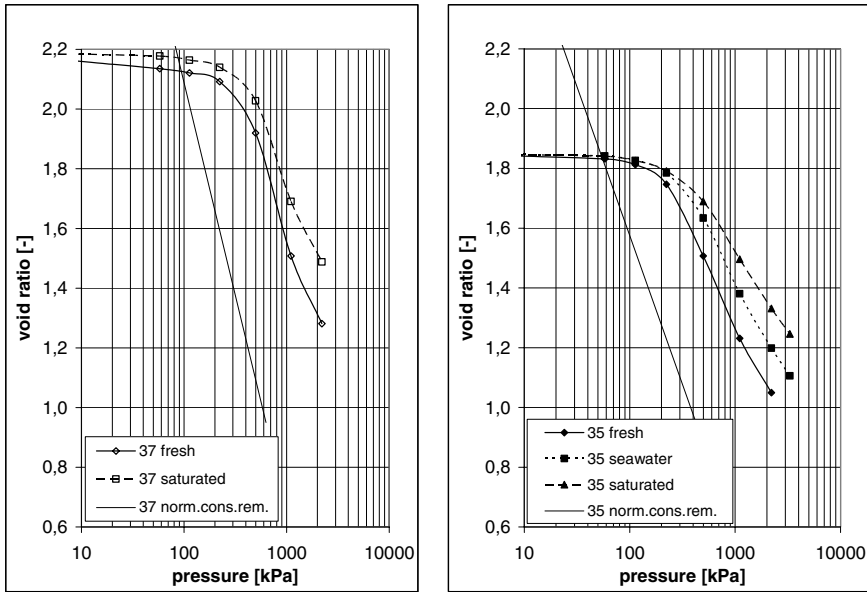


Fig. 6. Compression curves of clays from the Caspian Sea with different cell fluid salinity.

Table 1. Calculated overburden pressure for the Caspian Sea clay samples 35 and 37 for the normally consolidated remoulded condition and based on measured in situ moisture contents, compared to measured pre-consolidation pressures with different salinities of the permeant fluid in the oedometer cell.

		sample 37	sample 35
Calculated	normally consolidated remoulded clay	725	686
	from measured moisture content	525	507
Measured	fresh cell water	300	200
	seawater as cell water	-	370
	saturated cell water	400	400

pressure is in fact the yield-stress of the soil fabric. Above the yield stress the soil structure will gradually collapse and can even show a higher compressibility than expected. For example, if the sample depth was not known, the expected pre-consolidation stress of samples 35 and 37 would be approximately 80 kPa, based on the measured liquidity index and the correlations with compressibility and undrained shear strength (eq. 4 and 5), and thus far lower than the measured and real pre-consolidation pressures. This affirms that the measured apparent pre-consolidation pressures are in fact yield stresses of the soil fabric and that the

steep part of the compression curve is in fact gradual collapse of the fabric. This fabric collapse is accelerated due to sample disturbance, including leaching by a salinity difference between the sample and the oedometer cell.

Conclusions

Test results on remoulded clays proved that the pore fluid salinity does influence the compressibility and undrained shear strength of clayey soils. Soils with a high plasticity, with moisture contents above the plastic limit and with salinity around or below the salinity of seawater are influenced by the pore fluid salinity. Soils with low plasticity, with moisture contents above the plastic limit or with very high pore fluid salinities are hardly influenced by changes in pore fluid salinity.

An increase of the pore fluid salinity causes a decrease of the moisture content, decrease of the liquid limit, decrease of the compressibility. The results can be explained using the modified effective stress concept, which includes the repulsive and attractive electrochemical forces between clay particles. An increase of the pore fluid salinity, causes a decrease of the repulsive force and therefore an increase of the modified effective stress at particle level, concluding in a decrease of the moisture content, i.e. compression of the remoulded soil. For natural clayey soils the role of fabric and its stability has to be included to understand the compressive behaviour of the soil. A stable fabric can lead to higher moisture contents than expected for a normally consolidated soil. However, the increase of pore fluid salinity results in a higher undrained shear strength of the soil than expected from its liquidity index. Test results obtained in this research indicated that the value of pre-consolidation pressure measured in oedometer testing was significantly affected by the testing conditions. When testing structured marine soils the test conditions should be adapted to mirror actual conditions as closely as possible. In the case of thick clay deposits with elevated pore fluid salinity, it is thought that oedometer testing using a permeant with salinity closely resembling the pore fluid salinity will more closely predict in-situ consolidation of the deposit. The effect of construction practices on the performance of foundations in this type of soil were not investigated. It must be considered that the highly structured clays from the Caspian Sea site could be significantly altered by construction practices. For instance, installation of driven piles may disturb the edge-to-face structure in a zone around the piles, and the foundation performance could be affected accordingly. This issue requires further research.

Acknowledgements

The field results were made available by Fugro Engineers BV from an offshore geotechnical site investigation in the Caspian Sea. The laboratory tests were performed at the soil laboratories of the section Engineering Geology of the Department Applied Earth Sciences of Delft Technical University, supervised by ing. W. Verwaal and A. Mulder and of Fugro Engineers BV in Leidschendam, supervised by R.de Regt. Many individuals provided contributions throughout the course of

this research project, and we appreciate this opportunity to recognise their support: Peter Verhoef and Sytse Goedemoed for their guidance, constructive criticism and enthusiasm for my work, Marco Huisman, Thomas Keijzer and Victor Osipov for their interesting discussions and for providing useful articles, Reinier de Regt, Willem Verwaal, Arno Mulder, Theo Verkroost and Pascal Visser for assisting, performing and instructing the laboratory work.

References

- Barbour, S.L., (1990), The impact of sodium-chloride solutions on the geotechnical properties of clay soils, A review of clay-brine interactions, Minerals and Groundwater Program, Saskatchewan Research Council (unpublished).
- Bjerrum, L., (1967), "Engineering geology of Norwegian normally-consolidated marine clays as related to settlements of buildings", *Géotechnique*, 17, pp.81-118.
- Burland, J.B., (1990), "On the compressibility and shear strength of natural clays", *Géotechnique*, 40, No.3, pp.329-378.
- Carter, M. and Bentley, S.P., (1991), Correlations of soil properties, Pentech Press, London.
- Fugro Engineers BV, (1999), "Geotechnical parameters and analysis", Geotechnical report (Caspian Sea). (unpublished).
- Imai, G., Tsuruya, K. and Yano, K., (1978), "A treatment of salinity in water content determination of very soft clays", pp.84-89.
- Lambe, T.W. and Whitman, R.V., (1969), *Soil Mechanics*, John Wiley & Sons, New York.
- Mitchell, J.K., (1993), *Fundamentals of soil behaviour*, 2nd edition (1st ed., 1976), John Wiley & Sons, Inc., New York.
- Paassen, L.A. van, (2002), "The influence of pore fluid salinity on consolidation behaviour and undrained shear strength development of clayey soils", Memoirs of the Centre of Engineering Geology in the Netherlands, No. 216, MSc thesis at Faculty of Civil Engineering and Geosciences, Technical University Delft, ISSN 1386-5072.
- Pandian, N.S. and Nagaraj, T.S., (1990), "Critical reappraisal of colloidal activity of clays", *Journal of Geotechnical Engineering*, 116, No.2, pp.285-295.
- Skempton, A.W. and Northey, R.D., (1952), "The sensitivity of clays", *Géotechnique*, 3, No.1, pp.30-53.
- Skempton, A.W., (1970), "The consolidation of clays by gravitational compaction", *Quarterly journal of the geological society of London*, 125, Part 3, pp.373-411.
- Sridharan, A. and Prakash, K., (1999), "Influence of clay mineralogy and pore-medium chemistry on clay sediment formation", *Canadian Geotechnical Journal*, 36, pp.961-966.
- Sridharan, A. and Nagaraj, H.B., (2000), "Compressibility behaviour of remoulded, fine-grained soils and correlation with index properties", *Canadian Geotechnical Journal*, 37, pp.712-722.
- Terzaghi, K., Peck, R.B. (and Mesri, G.), (1948/1996), *Soil mechanics in Engineering practice*, 1st ed./3rd ed., John Wiley & Sons, Inc., New York.
- Wroth, C.P., (1979), "Correlations of some engineering properties of soils", BOSS'79, Second International Conference on Behaviour of Off-Shore Structures, Part 1, London, pp.121-132.
- Wroth, C.P. and Wood, D.M., (1978), "The correlation of index properties with some basic engineering properties of soils", *Canadian Geotechnical Journal*, 15, Vol.2, pp.121-132.
- Youssef, M.S., El Ramli, A.H. and El Demerey, M., (1965), "Relationships between Shear strength, Consolidation, Liquid Limit and plastic limit for remoulded clays", *Proceedings of the 6th International Conference on Soil Mechanics*, Part 1, Montreal, pp.126-129.

Hydraulic Monitoring of Low-Permeability Argillite at the Meuse/Haute Marne Underground Research Laboratory

Jacques Delay and Martin Cruchaudet

Agence Nationale pour la Gestion de Déchets Radioactifs (ANDRA), Laboratoire de Recherche Souterrain de Meuse/Haute-Marne, RD 960, F 55290 Bure, France
{jacques.delay,martin.cruchaudet}@andra.fr
Tel: +33 3 29 75 53 52; +33 3 29 75 67 52
Fax: +33 3 29 75 53 89

Abstract. ANDRA (Agence Nationale pour la Gestion de Déchets Radioactifs) has developed an electromagnetic permanent gauge (EPG) for long term monitoring of pore pressures in low permeability Callovo-Oxfordian argillites. The EPG is a pressure gauge that is permanently cemented into a borehole with no wire or tubing connections. The EPG transmits its data electromagnetically through the rock. Improvements in batteries have extended the life of the EPG to six years or more. Data from EPG installations in two holes near ANDRA's underground laboratory provide information on hydraulic conductivity and head. The heads in the argillites of the laboratory site are higher than heads in the two encasing carbonate units. These anomalous overpressures provide evidence for the very low permeability of the rock. Possible mechanisms for the overpressure include osmotic flows due to chemical potential gradients or delayed responses to the evolution of the regional groundwater hydrodynamics.

Keywords: pressure gauge, pore pressure, monitoring, anomalous pore pressure, argillite, hydraulic conductivity, hydraulic head, osmotic overpressure

1 Introduction

Argillite is a highly consolidated fine-grained sedimentary rock that has significant clay content. Argillite is an attractive candidate lithology for geologic disposal of radioactive waste due to its low hydraulic conductivity and its capacity for chemical retention of radionuclides. These low conductivity characteristics present challenges for developing hydrogeologic monitoring systems for rock characterization. This paper presents a new method for pore pressure monitoring that cements gauges permanently into the rock and monitors the pressures using electromagnetic transmissions, hence the name Electromagnetic Permanent Gauge, or EPG. In August 1999, the French government authorized ANDRA (Agence Nationale pour la Gestion de Déchets Radioactifs) to develop the Meuse/Haute-Marne Underground Research Laboratory (URL) approximately 300 km east of Paris (Figure 1 and Pigué, 2001). The site targets the Callovo-Oxfordian argillite a 130-m thick middle Jurassic stratum. The laboratory site was selected where the argillite would be between 400 to 600 meters below the surface and well away from known tectonic faults.

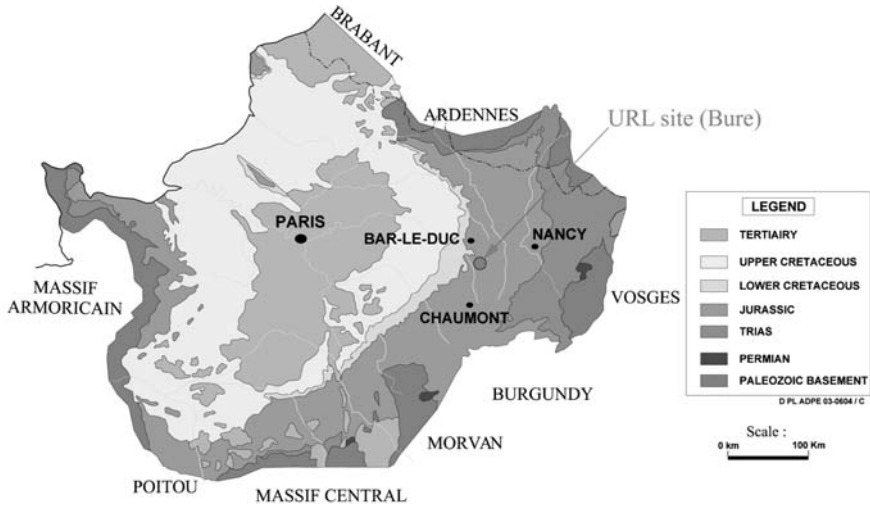


Fig. 1. Location of Meuse/Haute-Marne Underground Research Laboratory.

Figure 2 shows the site stratigraphy. Above the argillite are the Kimmeridgian marls and Oxfordian carbonates. The underlying formation is the Bajocian-Bathonian age Dogger carbonate.

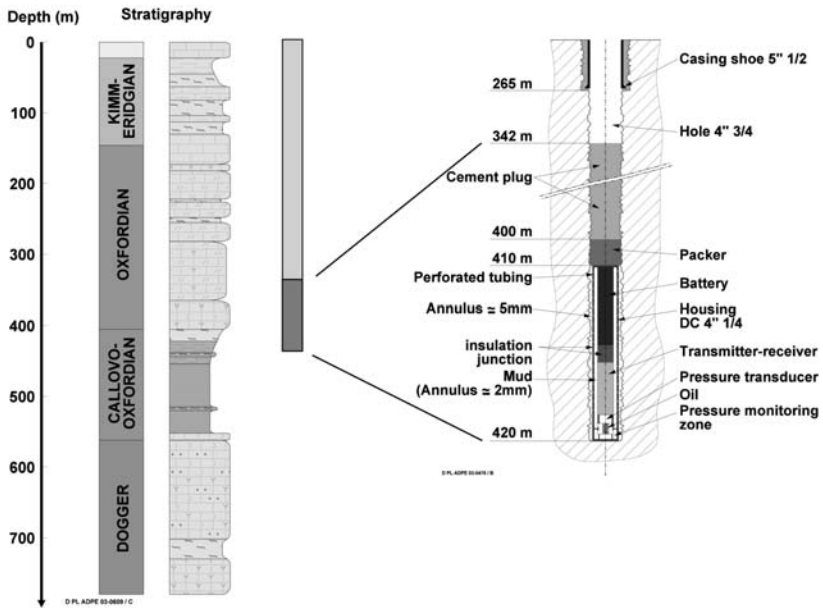


Fig. 2. Stratigraphy of the Meuse/Haute-Marne Underground Research Laboratory and EST 107 EPG installation.

2 Measurement of Pore Pressures and Hydraulic Properties in the Callovo-Oxfordian Argillite

Several deep exploratory boreholes were drilled at the Meuse/Haute-Marne site from 1994 to 1996. The borehole characterization program included packer tests in the Callovo-Oxfordian argillites, which gave information on hydraulic conductivity and initial pressures. Test durations were limited in part by concerns of borehole instability in the argillite. The hydraulic conductivities of eight packer tests averaged $2.2 \times 10^{-12} \text{ m s}^{-1}$. The well test analyses obtained estimates of initial hydraulic heads that exceeded those of the encasing units. Thick argillite units sometimes support unusual hydraulic heads that are significantly above or below those of the surrounding, more permeable rocks. These “anomalous” pore pressures are the result of coupled chemical, mechanical, or thermal processes. Alternatively, they may reflect long equilibration times, in the order of thousands to hundreds of thousands of years or more, to heads of the surrounding rocks. In any of these cases, anomalous pore pressures in argillites are a reflection of their low permeability at large scales (Neuzil 1995). Characterizing the anomalously high heads in the Callovo-Oxfordian argillite is therefore important for verifying the low permeability of the host rock. Packer tests may not meet this challenge. They typically have durations from a few hours to a few days, while stabilization of heads in argillites can require many months. Hence, the extrapolations of recovery using short-term tests to determine initial hydraulic head values are likely to have large uncertainties (Lavanchy et al., 1998, Croisé et al., 2000). These concerns led to a search for instrumentation that could support (1) longer duration recovery tests without concerns of borehole stability and (2) long-term monitoring of construction and other disturbances to the groundwater flow system.

3 Development of the Electromagnetic Permanent Gauge

To minimize well volumes and possibilities of leakage, ANDRA sought a technology for wireless data transmission and permanently cemented gauges. One data transmission technology, electromagnetic waves (DeGauque and Grudzinski, 1987; Soulier and Lemaitre, 1993), had been applied successfully in oil field settings but for shorter monitoring periods than ANDRA was seeking. The possibility of extending the monitoring life arose in 1994 with the introduction of longer-life batteries by SAFT, a French-based manufacturer of specialty batteries. ANDRA's contractor, Géoservices, was able to extend the expected gauge life to three years using the new battery sources and power-saving adaptations to the electronics. The resulting EPG tool in its full configuration is 9.66 m long. The pressure and temperature sensors, their electronics, the transmitter-receiver, and the batteries are housed in a 108-mm diameter stainless steel casing. Figure 2 shows a diagram of the gauge and its installation. The heart of the EPG is its Paroscientific quartz-crystal pressure gauge, which uses the crystal's pressure-dependent resonance properties as a basis for measurement. Such sensors are inherently stable over time and provide very high resolution (10^{-8} of full scale) thus allowing measurements

of very small pressure changes against a large background pressure. ANDRA's next concern was how to seal the sensor in the borehole. An initial review of cement products raised concerns of the cements being more transmissive than the rock. Dowell-Schlumberger was able to develop a borehole cement with a hydraulic conductivity of $7 \times 10^{-11} \text{ m s}^{-1}$ that met ANDRA's specifications. Finally, a cement-inflated packer was added from Baker Oil Tools to separate the sensor from the cement plug. A key feature of the EPG is the data acquisition by electromagnetic transmission through the rock. The transmitter-receiver system functions with two antennae using the casings of boreholes or stakes driven into ground at the surface. Different configurations will have different attenuation and signal-to-noise ratios. Testing of the antenna characteristics is important for setting the power of the signal. For a given quality of signal, a more efficient antenna configuration uses less battery power and prolongs the life of the gauge.

4 EPG Installations and Results

ANDRA has installed two EPG gauges, one in EST 107, a borehole about 3 kilometers from the laboratory site, and the second in EST 103, a borehole on the laboratory site. Both holes are drilled into the Callovo-Oxfordian argillite approximately 420 meters below the surface. The first EPG in EST 107 was installed in March, 1996. The gauge continued to transmit data for six years until April 2002. The EPG in EST 103 was installed in November, 2001, and it continues to transmit data as of November, 2003. The primary seal for the EPG is a low permeability cement plug, however, an additional cement filled packer provides a seal immediately above the gauge and isolates it from the cement (Figure 1). The EPG's in EST 107 and EST 103 lie at 83 meters and 24 meters below the top of the Callovo-Oxfordian respectively. The cement plugs in both holes extend from the packer a few meters upward into the Oxfordian. The chamber fluid volumes of the two holes are 29.2 and 49.6 liters for EST 107 and EST 103 respectively. Both installations use the casings of the installation well and a nearby well for antennae. The behaviours of the two installations are similar, hence a description of the EST 103 EPG's performance can be generalized to both installations. One difference between the two holes was installation of a multi-packer monitoring system above the EST 103 EPG to monitor hydrogeologic conditions in the overlying Oxfordian limestones (Delouvrier and Delay 2004). The monitoring intervals in the Oxfordian are water-conducting features and key stratigraphic horizons, such as the transition zone between the carbonate-rich Oxfordian limestones and the argillaceous Callovo-Oxfordian (designated C3a). The multi-packer system, developed by Westbay Instruments, complements the EPG by providing a profile of the head transitions from the carbonate rocks to the underlying argillite.

Since the EPG installation of November, 2001, daily measurements show the hydraulic head monotonically rising from about 300 mNGF to over 339 mNGF as of the end of May, 2003 (Figure 3). Conventional well test analysis methods can provide hydraulic properties and parameters for the Callovo-Oxfordian based on the pressure build-up. The analyses yielded the following parameters (given with

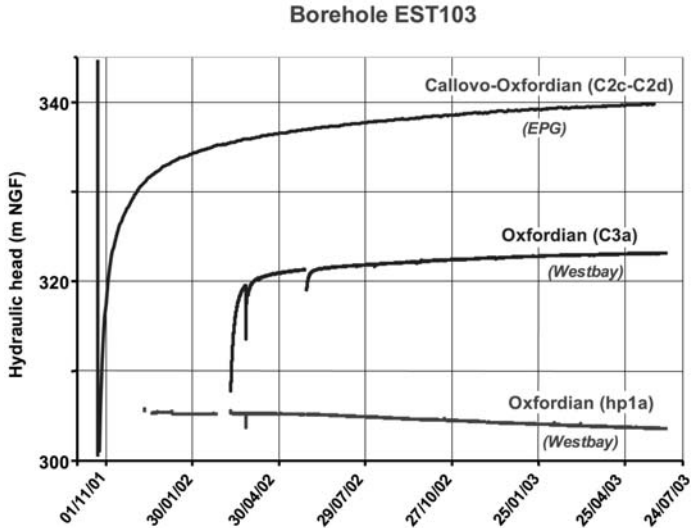


Fig. 3. Pressure data from EPG in EST 103 with responses from lower monitoring intervals of Westbay system.

confidence intervals): hydraulic conductivity of $2.1 \times 10^{-12} \text{ m s}^{-1}$ ($1.7 - 2.6 \times 10^{-12}$), specific storage of $1 \times 10^{-6} \text{ m}^{-1}$ ($1 \times 10^{-7} - 3 \times 10^{-6}$), and static head of 345.6 mNGF (343.7 – 347.1). Figure 3 also shows the hydraulic head history for the three lower intervals of the Westbay completions in the overlying Oxfordian. The C3a is a transitional unit between the Oxfordian carbonates and the Callovo-Oxfordian argillite extending 39 meters above the EPG. Hp1 is the deepest water-producing layer in the Oxfordian, at 124 m above the EPG. The head responses show that the C3a unit is a low permeability transition layer with similar build-up behaviour as the EPG, though with a lower hydraulic head. The Hp1 unit, on the other hand, shows an early stabilization at a head lower than the Callovo-Oxfordian at 305.3 mNGF followed by a drop to 303.7 mNGF in mid-June 2003. This drop may reflect effects of shaft sinking at the laboratory site.

5 Discussion and Conclusions

The results of the EPG monitoring show that permeability and hydraulic head characteristics can be successfully monitored and analyzed using data from permanently installed pressure gauges. The EPG overcomes the major drawbacks of conventional hydrogeologic tests in argillite, which are the short duration of the test and the difficulties of maintaining borehole stability. The EPG results confirm the anomalous pore pressure in the Callovo-Oxfordian argillite. At EST 107 the Callovo-Oxfordian support heads 27 meters higher than the overlying Oxfordian carbonates and 52 meters higher than the underlying Bathonian-Bajocian Dogger carbonates. Although a detailed discussion of the implications of these results is

beyond the space limitations of this paper, anomalous pore pressures in argillites are potentially indicators of large scale, low permeability properties (Neuzil 1995). Several possible mechanisms can create anomalous pore pressures, but a strong candidate is osmotic overpressures (Neuzil 2000, Gonçalves et al. 2004, Mitchell 1993) driven by chemical potentials arising from contrasting groundwater salinities in the Oxfordian (0.5 g L^{-1}), Callovo-Oxfordian (5 g L^{-1}), and Dogger ($4\text{-}5 \text{ g L}^{-1}$). Another possible source of the overpressure effect could be a long-lived delay in response of the heads in the Callovo-Oxfordian argillite to head changes in the encasing units (Gonçalves et al. 2004). Based on the encouraging results of EST 103 and EST 107, three additional EPG gauges are being installed to obtain a more complete head profile of the Callovo-Oxfordian at the laboratory site.

Acknowledgements

The authors gratefully acknowledge the contributions of Géoservices for the design of the EPG tool, Jean-Marc Lavanchy and Jean Croisé of Colenco for their analyses of the EPG build-up data, John Pickens of Intera for concept support, and Thomas Doe (Institut National Polytechnique de Lorraine and Golder Associates) for assistance with the manuscript preparation.

References

- Croisé J, Enachescu C, Frieg B, Lavanchy JM, Schwarz R, Schmid A, Wozniwicz J (2000) In-Situ Hydraulic Characterization of a Consolidated Clay Formation: Testing Approach, Results, Interpretation and Special Effects. Proc. of international conference on radioactive waste disposal, DisTec'2000, Sept. 4-10, 2000, Berlin.
- DeGauque P and Grudzinski R (1987) Propagation of electromagnetic waves along a drill-string of finite conductivity – SPE Drilling Engineering, 2:127-134.
- Delouvrier, J and Delay J (2004) Multi-level groundwater pressure monitoring at the Meuse/Haute-Marne Underground Research Laboratory. Proceedings EurEngeo, this volume.
- Gonçalves J, DeMarsily G, Violette S, Wendling J (2004) Analytical and numerical solutions for alternative overpressuring processes: applications to the Callovo-Oxfordian argillite in the Paris Basin, France, Journal of Geophysical Research, in press.
- Lavanchy JM, Croisé J, Tauzin E, Eilers G (1998) Hydraulic testing in low permeability formations. Test design, analysis procedure and tools. Application from site characterization programmes. Proc. of international conference on radioactive waste disposal, Sept 9-11., 1998, Hamburg.
- Mitchell JK (1993) Fundamentals of Soil Behavior, 2nd edition. Wiley Interscience, 437 p
- Neuzil C (1995) Abnormal pressures as hydrodynamic phenomena, American journal of sciences, 295:742-786.
- Neuzil C (2000) Osmotic generation of 'anomalous' fluid pressures in geological environments. Nature, 403:182-184.
- Piguet JP (2001) French Underground Research Laboratory – Construction and experimental programme. ICEM'01 – Brugge, Belgium, 2001.
- Soulier L and Lemaitre M (1993) E.M. MWD Data Transmission Status and Perspectives. Society of Petroleum Engineers Paper 25686 – SPE/IADC Drilling Conference, Amsterdam 23-25.

Hydrogeologic Exploration during Excavation of the Lötschberg Base Tunnel (AlpTransit Switzerland)

Marc Pesendorfer and Simon Loew

Engineering Geology, ETH Hoenggerberg, CH-8093 Zurich, Switzerland
{pesendorfer, loew}@erdw.ethz.ch
Phone: +41 16332742
Fax: +41 16331108

Abstract. Many tunnels that are currently being built through the Alps have to cross fractured and karstified formations at great depth and many hundreds of meters below the ground water table. The detection and characterization of permeable structures ahead of the advancing tunnel face is vital for these projects. We present new prediction and analysis methods and actual results from a deep Alpine tunnel in Switzerland, which has recently crossed 3.5 kilometers of karstified and fractured Limestones under an overburden of 1000 meters. The exploration programme in this part of the tunnel was unique and includes about 10'000 m of cored boreholes tested systematically with open hole and packer tests. From the high resolution transient pressure records of these experiments we derived not only standard formation properties but also diagnostic information including type, orientation and dimension of permeable structures. The subsequent tunnel excavation at these locations allowed to directly map the permeable structures and to evaluate the diagnostic model results.

Keywords: Lötschberg Base Tunnel, Karst, Fracture, Horizontal Borehole, Hydrogeology, Hydraulic Testing, Diagnostic Plot

1 Introduction

Karstification of limestones and dolomites can lead to various types of solution voids, among which many can lead to preferential pathways with very large hydraulic conductance. An underground excavation intersecting such structures in the saturated part of an aquifer can be confronted with extreme water inflows. Besides the karst structures water containing fractures and fracture networks with high hydraulic transmissivities can cause great problems during tunnel excavation especially if these fractures are hydraulically connected to karstified structures or deep Quarternary gravel infillings of valleys above the tunnel.

Many tunnels that are currently being built through the Alps have to cross such formations at great depth and many hundred meters below the regional ground water table. Therefore the detection and characterization of karstified zones, karst pipes and water-containing fractures ahead of the advancing tunnel face is vital for these projects. The determination of the spatial distribution of pressures, transmis-

sivities and storativities along the tunnel axes is of great practical interest especially in complex hydrogeologic situations.

The calculation and prediction of possible inflows into a tunnel excavated in hard fractured rocks is a difficult topic, mainly due to extreme spatial variability and range of hydraulic properties. Loew (2002) describes different conceptual and analytical models for tunnel inflows in homogeneous media. Raymer (2001) presents a prediction method which takes into account permeability distributions, measured from packer tests performed in exploration boreholes drilled from the ground surface during preliminary investigation phases.

For long and deep tunnels it might not be feasible to explore the detailed hydrogeological conditions from ground surface. In such a situation, drilling and testing from the advancing tunnel face (or adjacent caverns) is often more appropriate. However hydraulic testing in horizontal boreholes is not commonly used in underground excavations and the corresponding literature is very restricted.

On the other side horizontal well testing is very common in the petroleum industry. Interpretation methods have been developed by Kuchuck (1990), Kuchuck (1995) and others. Horne (2000) summarizes their papers in his book. Kaweck (2000) presented an interpretation method for hydraulic testing in horizontal boreholes which is based on theories developed in the petroleum industry.

In this paper, we present new hydrogeologic prediction and analysis methods and actual results from horizontal test boreholes of a deep alpine tunnel in Switzerland, the double tube Lötschberg Base Tunnel (LBT) of the Swiss AlpTransit project (Loew et al. 2000). This tunnel has recently crossed 3.5 kilometers of limestones (karstified and fractured) under an overburden of up to 1000 meters. The main focus of this paper is the description of the field testing conditions and data analysis methods of systematic hydraulic tests performed in nearly horizontal 250 m long exploration boreholes with a total length of about 10'000 meters drilled from the tunnel face during tunnel excavation.

2 Site

All hydraulic measurements were performed during excavation of the Lötschberg Base Tunnel (LBT). Figure 2.1 shows the location of the tunnel in connection with the European high velocity train network. A longitudinal geologic section is presented in Figure 2.2.

The LBT crosses from North to South the following tectonic units: The Helvetic Nappes consisting of sandstones and shists (northern part of the Helvetic Nappes), as well as limestones and marls (southern part of the Helvetic Nappes) and the Aar Massiv in the southern part of the tunnel consisting of granites, granodiorites, gneises and shists. In between the Helvetic Nappes and the Aar Massiv the short tectonic unit of the Autochthonous North consisting of sandstones, anhydrites and shists is located.

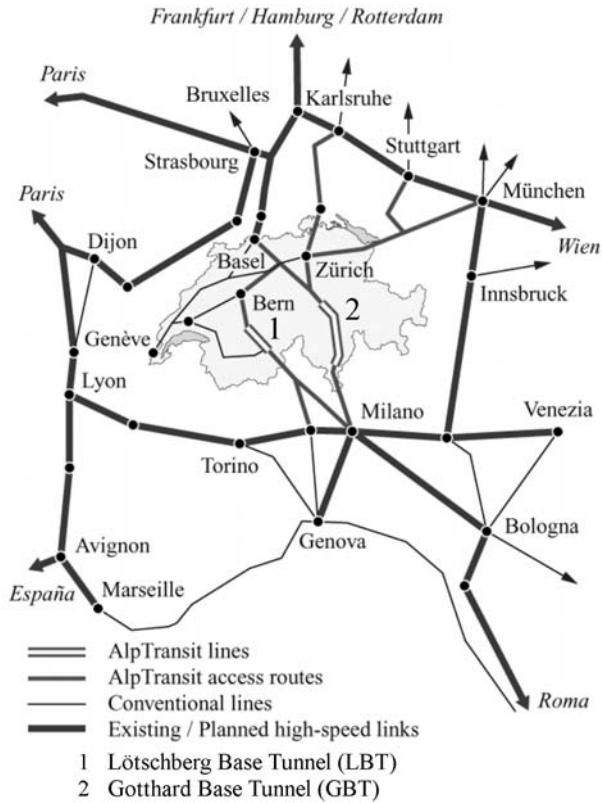


Fig. 2.1. Location of the Lötschberg Base Tunnel (LBT) with interconnection to the high velocity train network of Europe.

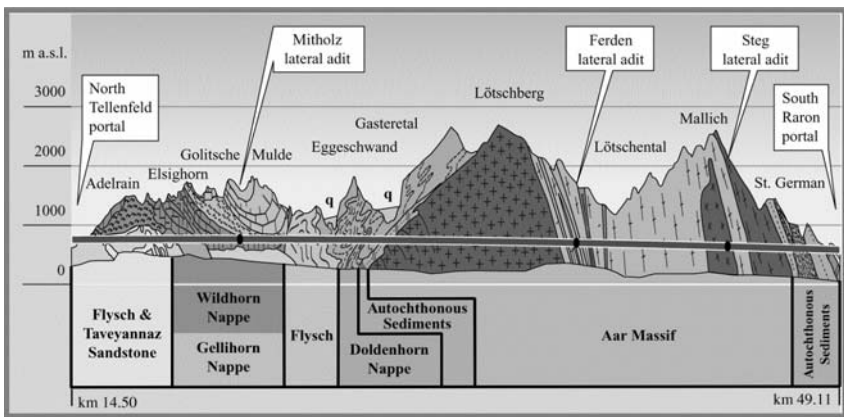


Fig. 2.2. Cross section of the Lötschberg Base Tunnel with main geological units.

The key zone for tunnel construction was the crossing of the limestones of the Doldenhorn Nappe with two deeply incised glacial valleys (Kandervalley and Gasteretal), filled with gravel. The ground water table is located several hundred meters above the elevation of the tunnel. A detailed profile (Figure 2.3) shows the limestones and marls of the Doldenhorn Nappe which occur over a length of about 3.5 km. These limestones and marls are heavily folded and truncated by several fault zones. Besides these faults and fractures the Limestones in the area burry a great risk of karststructures. In the Kandervalley so in the Gasteretal several large springs with a seasonal fluctuation in water flow can be identified in compact rock.

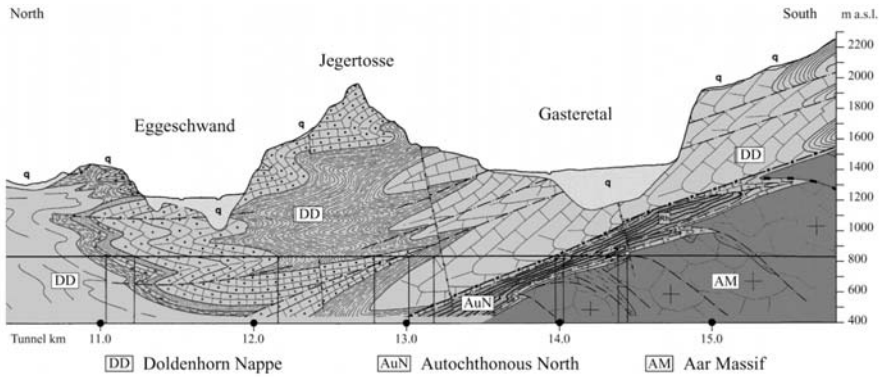


Fig. 2.3. Detailed cross - section through the Doldenhorn Nappe. In this area the risk of great water inflow into the tunnel was very high because of possible karst structures.

3 Exploration Programme

3.1 Exploration during Preliminary Investigation Phase

During the planning phase of the project several Karst scenarios including the maximum possible amount of water inflow into the tunnel have been evaluated. Especially the following items had to be answered before starting the tunnel excavation.

- Is there a possibility that water filled Karst cavities occur on the elevation of the base tunnel?
- What is the shape, orientation and opening of possible Karst structures on the elevation of the base tunnel?
- What is the maximum amount of water flowing into the tunnel from a Karst structure and what is the expected water pressure?

For answering these questions, detailed geochemical, hydrogeological and geological investigations were performed, including both field investigations and modeling. These models lead to the following “worst case” scenario: The tunnel

crosses a karst pipe in intact Limestones with an effective pipe diameter of approximately 1 meter. The inflow from such a system was calculated for a vertical pipe and a pipe with 30° inclination. With these models a maximum inflow of 8 m³/s resp. 5 m³/s into the tunnel was estimated.

3.2 Exploration during Excavation

Within the marl sections of the Doldenhorn Nappe exploration during tunnel driving consisted of 1 horizontal cored directional borehole per tunnel tube. The horizontal boreholes drilled from the tunnel face in direction of tunnel excavation were normally drilled to a length of approx. 300 meters. Water inflow into the borehole and the pressure were continuously monitored by the drilling crew. In potentially karstified limestone sections the exploration included at least two boreholes per tube including hydraulic open hole and packer tests as well as systematic borehole radar measurements. Most of the open hole hydrotests were performed as interference tests between two or more boreholes. Depending on the results of these first boreholes, drilling and testing was subsequently increased in zones showing indications for karstification and fracturing. Strongly karstified or fractured sections were tested with at least 4 nearly parallel cored boreholes before any decision regarding continuation of tunnel driving or injection was taken. During the entire exploration program in the Doldenhorn Nappe with a length of approx. 3.5 km, 41 cored and 10 destructive horizontal boreholes were drilled.

During core drilling normally only one, two or maximum three transmissive zones were intersected on a length of 300 m. The zone of water inflow into the borehole was not always clearly identifiable by the drilling crew. The transmissive zones could be grouped into three units:

- **Conductive Fracture Zones in Limestones:** 85 % of all conductive zones. These zones were not always clearly identifiable in the core.
- **Conductive Karstified Fractures in Limestones:** 10% of all conductive zones. These were clearly identifiable because of the alteration of the rock.
- **Sediment filled Karst Cavities in Limestones:** 5% of all conductive zones. These were clearly identifiable in the core because of sandy infills.

Transient open hole and packer based hydraulic tests were systematically performed in most of the horizontal exploration boreholes.

4 Testing Equipment and Methods

4.1 Testing Equipment

One of the objectives of the interference hydrotests was to gain transient pressure and flow data with high accuracy, a simple and robust equipment and within a short amount of time i.e. in a few hours in total. The main devices used for open

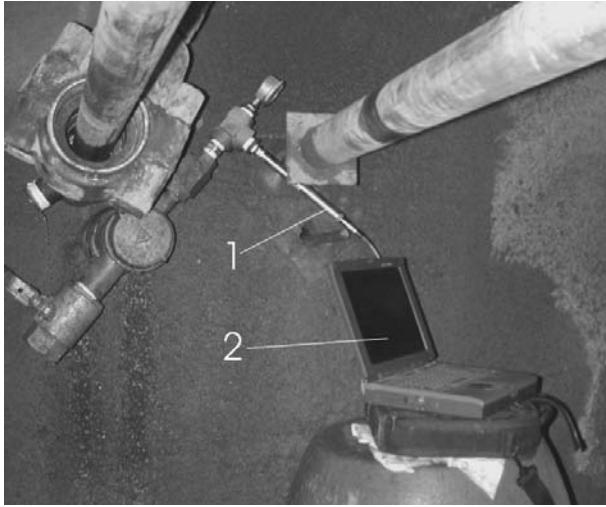


Fig. 4.1. Open hole testing equipment consisting of a piezoelectric pressure sensor with data logger (1) and a laptop (2).

hole tests consisted of a highly sensitive piezoelectric pressure sensor with data logger, a Laptop for reading out and controlling the pressure measurements, a calibrated tank and a stop watch for measuring the outflow (Fig. 4.1).

For packer tests a newly designed system that could be pumped through the drill string and that included downhole pressure and temperature sensors and a flow meter at the borehole head (Delouvrier and Buehler 2003) was used.

4.2 Methods

After completion of the boreholes with a length of approx. 250 to 300 meters, georadar reflection measurements for detecting cavities and fractures of bigger size were systematically accomplished in one of the boreholes. After a phase of pressure stabilization (all gate valves closed) which was allowed to last for about 1.5 hours, transient open hole tests were started, which mainly consisted of a constant rate outflow (pressure drawdown) phase followed by pressure recovery. All open hole tests were executed as interference tests (only one well is produced and pressure is observed in all the other closed boreholes). Such an interference test can be useful to characterize reservoir properties over a greater length scale than single well tests. After a drawdown phase of approx. 2 hours, the open gate valve was closed and the pressure recovery was monitored for a period of approx. 1 hour. Pressure were always recorded at intervals of 1 second. Open hole tests over the complete borehole length could only be performed systematically and successfully, because there was in most cases a limited number of discrete and closely spaced water containing zones. Otherwise packer tests for separating highly transmissive zones would have had to be used more often.

For the ongoing tunnel excavation, the hydrotests had to be analyzed within about 12 hours. Within this short period of time, so called “Quick Look Reports” resp. “QLR’s” were generated. For first order estimates of hydraulic properties it was assumed, that a confined, infinite extent, homogenous, and isotropic fracture (zone) of uniform thickness intersect the borehole at a large angle (radial flow). Jacob & Lohmann (1952) give the approximate solution for such a type of aquifer and test. Plotting the transient pressure data from the drawdown and recovery phases in suitable formats (e.g. semilogarithmic pressure drawdown vs. time) shows whether the model assumptions hold or not: For the aquifer type described above the log of drawdown vs. time leads to a straight line which is proportional to fracture transmissivity. As this was often not the case, most transmissivity values had to be treated as rough index properties only. For Quick Look Analyses the recovery curves were used to check the results from the drawdown phase. If the fracture in-between the active and passive boreholes could be treated as homogeneous, a storativity could also be estimated from simple straight line methods.

In a second phase of the data evaluation so called diagnostic plots were created for all hydrotests. A diagnostic (or derivative) plot consists of a simultaneous presentation of $\log(D_p)$ vs. $\log(Dt)$ and $\log(tD_p/Dt)$ vs. $\log(Dt)$. The advantage of a diagnostic resp. derivative plot is that it is able to display in a single graph many separate characteristics that would otherwise require different plots. In Figure 4.2 a idealized Diagnostic Plot is shown (after Horne, 2000).

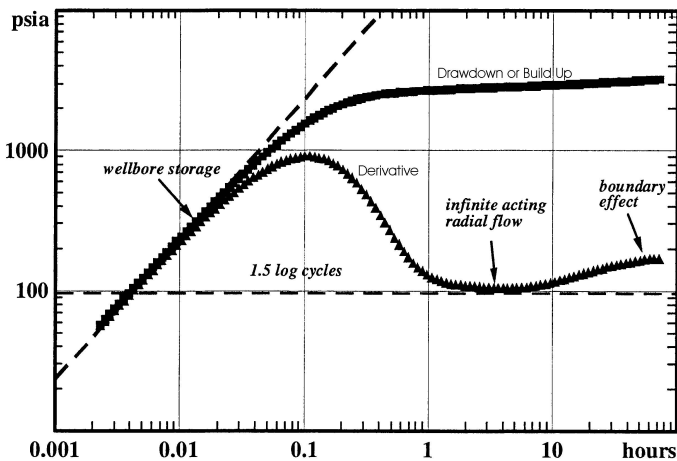


Fig. 4.2. Idealized diagnostic plot after Horne, 2000.

Several different flow periods can be identified on a diagnostic plot. This can for example include an early time borehole related response such as borehole storage or skin effects (caused by drilling), middle time responses such as Infinite Acting Radial Flow (IARF) and outer boundary effects.

5 Results

5.1 Comparison of Open Hole and Packer Test Results

At the beginning of the exploration programme it had to be demonstrated that the transient open hole tests are accurate enough to fulfill the expectations of the tunnel engineers, i.e. that open hole transient pressure tests performed over a length of approx. 250 m with one or two transmissive zones lead to the same results as if the transmissive intervals were packed off individually. Figure 5.1 shows a comparison between an open hole test and a packer test in the same borehole. It can be seen easily that the normalized drawdown curves (Drawdown [m] divided by Outflow [m^3/s]) have nearly the same slopes and therefore the same transmissivities. The difference between the both curves is probably based on the fact that the transient pressures are measured at different locations, and are influenced by pressure losses in the packer - drill - string - valve system.

We therefore can conclude that the transient open hole tests can be used to gain highly accurate data sets which absolutely can be compared with packer tests.

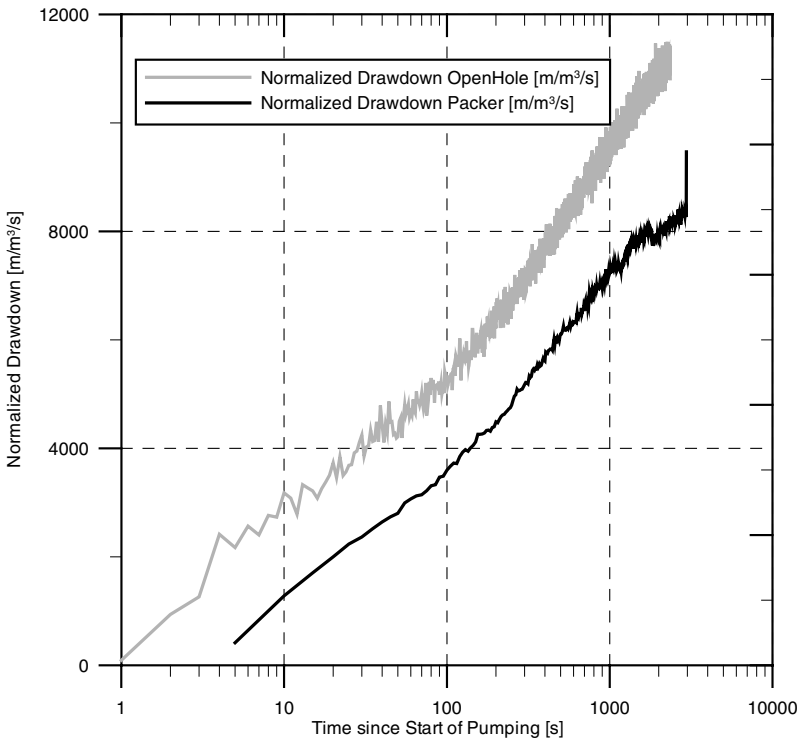


Fig. 5.1. Comparison between an open hole transient test and a packer test, both performed in borehole K12EB.

5.2 Results from Open Hole Transient Pressure Tests

The Quick Look Analysis results, consisting of first order transmissivity estimates, (quasi-static) formation fluid pressures, and indications of geometric properties of flowing structures were used successfully by the site engineers and geologists to decide about tunnel excavation schemes, supplementary explorations and injection procedures.

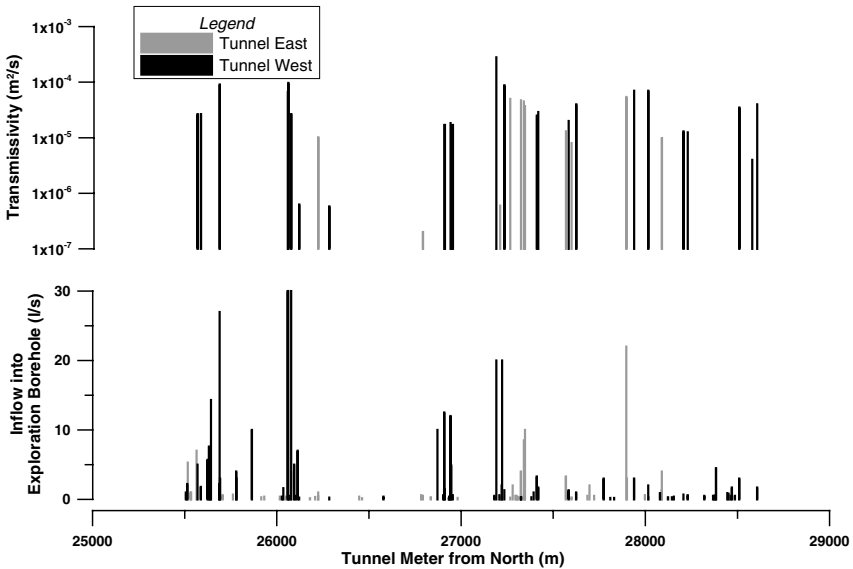


Fig. 5.2. Comparison between water inflow into the boreholes and transmissivity estimates.

Mainly due to these results and suitable geological conditions, the tunnel section was completed 6 months earlier than predicted, and only one karstified zone had to be grouted (an operation which required about 100 injection boreholes and 3 month of excavation stop).

Figure 5.2 shows initial transmissivity estimates (index properties) from open hole tests compared with measured water inflows into the exploration boreholes. It is clearly pointed out on this Figure, that low borehole inflows are not directly related to a low value of transmissivity. In Figure 5.3 a comparison between pressure head and measured water inflow into the borehole is plotted. From this plot it seems that pressure compartments are very common in the Doldenhorn Nappe. Comparing the pressure head with overburden topography it can be shown very clearly, that the pressure head at Tunnel elevation does not follow the overburden.

A systematic evaluation of all diagnostic plots shows several families of pressure responses with very characteristic patterns. Some of the tests follow simple classical flow models such as infinite acting radial flow (IARF) following well-bore storage without skin effects (Figure 5.4). On this type of pressure response, no late time boundary effect can be identified.

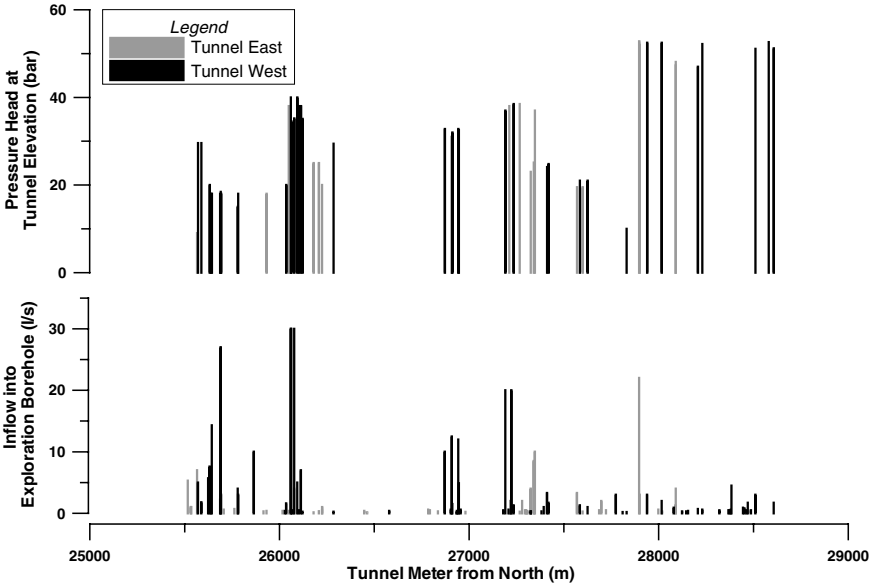


Fig. 5.3. Comparison between water inflow into the borehole and pressure head at the tunnel elevation.

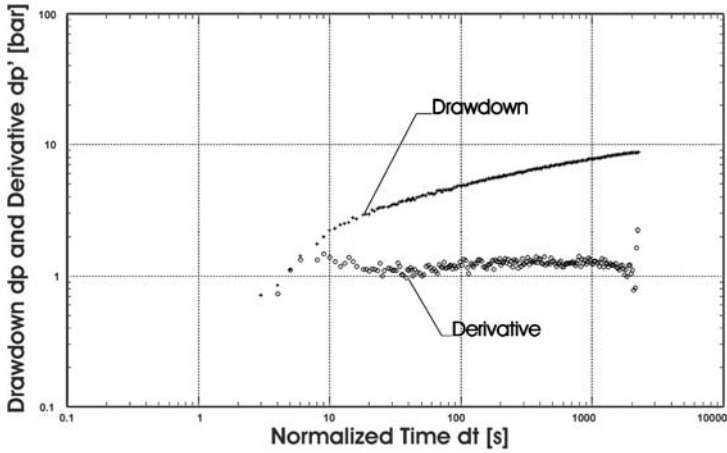


Fig. 5.4. Infinite Acting Radial Flow (IARF) indicated as a straight line on the derivative following borehole storage.

The pressure response seems to correspond to a steep and extended fracture or a fault zone that intersects the test borehole at a high angle.
 An example of a completely different aquifer response is shown on Figure 5.5. A 1/4 slope line on a log - log pressure plot, with the derivative showing the same

behavior. The separation factor between derivative and pressure plot is 4. From such a response one can conclude that the reservoir consists of a fracture of finite conductivity that intersects the test borehole along strike.

Many other tests show responses which can not easily be explained by such classical flow models. These “anomalous” responses are the focus of ongoing research investigations. In addition, the sites of all hydraulic tests (i.e. the locations of permeable features) are currently mapped in detail, in order to compare predicted flow models and tunnel inflows with reality.

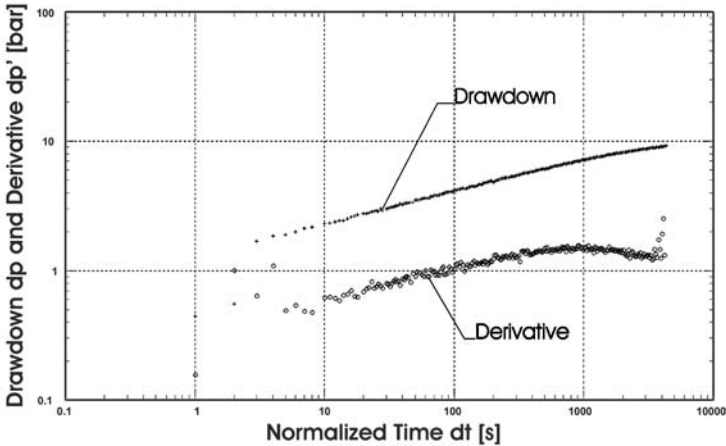


Fig. 5.5. Fracture flow indicated as 1/4 slope on the drawdown same on the derivative. Separation factor between the two lines is 4.

6 Summary and Conclusion

During tunnel excavation of the Löttschberg Base Tunnel, while passing through the Limestones of the Doldenhorn Nappe, we were able to gain unique hydrogeological data sets from a large number of hydrotests performed in horizontal exploration boreholes drilled through the tunnel face. The equipment used was simple and low cost but nevertheless lead to very high quality test data. As normally only one, two or maximum three closely spaced and discrete transmissive zones were intersected by a boreholes of approx. 300 m length, open hole pressure tests could be successfully performed in most of the drilled boreholes. For characterizing individual transmissive or complex zones, packer tests were used.

Single and crosshole pressure responses gave very valuable indications for local and far field hydraulic transmissivity, lateral extension and connectivity of permeable features, pressure head and drainable water volumes. Preliminary analyses indicate the existence of several wide pressure compartments along the length of the tested tunnel section. Further research needs to address the fact that measured pressure heads are substantially lower than the overburden. Flow in the

Doldenhorn Limestones is mostly controlled by fracture flow. The fracture orientations and their conductances can clearly be derived from diagnostic plots. Many tests exhibit anomalous behavior that can not be explained with classical flow models.

Acknowledgements

We would like to thank BLS AlpTransit AG for their support during excavation of the Doldenhorn Nappe. A special thanks goes to the geologists of the Lötschberg Base Tunnel project (H.J. Ziegler, R. Haenni, M. Lengacher and P. Zwahlen) and to Peter Hufschmied (Project Engineer). We also would like to thank Keller Druckmesstechnik AG, Winterthur (M. Gautschi and B. Vetterli) for supporting us with highly sensitive pressure sensors, N Morrisette (S. Brisson) for drilling long horizontal borholes in a very effective and precise way and Solexperts AG, Schwerzenbach (Ch. Bühler and M. Kech) for performing the packer tests.

References

- Delouvrier, J., Buehler, Ch., 2003: Using adapted testing tools and testing program to estimate water drainage from tunnels under construction and tunnels in service. Proceedings of Groundwater in Fractured Rocks, an international IAH conference in Prague. Editors: Krasny, J., Hrkal, Z., Bruthans J.
- Horne, R.N., 2000: Modern Well Test Analysis. A Computer - Aided Approach. Second Edition. Petroway Inc. ISBN 0-9626992-1-7.
- Jacob, C.E., Lohman, S.W., 1952: Nonsteady Flow to a Well of constant Drawdown in an extensive Aquifer. Transactions, American Geophysical Union. Volume 33, Number 4.
- Kawecki, M.W., 2000: Transient Flow to a Horizontal Water Well. Groundwater, Vol. 38. No.6, pp. 842 – 850.
- Kuchuk, F.J., 1995: Well Testing and Interpretation for Horizontal Wells. Journal of Petroleum Technology, January edition, pp. 36 – 41.
- Kuchuk, F.J., Goode, P.A., Brice, B.W., Sherrard, D.W., Thambynayagam, M., 1990: Pressure Transient Analysis for Horizontal Wells. Journal of Petroleum Technology, August edition pp. 974 – 984.
- Loew, S. 2000: AlpTransit: Engineering geology of the world's longest tunnel system. Proceedings of GeoEng2000, an international conference on geotechnical and geological engineering. Melbourne, Technomic Publishing Co.
- Loew, S. 2002: Groundwater hydraulics and environmental impacts of tunnels in crystalline rocks. Proceedings of the 9th Congress of the International Association for Engineering Geology and the Environment, Durban. In: van Roy & Jermy (eds): Engineering geology for developing countries.
- Raymer, J.H., 2001: Groundwater Inflow into Hard-Rock Tunnels. Proceedings of the Rapid Excavation and Tunneling Conference, 2001.

Coring Performance to Characterise the Geology in the “Cran aux Iguanodons” of Bernissart (Belgium)

Jean-Pierre Tshibangu, Fabrice Dagrain, Hughes Legrain, and Benoît Deschamps

Mining Engineering Department, Faculté Polytechnique de Mons (FPMs)
Rue du Joncquois 53, B-7000 Mons - Belgium
{jean-pierre.tshibangu, fabrice.dagrain, benoit.deschamps, hughes.legrain}@fpms.ac.be
Tel: + 32 65 37 45 18
Fax: + 32 65 37 45 20

Abstract. The “Cran aux iguanodons” of Bernissart is a sinkhole (or chimney caving) with a valuable paleontological deposit due to the exceptional quantity and diversity of fossils found during the excavation conducted from 1878 to 1881. In fact, bones have been discovered in a clayey geological formation when digging à mine gallery at the –322 m level. A subsequent extraction gave an overall production of 29 iguanodon’s skeletons. Referring to the available data at the Natural Sciences Museum of Brussels where the found skeletons are exhibited, one does not know the degree of depletion of the deposit after the extraction. A feasibility study (Tshibangu and Dagrain 1998) showed then the need to drill 4 exploration wells of 400 m depth with different objectives: to evaluate the chance of finding more fossils, understanding how and when the geological formations moved down, and testing a seismic geophysical technique for ground imaging. The typical geological formations concerned are: chalk, limestone, conglomerate, clays, and layers of silex nodules. In October 2002 the workings started with a completely cored well (the Number 3) using the PQ wire-line technique. During operations, different parameters have been recorded: rate of penetration, core recovery and a brief core description. Some problems have been encountered when crossing silex stones contained in a clayey matrix; and this paper gives some interpretations in terms of the relationship between the lithology and the drilling performances.

Keywords: wire-line core drilling, conglomerates, drillability, core recovery and quality.

1 Presentation of the Site

Collecting and treating of old mining documents of the former Bernissart Colliery and actual topographical data allowed a 3D-reconstitution of the studied site as presented in figure 1.1 (Tshibangu and Dagrain 2001). Geological informations were available in the mined out areas, but the knowledge of the sinkhole and the region above was very poor.

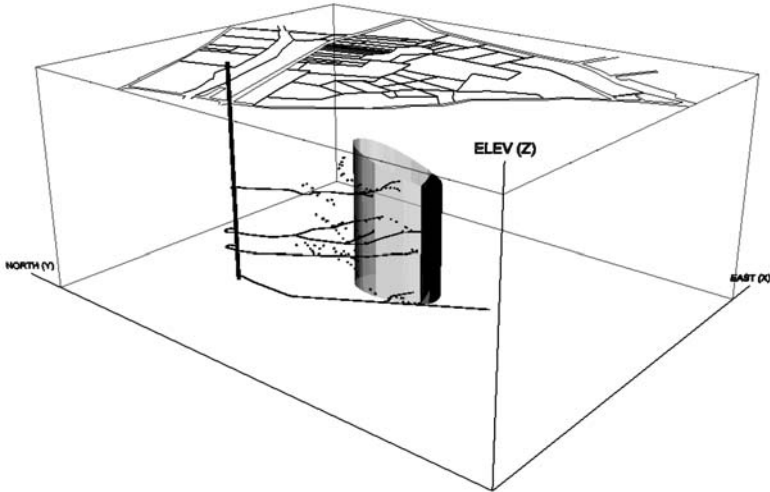


Fig. 1.1. 3D model of the Bernissart sinkhole including the cadastral plan and the mining infrastructure.

2 Drilling and Monitoring Operations

The wire-line coring technique was adopted, with a 3.10 meters long barrel. The PQ coring diameter (core 85 mm, hole 122 mm) has been chosen to maximise the chance of bones recovery and allow later geophysical operations. In the wealdian clays, the PQ3 barrel was used to enable an easy recovery of soft and swelling materials. The main operations proceeded as follows: drilling down to 33 m and installation of a PW casing to stabilise superficial geological formations; PQ coring down to 265 m; and finally PQ3 coring from 265 to 345 m. At the end of the coring operations, on the basis of a caliper log which did not show excessive collapse of the drillhole, a plastic casing (PVC type) has been placed.

Three types of coring bits were used: one surface set, some impregnated, and a surface set with polycrystalline thermostable cutters (TSD). The description is as follows:

- Bit Nr 1: DATC surface set bit, with round profile R, and nuance 35 (diamond of +/- 1,50 mm). Nuance 35 is planned for rocks with strength from 100 to 150 MPa.
- Bit Nr 2: Boart Longyear impregnated bit, with flat profile F, and nuance 6. It is suitable for very hard and fractured rocks and requires a high rotating speed.
- Bits Nr 3 and 4: DATC Impregnated bits, with conical profile T, and nuance 4. The conical profile is recommended in heterogeneous formations like conglomerates, chalks with silex, phosphates with flint, gravels...
- Bits Nr 5 and 6: DATC Impregnated bits, with conical profile T, and nuance 2.
- Bit Nr 7: DATC impregnated bit, with conical profile T, and nuance 4.
- Bit Nr 8: DATC TSD Bit, with cubical profile R.

The drilling rig was a GSB60 hydraulic type powered by a diesel engine of 227 kw at 2200 rpm. The mechanical characteristics are: a pulling capacity of 60 tons, a mast height of 13 m, and an overall weight of 34 tons. The drilling fluid was a mix of water and two polymers: Lubtub to avoid clay swelling, and polycol to stabilise the hole. The technical parameters were chosen as follows: the rotating speed ranged between 200 and 700 rpm, the Weight on Bit between 500 and 3000 kg, and the mud flow between 50 and 100 l/min. Unfortunately, the drilling rig was not equipped for a real time recording of these parameters.

Under the supervision of the Mining Engineering Department of FPMs a continuous monitoring has been achieved to describe the cores and record technical parameters: rotating speed, weight on bit (WOB), Rate of penetration (ROP), reached depth, time of the runs, drill string pulling out, bit changing, bit descent, and the standby time. The treatment of the collected data yielded results (Dagrain and Deschamps 2003) among which the curves of figure 2.1 are drawn.

3 Geological Description and Mechanical Characterisation

From the geological description that gave the lithology of figure 2.1D (Yans et al. 2003), the encountered formations are summarised hereafter with some comments drawn from mechanical tests performed in the laboratory:

- 0 to 8 m (L1): shallow ground
- 8 to 27.5 m (L2): white chalk.
- to 33.6 m (L3): white chalk with centimetric black flints.
- to 43.5 m (L4): gray chalks with siliceous nodules. Uniaxial compressive strength (UCS) varies from 14 (chalk) to 90 MPa (nodules). Nodules also show a high abrasiveness.
- to 56 m (L5): clayey chalk. UCS is about 10 MPa.
- to 75 m (L6): alternation of clay and marl. UCS varies from 2 (clayey marls and clay) to 20 (calcareous marls). The abrasiveness is very low.
- to 103 m (L7): glauconeous limestone with some layers of rollers and flints. UCS varies from 30 (limestone) to 180 MPa (flints). The abrasiveness is very low, except for flints.
- to 134.5 (L8): alternating conglomerate and sandy limestone. Conglomerates contain centimetric and sometimes pluri-decimetric rollers with a calcareous cement. UCS varies from 50 (glauconeous limestone) to 120 MPa (rollers). The abrasiveness is very low, except for some rare flints. Some conglomerates have a hard cement with weak rollers, while others are constituted with very hard flints in a soft matrix.
- to 165 (L9): glauconian limestone with UCS from less than 1 to 80 MPa. The abrasiveness is very low.
- to 170.7 m (L10): alternation of thin layers of calcareous sandstones and conglomerates with calcareous and clayey matrix. The matrix is often very weak to be tested and the roller are hard. The UCS is about 80 MPa.

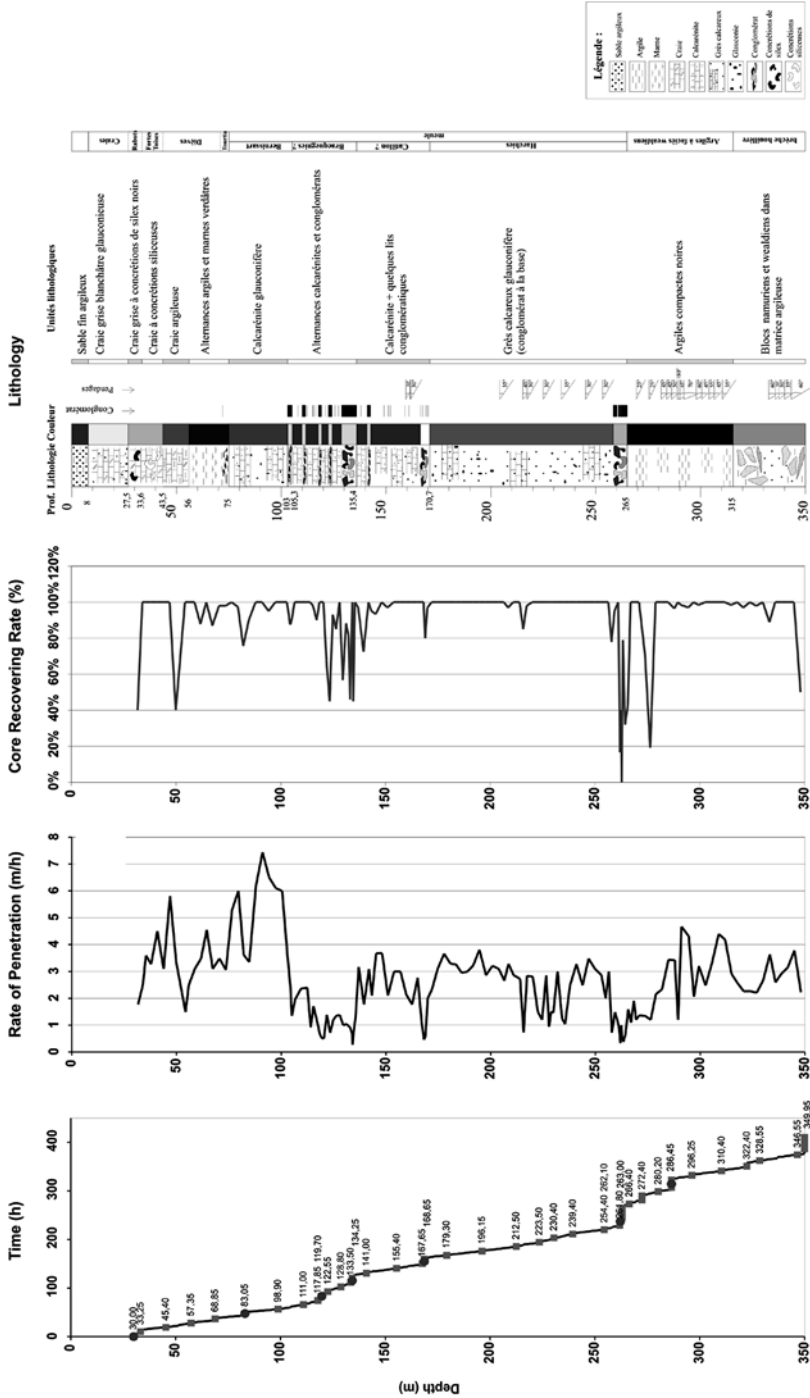


Fig. 2.1. Logs of measured parameters and lithology for the well BER3. A: Drilling time. B: Rate of penetration C: Core recovery. D: Lithology.

- to 260 m (L11): argillo-calcareous sandstone (UCS 4 MPa) and limestone (UCS 40 MPa).
- to 265 m (L12): conglomerate with centimetric rollers and an argillo-calcareous matrix.
- to 315 m (L13): homogeneous black hardened clay. UCS is 20 MPa.
- to 350 m (L14): Namurian rocks with a UCS of 15 MPa and low abrasiveness.

4 Results in Terms of Performances Achieved

4.1 Rate of Penetration (ROP)

This parameter has been measured on field by marking the drilling pipes and then recording the vertical displacement of the marks; figure 2.1B shows the ROP log. It is usual that when the drilling bit is wearing out, the ROP decreases with respect to the size of cutting elements. But, there is no such obvious result on figure 2.1B. This is a typical behaviour of impregnated bits thanks to the numerous layers of small diamonds contained. So, making a decision to change the bit will depend on the complete wear or some other problems as breakage. Table 4.1 presents the overall results obtained, showing the mean values of ROP with respect to the lithology or a particular bit.

According to the lithology, it can be seen that the poorest performance of 0.67 m/h has been achieved in the L12 formation (conglomerate with centimetric siliceous stones in a soft clayey matrix). A bit better results have been obtained in L3 (chalk with silex stones), L8 (alternating conglomerate and sandy limestone) and L10 (alternation of thin layers of calcareous sandstone and conglomerates with calcareous and clayey matrix). This set of rocks exhibit hardened stones contained in a soft clay or chalk cement, and the difference in the UCS of the components is high. Conversely, the highest performance of 5.33 m/h has been registered in L7 which is a sandy limestone with some layers of stones. The matrix material is stronger (UCS is 30 MPa) than for the previous formations and the abrasiveness of the stones is not so high. Other rock formations exhibit mean performance as the overall ROP is 2.42 m/h. According to the bits used, the bit 2 ran from 30 to 83 m gives the highest performance with an average ROP of 3.14 m/h. The drilled formations are mainly carbonates (chalks and limestone) containing clay or some nodules with low UCS. The bit 3 also shows a comparable performance but this is due to the very good results achieved in the lower part of L7 (5.52 m/h). The poorest results are given by the bit 4 which drilled in L8 (alternating conglomerate and sandy limestone), and bit 7 in L12 (conglomerate) and L13 (clay). The bad result obtained in this last formation could be due mainly to the non-suitability of impregnated bit for clay rocks (balling phenomenon because of the poor bit cleaning), but also the wear in L12. Using a more convenient bit 8 gave a quite high ROP in the clay (3.4 m/h).

Table 4.1. Relationship between the drill bit, the lithology and the coring performance.

Bit				Lithology			Averaged ROP			Averaged recovery
Bit number	Initial depth (m)	Final depth (m)	Metrage (m)	Lithology	Initial depth (m)	Final depth (m)	by bit & lithology (m/h)	by bit (m/h)	by lithology (m/h)	by lithology (%)
1	24.00	30.00	6.00	L1	0	8	-	-	-	-
				L2	8	27.5	-		-	
				L3	27.5	33.6	-		1.77	57
2	30.00	83.05	53.05	L4	33.6	43.5	3.50	3.14	3.50	100
				L5	43.5	56	2.72		2.72	69
				L6	56	75	3.22		3.22	96
				L7	75	103	4.93		5.33	96
				L8	103	134.5	1.95		1.20	88
3	83.05	117.85	34.80	L9	134.5	165	2.30	3.00	2.30	90
4	117.85	134.50	16.65	L10	165	170.7	1.12	1.89	1.09	97
5	134.50	168.65	34.15	L11	170.7	260	2.42	2.28	2.42	99
				L12	260	265	0.92		0.67	56
				L13	265	315	0.58		2.37	93
6	168.65	262.10	93.45	L14	315	350	1.69	1.38	2.37	93
				L14	315	350	3.40		2.42	93

4.2 Bits Metrage

The bit metrage is defined as the total length ran for a given bit with an acceptable ROP (i.e. economic) and this is a good measurement of the efficiency of a drilling process. When drilling in hard and abrasive rocks, impregnated bits have the ability of giving high metrages (usually some hundred meters). But in this project, the best result is given by the bit 6 with 93 m, while the poorest is that of bit 4 with only 17 m. For the surface set bit 1 the decision to change has been taken because it was not suitable for hardened material (especially silex). Figure 4.1 is a zoom of a part of the well ranging from 30 m down to 122m. On this interval three bits have been used, and comments in boxes give a detailed description of what happened during operations to explain the poor result achieved. In fact, most of the

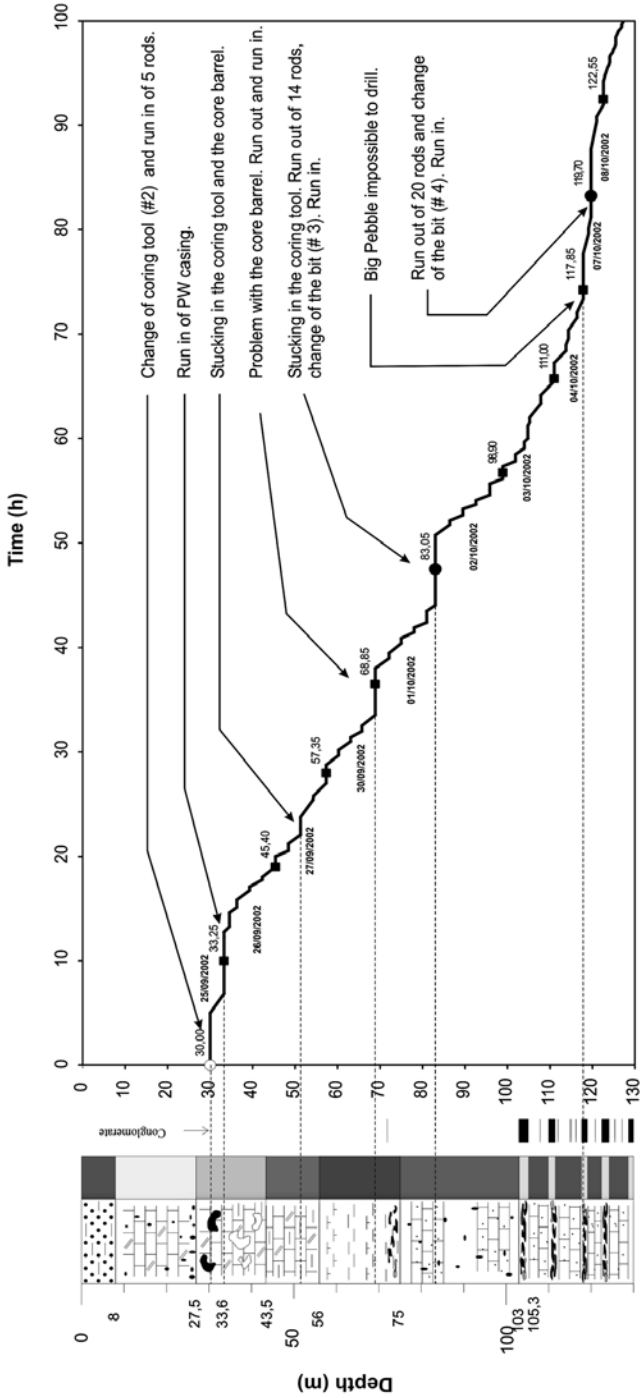


Fig. 4.1. An Example of the relationship between the performance and the drilling incidents.

bits have been changed not only for the wearing out but mainly because of damages caused by stones blocked in the core barrel. These free stones were detached from the original rocks by the core wash out which removed the soft materials. The small stones tend to enter directly in the core barrel, rotate inside and then damage the bit and barrel, while the biggest were cut partly or completely before detaching. A good choice in the drilling fluid and flow rate could help solve this problem, and this needs an accurate control of the pumping.

4.3 Cores Recovery

Figure 2.1C shows a sketch of the percentage of core recovery versus depth. Table 4.1 also gives the average recovery per geological formation. The overall result seems good with values generally greater than 80%, but in the conglomerates it is poor, this is a confirmation of the results on performance. In such difficult materials, the recovery felt to values as low as 20 % for certain passes. Figure 4.2 shows how the core looks like when crossing conglomerates with a soft cement, this is just a gravel because of the core wash out. The recovery in the wealdian clay is not very bad but exhibits more variability than in other formations, the overall result is 93%. As the clays materials are very important for the project, such cores have been enveloped in a thin aluminium sheet to keep the moisture. When reaching the depth of about 300 m, one of the main objective has been achieved by crossing some bones which, after appropriate studies revealed that the materials are from dinosaurs.



Fig. 4.2. An example of the core recovered in a conglomerate with a soft cement.

5 Geological Interpretation

To not spend too much money, this project has been designed so that just one well had to be completely cored. The two or three others will be destructive down to the top of the wealdian clays before coring in this formations. Monitoring the destructive drilling operations is more difficult than for coring (cuttings are collected in place of cores) and the challenge was to guess at which moment or depth the drilling bit will hit the clay materials. As this is not so obvious, an attempt can be made to try to correlate some drilling parameters and the geology. In fact, as stated earlier, typical layers containing hard pebbles in soft cement gave poor results, with values amounting less than 50% of the mean ROP. In the destructive drilling with roller cones bits, the ROP is higher than in coring. But, when analysing the performance of a destructive drilling, the variation of the result could give

an indication of the depth at which the conglomerates are found. Such comparisons, together with geophysical logging, will be used in the future to try building a 3D model of the sinkhole.

6 Conclusion

This paper presents the working methods and general results obtained when drilling a completely cored well in the Bernissart sinkhole. Abnormal wear problems have been encountered because of some layers of conglomerates composed by hard silica nodules contained in a soft cement. These layers gave very poor performance in terms of rate of penetration (ROP) but also with respect to the bit metrage. In fact, some coring diamond tools stayed in the hole for less than 20 m. The average ROP of 2.4 m/h obtained gives an idea of a commercial speed to be used when building project in such materials, but values as high as 5 m/h have been reached in limestones. Conversely, values as low as less than 0.6 m/h were registered in conglomerates. It is important to point out the contrast of strength between the cement and the contained nodules because this seems to be the main factor playing a role in the performance; furthermore, the so identified difficult formations can be used as reference levels when drilling by a destructive technique.

Acknowledgements

The authors thank the four organisms who funded the project: Royal Institute of Natural science of Belgium (IRScNB), Department of Technology, Research and Economy (DGTRE) of Walloonian (Belgium), Department of Territory Planning, Housing and Patrimony (DGATLP) of Walloonian, as well as the local authority of Bernissart (Belgium).

References

- Dagrain F, Deschamps B (2003) Sondages exploratoires dans le cran aux Iguanodons de Bernissart – Sondage #3. Internal report FPMs.
- Tshibangu KJP, Dagrain F (1998) Etude de faisabilité des travaux exploratoires pour l'évaluation du gisement aux iguanodons de Bernissart. Internal report FPMs.
- Tshibangu KJP, Dagrain F (2001) Pourquoi des sondages exploratoires dans le cran aux iguanodons de Bernissart ? Mines et Carrières Vol 83, pp38-45.
- Yans J, Spagna P, Vanneste C, Hennebert M, Vandycke S, Baele JM, Tshibangu KJP, Bultynck P, Streel M, Dupuis C (2003) Description et implications géologiques préliminaires de forages carottés dans le Cran aux Iguanodons de Bernissart. *Geologica Belgica*, submitted and accepted.

ConsoliTest – Using Surface Waves for Estimating Shear-Wave Velocities in the Dutch Subsurface

Rogier Westerhoff, Vincent van Hoegaerden, Jan Brouwer, and Richard Rijkers

Netherlands Institute of Applied Geoscience TNO – National Geological Survey, P.O. Box 80015, 3508 TA Utrecht, The Netherlands

r.westerhoff@nitg.tno.nl

Tel: +31 30 256 4862

Fax: +31 30 256 4855

Abstract. ConsoliTest is a geophysical method for estimating geomechanical parameters of the shallow subsurface. The procedure is based on the MASW method (Park et al, 1999) and has additional verification and validation modules. The Dutch subsurface can consist of an alternation of very stiff layers and weak layers. In these types of soils many non-standard waveforms are generated, which cannot be inverted properly by using only the MASW algorithm. By describing two case-studies we explain the developments at TNO-NITG for creating a surface wave method designed for the Dutch subsurface.

Keywords: geophysical, surface waves, geomechanical, geotechnical, shallow subsurface, ConsoliTest, MASW.

1 Introduction

In high resolution seismic (HRS) surveys, Rayleigh waves are considered annoying and unwanted noise. However, since Rayleigh waves contain by far the largest part (two-third) of seismic energy (Richart et al., 1970) and contain valuable information of the very shallow subsurface, TNO-NITG has started a research project in 2001, to investigate possibilities for a new geophysical tool. The purpose of this project is to create a shallow seismic field-procedure, which can compete with state-of-the-art commercial geotechnical techniques. In three years time, a method has been developed which can already be used for geotechnical evaluation of the Dutch subsurface: ConsoliTest.

The most important advantages of the ConsoliTest method are:

- the non-destructive character, contrary to CPT's, drilling, or borehole measurements;
- the ability to detect low-strength zones, transitions and stiffness contrasts in the subsurface;
- obtaining geomechanical information (shear wave velocities and shear modulus G);

- the ability to calculate soil properties in 2D contrary to a point measurement like a CPT.
- obtaining information from the surface up to a depth of approximately 30 m; the depth interval from 10 – 25 m used to be the “black hole” for geophysical measurements.

2 Theory

2.1 Theoretical Background

ConsoliTest is a geophysical method to estimate geomechanical parameters of the shallow subsurface from recordings of Rayleigh waves. Rayleigh waves are surface waves. They travel along the boundary of the earth and air. When we look at figure 2.1, we can see that the propagation of Rayleigh waves is subject to the layer properties in which the wave travels; the velocity of small wavelengths is influenced by the (mechanical) properties of the top layer(s) and velocities of large wavelengths are also influenced by the properties of underlying layers; this phenomenon is called dispersion. Similar to acoustic waves, Rayleigh waves come in more than one mode: the fundamental mode and several higher modes. The relative energy of the higher modes compared to the fundamental mode depends on the velocity distributions in the layer model (Foti, 2000).

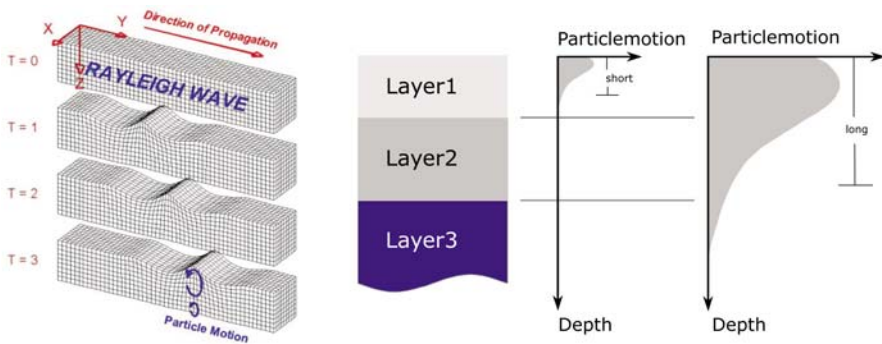


Fig. 2.1. The propagation of Rayleigh waves in two projections.

2.2 Data-Acquisition

For all seismic surveys TNO-NITG uses a digital seismic recording system capable of acquiring data with an unlimited number of recording stations. Usually, a weight of 40 kg is dropped for generating a seismic signal, but a large sledgehammer can also be used. The signal is recorded with geophones, which are evenly spaced in a straight line. Disturbance due to recordings of near-field effects are in general minimised by using a minimum offset of 5 m. A schematic drawing of the field procedure is shown in figure 2.2.

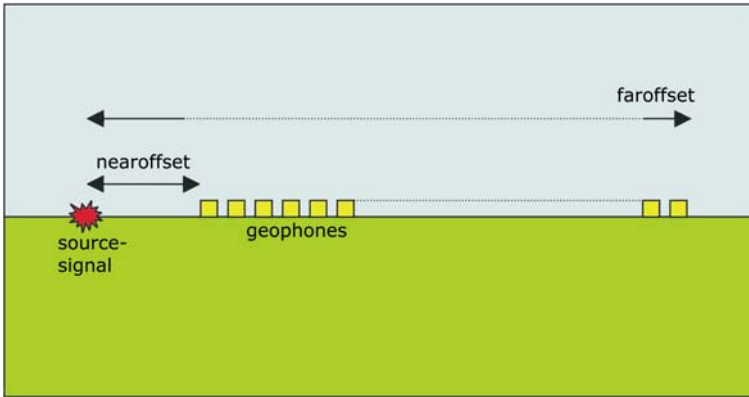


Fig. 2.2. Position of geophones and source in a surface wave measurement.

Processing

For processing the seismic data, TNO-NITG uses the MASW technique (Park et al., 1999), which consists of two important steps:

- creating a dispersion curve: seismic data in the space-time domain is transformed to the velocity-frequency domain as explained in Park et al. (1998). As is shown in figure 2.3, this plot shows dispersion and data quality (i.e. the relative amount of energy in Rayleigh waves) in a fast and effective manner. From this *dispersion plot* a dispersion curve for the fundamental Rayleigh mode can be calculated;
- calculating shear-wave velocity: an iterative calculation according to Xia et al. (1999) is used in the calculation, in which the Thomson-Haskell or propagator matrix method (Thomson, 1950; Haskell, 1953) is used in the forward modelling (from shear wave velocity to dispersion curve) and the Levenberg-Marquardt method (Levenberg, 1944; Marquardt, 1963) combined with Singular Value Decomposition for the inversion (from dispersion curve to shear wave velocity).

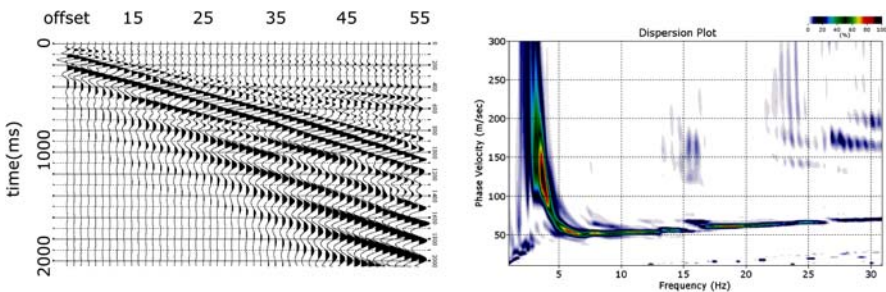


Fig. 2.3. Seismic data in the space-time domain (left) is transformed to the velocity - frequency domain (right) as described in Park et al. (1998). The resulting plot is called a “dispersion plot”.

2.3 Verification and Validation

Building upon the MASW processing steps, TNO-NITG has developed several tools for verification and validation of the dispersion curves and shear-wave velocity result. These steps are:

- definition of quality criteria. To improve consistency in data-interpretation, several quality-criteria are defined. A few of them are mentioned here:
 - do the wavelengths (=velocity/frequency) in the dispersion plot comply with the target depths?;
 - is there a low velocity layer at depth?;
 - is there noise from other waves (e.g. Lamb waves or higher mode Rayleigh-waves)?;
- forward modelling (**F1**) of dispersion curves; TNO-NITG has developed a software tool that can model an infinite number of dispersion modes for Rayleigh waves for an arbitrary layer model;
- forward modelling (**F2**) of seismic data; TNO-NITG has developed a finite-difference software tool that generates seismic data for an arbitrary measuring geometry and 2-D layer model.

The case studies in this paper will show the valuable contribution of the verification and validation steps.

2.4 Interpretation

For the interpretation of geophysical data, TNO-NITG uses a procedure that allows full interaction between geologists, geotechnical experts, and geophysicists. A rough estimation of soil parameters for shallow Dutch soil-types is given in table 2.1.

Table 2.1. Soil parameters for the Dutch shallow subsurface according to NEN6740 and TNO_NITG reports.

wet soils	ρ (kg/m ³)	V_p (m/s)	V_s (m/s)	σ	G (MPa)	v_R (m/s)
peat	1100 – 1200	1500	20 – 50	0.50	0,4 – 3	20 – 50
soft clay	1450 – 1750	1500	50 – 100	0.50	4 – 18	50 – 100
stiff clay	1700 – 1950	1600	100 – 350	0.47 – 0.50	17 – 240	95 – 330
sand	1850 – 2300	1700	150 – 325	0.48 – 0.49	40 – 240	145 – 310
gravel	2100 – 2450	1700	150 – 325	0.48 – 0.49	45 – 260	140 – 310
dry soils	ρ (kg/m ³)	V_p (m/s)	V_s (m/s)	σ	G (MPa)	v_R (m/s)
peat	100 – 600	200 – 400	20 – 50	0.47 – 0.50	0,04 – 2	20 – 50
soft clay	700 – 1300	400 – 600	50 – 100	0.47 – 0.50	2 – 13	50 – 100
stiff clay	1300 – 1600	600 – 800	100 – 350	0.24 – 0.49	13 – 200	95 – 330
sand	1400 – 2100	600 – 800	150 – 325	0.29 – 0.48	30 – 220	145 – 310
gravel	1800 – 2300	500 – 800	150 – 325	0.13 – 0.48	40 – 245	140 – 310

3 Case-Studies

3.1 Location A: Shallow Peat Layers

In the Northwest of the Netherlands, there are many locations with peat at or near the surface. The peat has developed in the Holocene under the influence of the high sea level and related high groundwater levels. Half of these locations have been excavated for domestic energy from the 16th to the 19th century. At locations where there still is a thick peat layer it is nearly impossible to construct stable infrastructure without using long pile foundations. The geological information of location A up to 20 metres depth can be roughly described as: a soft layer of 10 m on top of 10 m of river sediments (mainly sand). The upper 10 metres consists of 3 metres peat and 7 metres clay. ConsoliTest measurements have been performed at this location, with acquisition parameters as shown in Table 3.1.

Table 3.1. Acquisition parameters location 1.

Field recording parameters ConsoliTest	
Source signal	Dropweight: mass 800 kg, height 0.50 m
Receivers	4.5 Hz Geophones
Number of receivers	50
Receiver interval	1 m
Minimum offset	6 m
Sampling interval	1 ms
Opname tijd	2048 ms

When we look at the left part of figure 3.1 we see that the Rayleigh waves have a very slow dominant velocity of about 50 m/s. When we look at the dispersion plot at the right of this same figure, we see something that looks like a nice clear fundamental mode of a Rayleigh wave. Forward modelling F1 of five Rayleigh dispersion modes in the expected subsurface with modelling parameters as shown table 3.2 shows us that we are indeed looking at a fundamental Rayleigh mode.

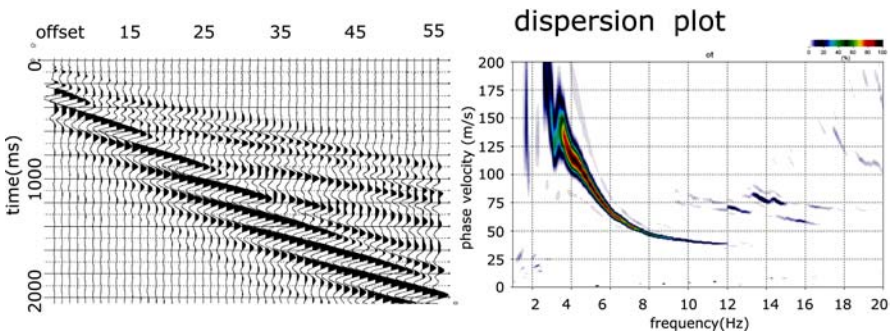


Fig. 3.1. Location A: seismic data (left) and the dispersion plot (right).

After this validation we calculate a shear wave velocity model to match with the fundamental dispersion curve. The result of this calculation and the con-resistance of the CPT at this location match very well: the sand layer at 10 to 13 metres depth and the stiff sand layer at 19 m depth show a distinct shear wave velocity increase. The peat layer from 0 – 3 m depth has shear wave velocities from 30 – 60 m/s.

Table 3.2. Modelling parameters for the forward modelling tool used for location A.

depth (m – surface)	density (kg/m ³)	s-wave velocity (m/s)	p-wave velocity (m/s)
0 – 1	1010	50	400
1 – 3	1010	25	1450
3 – 10	1400	100	1500
10 – 20	1800	125	1750
20 – 30	2000	150	1700

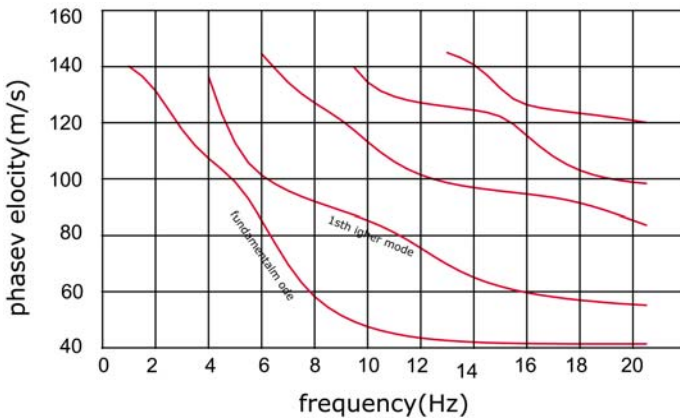


Fig. 3.2. Forward modelling F1.

Location B: Compacted Sand

This location in the Northeast of the Netherlands has a stiffness contrast that is very different from location A. The first two metres are Holocene clays and sands, followed by two metres of Pleistocene sands with cone resistances less than 15 MPa. From 4 to 8 metres under the surface lies a very stiff layer, which consists of very well sorted sand (eolian sedimentation). This layer has undergone compaction during a glacial period 150,000 years ago by several hundreds of metres of ice. Although these sands are still defined as unconsolidated, their cone resistance can reach up to 70 MPa. Underneath this layer softer clays and sands are found (cone resistance of max. 20 MPa).

Geophysical data has been collected with the same acquisition parameters as at location A.

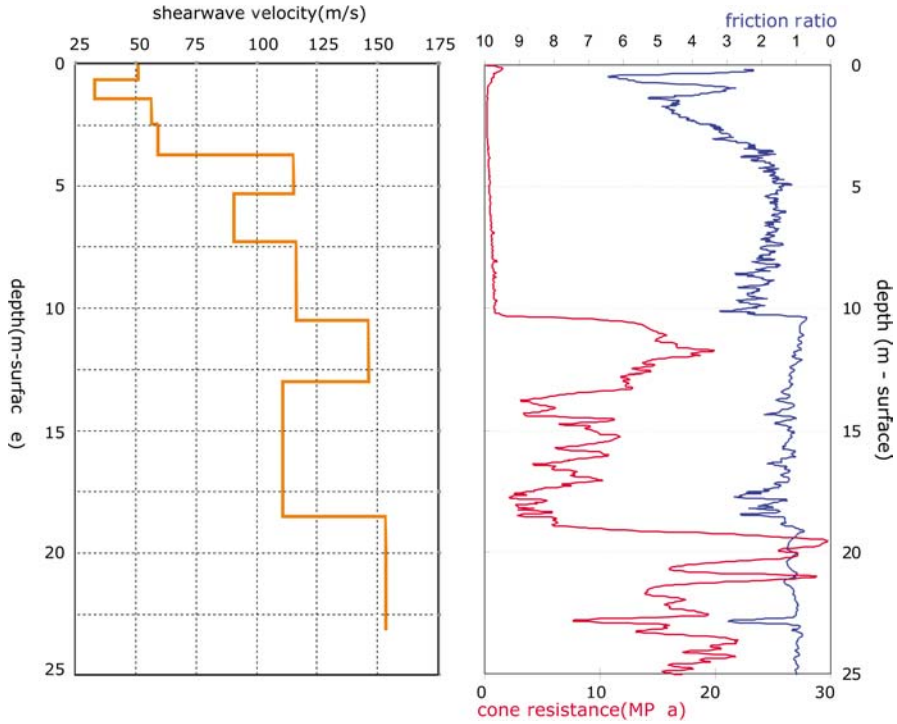


Fig. 3.3. Location A: calculated shear wave velocity (left) and CPT (right).

When we look at the seismic record (left in figure 3.4) dominant velocities are approximately 250 m/s. Thus, the fundamental mode of the Rayleigh wave must have a similar dominant velocity. The dispersion plot shown at the right of figure 3.4, however, shows a dominant velocity that is much higher. We assume that we are not looking at the fundamental Rayleigh mode, but at one of the higher Rayleigh modes. The inversion of higher modes has not been implemented in the MASW algorithm. This means that for this location we need an extra data-

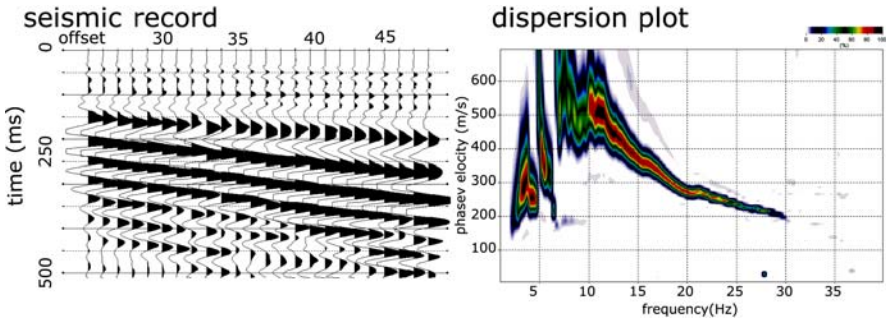


Fig. 3.4. Location B: seismic data (left) and the dispersion plot (right).

processing step to calculate shear wave velocity. The algorithm used in forward modelling tool F1 cannot calculate these extreme alternations of stiff and weak layers. Therefore, the tool F1 cannot validate our dispersion plot in this case. For these cases, the finite-difference forward modelling tool F2 with modelling parameters as shown in table 3.3 is used to create synthetic seismic data. After frequency filtering a dispersion plot is created from these data. The result is shown in figure 3.5. With this plot we can conclude that the layer model used for this seismic record, approximates the real data; although the MASW algorithm cannot solve for these types of soils and without knowing whether we are looking at a fundamental Rayleigh mode, soil parameters can still be estimated.

Table 3.3. Modelling parameters for location B used for the finite-difference modelling tool.

depth (m – surface)	density (kg/m ³)	s-wave velocity (m/s)	p-wave velocity (m/s)
0 – 2	1700	150	1500
2 – 4	1800	200	1500
4 – 8.5	2000	350	2000
8.5 – 18	1800	200	1500

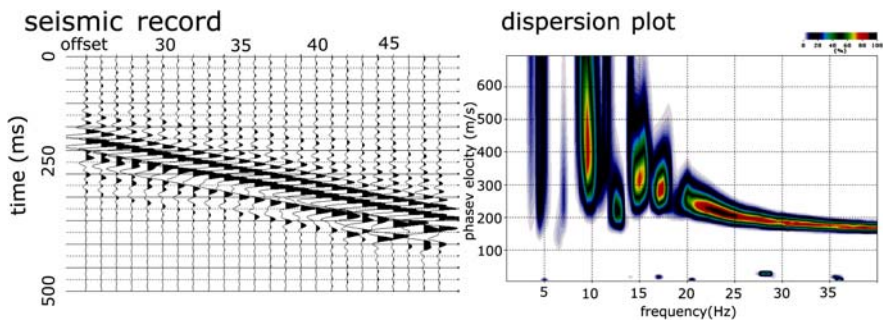


Fig. 3.5. Location B: finite difference modelling of seismic data (left) and a dispersion plot from these seismic data (right).

4 Conclusions

ConsoliTest is a method for geotechnical exploration of the shallow unconsolidated subsurface. This technique shows good results in detecting geological surfaces that show high stiffness contrast.

This method consists of the MASW method by Park et al. (1999) and additional verification and validation tools developed by TNO-NITG. Two of these extra tools are forward modelling tools. They can estimate the shear-wave velocities in cases where the MASW procedure does not work and can also give an extra quality check of MASW results. We have shown two cases of typical Dutch subsur-

face scenarios, in which velocity contrasts are rather large. In the first case, the forward modelling tool F1 gives valuable verification and validation of calculated results. In the second case, the forward modelling tool F2 can estimate shear wave velocities where other algorithms fail.

TNO-NITG is working on further development of the ConsoliTest method, in which the forward modelling of surface wave data will play an even more important role.

References

- Foti S (2000) Multistation methods for geotechnical characterization using surface waves, PhD Universita degli Studi di Genova, Universita degli Studi di Padova, http://www2.polito.it/research/soilmech/sasw/SF_PhD_diss.pdf.
- Haskell NA (1953) The dispersion of surface waves in multilayered media. *Bulletin of the Seismological Society of America*, 43, pp 17-34.
- Levenberg K (1944) A method for the solution of certain nonlinear problems in least squares. *Quart. Appl. Math.*, 2, pp 164-168.
- Marquardt DW (1963) An algorithm for least squares estimation of nonlinear parameters. *J. Soc. Indus. Appl. Math.*, 2, pp 431-441.
- Nederlands Normalisatie Instituut (1991) Nederlandse Norm (NEN) 6740, Geotechniek, TGB, Basiseisen en bepalingen.
- Park CB, Miller RD, Xia J (1998) Imaging dispersion curves of surface waves on multichannel records. 68th Ann. Internat. Mtg., Soc. Expl. Geophys., Expanded Abstracts, pp 1377-1380.
- Park CB, Miller RD, Xia J (1999) Multichannel analysis of surface waves. *Geophysics*, 64, pp 800-808.
- Richart FE, Hall JR, Woods RD (1970) *Vibrations of soils and foundations*. Prentice Hall, Inc.
- Thomson WT (1950) Transmission of elastic waves through a stratified solid. *Journal of Applied Physics*, 21, pp 98-93.
- Xia J, Miller RD, Park CB (1999) Estimation of near-surface shear-wave velocities by inversion of Rayleigh waves.

Multi-level Groundwater Pressure Monitoring at the Meuse/Haute-Marne Underground Research Laboratory, France

Jacques Delouvrier¹ and Jacques Delay²

¹ Hydro Équipements, 24, Av. Jean Cocteau, F-77000, La Rochette, France
jacques-delouvrier@wanadoo.fr

Tel: +33 1 64 37 60 45

Fax: +33 1 64 37 72 74

²Andra, Laboratoire de recherche souterrain de Meuse Haute-Marne
RD 960 F 55290 Bure, France

jacques.delay@andra.fr

Tel: +33 3 29 75 53 52

Fax: +33 3 29 75 53 89

Abstract. Multi-packer systems are an effective approach to groundwater monitoring, testing, and sampling. Multi-packer monitoring systems consist of (1) casing with packers, (2) ports to allow access from the casing to the rock, and (3) wireline probes to perform monitoring and sampling operations. Six Westbay multi-packer systems have been installed from the surface at the Meuse/Haute-Marne underground research laboratory to monitor the hydrogeologic effects of construction and operation. The data from the monitoring systems provide information on the hydraulic properties and geometries of conducting intervals. Anomalous pore pressure measurements in marls and argillites demonstrate the low permeabilities of these units.

Keywords: underground research laboratory, argillite, earth tide, groundwater, hydraulic conductivity, monitoring, packer, poro-elasticity.

1 Introduction

In August 1999, the French government authorized ANDRA (Agence Nationale pour la Gestion de Déchets Radioactifs) to develop an underground research laboratory (URL) approximately 300 km east of Paris. The laboratory targets the Callovo-Oxfordian argillite, a well-consolidated, clay-rich rock. The argillite is about 130-m thick and lies between 400 and 600 meters below the surface in the vicinity of the laboratory (Figure 1). The argillite's low hydraulic conductivity and chemical retention capacity for radionuclides make it an attractive candidate for waste disposal. Hydrogeologic measurements in the overlying Kimmeridgian marls and Oxfordian carbonates and in the underlying Dogger carbonates help to define the argillite's hydrogeologic properties by investigating its behavior as a barrier to groundwater flow. For an underground research laboratory, the construction itself is one of the most important experiments. Construction activities create mechani-

cal and hydraulic disturbances. Data from these perturbations constitute an important data set for determining rock mass parameters and for testing conceptual models of rock behavior. This paper focuses on one part of the monitoring activities – the monitoring of pore pressures in the Kimmeridgian and Oxfordian limestones using multi-packer monitoring systems. The limestones and marls overlying the Callovo-Oxfordian argillite contain multiple conducting strata that may have some degree of natural isolation from one another. To minimize the hydrogeologic disturbances of the boreholes themselves, the monitoring network needed to restore the hydrogeology to its original state to the extent possible by isolating each of the significant conducting intervals. In addition to the borehole systems, the underground workings of the laboratory are instrumented to record the water volumes that are extracted both as liquid water and as vapour by the ventilation system. The shaft construction includes sampling stations along the shaft lengths to record the volume and elevations of inflow.

2 Description of the Future Laboratory

Figure 1 is a schematic layout of the underground laboratory, which is currently under construction. At a depth of 490 meters, a network of galleries excavated in the argillite will constitute the heart of the URL (Piguet 2001). Galleries will be installed around the two shafts for measuring the effects of shaft construction on the rock and for housing laboratory infrastructure.

Eleven holes were drilled to monitor the laboratory's activities. Two were pilot holes for the two shafts and three were dedicated to monitoring the surficial materials. Multi-packer monitoring systems are installed in the remaining six holes –

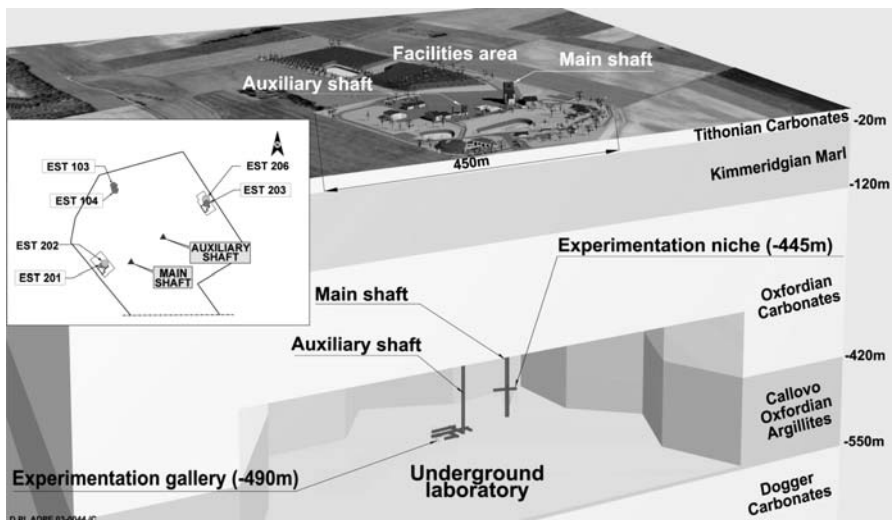


Fig. 1. Planned cross section of the Meuse/Haute-Marne laboratory showing stratigraphy.

two holes in the Kimmeridgian marls and four holes in the Oxfordian carbonates. Borehole investigations were carried out to identify the conducting sections of each hole. In addition to a standard wireline logging program, detailed investigations were performed including pumping tests, packer tests, fluid logging and sampling (Delay and Aranyosy 1994, Delay and Distinguin 2004, this volume). In the Oxfordian, these tests identified seven main conducting zones named Hp 1 to Hp 7 in order of decreasing depth. Due to their proximity to one another, Hp1-Hp2 and Hp3-Hp4 are monitored in common intervals. These five monitored intervals have transmissivities ranging from 2×10^{-7} to $3 \times 10^{-8} \text{ m}^2 \text{ s}^{-1}$

To monitor accurately the hydraulic disturbance caused by the sinking of the shafts, it was necessary to separately monitor each of the five porous zones in the Oxfordian formation as well as porous zones in the Kimmeridgian (Figure 2). After a review of available technologies, Andra chose the Westbay monitoring system for this task. Westbay systems have been used extensively at nuclear study sites worldwide (Davison 1984, Eldred et al. 1995, Stellavato 1995, Yanagizawa et al, 1991). Andra also had experience with six Westbay completions at a granite study site in the southeast of France.

3 The Westbay Multi-level Monitoring System

The Westbay MP System[®] is a multi-level groundwater monitoring system (Black et al., 1986) that works to restore the initial pressure and chemical conditions before drilling. The system has three components – the casing with packers, the access ports, and the measurement probes (Figure 2).

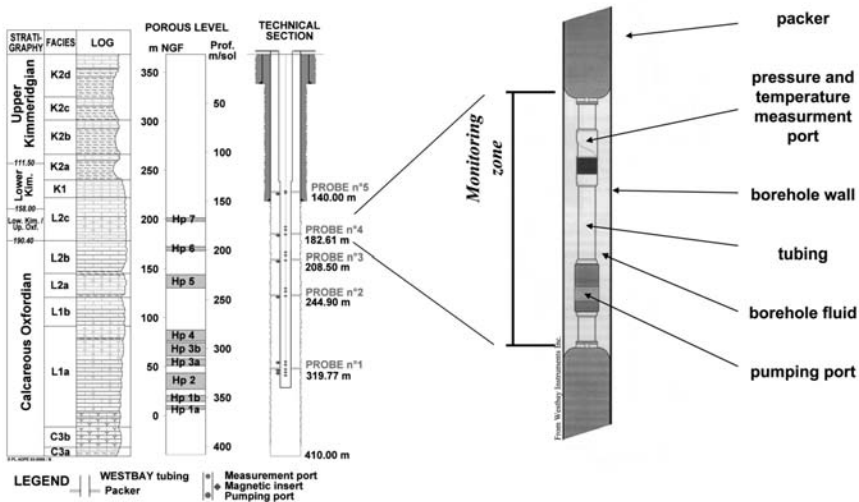


Fig. 2. Westbay multi-packer borehole completion.

The first part of the system is the casing equipped with packers, which seal the borehole into discrete zones as closely spaced as a few meters. For the Andra installations, the inflation of the packers is maintained with water. The second part of the system is the measurement port. Ports are installed between packers at the depths of interest for monitoring. Pressure measurement ports remain closed until opened by an instrument probe. The setting of the probe on a port is done with no volume exchange from the monitoring chamber and minimal pressure disturbances. The pressure ports use small openings in the casing, but for operations involving large flow rates, the casing may be equipped with pumping ports that have larger flow capacities. Pumping ports provide access for chemical sampling or hydraulic testing. The third part of the equipment system consists of the probes, which are tools run on a wireline cable to perform various functions in the ports. Probes monitor pressure and temperature as well as opening and closing the ports. The probes find the ports by sensing magnetic collars on the casing at the port locations. Once lowered to a port, an arm extends from the probe to guide and seat the probe on the port opening. Pressure probes may be run either singly to monitor ports sequentially, or the probes may be strung together to monitor several ports simultaneously. Andra uses this latter approach.

4 ANDRA's Monitoring Installations

4.1 Boreholes and Target Strata

Each monitoring interval in Andra's boreholes has a pressure port and a pumping port. Pumping ports are equipped with screens to allow pumping tests to be performed on one active zone while monitoring pressure in other monitoring zones. Since the beginning of July 2000, this system has been fully operational and connected to the laboratory's central data acquisition system which continuously collects the data from the pressure probes.

Figure 1 shows the locations of the monitoring holes and the shafts at the laboratory site. The Westbay monitoring network has the following holes:

- EST 201 and 203 are about 410 meters deep and isolate the five main flowing zones in the Oxfordian.
- EST103 is 453 meters deep and has three chambers between 319 and 416 meters monitoring the transition strata between the Oxfordian and the Callovo-Oxfordian argillite. This hole also has a wireless transmission pressure gauge cemented into the Callovo-Oxfordian argillite below the Westbay installation (Delay and Cruchaudet, 2004, this volume).
- EST104 is 358 meters deep with three chambers monitoring the lowest four conducting zones of the Oxfordian.
- EST202 is 150 meters deep and monitors pressures in the four zones of the Kimmeridgian.
- EST206, 55 meters deep, has two zones monitoring the transition from the shallow Tithonian (Barrois) carbonates and the Kimmeridgian marls.

Several types of responses have been recorded in the Westbay monitoring systems to date. These include the following:

- Responses to drilling activities before shaft construction,
- Responses to earth tide and barometric variations,
- De-pressurization responses to drainage by shaft construction,
- Pressure buildup in the Kimmeridgian, possibly due to poroelastic responses to shaft construction,
- Anomalous pressure buildups in the transition zones of the Oxfordian and Callovo-Oxfordian.

4.2 Responses to Drilling and Shaft Excavation

The main function of the Westbay installations is to monitor the shaft construction. Even before shaft construction started, the systems began to yield data, as the first installations recorded pressure effects from the subsequently drilled boreholes. The drilling activities could be treated as cross-hole pumping tests giving data on the transmissivity and storativity of the monitored intervals. The quantitative interpretation of some of these interferences has been performed by Colenco Power Engineering using a well test simulator, MULTISIM (Croisé et al. 2004). The Westbay systems produce data with clear responses from barometric effects and earth tides in the Oxfordian carbonate. Earth tides, themselves, can constrain the hydraulic properties of the rock, but for analyses of cross-hole responses, these effects and those of barometric variations are filtered. Barometric corrections are made using the barometric efficiency, which is determined from comparison of the pressure data from the boreholes and barometric measurements at the surface. The filtering uses a geostatistical, kriging approach (Matheron 1982). The barometric efficiency for the Oxfordian carbonates at the Bure site is between 0.2 and 0.3. The earth tide effects are filtered using a similar analysis. Once filtered, the data are used in MULTISIM to calculate transmissivity and storativity. The values from the Westbay data confirm the range of transmissivities obtained from borehole testing as between $4 \times 10^{-8} \text{ m}^2 \text{ s}^{-1}$ and $2 \times 10^{-7} \text{ m}^2 \text{ s}^{-1}$. The storativity has been also calculated, with a range between 1×10^{-4} and 1×10^{-6} . The responses to shaft construction can similarly yield information on the hydrogeology of the strata. Figure 3 shows the responses of several Westbay monitoring points to the drilling perturbations and the shaft construction. When the shaft penetrates a conducting stratum, the flow rates in the shaft increase, and the connected monitoring intervals record a strong response. Using the data from water inflows to the shaft, the transient responses of the Westbay piezometers provide additional measures of the transmissivities and storativities of the conducting layers using well-test analytical approaches embedded in MULTISIM.

The variability of the responses can indicate the heterogeneity of the conducting units. The similarity of responses among intervals in different conducting zones can indicate the vertical connectivity of the layers. To date, the Westbay responses to shaft inflows have provided hydraulic data on several conducting levels of the Oxfordian. For the shallowest conductor, Hp7 at about 170 meters

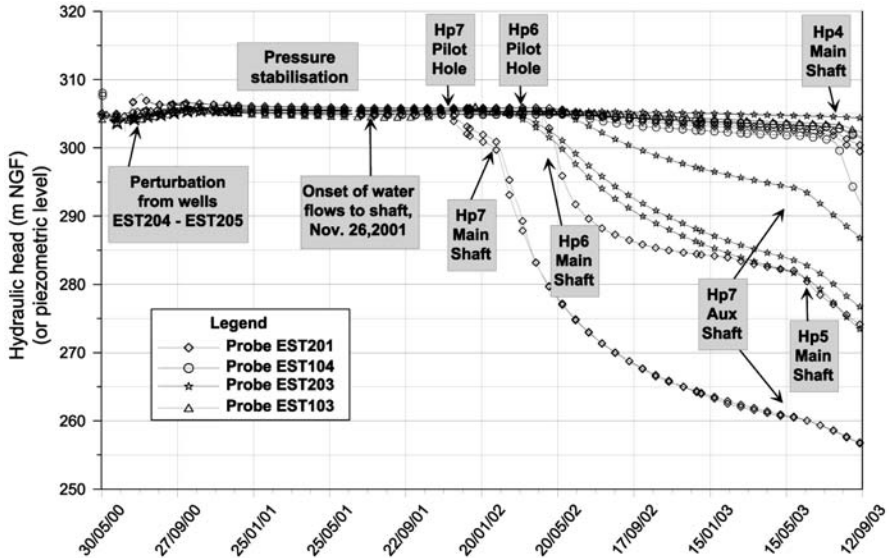


Fig. 3. Westbay monitoring responses to shaft construction activities.

depth, the transmissivity is 1×10^{-7} to $7 \times 10^{-8} \text{ m}^2 \text{ s}^{-1}$ with a storativity of 6×10^{-5} . Simultaneous responses in the next lower conductor, Hp6 at 200 meters, indicate that these conductors are vertically connected. Similar responses deeper in the shafts also allow calculation of properties of the Hp5 conductor (about 235 meters depth) of $4\text{--}6 \times 10^{-8} \text{ m}^2 \text{ s}^{-1}$ for transmissivity and $2\text{--}3 \times 10^{-5}$ for storativity.

4.3 Poroelastic Effects

During the passage of the shaft by the Kimmeridgian marls, lowest Kimmeridgian Westbay monitoring point in EST 202 observed a pressure increase. A similar smaller pressure increase was observed in the same monitoring interval when the shaft began producing water from the shallowest conducting interval of the Oxfordian. Pressure increases due to water withdrawal are clearly not a direct consequence of normal groundwater flow, and thus considered anomalous pressures. Such anomalous increases in response to pumping have been documented in low permeability materials, especially clays (Hsieh 1995). The phenomenon, known as the Noordbergum effect after a clay in the Netherlands, is caused by the deformation of the aquitard by water withdrawal in adjacent aquifers. The deformation results in a net compression of the aquitard creating a pressure rise. If verified, analyses of the phenomenon using poroelasticity can provide information on both the hydraulic and mechanical properties of the aquitard.

4.4 Osmotic Pressure Effects

Anomalous pressures are useful indicators of the large-scale, low permeability characteristics of an aquitard (Neuzil 1995). Another form of anomalous pressure, besides the Noordbergum effect, is one caused by osmotic flows. Argillites with very small pore sizes can act as osmotic membranes when the argillites are separating waters of different salinities (Neuzil 2000). Water flows towards higher salinity in response to gradients of chemical potential energy. At steady state, the osmotic flow and the Darcian flow balance one another producing an anomalously high pressure in the rock with the higher salinity water. The Callovo-Oxfordian argillite carries a pore pressure higher than both the Oxfordian and the Dogger carbonates as measured by wireless transmission gauges in the argillite. This elevated pore pressure also appears in Westbay measurements from EST 103 in the transition zone of the Oxfordian to the Callovo-Oxfordian argillite (Delay and Cruchaudet 2004, Figure 3). Analyses are continuing to evaluate osmosis as well as other possible causes of the anomalous pressures.

5 Conclusions

Multi-packer systems are a flexible and reliable approach to groundwater monitoring that is cost effective when compared with drilling separate holes for each monitoring depth. The quality and stability of the information acquired enables the identification of pressure changes down to 1 kPa, once the barometric effect and the tidal effects have been removed. The interpretation of interferences during the drilling of four wells in 2000, before the shaft sinking provide information on the hydraulic properties and geometries of conducting intervals. Anomalous pore pressures in marls and argillites demonstrate the low permeabilities of these units.

Acknowledgements

The authors thank Hydro Invest and William Black of Westbay Instruments for their advice and support concerning the technical aspects of this paper. Jean-Marc Lavanchy and Jean Croisé contributed the analyses of pressure responses. Thomas Doe of INPL assisted with the manuscript preparation.

References

- Black WH, Smith HR, and Patton FD (1986) Multiple Level Groundwater Monitoring with the MP System. Proc NWWA-AGU Conf on Surface and Borehole Geophysical Methods and Groundwater Instrumentation, Denver, Colorado, Oct 15-17, 1986, p 41-61.
- Croisé J, Schlickerieder L, Marschall, P, Boisson J -Y, Vogel P, Yamamoto S, (2004) Hydrogeological Investigations in a Low Permeability Claystone Formation: the Mont Terri Rock Laboratory, Journal of Geochemical Exploration, in press.

- Davison C C (1984) Monitoring Hydrogeological Conditions in Fractured Rock at the Site of Canada's Underground Research Laboratory. *Ground Water Monitoring Review*, 4: 95-103.
- Delay J and Cruchaudet M (2004) Hydraulic monitoring of low-permeability argillite at the Meuse/Haute-Marne Underground Research Laboratory, EurEngGeo, Liège, this volume.
- Delay J and Distinguin M (2004) Hydrogeological investigations in deep wells at the Meuse/Haute-Marne Underground Research Laboratory, EurEngGeo, Liège, this volume.
- Delay J and Aranyosy J F (1994) Les mesures hydrogéologiques dans les forages de reconnaissance des sites potentiels pour le stockage des déchets radioactifs. *Hydrogéologie* 4: 53-62.
- Eldred C D, Scarrow J A, and Smith A (1995) An integrated system for groundwater monitoring at Sellafield PNWR UK. *Proceedings 6th International High-Level Radioactive Waste Management Conference*, May 1-5, 1995, Las Vegas, Nevada, USA.
- Hsieh P (1995) Deformation induced changes in hydraulic head during ground-water withdrawal. *Groundwater* 34:1082-1089.
- Matheron, G (1982) Pour une analyse krigéante des données régionalisées. note interne, N-732 Centre de Géostatistique, Fontainebleau, France, p 1-22.
- Neuzil, C (1995) Abnormal pressures as hydrodynamic phenomena: *American Journal of Science*, 295:742-786.
- Neuzil, C (2000) Osmotic generation of 'anomalous' fluid pressures in geological environments. *Nature*, 403:182-184.
- Patton, F D, Black, W H, and Larssen, D (1991) A modular subsurface data acquisition system (MOSDAX) for real-time multi-level groundwater monitoring. *Proc 3rd Int'l Symposium on Field Measurements in Geomechanics*, Sept 1991, Oslo p 339-348.
- Piguet J P, (2001) French underground research laboratory – Construction and experimental programme. *ICEM'01 – Brugge Belgium*, 2001.
- Stellavato, N (1995) Westbay/MOSDAX Instrumentation of UE-25 ONC #1 and USW NRG-4 at Yucca Mountain, Nevada. *Proceedings 6th Int'l High Level Radioactive Waste Management Conference*, May 1-5, 1995, Las Vegas, Nevada, p 163-164.
- Yanagizawa, K, Imai, H, and Kawamura, H (1991) The Shaft Excavation Experiment: Development of Hydrogeological Model in Tono Research Field *Proceedings 2nd Int'l High Level Radioactive Waste Management Conference*, April 28-May 3, Las Vegas, Nevada p 1291-1298.

Application of Borehole Radar for Monitoring Steam-Enhanced Remediation of a Contaminated Site in Fractured Limestone, Maine, USA

Colette Grégoire¹, John W. Lane, Jr.², and Peter K. Joesten²

¹ KULeuven, Department Civil Engineering
Kasteelpark Arenberg 40, 3001 Leuven, Belgium
colette.gregoire@bwk.kuleuven.ac.be

² U.S. Geological Survey, Branch of Geophysics, 11 Sherman Place
Unit 5015 Storrs Mansfield, CT 06269, United States
Tel: +32 16 321651
Fax: +32 16 321988

Abstract. Steam-enhanced remediation (SER) has been successfully tested in porous media to remove DNAPL and LNAPL contaminants. This paper focuses on the use of borehole radar for geophysical monitoring of a SER pilot test in fractured limestone at the former Loring Air Force Base (Maine, USA). Theoretical calculations indicate that changes of dielectric and electric properties are expected due to the increase in rock matrix temperature and groundwater infilled fractures temperature during the SER test. Borehole radar reflection and tomography data were collected in two wells before the start of the steam injection, at the beginning of the injection, and near the end of the injection. Temperature logs were collected in several wells on the same days as the radar measurements. The frequency content analysis of the radar reflectors suggests that steam had not replaced water in the fractures. A significant attenuation of the signal was observed around the well where an increase of fluid temperature was observed at the end of the steam injection. After calibration of the tomography data, the inversion of the differences in travel-times indicates a small decrease of velocity, resulting from fractured rock heating. Based on this pilot test, it is concluded that borehole radar has potential to be used to monitor decrease of electromagnetic wave velocity and increase in attenuation in the fractured limestone due to steam injection.

Keywords: Borehole radar, tomography, steam-enhanced remediation, fractures.

1 Introduction

The steam injection technique (steam-enhanced remediation or SER) is an effective tool for remediation of dense nonaqueous phase liquid (DNAPL) and light nonaqueous phase liquid (LNAPL) contaminated sites in porous media (Steamtech Environmental Services, Inc. Bakersfield 2001). A SER pilot study was completed in a fractured limestone quarry at the former Loring Air Force Base, Maine, USA. The limestone is contaminated with volatile organic compounds. The radar technique has been used successfully for detecting and locating fractures in resis-

tive rocks away from the boreholes (e.g. Grasmueck 1996; Dérobert and Abraham 2000). In the last 10 years, the method has been tested as a monitoring tool to map contaminants in aquifers or to determine contaminant movement, based on the contrast in dielectric and electric properties (e.g. Brewster and Annan 1994).

When steam is injected into a rock formation, a change of medium properties is expected due to the heating. The heating of the water already present or the replacement of water by steam in the fractures should affect the radar response. The U.S. Geological Survey collected borehole radar during the SER pilot study at the Loring site to evaluate the effectiveness of radar methods for monitoring the effect of the steam injection on the limestone formation.

2 Theoretical Calculations of the Effect of Heat on Radar Wave Propagation and Reflectivity

The effect of temperature on electromagnetic wave velocity and attenuation is theoretically analysed in this study. The velocity and attenuation are directly related to the dielectrical permittivity and electrical conductivity of the fractured limestone. The replacement of water by steam in fractures results in a significant increase in velocity and a small decrease in attenuation.

The exact effect of heating on the limestone conductivity is not known. Therefore, the effects of changes in the limestone conductivity, water conductivity, and water permittivity on the radar wave velocity and attenuation were studied separately. The given assumed set of material properties includes: the water conductivity is 0.05 S/m, the water permittivity is 80.75 and the limestone matrix conductivity is 0.01 S/m. The limestone matrix permittivity assumed to be 7.2. A porosity of 2% was considered.

An increase in the electrical conductivity of the limestone matrix produces a decrease in the velocity, but a large increase in the attenuation (Grégoire et al. 2003). An increase in fluid conductivity does not significantly affect the velocity and the attenuation due to the low porosity of the fractured limestone. A decrease in water permittivity does not significantly affect the velocity and attenuation of the radar signals.

The reflection coefficient due to a thin layer is related to the contrasts in permittivity and conductivity between the fluid-filled fractures and the limestone; it is also related to the thickness of the layer, the frequency, and the angle of incidence (Hollender and Tillard 1998):

$$R = \frac{E_r}{E_i} = \frac{R_{12} + R_{23} e^{-i\varphi}}{1 + R_{12} R_{23} e^{-i\varphi}} \quad \varphi = 2 k_2 d \cos(\theta_m)$$

where E_r and E_i are the reflected and incident wave amplitudes respectively, R_{ij} is the reflection coefficient at the interface between two semi-infinite media i and j , k_2 is the wave number of medium 2 (fluid infilling the fracture), d [m] is the

thickness of the fracture (medium 2), and θ_m is the transmission angle at the interface 1-2, determined by Snell's law. The reflection coefficients are complex quantities. An increase in temperature should produce changes in the medium properties, and thus affect the reflection coefficient. When steam replaces water (a temperature of 100°C under normal pressure is taken as the condition for steam), the electric properties of steam are used in the calculations (the dielectric permittivity ϵ_{steam} of the steam is approximately equal to 1 and the electric conductivity σ_{steam} of the steam is equal to 0 S/m). The reflectivity is calculated for apertures of 1 mm and 5 mm (Fig. 1). For both apertures, the reflectivity decreases with an increase in temperature. When the steam replaces water, the reflectivity decreases by a factor of 10 for all frequencies.

Radar logging before steam injection remediation is critical to determine the location of fluid-filled fractures. A comparison of the fractures during remediation can determine the extent of the steam migration in the fractured rock. Steam replacement of the fluid-filled fractures during remediation can be measured by the sudden attenuation and lack of reflection in these fractures.

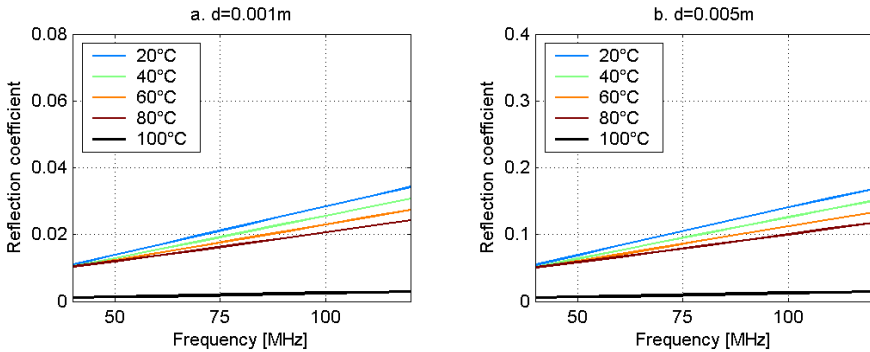


Fig. 1. Effect of temperature on the reflection coefficient for a fracture filled with water: (a) fracture thickness 0.001 m and (b) fracture thickness 0.005 m.

3 Data Acquisition

Single hole and borehole radar measurements were acquired at the Loring site using 100-MHz radar antennas in two wells (JBW-7816 and JBW-7817a). The distance separating the wells is 7.34 m (Fig. 3). Background data were collected in August 2002 before the start of the steam injection. Data also were collected at the beginning of the steam injection (September 2002) and at the end of the injection (November 2002). The acquisition of the radar tomography was completed with a step of 20 cm between every position of the transmitter and the receiver. In November, the acquisition was repeated using a step of 1 m to obtain an acquisition with a reduced number of rays. Crosshole acquisition (transmitter and receiver at

the same depth with an increment of 20 cm) also was completed before and after the tomography acquisition. Temperature logs were collected in several wells on the same days as the radar measurements. Between August and November, the temperature of the water in JBW-7817a increased about 40°C at depths below about 20 m. For the same period, the temperature of the water in JBW-7816 increased about 10°C, also at a depth of about 20 m. The larger temperature change in JBW-7817a is due to the proximity of a steam-injection well and the depth of the greatest temperature increase is due to the fact that the steam was injected between 20 and 40 m.

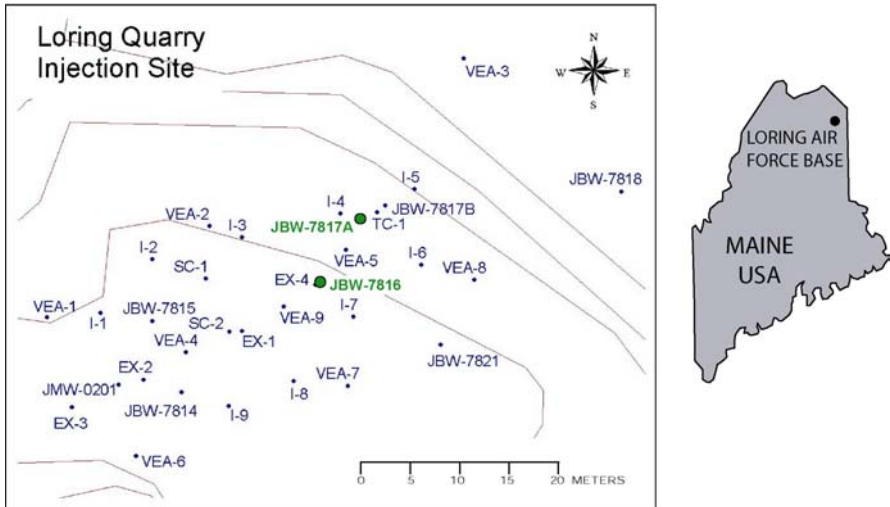


Fig. 2. Location of the wells at the Loring site (Maine, USA).

4 Reflection Data

The radar reflection profiles collected in well JBW-7817a are shown in Figure 3 because the variation of attenuation and reflectivity are more substantial around this well. A standard processing sequence - removal of the mean component, filtering, adjustment of the gain, and background removal - was completed to improve visualisation of the data. The effective central frequency is about 60 MHz. An analysis of the direct wave peak-to-peak amplitude shows that the output power of the first acquisition is larger than the output power of the two other acquisitions. For this reason, the shallow reflectors are more reflective on the background measurements. The reflectors R1 and R3 are visible on all datasets; the reflector R2 is not visible on the first dataset. The attenuation is significant for the November data collected in well JBW-7817a, and it is explained by an increase of the fractured limestone temperature in the neighbourhood of this well. A very strong reflector R appeared at the beginning of the injection in the September data

(Fig. 3b). This reflector was not visible before the injection or at the end of the injection. The presence of this reflector cannot be explained. There is no significant difference in travel-times between the different acquisitions. There is no significant change in the radar penetration in well JBW-7816.

A detailed analysis of the radar reflections was completed to characterise the reflectors affected by the steam injection and to investigate whether steam had replaced water in the fractures. The reflectors are indicated in Figure 3. Two reflectors around well JBW-7816 were also studied. Before analysing the amplitudes, a correction had to be applied to the amplitudes in the time domain to take into account the power variation of the transmitter. The correction term is based on the exponential decrease of the radar reflection with penetration. The selection of reflectors to be studied was not straightforward because many reflectors are affected by interference. The selected reflectors were chosen because they have a high energy level and they include enough traces. No change of polarity occurs for the observed reflections. After extraction of the reflections from the profile, the frequency spectra were calculated and are shown in Figure 4. The largest decrease of amplitude between the data collected at the end of the steam injection and the background data occurs in the reflectors located around well JBW-7817a (the

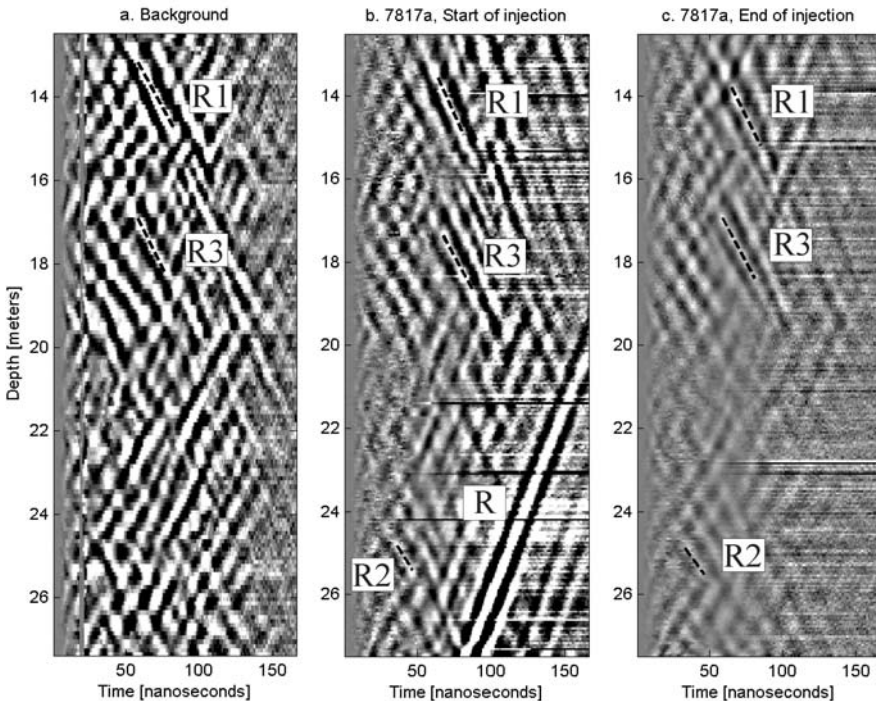


Fig. 3. Radar profiles collected (a) before the start of the steam injection (August), (b) at the beginning of the steam injection (September), and (c) at the end of the steam injection (November).

lowest ratio is 0.4). This value suggests that steam had not replaced the water present in the fractures, otherwise the ratio would have been much smaller ($<<0.1$). The results of this reflector analysis show no polarity change of the radar reflection, no significant change in travel-times, and a decrease in amplitude of less than an order of magnitude; all these results suggest that the steam did not replace the water in the fractures around wells 7816 and 7817a.

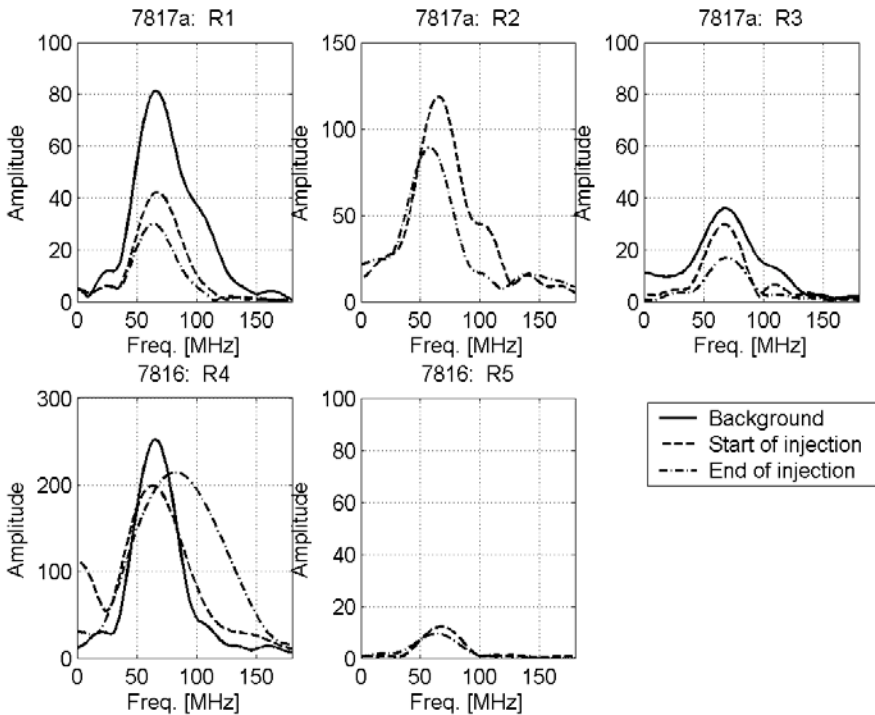


Fig. 4. Amplitude in the frequency domain of selected reflections. The amplitudes are given in V/m.

5 Inversion of Travel-Times (Tomography Data)

Before inversion, the tomography data needed to be calibrated due to the arbitrary position of the signal beginning. For the three datasets (August, September, and November 2002), the zero positions are different. Crosshole data were collected at each site visit, and were used for calibration of the tomography data. The rays of the tomography were corrected to have the same travel-times as the rays of the crosshole data following the same raypath.

After calibration of the data, the arrival times in the three datasets were compared. Because the property changes in the medium are small, the travel-time

differences were inverted to produce difference tomograms rather than differencing absolute tomograms generated from inversion of absolute travel-times. The inversion was done in several steps using a Matlab-based inversion tomographic software (Frederick Day-Lewis, U.S. Geological Survey, oral commun., 2003). The SIRT algorithm (simultaneous iterative reconstruction technique algorithm) was used. The inversion of the crosshole data was completed to obtain a starting model for the complete inversion of the travel-times. The results of the inversion were smoothed. The times of the crosshole data were again inverted to constrain the results and to obtain the final travel-time model.

The results of the travel-time inversion are shown in Figure 5. The results are presented in terms of slowness. An increase in travel-time can be observed at the end of the steam injection period (t_3 is greater than t_1), at depths greater than 22 m below the surface. This increase in travel-times, or decrease in velocity, is probably due to an increase in the limestone conductivity due to the increase in temperature.

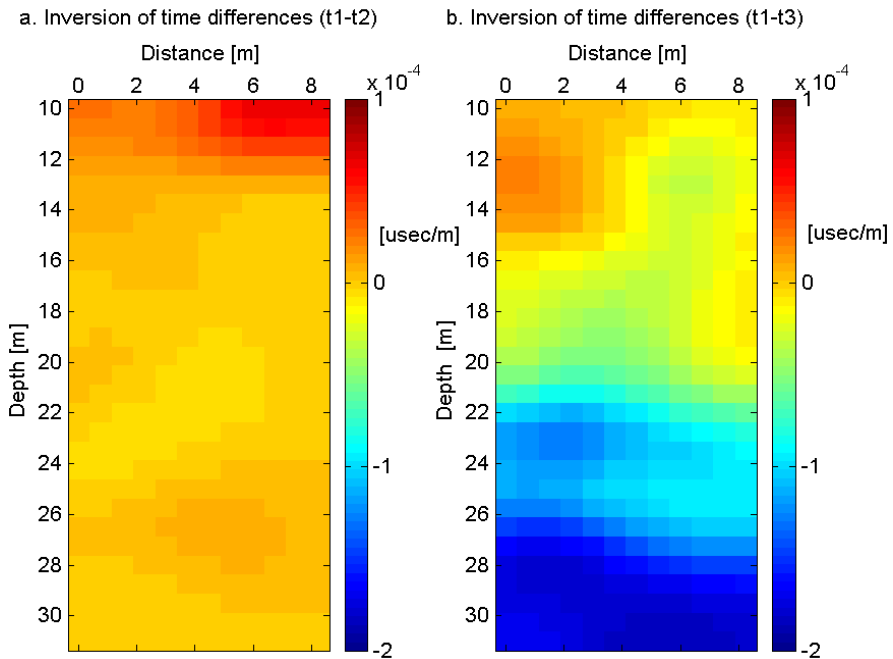


Fig. 5. Result of the inversion of time differences, in term of slowness: (a), t_1 - t_2 or August-September (b), t_1 - t_3 or August-November.

6 Conclusion

Analysis of radar reflection data collected during a steam injection at the Loring site shows no evidence that steam replaced water in fractures near these wells.

This interpretation is based on three observations: no change of polarity was observed in the radar reflections; there were only insignificant variations in the travel-times; and although a decrease in reflectivity was observed, it was not large enough to be explained by replacement of the in-situ water with steam. A decrease in amplitude was most significant in the data collected in well JBW-7817a, probably due to the higher heating around this well. Radar tomography data also were analysed. Prior to the inversion of the data, the travel-times were calibrated using the crosshole data. Due to the large time variation and changes in antenna power, the calibration process is an important step in the processing of the data. Because the property changes in the medium are small, the travel-time differences were inverted rather than inverting the absolute values. An increase in travel-times was correlated with an increase in temperature due to the steam injection for greater depths in the borehole. Although the variations of travel-times observed in this study are very low, our results demonstrate that radar tomography can detect thermally induced variations of medium properties.

Acknowledgments

The authors acknowledge the support of the U.S. Geological Survey (USGS) and the KULeuven (University of Leuven, Belgium). The study was funded by the U.S. Environmental Protection Agency (USEPA) Office of Solid Waste and Emergency Response, Office of Superfund Remediation and Technology Innovation and by the USGS Toxic Substances Hydrology Program. The authors thank F.D. Day-Lewis for the use of the Matlab-based inversion tomographic software. The authors are grateful to Chris Kochiss for his contribution in the field work. The authors are also grateful to F.D. Day-Lewis, Carole Johnson, Frederick Stumm, Lucien Halleux, André Vervoort and Alison Waxman for their suggestions concerning the manuscript.

References

- Brewster M.L., Annan A.P. (1994) Ground penetrating radar monitoring of a controlled DNAPL release: 200 MHz radar. *Geophysics* 59: 1211-1221.
- Dérobot X., Abraham O. (2000) GPR and seismic imaging in a gypsum quarry. *Journal of Applied Geophysics* 45: 157-169.
- Grasmueck M. (1996) 3-D ground penetrating radar applied to fracture imaging in gneiss. *Geophysics* 61: 1050-1064.
- Grégoire C., Lane J.W. Jr., Joesten P.K. (2003) Use of borehole radar to monitor a steam-enhanced remediation effort in fractured limestone - Results of numerical modeling and radar reflection data. Submitted to *Journal of applied Geophysics*.
- Hollender F., Tillard S. (1998) Modelling of ground penetrating radar wave propagation and reflection. *Geophysics* 63: 1933-1942.
- Steamtech Environmental Services, Inc. Bakersfield, CA (2001). Pilot study of steam enhanced remediation for mitigation of residual DNAPL in fractured rock, Loring Air Force Base, Limestone, Maine, 31 p.

Site Investigation for Abandoned Lignite Mines in Urban Environment

Paul Marinos¹, Harry Saroglou¹, Mark Novack², Maria Benissi²,
and Vassilis Marinos¹

¹ National Technical University of Athens, Faculty of Civil Engineering,
9 Iroon Politexneiou str., 157 80 Zografou, Greece
saroglou@central.ntua.gr
Tel: +30 210 7722440
Fax: +30 210 7723428

² Attiko Metro S.A., Mesogeion 191-193, Athens, Greece

Abstract. The existence of shallow coal mining in urban environments poses a great danger to engineering works due to either the creeping subsidence at the surface, the induced deformations at depth, or settlement at the surface in the case of potential roof collapse. The detection of such works requires detailed site investigations in order to acquire as much data as possible on the layout and extent of mined areas and the geotechnical quality and behaviour of the geological formations. In this context, a review of the site investigation methodology in re-developed former mining areas is made. The applicability and efficiency of geophysical methods is discussed. Site-specific information on the extent of lignite mining activity in Peristeri area, in the western outskirts of Athens, was gathered in view of the new proposed Metro extension. A three-dimensional plan view of the Peristeri Lignite Mines was produced, based on existing data, in order to define most accurately the depth of the exploitation works and their possible interaction with the tunnel construction works. During the site investigation that was planned as accurately as possible, the core borings encountered voids and backfill materials confirming the assessed depth of the galleries and allowed a validation of the model. Additional data were provided during construction. The depth of exploitation works is limited to 30 – 90 m, developed in three main levels in a rather scattered pattern due to the presence of faults. The geology of the site consists of marly deposits possessing soft rock behaviour. The results of this study lead to a prediction of the size of a potential roof collapse and an analysis of the subsequent distribution of the ground deformation.

Keywords: site investigation, lignite, urban, ground settlement, collapse.

1 Introduction

The existence of shallow coal mining in urban environments poses great danger to engineering works at the surface. The effect of mine roof collapse on surface structures, such as buildings, gas pipelines, and power lines is well documented (Bell and de Bruyn, 1999, Madden et al., 1996). An example of mining subsidence affecting the urban environment is that in the city of Norwich in the UK in 1988

where a hole of 10 m wide to 4 m deep immersed on the ground surface trapping a bus. Additionally, the design and development of structures, such as tunnels and deep foundations, in undermined areas is directly influenced by the space geometry of voids and shafts and reported by a number of authors (Price D. et al., 1969, Bucek et al. 2003). These are the cases where a “mining ground investigation” is required, in contrast to a “standard ground investigation”. A concise guide to the problems of construction over abandoned mine workings is given by Healy and Head (1984). They proposed a methodology for mining investigations, shown in Figure 1. that relies on a thorough desk study and archival search both to assess the probability that mining has taken place and to try to determine the extent of any mining activity.

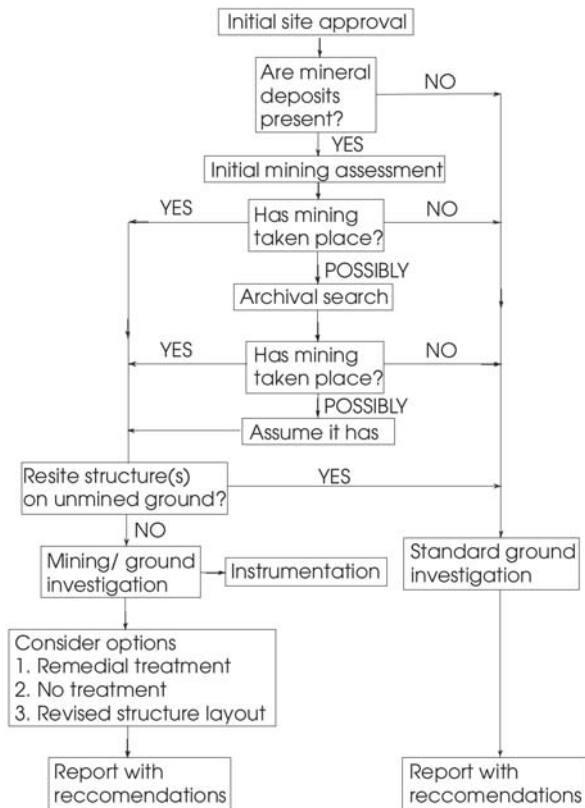


Fig. 1. Methodology for mining investigations proposed by Healy and Head (1984).

In our view the methodology should be expanded to include investigation methods that can determine all the critical parameters (Figure 4). These are: known past activity, extent of mining operations (geometry, depth, area, ageing of ground), method of mining and presence of backfilling, geological site features, geotechnical properties of host ground, and groundwater conditions of the area.

2 Coal Mining Site Investigation Methodology

The investigation consists of direct and indirect methods. Direct methods include desk study and borehole drilling while indirect methods include geophysical testing. The *desk study* must take into account the following:

- a) *Topographical maps* as they are useful in detecting the presence of mine workings by observation of spoil heaps, shafts or disturbed ground, or even signs of subsidence areas in the case that no mining records for a specific area exist.
- b) *Old mining maps, mining records, and local historical records* (newspapers etc.). These give information on the layout, extent of mines and on incidents of mine closure or collapse due to deterioration of support or fires.
- c) *Aerial photographs* at different dates, ideally before and after the mining activity. These usually indicate shallow partly-collapsed workings (Giles, 1987).
- d) On site investigation in order to identify signs of damages from subsidence.
- e) *Geological maps*. These identify probable past mining activity in areas that coal strata of significant thickness are exposed at the surface.

Following a precise desk study, *geophysical methods* can be used to detect the presence of mining but they require confirmation of features by drilling. Electromagnetic methods and radar are used for shallow depths and have limitations by background interference on urban sites. These are satisfactorily employed on open sites. The success of geophysics depends on a number of factors, namely: a) the heterogeneity and complexity of the site, b) the nature of overburden, c) presence of capping material of shafts, d) the presence of backfilling in galleries, and e) the presence of a groundwater table. In the following paragraph the main geophysical methods used in the detection of mining voids are presented:

Current-path electromagnetic prospecting is used for detecting voids at small depth and has been found suitable for locating features where the ratio of depth : diameter is of the order of 8:1 or smaller, while the depth of the feature cannot be exactly determined.

Ground penetrating radar (GPR) is generally used for the detection of shallow voids and its ability to detect a target depends on the contrast in dielectric properties. The depth of penetration may be strongly reduced or be null by conductive superficial layers.

Shallow seismic refraction. The depth of detection ranges from 2 to 100 m below surface. Its use for detection of a 60 m filled mineshaft (at St. Helens) and a shallow hole (at Radyr) has been reported by Hooper and McDowell (1977).

Magnetometric methods. The main use of magnetic methods in site investigation appears to be for the location of abandoned mineshafts, as reported by Raybould and Price (1966), Maxwell (1976), Dearman et al. (1977) and Hooper and McDowell (1977). The main problem in detecting abandoned shafts is that there is a great variety of anomalies associated with these features. Ideal sites for the use of magnetic methods are on open little-developed land, while limitations exist in heterogeneous ground that are often encountered in urban redeveloped areas.

Crosshole and Down-hole methods are reliable methods, but the cross-hole method has limitations in the spacing of the neighboring boreholes and in the sensitivity of void detection, while the down-hole method is unable to identify critical voids that are more than 1 to 2 m from a borehole.

In order to complete a "mining ground investigation" a special and detailed **borehole drilling** campaign is necessary. The planning and layout in coal mined areas relies upon the accuracy of data gathered at the stage of the desk study. The significance of selecting an accurate *prediction ground model*, based on mining maps and records, assists in the design of the borehole campaign and the confirmation of any uncertainties by borehole investigation and in the design of future engineering works. Old mining voids are normally located by drilling when penetration rate, fluid loss, core recovery and the R.Q.D. on cored holes are the most useful features to watch for. The depth and spacing of boreholes is suggested by a previous desk study and can be modified as work progresses, but should reach a depth at least 10 times the likely seam thickness or mine height (Healy and Head, 1984). Spacing of exploration holes will depend on site conditions, but should never be on a regular grid in case this coincides with a regular pattern of mine pillars. Taylor (1968) and Price et al. (1969) suggest that it is not unusual to employ spacings of 20 m and even 1 to 2 m in critical areas. Water absorption tests may assist in assessing potential grout requirements. Other methods of ground investigation, such as *downhole television* offer deep sounding applications and help to assess the size of encountered cavities. Ultrasonic scanners in boreholes can prove to be successful, while rotating ultrasonic scanners may be used within voids of flooded mines (Bell and de Bruyn, 1999).

3 Mining Ground Investigation during Tunnelling Construction

Methods of predicting voids ahead of the tunnel face have been proposed from various scientists (Yamamoto et al. 2001, Ashida, 2001) developed and applied by various companies. Tunnel Seismic Prediction (TSP) is a seismic acquisition and processing system primarily targeted at hard rock (Amberg Measuring Technique AG Switzerland). Sonic Softground Probing (SSP) is a seismic system that is mounted on the cutting wheel of a tunnel boring machine operates automatically while boring (Herrenknecht AG, Germany). Seismic Imaging is a seismic system for tunnelling (NSA Geotechnical Services Inc.). These rely upon imaging techniques and combined methods of reflection tomography and drill, velocity logging ahead of the advancing face. Probe drilling ahead of the tunnel face can be employed to assist in determining the size and geometry of voids, the presence of weaker material backfill and groundwater.

4 Issues of Tunnel Alignment of Athens Metro along Undermined Area

The initial alignment of the Athens Metro Tunnel Extension to Peristeri (Alignment 1 in Figure 2) was passing over an area where extensive lignite mining has taken place in the past. It was well established from historical data that mining in the Peristeri lignite basin initiated at 1930's and lasted until the early 60's (De Pian, 1949, Voreadis, 1940). The lignite deposits are mainly hosted in the layer of dark grey marls, which underlie the yellowish clayey marl horizon (Figure 3). These strike in NW-SE direction and have a dip of about 8° . The depth of exploitation works is limited to 30 – 90 m, developed in three main levels in a rather scattered pattern due to the presence of faults. The width of the exploited area ranges between 250 – 400 m. The area of mining activity is shown in Figure 2.



Fig. 2. Plan view of Metro Alignment, location of initial investigation boreholes (Marinos P., 2000).

Initially, the presence of lignite and mining works within the tunnel cross-section could not be estimated with the data available. A number of widely spaced boreholes were drilled along Alignment 1. A study for an alternative alignment (Alignment 2) was carried out for planning purposes, at the boundary of the mining field where shallow mining has taken place. The lignite formation was found at shallow levels in boreholes G11, G13 and G19 during the first phase. Specifically, borehole G11 encountered mining voids at a depth of 24 and 38 m below surface, in the close perimeter of the tunnel, while the lignite beds were found to lie between at a depth of 23 and 45-50 m (Figure 3).

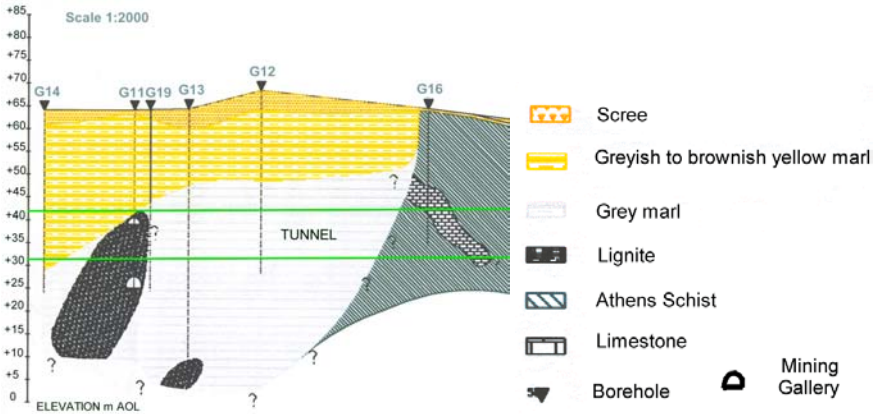


Fig. 3. Geological section along the initial Metro Alignment 1 (Kotzias – Stamatopoulos, 1998).

Based on the Mining Map of Peristeri (Greek Ministry of Industry), it was found that the green-field site area shown in Figure 4 was used for access to the mines by a number of vertical and inclined shafts and was extensively backfilled thereafter. The tunnel alignment (Alignment 1) was passing right through the

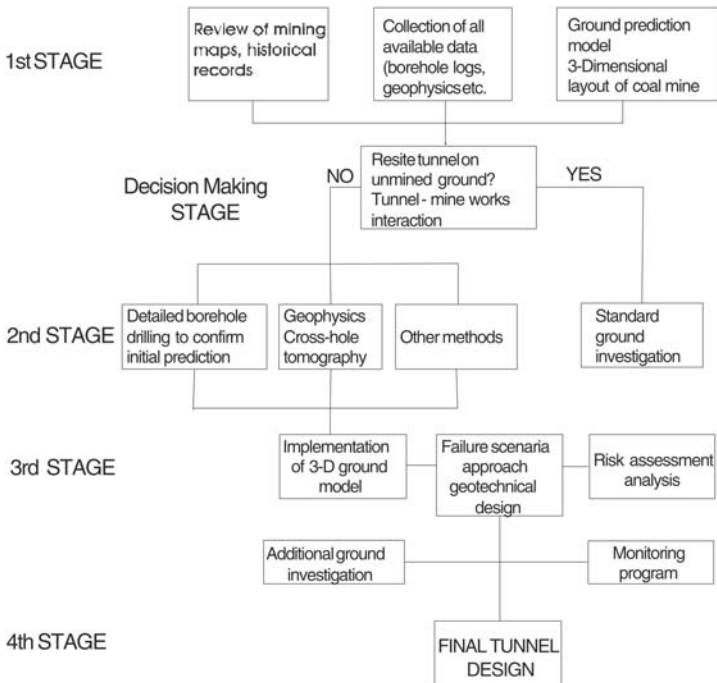


Fig. 4. Site investigation methodology for detection of mining voids along Athens Metro.

abandoned workings and would have to deal with empty or collapsed galleries and backfilled shafts. The tunnel construction along Alignment 2 was carried out successfully using an Open Face boring machine without encountering mining voids.

5 Mining Site Investigation Methodology Related to Tunnelling – Athens Metro Case

Although the alignment of the Metro Railway moved to Alignment 2 for purposes other than the risk of passing through the shallow mining field (Figure 2), the possibility of encountering voids in the vicinity of the tunnel section remained. At this stage, the design of the Metro tunnel along the Peristeri lignite field, required a careful geotechnical as well as risk-assessment approach in the undermined area.

In order to detect the mining voids a detailed site investigation was proposed. The methodology used is summarized in Figure 4.

Based on the Mining Map obtained by the Mine Survey Office, a three-dimensional layout of the lignite mine was designed, shown in plan view in Figure 5 and in three dimensions in Figure 6. The model was digitized in three dimensions, synthesized from all information and plan drawings available from different stages of exploitation. This depicted the three main levels of exploitation, as well as the vertical and inclined shafts access shafts in the area of interest. The method of exploitation was similar to that of room and pillar, extracting the coal partially. The shallow mining area (black color lines in Figure 6) situated at a depth of 35 to 40 m, was detected in the initial investigation.

The exploitation, after 1940, was planned in four main levels: 1) between +20 and +40 m AOL, 2) between 0 and +15 m, 3) between -15 and 0 m and 4) at level deeper than -15 m, shown with distinct colors on the layout. The galleries in the room and pillar section were 2.5 m high while the area at Chainage 2+600 was probably extracted using the long wall mining method (pink hatched area). A number of galleries at a level of 0 m and deeper could have been collapsed due to a fire incident in the history of the mine in 1942 (Trikalinos & Mousoulos, 1949), as well as filled with water. After the 1st stage of investigation it was decided to design a specific borehole campaign.

5.1 Specific Site Investigation

At this stage it was obvious, that a large number of galleries were not mapped at all or they were inaccurately recorded, resulting in a residual hazard. The investigation that was planned, for the tunnel stretch from the Open Face Shield Shaft to Thivon Station, would have to validate and implement the predicted mine layout and included:

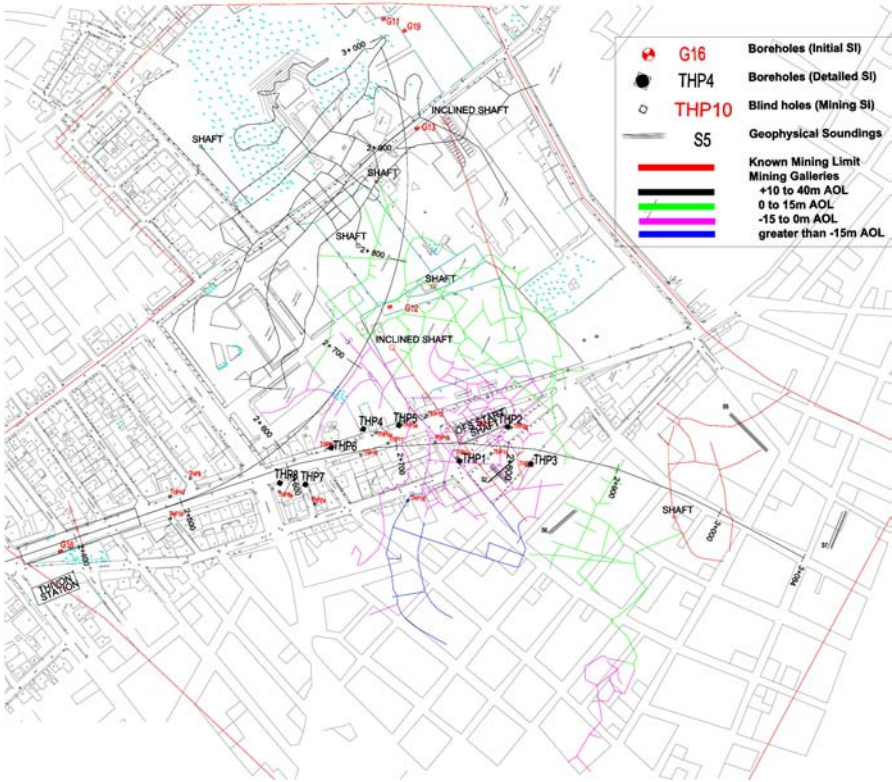


Fig. 5. Plan view of undermined area showing Peristeri mine layout on a synthetically digitized background from available data (Marinos P., 2000).

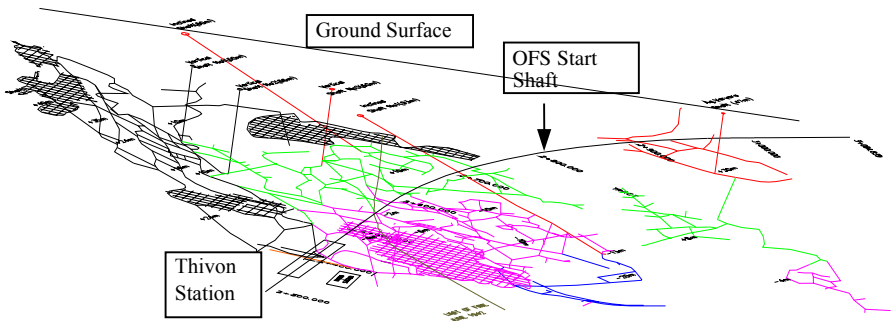


Fig. 6. Three dimensional layout of mine and Metro alignment.

1. 5 boreholes along the tunnel alignment and 3 boreholes in the location of the proposed Shaft to a depth of 100 m,
2. 18 open holes for void detection along the tunnel route, and
3. Crosshole tomography between boreholes at spacings of 50-80m. This was aborted as the data collected from the boreholes agreed well to the predicted voids.

5.2 Detection of Voids

The presence of lignite mine voids based in boreholes was encountered in two distinct levels, showing very good agreement with the predicted ones from the desk study (Figure 7):

- At the level of 0 to -10 m Above Ordnance Level (AOL). This level represents the shallow level of exploitation at a depth of 47 – 57 m below the tunnel invert and was found in boreholes THP4, THP13 and THP2. The mine voids were not usually backfilled (only in borehole THP2). The possibly backfilled voids were found in the form of sandy gravel in a marly matrix (borehole THP3 at a depth of 75 to 79 m).
- At the level of -17 m. This level represented the deep exploitation level at a depth of 64 m below the tunnel invert and was found in boreholes THP1 and THP1a.

Both levels lied in good agreement with the predicted ones: a) in THP4 a void and timber support (Figure 8) was encountered only 2 m above the predicted total extraction area, b) in THP1 and THP1a only 5 m below the predicted level and c) in THP13 it lied right within the area of predicted exploitation.

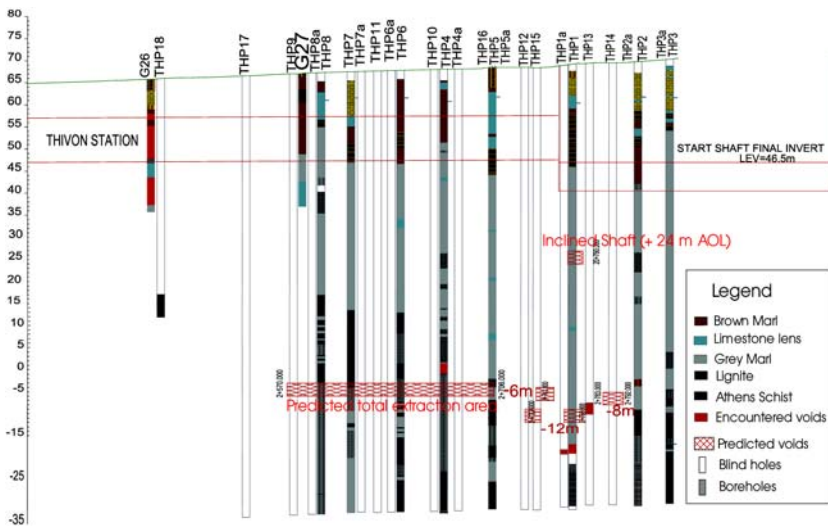


Fig. 7. Geological section showing levels of predicted and encountered past mining activity in relation to the tunnel vertical alignment (Marinos P., 2000).



Fig. 8. Part of timber support encountered in borehole THP-4.

The information was adequate to prove that the existence of voids was in the predicted depth and not shallower. All the data proved that the presence of voids would be expected at a level of 0 to -17 m AOL, which is 47 to 64 m below the tunnel invert. The case of voids encountered shallower was not likely, but if so it would only be due to an inclined access shaft.

6 Subsequent Effects on the Metro Tunnel Structure of a Potential Roof Collapse

The site specific investigations thus, showed that the most probable layout of the underground mine below the metro tunnel invert consisted of access galleries (typical cross section 2.5 m x 2.5 m) located at a depth of about 20 metres below the tunnel invert and large chambers (100-200 metres in plan and about 2 m high) supported by pillars at irregular spacing located at depths 50-60 metres below the tunnel invert. Under this scope it was possible to investigate the effects of a potential collapse of these cavities via a set of Finite Element Modelling analyses, which was performed by Prof. M.Kavvadas and included:

1. The potential collapse of a 2.5 m x 2.5 m gallery (100 m long) located 20 meters below the metro tunnel invert. Ground subsidence due to such an effect, extended up to a height equal to 1-2 times the width of the collapsing gallery, i.e., up to 4-6 metres above the gallery. Since the metro tunnel will be located at least 20 metres above such galleries, the effect of a potential collapse would escape undetected.
2. The potential collapse of one chamber, 100 m long, 25 m wide and 2 m high, located 47 meters below the metro tunnel invert. This would cause a settlement of the tunnel invert equal to 6-13 mm (if the collapse occurred exactly below the tunnel axis) and 3-6 mm (if the collapse occurred with an offset of 15m from the tunnel axis). Assuming that the settlement trough would extend in plan at a distance of about 50 metres (i.e., equal to the vertical distance between the collapsing chamber and the tunnel invert), the differential settlement (slope) would be less than 0.5 / 1000 and thus would be undetected at the elevation of the tunnel.

These two scenarios would be reasonably possible and conservative since a 25 m wide chamber seemed to be very large to maintain stability for 40 years without having collapsed. The initiation of such a collapse could be due to a large earthquake that might occur within the useful life of the Metro tunnels.

7 Conclusions

The design of engineering structures, such as tunnels, in redeveloped urban sites requires sound knowledge of the prevailing ground conditions. One of the major and unexpected hazards that can affect construction is the collapse of old mine-workings. In those cases, a detailed site investigation tailored to determine the controlling factors affecting the site is more than crucial. This was the case of the western extension of Line 2 of Athens Metro, aligned through an abandoned undermined area. The site investigation was designed, upon a precise ground model based on a thorough desk study, which predicted the extent of voids occurring in the tunnel proximity. Since, the predicted and encountered voids lied very close, the accuracy of the model was proved but this cannot substitute for a specific site investigation. The Metro tunnel was likely to encounter voids only due to the presence of access shafts, which could be investigated ahead of the face with probing holes. The mine voids lied 50 to 60 m below the tunnel invert. This information allowed for risk assessment in the case of potential roof collapses, while monitoring during operation of the tunnel would be crucial for detecting future deterioration and collapse of supporting pillars. The effect of a potential collapse using finite element analyses of a) a 2.5 m x 2.5 m gallery and b) a chamber, 100 m long, 25 m wide and 2 m high, located 47 meters below the metro tunnel invert would escape undetected for the first case while in the second case would cause a maximum settlement of 6-13 mm and a differential settlement of less than 0.5 / 1000 and thus would be undetected at the elevation of the tunnel. The tunnel construction along Alignment 2 was carried out successfully using an Open Face boring machine without encountering mining voids.

References

- Ashida Y. (2001) Seismic imaging technique for looking ahead of the tunnel face using 3-component receivers, Proc. Of Int. Symp. On Modern Tunneling Science and Technology, Kyoto, Vol.2, pp. 1119-26.
- Bell F.G. & de Bruyn I.A. (1999). Subsidence problems due to abandoned pillar workings in coal seams. Bull. Eng. Geol. Env. vol.57, pp. 225-237.
- Bucek M., Hert M. & Smida R. (2003) Tunnelling in an undermined area. Proc. of ITA World Tunnelling Congress, (Re)Claiming the Underground Space, vol.1, pp. 543-549.
- De Pian A. (1949) Aperche de la Mine de Peristeri, Athen.
- Dearman W.R., Baynes F.J. & Pearson R. (1977). Geophysical detection of disused mine-shafts in the Newcastle-Upon-Tyne area, N.E. England, Q.J.Eng.Geol., 10(3), 257-270.

- Greek Ministry of Industry, Mine Survey Office (unknown date of publication). Schematic drawing of the Underground Mining Works of Peristeri Lignite Mines, (Scale 1:1000).
- Healy P.R. & Head J.M. (1984). Construction over abandoned mine workings, Construction Industry Research and Information Association Special Publication 32, 94 pp.
- Hooper W. & McDowell P.W. (1977) Magnetic surveying for buried mine shafts and wells. *Ground Engineering*, 10(2), 21-23.
- Kotzias P., Stamatopoulos K. (1998) Geotechnical Investigations for the Extension of Line 2 to Peristeri. Design Study submitted to Attiko Metro S.A. (unpublished).
- Madden B., Van der Merwe J. & Oldroyd D. (1996). Effects of surface structures due to collapsed board and pillar workings, Eurock'96, Barla (ed.)
- Marinos P. (2000) Petroupoli Extension, Subsidence prediction and Peristeri coal mine 3-d layout. 2nd Consultant's note, (unpublished).
- Maxwell G. M. (1976) Old mineshafts and their location by geophysical surveying. *Q.J.Eng.Geol.*, 9 (4), 283-290.
- Price D.G., Malkin A.B. & Knill J.L. (1969) Foundations of multistorey blocks on Coal Measures with special reference to old mine workings. *Q.J.Eng. Geol.*, 1, pp.271-322.
- Raybould D.R. & Price D.G. (1966) The use of proton magnetometer in engineering geological investigations. *Proc. 1st Congress Int.Soc.Rock Mech.*, Lisbon, Vol.1, pp.11-14.
- Taylor, R.K. (1968) Site investigations in coalfields: the problem of shallow mine workings, *Q.J. Eng. Geol.* 1 (2), 115-133.
- Trikalinos I. & Mousoulos A. (1949) Lignite Mines of Peristeri, Stratigraphical and tectonic study of lignite deposits, Immediate and future exploitation planning, Athens.
- Voreadis G.D., 1940. Lignite deposits of Attica Lignite Mines S.A. in the Athens Basin.
- Yamamoto T., Shirasagi S., Inou M., Aoki K. (2001) Systems for forward prediction of geological condition ahead of the tunnel face. *Proc. Of Int. Symp. On Modern Tunneling Science and Technology*, Kyoto, Vol.2, pp. 237-242.

Behaviour of the Weak Rock Cut Slopes and Their Characterization Using the Results of the Slake Durability Test

Joan Martinez-Bofill^{1,3}, Jordi Corominas¹, and Albert Soler²

¹ Department of Geotechnical Engineering and Geosciences
Technical University of Catalonia, UPC. Barcelona, Spain
jordi.corominas@upc.es
Phone: 34 93 401 68 01
Fax: 34 93 40172 51

² Department of Crystallography, Mineralogy and Ore Deposits
University of Barcelona Barcelona, Spain
alberts@naturales.geo.ub.es
Phone: 34 93 402 13 45
Fax: 34 93 402 13 40

³ GEOMAR Engenharia del Terreny, Barcelona, Spain
martinezbofill@geomar.es
Phone: 34 93 424 27 05
Fax: 34 93 451 38 46

Abstract. Slopes excavated in argillaceous rocks often show degradation mechanisms and local falls which affect both safety and maintenance costs of the roads. However, such behaviour cannot be generalized. Some cut slopes remain unaffected for years while others degrade very rapidly. The degradation process occurs in both marine and continental geological formations, which involve a variety of lithologies and textures of a complexity that is not reflected in the simple terms used to designate them (i.e. claystones, siltstones, shales or marls). Previous investigations have shown that relationships between the materials properties and their long-term behaviour in cut slopes are not evident. In our research, we have used samples from 35 cut slopes distributed along several roads of the Catalan sector of the Ebro Basin in Spain. Both intact samples and samples aged by the action of drying-wetting and freeze-thaw cycles have been tested with the Slake Durability Test (SDT). The results have shown the importance of freeze-thaw cycles in the development of cracks and weakening of the sample matrix. Most durable materials show only a slight loss of weight in the SDT and a linear degradation trend when tested up to five cycles. Weakest samples degrade very fast, some of them may fall apart with only few cycles of the SDT while showing a non-linear trend. Aged samples are found to reproduce more adequately the long-term behaviour of the cut slopes. The ageing cycles increase the contrast between durable and weak rocks, thus allowing a much better prediction of their future behaviour. The results of the laboratory tests are in agreement with the observed degradation of the excavated slope, which have been classified taking into account the response to the degradation process.

Keywords: Slake Durability Test, Laboratory testing, cut slope, degradation, freeze thaw cycles, Catalonia.

Introduction

Slopes excavated in weak rocks have a complex behaviour. Blasting is often required to excavate argillaceous rocks (i.e. mudstones, claystones, siltstones, marls or shales), however, new slope faces are highly susceptible to physical weathering and may disaggregate in a very short span of time, often during the lifetime of the infrastructure. Breakdown and disaggregating of the rock structure is observable in some marly formations only few years after the excavation (figure 1a). Similarly, when interbedded layers of limestones, sandstones or conglomerates are present, disaggregating mechanism gives place to the development of overhanging layers, which may produce toppling of blocks, especially if vertical joints parallel to the slope face exist (figure 1b). On the other hand, stress release induced by excavation is also responsible for the development of listric joints. This type of discontinuities is seldom identified in boreholes or in field surveys as they develop mostly after the rock has been exposed. The presence of listric joints in cut slopes is a main source of instability (figure 1a). Finally, water plays a key role by changing the characteristics and properties of the argillaceous rocks. In particular, it may cause swelling and breakdown of the rocks, sometimes mobilising high swelling pressures.



Fig. 1. (a -left) Breakdown of marls, with fragments accumulation at the slope foot and generation of listric joints responsible for the failure. Cut slope near Vic (Barcelona); (b – right) Rock falls produced by overhanging and subsequent toppling of sandstone layers in a cut slope near Solsona (Lleida). The process is accelerated by rapid disintegration of the underlying mudstones.

Understanding degradation mechanisms of such materials has attracted the attention of many engineers because they can reduce the stability of the cut slopes, cause undesired settlements in embankments, and increase significantly the maintenance costs. Previous research works have shown that weak rocks and, in particular argillaceous ones, are much more heterogeneous than expected from the simple terms used to designate them (i.e. claystones, siltstones, shales or marls). Properties of the argillaceous rocks and their long-term behaviour in the cut slopes are strongly controlled by mineralogy of clay components, the overconsolidation history, nature and degree of cementing material and the texture (Morgenstern and

Eigenbrod 1974; Dick and Shakoor, 1997). Most of the indexes that have been proposed to characterize such materials are based on the Slake Durability Test (i.e. Franklin, 1981; Santi, 1997).

In our research we have characterized argillaceous rocks by means of the Slake Durability Index (SDI) taking into account the ageing effect caused by the weathering factor related to climate (freeze-thaw and wet-drying cycles). The aim of this paper is to present to what extent SDI obtained are in accordance with the observed behaviour of cut slopes. To this purpose, the interpretation of the SDI is critically discussed and a new field classification, based on the durability of the slopes, is proposed.

Study Area

The study area is located in the Central Catalan Basin, which forms the eastern end of the Ebro Basin, NE of Spain. This area has a Mediterranean-continental transition climate, showing a high thermal contrast between cold and foggy winters, with high humidity and freezing days, and hot and dry summers, with temperatures commonly rising over 30°C degrees. The Ebro Basin is the southern foreland basin of the Pyrenees range, filled with both marine and continental sediments. The latter come from the erosion of the Pyrenees during the first uplifting movements, which occurred at the end of the Cretaceous Period and continued until the middle of Miocene. The Catalan sector of the basin is formed by a thick sedimentary record. The northern sequences are affected by the orogenic building, while the southern ones, where this study is carried out, remain basically undeformed. The outcropping geological formations can be divided in three great sedimentary sequences that show the change from marine to continental environment: massive lutite formations of marine origin, including layers of mudstones-sandstones related to regressive and transgressive marine cycles (Ilerdian-Lower Lutecian age); transition from marine to continental conditions is made by a succession of evaporitic layers (gypsum, halite) interbedded with thin grey lutite layers. To the top of the sequence red marls and sandstones of continental origin appear (Upper Lutecian- Priabonian age); and thick and massive conglomeratic sequences of continental origin which progressively become a succession of sandstone and argillaceous layers towards the South (Upper Priabonian-Late Oligocene age). The slopes that have been described and sampled correspond to both marine and continental sequences.

Methodology

A total of 35 cut slopes were selected to analyze the long-term behaviour and its relationship with the lithological and durable characteristics of the outcropping materials. The selection of the slopes took into account several factors: (i) presence of argillaceous deposits; (ii) presence of either marine or continental forma-

tions; (iii) lithological variety that includes siltstones, claystones, marls, shales, in order to assess the influence of the mineralogical and textural components; (iv) the existence of roads with recently excavated slopes (less than 15 years), in order to observe the evolution of each slope face; (v) absence or a low degree of structural deformation of the layers that, otherwise, would introduce an additional scattering factor in the assessment of the durability of the materials. The working hypothesis is that degradation of cut slopes depends on both lithology (mineralogy and cementation degree), and the environmental conditions of the area. The argillaceous layers in the slopes were systematically sampled with a portable drilling machine. Cores of 30 mm diameter and 30 cm length were obtained and sent to the laboratory. The samples were first identified and then tested with the Slake Durability Test (SDT) as described by Franklin & Chandra (1972). From each slope, three sets of samples were tested. One set was tested without any treatment. To simulate the moisture changes in the slopes, a second set was first subjected to an ageing process of 15 drying-wetting cycles of 24 hours duration and then tested. Each cycle consisted in storing the samples in an oven at a temperature of 105° C for 12 hours and then placing it into a controlled humidity room at a temperature of 22° C for the same span of time. Finally, a third set of samples were subjected to an ageing process of 15 freeze-thaw cycles (ASTM, 1997) of 24 hours duration before testing. The samples were first soaked in a 0,5% isopropyl alcohol solution prior to the storage for 12 hours in a freezer at a temperature of - 18°C and then placed into a controlled humidity room at a temperature of 22° C for the same span of time. Cylindrical core samples of 30 mm of diameter, and 30 mm height, were used in order to compare visually the evolution of samples during the ageing process and after the SDT. Results are given by Sehudes Index, corresponding to the relation between the final and initial weight of the sample, expressed as percentage, after two slaking cycles. In this work, however, a total of five SDT cycles in each sample has been carried out, obtaining the durability index Id_5 . Samples showing low durability were also tested in the soil mechanics laboratory (Atterberg limits, grain size analysis, expanding test...).

On the other hand, we prepared an inventory of road cut slopes excavated in argillaceous rocks. At each slope, a form was filled annotating the morphological, geological, geomechanical and evolutionary characteristics of the excavated face. The most significant parameters recorded were the following: (a) morphology: orientation, length, height and slope angle; (b) geology: lithological description, thickness of the strata, orientation and dip; (c) geomechanical properties: RMR (Bieniawski, 1979); and (d) evolutionary features: nodular cracking of the surface, rock fall scars, erosion, rate of slope receding. A field classification of the rate of slope degradation was prepared:

- Type 1: Intact cut slope. Blast holes are clearly visible. Originally excavated slope surface is well kept. Stable slope and only sporadic rock falls.
- Type 2: Slightly weathered slope surface. Spheroidal exfoliation cracks may appear. Stable slope and local rock falls associated to listric joints. Blast holes are observable for most of the length. Originally excavated slope profile is kept in average.

- Type 3. Weathered slope. Slaking and disintegration of the rock surface. Debris starts accumulating at the slope foot. Frequent rock falls through listric joints. Blast holes poorly preserved. Stable but receding cut slope.
- Type 4. Heavily weathered slope. Intense slaking of the rock surface. Continuous falling of chunks prevents the slope from rock falls. Weathering and cracking of the rock reach a depth of up to 25 cm. Original rock structure can not be recognized. Blast holes have disappeared. Erosion and gulying of the slope surface. Receding slope profile. Steep slopes tend to be unstable.
- Type 5. Completely weathered slope. Original rock colour has vanished. Weathering and cracking of the rock reach a depth of more than 25 cm Usually composed of compacted but non cemented clays. Steep slopes are unstable with frequent rotational failures. Gulying even with low slope angles.

Results - Laboratory Results

As it has been already mentioned, although the standardized results of the SDT are usually expressed by the Sehudes index (Id_2) we have tested the samples up to five cycles (Id_5). The results have shown two main behaviours: on one side, there is a group of samples with a linear degradation (disintegration) trend, usually coinciding with the most durable materials while, on the other hand, other group of samples, that correspond to most friable materials, display a non-linear disintegration trend (figure 2). In the group of the most durable samples, the percentage of disintegration is less than 20% for the Id_5 . It corresponds to marine sediments and cemented continental claystones. The group of friable samples has a percentage of loss of material over 30-50 % after each cycle. Sometimes, the retained material is

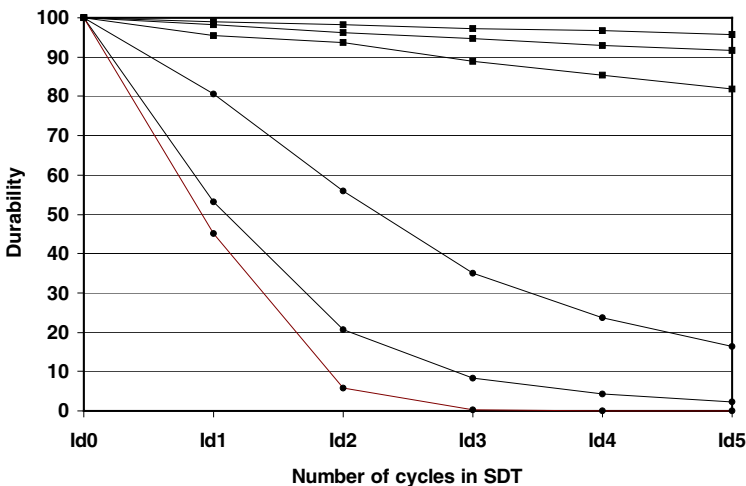


Fig. 2. Results of SDT in intact samples showing two different behaviours, a linear trend in more durable samples, and non-linear trend in weaker ones.

not enough to perform all the five cycles, and the general trend is to achieve an Id_5 with a constant value close to zero. This is the most common behaviour in continental argillaceous rocks. Performance of five cycles has shown that the percentage of material loss in the first cycle is variable. We assume that this is because the loss in the first cycle depends on the material durability but also on the degree of alteration during preparation of the sample (extraction procedure, sawing of the samples, etc). Damaged samples during either the extraction or the preparation procedure will experience a greater loss. Fitting a trend line between the first two cycles often does not give an appropriate insight of the durability of the material. Instead, in durable argillaceous rocks, loss percentages from second to fifth cycles fit quite well to a linear trend (correlation coefficient $> 0,95$) and explain much better the observed behaviour of these materials in the slopes (figure 2). In case of very friable argillaceous rocks, the great percentage of sample loss in each cycle is a good indicator of the behaviour in the slopes.

Influence of Sample Ageing

Ageing with drying-wetting cycles has not produced a marked effect on the SDT (figure 3). SDI obtained from samples after the drying-wetting cycles are very similar to those obtained without ageing process. For durable materials, only a slight decrease in the SDI can be observed. With the available information, we can not conclude whether such behaviour is due to the lack of influence of the humidity changes or to the small number of cycles that samples have been subjected to. This will be the goal of future research. Instead, samples aged with freeze-thaw cycles show a distinct decrease of the durability. However, two behaviours are

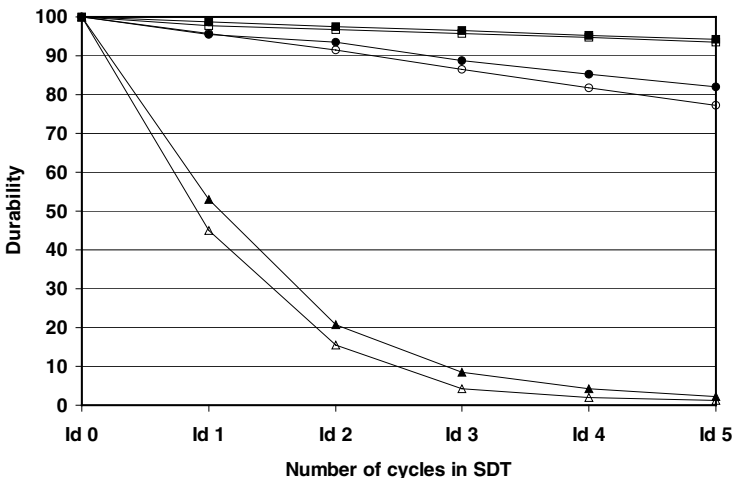


Fig. 3. Results of SDT on 3 representative intact samples (solid symbols) and on aged samples (open symbols) after 15 wetting-drying cycles. There are not remarkable changes in the durability of tested samples.

identified (figure 4). On one hand, there is a set of samples which, even though SDI (Id_5) has been reduced by the ageing process, it is still high, indicating that the materials are resistant to the weathering processes and can stay fresh in the long term (for instance, sample plotted with triangles in figure 4 decreases by ageing Id_5 only from 95% to 85%). Instead, other set of samples show a marked decrease of the durability after the freeze-thaw cycles. Some samples show high durability values ($Id_2 > 80\%$ and $Id_5 > 60$, solid circles in figure 4) in fresh intact samples, but their durability shows an important decrease after freeze-thaw ageing (open circles in figure 4). In the weakest samples, most of the disintegration is produced in the first cycle and sometimes, the retained material is not enough to perform all the five cycles.

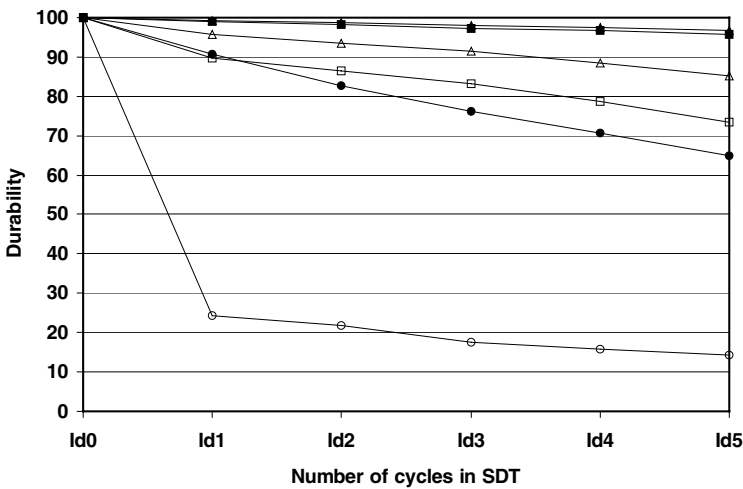


Fig. 4. Results of SDT on 3 representative intact samples (solid symbols) and on aged samples (open symbols) after 15 freezing-thawing cycles. In all the tested specimens, results show a decrease of durability after ageing.

Correlation between Field and Laboratory Results

Laboratory results have been checked with the observed behaviour of cut slope in the field, that have been defined previously (figure 5). Durability indexes tend to decrease in accordance to the slope degradation rate. It is interesting to note that, in some cases, the value of SDI for intact samples does not fit with the observed behaviour of the slope. For instance, intact sample 2 has a high Id_5 value that is not consistent with the cut slope category. However, if SDI values after freeze-thaw ageing test are incorporated to the plot, much better agreement is found. In fact, SDI values of aged samples defined a lower boundary of durability for each category of slope. Thus, the expected behaviour of a cut slope is better inferred from the SDI values of the aged samples.

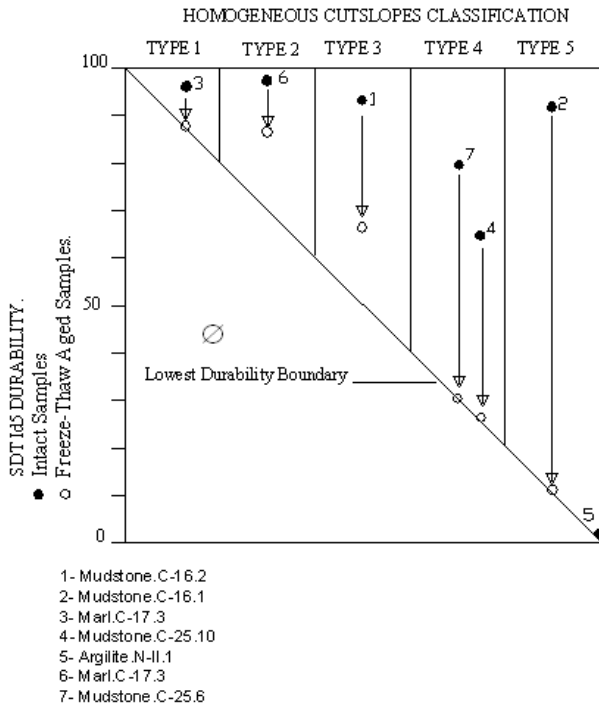


Fig. 5. Comparison between laboratory results and the observed behaviour of cut slope in the field. Results show how durability indexes tend to decrease in accordance to the slope degradation rate, especially when samples are tested after freeze-thaw ageing test. SDI values of aged samples define a lower boundary of durability for each category of slope.

Conclusions

The SDT results show that two slaking cycles are not enough to characterize the durability of samples, and four or five cycles reproduce more appropriately the behaviour of the argillaceous rocks in most of the cases. A linear trend in durability decrease can often be observed using second to fourth cycles. The best predictive capability of the slope behaviour from SDI is obtained by freeze-thaw ageing of the samples. This is particularly useful for some durable argillaceous rocks, some of which show a sudden disaggregating after freeze-thaw cycles. Consequently, ageing with freeze-thaw cycles allows a better discrimination of the mid or long-term expected behaviour of the slopes. The weakest samples show that most of the disintegration is produced during the first freeze-thaw cycle. Therefore, we conclude that cut slopes located in freeze-thaw areas, will show a faster degradation rate than the same materials in cut slope subjected to warmer/mild climatic conditions. There are no significant changes in rocks durability in drying-

wetting aged samples. Probably the number of cycles should be much greater than 15 cycles to affect rock durable properties. The observed behaviour of the cut slopes is in agreement with the results of the laboratory tests.

References

- ASTM. 1997. "Standard test method for evaluation of durability of rock for erosion control under freezing and thawing conditions". Designation D 5312 -92 (Reapproved 1997). pp. 190-192.
- Bieniawski, Z.T. 1979. "The geomechanics classification in rock engineering applications". Proceedings 4th Intern. Congress of Rock Mechanics. Montreux, vol.2: 41-48.
- Dick, J.C. & Shakoor, A. 1997. "Predicting durability of mudrocks from geological characteristics". In P.M. Santi & A. Shakoor (editors). *Characterization of weak and weathered rock masses*. Association of Engineering Geologists, Special Publication, 9: 89-105.
- Franklin, J.A. & Chandra, A. 1972. "The slake durability test". International Journal of Rock Mechanics and Mining Sciences. Vol. 9, pp. 325-341.
- Franklin, J.A. 1981. "A *Shale Rating System* and tentative applications to shale performance". In TRB Symposium on Properties and Performance of shales. Washington DC, 22 pp.
- Morgenstern, N.R. & Eigenbrod, K. D. 1974. "Classification of arcillaceous soils and rocks". Journal of Geotechnical Engineering Division. ASCE. Vol. 100, GT10: 1137-1156.
- Santi, P.M. 1997. "Comparison of weak and weathered rock classification systems". In P.M. Santi & A. Shakoor (editors). *Characterization of weak and weathered rock masses*. Association of Engineering Geologists, Special Publication, 9: 139-159.

Determination of the Failure Surface Geometry in Quick Slides Using Balanced Cross Section Techniques – Application to Aznalcóllar Tailings Dam Failure

José Moya

Dpt. of Geotechnical Engineering and Geosciences
School of Civil Engineering of Barcelona, Technical University of Catalonia (UPC)
Jordi Girona 1-3, UPC Campus Nord modulo D-2, 08034 Barcelona, Spain
jose.moya@upc.es
Tel: +34 934010736
Fax: +34 934017251

Abstract. In a landslide investigation, the location of the failure surface is a difficult task when measures of subsurface displacement are lacking, as it occurs in old landslides or in recent but quick ones. The subsurface geological data and ground surface displacement data may not be enough to formulate a unique interpretation of the failure surface. However, an accurate determination of the failure surface is possible when balanced cross section techniques are applied to preliminary interpretations. The former is proved by means of the example of Aznalcóllar dam failure (Seville, Spain).

Keywords: landslides, failure surface determination, balanced cross sections, Aznalcóllar tailings dam.

1 Introduction

The identification of the failure surface geometry is a critical task in landslide investigation. The failure surface can be located by measurements of subsurface displacements in moving landslides, a method that is, obviously, not applicable to stationary ones. That is the case of old landslides, and also of recent failures in which the movement elapses a time span too short for monitoring of subsurface displacements. Then, the exploration of the landslide morphology and structure becomes especially important. Logging of discontinuities and searching for structural features indicating displacement (like slickensided planes or shear zones) are the most common subsurface exploratory methods to locate the failure surface. Nevertheless, these methods may not be resolute enough; that is to say, the geological data may not be sufficient to deliver a unique interpretation of the failure surface. This may happen when several slip surfaces are identified at the boreholes. In that case, the lowest of the slip surfaces may not correspond to the failure surface (the surface from which the whole slid mass was detached) but to an old

tectonic feature or to a landslide slip surface with a short displacement (millimetres to decimetres).

A situation like the former mentioned arose during the geological reconnaissance of Aznalcóllar dam failure (Seville, Spain), carried out for the judicial investigation about the causes of the accident (Moya 2000). The use of balanced cross sections is a powerful method applicable to these situations, because it allows checking the geometrical consistence of the formulated interpretations. This method is currently used by structural geologists for the construction of complex geological cross sections (Dahlstrom 1969, Ramsay and Hubert 1988). For landslide investigation, Hutchison (1983) and Bishop (1999) describe simplified versions of the method to locate approximately the failure surface when subsurface geological data are not available. This paper shows, by means of the example of Aznalcóllar failure, that an accurate determination of the failure surface is possible by combining measurements of ground surface displacements, detailed surface and subsurface geological data and balanced cross section techniques.

2 Setting of Aznalcóllar Dam Failure

The Aznalcóllar impoundment, located at 35 Km of Seville (Spain), was used to stock the tailings of the Los Frailes mine. The impoundment is closed by a perimetral dam that encircles 16 ha (figure 1). The east flank of the dam is bordered by the flood plain of the Agrio River. At this flank the dam reached its maximum size (28 m high and 100 m wide at the base). The geology under the dam is simple. It consists of a horizontal terrace deposit of the Agrio River (terrace T3, with a thickness of 4 to 6 m and formed by gravel and sands), which overlies a 70 m thick blue clays formation of Miocene age (Guadalquivir Formation). At the east of the dam, the flood plain deposits form a 2-3 m thick layer of gravel and sands (terrace T0), which lies directly over the Miocene clays.

The dam rupture occurred on 25 April 1998 and was caused by a landslide that affected the SE sector of the dam. The landslide occurred abruptly, between 00:30 and 1:00 h, as can be deduced from the statement of some workers of the mine. The slide involved a band of 600 m long and 180m wide of the dam and its foundations, displacing them as a whole a maximum of 49 m towards the flood plain (figure 1). The slide created a big breach in the embankment through which contaminated water and tailings slurries spilled (figure 1).

3 Geological Reconnaissance

The reconnaissance involved a detailed geological-geomorphologic map of the area (at scale 1: 1000). Accurate measurements of surface displacements were available at the bench marks installed in 1997 on the dam top and at the electric towers located close to the foot of the dam. Additional ground surface displacements were gathered by comparing the pre- and the post-failure topographic maps

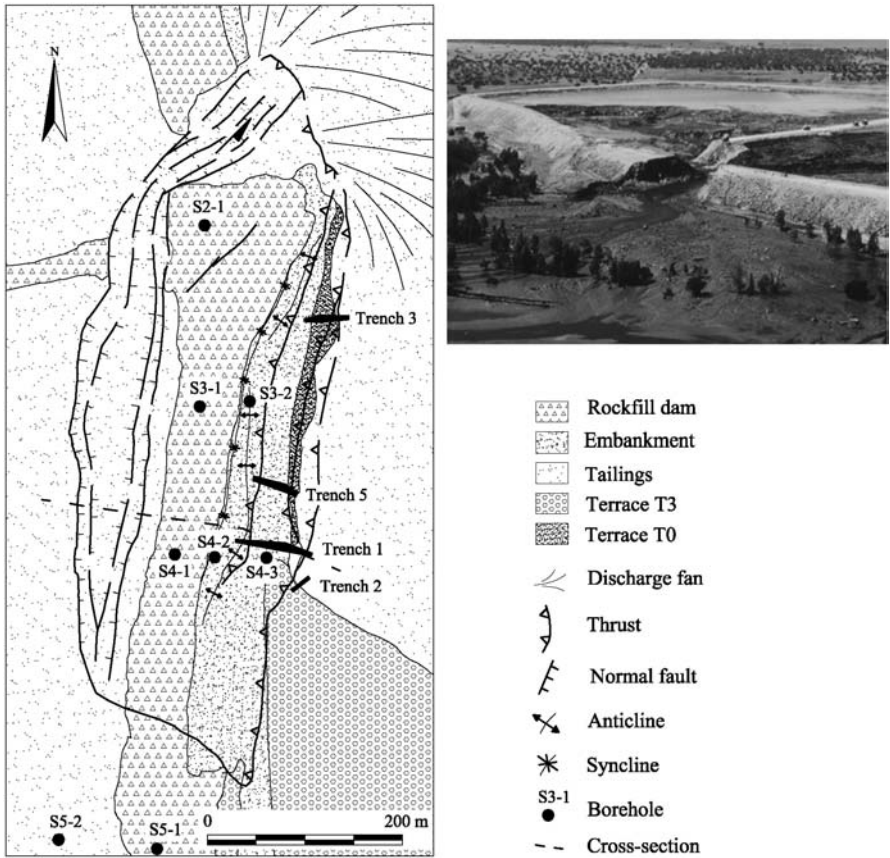


Fig. 1. Left: geological map of the Aznalcóllar landslide; the location of the cross-section of figure 3 is indicated. Right: Aerial view of the dam sector affected by the slide (photo taken towards the SW).

(scale 1: 1000). The subsurface investigation of the landslide was carried out by means of two trenches (located at the landslide foot) and 6 boreholes (figure 1). To ensure the undisturbed character of the cores of blue clays, and a high recovery, the clays were drilled with a Mazier tube, with a low rotation speed and a low pressure of drilling water. The characterization of the original discontinuities of the blue clays formation was carried out at several *fresh* outcrops, close to the tailings impoundment, and at two trenches and 5 boreholes located outside the landslide. In order to reconstruct the geological structure of the site, the subsurface data gathered for the judicial investigation were complemented with the stratigraphic data provided by other boreholes. They were drilled for the investigations ordered by the other parties involved in the judicial process.

3.1 Landslide Morphology

Three zones with different style of deformation can be distinguished at the landslide (figure 1).

The *head zone* is defined by a 70 m wide plain located inside the impoundment (between the head scarp and the dam). The plain is bounded by two sets of sub-vertical scarps, one corresponding to the head scarp (with a maximum accumulated height of 6 m) and the other one located close to the top of the dam (figure 1).

The *intermediate zone* or *dam zone* corresponds to the displaced dam. The dam was displaced towards the east with no major deformation. The horizontal maximum displacement (49 m) was observed at the central section of the dam and it progressively decreased towards the south. Northwards the horizontal displacement decreased to 24 m, close to the dam breach. Unlike the horizontal displacements, the vertical ones recorded at the dam top were very small; they involved a maximum descent of 2.4 m. It should be remarked that the dam moved without recording any tilting.

At the landslide *foot*, the ground surface bulged and rose up to 7 m. The horizontal displacements were of the same magnitude than those observed at the dam. The foot of the landslide invaded the flood plain of the Agrio River. The two trenches dug at the landslide foot showed that it was structured in two major units both incorporating blue clays, and terrace deposits. Each of these units corresponds to a thrust sheet bounded by a *west dipping* thrust fault through which the blue clays overrun terrace deposits. The frontal (easternmost) thrust marked the emergence of the failure surface and the toe of the landslide. Below this thrust, deposits of the flood plain (terrace T0) and the blue clays were found "in situ".

The displacements observed and the morphological features of the landslide indicated clearly that it corresponds to a *translational slide*, with a head consisting of a graben bounded on both sides by normal faults. The relatively small vertical displacement of the dam, and its downward sense, indicated that the movement occurred along a plane surface with a slight dip (2 to 3°) towards the east. The bulging and rising of the slide foot resulted from the splitting of the failure surface in two main branches, both of them with a westwards dip. The presence of blue clays on the slide foot shows that the failure surface developed within the clay formation.

3.2 Original Structure of the Blue Clays

The original structure of the blue clay can be observed at a few recent outcrops, made for mining works excavations. At these outcrops, the clays are only lightly weathered and do not show desiccation cracks. At the trenches and boreholes cores, the clays were saturated and the discontinuities were observed only after a drying of some days. The structure consists of several sets of sub-vertical fractures with predominant strikes N-S and NE-SW, and of almost horizontal bedding. The main characteristics of the bedding planes are: a) a strike of N050E to N070E



Fig. 2. Bedding of the Miocene blue clays at an outcrop of the Agrio River (left) and in a core taken below the dam and outside the landslide (right).

and a dip of 2 to 3° towards the SE; b) a spacing ranging usually between 0.5 to 3 m (figure 2); c) a continuity higher than 30 m; and d) a low roughness, sometimes showing slickensided or polished surfaces.

3.3 Borehole Data on the Location of the Failure Surface

Two inclinometer casings were installed at the foot of the slide (boreholes S3-2 and S4-2 in the figure 1). No significant displacements were recorded in any of them. Previous to the failure, four inclinometers casings were installed in the dam for stability control. One of them was located inside the area affected later by the slide. No premonitory signals of instability were detected on that inclinometer. After the failure a flexible tape with a plumb bob in one of the ends was lowered down the casing, but it jammed before reaching the base of the dam.

At the head of the slide, the failure surface was located without major difficulties. Here, the terrace T3 was lacking, and the tailings were directly in contact with the blue clays (figure 3). This disposition of the materials can be explained by considering the large displacement of the block formed by the dam and its foundations. The movement of this block created the graben observed at the head of the slide. The base of the graben had to coincide with the failure surface, which was developed within the blue clays. During the formation of the graben, the tailing deposits located in their flanks collapsed and progressively filled the graben basin.

To identify the failure surface below the dam and below the foot of the slide, a detailed logging of the discontinuities of the blues clays was carried out. Below the dam, a band with a high density of discontinuities was observed at depths between 17 and 12 m below the natural ground (that latter corresponds to the top of the terrace). Within this band there were several sub-horizontal slickensided planes and shear zones. The same base of the band was defined by a shear zone, which was bounded by slickensided planes. Beneath the band only some vertical joints and a few bedding planes were observed. A prominent feature found within

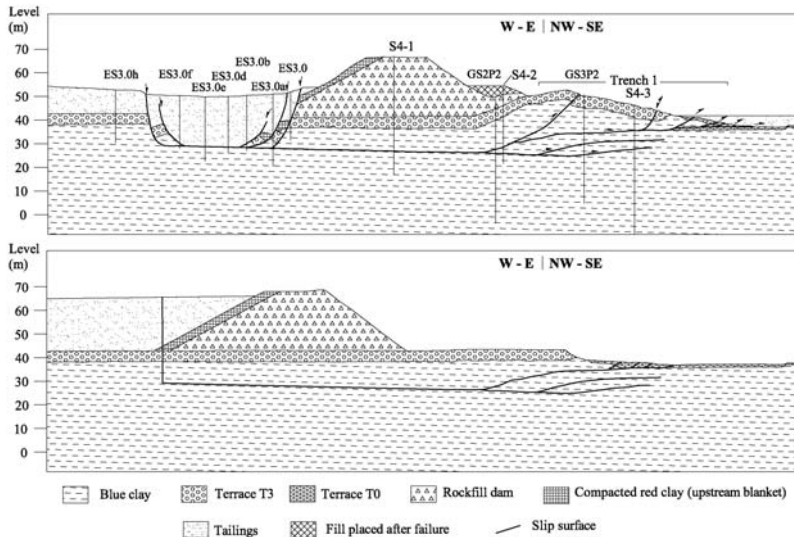


Fig. 3. Balanced cross-section (up) and restored cross-section (down) of the central sector of the slide. Only in the boreholes drilled for the judicial investigation (S4-1, S4-2 and S4-3 in this cross-section) the structure of the blue clays was analyzed.

the highly fissured band was a 1 m thick shear zone formed by horizontal (0 to 2° dip) shear surfaces showing a spacing in the order of millimetres. This shear zone was bounded by slickensided planes, which were located at 14 and 15 m depths below the natural ground. Two main interpretations are possible on the location of the failure surface in this zone of the slide: a) the failure surface locates at the base of the highly fissured band, then at a depth of 17 m below the natural ground; or b) it coincides with the shear zone showing high internal deformation which is located at a depth of 14-15 m.

At the foot of the slide several centimetre sized shear zones and slickensided planes were also detected (they are shown in figure 3). The former data indicate that several slip surfaces are present in all boreholes. Therefore, for a same cross-section multiple combinations can be drawn linking the shears observed in the boreholes. It is not possible to decide objectively which of the combinations correspond to the failure surface. It was especially important to decide the location of the failure surface at the dam zone (at 17 m or at 14-15 m depths below the natural ground). This problem was solved using the balancing of cross-section method.

4 Interpretation of the Failure Surface Geometry

4.1 Balancing of Cross-Sections

It consists in the construction of a geological cross-section in such a way that it can be restored to the situation previous to the deformation, with no changes of the

cross-sectional area. Balancing requires the following conditions to be accomplished (Dahlstrom 1969, Ramsay and Hubert 1988): a) the deformation does not involve a change of the volume of the materials; and b) the deformation is plane (two-dimensional) in the cross-section, that is to say, lateral migration of material does not occur from the cross-section. If the former conditions are fulfilled, then the area of the cross-section is preserved during the deformation, as well as the length and thickness of the beds.

4.2 Application to Aznalcóllar Failure

In Aznalcóllar case, the conditions required for balancing of cross-sections are accomplished. It is reasonable to assume that the volume of the landslide was conserved during the displacement. That is because the landslide was a translational slide, and no fluidal movements occurred (as, for example, happens in mudslides). The clays of the Guadalquivir Formation are swelling, but the error that this behaviour may introduce in the interpretation is negligible, if we take into account the magnitude of the displacements involved. On the other hand, although tailings escaped out from the head of the slide, for the reconstruction of the slide geometry it is not necessary to consider the existence of the tailings.

Severe geometrical restrictions controlled the balancing of the cross-sections of the slide. Main restrictions are defined by the location of the failure surface at the head and at the foot, and the depth of the slip planes detected in the boreholes. Other main restrictions were: the topography of the ground surface before and after the failure, the geometry of the terrace T3 before and after the failure, the observed surface displacements and the translational character of the slide. In particular, the two latter factors involved that the failure surface was a plane with a 2-3° dip below the head and the dam.

Cross-sections for three profiles were constructed; one of them is shown in figure 3. For each profile, the geometrical consistence of the preliminary interpretations of the failure surface was controlled by trying to balance the cross-section. In each trial, balancing was carried out conserving the length and local thickness of the terrace T3 and of the layer of blue clays located above the interpreted failure surface. It should be stressed that the cross-sections must be drawn following the displacement direction. This direction is N100E along the head and dam, but N128E along the foot of the slide. Finally, the balancing of each cross-section was possible only for one of the preliminary interpretations (figure 3). The final interpretation locates the failure surface at a depth of 14-15 m below the natural ground at the dam zone. The other main possibility for this zone, a location at 17 m depth, should require a rise of the ground at the slide foot several meters greater than the observed.

Another advantage of the use of balancing cross-section techniques, moreover of the test of the geometrical consistence of the interpretation, is that once a cross-section is balanced, it can be restored to the situation previous to the deformation (previous to the failure). Thus, in the case of the Aznalcóllar tailings dam, it was possible to deliver pre-failure cross-sections for the stability analysis (figure 3).

It should be remarked that at the head and dam zones of the landslide, the failure surface has the same orientation as the bedding of the Miocene clays (an average trend of N060E and a dip of 2 to 3° towards the SE), and that the dam failed *precisely* where the bedding of the Miocene clays had the most unfavourable orientation. This suggests that: a) the failure surface developed, for most of its extent, in a pre-existing discontinuity (a bedding plane), this explains the planar geometry of the failure surface which developed within a clay formation; and, b) the stability of the tailings dam was conditioned by the strength properties of the bedding of the clay formation, rather than those of the clay matrix.

5 Conclusions

The failure of the Aznalcóllar tailings dam was a consequence of a translational slide which affected to a sector of the embankment and to its foundations. The slide was very quick (it occurred in less than half an hour). Because of this the inclinometers installed after the accident provided no information about the location of the failure surface. On the other hand, the measurements of the surface displacements and the surface and subsurface geological data were insufficient to make a unique interpretation of the failure surface. From these data preliminary cross-sections can be drawn. The determination of the geometry of the failure surface is possible by testing the consistency of the preliminary cross-sections. This can be done using the balancing cross-section method. When the available data (topographical, surface displacement and geological data) are detailed enough, as in the study case, the failure surface can be located with a precision of 1 m. Balanced cross-sections can be restored to the situation previous to the deformation (previous to the failure) and used as the basis for the stability analysis.

The coincidence of the orientation of the failure surface with that of the bedding of the Miocene clays suggests that the rupture developed in a bedding plane of the clay formation, and that the stability of the tailings dam was governed by the strength of these pre-existing discontinuities.

References

- Dahlstrom DCA (1969) Balanced cross-sections. *Can. J. of Earth Sciences* 6: 743-747.
- Bishop KM (1999) Determination of translational landslide slip surface depth using balanced cross-sections. *Environmental and Engineering Geosciences* 5: 147-156.
- Hutchinson JN (1983) Methods of locating slip surfaces in landslides. *Bull. Ass. Eng. Geol.* 20: 235-252.
- Moya J (2000) Reconocimiento geológico de la rotura de la balsa minera de Aznalcóllar. Annex 3 of the expert report. Dpt. of Geotechnical Engineering and Geosciences, Technical University of Catalonia, 123 p.
- Ramsay JG and Hubert MI (1988) Faults and the construction of balanced cross-sections. In: Ramsay JG and Hubert MI, *The techniques of the modern Structural Geology*. Academic Press. Oxford. vol 2, pp. 543-559.

Obstacle Investigation RandstadRail in Rotterdam, The Netherlands

Robert Berkelaar and Melinda van den Bosch

Engineering Department Rotterdam Public Works, Projectbureau RandstadRail
P.O. Box 6633, 3002 AP Rotterdam, The Netherlands
r.berkelaar@gw.rotterdam.nl
Tel: +31 10 4896922
Fax: +31 10 4897855

Abstract. RandstadRail is a light rail project connecting the cities of Rotterdam, The Hague, and Zoetermeer in The Netherlands. Part of the project is the connection of the Rotterdam metro system to an existing railway line. This section is called the ‘Statenweg-tracé’, 3 km in length of which 2.4 km will be realised by two single track bored tunnels. Halfway a new underground station will be built. Part of the integral design was an extensive underground obstacle investigation programme carried out by the Engineering Department of Rotterdam, Public Works. The goal of the obstacle research was to assess the type and extent of subsurface objects along the alignment in general and more specifically in the bored tunnel sections. This in order to minimize the risks caused by subsurface obstacles and take preliminary actions against such an event. As part of the obstacle investigation a desk study was performed which included historical research in public and private archives. For two locations where foundation remnants were identified, an 18th century steam driven pumping station and an 19th century gas factory, this resulted in additional field-investigation consisting of geophysical techniques and “blind” cone penetration tests. A tailor made design philosophy was adopted because of the presence of wooden piles in the bored tunnel alignment. Both cases and design solutions are presented in this paper and will be concluded with recommendations of how to deal with obstacle investigation during the design process of large line infrastructure projects.

Keywords: RandstadRail, bored tunnels, urban area, obstacle investigation, geophysics, design solutions, Rotterdam, Netherlands.

1 Introduction

Four major cities of the Netherlands: Amsterdam, Rotterdam, The Hague, and Utrecht are situated in the western part of the Netherlands (fig. 1). Between these cities, many people travel each day resulting in traffic jams on highways and in the inner cities. There is also an increasing pressure on the public transport system to be more profitable as well as reaching a higher level of service. One of the projects to alleviate the mentioned problems is RandstadRail. RandstadRail is a

light-rail link between the cities of Rotterdam, The Hague, and Zoetermeer (close to The Hague). RandstadRail will make it possible to travel between these inner cities without transfer. In Rotterdam RandstadRail will be connected to the North-South line of the local metro system at Rotterdam Central Station (fig. 2). Rotterdam Central Station is labelled as a so called national “key-project” because of its great importance for public transport in the Rotterdam area. RandstadRail and the arrival of the High Speed Railway link Amsterdam - Paris are part of this key-project. The underground tunnel of RandstadRail in Rotterdam will be built in an urban area, which is unique for bored tunnels in the Netherlands. So far, only bored tunnels have been realised in non-urban areas. The RandstadRail alignment in Rotterdam will follow the “Statenwegtracé” called after the main street overlying the tunnel. This section will be 3 km in length of which 2.4 km will be realised by two single track segmented concrete lining shield driven bored tunnels. A new underground station and the start and receiving shafts will be made by conventional building techniques. The tender with detailed specifications took place in October 2003.



Fig. 1. Map of the Netherlands.

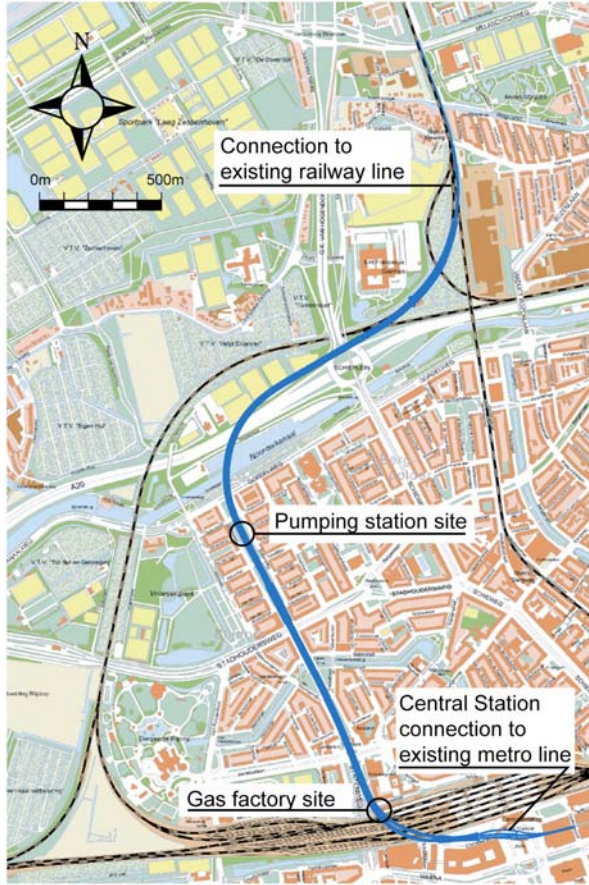


Fig. 2. Horizontal alignment of RandstadRail in Rotterdam.

2 Design

The design of RandstadRail in the Rotterdam area has been performed by the Engineering Department of Rotterdam Public Works. An important part of the design process was an extensive obstacle investigation programme. The goal of the obstacle research was to assess the type and extent of subsurface objects along the alignment in general and more specifically in the bored tunnel sections. This in order to reduce the risks caused by underground obstacles. Examples of these risks range from the tunnel boring machine (TBM) encountering an unknown obstacle to obstacles jeopardising the structural integrity of the tunnel. The research has been carried out following a systematic approach under supervision of a multi-disciplinary team including an archaeologist, geophysical experts, as well

as engineering geologists and civil engineers. The obstacle investigation started with an extensive historical research. With the results of the desk study, several locations were identified that required further (field) investigation to obtain answers concerning unresolved issues. Parallel a study was performed to identify and label obstacle investigation techniques that could be used in a later stage to detect and investigate obstacles in situ.

3 Ground Conditions – Vertical Alignment

The ground conditions in the Rotterdam urban area can be characterised as follows: first, a layer of antropogene sand, followed by soft Holocene clay and peat layers to a depth of 16 m below reference level (NAP). At this level, the Pleistocene sand strata starts and continues down to a depth of NAP -35 m. Below this layer the Kedichem formation is present. The surface level varies around NAP +0 m and the groundwater level is at approximately NAP -2.5 m. A simplified geological cross section is presented in the vertical alignment (fig. 3). The vertical alignment is dictated by costs (building and exploitation) and the geology of the area. From a financial point of view, a shallow vertical alignment would be most favourable. However, good foundation properties are required for the bored tunnel sections, which can be found in the Pleistocene sand strata. An advantage of a deep vertical alignment is less obstacle related risk. Locally, at locations where the tunnel connects to the shallow conventional elements, the bored tunnel crosses soft Holocene strata (fig. 3).

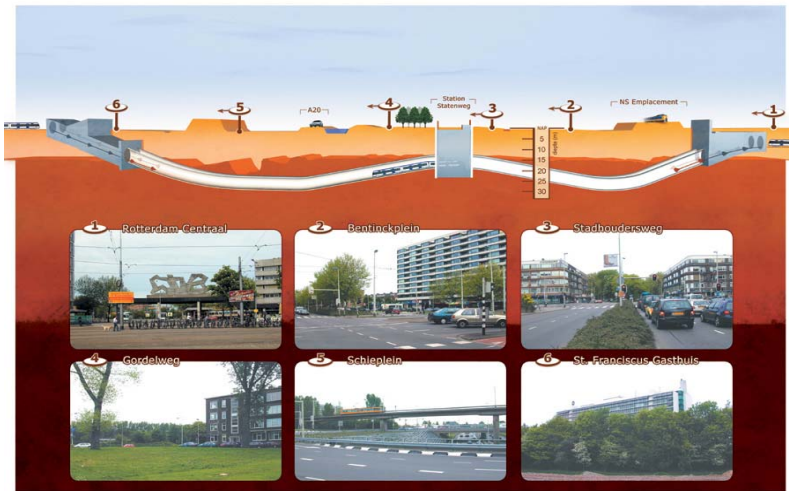


Fig. 3. Vertical alignment of RandstadRail in Rotterdam (source: MCW Studio's, Rotterdam).

4 History of the Project Area

To determine the presence of subsurface obstacles a detailed study was made of the history of the project area. With the aid of city plans dating back as far as the 19th century construction and demolition of building structures was determined. History books and archives concerning the construction of the railway tracks and train stations in Rotterdam were consulted. Authors of these books were interviewed to obtain all possible information on the subject. To gain further insight in the history of this part of Rotterdam during the middle ages the Archaeology Department of Rotterdam Public Works conducted an investigation. To go even further back in time engineering geologists researched the geology of the area to investigate the presence of natural subsurface obstacles like boulders.

During the last ice age (Weichselian) the ice sheets never reached Rotterdam, thus no boulders and only Pleistocene sand and gravel layers were deposited. Although subsurface river dunes have been documented in the area of Rotterdam before, none is known to exist in the project area. During field investigation, evidence of a river dune was found on the south side of the railway yard at Rotterdam Central Station. Remnants of human habitation were identified in samples taken of the river dune, which were dated by C14 analyses to 5.500 BC. The river dune has probably been used as temporary dwelling place meaning that wooden canoes, as well as fallen down tree trunks, can be present. It was not till dikes were constructed in the middle ages that permanent structures were built in the polders of Rotterdam. The polder of Blijdorp was created in the 14th century when the city of Delft commissioned the man-made canal "The Schie". These permanent building structures consisted of a few scattered farmhouses. The most prominent structure, with a wooden pile foundation, was a steam driven pumping station built in 1786. The city plans show that Rotterdam Central train station, with a gas factory on the northern edge of the railway yard, was built in the 1870's on the outskirts of the city in the polder. It was not until the 1920's that the Blijdorp polder north of the train station was made ready for building through hydraulic filling with dredged material. Shortly thereafter houses were built in this new urban area. During the 2nd World War the city centre south of the train station was heavily bombed. Consequently, temporary emergency stores and houses were built in Blijdorp. With the information of various potential obstacles in the alignment of the bored tunnel a detailed research was performed in the archives of the City of Rotterdam. However, some crucial documents were lost during the bombardments of the 2nd World War. Extensive research was done in local, private, and national archives to find the missing building plans and other relevant information.

5 Case Studies

To illustrate the obstacle research programme two case studies will be discussed in more detail. Firstly the foundation remnants of a 18th century steam driven pumping station and secondly the foundation remnants of a 19th century gas factory.

5.1 Desk Study: Steam Driven Pumping Station

One of the first Dutch steam driven pumping stations built in 1786, was located on the south bank of the canal “The Schie” (fig. 4 and 5). The pumping station was equipped with the first James Watt steam engine in Holland. The pumping station only served a short time not because of poor pumping qualities; these were actually amazing at that time with approximately 45.000 litres of water per minute, but mainly due to politics and resistance of local farmers. According to which the “devilish fire machine” would disturb the milk production of the cows and cause traffic jams! In 1797 the steam engine was sold and the building demolished. In 1904 the chief engineer of Rotterdam Public Works conducted a survey of the foundation before the area was made ready for building. Unfortunately, this specific bit of surveying information was destroyed in the 2nd World War. From other sources, the layout of the building and type of foundation became clear, however not revealing the exact location. The foundation consisted of 180 wooden piles with a maximum length of 15.7 m, installed from a building pit of 4.4 m depth. The approximate location as deduced from the desk study was confirmed during soil investigation. In a borehole, brick rubble was found and later identified by an archaeologist as originating from the 18th century. Knowing the approximate location and the range of depth where to expect wooden piles, the risk at hand became more prominent. This risk consisted of a conflict between the TBM and the wooden piles and, later after the tunnel is finished wooden pile remnants may possibly rest on the tunnel lining (fig. 5). In order to be able to assess the full extent of this potential problem and to reduce and/or control the risk, answers had to be found to the following questions: 1) what is the exact location of the foundation of the pumping station, and 2) what is the depth of the toe of the wooden piles.

5.2 Desk Study: Gas Factory

In 1870's the construction of a new train station at the location of the present day Rotterdam Central Station was commenced. The two railway companies that were to exploit the railway tracks each built their own buildings and railway tracks. As the terrain of the new railway yard was a polder a special canal from the canal



Fig. 4. Sketch of pumping station “Stoom-machine” (source: museum Atlas van Stolk, Rotterdam).

“The Schie” was made to transport sand from the dunes at the coast to the site. In total, an amount of 623,780-m³ sand was needed to create a solid underground on which to lay the railway tracks. At the northern edge of the railway yard, a gas factory was built. The gas was used for the illumination of the train carriages. In the 20th century the two companies merged to form the newly state owned ‘Nederlandse Spoorwegen’ and subsequently due to the changing times and need for expansion, all buildings, but not the foundation piles, in the railway yard became obsolete and were demolished (fig. 6). The gas factory, built in 1893, consisted of four buildings. According to the building plans 423 wooden piles with a length of 18 m were driven, theoretically, 5 meters in the Pleistocene sand layer. Extensive pile foundation calculations showed it could be possible that the piles could be driven to this depth. The original co-ordinates of the buildings were supplied by the Dutch land register, although in itself accurate there was some inaccuracy

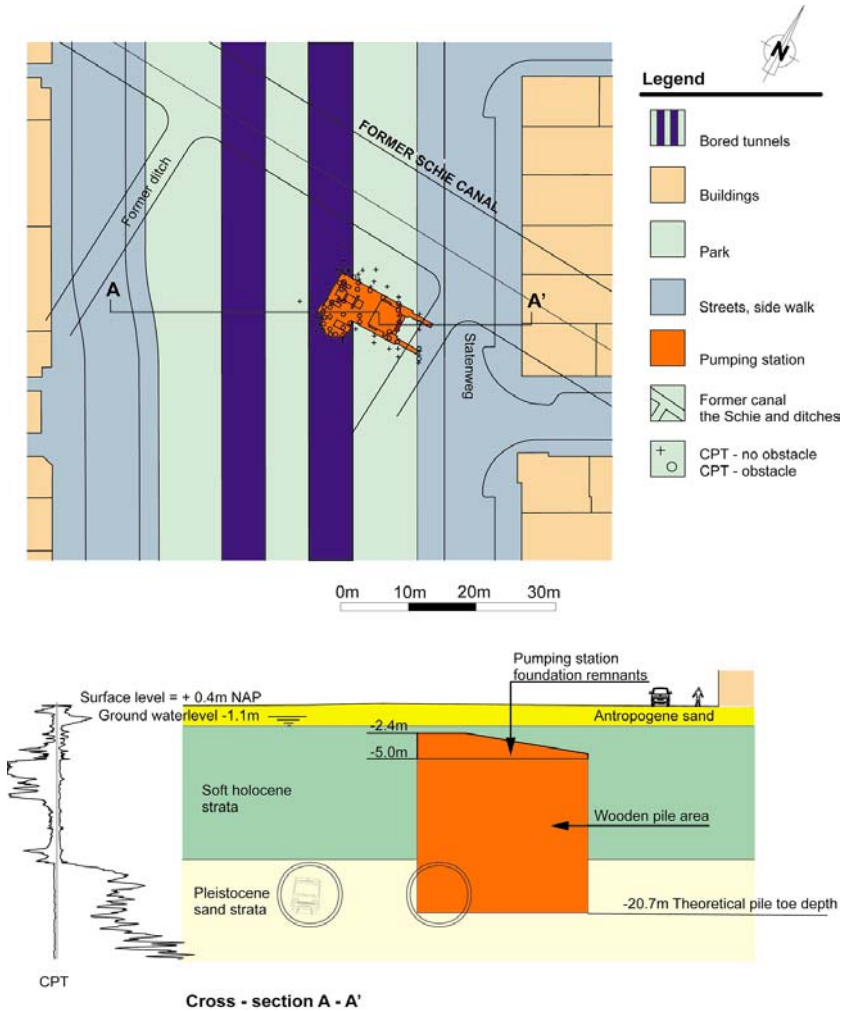


Fig. 5. Plan and cross-section at the pumping station site.

(approximately 30 cm) due to transformations. The resulting location of the buildings showed that the piles would be well within the proximity of the TBM (fig. 6 and 7). Since the construction of the railway yard, the ground surface level has been raised several times due to ongoing settlement. This means that the top of the wooden piles are situated at approximately 6.5 m beneath the surface. The risk at hand, similar to the pumping station site, became more prominent and more investigation was required to investigate the risk causing piles and in a way to reduce and/or control the risk.

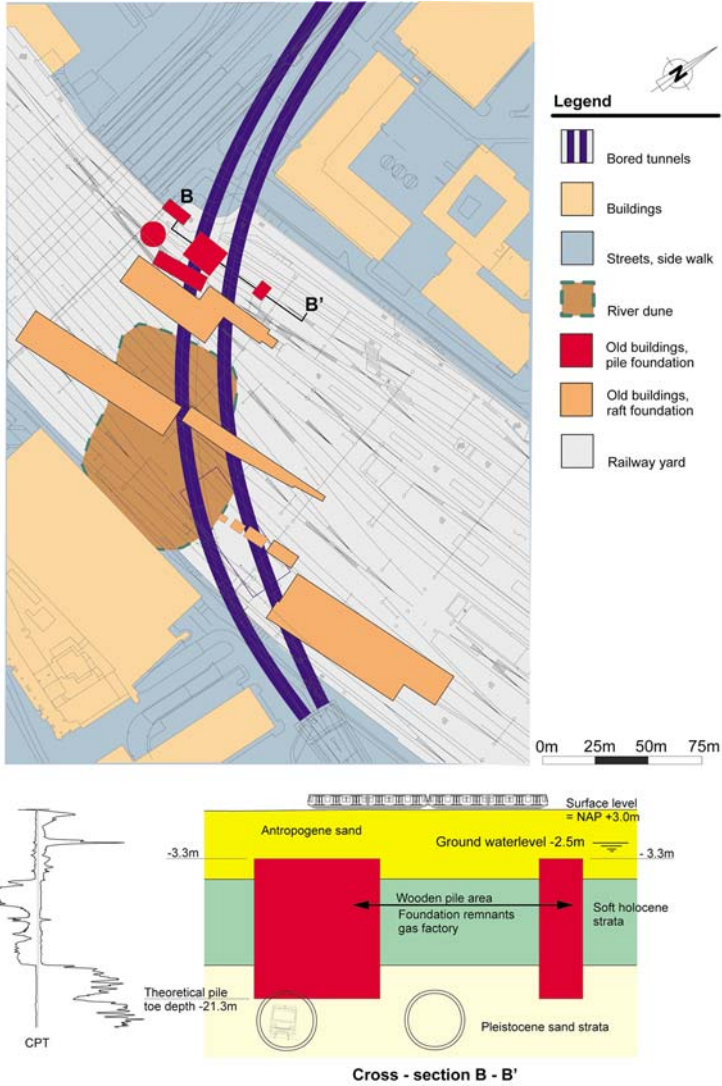


Fig. 6. Plan and cross-section at the gas factory site.

5.3 Field Investigation

It was decided to continue the obstacle investigation by additional field investigation since further historical research was not likely to give the required answers. The field investigation at the pumping station site was used as a test case to determine the best applicable field investigation techniques. Knowing the best tech-

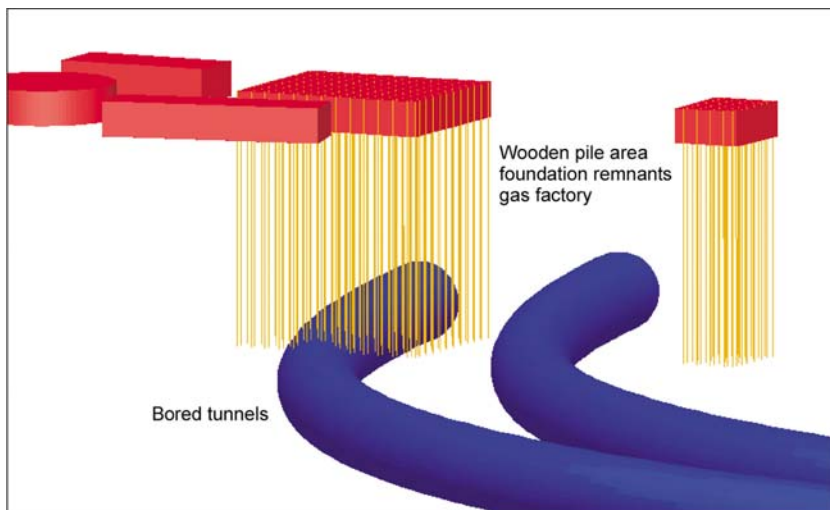


Fig. 7. 3D Representation of TBM and pile foundation at the gas factory site.

technique an efficient investigation would be possible at the site of the gas factory where difficult site conditions prevail due to the intensive exploitation of the railway embankment and the depth of the piles below the surface.

5.3.1 Part I – Where?

The question ‘Where?’ only had to be answered for the pumping station site since the location of the gas factory was known with an acceptable accuracy.

The potential area for the location of the pumping station had already been narrowed down by historical investigation and soil investigation to a circle with a radius of approximately 25 m. Because of the relatively favourable surface conditions, i.e. in a park, geophysical methods were applied first. After consulting geophysical experts it was decided to make trail runs with a pE 1000 ground radar system and a Campus Geopuls Resistivity meter. The penetration depth of the ground radar system proved to be less than 2.5 m below surface level thus not reaching the top of the foundation remnants. This is probably caused by the high groundwater table and due to peat and clay inclusions. The electrical resistivity method promised to be more successful after the first two trail runs. However, it was impossible to interpret a third run, made exactly over the location where the pumping station was identified by soil investigation. At this point, the geophysical surface methods were abandoned and it was decided to use probing techniques. A track mounted CPT truck was mobilised and the contours of the foundation were probed by executing “blind” CPT tests while registering the depth of refusal. In the end, this method proved quite efficient, the detected contours matched almost perfectly with the original building plan (fig. 5). The field investigation confirmed that the location of the pumping station was indeed located above the alignment of

the eastern tunnel tube. Further research concerning the depth of the wooden pile toes was necessary since it was not possible to change neither horizontal nor vertical alignment of the tunnels and thus divert from the obstacle.

5.3.2 Part II – How Deep?

The goal of the investigation was to find a technique capable of determining the pile toe depth with an accuracy of at least 0.1 m suitable for both sites.

An inventory was made of all potential techniques available to determine the depth of the wooden foundation piles resulting in the following possibilities:

- 1) Dig up the foundation and pull out a pile. This option was not very favourable, it might be possible at the location of the pumping station, regardless of the high costs and consequences for the nearby surroundings (removing trees, lowering groundwater table) but at the site of the gas factory this option would have an enormous impact for the railway traffic and is virtually impossible.
- 2) Dig up foundation and use sonic integrity testing techniques to measure the pile length. This option was not likely to work for wooden piles and still a considerable pit would be needed to reach the pile top and therefore not feasible at the gas factory site.
- 3) Use geophysical techniques. This option working with geophysical techniques was the only resulting and most practical option to investigate the pile toe depth. Surface techniques were not investigated in detail since these would not be applicable at the gas factory site due to the abundance of rails, cables etc. Thus, down-hole geophysical techniques were studied in more detail.

The down-hole techniques can be divided in 2 groups: 1) working with pulse reflection, and 2) tomography techniques. Seismic and radar techniques can be used in both configurations. Tomography was not considered to give good results since the rays (radar or seismic) would most likely follow the easiest way and bypass the wooden piles.

Seismic pulse reflection techniques were not considered in more detail because it would not be possible to reach the desired accuracy of 0.1 m. Radar electromagnetic pulse reflection techniques seemed to be very promising, especially the 3D radar of T&A Survey. This down-hole tool has a directional sensitive antenna and by doing measurements at different depths a 3D image can be created. Before this tool was to be applied in the field, tests were done to establish the penetration zone of the 3D radar. Sand and groundwater samples from the expected pile toe depth were taken and tested with the actual radar frequency. The results of these tests were, unfortunately, disappointing. The soil conditions in situ were such that a penetration depth with a maximum radius of 2 m was expected. However, the first 1.5 m was a so called 'blind zone', in this area the direct arrivals mask the reflected signals. The chance of successfully detecting the pile toe depth was too low and it was decided to abandon the geophysical investigation and end all in-situ investigation concerning the pile toe depth at the test site of the pumping

station. As a result, the design for both the pumping station and gas factory site had to be adjusted since the study and tests did not result in any potentially successful techniques to determine the pile toe depth.

6 Design Solutions

As a result, from the obstacle investigation the design philosophy had to be adapted in such a way that the uncertainties of the unknown pile toe depth and associated risks were coped with.

The following design philosophy was adopted. In general it is possible for a TBM to drill through wooden piles, if the piles are sufficiently horizontally fixated, the cutting wheel is prepared for wood cutting and the drilling speed is adjusted. This, however, creates extra risks, costs, and is a time consuming process. Therefore, if removal of the piles is possible and large numbers of piles are expected, the piles should be removed beforehand. But, if the removal of piles itself involves great risks and costs, boring through the piles is an acceptable option. With this design philosophy in mind the two cases were dealt with as follows.

6.1 Pumping Station

For the design, a worse-case scenario was adopted based on the maximum theoretical pile toe depth. It was decided that all piles have to be removed by the contractor before the TBM reaches the site based on following reasons:

- there are a large number of piles, probably more than 100 in the tunnel cross-section at this location;
- drilling through piles is very difficult because of the poor horizontal fixation of the pile top in the soft Holocene layers,
- the remainders of the piles, when drilled through by the TBM, might impose unfavourable forces on the tunnel lining in time caused by negative skin friction,
- at the pumping station site, a park, it is relatively easy to remove the piles from the surface.

The removal of the foundation remnants and pulling of the piles will be followed closely by archaeologists because of its historical value.

6.2 Gas Factory

For the gas factory site a similar worse-case scenario was adopted. However, at this site it was decided to drill through the piles because of following reasons:

- horizontal fixation of the piles seems sufficient at this location. The piles are fixated at the top in the thick antropogene sand layer,
- forces of pile remainders on the lining are tolerable if present at all. Because negative skin friction is distributed by overlying layers,
- pile removal is very difficult and complex since the site is located under a heavily exploited railway embankment.

7 Conclusions

The obstacle research programme as executed by the Engineering Department of Rotterdam Public Works seems to be very successful. However, the final judgement can only be given when tunnel boring is finished. At this time following recommendations can be given, identified as critical success factors:

- 1) make an early start with the historical investigation:
 - Although usually with time most of the required information such as building plans can be found in archives, it is not evident from the start where this specific information is contained. Therefore, much time is needed to follow up on leads concerning the various local, national, and private archives and find the relevant information. Most archives do not have on-line services and specific background information is needed to extract the required information from the immense amount of historical documents stored in all these archives.
 - An early start gives time to cope with unexpected results from the historical research.
- 2) Include different relevant disciplines in the obstacle research team:
 - As a result of the different views from the different disciplines (especially archaeologists) the problem can be seen in it's proper context.
 - By doing so different interests can be integrated in the contract in the way the obstacle is dealt with. I.e. giving the archaeologists time to do their fieldwork during construction.
- 3) High tech geophysical techniques are very promising and might be very useful in obstacle detection:
 - However, these techniques are very sensitive to surface conditions and unfavourable ground properties, as was the case with the two discussed locations. One should therefore not rely on geophysical methods only, especially when working in urban areas.
 - Furthermore the detection of wooden objects in soft soils is very difficult. One should not rely on positive results and think ahead in 'what if' scenario's.

Tunnelling in Urbanised Areas – Geotechnical Case Studies at Different Project Stages

Stefan Eder¹, Gerhard Poscher¹, and Bernhard Kohl²

¹ ILF Beratende Ingenieure ZT GmbH, Framsweg 16, A-6020 Innsbruck, Austria

Tel: +43 512 2412 0, Fax: +43 512 2412 200

Tel: +43 512 2412 171, Fax: +43 512 2412 200

{stefan.eder, gerhard.poscher}@ibk.ilf.com

² ILF Beratende Ingenieure ZT GmbH, Harrachstraße, A-4020 Linz, Austria

bernhard.kohl@linz.ilf.com

Tel: +43 732 784663 0, Fax: +43 732 784663 63

Abstract. Tunnelling in urbanised areas is always a challenge for the client and the contractor as well as for the designers, the engineers, and the geologists. The high demand for space and the disturbance of existing infrastructures by construction measures increasingly forces future infrastructure projects to be carried out underground. At the same time, interferences with human, natural or water resources shall be reduced and noise, dust, as well as site traffic shall be minimised. Quite frequently, politics also come into play. All these factors may lead to pre-determined routes, with ground conditions which may not always be very favourable. This article presents examples of different projects at different stages and emphasizes the importance of engineering geology in the route selection process. The most promising options are routes located in ground, which is not sensitive to settlement and/or water ingress. A longer route in favourable ground conditions is to be given preference over a shorter route in adverse ground conditions. In case of no alternative, the risk of surface settlements and exploding construction costs have to be taken into account. The first project presented is the railway line in the Inn valley / Tyrol, comprising four sections in urbanised areas, which – due to environmental and political reasons – have to cross infrastructure facilities and traffic lines, often in unfavourable ground conditions. There is a variety of construction methods in the tender design to be applied in urbanised tunnelling ranging from NATM tunnels with local groundwater draw-down and jet grouting enclosure against water pressure, to TBM-driven tunnels with hydro-shield. The second project is a planned by-pass for the city of Linz, which is at the environmental impact assessment stage. The alignment is dominated by geological considerations, avoiding unfavourable ground conditions to the greatest possible extent.

Keywords: tunnel, urban area, routing, NATM, TBM.

Geological Aspects of Tunnelling in Urbanised Areas

Without additional support measures, tunnelling or groundwater lowering works often lead to critical and uncontrolled surface settlements, which are the main hazards of tunnelling in urbanised areas (Schubert 2002, Vavrowsky and Pöttler

2002). Therefore, the geological analysis does not only concentrate on rock mass types and rock mass behaviour types including an evaluation of the geotechnical parameters for the excavation and the inner lining, but also focuses on ground improvement options and on hydrogeological aspects. Unfortunately, the alignment is often dominated by aspects other than geology and geotechnics. Political necessities, i.e. finding a route which will excite as little opposition by the resident population as possible, environmental considerations, i.e. safeguarding water resources, wildlife habitats, human interests and last but not least technical requirements – i.e. lining parameters, guidelines and regulations often force the engineer to resort to sites which are characterised by unfavourable ground conditions, with high groundwater tables, old foundations, sensitive soils, etc. If these ground conditions are unavoidable, additional measures will have to be taken to minimise the risk for buildings at the surface. In this case the engineering geologist will have to point out the risks resulting from the complex sedimentological environment. One example for a tunnelling project, which is predominantly located in unfavourable water-bearing gravel and sand – is the new railway line of the Munich – Verona railway axis in the lower Inn valley / Tyrol – the northern approach to the Brenner base tunnel.

Case Study 1: Railway Tunnels in the Lower Inn Valley / Tyrol

The Project

The existing railway line in this area has already reached its capacity limits, which should be solved by the construction of a new 43 km long high-capacity railway line (approx. 80 % in tunnels). The line is composed of seven individual construction lots, which – depending on the soil conditions encountered – are planned according to the NATM, cut-and-cover or shield tunnels (Eder et al. 2004). The following table gives an overview of the different construction methods and the sites in urbanised areas.

Route Sections in Urbanised Areas

As shown in figure 1 the urbanised areas will have to be crossed or underpassed in four locations. All other crossings, including the crossing of the river Inn, will be situated in the open field and shall not be discussed in this paper. Because of the extent of the planned construction measures in urbanised areas, this article shall only present an overview focusing on the results of the first tunnelling works in these sections.

Construction Methods and Geological Risk Assessment

All these tunnel sections lie in heterogeneous softrock (mostly gravel and sand) below the groundwater table. The option of groundwater lowering was eliminated

as a result of the environmental impact assessment and a mined excavation was demanded in the sections listed in the table. Because of the length of these sections, different construction methods were chosen for the tender design, firstly open pits using NATM tunnelling in urbanised areas and secondly hydroshield excavations.

Table 1.

Area	Geology	Construction method(s)	
Underpassing of a sports ground in the town of Brixlegg (length: 0.2 km)	Heterogeneous quaternary sediments	Pilot tunnel under a jet-grouting roof; running tunnel with groundwater lowering (pipe-roof)	
Crossing of the Inn valley motorway and the existing railway line near the town of Jenbach and the village of Stans (lengths: 0.7 km and 0.8 km)	Alluvial sediments of the Inn valley bottom – gravels and sands	TBM with hydroshield	Jet-groutig umbrella from the surface and compressed air
Undercrossing of the existing railway line and the station in the town of Wattens (length: 0.8 km)	Alluvial sediments of the Inn valley bottom – gravels and sands	Jet-grouting umbrella from the tunnel face and compressed air	

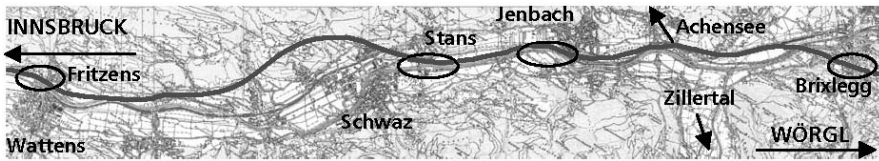


Fig. 1. Overview of sections in urbanised areas of the railway line in the lower Inn valley / Tyrol.

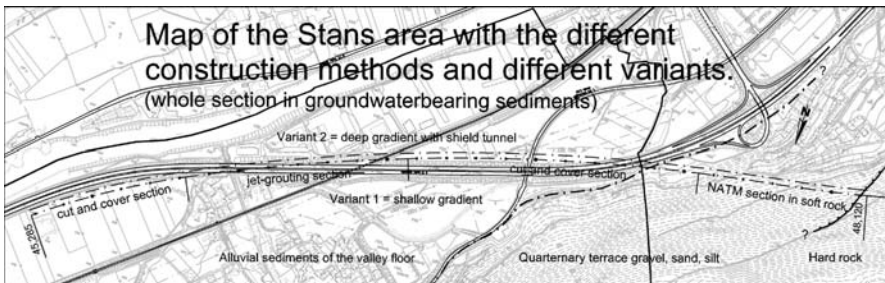


Fig. 2. Map of the Stans area with different construction methods.

The NATM requires an enclosure of the tunnel prior to the excavation to prevent water ingress. Jet grouting was thought to be the solution to this problem as it represents a construction method that can well be adapted to varying ground conditions.

The geotechnical risk assessment concentrated on the diameter of the jet-grouting columns depending on the ground conditions, the jet parameters, and the inclination of the column. For an advanced risk assessment in the form of an in-situ test, a pilot tunnel (see the following chapter) and different test columns – some in a test shaft – were constructed. All these tests revealed that with columns with an inclination exceeding 45°, unacceptable diameter variations tend to occur. In other words, the impermeability of the enclosure cannot be guaranteed in the heterogeneous ground of the Inn valley. Experiences acquired during construction showed the disastrous effect even of a minor water ingress (see the following chapter), which led to a new risk management philosophy for all project sections in urbanised areas. In light of these facts, additional measures were required if settlement risks due to soil erosion into the tunnel were to be avoided by all means. A redundant system comprising a jet-grouting enclosure to reduce the water and air permeability and to improve ground conditions and compressed air to control the water pressure was introduced.

The “Matzenpark” Crossing of the Radfeld – Brixlegg Tunnel

Geology of the “Matzenpark” Area

The alignment of the Radfeld - Brixlegg tunnel had to be planned in a way that the mineral water aquifer of the so-called Alpquell springs would not be adversely affected. It was for this reason that the NATM part of this tunnel with a length of approx. 5 km had to leave the hard-rock formations for a stretch of approx. 250 m – the so-called “Matzenpark” crossing (Nemec C. 2002). The “Matzenpark” (Figure 3) is an area used for recreation and sports by the local people, situated east of Brixlegg. Exploratory drillings revealed that the flat “Matzenpark” area was a syncline of the Inn river, formed by glacial erosion in the surrounding hills made up of dolomite. Shortly after the retreat of the mighty Inn glacier, remnants of this glacier remained stationary, which finally melted with different sediments ultimately accumulating in the resulting syncline. In the centre of this syncline, silts were deposited. The water content of this sediments is very variable but in some cases still high. The bottom layer of sediments is overlain by dipping sands and gravels of a foreset (deltaic sediments). This dipping was probably intensified by a surge of the nearby Inn glacier leading to vertical “faults” in the sediments.

Construction of the Brixlegg West Pilot Tunnel

From a hard rock cavern, which was reached through an access tunnel, the 5-m-diameter pilot tunnel was driven into the soft rock of the “Matzenpark” syncline. With the water table lying approx. 5 m above the roof of the ultimate running tunnel - jet-grouting columns were installed around the entire excavation to protect the tunnel against water pressure. Once this “umbrella” had been created by

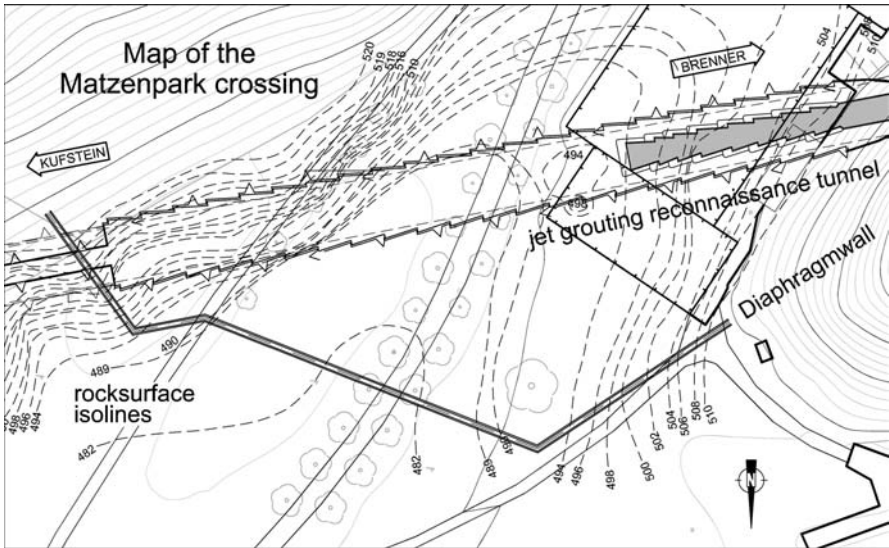


Fig. 3. Map of the “Matzenpark” crossing.

jet grouting, the end of the umbrella could be reached in 6 excavation sequences. For safety and soil improvement reasons, expensive additional injections were inevitable. But even with these additional injections with bentonite-cement slurry, erosion processes between the jet-grouting columns could not be prevented. Silty and sandy horizons, which reduced the planned diameter of the columns led to water and material ingress into the tunnel behind the 6th umbrella, producing a crater at the tennis court above. It was proved that even with extensive additional injections, water ingress could not be prevented in heterogeneous sediments. For this reason, the pilot tunnel was finally abandoned upon completion of umbrella no. 8. Once the final alignment approval for the route and an additional water authority permit had been obtained, the groundwater table could ultimately be lowered for the crossing. For this groundwater drawdown, the syncline was dammed against the groundwater from the Inn valley with a diaphragm injection wall, which was founded in the underlying rock. The groundwater lowering was accomplished by the installation of 8 wells. For reasons of cost reduction, the crossing was constructed in the ultimate profile of the running tunnel under a double-pipe roof. But even with the water table being situated beneath the lining, local horizontal water ingress still caused major problems by erosion of sand and gravel. This water ingress could not be drained even by closely spaced well pipes (distance 2 m!). Additional problems were experienced as a result of the high-plasticity silts encountered in the middle of the “Matzenpark” syncline. The danger of water ingress and settlement in soft rock manifested itself in two additional collapses. The lessons learned at this site were that with soft rock at the tunnel face even minor water ingress might lead to serious problems during tunnel construction, which may even include major threats of collapse. It is impossible to

drain efficiently horizontal water flows, e.g. on layers of silt or gravel with a high sand fraction, which cannot be identified by core drillings. If infrastructures have to be underpassed, additional injections, jet grouting or compressed air may become necessary to minimise the danger caused by water ingress and erosion. If NATM tunnelling in soft rock beneath the groundwater table may not be avoided, designers and clients must be aware of the additional measures, which might become necessary, and of the risks and costs possibly involved.

Case Study 2: Linz Western City By-pass

The Project

Another project where the attempt was made to minimise the geotechnical risk is the Linz city by-pass, which is approaching the environmental impact assessment stage in 2004. Even at the preliminary design stage, intensive soil reconnaissance works were carried out to determine the very alignment which least affects, both the resident population as well as existing buildings and traffic routes. This new motorway is part of the important traffic connection from the Czech Republic to Austria and for commuter traffic to the industrial region of Linz / Upper Austria. In the first stages of the project, two variants with different construction methods and different routes were discussed (Figure 4).

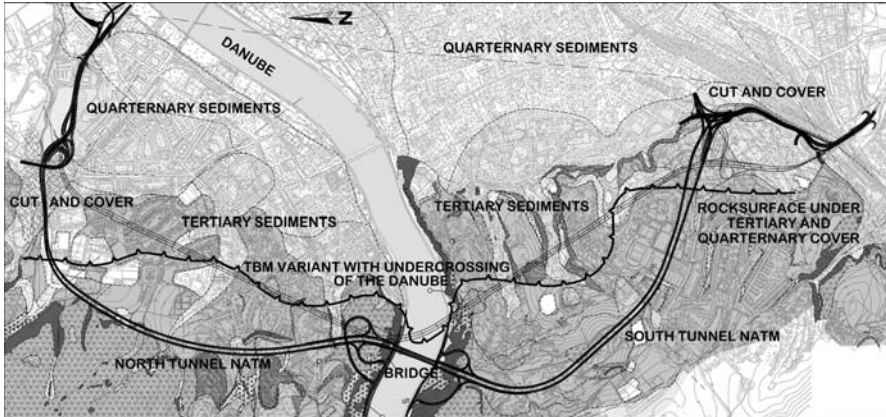


Fig. 4. Geological map with Variant1: Western city-by-pass Linz and Variant 2: direct TBM-variant.

The first variant, the alignment of which was optimised based upon the knowledge gained during two soil reconnaissance campaigns conducted in 2000 and 2002, consists of two double-tube highway tunnels with surface sections (length approx. 0.75 km), cut-and-cover sections (length approx. 0.55 km) and NATM sections (length approx. 5.35 km, 1.45 km in soft-rock). In the vicinity of the junctions, up

to 4 lanes will have to be constructed. The Danube shall be crossed by two 3-lane suspension bridges. A second variant was to shorten the entire length of the by-pass by a more direct route with a double-tube tunnel. This tunnel should be driven with shield machines, which will have to be adapted for hard-rock excavation. The bridge solution was abandoned in this variant, to be substituted by a subaqueous crossing of the Danube. All connection tunnels for the exits shall be advanced by NATM excavation.

The Geological Situation

The geology of the so-called “Bay of Linz” is dominated by three major formations. The “bay” was formed in paleozoic hard rock of the Bohemian massive – gneiss and granite. After a long period of erosion, tertiary sands and silts were deposited. This over-consolidated soft rocks are covered by gravel and silt of quaternary terraces with a mighty groundwater aquifer. It was the prime aim of the route selection process for Variant 1 to minimise the tunnel sections in tertiary and quaternary sediments and to construct the by-pass in hard rock.

Soil Reconnaissance and Route Selection

The following geological risks were – by means of core drillings (app. 2.900 m), in-situ tests, well pipes for pumping tests, geophysical investigations and surface mapping – identified in the reconnaissance campaigns for the environmental impact study (ILF-IBK 2000-2003):

- quaternary terraces, which are frequently covered by layers of silt and clay up to a thickness of 18 m
- large quantities of groundwater in the quaternary terraces, which serve as water resource for the city of Linz (the boundaries of a groundwater protection area extend into the northern project area)
- danger of settlement in weathered or disturbed silt and sand of the tertiary age
- existence of old cellar foundations in over-consolidated tertiary sands
- pronounced relief of hard-rock surface and different depths of weathered rock mass

It was for these reasons that, all routes with longer sections in quaternary and tertiary sediments were abandoned during the route evaluation process. The final route for the environmental impact assessment proceeds to the hard-rock formations in the shortest possible way. The connection tunnels for the subterranean junctions north and south of the banks of the Danube are also located in hard rock. In other geological units the connections are predominantly to be constructed as cut-and-cover tunnels. By adopting this approach, tunnelling works in silty, unconsolidated sediments could largely be avoided – i.e. there will mostly be cut-and-cover sections. All sections in quaternary sediments will definitely be cut-and-cover constructions with impermeable pits, which will neither threaten near-

by buildings by groundwater lowering nor harm the aquifer system supplying drinking water to the city of Linz. It was determined that both construction risk and construction cost could only be minimised with a wide by-pass route mostly in hard rock and a crossing of the tertiary sediments in terrain which would not affect any surface structures (underneath parks, etc). In contrast to Variant 1, the shield tunnels of Variant 2 underpass numerous highly-populated districts of Linz in quaternary and tertiary sediments, and might – judging by today’s knowledge – even be hitting a few old cellar foundations. The danger for the aquifer system is to be higher than with Variant 1 since water bearing gravel in the inflow area of the Linz Waterworks will be affected by the Danube crossing. The unknown relief of the hard-rock surface will require additional reconnaissance works to estimate the amount of sections with mixed face conditions – danger of vibrations, settlements. The measures, which will in addition be required with the NATM connection tunnels in soft rock to minimise the risk for surface buildings have as yet not been planned. It is in the light of these facts that at the present project stage Variant 1 is given preference.

Conclusion

Tunnelling in urbanised areas always involves a higher risk, as even minor settlements often lead to damage at the surface. For this reason, the underpassing of sensitive areas should be avoided to the greatest possible extent. Should this not be possible, the prime target for the engineering geologist should be to select a route where ground conditions, which are sensitive to settlement, will be reduced to a minimum. This implies avoiding silty and sandy sediments and preventing groundwater lowering in gravel. When ever possible hard-rock formations should be chosen in tunnelling. A project pursuing this strategy is the Linz city by-pass. With this project, preference was given to a considerably longer variant considering surface settlements and groundwater hazards. By choosing the by-pass, risky sections could be reduced to a minimum by longer hard-rock excavations. Taking the risk of urbanised tunnelling into account, the longer variant was determined to be less expensive than the shorter variant, which would directly have underpassed buildings in unfavourable ground conditions. Another project, where unfavourable ground conditions could not be evaded was the “Matzenpark” crossing of the railway line in the Lower Inn valley. Here the fact had to be accepted that water drainage in layered soils and sealing against water pressure with jet grouting is extremely difficult. Experience gained at this site revealed that in NATM tunnels with low overburden and water ingress, the stability of the excavation cannot be guaranteed due to the risk of erosion. This water ingress in combination with erosion constitutes an unacceptable risk for NATM tunnels in urbanised areas. As a consequence for the NATM sections of the railway line in the lower Inn valley, underpassing urbanised areas, compressed air will be used in addition to jet grouting enclosure in order to minimise the danger of water ingress.

References

- Eder S, Poscher G., Sedlacek C. (2004) An overview of the geotechnical aspects of the new railway line in the lower Inn valley (EurEnGeo 2004, Liege).
- ILF-IBK for the rural government of Upper Austria (2002 2003); reports on the soil investigation Westring Linz, 2002-2003. unpublished.
- Nemec C. (2002) Ausbau der Bahn im Unterinntal, Felsbau 5/2002, p. 87-95.
- Schubert P., (2002) Key elements of geotechnical risk management at shallow tunnels (International conference probabilistics in geotechnics, Graz 2002, p. 235-245.
- Vavrowsky.G., Pöttler R., (2002) Risk management by the client in the life cycle of a project: focus on geotechnical risk management in the design and construction stage (International conference probabilistics in geotechnics, Graz 2002, p. 167-179.

Geotechnical Characterization and Stability of a Slope in the Marnoso-Arenacea Formation for the Realization of an Underground Car Park in Urbino (Italy)

Umberto Gori, Ennio Polidori, Gianluigi Tonelli, and Francesco Veneri

Università degli Studi di Urbino “Carlo Bo”, Engineering Geology Institute
resort Crocicchia, 61029 – Urbino, Italy
g.ton@uniurb.it
Tel: +39 722 304239
Fax: +39 722 304260

Abstract. The plan of an underground car park located near the historical centre of Urbino town, has required characterizing the Marnoso-Arenacea Formation (Tortonian), from a geomechanical point of view. The project implies that the intervention will be insert inside the flank of the hill, in order to mitigate the effect of the environmental impact. It also involves an excavation front 42 m high and 100 m large. To analyze the mechanical behaviour of the soils, many samples both from the Marnoso-Arenacea Formation and from the cover, have been tested in laboratory. The anisotropy index evaluated by point load test in natural water conditions shows a higher value of the arenitic levels in comparison with the marls. On the contrary, the marls level tested in dry condition provides greater anisotropy index data. In the mono-axial compression test the arenaceous sediments show higher results. The stability analysis carried out with distinct element method shows the opportunity to retain the upper part of the cut with anchored bulkhead.

Keywords: Underground Car Park, Marnoso-Arenacea Formation, Geotechnical Behaviour, Slope Stability Analysis, Numerical Modelling.

Introduction and Action Outline

The city of Urbino, recently declared world heritage by UNESCO, is an internationally recognised cultural heritage. That calls for appropriate accommodation facilities, and it is therefore necessary for the city to have large car parks. The difficulty in finding suitable spaces near the old city centre as a result of the morphology and urbanisation of the area, together with the need to safeguard the city’s architectural complex, have led to the plan of an underground multi-storey car park. It will be built on either hill slope on whose top is Urbino, right outside the Renaissance walls (fig.1). Since it entails the digging of a deep hole in close proximity to monuments and streets, it is a technically demanding action (Godard & Tareau 1995; Aydan et al., 1997). Conversely, the entire structure is going to be embedded in the original slope profile, thus affecting the environment on its execution stages only. The area where the abovementioned action will take place corresponds to the northern slope of “Monte S. Sergio” (477 m a.s.l.); it is a rectilinear slope stretching c.ca E-W (fig.2), whose acclivity

linear slope stretching c.ca E-W (fig.2), whose acclivity ranges between 65% (on the top) and 43% (at the bottom), in the alti-metrical interval ranging from 410 m and 450 m a.s.l. As far as building works are concerned, the excavation will have to be about 100 m in width and 43 m in depth. The three excavation fronts are meant to be terraced, with a horizontal bench 22 m away from the excavation base which will divide the upper vertical wall from a surface sloping about 80 degrees downhill (fig. 4).

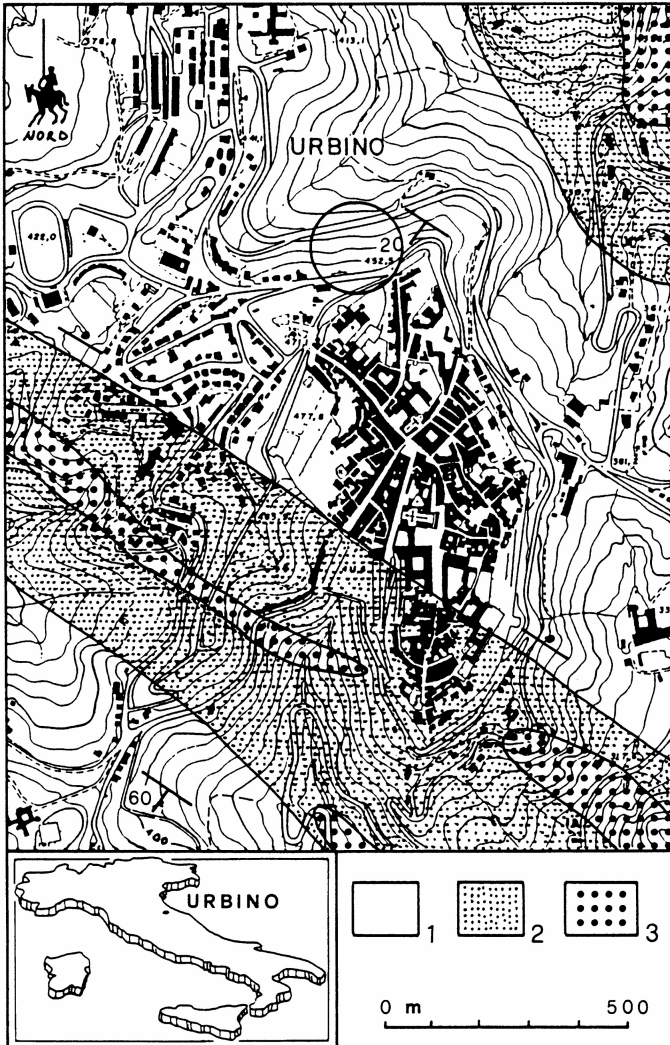


Fig. 1. Geological sketch map with location of investigated area. 1) Marnoso-Arenacea Fm (Serravallian p.p.-Tortonian p.p.); Schlier Fm (Burdigalian p.p.-Langhian p.p.); Bisciaro Fm (Aquitanian p.p.-Burdigalian p.p.).

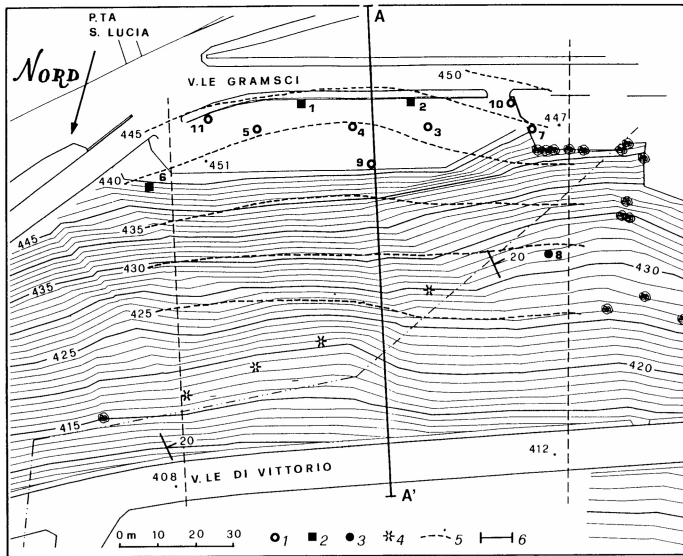


Fig. 2. Plan of the investigated area. 1) Borehole; 2) Borehole with inclinometer pipe; 3) Borehole with Casagrande piezometer; 4) Geomechanical survey station; 5) Contour lines of bedrock top; 6) Section trace.

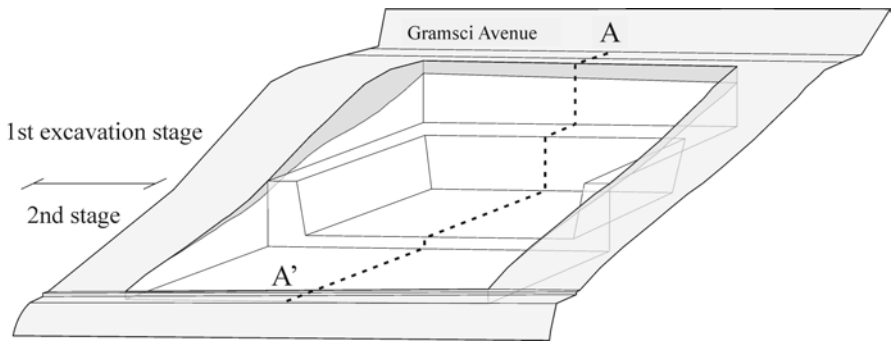


Fig. 3. Strike orientation rose diagram (a) and pole density contour plot (Schmid net, lower hemisphere) (b) of discontinuity planes.

Soil Characterization

Geomechanical Survey

A geomechanical survey was carried out of four purposely-made excavations in order to get the main parameters of the bedrock. It consists of Tortonian turbidite deposits of the Marnoso-Arenacea Fm (ARDANESE *et al.*, 1987; AA.VV., 1994)

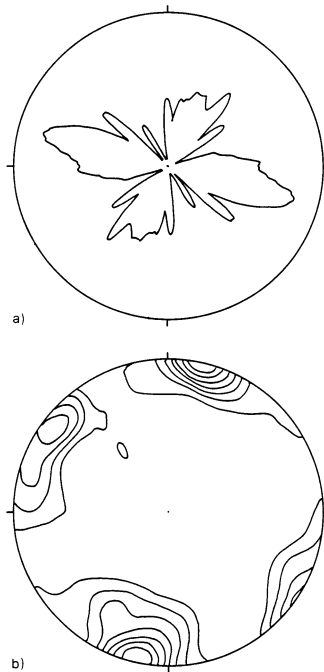


Fig. 4. 3D block-diagram of the excavation with the (A-A') examined section.

with dip direction N 240° E and dip ranging between 15° and 25°; the thickness of strata varies from 0,5 to 4,0 m, more frequently between 0,5 and 1,5 m. On its eastern side, the slope is affected by a N 5°÷10°E sub-vertical fault with a not assessable displacement. Several fractures, whose density varies from place to place, are also noticeable at the meso scale. Two prevailing trends (WNW-ESE and NNE-SSW) can be recognized in the discontinuities strike, as the rose diagram in fig. 3a clearly highlights. Such data match with the pole density contour plot shown in fig. 3b, with values of 307/06 for NNE-SSW striking discontinuities and 193/02 for WNW-ESE striking ones. The spacing ranges from 10 to 20 cm, except for station 4 where a stronger tectonic influence makes the spacing denser. The persistence of discontinuity sets (except for stratification) cannot be determined with precision, owing to the narrowness of the outcrops that are also affected by debris covers on the mid-upper part of the slope. However, the antiapenninic (NNE-SSW) discontinuity trends seem to be much limited in continuity. As a rule, the discontinuities show neither separation nor infilling. In fact, such features are sometimes difficult to assess because of the presence of weak lithotypes where sharp discontinuity planes are unlikely to form. The assessment of discontinuity planes alteration by means of the rock hammer test displayed values between 18 and 21 MPa. Moreover, slight water inflow has been noticed in some discontinuities in the lower part of the slope.

Drill Stratigraphy

Altogether eleven continuous coring boreholes with a total length of 250 ml have been drilled in order to get the subsurface stratigraphy (fig. 2), (descending) to a maximum depth of 40 m below ground level as regards drills No. 1 and 2. For reasons of accessibility, the drills were distributed along three preferential directions. Drills No. 1, 2, and 6, located outside the target area, have been equipped with inclinometer casings for monitoring possible slope movements which could happen both during the excavation/building stages or after the car park becoming operative. Furthermore, drill No.8 has been equipped with two Casagrande piezometric cells at a depth of 5.00 and 12.00 m below ground level (g.l.). All the drills clearly show that the whole area is covered by a debris cover whose thickness ranges from 2.6 m (drill No.8) to a maximum of 12 m (drill No. 9). The debris cover is both the result of bedrock weathering, and, for the most part, of a human activity (e.g. repeated filling of heterogeneous materials such as rubble, stones, earth, etc.). The bedrock is made up of arenites, characterised mainly by a brittle-plastic behaviour, and marly siltites with a pseudo-plastic behaviour. Moreover, the first lithotype shows both primary and secondary permeability connected to a low cementation degree and to fracturing respectively. The second lithotype is slightly permeable. Two lithozones can be recognized according to the previously mentioned lithotypes' distribution:

An arenaceous-pelitic sequence constituting the mid-lower part of the slope. It is typified by a planar, lenticular stratification, with a sandstone/mudstone ratio $\gg 1$. The arenite grain-size ranges from medium to fine, with a typical normal grading. The presence of current casts often shapes the base of strata in an irregular way. The transition from arenite to pelite is always gradual. Some pelites display a tight planar-parallel lamination.

A pelitic-arenaceous sequence constituting the mid-upper part of the slope. It is made up of medium-thin arenite beds alternated with much thicker pelitic strata. As far as such sequence is concerned, the sandstone/mudstone ratio is < 1 .

The drill core quality (RQD) is very high (over 90%) for any drill which has been carried out. Such a result might seem to contrast with the discontinuities' spacing values, which emerged from the geomechanical survey. It should be noted that the surface portion of the bedrock is commonly subject to unloading which produces sheeting phenomena and, therefore, a greater fracture density. In fact, unpublished data about recent excavations for Urbino's hospital extension showed that the discontinuities' spacing at greater depths is between 50 and 100 cm. The previously mentioned area is just a few hundred metres far from our target area, with bedrock belonging to the same geologic structural context. In the light of that, the number of discontinuities per unit volume (I_v) can be more exactly calculated on the basis of RQD's value, through the relation $I_v = (115-RQD)/3.3$ (Palmström, 1982; 1985), whose result (7.57) corresponds to medium-sized blocks. Far larger blocks may occur where the discontinuities' density is not remarkably high. At any rate, the geometrical relationship between discontinuities strike and dip and the excavation front should guarantee the blocks a fair stability, with the exception of the eastern excavation front, whose down dipping might generate instability

conditions. The subsurface is characterized by slight water circulation. It has been monitored by gauging the static level through the drill holes. The maximum height in the static level, namely 444 m a.s.l., has been measured in drills No. 1 and 2. As regards drill No. 8 (the only one equipped with piezometer), the static levels have been registered at a depth of both 429 m and 424 m a.s.l. The latter, pertaining to the bedrock (as one can infer from the contour line of the Marnoso-Arenacea fm top in fig. 2), proves that there is a groundwater circulation in this formation too.

Laboratory Tests

Many undisturbed samples of both the detritic cover (except for the coarse, heterogeneous anthropic layer) and the Marnoso-Arenacea fm. lithotypes have been collected from the drilled cores in order to set the building dimensioning parameters. Both terrains have been classified in accordance with international standards (ASTM, BSI, ISRM). Sample analysis outcomes are in tab. 1 and 2.

Table 1. Geotechnical parameters of detritic cover. w_L = liquid limit; I_p = plasticity index; γ = bulk density; γ_s = dry unit weight; w_n = natural moisture content; e = void ratio; ϕ' = effective internal friction angle; c' = effective cohesion; ϕ'_r = residual effective internal friction angle; c'_r = residual effective cohesion.

Dept (m)	Grain size			Atterberg limits		Physical parameters				Direct shear test			
	sand (%)	silt (%)	clay (%)	w_L (%)	I_p (%)	γ kN/m ³	γ_s kN/m ³	w_n (%)	e	ϕ' (°)	c' KPa	ϕ'_r (°)	c'_r KPa
Borehole 1													
4,00 - 4,30	62	29	9	30,6	10,0	18,4	26,4	23,8	0,77	32	10	23	0
5,00 - 5,50	-	63	37	52,6	25,0					26	15	14	4
Borehole 2													
5,70 - 6,00	12	50	38	42,5	20,0	19,8	26,8	22,6	0,66	27	15	22	5
Borehole 3													
3,00 - 3,50	35	47	13	31,6	11,0	19,6	26,7	18,8	0,61				
6,00 - 6,50	23	46	31	43,0	21,0	20,2	26,7	22,1	0,61	28	10	20	4
Borehole 4													
9,10 - 9,30	1	47	52	52,6	29,0	19,3	27,2	20,0	0,68	29	10	20	2
Borehole 5													
5,00 - 5,50	54	30	9	33,5	11,3	19,3	26,5	23,6	0,69	30	10	18	2

Detritic Cover

As regards grain size distribution, the samples at issue are remarkably different especially in their sand content. The next step in the geotechnical analysis was that of consistency limits determination: the average liquid limit and the average plasticity index are 41% and 18% respectively. Volumetric analysis provided quite

Table 2. Mean values of bedrock geotechnical parameters.

Dept (m)	Litology	Poit load test (MPa)			B (MPa)	UCS (MPa)		
		Is ₍₅₀₎ d	Is ₍₅₀₎ a	Ia ₍₅₀₎	σ _r	σ _r	Es _(rot.)	Es ₍₅₀₎
Borehole 1								
7,20 - 7,60	Sandstone	0,23	0,26	1,13				
12,10 - 12,50	Sandstone				2,74*			
13,10 - 13,60	Marlstone				6,34*	14,66*		
14,00 - 14,60	Sandstone	0,58	0,58	1,00				
17,40 - 17,60	Sandstone					1,87**	51,01**	38,26**
17,60 - 18,10	Sandstone	// 0,07	⊥ 0,15	2,14				
19,30 - 19,70	Sandstone	0,024**	0,064**	2,66**	0,15**			
19,70 - 20,00	Sandstone	2,28*	2,20*	0,96*	2,79*	34,92*	1118,3*	1064,4*
“ “	“					0,63**	13,44**	13,73**
21,20 - 21,50	Sandstone	0,43	0,45	1,04				
21,60 - 22,00	Marlstone				2,20*			
26,00 - 26,50	Sandstone	0,12	0,19	1,58	0,29			
28,20 - 28,60	Marlstone	0,31*	2,65*	8,55*				
36,40 - 37,00	Sandstone	1,02*	2,65*	2,60*	3,14*	22,17*	696,51*	578,79*
“ “	“	0,07**	0,21**	3,00**	0,20**	5,79**	255,06**	192,76**
Borehole 2								
8,70 - 9,00	Marlstone	0,52	0,98	1,88				
12,60 - 12,80	Sandstone	0,28	0,50	1,78	0,71	26,88*	1069,3*	1039,8*
“ “	“					14,03**	421,83**	412,02**
12,80 - 13,00	Marlstone					7,85	145,84	127,53
18,00 - 18,30	Marlstone	0,51	0,52	1,02	0,64			
20,50 - 20,80	Sandstone	0,32	0,59	1,84	0,41			
35,00 - 35,35	Marlstone	0,39	0,48	1,23	0,82	7,85	224,0	202,7
Borehole 5								
9,70 - 10,00	Marlstone	0,18	0,26	1,44	0,68			
Borehole 6								
15,15 - 15,40	Sandstone	0,42	0,75	1,78	0,96			
22,25 - 22,60	Sandstone	0,24			0,70			

7,85 = natural moisture condition specimen

7,85* = dry condition specimen

7,85** = saturated condition specimen

B = Tensile splitting test (Brazilian)

UCS = Unconfined compressive strength

homogeneous values as far as the natural and saturated unit weight: their average values are 19.4 kN/m³ and 19.9 kN/m³ respectively. Finally, the undisturbed samples have undergone consolidated drained direct shear tests. The effective internal friction angle and cohesion peak and residual values have been eventually calculated.

Bedrock

The following tests have been performed on both arenaceous and pelitic samples under natural, dry and saturated conditions: natural unit weight, point load test, tensile splitting test (Brazilian) and unconfined compressive strength. The average values of natural unit weight in arenitic and pelitic layers are 21.7 kN/m^3 and 22.9 kN/m^3 respectively. Moisture content varies from 8% to 12%, the highest values belonging to marly levels. The point load test, which was performed on the same lithotypes, aimed at calculating the point load strength index ($I_{s(50)}$). Being the tested rock an anisotropic one (because laminated and stratified) axial ($I_{s(50)a}$) and diametrical ($I_{s(50)d}$) tests were performed on it. The ratio of axial tests' average values to diametrical tests ones has permitted the calculation of the strength anisotropy index $I_{a(50)}$. It is between 1 and 2, under field moisture conditions, both for marls and arenites. A tensile splitting test has been performed on core samples undergoing the diametrical pressure of two opposite, facing surfaces. Moreover, the samples have undergone unconfined compressive strength tests, recording the axial strain. Data processing provided samples' maximum strength as well as secant elasticity Young' modulus at maximum strength and at 50% of it. The resultant average values have proved to be extremely variable, especially those pertaining to dry and saturated specimens. Such a difference is to be chiefly attributed to the low and irregular cementation of the arenitic levels and to the intense lamination of the marly levels.

Stability Analysis and Conclusions

The distinct element's numerical modelling (ITASCA, 1995) by means of UDEC code has been performed along the A-A excavation plan's profile in order to test the overall stability conditions of the excavation fronts. Five different materials have been taken into consideration: 1) dry debris cover; 2) wet debris cover; 3) dry sandstones; 4) wet sandstones; 5) marls. Such materials, whose behaviour is an elastic and thoroughly plastic one (Mohr-Coulomb's principle) have been assigned/given the following parameters: density, Young's modulus, Poisson's ratio, shear modulus, bulk modulus, internal friction angle, cohesion and tensile strength. Bedding planes have been assigned strength parameters gauged through correlative values, which were corroborated by literature data concerning similar lithotypes. (HUDSON, 1992; PRIEST, 1993; BERTI *et alii*, 1996). Such a choice implies that even if modelling results truly represent the overall behaviour of the rock formation, they seem to be less reliable as far as quantitative estimates are concerned. With regard to the geomechanical survey's data and to the excellent RQD values of cores, stratification has been recognised as the sole persistent discontinuity in the rock mass. Reduced values of elastic parameters (obtained through Singh's formula for rock masses with given spacing discontinuity, RQD and modulus of elasticity; Singh, 1973), were assigned to the rock mass because of sub-vertical joint sets affecting arenites and marls. The modelling was obtained

through the discretization (with the finite differences method) in a triangular grid that can deform with the material that it represents. Moreover, it was vertically overloaded with 20 kN/m^2 in view of the traffic of the overlooking road (Avenue Gramsci).

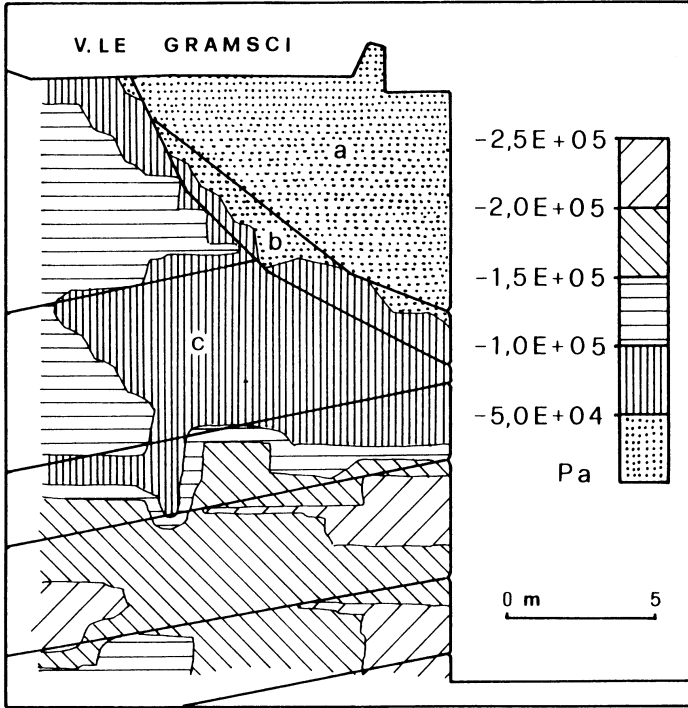


Fig. 5. Horizontal stress trend near the 1st stage excavation. a) detritic cover; b) detritic cover under saturated conditions; c) bedrock.

Stability analysis has shown the slope to be stable under the imposed conditions, thus confirming the assigned parameters accuracy. The first excavation stage simulation (vertical front) has caused the slope to undergo strong instability conditions (fig. 5), to such an extent that the detritic cover eventually slide. In order to simulate the second excavation stage (inclined front), the first excavation front was made stable. As the modelling shows, the inclined front is stable even without reinforcement works. However, some horizontal displacements (ca. 8.0-9.0 cm) also occur in the mid-lower part of the excavation front (fig. 6), thus requiring the use of tie rods. Moreover, because of both the fast uploading and the elastic behaviour of the model, the excavation base is affected by sheeting phenomena (fig. 7). To sum up, stability analyses results clearly emphasized the feasibility of the project on condition that reinforcement works were made to contain the upper part of the excavation front; it is also important for it to be terraced by means of a horizontal bench in order to contain the step height within 20 m.

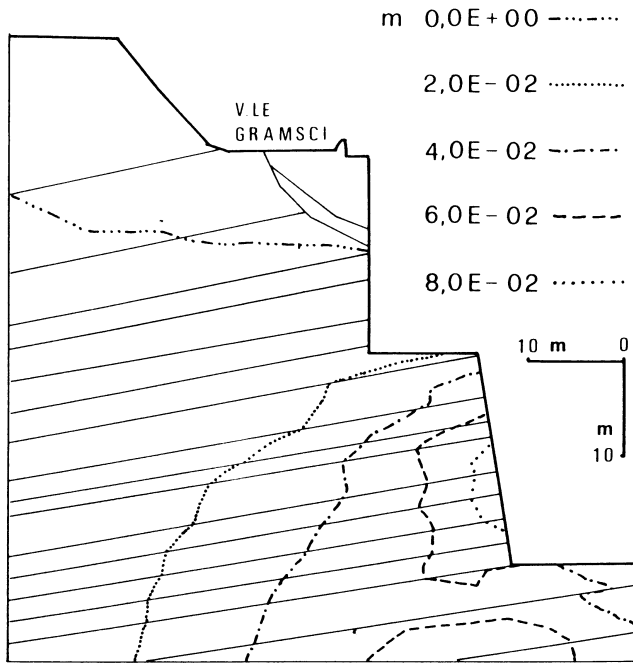


Fig. 6. Horizontal displacements' contour lines after the 2nd stage excavation.

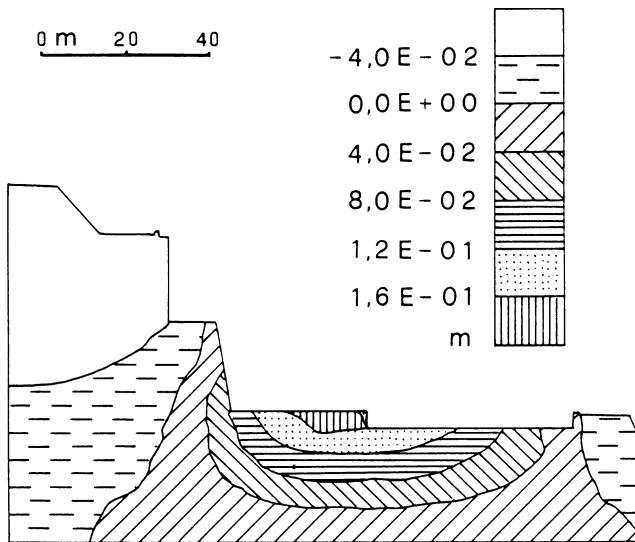


Fig. 7. Vertical displacements' contour lines at the end of excavation works.

References

- ARDANESE L.R., CAPUANO N., CHIOCCHINI U., CIPRIANI N., MARTELLI G., TONELLI G. & VENERI F. (1987) - Studio delle arenarie di Urbania e di Serraspino come contributo alla conoscenza dell'evoluzione paleogeografica del margine adriatico durante il Miocene medio-superiore. *Giorn. Geol.*, 49, 127-144.
- ASTM (1993) – Standard classification of soils for engineering purposes. Test Designation D2487. American Society for Testing and Materials, v. 04-08, Philadelphia.
- A.A.V.V. (1994) - Appennino Umbro-marchigiano. *Guide Geologiche Regionali. Soc. Geol. It.*, 7.
- AYDAN Ö., ULUSAY R. & KAWAMOTO T. (1997) - Assessment of rock mass strength for underground excavations. *The 36th US Rock Mechanics Symposium*, 777-786.
- BERTI M., GENEVOIS R., GHIROTTI M. & TECCA P.R. (1996) - Mechanical characteristics and behaviour of a complex formation by landslide investigations and analyses. VII Int. Symp. On Landslides, Trondheim, Norway, 17-21 June 1996.
- BSI (1990) – British standard methods of test for soils for engineering purposes. BS 1377. British Standards Institution, Milton Keynes.
- GODARD J.-P. & TAREAU, J.-P. (1995) - Underground Car Parks in France: a Case Study. French Tunnelling Association (AFTES) Working Group “Direct and Indirect Advantages of Underground Structures”. *Tunneling and Underground Space Technology*, 10 (3), 311-320.
- HUDSON J.A. (1993) - *Comprehensive Rock Engineering*. Ed. Brown E.T., Pergamon Press, Oxford.
- ITASCA CONS GROUP (1995) - UDEC: Universal Distinct Element Code (vers. 2.0), Itasca Cons. Group, Minneapolis, Minnesota.
- ISRM
- PALMSTRÖM A. (1982) – The volumetric joint count – a useful and simple measure of the degree of rock jointing. *Proc. 4th Int. Congress Int. Ass. Engng. Geol.*, Delphi, 5, 221-228.
- PALMSTROM, A. (1985) - Application of the volumetric joint count as a measure of rock mass jointing. *Proc. Int. Symp. on Fundamentals of Rock Joints, Björkliden*, pp. 103-110.
- PRIEST S.D. (1993) - *Discontinuity Analysis for Rock Engineering*. Chapman & Hall. Londra.
- SINGH B. (1973) - Continuum Characterization of Jointed Rock Masses. *Int. J. Rock Mech. Min. Sci. & Geomech. Abstr.*, 10, 311-335.

Cross Connections at Pannerdensch Canal Tunnel – Freezing Soil Mass Design and Execution Comparison

Hans Mortier¹ and Léon L.T.C. Tuunter²

¹ Comol Tunnelbouw, CFE Beton & Waterbouw, Dordrecht, The Netherlands

Hans_Mortier@cfe.be

Tel: +31 6 15082046

Fax: +31 180646465

² ARCADIS Infra BV, Amersfoort, The Netherlands

L.T.C.Tuunter@arcadis.nl

Tel: +31 6 27061384

Fax: +31 334772001

Abstract. The tunnel under the Pannerdensch Canal (The Netherlands) has two strongly differing cross connections. In this article the design of the freezing bodies, the strutting systems and the definitive structures are explained. The execution process is given, as well as the monitoring results. Finally some conclusions and recommendations for future similar projects are formulated.

Keywords: Ground freezing, tunnel, modelling, temperature, strain, monitoring, Pannerdensch Canal, Netherlands.

Introduction

The bored tunnel passing the Pannerdensch Canal (The Netherlands) is the third bored tunnel in the Betuweroute, the Dutch railway project dedicated to freight traffic connecting the North Sea with the German border. In this tunnel two cross connections are foreseen which the contractor, COMOL TUNNELBOUW, decided to realize by using ground freezing techniques. At the deepest point of the tunnel the first cross connection is made from out of a previously sunken concrete shaft to each of the two tunnel tubes. The shaft is also used as a leak water basin (Figure 1). The second cross connection is constructed from the north to the south tube (Figure 2). After an exhaustive soil investigation program, the design of the freezing was made. Inside these frozen bodies the excavations took place. Temporary support was realized by using shotcrete. After installation of the waterproofing, finally the definitive concrete structure of the connections could be made. An elaborate monitoring system was foreseen to measure all deformations of the existing tunnel lining and the evolution of the temperatures in the surrounding soil. To avoid excessive deformations of the lining two different steel strutting systems were designed. For the cross connections at the shaft there were struts inside the future cross connection, for the other cross connection a system of pre-stressed steel rings inside the tunnel tubes was placed (Figure 3). The contractor, the client

Projectorganisatie Betuweroute and the consultant ARCADIS, were interested to know which part of the loads were taken by the frozen soil mass, and which part went into the strutting systems. A series of strain gauges were installed upon the struts at the normative sections. The results of these measurements, in combination with deformation and temperature measurements gave a clear view upon the behaviour of the (frozen) soil.

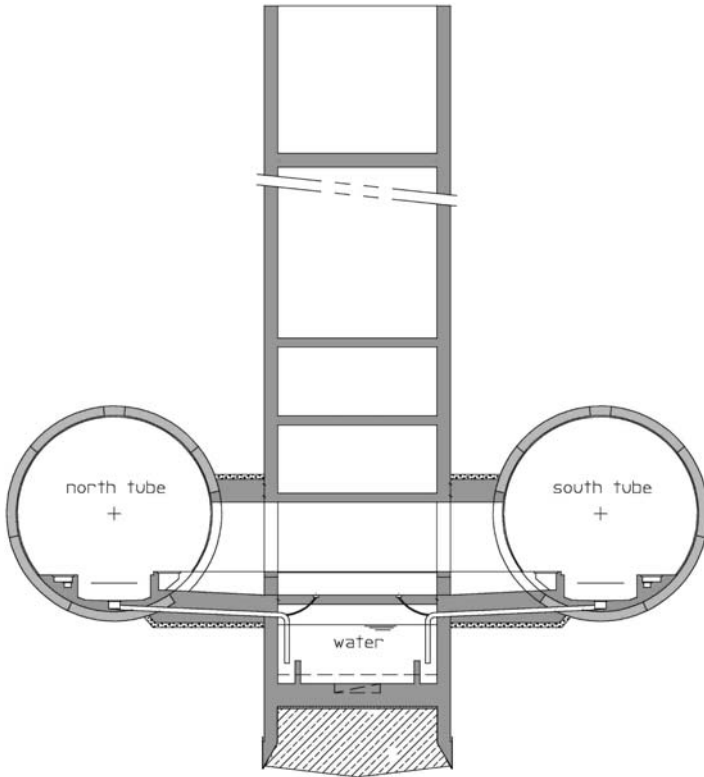


Fig. 1. Sketch of cross connection 1 including the Leakwatershaft.

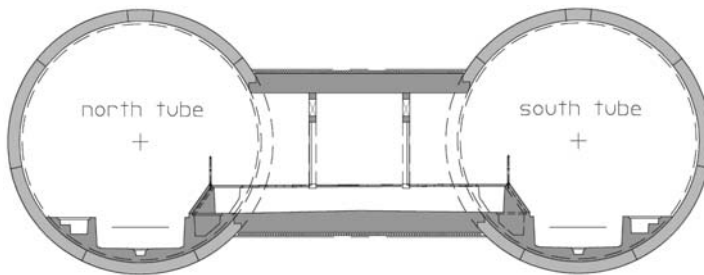


Fig. 2. Sketch of cross connection 2.



Fig. 3. Photo of prestressed steel rings at cross connection 2.

Design

Starting point for the design of the cross connections were the existing soil stress levels after realization of the two tunnel tubes. Due to the boring process of the vertical shaft and the twin tunnel, the soil at the future cross connection was subjected to stress changes. These changes were estimated by using finite element method calculations. These calculations showed a stress increase in the soil besides the upper part (crown) of the tunnels and a stress decrease at the lower parts (invert). The design of the freezing followed after an elaborate soil investigation. At the first cross connection three boreholes were sunk at the shaft location. These show a coarse to medium fine sand in the upper half of the foreseen cross connections, changing into very fine sand with a silt content below 10 % at the invert. The five performed cone penetration tests (CPT) at this location resulted in cone resistances of 10 to 50 MPa and a friction ratio of 0,7 to 1,5, which is typical for sandy gravel to medium sand. One CPT showed a fine layer with a cone resistance of 6 MPa and a friction ratio of 3, parameters correlated with clayey silty sand. At the second cross connection, the borehole data vary from gravelly, coarse sand at the crown towards slightly silty, medium to fine sand at the axis. At the invert the sand becomes again more gravelly and coarse. The cone resistances of 10 to 25 MPa combined with friction ratios of 0,3 to 1,0 confirm the borehole data. According to several recommendations, the strength of the frozen soil is dependent upon the following factors:

- The amount of unfrozen water contained within the soil. The coarser the sand, the less unfrozen water content and therefore the higher the (shear)strength of the frozen soil.
- The strength of the ice matrix. The strength increases with decreasing temperatures.

- The frictional resistance of the frozen material. The higher the friction angle, the higher the strength of the frozen soil. Thus once again, coarse sand is expected to be stronger than silty, clayey sand layers.
- The period for which the load must be sustained. The cohesive strength of the ice matrix is responsible for the often high instantaneous strengths of frozen soil. However ice deforms at low stress and transfers its stress to the soil skeleton up to the limit of its frictional resistance. The strength of the frozen soil mass exhibits time dependent creep properties. Therefore the recommended short term strength values are divided by two. Further on, the characteristic design strength is obtained by dividing the long term strength values by a material factor of 1,5.

In order to simplify the model, a uniform soil type is chosen for each cross connection. For the first cross connection this resulted in a silty sand with a characteristic strength of 1,87 to 3,40 MPa for a temperature range of -10°C to -20°C . At the second cross connection these values reached 2,50 to 4,35 MPa for the same temperature range for an expected fine to medium sand soil type. When water freezes, the volume of the ice is some 9% larger than the volume of water. A saturated material with a 35% porosity, therefore can have a swelling volume of about 3% and cause an important frost heave. In coarse-grained soils, frost heave is normally only observed in closed systems, conditions that will not occur in this project. For low permeability clays, the predicted frost heave problems become increasingly severe. However it should be noted that heave pressures, where present, develop normal to the freezing front, thus in an approximately radial pattern around the freezing pipe. In this project only full heave pressures can develop at the invert of the tunnel at the first cross connection. For fine sand the heave pressures were estimated to reach 25 to 100 kPa; for the silty sand values of 325 to 375 kPa were expected. As the ice wall is used to prop the main tunnel lining, the loads have to be sustained for longer periods. A conservative assumption is made to use for every load case the long-term elastic modulus of 145 MPa for the frozen soil mass.

The thickness of the ice shell and the required strength, thus temperature, is calculated by three semi-empirical methods; a plastic analysis including friction at the boundary of the excavation, a plastic analysis and an elastic analysis. Each of these methods neglect effects as temperature gradients and strength variations across the ice wall section and time related effects such as creep. The required ice wall thickness varies between 560 to 950 mm (fully plastic to fully elastic). Mostly the conservative thickness according to the elastic method is applied on site. For this project a core thickness of 900 mm at a temperature of -20°C is required at the first cross connection, where a thickness of 700 mm and -10°C is sufficient for the second cross connection. With the obtained ice arches, the loads of the existing water tables and the soil pressures according to Terzaghi's trap door theory could be encountered. After excavation in the frozen bodies, a 350 mm thick shotcrete shell was realized. Afterwards, a definitive reinforced concrete lining was installed within this shotcrete lining. This definitive lining was designed to sustain, besides all soil and water pressures, the normal forces that existed within the tunnel lining segments that were cut during the construction proc-

ess. These forces were introduced into the cross connection concrete by means of reinforcement ties and concrete compression struts. In order to enable differential settlements between shaft and tunnel tubes at the first connection, and between the two tunnel tubes at the second connection, non-reinforced cold concrete joints were foreseen. As the frozen soil was expected to deform too much during the excavation and therefore the risk for damages at the tunnel lining dowels between the rings was estimated fairly high, the necessity of strutting systems arose. This resulted in (very) heavy steel strutting systems between shaft and tunnel tubes (first connection) and inside the tunnel lining (second connection). To avoid numerous anchoring devices between cut lining rings and internal steel rings at the second cross connection, the certainty that all forces went into the steel rings was obtained by first pre-stressing these rings up to a level that the longitudinal joints between the lining segments nearly opened.



Fig. 4. Photo of the special drilling device.

Execution

After preparation of the shaft and the two tunnel tubes the construction of the connections could start. For the construction it is necessary to stabilize and seal the soil in the vicinity of these connections. Therefore, it is intended to freeze the soil by circulating liquid nitrogen through copper tubes, which are run into cases. These holes, 130mm and 250mm, are drilled with a special device (Figure 4) nearly horizontally over approximately 3 metres out of the shaft for cross connection 1. After setting the standpipes, the boreholes in the shaft are drilled with a small drilling-rig, moved on a steel platform up and down in the shaft. The boreholes are distributed regularly all around the future tunnel excavation. In the shaft 36 holes were drilled inclusive 4 holes dedicated for the installation of thermocou-

ples. Stainless standpipes with flanges of 114 mm are fixed and oriented in the concrete walls. A robotized theodolite controls the direction of the pipes. The pipes are fixed with a special epoxy resin.

In order to freeze the ground, liquid Nitrogen of temperature $-196\text{ }^{\circ}\text{C}$ is conducted through an insulated pipe and a distribution system into the freezing pipes. Nitrogen extracts the heat off the pipes and the soil by means of vaporization. It escapes from the freeze pipes and the exhaust pipe gaseous. The freeze time is based on the thermal conductivity of the soil. The thermal conductivity depends on the soil type. An approximate freeze duration of 9-14 days is typical time in this sandy soil in comparison to previous nitrogen freeze projects. Every freeze pipe is equipped with a temperature sensor. One dosage and magnet valve is installed in every supply pipe. The supplied amount of nitrogen conducted into the freeze pipes is regulated according to the temperature of the vaporized nitrogen. This ensures a customized frost solid and provides an efficient performance. Regulation parameters are determined in the engineering room for measurements and control. The movable temperature sensors serve to control the freeze wall thickness and the power of the refrigeration plant. The nitrogen supply is ensured by a truck, which refills the vacuum insulated supply tank at the surface of the tunnel. After the freezing is completed the sawing and coring works for the connection openings could start. In addition, inside the south and north tunnel at cross connection 1 and inside the southern tunnel at connection 2, the segmental lining is only opened after construction of the final lining. After two wall openings of $140\times 240\text{ cm}$ in the 600 mm thick shaft were made, the excavation works of the upper layer of frozen soil started. Because nitrogen was used the frozen soil body was very stiff and not easy to excavate.

The steel frame intends to control the deformations and internal forces in the tunnel lining during the construction stages. The support structure consists of two frames on each side of the door opening. Each frame contains five horizontal struts. The beams are composed of double channel profiles (Figure 5). The struts are fixed to the shaft. The lower three struts support the tunnel in radial direction, which means that these connections are made as sliding supports. The lower beams are pending on a diagonal tension device that is fixed to the struts with tenon-and-mortise joints. Because of the lack of space between the concrete constructions and the narrow door opening a special wooden template was made. This template had the actual dimensions and was used to see how the actual heavy steel struts could be handled. The template test showed that it was possible to position the struts in the narrow working space.

At cross connection 2, other factors must be taken into consideration. Huge steel rings were installed in the southern and northern tunnel tubes (Figure 6). The steel rings were linked together to minimize the longitudinal movement of the segments around the passage opening. The maximum movement of the ring at the joints must be limited to 10 mm , according to the contract. Finally, in each case part of the deformation at the joints are minimized by the concrete to concrete friction coefficient as well as the dowels in the segments. It can be concluded that the loss of continuity along two bars will have no effect. Besides, in order to detect eventual exaggerated movement, the joints stepping and the tunnel con-

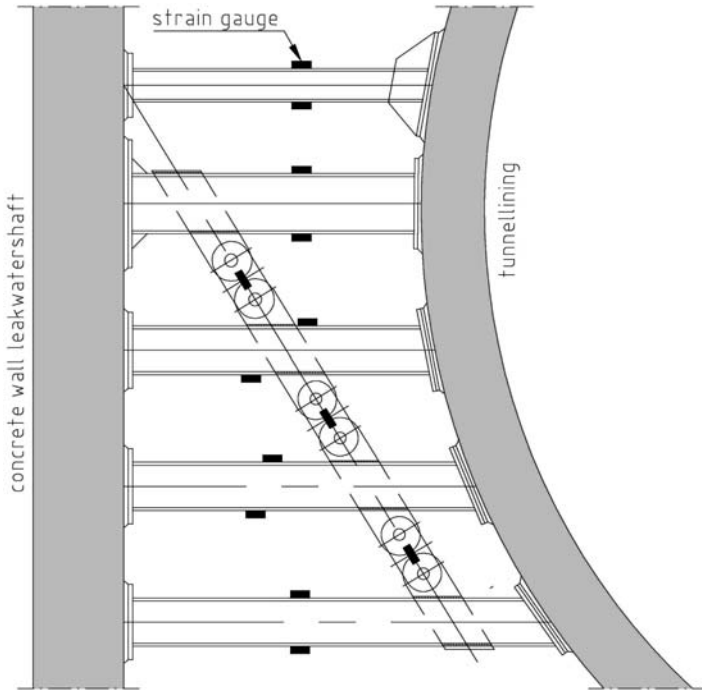


Fig. 5. Sketch of the steel strutting at cross connection 1.

vergence will be intensively monitored. After completion of the first excavation phase (Figure 7) the temporary shotcrete lining could be adapted. The temporary lining is designed as a temporary supporting structure with the consideration to the loads generated during the various excavation phases until the definitive lining is completed. The temporary lining consists of a first layer of 150 mm of shotcrete (75 mm for cross connection 2). It was the intention to spray directly against the frozen soil but because approximately 75% of the first layer came off during spraying, insulation was fixed directly against the frozen soil to prevent the shotcrete from falling. Finally after the first layer a set of steel lattice girders was installed and the last layer of 200 mm shotcrete was sprayed (145 mm for cross connection 2). The first 50 mm of the first layer is considered as 'lost' because it will be frozen and is not taken into account in the calculation. Because the use of the internal steel struts at cross connection 1 there was a lack of space the temporary lining was placed in three phases, the top part, side parts and the bottom part. Connection 2 was realized in two parts.

Monitoring

The temperatures are measured with platinum resistance thermometers, they offer an excellent accuracy over a wide temperature range. These sensors were placed

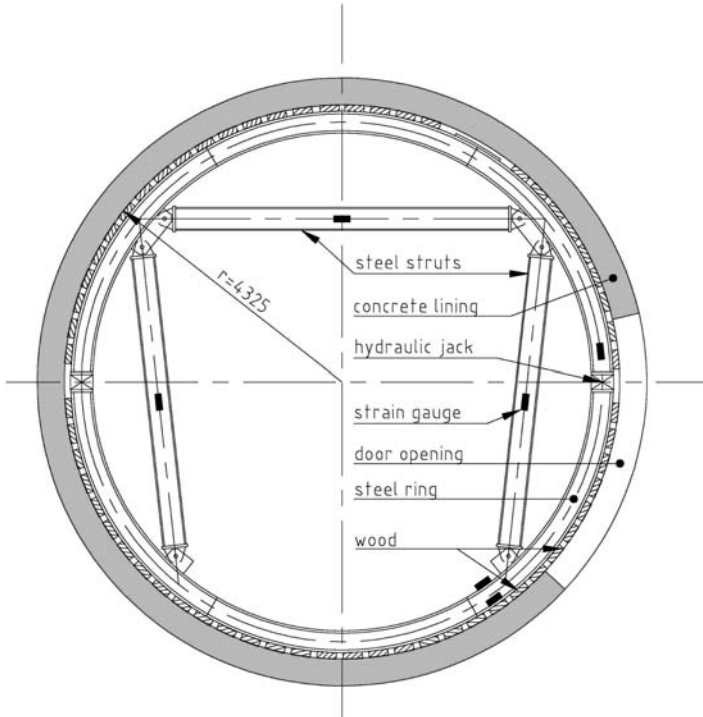


Fig. 6. Sketch of the prestressed steel rings at cross connection 2.

in 4 drilled tubes per connection, two of them parallel to the freezing tubes and the two at a certain angle to measure the temperature changes across the thickness of the (forming) ice wall. Also five additional sensors were placed in the tunnel segments to measure the temperatures in the lining. For the first connection a freezing time of 12 days was foreseen and needed to reach the required temperature of -20°C . At the outside of the ice wall a temperature of -2°C was obtained. For the second cross connection a freezing time of 9 to 14 days was foreseen, but after 7 days the required -10°C was measured over a wall thickness of 1,40 m. The forces in the strutting systems were monitored by strain gauges; 13 at the first cross connection and 7 at the second cross connection (Figure 5 and 6). The position of the strain gauges was well chosen to measure compression forces and bending moments in the horizontal struts and the tensile forces in the diagonal at connection 1. The maximum measured forces and moments varied between 20 to 80% of the calculated forces.

At the second cross connection, the sensors were placed in such way to measure bending moment and axial forces just below the door opening, the axial force in the steel ring just above the opening, the axial forces in the three inner struts and in the tie between two adjacent rings (Figure 8). In the calculation notes the construction process for this connection was simulated in three discrete steps. In



Fig. 7. Photo of the excavated cross connection 2.

the first step, all existing soil and water pressures were taken into account together with the prestressing force in the rings; a friction between adjacent rings of 25, 50 and 75% was modelled. In the second step the moduli of subgrade reaction were changed by the modulus of the frozen soil (creep inclusive) and the frost heave load was modelled. At the last step, the excavation was modelled by removing soil pressures and moduli of subgrade reaction. As the monitoring could only take place after the prestressing was already realized, and due to the fact that sensor 2 was damaged after some days of monitoring, it was very difficult to evaluate the measurements. However, it was remarkable that the axial forces in the rings were far below the calculated ones (but exact evaluation of these values are still ongoing) and the forces in the inner struts was equal to zero kN. Due to the severe demands of a required minimum temperature all along the calculated ice wall thickness, the realized ice wall was almost twice as thick. This combined with all applied safety factors, creep effects and possible arching effect of the soil at the non excavated side of the tunnel tube is probably the reason of the great differences between calculation and monitoring. Based upon the monitoring results, the moment of lowering the freeze capacity and the dismantling of the four outer rings could take place earlier than foreseen.



Fig. 8. Detail photo of the prestressed steel rings at cross connection 2.

During the whole process, the internal diameters of 24 rings were monitored. The maximum deformations were (of course) encountered at the rings where the excavation took place. The horizontal diameter increased for 7mm while the vertical diameter decreased for 6 mm (a horizontal ovalization) at cross connection 1; for cross connection 2 these values were + 9 mm and - 8 mm. The differential displacement between two adjacent rings (stepping) was 4 mm and 6 mm for cross connections 1 and 2. The contract required a stepping less than or equal to 10 mm. In the cross connections themselves, also a whole series of measurements took place. The most remarkable difference between the two systems was the interdistance between the tunnel tubes and the shaft or between the two tunnel tubes. At the first connection this length decreased for 3 mm while, at the second cross connection, a decrease of 9 mm was measured. This is due to the fact that at the first cross connection the tunnelling was only cut through after hardening of the definitive lining concrete, while at the second cross connection this had to take place before the excavation process.

Conclusions

Even though it is difficult to evaluate the measurements due to damages of the sensors and late installation moment, the whole set of measurements showed clearly that the strutting systems were necessary to limit the lining deformations. A major improvement in the future can be achieved by assuming a bigger and stronger ice body in the calculations. The amount of steel rings could be reduced by 67%. The design of freezing bodies for underground works proved to be a well known process as the predictions coped very good with the performed measurements.

References

Banon A, Payet J, Mirabile A, Fernex de Mongex A, & Abdelmoula A. “Tunnels Pannerdensch Kanaal: Construction des galeries de connexion – rapport d’activite” (not published).

Effects of Lime Stabilization on Engineering Properties of Expansive Ankara Clay

M. Celal Tonož, Resat Ulusay, and Candan Gokceoglu

Hacettepe University, Department of Geological Engineering
06532 Beytepe, Ankara, Turkey
resat@hacettepe.edu.tr
Tel: +90 312 297 77 67
Fax: +90 312 299 20 34

Abstract. With the existing expansive clay in Ankara (Turkey) metropolitan area, some light buildings, road pavements and buried lifelines have suffered some damages due to the heave of the clay. There has been very little work concerning the stabilization of smectite rich Ankara Clay, which is mainly the weathering product of the surrounding volcanic rocks. The main objective of this study is to investigate the performance of quick lime in powder form on laboratory-scaled models to improve physical, swelling and strength characteristics of the clay. The lime-soil mixture design technique was employed in the laboratory, and five different types of lime-clay mixture between 2% and 10% by weight were prepared. Engineering properties of the clay determined from natural and lime-treated samples cured for 3, 7, 14 and 28 days were compared. As a result of reactions uniaxial compressive strength (UCS) increased about 84% after 28 days. However, the results indicated that if the curing period is less than 28 days, the UCS values of the lime-treated samples are higher than those of natural samples. This suggests that the pozzolanic reaction is slower than flocculation in Ankara Clay, which achieves optimum stabilization at 4% lime content and 28 days curing time when swelling is considered.

Keywords: Ankara clay, Engineering properties, Lime stabilization, Swelling.

1 Introduction

Lime stabilization refers to stabilization of the soils by the addition of burned limestone products, either calcium oxide or calcium hydroxide (Bell 1988a). This technique is commonly employed in the construction of roads, airports, embankments, or canal linings by intimate mixing with clay subgrades to improve workability, strength, swelling characteristics and bearing capacity. The effects of lime stabilization on clay soils have been investigated by numerous researchers (e.g. Bell 1988b; Indrartna et al. 1995; Popescu et al. 1997; Afes and Didier 2000). Because the properties of soil lime mixtures depend upon character of the clay soil, type, and period of curing, the method and quality of construction, and the proper amount of lime to be used should be investigated before the application of lime stabilization. Approximately two-thirds of the settlement area of Ankara city is founded on the Ankara clay mainly consisting of smectite minerals. Some dam-

age to light one-storey buildings, garden walls, roads and buried utilities occurred due to excessive heave of the clay (Figure 1). Although there exist experimental investigations on the swelling properties of the Ankara clay (e.g. Birand 1963; Cokca 1991; Erguler and Ulusay 2003), there have been very limited works (e.g. Oral 1964; Tonož et al. 2003) concerning the stabilization of this clay. The main objective of the present study is to investigate the effects of quick lime in powder form as the stabilizing agent on index, strength, and swelling characteristics of the Ankara clay in laboratory conditions. For the purpose, five different types of lime-clay mixture were prepared, and engineering properties both of the natural and lime-treated samples waited for different curing times were evaluated.

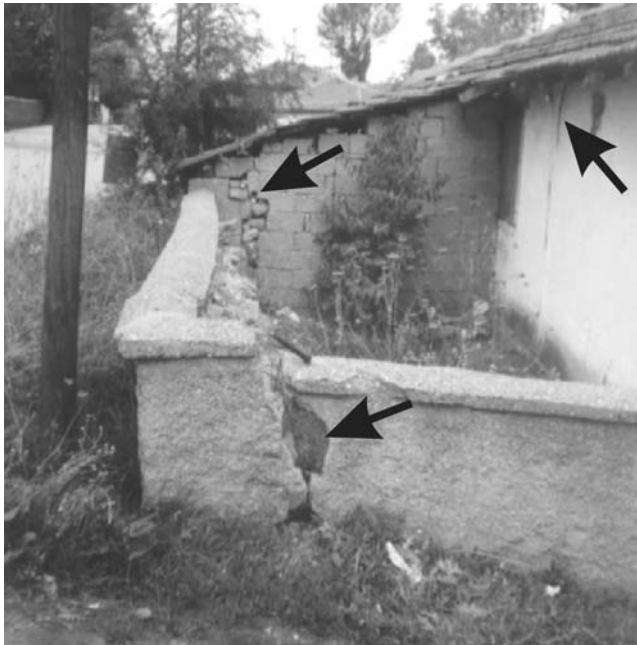


Fig. 1. Damages to a garden wall and a light building due to heave of the Ankara Clay.

2 Mineralogy and Engineering Properties of the Soil

The Ankara Basin is occupied by both fluvial red clastics of Late Pliocene and Quaternary alluvial deposits (Figure 2). The Late Pliocene sequence is mainly composed of clay and occasional sandy and gravely levels, and generally called as Ankara Clay (Birand 1963). This clay, with a typical reddish-brown colour, is mainly the weathering product of the volcanic rocks, particularly the andesites surrounding the basin. In this study, based on the results from a most recent work (Erguler and Ulusay 2003), a sampling location, where highest swelling pressures were experienced and typical damages to light structures are well observed, was

selected at the south-western part of Ankara city (Figure 2). The quantitative results of the XRD analyses revealed that the natural sample is mainly composed of clay (77%), quartz (11%), calcite (8%), and feldspar (4%) minerals. The abundant clay mineral in the sample is smectite. Physical properties, unconfined compressive strength, swelling pressure and compaction characteristics of the natural sample were determined in accordance with the procedures recommended by ASTM (1994) (Table 1). Based on the classification suggested by Seed et al. (1962), the clay has high swelling potential.

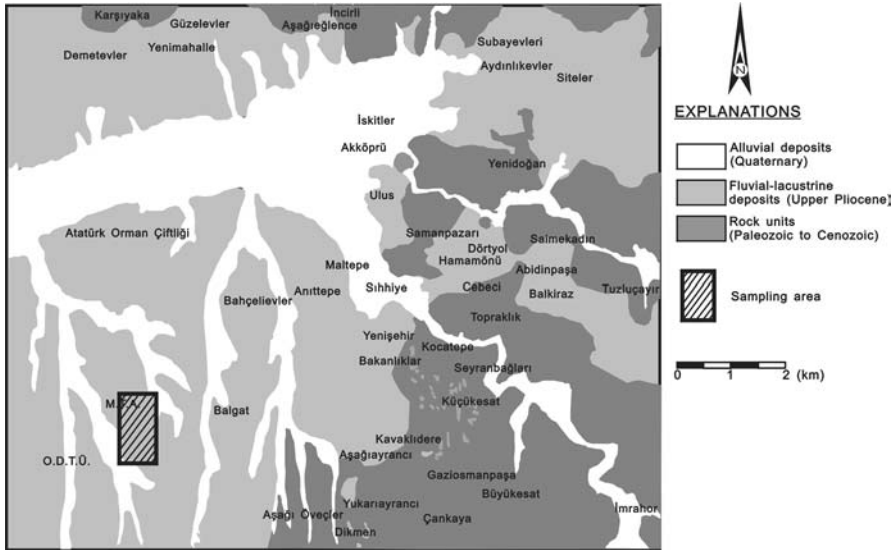


Fig. 2. Simplified geological map of Ankara city and sampling location (modified from Kasapoglu 1980).

Table 1. Physical and geomechanical properties of the natural clay sample.

Grain size										Soil class	γ_n	γ_d	A	UCS	SP
w_n	Grav.	Sand	Silt	Clay	G_s	LL	PL	PI	SL						
(%)	(%)	(%)	(%)	(%)	(%)	(%)	(%)	(%)	(%)						
29	8.5	16.5	20	55	2.64	75	43	32	18	MH	1.68	1.46	0.79	82	96

w_n : Natural water content; G_s : Specific gravity; LL, PL, PI, SL: Atterberg limits; γ_n and γ_d : Natural and dry unit weight, respectively; A: Activity; UCS: Unconfined compressive strength; SP: Swelling pressure.

3 Application of Mixture Design Procedure in Laboratory

During the laboratory studies, the mixture design procedure developed by Thompson (1966) was employed on disturbed soil samples. By using 100 kg sample, five

different type lime-soil mixtures (2%, 4%, 6%, 8% and 10% lime by weight) were prepared and engineering properties of each were determined after 3, 7, 14 and 28 days. Before the preparation of lime-treated samples, pH tests were also carried out in order to obtain general information on the amount of lime to be introduced into the soil. In this test, a pH value of 12.4 indicates most optimum lime modification (Eads and Grim 1966). A close pH value (12.2) to this value was achieved in the case of 6% lime mixture. The effects of the lime-mixture on engineering properties of the clay are assessed in the following paragraphs.

3.1 Grain Size Distribution

Flocculation of clay particles is one of the main effects of lime stabilization on clay soil. A change in soil texture through flocculation of the clay particles takes place when lime is mixed with clay. As the concentration of lime is increased, there is an artificial reduction in clay content. Variations in grain size distribution, depending on lime content and curing time, were evaluated by the grain-size distribution analyses. Variation in grain size distribution of the sample with 4% lime content in 28 days curing period is shown in Figure 3a as an example. It is evident from this figure that amount of clay falls below 10% when lime content achieves 4% or more. It is also noted that lowest clay content (2%) is obtained at 4% lime content for each curing period considered in the study. Because of this, percent of “sand and gravel” increases as lime content does (Figure 3b).

3.2 Atterberg Limits

In most cases, the effect of lime on the plasticity of a clay soil is instantaneous and the calcium ions from the lime result in a reduction in plasticity, therefore, the soil becomes more friable and more easily worked. The clay particles undergo flocculation to form aggregates, which behave like the particles of silt. Very small quantities (1 to 3%) of lime are required to bring about these changes in plasticity (Bell 1996). Because the amount of clay-sized particles considerably decreases in the case of lime contents equal to 4% and more, the effect of lime mixture treatment on Atterberg limits was only examined on a sample with a clay content of 2% for four different curing periods. Figure 4 suggests that the effect of lime stabilization on Atterberg limits is very quick and evident in the first seven days, while it gradually decreases between 7 and 14 days. For the curing periods longer than 14 days it tends to be stationary. Although an increase was expected in plastic limit, it tended to decrease. This behaviour is considered probably due to the presence of quartz (11%) and kaolinite (19%) in the sample.

3.3 Compaction Characteristics

The addition of lime to all clays results an increase in optimum moisture content and reduction of maximum dry density for the same compaction effort (Bell

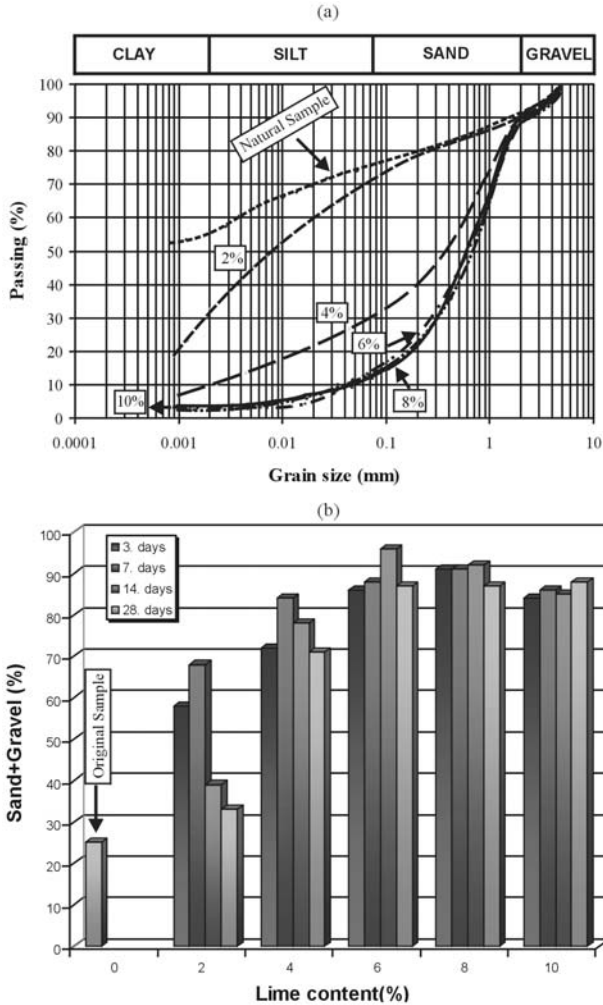


Fig. 3. (a) Variation of grain size distribution depending on lime content for 28 days curing time, (b) effect of lime content on “sand+gravel” percent.

1988a). The results obtained by Afes and Didier (2000), the optimum moisture content increased from 20.5% to 24.5%, while the maximum dry density decreased from 1.65 g/cm³ to 1.52 g/cm³. These results enable the soils in wetter than original condition to be compacted satisfactorily. In the present study, a series of compaction tests were performed on the lime-treated samples, and the moisture content-dry density curves are drawn (Figure 5). Decrease in the maximum dry density and increase in optimum water content after lime stabilization are evidently seen in Figure 5.

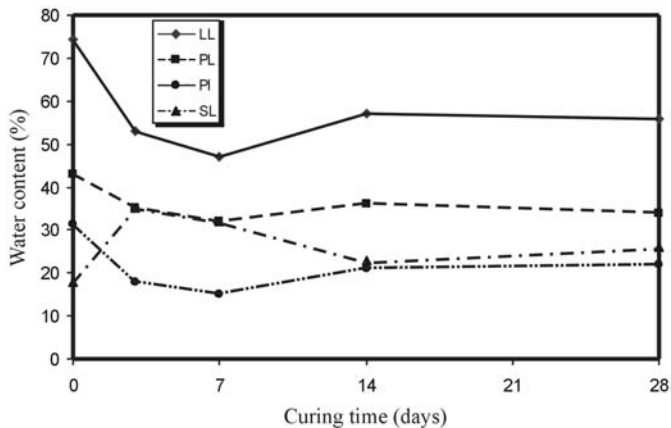


Fig. 4. Effect of curing time on the Atterberg limits with 2% lime content. (LL = Liquid Limit, PL = Plastic Limit, PI = Plasticity Index, SL = Shrinkage Limit).

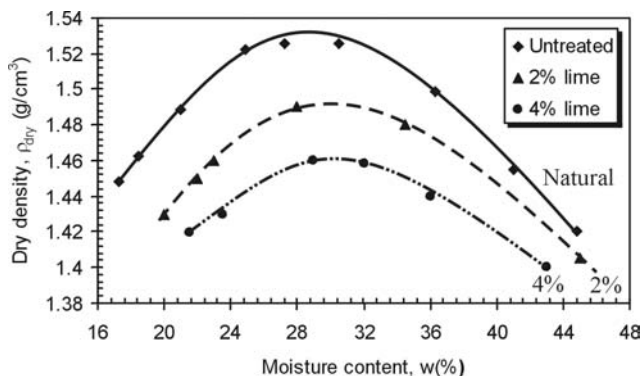


Fig. 5. Comparison of compaction curves of the natural and treated samples.

3.4 Unconfined Compressive Strength

Clays generally show a significant increase in strength when lime is used for stabilization. However, strength does not increase linearly with lime content and excessive addition of lime causes a reduction in strength, because lime itself has neither appreciable friction nor cohesion (Bell 1996). For this reason, determination of the proper lime content to be used as stabilizing agent is very important and another important factor controlling the increase in strength is the length of curing period. In this study, UCS tests were conducted on remoulded specimens to assess the effects of lime on the UCS of the Ankara clay. However, when 6% or more of lime was introduced into the soil, remoulded specimens could not be prepared. Due to this difficulty, only 2% and 4% of lime contents were experienced. As seen in Figure 6a, for the curing periods shorter than 28 days, the UCS of the untreated

sample is higher than those of the treated samples. This shows that the pozzolanic reactions are slower than the flocculation in the Ankara clay. The maximum improvement on the strength was obtained at 4% lime content and 28 days curing period. The stress-strain curve of the sample (4% lime and 28 days curing period) shown in Figure 6b demonstrates that the treated sample suffers lesser deformation when compared to the untreated sample, and therefore, Young’s modulus increases about 60% with lime stabilization.

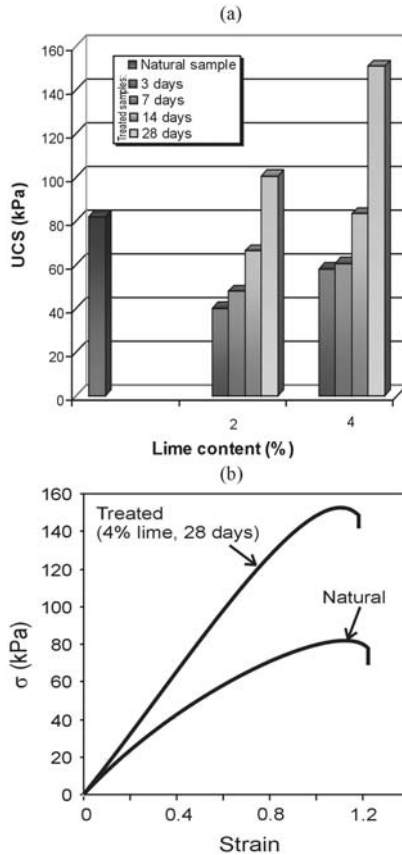


Fig. 6. Variation of UCS (a) and stress-strain behavior of clay (b).

3.5 Swelling Pressure

By considering the damages to light structures in Ankara city due to the swelling clay, effect of lime stabilization on the swelling behaviour was also evaluated for different lime mixtures and curing periods. Figure 7 indicated that swelling pressure sharply decreased at the end of 3rd days curing period, and 100% reduction in

swelling period was recorded for the sample with 4% lime content, which seems to be most suitable mixture composition. Basma and Al-Sharif (1994) suggest that lime contents between 3-9% are required to reduce the swelling pressure to zero depending on the properties of soils. The optimum lime content found in this recent study falls into the above-mentioned range.

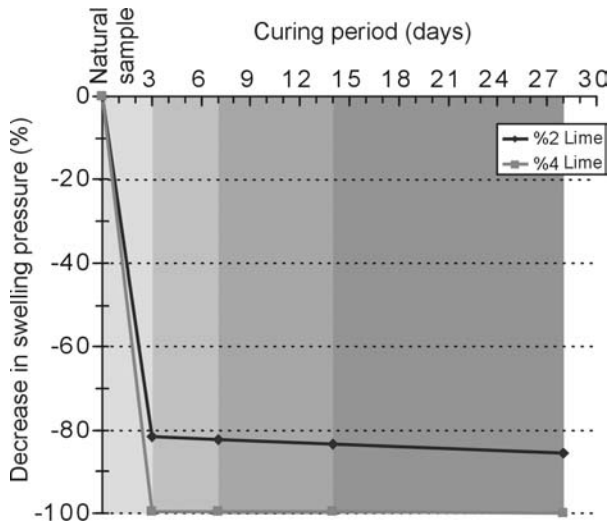


Fig. 7. Decrease in swelling pressure with lime content and curing period.

4 Concluding Remarks

In this study, the results of a laboratory-testing program for the expansive Ankara Clay stabilized with lime mixture method in laboratory scale are presented. The main conclusions from this study are as follows:

- Due to its mineralogical composition, the clay has a high swelling potential.
- In the case of a lime content of 4% in 28 days curing period maximum improvement in strength (84%) was achieved.
- The reduction of the clay content by the addition of lime resulted in a reduction of the amount of swelling, particularly at 4% lime content.
- The results suggest that the optimum lime content and curing period to provide a better improvement on engineering properties of the Ankara clay are 4% and 28 days, respectively.

Although this study is a preliminary work based on laboratory-scaled models, the results obtained may be considered as a useful guide for future in-situ lime mixture studies in the Ankara clay.

References

- Afes M, Didier G, (2000) Stabilisation des sols gonflants: cas d'une argile en provenance de Mila (Algerie). *Bulletin of Engineering Geology and the Environment*, 59: 75-83.
- ASTM (1994) Soil and rock, bulding stones, Section-4, Construction, vol 04.08. American Society for Testing and Materials, Philadelphia, 972 p.
- Basma AA, Al-Sharif MA, (1994) Treatment of expansive soils to control swelling. *Geotechnical Engineering Journal*, 25 (2): 3-19.
- Bell FG, (1988a) Stabilization and treatment of clay soils with lime, Part 1-Basic principles. *Ground Engineering*, 21 (1): 10-15.
- Bell FG, (1988b) Stabilization and treatment of clay soils with lime, Part 2-Some applications. *Ground Engineering*, 21 (2): 22-30.
- Bell FG, (1996) Lime stabilisation of clay minerals and soils. *Engineering Geology* 42: 223-237.
- Birand AA, (1963) Study of the characteristics of Ankara clays showing swelling properties. MSc Thesis, Middle East Technical University, Ankara, Turkey, 39 pp.
- Cokca E, (1991) Swelling potential of expansive soils with a critical appraisal of the identification of swelling of Ankara soils by methylene blue tests. PhD Thesis, Middle East Technical University, Ankara, Turkey, 323 pp.
- Eads JL, Grim RE, (1966) A quick test to determine lime requirements for lime stabilisation. *Highway Research Bulletin* 139:61-72.
- Erguler ZA, Ulusay R, (2003) A simple test and predictive models for assessing swell potential of Ankara (Turkey) Clay. *Engineering Geology* 67: 331-352.
- Indraratna B, Balasubramanian AS, Khan MJ, (1995) Effect of fly ash with lime and cement on the behaviour of a soft clay. *Quarterly Journal of Engineering Geology* 28:131-142.
- Kasapoglu KE, (1980) Ankara kenti zeminlerinin jeo-mühendislik özellikleri. Docentlik tezi, Hacettepe Üniversitesi, Yerbilimleri Enstitüsü, Beytepe-Ankara, Turkey, 206 pp (unpublished, in Turkish).
- Oral C, (1964) Stabilization of Ankara Clay. MSc Thesis, Middle East Technical University, Ankara, Turkey, Ankara, 96 pp
- Popescu ME, Constantinescu T, Ferrando C, Quintavalle F, (1997) Treatment of subgrade expansion soil at the extension of Bucharest-Otopeni International Airport. In: Proc International Symposium on Engineering Geology and the Environment, Athens, Greece, pp 331-338.
- Seed MB, Woodward RJ, Lundgren, R., (1962) Prediction of swelling potential for compacted clays. *Journal of the Soil Mechanics and Foundation Engineering Division ASCE*, 88: 53-87 pp.
- Thompson MR, (1966) Lime reactivity of Illinois soils. *J Soil Mechanics and Foundation Engineering Division ASCE*, 92: 67-92 pp.
- Tonoç MC, Gokçeoglu C, Ulusay R, (2003) A laboratory-scale experimental investigation on the performance of lime columns in expansive Ankara (Turkey) Clay. *Bulletin of the Engineering Geology and the Environment* 62:91-106.

The Belgian High-Speed Railway Soumagne Tunnel Project

Iwan Couchard¹, Alain Van Cotthem², and Servais Hick³

¹ Tuc Rail, 91 Rue de France 1070 Brussels, Belgium
icd@tucrail.be
Tel: + 32 2 5297850
Fax: + 32 2 5297943

² Tractebel, 7 Avenue Ariane 1200 Brussels, Belgium
alain.vancotthem@tractebel.com
Tel: + 32 2 7737581
Fax: + 32 2 7737990

³ Tunnel de Soumagne, 3 Rue des Heids 4630 Soumagne, Belgium
shick@tunnel-soumagne.com
Tel: + 32 4 3550955
Fax: + 32 4 3581074

Abstract. This paper aims at explaining the general context in which this 6.5 km single tube tunnel was planned, designed and is today under construction with full resources on 4 simultaneous attacks. First, the tunnel is set in the general rail infrastructure network spreading from Brussels to neighbouring countries. Its location near dense urban sites has prompted specific answers to environmental and organizational problems such as spoil removal, intermediate access shafts, East and West portal configurations. An overview on the regional geology is made to emphasize the complex hydrogeological context in which the excavation must safely proceed under an urban environment. Among the challenges are the presence of old exploited coal seams, unfavourable joints orientations and karstic limestones. The relatively shallow overburden (max 120 m) has allowed extensive exploratory campaign including geophysics and some 8000 m of core drilling with in situ and laboratory tests. The next item will explain the design methodology used to deal with the rock mass heterogeneity and variability (empirical, analytical, and numerical). The design leads to a limited number of typical temporary lining cross-sections. It will be focused on a comparison between the necessary simplification used in numerical analysis and the reality of the actual situation encountered at the faces. Finally, the work organization foreseen by the Contractor will be briefly developed to emphasize the crucial impact of rational working phases on the overall performance of the excavation process. This will cover the digging phase itself down to the curing of the cast-in situ permanent concrete lining.

Keywords: rock tunnel, high-speed train, railway, design, construction, Soumagne, Belgium.

1 Introduction

The Soumagne tunnel is part of the high-speed train link between Brussels and Aix-La-Chapelle in Germany, completing a dense national railway network at the

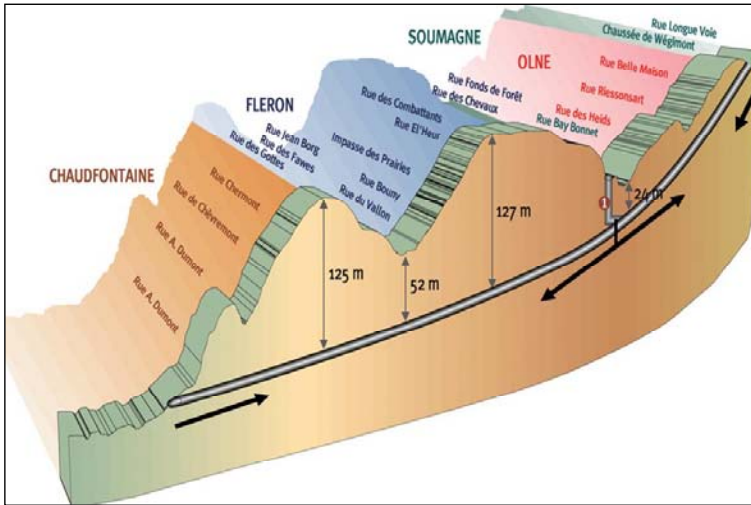


Fig. 1. Schematic tunnel layout and construction fronts

heart of Europe, operated by SNCB. Simultaneous works under Antwerp city will allow a high speed link with Amsterdam. Liège as destination requires plunging to the Meuse level at the Guillemins station from where several solutions were envisaged to ascend the 200 m climb to the Herve high ground. A direct route was chosen through the hills of Vaux-sous-Chèvremont requiring the construction of a double track tunnel while minimizing impacts on this relatively densely populated area. The tunnel is about 6.5 km long including two covered trenches at each end (fig 1).

For a 200km/h nominal speed, the required free section is 69 m² with an average 110 m² excavated section, depending on ground conditions (fig 2)

2 Geology

The tunnel crosses 3 types of rock formations, from west to east:

- The *Westphalien shales* on 3300 m, from the Herve massif
- The *Viseen limestone* on 650 m, from the Vesdre massif
- The *Namurien shales* on 1900 m, from the Vesdre massif

A major overlapping fault (Magnée) divides the Westphalien shale and the Viseen limestone. Several other faults are to be crossed (fig 3).

The geology encountered along the route presents some important features to be taken into account for the design and the construction procedures:

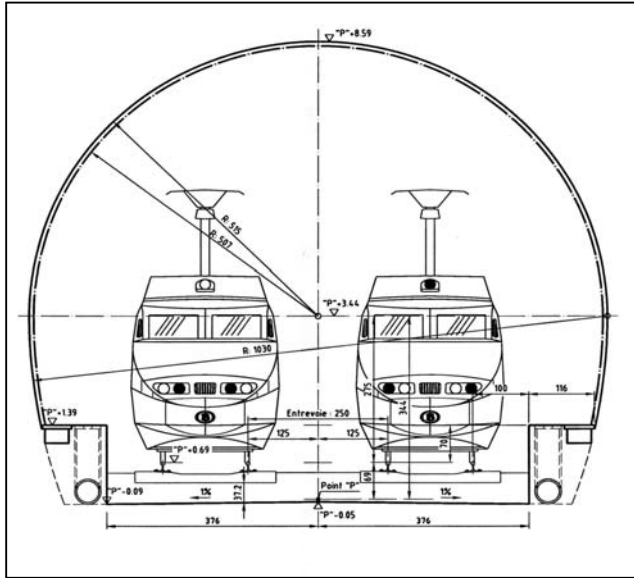


Fig. 2. Tunnel template.

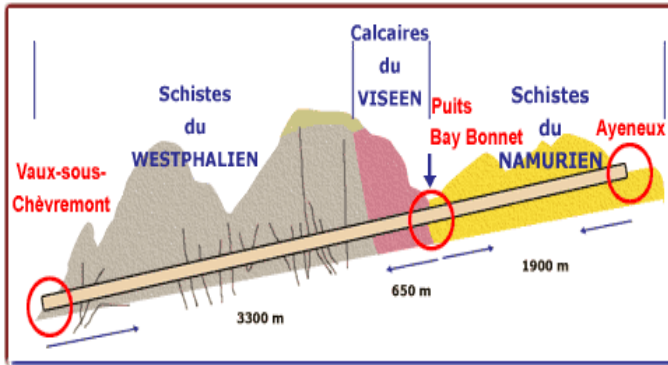


Fig. 3. Geology.

- The presence of old exploited coal seams in the Westphalien formation. Some of these seams are backfilled with poor materials or even not backfilled at all. The decompression caused by these works has erased any tectonically induced stresses and has led in the past to significant amount of settlements in the region. These “soft” layers may induce local instabilities, a lack of arching effect while excavating or ingress of water from the upper water tables. They can generate differential settlement near the foot of steel ribs or delayed creeping effects under the invert. A positive consequence of these mining activities is the presence of old drainage gallery under the tunnel levels, limiting total flow and reducing the risk of bursting at the face.

- The *tunnel direction is N 95° E while general bedding directions are mainly between N 80° E to N115° E*. This combined with sub vertical dips, lead to unfavourable conditions. This is particularly the case with the following features:
 - Hard sandstones layers, about a meter thick, calling for local drill and blast method, while adjacent softer shales could have been excavated with road header technology.
 - Badly backfilled coal seams, calling for systematic forepoling or grouting, slowing down the advance rate.
 - Digging trough the heart of dislocated synclines and anticlines.
- The limestone is encountered at its contact with the shale, featuring a *paleo-karst profile*, along with its local potential instabilities. On the other hand, these karsts are located above the aquifer and are mainly filled with cohesive materials with a sufficient standing time.

Prior to the tunnel bidding process, the geology was thoroughly investigated with an extensive in situ and laboratory program, made possible by the relatively shallow depth of the project:

- 105 core boring totalizing 8070 m of samples. Each boring was logged with an inclinometer. The in situ campaign included geophysics near the limestone contact, Lugeon tests and dilatometers test. Each boring was permanently equipped with a piezometer.
- The laboratory tests included compression (with modulus and Poisson ratio measurements) and Brazilian tests, Shore and Cerchar hardness, abrasivity (FPMS, Cerchar).
- A 70 m long exploratory adit, 4m in diameter, was built near the Namurien/Viséen interface in order to evaluate the importance of the karstic problem. To reach the level of the future tunnel, a 40 meters deep shaft was drill and blasted.
- For the limestone drill and blast optimum design, the ground attenuation law was derived in situ from specific unitary blasting tests.

As a result, the main design characteristics of each formation were inferred as followed:

Table 1.

<i>Lithology</i>	<i>Young's Modulus (MPa)</i>	<i>Intact compressive strength (MPa)</i>	<i>Wear factor</i>	<i>Cerchar Abrasivity</i>
Clayey shale	1700 – 4000	14	< 0.04	0.1
Slightly sandy shale	3000	20	< 0.1	0.1
Sandy shale	2300 – 7500	30	< 0.3	0.6
Sandstone	3000 – 7500	70 – 94	1 – 2	2.6 – 4.6
Limestone	10 000	100	-	0.7

3 Design

3.1 Cross Section

The Soumagne tunnel is the second hard rock tunnel recently build in the Liege region in the same type of shale formation, the first being the close by Cointe road tunnel. Accordingly, the basic design intended to be included in the tender documents was based on a similar approach: a three phases excavation (top heading, stross, invert) with heavy duty road headers. Drill and blast was foreseen to pass through limestones or locally massive layers of sandstones. The typical cross section is shown on fig 4.

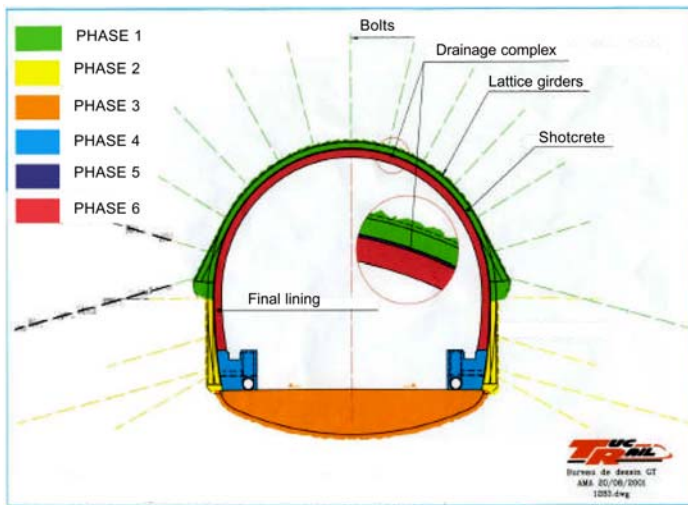


Fig. 4. Typical cross section.

The temporary lining components are:

- An outer *fiber reinforced shotcrete shell*, 20 to 30 cm thick, including an initial 5 cm safety layer, placed immediately at the face. The amount of fiber is about 35 kg /m³.
- Systematic *bolting* with Swellex-like immediate frictional expanded bolts.
- Steel ribs either light lattice girders or HEB heavy support in difficult conditions.

This shell is considered as being part of the long-term structural lining in combination with the cast in situ concrete. Being impervious, it is designed for the short-term effective ground pressure. The final lining is a continuous closed concrete shell made of:

- A cast in situ *concrete shell* with minimum reinforcement for practical reason
- A *reinforced concrete invert*

Between the two shells, an *impervious drainage layer* is placed. In the original design this drainage was classically foreseen only down to the stross lower level with two lateral drains imbedded in the sidewalk complex. The design has been changed during construction work to allow for additional demands for fire fighting equipments. As a consequence, it has been decided to drain the whole tunnel perimeter, including the invert under which the main drains, accessible through manholes, are then relocated. As a consequence and following a new risk assessment, the accidental load cases (drainage clogging) has been reduced allowing a flat shape invert, easier to install (fig 5).

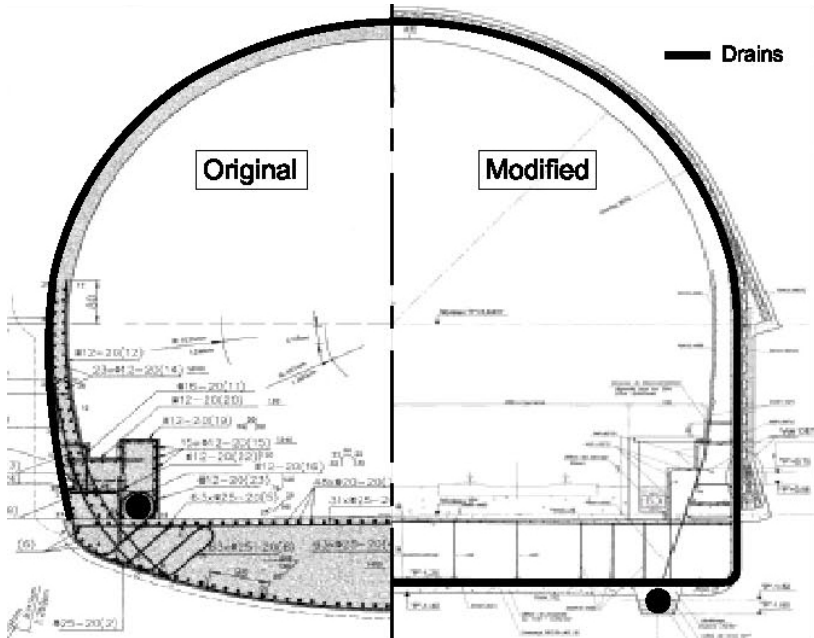


Fig. 5. Cast in situ lining – original vs. final design.

The drainage complex consist of:

- A drainage mat, 8 mm thick on the top and side walls, 20 mm thick under the invert.
- A geotextile as a buffer protection for.
- A continuous welded 2 mm polyurethane membrane, except under the invert.
- Two 400 mm drains, able to absorb the drained flow for the whole 6.5 km tunnel.

3.2 Design Methodology

The design was conducted according to the following methodology:

- Analysis of available information and choice of design parameters.
- Use of empirical methods – first draft of typical profiles.
- Analytical methods for cross checking of main parameters.
- Numerical methods (continuous and discontinuous) including sensitivity calculation, these methods were used for current section and in special geometrical configurations.

Analysis of Available Information and Choice of Design Parameters

There is approximately one boring each 100 m, each of them reaching the tunnel level. A fairly good representation of the geology was possible, although it poses more problems in the Namurien formation, later confirmed by the difficulties encountered in that zone. From there the proportion of each rock type likely to be met was deduced, mainly focused on the heading phase that is the most critical. Laboratory test results were compiled to derive a *range* of design parameters. The less obvious value to infer was the modulus of deformation, at the tunnel scale, for which the following information had to be analysed: laboratory value on intact specimen, “metric” dilatometers value in the three sensors direction in relation with the bedding and at different stress levels, empirical values.

Use of Empirical Methods

The use of Bieniawski empirical method was made in order to have a preliminary set of typical lining sections (shotcrete thickness, bolts lengths and spacing, unsupported span,...) in the different geological conditions encountered along the route. Although summarizing local situation by only one number (RMR, GSI) seems daring, it helped giving a limited number of options for such a complex geology and overabundant information. The method of Barton was not used due to the difficulties of characterizing all the joints types. This Rock Mass Rating was used in order to deduct the basic set of parameters characterizing the rock non linear behaviour at the scale of the tunnel; m and s values (by opposition to the soil c' and ϕ'). These two parameters are input data's in today's numerical or analytical calculation tools. They are deduced either from a modified RMR value of directly through double entry abacuses.

Analytical Methods

The convergence confinement method was then apply to infer the order of magnitude of some basic grandeur for different excavation scenario (full face or two-stages) such as the “plastic” or broken radius (to check bolt lengths), the initial displacement at the face (thus possible instabilities), the radial convergence and the average normal force in the lining. The main advantage of using this quick method was to be able to choose the deconfinement ratio by varying all parameters including the unsupported span. This ratio was set at 80 % (i.e.; the fraction of the overburden taken by the rock were the shotcrete lining is placed). This value was confirmed by a three dimensional calculation (FLAC 3D) that could take into account the excavation phases and the relations between the lining stiffness and the face behaviour.

Numerical Methods

Numerical analysis is essential to take into account:

- actual shape of the excavation and the characteristic of each lining components
- excavation phases
- three-dimensional effects at the face
- stress anisotropy
- ground heterogeneity
- discontinuity behaviour

Software validation was made by comparing results between Flac2D, Flac3D, and Phase². The effects of the choice of a behaviour law was made (Hoek-Brown, Mohr Coulomb) and systematic calculation was performed by varying K_0 , the overburden, the rock type, the rock class, the number of excavation stages and the lining components. The results given are:

- displacements field (face and current section)
- bolts tension
- plastic zone pattern,
- Bending moments and normal force in the lining, allowing for a classical concrete design according to Eurocode practice.

Particular models were made to include the systematic direction and dip along most of the tunnel route (ubiquitous joint, see fig 6) and the presence of low stiffness coal seams near or through the excavation profile.

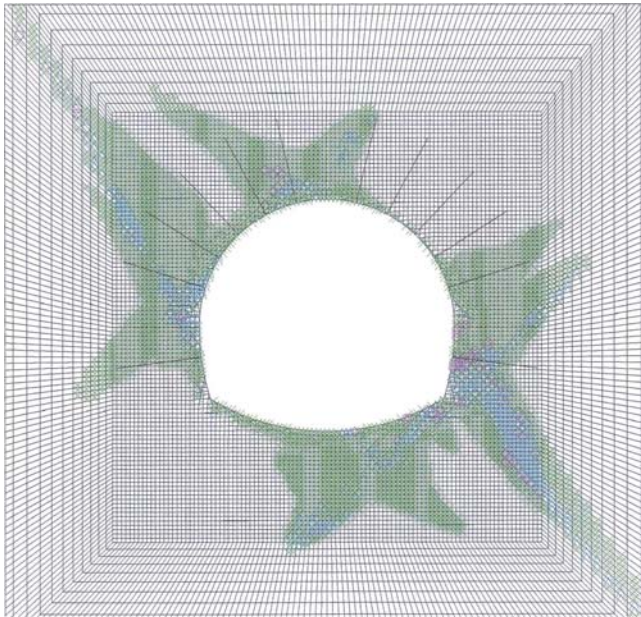


Fig. 6. Plastic zones for the ubiquitous FEM model – example.

The dimensioning of the limestone was made using discontinuous methods such as the Goodman and Shi critical block theory. By adding provision for ground treatment, the final results allow to compute all quantities and finalize the documents for tendering.

4 Construction Aspects

The contract has been awarded to the consortium "Tunnel de soumagne" (composed of CFE, Vinci, Eiffage et Duchêne, Galère and Wayss & Freytag A.G, Bouygues TP and Bouygues Belgium). The works started on 14.05.2001 and should be completed by 08.2005. This tight schedule is made possible by starting four almost simultaneous excavation fronts (as illustrated on fig 1) and a 24 h working day, 5 days a week on each front. At full peak, the total contractor's team amounted to about 330 people and 50 employees.

From Vaux-sous-Chèvremont, the work started upward from a covered trench which walls consist of large tangent piles closed by a flat concrete roof. The anticipated massive sandstone layers, parallel to the tunnel direction, proved from the start to be more difficult to dig out while keeping a reasonable advance rate. This situation has prompted the contractor to generalize the drill and blast technique for the whole tunnel length.

From Ayneux downward, the site is located in an open field. In order to start tunneling under sufficient overburden, a deep trench has been made, later completed with a precast concrete box structure poured in place with a large sliding formwork. The site will be given back to its original aspects.

At Bay Bonnet (fig 7), some 2/3 of the route, where the overburden is at its lowest, a temporary 30 m deep shaft 30 m in diameter has been built in order to start simultaneous excavation in both opposite directions. The face downward is located almost immediately at the top of the 600 m limestone formation. This site is also used as the main field office.

Although ideal for construction purposes, a number of arrangements have been made due to the densely populated neighborhood such as noise reduction equipments including a full roof on the shaft and a temporary bridge to reduce traffic on the existing road. The drill and blast operation were strictly limited to daytime and none on weekends.

The *generalized drill and blast technique* has proven to allow fast advance rate but has induced large over breaks and thus more shotcrete consumptions. On the other hand, the amount of costly ground treatment has been less necessary than initially foreseen except some systematic forepoling and a more heavy intervention at the Magnee fault crossing. Also, wherever feasible, a full section excavation was used. As a result, the financial equilibrium has been respected.



Fig. 7. Intermediate temporary construction shaft.

The *choice of each lining type* (type of steel beams, thickness of shotcrete, length and spacing of bolts, excavation span, blasting pattern,) is made on a day to day basis, in close cooperation between TUC Rail and the Contractor. The *basis for changes* are the daily convergence measurements, water ingress observation, geological features at each face, vibration measurements at each sensitive surface building or house and the results of a number of long exploratory boring (about 30 m in length) drilled each week end at each advancing face. Geologists are mapping all features either for as build purpose, to provide information for a subsequent excavation phase or for possible delayed ground treatment needs.

The *other monitoring aspects* include the surface settlements, the evolution of the water table ahead of the face, surface noise on the 3 sites, noise in the tunnel, methane and CO, CO₂, NO, NO_x contents in the tunnel.

At the date of this paper, the link has been made between the Eastern Aynex site and the Bay Bonnet temporary shaft. The two remaining fronts will meet around end of 2004.

The construction of the final lining is catching up on the excavation with an advance rate of 24 m of lining each day.

High Speed Lines in Belgium: Various Engineering Geological and Geotechnical Aspects

Keynote

Bernard Dethy and Saâd Bouhenni

Suez-Tractebel / Tuc Rail, Rue de France, 91, B1070 Brussels, Belgium
dyb@tucrail.be
Tel: +32 2 5297851
Fax: +32 2 5297943

Keywords: High Speed Railway, Infrastructure, karst, consolidation, piles in chalk, cavities, lime treatment.

1 Introduction

The High Speed Railway network in Belgium extends over 322 km of lines made up of 210 km of new line designed for speeds of 300 km/h and 112 km of conventional lines developed and upgraded for max. speeds up to 220 km/h. The estimation of the total budget of HSR lines is around 4,6 billion euros (1999). More specifically, the project can be divided into three parts:

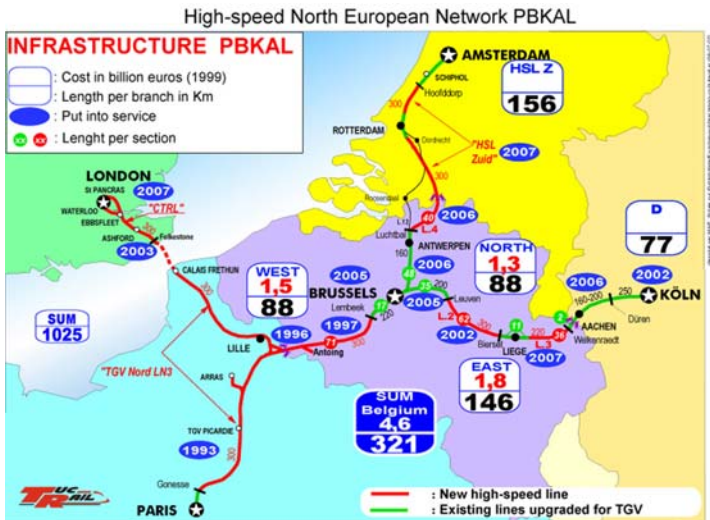


Fig. 1.

1.1 Western Branch

The branch to the West between Brussels and the French border connects up with the Paris-Lille high-speed line. It consists of a new 71 km line with its own right of way designed for a speed of 300 km/h and 17 km of upgraded line workable at up to 220 km/h. This section is fully operational: high-speed revenue service began between Paris and Brussels on December 1997 putting the two capitals at just 1 hour 25 minutes apart.

1.2 Eastern Branch

This branch links Brussels with Liège and the German border over a distance of 146 km, 98 km of which have dedicated right of way. The section between Brussels and Liège has been opened to traffic in December 2002 (the first 35 km between Brussels and Leuven and the last 10 km west of Liège consist of upgraded existing lines while the rest is a new line – 300 km/h – built along the E 40 motorway). The section under construction between Liège and Germany is scheduled to come into service in 2007.

1.3 Northern Branch

The branch to the North comprises the upgrading of the existing lines between Brussels and Antwerp, the construction of a new south-north tunnel link underneath the city of Antwerp and a new 40 km high-speed line between Antwerp and the Dutch border towards Amsterdam with dedicated right of way built parallel to the E 19 motorway. The branch is scheduled to come into service at the end of 2006.

Brussels will be at 1 hour 40 minutes from both Amsterdam and Köln.

2 Western Branch

2.1 Geological Aspects

The HSR line encounters, under a Quaternary cover, the soft formations of the Tertiary (Eocene) and of the Secondary (Upper Cretaceous) which are made up of marine deposits associated with transgressions interrupted by continental phases. These formations rest unconformable on the Primary substratum which is folded, eroded and peneplained. Between the French border and the Dendre valley, the Primary substratum belongs to the northern boundary of the Namur Synclinorium. It consists of (on the most part of the route) limestone and dolomite from the Carboniferous (Viséan, Tournaisian) generally very faulted and subjected to karstic phenomena. These formations crop out in the valleys of the Scheldt and the Dendre rivers. Immediately to the east of the Dendre, the substratum consists of calcareous sandstone of the Devonian (Famennian, Frasnian). Between the Dendre

and Brussels, the Primary substratum includes sedimentary rocks (schist, phyllite and sandstone) from the Cambrian and Silurian age, belonging to the Brabant Massif. These rocks crop out in the valleys of the Laubecq and the Senne. The Cretaceous formations which are present discontinuously between the French border and the Dendre start with lacustrine deposits (clays and sands) of the Wealdian. They are covered with Turonian marls. The Eocene formations form the hills which are cut by the HSR earthworks and consist of clays, sandy clays and fine clayey sands (Ypresian), glauconiferous sands and sandy clays (Landenian). The Quaternary cover is composed of continental deposits: silts and loams on the reliefs, recent alluvia in the valleys.

2.2 Karstic Phenomena

One of the characteristics of the HSR line between the French border and Brussels is the presence of a limestone substratum on the 40 first km in Belgium (up to the Dendre valley). This existing underlying rock raises the difficult problem of interfering with eventual karstic phenomena. In this region, the formation of natural shafts up to the surface caused by the collapse of underground cavities has often been observed. Due to their random property, these phenomena are not easily predictable in time and in space. The overexploitation of the groundwater table, the groundwater lowering in order to extend the quarries, the tectonics or the important vibration sources can contribute to their occurrence. The resulting risks have obviously been analysed by the authors of the HSR project, from the beginning of the studies, during and after the works. The general geotechnical investigation performed on the western branch (about a thousand in situ tests and more than 600 boreholes) was preceded by a seismic refraction survey on the whole length of the line. This very dense investigation has made it possible in a first phase to detect some clues about eventual risks of karstic phenomena. In a second phase, detailed geophysical and geotechnical investigations were carried out at these places before and during the civil works in order to locate cavities that may endanger the embankments foundations, the cutting beds and the bridges or viaducts:

- several embankment foundations were systematically injected by means of a dense mesh of destructive boreholes with instantaneous loggings;
- the cutting beds interfering with or close to the top of the carboniferous formation (in particular the cuttings located on each side of the Scheldt valley) were systematically investigated by means of radar and electromagnetic surveys. Locally, when anomalies were detected, boreholes with grout injections were executed;
- the bridges and viaducts are founded on the limestone substratum, some on direct footings, others on deep foundations (bored piles of large diameter except for the Arbre viaduct); before the construction of each footing and/or pile, destructive borings with instantaneous loggings were executed in order to find out eventual karstic phenomena and to perform grout injections. Moreover, each pile was equipped with reservation tubes allowing for a grout treatment at the base.

This methodology can be illustrated by some examples (Dethy and Detry, 1994, Halleux et al., 1994, Bustamante et al., 2002):

- the passage under the N 52 roadway in Antoing, which is supported by a thick raft allowing to bridge any deconsolidated zones within the limestone;
- the viaduct over the Scheldt river in Antoing, where extensive consolidation injections were performed at the location of one of the piers. A 16 m thickness of weathered and karstic limestone under the pile bases was treated in two phases: first a compaction grouting between the piles followed by a grouting by means of sleeve tubes (*tubes à manchettes*) through each pile;
- the bridge allowing the passage of the HSR under the existing main Walloon railway line where, due to the identification of local deconsolidated areas inside the carboniferous formation, some piles were injected at their periphery through sleeve tubes and/or at their base contact;
- the Arbre viaduct is undoubtedly the main civil engineering structure of the western branch in terms of its length, the poor characteristics of the subsoil and the size of its foundations.



Fig. 2.

This viaduct consists of 36 spans totalizing a length of 2 km and rests on the carboniferous bedrock, which is covered by a thickness of nearly 15 m of alluvial deposits. This bedrock is composed of locally dolomitised limestone, calcschist and dolomite generally fractured and including many karstic pockets with infilling sandy and clayey materials coming up from bedrock decomposition. The general geotechnical investigation along the viaduct (essentially boreholes and cone penetration tests) had to be completed by a detailed investigation at the location of each

pier: execution of 2 borings at each side of the footing associated with instantaneous loggings and pressuremeter tests followed by radar-tomography between these borings. The borehole radar-tomography systematically performed at each pier location made it possible to obtain a continuous picture of the bedrock, a realistic description of the geometry of the dissolved pockets and an evaluation of the quality of the subsoil. These measurements and data were used to extrapolate the locally performed pressuremeter characteristics, to elaborate the foundations and to plan and manage the injection operations.

The foundation technique was based on the execution under each footing of about 80 high pressure injected micropiles (diameter 170 mm) with a spacing of 1,5 m. More than 60 km of micropiles from 25 m to 30 m length were performed. This process made it possible on one hand to get a sealing between each micropile and the surrounding subsoil and on the other hand to grout the eventual voids existing between the micropiles. The obtained result is that each pier rests on a grouted foundation block under the whole area of the footing and on a mean depth of 30 m. It can be noted that, on the location of each pier, the realisation of destructive boreholes with instantaneous loggings before and after execution of each micropile, allowed us to confirm the presence or absence of deconsolidated or karstic areas. Since the completion of the structural works, the settlements of each pier have been monitored. No significant values have been detected till now.

2.3 Earthworks

The earthworks (embankments and excavations) concern mostly the postprimary cover formations: Quaternary silts and alluvial deposits, Ypresian clays, Landenian sands, Turonian marls (between the French border and the Scheldt river). The Primary basement was only locally excavated: the deep cutting in the Tournaisian limestones at Bruyelle (Scheldt valley). Apart from the problems of re-using the excavated soils and of constructing embankments on compressible soils, the following difficulties were encountered during the earthworks of the western branch:

- the execution of the track bed inside the very humid cuttings: poor soils had to be substituted by means of a 1 m thickness of crushed materials 0/300 mm reinforced with geosynthetics (reinforcing geogrid installed on a separation geotextile). This substitution, associated with the deep draining collector located longitudinally at each side of the track, allowed to solve the most critical problems of bearing capacity and drainage (Dethy et al., 2000);
- the slope stability of the cuttings had to be assured by adding draining blankets using 0/150 or 0/300 mm crushed materials. These reinforcements were systematically applied where the excavation met the interface between the Quaternary loams and the Ypresian clays which are characterized by a low permeability;
- surface protection blankets had also to be laid on the slopes where sensitive and evolutive materials like Landenian sands or Turonian marls were excavated in order to avoid any erosion damages.



Fig. 3.



Fig. 4.

3 Eastern Branch

3.1 Geological Aspects

The HSR line encounters under the Quaternary cover the tabular formations of the Tertiary (Oligocene and Eocene) and of the Secondary (Upper Cretaceous) resting unconformable on the peneplained Primary substratum. Between Brussels and Liège, the Primary substratum consists of rocks from the Siluro-Cambrian age belonging to the Brabant Massif. The line runs alongside the axial zone of this Massif and crosses, in the area of Voroux-Goreux, its southern border identified by the Horion-Hozemont fault where the contact zone between the Silurian and the Carboniferous of Namur Synclinorium exists. The Primary substratum crops only out in the vicinity of Liège and does not interfere with the HSR works on this branch. Between Liège and the German border, the Primary basement is composed of folded rocks belonging to the Verviers Synclinorium subdivided into 2 units: north, the Herve Massif and south, the Vesdre Massif. The 2 massives are separated by an overthrust fault which can be named differently depending on the locations: Magnée fault, Soiron fault... The Primary grounds are of different ages: from the Famennian to the Westphalian. They consist of schist and sandstone (Famennian), limestone and dolomite from the Dinantian (Tournaisian, Viséan) and schist or shale including sandstone massive layers and coal seams (Namurian, Westphalian). The main coal seams belong to the Westphalian stage: they have been exploited by mining works from the 19th century. The Cretaceous formations include the Gulpen, Vaals and Aachen formations. The Gulpen formation (Maastriechian, Campanian) present on the whole branch between Brussels and Liège consists of silex chalk. The chalk weathering has led to the formation of residual deposits (silex conglomerate, phosphate pockets). Old phosphate and chalk exploitations are present in the area, namely between Waremme and Liège. The Gulpen formation is also present between Liège and Battice where it comprises clays and silex silts which are dissolution residues of tufa and chalk. The Vaals formation (Campanian) consists of alternatively clays, glauconiferous sands and silts including sandstone layers (Herve smectite). It interferes with the HSR route between Liège and Battice. The Aachen formation (Santonian) includes fine sands and clayey silts with many vegetable debris and lignite lenses showing the properties of running sands when located under the watertable. This formation is present continuously between Battice and the Grünhaut wood and at some isolated places towards the German border. The Oligocene and Eocene formations consist of fine and micaceous sands (Tongrian), sandy marls (Heersian) and glauconiferous sands (Landenian). They are only present between Brussels and Liège. The HSR line encounters successively, from west to east, the Landenian grounds, the Tongrian sands at isolated locations on the reliefs. Before Waremme, these grounds are replaced by the Heersian marls up to the valley of the Geer. The Quaternary cover is composed by eolian loams or loess covering the uplands, colluvial soils as a result of the substratum weathering, silty and clayey alluvial deposits, sometimes peaty, within the valleys. Dumpings produced during the works of the motorway had also to be excavated for the HSR platform.

3.2 Crossing of Compressible Valleys

One of the specific and major geotechnical difficulties of the eastern branch is the crossing of the HSR line with various and several compressible valleys, taking into account the proximity of the existing E 40 motorway from Brussels to Liège. Three particular sites were chosen to illustrate the problems which had to be resolved: the valleys of the Gollard, the Petite Gette, the Mule and the Geer (close to the motorway's petrol and parking station near Waremme). A specific solution had to be found for each site, considering the subsoil, the distance separating the HSR line and the motorway and the height of the embankments (Dethy et al., 2000). The sites of the Gollard and the Petite Gette are similar with respect to the height of the embankments (nearly 10 m), the important estimated settlements (1,50 m for the Gollard where the thickness of the alluvial deposits varies between 8 and 10 m; more than 2 m for the Petite Gette where the thickness of the alluvial deposits varies between 12 and 15 m). The 2 sites are not the same in terms of their respective distance from the motorway:

- in the case of the Gollard, the distance between the HSR line and the motorway is sufficient to apply the classic solution of consolidating the subsoil by means of vertical drains and overload.

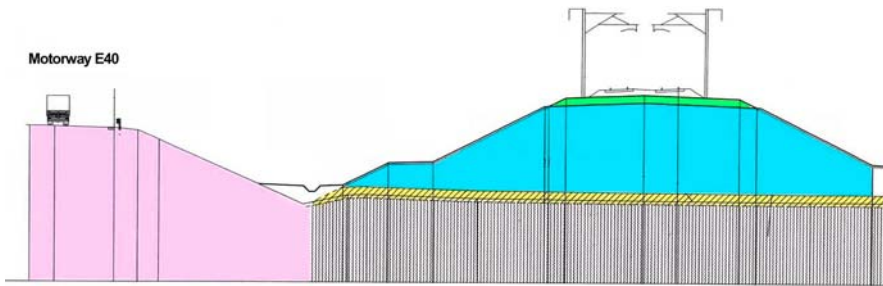


Fig. 5.

The prefabricated drains were driven through a draining platform (crushed material 0/80 mm) in a triangular mesh of 1,30 m. The embankment was performed in 3 phases; a total period of 10 months of consolidation was estimated in order to obtain a settlement of 1,50 m. The embankment monitoring, during and after the filling, was based on the measurements of hydrostatic profile gauges, inclinometers and pore water pressure gauges. The results have confirmed the calculated deformations;

- in the case of the Petite Gette, the embankment, which had to be executed for the HSR track, rests mainly on the slope of the motorway; finite element modelling showed that this configuration could lead to unacceptable fissurations of the motorway: the settlements had to be avoided by means of reinforcing the subsoil basement of the new and existing embankments through rigid piles, able to support the weight of the fill via a crushed material platform reinforced with geogrids.

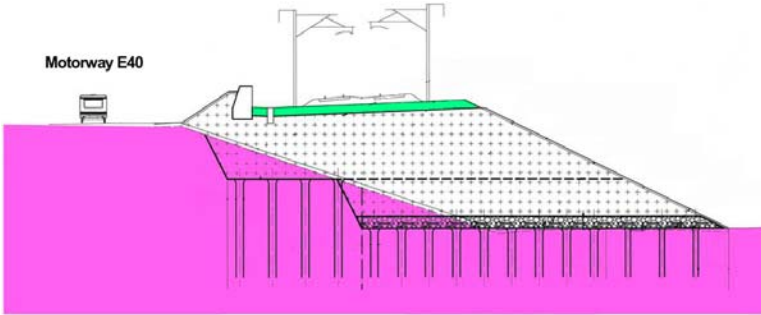


Fig. 6.



Fig. 7.

Two geogrid layers (PP) were incorporated inside the platform (1 m thick). The inclusions (executed as screw piles with partial excavation) are supported by the silex conglomerate located at the weathered top of the chalk bedrock (piles of 40 to 60 cm diameter are about 15 m long in a triangular mesh of 2 to 3 m).

The third site has to be distinguished from the others by the height of the embankment which is limited to 1 to 2 m. The alluvial deposits of the Mule and the Geer, the thickness of which varies between 8 and 10 m, interfere with the HSR line on a length of nearly 3 km and cover the silex conglomerate located at the top of the chalk bedrock. The presence of several peat pockets and the small height of the embankment result in a great sensibility to dynamic effects. Moreover, the



Fig. 8.

existing motorway along the project does not permit to opt for a consolidation by means of static overload. Consequently, a viaduct close to the ground level was designed (2750 m length) resting on more than 2400 piles which are 15 to 20 m long and anchored into the chalk.

One of the particularities of the site is that the HSR line design had to take into account the existing petrol and parking station: new access ways were built to create passages over the new railway track involving the erection of high embankments. Different techniques were used depending on the amplitude of the allowed settlements:

- in the areas close to the motorway, for the embankments higher than 4 m, rigid inclusions and reinforced platforms were used to avoid any settlement; for lower embankments, weight reduction was reached by incorporating low density (250 kg/m^3) blocks made up with re-used compressed and locally thermomelted plastic materials (bottles);
- in the areas far from the motorway, consolidation by means of vertical drains and overload was applied.



Fig. 9.

3.3 Pile Foundations in Chalk

The first load pile tests performed on the eastern half part of the Waremme viaduct, on lost steel tube cast in situ driven piles, showed important shortage of bearing capacity due to the high variations of the thickness and density encountered within the silex conglomerate and the significant weathering of the underlying chalk. The low base resistance offered by the tested piles could not be compensated by the negligible friction between the steel pile shaft and the chalk formation. For this part of the viaduct, the planned piles had to be replaced by vibro-driven cast in situ piles. The piling system comprises the following steps: first, a temporary casing with enlarged lost base is driven by means of a vibrator through the compressible layers; then an HP profile (305 x 305 mm, 88 kg/m) equipped with concrete injection tube is inserted in the casing and the void filled with concrete; afterwards, the HP profile is vibro-driven down to the required depth (with concreting under pressure occurring at the same time).



Fig. 10.

The concrete coating of the HP profile, in contact with the chalk, provides a remarkable high shaft friction allowing to support more than 80 percent of the total load pile. As shown by the instrumented load pile tests (using removable extensometers) carried out by the LCPC, the unit values for shaft resistance (q_s) can vary from 120 kPa for weathered chalk to more than 200 kPa for good quality chalk (Bustamante and Gianceselli, 1999).

3.4 The Underground Cavities

Between Waremme and the connection of the HSR with the existing line just before Liège, the route interferes with an area where risks of collapse of the sub-

soil exist due to the chalky nature of the substratum and the presence of old phosphate exploitations. Under the Quaternary silts and a variable thickness of silex conglomerate, the bedrock consists of Cretaceous chalk. At the top of this chalk, a phosphate layer may be present and has been randomly exploited in the past times. Moreover, dissolution phenomena can affect the top of the chalk in relation or not with the old exploitations. These cavities or voids can migrate up to the surface and induce collapses. This process can be accentuated by the presence of water infiltration or vibrations. In order to identify the presence of such phenomena, several investigations were performed. A microgravimetry survey was carried out before the works along the route on a length of more than 9 km (Schroeder et al., 2000). In addition, cone penetration tests were performed at the locations where significant microgravimetric anomalies were observed. Unfortunately, these investigations failed to give any clear result in order to locate dissolution pockets or old exploitations before the starting of the civil works. However, during the earth-works, several old shafts giving access to underground phosphate exploitations were discovered. The exploration of these shafts permitted to identify a network of galleries often quasi intact and excavated at the top of the chalk about 10 m depth under the ground level. After investigation, these shafts and galleries were filled with concrete.

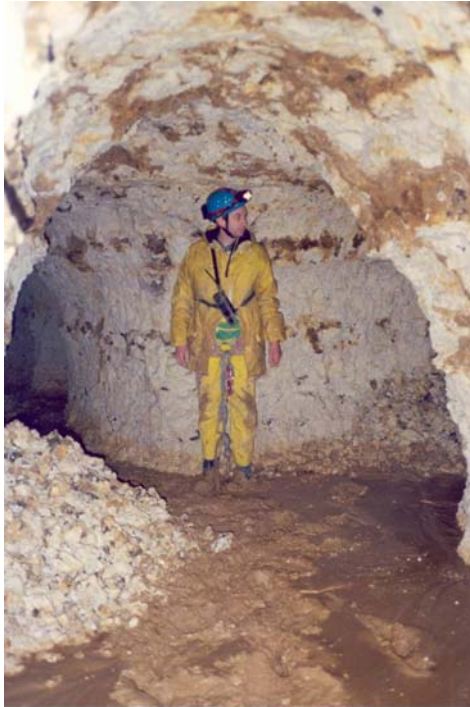


Fig. 11.

Before the filling of the first network of galleries, a radar tomographic panel test was carried out from 2 boreholes located on both sides of a previous plotted gallery: the identification of the cavity by this method was clearly successful as shown on the figure.

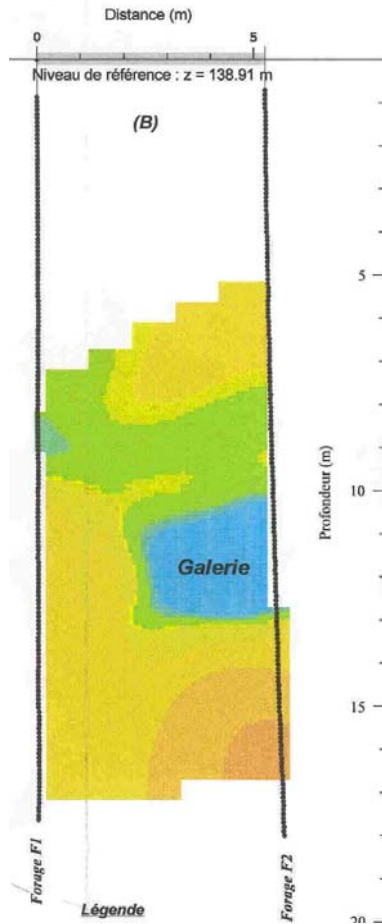


Fig. 12.

Based on this positive result, this method was also used at the location of micro-gravimetric anomalies and at the places where discovered galleries partially collapsed and did not allow a complete exploration of the underground cavities. In this manner, the presence of a network under the platform was identified, plotted and filled. The track platform was reinforced by means of a concrete slab on a length of about 100 m. In the areas where the earthworks did not discover anything but where nevertheless indications of the presence of old exploitations exist (based on old existing documents), the option was to improve the stiffness and the

impermeability of the platform's last meter, immediately under the structural layers, in order to avoid any deformations caused by the evolution of potential cavities located in the subsoil under the track. The improvement was obtained by a mixed treatment (with lime and cement).

3.5 Works between Liège and the German Border

The civil works between Liège and the German border are still in progress. East of Liège, the route leaves the urban area and the Vesdre valley by the Soumagne tunnel in order to reach the Herve plateau with a nearly 2 percent gradient. The Soumagne tunnel, about 6 km long, is being excavated through the Carboniferous shales formation of the Westphalian and the Namurian separated by 600 m of Viséan limestone (Couchard et al., 2004). The coal seams, included in the Westphalian formation, encountered by the tunnel on the first 3 km from the downstream portal, were extensively exploited in the past. In addition to these coal seams, several dislocated synclines and anticlines, several faults have to be carefully crossed by the tunnel whose breakthrough is foreseen for next autumn 2004. From the end of the tunnel (upstream portal), the HSR line joins the existing Liège-Köln motorway by means of a mostly underground route (5 cut and cover tunnels using secant piles walls within the shale substratum and diaphragm walls within the Cretaceous formations).



Fig. 13.

Along the motorway towards Germany, the hilly country of the “Pays de Herve” results in the execution of a succession of important cuttings and embankments. Some valleys need also to be crossed by viaducts like the one of Battice which bypasses the motorway interchange over more than 1200 m long.



Fig. 14.



Fig. 15.

Each pier of the 4 viaducts to be built rests on 30 bored piles (mostly 10% inclined, diameter 60 cm) executed with temporary casing. Their reinforcement consists of a wide flange HP profile (305 x 305 mm, 110 kg/m). After installation of this profile inside the casing and before concreting, the contact with the excavated bottom is ensured by means of a piling hammer which drives the HP toe in the subsoil over a depth of about 5 to 10 cm.

The length of these piles varies from 10 to 30 m. The instrumented load pile tests (using removable extensometers) performed by the LCPC have shown that this type of piles was perfectly appropriate to transmit the loads to the shale substratum. The cuttings have to be excavated within evolutive soils (Vaals and Gulpen clays, Aachen sands, shales...) and therefore have to be covered with anti erosion crushed stone blankets. If necessary, the stability has to be locally secured by adding thick crushed stone blankets on the slopes. As for the Soumagne tunnel, the substratum of the HSR line towards the German border is subjected to old mining works (coal seams) but also locally to karstic phenomena where limestone is present.



Fig. 16.

For this reason, the track platform has to be reinforced by the construction of a concrete slab designed to be able to bridge over cavities (max. 4 m diameter) liable to collapse within the subsoil. In this case, the classic track structural layers (track bed and sub-layer) are replaced by the concrete slab.

4 Re-use of Excavated Materials

On all branches of the Belgian HSR lines, the optimisation of the re-use of the excavated soils was obtained by means of lime treatment. The Quaternary very



Fig. 17.



Fig. 18.

humid silts (with low plasticity index) were extensively re-used by adding 1 to 3 percent lime, this in conjunction with the weather conditions prevailing during the earthworks. The soil treatment with quicklime provides short time benefit enabling the quasi-immediate re-use by drying, flocculating and improving the bearing capacity.

The Tuc Rail specifications regarding the soil treatment by quicklime in view of their re-use for the embankments of the HSR platforms are essentially based on the recommendations of 2 French technical guides (LCPC – SETRA, 1992 and

2000). The alternative for the treatment was the supply of quarry materials for embankments in addition to unacceptable quantities of on site excavated materials to be placed into landfill sites. The economical and environmental interests are obvious. But the execution of the landfills with lime treated soils showed the necessity to provide a thorough preparation for the ground investigations and the laboratory analyses (Dethy, 2001, Dethy and Verhelst, 2003). For the site works organisation, the stakes are high both on the technical level (quality of treatment) and on the economical level (optimisation of the lime dosage).

5 Conclusions

The present keynote lecture allowed to briefly review the most specific problems encountered during the realisation of the HSR lines in Belgium between the French and the German borders. The various and specific aspects of Engineering geology and Geotechnics were illustrated by:

- the presence of karstic phenomena and their influence on the earthworks and the civil works (bridges and viaducts foundations);
- the earthworks problems encountered during the excavation within very humid cuttings in order to secure the bearing capacity and the drainage of the track platform and to preserve the stability of slopes interfering with a low permeable interface;
- the crossing of compressible valleys taking into account the vicinity of an existing motorway;
- the realisation of special deep foundations necessary for several viaducts along the HSR lines;
- the occurrence of underground man-made cavities (coal or phosphate mining exploitations);
- the re-use of excavated materials by means of lime treatment.

References

- Bustamante M. & Gianceselli L. (1999) Train à très grande vitesse: les fondations du viaduc de Waremme. *Geotechnical Engineering for Transportation Infrastructure*, Barends et al., pp 1743-1748.
- Bustamante M., Borel S., Gianceselli L., Couchard I., Detandt H. and Dethy B. (2002) Foundation behaviour of a large HS-train viaduct after 4 years operation. *DFI, Nice*.
- Couchard I., Van Cotthem A. and Hick S. (2004) The Belgian H.S.T. Soumagne Tunnel Project. *EurEnGeo, Liège*.
- Dethy B. & Detry P. (1994) Fondations en zones karstiques. *CBGI, Louvain-la-Neuve*, pp III 44 - III 60.
- Dethy B., Theys F. and Miller J.P. (2000) Utilisation des géosynthétiques comme renfort dans les ouvrages de génie civil - Travaux sur les lignes du TGV en Belgique. *CERES, Liège*, pp 77-98.

- Dethy B. (2001) Les spécifications propres au traitement à la chaux des sols en vue de leur réutilisation au droit des remblais de plateforme du TGV belge. *Centre de Recherches Routières, Bruxelles*.
- Dethy B. & Verhelst F. (2003) Soil improvement for the construction of the platform for Belgian High Speed Train in urban areas. *IABSE, Antwerp*.
- Halleux L., Bouhenni S., Corin L., Couchard I., Dethy B., Dijkshoorn P., Monjoie A., Richter Th. and Wauters J.P. (1994) Tomographie radar appliquée à la reconnaissance des terrains de fondation du futur viaduc d'Arbre. *CBGI, Louvain-la-Neuve*, pp II 98 - II 109.
- LCPC-SETRA (1992) Guide Technique - Réalisation des remblais et des couches de forme.
- LCPC-SETRA (2000) Guide Technique - Traitement des sols à la chaux et/ou aux liants hydrauliques.
- Schroeder C., Thimus J.-F. and Dethy B. (2000) Detection of collapse hazards related to underground quarries. *GeoIng, Melbourne*.

An Overview of the Geological and Geotechnical Aspects of the New Railway Line in the Lower Inn Valley

Stefan Eder¹, Gerhard Poscher², and Christoph Sedlacek³

¹ MAG., ILF Beratende Ingenieure ZT GmbH, Framsweg 16, A-6020 Innsbruck
stefan.eder@ibk.ilf.com

Tel: +43 512 2412/0

Fax: +43 512 2412/200

² DR., ILF Beratende Ingenieure ZT GmbH, Framsweg 16, A-6020 Innsbruck
gerhard.poscher@ibk.ilf.com

Tel: +43 512 2412-171

Fax: + 43 512 2412-200

³ MAG., Brenner Eisenbahn GmbH., Industriestraße 1, A-6172 Vomp
pm_beg@beg.co.at

Tel: +43 5242 71481-0

Fax: +43 5242 71481-110

Abstract. The new railway line in the lower Inn-valley is part of the Brenner railway axis from Munich to Verona (“feeder north”). The first section between the villages of Kundl and Radfeld, west of Wörgl, and the village of Baumkirchen, east of Innsbruck, will become one of the biggest infrastructure projects ever built in Austria, with a length of approx. 43 km and an underground portion of approx. 80%. The article gives an overview of the various geologic formations - hard rock sections in the valley slopes, different water-saturated gravel and sand formations in the valley floor and geotechnically difficult conditions in sediments of Quaternary terraces. It also describes the methodology of the soil reconnaissance using groundwater models for hydrogeologic estimations, core drillings for evaluating geologic models and describes the experiences gained from the five approx. 7.5 km long reconnaissance tunnels for geotechnical and hydrogeological testing. The results of the soil reconnaissance were used to plan different construction methods, such as excavation in soft rock under a jet grouting roof and compressed-air, as well as mechanised shield with fluid support.

Keywords: tunnelling in soft rock, groundwater, jet grouting, geomechanical planning

The Geology of the Lower Inn Valley

Hard Rock Formations

This paper focuses on the Tyrolean lower Inn valley from Innsbruck to Wörgl. The hard rock formations encompassing this area are composed of carbonate rocks of the Northern Calcareous Alps to the north and carbonates south of the river Inn. The development of the valley took place along one of the large inner alpine shear

zones. In the hard rock this results in mainly tectonic transitions, which constitute a high risk potential for the tunnel due to the parallel course to the valley and to the axis of the structures. Water is present in partly geotechnically difficult rock such as the carbonates and shale of the Raibler Formation. The hard rocks of the Raibler Formation and the Wetterstein Formation also contain important groundwater resources, which should not be impaired by the excavation works.

Sediments of the Quaternary Terraces

Another characteristic of the Inn valley are the Quaternary terraces that accompany the valley on one or both sides at an elevation of about 250 m above valley floor. They are generally believed to have evolved on account of the advance of marginal tributary glaciers during the Hochwürm glaciations, damming up the Inn river in the main valley and thus effecting the complex internal structure. The lithological sequence can be divided into a lower, lacustrine section (banded silts) and an overlying, fluvial section (sands und terrace gravel). The whole sequence is covered with till deposits. Post glacially these sediments were eroded, partly to the base of the terrace, or re-deposited (disturbed terrace gravels) and covered by gravel, sand, silt, sedimented near the ice margin. Fine-grained, impermeable and coarse-grained, permeable horizons lead to highly variable groundwater conditions, which are very difficult to forecast and to handle during excavation works.

Sediments of the Valley Bottom

The sediments of the valley bottom reflect the change from fine-grained sediments (clayey silt, fine sand, and sand) in former quiet water zones to coarse-grained or sandy gravel in fluvial zones (Inn river gravel, alluvial fans). The geotechnically difference lies within the probability of the occurrence of boulders, sand-silt layers and zones with high permeability (kf up to $10 \cdot 10^{-2}$ m/s). Along the entire route, the groundwater level is 2-5 m below ground surface.

The Project

An Overview of the Route

The lower Inn valley is one of Europe's main traffic arteries and an important route both for traffic from Eastern to Western Austria and across the Alps from Italy to the Northern EU countries, and vice versa (Figure 1). The existing railway line in this area, which serves as the northern approach ("feederline") to the Brenner Base Tunnel (Köhler and Bartl, 2000), has already reached its capacity limits. In the endeavour to encourage a modal shift from road to rail, the rail capacity between Kundl south of Kufstein and Baumkirchen east of Innsbruck shall, in a first step, be increased by the construction of a new 43-km-long high-capacity railway line.

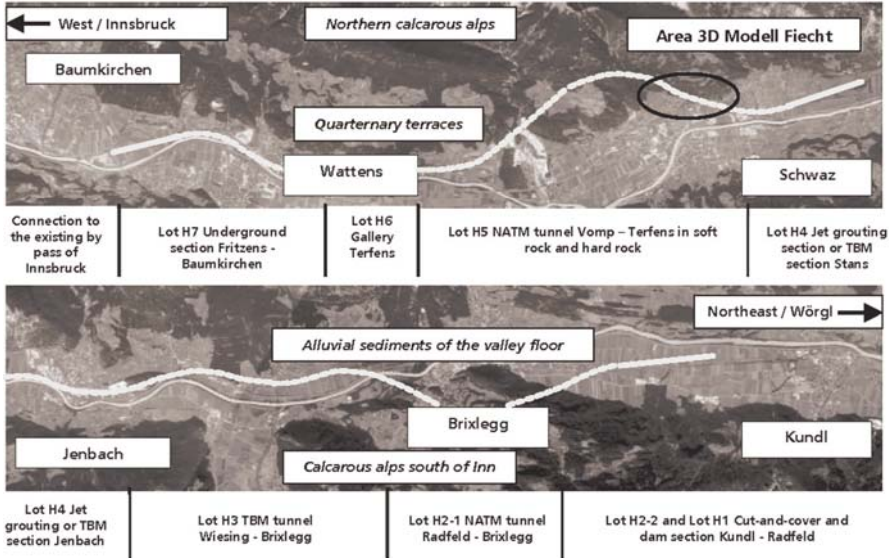


Fig. 1. Overview of the project area.

As a project area, the Lower Inn valley imposes numerous restraints on the alignment of a high-capacity line, not only due to the alignment criteria resulting from the high building density in the valley (residential and commercial facilities, Inn valley motorway and existing railway line) but also due to partially unstable valley slopes. Further restraints result from the intensive utilization of the project region as water supply area. A characteristic of the planning process to date is the tender design of two alternatives with partly marked differences regarding gradients and construction methods (Gangkofner et al. 2003). The most significant difference regarding the construction method is found in the route section between Jenbach and Stans. Variant 1 is designed with shallow gradient and cut-and-cover construction methods, with special measures for crossing the motorway, the existing railway line and sensitive structures, while variant 2 proposes a deep gradient and shield tunnelling methods. Table 1 provides a brief overview of the planned construction methods.

The Environmental Impact and Route Selection

The demands made on the geologists mainly concerned the water resources assessment during the environmental impact statement and route selection (Fisch et al 2003, Poscher et al 2002). The groundwater flowing parallel to the river Inn in the Inn valley is intensively used to provide water both to private households and industrial enterprises. The Quaternary terraces are also the site of extensive groundwater resources (groundwater protection area at Gnadenwalder Plateau). The affected zones of hard rock contain no extensively exploited joint water aqui-

Table 1.

Constr. Lot	Construction method	Length
H1	Earthworks with bridges and dams	app. 3 km
H2-2	Cut-and-cover section	app. 2.5km
H2-1	NATM tunnel (0.6 km already excavated)	app. 5 km
H3-1 shallow gradient	TBM tunnel with a gallery and a cut-and-cover section; a short NATM tunnel (0.5 km)	app. 7 km
H3-2 deep gradient	Replacement of the cut-and-cover section and the gallery with a shield driven tunnel	app. 7 km
H4-1 shallow gradient	Cut-and cover sections, two jet-grouted columns to protect NATM tunnels under the motorway and railway, earthworks	app. 3.7 km, 1.5 km and 3 km
H4-2 deep gradient	Two shield driven tunnels, short cut-and-cover sections and earthworks	see above
H5	NATM tunnel in hard and soft rock	app. 7.7 km
H6	Gallery	app. 1.3 km
H7-1 / H7-2	Cut-and-cover sections in Lot H7-1; jet-grouted columns to protect NATM tunnel under the existing railway	app. 4.6 km

fers in the immediate route area, however, the affected groundwater resources are used for local water supply. Separated from the tunnel structures by impermeable rock units parallel to the route, water resources of supra-regional significance occur both to the north (groundwater protection area “Inntaldecke Karwendel”) and to the south (Alpquell mineral water aquifer). The route submitted for the environmental impact assessment does not affect these important water resources. Because of the importance attached to the protection of people and water resources in the densely populated Inn valley, restrictions were imposed in addition to railway and alignment requirements, which made it imperative to design the route in tunnels in the groundwater and in the valley slopes. For the sections in the valley bottom it was an essential precondition to ensure that there would be no impact on the groundwater flow, necessitating the construction of sealed construction pits without any lowering of the water table and / or shield tunnelling.

Soil Reconnaissance and Resulting Construction Methods

The NATM Tunnels

Four route sections are driven according to the NATM. While the “Tiergarten tunnel” in Wiesing (Lot H3) with a length of approx. 0.5 km is located in simple geological conditions (Wetterstein-limestone), the two long NATM tunnels to be

advanced from Radfeld to Brixlegg (length approx. 5 km), and the Vomp-Terfens tunnel (length approx. 8 km) made high demands on the geologic-hydrogeologic subsoil models. The attendant circumstances and complex hydrogeological conditions made exploration by means of reconnaissance tunnels the most appropriate approach.

The tunnel from Radfeld to Brixlegg traverses mainly carbonate rocks of the Wetterstein and Raibler Formation of the so-called Hauskogel and Hohenegg Nappe (Tirolikum, Northern Calcareous Alps) (Sausgruber and Brandner 2003) south of the Inn River. Subordinately, rocks of the basement occur – completely tectonised phyllites - and the lower Triassic - anhydrites of the Reichenhall Formation. While driving the Brixlegg East reconnaissance tunnel, which will be used as escape tunnel during operation, the existence of fault zones with non cohesive, water saturated kakirites, running sub-parallel to the Inn valley and thus at an acute angle to the route alignment, was confirmed. In the course of an extensive exploration of different sealing and drainage measures groundwater draw-down turned out to be the only economically solution (approx. 5 bar), especially as the effects in the hydrogeologically sensitive area (spa water aquifer system in the branched fault zones) turned out to be largely reversible. A 600 m long section including access tunnel has already been erected, with the tunnel having to traverse about 120m of soft rock which will not be discussed in more detail. For this section the following reconnaissance methods can be summarised:

- Lot H2-1: NATM tunnel – reconnaissance tunnels with in-situ testing, core drillings, 3D-model, geophysics

No serious construction problems are expected for the approx. 3km long hard rock section of the Vomp-Terfens tunnel since the questions on the hydrogeological influence on the groundwater aquifer have been clarified by means of the accompanying reconnaissance / escape tunnel (Poscher et al. 2002). In contrast, the marginal areas with a length of about app. 4,7 km of this tunnel have to be classified as technically difficult with regard to the advance through the slope of an inner alpine terrace. The eastern section of softrock mainly comprises a 600 m long excavation section in gravelly sediments of the ice margin to sandy-silty sediments of the main terrace. The main problem is to controll the groundwater inflow. The results from the soil survey and the Fiecht reconnaissance tunnel, located above the actual tunnel site, were evaluated in a 3D model with numerical groundwater modelling (see fig. 2). Both the recorded long-term conditions and the changes caused by the excavation of the reconnaissance tunnel and the large-scale pumping tests were modelled. The effectiveness of different drainage measures was tested, resulting in the development of an excavation concept in stages, adjustable to different hydrogeological conditions. The following reconnaissance methods can be summarised:

- Lot H4-Fiecht: reconnaissance tunnel, exploratory and groundwater testing wells in a cavern, large scall groundwater pumping tests, hydrogeological numerical modelling

In the western softrock section, the overburden ranges from a few meters, in cohesionless terrace gravels up to 200m, in highly consolidated gravels of a Quaternary delta complex. Here, the entire lithofacies spectrum of an inner alpine terrace is expected for the excavation, ranging from basal silts, water-bearing sands and gravels of the principal terrace, over-consolidated till, to postglacial terrace gravels (redeposition products of the principal terrace). The shift from slightly to highly permeable rock may lead to layered groundwater horizons which are difficult to control during excavation. This tunnel is the first to be excavated according to the principles of the so called Austrian Geomechanics Guideline (Österreichische Gesellschaft für Geomechanik 2001) and has been under construction since October 2003. It was the documentation of the reconnaissance tunnels that allowed the rock mass to be classified in detail in line with the guideline and as verified by tests (Eder et al. 2003).

- Lot H5: reconnaissance tunnel, in-situ testing, core drillings

It has become evident that the spectrum of rock mass types and rock mass behaviour types encountered could not have been ascertained without the reconnaissance tunnels, both the fault zones at Brixlegg with their hydrological impacts, and the Quaternary deposits of deltaic sediments and intermediate terrace gravels in Vomp.

The TBM Tunnels

In addition to the route sections in the slope, for noise control purposes and to minimise the use of land, tunnel structures will be located in the valley bottom and thus below groundwater level. Differing from the design phase of the EIS (environmental impact study), alternatives with shield driven tunnels were planned for these sections. They replace up to 30 m deep pits for tunnels constructed using the cut-and-cover technique, and a tunnel to be driven using mining methods in softrock with fluctuating groundwater levels. What were essential for the decision to use TBM excavation was the positive experience as well as the requirements of the EIS which prohibited an open crossing of the river Inn (Lot Nr. 3 between Brixlegg and Jenbach).

The shield driven tunnel between Brixlegg and Wiesing (Lot H3) predominantly intersects gravel sediments of the Inn River. In its western section the postglacial alluvial fan at Bradl is under passed. It is forecast to be geotechnically difficult due to the high permeability of the Inn gravels, the presence of boulders and interlayered silt. Alternatives with deep gradient in which the base of the alluvial fan does not extend into the cross-section minimise the risk of hitting boulders. To the west intercalations of medium grained sands and coarse grained, clayey silts are encountered which form several aquifers with partly increased sulphate concentrations. In these sections the subsoil survey was done by means of core drillings, with a number of large diameter drillings (DN 800 mm) to determine the maximum grain size.

The shield-driven sections between Jenbach and Stans (lots H4) are expected to intersect mainly gravely deposits of the Inn River and its tributaries. The geotechnical problems encompass crossing of the motorway and existing railway line (in total six times) at an acute angle, the low distance to partly sensitive buildings (high-rise storage facilities) and route sections in the former riverbed of the Inn.

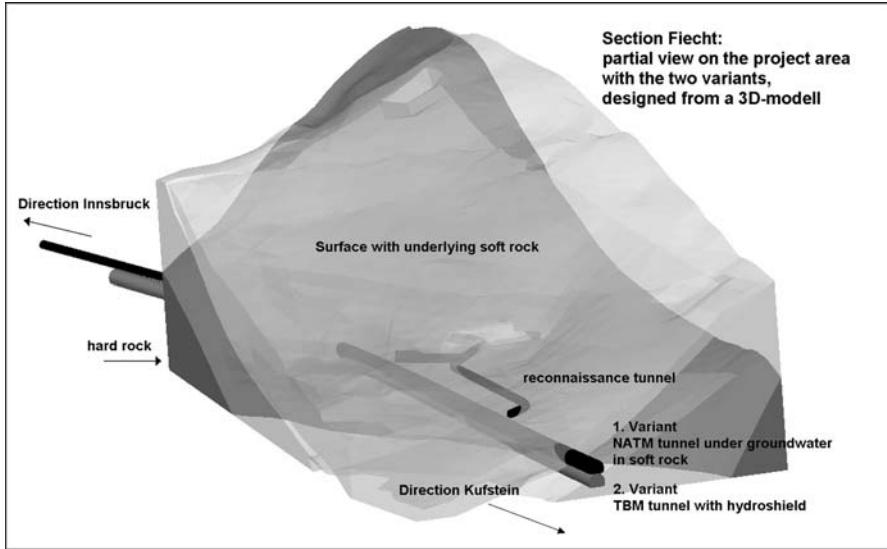


Fig. 2. 3-D model of the Fiecht area with different variants (NATM and shield tunnel).

The western end of this lot, the transition to the solid rock (see fig. 2), is also considered to be geotechnically difficult. In summary, the following reconnaissance measures were carried out for the shield driven sections:

- core drillings, in-situ testing, test wells, numerical groundwater modelling, mineralogical analyses

The Cut-and-Cover and Jet-Grouted Sections

A total of four lots (H2-2 in Radfeld, the shallow variants of lot H4 in Jenbach and Stans and lot H7 in Fritzens) will be designed as cut-and-cover tunnels with a shallow gradient and with sealed pits as an alternative to the shield-driven sections. The depth of these pits will be up to 30 m, with the sheeting to be selected by the contractor. As a relocation of the existing line and the A12 Inn valley motorway was not possible for all sections, solutions comprising mining methods had to be found for those sections. It is planned to do this with jet-grouting columns, which protect the construction area against groundwater. The subsoil conditions were explored at the crossings by complementary inclined drillings (see fig. 3).

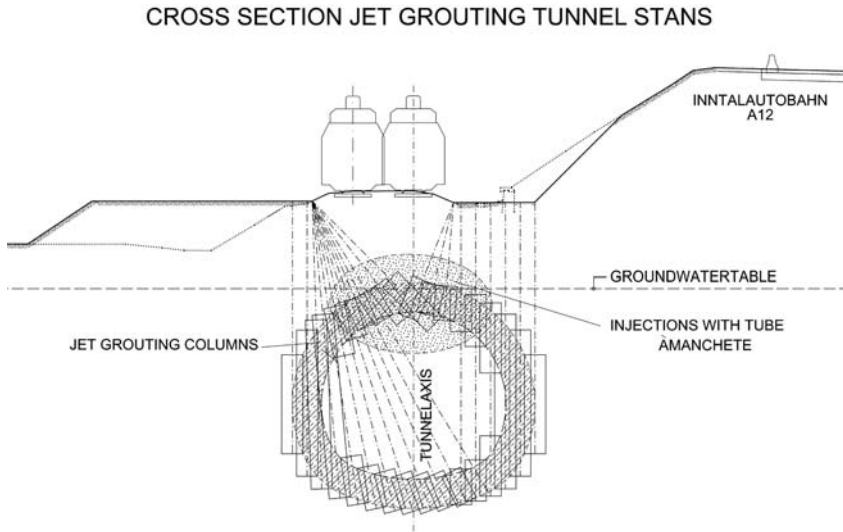


Fig. 3. Cross section of the jet-grouting enclosure.

Furthermore, construction specific tests were conducted with 3 test fields for jet-grouted columns and 2 pile driving tests for different types of sheet. The results, particularly those of the inclined test columns that were exposed, resulted in planning complementary risk reducing measures to avoid the hazard of water ingresses. The main risk is the fact that the columns have unpredictable, varying diameters. Therefore dewatering with compressed air was found to be necessary. In summary, the following soil reconnaissance measures were carried out for the cut-and cover sections and jet grouting tunnels:

- core drillings, in-situ testing, test wells, numerical ground water modelling, jet-grouting tests, test shaft, sheet piling test

Concluding Remark

The commencement of tunnelling works for the Stans-Terfens tunnel in October 2003 comprised the start of construction of the first section of the largest European infrastructure project - the railway axis from Munich to Verona. From the engineering geologist's point of view, extensive experience was and is continuously gained in the field of soil reconnaissance, in tunnelling in unconsolidated soft rock, and in tectonically stressed and faulted carbonates. The subsoil conditions range from alluvial silt, gravels of different origin and consolidation, to conglomerated Quaternary coarse gravel and overconsolidated glacial sediments. The required construction measures range from a NATM tunnel, shield tunnelling, special underground engineering measures for up to 30 m deep pits and jet-grouting supported excavation methods with compressed air. The subsoil survey comprised:

- structural geological and Quaternary geological mapping
- documentation of a total of 5 reconnaissance tunnels with a length of approx. 7,5 km,
- in total app. 25,000 linear metres of core drillings with borehole and soil geophysics
- long-time monitoring of 2000 groundwater measuring points,
- hydrogeological (pressure relief test at Brixlegg Ost, large-scale pumping tests) and
- geotechnical (jet-grouted columns –test fields, grouting tests, sheet piling tests, test shaft) tests
- with 3D and numerical simulation

This construction provides extensive experiences and it is necessary to continue the evaluation of geological data to enhance the knowledge for future projects.

References

- Bartl M & Köhler M (2000) Munich-Verona Rail Link, Investigations for the northern approach in Austria and for the Brenner Base Tunnel. In: Felsbau 18, No. 4, pp. 7-13. Essen.
- Eder S, Poscher G & Schwarz L (2003) Baugrundmodelle und hydrogeologische Modelle für Tunnelvortriebe in quartären Sedimenten am Beispiel der Zulaufstrecke Nord der Eisenbahnachse Brenner. 14. Tagung für Ingenieurgeologie, pp. 77-82. Kiel.
- Gangkofner T, Keinprecht M & Pellizari M (2003) Baumethoden im Unterinntal, tunnel 1/2003.
- Poscher G., Fisch H., Mammel R., Sedlacek C. (2002) Konfliktfeld Untertagebau und alpine Wasserressourcen. In: Felsbau, Vol. 20, No. 5, S. 101-111, Salzburg, Austria.
- Fisch HR., Mammel R., Poscher G., Reichl I. (2003) Methods of fractured aquifer characterisation using an example of a brittle fault zone in calcareous rock. In: IAH International Conference on Groundwater in fractured rocks Prague, 15-19 September 2003.
- Österreichische Gesellschaft für Geomechanik (2001): Richtlinie für die Geomechanische Planung von Untertagebauwerken mit zyklischem Vortrieb. Salzburg.
- Sausgruber T, Brandner R (2003): The relevance of Brittle Fault Zones in Tunnel Construction – Lower Inn Valley Feeder Line North of the Brenner Base Tunnel, Tyrol, Austria. Mitt. Österr. Geol. Ges. 94: 157-172.

Stability and Serviceability of a Gas Pipeline at the Base of a Steep Creeping Slope

Rolf Katzenbach¹, Matthias Seip², and Johannes Giere¹

¹ Institute and Laboratory of Geotechnics
Technische Universität Darmstadt
Petersenstraße 13, 64287 Darmstadt, Germany
{katzenbach, giere}@geotechnik.tu-darmstadt.de
Tel: +49-6151-162149

² Ingenieursozietät Professor Dr.-Ing. Katzenbach
Robert-Bosch-Straße 9, 64293 Darmstadt, Germany
seip@katzenbach-ingenieure.de
Tel: +49-6151-1301360

Abstract. The disposals of potash mining are stored on huge heaps with heights up to 200 m and a ground view of more than a square kilometre. The material behaviour of the piled salt is strongly visco-plastic, so that the slopes are moving constantly at slow rates. As the strength of the salt is rate-dependent, structural analysis of the slope stability has to consider the deformations and deformation rates of the slopes as well as the deformation behaviour of the subsoil. Due to the complex material behaviour, the structural analysis is accompanied by an extensive measuring programme, according to the Observational Method. The paper focuses on a high-pressure gas-pipeline situated at the baseline of the slope of a heap with a height of 190 m.

Keywords: gas, pipeline, slope, heap, visco-plastic, potash mining, rock salt, serviceability, creep, observational method, inclinometer, slip, deformation, stability.

Introduction

In German potash mining 50 % to 75 % of the mined salt is left as waste which mainly consists of rock salt (Halite, NaCl) and small amounts of various other salts (Beer 1996). The waste material is piled on huge heaps, with heights of up to 240 m. With a density of up to approx. 1.9 t/m³ they induce very high loads to the ground and especially to the basis of the slopes. The visco-plastic behaviour of salt requires special considerations and calculations for the design of these heaps. Especially when dealing with the serviceability, one has to take into account the permanent movement of the slopes, which often leads to problems concerning the serviceability of adjacent structures. In this paper a case is presented, where it was required to deal with these properties and conditions in special ways.

1 Material Behaviour of Rock Salt

Rock salt exhibits a strongly time- and load-dependent non-linear behaviour. Exposed to deviatoric stresses the salt will creep at a constant rate. With time passing and under the influence of water and overburden, the granular rock salt with an initial density of $\rho = 1.4 \dots 1.5 \text{ t/m}^3$ gradually transforms into a rather compact rock salt with a density of up to $\rho \cong 1.9 \text{ t/m}^3$, what is near to the original density of $\rho = 2.2 \text{ t/m}^3$. Material strength of rock salt strongly depends on the stress level and the deformation rate. In figures 1 and 2 the results of two strain driven triaxial tests on rock salt are given. The cell pressures are the same, whereas the strain rates vary by the factor 1000. Whereas the specimen with the higher strain rate of $d\epsilon_1/dt = 10^{-8} \text{ 1/s}$ shows the typical behaviour of a dense granular material (peak strength q_{fr} followed by a decrease of deviatoric stress), the second specimen submitted to the same strains at a lower strain rate of $d\epsilon_1/dt = 10^{-5} \text{ 1/s}$ does not fail. This specimen creeps at a constant rate with a constant stress level q_{stat} . Creep is driven by stresses. Submitted to a deviatoric stress state, rock salt begins to creep at an initially high rate, slowing down asymptotically to a constant rate, which is called the stationary creep rate ϵ_{cr}^{stat} (fig. 2). At this rate micromechanical creep mechanisms (dislocation creep, diffusion creep) take place, allowing the specimen to bear large strains without macroscopic failure.

Creep rates and corresponding stresses are connected by the creep function, considering both volumetric and deviatoric creep mechanisms. Based on extensive experimental data from rock salt of several potash mines in Germany, Boley formulated new constitutive equations describing creep and strain rate dependent failure of rock salt (Boley 1999). For a more detailed discussion of the material

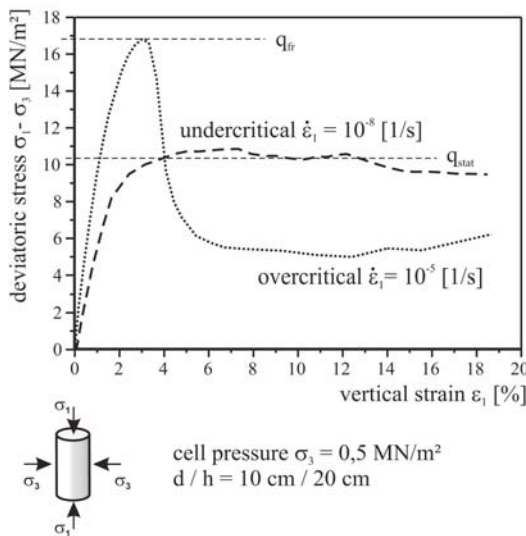


Fig. 1. Typical triaxial tests on rock salt.

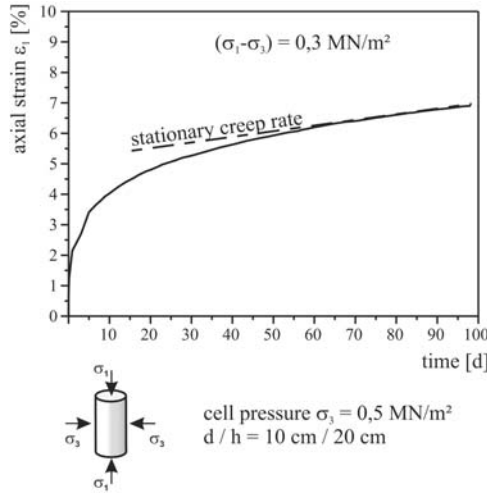


Fig. 2. Typical creep curve of rock salt.

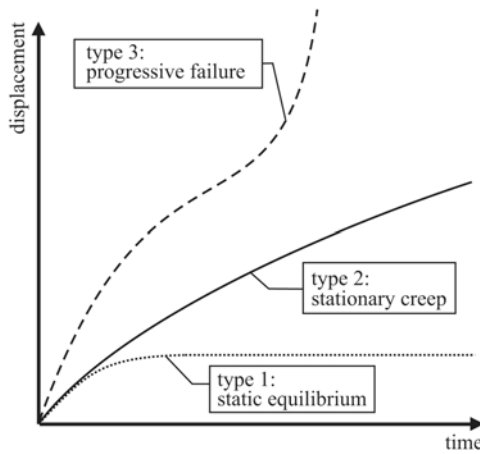


Fig. 3. Time-Displacement for time-dependent material behaviour.

behaviour of rock salt see for example Chumbe et al. (1996) Fordham (1988), Munson & Wawersik (1991) and Boley (1999).

Structures built of material with time dependent behaviour are stable although they may be moving at a constant rate (fig. 3). A collapse of the structure is preceded by an acceleration of the movements (type 3 in fig. 3). The bearable acceleration of the structure and the distance from collapse depends on site conditions and parameters, which are hard to determine with appropriate accuracy. It is crucial to observe the movements by geodetic and geotechnical measuring devices

and to review the measuring results regularly. The theoretical models for prediction have to be validated and updated in order to assess the risk of failure of these structures and are applied within the framework of the Observational Method (Brandl 1979, Katzenbach & Hoffmann 2003).

2 Deformations of a Gas Pipeline

2.1 Location and Problems

The gas pipeline is situated within a distance of less than 25 m at the base of the slope of a heap 190 m high. The base of the heap has the shape of a kidney. The length of the heap in southeast to northwest direction is about 1200 m. The width from northwest to southeast is 550 m. The gas pipeline with a soil cover of 1 m and a diameter of 0.35 m passes along the northwest side of the heap (fig. 4a).

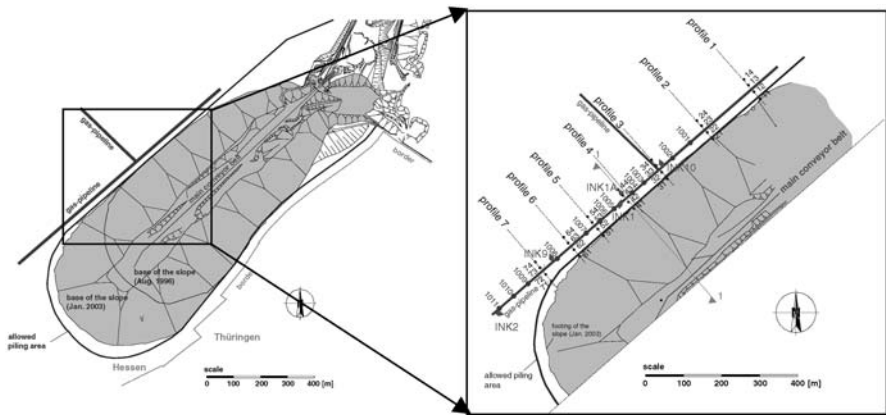


Fig. 4a. Ground view of the heap.

Fig. 4b. Ground view (detail) with measuring system.

In the more detailed figure 4b the locations of the gas pipeline and the measuring system is shown. According to the Observational Method the horizontal and vertical deformations of the gas pipeline are surveyed by several profiles of geodetic measuring points (profiles 1 to 7) and by inclinometers placed along the side of the tailing heap within a distance from 10 m up to 50 m (INK 1 to INK 10). The inclinometers have a depth of 30 m. Furthermore several points along the baseline of the slope are measured geodetically (points 1001 to 1011).

2.2 Deformations

The subsoil below the heap consists of quaternary loam (sand, silt, and clay) down to a depth of 2 m. Under the quaternary soil follows the Bunter Sandstone with partly weathered layers and two natural slip surfaces in a depth of 5 m and 10 m.

Due to high loads caused by the waste in conjunction with natural slip-surfaces and weak zones respectively in the subsoil, large deformations, partly at accelerating deformation rates, occurred. The deformation may cause stability and serviceability problems of the gas pipeline in the long term. In figure 5 some measuring results from the inclinometer INK 1 based on the zero measurement from June 1997 are shown. The inclinometer shows the two natural slip surfaces in depths of 5 m and 10 m. Fig. 9 shows the results of the geodetical surveying in profile 4, beginning with the point nearest to the slope (point no. 41). Profile 4 shows the largest deformations of all profiles. As can easily be seen from the direction of the deformations the movement became stable in 1999 (point no. 41 and 42) with a direction of approx. 350 gon (NW). It was not before 2001 that the movement reached point 43 and in point 44 the movement does not show a stable direction up to now. Deformation rates of approx. 10 cm/a in points 41 to 43 (fig. 6) do not increase any more.

Having a look at the horizontal deformations along the baseline of the slope in the points 1001 up to 1011 (fig. 7) the localization of the deformations can be noticed. The maximum of the deformations is noted between the points no. 1004 and 1005 where profile 4 is situated. The horizontal extension of the moving part of the subsoil parallel to the baseline of the slope can be estimated to approximately 300 m.

Taking into consideration all available data, the observed movements have to be concluded as follows:

- The upper 5 m to 10 m of the subsoil are moving at a rate of 100 mm/a in direction NW, orthogonal to the baseline of the slope.
- The movements take place on two slip surfaces in the Bunter Sandstone.
- The movements are localized to an area of approx. 300 m along the baseline of the slope and to less than 100 m orthogonal to it.

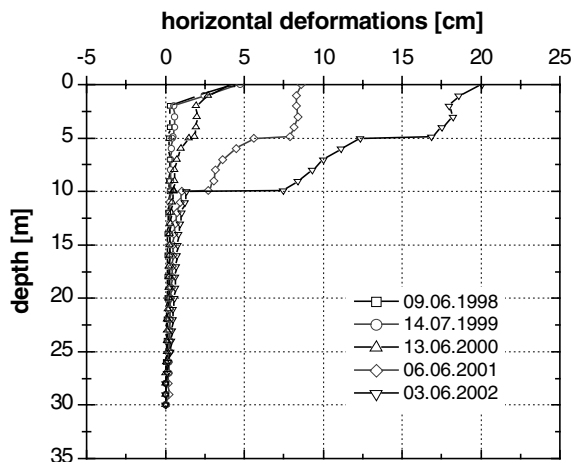


Fig. 5. Horizontal deformations measured in INK 1.

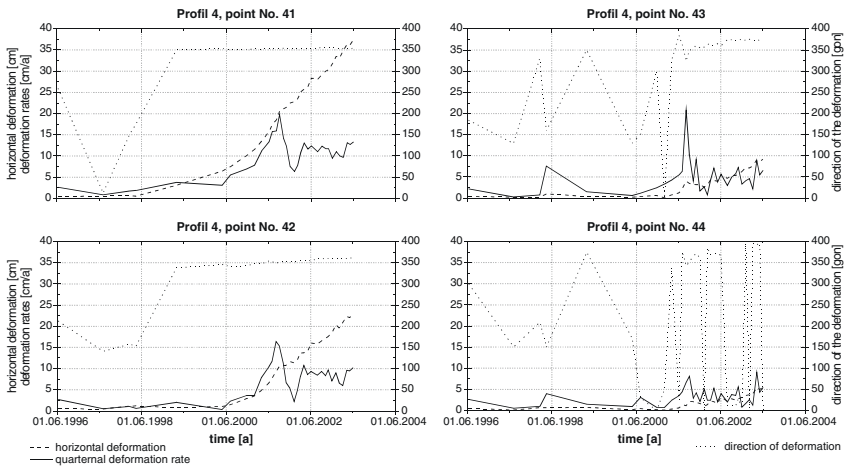


Fig. 6. Deformations, deformation rates and direction of deformation in Profile 4.

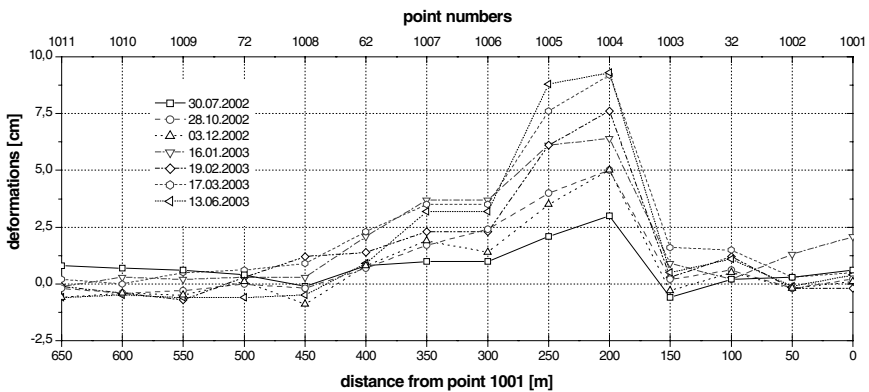


Fig. 7. Horizontal deformations along the baseline of the slope.

2.3 Application of the Observational Method

With respect to the very high sensitivity of the gas pipeline to induced deformations a concept of safety as well as a monitoring and restoration concept has been developed. One component of the monitoring concept is the numerical simulation based on the results of the measuring programme to improve the prediction of deformations of the gas pipeline that had to be expected. The discretization of the Finite-Element-Model is shown in figure 8. Visco-plastic material behaviour for the salt has been considered using the constitutive equations of Boley (1999). Bunter Sandstone and weathered Bunter Sandstone are modelled using elastoplastic material behaviour. The slip surfaces in a depth of 5 m and 10 m are modelled as contact pairs using the master-slave-concept to allow large deformations.

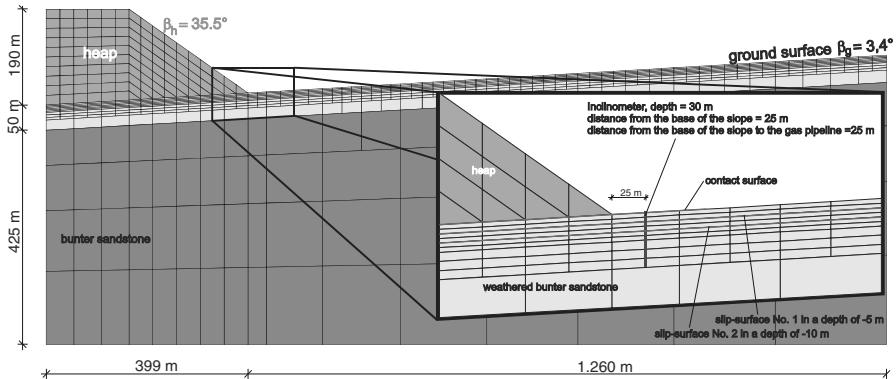


Fig. 8. Finite-Element-Model of the heap.

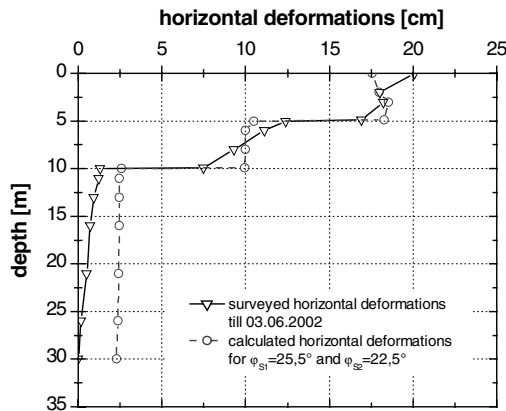


Fig. 9. Calculated and measured horizontal deformations of inclinometer INK 1.

With the calibrated model numerical simulations for an improved forecast of the expected deformation have been executed. Fig. 9 shows the comparison between measured and calculated horizontal displacements in inclinometer INK 1. The angles of friction ϕ_s in the slip surfaces have been back calculated. Both curves correspond well. With the calibrated and validated model a tool to predict the future deformations and to assess risk of failure is at hand. Along with the extensive surveying programme the induced deformations to the gas pipeline can be predicted. Thus a safe operation of the tailing heap and its adjacent structures is ensured in spite of the observed movements. If the deformation of the gas pipeline reaches a critical range the following structural measures are provided:

1. Uncovering the gas pipeline for stress relief and to reset the occurred elastic deformations.
2. Installation of a bellow expansion joint at the branch line.

3. Setting down the gas pipeline and ensuring the gas supply with an existing alternative pipeline system.
4. Passing a new pipeline in a greater distance.

The critical deformation of the gas pipeline has been calculated against the distance of the measuring points. For this, the horizontal deformation must not exceed 60 cm within the range of 50 m (distance of two measuring points).

References

- Beer, W. (1996) Kalilagerstätten in Deutschland. *Kali und Steinsalz* 12 (1), 18-30, Glückauf, Essen.
- Boley, C. (1999) Untersuchungen zur Viskoplastizität und Festigkeit von Steinsalz. *Mitteilungen des Institutes und der Versuchsanstalt für Geotechnik der Technischen Universität Darmstadt*, Heft 48, 1-236, Darmstadt.
- Brandl, H. (1979) Design of high, flexible retaining structures in steeply inclined unstable slopes. *Proc. 7th ECSMFE* 3, 157-166, Brighton.
- Chumbe, D., Lloret, A., and Alonso, E. E. (1996) Creep and Permeability Tests on Compacted Granular Salt. *The Mechanical Behaviour of Salt, Proceedings of the Fourth Conference on the Mechanical Behaviour of Salt*, Montréal, 331-339, Aubertin, M. and Hardy, H. R. (Eds.), Trans Tech Publications, Clausthal-Zellerfeld.
- Fordham, C. J. (1988) Behaviour of Granular Halite for Use as a Backfill in Potash Mines. 1-181, Dissertation, University of Waterloo, Ontario, Canada.
- Katzenbach, R. und Hoffmann, H. (2003) Möglichkeiten und Grenzen der Identifikation und der Beherrschung von Massenbewegungen von Boden und Fels (Rutschungen). *Bauingenieur* 78 (7/8), 381-386, Springer, Heidelberg, Berlin.
- Munson, D. E. and Wawersik, W. R. (1991) Constitutive Modelling of Salt Behaviour - State of the Technology. *Proc. 7th Int. Congress on Rock Mechanics, Workshop on Rock Salt Mechanics*, 1797-1810, A.A.Balkema, Rotterdam.

Investigation of Karst Cavities and Earth Subsidence with Combined Application of Boring and Geophysics in the Progress of High-Speed Railway Routes

Bodo Lehmann¹, Rudolf Pöttler², Alexander Radinger³, and Manfred Kühne¹

¹ Deutsche Montan Technologie GmbH, Am Technologiepark 1, D-45307 Essen
lehmann@dmtdt.de
Tel.: +49 201 172-1980
Fax: +49 201 172-1640

² ILF Beratende Ingenieure, Framsweg 16, A-6020 Innsbruck
Rudolf.Poettler@ibk.ilf.com
Tel.: +43 512 2412 141, +43 512 2412 200

³ Verbundplan Prüf- und Meßtechnik GmbH, Rainerstraße 29, A-5020 Salzburg
Alexander.Radinger@verbundplan.at
Tel.: +43 662 8682-22325
Fax: +43 662 8682-122325

Abstract. In Germany there are a lot of new high-speed railways in planning or under construction. One of these is the new Nuremberg – Ingolstadt railway line and the updated line from Ingolstadt to Munich. These two lines will form part of a high-speed trans-European railway link from Scandinavia via Berlin to Munich and Verona. The 78 km railway line construction project has been divided into three contract sections: Contract Section North, mainly characterised by pure earth and bridge works; Contract Section Centre, with the emphasis mainly on tunnel construction; and Contract Section South, combining earthworks and tunnelling. Extensive geophysical investigations combined with borings are carried out in critical areas between Nuremberg and Ingolstadt. The target of this geological exploration phase is mainly the detection of karst pits and earth subsidences (dolines). In this area these geological objects are an important aspect for the stability and permanent serviceability of the high-speed railway routes. The exploration concept on the open stretch consists of combined geological enquiry, geotechnical work, geophysical investigations and borings, which are positioned at the found anomalies of geophysics. The survey leads to a common interpretation of all information and results. After several test campaigns the combination of at least two geophysical methods yields to the best results. Dependent on the thickness of the overburden layer seismics, micro-gravity and/or georadar are applied from the surface. Additionally tomographic methods are used between boreholes for special topics. Important for the success of the investigation in difficult geological areas are the excellent co-operation between all scientists, engineers and technicians (geologists, geotechnicians, geophysicists, driller, consultants, etc.).

Keywords: karst cavities, boring, geophysics, high-speed railway routes.

Introduction

A high-speed railway route construction in karst geology is a very complex procedure. Between technical and economic solutions a fine balance is required, including geological and hydro-geological exploration campaigns, numerical analysis, design, and final operation of the construction process. In as early as the concept stage, when preparing the project and the design sequences, it has to be taken into account that it may not be possible to explore fully all karst and sinkhole structures prior to construction. A full and detailed description of the ground, which would subsequently permit an accurate tailor-made design as the basis for reliable tendering and a well-defined construction process, may simply not be feasible (Pöttler and Wegerer 2003). Exploration performed to provide a comprehensive description of the ground is best carried out according to a multi-stage concept. A distinction has to be made between pre-construction exploration and exploration and documentation that is carried out during excavation and construction. It should be the aim to get a good knowledge of the geotechnical properties of the subsurface already during the early phase of the construction project. Geotechnical exploration is traditionally made by drilling boreholes, examination of cores, laboratory measurements on cores, and mechanical and hydraulic tests in boreholes beside the description of the geological situation according to outcrops and prospecting pits, shafts or tunnels. The results of geophysical surface measurements can be used to define the optimum distribution of borehole positions. This approach often reduces the number of boreholes to be drilled. So the optimum underground model can be developed by a combination of geophysics and drillings. The following factors should be taken into account when defining the exploration specification:

- Technical constraints for the application of different exploration methods.
- Technical limits of different methods under the given boundary conditions: geology, vibrations, etc.
- Costs for direct and indirect methods of exploration, which increase disproportionately with decreasing limit sizes.
- Cost for covering the effects of undetected cavities the size of which is below the above-mentioned limit.

The Nuremberg-Ingolstadt high-speed railway line is part of the high-speed network being newly developed in Germany. The overall length is 89 km and 6 tunnels with a length of 22.7 km. Several tunnels have been designed to solve the alignment passing across the Jura mountain range. One of these is the Irlahüll tunnel with a length of 7.260 m. This tunnel passes from its southern gate through the Tertiary clayey-sandy sediments, followed by the Mesozoic (Jurassic) and dolomite limestones. All excavation took place in carbonates specified by a high degree of karstification, which manifested itself through underground cavities occurrence. The cavities sizes often achieved several meters. Some karst structures were filled with slipped loamy detritus containing limestone blocks, other were freely passable. A formation of bedded (locally even massive) limestone, practically unaffected by the karstification, followed after the karstified limestone.



Fig. 1. Karst cavity on the planed railway line (source: construction supervision BÜZ Süd).

Karst Geology and Its Effects on Tunnelling, Leading to a Wide Demand upon the Investigation of Underground Constructions

From the various geological and hydrogeological boundary conditions the following hazard scenarios for buildings in karst areas were conceived (Höwing et al. 2003):

- Open, filled and partly filled karst cavities: cavities in the vicinity of the tunnels, embankment and gaps are relevant for the building.
- Erosion in karst structures: the mobilisation of cavity fills, owing to a change of the groundwater conditions in the karst formation, may result in a loss of bedding in the rock mass.
- Instability of cavities: karst cavities in the bedrock may lead to dynamic loads on the final lining due to blocks falling onto the lining.

Surveying the underground on foundation conditions should follow several phases (Pöttler et al. 2002). After defining the type of construction (tunnel, embankment, gaps) the first steps are direct (drillings) and indirect (geological mapping, geophysics) underground exploration as well as a historical research. An exemplary working flow of the indirect and direct investigation is shown in Figure 2.

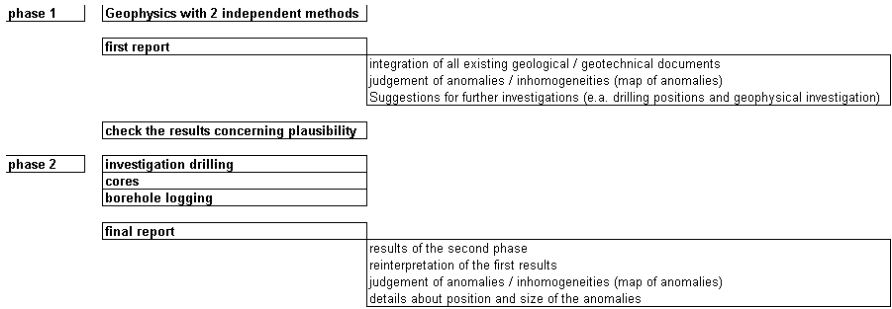


Fig. 2. Exemplary working flow for a combined survey of karst structures.

Experiences and Results

On extensive testing surveys in prestigious areas with known cavities and inhomogeneities a complex investigation concept was evolved being a combination of geophysical methods compositely and drillings (Radinger et al. 2003). The geophysical methods are seismics, micro-gravity, georadar and resistivity.

Changes of measured physical parameters (P/S-wave velocity, density, frequency effect) can interpreted as an indirect information to a cavity suspicion in the methodical limits. Similar anomalies (geophysical effects) can cause various geological inhomogeneities (e.g. filled cavities). It also is conceivable that a method shows a suspicion area and the second method shows none or only very weak indications in a suspicion area. The refined combination of reconnaissance



Fig. 3. Seismic measurements using a weight drop for generating elastic waves and the SUMMIT data acquisition system.



Fig. 4. Micro-gravity surveys for cavity detection along the Irlahüll tunnel.

methods therefore is just one guarantor (redundancy) for successful use. The geophysical anomalies are verified and investigated with drillings. This synergy effect makes it possible to develop a reliable and dependable underground model. The aim to characterize the anomalies and give information about the extension (length, width, and height). The following method combinations are successfully applied:

- Top of the rock layer - Seismics, micro-gravity, (georadar for special topics), investigation drillings.
- Building relevant karst structures (to 10 m under the basis of the gaps or 8 m under embankments) - seismic, micro-gravity (georadar in case of low overburden layer), investigation drillings
- Filled karst structures or weakness zones - Seismics, micro-gravity (georadar in case of low overburden layer), investigation drillings.
- Weakness zones in the rock containing the karst structures (to 10 m under the top of the rock layer) – Reflection / refraction seismics, micro-gravity (georadar in case of low overburden layer), investigation drillings, 2-D modelling, seismic tomography.
- Investigation of the basis of the embankments with built in gravel columns - Reflection / refraction seismics, micro-gravity, investigation drillings.

Following working phases are successful:

- Performing geophysics with 2 redundant methods.
- First report with results of the geophysical investigation including all existing geological and geotechnical information, evaluation of the anomalies (mapping), suggestion for further steps (position of drillings, additional geophysical investigations).
- Checking the plausibility of the first report with regard to e.g. completeness of the results and correctness of the figures.

- Extensive proofing and evaluation of the content of the reports containing the geophysical results and the suggested steps (drillings, camera logging, etc.).
- Carrying out the proposed drillings with mining the cores, camera logging, etc.
- Final report including all existing and extracting information, reinterpretation of the geophysical anomalies, photo documentation of the cores and final evaluation of the inhomogeneities with regard to location and extension.

Beside the successfully developed and applied concept for surveying karst structures, the most outstanding point is the fact that only the cooperation of customers, clients, planners, building supervision, geotechnicians, geologists, civil engineers, drilling technicians and geophysicists could lead to a maximum knowledge of the underground situation.

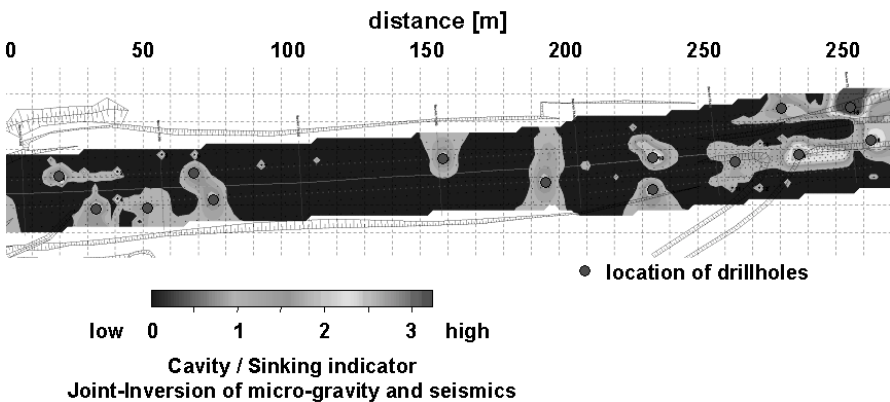


Fig. 5. The joint-interpretation of micro-gravity and seismics shows a cavity and sinking indicator respectively and the locations of drill holes.

References

- Höwing, K.-D.; Eder, S.; Plank, M.: Baugrunderkundung für Verkehrswege in Karstgebieten. Felsbau 21 (2003) 13-21.
- Pöttler, R. Schneider, V., Rehfeld, E., Quick, H. (2002): Grundkonzept zur Lösung der Karst- und Erdfallproblematik für den Bau von Verkehrswegen - Felsbau 20 (2002), Nr. 3, S. 10-21.
- Pöttler, R., Wegerer, P. (2003): Empfehlungen für Planung und Bau von Verkehrswegen in karst- und erdfallgefährdeten Gebieten, In: Felsbau 21, Nr. 1, 8-12.
- Radinger, A., Scheibe, R., Lehmann, B., Kaus, A. (2003): "Die Geophysik im Einsatz zur Karst- und Erdfallerkundung im Zuge von Hochleistungsstrecken – Erkundungskonzepte und grundsätzliche Überlegungen" – Felsbau 21, Nr.1, 42-49.

Engineering Geological Considerations in Tunnelling through Major Tectonic Thrust Zones – Cases along the Egnatia Motorway, Northern Greece

Vassilios P. Marinos¹, Georgios Aggistalis², and Nikolaos Kazilis¹

¹ National Technical University of Athens, Faculty of Civil Engineering
9 Iroon Politechniou str., 157 80 Zografou, Greece
vmarinos@central.ntua.gr
Tel: +30 210 7722442,
Fax: +30 210 7723770

² Egnatia Odos S.A., 6th km Thessaloniki-Thermi, 57001, Thessaloniki, Greece
{nkazilis, gaggistalis}@egnatia.gr

Abstract. Tunnelling through tectonic shear zones is always a challenge due to the geometrical complexity and the presence of poor quality rock masses with high variability in their occurrence. Based on the experience from the Egnatia motorway, in Northern Greece, the paper aims to give some general concepts, on the main failure mechanisms of the deformed materials and discuss guidelines for the design. Two case studies are presented, the first when the rock mass is brecciated derived from brittle rocks and the second when the rock mass is sheared from the compression of weak rocks with plastic characters. In the first case the rock mass is composed of interlocking angular pieces of strong rock and can exhibit satisfactory stability under confined conditions. Unless immediate support is provided, the cohesionless rock mass does ravel in tunnel excavation. In the second case heavily sheared clayey flysch exhibits squeezing behaviour even under tens of meters of overburden. In this case there is a variability of the material and it is not suggested to provide a number of support categories for each of the erratically alternating various geotechnical conditions that may be present but it is preferable to design an excavation and support system and sequence which are capable to deal with the worst anticipated conditions.

Keywords: tunnelling, thrusts, weak rock masses, ravelling, squeezing, design, Egnatia, Greece.

1 Introduction

Egnatia Highway, today under construction, composes a very important and modern infrastructure for the communication of Greece with Europe, the Balcans, and the East. It starts from Igoumenitsa at the west, runs across the northern part of the country, ending to the east to the Greek-Turkish borders (Fig.1.1). The Motorway will be 680Km long, providing to the European Union access to the east with no border crossing and belongs to the 14 projects of a Trans-European network. Until know 449Km have already been constructed. When complete, the Egnatia Motor-

way will have a total of 76 road tunnels of an overall combined length of 99km. The majority will be bored tunnels. The excavation diameter of the tunnels is about 12m and among those already finished, most were opened by the method of top heading and bench. The Egnatia Motorway runs across the entire width of Greece traversing almost perpendicularly the main geotectonics units of the country crossing perpendicularly major tectonic contacts and thrusts. Thus, there is a great variety of geological situations and each geotectonic unit displays different particularities in terms of occurrence of weak rock masses, tectonic structure, and therefore the possibility of unstable arrangements of rocks. The weak rock masses produced by such thrusts are originated from both strong or weak intact rock. They are present to a large scale and may cover the whole tunnel length. In that case, the discrimination of the different engineering geological units and qualities with specific characteristics and parameters along the tunnel is very difficult. The quality of the rock mass in such environment can change dramatically in few meters and in such cases; a swift to a radical change of the support can be dangerous if temporarily a better quality of the rock mass appears.



Fig. 1.1. Location of the Egnatia motorway and its connections to the rest of Europe (in an informative article, Greeman 2001).

2 Geological Model in Major Tectonic Thrusts

2.1 General

The geological model is the basic initial step on which the design of the tunnel will be based. As a result, the geological conditions to be encountered in terms of quality of the ground can be defined and the type, location, and size of potential hazards can be identified. In the case of major tectonic thrusts the alignment, even crossing them perpendicularly, deals with a rock mass disturbed in a very wide

zone often extended by satellite shears. An important factor for the establishment of the geological model is the site investigation. This investigation has to be derived into several phases: a) review of the regional geology, b) surface exploration, c) subsurface investigation and testing. Many problems arise during the geological investigation when searching for the specific location, the extent, and the frequency of the tectonic zones. This becomes more true in flat areas or in urban environment. Many times tectonic zones cannot be determined exactly with boring because of low core efficiency. In such cases the disturbed material, when clayey, is washed out and these sections cannot be quoted. Moreover, when fault zones, mainly normal, are in a vertical orientation, boreholes cannot detect them. In this kind of investigation, further information on the rock mass properties can be obtained by the use of down hole cameras, air photographs, appropriately inclined boreholes, geophysical surveys and, in case of areas close to surface, trial shafts (Dalgic, 2000). In mountainous areas due to morphological changes it may be possible to map tectonic zones such as thrusts or faults based on differences of vegetation, while the existence of a “pilot” strata affected by shearing and displacing is of great help.

2.2 Complex Geological Models in Egnatia Motorway

Egnatia is crossing perpendicularly almost all the main geological zones of Greece. These zones have been differentiated by their lithology and tectonic history and many of them are placed one beside the other by big thrusts. The rock mass consists mainly of limestones and flysch in the western part whether ophiolites, gneiss, marbles and phyllites are present in the central and eastern part. In this paper, two case studies of different geological structure in a thrust environment are presented. The first when it is derived from the brecciation of brittle rocks and the second when the rock mass is derived from a sheared weak rock mass such as flysch. These cases were chosen because their behaviour in tunnelling is completely different, based on structurally control stability in the first case and stress controlled stability in the second.

Case Study 1: Tunnelling in heavily fractured and brecciated limestones.

The area is at the edge of the cliff of a “balcony” overlooking the plain of Paromythia and dominated by the mountain of Khionistra in the western part of the motorway (fig.2.1). The rock mass of the area is a heavily fractured and brecciated limestone resulting from thrusting and from tectonic rugs. The Greek Geological Survey and the Institut Francais du Petrol, studied the broader area, during the early 60s, and have produced an excellent publication (1966). In figure 2.1 a block diagram, is shown, illustrating the geological model in which a series of tunnel are bored.

Case Study 2: Tunnelling in heavily sheared flysch.

The motorway runs through a contact of the huge overthrust of the Pindos Unit formation over the Ionian Flysch in Metsovo area. The base of the overthrust-

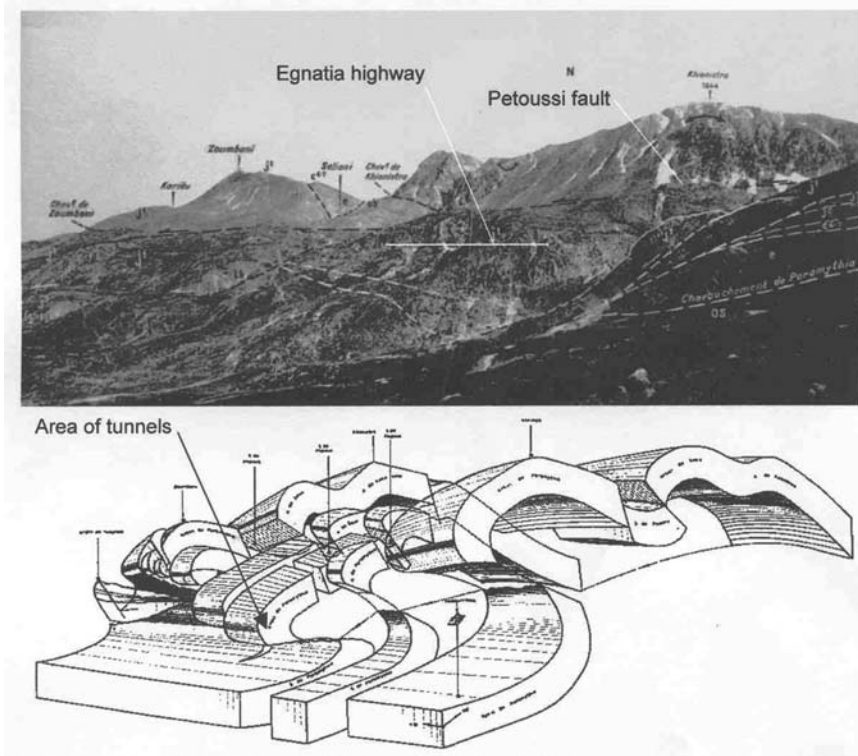


Fig. 2.1. The geological model for the Khionstra-Paramythia thrust and the Petoussi fault (from IGME – IFP, 1966). Western part of Egnatia Motorway.

sheared material is mainly in the Pindos flysch. This flysch is characterized by different alternations of siltstones and sandstones. Within the area of one of the tunnels, the flysch is of a more clayey nature and often exhibits a chaotic structure.

The main thrust movement is associated with satellite shears within the thrust body. These shears are generally marked by a reddish siltstone sequence of the Pindos flysch, which acted as a 'soap layer' for these internal thrusts and when vegetation is absent, these shears can be mapped. The flysch has thus suffered from large compression and very weak rock masses have been produced. A conceptual model has been drawn to picture the geological structure of the area in figure 2.2. Inside the body of the sheared mass, it is reasonable to expect less deformed sandstone flysch with more rock-like behaviour. However, this material is likely to be cut by small shears. Consequently, frequent shifts from good to weak flysch with a significant presence of sheared and very weak siltstone or clay shales are a common practice. Another tunnel, in the same area, crosses a series of thrusts and faults associated with weak flysch material. The programme except of the geological mapping and the lab tests involved geophysics and boreholes. Moreover, the kinematic analysis of the thrusts was verified by the tectonic analysis of the fold axis (Sotiropoulos and Mourtzas, 1999).

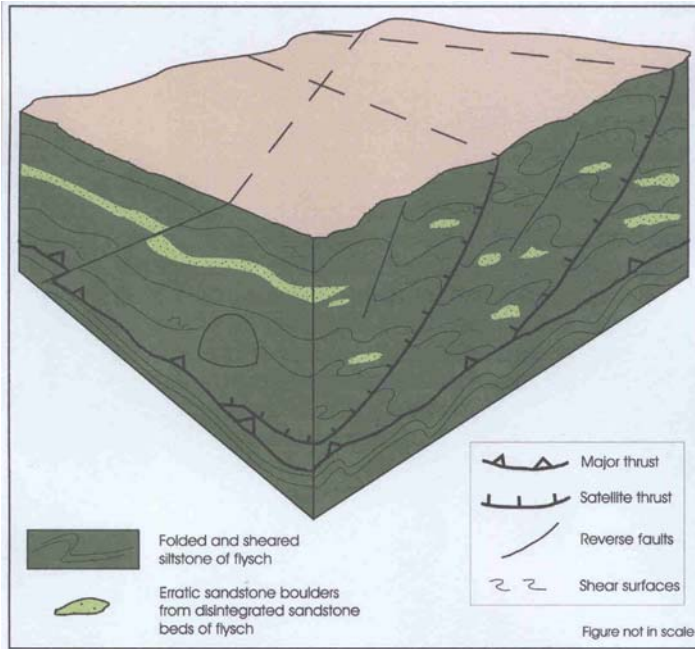


Fig. 2.2. Geological model in a tectonically sheared zone with weak rock masses (flysch).

3 Rock Mass Model and Mechanisms of Failure in Tunnelling in an Environment of Thrusts

3.1 General

Having defined the basic geological model, design can start on a sound basis and selection of rock mass properties is the next step. Estimation of rock mass properties can be achieved by one of the following methods: a) laboratory testing, b) in situ testing, c) back analysis, and d) use of rock mass classifications (RMR, Q, GSI etc.). However, the outcropping geological materials do not permit high quality sampling and consequently performance of laboratory tests to derive the design geotechnical parameters is difficult. Moreover, sampling is not representative of the rock mass due to the disturbance, jointing, and the heterogeneity of most formations. Additionally, it is often not realistic or always feasible to carry out in situ tests. On the other hand, back analysis, although the best way to estimate the geotechnical parameters can be done only during construction and by evaluation of the deformation measurements. Thus, the remaining solution in order to estimate reasonable geotechnical parameters is to rely upon the use of the rock mass classifications schemes that are correlated with the basic parameters needed for the design. However, someone must always have in mind their limitations; their

proper use is assured if the engineering geological behaviour during tunnelling is understood.

If the problem is stress dependant, having defined the parameters of the Geological Strength Index, GSI, (mainly used in Egnatia project- Marinos and Hoek 2001) the unconfined strength of the intact rock σ_{ci} and the material constant m_i , are defined for the assessment of the mechanical properties of the rock mass. On the contrary, when failures are structural dependant the persisting influencing discontinuities have to be defined and their properties accessed.

Regarding groundwater, its most basic impact is upon the mechanical properties of the intact rock, when this is of clayey nature. Furthermore, when the water is not drained it reduces the effective stresses and finally, in all cases, the strength of the rock mass. This is the case of clayey flysch. In more permeable masses (e.g. limestones, fractured sandstone flysch) free drainage helps but groundwater in-flows must be controlled.

3.2 The Cases of Egnatia Motorway

Case Study 1: Tunnelling in heavily fractured and brecciated limestones

The predominant rock mass of the area is a heavily fractured and brecciated limestone. Under confined conditions this tightly interlocked, highly frictional but cohesionless material behaves in a stable manner. This is evident in many of the steep slopes in such material that were cut in the site. However, when confinement is released, as for example in the roof of a tunnel, the rock mass dilates and individual pieces fall under gravity loading. If left unconfined, this ravelling will continue and a chimney will be formed, until, and if, arching is achieved. As a result, the local stability of the rock mass immediately above the roof has to be dealt with in an entirely different manner since the failure mechanism involved is driven by gravity rather than by stress. In these conditions the “blind” application of rock mass classifications for support selection can be very misleading since these classifications were developed for different failure mechanisms. The rock mass classifications remain a useful qualitative tool for communication between those involved in the project but the selection of the excavation method and the choice and sequence of support installation must be based on a clear understanding of the mechanics of rock mass failure due to loss of confinement. In this kind of material it is very conservative to give low geotechnical parameters and to use a rather “heavy” support system. The prime concern of the design of the supporting shell has to cope with a mass that must first be protected against disintegration and ravelling.

Case Study 2: Tunnelling in heavily sheared flysch.

As it is described in the geological model, flysch has suffered from large compression-shearing and very weak rock masses are likely to be found close to the shear zones. The original structure is no longer recognisable and blockyness is lost. The rock mass may contain small pieces of strong rock (sandstones) floating in the surrounding weak material. However, in the scale of the tunnel, these boulders do not contribute significantly to the overall strength of the rock mass and addition-

ally, due to the heterogeneity in both horizontal and vertical direction these better conditions may not encounter to the whole tunnel section (e.g. foundation area of the elephant foot of the top heading). The normal tunnel design process, in which a number of support categories are provided for the different geological and geotechnical conditions predicted or observed in the tunnel, may not be applicable to this case due to the heterogeneity of the mass and the rapid changes from better to worst rock mass. It is preferable to design an excavation, support system and sequence, which are sufficiently robust to deal with the worst anticipated geological-geotechnical conditions and which are therefore practically independent of the precise geological conditions encountered. The problem that has to be anticipated in this weak rock mass is the expected large deformations when the tunnel is under high overburden (in the Egnatia motorway, up to 250m). An indicator of potential tunnel squeezing problems is the ratio of uniaxial compressive strength σ_{cm} of the rock mass to the in situ stress p_o . Its relation to the “strain” of the tunnel is shown in figure 3.1. To proceed to such an analysis the correct geotechnical parameters should be chosen. The Geological Strength Index (GSI), σ_{ci} and m_i , of the predominant sheared clayey siltstone, suggested for this purpose, for these tunnels, were $GSI=15-20$, $\sigma_{ci}=5-8$ MPa and $m_i=5-7$. These parameters can be validated or reevaluated from the deformation measurements during construction and support to be optimally adjusted to the rock mass structure. Thus, monitoring is of essential importance.

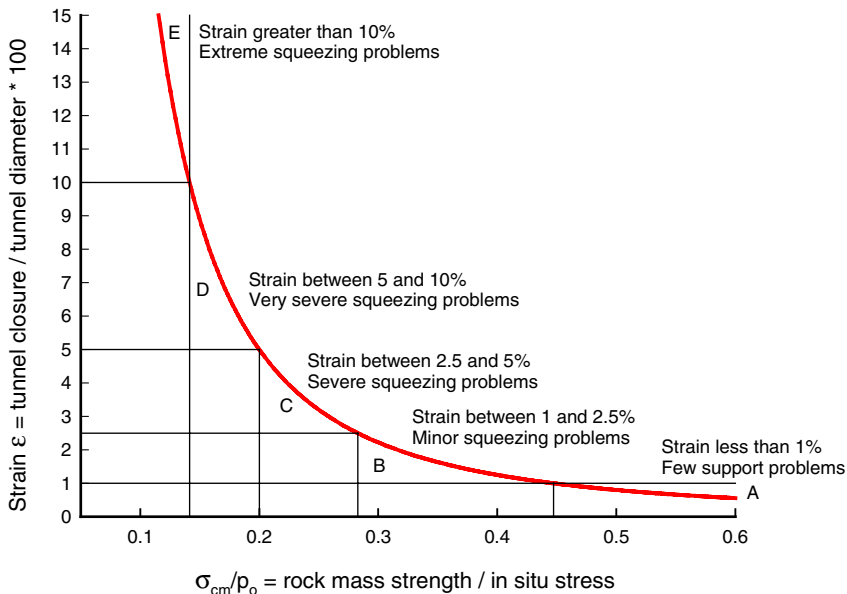


Fig. 3.1. Squeezing conditions depending on the ratio of rock mass strength to in situ stress related to strain. The example of Anthochori and Anilio tunnel in Egnatia highway (based on Hoek and Marinos 2000).

4 Design Guidelines

4.1 Design Features in Tectonic Zones with Application in Egnatia Highway

In this paragraph it is not attempted to give precise design categories and support measures for the rock mass qualities here discussed, but to focus on guidelines and describe the features from the design philosophy based on the understanding of the behaviour of these particular rock masses.

Case Study 1: Tunnelling in fractured and brecciated limestones

From a practical point of view it is believed that it is essential that the rock mass ahead of and above the advancing tunnel face should be treated by grout injection in order to provide sufficient cohesive strength to prevent the ravelling process described in paragraph 3.2. This would create a stable arch in the pervious brecciated limestone and this would permit tunnel advance with shotcrete and rock bolt support only. An alternative solution could be the excavation of an annular peripheral slot that is shotcreted in the beginning of every excavation cycle. Shotcrete is a very effective support medium in this type of rock mass since it prevents the start of the ravelling process. Furthermore, where this pre-conditioning of the rock mass is not absolutely necessary, the use of self-drilling rock bolts with immediate grout injection could be sufficient. Additionally, it is very important to excavate in a small advance step in order not to disturb the surrounding rock mass and to use an excavation method that induces as little disturbance as possible. In case water is present, ravelling is easier to take place by flowing process. In order not the shotcrete to wash out, accelerating admixtures should be used or the thickness of the shotcrete should be increased. In this tunnel the ground water table is below the tunnel and problems of this type were absent. Usually, it is very difficult to identify the exact place of the more brecciated zones that will more easily ravel during excavation. More tectonised zones may be found during construction by drilling ahead of the face with probe-holes.

Case Study 2: Tunnelling in heavily sheared flysch.

The main issue that has to be faced in dealing with this support design is how to control the large deformations that occur from the squeezing of the tunnel. In order to control these deformations, it is necessary to install a heavy temporary support in the form of steel sets, shotcrete or rock bolts or a combination of these systems. Face stability is also a main issue. The addition of forepoles is very effective in controlling the deformation ahead of and at the tunnel face but of course has little influence upon the deformations behind the face and the shell has to carry the load of the poles too. In such a support system, in a weak rock mass and high overburden, it is very important to make a good foundation of the support cell and to close the excavation phase with a temporary invert. If, however, these large deformations cannot be accommodated by simply making the support system stronger and more rigid, particularly for a top heading and bench method of excavation where it is impossible to achieve a closed support ring in one step, a much

more effective approach is to allow the support system to yield while, at the same time, retaining sufficient capacity to support the loads imposed by the overburden. This flexible support system can be provided by different sophisticated yielding systems. The theoretical basis for this approach is illustrated in Figure 4.1 (from Hoek and Marinos, reports to Egnatia S.A.1998-2003). The “soft” support system follows the reaction curve that starts with yielding at very low load. The amount of this yielding can be controlled and the support system is locked and will react in the same way as a “stiff” system when the pre-determined tunnel deformation is achieved.

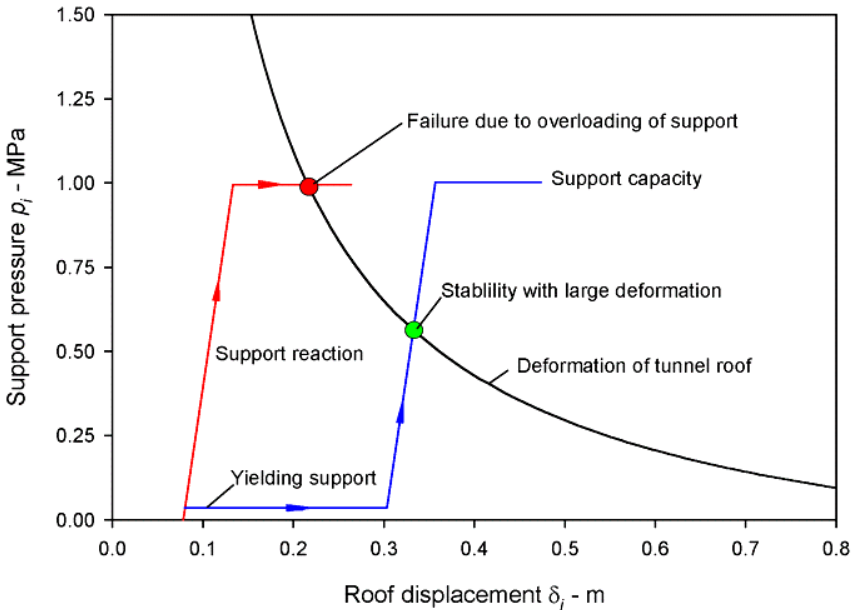


Fig. 4.1. Rock-support reaction curves for the top heading of a tunnel subjected to squeezing conditions. The “stiff” support system fails due to overloading while the “flexible” system yields and achieves stability at a displacement of about 0.3 m in this example (from Hoek and Marinos, reports to Egnatia S.A.1998-2003).

5 Conclusions

The paper discusses some general concepts in tunnelling through thrusts zones, from the definition of the geological model to the main failure mechanisms and the guidelines for the design. Tectonic zones produced by big thrusts or satellite shears within the thrust body are very difficult to access as far as the conceptual model is concerned. Due to high geometrical complexity, heterogeneity and big scale tectonic disturbance, it is difficult to precisely specify by the zones of weak rock masses. The rock masses are heavily deformed in a greater scale, producing

Table 1. Tunnelling through tectonic thrust zones. Summary of the two cases of weak rock mass derived from either brittle or soft initial rock.

<i>Rock Mass Type</i>	<i>Brecciated limestones</i>	<i>Sheared siltstones or shales</i>
<i>Rock Mass Characteristics</i>	Interlocking angular pieces of strong rock. No clayey material	No sign of initial structure. Shear surfaces-slickensides. Interlocking of rock pieces is absent. Boulders of more competent rock floating into the chaotic clayey mass
<i>Water Effect</i>	If present, reduction of effective stresses. Possible inflows into the tunnel	Reduction of the mechanical properties of the intact rock and of the condition of the discontinuities. Reduction of effective stresses
<i>Failure Mechanism</i>	Ravelling, driven by gravity rather than by stresses	Large deformations. Squeezing conditions
<i>Possibility in predicting rock mass quality ahead of the face (when inside the thrust zone)</i>	Probe drilling	Limited options due to heterogeneity (rapid changes and alternations in short lengths)
<i>Design concept</i>	Keep confinement	Control deformations of perimeter and face
<i>Design guidelines</i>	Pre-grouting of the surrounding rock mass through perforated spiles. Alternatively, create perimeter slot ahead the face associated with spiles. Immediate application of shotcrete. Buttress on the face and short advance step. Then apply required temporary shell	Forepoles or spiles, face nailing, heavy shell (e.g. steel sets embedded in shotcrete). Temporary invert necessary. Short advance step. Alternatively flexible support system with yielding elements (for the cases of large deformations)
<i>Measures to prevent adverse respond of the surrounding rock mass in order to provide assistance to the shell of temporary support</i>	Grouting	Anchoring well beyond the plastic zone if necessary may assist

either heavily fractured, brecciated mass from brittle rocks or sheared melanges and chaotic masses if the initial rocks were soft or heterogeneous. The site investigation programme must be soundly based on the guidelines provided by the knowledge of the regional geology. To specify the geotechnical parameters of these rock masses to use for the design, the use of the rock mass classifications offer the main tool. Given their limitations their proper use depends on the under-

standing of the behaviour of the rock mass during tunnelling. Rock masses tectonically disturbed but with different lithology may have similar geotechnical parameters. However their behaviour in underground excavation can be very different. Thus, support measures should not only consider the stress problem but also the mechanism of failure of the rock mass especially in brecciated brittle rocks. In other cases of sheared chaotic rock mass, subject to plastic deformations, it is preferable to design an excavation, support system and construction sequence, which are capable to deal with the worst anticipated geotechnical conditions and which are therefore practically independent of the geological conditions encountered. However, this conclusion must not be misunderstood because this independency from the geological conditions is imposed just because of these geological conditions. In table 1 are summarized the two cases, discussed in this paper, as far as the main failure mechanisms, the water effect, the intervention to the surrounding rock mass and the guidelines for the design are concerned.

References

- Dalgic S (2003) Tunnelling in fault zones, Tuzla tunnel, Turkey. *Tunnelling and Underground Space Technology*, 18:453-465.
- Greeman A (2001) Ancient route to the East revived. *Tunnels and Tunneling International*, 33, (5): 26-30.
- Hoek E, Marinos P (2000) Predicting tunnel squeezing problems in weak heterogeneous rock masses. *Tunnel and Tunneling International*, 32 (11):45-51, part one and 33(12):33-36, part two.
- Marinos P, Hoek E (2001) From the Geological to the rock mass model. Driving the Egnatia Highway through difficult geological conditions. Proc. 4th Congress of the Hellenic Society for Soil Mechanics and Foundation Engineering.
- Sotiropoulos I, Moutzas N (1999) Anilio tunnel: Geological structure and classification of the rock mass. Proc. 1st Conference on Tunnels of Egnatia Highway, Ioannina, Greece.

Tunnelling Problems in Older Sand Formations

Jan Dirk Nieuwenhuis and Arnold Verruijt

Delft University of Technology, Faculty of Civil Engineering and Geosciences
P.O. Box 5048, 2600 GA Delft, the Netherlands
j.d.nieuwenhuis@citg.tudelft.nl
a.verruijt@planet.nl
Tel: +31 15 2782811
Fax: +31 15 2785124

Abstract. In its deepest stretch, 60 m below o.d. and water level, the Westerschelde tunnel trace below the estuary in the Southwestern part of the Netherlands, crosses the lower Oligocene Rupel clay (Boom clay) and the Sands of Berg. Expected problems such as small penetration rates and difficult steerability of the TBM did not occur but surprisingly high radial pressures deformed the shield's tail section to such an extent that concrete rings of the permanent tunnel could not be emplaced. In retrospect after finishing the tunnel and cumbersome remedial measures the sands of Berg, known to be dense and strong, appear to exhibit very strong dilatancy when axially sheared by the TBM. Some buckling computations and an estimate of dilatant effects are presented together with educated (and now confirmed) guess work on diagenetic effects such as recrystallization and cementation. It seems wise to warn designers of shallow tunnels crossing tertiary sand formations for unexpected forces on shield and cutting wheel due to diagenetic structuring of these old sands.

Keywords: bored tunnel, tunnel shield, tertiary sand, dilatancy.

1 Introduction

Between 1998 and 2003, a road traffic tunnel was constructed below the Westerschelde (Engl. Western Scheldt) estuary in the South Western part of the Netherlands (fig. 1). The Westerschelde forms the seaward outlet of the Scheldt-river in Belgium; it has a length of 60 km and a variable width between 5 and 10 km. The bottom consists of shoals and tidal channels, locally 40 m deep, underlain predominantly by young Holocene sand deposits. The navigation channel of the large Belgian harbour Antwerp runs along the deeper parts of the estuary. The tunnel crosses the estuary at a relatively narrow and relatively deep stretch; it connects the Western part of Holland and the Province of Zeeland with the Dutch part of Flanders and with Belgium. The Westerschelde tunnel consists of two separate bored tubes, approximately 10-20 m apart and connected every 250 m by transverse tunnels for inspection and escape (fig. 2). Each tube is 6 km long and has a diameter of 11.4 m. Each carries a single direction dual lane carriage way. Both tubes were made by separate TBM's running at cross-courses. The construction was relatively standard: single cutting wheel followed by a 10 m long steel liner with a tail section accommodating the last permanent concrete tunnel ring. After assembling the sector parts into a ring and doweling it to the next-to-last concrete



Fig. 1. Large-scale geological and tectonic setting of the Westerschelde area.

ring, the steel liner shield is pushed forward hydraulically from the last tunnel ring against the cutting front to continue boring. The tunnel dives down to 60 m below the water surface in a relatively steep descent from the south bank of the estuary to climb up more gently to the north bank (fig. 3). For more than 4 km, along the deeper part of the trace, the tunnel crosses older sediments. From top to bottom: Miocene glauconitic sands (GZ1, Formation of Breda), Oligocene Rupel clay (Boom clay) and lower Oligocene glauconitic sand (sand of Berg; modern name: Layers of Vessem). Problems arose during the passage through the Layers of Vessem. Deformations of the tunnel shield occurred during both courses but for one tube the radial deformations (roughly said: the ovalizing) became so large that it was impossible to install the permanent concrete rings. Boring had to be stopped and divers attached radial extensions to the cutting wheel in the form of scraping

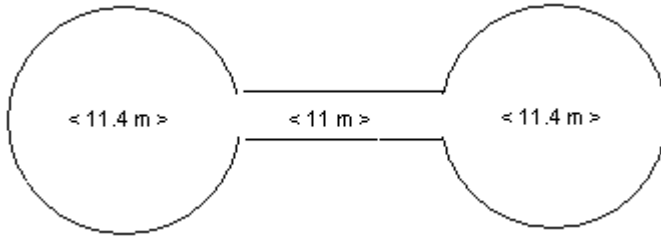


Fig. 2. Cross-section of the Westerschelde tunnel.

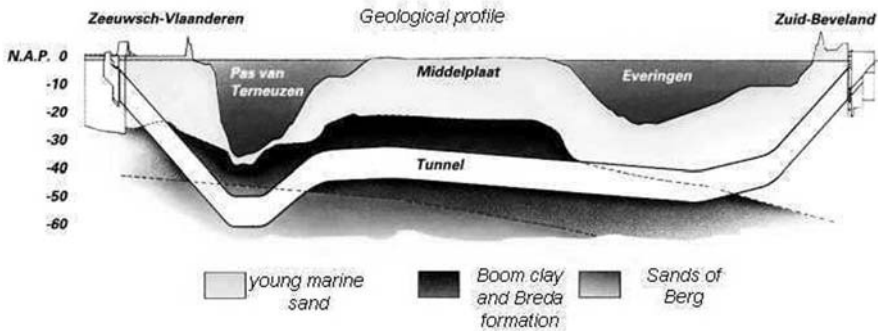


Fig. 3. Simplified longitudinal profile of the tunnel trace.

knives. This had to be done several times in very muddy water at 60 m of depth because the knives could not be made as solid as the cutting wheel itself and broke down occasionally. The enlargement of the diameter of the wheel was achieved and the shield deformations did no longer prevent the emplacement of the concrete rings, but the adaptations resulted in many months of delay and involved very costly and dangerous repair works. Both the designer and the contractor were anxious about the strength and solidity (low porosity) of the sands of Berg but this anxiety concerned rather the penetration rate and steerability of the cutting wheel than the unexpected deformations of the tail end of the shield.

For very long geological epochs up to this day the Netherlands form a subsidence basin bounded to the south by the Palaeozoic socles Brabant Massif and Rhein-Schiefer Gebirge (fig. 1). The socles were stable or slightly rising most of the time. This location implies a both strong variations in facies and increasing thickness of layers in the direction of the basin. The Westerschelde area is situated in the hinge region between basin and Brabant Massif. The formations present in the tunnel trace area therefore consist of beach or shallow sea sediments subjected to prolonged periods of subaerial weathering and erosion (Van Adrichem Boogaert, Kouwe, 1997; Kruse, 1995). The sands of Berg and the overlying Boom clay were deposited in the lower Oligocene (Rupelien) roughly 30-25 million years ago. For 20 million years or more, due to eustatic sea level drop, these formations had a terrestrial position and were eroded. In Miocene and Pliocene times, from 10-5 million years ago, the sands of the Breda formation were deposited

discordantly over the Boom clay in quiet shallow sea conditions as witnessed by the glauconite content and the presence of digging traces of marine organisms. Pleistocene deposits are lacking and the top 25 to 30 m consist of Holocene marine sands. The 40 m deep tidal channel, the Pas van Terneuzen, below which the tunnel passes at 60 m below o.d., is not older than 1000 years (De Mulder et al, 2003).

2 Field and Lab Estimates of Parameter Values

a. Parameters Needed for the Analysis of Tunnelling Performance

To warrant smooth operations designer and contractor requested soil parameters to assess the penetration rate and steerability of the cutting wheel, normal and shear forces on the shield and the risk of leakage to and from the estuary's bottom. Cone penetration tests (cpt's) with piezo-cones were conducted on land and from floating platforms. The parameters obtained are q_c (tip resistance) used to estimate shear strength and deformation moduli (modulus of elasticity, coefficient of sub-grade reaction); f (local friction) used to define soil type (sand, clay etc.) and layering; u (pore pressure) used to distinguish dilatant/contractant behaviour and very roughly estimate the permeability. Up to 10 m long cores were taken with the Begemann sampler of GeoDelft and in the deeper parts with shorter piston samplers. Samples from the cores were used to perform oedometer tests (clays), triaxial tests (strength, elasticity) direct shear tests (strength), unit weight, porosity. Remoulded samples were used to determine relative density, permeability, and microscopic analysis. The focus of concern was on the Boom clay, a stiff and strong clay, well-known from Belgium and feared for its stickiness. The sands of Berg appeared to be variable both in vertical and lateral direction, dense (95-100 % relative density) and strong in places (q_c up to 80 MPa). They are fine sands (D50 100-130 μm) containing glauconitic and lime concretions. The cutting wheel was (and later appeared to be) sufficiently powered to cut its way through the strong sands and clays. The shield deformations have been estimated by the method of Duddeck (1980) based upon overburden pressure, neutral earth pressure, water pressures, and soil stiffness expressed as spring constants. Apart from the neutral earth pressure, estimated at 0.5-0.8 of the overburden pressure, all soil parameters could be estimated sufficiently accurate to make an acceptable analysis. The glauconitic content, glauconite being a friable phyllosilicate aggregated into sand-size particles, being harmful when sheared to the over-all permeability and to pile driving, was not considered detrimental to the scraper-like penetration of the cutting wheel. This appeared to be correct, but the deformation problems of the tail section of the shield were not foreseen.

b. Parameters Needed for the Analysis of Unexpected Shield Deformations

The harmful shield deformations required both a closer look at the computations and at the sands of Berg. Duddeck's method, though quite acceptable for shield dimensioning, is too rough to estimate deformation distributions along the shield's

parameter. Moreover, it does not do justice to dilatancy/contractancy if that occurs. Dilatancy is the tendency of densely packed, overconsolidated sands (and clays) to increase in volume when sheared. Contractancy is the opposite. A more sophisticated computational analysis, analytical or numerical, however, immediately requires more sophisticated and more accurate estimates of the soil parameters:

- neutral earth pressure to define in situ stresses as starting point for the analysis,
- in-situ permeability,
- stress-strain relations, including dilatancy/contractancy, to model strains and stresses along the shield perimeter due to the increasing shear stresses as the tunnel shield slides forward along the surrounding sands.

Parameter estimates of this kind can only be obtained from tests on high quality samples or from complicated field tests such as pressuremeter tests in "undisturbed" boreholes. Piston samples or Begemann samples for continuous cores are good enough to produce quality samples from clays and from sands when the operational conditions are easy: on land, not too deep and not too variable a subsoil. The same is true for sophisticated pressuremeter tests. The sands of Berg in the problem area, however, lie more than 10 m below the channel bottom below 40 m of water depth in a tidal area. Only a bottom-seated diving bell, such as GeoDelft deployed for the Oosterschelde storm surge barrier could have had a chance if it still would have existed. But even then the Oosterschelde sands and silts where the diving bell demonstrated its value, are simple soils compared to the hard, old and structured sands of Berg. Only after mastering the operational difficulties, some good samples could be taken through openings in the wall of the finished tunnel tube in sands locally frozen to facilitate the construction of the transverse escape and inspection tunnels.

3 Deformations of a Tunnelling Machine

a. Buckling of a Circular Shell

In the design of tunnels and tunnelling machines an important element is the prediction of the deformations due to the pressures from the surrounding soil. Early on, it was realized by Schulze and Duddeck (1964) that in this analysis the dependence of the soil reaction on the tunnel deformation should be taken into account, for instance by using a spring constant model for the soil, perhaps with some modification for the variation with depth (Duddeck, 1980). Without the effect of the spring stiffness of the soil the deformations of the tunnel, and the bending moments in it, would become unacceptably high. For a tunnel below a deep water channel it may also be important to consider the possibility of buckling of the shell under the influence of a rather high isotropic pressure and some initial anisotropic deformation, see Figure 4. In order to present this buckling analysis in a simplified form it will be assumed that there is some initial deformation of the form $w = w_j \cos j\theta$, where j is an integer number indicating the number of waves in circumferential direction, $j \geq 2$.

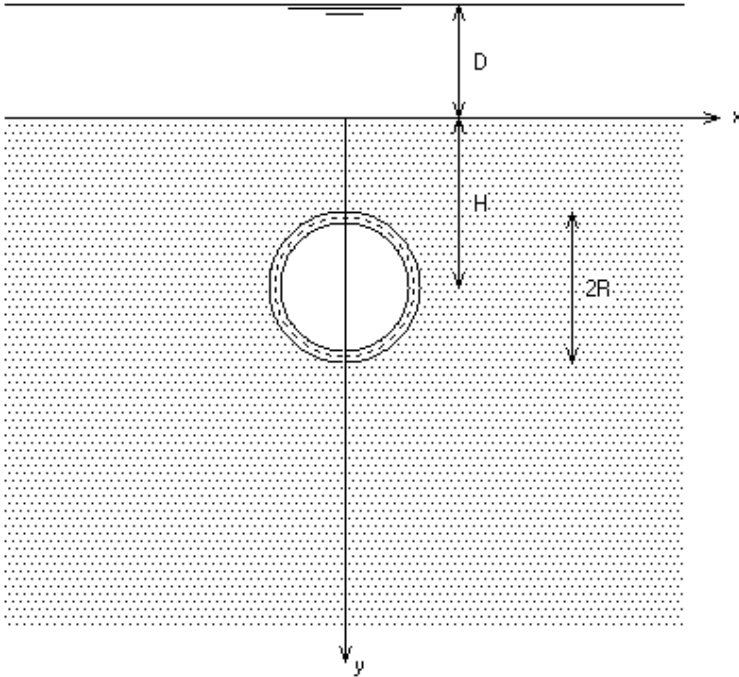


Fig. 4. Tunneling machine below water channel.

It is assumed that the tunnel (a shell of the form of a circular cylinder) is also loaded by a uniform pressure of magnitude p_0 , while being supported by uniform soil springs of stiffness k_0 . For this case the deformation of the circular shell is written as $w = w_j' \cos j\theta$. The uniform radial compression of the shell is neglected, as the shell is very stiff to such a deformation. The relation between the loads and the displacement of the shell can be derived using methods described by Timoshenko & Gere (1961). The result is

$$\frac{w_j'}{w_j} = \frac{1}{1 + (k_0 / k_r) / (j^2 - 1)^2 - (p_0 / p_r) / (j^2 - 1)}, \tag{1}$$

where k_r is a reference spring constant, defined by the properties of the shell, and expressing its stiffness,

$$k_r = \frac{EI}{R^4},$$

and where p_r is a reference pressure, defined as

$$p_r = \frac{EI}{R^3}.$$

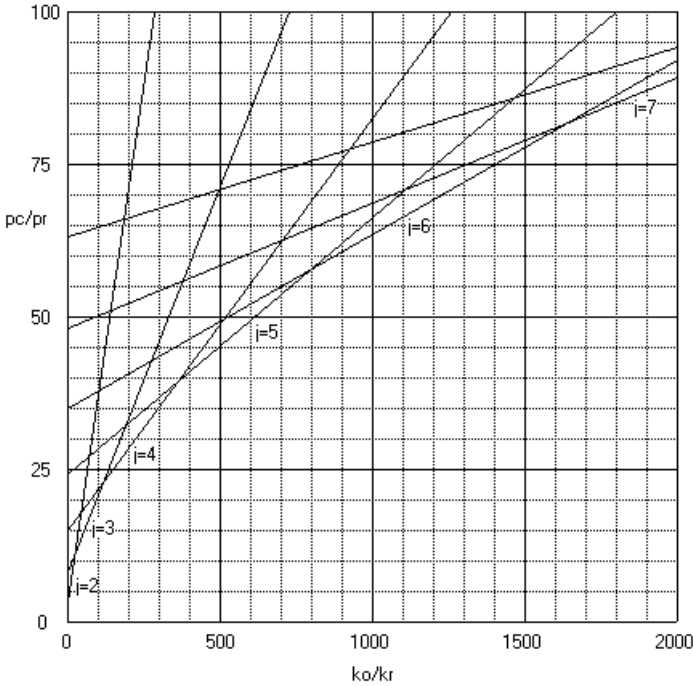


Fig. 5. Buckling of a shell with elastic support.

In these expressions R is the radius of the tunnel, and EI is its bending stiffness.

It can easily be seen from equation (1) that in the absence of spring support ($k_0 = 0$) and isotropic load ($p_0 = 0$) the amplitude of the displacement remains equal to its initial value ($w'_j = w_j$). Buckling may occur if the load p_0 is so large that the expression in the denominator of equation (1) becomes zero. This buckling load p_c appears to be

$$\frac{p_c}{p_r} = (j^2 - 1) + \frac{k_0 / k_r}{j^2 - 1}. \tag{2}$$

For a shell with no lateral soil support ($k_0 = 0$) the buckling load would be

$$k_0 = 0 : p_c = (j^2 - 1)p_r = \frac{(j^2 - 1)EI}{R^3}. \tag{3}$$

This is a well known result (Timoshenko and Gere (1961), p. 300).

In case of a definite elastic soil support, the buckling loads are much larger, as indicated by equation (2). This is illustrated in Figure 5, which shows the behaviour of equation (2) for various values of the wave number j . It appears that the elastic support may significantly increase the buckling load, thus preventing large deformations. If it is assumed that any form of initial deformation is possible, it

also appears from Figure 2 that the number of waves in the buckling mode (the parameter j) will increase when the stiffness of the support increases. This is a well known phenomenon in the buckling of structures on an elastic foundation (Hetenyi, 1946). As an example, consider a steel tunnelling machine of radius $R = 5.63$ m, and wall thickness $d = 0.07$ m. Then $k_r = 5.97 \text{ kN/m}^3$, and $p_r = 33.6 \text{ kN/m}^2$. A representative value for the spring constant of a sandy soil at a reasonable depth is $k_0 = 3000 \text{ kN/m}^3$, so that $k_0 / k_r \approx 500$. It then follows from Figure 5 that the smallest buckling load occurs for $j = 5$, and that this buckling load is about 45 times the reference value p_r , that it is about 1500 kN/m^2 . Such high values of the isotropic load, corresponding to a water depth of 150 m, are unlikely to occur in engineering practice. To estimate the actual displacement from equation (1) it may seem to be necessary to assume a value for the initial displacement amplitude w_j , but this is not really necessary. Actually, by taking $k_0 / k_r = 500$, and $p_0 / p_r = 20$ (which corresponds to a rather large water depth of about 65 m), it follows from equation (1) that the smallest value of the denominator occurs for $j = 7$, and results in a displacement $w'_j / w_j = 1.25$. Thus the final displacements will hardly be larger than the initial displacements, which may be assumed to be rather small, say a few mm.

b. Dilatancy

A phenomenon usually neglected in the design of tunnels is the possible dilatancy of the soil, a volume increase during shear deformation. This is a phenomenon that may be observed in very dense soils. It may be of great importance for the response of the soil, as it may increase the radial compressive stress on the tunnel during axial shearing of the tunnel through the surrounding soil. It is certainly not an easy matter to reliably quantify this effect, but it may be estimated that it can amount to a relative volume change of the order of magnitude of 5 %, for extremely dense sands. If this is compared to the relative volume change caused by a uniform radial displacement, $\Delta V / V = 2w / R$, such a dilatancy would be equivalent to an additional radial displacement of about $0.025 R$. For a tunnel of radius 5.63 m this would be about 14 cm, which probably would be unacceptable.

4 Some Geological and Geotechnical Characteristics of the Oligocene and Miocene Sands

a. Characteristics

As demonstrated in the previous paragraph the elevated radial stresses needed to generate the observed deformations of the tunnel shield require the soil surrounding the shield to be either very stiff or heavily loaded horizontally (high neutral earth pressure) or both. In the near field, moreover, the soil must be strong (devel-

opment of large contact shear stresses between shield and soil) and strongly dilatant (development of high radial soil stresses at the shield wall). The simple shear tests conducted by GeoDelft (2001) on the samples borrowed from the frozen sand have shown the strong dilatancy by presenting angles of dilatancy of 9-17° and volume strains up to 8% (more incidentally than the 5% used in par. 3). In the soil reconnaissance phase of the design the sand of Berg generated some concern due to the high q_c values and high f -values of the cpt-tests and even penetration refusals, the high relative densities (95-100%), evidence of cementation from the piston samples and the glauconite content (10 % of the sand fraction). Now, in retrospect and after completion of the tunnel, the geotechnical properties appeared even more cumbersome for tunneling. The relative density, as obtained from the frozen samples, did not stay below 100% but showed values of 100-120% and the angle of dilatancy not only was large but it also appeared to increase with increasing stress level (fig. 6).

sample	σ_v (vertical stress) [kPa]	ψ (angle of dilatancy) [°]
SSZ1	300	8.7
Z2	600	16.8
X1	300	13.3
X2	600	15.4
Y1	300	12.1
Y2	600	17.0

Deduced from GeoDelft (2001)

Fig. 6. Angle of dilatancy as a function of vertical (and isotropic) stress.

What kind of sand must we imagine to produce such extreme soil parameter values?

In the first place a sand very sensitive to disturbance implying that sampling has shattered brittle particles and has broken silicate or lime bonds between the particles. The shattered fragments, being generally smaller than 63 μm , were thus lost before the relative density measurements were done. In the second place a peculiar aggregate of particles exhibiting increasing dilatancy with increasing isotropic stress level. Normally dilatancy decreases with stress level. If we imagine dilatancy to be due to densely packed particles forced to roll and slide over each other when subjected to shear stress then decreasing dilatancy with stress must be due to breaking of the weaker and unfavourably shaped particles (instead of rolling) and/or to concentration of the shear strains in smaller zones separated by rigidly packed strong-particle areas which stay unsheared. The sands of Berg apparently did not react in this way to increasing stress level. The aggregate of quartz and weaker grains and silicate bonds must have been insufficiently friable to break enough particles to suppress the increase of dilatancy with stress and sufficiently homogeneous to prevent the development of continuous friable and rigid areas. If one was requested to make such an aggregate he would probably spread the weaker and stronger grains evenly over the aggregate (no continuous weak zones), prevent the silicate bounds to get so strong that they cement large areas together (no continuous rigid zones) and to match the shapes of weak and

strong particles so perfectly (like good rock masonry) that breaking of the weaker grains does not fully exclude them from participation in the rolling-over-each-other of all grains but that breaking occurs enough to preclude the formation of large rigid zones. Most probably natural processes have proceeded in a similar way in the sands of Berg!

b. Diagenesis in the Sands of Berg

The sands of Berg are not simple quartz sands as the Pleistocene river sands and Holocene marine sands formed at or near the surface in The Netherlands. They consist of quartz and at least 25% of weaker feldspars, glauconites and other minerals. All minerals are evenly dispersed over the sediment. The sands of Berg are old, lower Oligocene, and underlying the Boom clay. Age and position have given rise to diagenesis, alteration of the sediment in the course of time (Pedro, Siefferman, 1979). The overlying Boom clay, for millions of years at or near the surface in a terrestrial position, weathered and eroded, has furnished a continuous supply of silica-ions and positive ions to the underlying sands. The chemically weaker and more reactive feldspars and glauconites exchanged ions with the pore water and included ions in their crystal lattices and by doing so improved their crystallinity and adapted their shapes to adjacent particles (Bornand, 1978). Even the harder, less reactive quartz grains are subjected to these reactions especially in the contact points with other particles. The overall effect of the described solution and recrystallization is a much better pointed, and denser, aggregate than the original sediment. In case of a relative abundant supply of silicate (or carbonate) ions the particles may be connected by cement or lime bridges. This cementation adds some extra strength and some extra decrease of porosity to the sediment, but in the sands of Berg cementation is less important for their strength and dilatancy than recrystallization. Electron-microscopical images of the sands exhibit an impressive amount of diagenesis (oral communication GeoDelft-collaborators). The composition of the sands of Berg (a large proportion of particles weaker than quartz grains), their position below the Boom clay (supply of ions includable in the particles' crystal lattices) and their age (ample time for the very slow recrystallization processes to operate) have turned the sands into a strong, very dense and strongly dilatant aggregate capable of exerting strong radial stresses on a tunnel shield when sheared by the forward movement of the TBM.

5 Conclusions

Tunnelling in unconsolidated sediments such as clays, sands or gravels is always a bit hazardous due to the low cohesive strength of these sediments.

In the case of old, diagenetically altered, sandy sediments their apparent shear strength and dilatancy must be added to these hazards. During the construction of the Westerschelde tunnel in The Netherlands neither the penetration nor the steerability of the TBM's gave problems, but the radial deformations of the tunnel shield, which was not underdimensioned according to the international state-of-

the-art, prevented the emplacement of the permanent concrete rings in the shield's tail section and caused many months of delay and cumbersome and dangerous remedial measures. Computations with simplified stress-strain relation but including dilatancy reveal that the radial deformations of a "normal" shield become unacceptably large. In view of the large number of shallow bored tunnels world wide under design or in construction it seems wise to warn for the crossing of Tertiary or older sandy sediments.

References

- Bornand M (1978) *Altération des matériaux fluvio-glaciaires*. Thèse Doct. d'Etat USTL Languedoc Publ. SES-INRA, Montpellier 444, 329 p.
- De Mulder EFJ, Geluk MC, Ritsema I, Westerhoff WE, Wong TE (2003) *De ondergrond van Nederland (The subsoil of the Netherlands)*, NITG-TNO, 379 p.
- Duddeck H (1980) *Empfehlungen zur Berechnung von Tunneln im Lockergestein*. Bau-technik, vol. 10, p 349-356.
- GeoDelft Rpt CO-364110/755 (2001) *Laboratory investigation of glauconitic sand*.
- Hetenyi M (1946) *Beams on elastic foundation*. University of Michigan Press, Ann Arbor.
- Kruse GAM (1995) *Subsidence at the transition from massif to basins in the southwestern Netherlands*. Proc. 5th Symp. on Land/ Subsidence, The Hague, 59-68'.
- Pedro G, Siefferman G (1979) *Weathering of rocks and formation of soils. Review of modern problems of geochemistry*. F. Siegen (Ed.) Unesco 39-55.
- Schulze H, Duddeck H (1964) *Spannungen in schildvorgetriebenen Tunneln*. Beton- und Stahlbetonbau, vol. 8, p 169-175.
- Timoshenko SP and Gere JM (1961) *Theory of Elastic Stability*. 2nd ed., McGraw-Hill, New York.
- Van Adrichem Boogaert HA, Kouwe WFP (1997) *Stratigraphic nomenclature of the Netherlands*. Revision and update by RGD and NOGEPa. Mededelingen Rijks Geologische Dienst, 50.

Engineering Geological Model of the Contact between Two Petrographic and Stratigraphic Units along the Zagreb-Split Highway, Croatia

Tomislav Novosel¹, Željko Mlinar², and Damir Grgec³

¹ Institute of Geology, Sachsova 2, Zagreb, Croatia
novosel@igi.hr

Tel: +38516160888

Fax: +38516144713

² Institute of Geology, Sachsova 2, Zagreb, Croatia
mlinar@igi.hr

Tel: +38516160888

Fax: +38516144713

³ Civil Engineering Institute, J. Rakuše 1, Zagreb, Croatia
dgrgec@zg.igh.hr

Tel: +38516144111

Fax: +38516144732

Abstract. The highway route Zagreb-Split, section through Lika region, was designed along the valley of the River Gacka. In this section the highway level line often crosses or goes along the contact zone between two lithological types. The significant differences of rock mass properties of two types would represent the geotechnical problem. The type of contact was also not known as well as the possible weathering degree. Investigation results showed no significant difference in characteristics between Cretaceous limestones and Eocene-Oligocene breccias. Using the results of comprehensive investigations engineering geological model was made.

Keywords: highway design, contact between two rock types, engineering geological model, Zagreb, Split, Croatia.

1 Introduction

The highway Zagreb - Split is the largest infrastructure project in Croatia in the last ten years. In its greater part, the highway passes through a karst region. Numerous structures (such as tunnels, viaducts, bridges, and cuttings) have been designed because of distinguished relief. Extensive multidisciplinary investigations had to be done, such as geological mapping, geophysical measurements, investigation boreholes, laboratory tests on samples, etc. The investigation results enabled the production of engineering geological and hydrogeological maps, prognostic cross-sections and models, which were used for the geotechnical design. In the part of the highway that passes through the Lika region along the valley of the river Gacka, the complex of sediments is characterised by exchange of

two petrographic units: Cretaceous limestones and Eocene-Oligocene breccias. During the investigations, the problem of defining their contact and relation emerged, because the highway level line often passes this zone.

2 Geological Evolution

Lower Cretaceous limestones are of mudstone type, mostly massive and rarely layered along the stilolites. The layers are very thick, with a thickness up to several meters. In some parts, limestones are thickly layered and in some stratigraphic stages, emersion breccias and thinner layers (50-80 cm) appear. Eocene-Oligocene deposits ("Jelar") are represented by breccias. The breccias are fine grained. Grains are predominantly smaller than 1 cm, locally up to several cm and semi-rounded, of various lithology and stratigraphic age. This implies to significant transport and mixing of detritus of various origins. The breccias are strongly cemented with a carbonate matrix of red to grey colour. Because of various grains and matrix, breccias are characteristically multi-coloured. The contact zone with the bedrock is marked with a distinguished tectonic disturbance. In the wider zone there are disturbed, cataclastic, recrystallized and late diagenetically dolomitized bedrock deposits (Lower Cretaceous limestones), in which the deep, open joints are filled with Jelar deposits. The sediment complex is deeply karstified with sub-vertical joints with an aperture up to 1 m at surface. Joints are filled with red soil up to the depth of over 5 m. In the fault zones, the rock is additionally fractured and the joints are mostly filled with clay and rock fragments.

3 Investigation Results

Based on the investigation results the engineering geological map with the scale 1:5000 and longitudinal cross-section with the scale 1:5000/500 were made (Mlinar, et. al, 2002). Figure 1 shows the part of this map. Looking at the appearance of Jelar deposits it is obvious that they have been deposited along the discontinuities with strike NE-SW and N-E. Figure 2. Shows the process of sedimentation of these deposits in several phases. Figure 3 shows a part of the core from one of the boreholes, in which the contact between limestone on the left side and breccia on the right side is visible.

Strong bonds between two rock types are established and the discontinuity from the later tectonic phase was not formed along the contact, but continuously passes from breccia into limestone and vice versa.

The results of the laboratory tests (uniaxial compressive strength) showed that there are no major differences between limestones and breccias (Vrkljan & Sesar, 2002). Taking into account all the investigation results, the categorization of sediments (Singh & Goel, 1999) according to GSI system and considering lithotype, tectonic blocks and placement within the structure, was made. Because of the type of investigation and designers requirements, the values were given in

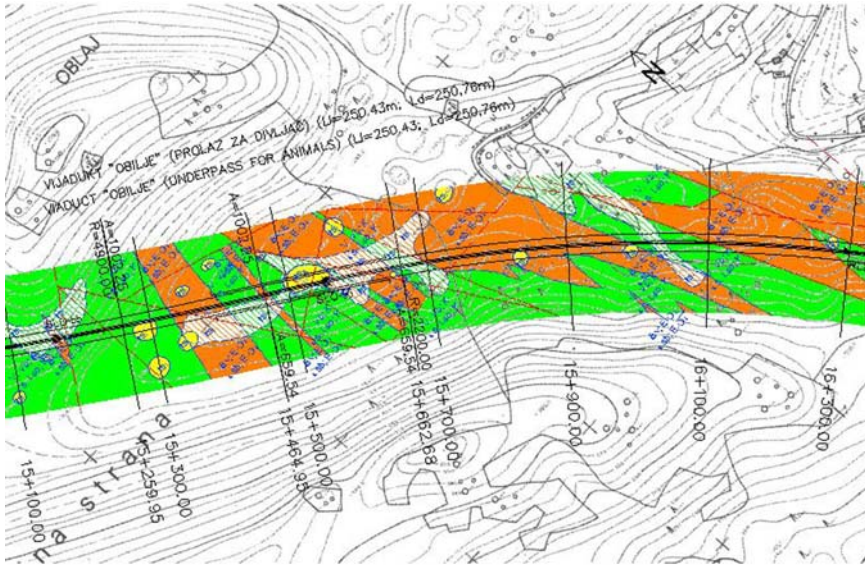


Fig. 1. Engineering geological map.

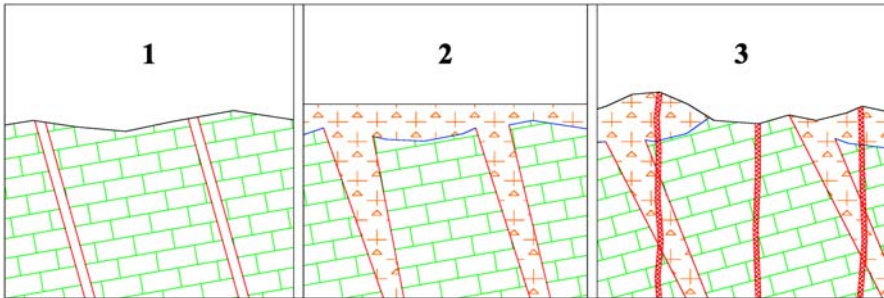


Fig. 2. Phases of sedimentation. A) After the sedimentation of the limestones the emersion phase begins. The deposits are mildly folded and discontinuities - joints are created; B) Limestone breccias are deposited in newly developed basins. Contact with the limestones in the base is discordant and the breccias are filling the open joints. Carbonate matrix strongly cements the breccias and at the same time, strong cementation bonds are established between breccias and limestones; C) In the last phase, the today's relief is formed and the newly created joints continuously pass from one sediment type to the other.

ranges. Calculated GSI values for Jelar breccias are in the range from 50 to 77. Calculated GSI values for limestones are in the range from 52 to 74. Engineering geological mapping, geophysical investigations and core drilling showed that the Quaternary deposits in various forms of appearance are present in the whole area (Vrkljan et al., 2002). High fractured carbonates susceptible to weathering combined with the tectonic activity lead to forming of the distinguished relief. Cover deposits (red soil - mostly clays) were sedimented in depressions, where they



Fig. 3. Borehole core with contact between two rock types.

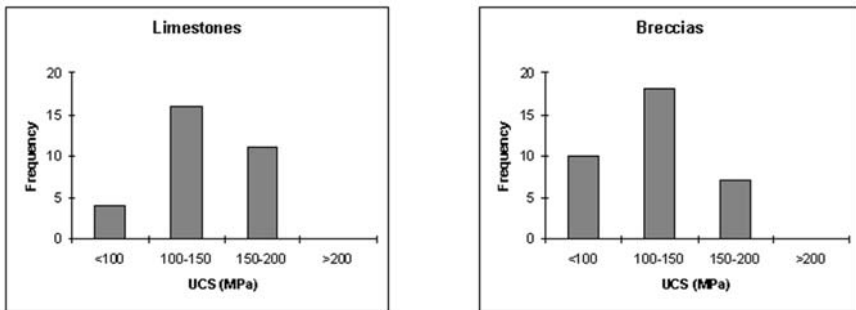


Fig. 4. Results of uniaxial compressive strength laboratory tests.

reach the significant thickness (over 5 m). These deposits also fill the open joints that locally exceed the depth of 5 m. Weathering zones in these rocks are of various thickness and wideness. Because of the tectonic activity, the fractured and weathered zones have a significant thickness in some places. In such zones the GSI values are 20-50% lower than those previously mentioned. Geophysical investigations, mainly electrical tomography and WET tomography, were used in critical locations to determine the thickness and wideness spreading of the cover deposits, the weathering zones and the fractured zones. The characteristic cross-section is shown in figure 5.

4 Engineering Geological Model

Compilation of all investigation results enabled the creation of the engineering geological model of this part of the future highway route.

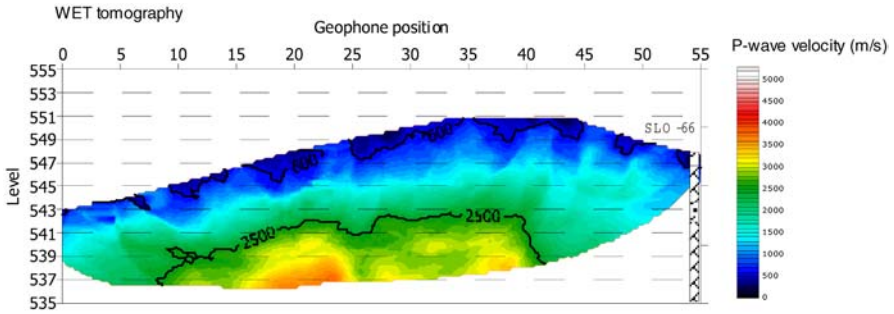


Fig. 5. WET tomography cross-section.

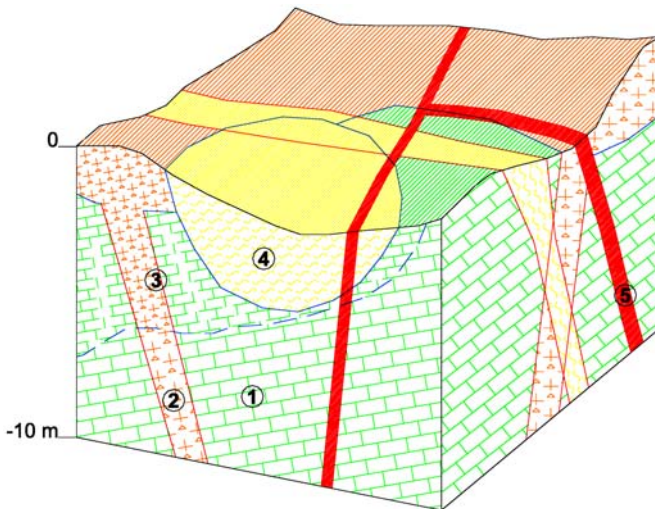


Fig. 6. Engineering geological model. 1) Limestones, slightly weathered or fresh, GSI = 52-74, P-wave > 2500 m/s; 2) Breccias, slightly weathered or fresh, GSI = 50-77, P-wave > 2500 m/s; 3) Limestones or breccias, medium to high weathered, GSI = 30-50, P-wave = 600-2500 m/s; 4) Clays, stiff to firm, CH, P-wave < 600 m/s; 5) Faults and joints of the latest tectonic phase.

5 Conclusion

The results show that the contact between two rock types would not present a geotechnical problem. However, because of the similar characteristics of both types, especially in the way of weathering, the main problem will be the zones of highly weathered rock and wide joints and the distinguished paleo-relief filled with cover deposits that are hard to predict. These problems will have to be dealt individually during the construction phase of the highway.

References

- Singh B & Goel RK (1999) *Rock Mass Classification A Practical Approach in Civil Engineering*, Elsevier, Amsterdam.
- Mlinar Ž, Novosel T, Pollak D & Larva O. (2002) IPZ-IIIIC-2-B-Y-0021-0 Inženjersko-geološki istraživački radovi, archive IGI, Zagreb.
- Vrkljan I & Sesar S (2002) IPZ-IIIIC-2-B-Y-0030-1 Laboratorijski istraživački radovi, Elaborat laboratorijskih rezultata, archive IGH, Zagreb.
- Vrkljan M, Bruneta I, Sapunar N & Matković I (2002) IPZ-IIIIC-2-B-Y-0010-1 Geotehnički istraživački radovi, archive IGH, Zagreb.

Overconsolidated, Early-Pleistocene Clays in Relation to Foundation Design and Construction of HSLSouth, Province of Brabant, The Netherlands

Floris Schokking

GeoConsult bv, P.O.Box 2296, NL-2002 CG Haarlem, The Netherlands
floris.schokking@geoconsult-haarlem.nl
Tel: +31 23 5269765
Fax: +31 23 5269767

Abstract. The High Speed Line connecting Amsterdam to Brussels (HSLSouth) requires a link to the existing railway system at the City of Breda, Province of Brabant. Shuttle connections to the North (Rotterdam) and to the South (Antwerp) will join and exit the HSLSouth near Breda. Accommodation of existing and new railway tracks necessitate the construction of several fly-overs and underpasses in the area between Breda and the tributary of the River Meuse, the Hollandsch Diep, further to the North. Throughout the area occur Early-Pleistocene fluvial clay layers at a depth of approximately 19 to 23 m – GS, below a cover of sandy deposits and towards the North also below an additional 2 to 8 meters thick cover of Holocene clays, sand and peat. The deep clay layers show overconsolidation ratios of OCR=1.1 to 2.1. Geotechnical properties of the clays are up till present badly documented and the cause of overconsolidation is still poorly understood. In the design of the structures for the shuttle connection to the HSLSouth the clays come into play in various ways: as an aquiclude forming the bottom of a sheet piled construction pit and as a settlement prone layer below slab or pile foundations, and in some cases additionally loaded by adjacent earth embankments. The character and cause of the overconsolidation is discussed in relation to the geological history. The role of the overconsolidated clays in foundation design and construction is elucidated using case studies of two underpasses near Breda and a fly-over near Den Hoek, between Breda and Hollandsch Diep.

Keywords: overconsolidated clay, foundation design, HSL.

Introduction

In design problems related to settlement of overconsolidated clays, the variation or consistency in OCR values is often critical. The construction of a local or regional model in which the cause of overconsolidation becomes clearer can be a helpful instrument. In dewatering for construction the continuity of clays is often essential for the working of clay layers as aquicludes. During the building the HSLSouth in Brabant many geotechnical data gathered in three successive site investigations by the Projectbureau HSLZuid, as principal, and in additional site investigations by the construction joint ventures involved, HSLInfraRail, for which GeoConsult carried out the geotechnical engineering, and HSL Brabant Noord. In three case-

studies of structures, designed and built by HSLInfraRail, is described the role which the overconsolidated clays played in the design and in the choice of construction methods.

Early-Pleistocene Fluvial Sedimentation

Along the route of the HSLSouth from the Hollandsch Diep to the City of Breda Early-Pleistocene fluvial sediments are deposited over marine sandy sediments (Fig. 1). Apart from the geological map (RGD, 1975) shown no other compiled public geological information about the area is available.

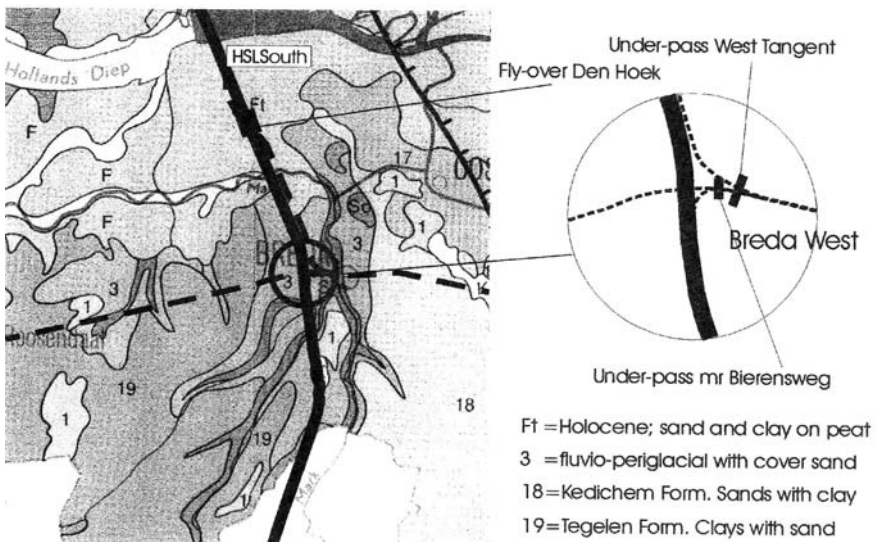


Fig. 1. Geological Map of Project Area (RGD, 1975), HSLSouth, IC-railway lines and discussed constructions.

During the sedimentary sequence of the Early-Pleistocene large river channels with overflow deposits were formed in various stages, which are related to alternating colder and warmer periods. Erosion and deposition alternated depending on climate variations. These also influenced the character of materials deposited, in combination with sea level rises and falls and tectonic movements influencing river gradients and water depths. The following fluvial deposits characterise the whole area (Fig. 1):

- During an early fluvial sequence mainly clay and loam layers, interlayered with fine sands, were deposited (Tegelen Formation) and situated at levels from 14 to 21 m – GS.
- Mainly fine sands interlayered with clay and loam layers were deposited subsequently (Kedichem Formation) ranging in thickness from 10 to 15 m.

The ground surface of the existing sedimentary plain during the latter deposition phase may have been considerably higher than the present ground level, so influencing the maximum past effective stresses, which will be discussed in the next section. There are several indications found in the site investigation of the HSL project, that strong erosion and redeposition, during the latter fluvial sequence can have occurred. An example of this is a deep clay filled gully of up to 13 m - present GS in depth and with a width of 1 to 1.5 km located just North of the present River Mark and South of Fly-over Den Hoek. This may have been the former channel of the River Mark, which has at its present location an incision of similar depth, but filled with mainly silty sands and some clay layers. At the end of the Pleistocene period fluvioglacial deposits, loam and fine to medium coarse sands, covered the fluvial deposits all along the route of the HSLSouth. Holocene deposits, silty clays and peats and locally fine sands, overlaid the Pleistocene deposits from around the River Mark up till the Hollandsch Diep. The thickness of these deposits ranges from 2 to 3 m in the South to some 8 m in the North.

Engineering Geology of Overconsolidated Clays

Geotechnical Properties

The overconsolidated clay layers, as discussed in this paper, have not been described in literature before. During this HSLSouth project considerable data sets became available in the area concerned from successive geotechnical site investigations by firstly the Projectbureau HSLZuid and later by Construction Joint Ventures: HSL Brabant Noord, HSL Brabant Zuid and HSLInfraRail. For the area Breda West and between Breda and the Hollandsch Diep these data has been interpreted and analysed and is presented in Table 1 and in the diagrams of Fig. 2 and 3. Of the Pleistocene overconsolidated cohesive layers about 90 % can be defined as clay, according to the Dutch norm on soil description (*NEN, 1990*), with a clay fraction larger than 8 %. The remaining 10 % has to be classified as loam. For matter of clarity the term clay is used in this paper for all cohesive layers concerned.

Table 1. Geotechnical properties of overconsolidated clays.

	γ_s KN/m ³	γ_d KN/m ³	w_N %	<2 μ m %	p_i %	w_L %	C_p	C_s	C'_p	C'_p	C_c m ² /s
Breda West	18.2 – 21.4	13.1 – 18.2	39 – 18	7 –57	7 – 38	28 – 72	21 – 126	460 – 1640	18 –63	225 – 840	2.1*10 ⁻⁸ – 1.9*10 ⁻⁶
Breda – Hollandsch Diep	16.4 – 21.6	-	-	-	11 – 53	25 – 80	40 – 210	340 – 1650	21 –62	180 – 910	-

The clays are in general to describe as inorganic clays with low to medium plasticity with variable silt and sand contents, from their position in the Plasticity Chart. The variation in geotechnical properties between the Breda West area and the area further North is marginal. In most of the design applications the loading of the clay falls within the trajectory above the preconsolidation load. The range of the

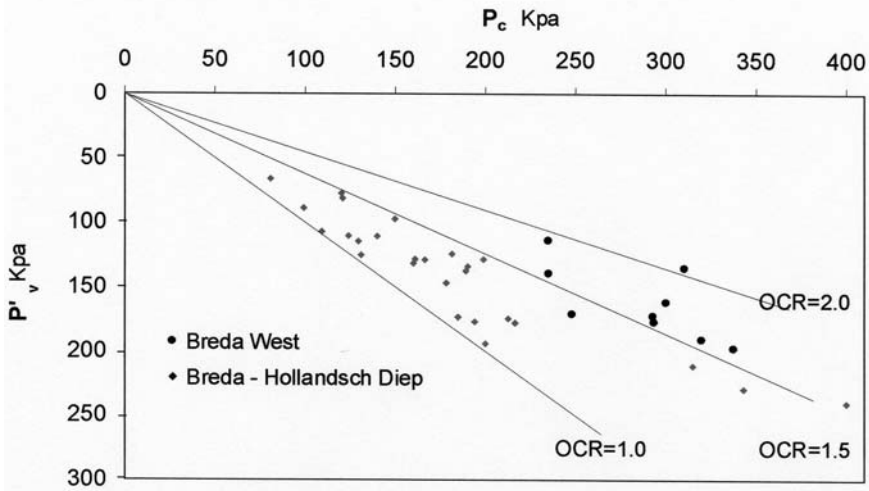


Fig. 2. Pre-Consolidation Stress vs. In-situ Effective Stress.

range of the consolidation parameters C_p and C_s , as used in the Terzaghi-Buisman-Koppejan formula (Koppejan, 1948) is on average identical in both areas for this trajectory.

Overconsolidation

The Pleistocene clay layers are overconsolidated from their occurrence in the Breda West area up to the Hollandsch Diep, as observed in CPTs and in oedometer tests (Fig. 2 and 3). A definite trend in decrease of OCR values can be observed from the Breda Area (OCR from 1.45 to 2.1) to the Hollandsch Diep (OCR from 1.05 to 1.55). Further can be recognized, supposing overconsolidation by additional sediment loading in the past, that in the Breda West area sediment levels have been 11 to 15 m higher than present ground levels for the deep clay layers and for the higher positioned clay layers above approximately 9.0 m - GS values are from 9 and 10 m. For the area towards the Hollandsch Diep these values for the deep layers range from 2 to 4 m and for the higher positioned clay layers from 3 to 7 m.

These observations appear to indicate, that the supposition of the additional sediment loading in the past as the cause of the overconsolidation for these layers, is justified. The inferred indication of sloping of the sedimentation plain towards the North or the Northeast fits into the regional picture for the fluvial system during the Early-Pleistocene. Aging, drying, or the influence of frost action in a periglacial environment are much less probable as a cause of overconsolidation, although some influence of these can not be excluded, especially where the large variation in the values in the area towards the Hollandsch Diep is concerned. Apart from additional sediment loading, also the influence of a lower ground wa-

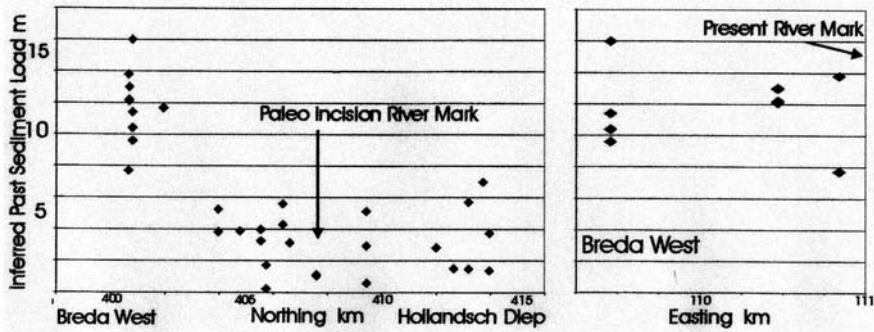


Fig. 3. Inferred Past Sediment Load vs. Sample Location

ter level, increasing effective stresses, possibly during colder periods, must be considered to have played a role in the overconsolidation. A further tentative deduction from the above observations, is that the upper clays, after a phase of considerable erosion, are loaded to a less elevated ground level in the past, as to what the deeper clay layers have experienced and that slopes or possibly slope directions are different from those of the earlier phase, which supports the dynamics of the fluvial system under changing climatic and tectonic conditions. Expressions of previous (and in Breda possibly still present day) channels of the River Mark appear to be observable from the diagrams of Fig. 3. In the Breda Area sand layers directly overlying and underlying the early clay layers are overconsolidated, indicated by CPT values between 30 and 50 MN/m², which supports the above tentative deductions about overconsolidation by additional sediment loading.

Foundation Design and Construction

Underpass West Tangent, Breda

The Underpass West Tangent is the connection of the Western ring road around Breda under four rail tracks, a secondary road and a cyclist path. The depth at the lowest point is 6.2 m - GS and 10.5 - GS at the pump room, the maximum width is 24.8 m, and the overall length 275 m. The central part of the underpass has a piled foundation, with piles mainly loaded in tension to prevent floating up, and partly in compression under the walls. Both underpass entrances have a slab foundation.

During the tender phase three alternatives for foundation design and the construction of the central part of the underpass were considered as presented in Table 2 and Fig. 4.

Table 2. Alternatives for Foundation Design and Construction of Underpass West Tangent, Breda.

Alternatives	Sheet piling	Tension piles	Dewatering	Risks	Costs
Dry	Deep sheet piling *, "Polder"-solution	For permanent situation, Vibrocom Ø 610 mm, short (above deep clay layers)	Infiltration water only	Discontinuity of deep clay layers - Problems with driving of sheet piling through overconsolidated sands and leaks developing - Problems with retrieval of pile casings from overconsolidated sands	++
Dry	Shallow sheet piling ** and confined dewatering	For permanent situation, Vibrocom Ø 457 mm, short (above deep clay layers)	Confined to $\Delta h = - 4.5$ m	Discontinuity of shallow clay layers - Pumpability of fine, overconsolidated sands - Damage to environment resulting of lowering of phreatic surface	Base
Wet, Underwater Concrete	Shallow sheet piling ** and tension piles	For temporary and permanent situation Vibrocom Ø 610 mm, long (below deep clay layers)	Infiltration water only	- Problems with retrieval of pile casings from overconsolidated sands	+

* in deep clay layers at 20.5 m – GS ** in shallow clay layer at 9.0 m – GS

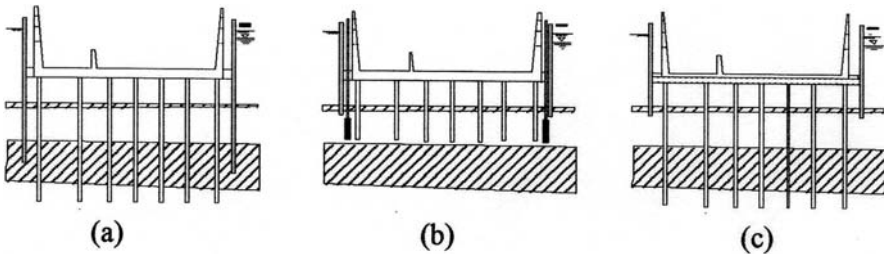


Fig. 4. Underpass mr Bierensweg and geotechnical section.

For the dry alternatives the uncertainty about the working as aquicludes of the overconsolidated shallow and deep clay layers formed a considerable risk, mainly with respect to their continuity. The first step in the investigation of this risk, was carrying out 11 CPTs and 3 boreholes to approximately 21m – GS into the lower Pleistocene sands below the overconsolidated clays, additionally to CPTs and boreholes, which had been made in two earlier site investigation stages by the Projectbureau HSLZuid. The upper layers of the deeper clays appeared absent under the central part of the planned underpass, unfortunately just beside a 10 m wide stretch where no investigation could be carried out as a result of the presence of the existing railway tracks. As there was still concern about the continuity of the whole unit of clay layers it was decided to perform a pumping out/ recovery test with a pumping filter within the overconsolidated sands from – 8 to -12 m GS. The pumping test would also gain information on hydraulic conductivity of the deposits for the hydrological modelling, besides the estimation thereof in in-situ and laboratory tests in the additional boreholes. It appeared, that both shallow and deep overconsolidated clay layers would function adequately as aquicludes with

permeabilities of approx. $K = 8 \text{ to } 6 \cdot 10^{-8} \text{ m/s}$, and in general being continuous over the area of the underpass. In the south-eastern part of the underpass the shallow clay layer appeared thin or was absent. The continuity of the deep clays has been proven as well for the HSLSouth constructions further West and South (Bouwcombinatie Brabant Zuid; pers. comm.). The dry solution, with confined dewatering and short precast concrete piles in the overconsolidated sand was chosen in the end for reasons of lower costs and low risk.

Underpass mr Bierensweg

A secondary road with cyclist path runs under four railway tracks at the Underpass mr Bierensweg. The depth at the lowest point is 4.1 m – GS and 5.7 m – GS at the pump room, the maximum width is 23 m in the central part, and the overall length 185 m.

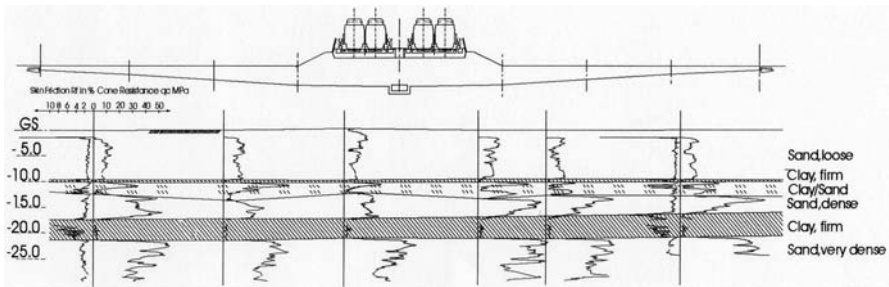


Fig. 5. Underpass West Tangent; Alternatives: a) Dry, “Polder”-solution; b) Dry, Confined dewatering; c) Wet, Underwater Concrete.

The underpass has a slab foundation over its whole length. The central part, which carries the railway tracks, is made in one unit of 41 m length (Fig.5). The units comprising the entrances have lengths varying from 17 to 19 m. The excavation for and the construction of the central unit and two adjacent units is carried out within sheet piling, with a toe level below a clay layer at a depth of approx. 10 m – GS. For dewatering wells above the clay layer were used. The main foundation problem is associated with settlements within the overconsolidated clay layers, resulting from the railway embankments, to be placed directly against the walls of the underpass to a level of 3 m + GS. The earth embankment can be placed only after the construction of the central unit and therefore the settlements apply a forced deformation to the concrete wall and floor. As a result of settlements in the clay layers, which are largest under the centre of the embankment, the concrete wall will experience a differential settlement of approx. 30 mm. The wall will not be able to withstand these differential settlements, which are largest at the ends of the wall, where the embankment is sloping down, not even with additional reinforcement. To reduce the differential settlements a preconsolidation load of 3 m of sand was applied, realising a reduction in differential settlement to approx. 5 mm. As the clay layers are overconsolidated with OCR values from 1.9 to 2.1 the effect

of the preconsolidation will not be diminished during the excavation and the construction of the central unit. For overconsolidated clays the Skempton A factor decreases with increasing OCR (Bishop & Henkel, 1962). Therefore the reduction of the pore water pressure upon unloading becomes smaller with increasing OCR, so reducing the swell and swell velocity which can occur. Settlements during preconsolidation varied from 26 to 60 mm and measured swell values after removal and excavation were neglectable.

Fly-over Den Hoek

Between the City of Breda and the Hollandsch Diep a northbound shuttle connection, firstly using the IC-tracks, passes at Fly-over Den Hoek over the HSL tracks, to join the left track shortly after it. The fly-over consists of 29 intermediate columns and 2 end columns, with an overall length of 500 m. The Fly-over is connected at the end columns to earth embankments with a height of approx. 7.5 m + GS, which are supported by L-shape retaining walls where the HSL- and the IC-tracks are running close to the ends of the fly-over (Fig. 6). The deep overconsolidated clay layers play an important role in the design of:

- 1) the end column foundation piles in the sands below the clays
- 2) the foundation of the retaining wall on piles in sands above the clays
- 3) the HSL track concrete slab on an earth improvement of sand on the top of the Pleistocene sands

Each of these geotechnical structures experiences the consolidation of the deep clay layers resulting from the load of the earth embankment in a different way, and at different moments in time, depending on the construction sequence. The interaction between these structures is made even more complicated, where the design and construction of the HSL and the Fly-over Den Hoek are performed by two different construction joint ventures.

The end columns of the fly-over (1) have to be founded on piles in the sands below the overconsolidated clays. With piles with toe levels above the clays, the

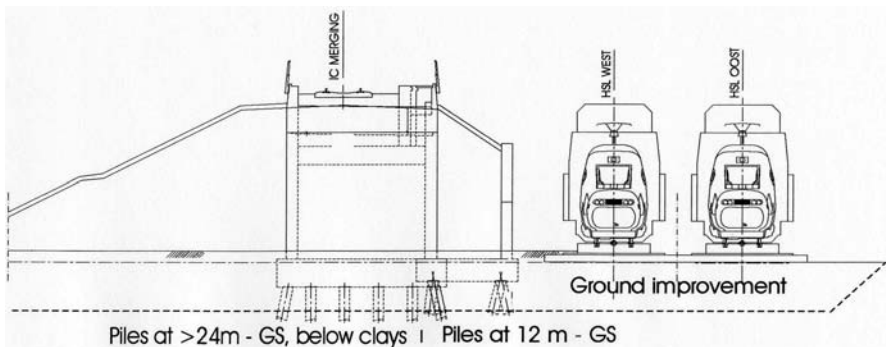


Fig. 6. Fly-over Den Hoek; Section at End Column North with Retaining Wall and HSL Settlement Poor Construction.

combination of settlements from the earth embankment and the pile loads from the end column would result in settlements in the order of more than a decimetre, with moreover an asymmetrical pattern over the foundation slab, which induces undesirable stresses in and rotation of the slab.

Choosing deeper piles, having a length of 23 to 26 m, the problem of negative skin friction under influence of settlements in the order of magnitude of several centimetres resulting from the load of the earth embankments arises. This problem is occurring at many of the crossing road infrastructure constructions with the HSL and in the re-routed A16 motorway, along this stretch of the HSL. One of the solutions to this problem is allowing the piles to fail in end bearing under the actual load with the additional load from the skin friction. After a displacement in the order of centimetres, the skin friction load will diminish or disappear. For road construction the then resulting vertical deformation and rotation of the end column will be, in general, within an acceptable range. For the "low-founded" foundation slab of the end column the asymmetrical deformations, increasing in the direction of the earth embankment, would give too large a horizontal deformation at deck level, resulting from the rotation of the slab and the column. For this reason the decision was taken to apply a preconsolidation load during a 3 month period at the end column, which resulted in settlements from 0.03 to 0.04 m. The retaining wall along the earth embankment (2), constructed in units of approx. 20 m, can be supported on piles with toe levels above the clay layer. One problem resulting from settlements in the order of magnitude of centimetres related to the earth embankment and with a decreasing trend away from the centre of the embankment and towards the retaining wall, is the development of unwanted stresses in the concrete of the bottom slab. Moreover at the location of the end column the loading of the wall in a confined situation where arching of the earth embankment will probably occur, the deformation will be less than at the other end of the unit, giving undesirable stresses within the slab. These were other reasons to decide on preconsolidation at and in the surrounding of the end column. In this stretch of the HSL South the tracks have a slab foundation (3) (Settlement Poor Construction (SPC)), where further North and all the way to Amsterdam a pile foundation under a concrete slab is used (Settlement Free Slab), in areas where no special constructions are made. The foundation of the slab consists of a ground improvement of densified sand, resting on the top of the Pleistocene surface, from which 3 to 5 m of Holocene clay, peat and sand have been removed.

Apart from an increase in effective stress from the own weight of the slab and the additional weight of the sand, the SPC experiences the settlement in the deep overconsolidated clays resulting from the earth embankment and from loads on the piles of the retaining wall with toe levels above the clays. As total settlements of the SPC would be beyond the residual settlement requirement of 30 mm/100 years, part of this settlement must have been achieved prior to track fixation to the slab. The preconsolidation around the end column of Fly-over Den Hoek, as used for to solve the problems in (1) and (2), is necessary, due to the time constraint of the construction planning, to reduce the resulting residual settlements to the required limit.

Conclusions

The main cause of overconsolidation of Early-Pleistocene clays between Breda and the Hollandsch Diep is additional sediment loading, with OCR values ranging from 1.1 to 2.1.

In the area West of Breda form the deep overconsolidated clays continuous sheets on the scale of engineering constructions with lengths up to at least 500 m.

Acknowledgements

The author is thanks indebted to the Projectbureau HSLZuid and HSLInfraRail for allowing the information about the project to be used in this paper. Further he is grateful to H. van der Velden, Bouwcombinatie HSL Brabant Noord, for supplying some of the geotechnical data presented.

References

- Bishop AW & Henkel DJ (1962) The measurement of soil properties in the triaxial test, 2nd ed. London: Edward Arnold.
- Koppejan AW (1948) A formula combining the Terzaghi load-compression relation and the Buisman secular time effect; Proc. 2nd Int. Conf. on Soil Mech. and Found. Eng., Rotterdam, Vol. 3.
- NEN (1990) Geotechnics – Classification of unconsolidated soil samples. NEN 5104:1989/C1:1990 nl.
- RGD (1975) General Geological Map of The Netherlands; In: Geologische overzichtskaarten van Nederland, Eds. W.H. Zagwijn en C.J. van Staaldunin, Rijks Geologische Dienst, Haarlem.

Location of Buried Mineshafts and Adits Using Reconnaissance Geophysical Methods

Martin Culshaw¹, Laurance Donnelly², and David McCann³

¹ Urban Geoscience and Geological Hazards Programme, British Geological Survey
Kingsley Dunham Centre, Keyworth, Nottingham, NG12 5GG, UK and
School of Property and Construction, The Nottingham Trent University, Newton Building
Burton Street, Nottingham, NG1 4BU, UK

² Halcrow Group Ltd., Deanway Technology Centre
Wilmslow Road, Handforth, Cheshire, SK9 3FB, UK and
Research Fellow, British Geological Survey, Kingsley Dunham Centre
Keyworth, Nottingham, NG12 5GG, UK

³ British Geological Survey, Kingsley Dunham Centre
Keyworth, Nottingham, NG12 5GG, UK and
School of Engineering and Electronics
Institute for Research in Infrastructure and Environment, Crew Building
West Mains Road, Edinburgh EH9 3JN, UK
mgc@bgs.ac.uk
Tel: +44 115 936 3380
Fax: +44 115 936 3460

Abstract. Britain has a long history of mining activity, which stretches back some 3000 years to the excavation of flint in East Anglia. The legacy of this long period of activity is the presence of many buried mineshafts and adits, whose location is often unknown precisely and in many cases not even recorded in historical mining records. As has been shown by Donnelly et al (2003) the discovery of a mineshaft in an area of housing development can have a profound effect on property values in its vicinity. Hence, urgent action must be taken to establish at the site investigation stage of a development to determine whether any mineshafts are present at the site so that remedial action can be taken before construction commences.

A study of historical information and the drilling may well enable the developer to locate any suspected mineshafts and adits on his site. However, the use of geophysical reconnaissance methods across the whole site may well provide sufficient information to simplify the drilling programme and reduce its cost to a minimum. In this paper a number of rapid reconnaissance geophysical methods are described and evaluated in terms of their success in the location of buried mineshafts and adits. It has shown that a combination of ground conductivity and magnetic surveys provides a most effective approach on open sites in greenfield and brownfield areas. Ground penetrating radar and micro-gravity surveys have proved to be a valuable approach in urban areas where the use of many geophysical methods is prevented by the presence of various types of cultural noise. On a regional scale the infrared thermography method is being increasingly used but care must be taken to overcome certain environmental difficulties. The practical use of all these geophysical methods in the field is illustrated by a number of appropriate case histories.

Keywords: mine entrances, radar, microgravity, magnetometer survey, electromagnetic surveying.

1 Introduction

Buried mineshafts, adits, and mineworkings are a major problem in the United Kingdom for the civil engineering industry both during the execution of a project and in the years following its completion. Urban housing developments that often cover large areas of land in previously mined areas are particularly vulnerable to sudden collapses of the ground surface as a result of the presence of old, abandoned mineshafts. Normal site investigation procedures based on the drilling of a number of boreholes often fail to delineate the position of these abandoned mineshafts and consequently development proceeds without the construction company being aware of this potential hazard on the site.

The detection of man-made cavities is essential at the site investigation stage of all civil engineering construction work. A suitable investigation procedure for the location of mineshafts and natural cavities was introduced by Culshaw and Waltham (1987) and this is summarized briefly below:

- (1) Desk study documents, maps, aerial photographs
- (2) Field study (reconnaissance), geochemical survey, geophysical survey
- (3) Field investigation, drilling and/or excavation
- (4) Further, more detailed, geophysical surveys, possibly followed by drilling.

It is most important to realize that a comprehensive desk study of the area of interest must be carried out before starting any activity in the second and third stages given above. Once this first-stage investigation has been completed, the desk study may well have yielded sufficient information for the civil engineer to proceed to the drilling and/or excavation stage. The possible presence of mineshafts will have been assessed since all the available information will have been studied. However, the use of boreholes and trial pits is often initiated without introducing the second phase of the investigation in the form of a reconnaissance geophysical survey, despite the fact that geophysical methods can provide information on the whole of the ground mass while intrusive methods sample only a tiny proportion. For example, 100 boreholes of 100 mm diameter each drilled to a depth of 10 m and located on a 10 m grid sample less than 0.01% of the ground.

Abandoned mineshafts may vary considerably in terms of their dimensions (diameter), cross sectional shape, type of lining (if any) and composition of any infilling. Older and shallower shafts were often timber lined, though this was superseded by brick lining. Filling of shafts on abandonment was not carried out consistently; a wooden platform might be built at the top of the shaft, just below the ground surface, which was then topped up with fill. In time, the wood will decay with subsequent collapse. If the shaft was not sealed off from the workings, fine fill material could flow into the workings leaving voids within the shaft (Bell 1975).

The variable nature of abandoned shafts can influence the capability of any geophysical method to locate their presence. For example, if a mineshaft is of small diameter (about 1 m or less), and the original site of the mineshaft has been covered by foundations or other artificial material, it may be difficult for the

anomaly of a partially infilled void to be resolved. Similarly, a mineshaft through shale/clay, that has been backfilled with the same material, will be difficult to identify.

2 Reconnaissance Geophysical Surveys

If, following a desk study, it is decided to move to the second investigation phase, then a decision has to be taken whether a geophysical survey is necessary. A reconnaissance geophysical survey measures the variation of a physical property, such as electrical conductivity on a grid basis over the ground surface. Contouring of this data will locate anomalous zones, which may be associated with the presence of a buried mineshaft. Selection of the line and station separation used in the survey must be appropriate to the anticipated dimensions of the target. Further investigation of the anomalous areas with boreholes or trenches is often required unless historical information exists that indicates the likely cause of geophysical anomaly. It is usually assumed that the geophysical equipment used in a reconnaissance survey does not require direct contact with the ground surface. This does not preclude the use of an electrical resistivity survey using a constant electrode separation, in which the electrodes are pushed into the ground surface or a seismic refraction survey using geophones, which also have to penetrate the ground surface. However, the major criteria for the geophysical reconnaissance survey have to be high speed of movement over the ground surface and rapid measurement of the data at each station.

Some knowledge of the types of mineworking that may be present on the site will be available from the initial desk study, so that consideration can be given to the most suitable geophysical method. It is important to realize that the choice of the correct geophysical method is absolutely essential from the point of view of maximizing the success of the survey. Lack of collaboration between the site geologists and engineers, and the geophysicist can lead to an unsuccessful survey, since it is usually the combination of all the available information with the geophysical survey data, that finally locates the mineshaft or anomalous ground conditions associated with it. The consulting engineer should have access to an expert geophysical consultant who, in addition to advising on the suitability of the various geophysical methods, will plan and oversee the geophysical survey work with geological advice (McCann *et al.* 1995).

The various geophysical methods that have been used in reconnaissance surveys for the location of mineworkings have been described by several authors including Telford *et al.* (1990), Reynolds (1997) and McDowell *et al.* (2002). In general, the case histories below have been orientated towards the detection of anomalous zones down to depths of about 10 m, which is the main area of interest for site investigations for shallow foundations and excavations. In many cases, the mineworkings or shafts, result in some disturbance at the surface that can be detected by the standard geophysical methods. It must be emphasized that for a geophysical anomaly to be detected by a geophysical surveying method, the zone or area associated with it must have physical properties that are significantly different from those of the surrounding rock mass.

The presence of an anomaly in the survey area resulting from the presence of a mineshaft is controlled by its physical dimensions, shape and depth of burial, and the properties of the material that it contains in relation to those of the surrounding rock mass. All these parameters influence the performance of the geophysical technique used in relation to the four fundamental controlling factors, namely:

- (1) penetration;
- (2) lateral and vertical resolution;
- (3) signal-to-noise ratio;
- (4) contrast in physical properties.

The geophysicist must be satisfied that the technique proposed to locate a mineshaft is capable of resolving the smallest significant anomaly that is likely to occur at a given depth. This must be established before the survey commences, so that the survey can be designed to locate mineshafts with known minimum specifications with regard to physical dimension, depth of burial, etc.

3 Geophysical Methods Used in Mineshaft Location

3.1 Micro-gravity Case Study: Abandoned Coal Mineshafts Close to a Housing Estate, England

Figure 1 shows a site plan of a typical mining area in Britain with three suspected abandoned mine shafts. The attention of a local authority was drawn to a playing field after members of the public reported ‘noises and vibrations’ from underground. Since the area was known to have been subject to past mining it was feared that the disturbances were associated with abandoned mineworkings as a result of collapsing mineshafts. The collapse of the ground over one of these shafts resulted in the generation of a 30m deep crown hole. Due to the relatively large size of the playing field, a programme of speculative drilling and trenching was considered to be too expensive and time consuming. Instead, a micro-gravity was carried out to determine the location of the other two shafts.

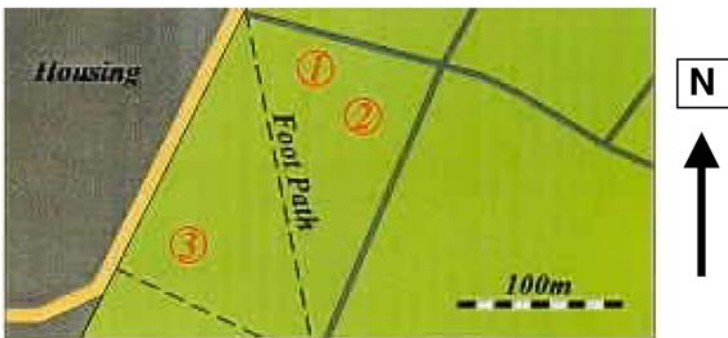


Fig. 1. The anticipated locations of three mineshafts (1, 2 and 3) adjacent to housing in a former coal mining area in the UK (courtesy of IMC Geophysics Ltd).

The microgravity survey was designed and implemented over the area to look for any evidence of voiding at depth. Contouring of the microgravity data after standard corrections were applied indicated low gravity anomalies at points A and B (Figure 2). These results showed that the shaft was filled with a very low-density material or was partially filled with spoil but had an extensive void at depth. Subsequent drilling confirmed that the microgravity anomaly did actually represent the position of a mineshaft that had a brick lining. The shaft located at position A was subsequently remediated by infilling and capping.

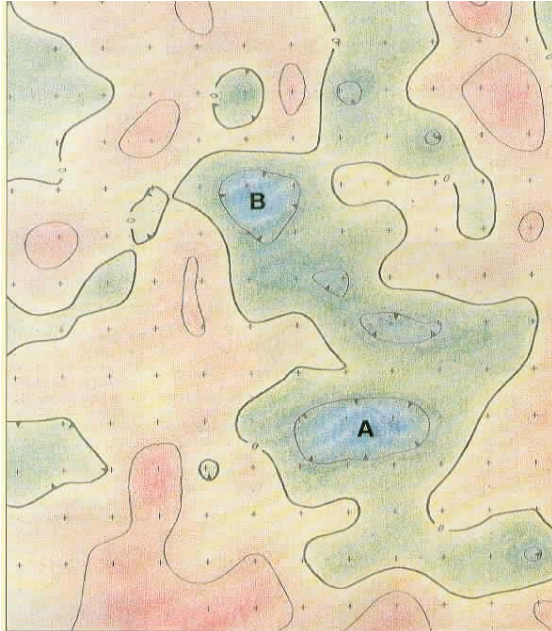


Fig. 2. Residual gravity indicating low gravity points at A and B. A buried shaft was subsequently located at point A and appropriately remediated (courtesy of IMC Geophysics Ltd).

3.2 Magnetic Surveying Case Study: Abandoned Mineshaft in Hematite Deposits, North West England

Dalton-in-Furness is an area in north west England where extensive hematite mining formerly took place. Access to the mines included vertical mineshafts. Development in the area needs to take account of the presence of these abandoned shafts. The hematite is present as veins, lenticular bodies parallel to the bedding and sops infilling dissolution hollows in the Dinantian (Lower Carboniferous) limestone. The limestone is overlain by Quaternary glacial clayey till with bands of sand and gravel. A magnetometer survey, using a bottle height of 1.5 m, was carried out in the area of Thwaites Flat to the west of Dalton-in-Furness. Figure 3 shows the results of the survey. Two clear, positive anomalies can be seen against

a background that slowly increases to the north east as the superficial deposits change from a clayey to a sandier soil (Jackson *et al.* 1987).

The smaller anomaly, to the south east, is centred within 2 m of a known shaft while the larger anomaly was not associated with any known workings. In practice, both anomalies would be treated as being related to the presence of mine-workings, to be proved by direct investigation. Using pitting and/or drilling.

3.3 Electromagnetic Surveying Case Study: Abandoned Coal Mine Shaft West of Nottingham, England

A ground conductivity survey is often carried in conjunction with a magnetic survey since, even if there is no magnetic response at the location of a suspected buried mineshaft, its presence may be detected from the change in the groundwater drainage pattern that will cause a variation in ground conductivity.

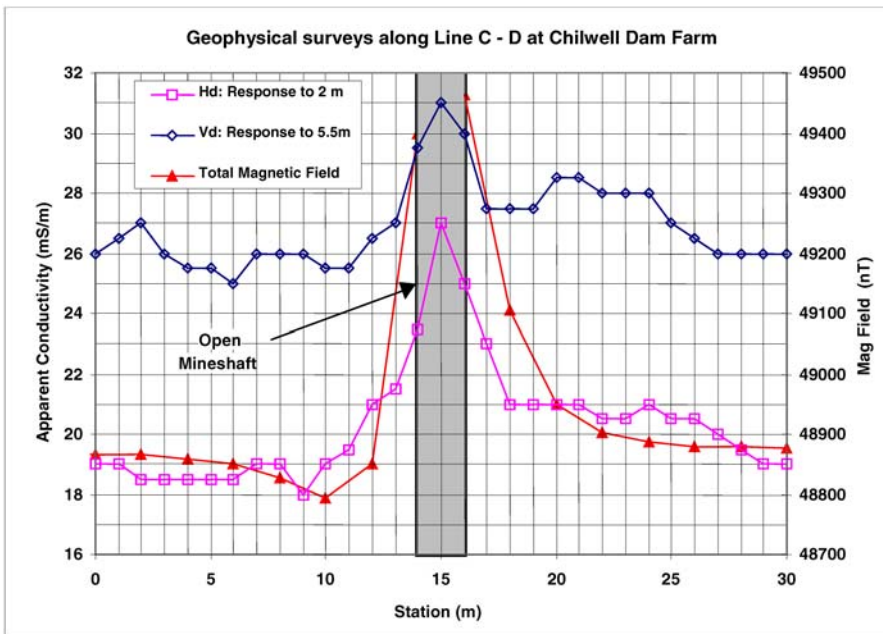


Fig. 3. Electromagnetic (EM31) and magnetic profiles over a bricklined mineshaft at Chilwell Dam Farm, Nottingham.

Figure 3 shows an electromagnetic (using a Geonics EM31 instrument) and a magnetic traverse over an open, abandoned coal mineshaft at Chilwell Dam Farm, west of Nottingham, England. The line is 30 m in length and the mineshaft is positioned at its centre. No coal spoiling was observed in the reddish-brown soil immediately surrounding the shaft. In the vertical dipole orientation, the EM 31 profile shows the averaged conductivity of the ground down to about 5.5m depth.

This profile has a peak of higher apparent conductivity (around 8% higher than the end line conductivity) that coincides with the centre of the shaft. In the horizontal dipole orientation, the EM 31 profile shows the averaged conductivity down to about 2 m depth. This has a peak of higher apparent conductivity (around 35% higher than the end line conductivity) that coincides with the centre of the shaft. The horizontal dipole survey is strongly affected by the presence of metal objects at the top of the mineshaft and has a similar signature to that caused by an extended conductor. Many of the metal objects had rusted over indicating the presence of ferrous materials. There is a very strong magnetic anomaly over the mineshaft, which indicates a sub-vertical magnetic dipole within the mineshaft. A near-vertical standing, iron scaffolding bar was observed in the shaft. It should be noted that kiln-baked brick wall structures within the ground can also produce geophysical anomalies of a similar character. However, because of the strength of this peak, it is suspected that the metal objects have a very significant influence on this magnetic anomaly.

3.4 Infrared Thermography

Airborne geophysical methods are widely used in regional surveys associated with hydrocarbon and mineral exploration. They currently have little application in engineering studies since their overall cost would be prohibitive in most cases. However, in a large engineering project, which involves a significant requirement for regional geological information, the use of airborne methods might well be both practical and economically viable.

Donnelly and McCann (2000) described the use of infrared thermography for the aerial surveying of development sites on which buried abandoned mineshafts were suspected. The method produces an image of temperature variations over the ground surface. As result of advances in the development of portable, high-sensitivity thermal imagers it is possible to assess a number of sites at economic cost by combining this equipment with the mobility of a helicopter to detect heat anomalies associated with the presence of a mineshaft. Ground investigations are essential to calibrate any temperature anomalies.

Culshaw *et al.* (2004) described the use of thermal imaging to locate mineshafts at a site just to the west of Nottingham, UK. 23 of 36 known mine shafts were identified and a further nine were obscured by vegetation. Only four shafts located on open ground did not produce an anomaly. The method should not be confused with infrared photography, which is used widely in surface vegetation studies.

4 Discussion

The key to locating buried mineshafts and adits is the carrying out of a comprehensive review of all available historical information on the mining activities carried out in the past on the site under investigation. This not only helps to determine the possible presence and approximate location of any mineshafts but also assists in the design of the most appropriate geophysical survey. For example, it is

often the case that much of the evidence relating to the presence of infilled mine-shafts has been buried by later building and construction activities that have covered the top of the mineshaft with a considerable thickness of made ground. In this situation the geophysical method proposed might lack the penetration required to resolve any anomalous ground conditions relating to the presence of the mine-shaft.

In general any site, on which it is proposed to carry out a reconnaissance geophysical survey does require that the survey area has been cleared of debris, such as old machinery, building rubble, etc., since it is extremely difficult to lay out the survey lines if the ground surface is not reasonable flat and unobstructed. The presence of any ferrous material can prevent the effective execution of a magnetic survey while an uneven ground surface can be a problem when setting up a micro-gravity station.

All the survey methods can be carried out in conjunction with a global positioning system (GPS) and this enables the data to be accurately plotted and contoured in map form. The geophysical map can be superimposed on the topographic map for the area or on the site plan showing field boundaries, buildings, tracks, and roads. This enables the geophysicist to identify the position of anomalous areas on the ground surface prior to further investigation with trenches or boreholes.

5 Conclusions

Mineshafts can be a particular problem for the development and regeneration of former mining areas. The abandoned shafts may have been partially or wholly backfilled, but not in an engineered manner, and subsequently, the site may have been covered over with artificial materials. The use of direct pitting or drilling to locate mineshafts that can be as little as a metre in diameter, is likely to be rather 'hit or miss' and, so, not usually cost effective.

Geophysical methods such as micro-gravity, magnetic, electromagnetic, ground probing radar and thermography, particularly when used in an appropriate combination, provide a quick and relatively cheap approach to identifying the possible presence of a shaft. However, it must be emphasised that the success of a geophysical survey is likely to be enhanced if a thorough desk study is carried out first. Not only might this identify potential shaft locations, but it will also ensure that the geophysical survey is designed as well as is possible.

New geophysical techniques are regularly being developed and these, coupled with vast increases in computer power are likely to increase the success of geophysical methods in locating mineshafts in the future.

Acknowledgements

The authors would like to express their gratitude to IMC Geophysics Ltd for the provision of some of the data and case studies mentioned in this paper. The paper is published with the permission of the Executive Director of the British Geological Survey (NERC).

References

- Bell, F. G. (ed.) (1975). *Site investigations in areas of mining subsidence*. London: Newnes Butterworths, 168p.
- Culshaw, M. G. and Waltham, A. C. (1987). Natural and artificial cavities as ground engineering hazards. *Quarterly Journal of Engineering Geology*, 20, 139-150.
- Culshaw, M. G., McCann, D. M., and Bell, F. G. (2004). Modern reconnaissance methods for geohazard detection and monitoring in site investigation. In: Proceedings of the A W Skempton Memorial Conference, London, March 2004. (In press).
- Donnelly, L. J. and McCann, D. M. (2000). The location of abandoned mine workings using thermal monitoring techniques. *Engineering Geology*, 57, 39-52.
- Donnelly, L. J., McCann, D. M., and Culshaw, M. G. (2003). Abandoned mineshafts and the problem of defining a reasonable 'search' distance for conveyancing purposes. In: Proceedings of the 10th International Conference on Structural Faults and Repair, Editor M. C. Forde, Commonwealth Institute, London, 1st to 3rd July 2003. CD ROM.
- Jackson, P. D., McCann, D. M. and Russell, D.L. (1987). Geophysical mapping during the planning of new roads: an aid to the detection of mine workings. In: Culshaw, M.G., Bell, F.G., Cripps, J.C. and O'Hara, M. (Eds), "Planning and Engineering Geology." Engineering Geology Special Publication, No.4, London: Geological Society. 447-452.
- McCann, D. M., Culshaw, M. G. and Fenning, P. J. (1995). Setting the standard for geophysical surveys in site investigation. In: McCann, D. M., Fenning, P. J., Reeves, G. M. and Eddleston. M. (eds.), "Modern Geophysics in Engineering Geology." Engineering Geology Special Publication No. 12, London: Geological Society. 3-34.
- McDowell, P. W., Barker, R. D., Butcher, A. P., Culshaw, M. G., Jackson, P. D., McCann, D. M., Skipp, B. O., Matthews, S. L. and Arthur, J. C. R. (2002). Geophysics in engineering investigations. Construction Industry Research and Information Association (CIRIA) Report C562 and Geological Society Engineering Geology Special Publication No. 19. CIRIA, London. 252p.
- Reynolds, J. M. (1997). *An introduction to applied and environmental geophysics*. Chichester: John Wiley and Sons, 796p.
- Telford, W. M., Geldhard, L. P., and Sheriff, R. E. (1990). *Applied Geophysics*. 860p. Cambridge: Cambridge University Press.

Geological-Technical and Geo-engineering Aspects of Dimensional Stone Underground Quarrying

Mauro Fornaro¹ and Enrico Lovera²

¹ Scienze della Terra Dept., Università degli Studi di Torino, 35, Via Valperga Caluso
10125 Torino, Italy

mauro.fornaro@unito.it

Tel: +39 011 670 7114, Fax: +39 011 670 7155

² Georisorse e Territorio Dept., Politecnico di Torino, 24, C.so Duca degli Abruzzi
10129 Torino, Italy

enrico.lovera@polito.it

Tel: +39 011 564 7652, Fax: +39 011 564 7699

Abstract. Underground exploitation of dimensional stones is not a novelty, being long since practised, as proved by a number of historical documents and by a certain number of ancient quarrying voids throughout the world. Anyway, so far, open cast quarrying has been the most adopted practice for the excavation of dimensional stones. One primary reason that led to this situation is of course connected to the lower production costs of an open cast exploitation compared to an underground one. This cheapness has been supported by geological and technical motives: on the one hand, the relative availability of surface deposits and, on the other, the development of technologies, which often can be used only outdoor. But, nowadays, general costs of quarrying activities should be re-evaluated because new, and often proper, restrictions have been strongly rising during recent years. As a consequence of both environmental and technical restrictions, pressure will more and more arise to reduce open cast quarrying and to promote underground exploitations. The trend is already well marked for weak rocks – for instance in the extractive basin of Carrara, where about one hundred quarries are active, 30 per cent is working underground, but also in Spain, Portugal and Greece the number of underground marble quarries is increasing – but not yet for hard rock quarrying, where only few quarries are working underground all around the world. One reason has to be found in cutting technologies traditionally used. In weak rocks, diamond wire saw and chain cutter are usable, with few adaptations, in underground spaces, while drilling and blasting, the traditional exploitation method for hard stone, is not easily usable in a confined space, where often only one free face is available. Many technicians and researchers agree that two technologies will probably open the door to underground quarrying in hard rocks: diamond wire and water jet. The first one is already available; the second should still be improved. The paper refers to some of the most important and significant examples in Italy, and underlines the possibility of extending, by underground quarrying, the exploitation of important and well-appreciated natural stones, as the quartzite-sandstone of the Tosco-Emiliano Appennini (“Firenzuola Stone”) and the Alpine gneisses. In order to pass from the simple experimental stage (explorative drift) to the more complex 3D design of the underground voids, detailed geo-structural reconstruction of the rock body and specific lithological *in situ* surveys are needed: such important aspects represent a very interesting common field between mining engineers and geologists.

Keywords: natural stone; dimension stone, underground exploitation; technical development.

1 General Aspects

Underground exploitation of dimensional stones (the term dimensional and ornamental stones are used as synonyms hereinafter) has very ancient origins: for example, it was carried out more than one thousand years B.C. in some Egyptian quarries; the statuary marble of the island of Paros, in Greece, was exploited underground; in the Roman age many underground quarries were opened in the Italian Karst limestones; etc. (Fornaro and Bosticco 1999). Probably, the technical impossibility for ancient quarrymen to remove thick overburdens recommended, in these situations, to “follow in the mountain” the rock portions with the best qualities. Today there could be many reasons for moving underground a stone exploitation, even in spite of the technical difficulty and the higher costs (at least at the beginning) that such option usually involves (Table 1). First of all, the structural condition of the rock body can make an open cast quarrying problematical, because of the high superficial fracturing or of the occurrence of non-exploitable cap rocks covering the workable portion: if the general condition of the rock mass are suitable, a selective exploitation allows to quarry mostly the soundest materials, with an higher overall blocks yield. Sometimes, an open cast quarry could present also problems related to the rational exploitation of the rock deposit, which is a valuable and limited natural resource. For instance, where free areas are few and authorized quarrying sites are strictly defined, open cast excavation could bring to unacceptable situations, from both a technical and safety point of view, with too deep pits and potentially instable walls. Besides, the elimination of the costs connected to the removal of cap rocks and the general reduction of materials to be disposed in dumps are certainly positive aspects, to which less impacts on the landscape and local environment should be added: actually, only adits and possible plants on the quarry yard are visible. Moreover, underground operations could be performed independently of the weather conditions, avoiding unproductive stops. Finally, the creation of wide stable voids can be an economically positive factor in forecast of possible reuses at the end of the exploitation. For example, waste rock can be properly relocated into the exhausted voids: such operation could help the long-term stability of the mining voids and represents a final mitigation of the visual impact of the debris dumps grown along the slopes or over the flat areas around the quarries. Anyway, the underground option has to consider different onerous aspects of the creation and control of the structures. Obviously, long term stability of the voids must be guaranteed, demanding for suitable rock mechanics studies and verifications, monitoring and intervention in course of works, which couldn't be committed only to the experience (or, sometimes, irresponsibility) of the workers. Higher costs in the early stages of the opening should be evaluated, considering also that a part of potentially exploitable material has to be leaved in pillars. Moreover, necessity of lighting and ventilation systems in the underground quarries must not be neglected, in addition to safety and health problems which could be amplified in confined spaces.

Table 1. Main pros and cons of an underground exploitation of dimensional stones.

Motives	Positive aspects	Negative aspects
<i>characteristics of the rock body</i>	<ul style="list-style-type: none"> - more selective exploitation - impracticability of an open cast exploitation 	<ul style="list-style-type: none"> - more accurate prospecting and geotechnical investigation; - difficult characterisation of the rock body - possible complication during the exploitation (presence of faults, ground water, etc...)
<i>technical and operational</i>	<ul style="list-style-type: none"> - no stability problems of high and steep slopes - possibility of working independently on weather conditions 	<ul style="list-style-type: none"> - detailed studies for the opening stages - stability analysis of rooms and pillars - need for technical direction with underground experiences
<i>economical</i>	<ul style="list-style-type: none"> - removal of overburden is avoided - less production of waste rock and - possibility of disposing them into the exhausted voids - reduction of costs for environmental rehabilitation - possible economical re-use of the voids - nearly unchanged value of surface soil 	<ul style="list-style-type: none"> - higher cost of the project - higher cost and less production in the early stages - bigger investments - costs of possible systematic works of consolidation (bolting, etc.)
<i>environmental</i>	<ul style="list-style-type: none"> - less visual impact - reduction of rock volumes to be disposed in dumps - possibility of quarrying even in protected areas 	<ul style="list-style-type: none"> - possible long term stability problems - possible interference with ground waters

As a consequence of both environmental and technical restrictions many pressures will be more and more brought to reduce open cast quarrying and to promote underground exploitations. But so far, underground quarrying has been positively adopted only for “soft rocks”, such as marbles, limestones and slates, while for “hard rocks” some technological improvements are still needed (Mancini et al. 2001). Around Europe different soft stones are underground quarried at present: pink marbles and brown limestones in Portugal (Alentejo), slates in UK, France and Italy, yellow limestones in Croatia and different lithotypes in Italy (Figure 1). Technologies adopted are always chain (or sometimes diamond belt) cutters and diamond wire saws. On the contrary, very few experimental underground quarries are opened in hard stones, adopting different technological solutions: for example, one granite quarry in Japan is developed using water-jet and diamond wire saws (Agus et al. 2000), one blue quartzite quarry in Brazil uses only diamond wire; one green quartzite quarry in Italy is experimenting diamond wire saws combined to dynamic splitting by blasting and one gneiss quarry in Switzerland uses only explosives.

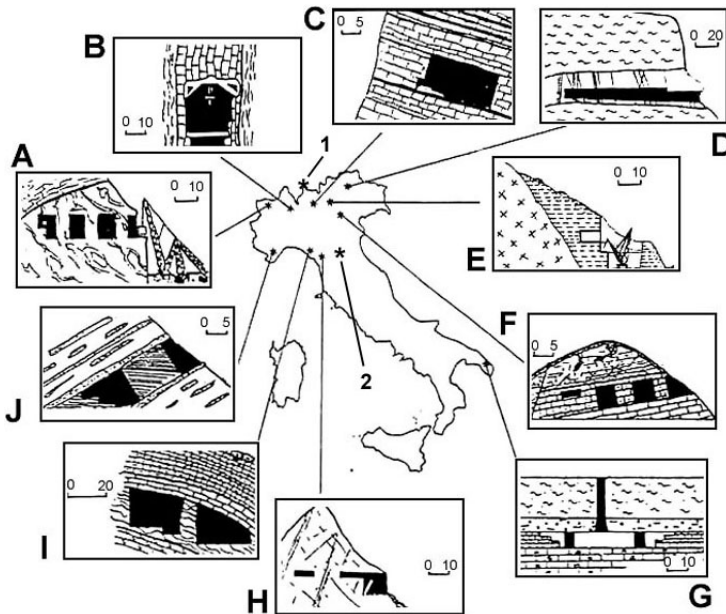


Fig. 1. Main Italian underground quarries for dimensional stones: A) Green ophicalcite of Aosta Valley; B) Cardoglia pink marble; C) Breccia Orobica; D) Lasa white marble; E) Conglomerate of Iseo Lake; F) Arenaceous limestone of Vicenza; G) Tuff limestone of Lecce; H) Carrara marble and Cardoso stone basins; I) Portoro black marble; J) Slate of Liguria. The localisation of the two case studies is indicated by the star: 1) Green Quartzite of Spluga Valley; 2) Pietra Serena of Firenzuola.

2 Technical and Technological Developments

Many aspects have a strong influence on the design and development of underground stone quarries: some of them are consequence of geological and geomechanical characteristics - the rock type, the structure of the rock mass, the topographic surface - others depend on production and economical issues - large size of the voids, limited artificial supports, etc. The definition of the geological and geotechnical set of the area where the quarry is supposed to work should be based on a series of investigations, which include: surface survey of the site, survey of the rock mass structure, measurement of absolute and relative stress conditions, geophysical surveys, test laboratories on cored samples. Of course, an accurate initial characterisation provides a better correspondence between the chosen design method and the actual working conditions; anyway investigations should not be performed only before the exploitation, to collect data project, but also in process, to verify the project and to control the evolution of the quarry and, if necessary, after the exploitation to monitor the general stability of the structures over time. The hypothesis about the underground structure have also to be confirmed by geotechnical coring and geophysical techniques: a planned series of coring (mini-

imum diameter 54 mm) is essential to get direct information, such as frequency and characteristics of discontinuities, description of lithotypes, etcetera. and to define different indexes (RQD, Is, L-Hammer) related to the mechanical properties of the rock matrix. These data supply the input for some empirical design methods based on rock mass classifications (Q-System, RMR). Anyway the laboratory analysis of specimen volumes can not supply a prediction of the *in situ* stress state acting within the rock mass; its measurement is important in the design stage to evaluate the stability condition of the excavation, and during the excavation to check the stress variation induced by the activity. If a rock wall is directly accessible the stress state can be assessed through load tests (flat pressure cells); otherwise suitable boreholes coring is used (cylindrical pressure cells, borehole deformation gauges, bi/triaxial strain cells, hydraulic fracturing): stress is always measured indirectly, derived from physical quantities (displacements, strains, etc.). Once the rock mass structure and rock matrix features are properly characterised, the static behaviour of the underground quarry can be investigated with different methods (analytical or numerical) based on different modelling approaches: discontinuous or equivalent continuous. The first approach fits well when the rock mass behaviour is ruled by the presence of discontinuities which identify elements whose volumes are not much smaller than excavation volumes; the latter is indicated with heavily jointed masses, where the strain-stress behaviour of the material could be described as continuous, assuming homogeneous characteristics of the discontinuities-rock matrix system. Analytical methods (e.g. tributary area, etc...) are mainly applied in case of regular geological and geometrical situations or to assess the stability of local rock elements, while if the interaction between underground geometries and complex rock mass structures is concerned the application of numerical methods is recommended. In particular, numerical codes based on Finite Elements Methods (FEM) or on Boundary Elements Methods (BEM) follow the continuous approach, whilst numerical codes based on discrete block models, such as Distinct Elements Methods (DEM), follow the discontinuous approach (Oggeri 2002). Different approaches can be adopted in the same case study: for example, BEM can be selected in a preliminary stage to assess the stress and strain evolution due to the excavation, in order to define a suitable monitoring scheme; then, after detailed rock mass surveys and geometrical modelling of fracturing set is obtained from an experimental panel, 3D DEM can be performed in order to validate the quarry exploitation layouts. It is evident that geotechnical measurements should be performed also during the excavation to validate the hypothesis formulated in the design stage (back analysis) and to control the behaviour of natural structures (stability and safety). Monitoring operations include the use of different devices - for surveying displacements, rotations, convergence (e.g. small or long-basis extensometers) strain and stresses (e.g. potentiometric and inductive transducers), loads and pressures (e.g. soft or hard inclusion pressure cells) - installed in appropriate section of the excavation, especially where the rock behaviour is more uncertain (high fractured areas, portals, pillars and walls). Some innovative monitoring methods, still at an experimental stage, have to be just mentioned: they include acoustic emission, time-domain and optical time-domain reflectometry, low-coherence interferometry, as well as radar (Ferrero and Iabichino 2003).

3 Case Studies

In the following lines two very recent case studies are described. The first one refers to a successful experimental exploitation in a hard and abrasive quartzite, located in the Northern Italy; the second one refers to a feasibility study for a challenging underground quarry in a layered silicate sandstone in the Central Italy.

3.1 Green Quartzite of Spluga Valley

The green quartzite commercially known as “Verde Spluga” is traditionally excavated in open cast quarries, located in Valchiavenna (Province of Sondrio - central part of Italian Alps) at a height of about one thousand and five hundreds meters above the sea level. The stone is a metamorphic green quartzite and the exploitable body is represented by a 30 m thick bank outcropping within a 80 m height vertical slope. The morphologic and structural situation did not allow a further surface activity and so an underground exploitation has been experimented (Figure 2). A blind drift was first driven, with a height of 6 m, a width of 5 m and a



Fig. 2. The thick rock cap above the exploitable bank where the underground experimentation has been driven.



Fig. 3. The complex “reverse catenary” arrangement adopted to make the first blind cuts with the diamond wire.

length of 5 m; then the excavation advanced with heading, lowering and widening of the first tunnel (Figure 3). Today a long room has been created in the mountain, with a width of 10-12 m, an height of 20 m and a length of 30 m.

The technique so far adopted involves the drilling of 4 holes (diameter 255 mm), at the edges of the rock volume to be extracted, using a down the hole hydro-pneumatic perforator: large diameter holes are necessary to hold the down-the-hole pulleys needed to realize blind cuts by diamond wire in “reverse catenary” arrangement. The diamond wire used is the standard one for granite, with 40 sintered beads per meter and rubber coating. Cutting speed is quite low (about 1 m²/h) because of the complex arrangement and the difficulty to keep the wire well refreshed by water during the cut. Being impossible to make the back cut with the wire, it’s necessary to extract a wedge of rock, splitting it by explosives: a sequence of aligned and spaced holes are drilled and charged by pentrite detonating cord. The productive phase follows the same steps: first, an upper wedge is cut and then the lower prism is split by explosive. Side cuts of the upper wedge are made by diamond wire, just drilling an inclined hole (diameter 90 mm), which intercepts the bigger horizontal hole. Because of the very narrow angle of the wedge, the wire presents a high wearing and so it’s preferred to keep a very low pull on the wire and a higher speed (about 30 m/s). The lower prism is cut just like in an open cast quarry: side cuts by diamond wire and back and horizontal cuts by dynamic splitting (Figure 4). Cutting speed by wire is about 2,5 m²/h with a service life of 10 m²/m. In such operation, wire tension pull is kept high, with a lower wire speed (about 22 m/s).

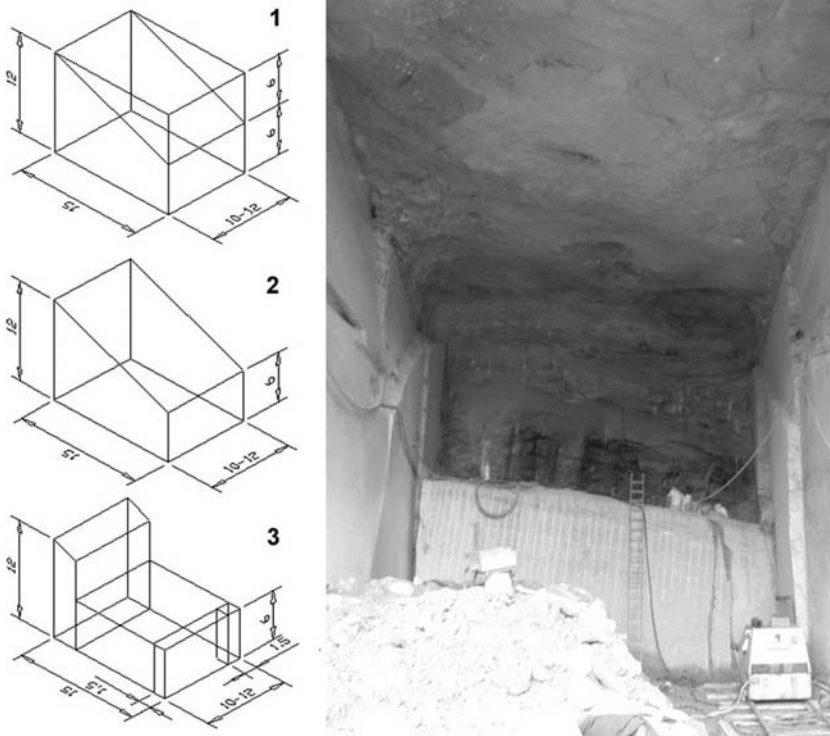


Fig. 4. Sketch of the different steps of the productive phase. On the right a picture of the present underground room; a diamond wire saw is making the side cut of the bench.

After the experimental stage, which proved to be quite promising for the production, the quarry will develop with a series of traverses following the dip of the bank, in order to create a second addit to the underground voids. So far, block yield is on average 50% but in the future productive lowering a 70% blocks recovery is expected. The competent Public Administration is supporting such experimental activity, with the aim of spreading the underground option in other suitable situations.

3.2 “Pietra Serena” of Firenzuola

The stone commercially called “Pietra Serena” is open cast quarried in the municipality of Firenzuola (Province of Florence, in the Tosco-Emiliano Appennines). It is excavated from beds of sandstones alternated with marl and siltstone deposits, in the “*Marnoso Arenacea*” formation (Casagli et al. 2002). The overall thickness of the exploitable body is about 60 m, but only 10-15% of the extracted material is usable, being about 5 m the maximum thickness of the sandstone beds (Figure 5).

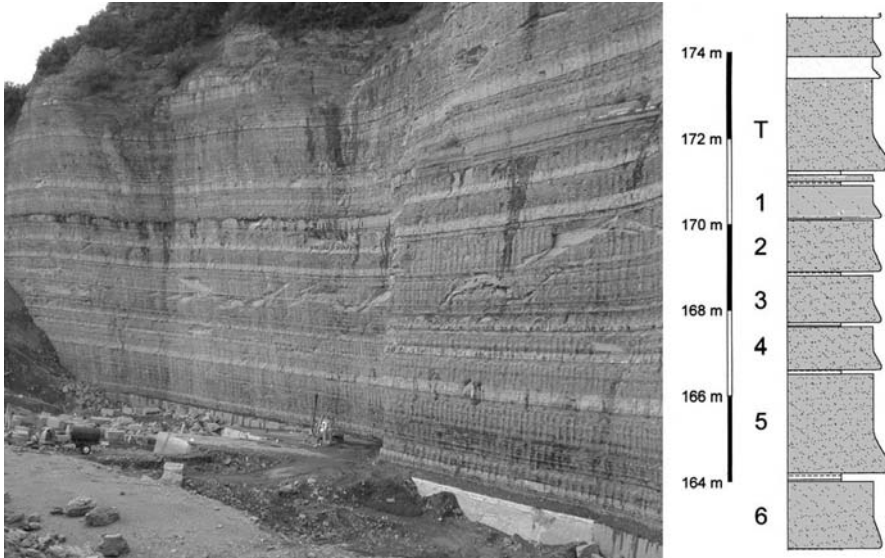


Fig. 5. A typical front of an open cast quarry of “Pietra Serena”. Exploitable beds of sandstones are alternated with marl, as illustrated in the stratigraphic sketch (I. Parenti) of the area investigated for the experimentation. Workable “filaretti” are progressively numbered; T indicates the possible roof of the underground room.

Underground exploitation can give the possibility of quarrying only the best sandstone layers, avoiding very expensive and environmental unfriendly preparation works, but the layered structure of the rock body represents an additional difficulty for the experimental quarry, whose feasibility project is in progress at present. First of all the technical feasibility has to be assessed, verifying the self stability of the thin layers (few decimetres – locally called “*filaretti*”) that will be leaved as roof of the void, and investigating the strength of pillars that will sustain the structure, given the alternate sequence of sandstones and plasticizable marls. So far the rock mass has been characterized and classified on the basis of *in situ* geological-structural surveys, while the characteristics of the different intact material are going to be measured in laboratory. But also the technological feasibility has to be demonstrated because of the abrasive quartzeous lithotype to be cut: the use of tunnel chain cutters for the blind cuts (both vertical and horizontal) and of diamond wire saws for the back cuts is planned, but service life and production performances of tools have to be verified (Figure 6). Last but not least, the economical feasibility, especially in the early stages, has to be proved, because the general productivity will be less than an open cast activity.

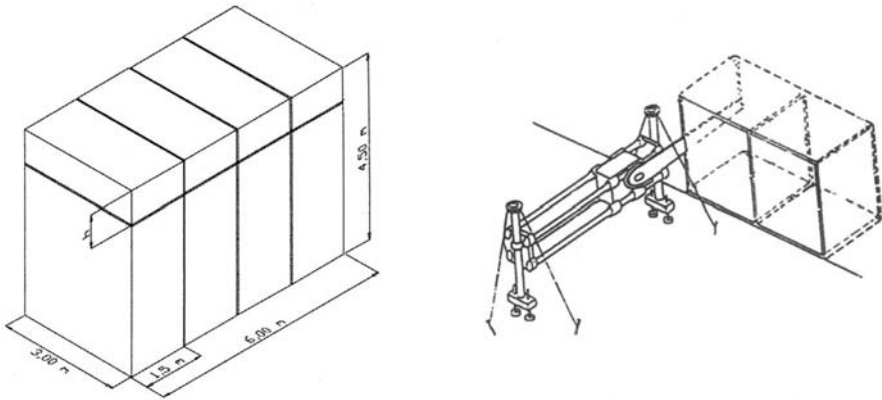


Fig. 6. Sketch of the underground exploitation scheme using a tunnel chain cutter.

4 Concluding Remarks

Environmental issues - and consequently administrative authorization possibilities - will more and more press towards underground quarrying activities. It is then essential that a scientific methodology, based on methodical observations and experimental controls, is established to investigate the physical phenomena involved in the opening and managing of a stone quarry. The target is the minimisation of the environmental impact and of the geological risk, maximising the production results at the lowest cost. In other terms, the cooperation of geological and engineering competences should not be occasional and connected to particularly difficult conditions, but have to become the rule for the sustainable future of this important activity.

Acknowledgments

Authors would like to thank dr. S. Guerra, dr. I. Parenti and ing. D. Valentino for their important contribution to the reported studies.

References

- Agus. M., Bortolussi A., Ciccu R., Cuccu W., Grosso B. (2000) L'estrazione in sotterraneo dei blocchi di granito con tecnologie avanzate. In: *Le cave di pietre ornamentali*, GEAM, Torino, pp. 185-192.
- Casagli N., Focardi P., Lombardi L. Parenti I. (2002) *Le cave di Pietra Serena nel Bacino di Brento Sanico*. In: Baldassarre G., Fornaro M. (eds) *Controllo ambientale delle attività di cava per lapidei ornamentali in importanti bacini estrattivi*. GEAM, Torino, pp. 31-42.

- Ferrero A.M., Iabichino G. (2003) Control and monitoring of stability conditions in dimension stone exploitation: methods and instruments. In: Terezopoulos N., Paspaliaris I (eds) Dimension stone quarrying in Europe and stability of quarrying operations. OSNET, Athens, pp. 61-159.
- Fornaro M., Bosticco L. (1999) La coltivazione in sotterraneo delle rocce ornamentali. Quaderno n. 22, GEAM, Torino.
- Mancini R., Cardu M., Fornaro M., Lovera E. (2001). Technological and Economic Evolution of Diamond Wire Use in Granite or Similar Stone Quarries. In: 17th Mining International Congress and Exhibition of Turkey, Ankara, pp.543-548.
- Oggeri C. (2002) Design methods and monitoring in ornamental stone underground quarrying. In: Baldassarre G., Fornaro M. (eds) Controllo ambientale delle attività di cava per lapidei ornamentali in importanti bacini estrattivi. GEAM, Torino, pp. 85-90.

Leibis/Lichte Dam in Germany

Markus Kühnel

Hydroprojekt Ingenieurgesellschaft, Dittelstedter Grenze 3, 99099 Erfurt, Germany
Kl@hydroprojekt.de
Tel: +49 36730 310 14
Fax: +49 36730 310 40

Abstract. In Thuringia the second highest dam of Germany is under construction (figure 1). The new Leibis/Lichte dam is a 370 m long and 102.5 m high gravity dam of concrete with straight axis. With the completion of the Leibis/Lichte dam in 2005 more than 300.000 inhabitants of the Eastern Regions of Thuringia will be supplied with high quality drinking water. The foundation rocks at the dam site are exclusively greyish-blue argillaceous schist, silt schist and cleaved fine sandstones from the Ordovician period (phycode schist). The main joint system consists of three differently orientated joints. Geomechanically of main interest is the shallow dipping bedding, especially in the left abutment because of its down-hill dip. The other joints show a generally steep dip. Wide extending faults with thick mylonites or fractured zones, which could influence the foundation of the dam, do not exist within the dam site. The engineering geological field mapping of the foundation surface confirms the rock mass parameters. The excavation works are carried out in four different stages to avoid loosening of the foundation rock. Great care is taken to assure that the foundation rock is protected against weathering. Based on the results of preliminary investigations the foundation level was planned in a depth of 4 to 14 m. The abutments of the dam correspond to the expectations. Predominantly the argillaceous rock shows a low permeability. The permeability is exclusively linked to faults respectively few large joints. In order to prevent seepage and to reduce the uplift pressure, a grout curtain in two rows is arranged with a depth of 5 to 44 metres.

Keywords: dam, bedding conditions, joint system, excavation, grout curtain.

1 General Data of the Dam

1.1 Purpose

With the completion of the Leibis/Lichte dam in 2005 more than 300.000 inhabitants of the eastern regions of Thuringia will be supplied with high quality drinking water. The stabilisation of drinking water supply as well as flood protection and power production with two small size turbines are the objective of the dam. The flood storage capacity is 5.6 million m³.

1.2 Technical Data

The Leibis/Lichte dam is a gravity dam of concrete with straight axis and a vertical upstream face. The downstream face has a slope of 1:0.78 (figure 2). The dam

has a volume of 620,000 m³, it is 102.5 m high with a crest length of 370 m. At the crest the dam is 9 m wide and its toe is 80.6 m wide. Construction joints divide the dam corpus into 35 fields with a normal width of 10 m (maximum 15 m). The reservoir has a gross storage capacity of 39.2 million m³. The dam has a crest spillway with downstream race and ski jump designed for a maximum discharge of 86.5 m³ s⁻¹. Three bottom outlets (diameter 1200 mm) are arranged for a planned discharge capacity of 35 m³ s⁻¹. The extraction of raw water from the reservoir is managed by five intakes staggered height wise. The raw water flows through a 10 km-long tunnel to a drinking water treatment plant. The main inspection gallery is located at a distance of 5.05 m from the upstream face (dam axis). Different measurement and monitoring devices (auto centering device sounders, extensometers, uplift pressure and seepage water measurements etc.) are provided within the gallery. Furthermore the drilling and grouting works will be executed from the gallery. With the completion of the Leibis/Lichte dam in the year 2005 the test impoundment will start and last two years minimum.



Fig. 1. Aerial view of the dam site.

2 Geological Site Investigation

The dam site was investigated in different phases in the 1970th and 1980th. Complementary geological investigations were executed in the years 1992-1995. Four investigation tunnels with a total length of 230.5 m containing chambers for in situ shearing and compression testing were excavated by drilling and blasting. Three

shafts (33.6m) were sunk and the raw water tunnel (326 m) was driven. The sub-soil of the dam was investigated through exploratory drilling with more than 5.600 drilling meters. Within several of the boreholes special tests such as water pressure tests and trial injections with different orientated directions to the main joint system were performed. An extensive geotechnical investigation program was executed with the drill cores to determine the decisive rock parameters. At the end of the investigation program in 1994/95 an exploratory pit was excavated at the left abutment, where the most difficult geotechnical situation according to the preceding results was expected. The exploratory pit had an area of 5.270 m² and was up to 12 m deep. The pit confirmed the geological model and gave precise information about location, thickness and outcrop length of faults. For the design of the foundation of the dam important information was obtained.

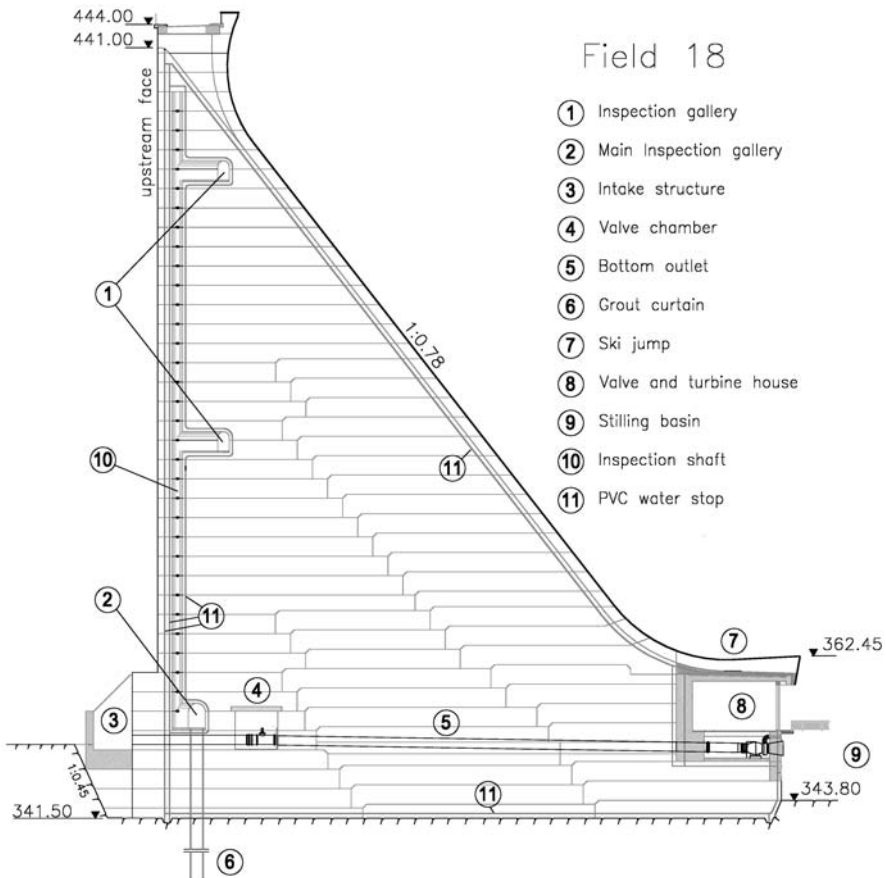


Fig. 2. Cross section.

3 Geological Situation of the Dam Site

The dam site is situated with respect to the local geology on the SE flank of a saddle, the so called Schwarzbürger saddle, which is the northwestern structural element of the East-Thuringia Slate Mountains. The subsoil of the reservoir is covered by Ordovician terrigene, clastic sediments (mud-, silt- and sandstones), which sedimentated 400 mio years ago within a relative shallow border sea. During the Variscan orogenesis these sediments were folded, cleaved, jointed and disintegrated into mosaic-like blocks. The foundation rocks at the dam site are exclusively greyish-blue argillaceous schist up to an explored depth of 80 metres. The rock in place shows low-grade epimetamorphic superimposed clayish siltstones, silty mudstones and fine sandstones, which have a dense cleavage due to the orogenetic pressure.

3.1 Bedding Conditions

The foundation area of the dam is divided into the following three homogeneous zones – left abutment, valley bottom and right abutment. The bedding represents the most important fabric element for the division into homogeneous zones. Due to the regional-geological location of the dam site on the SE-flank of a saddle, the bedding shows generally a gentle dip in E to NE-direction. The left abutment shows the most difficult conditions for the foundation of the dam because of the downhill dipping of the bedding. Within the zones valley bottom and right abutment the bedding has an uphill dipping. The cleavage and the Q-joints have generally a steep dip (angles higher than 70°) and are therefore geomechanically less important. The comparison of the joint orientation used for the design with the in situ data shows a good agreement (table 1).

Table 1. Joint orientation of the zone valley bottom, dam fields 17 to 21.

Joints	Construction	Design
Bedding ss	065/13°	038/18°
Cleavage sf	306/78°	305/80°
Q-joints (Q ₁)	213/75°	215/75°
Q-joints (Q ₂)	-	036/64°
Transverse faults	194/77°	215/75°
Longitudinal faults	325/79°	305/80°

3.2 Joint System

The joint system of the subsoil is characterized by three main joints – bedding, cleavage and Q-joints. A large amount of the bedding planes has no geomechanical significance. But in a greater distance (approximatly every 2 m) these bedding planes have a low shear and tensile strength and therefore detach from the rock

mass. These detachment planes can extend some metres (surface areas of 100 m²), especially on the left abutment those continuous bedding planes are visible. The bedding is from medium- to thick-layered and has a ripply and rough surface. The ripples are as high as 5 cm. Frequently a clayish-silty filling can be found on the bedding planes, which is caused by illuviation from the overlapping soil. The mapping of the foundation rock shows that the ripples are normally higher than the fillings. The cleavage is the most significant fabric element. It has a dip from steep to very steep (70° to 85°) in NW-direction. The cleavage planes have a slight undulation and even surface with partial haematitic films. Clayish-silty fillings are very rare. The cleavage planes appear in a distance of some centimetres, major detachment planes exist in a distance of 1 to 2 metres. The Q-joints run perpendicular to the other joints. They have mainly a steep dip in SW-direction (Q₁-joints), rarely in NE-direction (Q₂-joints). The Q-joint surfaces are as well undulating, benched and rough as plane and smooth. Haematitic films can be found very often. The joint fillings consist of clayish-silty material with fine detritus, sometimes small quartz dikes as thick as 20 cm can be found.

3.3 Faults

Wide extending faults with thick mylonites or fractured zones, which influence the foundation of the dam, do not exist within the dam site. The tectonic system is characterized by hercynian trended (NW-SE) disturbances, which dominate within the foundation area. Longitudinal disturbances, which run sub-parallel to the cleavage, do exist subordinated. The disturbances are largely thin-schistous zones of 10 to 50 cm, the boundary is frequently filled with mylonites of some millimetres thickness. A special filling of the disturbances are some centimetres thick brecciated quartz dikes, which exist very often with a typical red-violet (iron-bearing) breccia. The genesis of the breccia is possibly connected with the emplacement of a near-by andesite. It is remarkable that the fillings do never exist all over the entire length of the longitudinal and transverse disturbances, but show repeatedly dislocations.

4 Geomechanical Parameters

The strength and deformation behaviour of the rock in place is determined by the different planes of the joint system. The total shearing strength of the joint planes is composed of the shear resistance both of the rock and the separated joint [Egger and Reik 1996]. The characteristic parameters for the design are listed in table 2 and 3. Within planes that are not running parallel to the main joint system, the strength parameters of the jointed rock mass have to be used.

Table 2. Characteristic strength parameters of the joints.

	Bedding	Cleavage	Q-joints	Faults
Friction angle [°]	30.2	30.9	28.5	25.0
Cohesion [kPa]	33	400	400	0
Tensile strength [kPa]	8.5	100	100	0
Degree of separation	0.9	0.6	0.6	1.0

Table 3. Strength parameters of the rock mass.

	Peak shear strength	Residual shear strength
Friction angle [°]	30	30
Cohesion [kPa]	780	195
Tensile strength [kPa]	100	0
Uniaxial compressive strength [kPa]	2700	675

5 Excavation of the Pit

The excavation works are carried out in four different stages to avoid loosening of the foundation rock. Great care is taken to assure that the foundation rock is protected against weathering. The four stages are described as follows:

- Stage 1: Excavation of loose rock mass (average thickness 1.5 m).
- Stage 2: Excavation of hard rock up to 1 m above planned foundation level with pre-split and loosening blasting. Rock slope stabilization works with rock bolts, shotcrete and nets.
- Stage 3: Final excavation by hydraulic excavator equipped with transverse cutting head.
- Stage 4: Cleaning of the foundation level with a mixture of water and compressed air just before casting. Removing of all loose rocks.

The final excavation (Stage 3 and 4) takes place maximum four weeks before casting to protect the foundation against weathering.

6 Foundation Depth

Concerning the foundation depth it is specified, that the dam is founded at least two metres in sound rock. The definition of the top of the sound rock was determined by the number of joints per bore hole meter. Essential knowledge for the determination of the foundation depth was also given by the examination of the foundation level of the exploratory pit (1994/95) on the left abutment. Seismic refraction investigations and dilatometer tests on the other hand gave no useful results for the determination of the foundation depth. The foundation of the dam is executed in depths from 4 to 18 m.

7 Grout Curtain

The purpose of the grout curtain is to seal the subsoil of the dam site and to reduce the uplift pressure. The injection works are carried out from the main inspection gallery (height 3.4 m, width 2.2 m). During the geological site investigation the permeability of the ground and the injection behaviour were determined on the basis of many water pressure and injection tests. The design of the grout curtain was arranged on the basis of these data. The grout holes are arranged in two rows with borehole spacing of 2.5 m and a row distance of 1.6 m. The injection depth ranges between 5 m (right abutment) and 44 m (left abutment) dependent on the natural permeability of the ground. The length of the grout sections is generally 3 m, the grouting pressure of 1 to 3 MPa depends on the rate of take of grout material. The grout mix consists of a cement suspension with the following parameters:

- w/c ratio : 0.8 to 2.0
- bentonite percentage distribution: 2-3 % of the cement weight
- viscosity (Marsh-funnel): 35 to 40 seconds
- sedimentation: maximum 5 % per hour
- Blaine value of cement: $\geq 4.000 \text{ cm}^2 \text{ g}^{-1}$
- Maximum grain size of cement: $\leq 100 \mu\text{m}$

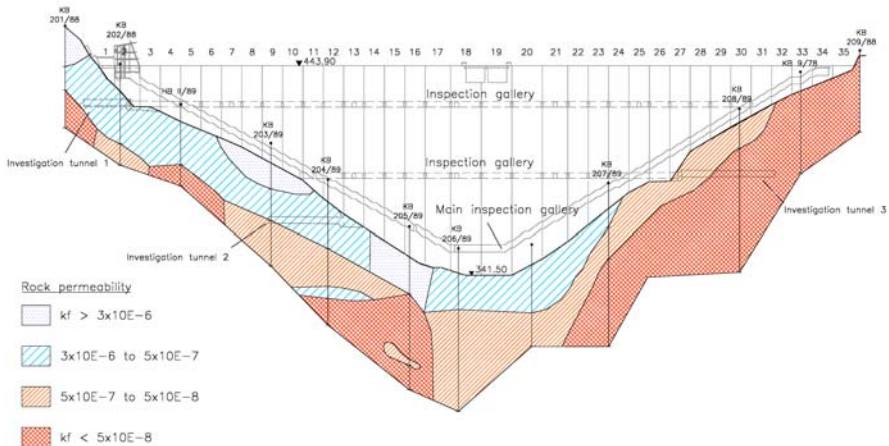


Fig. 3. Rock permeability in m s^{-1} .

The subsoil of the dam site exposes demanding conditions for grouting. Predominantly the argillaceous rock shows a low permeability. Wide areas of the subsoil consist of nearly impermeable rock, and it is expected that these areas will have no grout take. The water conductivity is exclusively linked to fault respectively few large joints. The left abutment shows the highest permeability because of the downhill dip of the bedding planes. An overview of the permeability of the dam site shows figure 3. The aim is to reduce the permeability at least to $5 \times 10^{-7} \text{ m s}^{-1}$.

Especially in the right abutment it is expected, that the injection works will not lead to a substantial reduction of the water permeability. Therefore, it is necessary to reduce the uplift pressure with drainage bore holes. The drainage holes are arranged on the downstream side of the main inspection gallery. They are inclined with 20° to the downstream side and put down 5 m deep below foundation level. The number of drainage holes and the bore hole spacing will be defined on the basis of the water pressure testing results. As experience shows it is necessary to sink drainage holes every 1.5 to 3.0 metres.

References

Egger P and Reik G (1996) Talsperre Leibis/Lichte – Abschließendes Gründungsgutachten (not published).

Creep Behaviour of Alpine Salt Rock and the Influence of Insoluble Residues in Solution Mining

Gerhard Pittino and Johann Golser

Department of Geomechanics, Tunnelling and Heavy Construction Engineering
University of Leoben, Parkstrasse 27, A-8700 Leoben, Austria
{pittino, geomech}@unileoben.ac.at
Tel: +43 3842 402 3401
Fax: +43 3842 402 3402

Abstract. In Austrian salt mining, brine is won by way of solution mining with the borehole well method. The Alpine salt rock (Haselgebirge) consists of a high share of insolubles, and therefore leached caverns are filled with clay residues, as so-called Laist, a natural backfill, according to the salt content. The creep deformations of the Haselgebirge mainly correspond with a rupture-free flow and are calculated by means of an elasto-viscous model (power-law). These deformations mobilize the passive fill-pressure in clay residue that is described as elastoplastic with isotropic hardening by means of a modified Cam-clay model. The long-term laboratory tests are supported through calculations of the creep parameter via measured convergences of drifts at various depths. The long-term behaviour of the caverns is evaluated based on numerical calculations by the volume convergence and the degree of utilization of pillar.

1 Introduction

The Alpine salt rock (Haselgebirge) is composed of mixed rock similar to a conglomerate formed of salt, clay and anhydrite, thus the leached caverns are filled with clay residue (Laist), a natural backfill, according to the salt content. The development of leaching techniques in Austrian solution mining enables caverns with a 100 m diameter and a height of several hundred metres (Gaisbauer 2000). Therefore with the endeavour to increase the amount of brine that can be deployed per solid and cropped-out deposit volume, a geomechanical perspective of the cavern system involving the clay residue was necessary. Salt mining is performed by the borehole well method through the leaching of thin slices. After the sinking of the production bore, cementation of the standpipe, installation of the well head, tubing of the borehole with an outer and inner pipe, running of water and brine conduits and after installation of measuring and regulating devices, the production process can be assumed. In the developing stage a fast cavity formation is targeted in the width, during the central stage the cavern is supposed to develop cylindrically upward and in the ultimate stage the final cavern roof is created (see

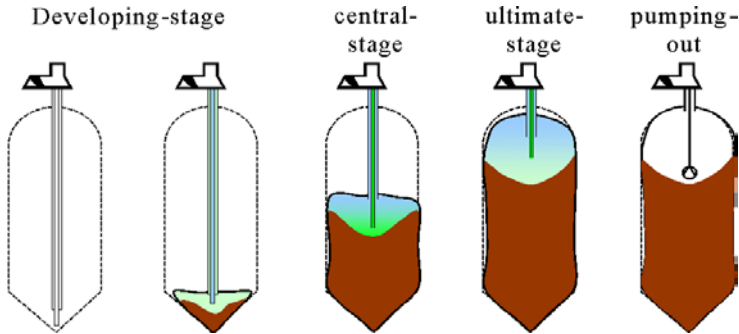


Fig. 1.1. History of borehole well.

fig. 1.1). Insertion of leaching liquid into the borehole is prevented through an inhibiting medium (blanket). Through the optimal combination of water insertion, specification of a measure for cauterisation (Ätz-maßvorgabe) and blanket, the leaching process can be regulated horizontally, as well as vertically.

2 Constitutive Laws and Material Parameters

The constitutive model and respectively its correct choice, determines the description of the material behaviour. The necessary material parameters must be definable by laboratory tests or in situ tests or at least estimable with monitored measurements according to project requirements.

2.1 Salt Rock – Laboratory Tests

The leaching process of a cavern is very slow, only by 2 cm vertically per day and causes stress redistributions. Due to the creep behaviour of salt rock the deviator stresses decrease and in addition the volume convergence increases and mobilizes the passive fill-pressure in the clay residue. The creep deformations observed in salt rock correspond particularly with a deformation free of fraction. Thus, long-term tests are evaluated based on an elasto-viscous power law describing the secondary creep process.

$$\dot{\epsilon}_s = A \cdot \bar{\sigma}^n = 0.27 \cdot \bar{\sigma}^{1.14} \quad (\mu\text{mm}^{-1}\text{h}^{-1}) \quad (2.1)$$

In figure 2.1 steady state creep-rates that were assessed through tests (Pittino and Golser 1997) are described as a function of Mises's equivalent stress $\bar{\sigma}$ applying power law and furthermore, are compared to exponential law.

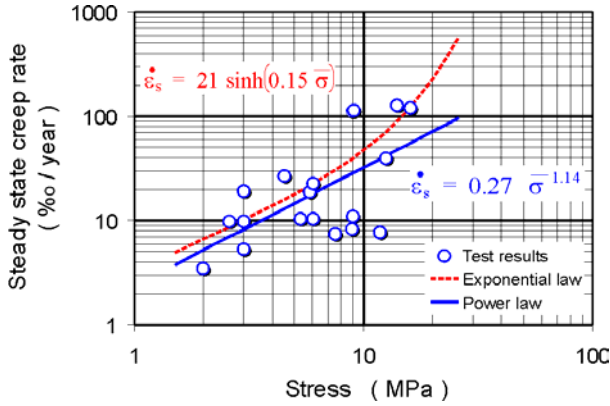


Fig. 2.1. Comparison of steady state creep-rates for Haselgebirge – power and exponential law.

2.2 Salt Rock – Creep Properties, Calculated from Measured Convergences

Relatively few long-term investigations concerning the four salt rock types, the five salt “stone” types, as well as in respect to the general salt concentration of the Haselgebirge exist and thus were supported through calculations of the creep parameter via measured convergences of drifts of various depths (see fig. 2.2).

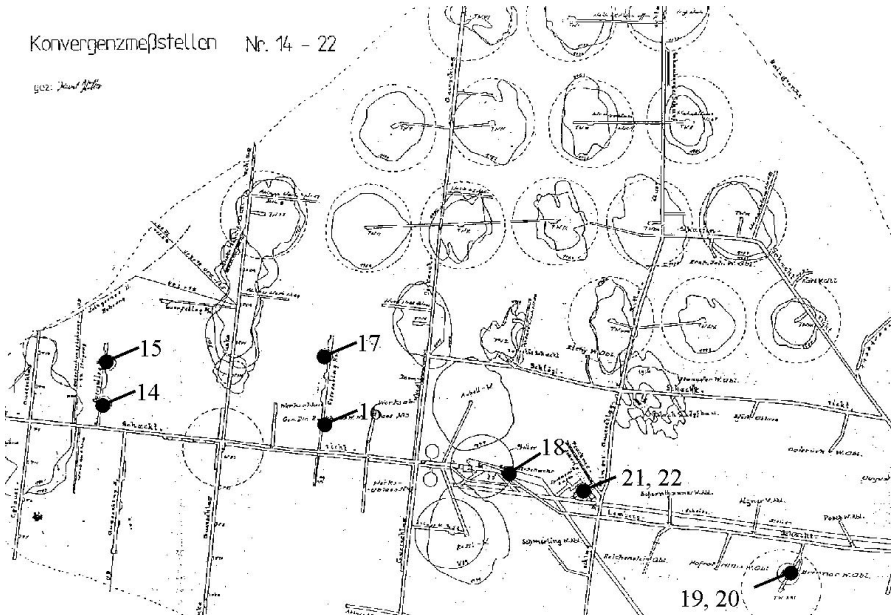


Fig. 2.2. Mine layout with convergence-monitoring points.

Numerical calculations with the Finite Difference code FLAC 3.4 (Itasca 1999) and the elasto-viscous constitutive model “power law“ (equation 2.1) demonstrate how the stress-dependent creep behaviour can be determined by monitoring convergence of different drifts in various depths (Pittino 2002). According to Dreyer (1974) depth pressure has an effect on the volume-convergence rate based on power law.

In the example depicted in figure 2.3, the creep parameters A and the stress exponent n are pre-assigned. The cavern is excavated in one step, subsequently the secondary stress state is calculated, as well as the vertical and horizontal convergence for the duration of 10 years respectively for a depth of 250, 350 and 450 m. The convergence rates result, outlined double logarithmic as a function of the depth, into the stress exponent $n = 2.5$, which is the pre-assigned creep parameter in the calculation, as the slope of the best-fit line. According to this method a stress exponent of $n = 1.2$ could be obtained for the cavern system Altaussee. This however, only with the inaccuracy of stress states in regions of measuring cross-section that are dependent upon the constellation of the cavern system to a large extent. The stress exponent of rock salt is in comparison at 5.

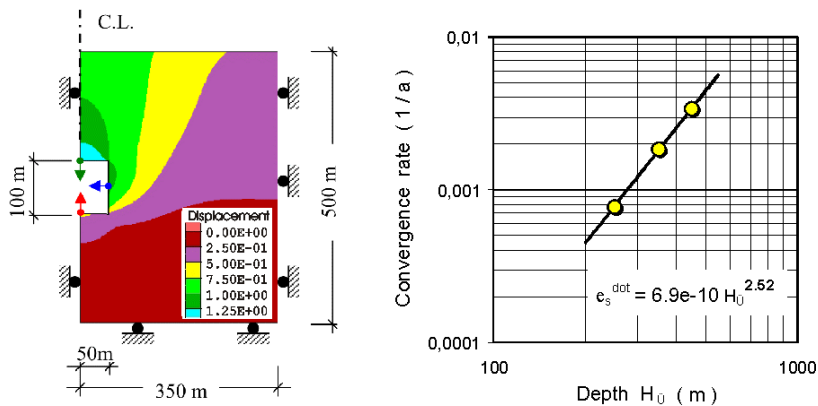


Fig. 2.3. a) Model geometry and displacement contours; b) Stress dependent creep rate.

2.3 Clay Residue – Laist

The method of Laist-sampling was performed with a telescopic core drilling with a single tube core barrel, from 180 to 101 mm, without drilling fluid 55 m in the Laist of a cavern with a drilling performance of approx. 2.5 metres per day. Distributed across the borehole dilatometer tests were carried out. The core analysis was supplemented by the pocket penetrometer and vane shear test (see fig. 2.4). Table 2.1 illustrates the results of field test.

The material behaviour of cohesive soil generally depends on the content of pore fluid. Determining of water content via a drying oven, however, only yields

small values due to the crystallization of salt during the drying phase and thus becoming part of the dry mass. Therefore, the soil's physical properties were determined in consideration of the brine content in the Laist (see table 2.2).



Fig. 2.4. Vane shear test and pocket penetrometer.

Table 2.1. Results of the field tests in MPa for Laist.

Pocket-penetrometer	Uniaxial compressive strength	$\sigma_{FD} - \text{radial}$	0.24
		$\sigma_{FD} - \text{axial}$	0.33
Vane shear test	Undrained shear strength	τ_{FS}	0.05
Dilatometer test	Deformation modulus	G	3.7
	Un-/reloading modulus	G_{UR}	37

Table 2.2. Soil physical properties of Laist concerning brine content ($w = m_{\text{brine}} / m_d$).

Drying Oven	Brine content	w	32.7 ± 5.7	%
Capillary pycnometer	Density of brine	ρ	1.2	g/cm^3
	Density of solids	ρ_s	2.87 ± 0.05	g/cm^3
Underwater weighing	Bulk density	ρ	2.08	g/cm^3
	Dry density	ρ_d	1.57	g/cm^3
	Degree of Saturation	S_r	94	%
	Porosity	n	45	%
Consistency	Void ratio	e	0.83	1
	Liquid limit	w_{LL}	47	%
	Plastic limit	w_{PL}	32	%
	Plasticity index	I_p	15	%
	Consistency index	I_C	0.93	1

The objective of the geotechnical tests was to determine the material behaviour of Laist and to describe it through parameter-based Mohr-Coulomb and modified Cam-clay constitutive models. The results are illustrated in table 2.3 according to the denominations in figure 2.5. In the yield function $F = q^2 + M^2 \cdot p(p - p_c) = 0$

Table 2.3. Soil mechanical parameters of Laist.

Friction angle	ϕ'	$27 \pm 5^\circ$
Cohesion	c'	0.051 ± 0.043 MPa
Loading:	E_s	$18 \sigma'$ MPa
Unloading:	E_s	$176 \sigma'^{1.33}$ MPa
Consolidation coefficient:	C_v	$1.75e-7$ m ² /s
Hydraulic conductivity:	k	$2.2e-9 \sigma'^{-1.5}$ cm/s
Void ratio for:		
Initial state	$e_{a,m}$	0.91
$\sigma'_v = 600$ kPa	$e_{0.6,m}$	0.70
NCL at $p = 1$ kPa	$e_{\lambda}^{1\text{kPa}}$	1.183
CSL at $p = 1$ kPa	$e_{\Gamma}^{1\text{kPa}}$	1.136
CSL at $p = 1$ lb/in ²	$e_{\Gamma}^{1\text{lb/in}^2}$	0.980
Compression index	$C_{c,m}$	0.186
Slope of NCL	λ_m	0.081
Swelling index	$C_{s,m}$	0.030
Slope of elastic swelling line	$\kappa_{,m}$	0.013

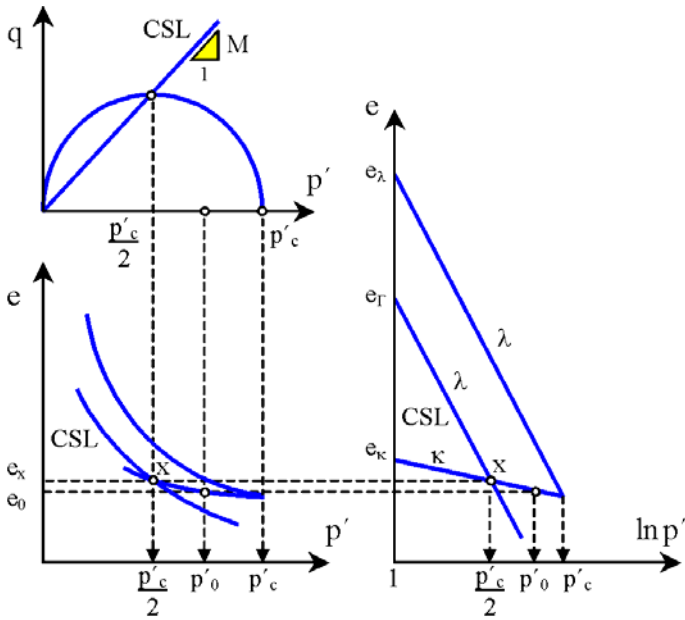


Fig. 2.5. Modified Cam-clay failure criterion. Normal consolidation line (NCL), swelling (slope κ) and critical state line (CSL); according to Budhu (2000).

of the modified Cam-clay, Model M is the stress ratio q/p for the critical state, thus corresponding with the CSL (critical state line) and p_c being the preconsolidation pressure. This material model describes against the volumetric plastic strain for normally and slightly over-consolidated soil, an isotropic strain hardening and for highly over-consolidated soil a softening occurring from the maximum shear strain. Table 2.4 shows Laist in comparison to known soil types.

Table 2.4. Laist compared with known soil types.

Parameter	Laist	Klein Belt Ton	Wiener Tegel V	London Clay	Weald Clay	Kaolin
λ	0.081	0.356	0.122	0.161	0.093	0.26
$\Gamma^{-1} \text{ lb/in}^2$	1.980	3.990	2.130	2.448	1.880	3.265
ν for $p = 100 \text{ lb/in}^2$ $= 0.69 \text{ MPa}$	1.607	2.350	1.558	1.700	1.480	2.065
M	1.07	0.845	1.01	0.888	0.95	1.02
ϕ ($^\circ$)	27	21.75	25.75	22.5	24.25	26
κ_m	0.013	0.184	0.026	0.062	0.035	0.05
$\Lambda = 1 - \kappa/\lambda$	0.778	0.483	0.788	0.614	0.628	0.807
w_L	0.47	1.27	0.47	0.78	0.43	0.74
ν_L	-	4.520	2.300	3.144	2.180	2.930
w_p	0.32	0.36	0.22	0.26	0.18	0.42
ν_p	-	2.00	1.607	1.715	1.495	2.108
l_p	0.15	0.91	0.25	0.52	0.25	0.32
$\Delta\nu_p$	-	2.52	0.693	1.429	0.685	0.822
ρ_s	2.87	2.77	2.76	2.75	2.75	2.61
Source	PITTINO	HVORSLEV		PARRY		LOUDON

3 Numerical Analysis of Volume Convergences

The influence of cavern-fill-pressure on the long-term behaviour of the cavern system was evaluated using numerical calculations, whereby the creep behaviour of the salt rock was described by the elasto-viscous power law and the clay residue by the modified Cam-clay model. 60% salt content and a corresponding swell factor lead to a cavern that is filled with up to 65% Laist.

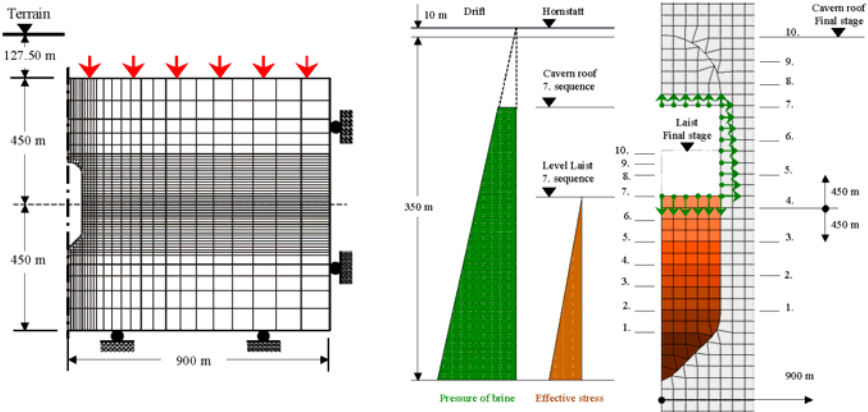


Fig. 3.1. a) Model geometry; b) load assumption and time-dependent leaching model.

3.1 Single Cavern

The leaching process of a cavern containing 2 million m³ lasts for a duration of 2 cm per day in its vertical leaching rate at around 40 years and is **time-dependent** simulated through 10 leaching sequences. The content of the cavern is modelled through Laist as a modified Cam-clay and brine with a unit weight of 12 kN/m³. The brine level is at 10 m above the final cavern roof at the pertaining drift (see fig. 3.1). Due to the low convergence rate of the cavern as compared to the permeability of Laist and the slowly increasing Laist level (0.12 kPa/d) a steady-state brine-pressure distribution is assumed. Thus, a coupled hydro-mechanical analysis can be disregarded. Effective stresses and brine pressure are taken into consideration by the utilization of FLAC-configurations such as “config groundwater” and “flow off”. For every Cam-clay-element the preconsolidation pressure and the total stresses are initiated through the FISH-Routine. In the time-independent leaching simulation, Laist is modelled according to the description above, with the variation that the termination of the production process is equated to the beginning of the creep time, which means that the designed cavern is “leached” in an elastoplastic analysis.

Figure 3.2 illustrates the volume convergence by time-dependent and time-independent leaching using the creep parameter $A = 6.75 \cdot 10^{-13} \text{ (Pa}^{-1.2} \cdot \text{year}^{-1})$ and $n = 1.16$, and furthermore the time-dependent modelling of leaching is not necessary. Therefore, further analysis will be performed by means of time-independent leaching.

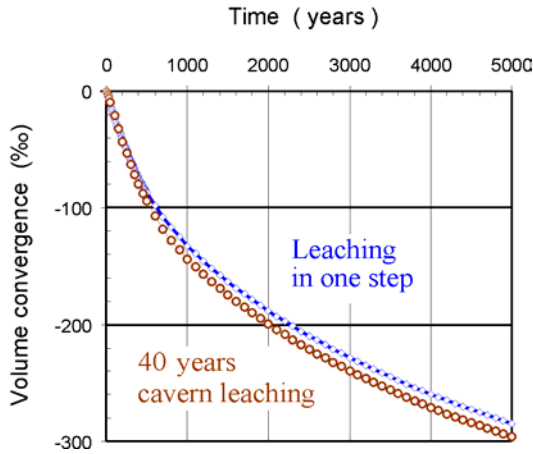


Fig. 3.2. Volume convergence by time-dependent and time-independent leaching.

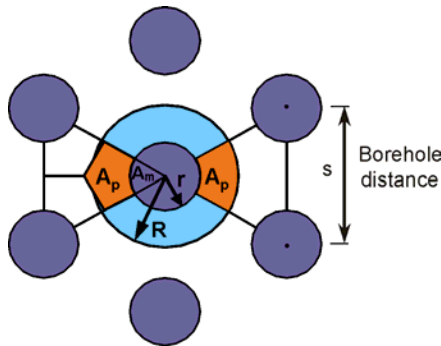


Fig. 3.3. Hexagonal cavern system with “tributary area” = $6(A_p + A_m)$.

3.2 Hexagonal Cavern-Layout

The mining layout is supposed to help in utilizing the limited salt deposit economically and safely. Through a hexagonal cavern constellation mining claims are evenly loaded. In the case of a concurrent leaching of all caverns the limits of tributary areas represent planes of symmetry. Thus, the 3D-problem can be approached axisymmetric, in the form of a vertically loaded, hollow cylinder (see fig. 3.3). On the outer radius, transverse strain is prevented, with the inner one corresponding to the cavern radius r . Through the tributary area of a cavern for a borehole distance of $s = 4r$ the outer radius is calculated at $R = 0.525s$ and the

percentage of the remaining area at 0.773. The numerical analysis exhibits the same distribution concerning volume convergence as a single cavern.

The Laist is mobilized corresponding to the fill-pressure through the creep behaviour and the resulting lateral deformation of the pillar. The average degree of utilization (see equation 3.1) of pillar, weighted according to the axisymmetric through the volume, is calculated for the 200 m high hollow cylinder (λ_{200}) and for the unsupported 60 m high pillar range (λ_{60}).

$$\lambda = \frac{\sigma_1 - \sigma_3}{2 \cdot \sigma_3 \cdot \sin \varphi - 2 \cdot c \cdot \cos \varphi} \cdot (1 - \sin \varphi) \tag{3.1}$$

where λ = degree of utilization; φ = friction angle; c = cohesion; σ_1 and σ_3 = principal stresses. λ decreases from 45% in the secondary stress state e.g. after 1 year to approx. 40% (see fig. 3.4).

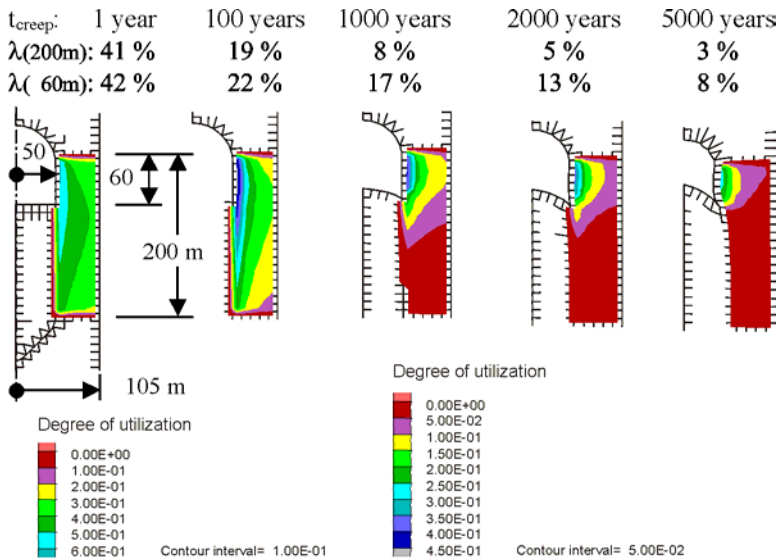


Fig. 3.4. Degree of utilization λ of pillar.

4 Conclusions

Along with the development of leaching techniques in Austrian salt mining that enables caverns with a 100 m diameter and a height of several hundred metres, a geomechanical perspective of the cavern system involving the clay residue was necessary. The research programme for assessing relevant parameters in respect to

short, as well as long-term behaviour was presented for the Haselgebirge and for the Laist. Part of it was the results of the field tests performed with help of a dilatometer, penetrometer, as well as a vane shear test and soil mechanical laboratory analyses. Soil physical parameters were determined with the inclusion of brine contained in Laist. The creep deformations of the Haselgebirge mainly correspondent to a rupture-free flow throughout centuries were calculated by means of an elasto-viscous power law, solely characterizing steady-state creep behaviour. These deformations mobilize the passive fill-pressure in Laist that was described as elastoplastic with isotropic hardening by means of a modified Cam-clay model. It was demonstrated that the creep behaviour of a material, which can be described via the Norton power law, could additionally be obtained from the convergence rates of drifts in different depths. The choice of the material model considerably influences the quality, respectively, the reliability of statements of numerical calculations besides the efforts to determine the true measured quantity. Time-dependent calculations over long periods must be verified by long-term monitoring, respectively, through long-term measurements.

References

- Budhu M (2000) *Soil Mechanics & Foundations*. John Wiley & Sons, New York.
- Cristescu ND (1998) *Time Effects in Rock Mechanics*. John Wiley & Sons, Chichester.
- Dreyer W (1974) *Gebirgsmechanik im Salz*. Ferdinand Enke Verlag, Stuttgart.
- Gaisbauer E (2000) Experiences with blanket level measurement in solution mining caverns of Saline Austria. 8th World Salt Symp The Hague, The Netherlands.
- Itasca (1999) *FLAC – Fast Lagrangian Analysis of Continua, Manual Version 3.4*. Itasca Consulting Group Inc, USA.
- Pittino G (2002) *Tragverhalten des Gesamtsystems Alpines Salzgebirge – Grubengebäude – Laugungsrückstand*. Doctoral Thesis, University of Leoben.
- Pittino G, Golser J (1997) *Gebirgsmechanisches Dimensionierungsmodell – Projekt Laist*. Institut für Geomechanik, Tunnelbau und Konstruktiven Tiefbau, unpublished .
- Schofield A, Wroth P (1968) *Critical State Soil Mechanics*. Mc Graw Hill, London.

Assessment of Rock Slope Stability in Limestone Quarries in the Tournai's Region (Belgium) Using Structural Data

Jean-Pierre Tshibangu, K. Pierre-Alexandre Deloge, Benoît Deschamps, and Christophe Coudyzer

Mining Engineering Department
Faculté Polytechnique de Mons (FPMs)
Rue du Joncquois 53
B-7000 Mons, Belgium
{jean-pierre.tshibangu,benoit.deschamps,
christophe.coudyzer}@fpms.ac.be
Tel: + 32 65 37 45 18 or 19
Fax: + 32 65 37 45 20

Abstract. The Tournai's region is characterised by famous outcrops of carboniferous limestone which is mined out for cement and raw material production. The four main quarries found in the Region, i.e. Gaurain-Ramecroix, Milieu, Antoing and Lemay; are owned by the three main cement producers in Belgium: Italcementi, Holcim and CBR. The global production of limestone is about 20 millions tons per year, giving big pits with depths up to 150 m. With the growth of the pits, the quarries are approaching each other leading to the problem of managing the reserves contained in the separating walls and their mechanical stability. The limestone deposit is composed of different seams having varying thickness, chemical composition and even mechanical properties. The deposit has an overall horizontal dip and is intersected by two main sets of discontinuities with a spacing of about 10 m or less. It is also crossed by a set of east to west faults but the quarries are implanted in the in between areas, so to not be crossed by these faults. The layers and specially the shallow ones are characterised by a typical karstic weathering giving open or filled cavities. This paper presents the global work quarried out in order to study the stability of the Lemay's quarry. First a description of the orientation and spacing of discontinuities is presented, and an attempt made to correlate to the development of weathering. Mechanical laboratory tests have been performed and a qualification of the rock mass assessed. A coupled approach is then presented using a mining planning analysis and mechanical simulation (i.e. Finite Element method).

Keywords: Rock mass quality, mining planning, Numerical modelling, Quarry.

1 Presentation of the Site

Figure 1 presents, in the actual situation, the wall separating two pits with on the northern side the Milieu's quarry with a steep cut, and on South the Lemay's one. This last quarry is interested in recovering a maximum reserves in the wall.

The Tournai's limestone outcrop belongs to the Carboniferous formations of the northern border of Namur's Synclinorium (Belgium). This is a strip lying from

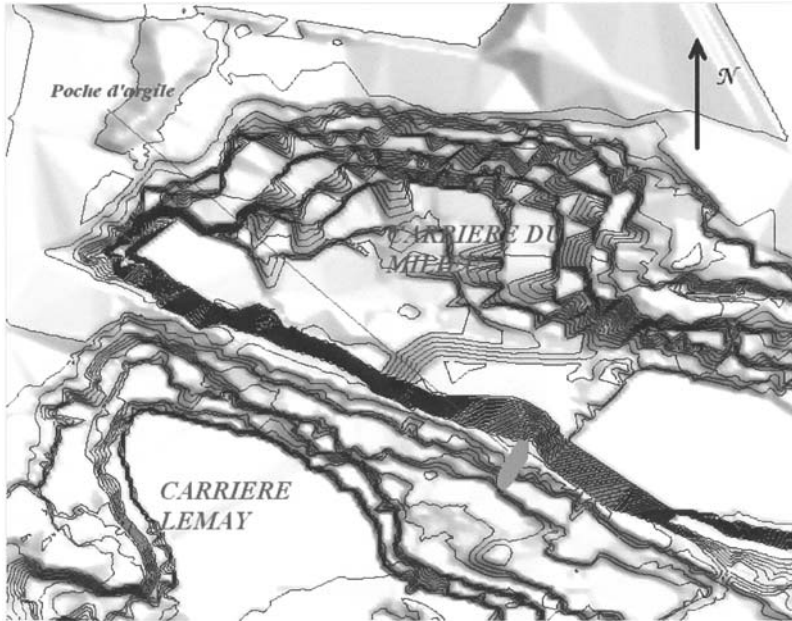


Fig. 1.1. Overview of the Region under study.

eastern Namur to western Lille in France. In the Western part of this synclinorium the structure is characterised by the Roubaix's synclinal followed by the Mélan-tois-tournais anticline in which the quarries of the tournasian basin have been opened. The outcrop is characterised by argillaceous limestones which sometimes contain hard silica nodules. When looking the deposit from the top to the bottom of limestone materials, the identified seams are:

- The Calonne unit with a thickness of 50 m. The upper part is composed of a fine grained limestone with clay and silica content. The part beneath is similar to the precedent but is richer in silica nodules (cherts). The bottom of this formation is characterised by the so called "Gras Délit" which is a typical thin clay layer.
- The Vaulx and Chercq unit (32-35 m): at the top one find also a fine grained silica-argillaceous limestone containing rows of silica nodules known as "carboniaux".
- The Pont-à-Rieu unit (21-22 m) : it is a grained limestone with high content in CaCO_3 .
- The Providence unit (35 m) : composed of fine grained silica-argillaceous limestone. Black cherts are present in most of the contained seams.
- The Allain unit (30 m) : composed of stratified silico-argillaceous limestones in which the seams are separated by thin layer of calcareous shales.
- The Crampon unit (12 m) : succession of small layers of silico-argillaceous limestones (about 10 cm thickness) with numerous calcareous shale joints.

- The limestone is generally covered by sandy and clayey sand formations. The top of the limestone is generally horizontal but is affected by karstic phenomena.

The Lemay's quarry is actually mined in four benches of varying heights depending on the thickness of the mined layers, and the deepest mined seam actually is the Pont-à-Rieu, but the Company intend to mine down to the bottom of the Crampon's formation.

On the tectonic point of view, the Mélantois-tournaisis anticline is crossed by numerous faults parallel to its axis; this is a typical horst structure named "Tournaisis Horst". These faults subdivide the deposit into many compartments oriented according the East-West or NW – SE directions. The faults do not cross the Lemay's quarry, this gives a uniform dipping of limestone layers all over the mined area, but the deposit is crossed by a net of joints. On the hydro-geological point of view the limestones contain an important water reserve because of the macro-permeability, and the water table draw-down ranges from 60 to 100 m in the area of quarries.

2 Fractures Surveying

In the Tournai's basin, the limestone rock masses are intersected by two families of mechanical joints to which can be added the stratification. The three sets of discontinuities cut rock masses into prismatic blocks with sizes as low as some decimetres depending on the local weathering. Measurements have been carried out along the studied wall leading to typical results shown in tables 2.1 and 2.2. Depending on the area, the mean joint spacing along the wall ranges from 0.32 m to about 2 m.

Table 2.1. General description of a profile along the wall on the Lemay's side.

<i>Interval</i>			<i>Characterisation</i>
Start (m)	End(m)	Width (m)	
0	28.7	28.7	Massive rock. metric fracturing
28.7	78.7	50	Black clay pocket +weathered rocks
78.7	83.5	4.8	Massive rock. metric fracturing
83.5	84.3	0.8	Light clay pocket
84.3	93.6	9.3	Massive rock. metric fracturing
93.6	107.2	13.6	Clay pocket
107.2	125.7	18.5	Very disturbed rock mass
125.7	146.5	20.8	Massive rock. metric fracturing
146.5	193.5	47	Very disturbed rock mass
193.5	211.3	17.8	Light clay pocket
211.3	223.1	11.8	Massive rock. metric fracturing
223.1	228.1	5	Light clay pocket
228.1	233.6	5.5	Disturbed mass. infra-metric fracturing
233.6	240.3	6.7	Clay pocket

Table 2.2. Typical dip measurements (Positions have been measured by a GPS device).

<i>Position (X-Y)</i>	<i>Measures</i>	<i>Observations</i>
(142215.85095)	N008E 85E N130E	Western part of the clay pocket. perpendicular to the wall
Idem	N120E 85E	Western part of the clay pocket. weathered surface
Idem	N008E 85E	Western part of the clay pocket. measurement of another direction
(142250.85000)	N135E 75E N040E 85E N180E 90	East of the main lay pocket
(142240.84980)	N135E 70E	Eastern weathered zone. dip of the wall
(142180.85100)	N140E N130E	On the second bench. directions of two lines showing weathering

The rock mass shows two main sets of discontinuities with a dipping close to vertical:

- The first family (S1) with metric spacing has a strike close to North-South;
- The second one (S2) with higher spacing (usually more than 10 m) is oriented N120°E to N135°E. Some conjugate joints oriented N50°E have also been observed.

This net is crossed by a horizontal stratification as a third family (S3). Figure 2.1 is a polar diagram of the measurements. The directions of fracturing are correlated to the development of the weathering, giving oriented filled caves. A big black clay pocket of about 50 m wide has been identified on the first bench of the quarry. The filling material is the residue of an equal-volumetric weathering of limestone, because this contains tracks of typical limestone fossils. This material is named as “ghost rock” by geologists (Quinif et al. 1997).

3 Geo-technical Qualification

Based on the density of fracturing, the deposit has been subdivided into two geo-technical zones: the first one corresponding to the first bench of the Lemay's quarry, and the second, to the remaining limestone layers (named as “massive fractured rock”). Uniaxial and triaxial compression tests have been performed on samples collected on each bench, results are presented in tables 3.1 and 3.2.

Some quality indexes of the rock mass have also been assessed (Tshibangu et al. 2003b), these are RQD (Rock Quality Designation from Don Deere), RMR (Rock Mass Rating from Bieniawski) and GSI (Geological Strength Index from Hoek and Brown). The RQD has been calculated using a virtual horizontal well corresponding to the description of table 2.1, while table 2.2 and the spacing measurements led to the assessment of RMR and GSI. Table 3.3 summarises the results together with the estimated mechanical properties on the basis of Bieniawski and Hoek & Brown formulas (Hoek and Brown, 1997).

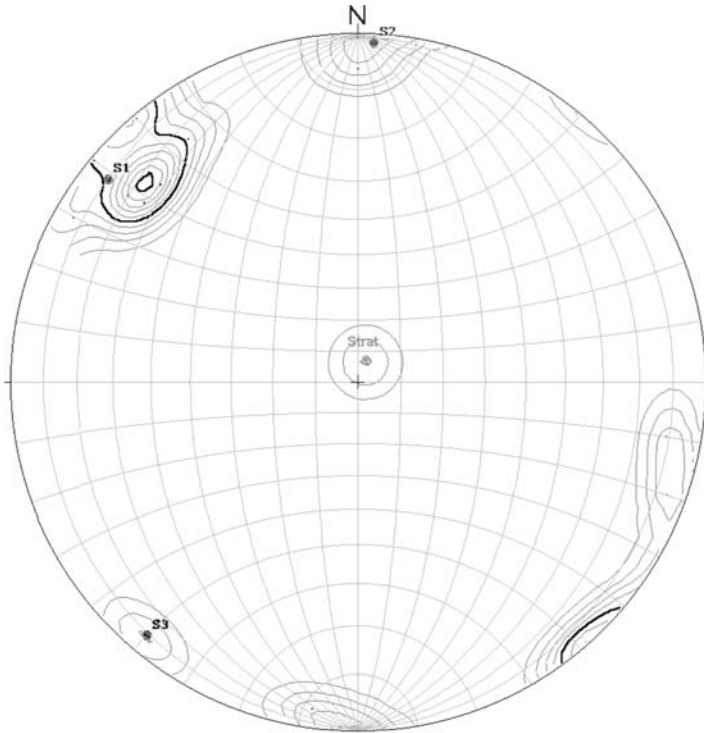


Fig. 2.1. Polar stereonet showing the directions of fracturing in the Lemay's quarry.

Table 3.1. Mean results of uniaxial compression and traction tests.

<i>Sample Nr.</i>	<i>UCS (MPa)</i>	<i>Tensile strength (MPa)</i>	<i>Young's Modulus (MPa)</i>	<i>Poisson's ratio ν</i>
1	99.1	8.5	47780	0.31
2	112.4	7.2	12389	0.305
3	116.3	10.2	21941	0.41
4	74.0	6.5	14260	0.415

Table 3.2. Mean results of triaxial tests(σ_1 is the value of the major principal stress at failure).

σ_3 (MPa)	Sample 1	Sample 2	Sample 3	Sample 4
	σ_1 (MPa)	σ_1 (MPa)	σ_1 (MPa)	σ_1 (MPa)
5	171.4		157.3	250
10	198.6	228.8	176.8	258.1
15	208.8		201.6	264.1
0	260.1	300.2		280.2
25	239.9		284.3	354.8

Table 3.3. Quality indexes and mechanical properties of the rock masses.

PARAMETER	MASSIVE ROCK			FIRST BENCH
	Samp. 2	Samp. 3	Samp. 4	
Rock mass quality :				
RQD		95		63
RMR		93		63
GSI		70		35
Parameters of the Hoek & Brown criterion :				
σ_{ci} (MPa)	100	99.3	108.85	84
m_i	26.8	7.45	30.97	22.4
m_b	9.193	1.493	10.609	2.197
S	0.036	0.006	0.036	0.0007
A	0.5	0.5	0.5	0.5
Deformability (GPa) :				
Hoek & Brown relationship		31.6		3.2
Bieniawski relationship		86		26
Serafim et Pereira relationship		20.7		13.2
Parameters of the Mohr-Coulomb criterion :				
Uniax. comp. strength σ_{cm} (MPa)	38	25.7	43.6	12.7
Friction angle φ (°)	45	33.1	46.9	34.4
Cohesion C (MPa)	7.8	6.7	8.6	3.3
Tensile strength σ_{tm} (MPa)	-0.38	-1.38	-0.37	-0.03

4 Mining Planning

Figure 4.1 shows the actual configuration of the Lemay's quarry with the closed polygonal line symbolising the wall under study. One can see that on the northern side of this wall, the slope is steep and the deposit has been mined down to the -115 m level, while on the southern part, there is a considerable amount of limestone to be recovered. To reach this goal, a mining project has been carried out to meet the following criterions (Tshibangu et al. 2003a, 2003b): (1) Recover a maximum rock down to the bottom of the Crampon's layer (-115 m below sea level), (2) Keep an access ramp down to the lowest bench, (3) Keep a separating wall between the two quarries to hold the backfilling planned on the northern side, (4) Have a junction between the eastern and western sides of the Lemay's quarry. Different scenarios have been computed with the top of the wall quoted at +30 m or -60m, allowing the estimation of the amount of the rock to be retrieved in the pit. Figure 4.2 is one of the calculated situations showing the pit in the final stage with the bottom plane at -115 m. Such computations enable an estimation of the removed rock between an initial state corresponding to the actual topography, and a final stage giving the depleted pit. An access ramp has been placed along the wall to give a good stability because of a lower pit angle.

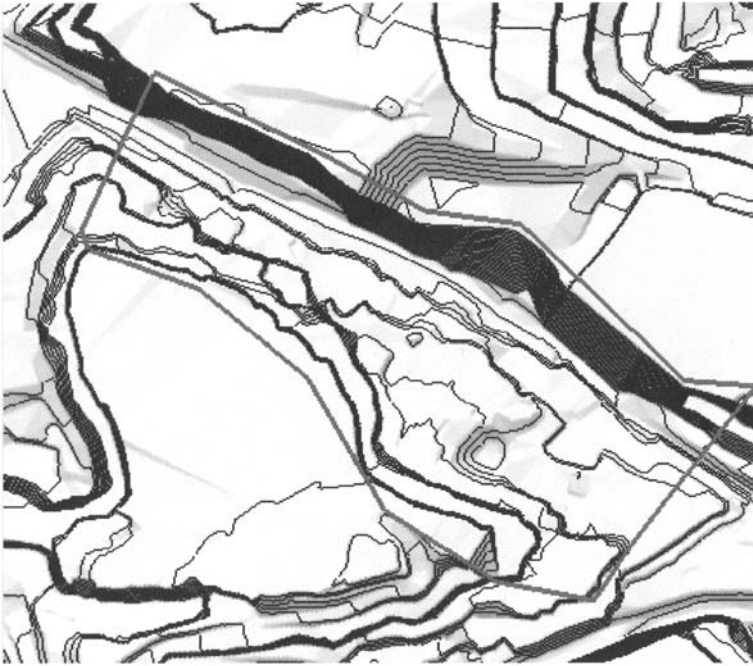


Fig. 4.1. Actual situation of the Lemay's quarry.



Fig. 4.2. Lemay's pit as computed in the final stage of mining.

5 Mechanical Analysis

Building such a mining project is a trial and error process during which different combinations of mining parameters (slope height and angle of the benches, width of horizontal platforms) will be used in conjunction with mechanical parameters of the rock mass. These analysis have been carried out simultaneously. The stability analysis has been conducted using 2D finite element method (plan strain) with either Hoek and Brown or Mohr-Coulomb elasto-plastic materials. The mining excavation has been studied as a sequential process starting by a flat ground, than using the following steps: (1) mining the Milieu's quarry down to about -100 m, (2) mining the Lemay's quarry down to the actual situation, (3) deepening the Lemay's pit down to -115 m as planned, with the ground surface at $+30$ m, (4) mining the separating wall to fix the top at -60 m as an alternative to the precedent scenario. During the analysis, different variables have been studied: horizontal and vertical stresses, deformed shape, and plastic function. Dealing with possible failure, we focussed especially on horizontal stresses σ_x and plastic function. The first of these two parameters was important because of the near-vertical dip of the joints and the possible subsequent toppling failure. Figures 5.1a and 5.1b present some results in terms of horizontal stresses in the two possible final stages of the pit. With top of the wall at $+32$ m (tall wall), region in tensile state is more pronounced on the Lemay's side and this is due specially to the steep angles used for the benches. When fixing the top of the wall at -60 m, one can observe a balanced behaviour on the two sides. This shows that the second case is preferable, but, to avoid any risk of failure, the slope angles in this final stage can be chosen to be lower depending on the state of fracturing when mining the three deepest benches.

6 Conclusion

This study started with a field job to point out the main joints families and take measurements. In a second stage, rock samples have been collected to perform laboratory mechanical tests and, following this stage, quality indexes have been assessed based on the spacing measurements along the wall of the pit, this led to a correction of the mechanical properties using some classical relationships. With the so defined mechanical parameters, a mining study has been performed simultaneously with finite element modelling to assess the geometry of the future pit in its final stage. The combination of different tools and methods showed how the complex problems of the slope analysis in mining projects can be approached by a simultaneous use of modelling tools. This method is intended to solve the problem of the overall understanding of mining projects in which people working in project design and those working in geo-mechanics need have a close collaboration.

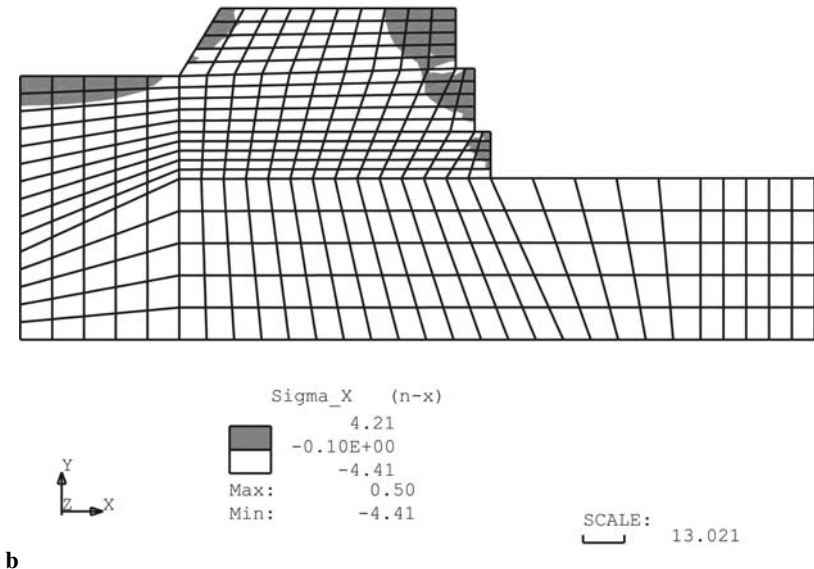
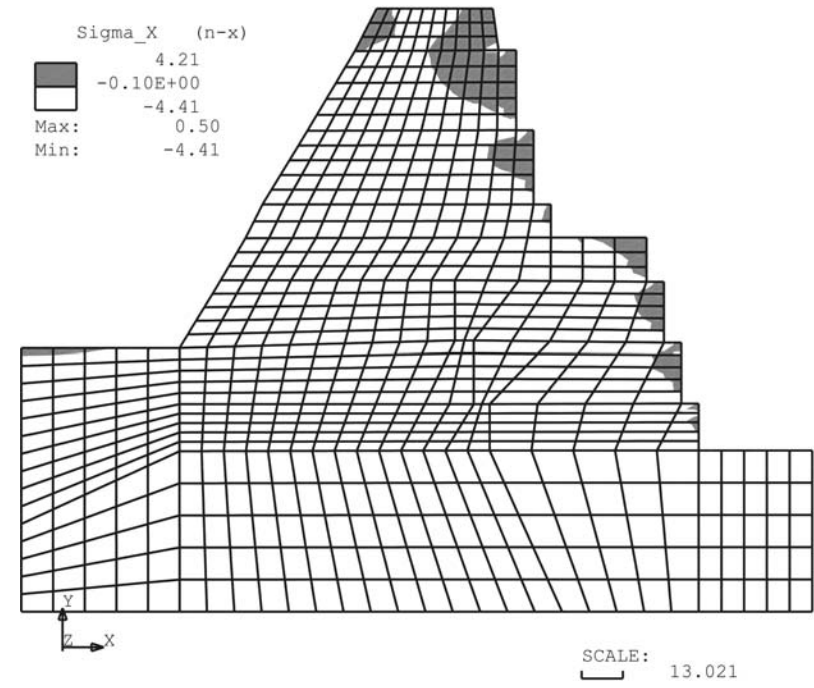


Fig. 5. a: Excavation of Lemay's pit down to -115 m; b: Scraping of the wall down to -60 m.

Acknowledgement

The authors would like to thank the Lmay's quarry Managers for allowing and supporting the study.

References

- Hoek E & Brown ET (1997) Practical Estimates of Rock Mass Strength. *Int. J. Rock Mech. Min. Sci.* Vol 34, No 8, pp 1165-1186.
- Quinif Y, Vandycke S & Vergari A (1997) Chronologie et causalité entre tectonique et karstification - l'exemple des paléokarsts crétacés du Hainaut (Belgique). *Bull.Soc.Géol.Fr.*, 168, 4, pp 463-472.
- Tshibangu KJP, Deschamps B, Herbinaux Q & Legrain H (2003a) Utilisation des techniques modernes de conception, planification et suivi des exploitations. *Revue les Techniques de l'Industrie Minérale*, No 19, pp 18 – 23, 105-107.
- Tshibangu KJP, Deloge PA, Deschamps B (2003b) Conception de l'exploitation et étude de stabilité à la Carrière Lemay s.a. Internal report FPMs-GM.

Studying Underground Motions in the Ramioul's Cave – Belgium

Jean-Pierre Tshibangu¹, Michel Van Ruymbeke², Sara Vandycke³,
Yves Quinif³, and Thierry Camelbeek²

¹ Mining Engineering Department, Faculte Polytechnique,
53 rue du Joncquois, B-7000 Mons, Belgium
jean-pierre.tshibangu@fpms.ac.be
Tel: + 32 65 37 45 18 or 19

Fax: + 32 65 37 45 20

² Royal Observatory of Belgium

³ Fundamental and Applied Geology Department, Faculte Polytechnique de Mons, Belgium

Abstract. The show-cave of Ramioul is situated close to Engis in Belgium in Dinantian. Beside the natural cavities, a quarry is being mined out and the tourist guides observed some ground motions since more than 6 to 7 years. In order to understand the motion of the geological Ardennes's base in Belgium a research team has been built including geologists, rock mechanics engineer, and physicists from Mons Faculty and the Royal Observatory of Belgium. This team funded by the FNRS (Fonds National de la Recherche Scientifique) chose to study the Ramioul cave to assess the direction of motion and try to correlate with either tectonic stresses or quarrying operations. A structural description of the rock mass containing the cavity has been achieved using typical software to model the topography and orientations of discontinuities. Some rock samples have then been collected for performing laboratory tests i.e. uniaxial and triaxial compression tests. A numerical model has been built to understand the kinematics of the rock mass depending on the sequence of quarry digging. Some displacement transducers as well as a seismic station have also been installed in the cave and data have been registered for more than two years. During the period covered by the measurements, a mechanical slope failure of toppling type occurred, and this has been registered by the transducers. The interpretation of the results showed the important role played by the quarrying operations.

Keywords: Cave, Rock mass quality, Quarry, Stability, Numerical Modelling.

1 Introduction

According to Quinif and Vandycke (Quinif et al. 1997), the structural analysis enables a good understanding of the global geo-dynamics in which the natural caving occurs; this is achieved by micro-tectonic analysis and also by the so-called paleo-stress assessment. In fact, studying the geometry of tectonic marks encountered in natural caves allows a differentiation of different tectonic stages that gave the actual net of caving, and understand, with respect to time, which structures have been inherited from old tectonic thrusts, and which are actually active. This

approach can be used to try understanding the actual deformation exhibited by cave structures, and perhaps, assess the direction and magnitude of the tectonic forces. Estimating the direction of these forces can be performed thanks to the classical tectonic approaches using direction of conjugate faults; but calculating their magnitude needs a good knowledge of the mechanical rock mass behaviour on large scales, this is not very easy, but in numerical modelling this can be considered as a parameter. During the observations on this so complex structure, some fault directions were measured, but obvious outcrops of conjugate structures were not found. It was then difficult to assess any tectonic force direction.

2 Description of the Studied Site

2.1 Geometric Model

The study focuses on the artificial “hill” containing the Ramioul Cave. This hill results from mining excavations at the West and South by the Engis quarry of the Carmeuse s.a., and on the northern part by an ancient quarry. The picture of figure 1 taken from the West gives an image of the field configuration and also shows the nearly vertical dipping of the stratification joints.

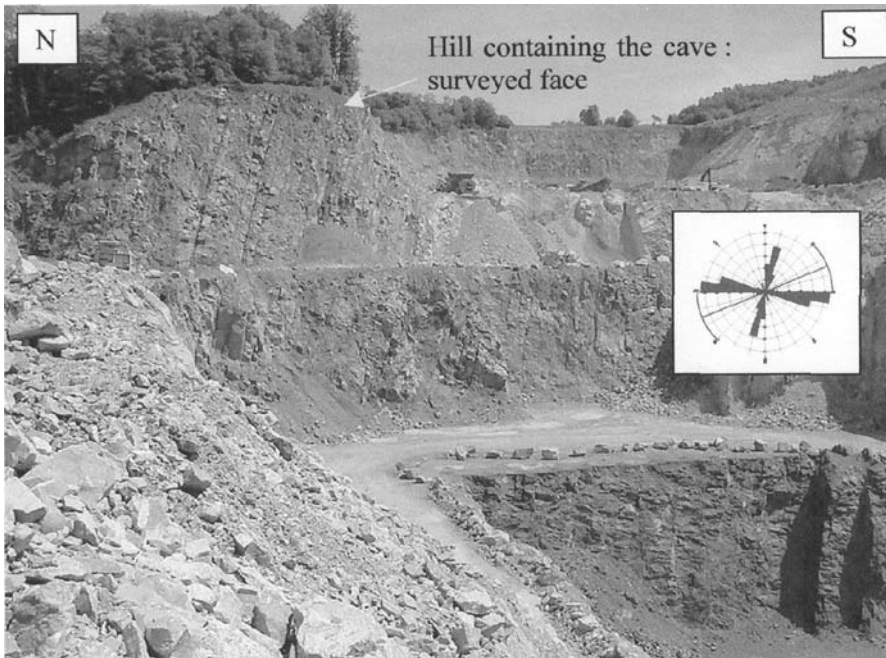


Fig. 1. General view of the studied site showing the wall which has been surveyed.

To model the mechanical behaviour of the rock mass containing the natural cave an actual topographic model was needed. This has been achieved by using the quarry plan view that was supplied gratefully by the Carmeuse's engineers. Selection of about 500 points and introducing these in the Rockworks2002 software gave a geometric model that can be seen in figure 2, lines A and B representing the profiles were surveyed during the geotechnical studies (Tshibangu, 2003).

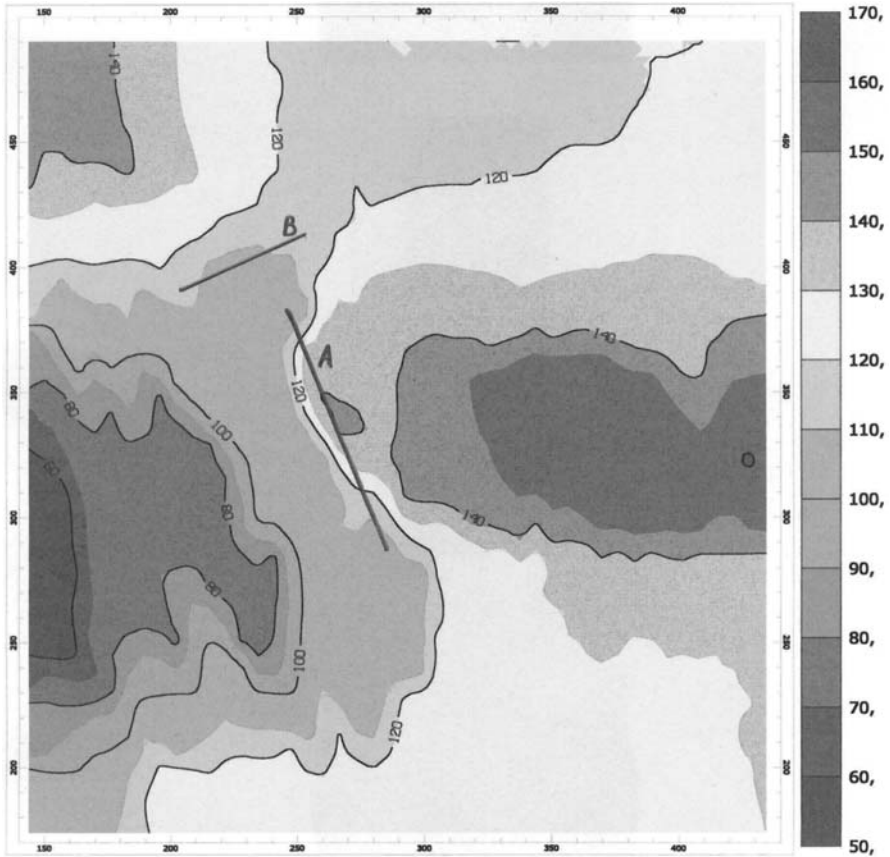


Fig. 2. Topographic model of the area containing the Ramioul's natural cave.

2.2 Quality of the Rock Mass and Mechanical Properties

Figure 1 and the plan view of figure 2 show the face and track of profile A that was studied. Figure 3 presents the joint spacing as measured.

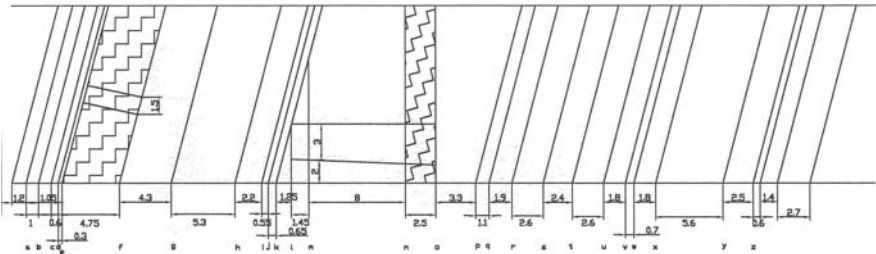


Fig. 3. Representation of observed discontinuities on the profile A (spacing in meters).

Table 1 summarises the description of some chosen discontinuities in the profile. Some rock samples have been collected and tested to give the results summarised in Table 2.

Table 1. Description of some chosen discontinuities in the surveyed profile A.

<i>Discontinuities</i>	<i>Description</i>
A	Few weathering, dry, rough, some rock debris in the fracture
B	Tracks of fluids circulation, rough (thin lime depot on the surfaces)
C	Rough with lime depot
Interval e-f	Crushed zone, without weathering between blocs (4,75 m)
F	Karstic concretions, clay filling (5 à 10 cm)

Table 2. Uniaxial compression and traction mean results.

	<i>UCS</i> <i>[MPa]</i>	<i>Young's modulus</i> <i>[MPa]</i>	<i>Tensile Strength</i> <i>[MPa]</i>
Sample 0	152	98987	-4.9
Sample 1	99	47887	-4.8
Sample 3	136	63393	-5.5
Concretion	23		-1.7

The uniaxial compressive strength of the limestone can be qualified as high to very high; while the tensile strength, which is relatively homogeneous, is a mean value. To take into account the presence of discontinuities and other flaws, the Rock Quality Designation (RQD), and the Rock Mass Rating (RMR) were used. The RQD from Don Deere (1963) is defined as the ratio (in percent) of the sum of lengths of unbroken pieces of core having a length of more than 10 cm to the total length of the core drilled. It is important to notice that the value of the RQD is direction dependent and the coring technique used can have a great influence on the obtained results. A virtual coring wellbore was created by drawing a horizontal line on the front studied as shown on figure 1, and the thickness of intact and weathered materials was used to calculate the RQD. As most of the surveyed layers show a thickness of more than 10 cm, it was considered that only the total

thickness of the weathered material (located mainly in joints) will have to be removed from the coring pass length to get the cumulative length of the cores longer than 10 cm. The ratio between this total thickness of weathered materials and the total length of surveyed face gave a RQD of about 85%. To take into account more parameters the RMR (Bieniawski 1976) was estimated using 5 parameters that are: the Uniaxial Compressive Strength, the RQD, the joint spacing, the nature of joints, and the water flow. Each parameter is weighted to obtain, after summing, a global reference note with respect to 100. This global note has to be corrected according to the orientation of the studied structure. Depending on the description given earlier, the RMR of the rock mass can be assessed as follows (table 3):

Table 3. Estimation of the global RMR note on the studied rock mass.

<i>PARAMETER</i>	<i>VALUE</i>	<i>NOTE</i>
Uniaxial Compressive Strength (MPa)	100	12
R.Q.D. (%)	80	17
Joints spacing (m)	0,6 – 2	15
Nature of joints	Continuous joints	10
Water flow	No water, except when raining	10
Global note		64

The orientation of the surveyed wall being unfavourable we adopted a RMR value of 60%, so qualifying the rock mass as of mean quality. Based on this quality we can use the Hoek and Brown (Hoek and Brown 1997) recommended parameters summarised in table 4:

Table 4. Mechanical parameters recommended by Hoek & Brown for rock masses.

<i>PARAMETER</i>	<i>MEAN Quality</i>	<i>POOR QUALITY</i>
Strength of the intact rock σ_{ci} (MPa)	80	20
Internal friction angle φ (°)	33	24
Cohesion C (MPa)	3,5	0,55
Compres. Strength of the rock mass σ_{cm} (MPa)	13	1,7
Tensile Strength of rock mass σ_{tm} (MPa)	-0,15	-0,01
Deformability modulus E_m (MPa)	9000,0	1400,0
Poisson's ratio ν	0,25	0,3
Dilatancy angle α (°)	$\varphi/8 = 4$	0
Residual angle of friction φ_r (°)	-	-
Residual cohesion C_r (MPa)	0	0,55
Residual deform. Modulus E_{mr}	5000	1400

3 Mechanical Modelling

The BEFE software (Boundary Element and Finite Element) was used for a plan-strain analysis using a North-South plane crossing the cave. The rock mass has

been considered as homogeneous with an elasto-plastic behaviour of the materials. The stresses in the rock mass will be due only to gravity and excavation process. This will start with a flat surface symbolising the ground prior to any excavation and creating the following excavations: the underground cave, the ancient quarry on the northern part, and finally the actual quarry on the southern side by Carmeuse s.a. excavated in two stages. We would like to point out that the tectonic thrust that could have occurred prior to the cave excavation was neglected. As stated earlier, two types of material will be analysed in the computations: this is the material corresponding to the mean quality rock mass, and that corresponding to the poor quality according to the Hoek and Brown recommendations. Following stages will be used in the calculations:

- I. Calculate the virgin state of stress (due to gravity) with the ground surface located at +160 m (with respect to the sea level);
- II. Excavate the cave;
- III. Excavate the ancient quarry on the North;
- IV. Excavate the Carmeuse quarry down to +152 m with a smooth slope beside the cave;
- V. Excavate the Carmeuse quarry down to +120 m with a steep slope (angle of about 85°);

The observations focussed on the following parameters:

- The horizontal stress (σ_x) the importance of which is justified by the possibility of traction forces in the steep wall of the structure;
- the displacements and the deformed shape which allow a good understanding of the difference between the directions of displacements when using a single gravity model (i.e. a model in which the final geometry is used and gravity forces applied) and an excavation model;
- the plastic function and the associated plastic points showing if the model undergoes plastic strains and the dimension of the failed zone.

Figure 4 illustrates the horizontal stress σ_x in the final stage of excavation which corresponds to the actual state of the site. This shows that possible tensile horizontal stresses are concentrated in the upper part of the model (positive values of σ_x); and it can be emphasised that the excavation of the Carmeuse quarry (right side on the figure), induces a zone with such stresses including the cave. Remembering that the rock mass material is jointed with dipping angles close to 90° towards North direction, one can assess the risk of toppling failure towards the Carmeuse opening.

When performing calculations with the mean quality materials (see table 4), no failure was obtained in the model, but in case of poor material, some points showed plastic behaviour (figure 5). This shows that around the cave, most of the points are concentrated on the right side wall, and in the roof. It can also be seen that some failed points occur in the steep slope of the Carmeuse quarry. The right side wall of the cave will be used for a displacement monitoring because many broken concretions have been observed in this area.

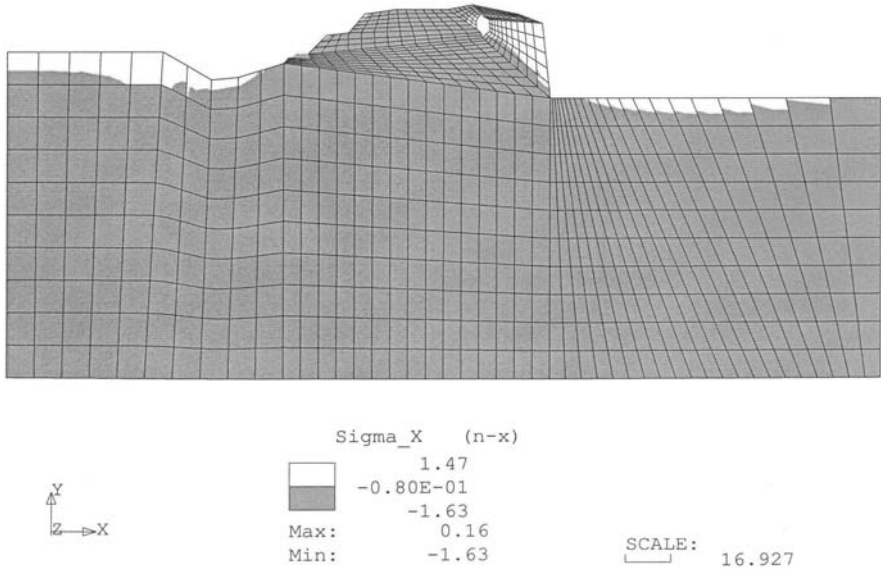


Fig. 4. Final result obtained in terms of horizontal stress after the excavation of the ancient quarry (left) and the Carmeuse's one (right) down to +120 m. Areas developing tensile stresses are in white color.

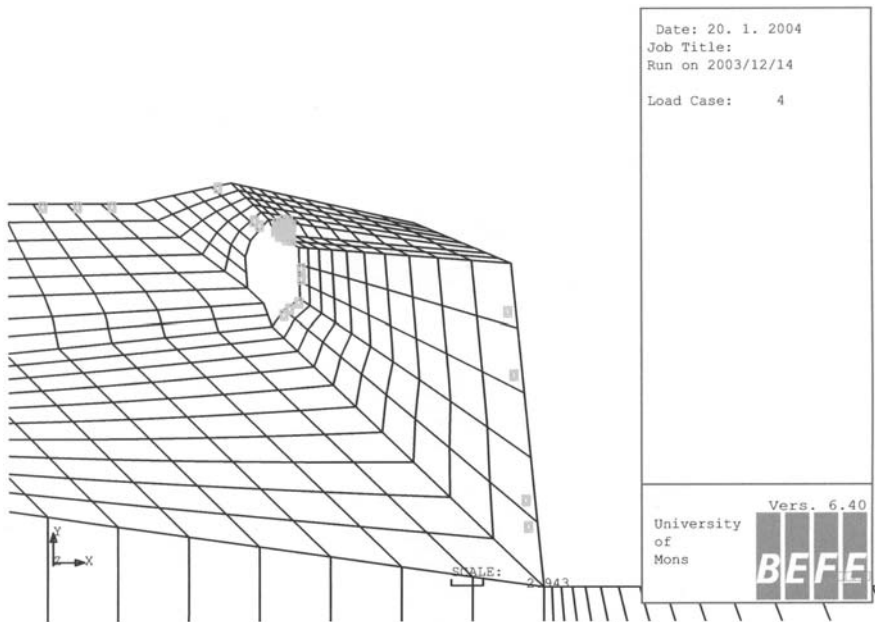


Fig. 5. Plastic points occurring in the actual stage of excavation with a poor quality material.

Another interesting result to be pointed out is the deformed shape of the rock mass, especially in the final stage (light grey mesh on figure 6). The overall displacements obtained are oriented towards the excavation with horizontal surfaces being curved downward. This induces tensile stresses that are responsible of the joint opening that can be observed in the quarries. One must then understand that the joint opening observed in the actual situation was not so obvious prior to excavation, but this has been induced by the material removal.

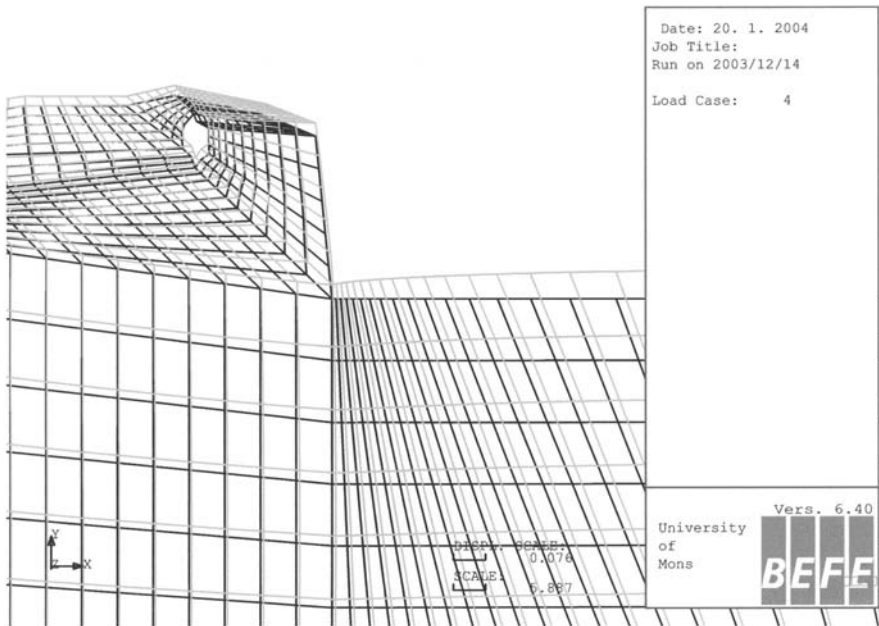


Fig. 6. Deformed shape of the mesh (light grey) in the actual stage of excavation.

4 Displacement Measurements

Working with the ORB (Royal Observatory of Belgium) team, some electrical Edas extensometers (Van Ruymbeke 1990) were installed to monitor displacements around the cave. Figure 7 shows the result obtained on an extensometer located on a moving joint in the southern wall of the cave and oriented North to South. The measurements exhibit a steady-state increasing of the displacement on the device for a period ranging from August 01 to March 02.

On 09 January 2002 a toppling failure occurred on the slope beside the Carmeuse quarry. This has been recorded by the extensometer, with a jump of about $10 \mu\text{m}$, which is shown by the second graph of figure 7 as a zoom of the first one for the targeted day.

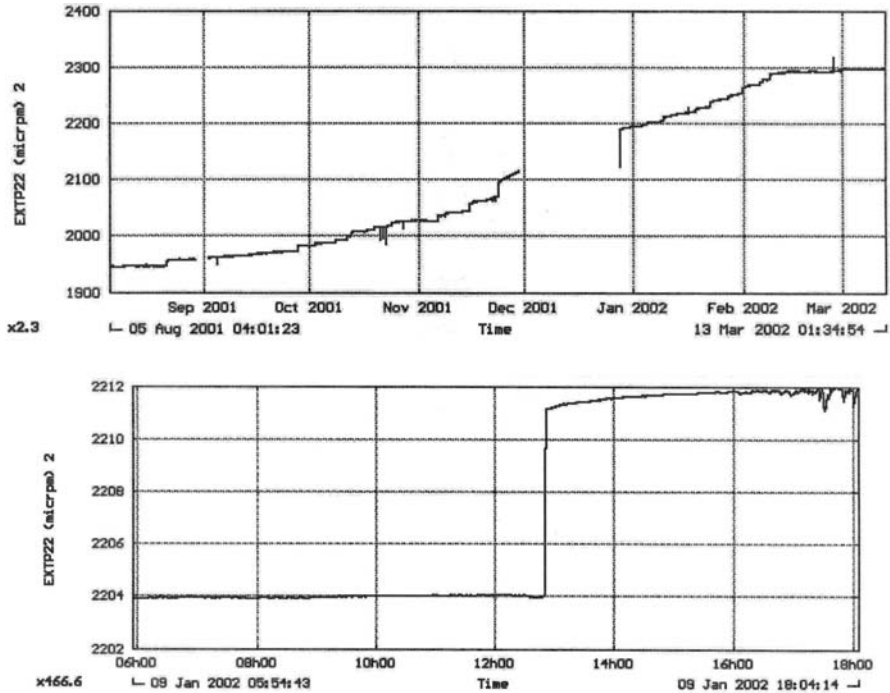


Fig. 7. A curve showing the signal of extensometer EXTP22 in the Ramioul cave (measurements are in μm). The bottom graph is a zoom on 09 January 2002.

5 Conclusions

This paper summarises the geo-mechanical study achieved on the Ramioul's cave in order to understand the cause of ground motions observed. The work to reach such a goal comprised of a geometric modelling, a structural description, an assessment of the quality and, hence, the mechanical behaviour of the rock mass, and a numerical model. Some displacement measurements have also been performed in the cave during the studies. Even if structural data show that the tectonics affected the area in the past (dipping of layers and occurrence of faults), the interpretation of obtained results leads to the observation that the main role in the actual ground motions is played by the quarrying operations. This has been confirmed by the toppling failure measured on the transducers on 9 January 2002. The study shows that not only the tectonic stresses, but also the topography and the induced stresses can play a role in the formation and evolution of karst. For future studies of the research team, a working method involving the main tectonic events as well as topographic evolution will be useful.

References

- Bieniawski ZT (1976) *Exploration for Rock Engineering*. Balkema Rotterdam.
- Hoek E, Brown ET (1997) Practical Estimates of Rock Mass Strength. *Int. J. Rock Mech. Min. Sci.* Vol 34, No 8, pp 1165-1186.
- Quinif Y, Vanduycke S, Vergari A (1997) Chronologie et causalité entre tectonique et karstification - l'exemple des paléokarsts crétacés du Hainaut (Belgique). *Bull.Soc.Géol.Fr.*, 168, 4, pp 463-472.
- Tshibangu KJP (2003) *Projet FRFC – Karsts à Ramioul, Rapport géomécanique*. Internal report FPMs.
- Van Ruymbeke M (1990) Instrumentation développée à l'Observatoire Royal de Belgique pour la mesure des déformations lentes du sol. *Annales de la Soc. Géologique de Belgique* tome 112, fasc. 2, pp 459-466.

Drying-Up of a Natural Spring for Ensuring Stability of an Artificial Slope: Is It Sustainable Development?

Marie Dachy¹, Sandrine Sage², and Alain Dassargues^{1,3}

¹ Hydrogeology & Environmental Geology, Dpt Georesources
Geotechnologies and Building Materials (GeomaC), University of Liège

² Geophysical Prospecting, Dpt Georesources

Geotechnologies and Building Materials (GeomaC), University of Liège

³ Hydrogeology & Engineering Geology, Dpt Geology-Geography, KULeuven
Marie.Dachy@ulg.ac.be

Tel: +32 4 366.23.58

Fax: +32 4 366.95.20

Abstract. Near a small city of the Belgian ‘Ardennes’ (East of Belgium), modification of a natural slope for extension of industrial activities has required an extensive drainage in a weathered zone composed of colluvium and weathered claystones and quartzites. After a few days, the drain at the foot of the artificial slope was producing about 1000 m³/day while a natural spring located at a 200 m distance on the hillside was completely dried up. This spring was used for drinking water by the local community. A shallow geophysical prospection by refraction seismics and 2D geoelectrical tomography, associated to geological, morphostructural and hydrogeological observations have lead to a clear understanding of (1) the spring occurrence; (2) the feeding conditions of the spring and consequently (3) the ‘lateral’ hydraulic impact of the drain. In the hill, the bedrock is changing from quartzites (uphill) to claystones (downhill) inducing changes in hydraulic conductivity and thickness of the overlying weathered zone. On the basis of these hydrogeological conditions, associated to the specific topographic conditions, different possible remediation schemas have been proposed to the decision makers. Unfortunately, the full restoration of the natural spring appears to be one of the most technically and financially difficult option ...while it is surely the most suitable in the name of a sustainable development.

Keywords: hydrogeology, geoelectrical tomography, impact of drainage, drying up a natural spring.

1 Introduction

In order to create an horizontal platform for extension of its industrial activities, a private company has received the authorization to modify the natural slope of a hillside. The local geology of the area consists of quartzitic rocks and schists belonging to lower Salmian age (Cambrian). The direction of the layers is more or less parallel to the direction of the valley (SW-NE) with a dip towards the south. The schematic SE-NW cross-section of figure 1 illustrates the relation between

geomorphology and geology in this region. Quartzites are generally observed at the top and higher parts of the hills while schists are found back in the lower parts of the valleys. Usually, in that region, the transition zone between quartzites and schists is observed to be relatively sharp. Here, however, the hillslope seems uniform, not showing any clear transition zone. Works of extension of the company required an earthwork platform. Topographically, the ground surface, originally inclined towards NW, has been transformed for presenting a platform at the absolute level of 417 m, the top of the remaining slope being at 428 m (figure 2). However, very soon, groundwater seepage from the reshaped slope was observed. It was also threatening the slope stability. A drain was placed at the base of the slope, along the entire width of the extension zone. The base of the drain is at the absolute level of 415 m. This drain presents a slope of 0.5 % and the water is collected east of the site. After a few days, the approximated daily water drained flow rate reached a value of 1000 m³/day.

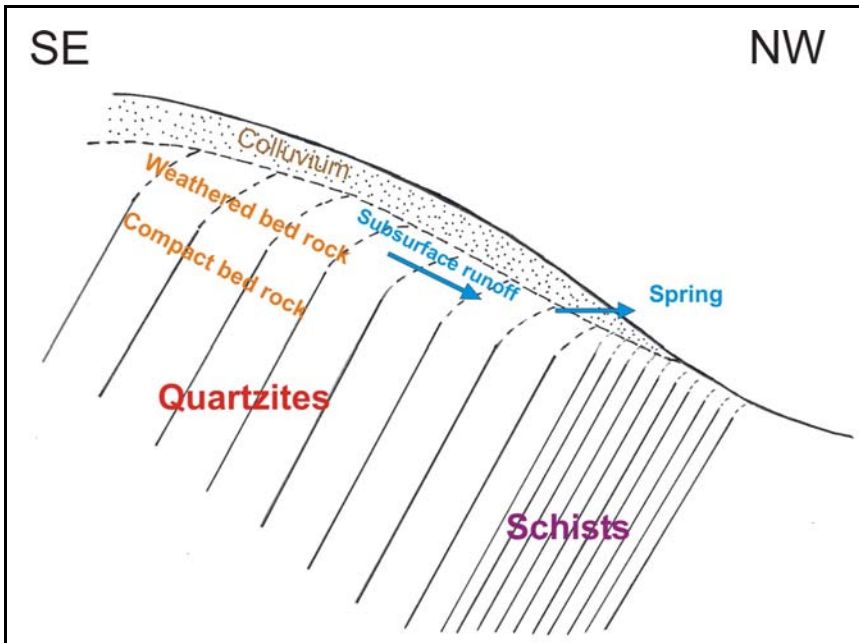


Fig. 1. Schematic SE-NW geological cross-section normal to the layer direction and transverse to the valley.

At the same time, the flow rate of a natural spring, located at a lateral distance of about 200 m from the drain on the same hillslope, brutally dropped and the spring eventually completely dried up. Previously, the averaged daily flow rate was comprised between 200 m³/day and 350 m³/day. The emergence of this spring was flowing at an absolute level of 422 m. Another spring is emerging further on the same hillslope at a distance of more or less 1 kilometer and at the absolute level of

405 m. The averaged daily flow rate of this last spring changed from 1330 m³/day to 1036 m³/day in fourteen days. Both of these springs were exploited by the local community for drinking water. A study was needed to determine the local hydrogeological context explaining the impact of the new drainage on the springs and to propose, if possible, sustainable alternatives.

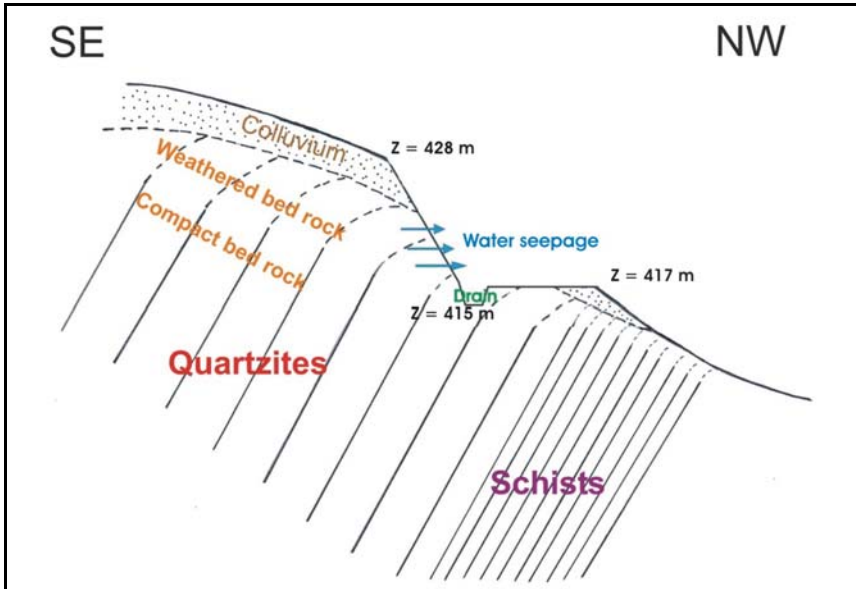


Fig. 2. Schematic SE-NW transverse cross-section showing the reshaped slope and the position of the drain.

2 Analysing and Investigating Hydrogeological Conditions

On the basis of the geological conditions indicated on the transverse cross-sections of figures 1 & 2, a crucial issue consists in accurately determining where the bedrock lithology changes from quartzites to schists. This matter is actually very important because of its considerable impact on the local colluvium characteristics. The weathering of quartzites mainly produces a sandy colluvium with relatively high hydraulic conductivity. This permeable mantle makes the water infiltration easier and thus allows further weathering and decomposition of the underlying quartzites. This process generates a relatively thick and permeable unit composed of weathered bedrock and colluvium. On the other hand, it is expected that the weathering and decomposition of the schists provide a more clayey colluvium. The low hydraulic conductivity of this layer does not favour deeper weathering and decomposition of the bedrock, thus resulting in a thin and relatively low permeability colluvium overlying the argillaceous schists bedrock.

Within the sandy weathered bedrock and colluvium an important groundwater flow is possible. Considering that the slope of the valley is relatively long, the quantity of groundwater accumulated in the weathered bedrock and colluvium is significant. The presence of springs along the slope is most likely explained by the appearance of clays derived from the decomposition of the underlying schists. This change in permeability associated with a reduced thickness induces the emergence of groundwater at the surface. This change in the colluvium could normally provide indication on the contact between the quartzites and schists. However, a possible creep effect must also be considered. Examination of the topographic maps shows an alignment of the sources in that area along the hill-slope between levels 400 m and 425 m. Among the possible causes of the drying up, the abnormally dry climate conditions of this beginning of year 2003 were evoked. However, the history of the gaugings showed that the nearest spring was never dried up in the past, even at the time of the 1976 drought, and that its flow rate was never below 190 m³/day. Moreover, the drying up of the nearest spring and the flow rate decay of the spring located 1 km further were observed shortly after the installation of the litigious drain. There was no other civil engineering work undertaken in the area at that time.

It thus clearly appears that the drying up of the nearest spring results from the installation of the drain within the weathered bedrock and colluvium in the extension zone of the company. Indeed, if the conceptual hydrogeological schema presented hereabove prevails in this hillslope, the drain and the spring are both supplied with the shallow groundwater flow which was at the origin in the SE-NW direction. The drain being at a 200 m distance from the spring, but at a lower absolute level (base of the drain at 415 m, spring at 422 m), it makes it possible for the groundwater to be drained at a considerable flow rate (1000 m³/day). This new exit point must probably influence the local water table and the groundwater streamlines towards the drain. A local water table lower than the spring level (415 m) caused the drying up of the nearest source. However, the lowering of the water table is probably sufficiently laterally limited to induce a flow rate decay of only 30 % at the spring located about 1 km further.

3 Groundwater Quality as an Indicator of a Shallow Groundwater System

In terms of hydrochemistry, temporal evolution of the in situ measured pH, temperature and conductivity showed an average pH of 6.07 at the nearest spring (before drying up). This slightly acid pH value is current in that region of the Ardennes. Average conductivity is of 73.16 $\mu\text{S}/\text{cm}$ (20°C), which is characteristic of a groundwater with low mineralization. The seasonal fluctuations of the temperature (more than 6° between 9°C and 16 °C) on the one hand and the weak mineralization, on the other hand, indicate that the spring is fed primarily by a shallow groundwater system. This observation is fully consistent with the conceptual hydrogeological schema described here above. The second spring located

1 km further has an average pH of 6.06 and an average conductivity of 92.35 $\mu\text{S}/\text{cm}$ (20°C). The average temperature is of 10.54 °C fluctuating in the same way as for the other spring (maximum of 17°C reached in summer). The temperature fluctuations and the weak mineralisation also indicate a relatively short and shallow groundwater flow path. Results of the hydrochemical analysis performed for the drained water and for the water at the remaining spring, are illustrated in the Piper diagram of figure 3.

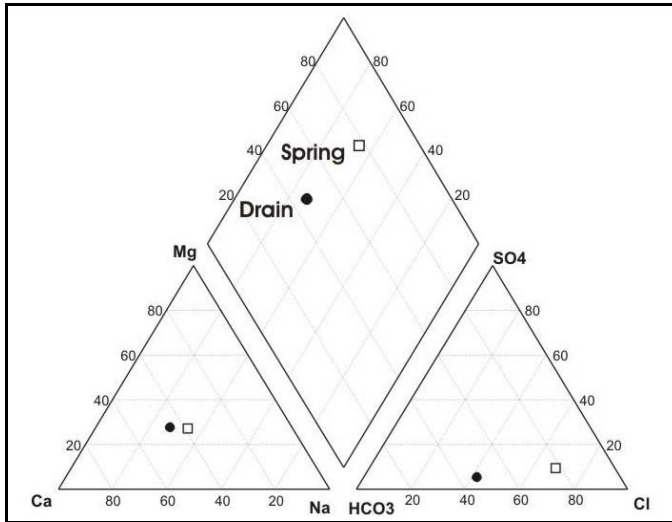


Fig. 3. Piper diagram showing the relative hydrochemical characteristics of the groundwater in the drain and in the spring located 1 km further.

4 Shallow Geophysical Prospecting

An hydrogeological model was proposed to explain the drying up of the nearest spring. A shallow geophysical study was proposed in order (1) to confirm the location of the bedrock lithological change from quartzites to schists, implying possible changes in the weathered bedrock and colluvium; (2) to determine the thickness of this colluvium and weathered zone overlying the bedrock (with an anticipated maximum thickness of about 10 m). Refraction seismic and electric profiling were selected. The electric profiles are used in order to determine lithological changes resulting in different resistivities. The resistivity of quartzites is higher than that of schists. An electric profile with a 'dipole-dipole' or 'pole-dipole' configuration is usually able to detect lateral in-depth resistivity differences along a profile. The seismic refraction is currently used to detect the interface between the loose sediments and the bedrock. This method is used here to determine the thickness of the loose materials (weathered bedrock + colluvium) overlying the bedrock. Seismic velocity in the basement is indeed higher than in the overlying materials. A seismic profile was carried out along the hillside and

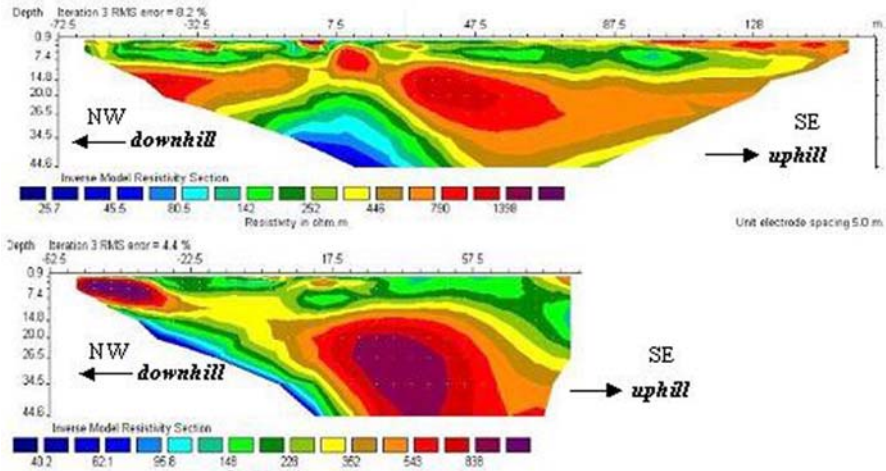


Fig. 4. Modelled resistivity profiles near the dried spring (top) and near the drain (bottom).

two electric profiles were carried out along the slope : the first electric profile was close to the dried spring and the second one was close to the drain. Results are given in figure 4.

On the first profile, a first horizon is characterized by apparent resistivities ranging between $100 \Omega\text{m}$ and $300 \Omega\text{m}$. It corresponds to an unconsolidated layer. This unit is thicker uphill and a local thinning is observed very close to the dried spring in the hillslope : a bed of very resistive rock, probably quartzitic, is nearly outcropping. The incomplete second profile only investigates the downhill part of the slope. Nevertheless, both profiles seem to indicate a lithological change from a resistive material uphill to a conductive material downhill. From the seismic results, a longitudinal (along the hillside) cross-section can be interpreted as shown on figure 5. A first layer of unconsolidated granular material having a maximum thickness of 2 m is overlying a second layer that can be identified as a weathered bedrock. The interface between this weathered zone and the bedrock seems very irregular and globally describes a thickening in the direction of the drain.

5 Summary, Conclusions and Perspectives

The various investigations indicate that the constructed drain induces the drainage of a shallow groundwater system mainly included in the colluvium and the weathered bedrock overlying a Primary bedrock composed of quartzites changing downhill to schists. The geophysical prospection results have highlighted the presence of a quartzite bed nearly outcropping close to the dried spring. The presence of the spring would thus be related to a local thinning of the weathered bedrock which is the main aquifer layer. Additionnaly, less resistive materials appear downhill on the electric profiles. This resistivity change could be related to the

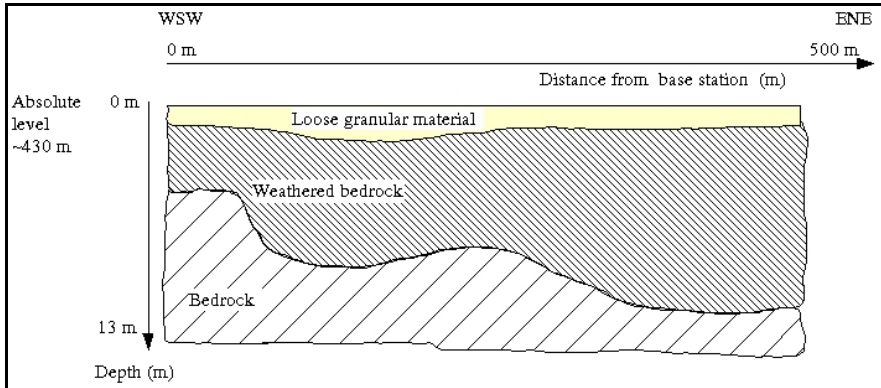


Fig. 5. Interpretative profile from seismic results: a thickening of the weathered bed-rock is observed from the dried spring to the drain.

change from quartzites to schists. The excavation of the platform and the drain at a very short distance from the spring, especially at an absolute level located 7 m below the outlet of the spring, caused the drainage of the saturated zone within the weathered bedrock. The induced drawdown is such that now the spring is completely dried up and located above the saturated zone. Unfortunately, the definitive conclusion is that the construction of the drain obviously has a disastrous impact on the spring feeding system. On the basis of these conclusions and considering the specific topographic conditions, different possible remediation schemas have been proposed to the decision makers.

a) Being given that the company does not plan to exploit the totality of the water volume tapped by the drain, a first solution could be to use the drain itself for producing drinking water. However, this a priori tempting solution is not possible in practice due to the local legislation on protection zones.

b) A second solution could consist in trying to cancel the effect of the drain by installing a grout curtain or a slurry wall located just upstream of the drain in order to restore the initial feeding mode of the spring. It is a very expensive solution, which, in addition, would be accompanied by many technical difficulties and uncertainties (i.e. stability of the slope and of the wall by a rise of water pressure, uncertainties about the actual rebirth of the spring). Although this schema is about the only solution to try to restore the spring, it seems practically infeasible.

c) Another solution consists in setting up a new collecting drain or well (in conformity with the local legislation with regards to the protection zones) upstream of the existing drain. The drilling of a well (or a series of wells, if need be) would make it possible to restore the water supply of the village with legal protection zones. However, it is clear that the drilling would be preceded by more detailed investigations (geophysical prospection) in order to determine optimal locations.

Unfortunately, the full restoration of the natural spring appears to be one of the most technically and financially difficult option ...while it is surely the most suitable in the name of a sustainable development.

Suitability Maps of Underground Construction in the Province of South-Holland

Jurgen Herbschleb¹, Brecht B.T. Wassing², and Henk J.T. Weerts²

¹ Royal Haskoning, P.O. Box 705, 3000 AS Rotterdam
j.herbschleb@royalhaskoning.com

Tel: ++31104433472

Fax: ++31104433688

² TNO-NITG National Geological Survey, P.O. Box 80015, 3508 TA Utrecht
{b.wassing,h.weerts}@nitg.tno.nl

Tel: ++31302564850

Fax: ++31302564855

Abstract. Subsurface suitability maps give an insight in both the geology and the physical and chemical soil properties. The geology and soil properties together with the groundwater conditions determine technically speaking the way subsurface activities can take place. In the project described in this article a set of maps was created which indicate the suitability of the soil conditions for underground constructions. A common way to create underground constructions in the Netherlands is to use building pits and the degree of difficulty (or suitability) of underground construction is directly related to the design of the building pit. With the geological knowledge and boundary conditions that apply to the design of a building pit, a common classification of the soil properties has been made based on the type of soil (sand, clay, and peat). The combination of the strength and stiffness properties together with the thickness of the soil layers is used to obtain three suitability scores, (1) score underneath the building pit, (2) score adjacent to the pit, and (3) ground water score. These scores are added to obtain an overall suitability score. In this way, a suitability score is calculated for every site where borehole-descriptions of sufficient depth are available and groundwater conditions are known. Based on the data in the DINO-database of TNO-NITG a suitability map for subsurface building/construction was made for the province of South Holland.

Keywords: engineering geological maps, suitability maps for underground construction, databases.

1 Introduction

Recently in the Netherlands awareness has grown that when the (shallow) subsurface is visualised, opportunities within the subsurface can be created (COB, 2002). The Province of South Holland decided two years ago that in addition to existing maps of the surface, which display groundwater conditions, archaeology, etc., other engineering geological maps that display the usability of the sub-surface should be used for policy plans. Those maps are amongst others suitability maps for underground storage of groundwater for cold-heat storage, workable sand

deposits, and suitability for underground constructions. In a project executed in co-operation between NITG-TNO and Royal Haskoning and financed by the province of South-Holland, maps have been created which reflect the suitability for underground construction activities.

2 Engineering Geological Maps

A map using a spatial classification to transmit information about geological features at or near the earth's surface that has a role in the use of the subsurface for the design, realisation, and maintenance of constructions, is often called an Engineering Geological Map. The added value of Engineering Geological Maps is to visualize the "unknown" subsurface, not by using "complex" geological features and terms, but by translating the geology into physical properties. Such maps are primarily instruments for arranging, storing, transmitting, and analyzing information about the spatial distribution of attributes, and are both prepared and modified through four principal types of operations: generalization, selection, addition or superposition, and transformation (Varnes, 1974). Engineering geological maps can be used for further technical interpretation, policy plans, planning building activities or prior knowledge to areas where care to site investigation is to be taken. In the Netherlands Engineering Geological maps have been created in the past by the Dutch Geological Survey (Krajcicek, et al 1984) and the municipality of Amsterdam (Philippart, 1990).

3 Building Underground

3.1 Main Factors

The province South-Holland in The Netherlands is one of the most densely populated areas in the world. Many building activities will have a subsurface component in the (near) future, see figure 1. Generally speaking there are the following reasons to build underground, ranging from the aesthetic, to preservation conservation, to finances (Trinity, 2002):

- An underground building has a low visual impact. For example, if an industrial building needs to be located near a residential location, an option would be to put the building underground to preserve the residential scene.
- Underground construction affords more efficient landuse. Land near to highways can become useable for office buildings because the ground itself prevents the infiltration of noise from the outside.
- Underground buildings are protected from natural disasters. High winds, hail, tornadoes, earthquakes and fires all cause less damage to an underground building than to an above surface building.



Fig. 1. Artist impression Tramtunnel, the Hague.

- Underground buildings may have a lower life cycle costs (Trinity, 2002). For instance, soil will show less extreme temperature variations than air.
- Underground construction has the potential to save money. With proper planning, some buildings could cost less if built underground rather than above-ground (Trinity, 2002). For example, with an underground building, depending upon design, there would be fewer facades than for a building on the surface.

There are drawbacks for building below surface that should be carefully considered:

- Underground buildings can cause psychological stresses. Some people have severe adverse effects to being underground for extended periods and there is less potential for natural light and “a view”.
- Repairing an underground building is expensive. It will be very costly to repair an underground building if any leaks or structural damage occurs.
- Adding an extension to an underground building is difficult and very costly. The protection of the original building and its foundation will be very difficult and will raise construction costs considerably.
- Site conditions can cause complications and may discourage underground construction at certain sites. For instance, a high groundwater table, which is often encountered in the Netherlands, discourages underground construction. If adjacent buildings are too close, temporary retaining walls will need to be constructed.

Many of the above positive and negative factors to build underground can be influenced and differ per project. However, the soil conditions are static and have a large influence on the success and costs of a project, which means that the suit-

ability of underground construction is strongly related to the soil conditions. Because the soil conditions are static, a map that incorporates the soil conditions has a “timeless” validity, which makes such a map suitable for long-term government decisions.

3.2 Building Pit

In the Netherlands, so-called building pits are very often used for underground construction to overcome the problems with (soft) soil conditions and high groundwater tables. The building pit usually consists of an excavation supported by vertical walls (sheet piles, diaphragm walls, etc.), which support the soil, prevent water inflow and limit the construction area. During construction, the inflow of water from the bottom of the building pit must be prevented and during the building stages the so-called condition of vertical equilibrium must be satisfied. To prevent the inflow of water and maintain vertical equilibrium several options are available. The simplest option is provided by nature itself when a soil layer of very low permeability (clay or peat) is present. If such a layer is absent or too deep, other options are lowering the water table or creating an artificial layer (underwater concrete, water glass, grout, etc) that prevents the water from flowing into the pit. The amount of measures needed to satisfy the condition of vertical equilibrium and the depth of excavation are the main cost factors in the design of a building pit. For example if thick and deep clay layers are present, the length of the vertical walls may be adapted to create a closed environment. On the other hand, if only soft soils are present extra measures must be taken to maintain horizontal stability of the walls. From the research carried out in this project it is concluded that creating a map of the global design of a building pit reflects the suitability to build underground because of the following reasons:

- building pits are necessary for most underground projects in the province of South-Holland
- the design of a building pit is independent of the structure to be build
- the costs of a building pit are mainly a function of the soil conditions present
- soil conditions are static.

4 Suitability Maps of Underground Construction

4.1 Introduction

Underground constructions can be subdivided as follows:

0 - 1m	cables and mains
1 - 8 m	cellars, parking garages, water storage, underground shopping, etc
8 - 16m	tunnels and (metro) stations
16 - 40m	special projects (deep tunnels and stations)

For this project it was decided to create two maps which can be used for common projects in the province: one map depicts the suitability of the soils for construction of 6 m deep building pits (representative of the second category of cellars, parking garages, etc.). The second map shows the suitability for construction of 10 m deep building pits and can be used for the third category of underground constructions: tunnels and underground railway stations. Table 1 gives an indication of the accuracy of both maps, when used to predict soil suitability for building pits with depths other than 6 or 10 m.

Table 1. Accuracy of predicted suitability (white=high reliability, black = not reliable).

Depth of underground construction [m]													
1	2	3	4	5	6	7	8	9	10	11	12	13	14

The process of creating the suitability maps of underground construction for the province of South-Holland has been as follows:

1. Defining the factors of influence on building pit design (generalisation).
2. Extraction of borehole data from DINO database (selection).
3. Calculation of suitability score per borehole (addition).
4. Mapping of suitability score (transformation).
5. Check with “real” projects (validation).

4.2 Generalisation

The complexity of the building pit structure depends on the following soil properties:

- composition of the subsoil (sand, clay, peat) underneath the building pit;
- composition of the subsoil adjacent to the building pit;
- groundwater level.

During construction of the building pit, vertical equilibrium of the building pit floor has to be maintained. Vertical equilibrium depends on the composition of the subsoil underneath the bottom of the pit and the local groundwater conditions. Furthermore, the bottom of a building pit must be closed and the inflow of excessive groundwater must be prevented. This means that when a clay layer of sufficient thickness is present at a suitable depth beneath the bottom of a building pit, soil conditions are considered “suitable”. When such a layer is only thin and too close to the bottom of the building pit for vertical equilibrium, soil conditions are considered (much) less suitable, see also figure 2. The soil adjacent to the building pit determines the horizontal stability. Sheet pile walls will be, for instance, much shorter in dense sands than in soft clays. The presence of peat with a thickness of at least 1.0 m is always considered as unfavourable. The groundwater level is important as it determines the water pressure both outside and underneath the building pit. A higher groundwater level is considered as unfavourable.

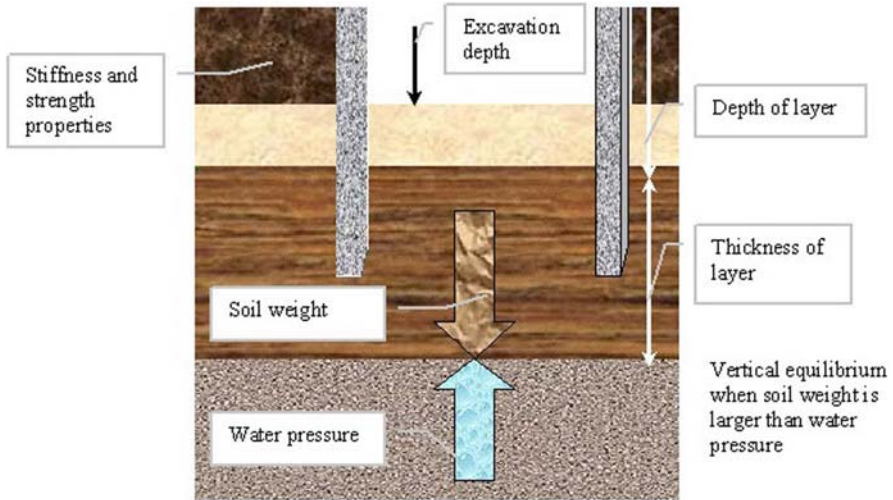


Fig. 2. Design aspects of building pit as used in calculating the scores.

4.3 Selection

Borehole data with good quality and a sufficient depth range were selected in the DINO-database (Data and Information of the Netherlands' Subsoil) of TNO-NITG and stored in a special project database. DINO contains all the digital borehole-descriptions and groundwater level maps of TNO-NITG. For each score to be calculated a so-called database query was developed to calculate automatically the score.

4.4 Addition

Based on geological knowledge, the different layers of sand, clay, and peat are classified in strength and stiffness categories. The combination of the strength and stiffness categories together with the thickness and depth of the layers is used to obtain three suitability scores, underneath the building pit, adjacent to the building pit and a ground water score. The three scores are added to obtain a total score for the suitability of the soils for underground construction. The scores are calculated for every borehole location of sufficient depth available, if the groundwater level is known. Table 2 gives an example of the relative suitability scores assigned for the soil conditions adjacent to the building pit.

4.5 Transformation

When the calculation of scores is completed, at each borehole location the suitability of underground construction is known. To determine the suitability at locations where no boreholes were present an interpolation technique was used. To construct this map a combination of interpolation (inverse distance) and geological

information is used. By using the geological information, interpolation over sharp geological boundaries of, for instance, tidal and fluvial channels is not allowed. Figures 3 and 4 show the effect of the geological information on the interpolation process.

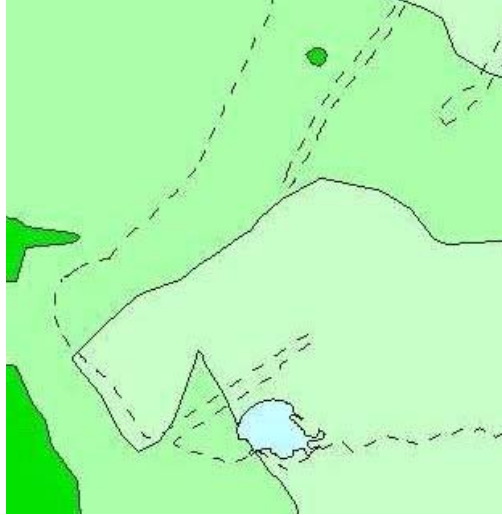


Fig. 3. Part of interpolated geological map without (geological) knowledge. The different colours indicate different geological formations.

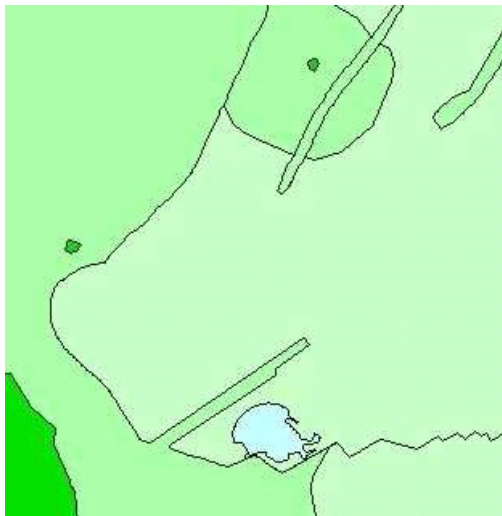


Fig. 4. Part of interpolated geological map using geological boundaries (knowledge). The different colours indicate different geological formations.

Table 2. Relative score shallow (fictive) building pit adjacent to building pit.

Soil type	Stiffness/strength	Thickness soil layer [m]		
		1 to 4m	4 to 8 m	≥ 8m
Clay	Soft/Weak	- / +	-	--
	Stiff/Moderately strong	- / +	- / +	-
	Very stiff/Strong	+	- / +	-
Sand	Dense/Moderately strong	+	+	- / +
	Very dense/ very strong	+	++	++
Peat		-	--	--

4.6 Validation

The initial suitability scores and maps have been tested on real designs of building pits and soil conditions within the province. In total 19 designs of various building pits have been used to test and validate the scores and maps. After this test, changes to the process were made to refine the outcome and to obtain a higher degree of accuracy and usability. Table 3 gives the translation of the suitability score into design aspects. Generally, the complexity of construction increases with the depth of construction. For this reason, the map at a depth of 10 m shows far more “fair” to “complex” and even “very complex” locations than the map at depth of 6 m.

Table 3. Relation between building pit design and suitability score.

Examples of building pit	Global suitability score
Concrete floor, light weight walls, no support or little support, no water drainage.	Very simple to simple
Concrete floor, light to medium weight walls, little single support no to little drainage.	Simple to fair
Underwater concrete or heavy drainage, medium weight walls, tension piles, single support.	Fair to complex
Underwater concrete and/or heavy drainage, high load tension piles, heavy weight walls, multiple support.	Complex to very complex.

4.7 Result

Although it is always possible to build underground constructions, at some sites underground construction is more difficult than at other sites. For instance, underground construction in the area in the southeastern part of the map in figure 5 is classified as ‘easy to very easy’. In this area, thick impermeable clay layers are encountered at a convenient depth below the bottom of the pit. In other areas this clay layer is absent or situated too deep; in those areas the suitability for underground construction decreases.

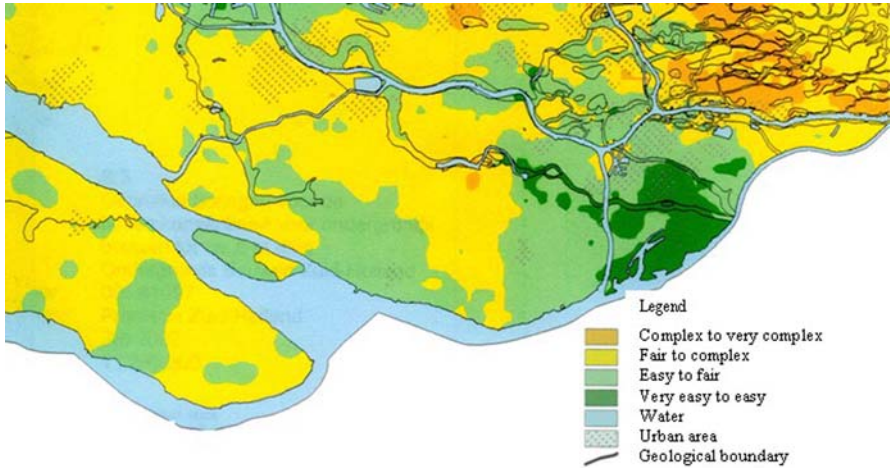


Fig. 5. Suitability map of part of the province of South-Holland at a depth of 10m.

5 Conclusions

In the (near) future, the use of the underground space will become more and more accepted in The Netherlands. Engineering geological maps that show the possibilities of the subsurface on a local and regional scale will be of great value to (urban) planning. For the province of South-Holland a set of maps was created that will not only be of use to urban planning but also to feasibility studies. The created maps of the suitability of underground construction in the province of South-Holland show a similarity with the geology and have a good validity. Furthermore the classes will give an indication of the type of design to be expected for the building pit and thus for the initial costs of underground construction.

References

- COB, Kansenskaart ondergronds Ruimtegebruik. Handreiking voor beleidsmakers, Gouda (2002).
- Maurenbrecher PM & Herbschleb J (1994) The Potential Use of Geotechnical Information Systems in the Planning of Tunnels for Amsterdam. *Tunnelling and Underground Space Technology* Vol. 9, pp 357-365.
- Trinity, A, Architecture art philosophy, *Underground Architecture and Construction*, Design Proposal for the Brewster Historical Society Athenaeum, <http://www.ceardach.com/architecture/underground.htm>. 2001.
- Varnes BJ (1974) The logic of geological maps, with reference to their Interpretation and use for Engineering purposes. U.S. Geological Survey Professional Paper 837.
- UNESCO (1976) *Engineering geological maps: a guide to their preparation*. UNESCO publishing.

- Weerts HJT, Wassing BBT & Herbschleb J (2002) Ondergronds bouwen in Nederland. Het gewicht van de bodem. *Civiele Techniek*, jaargang 57-2.
- Krajicek PVFS, Bakker JG, & de Lang FD (1984) Bisschops J.H. Ingenieursgeologische kaarten van Nederland, Geological Survey, Haarlem.
- Philippart MA (1990) Results of the pilot study of Ingeo-kaart Amsterdam. Proceedings of the Sixth International Congress of the International Association of Engineering geology.

Liquefied Natural Gas Terminal Siting in a Highly Seismic Region on the Mexican Pacific Coast

Yannick Zaczek and Nicolas Lambert

Tractebel Engineering, Avenue Ariane, 7, Brussels, Belgium
{Yannick.zaczek,nicolas.lambert}@tractebel.com
Tel: +32 2 773 70 69, +32 2 773 83 73
Fax: +32 2 773 79 90

Abstract. A new LNG terminal should be built on the Pacific coast of Mexico, one of the most seismic regions in the world. According to International codes, a siting process must be carried out to insure the feasibility of the project, which involves, in a first step, a data collection of all existing documents related to geology, seismicity, and geotechnics. As a second step, a seismo-tectonic study has been performed, with localisation of active faults on or close to the site (aerial and satellite imagery, geophysical investigations) and determination of OBE & SSE levels. Afterwards, the site was globally characterised, with a first geotechnical report, dealing with liquefaction risks, typical soil layers, and general foundation methodology. The general site layout, the general stability of buildings, the detailed soil investigations, and the detailed foundation design are performed in the phases as described in this paper.

Keywords: gas terminal, siting, LNG, earthquakes, geophysics, seismic risk, active faults.

Introduction

In 2003, the Tractebel Group has initiated the search for a new LNG terminal site on the Pacific coast of Mexico, one of the most seismic regions in the world. The candidate area has been located around the Lázaro Cárdenas harbour (Michoacán State) according to economic-strategic studies. Tractebel Engineering has been appointed to select one or more potential sites within the candidate area, following the siting process used for LNG (Liquefied Natural Gas) or NPP (Nuclear Power Plant) plants as prescribed by international codes to insure the feasibility of the project. After a description of the general siting methodology, presentation of the 2 first steps already carried out in 2003 is provided. The next steps of the siting process are going on in 2004.

Siting Methodology

The siting methodology is applied to a candidate area, which can be as large as hundreds of km², while the potential sites are of few km². The siting can be split

into 6 steps, as described hereafter. The first 2 steps can be developed without buying the land in order to assure the feasibility of the project. Indeed, there are hazards that can make the site rejected like active faults, wide karst, swelling clays or collapsible soils etc.

Phase 1. Data Collection

First, all available documents related to geology, hydrogeology, seismicity, and geotechnics are collected for the region including the candidate area. Secondly, site visits and visual inspection of buildings in the region are made. Meetings are organised with local companies to collect information about geotechnical data, foundation types and problems or damage due to previous earthquakes. No field or laboratory tests are carried out at this step. Geology, tectonics, earthquake activity and local foundation information are summarised and potential site(s) is (are) selected. This step is of relatively low cost and short duration.

Phase 2. Rejection Criteria

The potential site(s) has (have) not to be bought yet, but must be accessible for some field investigation. It (they) should be located more precisely in order to focus the investigation within the potential site area(s) and therefore limit the investigation cost. The first objective is to detect all geo-hazards that could make the site unsuitable. The geo-hazards could be large geological phenomenon like karst or important deposits of bad material like swellings clays or collapsible soils, but mainly tectonic accidents. Especially the active faults in the region are detected and potential sites are located outside of their influence. Satellite image and aero-stereo photos are interpreted to detect any evidence of faults (lineations) in the site region, prior to realise complementary geophysical investigations. When deep enough waterways are found close to the site(s), cheaper and faster offshore seismic tests can be conducted. The second objective is to evaluate preliminary values for the Operating Basis Earthquake (OBE) and Safe Shutdown Earthquake (SSE) levels on the site(s). The OBE is mainly an internal decision of the Owner while the SSE determination is ruled by international codes, such as NFPA59A and EN1473. Seismic risk analyses (probabilistic and deterministic) shall determine the SSE level, and help in OBE selection.

Phase 3. Global Site Characterisation

The site(s) should be located at few hundreds of meters accuracy and be accessible for soil tests. Type of buildings, typical loads, settlement criteria and earthquake levels must be established. Detailed review of the earthquake level shall be carried out in order to issue accurate OBE and SSE levels to be applied for the site qualification. During this step, field tests (e.g.: borings, CPT, pressuremeter tests) are

realised on site to characterise the typical soil layers affected by the construction. Liquefaction risk, bearing capacity, settlement, and any geotechnical hazard detection are estimated. A general foundation methodology (shallow or deep foundation, soil improvement...) shall be issued.

Phase 4. General Stability

The general stability of the buildings is studied, taking into account general layout, seismic and geotechnical data. The layout, sizes and loads of the buildings (including the tanks) are adapted in consequence, for both static and dynamic conditions; settlement criteria of BS7777 must be followed. Displacements of the buildings during earthquake must be controlled. Typical piles and soil improvement methods shall be established, and finally, general cost estimates are elaborated. No geotechnical tests are carried out in this phase.

Phase 5. Site Characterisation

The site must have been bought now. Soil investigation (geotechnical, geophysical, cross-hole borings) is realised on a regular grid mesh covering the building areas in order to elaborate geotechnical report, to be used for the project design and to elaborate LNG plant budget. The plant layout can be adapted, and technical specifications for foundations and soil improvements are issued according to this report.

Phase 6. Detailed Soil Investigation

The plant layout must be fixed and approved. Detailed soil investigations are carried out either to analyse local soil hazards or to elaborate very specific foundation design. The better the site characterisation is detailed, the less important is this last step of the study.

Lazaro Cardenas LNG Site

The first two steps followed for the Lázaro Cárdenas site have been developed into the data collection and the sub-steps needed to verify the rejection criteria.

Data Collection

During several trips in Mexico City and in Lázaro Cárdenas, geology and tectonics maps & documents, aerial photographs, earthquake data and reports, soil data and foundation information have been collected from University departments

(UNAM – Universidad Autónoma de México), from official Mexican institutions (INEGI, SMSS) and from local contractors/companies. All companies located within a 10-kilometre radius around the potential site have been visited to review the foundation types, the damage due to previous earthquakes, and to collect geo-technical/soil test reports. Specific data have been collected about major historical earthquakes around Lázaro Cárdenas (e.g. 1985 – thousands of people were killed). These data have been collected in local seismological centre, but also in La Villita dam, Petacalco power plant, Carbonser coal storage, where accelerometers are placed.

Geological and Tectonical Study

The Lázaro Cárdenas region is governed by the subduction of the Cocos Plate underneath the North-American plate. The main tectonic features are the Mid-America Trench (subduction of Cocos plate below the North-American plate), the East Pacific Rise (accretion zone, normal shallow faulting, some intermediate magnitude events), the Orozco Fracture Zone (slip faulting) and the Trans-Mexican Volcanic Belt. Seismicity is induced by the subduction of Cocos Plate underneath the North-American plate:

- Small to large earthquakes are due to shallow thrust faulting at the Mid-America Trench interface located more than 50 km offshore in the Pacific ocean. They are the most frequent ones with the largest magnitudes and at a depth smaller than 50 km.
- Deeper earthquakes (depth over 80km) occur in normal faulting within the subducted slab. They are generally of smaller magnitude, but of high intensity on the continental area because they are closer.

Very high magnitude event have already occurred ($M_w = 8.1$ in 1985, 8.2 in 1932). Twenty events ($M_w > 7.0$) have been recorded during the last century. A preliminary seismic spectrum has been computed using CRISIS95 software, taking into account attenuation laws for subduction, intermediate depth and crustal earthquake as well as the seismic zones of Mexico. The calculated Peak Ground Acceleration (PGA) is estimated around 0.7 g. Due to the presence of quaternary deposits related to the Balsas River delta on the potential sites, fault information does not appear in geological study. Anyway, morphological features, seismicity alignments and the occurrence of uplifted marine terraces in the vicinity of Lázaro Cárdenas indicate the possible presence of faults.

Analysis of Satellite and Aerial Imagery

Aerial photographs and SPOT satellite image have been analysed in order to detect faults and lineaments (see figure1). As expected from the geological study, lots of faults and lineaments have been evidenced. However, due to the presence of Quaternary sediments, no faults or lineaments appear below the city of Lázaro

Cárdenas and below the harbour. Even if no significant lineation has been detected towards the potential sites, it was unfortunately not possible to conclude, at this stage, that no fault is present below or in the vicinity of the possible terminal sites (see hatched areas on figure 1).

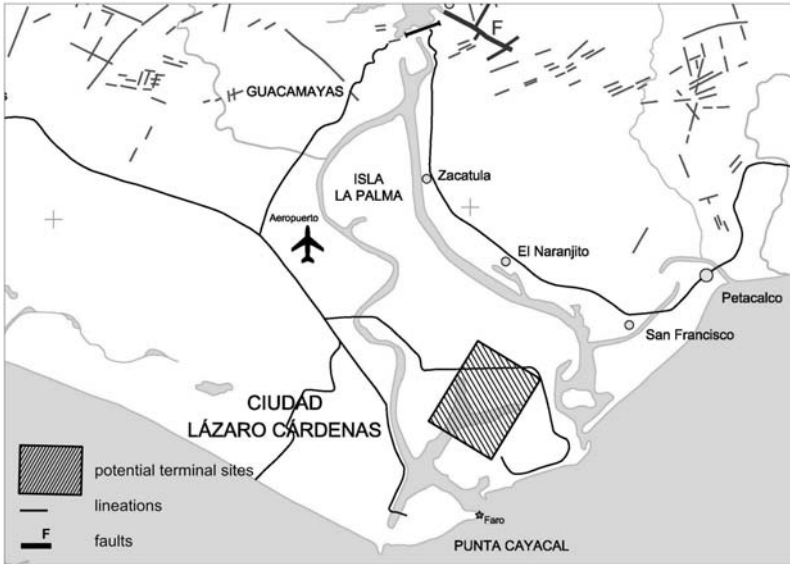


Fig. 1. Potential site and lineations detected by aerial and satellite images.

Magneto-telluric Survey and Gravimetric Profile

Some Acoustic Magneto Telluric (AMT) tests have also been realised on the site (figure 2) in order to confirm or discard the presence of faults below the potential site and to evaluate the bedrock depth (around 250m deep). The AMT results have also allowed power adjustment of the ignition shot for the offshore seismic tests. Tests have been located along a North to South profile, taking into account accessibility and available surface. An open area of at least 50 x 50 m² is needed for the AMT tests.

AMT tests are providing a profile of the electrical resistivity of the soil, while gravimetry is used to detect mass anomalies regarding to the normal gravity. Like AMT survey, a microgravity profile has also revealed bedrock dipping continuously towards the ocean (Southern border). According to the gravity profile, no geological fault appears in the area of interest. The resistivity profile, interpreted in terms of geological units (see figure 3), also shows a dipping basement from North to South. However, the basement rises anew from test point LCA-01 towards the south, leaving the possibility of a buried channel or accident to the north of this test point.

According to these tests, the basement could be as deep as 400 metres.

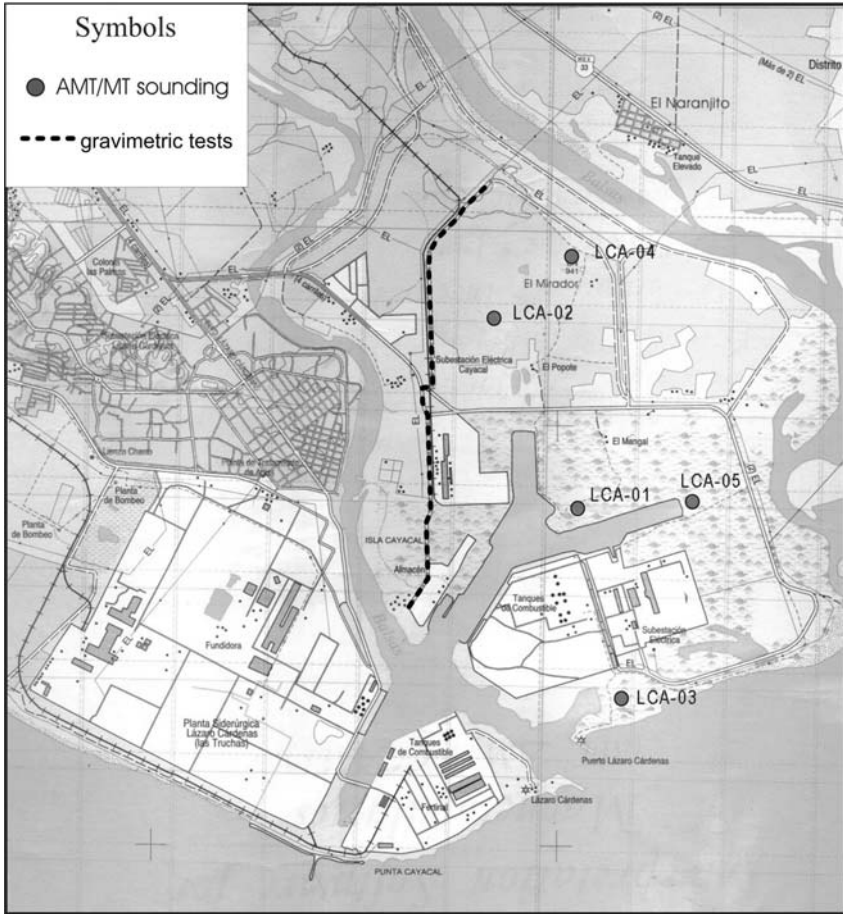


Fig. 2. Location of AMT and gravimetric tests.

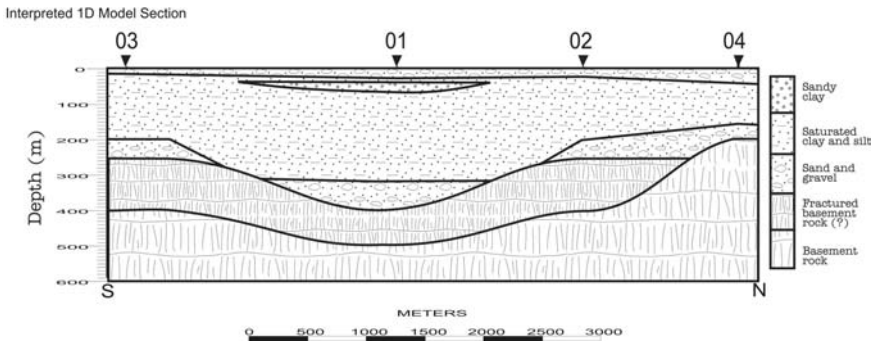


Fig. 3. Soil profile deduced from AMT tests.

Seismic Reflection Survey

In February and March 2003, a high-resolution offshore seismic reflection survey has been performed in the ocean and inside the Lázaro Cárdenas harbour. The purpose of that survey was, once more, to verify the presence of faults below or in the vicinity of the possible sites. Approximately 50 km of data were collected with sparkler and bubble pulser sound sources. These devices were pulled by a boat, together with a hydrophone streamer that collects the reflected waves. The sparkler produces pulses with higher energy and lower frequencies, allowing greater penetration than the bubble pulser, but with a lower resolution. Precise position of the ship was determined by using a GPS and stored with the reflection data. Pulses were fired at a rate of 4 shots per second (bubble pulser) or every 1.5 s (sparkler). Surveyed profiles are plotted on fig. 4.

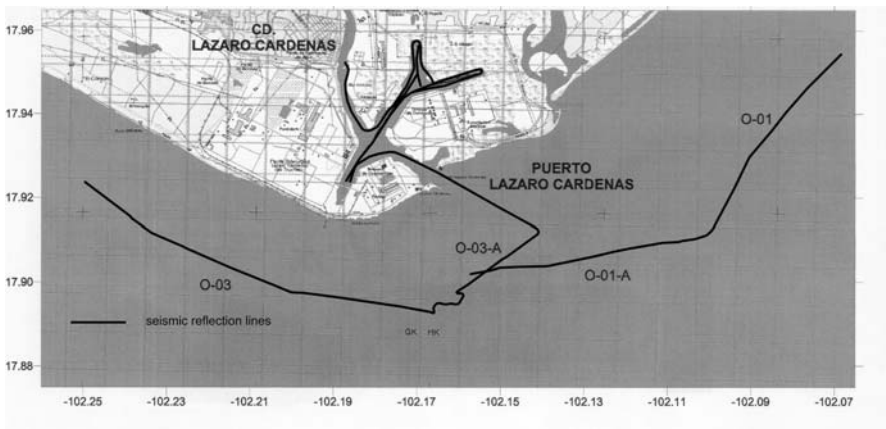


Fig. 4. Seismic Reflection lines.

Data have been processed to remove dead traces, and random, high amplitude noise bursts. Filters have been applied (band pass-notch filter, DC bias removal, early mute procedure, spherical divergence correction, automatic gain control, instantaneous phase). Based on this, it has been deduced that two major soil sequences can be found in the harbour: the upper one consists in unconsolidated sediments, the lower one being the pre-deltaic rocks (basement), consisting in parallel rock/sediment layers. Faults have been located in the basement (disruptions). However, near the possible sites, these faults appear to be non-active nowadays, because they do not cut through the Quaternary sediments. The basement gently dips southward, but several channels (erosion) have been detected in the basement close to the possible sites. The unconsolidated sedimentary sequence can be divided into two parts: a five-metre thick top layer composed of clastics and muds (continuous internal reflectors), and another layer composed of sands and gravels (discontinuous to chaotic reflectors). The thickness of sediments increases southward and should be less than 100 metres (to be confirmed by drill-

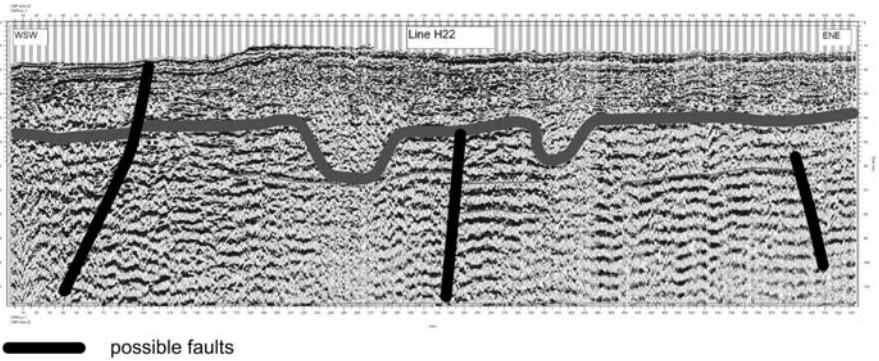


Fig. 5. Interpretation of one seismic profile.

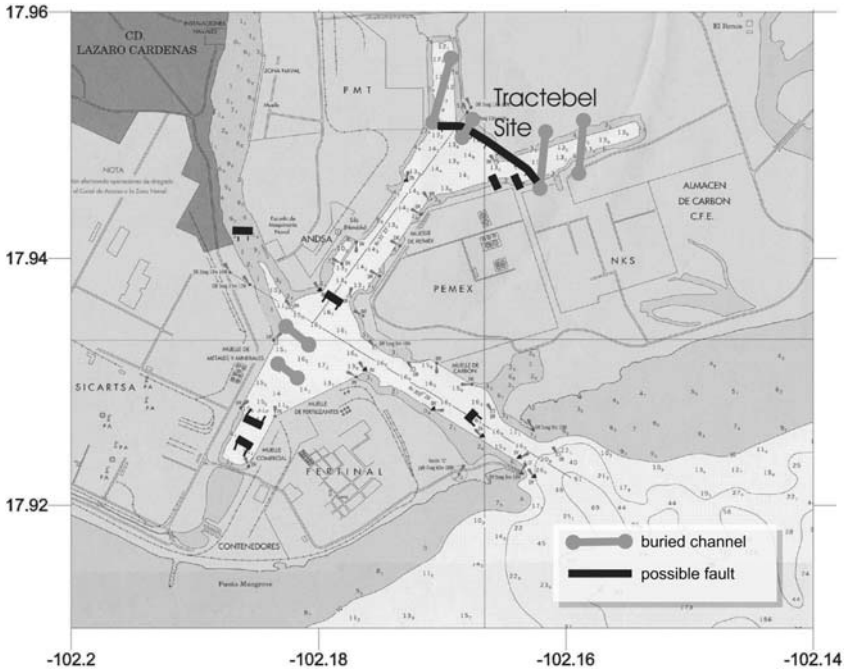


Fig. 6. Location of buried channels and small faults or accidents by seismic reflection.

ings). Around possible sites, unconsolidated sediments should be limited to 45 – 70 metres (80 metres within the channels) by a highly compacted clay layer.

A possible active fault has been detected (see figures 5 and 6) close to the possible sites. However, the data indicating that fault could be due to effects of dredging works within the harbour. This possible fault should be a local accident since it has not been discovered in the surrounding profiles. It should be confirmed by additional tests.

Conclusion

At this stage, the following conclusions can be drawn:

- A potential site has been selected without hazards that could make the site rejected.
- At the potential site, the subsoil seems to be composed of 45 to 70 (locally 80) metres of unconsolidated sediments (clastics and muds, sands and gravels), lying on rock basement.
- A possible fault has been detected close to the possible sites. Anyway, its presence should be confirmed by additional tests. In any case, it seems that this fault is far enough from the tank sites and would not prevent the construction of the terminal.
- Preliminary Peak Ground Acceleration value and hazard spectrum for Operating Basis Earthquake (475-year return period) have been computed. The PGA of 0.7 g is very important but is in agreement with the very high seismicity in the region. Anyway, detailed probabilistic and deterministic analyses of the seismic hazard still have to be performed to confirm the OBE values and to determine the SSE values.
- Based on the previous items, the siting process (site characterisation, general and detailed stability, and general and detailed soil investigation) can be continued after administrative actions.

National Environmental Monitoring of the Slovak Republic – Part Geological Hazards

Alena Klukanová and Pavel Liscak

Geological Survey of the Slovak Republic, Mlynská dolina 1, 817 04 Bratislava, Slovakia
{klukan,liscak}@gssr.sk

Tel: +4212 59375162

Fax: +4212 54771940

Abstract. The Concept of the National Environmental Monitoring of the Slovak Republic defines the environmental monitoring as a systematic, spatially and temporarily defined observation of precisely defined attributes of the environmental components or influences upon the environment (usually in monitoring network points). To a certain degree of reliability the Concept is able to characterise given areas under study and, to a higher level, a larger region within the Western Carpathians. The National Environmental Monitoring consists of 10 essential systems. One of them is Monitoring of Geological Hazards. It is co-ordinated by the Geological Survey of the Slovak Republic. Thematically it is focused on those geological factors and outputs, which seem to be convenient as the input data for issues of protection of the environment and for optimum utilisation of Slovakia territory geopotentials. The monitoring serves for observations and assessment of the mechanisms of negative changes within the rock environment. Recently, Monitoring of Geological Hazards consists of 13 autonomous subsystems, defined according to different types of the influencing geological process activated by natural or artificial factors.

Keywords: environmental monitoring, geological hazards, slope deformations, erosion, weathering, volume unstable sediments, neotectonic activity, stream sediments, radon activity, information system.

Introduction

Among general terms at the accession process of the states of Central and Eastern Europe into the European Community, the acquisition of quality data about the environment at a national level, their processing into system information and mutual exchange of information play a major role. Taking into account, that there until the nineties of the last century there was no complex monitoring system of the environment within the Slovak Republic, the Slovak Government by its Resolution Nr. 623 dated 21st December 1990 directed to the former president of SK P (Slovak Commission for the Environment) to elaborate a concept of the monitoring of the territory of the Slovak Republic in co-operation with involved ministries, including its organisational, technical and financial support. The Government of the Slovak Republic approved this concept by its Resolution No 449 dated 26th May 1992. The government directed to the ministries to realise a territory

monitoring system of the Slovak Republic and partial monitoring systems in terms of designed projects. Further, the Minister of the Environment was directed to inform annually by 31st March the Government on the advance of the realisation of the monitoring and information system of the environment. By the Resolution of the Government of the Slovak Republic Nr. 620 dated 7th September 1993 directed the Ministry of Environment of the Slovak Republic, Ministry of Agriculture of the Slovak Republic and Ministry of Health of the Slovak Republic to safeguard the performance of the functions of the centres of partial monitoring systems and to co-ordinate the realisation of the partial monitoring systems and partial information systems. This concept is based upon two essential ideas: firstly, realising of the actual state of performance of previous tasks, which have been carried out in terms of the Concept of the Monitoring System of the Environment of the Slovak Republic and secondly the Concept of Integrated Information System of the Environment of the Slovak Republic from 1992, and, those requirements, which the Slovak Republic is obliged to fulfil in preparedness process for European structures. The Information system is closely linked with the monitoring system. The monitoring and information systems have to be perceived as important tools for safeguarding of the environment protection and creation. Simultaneously, they provide a fundament for decision-making about recent activities, as well as about further perspective intents in the environmental disciplines. The realisation of the territory monitoring system of the environment SR itself was established on organizational and methodological unification in the frame of single partial monitoring systems and their mutual harmonisation. By the harmonisation of individual monitoring activities, performed in the frame of available sources it is possible to reach a substantial step forward in the state of the art and trends of the environment issues on the territory of the Slovak Republic.

National Environmental Monitoring of the Slovak Republic

The Concept of the National Environmental Monitoring of the Slovak Republic and the Concept of Integrated Information System on the Environment of the Slovak Republic define the environmental monitoring as a systematic, spatially and temporarily defined observation of precisely defined characteristics (attributes) of the environmental compounds or influences upon the environment (usually in monitoring network points). To a certain degree of reliability the above concepts are able to characterise a given area and, to a greater degree a larger region with similar environmental conditions. The main objective of the monitoring is observation of a certain phenomenon, or chosen parameter in precisely defined temporal and three-dimensional conditions. Monitoring serves for objective knowledge of characteristics of the environment and evaluation of their changes in monitored three-dimensional space. Recently, the National environmental monitoring of the Slovak Republic consists of the following 10 essential systems: Atmosphere, Meteorology and climatology, Water, Geological factors, Biota (fauna and flora), Wastes, Radioactivity of the environment - the Guarantee is the Ministry of Environment of the Slovak Republic (ME SR); Soil, Forests, Contaminants

in edibles and forages – the Guarantee is the Ministry of Agriculture of the Slovak Republic (MA SR). The performance and co-ordination of monitoring activities in the frame of individual partial national environmental monitoring systems provide Centres of Partial Monitoring Systems (PMS). The PMS Geological Hazards centre is at GS SR.

Partial Monitoring System of Geologic Hazards of the Environment

The Concept of Partial Monitoring System - Geological Hazards is derived from the Concept of the National Environmental Monitoring of the Slovak Republic. Thematically it is focused on those geological factors and on such outputs, which seem to be convenient as the entry data for issues of protection of the environment and for optimum utilisation of geopotentials of the country. The monitoring is focused mainly on geological hazards, harmful natural or anthropogenic processes, which jeopardise the environment, as well as humans. The monitoring serves for observations and assessment of the mechanisms of negative changes in the geological environment. Recently, Partial Monitoring System of Geological Hazards consists of 13 autonomous subsystems, defined according to the different type of the influencing geological process activated by natural or artificial factors. Each subsystem is solved individually, but the optimum solution is a mutual link among several subsystems in such a way, that individual measurements complement each other and provide sufficient data to obtain an optimum image of the state of the rock environment as a whole. The selection of monitoring sites, frequency of sampling and data collection, as well as the many ways of rock sample testing and acquisition of data are subdued to this essential philosophy. Table 1 provides information on the fundamental structure and content of the Partial Monitoring System of Geological Hazards. Localisation of the sites solved in the frame of PMS Geological Hazards is on Figure 1. The results of the monitoring from the period 1993 to 2001 are presented in the Final report Partial Monitoring System of Geological Hazards of the Environment SR (Klukanova et al. 2002) and in the monothematic issue *Geologické práce, Správy 106* (Klukanova ed. 2002). Among the most significant results of the long-term observations we have to mention: In the frame of **monitoring of slope deformations** the sites Velka Causa, Handlova, Lubietova, Fintice, Okolicne (Fig. 1) are jeopardised by slope movement activation. The real threat to inhabitants and their property have led to the extension of the monitoring network. On the other hand, the frequency of measurements at the sites Bojnice, Diviaky, Dolna Micina could be reduced and at the sites Slanec and Harvelka even minimised. Regarding the state of disrepair of several sites we propose to incorporate them into the system (Wagner et al. 2002). The most distinct activity of the **erosion processes** has been observed at the Novaky site – 2,32 km of erosion gullies per 1km² (Ondrasik 2002). The most intense **weathering process** has been monitored within the section of the road-cut from Harmanec to Sturec. Here, the retreat of the rock massif in dolomites reached a

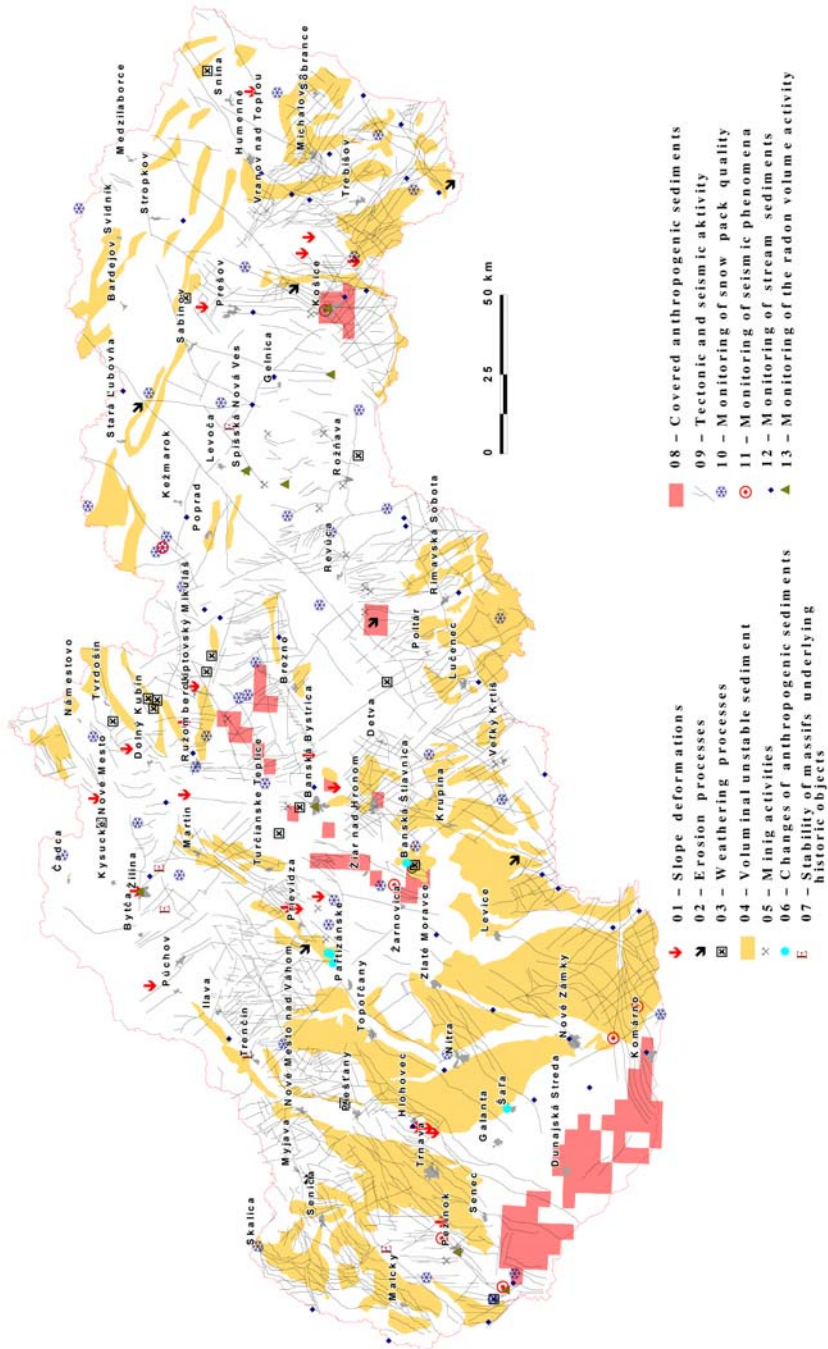


Fig. 1. Schematic map of monitoring localities.

Table 1. Structure and content of the territories solved in the frame of National environmental monitoring of Slovak Republic - Part Geological Hazards.

N ^o	Name of subproject	Solved issue
01	Landslides and other slope deformation	Continuous site monitoring of selected sites at exactness level corresponding to the site significance and its localisation within regional geological units. Extrapolation of acquired results to territories with analogous geological setting and climatic conditions according to defined criteria. Monitoring of territories prone to hazardous landslides and verification of corrective measures issues.
02	Erosion and abrasion processes	Study of genesis, trends and dynamics of processes influencing the relief evolution at present geomorphologic cycle with consequences on changes due to construction impact.
03	Weathering processes	Issues of road-cuts stability influenced by contribution of weathered material from non-protected rocky walls
04	Volume unstable sediments	Issues of behaviour of volumetric unstable sediments, in which due to over-moisturising normal over-load deterioration of their structure and volume changes take place
05	Influence of minerals exploitation upon environment	Identification and monitoring of environment damage due to mining activities (manifestations of undermining and sinking of territory, cave-ins, changes in hydrogeologic water regime, chemical composition of waters in the vicinity of deposits and treatment plants).
06	Changes of anthropogenic sediments	Study of changes in fine-grained materials of tailings of various origin.
07	Stability of massifs underlying historic objects	Study of the activity of slow slope gravitational phenomena, evaluation of causes of their origin and specification of secondary influences (climatic).
08	Covered anthropogenic sediments	Identification of empty spaces after exploitation filled with wastes of various types: communal and industrial wastes, materials from mining and treatment activities.
09	Tectonic and seismic activity of the territory	Territory monitoring and assessment of movements activity of geological structures and of the relative rate of movements along faults.
110	Monitoring of the snow pack quality	Territory evaluation of chemical composition of the snow pack in Slovakia focusing on its influence on accumulation of reserves and chemical composition of groundwater, acidification of soils, degree and character of contamination of the environment of SR.
111	Monitoring of seismic phenomena on the territory of SR	Continuous registration of seismic events on the territory of SR.
112	Monitoring of active alluvial sediments	Monitoring of anthropogenic loads of active river sediments and their influences upon the quality class of surface streams.
113	Monitoring of the radon volume activity	Radon contained in soils is monitored in selected cities with prognosis of increased radon risk, radon in waters of selected mineral and thermal springs, radon along faults.

mean annual value of 19,24 mm per year (Janova and Liscak 2002). Failed objects have been identified on the territory of the Podunajska nizina Lowland, where the buildings are founded in 72 municipalities upon the **volume unstable sediments**. On the territory of the Vychodoslovenska nizina Lowland similar failures are known from 54 municipalities (Klukanova and Frankovska 2002). It is supposed that the changes of the properties of **ashes from tailings** take place due to their gradual compaction and hydration. The change of their mineralogical composition plays also an important role (Matys 2002). The measurements are carried out on the church (**historic objects**) in Kostolany pod Tribecom using the SOMET gauge. In the last quarter 2000 the recorded settlement of the tower of the church reached 3,03 mm (Vlcko et al. 2002). In accordance with new knowledge on old ecological loads new ways of **covered anthropogenic sediments** sites assessment were elaborated (Kovacikova 2002).

The results of the **monitoring of neotectonic activity** have confirmed a vertical tendency of the surface movements in the territory of Slovakia, namely slow uplifts of the central parts, Carpathian Flysch and Klippen Belt in the section from Bytca to Bardejov and sinkage of western and eastern part of the Inner Western Carpathians, as well as the prevailed sinkage of the rest of the Flysch and Klippen Belt (Hrasna 2002). In the frame of the **snow pack quality monitoring** global and local influences on the chemical composition of snow and relations among individual ions have been identified. Global influences are typical mainly for so-called mountaineous sites like Certovica, Chopok-S and N, Donovaly, Lomnický štít, Tatranska Lomnica, Skalnaté and Strbské pleso. The local influences are typical for so-called lowland areas Bratislava and its surrounds, Patince, Prievidza-Handlova, Ziar, Vojany etc. (Bodis et al. 2002). From 1.1.1995 to 31.12.2000 35 **earthquakes** were macroseismically observed, of this number, 29 had their epicentre in the territory of Slovakia. Seismometry identified and localised 18 micro-earthquakes (magnitude > 2.5-3) with their epicentre in the territory of Slovakia (Cipcjar et al. 2002). In the frame of monitoring of **active stream sediments** the most contaminated areas are Nitra-Chalmovec, Stiavnica-mouth into Ipelský Sokolec, Hornád-Kolinovce, Hnilec-inlet into the Ruzin reservoir. They are influenced mainly by the anthropogenic activities past and recent mining metallurgical industry, which has led to distinct increased contents of Cu, Zn, Hg, Cd above the valid limit values (Bodis et al. 2002). The radon contents are subdued to seasonal variable changes. These changes will lead to their incorrect interpretation, and hence blunders could occur while assessing the radon risk of the sites measured (Smolarova, 2002). **Partial Information System** of geological factors serves for data collection and storage. Supported by a unified approach in data processing in the form of Geographic Information System (GIS) a complex set of information on the negative effects of geological factors on the environment has been created (Iglarova and Paudits 2002).

References

- Bodis D., Lopasovska M., Lopasovsky K., Rapant S.: Monitorovanie kvality snehovej pokrývky (*Monitoring of Snow Pack Quality*). Geologicke prace. Spravy 106. Vyd. D.Stura, Bratislava, pp.115-121, 2002.
- Bodis D., Rapant S., Slaninka I., Kordik J.: Monitorovanie kvality riecných sedimentov (*Monitoring of Stream Sediments Quality*). Geologicke prace. Spravy 106. Vyd. D.Stura, Bratislava, pp. 133 –138, 2002.
- Cipcjar A., Labak P., Moczo P., Kristekova M.: Monitorovanie seizmických javov Národnou sieťou seizmických staníc (*Monitoring of Seismic Phenomena by National Seismic Stations Network*). Geologicke prace. Spravy 106. Vyd. D.Stura, Bratislava, pp.123-132, 2002.
- Hrasna, M., 2002: Tektonicka a seizmicka aktivita uzemia (*Tectonic and Seismic Activity of the Territory*). Geologicke prace. Spravy 106. Vyd. D.Stura, Bratislava, pp.103-114, 2002.
- Iglarova L., Paudits P.: Parcialny informacny system (*Partial Information System*). Geologicke prace. Spravy 106. Vyd. D.Stura, Bratislava, pp.15-19, 2002.
- Janova V., Liscak P.: Monitoring procesov zvetravania (*Monitoring of Weathering Processes*). Geologicke prace. Spravy 106. Vyd. D.Stura, Bratislava, pp.53-60, 2002.
- Klukanova A., Frankovska J.: Objemovo nestále zeminy a ich vlastnosti (*Volume Unstable Sediments and Their Properties*). Geologicke prace. Spravy 106. Vyd. D.Stura, Bratislava, pp. 61-68, 2002.
- Kovacikova M., 2002: Antropogenne sedimenty pochovane (*Covered Anthropogenic Sediments*). Geologicke prace. Spravy 106. Vyd. D.Stura, Bratislava, pp.97-102, 2002.
- Matys M.: Zmeny antropogenných sedimentov v odkaliskach (*Changes of Anthropogenic Sediments in Tailings*). Geologicke prace. Spravy 106. Vyd. D.Stura, Bratislava, pp.123-132, 2002.
- Ondrasik M.: Monitoring erózných procesov – hodnotenie vymolovej erózie z leteckých meracských snímok (*Monitoring of Erosion Processes – Assessment of Gully Erosion by Air-Bound Photos*). Geologicke prace. Spravy 106. Vyd. D.Stura, Bratislava, pp.43-52, 2002.
- Smolarova H.: Monitorovanie radonu v geologickom prostredí (*Monitoring of the Radon Volume Activity within Rock Environment*). Geologicke prace. Spravy 106. Vyd. D.Stura, Bratislava, pp.139-145, 2002.
- Vlcko J., Petro L., Baskova L., Polascinova E.: Stabilita horninových masív pod historickými objektami (*Stability of Massifs Underlying Historic Objects*). Geologicke prace. Spravy 106. Vyd. D.Stura, Bratislava, pp.89-96, 2002.
- Wagner P., Iglarova L., Petro L., Scherer S.: Monitorovanie zosuvov a iných svahových deformácií (*Monitoring of Landslides and other Slope Deformations*). Geologicke prace. Spravy 106. Vyd. D.Stura, Bratislava, pp.21-42, 2002.

Stability and Subsidence Assessment over Shallow Abandoned Room and Pillar Limestone Mines

Roland F. Bekendam

GeoControl, Meidoorn 93, 6226 WG Maastricht, The Netherlands

geocontrol@planet.nl

Tel: +31 43 3628523

Fax: +31 43 3628524

Abstract. In the region of Maastricht, both in The Netherlands and in Belgium, many areas are underlain by abandoned room and pillar mines, which have been excavated in weak limestone to produce building stone. Several of these mines are kept open now to serve as an important tourist attraction. However, there have been both local and large-scale collapses up to the present, resulting in extensive surface subsidence, faulting, and sinkhole formation. For many mines the stability needs continuous attention. Depending on rock overburden thickness, mine span and density of joints, different collapse and subsidence mechanisms can apply. This contribution describes these mechanisms and then concentrates on how to assess the potential of a large-scale pillar collapse of a room and pillar mine. This quantitative assessment is based on short- and long-term laboratory tests on model pillars, numerical experiments and numerous field observations, taken during more than 20 years. Only taking the stability of individual pillars into account cannot assess the collapse potential of a mine. Particularly large-scale pillar stability, which considers the load carrying capacity of all pillars together, and general mine stability, which concerns the arching capacity of the overburden, are important. In the recent past, the method was applied successfully to several mines, in order to investigate the necessity of underground support measures to protect existing infrastructure and planned infrastructural projects. It is expected that at least a major part of the method applies to shallow room and pillar mines in other regions and rock types.

Keywords: subsidence, room and pillar mines, large-scale collapse.

1 Introduction

The limestone has been mined underground since the Middle Ages, mainly to produce building stone. The rock is of Maastrichtian age (Upper Cretaceous) and can be characterised, at the mined levels, as a calcarenite of high porosity (40-50%). The low strength (UCS generally of 1.5-3 MPa) allowed mining by means of handsaws, picks and chisels. At present, the building stone is mined only in one underground quarry using electric chainsaws. In the Dutch and Belgian provinces of Limburg at least 300 room and pillar mines exist, which range in size from a few galleries to labyrinths of 85 hectares (Fig. 1.1). Contrary to many other areas,

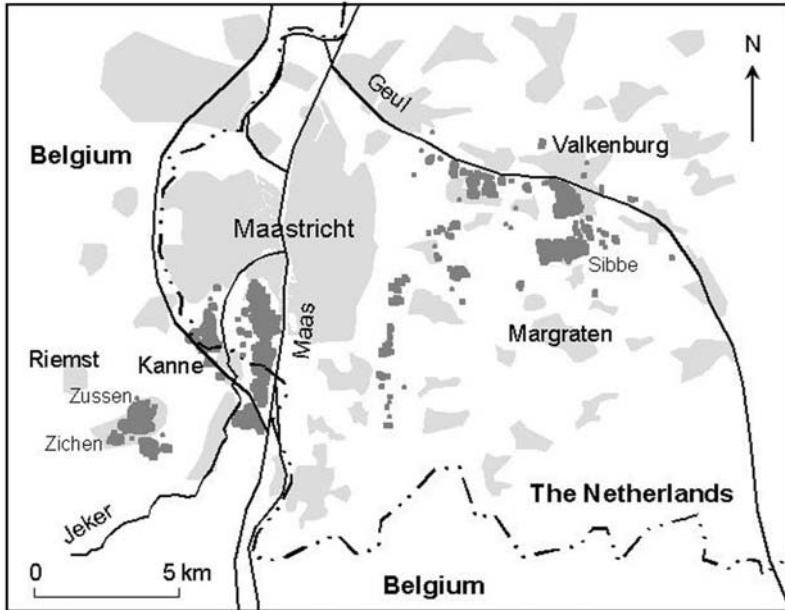


Fig. 1.1. The area of Limburg, underlain by room and pillar limestone mines (indicated by dark-colored zones; Courtesy of J Orbons).

in Limburg more or less all limestone mines are known and have been mapped at a reasonable degree of accuracy. The limestone was mined at levels relatively free of flint nodules, and roof and floor are normally formed by hardgrounds, locally known as “tauwlagen”. In most mines the pillar height varies between 2 and 3 m, but often the hardground was excavated to exploit deeper levels. In this way up to more than 15 m high mine systems resulted. The floor of most mines is covered with some dm to m of pulverised waste rock material, remaining from the excavation. This material has been compacted in the course of time and is now stabilising the pillars with its lateral support. The pillars are generally rectangular and show horizontal dimensions of typically 4 to 20 m (Fig. 1.2). According to the variation of the level of organisation of the exploitation and of the local geology (joints, faults, earth pipes), in some mines the room and pillar pattern is fairly regular, while in other ones pillar outlines are highly irregular. Joints, mostly subvertical, exist, but not at regular intervals. Their spacing is usually tens of meters and their persistence rarely exceeds 200 m. Faults are relatively rare.

The direct rock overburden is mostly 5 to 30 m thick, but some mines, especially in Belgium, show a limestone roof of just a few dm thickness. The limestone is overlain by clayey sands, gravels and loess deposits of the Tertiary and Quaternary. The total overburden thickness does not exceed 50 m in general. The now abandoned mines, often containing paintings, drawings and sculptures, are of great historical and cultural value, and their touristic exploitation (at least 500,000 visitors per year) is economically important for the region. The stability of the

mines is not only important because of the touristic exploitation but also because of the location of a number of these excavations below buildings, roads and other surface structures. Mine collapse and surface subsidence can develop in several ways, which is dealt with in the next section. This paper concentrates then on the assessment of the potential of a large-scale collapse as a result of pillar instability, because, of all types of collapse, its consequences are felt in the most extensive area both underground and at the surface.



Fig. 1.2. The Heidegroeve near Valkenburg before the collapse of 1988. Two mining levels can be distinguished separated by a hardground. The total pillar height is 4.6 m (Courtesy of J Silvertant).

2 Outline of the Stability Problems of the Mines

2.1 Types of Local Instability

In this paper, local instability is distinguished from large-scale instability. Local instability only affects one pillar or gallery, while large-scale instability involves a whole mine or a major part of it. Three major types of local instability can be recognized (Bekendam 1998; Fig. 2.1):

1. *Instability of pillars.* If the average vertical stress on a pillar exceeds its strength, pillar cracking, starting at the top and bottom edges, and spalling occur. At a certain amount of strain pillars are separated into an hourglass shaped core and parted pillar sides. Such a pillar is denoted as completely failed (fig. 2.2). However, such a pillar still has some residual strength. Joints may weaken a pillar. The amount of strength reduction depends on the position and

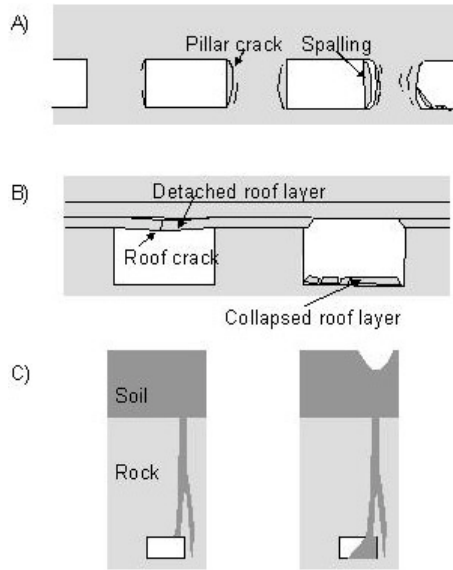


Fig. 2.1. Three main types of local instability: a) pillar cracking and spalling b) failure and collapse of immediate roof layers c) earth inflow from organ pipes.

orientation of the joints relative to the pillar boundaries. Local pillar deterioration normally does not represent an acute danger to people in the mine, except when large slabs threaten to fall into the gallery.

2. *Instability of the roof.* Immediate roof layers may tend to detach from the main roof and then collapse into the gallery at an unpredictable moment. Several collapse modes have been observed. Often detached roof layers cannot be recognized visually by downward deflection and tensional cracks. Gentle “tapping” with a steel rod against the mine roof (only by experienced miners!) is a well-known method to detect dangerous roof conditions. As for pillars, joints may reduce roof stability. Particularly near the mine entrance, where both the rock and soil overburden are thin, plant roots may invade the mine through joints and weaken the immediate mine roof. Widening of the joint planes due to karst facilitates the growth of plant roots. In the Geulhemmer Groeve interbedded clay layers, marking the Cretaceous-Tertiary boundary, have weakened the roof, resulting in many roof collapses. For people inside the mine roof falls represent the major hazard. Many miners were killed or severely injured, when they were excavating the limestone.
3. *Earth inflow from organ pipes.* More or less vertical and cylindrical solution pipes, filled with soil material from the layers on top of the limestone, often extend some tens of meters into the rock. Once intersected by a gallery, the earth may flow into the mine, until a cone has been formed at an angle of about 40° . People inside the mine could be trapped by the invading earth, but this has not happened until now. Organ pipes locally reduce pillar stability.



Fig. 2.2. A completely failed pillar with an hourglass geometry.

Local instability may extend both laterally and vertically, with surface subsidence as one of the consequences.

2.2 Consequences of Local Pillar Instability

The vertical strain of a failed pillar, reduced in strength, is often limited due to stress transfer to surrounding pillars, and collapse, i.e. compression of several dm to m and disruption does not occur. However, due to this load transfer other pillars may start to fail as well. By this domino effect pillar failure may affect a whole mine or a major part of it. Downward deflection of the main roof is maximal in the centre of the mine, and shortening of the failed pillars, and thus pillar damage, is often observed to increase from the boundary towards the centre. Eventually a sudden large-scale collapse may result and in a few seconds several hectares of a mine system are destroyed. Creep deformation must be of importance, because several collapses occurred tens of years or even more than 100 years after the end of the excavation. In Limburg, at least ten of such events have occurred in the past. The most recent collapse happened in 1988 in de Heidegroeve near the Dutch

town of Valkenburg (0.5 hectares; Price, 1990). Fortunately, nobody was injured because the mine was closed and abandoned at that time. The most tragic collapse (4 hectares) was in 1958 in the Roosburg mine near the village of Zichen in Belgium, when 18 persons, working in the mine as mushroom-growers, were killed. On the short term (weeks, months), such collapses are preceded by a striking acceleration of pillar- and roof-fracturing and spalling, by cracking sounds and by rock dust falling from the roof.

Field studies revealed the existence of two types of large-scale pillar collapse (Fig. 2.3). The most common type is characterised by downward movement of the rock overburden along collapse-induced faults at the collapse limit. These faults dip towards the area still standing and intersect the whole rock overburden. The overlying soil flows into the rock depression, and a subsidence trough is formed according to an angle of draw of about 45° , bounded by sinkholes and extensional faults with vertical offsets of up to more than one meter. The other type of collapse occurs by mere deflection of the rock overburden, without disruption over its full height at the margins. This type was observed at two collapses of relatively wide, more than 150 m, mined areas. The surface expression is more or less the same as for the first type.

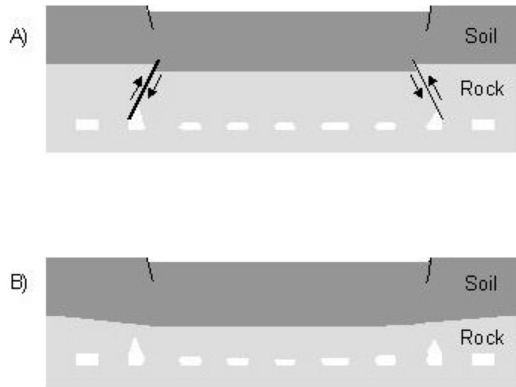


Fig. 2.3. The two main types of large-scale pillar collapse in the limestone mines: downward movement of the rock overburden along collapse-induced faults (a) and by mere deflection of the rock overburden (b).

Inside a collapse area often some open space remains, enabling an investigation of the zone. Pillars show severe spalling, often extending to the pillar core. Pillar slabs are pushed into the gallery and extensive collapses of roof layers are common. It is often to be seen that pillar slabs have rotated partly into the gallery, but became trapped under the rapidly subsiding overburden (Fig. 2.4). The collapse is finally arrested by the confining effect of the pillar and roof debris, which support the pillar walls. Sometimes a large part of the roof disintegrates in roof layer fragments, which fill up the galleries completely, due to the bulking effect. Such areas are no more accessible. This was the case for the Roosburg collapse, and a rapid access to the victims was therefore impossible.



Fig. 2.4. Inside the collapse area of the Muizenberg near Kanne. Segments of opposite pillar walls moved into the gallery partly by rotation, and were crushed by the rapidly descending overburden.

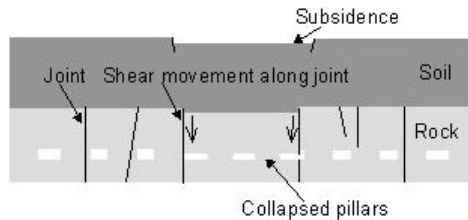


Fig. 2.5. Collapse of a limited number of pillars due to a densely jointed overburden of moderate thickness.

In some cases a small-scale pillar collapse, involving just a few pillars, may occur (Fig. 2.5). This can happen if the failed pillar(s) are more or less completely surrounded by joints, which intersect the whole rock overburden. Then the limestone roof may slide downwards along the joints, as occurred in the Scharnderberg and the Heerderberg just to the east of Maastricht. Clay-infill and openings of the joint plane due to karst, make such a collapse more likely. A small-scale pillar collapse is possible as well if the rock overburden is so thin that there is no arching effect across the pillar(s).

A large-scale pillar collapse is not only lethal for people who happen to be in the collapsing area. The strong air blast, which is always generated by the collapse, may kill people in other parts of the mine outside the collapsing area, and even people outside the mine near the entrance. During the collapse of the Muizenberg near the village of Kanne (Belgium) in 1926 three of the five casual-

ties were due to the air blast, including two men who had already fled out of the mine (Breuls, 1984). Additionally, the accompanying surface subsidence described above may severely damage buildings, roads, waterworks and other surface structures.

2.3 Consequences of Local Roof Instability

In general roof collapses in the mine do not bring about surface subsidence, because eventual stoping, a series of subsequent roof layer collapses, is normally arrested by the formation of a stable arch. Only where the rock overburden is thin, a roof collapse results in earth inflow into the mine and the forming of a sinkhole of several meters depth at the surface. This situation particularly applies to the area of the village of Zussen (Belgium), where the total limestone roof is often just a few decimeters thick. Here several craters have formed and are still forming now and then. In August 2002 a roof collapse expanded over an area of 0.4 hectares just outside this village. This large-scale roof collapse brought serious subsidence, partially bounded by faults with a vertical offset of up to more than 8 m, over the same area as the underground collapse (Figs. 2.6, 2.7). Inspection underground revealed that the pillars were undamaged. A strong air blast did not develop because earth inflow occurs less rapidly than subsidence of the complete limestone overburden during a large-scale pillar collapse.

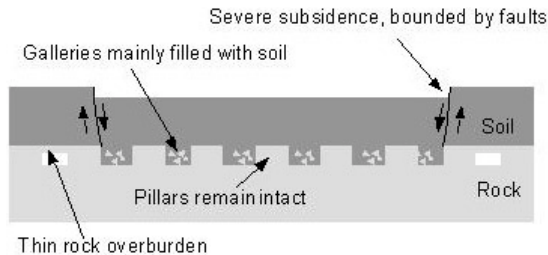


Fig. 2.6. Geometry of a in 2002.

2.4 Consequences of Earth Inflow from Organ Pipes

As a result of the earth inflow into the mine, the solution pipe has become empty over part of its height. This open space may migrate upwards during subsequent flows, with eventually the creation of a sinkhole at the surface of a depth and a diameter of some m. Such a sinkhole develops suddenly without any precursory subsidence and the time span between inflow into the mine and sinkhole formation is impossible to predict. In 1988 a sinkhole of 6 m diameter and 5 m depth emerged above the Geulhemmer Groeve just in between two private houses.



Fig. 2.7. Severe subsidence as a result of the large-scale roof collapse near Zussen, with faults of some m width and up to 8 m vertical offset.

3 Assessment of Large-Scale Pillar Collapse Potential

3.1 Individual Pillar Stability

The stability of an individual pillar is expressed by a *safety factor* SF , which is the ratio of the *pillar strength* S_p and the *mean vertical pillar stress* S :

$$SF = \frac{S_p}{S} \quad (1)$$

S is calculated by the well-known *tributary area method*, which considers the total overburden load directly over the pillar and the portion of the galleries at its perimeter:

$$S = S_{ov} * \frac{A_t}{A_p} \quad (2)$$

where $S_{ov} = \sum \gamma_i h_i$ is the overburden stress with unit weights γ_i and thickness h_i of the subsequent overburden layers. A_t and A_p denote tributary area and horizontal pillar area respectively. This method gives a slight overestimation of S , because partial load transfer from the pillars to the abutments or to relatively large barrier pillars is not taken into account. This overestimation decreases with an increase of the total mine span. Nevertheless, a bit conservative approach is to be preferred above applying a value of pillar stress with an unknown underestimation. However, this often used equation above has to be modified for pillars of considerable height relative to the total overburden thickness, because now the vertical stress due to the weight of the pillar itself significantly affects the mechanical behaviour of the bottom part of the pillar. In some mines the pillar height is 10 to 15 m, with an overburden of about 40 m. Application of Eq. 2 would result in an overestimation of SF. In this regard it has to be noted that failure starts at the top and bottom of the pillar near the edges, where the state of stress is relatively unfavourable. Now Eq. 2 becomes:

$$S = S_{ov} * \frac{A_t}{A_p} + \gamma_p H \quad (3)$$

where γ_p and H are the unit weight of the pillar rock and the pillar height respectively. Pillar strength S_p is commonly expressed as a product of unconfined compressive strength, on a cylindrical core or block sample on a laboratory scale, and a function, which relates size and shape of the pillar to those of the specimen tested in the laboratory. Hustrulid (1976), Hoek & Brown (1982) and Bekendam (1998) reviewed such relations suggested by various authors for several rock types. Extensive laboratory testing on calcarenite prisms by Dirks (1990) and Vink (1991) revealed that pillar strength for this rock is well described by the formula of Hustrulid, revised by Goodman et al. (1980):

$$N_{shape} = S_p / UCS = 0.875 + 0.250 W/H \quad (4)$$

where W and H are pillar width and height, and UCS is the unconfined compressive strength of a cylindrical core. For this continuous and homogeneous rock there proved to be no scale effect. This equation is derived for width/height ratio's of up to 4, which applies to the majority of pillars in the mines. In order to describe the strength of pillars with a non-quadrangular basal plane, $4 A/C$ is used as an effective width, where A and C denote the area and circumference of the basal plane of the pillar. Wagner (1974) had also proposed this concept. Thus Eq. 4 now becomes:

$$N_{shape} = S_p / UCS = 0.875 + A/CH \quad (5)$$

To delineate the residual strength of failed pillars of width/height ratio's between 1 and 4, the following shape factor was advanced by Bekendam (1998):

$$N_{shape, r} = S_{p, r} / UCS = 0.118 + 1.40 A/CH \quad (6)$$

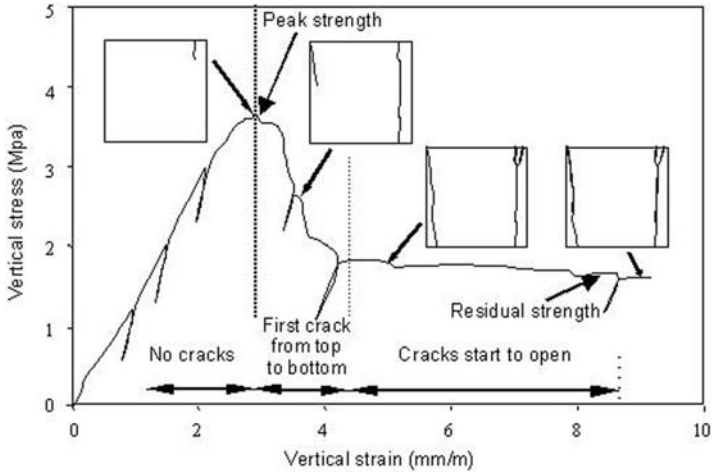


Fig. 3.1. Stress-strain diagram of a compression test on a cubical limestone prism of 15 cm width, and drawings showing crack development.

Stress-strain diagrams of model pillar compression tests (Fig. 3.1) show that one unique value of residual strength does not exist. However, at a certain strain beyond failure the stress hardly decreases anymore. It was decided to consider the stress at three times the strain at failure as the residual strength. Eq. 6 does not apply to pillars of W/H ratio's of less than 1, because such pillars commonly fail along one shear plane or a system of shear planes that intersects the whole pillar width. Accordingly, such pillars show hardly any residual strength.

In order to assess the amount of pillar damage more or less quantitatively by visual inspection and to validate calculated safety factors, a pillar classification system was presented by Bekendam & Price (1993). This system has been refined and extended during later research projects (Bekendam 2002). Pillars of class 0 are not affected at all by fracturing, and class 1 pillars do not show fractures of more than 1 mm width and more than a few dm length. In a stability analysis these pillars are considered as intact and their actual strength is described by Eq. 5. The amount of fractures and their width and length increases from class 2 to 6. From class 4 onwards major (more than 1 dm deep) spalling has arisen. Class 2 to 6 pillars are considered as failed and Eq. 6 applies here. Taking pillar damage into account in this way results in the actual shape factor $N_{\text{shape, act}}$ and the actual pillar strength $S_{\text{p, act}}$. Regarding the classification and pillar dimensions to be used in the calculation, corrections have to be made for small pillar projections, incisions in the pillar walls, fracturing due to the presence of joints, etc. Large, irregular pillars should be subdivided. However, explaining such aspects in detail is out of the scope of this paper.

In the calculation of safety factors various random and systematic errors exist. As an example of a systematic error, resulting in an overestimation of safety factors, creep deformation is important. The analysis presented above results in a

short-term strength. Due to creep a pillar can fail on the long term at a stress well below this value. Creep tests showed that an increase in stress of only 5% can reduce the time to failure about one order of magnitude (Bekendam 1998). An example of an important random error is the variation of UCS. Therefore a pillar safety factor should be well above one. According to practice, a value of more than 1.5 to 2 can be considered safe.

3.2 Large-Scale Pillar Stability

A large-scale pillar collapse is preceded by instability of individual pillars, but can only develop if the load carrying capacity of all pillars together is insufficient for the studied area of the mine. Here the *large-scale pillar stability* must be taken into account, which is defined by Bekendam (1998) as a safety factor, to be achieved by dividing the total load carrying capacity by the total overburden load:

$$SF_{\text{tot},0} = \frac{\Sigma(S_p * A_p)}{\Sigma(S_{\text{ov}} * A_t)} \quad (7)$$

This expression describes the total safety factor for the situation, where all pillars are still intact. The actual total safety factor is equal to:

$$SF_{\text{tot,act}} = \frac{\Sigma(S_{\text{p,act}} * A_p)}{\Sigma(S_{\text{ov}} * A_t)} \quad (8)$$

According to practice, a $SF_{\text{tot},0}$ of more than 2 can be considered as safe, while a value of less than 1.5 is definitely unsafe. It is important to subdivide the mine correctly in sufficient areas, to prevent that potential collapse areas are masked by a safe value of $SF_{\text{tot},0}$ for the whole mine.

3.3 General Mine Stability

A mined area of insufficient large-scale pillar stability, comprising mainly failed pillars, does not necessarily collapse. Now the *general mine stability* must be considered: are the roof strata strong and stiff enough to prevent a large-scale collapse, despite widespread pillar failure? Are the roof strata capable of transferring the vertical pressure on the pillars towards areas of unmined rock by means of a pressure arch? It is known that the maximum width of a pressure arch increases with depth (e.g. Adler 1973; Stacey & Page 1986). Since the soil overburden is hardly contributing to the arching action, only the rock overburden should be taken into account. To delineate general mine stability, rock overburden thickness is depicted vs. mine span for 15 areas of extensive pillar failure, comprising 5 cases of collapse and 10 without collapse (Fig. 3.2). An approximate line can be drawn separating collapsed and not collapsed areas. Obviously, this figure should be considered with care, because pillar layout, thickness and weight of the soil overburden, strength and stiffness of the roof rock formations and pillars are not incorporated. To increase the confidence in the assessment of general mine stabil-

ity, a numerical study is planned and data points from each new analysis are added to the figure. It should be noted that, if the overburden rock is relatively thin, densely jointed and affected by karst, an effective arching effect may be prevented. In such a case also pillar collapses on a small scale are possible as depicted in Fig. 2.5.

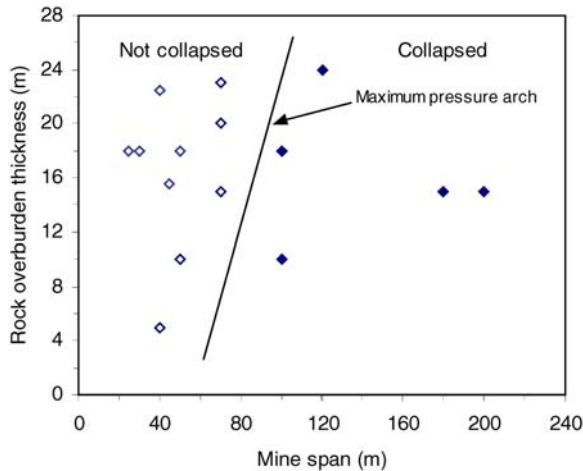


Fig. 3.2. Rock overburden thickness versus mine span for areas of widespread pillar failure. An approximate line separates collapsed and not collapsed areas.

4 Outlook

In the past 5 years the method presented above has been applied to more than 15 mined areas, in view of the safety of visitors to the mine and/or in consideration of existing or planned buildings and other surfaces structures like roads, service-pipes and reservoirs of drinking-water. Depending on the outcome of the assessment of the total safety factor and the general mine stability, different actions can be recommended. These may vary from just regular visual inspections, to regular or continuous pillar convergence measurements or support measures like filling up of galleries. Pillar convergence is measured now in a number of mines since a few years ago and parts of some mined areas were filled up, partly through boreholes, with a material of low viscosity and of a strength and stiffness, after hardening, close to those of the pillar rock. The method was also adapted to establish optimal support plans and to determine their effect in terms of stability improvement.

Acknowledgement

An important part of the study was performed at: Delft University of Technology, Faculty of Civil Engineering and Geosciences, Section Engineering Geology, Postbus 5028, 2600 GA Delft.

References

- Adler L (1973) Roof and ground control. In: SME mining engineering handbook (ed. by A.B. Cummins & I.A. Given), Vol. 1, 13-9 to 13-36.
- Bekendam RF (1998) Pillar stability and large-scale collapse of abandoned limestone room and pillar mines in South-Limburg, The Netherlands, PhD-thesis TU Delft (pp 361).
- Bekendam RF (2002) The "Gemeentegroeve" under the "Kop Cauberg", stability and support measures (in Dutch), GeoControl report M0027, 74 pp.
- Bekendam RF & Price DG (1993) The evaluation of the stability of abandoned calcarenite mines in South Limburg, Netherlands. In Proceedings of Eurock'93 (ed. by L. Ribeiro e Sousa & N.F. Grossmann), Balkema, Rotterdam, 771-778.
- Breuls T (1984) The collapse of the Muizenberg near Kanne (in Dutch). SOK Mededelingen, 5, 30-38.
- Dirks WG (1990) The influence of pillar geometry on calculating pillar strength; the Hoorensberg groeve as a case study. Doct. thesis, Delft University of Technology, 68 pp
- Hoek E & Brown ET (1982) Underground excavations in rock, The institution of mining and metallurgy, London, 527 pp.
- Goodman R, Korbay S & Buchignani (1980) Evaluation of collapse potential over abandoned room and pillar mines. Bull.Ass.Engng.Geol., 17, 27-37.
- Hustrulid WA (1976) A review of coal pillar strength formulas. Rock Mechanics, 8, 115-145.
- Price DG (1990) The collapse of the Heidegroeve: a case history of subsidence over abandoned mine workings in Cretaceous calcarenites. In Proceedings International Chalk Symposium, Brighton, Thomas Telford, London, 503-510.
- Stacey TR & Page CH (1986) Practical Handbook for Underground Rock Mechanics, Trans Tech Publications, Clausthal, 144 pp.
- Vink D (1991) Estimating pillar strength in stability analysis, a survey of the Geulhemmer mine. Memoirs of the Centre for Engineering Geology in The Netherlands, 89, Delft university of Technology, 141 pp.
- Wagner H (1974) Determination of the complete load-deformation characteristics of coal pillars. Proc. Third Congr. Int. Soc. Rock Mech., Vol. 2(B), 1076-1081.

Numerical Modelling of Seismic Slope Stability

Céline Bourdeau¹, Hans-Balder Havenith², Jean-Alain Fleurisson¹,
and Gilles Grandjean³

¹ Centre de Géologie de l'Ingénieur, Université de Marne-la-Vallée, Bâtiment IFI
Cité Descartes, 5, boulevard Descartes, Champs-sur-Marne
77454 Marne-la-Vallée cédex 2, France
celine.bourdeau@ensmp.fr

Tel: + 33 1 49 32 90 09

Fax: + 33 1 49 32 91 28

² Dep. GeomaC, University of Liege, B52, 4000 Sart Tilman-Liege, Belgium

³ BRGM/ARN, BP 6009, 45060 Orléans, France

Abstract. Earthquake ground-motions recorded worldwide have shown that many morphological and geological structures (topography, sedimentary basin) are prone to amplify the seismic shaking (San Fernando, 1971 [Davis and West 1973] Irpinia, 1980 [Del Pezzo et al. 1983]). This phenomenon, called site effects, was again recently observed in El Salvador when, on the 13th of January 2001, the country was struck by a $M=7.6$ earthquake. Indeed, while horizontal accelerations on a rock site at Berlin, 80 km from the epicentre, did not exceed 0.23 g, they reached 0.6 g at Armenia, 110 km from the epicentre. Armenia is located on a small hill underlaid by a few meters thick pyroclastic deposits. Both the local topography and the presence of surface layers are likely to have caused the observed amplification effects, which are supposed to have contributed to the triggering of some of the hundreds of landslides related to this seismic event (Murphy et al. 2002). In order to better characterize the way site effects may influence the triggering of landslides along slopes, 2D numerical elastic and elasto-plastic models were developed. Various geometrical, geological and seismic conditions were analysed and the dynamic behaviour of the slope under these conditions was studied in terms of creation and location of a sliding surface. Preliminary results suggest that the size of modelled slope failures is dependent on site effects.

Keywords: earthquake, slope failures, site effects, numerical modelling, parametric analysis.

Introduction

During the last 50 years, the phenomenon of slope instabilities in seismic areas has resulted in a long history of dramatic disasters worldwide. One of the recent most tragic events was induced by a debris flow (200 000 m³) at Las Colinas (El Salvador, Central America) which destroyed many houses and caused more than 500 deaths. This landslide was triggered by the $M=7.6$, January 13, 2001, El Salvador earthquake. Apart from this tragic event and the San Vicente debris slide (East of San Salvador) which blocked the Pan American Highway, the intense shake was responsible for nearly 500 landslides nationwide which inflicted great damage to

roads and buildings. Among the possible factors contributing to these dynamic failures, site effects were often mentioned. Indeed, many ground-motion recordings, especially those made on volcanic soils such as the Tierra Blanca -a pyroclastic ashfall deposit very common in El Salvador- revealed high ground-motion amplifications. According to Murphy et al. (2002), "*The largest PGV - peak ground velocity- was obtained at the Santa Tecla Station (Te) with a value of approximately 57 cm/s. This ground-motion was large enough to trigger the big landslide at Las Colinas. It must be said that the Te recording is located approximately 1 km away from the Las Colinas site.*" The significant influence of site effects on landslide occurrence was also pointed out for landslides triggered by large earthquakes in the Tien Shan (Central Asia), such as the Ananevo rockslide induced by the M=8.2, Kemin (Kyrgyzstan) earthquake in 1911 (Havenith et al. 2002). This is supported by extensive field observations and numerical modelling results. The comparison between both approaches revealed that the presence of surficial low-velocity layers of varying thickness is the key factor controlling ground-motions around the rockslide (Havenith et al. 2002). Connecting this result with slope failure susceptibility, it could be concluded that the main landslide rupture results from large ground-motions and deformations induced by wave focusing effects (Havenith et al. 2003).

In order to detect the most important parameters controlling both the occurrence and the size of such seismic landslides, the dynamic behaviour of slopes is studied for various geological and seismic conditions. The study aims in particular to detect a relationship between the size of earthquakes and the size of the induced landslides.

1 Numerical Modelling

The work presented hereafter is based on a parametric analysis of dynamic slope failures with respect to varying geological and seismic conditions. Numerical models were carried out by using the 2D finite difference (FD) code FLAC developed by Itasca Consulting Group. Three parameters (i.e. one geological parameter and two seismic parameters) considered as relevant to seismic slope stability assessment were varied and the susceptibility to failure was calculated as well as the area of the sliding mass.

1.1 Source

The input seismic motion is a vertically propagating SV wave applied at the bottom of the model. Two different acceleration waveforms were selected (Fig. 1.1): a mono-frequency waveform (signal 1: sinusoidal waveform) and a multiple-frequency waveform (signal 2: Ricker waveform). Therefore, the impact of the amplitude-frequency content of seismic waves on the slope stability could be assessed. Note that, in the following, the word "frequency" used for signal 2 will refer to the central frequency of the acceleration waveform.

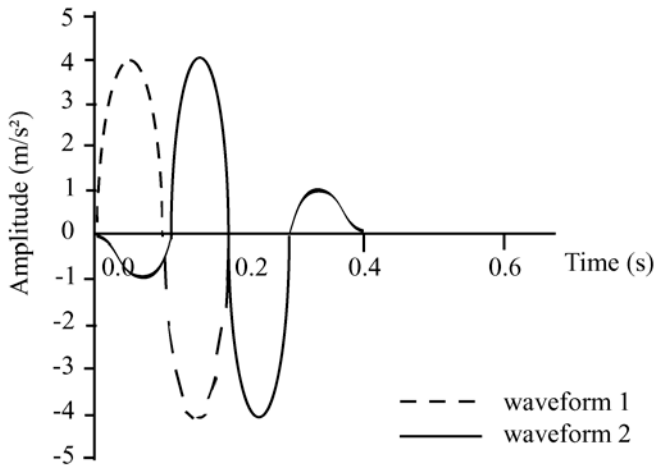


Fig. 1.1. Acceleration waveforms : (1) is a sinusoidal waveform; (2) is a Ricker waveform.

1.2 Boundary Conditions

Absorbing boundaries were applied on the vertical sides and at the bottom of the model in order to prevent artificial wave reflections.

1.3 The Models

The numerical simulations were performed with two types of models: elastic models simulating small deformations for site effects calculations and elasto-plastic models simulating large deformations for slope stability assessments.

With respect to finite difference methods, numerical distortion of the propagating waves can occur in a dynamic analysis if the spatial resolution of the models is not designed to accurately propagate the frequency content of the input waves. For an accurate representation of wave transmission through a model, the spatial element size must be smaller than approximately one-tenth of the wavelength associated with the highest frequency component of the input wave that contains appreciable energy. For example, the largest element size allowed in a model with an S-wave velocity equal to 250 m/s is 25 m when the highest frequency component is equal to 1 Hz, 5 m when the highest frequency component is equal to 5 Hz and 1 m when the highest frequency component is equal to 25 Hz. Therefore, the FD mesh has to be finer and finer when the resonance frequency of the surface layer gets higher, which leads to relatively high calculation costs.

1.3.1 Geometry and Geology of the Models

The geometry and the geology of the models refer to figure 1.2: a Tierra Blanca surface material with a thickness of H_1 m overlaying a basaltic bedrock.

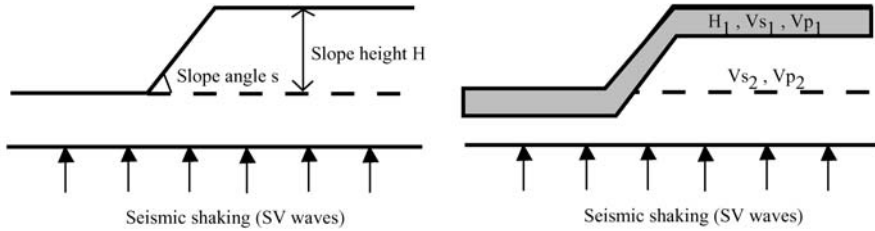


Fig. 1.2. a) Geometry of the slope; b) Geology of the slope.

1.3.2 Failure Criterion for Slope Stability Assessment (Elasto-Plastic Modelling)

The failure criterion used in the numerical simulations is a Mohr-Coulomb criterion expressed by two parameters: the cohesion and the friction angle. According to Bommer et al. (2002), the Tierra Blanca “possesses a shear strength that is very prone to drastic reductions when subjected to remoulding and/or wetting. [...] This creates a great potential for the soil to fail or collapse under the effect of disturbances such as those generated by seismic activity or heavy rainfall”. In the modelling, this softening behaviour of the Tierra Blanca is accounted for by decreasing the cohesion and the friction angle of the Tierra Blanca from initial to residual values (shear-strain-softening model) as soon as the plastic strains in one element reach a threshold value (Fig. 1.3: arbitrary threshold value = 3% of plastic strains).

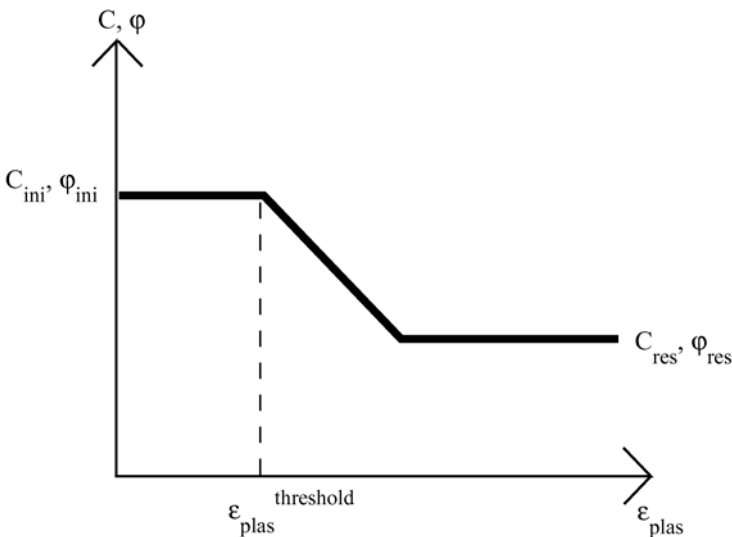


Fig. 1.3. Reduction of the cohesion and the friction angle of the Tierra Blanca as soon as the plastic strains in one element reach a threshold value.

1.3.3 Choice of the Fixed Parameters

The slope angle and the slope height have constant values: 50° and 25 m respectively. Based on previous studies of the Tierra Blanca (Mavrommati 2000, Faccioli et al. 1986) the following properties were adopted for the Tierra Blanca: V_p (P-wave velocity) = 467.5 m/s; V_s (S-wave velocity) = 250 m/s; density = 1300 kg/m^3 . For the basaltic bedrock, $V_p = 780 \text{ m/s}$; $V_s = 450 \text{ m/s}$; density = 2000 kg/m^3 . The duration of the input acceleration is 6 s. Shear strength parameters of the Tierra Blanca are provided by Bommer et al. (2002): $C_{\text{initial}} = 30 \text{ kPa}$; $C_{\text{residual}} = 10 \text{ kPa}$; $\varphi_{\text{initial}} = 39^\circ$; $\varphi_{\text{residual}} = 35^\circ$ (note that laboratory tests have shown that the residual shear strength parameters could even be much smaller). Shear strength parameters of the basaltic bedrock are: $C = 300 \text{ kPa}$; $\varphi = 40^\circ$.

1.3.4 Choice of the Variable Parameters

In a first attempt to analyse seismic slope failure occurrence and its size, the three following parameters were varied:

- the geometry of the Tierra Blanca surface layer with H_1 taking the following values: 2.5 - 5 - 10 - 20 - 30 m; 5 models corresponding to the 5 different H_1 values were therefore created (model 1: $H_1 = 2.5 \text{ m}$; model 2: $H_1 = 5 \text{ m}$...);
- the frequency content of the signal f (central frequency): 1 to 6 Hz (every 1 Hz);
- the amplitude of the signal: the PGA (peak-ground acceleration) of the input acceleration lies in the range [0.1 to 0.5 g] (every 0.1 g).

150 (i.e. $5 \cdot 6 \cdot 5 = 150$) different combinations of these three parameters were analysed for each waveform.

The next step consists of changing the geometry of the slope (slope angle and slope height).

The presentation of the results will address two different topics: the evaluation of the failure potential (i.e. creation or not of a sliding surface) and the calculation of the area of the sliding mass.

2 Results

Table 2.1 describes the static stability of each model. The 30 different dynamic simulations done per model correspond to all the possible combinations of the 6 different values of the signal frequency and the 5 different values of the input acceleration (i.e. $6 \cdot 5 = 30$ different simulations). As expected, the number of dynamic failures is higher for low FS (static factor of safety).

2.1 The Slope Failure Potential

2.1.1 Influence of the Amplitude of the Signal

Figures 2.4 to 2.7 describe the slope failure susceptibility with respect to varying seismic conditions (amplitude and frequency) for the models 2 to 5. The wave-

Table 2.1. Characteristics of the two seismic layers (i.e. S- and P-wave velocities, slope height, resonance frequencies, static factors of safety and number of instabilities simulated) for the five different models

Model	V_{s1} (m/s)	V_{s2} (m/s)	H_1 (m)	f_{res} (Hz)	FS (static factor of safety)	N° of instabilities modelled ("30" means that for each H1, 30 different simulations were done)	
	(Tierra Blanca)	(Basaltic bedrock)				Waveform 1 (sinusoidal waveform)	Waveform 2 (Ricker waveform)
	1	250					
2	250	450	5	12.5	1.9	11/30	8/30
3	250	450	10	6.3	1.7	17/30	12/30
4	250	450	20	3.1	1.7	18/30	15/30
5	250	450	30	2.1	1.7	20/30	16/30

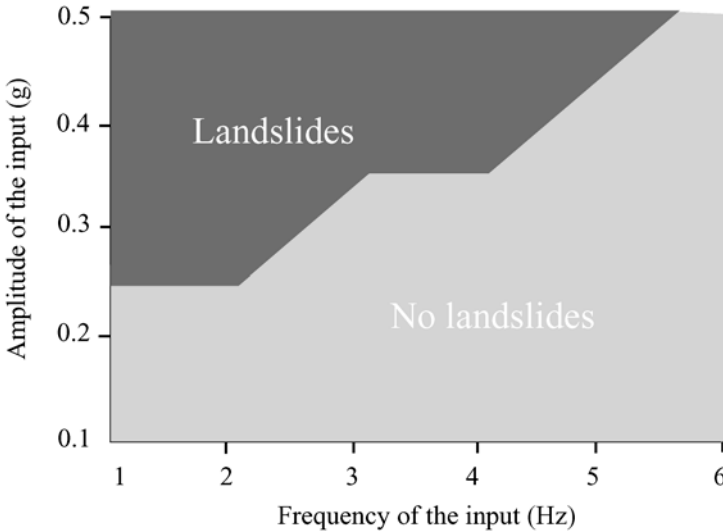


Fig. 2.4. seismic conditions (amplitude and frequency) leading to a landslide for model 2. The waveform considered is waveform 1.

form considered is signal 1. These plots demonstrate that for any given frequency of the input the slope failure potential increases with the intensity of the seismic shaking.

Note that figures 2.4 and 2.7 also show that the lower the FS value, the higher the susceptibility to slope failure.

2.1.2 Influence of the Frequency Content of the Signal

In this section, the PGA is constant as well as the Arias Intensity (I_a) incorporating all of the amplitude, frequency and duration information into a single value pro-

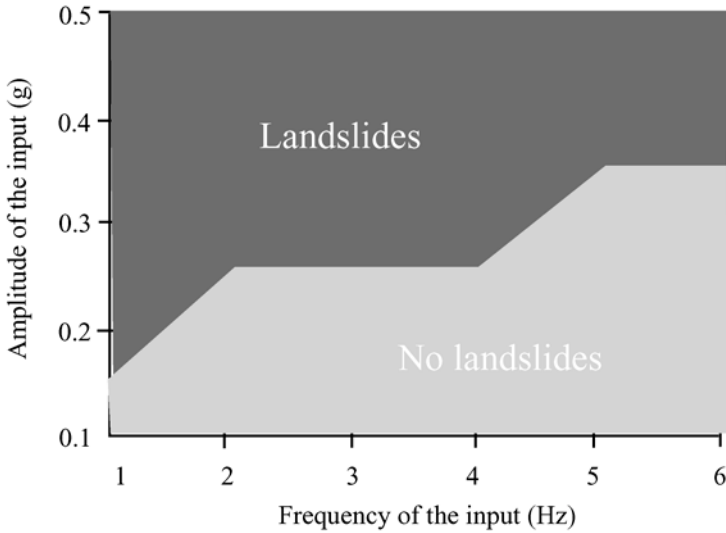


Fig. 2.5. Seismic conditions leading to a landslide for model 3. The waveform considered is waveform 1.

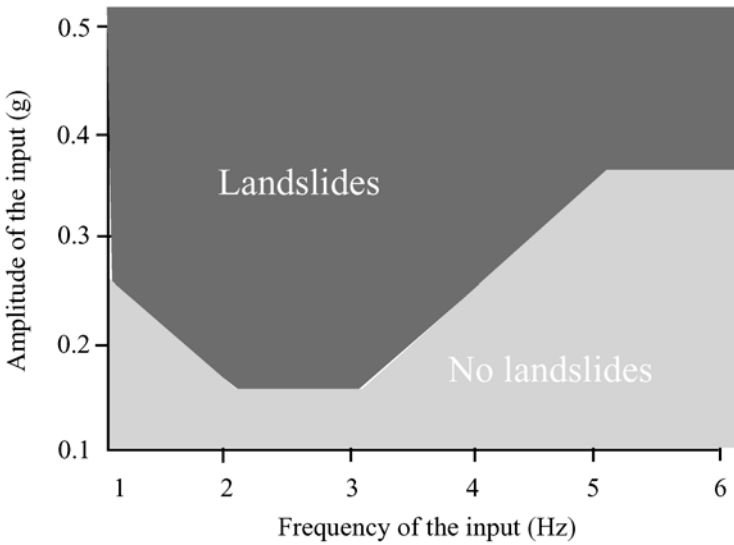


Fig. 2.6. Seismic conditions leading to a landslide for model 4. The waveform considered is waveform 1.

portionate to the total energy dissipated at the recording site. According to figures 2.4 to 2.7, models 4 and 5 follow the same trend whatever the seismic waveform may be: for the smallest shaking able to trigger a landslide (0.1-0.2 g), instabilities

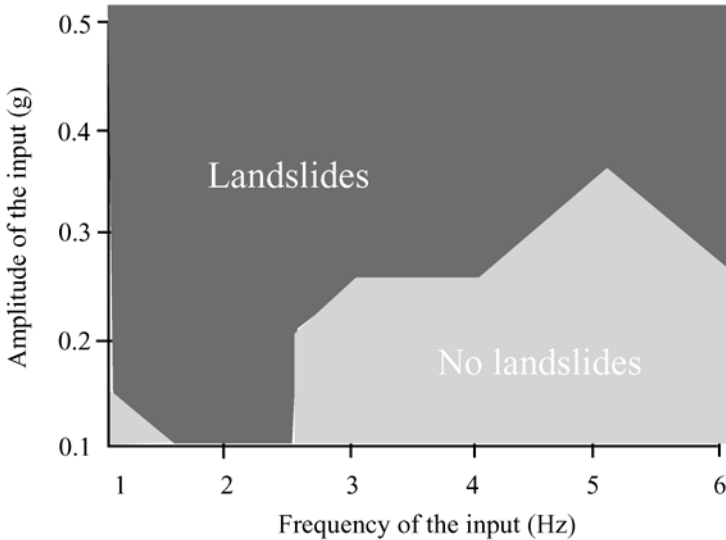


Fig. 2.7. Seismic conditions leading to a landslide for model 5. The waveform considered is waveform 1.

are only observed when the frequency of the input acceleration is close to the resonance frequency of the soil ($f = 2\text{-}3$ Hz for model 4 -Fig. 2.6-; $f = 2$ Hz for model 5 -Fig. 2.7-). The resonance frequency (f_{res}) is the signal frequency which leads to a period ratio $T_{\text{soil}} / T_{\text{earthquake}}$ equal to one where $T_{\text{soil}} =$ natural period of the soil $= 4 * H_1 / V_{s1}$ and $T_{\text{earthquake}} =$ dominant period of the earthquake $= 1/f$ (see Tab. 2.1). The large failure potential can be attributed to the amplified ground-motions at the resonance frequency. An illustration of this phenomenon is given in figures 2.8 (signal 1) and 2.9 (signal 2), in the time domain: horizontal ground-motion amplifications were calculated at the crest of the slope by reference to free-field motions (i.e. peak ground-motions recorded on a rock site). High ground-motion amplifications develop around the crest of the slope and their values depend on the seismic input (i.e. signal 1 or signal 2). This first result shows that site effects control the occurrence of a landslide. However, models 1 to 3 do not follow the same trend. Indeed, figures 2.4 and 2.5 show that for the smallest shaking able to trigger a landslide (0.1-0.2-0.3 g), the slope instability is only well developed at low frequencies (1-2 Hz). To understand this result, the distribution of horizontal ground-motion amplifications in and along the slope of model 2 was calculated, in the time domain, for signal 1 and various frequencies 2, 4, 6 Hz (Fig. 2.10 to 2.12 respectively). Figures 2.10 to 2.12 clearly show that the strongest ground-motions develop around the crest of the slope where wave focusing seems to be more intense for high-frequency sources. On the other hand, inputs with a lower frequency content induce higher amplitudes over a larger area below the crest (cf. for example the location of the line corresponding to an amplification of 1). The larger extent of the zone characterized by strong ground-motions may

explain why the simulated landslides preferentially develop for low frequency inputs, while only locally increased amplitudes are less likely to trigger failure. This result is another illustration of the dependency of the slope failure potential on the frequency content of the signal. It points out the importance, in slope stability assessment, to consider not only crest motions but also the distribution of the motions in the volume.

As a conclusion to this slope failure potential analysis, it may be interesting to have a look at the characteristics of large magnitude earthquakes. These seismic events are generally defined by high accelerations and low-frequency content. The preceding results show that larger earthquakes are more prone to trigger numerous landslides than smaller ones.

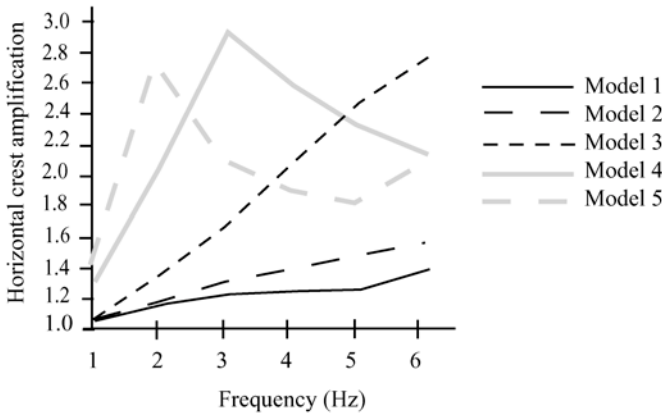


Fig. 2.8. Horizontal ground-motion amplifications at the crest of the slope for various frequencies of the input acceleration. The waveform here considered is signal 1. The reference motion is the free-field motion.

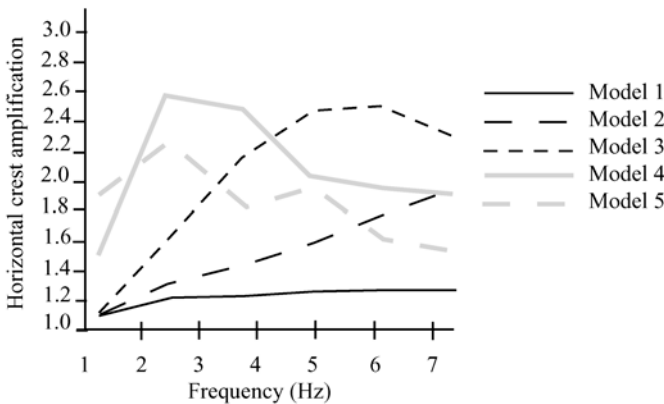


Fig. 2.9. Horizontal ground-motion amplifications at the crest of the slope for various frequencies of the input acceleration. The waveform here considered is signal 2. The reference motion is the free-field motion.

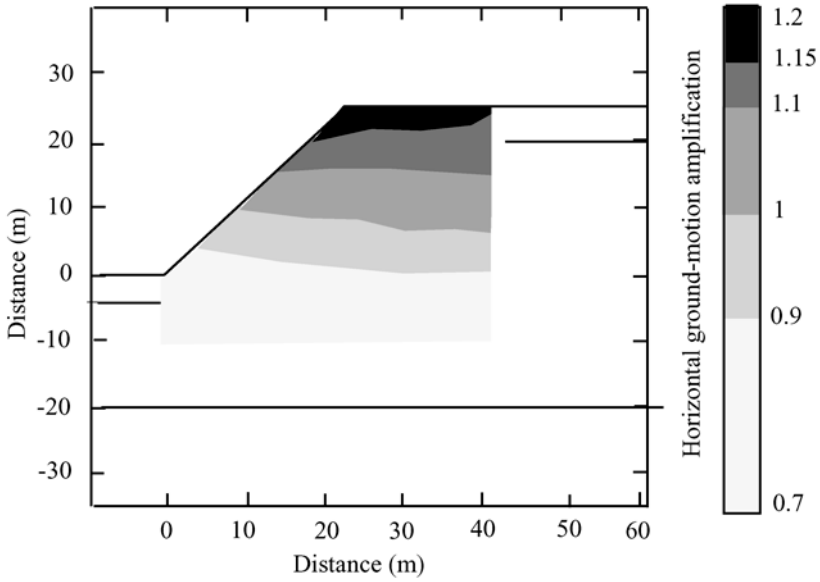


Fig. 2.10. Distribution of horizontal ground-motion amplifications in and along the slope of model 2 for a frequency equal to 2 Hz. The waveform here considered is signal 1.

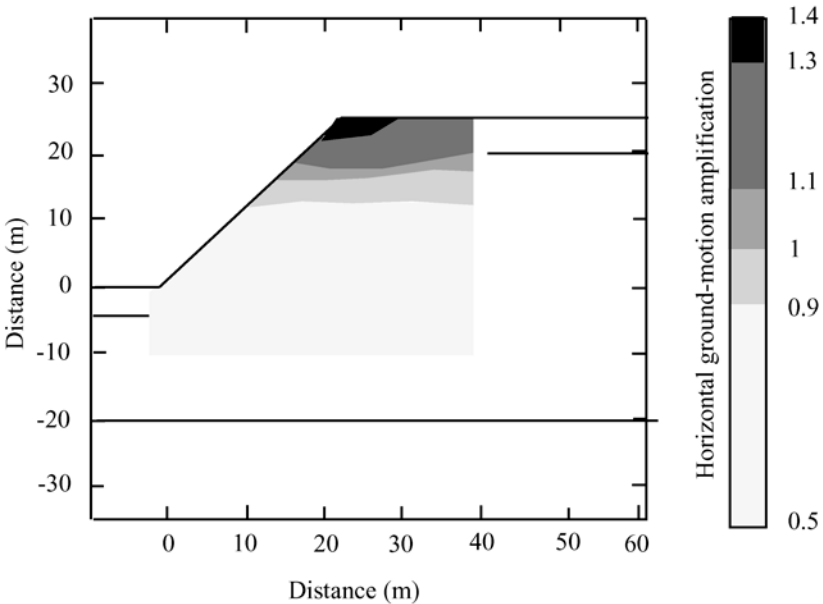


Fig. 2.11. Distribution of horizontal ground-motion amplifications in and along the slope of model 2 for a frequency equal to 4 Hz. The waveform here considered is signal 1.

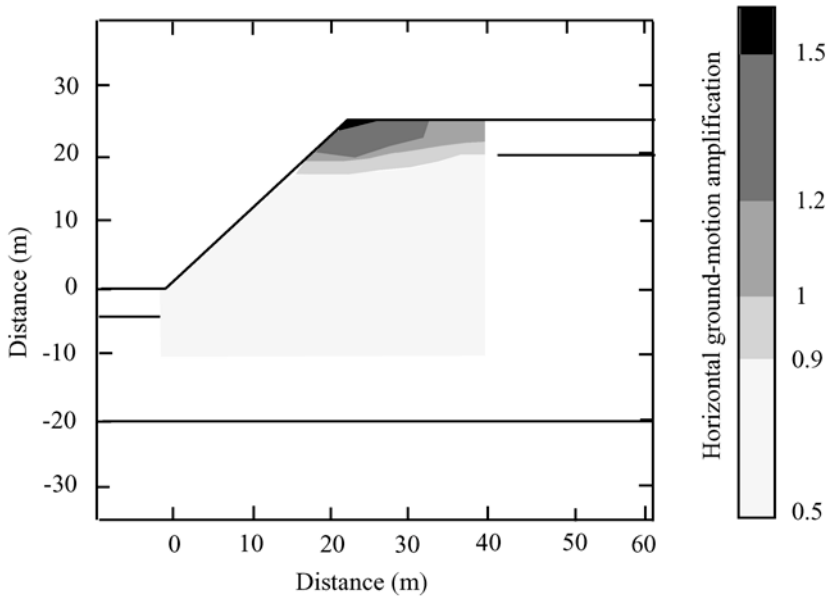


Fig. 2.12. Distribution of horizontal ground-motion amplifications in and along the slope of model 2 for a frequency equal to 6 Hz. The waveform here considered is signal 1.

2.2 Area of the Sliding Mass

In order to better characterize the landslide potential, the area of the sliding mass (2D approximation of the 3D volume of the landslide) was calculated for all the configurations leading to an instability. This analysis aims at defining how the size of a slope failure may be linked to the intensity of the seismic shaking and to the size of a seismic event, large events producing strong ground accelerations in a lower frequency range.

Figure 2.13 gives a schematic representation of the sliding surface with the location of points A and B, the lower and upper limits of the sliding surface, respectively. The sliding areas computed for various signal amplitudes and frequency contents (signal 2, Ricker wavelet) are represented in figure 2.14 for model 3 and in figure 2.15 for model 2.

2.2.1 Influence of the Amplitude of the Signal

Figure 2.14 shows that, just as the failure potential, the area of the sliding mass rapidly increases with the intensity of the seismic shaking. This increase is limited, in most of the cases, by an area value (plateau) corresponding to the area of the pseudo-static failure induced by large ground-motions (calculated with Flac under pseudo-static conditions). Indeed, the static and the pseudo-static sliding surfaces are, in general, deeper than the dynamic sliding surface.

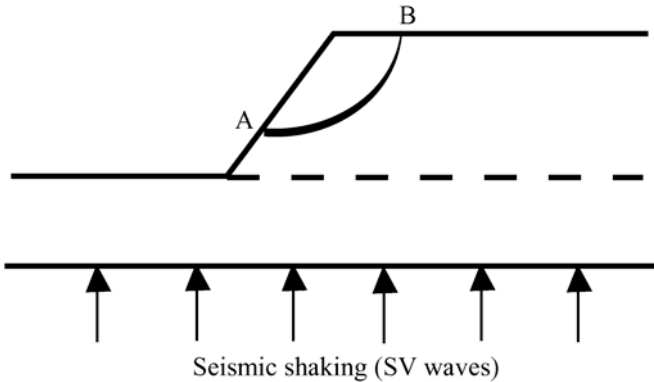


Fig. 2.13. Schematic representation of the sliding surface with the location of points A and B, the lower and upper limits of the sliding surface, respectively.

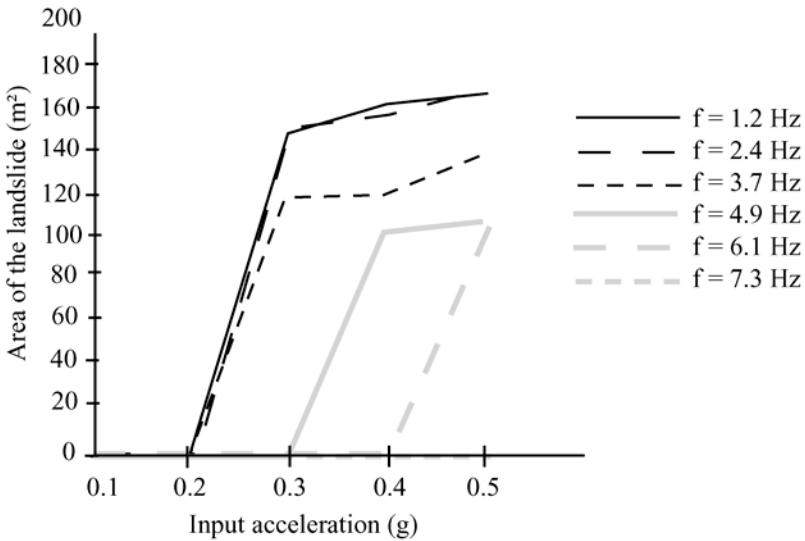


Fig. 2.14. Calculated landslide areas for the whole ranges of frequencies and input accelerations (signal 2). The model here considered is model 3.

The area of the sliding mass is also dependent on the geology of the profile as larger values were obtained for models 3 (Fig. 2.14) to 5 with a thicker surface layer and a related lower factor of safety than for model 2 (Fig. 2.15).

2.2.2 Influence of the Frequency Content of the Signal

Both figures 2.14 and 2.15 show that in addition to the amplitude also the frequency content of the signal has an influence on the sliding area. The area is generally larger for lower frequencies which may be a consequence of the distribution

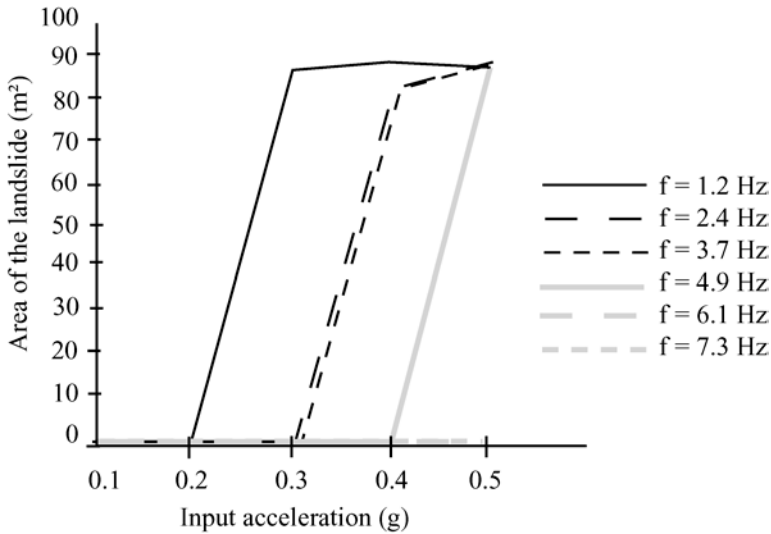


Fig. 2.15. Calculated landslide areas for the whole ranges of frequencies and input accelerations (signal 2). The model here considered is model 2.

of ground-motions in the slope (see section 2.1.2). Note also that a correlation can be established between the extent of the zone of high amplifications as described in section 2.1.2 and the intersection of the sliding surface with the topography behind the crest of the slope. The failure moves away from the crest of the slope and gets deeper when the frequency content of the input acceleration is relatively low. This also implies a larger volume of the landslide. This result points out that the location and the volume of a landslide are likely to be dependent on varying site effects.

From this analysis of the seismic factors controlling the area of the sliding mass, it can be inferred that large magnitude earthquakes tend to trigger larger landslides because of the larger ground accelerations and the low-frequency content.

3 Conclusion

Earthquake-induced landslides represent an important risk in all seismically active mountain regions. This calls upon scientists to get a better understanding of the conditions leading to such instabilities. The work presented in this paper revealed that site effects may contribute to the triggering of landslides. Indeed, it was shown that the formation of a failure strongly depends on the distribution of ground-motions along and below the slope. Therefore, considering only surface ground-motions when assessing slope stability is not satisfactory. For high-frequency inputs, strong ground-motions are confined to the crest of the slope

inducing a minor susceptibility to failure than for low-frequency shaking which produces relatively stronger ground-motions at depth. Combining a low-frequency input with a resonance phenomenon in the low-frequency range (1 to 3 Hz), the slope failure potential takes its highest values. In fact, this situation is the most critical as ground-motions are strongly enhanced at the resonance frequency. As expected, the area of the sliding mass (volume in 3D) increases with the ground-motion amplitude up to a certain threshold input acceleration above which the area of the landslide becomes constant.

Finally, it should be underlined that, unlike the assessment of the direct effects of an earthquake (destruction of buildings for example) where only surface ground-motions are important, the understanding of the induced effects of an earthquake (i.e. landslides) requires the study of the whole distribution of peak ground-motions also at depth.

References

- Bommer JJ, Rolo R, Mitroulia A, Berdousis P (2002) Geotechnical properties and seismic slope stability of volcanic soils, Elsevier Science Ltd.
- Davis LL and West LR (1973) Observed effects of topography on ground motion, *Bulletin of the Seismological Society of America*, 63 (1), 223-298.
- Del Pezzo E, Iannaccone G, Martini M and Scarpa R (1983) The 23 November 1980 Southern Italy earthquake. *Bulletin of the Seismological Society of America*, 73 (1), 187-200.
- Faccioli E, Battistella C, Alemani P and Tibaldi A (1986) Seismic micro-zoning investigations in the metropolitan area of San Salvador, El Salvador, following the destructive earthquake of October 10, 1986, *Proceedings of International Seminar on Earthquake Engineering*, Innsbruck, 1988, 28-65.
- H-B Havenith, D Jongmans, E Faccioli, K Abdrakhmatov and P-Y. Bard (2002) Site effects analysis around the seismically induced Ananevo rockslide, Kyrgyzstan, *Bulletin of the Seismological Society of America*, 92, 3190-3209.
- H-B Havenith, M Vanini, D Jongmans and E Faccioli (2003) Initiation of earthquake-induced slope failures: influence of topographical and other site specific amplification effects, *Journal of Seismology*, 7, 397-412.
- Mavrommati ZC (2000) Seismic behaviour of slopes in an unsaturated volcanic soil, MSc dissertation Imperial College.
- Murphy W, Bommer J and Mankelov JM (2002) Mechanisms of slope failure in volcanic soils during earthquakes, *Proceedings of the 12th European Conference on Earthquake Engineering*, London, 9-13 September 2002, Paper N° 782.

A Multidisciplinary Approach for the Evaluation of the “Bottegone” Subsidence (Grosseto, Italy)

Otello Del Greco, Elena Garbarino, and Claudio Oggeri

Politecnico di Torino, Dept. of Georisorse e Territorio
C.so Duca degli Abruzzi 24, 10129 Turin, Italy
{otello.delgreco, elena.garbarino, claudio.oggeri}@polito.it
Tel: +39 11 564 7609
Fax: +39 11 564 7699

Abstract. In January 1999 a subsidence phenomenon took place in Maremma (Italy): an elliptical shaped sinkhole formed, characterised by a diameter of 140 m and by vertical lateral slopes. The subsidence was put down to a natural cause, connected to the collapse of a hypogeal karst void located in the calcareous bedrock. The phenomenon study was based on some geostructural considerations and some geophysical analysis. The event dynamics was subjected to a first modelization, for understanding the phenomenon and extending this approach to nearby areas for territorial planning and risk management.

Keywords: subsidence, karstic sinkhole, numerical modelling, site investigation, Grosseto, Italy

1 Description of the Subsidence Phenomenon

A pseudo-circular shaped sinkhole, characterised by a diameter of 140 m with vertical walls and a maximum subsidence of 15 m in the S-SW area, formed in January 1999, over a period of just a few hours, in the plain north of Grosseto (Tuscan Region, Central Italy) in an area named “Bottegone”(fig.1). On the western side of the sinkhole, the slopes were less steep as a terracing of the edges occurred till the connection with the deeper and central portions. This phenomenon, apart from the almost uniform subsidence of the ground, was accompanied by disturbances of the hydrogeological regime of the artificial wells and of the natural springs in the surrounding area. The morphology and dimensions of the sinkhole and the presence of water on the inside changed over a period of time, after the phenomenon and the triggering of natural remodelling phenomena finished.

The reasons behind the phenomenon were studied and some of these aspects are still being studied; it can be stated, that the origin of the event can be put down to natural geological situations which have no links with intense rainfalls or ground flows, nor with the presence of tapping wells in the area (used for agricultural purposes and with limited depths). These considerations would lead one to think of natural and deep origins, caused by the collapse of a karstic void in the calcareous substratum. The study was therefore aimed at analysing the type and causes of the event and, consequently, at planning the investigations and measurement campaigns that had to be carried out around the subsidence basin.



Fig. 1. “Bottegone” sinkhole.

The dynamics of the event could be linked to the collapse of an asymmetrical shape void, in the bedrock formation, with greater dimensions in the southern portion. The collapse of the hypogeal structure, on the other hand, might not have occurred in a geometrically regular way in the vault of the cavity, leading to slightly asymmetric subsidence overhangings.

In the area north of the sinkhole, the presence of thermal water under pressure could be seen on the surface, which came from the deep karstic aquifer. The minor phenomena connected to this collapse were the increase in the piezometric level and discharges of three neighbouring thermal springs and the rise in water in the surrounding wells, which could indicate an outplating phenomenon of the waters at a depth, with an easier downflow towards the surface network.

The phenomenon was classified, according to the Jennings classification (after Beck and Wilson, 1987), as a dolina of karstic subsidence, which is also called “sinkhole”.

During the research, a fundamental reference, though of a local nature, was supplied by the results of a geognostic probe that was carried out in the vicinity of the sinkhole and was performed to a depth of 170 m without encountering the calcareous substratum. The objectives of the research can be outlined as follows:

- Identification of the depth of the calcareous substratum: the volumetric analysis of the sinkhole depends on this value in that an increase in the overburden would involve greater dimensions of the volume of the void;
- Definition of the tectonic structure of the analysed region, in particular the identification of the possible fault systems that are contact with the calcareous substratum, which represent the preferential paths for the underground thermal water flow but also elements of structural instability;
- Setting up of interpretation models of the phenomenology in order to evaluate the dimensions and the morphology of the underground void;
- Territorial planning that establish the possible risk;
- Identification of further investigations and monitoring to support the territorial planning, on the basis of findings from the specific case.

2 Geological and Hydrogeological Layout

An area of about 10 km² around the subsidence was studied. The ground used for agricultural purposes (b) makes up about 90 % of the area and entirely borders the subsidence area. Cavernous limestone (cv) can be found in important seams with intervals of anidrite -chalk cemented gravel; it can be found on the outcrops in the western part, where it appears quite altered and friable with a gravel-shaped structure. The limestone of “Poggetti Vecchi”, from which one thermal spring spouts, can be found in the southern part: the limestone appears to be more massive and crystalline. From the hydrogeological point of view, the area is not very permeable and the freatic aquifers are suspended or bordered on the inside by sandy-gravelly horizons bordered by the clay layers below. There are no hydropotable wells, these being the only infrastructures that could cause macroscopic events due to the over-exploitation of the water resources. The hydrogeological condition is also characterised by the presence of three thermal springs, connected by the deep aquifer flow.

3 Geophysical and Geotechnical Investigations

Geophysical investigations are fruitfully employed in structurally complex situations, above all in consideration of the size of the area that is involved. The use of different methodologies supplies cross-information which helps to obtain the final interpretation of the desired geological and structural layout. The following investigations were carried out: TDEM (Time Domain Electro Magnetism), magnetotelluric, geoelectric, electrical tomography and gravimetry. Geochemical analysis of the endogenic gases were also performed and, finally, seismic reflexion and refraction. The results of these investigations have convalidated the geostructural hypothesis of a limestone basement that becomes deeper as one goes from the calcareous hills on the East of the area of the subsidence towards the Tyrrhenian coast and on the West, due to a system of parallel faults according to a tectonic extension scheme (fig.2).

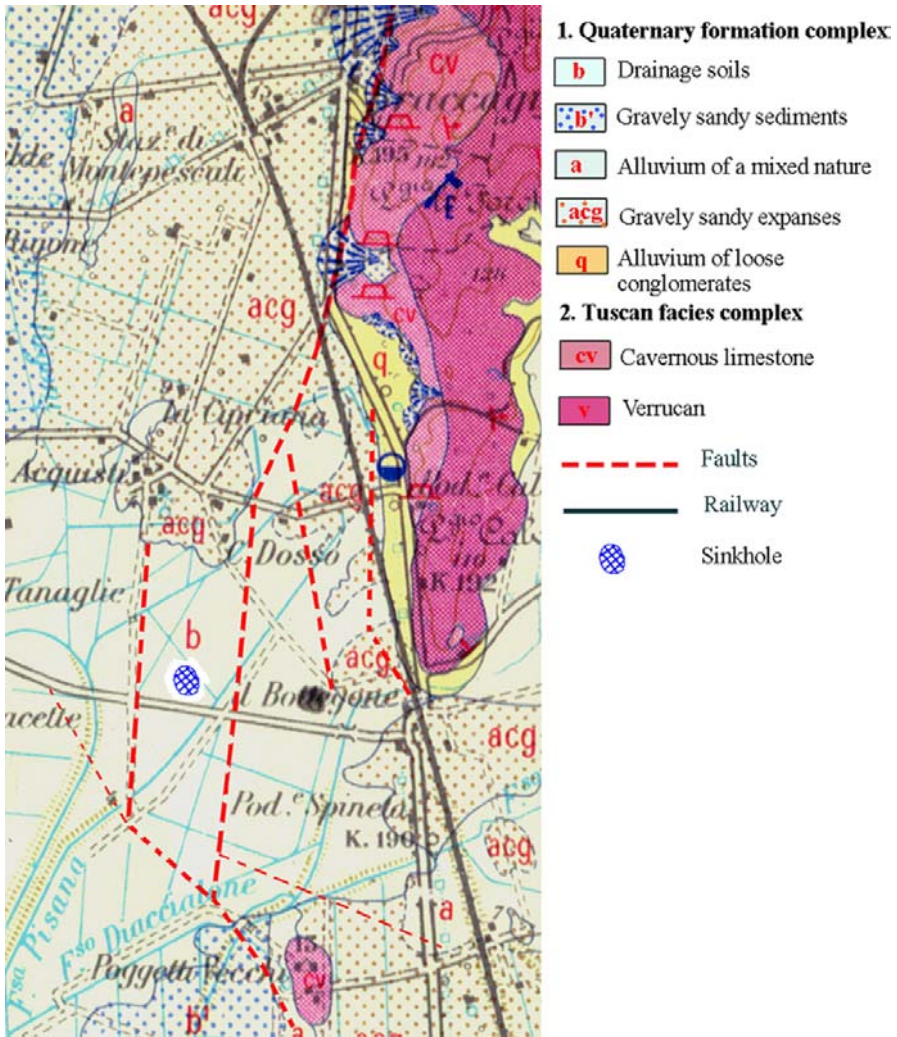


Fig. 2. Hypothesis of bedrock trend.

The geoelectric and gravimetric measurement campaign confirmed the electrostratigraphic succession, compatible with the characteristics of the soils, shown by the magnetolectric results. As far as the tomographic investigation is concerned, two profiles were prepared close to the sinkhole which identified a circular anomaly at a depth of 40 m below the SW portion of the sinkhole, which had a diameter of 100 m and interesting reworked soils of greater porosity; this anomaly seems to have identified the ground disturbed by the sinkhole collapse process. The interpretation of the data obtained with the seismic measurements offered a further indication of the depth of the substratum, with an evident degree of corre-

lation with the data of the previously carried out geophysical investigations. The results of the geophysical measurement campaign fixed the possible interval of variations of this depth at between 200 and 250 m. This depth also being supported by the geognostic drilling, extend down to 170 m. Laboratory tests were carried out on the materials that were found in the stratigraphic column of the cores: most of this material was prevalently made up of clay components. A representative sample was taken from each of the most evident stratigraphic units and classification tests were performed on these samples. The soils were clayey soils of variable plasticity, which were classified, according to the “Unified Soil Classification” (Wagner, 1957) with the initials “CH” to a depth of 50-60 m and with “CH” or “CL” in the lower layers to a depth of 130 m. Their shear strength angle was then calculated through an empirical correlation with the plasticity index of the soils and it varied between 24° and 30°.

Finally, uniaxial compression strength tests were carried out on calcareous rock samples taken from the bottom portions of the probe or from the nearby hills where the limestone massif outcrops. The following results of the compression strength were obtained from these tests: cavernous limestone, 5-10 MPa; calcareous gravel, 13-18 MPa; massif limestone, 50-60 MPa.

4 Interpretative Models

Resource was made of analytical, empirical and numerical solutions that are able to interpret the observed phenomena. In the case of the “Bottegone” sinkhole, the origin was not anthropic, nor were the geometric characteristics known, however the use of the solutions elaborated for mining situations allowed an evaluation of the dimensions of the void and a numerical modelling of the structure to be made.

In both natural and mining collapses, pipes of subsidence form whose evolution occurs because of subsequent rupture on the roof of the void and sliding of the soils from above, an increase in volume of these soils and an extension of the phenomenon up to the surface. The void remains stable until the stresses, which are distributed around the void according to an arch scheme, exceed the strength of the roof. The hypotheses for the setting up of interpretative models of the phenomenon took into consideration the shape of the subsidence on the surface, where the boundary on the South-West has one clear step, while on the other side there was a gradualist in depth of the hole. The sinkhole underwent greater changes over time on this side with an enlargement of the border towards the North-East. The numerical models provided both a regular geometry with a constant height of the void and an irregular shape with a variable hole height.

4.1 Analytical Modelling

The analytical solutions that were used to evaluate the dimensional characteristics of the underground void were: the Lehmann method, the U.K. empirical method and the subsidence pipe method. The Lehmann theory (Lueger, 1967) allows a

forecasting calculation of the surface displacements due to mining excavations to be made. This method can be applied in cases of mining on long faces and it considers the effects of surface subsidence as a consequence of the capacity of the orebody, without taking into consideration the dynamics that the overburden is subjected to. This method becomes even more valid if applied to phenomena that occur over a long period of time. The method also considers the perpendicular dimension of the excavation section as being infinitely extended and proposes a very regular geometric schematisation. A mean depth of the calcareous basement of 250 m with respect to the ground level was therefore hypothesised and an evaluation of the void dimensions was obtained with a width that varied between 90 and 120 m and a height between 24 and 39 m. The U.K. empirical method (Whittaker and Reddish, 1993) allows the subsidence produced by a void to be evaluated and it is based on observations of real mining situations. Abacuses are used for this purpose (fig.3) which present the ratio between the entity of the subsidence S and the excavation height of the mined layer M on the ordinate axis and the ratio between the width of the excavation w and the height of the overburden h on the abscises axis.

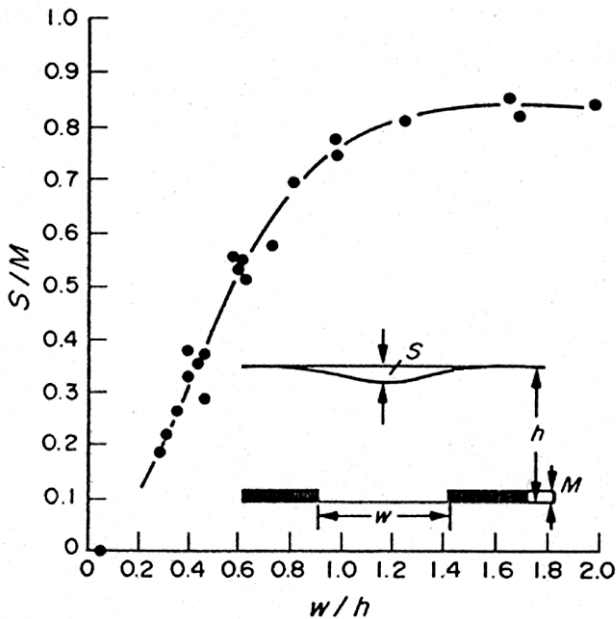


Fig. 3. Abacus for the "U.K." empiric method (Forrester and Whittaker, 1976).

It is an evaluation method that still makes use of bi-dimensional models, which mainly refer to coal mining on long faces, but it has the great advantage of being based on a large collection of real cases. The evaluation still has the restrictive hypothesis of a regular geometry of the void, which does not allow the slope of the basement or the irregularities of the void to be considered; furthermore, it does not

consider the development of the subsidence in the overburden soils. The entity of the surface subsidence being known and having hypothesised that the depth of the original void is of the order of 250 m, an application of the method gave a width of the void of between 110÷140 m and a height that varied between 30 ÷43 m. The study of the evolution mechanism of the subsidence pipe appeared to be more pertinent to the case under examination in that it considers a subsequent slide of overburden materials and their increase in volume through a coefficient k , which can be between 1.1-1.3. This method is also able to consider a void of greater dimensions than the entity of the surface sinkhole. The main drawback of this method is the symmetry that is imposed by the cylindrical geometry of the development, of a width that is close to the extension of the circular area of the sinkhole (fig.4) and the slope of the substratum is only qualitatively considered. The method involves the determination of the volume of the collapse pipe and of its increase through the coefficient k . The minimum volume of the underground void is made equal to the sum of the known volume of the sinkhole and of the increase in volume of the collapse pipe; in this way it is possible to evaluate the height of the void, the diameter of the development being known (fig.4) and made equal to that of the underground void. The depth of the calcareous substratum X was varied from 200 to 300 m, the variation interval of the width w of the void was placed between a minimum value of 90 m, which was established using the Lehmann method, and a maximum value of 160 m, which corresponds to the mean transversal dimension of the surface of the sinkhole. By applying the model, more probable values of the dimensions of the void are obtained (fig.4).

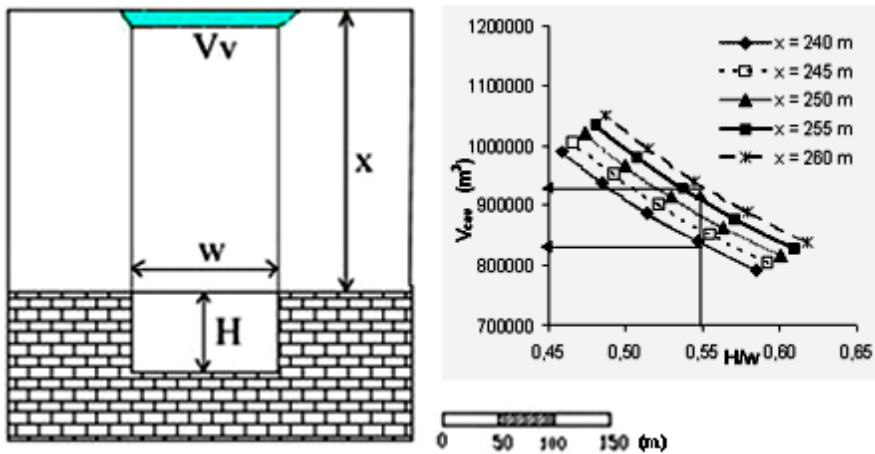


Fig. 4. Layout of the analytical method for the sinkhole.

4.2 Numerical Models

Two structural models were proposed, on the basis of the results of the geophysical investigations and the application of the analytical methods, both of which had

the depth of the substratum at 250 m (fig.5). A finite element numerical modelling of the hypothesised configurations was then carried out through the use of the Phase 2 calculation code. This code does not allow the very high displacements that were observed on the site to be analysed, however the modelling proved able to show the trend of the development of the vertical and horizontal displacements. A more complete modelling is at present being set up which, with a more appropriate calculation code, will be able to evaluate the large displacements through the deformation of the discretisation network, or by making use of meshless methods. Many requirements are necessary for the modelling in this case and these requirements sometimes “co-exist” with difficulty: the rigid transfer of portions of overburden, large displacements in the rock and in the ground and swelling of granular materials have to be allowed.

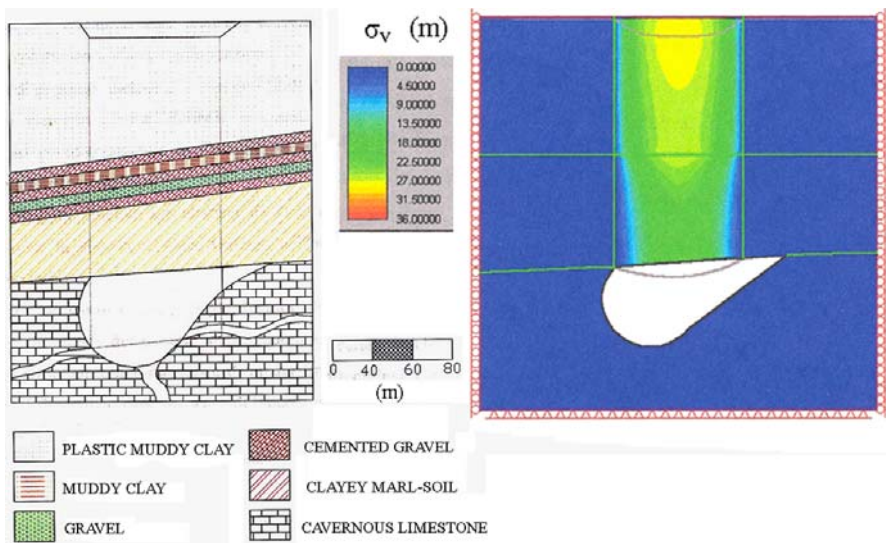


Fig. 5. Interpretative model with a sloped basement and numerical model of vertical displacements. σ_v .

5 Conclusions

The subsidence phenomenon that was studied can surely be put down to natural causes. It is very likely that the original underground void did not have a regular and symmetrical geometry as it originated from disintegration phenomena of the calcareous mass which caused a deep karsism along fault areas or even more so at the points where the faults cross. The objective of the study was to extend the investigations from a territorial planning point of view which, following the precise organisation of the geological and structural layout of the area and of the possible presence of other underground voids, establishes the possible risk areas

and assigns the utilisation classes of the territory, in the administrative context of the Town Plans, also in consideration of the fact that important structures such as the railway line and a busy national road can be found inside the area involved in the subsidence. The sub-division of the territory into areas with different criticalities is of a qualitative type. The guiding element that led one area to be more critical than another was the identification of possible faults, which represent elements of structural instability and underground thermal water flow paths. In order to supply a warning instrument for the management of the infrastructures (the railway line and the Aurelia national road) it would be possible to set up a monitoring system that would involve measurements of the altimetry variations of certain reference points which, in turn, would be connected to an alarm system that would be able to interrupt the traffic whenever signs of an incipient collapse would appear. In the case under examination, the monitoring of a section of the railway line of a length no longer than 4 km. The control measurements should be of a continuous type, for example, through GPS antennas together with a system of micro-sensors applied to the tracks. On the basis of experience gathered during the study, it is surely possible to make the adoption of investigation techniques systematic on large areas not joined by correlated parametric numerical analyses to show the potential concomitance of geological structural situations at risk. From this point of view, the modelling could be aimed at overcoming the drawbacks of the first stages of the study, introducing the typical behaviour of granular materials. In this way, and in not so urgent times, a better zoning of the areas resting on the Tuscan Cavernous formations could be obtained.

References

- Beck BF and Wilson WL (1987) Karst hydrogeology: engineering and environmental applications In: Proceedings of the second multidisciplinary conference on sinkholes and the environmental impacts of karst (Orlando, Florida, 9-11/02/1987). Balkema, Rotterdam.
- Forrester DJ and Whittaker BN (1976) Effects of mining subsidence on colliery spoil heaps. In *Int. J. Rock Mechanics Mining Sciences and Geomechanics*, pagg. 113-120.
- Lueger E (1967) *Enciclopedia della tecnica. Ingegneria mineraria*. Ed PEM, Roma, pagg 379-380.
- Wagner AA (1957) The use of unified soils classification system by the Bureau of Reclamation. In: *Proceedings of the forth International SMFE Conference*. Vol.1, London.
- Whittaker BN and Reddish DJ (1993): "Subsidence behaviour of rock structures" *Comprehensive Rock Engineering, Vol 4 (Excavation, Support and Monitoring)*. Pergamon Press.

Influence of Underground Coal Mining on the Environment in Horna Nitra Deposits in Slovakia

Jozef Malgot and Frantisek Baliak

Department of Geotechnics, Slovak University of Technology
Faculty of Civil Engineering, Radlinskeho 11, 813 68 Bratislava, Slovakia
{malgot,baliak}@svf.stuba.sk
Tel: +421 2 59274624
Fax: +421 2 59274264

Abstract. Mechanical mining of brown coal takes place in the complicated engineering-geological conditions below the volcanic mountain range Vtacnik and under the Novaky tectonic basin of Neogene age. Vtacnik Mts is affected by huge gravitational slope deformations. The main mass of the mountain range is 300-800 m thick (andesites, agglomerate tuffs) it rests upon plastic clays in which lie coal seams of 9 m thick. After excavation of the coal seams without backfilling, reactivation of extensive slope deformations (blocks, landslides) takes place. These are 100-400 m thick. This process has a large negative influence on the environment of the whole undermined area. In the Novaky basin, after mining out of the coal seam, occur large depressions on the surface. There are several villages, highways, and railways in endangered area. This paper deals with the negative influence of the activated landslides and subsidence on the environment. The methods to quantify the influence are based on engineering-geological mapping and special methods of monitoring.

Keywords: Slovakia, Horna Nitra, mining, brown coal, landslides, zoning maps.

1 Introduction

The Horna Nitra brown coal deposits are situated in Central Slovakia (Fig. 1). The eastern part of the deposits (Handlova deposit) lays below the Vtacnik volcanic mountain range. Coal mining in the Handlova deposit takes place in the region with extremely complicated geotechnical conditions under the volcanic massive that is intensively affected by various types of deep gravitational slope deformations (Figure 2B). The western part of the Horna Nitra deposit is mining in the Horna Nitra tectonic basin. In this area are quite different geotechnical conditions of mining and quite different influences on in environment (Figure 2A).

The area of Horna Nitra covers about 250 km², from which about 160 km² slope movements of various types affect more than 60 %. In the endangered area there are 16 villages, 26 km of roads, 4 km of railway tracks, a high-voltage line, industrial and mining enterprises and various kinds of long-distance pipelines.



Fig. 1. Situation of Horna Nitra brown coal Deposit in Central Slovakia.

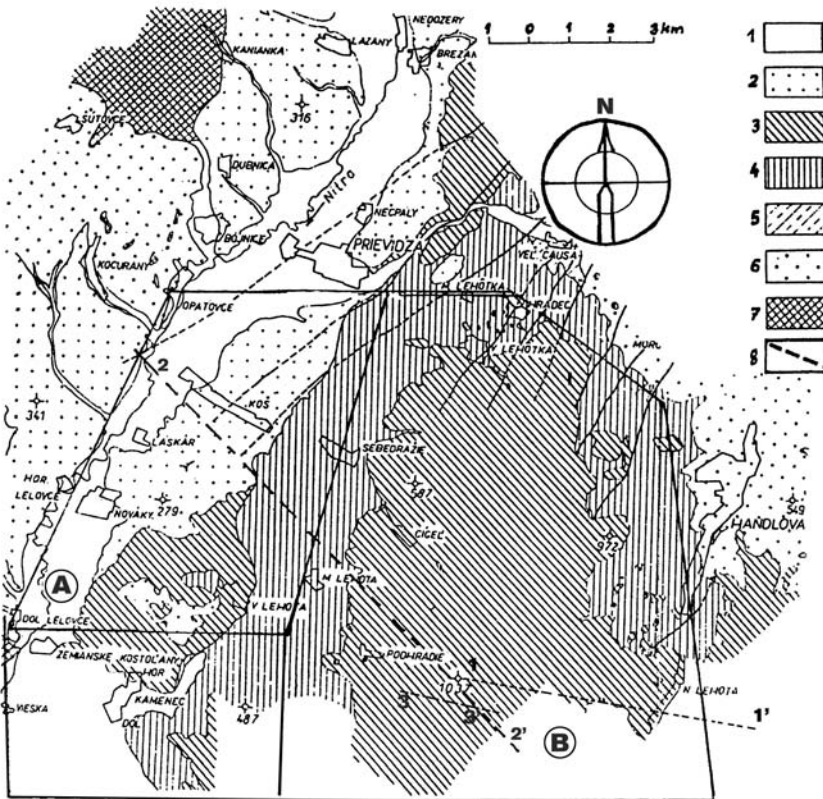


Fig. 2. Geological map of the Horna Nitra deposit (A-Novaky Deposit, B – Handlova Deposit 1-Quaternary, 2-3-Andesite, agglomerate tuffs – Sarmatian, 4-clays, tuffaceous clays with coal beds – Badenian, 5-Gravels with clays – Lower Burdigal, 6-sandstones, marly shales – Eocene, 7-Mesozoic and Paleozoic rocks, 8-Cross – section 1-1', 2-2', 3-3).

2 Influence of Mining on the Environment in Handlova Deposit

2.1 Geological Conditions

The geological-tectonic structure of the Handlova deposit is very complicated. The coal seam represents a horst, whose axis is parallel to the Vtacnik Mts water-divide. From the central part of the horst structure the seam is disturbed to the east and west by deformations of a subsidence character, which, till recently, were considered as typical gravitational tectonic subsidence. The deformations of the seam are a typical example of “gravitational tectonics” (Figure 3).

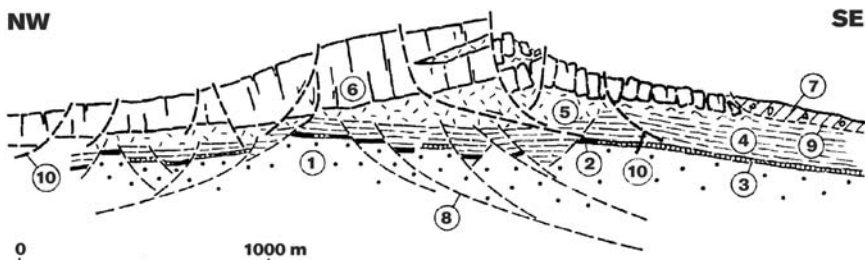


Fig. 3. Example of a profile of the brown coal deposits under the Vtacnik Mts (1-underlying conglomerates, 2-coal seam, 3-coal seam, partially affected by subsurface mining, 4-overlying clays, 5-tuffites, 6-andesites and agglomerated tuffs, 7-dispalced material, 8-surfaces of rupture in neovolcanic sediments of the gravitational tectonic origin, 9-sliding surfaces of recent natural landslides, 10-sliding surface activated by subsurface coal mining).

The middle and lower parts of the slopes are built by Paleogene clayey and loamy shales in the northeastern part or by clays and claystones of the Badenian also in the north-eastern part or the whole area of Horna Nitra . Under these layers there are 3 to 10 m thick of brown coal seams. The plastic beds are covered by hard volcanic rocks which form the rock mass of the Vtacnik Mts. These consist predominantly of andesite flows that alternate with agglomerate tuffs. The original thickness of volcanic rocks was more than 1000 m. Today it is 200 to 800 m thick. The volcanic activity took place during the Sarmatian. Later the whole area was uplifted and tectonically disrupted. The rock mass is deformed by faults of predominant NW-SE and NE-SW strike. The underground coal mining is carried out in irregularly distributed underground spaces. Presently about 50 percent of the Vtacnik Mts surface is undermined. The coal seams are mined by mechanized long-wall mining (Malgot and Otepka, 1977)

2.2 Types of Slope Deformations on the Vtacnik Mts.

The gravitational disintegration of the Vtacnik mountain range continues until today. The hard volcanic rocks submerge slowly into the plastic basement (clays) and displace slowly along the slopes down to the valleys, to the east, north and west. These are manifested by block type failures, landslides, earthflows and rock falls. The permanently unbalanced state is continually renewed by deep and lateral erosion of rivers and streams. Man-made influences are above all the influences of undermining of the slopes of the Vtacnik Mts, ballast fills, construction of urban units, communications, waste dumping, and excavations for underground mine. A more detailed description of the Vtacnik Mts gravitational deformation is to be found in the work of Malgot et al. (1986).

2.3 Influence of the Undermining on the Constructions and Environment

The activated horizontal movements of rock masses in the Vtacnik Mts area are of very large dimensions (Figure 4).

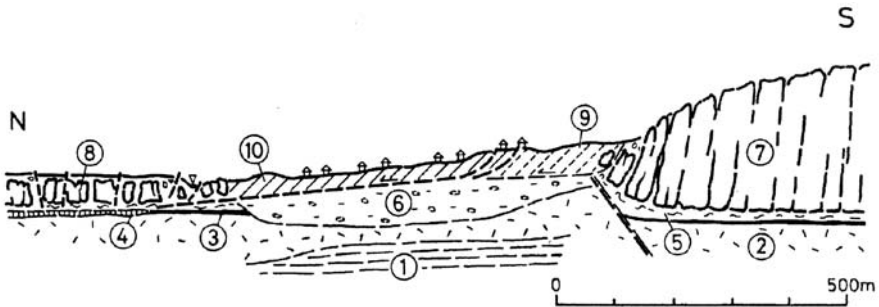


Fig. 4. Landslide profile on the western foots of the Vtacnik Mts (Burdigal: 1-claystones, Torton: 2-tuffits, 3-strata series, 4-strata series, partially affected by subsurface mining, 5-clays, Sarmat: 6-gravels and clays, 7-vulcanites, 8-cutting, fissures above undermined area, 9-landslides activated by subsurface mining, 10-ancient displaced material

After mining out a certain area of caving gradually takes place. When a sufficiently vast space is mined out, a subsidence basin develops on the surface. Its perimeter is limited by the angle of draw that under normal conditions is about 30° to 60°. In the Handlova deposit, however, subsidence brings about the revival of slope movements.. The scar walls of induced deformations may reach far beyond the boundaries of theoretically established subsidence basins. Based on the complex works mentioned in the Handlova Dep (Malgot et al., 1986), the behaviour of undermined slopes, the results of detailed mapping, extensive boring and laboratory tests, and field experiments and measurements, a special map of evaluation and prediction of slope deformations of the Vtacnik Mts was produced. From the profiles, it is apparent that activation of movements of large dimensions seriously

influences all the surface and subsurface mining objects. The activated movements devastate the surface structures and destroy forests. The cost of their stabilisation is considerable. The vertical mining structures (hauling shafts, ventilation shafts) are extremely sensitive to induced movements. In the past, there occurred shearing through several shafts at depths of 100 to 300 m. For example, in 1967, the ventilating shaft was sheared at the depth of 120 m on the contact plane of an andesite block and the underlying clays. In 1974, another shaft was sheared off at the depth of even 230 m. In 1981 an induced landslide destroyed the shaft at the depth of 20 m. Repair of deformed shafts is technically almost impossible. As a preventive measure it is possible to avoid their deformation by a suitable choice of mining process. Interesting landslides occur on the peripheral shear planes on the edges of a subsidence basin. A model example is the landslide on which lies the village of Podhradie (Figure 4). The landslides were explored by Malgot et al (1986) and by Fussgänger (1983). The volume of the activated landslide is about 24 mil. m³. The movement of the landslide on which is situated a whole village, is taking place on almost a flat shear plane, so that the objects lying on the moving mass manifest only slight signs of deformation. Their total movement reaches about 2-3 m. The most significant deformations occurred in 110 houses that are situated on the main scar, or on the lateral outlets of shear planes.

2.4 Prognosis of the Mining Impacts in Handlova

The prognosis of the influence of coal mining upon the Vtacnik Mts. was based upon detailed engineering-geological research focused on the behaviour of gravity deformations at their undercut. The prognosis of mining-controlled deformations was done in a cartographic form: three zones with three subzones each and 26 districts were delimited in detailed engineering-geological maps.

Zone I – “Areas not and not to be affected by mining”. This zone comprises the areas with no past and no future mining activities. It consists of three subzones – the subzone “Unstable slopes” with districts comprising landslides of variable activity (active, potential, stabilised), the subzone “relatively stable slopes” with the districts of block field and block rifts, and subzone “stable areas” whose districts comprise flood plains and alluvial fans, flat slopes consisting of loose sediments, and slopes consisting of rocks.

Zone II – “Areas of maximum influence of mining activities” have been distinguished according to the intensity of surface deformation caused by mining. The subzone “Strongly deformed slopes” comprises intensive surface deformation, landslides with only peripheral shear planes, block fields intensively disturbed by cracks, areas disturbed by vertical wedge like subsidence and areas affected by initiated rock falls. The subzone “Medium-deformed slopes” comprises in its districts areas consisting of loose sediments disturbed by cracks, and valley bottoms disturbed by pressure deformations. The last subzone comprises “Undisturbed areas” without surface influence of mining activities. On analogy with the zone II we can presume that consequences of the prepared mining in the

Zone III – “Areas affected by planed mining” will be identified with indications of undercut in the Zone III. This is why the names and description of subzones and districts are the same in these two zones. The results of this research will be applied for protection of four villages. The investigations result in basic data for the optimal ways of mining and four suggestions of protective zones around significant constructions on the surface. In the field investigation, a special attention was paid to the study of those slopes that are affected to a maximum by underground mining.

In the model of ‘pilot areas’, the special attention was paid to precise mapping of signs of undermining on the surface. On the map, the visual signs of vertical subsidence of slopes, shear, tensile and compression movements due to mining in the subsidence basins are indicated. For a more precise detection of the geological and hydrogeological conditions and for the quantification on the necessary data, a detailed investigation was made by boreholes in a certain selected areas. From the boreholes, numerous samples of rocks were taken for laboratory analyses. The boreholes have been equipped with special instruments to monitor slope movements (strap conductors, graduated tubes, geoacoustic and radionuclide measurements). On the terrain surface, networks of geodetic points were built in boreholes for trigonometric observations. Photogrammetry of the earth surface was used to monitor the activity of movements. The residual surface stress was also detected. Based on the investigations, it could be defined that each slope deformation reacts differently. Therefore, the influence of coal mining on the surface depends above all on the degree of its gravitational deformation, on the type slope deformations, and on the degree of its activity and development. From the study of the behaviour of slopes in the pilot areas undermined, it is possible to predict with a relatively high precision the behaviour of similar slopes, under similar conditions and with a similar type of deformation.

3 Influence of the Mining on Environment in the Novaky Deposit

The geotechnical conditions in this deposit are quite different from Handlova. The mining of brown coal is going on below the tectonic depression. The coal seams are relatively shallow. In this deposit, which has the same origin as the Handlova deposits, here are two coal seams (Fig. 5). The main seam has 2.5-12.0 m of thickness. This seam is gradually sinking down to the west at the depth of 400 m. Clay and gravel material cover the seam. This causes a problem with drainage before the start of mining.

If the underground mining is shallow, it appears small sinkholes on the surface. Mining of the coal in the deeper areas causes large depressions on the surface. The subsidence of the surface has a negative influence on the environment, in particular, the arable soils due to a change in the underground water regime. The depressions on the surface negatively influence the building of the villages Kos and Laskar, the state highway, railroad, rivers Nitra and Handlova, the electric lines

and the other line pipe structures (gas, water, etc.). Engineering geological research, monitoring, and prognosis of their influence on preventive works control the negative influence of mining activity. A very important role has the protection of the well-known historical monuments and the protection of mineral springs in Bojnice spa.

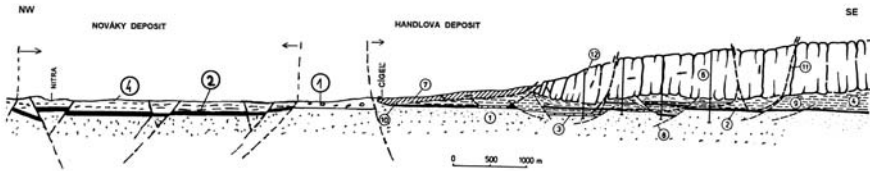


Fig. 5. Profil 1-1) Handlova deposit (1-Sandstones, shales – Paleogene, 2-coal seam, 3-coal seam, partially affected by underground mining, 4-overlying clays – Badenian, 5, 6-andesites, agglomerate tuffs – Sarmatian, 7-body of landslides, 8-surfaces of rupture in neovolcanic sediments of the gravitational tectonic origin, 11-sliding surface activated by underground coal mining, 12-boreholes Novaky deposit

Conclusions

Mining of the brown coal in Horna Nitra Deposit has a great influence on the environment. The deposit is divided into two parts. In Handlova part a complicated research has to be accomplished to know that influence. From the study of the behaviour of under mined slopes it is possible to predict with a relatively height precision the response of similar slopes disturbed by the similar slope deformations. In the Novaky deposit originate only subsidence with a small influence on the surface.

References

- Fussgänger E, Kuchar S. & Jadron D.(1983) Zosuvy pri Podhradi (Landslides near Podhradie), Report, Geofond Bratislava.
- Malgot, J & Otepka J (1977) Gravitational slope deformations near Handlova, Bull. IAEG, Krefeld, 15, pp. 63-65.
- Malgot J, Baliak, F, & Mahr T. (1986) Prediction of the influence of underground coal mining on slope stability in the Vtâènik Mts. Bull. IAEG, 3, Paris, pp. 57-65.

Sustainable Passive and Active Remedial Measures of Creeping Bedrock Slopes: Two Case Studies from Austria

Michael Moser and Stefan Weidner

Friedrich-Alexander Universität Erlangen, Schloßgarten 5, 91054 Erlangen

moser@geol.uni-erlangen.de

Tel: +49 9131 85 – 22 697

Fax: +49 9131 85 – 29 294

Abstract. Two case studies involving the large-scale and deep-seated creeping of slopes in southern Austria are discussed. In both instances passive and active remedial measures were applied to help mitigate the landslide hazard. At the first site, geodetic and extensometer measurements indicated movements averaging up to > 50 cm/year with a maximum of 352 cm occurring in one year. Previous active measures consisting of rigid structures were destroyed and replaced by flexible protective engineering works. The second case study involves an intensive geodetic monitoring program. Here, averaged yearly velocities are found up to > 30 cm/year. Active remedial measures consisted of stream diversion and protective engineering works. Both cases show the importance of a comprehensive passive remediation program.

Keywords: landslide hazard, passive and active remedial measures, deep-seated, large-scale, creep.

1 Introduction

An on-going assessment of landslide hazard resulting from deep-seated slope movements in southern Austria (Fig. 1.1) is outlined herein. The research is directed towards remedial measures and subsequent effects on the toe zones of two case studies and is one of many that address slope stability issues in Carinthia, conducted since the 1980's by the authors (e.g. Moser 1994; Weidner, Moser and Lang 1998). The effectiveness of both passive and active remedial measures is discussed.

Such efforts in understanding the processes and effects of large-scale and deep-seated slope movements in alpine regions, for instance sagging mountain slopes, on the environment, infrastructure, and engineering works is of great importance (Huder 1976; Bonzanigo 1988). Of particular interest is the large-scale detachment of bedrock slopes by deeply penetrating creep that are generally restricted to areas of recent deglaciation. These conditions cause the lowering of the local erosional base level and thus induce substantial gravitational forces within the mountainsides. This environment leads to strains and other negative impacts applied

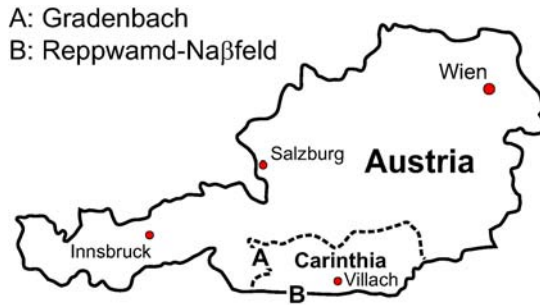


Fig. 1.1. Overview map of Austria showing the location of the two case studies, Gradenbach (A) and Reppwamd-Naßfeld (B).

over long durations to engineering works and infrastructure over broad areas. Continuous slope movements with rates up to several metres per annum alter the geotechnical properties of the parent material and result in the disintegration of rock masses. Protective engineering works and other remedial measures conventionally employed are ineffective in such situations, largely due to the scale of deformation (up to 200 m deep and 1000 m relief) opposed to shallow soil slips and slumps (in the order of metres or tens of metres) that can be more easily mitigated.

2 Remedial Measures

The experience acquired over the past 20 years in the Alps has shown that sustainable protective engineering works, designed for deep-seated slope movements, requires an extensive and long-term program of examination and measurements in order that these works be implemented successfully. The engineering works themselves are considered active remedial measures while the investigation preceding and following their implementation are passive remedial measures (Grubinger 1976). Active remedial measures are well documented in such publications as Kronfellner-Kraus (1978) and Kronfellner-Kraus (1988) and are therefore only mentioned in passing. Those that apply to the case studies are the: external (ditch) or internal (drain pipes) dewatering of slopes; drainage of sag ponds, and; construction of toe retaining walls, check dams (some with movable wings), and torrent diversion channels. Passive remedial measures can be grouped into three main categories, namely, those that describe the: nature of material involved in failure; characteristics of the failure itself, and; external factors influencing failure. The first category is primarily concerned with the geomorphologic, geologic and geotechnical properties of the rock mass. The second includes the type of failure, spatial distribution of rates of motion, and the exact course of motion. The final category revolves around climatic, hydrologic, and other environmental factors that affect large-scale creeping movements. The passive measures applied within this study are primarily those of the first and second kinds.

As a first step towards sustainable protective engineering works, detailed geomorphological, geological, and geotechnical mapping of the instable valley slopes was undertaken. This included the delineation of loosened and shattered rock masses, scarp exposures, outcrops of dilated shear zones, trenches within sagging masses, and other features related to slope instability. The preliminary, qualitative information collected was useful for describing the spatial distribution of the activity of the slopes. The preliminary mapping acted as a guide for the application of more costly, quantitative analytical methods. Unfortunately, due to the financial constraints of the project, the realization of such methods could only be carried out in limited quantities and so supplied only few reliable data. This portion of the investigations was centred about displacement velocities as these strongly influence the degree of hazard. Long-term monitoring using a combination of geodetic (areal) and steel tape, wire, and continuous recording extensometers (point-wise) was implemented. Thus the rates of deformation at the surface and the orientations of the movements could be recorded. For more detailed information the reader is referred to Moser (2003). The analysis of the accumulated data is then used for making decisions on the types of protective engineering works (active remedial measures) required, land-use zoning, and future passive remedial measures.

3 Case Study 1: Gradenbach (Fig. 3.1)

This site consists of a slope with an average inclination of 26° over 1000 m of relief (with a maximum elevation of 2100 m a.s.l.). The area of disturbed material is approximately 2 km^2 and is underlain by phyllites, calcareous schists, chloritic schists, and quartzite. Slope deformation is suspected to depths of approximately 200 m.

In 1966, a severe flood caused heavy erosion in the toe zone of the sagging slope and threatened accelerated slope movements. Subsequently, attempts were made at reconstructing the toe in hopes of stabilizing the slope and protecting the nearby village of Putschall. Active remedial measures in the form of reinforced check dams were constructed at a cost of 4 million €. Starting in the early 1970's, passive remedial measures such as steel tape, continuously recording, geodetic, and wire-extensometers were implemented (e.g. Kronfellner-Kraus 1974, 1990; Moser 2003). Observed high rates of movement (eg. 88 cm in 1972 and 352 cm in 1975, Fig. 3.1) are indicative of the extreme lateral pressures experienced within the toe. The result is the lateral displacement of check dams and uplift in the order of a metre. Where provisions for displacements were not incorporated within the design of the check dam (i.e. movable wings), cracks appear in conjunction with displacements. Ultimately, the structure is completely destroyed. By the end of the 1970's, effectively all check dams had been destroyed, demonstrating how such protective engineering works are an ineffective defence against toe erosion under these circumstances. With this realization and based on the observations from long-term passive remedial measures, new active remedial measures were introduced in the 1990's. Dams that consist of large boulders tightly connected by steel cables were substituted for the rigid check dams (Fig. 3.2). The concept of counter measures with flexible interconnected boulders was designed to compensate the

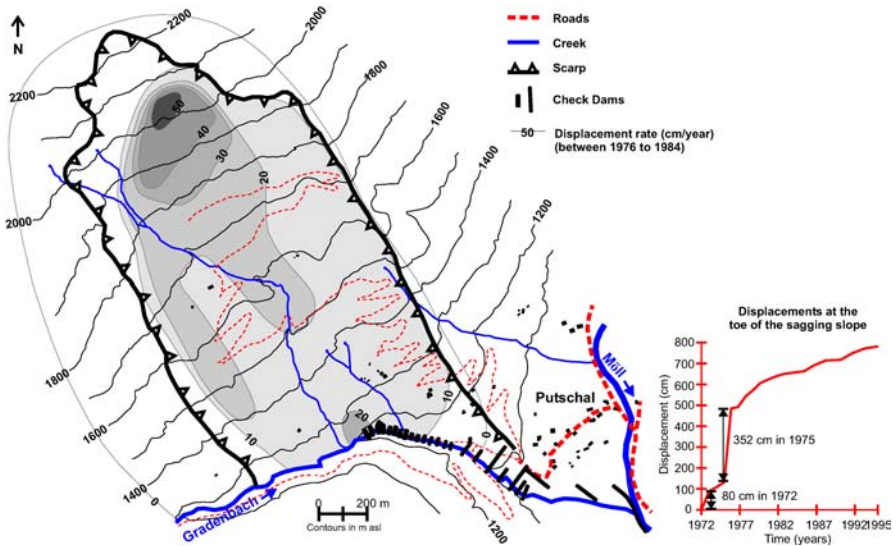


Fig. 3.1. Displacement rates for the unstable slopes at the Gradenbach site. Velocities are averaged over the period 1976 to 1984. The locations of protective engineering works within the toe zone are also given. Accompanying graph shows the yearly displacements measured at a site on the toe by a steel tape extensometer for the period of 1972 to 1995 (modified after Weidner 2000).

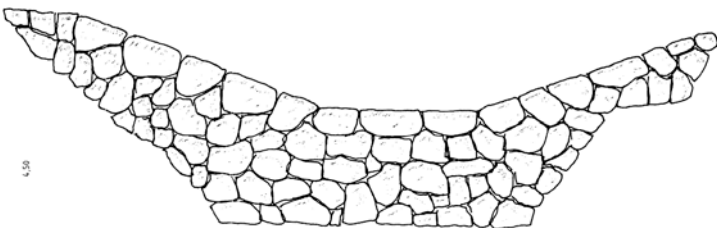


Fig. 3.2. . Example of a flexible check dam constructed boulders tightly connected by steel cables in the toe zone at the Gradenbach site (modified after Weidner 2000).

strains much longer than possible with the conventional check dams. The relative success of these measures have not yet been evaluated.

4 Case Study 2: Reppwand-Naßfeld (Fig. 4.1)

This site consists of a slope with an average inclination of 17° over 700 m of relief (with a maximum elevation of 1400 m a.s.l.). The area of disturbed material is approximately 1.7 km² and is underlain by calcareous sandstone and claystone.

Slope deformation is suspected to depths of approximately 150 m. In August 1983, an extremely heavy rainstorm resulted in the undercutting of the slope and caused 300 m of a road located in the toe zone to be destroyed by deep-seated bedrock failures. It was soon recognized that large vertical and horizontal movements were occurring and that a comprehensive control program was needed (Skolaut 1985). Subsequently, passive remedial measures in the form of a geodetic monitoring program was implemented (Fig. 4.1). The focus was on active portions of the toe and was meant to give basic guidelines for the construction of protective engineering works.

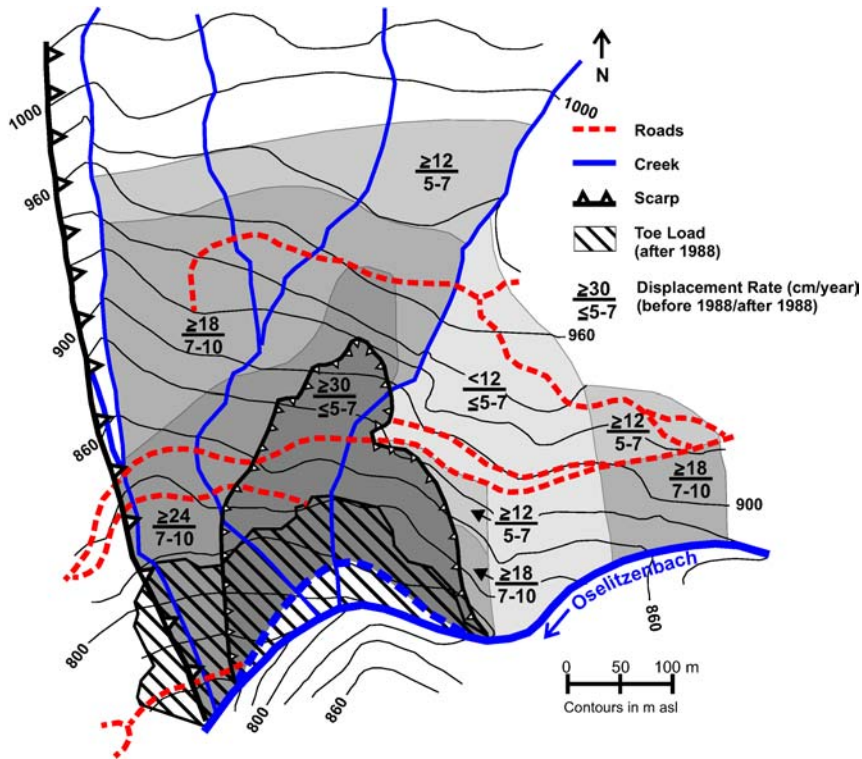


Fig. 4.1. Displacement rates for the unstable slopes at the Reppwand-Naßfeld site. Velocities prior to the implementation of active remedial measures and those that occurred afterwards are shown. In addition, the former course of the stream at the base of the slope is shown (modified after Weidner 2000).

In 1988, active remedial measures were undertaken that consisted of shifting the position of the stream found at the toe of the sagging slope to a 400 m channel made of competent bedrock (Fig. 4.2). This, in turn, created an embankment 80 m high opposite to the sagging slope. The material removed from the channel and the newly created embankment (ca. 170,000 m³) was used as a toe load for the unsta-

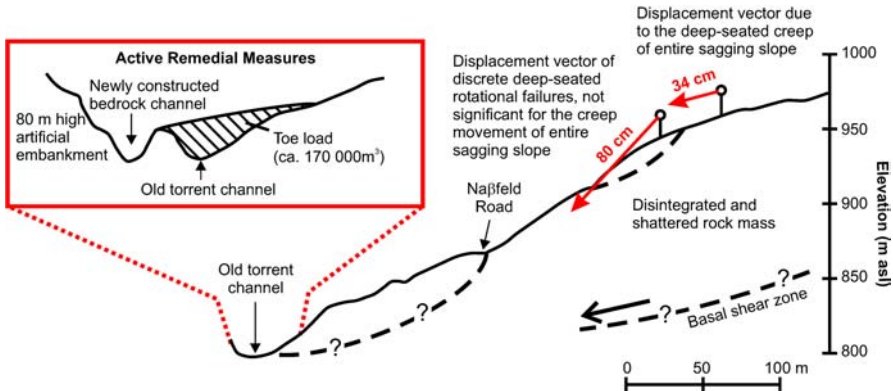


Fig. 4.2. Slope profile and remedial measures of the Reppwand-Naßfeld site. Displacement vectors are for the period 1988 to 1992 (modified after Weidner 2000).

ble flank of the slope. In addition, check dams with movable wings were constructed further upstream where rates of slope movement were substantially less. Costs for mitigation amounted to 1 million € (Moser and Weidner 1998).

The highly invasive measures (i.e. stream diversion and toe load construction) resulted in displacement rates being strongly reduced. In contrast, where only check dams were constructed, rates of displacement were only partially reduced (Fig. 4.1). Incipient cracks soon opened on transverse-channel structures and it is thought that the total destruction of these protective engineering works is inevitable (Moser 2003).

5 Conclusion

The assessment of landslide hazard due to deep-seated slope movements must be a dynamic and long-term process. The mitigation of the hazard requires in-depth knowledge of past and recent movements of the slope in order that future behaviour can be anticipated. This information is only obtainable from comprehensive passive remedial measures. The success of the mitigation is determined by the ability to understand these observations and compensate their pending affects with appropriate measures. The first step toward achieving sustainable protective works is therefore the collection and analysis of detailed geomorphic, geologic and geotechnical features and the creation of large-scale maps and cross-sections. These largely qualitative maps are then used for the systematic planning of more detailed studies, such as velocity analysis. The measuring program often includes both extensive, discontinuous measurements over the entire area effected by slope deformation, as well as continuous measurements, typically restricted to problem areas. Ultimately, the accumulated data is used for determination of the number, position, and types of active remedial measures. The past 20 years of experience investigating slope stability issues within alpine regions has provided numerous

instances of damages and total destruction of protective engineering works. Often, the outcome could have been avoided by the use of more extensive, passive remedial measures before the implementation of active remedial measures. Nevertheless, such monitoring programs are often postponed due to financial constraints and are only implemented after active remedial measures have been implemented. In the worse cases, no monitoring programs were ever initiated.

References

- Bonzanigo, L. (1988) Etde des méchnanismes d'un grand glissement en terrain cristallin: Campo Vallemaggia. In: C. Bonnard (ed) Proceedings of 5th International Symposium on Landslides, Volume 5, Lausanne, 10-15 July 1988.
- Grubinger, H. (1976) Der Schutz alpiner Lebensräume. *Österreichisches Wasserwirtschaft*, 28: 41-46.
- Huder, J. (1976) Creep in Bündner Schist. In: N. Janbu, J. Jorstad, B. Kjoernsli (eds) Laurits Bjerrum memorial volume; contribution to soil mechanics, Norway Geotechnical Institute, Oslo.
- Kronfellner-Kraus, G. (1974) Die Wildbacherosion im allgemeinen und der Tazuschub im besonderen. In: 100 Jahre Forstlichen Bundesversuchsanstalt.
- Kronfellner-Kraus, G. (1978) Geschiebepotential und Verbauungstechnik im Bereich von Talzuschuben. *Mitteilungen der Forstlichen Bundesversuchsanstalt*, 125: 58-71.
- Kronfellner-Kraus, G. (1988) "Der Durnbach im Oberpinzgau und seine Verbauungstechnischen Probleme". *Mitteilungen der Forstlichen Bundesversuchsanstalt*, 161: 9-10.
- Kronfellner-Kraus, G. (1990) Einige aktuelle Probleme und Ergebnisse der Wildbachforschung in Österreich. *Mitteilungen der Forstlichen Bundesversuchsanstalt*, 9: 7-24.
- Moser, M. (1994) Geotechnics of large-scale slope movements ("Talzuschübe") in alpine regions. In: R. Oliveira, L.F. Rodrigues, A.G. Coelho, A.P. Cunha (eds) Proceedings of the 7th International IAEG Congress, Volume 3, Lisbon, 5-9 September 1994.
- Moser, M. (2002) The effects of deep-seated mass movements on the alpine environment. In: Proceedings of the International Conference, Interpraevent 2002, Matsumoto, 14-18 October 2002.
- Moser, M. (2003) Geotechnical measurements for the assessment of the kinematic and long-term behaviour of unstable mountainsides. *GeoTechnical Measurements and Modeling Workshop, Karlsruhe 2003*.
- Moser, M. and Weidner, S. (1998) Die Auswirkungen von Talzuschüben auf die alpine Umwelt. *N.Jb. Geol. Paläont. Abh.*, 208: 531 – 548.
- Skolaut, H. (1985) Technischer Bericht für das Ausführungsprojekt Oselitzenbach. Villach
- Weidner, S. (2000) Kinematik und Mechanismus tiefgreifender alpiner Hangdeformationen unter besonderer Berücksichtigung der hydrogeologischen Verhältnisse; Diss.-Universität Erlangen-Nürnberg 246 S., Erlangen.
- Weidner, S., Moser, M. and Lang, E. (1998) Influence of hydrology on sagging of mountain slopes ("Talzuschübe") – new results of time series analysis. In: D.P. Moore, O Hungr (eds) Proceedings of the 8th International IAEG Congress, Volume 2, Vancouver, 21-25 September 1998.

Problems in Defining the Criteria for an Earthquake Hazard Map – A Case Study: The City of Haifa, Northern Israel

Ram Ben-David

ADAMA, Environmental and Geological Studies, PO Box 901, Shoham, Israel 73142

ram@adam-ma.co.il

Tel: +972 3 9739911

Fax: +972 3 977

Abstract. This paper deals with the problems of defining the criteria for an earthquake hazard map in the city of Haifa, Israel - an area where an active geological fault crosses a very densely populated urban zone that is situated in close proximity to a large industrial zone where a number of heavy and hazardous industries operate. The minimum acceleration rate in this area as defined by the map attached to the Standard Code 413 (Design provisions for earthquake resistance of structure) is 0.175. Since many geological sources indicate that this figure does not satisfy the structural design for building, a more comprehensive assessment was required regarding the local situation. Therefore, the following set of criteria (from low risk to high) for the earthquake hazard map were selected: 1) The minimal criteria is that of the Code 413 map, 2) Additional hazard due to geotechnically soft strata, 3) Additional hazard due to topography, 4) Additional hazard due to landslide, 5) Additional hazard due to liquefaction, and 6) Additional hazard due to proximity to an active fault. The Yagur Fault divides the city of Haifa to two very distinct regions – the Carmel Ridge and the Zevulun Valley. Therefore the earthquake hazard map is an important tool for appropriate planning of new quarters as well as the maintenance and emergency needs of the existing industrial zones and residential areas.

Keywords: Haifa, Northern Israel, earthquake hazard map.

1 Introduction

1.1 Different Approaches

Generally speaking, when editing an earthquake hazard map the author is presented with a serious challenge. On the one hand, there is the problem of trying to summarize earth sciences data (mostly geological and geophysical data) vis-à-vis the existing urban situation or future planning on the other hand. Different approaches were developed to deal with these problems, according to the planning and statutory culture in each country or state. Here are a few examples of these different approaches. In Basel, Switzerland, the earthquake hazard maps are focused on microzonation data and the probable damage due to an earthquake (e.g. Fäh, et al., 1997; Fäh, 2000). By contrast, the state of California happens to be

very tectonically active, so the law requires the State Geologist to establish regulatory zones (known as Earthquake Fault Zones) around the surface traces of active faults and to issue appropriate maps. The maps are distributed to all affected cities, countries, and state agencies for their use in planning and controlling new or renewed construction (Alquist-Priolo Earthquake Fault Zoning Act, 1972; Seismic Hazards Mapping Act, 1991¹ ext.). In Israel, the Israeli Code 413 elaborates the design requirements for the engineer with regard to the earthquake load condition. A map of different potential accelerations (PGA) is attached to the code (Fig. 1). This map mainly takes into account the distance from the most tectonic activity (primarily the Dead Sea rift valley and secondarily the Yagur Fault system). Due to new data of recent years this map is under revision today and the general approach is to use more conservative figures in construction design. Since the map attached to the Israeli Code 413 is too generalized, the Geological Survey of Israel (GSI) initiated a detailed earthquake map of the city of Jerusalem (scale of 1:12500). This map takes into account the acceleration potential due to strata composition, topography, slope stability, artificial slope stability and historical earthquake events (the 1927 earthquake)(Solomon et al. in prep.).

1.2 The City of Haifa and Its Unique Problems

The city of Haifa is situated at the southern rim of the bay of Haifa, in the north of Israel (Fig. 2). It is a city of about 290,000 habitants, and the considered surface is about 80 km². The topography divides the city area into two major parts – the Carmel Mount ridge (and slopes), of which its axis is from SW to NW and the Zevulun Valley, which lies north of Mount Carmel and on the Haifa Bay seashore. Modern day Haifa was developed from very ancient cultures that lived here since the Bronze Age (4000-1200 years Before Christ - yBC) through the Iron Age (Biblical time) and the Persian Age (at which time a fortress was built). Since the Hellenistic period (around 100 yBC) the name Haifa is found in the ancient Jewish religious books (Mishna and Talmud), up to the 6 Century AD – the time of the invasion of the ancient Arab tribes. The city of Haifa slowly developed since then up to the time of the British Mandate (1917-1948). The British developed the Haifa harbor side by side with heavy industry, such as refineries. Since the creation of the state of Israel in 1948 the industrial zone has grown become larger and larger. Today the city of Haifa is primarily an industrial city, with refineries, chemical factories and a very busy harbor. Large volumes of hazardous liquids and gases are stored there in tanks and transported via many kilometres of pipelines. The industrial activity is mostly in the Zevulun Valley and the Haifa bay seashore. Secondly, Haifa is a commercial and academic center. These activities are mainly focused along the Carmel ridge and slopes. Geologically speaking, the area of Haifa is situated in an area of earthquake hazard area due to a major fault

¹ Guidelines for Evaluation and Mitigating. Seismic Hazards in California. Special Publication 117.

Recommended Criteria For Delineating Seismic Hazard Zones in California. Special Publication 118.

line – the Yagur fault - that is considered to have been active during the Late Pleistocene – Holocene. This fault, and its sub-lineaments, divides the city to two major topographic parts mentioned above.

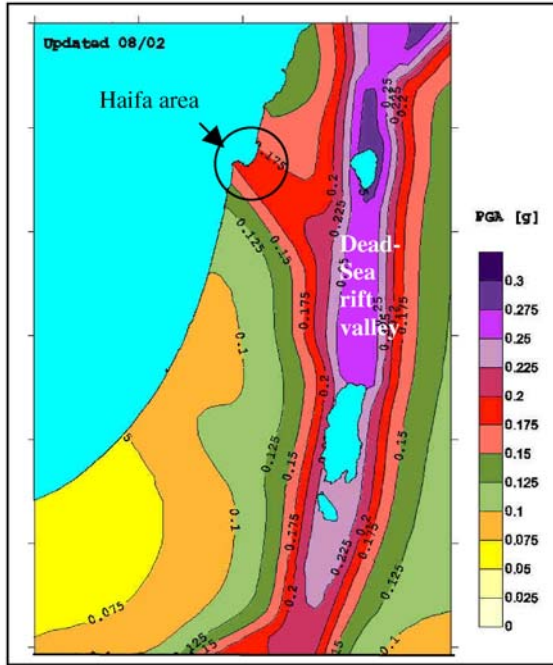


Fig. 1. The proposed new acceleration areas attached the Israeli Code 413 (edited by the Geophysical Institute of Israel).

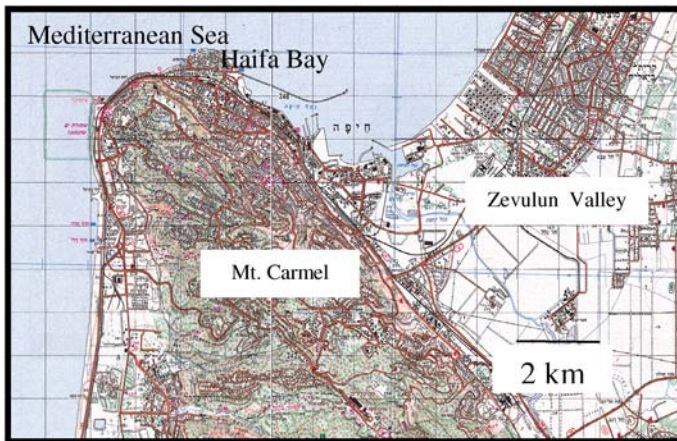


Fig. 2. Location map of Haifa and the surroundings.

2 The Research Question

The tectonically active area of Haifa and the heavily industrialized zones raise the following question – what criteria should be used for the establishment of an earthquake hazard map, and how to decide what is the value of each parameter in this map?

3 General Geology (Mostly from Karcz 1959; Kafri & Ecker 1964) (Fig. 3)

As mentioned above, the Yagur fault is the main reason for the very distinctive topographic elements. This fault system divides Mount Carmel and the Zevulun Valley. The geological strata of the Carmel ridge are composed of the Late Albien to Turonian strata, consisting mainly of dolomite and limestone to chalk (C1 and C2-t respectively). During the Upper Cretaceous time period volcanic eruptions occurred, leaving basalt and tuff remnants. The Zevulun Valley is a graben in which hundreds meters of its upper section is composed of Quaternary alluvial sediments of clay, calcareous sandstone and some gravel lenses (Table 4.1; Fig. 4).

4 The Suggested Parameters and Their Implications in the Earthquake Hazard Map of Haifa

4.1. The Geological Survey of Israel (GSI) parameters, used for the city of Jerusalem (Salomon et al. in prep.), were established on the basis of the proposed Haifa earthquake hazard map. Modifications were made due to differences between these two cities. These modifications are due to the fact that no active fault is found in Jerusalem and the earthquake hazards there are due to the Dead Sea valley rift tectonic activity. In Haifa, the main issue was to determine if the Yagur Fault is an active fault. Evidence that indicate that the fault is an active fault are as follows:

- Deviations of the riverbeds while crossing the Yagur Fault are interpreted as being due to horizontal displacement of the main fault during the Quaternary (Achmon 1986).
- Displacement of Pliocene to Recent sediments as criteria for young faulting was found in few sites. For example, evidences of a 55kaBP reversal faulting were found due to an investigation for fuel tanks in the vicinity of the main fault (Salomon et al. 2001).
- History of measured earthquake – The Geophysical Institute of Israel (GII) has measured earthquake activity for the last 3-4 decades. From these measurements it is clear that many earthquakes were produced in association with the Yagur Fault system (Fig. 5 – from Ron et al. 1990).
- Seismicity was noted in the Seismic Zonation map of Israel, in the Haifa area and Zevulun Bay (Shamir et al. 2001).

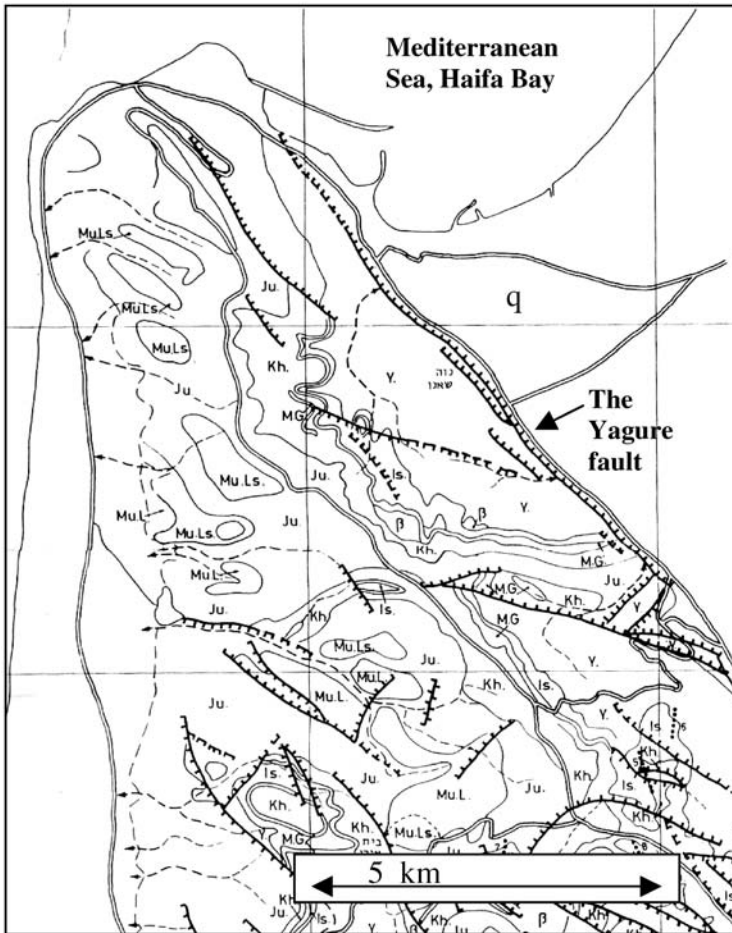


Fig. 3. Generalized geological map of the Haifa area (Source- Karcz 1959). Legend – Y= Yagur dolomite; Is= Isfiye chalk; β= volcanic; M.G.= “Gryphea” limestone; K.H.= Khurebe chalk; Ju= Jundiye chalk.

4.2. In the other hand, the evidence that suggests that the Yagur Fault cannot produce an earthquake of a magnitude larger than 6 are found in a detailed work that was carried out by Heimann et al. (2000). The data provided by this research is based on the bay area’s high potential for liquefaction due to mostly sandy deposits (sea shore dunes and alluvial deposits) and very shallow water table ($5 > m$). The results of this research are still under debate. The conclusions drawn by this research may be due to the fact that the deposits in the area under investigation are very young (mostly Holocene).

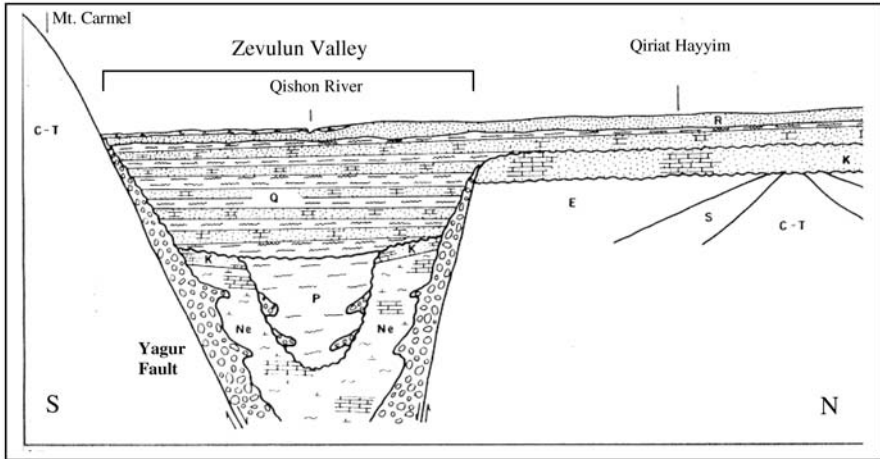


Fig. 4. Geological cross section of Haifa area – the Zevulun valley and Carmel ridge. C-T= Cretaceous to Tournian; S= Senonian; E= Eocene; Ne= Neogene; K= Ne calcareous Kourdani Fm.; P=Pliocene; Q= Quaternary; R= Recent (for location see Fig. 2).

4.3. Thus, the most likely conclusion and the assumption of this work is that the Yagur Fault should be considered as active.

4.4. The relative sensibility of the area with regard the acceleration map rate attached to the Israeli Code 413 (Fig. 1) should be evaluated according to the following stages, from mild to strong (modified from Salomon et al. in prep.):

- No additional hazards (indicates compatibility to Israeli Code 413 map – 0.175 – 0.2 g);
- Additional hazard due to geotechnically soft strata of the upper 30 m;
- Additional hazard due to topography, in which this factor is divided to sub stage – a) 10-30°, b) >30°;
- Additional hazard due to potential landslide and hydrological regime;
- Additional hazard due to liquefaction potential;
- Additional hazard due to proximity to an active fault.

4.5. The parameters detailed in 4.4 that were used to define the Haifa earthquake map criteria are as follows:

- The geological setting of the Haifa area – including the distance from the active Yagur Fault, and the strata composition along the Carmel ridge and slopes, and in the Zevulun Valley;
- The strata composition of the Carmel ridge and the Zevulun Valley), geotechnical data of the strata;
- The topography with regard to the differences in height between the Carmel ridge and the Zevulun Valley, and the local differences regarding the incised creeks on the Carmel ridge;
- History of landslides as potential areas to re-slide due to earthquake;

- Geophysical data, including recorded earthquakes related to the Yagur Fault and estimation of the accelerations in the Haifa area and local measured site effects;
- Depth of water table in the Carmel ridge and as related to its depth regarding landslide and liquefaction potential.

4.6. The data upon which is based the earthquake hazard map with regard to the criteria parameters mentioned in section 4.3 and 4.4 are as follows:

- Geology:
 - The distance from active faults – This is always considered as a major hazard parameter (as mentioned in the Californian law – see foot note 1). The Israeli Code 413 also forbids construction of any building on a known active fault. This instruction is in many cases difficult to achieve due to the lack of geological information and due to the lack of agreement about the meaning of the term “active fault”. In the case of Haifa, and from the Quaternary geology of the Haifa bay, we have to assume that the Yagur Fault is active. Yet only future research will be able to conclude whether or not this assumption is correct.
 - Rock composition implications – The differences between the rock mass of the Carmel ridge and the Zevulun Valley fill is very clear. If we use the US grading system of the rock mass, the shear wave speeds (V_s30) within the upper geological section at the Carmel ridge should be considered usually high ($V_s30=1000$ to >1500 m/sec which equivalent to class B, AB and A – Wills et al., 2000) due to the relatively hard rock which composes the upper part of ~80% of the city surface (Table 4.1).
 - Soil composition implications - The rock layers, which form the Carmel ridge, are found very deep in the Zevulun Valley due to its graben shape (Fig. 4).
- Geotechnical:
 - The Carmel ridge - The geotechnical data of the Carmel ridge strata is based mostly on boreholes performed for a ~6 km long tunnel, which was intended to cross the mountain E-W. The data indicates, from uniaxial and tensile strength tests, that the entire section is composed of moderate to strong rock layers (mostly chalk to dolomite respectively). The exceptions to that are few tuff layers or lenses (Geoprospect 1999).
 - The Zevulun Valley – The depth of the Pliocene-Holocene valley fill above the rock layer reaches down hundreds of meters (Kafri and Ecker 1964). The upper 50 m or more of the geological section is composed of unconsolidated material. Along the sea bay unconsolidated sand dune covers large areas up to about 8 m above sea level, which is the level of water table.
- Topography:

The Carmel ridge forms a moderately flat surface, at which the water divide inclines gently from ~+450 at its SE to ~+220 above the seashore cliffs at its NW side. Along the mountain's slopes creeks are incised. At the western side of the

mountain these creeks continue to the Mediterranean Sea, while at the NE side they flow into to the Qishon River, which crosses the Zevulun Valley to its base level in the Haifa bay. The SE Carmel slopes are much steeper than the W side, but on both sides steep cliffs (>300) were formed along the creeks' shoulders. The Zevulun Valley is a near shore plain rising very gently towards the SE up to an elevation of ~+8 m above sea level. It is important to note that the most populated areas are along the NNE slopes while the heavy industry is situated in the Zevulun Valley at the vicinity of the seashore.

Table 4.1. Geological and geophysical data of the Haifa area.

Formation ⁱ	General Lithology	Field Hardness	Generally exposed	Field evid. Of slope stability ^{vi}	Estimated Vs30 M/sec ⁱⁱ	American Definition ⁱⁱⁱ	Gradient Velocity ^{iv}
Saqiye to Kurkar	Sand on clay	soft	Zevulun Valley	_____	110-300 ^v	D-DE	Low
Alluvial fill	Clay and gravels	Moderately soft	Along creeks	_____	<180	E	Moderate
Muhraqa	limestone & dolomite	strong	Hills along water divide	Sliding upon Shamir Fm.	1000-1500	AB	Low
Shamir	chalk +flint	Moderately strong	Along water divide and W slopes	Ancient slide along exposure	555-1000	B	Low
Volcanic	Tuffs	Moderately soft	S part of Carmel ridge	Ancient slide along exposure	360-900 ^{vi}	C	Moderate
Khureibe	chalk	Moderately soft	Along water divide	Few small signs	555-1000	B	Low
Melecke	limestone	Moderately strong	Upper NE slope	No evidence	1000-1500	AB	Moderate
Isfye	chalk	Moderately soft	S Carmel ridge	Few small signs	555-1000	B	High
Yagur	dolomite	strong	NW Carmel slopes	No evidence	>1500	A	low

ⁱ According to the geological map of the Haifa area (Karcz, 1959, Fig. 3).

ⁱⁱ Source - Wax and Siman-Tov., 1991; Sneh et al., 2001.

ⁱⁱⁱ Extrapolated from Solomon et al., in prep.

^{iv} According to Willis et al., 2000 and NEHRP, 1994.

^v Gradient velocities are regarded when a low velocity formation covers a higher velocity formation. When a low velocity formation is exposed on surface increase of shear waves are expected.

^{vi} Source Yazreski, 2003.

^{vii} High values might be correct on a less altered tuff or basalt rock.

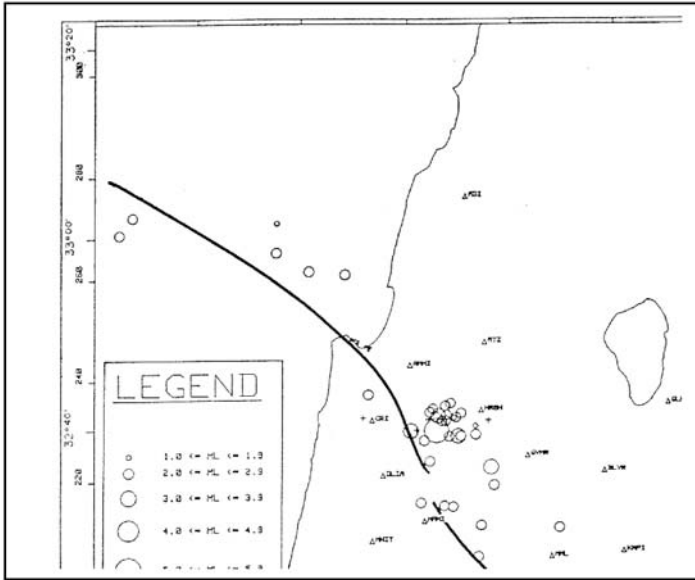


Fig. 5. Recorded earthquake as regard the Yagur Fault (from Ron et al., 1990).

- Landslide

In Haifa, a few areas were detected to have historical prints of landslides. Nevertheless, it seems that at present most of them can be defined as non-active landslides. Due to the dense urbanization it is very difficult to conclude whether or not these landslides may slide due to a strong earthquake.

- Geophysical data:

- Recorded earthquakes along the Yagur fault system – about 50 years of records exist although the modern seismic and acceleration measurement network has been in existence since 1982. Small to moderate earthquakes were felt throughout all these years, very clearly associated with the Yagur Fault (Fig. 5 – from Ron et al. 1990).
- Estimated acceleration of soft soils in the Haifa area - The younger fill, which is composed of clay and sand may produce shear velocities (from bottom at ~250m deep to surface) of 700-200 m/sec respectively (Zaslavsky et al. 2003). This is also true in the vicinity of the fault (less than 100 m from fault line), although a gravelly alluvial fan exists at the creek's outlets.

- Water table (source- the Hydrological Services of Israel):

- Along the Carmel ridge – In general, the water table along the Carmel ridge is ~3-5 m above sea level, at the western side while at its NE side the water table is ~1-3 m above sea level. Perched water may be found locally due to marl or clay layers.
- The Zevulun Valley - In the Zevulun Valley and Haifa Bay the water table is 1-3 m above sea level, which generally speaking is 2-4 m below surface.

- **Liquifaction potential** – As mentioned above the sand cover along the sea-shore of Haifa Bay and the very shallow water table indicate that the potential for liquifaction in this zone is high. This conclusion is important because of the heavy industry situated on this terrain.

5 Summary and Conclusions

An earthquake hazard map should take into account (from mild to strong) additional hazards based on the Israeli Code 413 due to strata geotechnical properties, to topography, to landslides, to liquefaction and to the proximity to an active fault. The city of Haifa is divided to two very distinct provinces the Carmel ridge and the Zevulun Valley. This sharp distinction is due to an active fault – the Yagur Fault -, which crosses the city along the foot of the mountain. Thus, the area of the city of Haifa is situated in an area, which may suffer severe damages because of a strong earthquake. Special attention is required in areas of heavy, hazardous industries and pipelines areas, which may multiply the damage caused by an earthquake. The map will serve as a major tool for the emergency services planners, especially regarding availability and accessibility to hospitals and for the fire department and hazardous materials teams. The map will be used to minimize earthquake hazards in recently planned areas within the city. The map will be used as part of the database to reinforce buildings in areas, which are more likely to be damaged due to earthquake. The map should be revised from time to time according to new geological data.

Acknowledgments

The author wishes to thank the Ministry of Interior, the Haifa Municipality and above all Architect Y. Freund for their acceptance to publish this work although it is still in process.

References

- Achmon M. (1986). The Carmel border fault between Yoqneam and Nesher. *MSc Thesis. Hebrew Uni., Jerusalem, 54 p. (in Hebrew).*
- Fäh D., Rüttener E., Noack T., Kruspan P. (1997). Microzonation of the city of Basel. *Journal of Seismology*, 1, 87-102.
- Fäh D. Kind F., Lang K., Giardini D. (2000). Earthquake scenarios for the city of Basel. *Soil Dynamics and Earthquake Engineering, in press.*
- Geoprospect (1999). Geotechnical geological report on core drillings along Carmel tunnels alignment. *Geoprospect LTD, Jerusalem, 30 pp.*
- Heimann A., Frydman S., Wachs D. and Talwani P. (2000). Late Quaternary seismic history of the Haifa and Elat bay areas evidenced by paleo liquefaction features: implications for seismic hazard evaluation. *TR-GSI/7/2000, Geol. Surv. Israel, Jerusalem, 18 p.*

- Kafri, U and Ecker, A. (1964). Neogene and Quaternary subsurface geology and hydrogeology of the Zevulun plain. *Bull. 37, Geol. Surv. Of Israel, Jerusalem, 13 p.*
- Karcz Y. (1959). The structure of the northern Carmel. The Bull. Res. Council of Israel, Aug.-Nov. 1959, pp: 119-130, Jerusalem.
- Ron H., Nur. A., Hofstetter A. (1990). Late Cenozoic and recent strike slip tectonics in Mount Carmel northern Israel. *Ann. Tecton., 4., pp: 70-80.*
- Rozen A. (1992). Evaluation of the seismic hazard to the Carmel tunnel due to the Yagur fault. *State of Israel, Mins.of Finance and Mins. of Transportation, Netivei-Carmel – Ayalon Highway Co. Ltd., App. B-13, 20 p. (in Heb).*
- Salamon A., Zaslavsky Y., Shtivelman V. Rockwell, T. (2001). Seismic Hazards analysis in the Neshet site: Bay of Haifa, Israel. *Isr. Geol. Soc. Ann. Meet., p: 101.*
- Shamir G., Bartov, Y. Sneh A., Fleischer L., Arad V., Rosenfeld, M. (2001). Preliminary seismic zonation in Israel. *GII, Rep 550/95/01(1).*
- Sneh A, Rozenpat M., Hoyland S. (2001). The geotechnical characteristic map of the Haifa area. *Geological Survey of Israel, Internal Report, 8 p.*
- Yazreski M. (2003). Seismic refraction survey of the Yadin and 75 interchange roads in the Quishon area. *The Geoph. Inst. Of Israel, Rep. 243/242/02.*
- Wax D., Siman-Tov O. (1991). First estimations of the seismic hazard in the city of Haifa and the Zevulun valley. *Geol. Surv. Israel, Rep.GSI/31/91, 25 p.*
- Wills C.J., Petersen M., Bryant W.A., Reichle G.L., Saucedo G.J., Tan S. Taylor G., Treiman J. (2000). A site condition map for California based on geology and shear wave velocity. *Bull. Seismo. Soc. America, Vol: 90, 6B, S187-S208.*

Some Positive and Negative Aspects of Mine Abandonment and Their Implications on Infrastructure

Laurance Donnelly¹, Fred Bell², and Martin Culshaw³

¹ Halcrow Group Ltd., Deanway Technology Centre
Wilmslow Road, Handforth, Cheshire, SK9 3FB, UK and
Honorary Research Fellow, British Geological Survey, Kingsley Dunham Centre
Keyworth, Nottingham, NG12 5GG, UK

² British Geological Survey, Kingsley Dunham Centre
Keyworth, Nottingham, NG12 5GG, UK

³ Urban Geoscience and Geological Hazards Programme, British Geological Survey
Kingsley Dunham Centre, Keyworth, Nottingham, NG12 5GG, UK and
School of Property and Construction, The Nottingham Trent University
Newton Building, Burton Street, Nottingham, NG1 4BU, UK
mgc@bgs.ac.uk
Tel: +44 115 936 3380
Fax: +44 115 936 3460

Abstract. Many urban and greenfield environments throughout the United Kingdom are located in regions where mining has occurred. Mining dates back to pre-Roman times and includes metalliferous minerals (such as gold, copper, lead & zinc), bulk minerals (such as sandstone, limestone, gypsum & halite) and coal, the latter being the most important mineral mined both quantitatively and in terms of value. Due to this long mining history, this had resulted in a legacy of 'mining relics' and hazards (such as mine entries, abandoned workings and contaminated land), with presumably many of these sites remaining, as yet, unknown. However, the mechanisms of failure and ground deformation, in general, are appreciated. Over the past few decades the British coal mining industry has experienced a gradual decline. However, individual closed and abandoned mines, as well as entire coalfields can, under appropriate investigations and a favourable economic climate, offer alternative energy resources. These include for instance, for coal bed methane (CBM), coal mine methane (CMM), underground coal gasification (UCG). The objectives of this paper are to draw attention to some less well-documented 'positive' aspects of mine closures and coalfield abandonment.

Keywords: abandoned mineworkings, reuse of mineworkings, Great Britain.

1 Introduction

Although mining in Britain has not been restricted to coal, it also involving the underground extraction and opencasting of metalliferous orebodies and industrial minerals, it is the decline of the coal mining industry that presents the most diverse and widespread range of mining-induced geological and environmental pro-

blems. In fact, coal mining in Britain primarily dates back to the twelfth century and has left a legacy of mining relics and mining-induced geological hazards. Geological problems associated with past coal mining include the following:

- Collapse of abandoned mine workings, shafts and adits
- Subsidence
- Fault reactivation, fissuring and compression
- Reactivation of landslides and the first time initiation of natural slopes and colliery waste tips
- Spontaneous combustion of insitu coal seams and tips
- Minewater rebound and acid mine water drainage
- Emissions of toxic, noxious, explosive and asphyxiant gas (mainly methane, sythe, carbon monoxide, carbon dioxide and hydrogen sulphide).

All of the above can represents serious problems when associated with land that is scheduled for regeneration land or to be developed for infrastructure projects. Further information on these types of geohazards and mining-induced hazards can be found in Bell 1999, Bell and Donnelly 2002, Bell *et al.*, 2000, 2002, Culshaw *et al.*, 1999, 2000, Donnelly 2000a, 2000b, Donnelly and Rees 2001, Donnelly *et al.* 1998. Less well known are the potential positive aspects associated with coal-field areas. These include the potential recovery and use of mine gases for power generation, and the alternative use of abandoned mine workings for storage of waste and other materials.

2 Clean Coal Technology and Alternative Energy from Abandoned Mines

Abandoned coal mines may not necessarily always be considered as a liability, but can potentially provide alternative resources of energy in the form of the following:

- Coal mine methane, coal bed methane, abandoned mine methane;
- Underground coal gasification;
- CO₂ sequestration.

2.1 Coal Bed Methane (CBM), Coal Mine Methane (CMM) and Abandoned Mine Methane (AMM)

Due to its susceptibility to explosions (when mixed with air in concentrations of 5-15%), methane gas is routinely removed from underground coal mines. This occurs in advance of planned mining operations, during mining, and after mining has been completed. It is achieved through degasification and by the use of vertical and horizontal drillholes into the coal, as well as by mine ventilation systems. This often is referred to as 'methane drainage'. If this occurs in association with any mining activities, it is referred to as coal mine methane (CMM). Coal bed methane

(CBM) on the other hand, involves the recovery and utilisation of methane, from a drillhole, or an array of wells drilled into coal seams, which have not been disturbed by mining. Following the abandonment of mining, the recovery of gas for energy purposes is referred to as abandoned mine methane (AMM). There is, however, some overlap between these three categories. It should be noted that coal has a very large surface area (some 93,000 000 m² per tonne of coal) and, as methane can exist as a tightly packed monomolecular layer adsorbed on the internal surfaces of the coal matrix, coal is able to hold two or three times more gas than conventional reservoirs. Indeed, higher rank coals may have a gas content of between 14 and 17 m³ per tonne. In addition, methane may be trapped in gas pockets or dissolved in groundwater.

The development and utilisation of coal mine methane is similar to that of conventional natural gas drilling and production in hydrocarbon reservoirs. Historically, methane gas drained from mines was 'flared' since it was considered as a hazardous waste by-product. However, where the gas recovered is of high quantity and quality it can be used for industrial and domestic purposes.

Following the abandonment of mining, methane continues to accumulate in the mine workings and voids in the rock mass, this is often referred to as 'gob gas', or in the fractured and displaced rock mass above collapsed panels in longwall workings (goaf gas). Vertical and horizontal wells are often drilled to recover this gas. Methane also may be extracted from ventilation air that is driven from underground mine workings. Bell *et al.* (2000) described the utilisation of methane from an abandoned mine in Herne-Sodingen, Germany, to heat new buildings. The gas is collected in sealed chimney-like units at the top of the shafts from which it is piped to a storage tank and from there to an electricity generating plant.

During falling atmospheric pressure conditions, methane gas may flow from fractured rock masses into abandoned mine workings (Donnelly and McCann 2000). However, the factors controlling gas recovery are dependent on several factors such as the following:

- Pressure of gas in the seam
- Volume of gas content in the seam
- Resistance of the gas pathways and permeability of the coal
- Increased rock mass permeability induced by mining
- Pressure in the mine workings
- Atmospheric pressure fluctuations.

Estimates of gas reserves associated with abandoned mine workings indicate that the gas remaining *in situ* is probably less than 50% of the initial volume. A general view of the maximum recoverable gas is 30% of the available reserves. However, rising minewater significantly influences the volume of gas available in abandoned mine workings, and it may be depleted below an economic recovery level. For instance, minewater rebound may cause the migration of mine gas, resulting in diffusion to the ground surface, for example, along faults, permeable sandstones, mining induced fractures, mine shafts and adits, or it may accumulate in subsurface pockets or traps. A vent installed in northern England has shown emissions

rates 4 litres an hour for every 10 m² of gas saturated sandstone in contact with abandoned mine workings. At another site, over 1000 tonnes of methane was emitted over a period of seven months. There are a variety of profitable markets for CMM & CBM, these include suppliers of natural gas, use as an on-site fuel, and for off-site electricity production. In the USA in particular, substantial progress has been made in the recovery and use of CMM & CBM (Robert *et al.*, 1995).

2.2 Underground Coal Gasification (UCG)

Gasification is a chemical process that involves converting a solid (or liquid) fuel into a combustible gas. This gas is then subsequently utilised as an energy resource or to produce heat. Underground coal gasification involves the in-seam gasification of strata-bound coal reserves, by drilling into the coal horizons, injecting air or oxygen, igniting the seam and therefore gasifying the coal. The gaseous products then are transported to the surface where they undergo processing, transportation and utilisation.

UCG may be favourable in recently abandoned coalfields. In-seam coal gasification, however, has been an area of research in the UK since the early 1920s, in the former Soviet Union since the 1930s, and throughout the 1940s to 1980s in Europe and the USA. These trials and experiments established the technologies involved with UCG. By the start of the 1990s UCG was considered in the USA to be a commercially viable technology. Commercial operations have since been established in parts of Russia and Uzbekistan and trials have been undertaken in Spain (1992-1999), Belgium (1982-1987) and the UK (1999-2003) to evaluate directional drilling capabilities and well configuration, and to assess the geological and environmental considerations. In this context, research is being undertaken in the UK and Europe to evaluate the coal reserves, both onshore and offshore, in former coal mining regions. The benefits of UCG include the following:

- The utilisation of coal reserves in otherwise abandoned coal fields
- Efficient power generation
- Production of clean gas, with reduced processing.

However, the potential environmental and geological concerns include:

- Underground contamination caused by small quantities of phenols and benzenes produced as a by-product of UCG. Some may reach the ground surface and a proportion may be absorbed by the coal. Dispersion of any contaminants will depend on several geological and mining factors such as the hydrogeology, proximity and state of abandoned workings, depth of seam, permeability of rock mass, etc.
- Surface watercourse contamination
- Control and prediction of subsidence, fault reactivation and fissuring
- Gas emissions, although this might be reduced in deeper coal seams
- Control of ignitions and in-seam combustion.

2.3 Carbon Dioxide Sequestration

Carbon dioxide sequestration is aimed at reducing the volumes of CO₂ emitted into the atmosphere. This involves the capturing of the gases after combustion and reinjecting them into the ground where they can remain for large periods of geological time. Potential storage sites for carbon dioxide include brine formations and salt domes (below land and sea), abandoned hydrocarbon reservoirs and former mining regions. One possible solution is that CO₂ sequestration could be undertaken in conjunction with UCG. A continuous system of UCG would result in highly fractured and porous strata. Abandoned cavities could be penetrated by drillholes, and the CO₂ could be injected under high pressure for storage.

3 Alternative Uses of Abandoned Mine Workings

Abandoned mine workings are usually perceived as a liability, but under favourable circumstances may actually represent an asset and provide commercially viable opportunities. The conversion of an abandoned mine for practical commercial purposes will depend upon several factors such as geology, hydrogeology, mining, environmental matters, public perception, economics and politics.

The use of abandoned mines as underground storage facilities was given an impetus during the world wars. Subsequently, the oil, gas and chemical industries, in particular, have used such facilities for economic storage for their products. Use has also been made of abandoned mines for the storage of waste, a good example being provided by the salt industry in Cheshire, England. Probably the most noteworthy example of the use of abandoned mines is that found in Kansas City, USA, where the old workings in the Bethaney Falls Limestone provide warehouse space and offices.

Many countries have been considering the use of abandoned mines for the long-term disposal of radioactive waste materials. In the UK, the NIREX project was aimed at the storage of nuclear waste in the Borrowdale Volcanic Formation beneath Cumbria. At Hasse, near Hannover, Germany, one such repository was operational between 1967 and 1978. Approximately 25,000 m³ of low-active and intermediate-active waste were routinely deposited in salt caverns, which were subsequently backfilled with salt, and sealed.

Some of the following represent other possible uses of abandoned mine workings:

- *Mining and power plant waste storage.* In some parts of the world, such as the Jiu valley in Romania, in Hungary and the Czech Republic, disposal of these types of waste has taken place in abandoned mine workings, which subsequently were backfilled and stowing. The materials used for backfill were tested and classified according to their safety for such use. The wastes investigated included slags and ashes from coal-fired power stations and waste incinerators, foundry waste, sandblasting waste, fly ash, bottom ash and construction waste).

- *Storage of consumables and foodstuffs.* In areas where surface space is in short supply and therefore valuable, underground storage will help conserve such surface areas for other uses. This may be important in and around populated urban areas, or where industrial space is required. Some mines are currently being used to store a range of items such as foodstuffs (ice cream and confectionery), deep-frozen products and drinking water. Yet another example is the use of abandoned mines as mushroom growing facilities, as illustrated by the Tennants Mine in Carrickfergus, Northern Ireland, and as nurseries as occurs in some old chalk mines in Kent.
- *Medical research.* Medical research may benefit from an anhydrite mine atmosphere, such as research into bronchitis. There have been some suggestions that this is currently being undertaken in a disused mine in Poland.
- *Oil well research.* Oil well research involving sensors used in oil wells, is practised in some abandoned gypsum and anhydrite mines in the English Midlands, where the underground mine atmosphere provides a shield from radio-wave interference.
- *Scientific research.* Research that requires protection from cosmic radiation and weather fluctuations may be suited to abandoned mine workings, where the temperature and humidity remains relatively constant.
- *Storage of documents.* Storage of paper documents may be possible in some mines due to the low humidity.
- *Secure storage.* Storage of sensitive and valuable documents, artwork or military data may be more secure in mines than in surface structures. In particular, some abandoned mines in Europe were used for these purposes during the first & second world wars, including the UK, Germany and Austria.
- *Museums.* Museums, and sites of industrial archaeological and historical value often are based in abandoned mine workings. In the UK, mining museums exist for metalliferous deposits, coal and evaporite rocks, an example of these being the Northwich Salt Mining Museum and the Caphouse Coal Mining Museum.
- *Site of Special Scientific Interest (SSSI) and Regionally Important Geological Sites (RIGS).* Abandoned mines in favourable circumstances may be designated as sites of special scientific interest, for example, where rare ore minerals or unique geological conditions occur.
- *Rock mechanics research.* Research facilities for drilling, cutting and digging machines (i.e. excavating equipment), for the testing rock stabilisation methods such as rock bolts, for support systems in tunnelling and for ventilation equipment may take place in abandoned mines.
- *Storm water channels.* Storm water channels and water reservoirs may be constructed in some abandoned mine workings that are located near to the coast, for storage and then subsequent discharge to the sea, in areas prone to flooding, or at sites where the surface storage of water is difficult.

4 Conclusions

Former mining areas in Britain are susceptible to a range of geological and mining related hazards. These are well documented, and are likely to continue to represent problems when developing land or planning for future infrastructure. In short, mine working can cause blight and in general this may contribute to the overall negative perception and stigma in former mining areas. This paper has drawn attention to some positive aspect of mine closure and coal field abandonment by the provision of alternative energy, or by the alternative use of abandoned mines. Research and trial have shown that methane gas, associated with in situ coal reserves, can be utilised as an energy resource. However, the environmental and economic constraints associated with coal mine methane, coal bed methane and underground coal gasification, will determine whether these techniques become commercially viable options. The adaptation and conversion of abandoned mine workings, under favourable conditions may also provide commercial opportunities; mainly for the storage of wastes, but also for other industrial purposes.

Acknowledgements

This paper is published with the permission of the Executive Director of the British Geological Survey (NERC).

References

- Bell, F. G. (1999). *Geological Hazards: Their assessment, avoidance and mitigation*. E&FN Spon, London & New York.
- Bell, F. G. and Donnelly, L. J. (2002). *The Problem of Spontaneous Combustion Illustrated by Two Case Histories*. 9th Congress of the International Association of Engineering Geology and the Environment, Durban, South Africa, 16-20th September 2002. South African Institute of Engineering and Environmental Geologists, Pretoria. On CD-ROM only.
- Bell, F. G. and Donnelly, L. J., and Genske, D. D. (2002). *The Impact of Subsidence: Some Less Usual Examples from Britain and Germany*. 9th Congress of the International Association of Engineering Geology and the Environment, Durban, South Africa, 16-20th September 2002. South African Institute of Engineering and Environmental Geologists, Pretoria. On CD-ROM only.
- Bell, F. G., Genske, D. D. and Bell, A. W. (2000). *Rehabilitation of industrial areas: case histories from England and Germany*. *Environmental Geology*, 40, 121-134.
- Culshaw, M. G., McCann, D. M. and Donnelly, L. J. (1999). *The Impact of Natural and Humand Ground Processes on the Stability of Buildings and Structures*. In: Forde, M. C. (ed), *Proceedings of the 8th International Conference on Structural Faults and Repairs*. The Commonwealth Institute, Kensington, London, 13-15th July 1999. Engineering Technics Press, Edinburgh. CD-ROM publication only, 10p.

- Culshaw, M. G., McCann, D. M. and Donnelly, L. J. (2000). Impacts of abandoned mine-workings on aspects of urban development. *Transactions of the Institution of Mining and Metallurgy*, 109, A131-A130.
- Donnelly, L. J., Dumbleton, S, Culshaw, M. G, Shedlock, S. L. and McCann, D. M. (1998). The Legacy of Abandoned Mining in the Urban Environment in the UK. In: Forde, M. C. (ed), *Proceedings of the 5th International Conference on Polluted and Marginal Land*, Brunel University, UK, 7-9 July 1998. Engineering Technics Press, Edinburgh. 559-572.
- Donnelly, L. J. (2000a). The Reactivation of Geological Faults during Mining Subsidence from 1859 to 2000 and beyond. *Transactions of the Institution of Mining and Metallurgy*, 109, A179-A190.
- Donnelly, L. J. (2000b). Fault Reactivation Induced by Mining in the East Midlands. *Merican Geologist*, 15 (1), 29-36.
- Donnelly, L. J. and McCann, D. M. (2000). The Location of Abandoned Mine Workings using Thermal Techniques. *Engineering Geology*, 57, 39-52.
- Donnelly, L. J. and Rees J. (2001). Tectonic and Mining-induced Fault Reactivation around Barlaston on the Midlands Microcraton. *Quarterly Journal of Engineering Geology and Hydrogeology*, 34, 195-214.
- Robert, M. D., Sloss, L. L. and Clarke, L. B. (1995). *Coalbed methane extraction*. IEA Coal Research, London.

Seismic and Flood Risk Evaluation in Spain from Historical Data

Mercedes Ferrer¹, Luis González de Vallejo², J. Carlos García¹,
Angel Rodríguez³, and Hugo Estévez¹

¹ Instituto Geológico y Minero de España, Ríos Rosas, 23. Madrid 28003
m.ferrer@igme.es

² Universidad Complutense de Madrid, Fac. CC. Geológicas, Ciudad Universitaria
Madrid 28040
vallejo@geo.ucm.es

³ Prospección y Geotecnia, S.A. Pedro Muguruza, 1, Madrid 28036
Tel: +34 91 349 5776
Fax: +34 91 349 58 34

Abstract. Floods and earthquakes are two of the natural processes that cause in Spain economic and social losses, with major effects on the first ones. In order to evaluate the risk (social damages and economical losses) associated with these processes, the available historical data and information on happened events (from bibliographical and documentary sources, press, files, data bases, etc.) has been compiled and analysed exhaustively, including also the information related to the economic and social losses (damages, victims, direct and indirect economical losses, governmental and insurance companies data, etc.). The analysis of the historical information has allowed to estimate the distribution and extent of the damages and losses due to floods and earthquakes in Spain, as well as the vulnerability of the national territory. The estimation of the damages and losses for the next three decades has been approached from the study of the flood and earthquake potential hazard in Spain, estimating the probabilities of occurrence of these processes with different magnitude/intensity for the period of reference. The present economic and social conditions of the territory have been considered, carrying out probabilistic estimations and valuing hypothetical situations of potential damage scenarios. The results allow to know the hazard (probability of occurrence of processes of certain magnitude) and risk degree (potential damages and losses) of every municipality of the country.

Keywords: natural hazards, geological hazards, risk evaluation, floods, earthquakes, Spain.

Introduction

The geological and climatic characteristics of Spain originate natural hazards such as floods, landslides, earthquakes, etc. These processes give rise, in many cases, to important economical losses and social damages. However, these negative consequences are not inevitable and they must not be accepted like the price to pay by the use of the territory, land occupation or natural resources exploitation. The present damages and losses, and the associated reconstruction and reparation costs, can be reduced in an effective way. The geological hazards in Spain fre-

quently affect populations and infrastructures, and most of times damages are due to the occupation of hazardous areas and the lack of prevention measures and mitigation strategies. The prevention is the most effective way to avoid the social and economical damages. The preventive measures must be applied to the different scopes of the society, including the citizen information, the urban planning, and the design of safety infrastructures in hazard areas.

For the development and implementation of the different preventive measures it is necessary to have a complete and updated data base of the geological and hydrometeorological events and their incidence, what allows the analysis of the present losses and damages and the evaluation of the potential risks. This paper presents the study carried out for the evaluation of present (last 15 years) and future (next 30 years) risks due to floods and earthquakes in Spain, from the analysis of the geological and physical aspects and the economical, social and environmental factors which could be affected. Probabilistic estimations have been developed, as well as benefit-cost analysis and valuation of hypothetical situations of possible risk scenarios. The results of the study allow different practical applications, such as the definition of hazard and risk criteria for insurance companies, urban and land planning, building and industrial installations specifications, infrastructures and life lines, prevention environmental risks, etc. Because of the national scale of the study, and the necessary degree of detail required, a specific methodology has been developed for the losses evaluation from the historical damages and losses compilation and inventory. It mainly consists in:

- Collection and compilation of historical data and information
- Data base preparation
- Analysis and evaluation of the present risk (based on last 15 years data) and the historical maximum risks in Spain due to floods and earthquakes.
- Potential risk evaluation for the next 30 years due to floods and earthquakes.

The work has been developed at a provincial and municipality level. The collected information has been introduced in a data base and treated with ARCVIEW. For the evaluation of the economical losses, both economical and social data have been used for the municipalities, updated at 2003. All the results have been represented in maps showing the distribution of the different hazard parameters and losses at municipality scale.

Seismic Risk Evaluation in Spain from Historical Data

Seismicity Analysis

The information related to earthquakes has been obtained from:

- Data bases and catalogues carried out by the Geological Survey of Spain (IGME, 1988a), including historical and recent data (from 565 to 1987).
- Seismic catalogues from the Geographical Institute of Spain for the national territory and north of Africa for the period 1987-2002.

- Seismic catalogue of the simulation program SES 2002 (Civil Protection of Spain), including historical and recent earthquakes with intensity \geq VI and/or magnitude \geq 4.0.
- Paper news related with earthquakes in Spain for the last 15 years.

The selected information has been classified and homogenized, including the data related to losses and damages in the affected areas, and the data have been introduced in a database. 547 earthquakes have been collected, though 22.000 events were analysed with a minor intensity or magnitude than those causing damages. For each of the selected events the maximum distance to the epicenter has been calculated where the earthquake causes damages, getting concentric circles of “damage degree” corresponding to different intensities. For this, the different attenuation laws corresponding to the different regions of Spain were applied. The great scope of earthquakes generated in the Azores – Gibraltar zone stands out, in which the historical earthquakes that have taken place, though of big intensity, were felt in the opposite end of Spain, beside causing serious damages in cities of the south of Spain. These intensity or damage circles were represented for all the earthquakes in order to define areas with different seismicity degree. It was also prepared a map with the maximum intensity affecting each municipality for the period 1900-2002, when the historical data are better and homogeneous. With the information included in the data base and implemented in a GIS system (ARCVIEW), it was possible to cross the data corresponding to each earthquake for the period 1900-2002 and the different data corresponding to the municipalities, obtaining next information:

- Number of earthquakes and their intensity (\geq VI) affecting each of the municipalities.
- Classification of the municipalities according to their seismic activity in the last 102 years.
- A seismic hazard map of Spain at municipality scale based on the maximum registered intensity.
- Definition of the return period for different intensity earthquakes for each municipality.
- A potential seismic hazard map for the next 30 years based on the historical and recent seismicity (last 102 years).

Losses Evaluation

In Spain there is not a complete information related to losses caused by historical earthquakes, including those of biggest intensity. Most of times, the data refer to general descriptions and, only in some few cases, the number of buildings affected, injured and killed people. It only exists detailed information of the economic losses caused by the Mula earthquake (Murcia, SW Spain, 1999). For this reason, for the losses evaluation it has been mainly considered the data corresponding to the Mula earthquake and some well documented recent big magnitude earthquakes in Italy with complete and detailed information about the provoked

losses: Friuli (1976), Campania (1980) and Umbria (1997); (Trímboli, 2002). It has been considered that these earthquakes and their social and economical consequences present characteristics extrapolable to the Spanish territory. Apart from these case studies, for the evaluation of the potential losses it has been used the “Simulación de Escenarios Sísmicos SES-2002” program (developed by the Civil Protection of Spain and the Geographical Institute of Spain), which has allowed the simulation of the main historical earthquakes occurred in Spain (Table 1). This program has been also used to simulate the effects of the Italian earthquakes, demonstrating the representatives of the available data.

Table 1. Historical earthquakes in Spain and Italy for the evaluation of losses.

Earthquake	Mula 1999 (1)	Umbria 1997 (2)	Friuli 1976 (2)	Campania 1980 (2)	Arenas del Rey 1884 (3)	Cehegin 1948 (3)	Queralps 1428 (3)	Adra 1993 (3)	Sarria- Becerrea 1995 (3)
Magnitude	4,8	5,8	6,5	6,9	6,8	5	5,9	5	4,6
Intensity	VII	IX	X	X	X	VIII	IX	VII	VI
Total Losses*	60,09	735,75	8.407,92	50.096,3	34.004	698,57	1.224,09	550,22	9,45
Population affected**	60.109	112.412	500.000	4.641.620	2.674.639	81.564	256.793	109.227	19.502

(1) Spanish earthquake: real losses; (2) Italian earthquakes: real losses; (3) Spanish earthquakes simulated with SES-2002 program considering present conditions.

(*) Million euros; (**) Population living in the areas affected by intensity \geq VI.

The information related to the real losses has been studied in detail. For the evaluation of losses in the simulated earthquakes it has been considered:

- The extension of the affected area, determined on the basis of the laws of attenuation of the intensity with the distance
- The population affected in every municipality
- The types of buildings in the affected zones, classified depending on the type of construction and the use
- The vulnerability of the buildings
- The vulnerability of the persons.

The information obtained about the damages caused by every earthquake has been:

- Affected area (km²)
- Number of inhabitants affected / Density of population
- Total losses / Losses per km² / Losses per Inhabitant
- Number of killed people / Number of injured people / Number of displaced persons
- Destroyed buildings / damaged buildings.

All the values of economic losses are up-to-date at 2003.

The previous information has allowed to study the degree of correlation among parameters as the intensity or the magnitude of the earthquakes with the losses, area and people affected, etc., and to define the corresponding mathematical ex-

pressions that correlate the magnitude or intensity with the losses. Also to correlate the magnitude with the intensity expressions were used that allow to use both parameters indistinctly. The losses produced by earthquakes can be represented graphically and study their correlation and degree of adjustment with regard to equations of exponential and potential type. Figures 1 and 2 represent two examples of the functions of correlation: total population affected by earthquakes and total losses caused by earthquakes (Table 2).

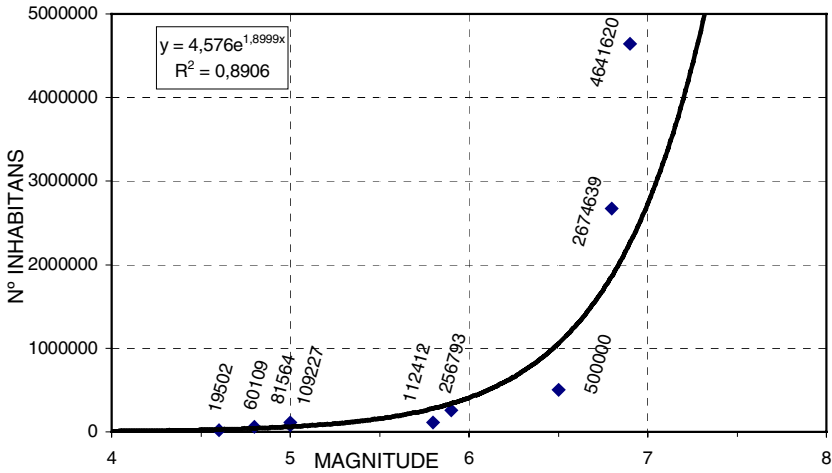


Fig. 1. Relation between population affected by earthquakes and magnitude.

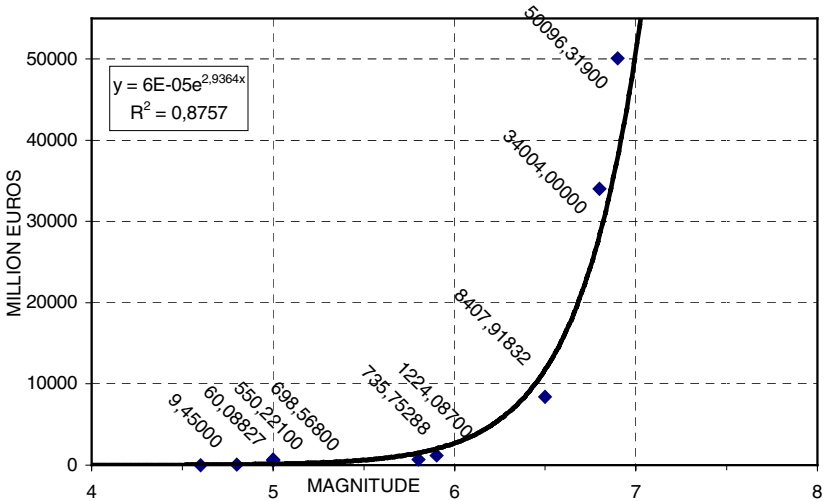


Fig. 2. Relation between total losses by earthquakes and magnitude.

Table 2. Estimation of damages and losses by earthquakes.

Losses and damages	Correlation with magnitude (M)	Correlation with intensity (I)
Affected population (n° Inhabitants)	$n^{\circ} \text{ Inhab} = 4,576 e^{1,8999 M}$	$n^{\circ} \text{ Inhab} = 4,576 e^{1,8999 (0,035 I^2 + 2,907)}$
Total losses TL (€ x 10 ⁶)	$TL (\text{€} \times 10^6) = 6,038 \times 10^{-5} e^{2,9364 M}$	$TL = 6,038 \times 10^{-5} e^{2,9364 (0,035 I^2 + 2,907)}$

Losses for the Period 1987-2002

From the collected earthquakes occurred between 1987 and 2002 those with intensity > V or magnitude > 4 were selected, that is, those causing notable damages. These earthquakes are 10: 2 with intensity VII, 1 with intensity VI-VII, 3 with intensity VI and 4 with intensity V - VI. This information emphasizes the low rate of seismicity observed in Spain in the period of study (1987-2002) in comparison with the registered in the last 102 years (1900-2002). Apart from this, 61 earthquakes have been selected with losses that have been an object of indemnification by the insurance companies. The calculation of the losses for the last 15 years (1987-2002) has been carried out by two different methods:

- Correlation between the quantities (indemnifications) paid for the insurance companies and the total losses.
- Calculating the potential losses for every maximum intensity felt in every municipality.

The quantities paid by the insurance companies represent around 2,24 % of the total losses until the year 1996, and 20 % from 1997. The values obtained by both methods are similar, emphasizing the representatively of both: 204 x 10⁶ Euros and 210 x 10⁶ Euros.

Seismic Risk Evaluation for the Next 30 Years

A total of 374 earthquakes have been studied of $I \geq VI$ and/or magnitude ≥ 4.0 happened in Spain in the period 1900-2001, most of them with intensity VI and VII. The analysis has allowed to know which are the municipalities affected by the earthquakes, the intensity felt for every earthquake and the number of times that a municipality has been affected by earthquakes of different intensity. Knowing the seismicity affecting the national territory in the last 102 years, in absolute value, that is, total number of earthquakes of different intensity, as in a detailed way, number of earthquakes of different intensity for municipality, it is possible to predict the seismicity that will concern to Spain in the next 30 years. For this it is necessary to determine the probability of occurrence of the earthquakes of different intensity in the next 30 years, departing from a period of observation of 102 years. So, there is obtained the number of earthquakes of different intensity predicted for the next 30 years. From these data there have been calculated the losses

that they might cause using the expressions previously obtained of the study of the earthquakes in Spain and Italy and the program of simulation of seismic scenarios SES-2002 (Table 3).

Table 3. Number of potential earthquakes in Spain for the next 30 years (2003-2032).

Intensity	Number of earthquakes
VI	70
VII	19
VIII	6
IX	1

As an example of the obtained results, Table 4 shows the total potential losses in Spain for the next 30 years by earthquakes of maximum intensity VII and VIII.

Table 4. Potential losses by earthquakes with intensity VII and VIII in Spain for the period 2003-2032.

Losses and damages	Intensity VII (19 earthquakes)		Intensity VIII (6 earthquakes)	
	Unit Losses	Total Losses	Unit Losses	Total Losses
Affected area (km ²)	766,92	14.571,5	1.511,55	9.070
Affected population (n° inhab.)	29.797	566.143	80.790	484.740
Total losses (€ x 10 ⁶)	47,332	899,31	221,14	1.326,84
Losses (€) / km ²	49.508	940.652	141.279	847.674
Losses (€) / Inhabitant	1.465	27.835	2.803	16.818
Destroyed buildings	1	19	22	132
Damaged buildings	3.225	61.275	9.018	54.108

Unit losses: losses corresponding to one earthquake

Total losses: losses for the total number of potential earthquakes (19 for I= VII and 6 for I = VIII)

In Table 5 appear the results of integrating the potential or predictable losses for the next 30 years for all the potential earthquakes (VI < Intensity = IX).

Table 5. Estimation of total losses for earthquakes in Spain for the period 2003-2032.

Total losses	
Affected area (km ²)	56.719
Affected population (n° inhabitants)	2.179.802
Total losses (€ x 10 ⁶)	4.366,122
Destroyed buildings	813
Damaged buildings	236.914

The losses have been calculated to regional, provincial and municipal level. Most of the losses correspond to Andalusia, Murcia, Galicia and Valencia regions.

Flood Risk Evaluation in Spain from Historical Data

Historical Data Collection

The information related to floods has been obtained from:

- Available data bases and catalogues carried out by the Geological Survey of Spain (IGME, 1988a), including historical and recent data (from 420 to 1987).
- Data from Civil Protection of Spain.
- Documents and publications on floods happened in the different Spanish hydrographic basins.
- Flood risk map of Spain (CEDEX, 1988).
- Governmental floods losses reports at provincial scale.
- Data from insurance companies.
- Press news related with floods in Spain for the last 15 years.

The selected information has been classified and homogenised, including the data related to losses and damages in areas affected by floods, and the data have been introduced in a database, including date, duration, area affected, river, hydrographic basin, flood causes, flow, precipitation data, etc. 2534 floods causing damages have been collected, 217 corresponding to the period 1987-2002. The damages caused by floods have been classified:

- Infrastructures, including hydraulics, and public buildings
- Private properties: houses, vehicles, goods, etc.
- Industrial and commercial properties
- Agriculture and cattle losses.

Losses Evaluation for the Period 1987-2002

Once collected the events occurred in the period 1987-2002, it was assigned to each of them the corresponding economic losses. In this way, 197 floods were selected for the period 1987-2002, with detailed descriptions of the events and the caused damages and losses. Neither the social damages nor the indirect economical losses were considered, because of the impossibility to obtain this information. By means of the correlation between the degree of damages declared (governmental reports) for every flood and the corresponding economical data from the insurance companies, the floods have been classified with a different degree of damages. Figure 3 present the relation between the economic losses declared and the quantities paid by the insurance companies. Three definite well defined lines can be observed corresponding to:

- Urban floods
- Non urban floods
- Mixed type floods

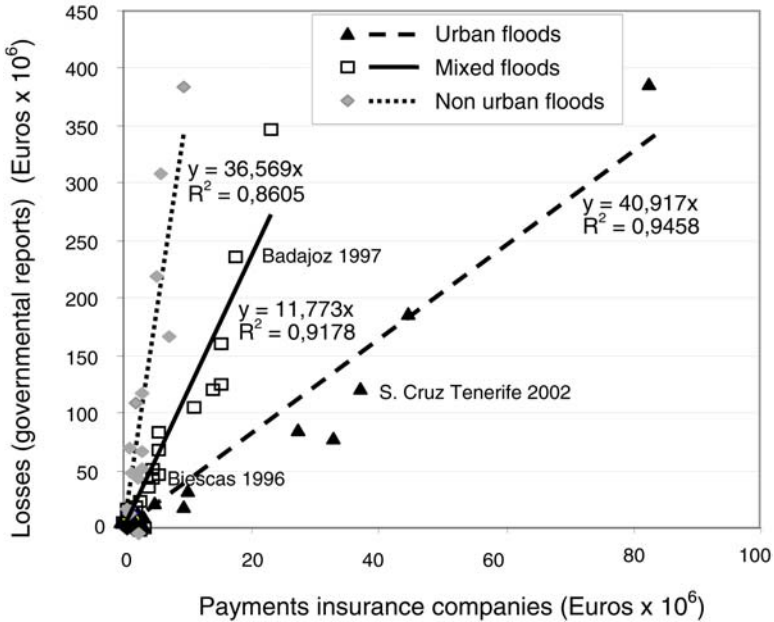


Fig. 3. Relation between the actual economic losses f floods and the quantities paid by the insurance companies.

From these correlations, and depending on the type of flood, the losses have been estimated for those events not considered in governmental reports but paid for by the insurance companies. By this way, either by direct assignment (from the governmental reports) or correlating with the insurance data, the economic losses corresponding to every flood between 1987 and 2002 have been obtained; the economic losses have got up-to-date to 2003. They represent 12.000 Euros x 10⁶ for the complete national territory. The economical losses have been represented by provinces in a national map, and a complementary map has been prepared with the municipalities affected by floods in the period 1987-2002.

Flood Risk Estimation for the Next 30 Years

For the estimation of the losses that can cause the floods in Spain in the next 30 years (2003-2032), there have been considered the floods occurred in the national territory from 1950, since for this period the available information about floods and the damages caused is complete. First, it has been carried out a classification of floods depending on the losses caused, that is, depending on the risk. 6 types of relative risk have been defined:

Table 6. Classification of floods depending on the losses, both for event and province.

Risk degree	Losses per event (Euros x 10 ⁶)	Losses per province (Euros x 10 ⁶)
I	0 – 1	0 – 0.5
II	1 – 5	0.5 – 4
III	5 – 50	4 – 30
IV	50 – 150	30 – 70
V	150 – 300	70 – 120
VI	> 300	> 120

This degree of risk has been used to estimate potential losses at provincial level, from the number of floods of every risk degree per province for the period 1987-2002 and the corresponding losses. The number of floods and the corresponding degree of relative risk for every province has been also evaluated for the period 1950-1987, from the available information on losses or from the qualitative descriptions of the damages. Also there has been calculated the number of floods of every degree of risk for year and province, for the period 1950-2002, and the average value of economic losses that causes a flood of “x” degree of risk in every province. The estimation of losses per province for the next 30 years has been carried out from the expression:

$$L_{30} = 30 [(R^I \times L^I) + (R^{II} \times L^{II}) + (R^{III} \times L^{III}) + (R^{IV} \times L^{IV}) + (R^V \times L^V) + (R^{VI} \times L^{VI})] \quad (1)$$

in which L_{30} = losses for the next 30 years; R^x = Number of floods per year of “x” risk degree estimated for the province. On determining the number of floods per year of risk x a conservative criterion has been followed; L^x = Economic losses caused by a flood of risk “x” in the province.

The estimated economic losses for floods for the period 2003-2032 in the whole national territory ascend to 26.000 x 10⁶ Euros, being the most affected regions those of Valencia, Andalusia and Catalonia. The losses estimated per province for next 30 years have been distributed by municipalities depending on the degree of risk estimated for each of them, as the product of the hazard (obtained from the number and intensity of the floods occurred in the municipality) and the vulnerability (considering the number of inhabitants and the index of economic level of each of them). The degrees of potential risk for municipalities are: 0 (nule or very low risk), 1 (low risk), 2 (moderate risk), 3 (high risk). Therefore, the losses estimated for every province (potential risk) distribute among the municipalities depending on the hazard degree and the vulnerability (population and economic level).

Conclusions

The study has allowed to have the following information and documentation:

- Valuations to national and municipal level of the impact of the geological risks in Spain and future losses predictions.
- Potential earthquakes and floods risk maps at national and municipal level.
- Data bases georeferenced, complete and updated at 2003 on the risks caused by earthquakes and floods in Spain.
- Detailed catalogues of the damages associated with these processes in the period 1900-2002, with homogeneous information updated to Euros of 2003

The estimations losses/intensity carried out for earthquakes have been validated and compared with real cases in Spain and Italy, which similar characteristics with Spain allow an acceptable correlation. An acceptable correlation has been defined between the intensity or magnitude of the earthquakes and the caused losses, depending on factors as the density of population or the economic level of the affected areas. The deduced mathematical expressions that relate these parameters allow to realize quantitative analyses that improve other empirical procedures used for evaluation of losses. The results of the study are of great usefulness for the insurance companies, for civil protection and for activities related to territorial planning and land use.

Acknowledgment

This research project has been supported by the Geological Survey of Spain (IGME) and the Consorcio de Compensación de Seguros (CCS).

References

- CEDEX (1988). Flood risk map of Spain. Scale 1/1.000.000.
- Civil Protection of Spain - IGN (2002). "Simulación de Escenarios Sísmicos SES-2002" Program.
- IGME (1988a). Catálogo Nacional de Riesgos Geológicos. 263 pp.
- IGME (1988b). Impacto económico y social de los riesgos geológicos en España. 138 pp.
- Trímboli, M. 2002. Reports on the Friuli (1976), Campania (1980) and Umbria (1997) earthquakes. Unpublished.

Landslide Risk Assessment in Italy: A Case Study in the Umbria-Marche Apennines

Mario Floris and Francesco Veneri

Institute of Engineering Geology, University of Urbino, Scientific Campus
I-61029, Urbino, Italy
geoappl@uniurb.it
Tel: +39 722 304235/304258
Fax: +39 722 304260

Abstract. This paper reports the study of a training area aimed to develop a methodology for assessing the landslide risk on the basis of landslide movements characterization and of the definition of lithotechnical features. “Risk” areas were identified on the basis of guidelines established by Italian laws which have been enforced since 1989, often following major natural disasters. Particular emphasis was placed on the assessment of the activity of landslides, which gives insights into their probability of occurrence (hazard). In this sense, the multi-temporal analysis of aerial photos proved to be an effective investigating tool. The study also emphasised the importance of the choice of geomechanical properties as one of the “primary” factors of landslide susceptibility.

Keywords: multi-temporal analysis, landslide hazard, risk assessment.

1 Introduction

In the past 15 years, the Italian Government enacted numerous laws on land planning and management, some of which (in 1989, 1998 and 2000) focusing on landslide risk mitigation plans. Law no. 183 of May 1989 urged the development of countrywide hydrogeological plans and attributed their formulation to the Basin Authorities. The law-decrees no. 180 of June 1998 and no. 279 of October 2000, issued after catastrophic events in Campania and Calabria Regions (Southern Italy), stipulated that landslide-prone areas and their boundaries should be immediately identified. During the last 5 years the Basin Authorities built the Landslide Risk Maps for the entire Italian territory; in accordance with the above legislation, 4 risk classes were defined on the basis of the expected damage or loss (negligible, mild, significant, severe) and of the potentially affected element (people, property, human activities and environmental heritage). For risk assessment, reference was made to landslide hazard, which was assessed on the basis of the main morphometric and kinematic features, as well as of the activity distribution (Cruden & Varnes classification, 1996) of landslide movements.

The study reported in this paper was aimed at developing a methodology for assessing the risk of landslides over wide areas, on the basis of landslide movements

and of the definition of engineering-geology scenarios where such instabilities occur.

The risk areas in the training area of Pergola (Umbria-Marche Apennines) were classified according to the guidelines set forth in the above-mentioned law-decrees. However, emphasis was placed on the use of rigorous criteria for assessing the activity of landslides and thus their probability of occurrence. Four maps at a scale of 1:10,000 (Lithotechnical Map, Landslide Inventory Map, Landslide Susceptibility Map and Landslide Risk Map), gathering all the data collected on the study area were built, but not shown in this paper. Here we report some of the main results achieved in the training area as an illustration of the criteria and methodologies adopted. Anyway, given the variety of lithologies, geomorphological features and types of landslides, this area was regarded as adequately representative of different situations.

2 Methods and Results

The study area (Fig. 2.1), located in the Umbria-Marche Apennines, is dominated by hills, which are broken by the alluvial plains of its main rivers (Cinisco and Cesano). The town of Pergola lies at the confluence of the two rivers. This zone is characterized by the Paleogene-Neogene terms of the Umbria-Marche sequence (Barchi et al. 2001). Lithologies consist of alternating calcareous, calcareous-marly and siliceous layers (Scaglia Rossa, Scaglia Variegata, Scaglia Cinerea and Bisciaro formations) and of pelitic to arenitic clastic deposits (Schlier, Gessoso-Solfifera and Arenarie e Marne di Serraspina formations). The prevailing structural style is of the folding type; two Apennine-trending anticlines represent the main structures. The slopes are affected by both shallow and deep landslide phenomena of various types.



Fig. 2.1. Geological sketch of the Pergola area. 1) Limestones, marly limestones, marlstones and cherts (formations between Calcare Massiccio and Schlier, Lias-Miocene p.p.); 2) Arenites, pelites and evaporites (formations between Marnoso-Arenacea and Colombacci, Miocene p.p.); 3) Chaotic complex clays of the Marecchia valley; 4) Clayey, sandy and gravely deposits (Plio-Pleistocene).

The spatial data were collected, processed and stored into a Geographic Information System. The use of alphanumeric software and of graphic interfaces made it possible to produce georeferenced maps to a scale of 1:10,000 (map of structures and infrastructures, lithotechnical map, landslide inventory map). The base maps and their topology were combined through "map crossing" processes in order to produce derived maps (e.g. landslide susceptibility maps) showing the importance of the individual geographic parameters in landslide susceptibility.

The analysis of geological aspects was the starting point of the study. Taking into account the aim of the study, the local sedimentary sequence was characterised according to lithotechnical criteria (Bieniawski 1975; Spagna 1998), by grouping the soils into classes having the same mechanical behaviour (Tab. 2.1) and dividing the land into areas having similar morphologies and types of landslide. In our opinion, lithotechnical features represent the primary features to be assessed in the study of landslide susceptibility. A recent study, conducted on the same sector by Guastaldi & Ridinella (2003), substantiated the above assumption: the Authors have considered various factors (lithotechnical, elevation, slope, aspect, bedding related to slope face, land use) and they have indicated that the information layer most correlated to landslide phenomena is the lithotechnical map.

Table 2.1. Lithotechnical classes. (Extract from the Lithotechnical Map).

Lithotechnical class	Description
RCS	Bedded competent rocks, high compactness ($4 \text{ Mpa} < I_s^* < 8 \text{ MPa}$). Calcareous member of <i>Scaglia Rossa</i> formation.
RC/T	Dominantly competent rocks, alternating with weak layers, medium compactness ($2 \text{ MPa} < I_s < 4 \text{ MPa}$). Marly member of <i>Scaglia Rossa</i> formation.
RT/C	Dominantly weak rocks alternating with strong layers, low compactness ($1 \text{ MPa} < I_s < 2 \text{ MPa}$). <i>Scaglia Variegata</i> and <i>Bisciaro</i> formations.
AMS	Dominantly cohesive weak rocks, very low compactness ($I_s < 1 \text{ MPa}$). <i>Scaglia Cinerea</i> , <i>Schlier</i> and <i>Arenarie e Marne di Serraspino</i> formations.
ecg	Materials of the eluvial and/or colluvial cover, poorly consolidated and consisting of sandy-gravely granular elements in poor silty-sandy matrix.
ecf	Materials of the colluvial cover, poorly consolidated and consisting of a dominantly silty-clayey fraction with subordinate inclusions of sandy-gravely material and/or of stone blocks.
ags	Materials of fluvial origin with dominantly gravely-sandy grain size.

*Point Load Strength

The following parameters were thus investigated for the 92 landslide phenomena identified: geometry, distribution, frequency and intensity (type and areal extent). All the data concerning the local slope movements were reported in a "Landslide Inventory Map". The map shows the forms and processes which are

mainly dependent on gravity and other morphogenetic processes related to both on-going and potential gravity-induced deformations. The map was built through field surveys (2000-2001) and interpretation of aerial photos taken during 6 flights conducted in 1954, 1974, 1977-1979, 1983-1984, 1988-1989, 1991 and 1994.

The multi-temporal analysis of aerial photos led to identify 293 landslide events and thus to determine the frequency of reactivation (or activation in the case of 1st-generation landslides) (see Tab. 2.2). It is worth stressing that, in the investigated sector, reactivations accounted for 90% of the total events recorded (Fig. 2.2); this finding is consistent with national data.

Table 2.2. Sketch of summary table of data obtained from analysis and interpretation of aerial photos.

Land-slide code	Litho-technical class	Type of movement (*)	LANDSLIDES EVENTS							Min. Return Period T (y)	
			Flight 1955	Flight 1979	Flight 1983	Flight 1989	Flight 1991	Flight 1994	Field Survey 2001		
038	ags	Rotational slide		F	R				R		3-10

F= 1st generation

R= reactivation

(*) CRUDEN & VARNES classification, 1996.

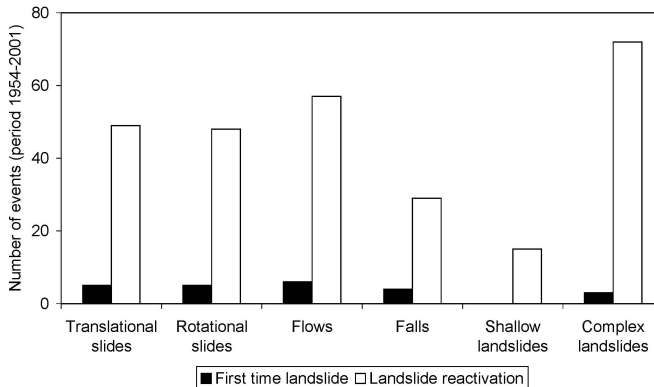


Fig. 2.2. Distribution of 1st-generation events and reactivations vs. types of movements. (Extract from the Landslide Inventory Map).

In order to quantify the landslide hazard, use was made of the minimum return period parameter (expressed in years) and 5 decreasing hazard classes were distinguished: $T < 3$ yrs (P1), $3 < T < 10$ yrs (P2), $10 < T < 20$ yrs (P3), $20 < T < 50$ yrs (P4), $T > 50$ yrs (P5). As these classes are based on static aerial photos, they necessarily refer to a time range and not to an absolute value of the return time. This is the

reason why a precautionary criterion, i.e. indicating the periods with the highest frequency of the phenomena, was selected.

In the case of reactivations, the assessment of the return time enables to estimate the probability of occurrence and the periods elapsing between two successive movements.

In the case of 1st-generation landslides (more hazardous since they may involve slopes with no clear signs of instability or indications on the intensity of potential movements), the assessment may be made by referring to the “Landslide Susceptibility Map” derived from the two basic maps previously described (“Lithotechnical Map” and “Landslide Inventory Map”). The graphical and topological combination of landslides and lithotypes gives a general view of the relations between landslide phenomena having given features (intensity, based on size and type of landslide, and hazard) and the lithotechnical properties of the materials (Fig. 2.3). This procedure yields clear data on the proneness of the various sectors of the investigated area to both 1st-generation landslides and reactivations.

Finally, the boundaries of the landslide risk areas in the Pergola area were defined on the basis of the guidelines set forth in the applicable legislation. With a view to refining the tools suggested by the legislation, namely those used for the assessment of landslide hazards, the 4 risk classes R_n were combined with the 5 hazard classes previously described, thereby obtaining 20 P_nR_n classes and thus a more rigorous assessment tool. This procedure highlights the landslide phenomena – and their damage – which have the highest probability of occurrence vs. those having return times of more than 10 years.

3 Conclusions

The methodology adopted for assessing the landslide risk in the Pergola area proved to be reliable and easy to use even for areas different from the investigated one.

The findings from the study emphasised the importance of the choice of the lithotechnical features of rocks and soils as one of the main factors of landslide susceptibility. This choice was dictated by strictly geological considerations rather than by the application of time-consuming and complex statistical processes. In effect, the geomechanical properties of materials are “primary” features, in contrast to other features (e.g. slope gradient) which represent a derived attribute, often due to the same landslide phenomena.

The study also stressed the importance of assessing the probability of occurrence of landslides, which heavily conditions the assessment of the actual risk induced by them. In this sense, the multi-temporal analysis of aerial photos proved to be an effective investigating tool.

Future research will be targeted at analysing the role of rainfall and earthquakes in the triggering conditions of landslides that affect representative slopes of the investigated area. In effect, while the assessment of the landslide risk on wide areas significantly contributes to land planning and management policies, the need arises for developing forecasting and warning tools, especially in cases of high risk in terms of potential loss of human lives.

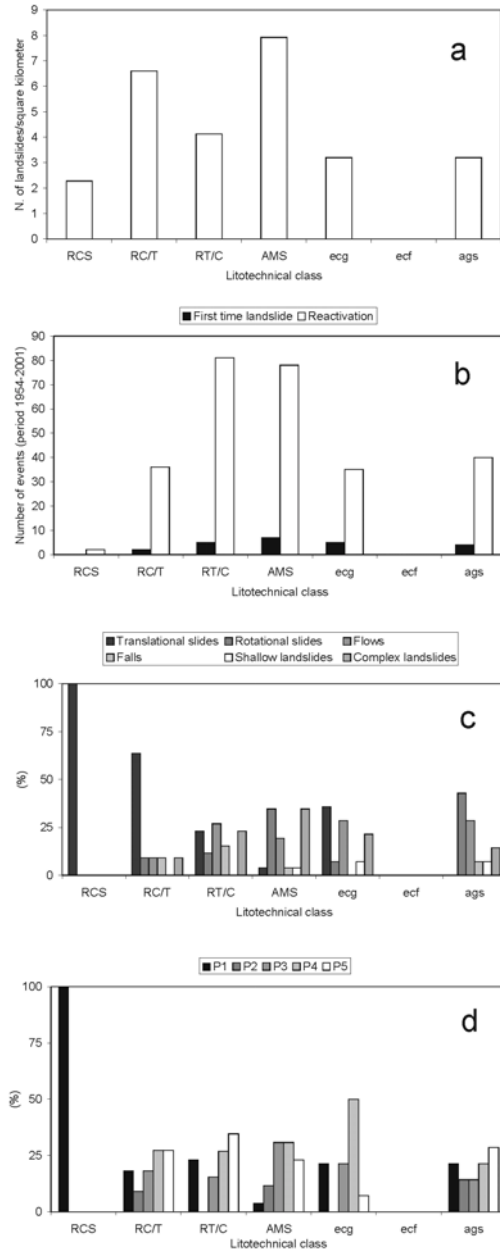


Fig. 2.3. Landslide index referred to each lithotechnical class (a); distribution of 1st-generation events and reactivations vs. lithotechnical classes (b); distribution of types of movement vs. lithotechnical classes (c); distribution of hazard classes vs. lithotechnical classes (d). (Extract from the Landslide Susceptibility Map).

A last consideration concerns the results achieved so far in understanding the land and its risks. It is certainly desirable to gain greater insight into the land and to further refine assessment tools. However, in the past 5 years, thanks to stricter and stricter laws, major steps forward were taken in the area of forecasting and prevention of geological risks (landslides, earthquakes, floods, volcanic eruptions), especially in terms of improved understanding of ongoing and potential phenomena.

Acknowledgements

The research is financially supported by CNR-GNDICI grant, contract n. 03.00044GN42, responsible Prof. U. Gori.

References

- Barchi M, Landuzzi A, Minelli G, Pialli G (2001) – Outer Northern Apennines. In: Martini P & Vai G (eds) “Anatomy of an orogen: The Apennines and adjacent Mediterranean basins”. Kluwer Academic Publisher, Dordrecht, NL, pp. 215-254.
- Bieniawski ZT (1975) - The Point-Load Test in Geotechnical practice. Eng. Geol., vol 9, pp 1-11.
- Cruden DM & Varnes DJ (1996) – Landslide Type and processes. In: Landslides investigation and mitigation. (Ed. A.K. Turner, L.R. Schuster). Transp. Res. Board, Spec. Rep. 247, pp 36-75.
- Guastaldi E & Rindinella A (2003) – Landslide hazard prediction in Pergola area (Marche, Italy). Proc. of the 1st National Congress AIGA (Engineering and Environmental Geology Italian Association), Chieti (Italy), 19-20 February 2003, pp 715-717.
- Spagna V (1998) - The Municipality General Master Plan as a tool for the geological risk mitigation. Journal of Technical & Environmental Geology, vol 1/98, pp 3-13.

Modelling of Landslide-Triggering Factors – A Case Study in the Northern Apennines, Italy

Mario Floris, Milena Mari, Roberto W. Romeo, and Umberto Gori

Institute of Engineering Geology, University of Urbino “Carlo Bo”, Campus Scientifico
Loc. Crocicchia, 61029 Urbino (PU), Italy
geoappl@uniurb.it
Tel: +39 722 304235/304258
Fax: +39 722 304260

Abstract. The paper describes a study which was conducted on a landslide-prone slope of the Northern Apennines (Italy). The slope, which dominantly consists of clayey and clayey-marly terrains, has been affected by landslide phenomena, whose frequent reactivations have involved wider and wider areas, destroying one home and causing significant damage to an important local road.

In order to analyse the correlation between rainfall and landslide reactivation, data were collected on the main stages of landslide activity and on the trends of rainfall in the same periods.

The study was expected to identify landslide-triggering rainfall thresholds, which may lead to the development of prediction, prevention and warning systems for landslide risk mitigation.

Keywords: landslide, rainfall, hydrological variables, Northern Apennines.

1 Introduction

The analysis of landslide-triggering factors (rainfall and earthquakes) may be a useful tool for assessing landslide hazards, if it combines the results of both deterministic and probabilistic models. Deterministic models describe the physical and mechanical behaviour of slopes under various boundary conditions (hydraulic and seismic), analysed in terms of steady-state and/or transient loading conditions. Probabilistic models, based on the recognition of rainfall and seismic thresholds as triggers of past landslides, may give insight into the recurrence of such critical conditions over time. In this way, an answer can be given to the crucial question of “when and where a landslide may occur” in view of landslide hazard assessment and mitigation.

Studies carried on by our research team include field investigations coupled with slope stability analyses, so as to determine the basic conditions of landslide reactivation and their impact on human settlements, leading to a comprehensive approach to landslide risk assessment.

This paper reports the preliminary findings from a study conducted on a training landslide-prone slope (Valzangona landslide) located near Urbino (Fig. 1.1) and discusses hydrological-statistical criteria for analysing the relationship be-



Fig. 1.1. Geological sketch of the Urbino area. 1) Limestones, marly limestones, marlstones and cherts (formations between Calcare Massiccio and Schlier, Lias – Miocene p.p.); 2) Arenites, pelites and evaporites (formations between Marnoso-Arenacea and Colombacci, Miocene p.p.); 3) Chaotic complex clays of the Marecchia Valley; 4) Clayey, sandy and gravelly deposits (Plio-Pleistocene). (From Antonini et al. 1993, modified).

tween landslides and rainfall, with a view to identifying landslide-triggering rainfall thresholds and develop appropriate alert/warning systems.

2 The Valzangona Landslide

The investigated area, located in the northern Apennines (Marche region, Italy), has outcrops of Pliocene clays and of the *Colombacci* geological formation (Fig. 2.1), i.e. stratigraphic units with a high spatial and temporal frequency of landslide phenomena (Gori and Tonelli 1992).

The landslide body rests on the terrains of the *Colombacci* formation. Two sub-units may be distinguished inside this formation. The lower portion is dominated by clayey, clayey-marly and clayey-silty lithotypes of grey-blue colour in 5- to 20 cm-thick layers, interbedded with grey-green laminated clays and thin yellowish arenaceous levels. The upper member consists of medium- to coarse-grained grey-yellowish sandstones in 20- to 60 cm-thick layers, intercalated with thin clayey-marly levels.

Tectonic activity and structural elements play a key role in slope instability, as they determine direction, dip, deformation and jointing of strata, as well as groundwater circulation. The slope under study lies on the outer side of an Apennine-trending syncline and consists of a number of west-dipping beds, occasionally taking on a chaotic appearance owing to minor folds. The compressive tectonic style is associated with a number of chiefly NW-SE-trending discontinuities. The most important of these faults, lying north of the landslide, puts the *Colombacci* clays in contact with the arenaceous member of the same formation. The permeability due to jointing and porosity of the arenaceous member is from average to low. Instead, both the clayey member of the *Colombacci* formation and the Pliocene deposits have a low or very low permeability, which favours runoff. The combination of runoff and of an easily erodible bedrock gives rise to a dense and hierarchised watershed.

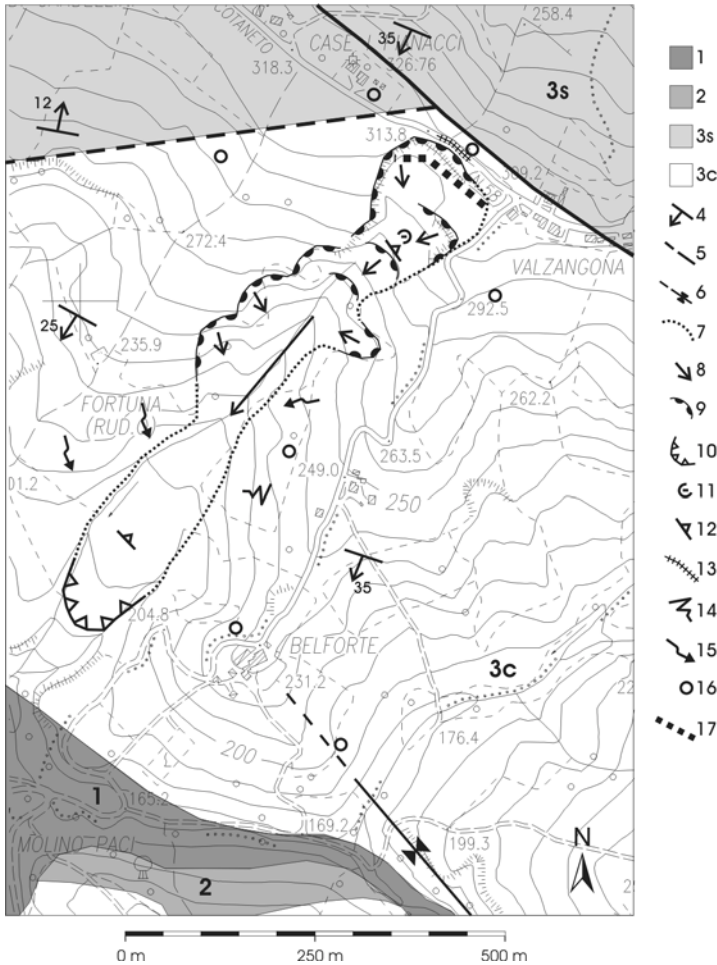


Fig. 2.1. Geological and geomorphological sketch of the Valzangona area. 1) Present and recent alluvia (Holocene); 2) Pliocene clays (lower Pliocene); 3s) *Colombacci* formation – sandy member (Messinian); 3c) *Colombacci* formation – clayey member (Messinian); 4) direction and dip of strata; 5) fault (dashed line if the fault is supposed); 6) syncline axis (dashed line if the syncline axis is supposed); 7) boundary of landslide body; 8) main direction of movement; 9) landslide scarp; 10) landslide deposit; 11) depressed area; 12) counterslope; 13) tension cracks; 14) widespread runoff; 15) surface movements; 16) well; 17) gabion walls.

The landslide occurred on the dominantly clayey member of the *Colombacci* formation, which has a low shearing strength ($c' = 19$ kpa, $\phi' = 25^\circ$; $c_{res} = 8$ kpa, $\phi_{res} = 14^\circ$) and is highly exposed to weathering. Despite low permeability of the lithotype, tectonisation and jointing allow the constant presence of water. Monitoring of the local groundwater level in the wells located near the landslide showed

variations of up to 1 m, with an average depth of the piezometric level ranging from 1 to 3 m from ground level for the wells located in the immediate vicinity of the landslide. The variations in the piezometric level recorded in the various wells demonstrated a close correlation with precipitation.

The examination of aerial photos taken in 1955 indicated that the Valzangona landslide is the result of a dominantly erosional process at the toe of the slope, followed by successive stages of gravitational movements which started in 1981 (Table 3.1). These movements caused the retreat of the crown area of the landslide and its lateral and down slope spread. The Valzangona landslide may be classified as a complex phenomenon, featured by roto-translational movements evolving into flows in the intermediate-lower portion of the slope. At present, the landslide has an approximately 150 m-wide crown and extends for about 800 m. The thickness of the landslide body is 8 to 10 m in the upper and central portions, respectively and about 15 m in the depositional area. The profile of the landslide is fairly irregular, with small scarps, steps, trenches and counter slopes (especially at the top), and displays an average gradient of 30-40%. Downhill, near the depositional area, the morphology of the landslide becomes more regular and takes on a convex trend upwards, with a slope gradient of about 15%.

It should be pointed out that the phenomenon is still active, in spite of mitigation works (gabion walls and drainage systems); landslide reactivations cause recurrent damage to a local road and to remedial works in the crown area.

3 Landslide-Rainfall Relationship

This section describes the methodology adopted and the results obtained from the implementation of a hydrological-statistical model for the Valzangona landslide. The model relies on empirical relations between hydrological variables and landslide movements: within a well-defined region and for a given type of landslide, they seek to identify threshold values of precipitation or other precipitation-derived quantities, above which instability phenomena may take place. The methods and relations used by the various authors are all based on the availability of historical data on the investigated landslide phenomena and on the analysis of the hydrological scenario preceding and accompanying their initiation.

The model developed for the Valzangona landslide takes into account the exceptional character of the meteoric events related to landslide reactivation. For this purpose, use was made of daily rainfall data recorded by the Petriano (1951-1986) and Urbino (1987-1999) hydrographic stations (Fig. 1.1). The landslide reactivation data (Table 3.1) were retrieved from the literature, the archives of the Municipality of Petriano, other dedicated archives (Guzzetti et al. 1994; <http://avi.gndci.cnr.it/>) and daily papers.

Graphs (Fig. 3.1) were built to analyse the hydrological scenario preceding and accompanying landslide reactivation. They show the cumulative rainfall prior to landslide initiation (day 0) and the rainfall probability curves for different return times. The latter curves, i.e. a kind of “probabilistic precipitation abacus”, enable to assess the return time of any cumulative curve for each reactivation and thus to

estimate whether it has an exceptional character or not. They also offer the opportunity: (i) to identify rainfall events, significant in terms of quantity and duration, which did not take place immediately before the landslide, but which may have played a role in its onset; and (ii) to assess their return time with simple graphic operations.

Table 3.1. Historical news on reactivations of the Valzangona landslide.

Month	Day	Year	Source	Excerpts from the news
11		1981	Literature	<i>...first important landslide movement ...</i>
4		1982	Literature	<i>... landslide reactivation with earth and mud flows ...</i>
12	11	1982	Municipal Archives	<i>... reactivation after last meteoric event ...</i>
3	5	1986	Municipal Archives	<i>...further developments ...</i>
2	18	1992	Municipal Archives	<i>... reactivation after last meteoric events ...</i>
3	2	1993	AVI Archives	<i>... partial collapse of Francini's house located at the crown of the landslide ...</i>
1	3	1994	Literature, Municipal Archives	<i>... the landslide involved the road and the house located at its crown ...</i>
4		1996	AVI Archives, daily paper	<i>...Francini's house completely destroyed ...</i>
8	30	1996	Municipal Archives	<i>...reactivation after last meteoric events ...</i>
10	17	1996	Municipal Archives	<i>... road cracks after recent rain ...</i>

The observations deriving from the examination of Fig. 3.1 are summarised in Table 3.2, which shows that the Valzangona landslide reactivations are connected to exceptional rainfall events, which occurred in periods of time even very distant from the day of initiation of the landslide.

The hydrological variable, which is significant in terms of landslide initiation, is the rainfall cumulated in short periods (3-20 days, Bold characters in the Table) with high average intensity (up to 43 mm/day) and/or the rainfall cumulated during longer periods (30-135 days, Italic characters in the Table). These considerations are explained in the diagram of Fig. 3.2, which correlates intensity and duration of potentially landslide-triggering rainfall events. The interpolation curve drawn in the Figure is a first-cut rainfall threshold, above which the landslide may be triggered. This threshold should be validated by a deterministic model taking into account the changes in pore pressures, as a function of meteoric events not necessarily exceptional and of the effects of such changes on slope stability.

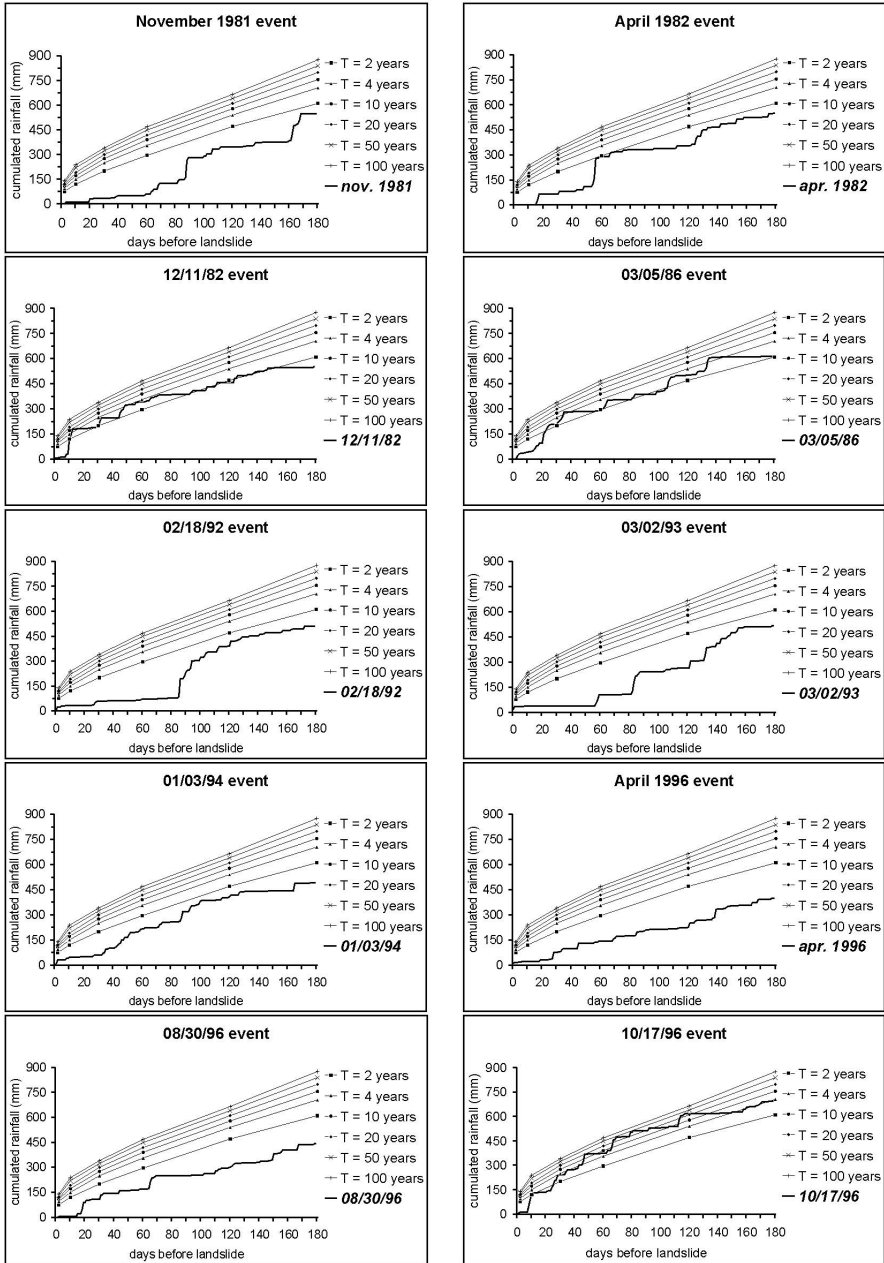


Fig. 3.1. Comparison of cumulated rainfall curves for different return times (T) computed with the GEV function (Jenkinson 1955; Hosking et al. 1984) and of cumulated rainfall curves associated with reactivations of the Valzangona landslide (day 0).

Table 3.2. D (days): duration of potentially landslide-triggering rainfall events, (*) period when the rainfall event occurred, calculated backwards starting from landslide initiation (day 0); Q (mm) = quantity of rainfall; T (years) = return time; I (mm/day) = average intensity.

Landslide event	D(*)	Q	T	I=Q/D
30(?) Nov. 1981	30 (59-89) 3 (86-89)	228 130	2-4 50	7.6 43
30(?) Apr. 1982	59 (0-59) 6 (53-59)	290 181	2-4 >100	~5 30
11 Jan. 1982	12 (0-12) 5 (7-12)	178 165	10 50-100	~15 33
5 Mar. 1986	35 (0-35) 135 (0-135)	281 604	4-10 4-10	~8 ~4.5
18 Feb. 1992	20 (84-104) 46 (84-130)	272 367	50-100 10	13.6 ~8
2 Mar. 1993	32 (56-88) 7 (81-88)	204 135	2-4 10	~6 ~19
3 Jan. 1994	20 (32-52)	135	<2	~7
30(?) Apr. 1996	8 (26-34)	60	<2	7.5
30 Aug. 1996	7 (14-21)	98	4	~14
17 Oct. 1996	82 (0-82) 4 (7-11) 40 (7-47)	512 118 368	50 10 50	~6 ~30 ~9

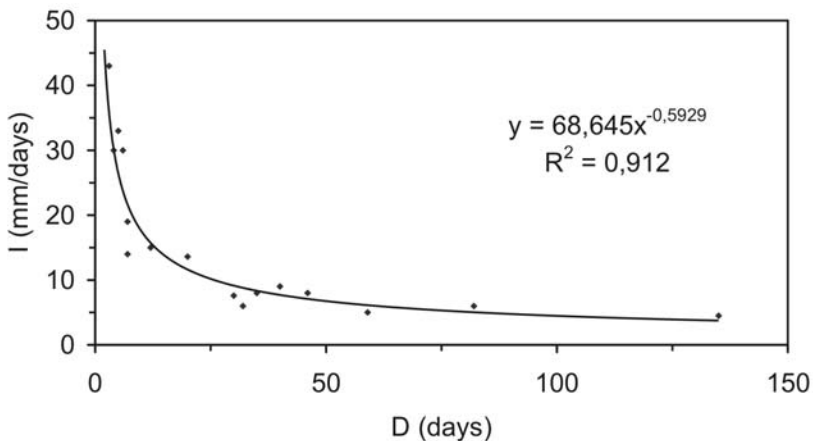


Fig. 3.2. I-D diagram of potentially landslide-triggering rainfall events.

It is worth stressing that the validity of a landslide-forecasting model, based on the rainfall-landslide relationship, is highly conditional upon the choice of the hydrological variable which can “justify” the onset of the investigated slope instabilities. This choice may follow an assessment criterion based on the exceptional

character of the rainfall event related to the landslide phenomenon, but it should also consider the possible impact of “normal” rainfall. In effect, if the exceptional character of a given hydrological variable strengthens the relation between the cause (rainfall) and the effect (landslide), a correlation between a landslide and “normal” hydrological events provides much more significant insights into the behaviour of unstable slopes (Iritano et al. 1998).

4 Conclusions

The study of the Valzangona landslide evidenced that hydrological-statistical models play a crucial role for an improved understanding of the relations between landslides and rainfall. Such models can be used for both landslide prediction and prevention, if the physical phenomena occurring in slopes are replicated in deterministic models.

In the case of the Valzangona landslide, the hydrogeological conditions of the site and the geotechnical properties of the materials involved suggest a more dramatic impact of exceptional rainfall cumulated over long periods, rather than of short and intense rainfall. At any rate, such correlation should be substantiated by the modelling of the destabilising effects - i.e. the future focus of this research - of the identified rainfall thresholds. After establishing the impact of exceptional rainfall on slope stability, an alert/warning system may be developed based on the quantity of rainfall recorded by rain gauges. For this purpose, use may also be made of the rainfall probability curves (Fig. 3.1), by assigning increasing alert conditions to increasing values of the return time.

Acknowledgements

The research is financially supported by a CNR-GNDCI grant, contract no. 03.00044GN42, project co-ordinator Prof. U. Gori.

References

- Antonini G, Cardinali M, Guzzetti F, Reichenbach P and Sorrentino A (1993) Carta inventario dei fenomeni franosi della regione Marche ed aree limitrofe. GNDCI, Publ. n. 580, scala 1:100.000, 2 Fogli, Arti Grafiche L. Salomone, Roma.
- Gori U and Tonelli G (1992) Flow slide movements in clayey terrains of the Italian northern Apennines. Proc. of the Chengdu Symposium, China, July 1992. IAHS Publ. n. 209, pp 227-236.
- Guzzetti F, Cardinali M and Reichenbach P (1994) The AVI Project: A bibliographical and archive inventory of landslides and floods in Italy. *Environmental Management*, 18, 4, pp 623-633.

- Iiritano G, Versace P and Sirangelo B (1998) Real-time estimation of hazard for landslides triggered by rainfall. *Environmental Geology*, 35, 2-3, pp 175-183.
- Hosking JRM, Wallis JR and Wood EF (1984) Estimation of the generalized extreme value distribution by the method of probability weighted moments. *Inst. of Hydrology, Report 89*, Wallingford, England, 27, pp 251-261.
- Jenkinson AF (1955) The frequency distribution of the annual maximum (or minimum) values of meteorological events. *Quarterly Journal of the Royal Meteorological Society*, 87, pp 158-171.

Management of Combined Natural Risks – A New Approach

Keynote Address

Jörg Hanisch

Federal Institute for Geosciences and Natural Resources
Stilleweg 2, D-30655 Hannover, Germany
joerg.hanisch@bgr.de
Tel: +49-511-6434231
Fax: +49-511-6343694

Abstract. A new attempt is made to illustrate and to quantify the relationships of individual natural hazards, their combinations and the human vulnerability to natural hazards. During many catastrophic events, combinations of different natural events aggravate their occurrence substantially. Earthquakes are frequently associated with heavy landsliding (El Salvador 2001) and heavy rainstorms are able to trigger fast running debris flows and not only floods (like during the Mitch disaster in Central America in 1998). That signifies that natural hazard maps should show the combinations of different hazards and their genetic relationships. To put into effect this, first, the individual hazards have to be assessed and presented in hazard zones (0 to 3). Then these hazards zones will be overlain using GIS techniques. In this way, e.g., an earthquake-prone area which coincides with an area susceptible to landslides (ranking 0 to 3 as well) can show hazard concentrations of up to a value of 6, simply adding the individual hazard zones. To get the result of the corresponding risk zones, the vulnerability maps of human settlements and infra-structure have to be overlain on the maps of these combinations of natural hazards.

Keywords: hazard, vulnerability, earthquake, flooding, zoning, GIS, mapping

Introduction

Numerous types of geologic, geomorphologic, engineering geologic maps have been developed during the past two decades to cover natural risks. The need for such thematic maps has been rising continuously because of increasing natural hazards and increasing vulnerabilities of human settlements and installations. Most of these maps concentrate on one of the hazards or treat them separately (Hanneberg et al. 2002). Engineering geologic maps show mainly the bearing capacities of the ground and hazards arising from landslides or hidden caves able to develop sinkholes. Geomorphologic hazard maps usually delineate landslide and erosion prone areas mainly based on slope inclination maps (Kienholz et al. 1984, Kienholz and Krummenacher 1995). Maps of volcanic hazards provide the zoning of several hazards: lava flows, ash fall, pyroclastic flows, and lahars (e.g.

Latter 1989). Maps of the combination of various natural hazards, such as, earthquake and landslide hazards or volcanoes combined with typhoon prone areas have not been elaborated hitherto.

Natural Hazards

A great variety of natural hazards are able to threaten areas of human settlements and infrastructure: earthquakes, volcanic activity, all kinds of mass movements, storm-induced floods. To present them in hazard maps, the individual hazards have to be recognized and assessed. All available data have to be collected, where data are missing the gaps have to be filled by own investigation. Data bases have to be generated where the data gathered from a multitude of sources will be stored and assessed. Using GIS techniques, the spatial distribution of hazards then results in zoning maps showing the ranking of each individual hazard. Usually, because of scarcity and incompleteness of available information a hazard ranking from 0 to 3 meaning from zero to high is the maximum achievable. In many cases the poor-ness of data available only allows a rating of 0 to 2 meaning negligible, medium, and high.

Stability and Engineering Properties of the Ground

The coordinated use of the available land should always be based on the knowl- edge of the ground properties such as bearing capacity, permeability and shear resistance. Depending of the scale of the map to be compiled, the density of pri- mary data of soil properties varies considerably but normally is found to be quite limited. Therefore, the zoning of areas of poor foundation conditions has to be rather simple if no campaign of detailed engineering geological mapping is possi- ble.

Sinkholes

The same is true for potential sinkhole areas. Areas with underground cavities originating from karst phenomena and ongoing or former underground mining activities have to be delineated in hazard maps rather roughly. Details of this haz- ard cannot be shown in such maps but have to be examined by geophysical meth- ods and drilling.

Landslides

The landslide hazard is among the most threatening especially in mountainous regions. According to the convention of the international geotechnical societies, all kinds of mass movements on slopes (except snow avalanches) belong to the general term 'landslides'. That means that also fast running debris flows with much higher reaches than typical landslides are grouped under this category. The

consequence of this is that areas under the threat of landslides cover far larger zones than according to the former definition of landslide. Accordingly, areas believed to be safe, because of their location far from steep slopes, may well be threatened by such types of mass movements (Plafker and Ericksen 1978, Eissbacher and Clague 1984, Grabs and Hanisch 1993, Reynolds 1995).

Numerous concepts to evaluate landslide hazards have been elaborated (Kienholz et al. 1984, Varnes 1984, Einstein 1988, Van Westen and Alzate 1990, Rengers et al. 1992). The more recent approaches use GIS. The gathering of data handled by this technique in most cases is a combination of remote sensing, fieldwork, and slope stability calculations. There is still a considerable quality gap of landslide data produced by detailed landslide mapping in the field and those from the interpretation of aerial or satellite images. It has to be stated clearly that filling this gap is a fundamental task for future landslide mapping techniques.

Earthquakes

The reliable hazard zoning of earthquake-prone areas is still a widely unsolved problem. In general, three approaches are being applied, (i) collecting data from historic events and data gathered from instrumented networks and compiled in distribution maps of earthquake epicentres, (ii) analysing patterns of recent and active faults with the help of satellite and aerial images, (iii) mapping of unconsolidated sediments susceptible to liquefaction from seismic shaking. Tectonically active zones normally are well known and the associated concentration of epicentres can be obtained from geological and geophysical surveys all over the world. Most of the known regions of active faulting have been mapped carefully and the areas of high susceptibility of liquefaction usually are well established as well. The key problem, however, to predict what will happen during the next major earthquake and where, is a totally unsolved dilemma. Neither can be predicted which of the existing active fault line will be triggered by the next wave, nor what type of wave will cause the most damage when an earthquake will originate from movements of a nearby epicentre. More than a macro-zoning of earthquake-prone regions seems to be unachievable at present.

Volcanism

Compared to the hazard zoning of earthquakes the endangered zones around active volcanoes can be delineated rather straightforwardly (e.g. Latter 1989). The witnesses of former events like lava flows and all types of pyroclastic sediments combined with age dating enable to reconstruct the history of each individual volcano quite accountably. On the basis of this, prediction of future volcanic activities and of the reach of volcanic materials can be established rather reliably. Advanced methods of volcano monitoring are available to give early warnings when the next expulsion will be approaching keeping in mind that most of the casualties and damage during volcano eruptions are caused by unpredictable and far-reaching pyroclastic flows or lahars and not by lava flows and ash fall.

Floods

Flood hazards have become an extreme risk for the people living in flood or deltaic plains. Not only the frequency of events seems to have increased considerably, but also the vulnerability of the settlement areas has risen to a hitherto unknown level simply because population growth has forced people to settle in areas avoided before. Other reasons for flood disasters are merely man-made: river regulation including the restriction of natural flood areas or deforestation of hill slopes are the most important ones. Mapping of flood hazard zones is a comparably easy task.

Combinations of Natural Hazards

During many catastrophic events, the combinations of different natural events aggravate their impacts substantially. Earthquakes are frequently associated with heavy landsliding (as 2001 in El Salvador where about two thirds of the casualties were caused by landslides and not by the collapse of their homes); rainstorms are also able to trigger huge landslides and especially the fast running debris flows (or hyper-concentrated flows) like in Central America during the Mitch disaster; most of the casualties and damage during volcano eruptions often are caused by mass movements like the unpredictable pyroclastic flows or lahars (Casita Volcano, Nicaragua 1998) and not by lavas. That signifies that geohazard maps have to show the combinations of hazards and their genetic relationships. The delineation of singular hazards often results in hazard and risk maps which might be quite misleading.

		HAZARD →			
		0	1	2	3
VULNERABILITY ↓	0	0	0	0	0
	1	0	1	2	3
	2	0	2	4	6
	3	0	3	6	9

Fig. 1. Matrix of the formula risk = hazard x vulnerability.

Therefore, in a second decisive step, the layers of the individual hazards are put above each other thus producing synoptic maps of geohazards. This technique allows recognising not only coincidences of hazards, such as, earthquake hazard zones with landslide-prone sediments but also genetic coherences of the individual

hazards: floods produce landslides by lateral erosion and landslides can provoke temporary dams able to produce devastation floods.

Risk has been defined to be the product of hazard and (human) vulnerability (Varnes 1984). This simple formula clearly demonstrates that without the presence of human settlements or infra-structure even the greatest natural hazard does not present any risk (from the limited viewpoint of mankind). Figure 1 visualises this distinctly. To include the concept of combined natural hazards, a new attempt is made in Figure 2 to illustrate and to quantify the relationships of individual hazards, their combinations and the human vulnerability to natural hazards. If each of the individual hazards and the vulnerability are given a ranking of, say, 1 to 3, a semi-quantitative approach for the risk zones can be attempted. For example, a well-known area highly prone to earthquake activity coincides with an area which has been found to be medium landslide-prone, a zone of combined hazards with factor 5 results. If this zone should fall into a densely populated area with a vulnerability factor 3, the resulting risk zone is given a factor 15 simply applying the formula $\text{risk} = \text{hazard} \times \text{vulnerability}$ (Fig. 2).

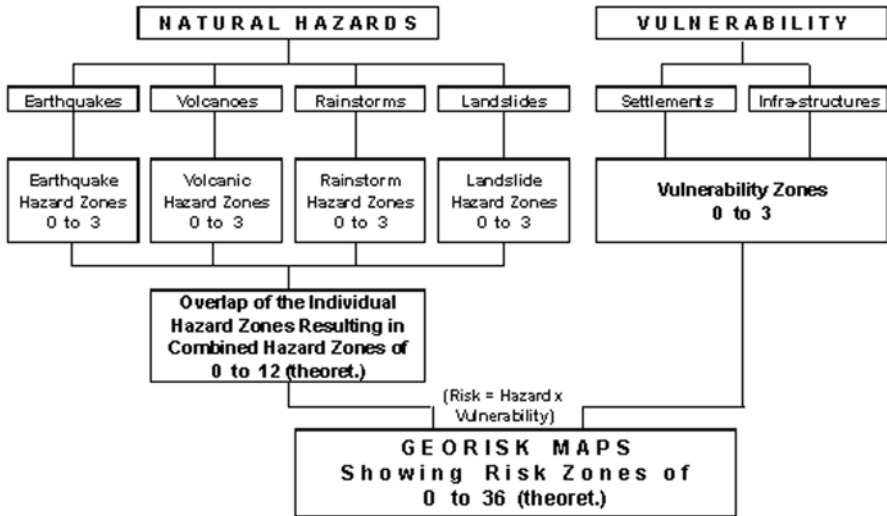


Fig. 2. Scheme to quantify risk zones from combined hazard zones and areas of different human vulnerabilities.

Discussion and Outlook

The semi-quantitative method proposed here cannot resolve all kinds of problems connected with the assessment of natural risks. Obviously in first order it depends on the quality of the individual hazard and vulnerability assessments. The dozens of existing landslide-hazard approaches clearly demonstrate that the final truth has

not yet been found in this field. Or, as another example, the prediction of which one of the faults of a known active fault pattern will move during the next heavy earthquake still remains an unsolved problem.

Another problem arises when low-frequency/high-hazard events have to be combined with high-frequency/low to medium-hazards in one singular map, such as, devastating volcanic eruptions with a recurrence of several hundreds of years and ordinary landslide events which might occur with every major rainstorm. Only experience during working with the method proposed will show in which way such apparently controversial topics can be handled satisfactorily. This is especially the case if, e.g., three natural hazards are present in a certain area of high vulnerability (meaning that risk zone ratings of up to 27 are possible theoretically) and in a nearby area only one hazard threatens a densely populated area (signifying that a maximum risk rating of 9 can result of this risk assessment method). The juxtaposition of such very diverging risk ratings requires special explanation in the legend of the map.

On the other hand, the proper evaluation of vulnerabilities is deeply influenced by social aspects especially in rural areas: For example, if a farmer owning, let's say, a livestock of 1000 cattle will lose 50 % of his animals during a natural disaster and, at the same time, a poor farmer family owning 4 cows and 20 chicken will lose 50 % of his livestock – which of the two families is more vulnerable? The usual method of vulnerability assessment simply counting the numbers of inhabitants per square kilometre and estimating values at risk quickly comes to its limits.

References

- Eisbacher GH, Clague JJ (1984) Destructive mass movements in high mountains - Hazard management. Geol. Surv. Canada, Pap. No. 84-16, 230 pp.
- Grabs WE, Hanisch J (1993) Objectives and prevention methods for glacier lake outburst floods (GLOFs). IAHS Publ. 218, pp 341-352.
- Hanneberg WC, Bauer PW, Chávez WX jr (2002) Multilevel geologic hazard assessment mapping in Rio Grande gorge, northern New Mexico, USA. In: Bobrowsky PT (ed) Geoenvironmental mapping – methods, theory and practice. Balkema, Lisse, pp 75-91.
- Kienholz H, Krummenacher B (1995) Dangers naturels - Légende modulable pour la cartographie des phénomènes. Comm. Off. Fédér. Économie des Eaux, Berne, 19 pp.
- Kienholz H, Hafner H, Schneider G, Zimmermann M (1984) Methods for the assessment of mountain hazards and slope stability in Nepal. In: Erlenbach W (ed) Natural environment in tropical mountain ecosystems. Erdwiss. Forschg. 18, pp 147-160.
- Latter JH ed (1989) Volcanic hazards. Springer, Berlin, 762 pp.
- Plafker G, Ericksen GE (1978) Nevados Huascarán avalanches, Peru. In: Voight B (ed) Rockslides and avalanches 1. Devel. Geotechn. Engineering 14A, pp 277-324.
- Rengers N, Soeters R, van Westen CJ (1992) Remote sensing and GIS applied to mountain hazard mapping. Episodes 15, pp 36-45.
- Reynolds JM (1995) Glacier lake outburst floods (GLOFs) in the Himalayas: an example of hazard mitigation from Nepal. Geoscience and Development 2, pp 6-8.
- Van Westen CJ, Alzate JB (1990) Mountain hazard analysis using a PC-based GIS. Proc. IAEG, vol. 1, pp 265-272.
- Varnes DJ ed (1984) Landslide hazard zonation: a review of principles and practice. UNESCO Ser. Natural Hazards 3, 63 pp.

Technique of Quantitative Assessment of Karst Risk on the Local and Regional Levels

Alexei Ragozin and Vladimir Yolkin

Institute of Environmental Geoscience, Russian Academy of Sciences
Ulansky lane 13, building 2, P.O.Box 145, 101000 Moscow, Russia
risk@geoenv.ru
Tel: +7(095) 2089605
Fax: +7(095) 9231886

Abstract. Meaning of terms “karst hazard” and “karst risk” is discussed. Quantitative measures of considered risk at any level of forecast assessment are the following: probable damage from karst deformations, frequency (probability) of its realization, and also product of the mentioned parameters characterizing annual physical, economic, social or ecological losses within certain territory. The general procedure of local and regional assessment of karst collapse intensity (cases of failures / years · km², m²/ years · km²), vulnerability of objects of national economy and population for these deformations, as well as karst economic (\$/year, \$/km² · year), social (per. /year) and individual (per. /per. · year) risks of losses is considered.

Keywords: karst hazard, karst risk, GIS.

1 Introduction

Karst is a significant hazardous natural process on the earth because it is manifested in the form of collapses and subsidence of the ground surface sometimes reaching 100 m and more in diameter and depth. About 13% of the Russia area including more than 300 towns and thousands of smaller settlements with 19% of the total population of Russia, are subject to karst deformations. In Russia, the total economic damage caused by karst and closely related suffosion is \$1-1.5 billions per year according to expert evaluations (Ragozin 1994).

By *karst hazard* we mean a menace of forming karst and (or) karst-suffosion collapses and surface settlements of certain dimensions in a specific area during a given time period, which can result in negative consequences for economic facilities and population.

In contrast to karst hazard, *karst risk* is the probable index of hazard of karst and karst-suffosion collapses and surface settlements established for a certain object as it possible losses in various spheres for a given time period.

A mean annual collapse-formation intensity (the number of collapses per km² per year) proposed by Makeev (1948) is the generally accepted integral measure of the considered hazard in Russia. Several classifications and methods for quantitative prediction of karst hazard were elaborated by Savarenskii (1995); Tol-

machev (1980); Reuter et al. (1981); Hu et al. (2001); Lei et al. (2002) mainly at a scale of 1: 25 000 and larger.

Up to recently, the regional karst hazard assessment has been only qualitative. It was mainly performed by analyzing the main factors of karst development and by a special zoning of areas, which sometimes took into account actual damage of these areas by karst deformations. Until recently all this caused lacking techniques and examples of a quantitative assessment of karst risk both on the local and regional levels.

2 Local Risk Assessment

The basic objects of the assessment at a local level are natural-technical systems (NTS) various in area and volume, including all buildings, located in their limits, structures and other economic objects, ranging from individual building up to their systems within the limits of small municipal formations and settlements occupying rather small area, which is usually mapped upon solving town-planning, design and other problems at a scale of 1:10000 and larger.

Therefore, a relative uniformity of geological, hydrometeorological, technical, ecological, social and other conditions of karst development are characteristic for them. Within NTS, karst risk can be evaluated on the basis of intensity or frequency of formation karst or karst-suffusion deformations preliminarily assessed from their age and size both within the limits of estimated object, and at adjacent territories. In case of absence of karst intensity data for estimated territory it is necessary to use the information obtained from the analogue site having preliminarily proved their similarity by the basic conditions of karst development.

The general formulas for estimation of total and specific (over area) karst economic risk of the losses caused by destruction or damage of the typical objects by karst hazard – C of the certain size, look as follows:

$$R_e(C) = P^*(C) \cdot P_s(C) \cdot V_e(C) \cdot D_e, \quad (2.1)$$

$$R_{se}(C) = R_e(C) / S_e, \quad (2.2)$$

where $P_s(C) = S/S_t$ – geometrical probability of destruction of estimated object by hazard C in space, $V_e(C) = D_d/D_e$ – economic vulnerability of estimated object for hazard C, calculated or determined by analogy, D_d is the cost of reconstruction of the destroyed object, D_e is the cost of object before destruction (\$), S_e and S_t are the area of object and estimated territory (m^2 , hectare, km^2) respectively.

If the object of estimation coincides in area with the territory, on which the hazard C can be manifested, probability $P_s(C)$ in formula 2.1 is equal to 1. The economic vulnerability is calculated separately for territories, various objects and structures, and is expressed as shares of physical and economic losses.

Karst social risk is determined as individual and total possible losses of the population with fatal outcome according to following formulas:

$$R_i(C) = P^*(C) \cdot V_s(C); \quad (2.3)$$

$$R_s(C) = R_i(C) \cdot D_p, \quad (2.4)$$

where $R_i(C)$ is the individual risk of population damage numerically equal to probability of such event for one person from group of people, which are located within the limits of estimated object (per./per.· year), $P^*(C)$ is the frequency of occurrence of hazard with certain sizes (cases / year), $V_s(C)$ is the social vulnerability of the population for hazard C , determined by computations (fractions of unit, f.u.), $R_s(C)$ is the total social risk of population damage from hazard C , equal to the number of fatal outcomes from this hazard within one year (per./year), D_p is the total number of people within the limits of estimated object (per.).

3 Regional Risk Assessment

The regional quantitative assessment of karst risk on a scale 1:50 000 – 1: 500 000 should include the following operations:

1. Identification of natural and technogenic conditions, factors of karst development on the basis of collecting and the analysis of all known materials on karst deformations in estimated and adjacent territories.
2. Spatial GIS analysis (MapInfo, in particular) allowing us to expand statistical bases of studied hazard, to define karst collapses, its sizes and relationship with geologic structures and geomorphologic elements, tectonic faults, economic objects.
3. Implementation of field researches at key sites with the purpose of specification or the establishment of the percent ratio of the total area of all registered surface karst forms to the site area (karstification coefficient), regularities and the age of karst deformations using radiocarbon, geologic, geomorphologic, pollen and other methods.
4. Zoning of the affected areas on regional-geological, zonal-climatic and technogenic factors of karst development and distribution on this basis of the data obtained at key sites over entire estimated territory.
5. Producing local assessment of karst hazard on key sites and then for entire estimated territory and tasks pointed in 1–3.
6. Typification of karst risk recipients with construction of corresponding map and assessment of its vulnerability to karst and karst-suffosion collapses and ground surface depressions of certain sizes.
7. Assessment, ranking and mapping of karst hazard as well as karst economic, social and individual risks of losses.

The karst hazard was estimated from the following modified formulas proposed by Ragozin (1994, 1998) for determining a degree of hazard or physical risk of area damage by single-moment natural processes of any genesis:

$$H(C) = R_f(C) = \sum_{i=1}^n P^*(C_i) \cdot S_i \approx S_c/t; \quad (3.1)$$

$$H_s(C) = R_{fs}(C) = R_f(C)/S \approx S_c/S \cdot t, \quad (3.2)$$

where $H(C)$ and $H_s(C)$ are the total and normalized (over area) karst hazards, which are identical to the total $R_f(C)$ and specific $R_{fs}(C)$, respectively, physical risks of damage by karst deformations ($m^2/year$ and $m^2/km^2 \cdot year$); $P^*(C_i)$ is the frequency of development of the i th-type karst forms (event/year); S_i is the average area destroyed by this deformation (m^2); S_c is the total area of karst deformations within the considered territory (m^2); t is the time interval of generation of these deformations (years); and S is the area of the considered territory (km^2).

Karst economic risk is the probabilistic index of karst collapse hazard evaluated for a certain object in the cost expression of its possible losses for a given time period. The specific losses of object reduced to a time unit (usually by one year) are referred to as name a total economic risk, and, in addition, normalized over area – specific economic risk (Ragozin 1994, 1998).

It is necessary to carry out estimation of karst total and specific economic risk according to the developed technique on the basis of the preliminarily determined square intensity of collapse formation ($m^2/km^2 \cdot year$) or karst risk of specific physical losses by the following formulas:

$$R_{fj}(C) = R_{fs}(C) \cdot S_j; \quad (3.4)$$

$$R_*(C) = R_{fj}(C) \cdot V_e(C) \cdot d_e; \quad (3.5)$$

$$R_{*s}(C) = R_*(C)/S_j, \quad (3.6)$$

where $R_{fj}(C)$ and $R_{fs}(C)$ are the karst risk of physical total ($m^2/year$) and specific ($m^2/km^2 \cdot year$) losses of the territory, respectively, within the j th risk recipient; S_j is the area of this recipient (km^2); $R_*(C)$ and $R_{*s}(C)$ are the total ($\$/year$) and specific ($\$/km^2 \cdot year$) karst economic risk respectively; $V_e(C)$ is the economic vulnerability of j th recipient of risk for karst failures (fractions of unit, f.u.); d_e is the density of national wealth within the limits of this recipient ($\$/km^2$).

Density of national wealth within the separate recipients of karst risk depends on cost of basic assets received from various departmental sources and the statistical databases. The value of economic vulnerability to karst failures of various size is determined separately for individual cities, settlements, agricultural lands, highways with a covering and without one, etc. Thus designed meanings of karst economic risk are applied at the final map. The fragment of this map for karst area of Republic Tatarstan (Russia) is presented in figure 1.

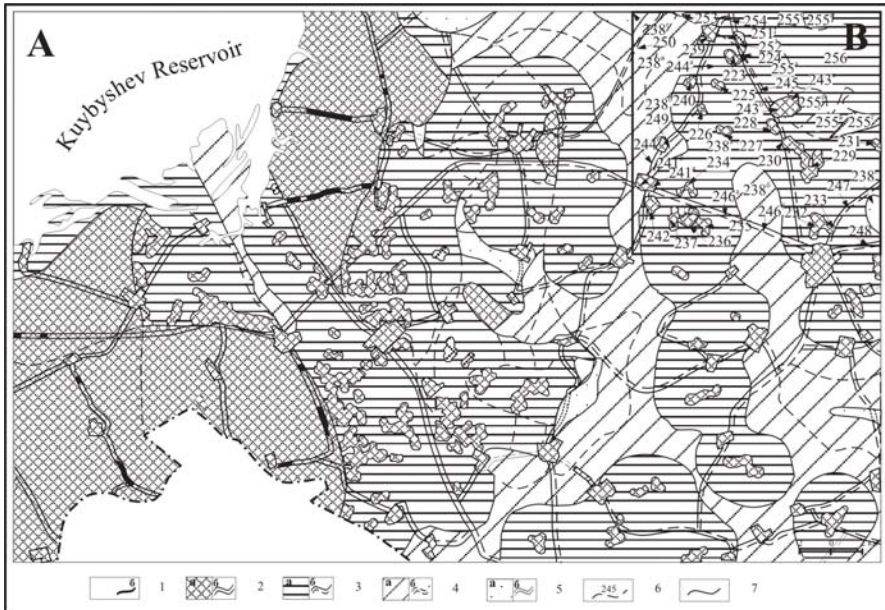


Fig. 1. Fragment of the map of karst economic risk of Republic Tatarstan at a scale 1:200 000 (schematized (A) and total (B) versions).

Karst economic risk in limits of square (a) and linear (b) objects ($\$/\text{year} \cdot \text{km}^2$): 1 – (1 - 0,1); 2 – (0,1 - 0,01); 3 – (0,01 - 0,001); 4 – (0,001 - 0,0001); 5 – (0,0001 - 0,00001). Boundaries: 6 – the second-order NTSs (and their numbers) with different square intensity of collapse formation, $\text{m}^2/\text{km}^2 \cdot \text{year}$; 7 – the second-order NTS groups of different economic karst risk categories.

Karst social or group risk is the probabilistic index of karst collapse hazard calculated for a certain population group in the zone of a possible karst deformation in the form of average annual losses of this group with different outcomes (death, injury, loss of health, moral injury, etc.), reduced, as in the assessment of economic risk, to one year. Thus, social risk reflects (in a form normalized in time) possible population losses due to karst collapses within individual areas of the considered territory. Such a risk directly depends on the group population permanently or temporarily located in the zone of possible destruction, which does not permit us to compare its values calculated, e.g., for different settlements. Therefore, Ragozin (1994) proposed a more indicative characteristic of the natural social risk - individual risk - for evaluating and subsequently mapping the degree of hazard caused by karst collapses and other negative natural and natural-technological processes. A karst or any other natural individual risk is calculated for a typical representative of a certain population group in the zone of possible destruction in the form of death, injury, or other negative outcomes during one year.

The social and individual risk of population damage by karst is evaluated during regional studies based on the preliminarily determined values of the collapse

formation square intensity and on the physical or economic vulnerability of risk recipients for karst deformations estimated from the following general formulas:

$$R_{fj}(C) = R_{fs}(C) \cdot S_j; \quad (3.7)$$

$$R_s(C) = R_{fj}(C) \cdot d_s \cdot V_t(C) \cdot V_s(C); \quad (3.8)$$

$$R_{si}(C) = R_s(C) / D_p, \quad (3.9)$$

where $R_{fj}(C)$ and $R_{fs}(C)$ are the karst risk of physical total ($m^2/year$) and specific ($m^2/km^2 \cdot year$) losses of the territory, respectively, within the j th risk recipient; S_j is the area of this recipient (km^2); $R_s(C)$ is the total social risk of population damage by karst with a certain outcome in the considered area (persons/year); d_s is the population density in this area (persons/ km^2); $V_t(C)$ is the population vulnerability to karst collapses in time on this territory (in and outside buildings and structures, on roads, etc.) (fractions of unit, f.u.); $V_s(C)$ is the population spatial vulnerability to karst collapses within the same risk recipients (f.u.); $R_{si}(C)$ is the karst individual risk of population damage with a certain outcome in the considered territory within the same risk recipients (persons/persons-year); and D_p is the population amount in this territory (persons).

4 Conclusion

The presented technique of local and regional assessment of karst risk allows us to obtain forecast meanings of possible losses in various spheres and to elaborate on this basis scientifically proved decisions on reduction of negative consequences from the development of karst and karst-suffosion processes. Among poorly developed questions it is necessary to point the procedure of vulnerability estimation of various recipients, including people to karst deformations of different intensity that requires performance of additional research on the basis of scenario modeling.

References

- Makeev ZA (1948) Principles of engineering geological zoning of karst regions. In: Molotov Conference on Karst (Molotov State Univ.), pp 4.
- Ragozin AL (1994) Basic principles of natural hazard risk assessment and management. In: Proceeding Seventh International Congress International Association of Engineering Geology. Rotterdam: Balkema, vol III, pp 1277-1286.
- Ragozin AL (1998) Theory and practice of geological risk assessment and management. In: Proceedings Eighth International Congress International Association for Engineering Geology and the Environment. Rotterdam: Balkema, vol II, pp 879-886.
- Savarenskii IA, Mironov NA (1995) Handbook of engineering geological survey in karst regions. PNIIS, Russian Committee on Construction. Moscow.

- Tolmachev VV (1980) Probabilistic approach to the stability assessment of karst regions and anti-karst designing. *Engineering Geology* 3: 98-107.
- Reuter F, Stoyan D, Oleikewitz P (1981) Einsatz mathematisch – statistischer Methoden zur Beschreibung von Gesetzmässigkeiten in Gebieten des Sulfat und Chloridkarstes. *Neue Bergbautechnik* H. 10.
- Hu RL, Yeung MR, Lee CF, Wang SJ, Xiang JX (2001) Regional risk assessment of karst collapse in Tangshan, China. *Environmental Geology*, vol 40, pp 1377-1389.
- Lei M, Jiang X, Yu L (2002) New advances in karst collapse research in China. *Environmental Geology*, vol 42, pp 462-468.

Cut-and-Cover Tunnel below Boulevard River Meuse, Maastricht, The Netherlands

Joost S. van der Schrier and Rijk H. Gerritsen

Royal Haskoning, Postbox 151, 6500 AD Nijmegen, The Netherlands
j.vanderschrier@royalhaskoning.com
Tel: +31 24 328 46 57
Fax: +31 24 360 96 35

Abstract. Paper describes the geotechnical risks and soil investigations related to design and construction of the cut-and-cover tunnel below the western boulevard of the river Meuse in Maastricht, the Netherlands. Relevant soil investigation results are shown and discussed in relation to the risks addressed. The quantification of the risks involved has led to a clear contract basis and resulted in transparency concerning pricing and project costs.

Keywords: Cut-and-cover tunnel, geotechnical risk assessment, limestone, de-watering, soil and rock mass properties, diaphragm walls, contracting, Meuse, Maastricht, Netherlands.

Introduction

In 2003 the construction of a cut-and-cover traffic-tunnel below the western boulevard of the river Meuse has been completed successfully. The construction of this tunnel was considered necessary to make the boulevard free of traffic and to provide direct access to the underground parking and floors of the adjacent shopping/office building currently under construction. The local site geology is dominated by limestones overlain by a 10 to 15 m thick layer of recent coarse-grained river deposits. These limestones consist mainly of Calcarene, but are known to include also hard grounds and flint layers. The combination of the highly permeable river deposits with the nearby river Meuse and the presence of detrital limestones, possibly containing hard-grounds and flint, were considered to pose specific risks to the project. These risks concern the de-watering of the site and the constructability of the building pit, including the excavation process and the installation of the diaphragm walls. An early quantification of the risks was considered necessary from both, a technical and financing point of view. Design considerations, the (specialised) site and laboratory investigations, and contractual implications (risk) are discussed from an engineering geological point of view.

Project Description

The Wilhelmina Bridge crosses the river Meuse almost perpendicularly and enters straight into the hearth of the city Maastricht (Figure 1).



Fig. 1. River Meuse, Maastricht. Bird view on the western Meuse boulevard (situation before construction of the cut-and-cover tunnel). The Wilhelmina Bridge is located north (right on the picture), the St.-Servaas Bridge is located south (left).

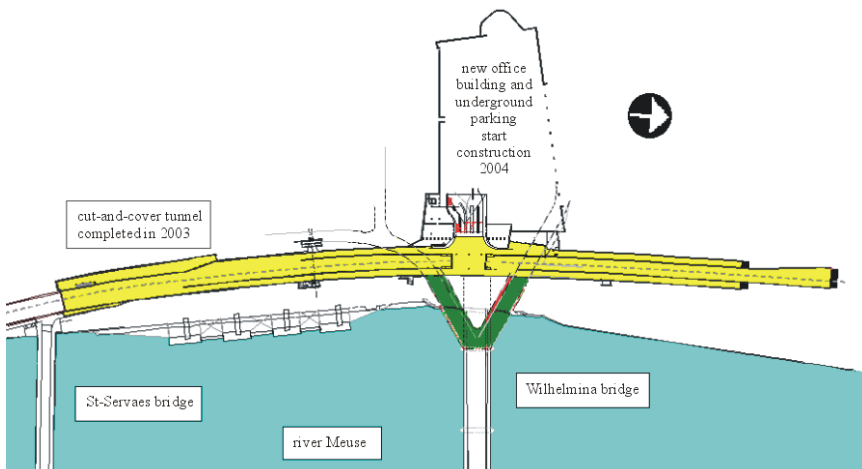


Fig. 2. Cut-and-cover tunnel, new office building/underground parking, and reconstruction of the western abutment of the Wilhelmina Bridge.

The cut-and-cover tunnel passes the Wilhelmina Bridge underground, frees the Meuse boulevard from traffic (attractive from a tourist point of view), and provides on its deepest point underground access to the car-parking and supply facilities of a 'new office building'. The "new office building" that will be constructed in 2003-2004 is located directly in front of the Wilhelmina Bridge, enforcing the reconstruction of the western abutment (Figure 2).

The tunnel is constructed in a building pit supported by soil retaining diaphragm walls. These walls were extended in to the relatively impermeable limestone, thus cutting off the (very) permeable coarse grained river deposits, preventing direct inflow of water from the river Meuse (Figure 3).

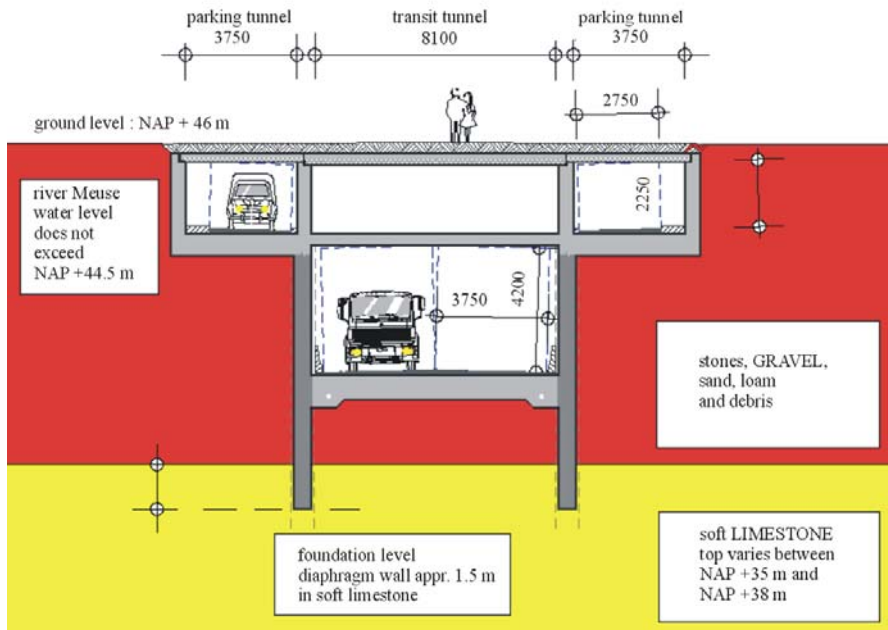


Fig. 3. Cut-and-cover tunnel, typical section. Measures in mm.

Geotechnical Risks and Site Investigations

The type and extent of the site investigations were optimised based on an interdisciplinary risk assessment (Gerritsen, 2001). The results, focussing on geotechnical risk, are given in Table 1.

Based on the outcome of the risk-assessment (Table 1), it was decided to focus the site investigations mainly on:

- The presence of debris and old construction works in the top of the soil profile (manipulated by human action);
- The particle distribution of the coarsely grained river deposits, particularly the amounts of fines (to great extent determining the formation's permeability), and the presence of large stones/boulders (from natural origin);
- The flow-velocity through the coarsely grained river deposits during periods of large river discharge;
- The location of the top of the limestone and its mass properties, including strength, permeability of the limestone (primary and secondary) and the possible presence of hard-grounds and/or flint layers.

Table 1. Risk bearing elements (from a geotechnical point of view).

Stage/process	Event	Possible consequence
Excavation.	Wrong choice excavation equipment (bucket, cutter wheel, etc.), unable to penetrate properly (due to presence large stones, hard bands, flint). Obstruction of building process by debris and/or old construction works.	Excessive wear (delay). Slow progress (delay). Hole instability (damage), caused directly or indirectly (by loss of mud/support pressure).
Excavation.	Large (water) flow velocities in coarsely grained river deposits during periods of large river discharge.	Hole instability (damage).
Excavation.	Instability of bottom building pit due to high pore pressure in water bearing layers /discontinuities (uplift).	Too large de-watering quantities (costs and permits).
Support (excavation front).	No mud-cake, loss of mud, lack of support pressure, de-flocculation (by chemical reaction), due to composition excavated soil (chemical components and/or grain size distribution).	Hole instability, collapse of excavation front, settlements, (damage).
Foundation.	Too low strength and/or stiffness of the (top of) the soft limestone e.g. due to excessive weathering.	Foundation failure (bearing capacity insufficient or too large deformation).
Building pit and/or de-watering.	Too large amounts of seepage e.g. due to water bearing faults crossing tunnel alignment (soft limestone) or due to a too shallow penetration of diaphragm wall into soft (relatively impermeable) limestone (due to large variations in bedrock depth or by large deviations from the predicted (mass) permeability.	Legal objections, e.g. permits not valid (anymore) or not present. Additional deep-well(s) required. Displacement of near by (present) pollution(s) due to the de-watering in too large quantities. Under-water concrete required.

Debris and Old Construction Works

Archive research revealed that the remains of old canal works could be present, almost coinciding with (parts of) the alignment (Figure 4).

Their potential location has been investigated by archive and field research (trial ditches to confirm field dimensions) and were plotted on a 'risk map' (part of the Tender documents). The alignment was fixed, taking into account other (restricting) boundary conditions, trying to avoid old construction works (quay walls, bridge foundations, sewage systems, etc.) as good as possible.

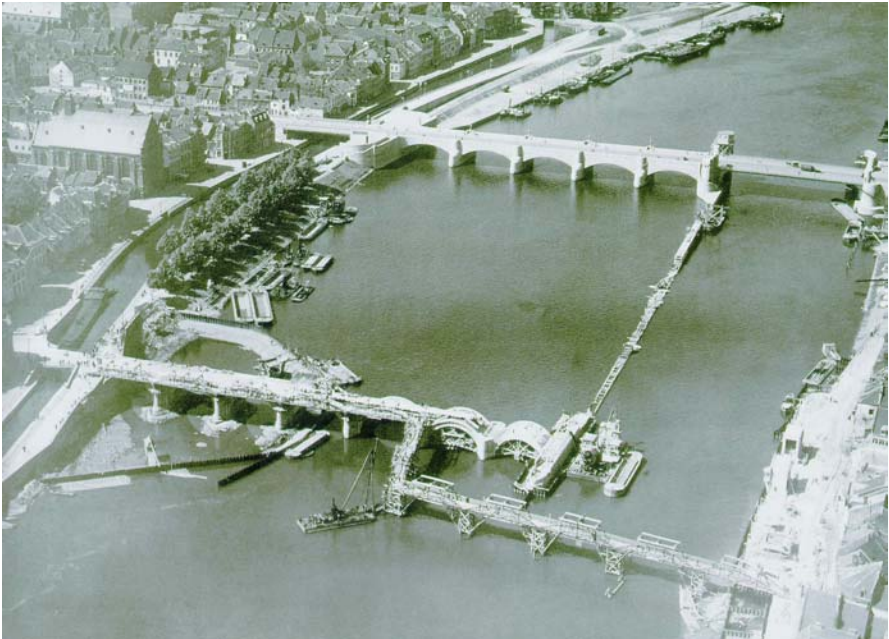


Fig. 4. Former lateral canal (filled early in the 20th century), located somewhere in the tunnel alignment.

Particle Distribution Coarse River Deposits

The particle distribution of the coarsely grained river deposits is considered of great importance in view of the constructability of the diaphragm wall. A too coarsely grained material, specifically if it includes big stones and large boulders, would hinder the excavation process. An open particle structure, combined with too large particle sizes, could hinder the formation of a proper mud-cake (with or without additives). Consequently, the lacking of a proper support pressure would endanger the stability of the excavation front. Finally, the replacement of mud by

concrete could become difficult, adversely affecting the wall's (structural) quality. Granular analyses on remoulded bulk samples of granular material, obtained by pulse boring, indicated initially that the amounts of fines would be relatively limited. Whether the first samples taken were representative was, however, doubted because of the difficulties encountered during sample taking (washing out of fines, length of core runs and debris). Eventually, representative (remoulded) soil samples could be obtained, but only after the implementation of special precautions to avoid "loss of fines", and by a careful collection of all materials sampled per metre progress and per change of soil layer (if any). Although, no indications were obtained pointing to the presence of large stones and boulders in the project area, their presence could not be excluded on basis of the bore campaign. Consultancy of TNO-NITG (Gruijters, 2001) revealed that the gravel formation encountered in the project area belonged to the Formation of Beegden (layer Oost Maarland) that usually contains 0 to 5 % silt, 10 to 15% sand, and 80 to 85 % gravel (classified according to NEN 5104). It was noted also that exceptions on these "regular rules" could be expected. In specific areas (but limited in size), part(s) of the sand fraction could lack. Furthermore, layers could be present at various levels in the formation with a relatively good gradation but containing mainly the coarser particle sizes of the spectrum. Finally, some layers (though relatively limited in number) could contain over 80 % of coarsely grained material (> 31.5 mm), but would be limited in thickness (< 0.5 m). On basis of the data available in the TNO/NITG database envelopes were constructed showing outer boundaries (with a certain probability to be exceeded) for possible gradation curves (Figure 5).

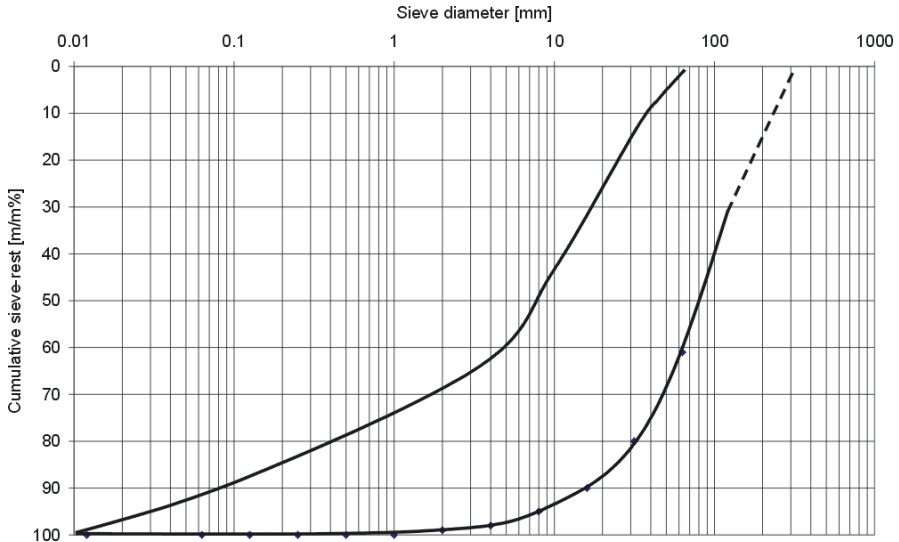


Fig. 5. Envelope of possible grain distributions of the coarsely grained river deposits of the Formation of Beegden, based on available sample material. Dashed boundary is uncertain due to sampling limitations and hence the number of observations available (Gruijters, 2001).

These envelopes specific for the project area were included in the Tender documents. The probability that 'real big boulders' (diameter > 600 mm with volumes larger than 1 m³) would be encountered, was considered small in view of their origin (ice rafted sediments), but should be considered in the Tender documents as their presence could not be excluded.

Flow through Coarsely Grained River Deposits

To monitor the relationship between the groundwater table and the water table of the river Meuse, five standpipes were installed with electronic data-loggers for a period of 3 years. The measuring frequency was set at 48 measurements each day in order to obtain a representative recording of the changes of the piezometric head relative to the change of the river level. Measured groundwater levels were linked to recorded river levels up and downstream. The measurements revealed that the water infiltrates at high river levels and at low river levels. The latter occurs because the water is kept high by the weir Borgharen. The water level in the project area responded with some delay. A response factor of 0.6 was calculated proving an 'infiltration resistance' being present due to river bottom sediments and quay structures along the river. High flow velocities through the coarsely grained river deposits were considered possible at large river discharges (possibly resulting in loss of bentonite and/or instability of excavation trenches). To assess flow rates in the coarsely grained river deposits measurements have been carried out with the Geoflo™-system (Telkamp, 2001). With this method, both the ground water flow and the direction of flow can be determined in a special standpipe filter of 4-inch diameter. The measurements were taken at several depths. Flow velocities of 0.9 to 3.0 m/day have been recorded. The above-mentioned risk concerning the stability of the excavation trench was considered acceptable (also because generally large amounts of fines were encountered in the soil samples).

Mass Properties Soft Limestone

The strength and stiffness of the soft limestones were considered of interest in view of the bearing capacity of the diaphragm wall. However, the permeability of the limestone formation (primary and secondary) was considered the main parameter, together with the possible presence of hard-grounds and/or flint layers.

Too large formation permeability would lead to excessive seepage into the building pit, limiting the possibility to de-watering the building pit with deepwells and/or drains with pumps. The quantities would be come too large from both economic and environmental point of view. The alternative however, being the constructing of an 'underwater concrete floor' to seal the bottom (including installation of tension piles), would be very expensive. The presence of hard-grounds and/or flint layers would hinder the excavation process. Literature review revealed that the permeability of the limestone could vary between 10⁻² and 10⁻⁴ m/day, if determined on fresh limestone cores, and between 1 m/day and 10 m/day in-situ,

depending on the degree of weathering and/or the characteristics of discontinuities present. At the other hand, if water-bearing tectonic faults or discontinuities or permeable sub-layers (flint) would be present, locally large flow quantities could be expected (Gerritsen, 2001). The limestone was found to be relatively homogeneous, only in the top a yellow colour was observed, indicating oxidation by water comprising relatively large amounts of oxygen. This yellow colour was interpreted as proof for weathering in the top layers of the soft limestone encountered. The eroding action of river water flowing through the coarsely grained river deposits, specifically at times of large river discharges, could have affected the particle bonding (due to cementation) and could have taken away the smallest particles ($< 1\mu\text{m}$), leaving a relatively permeable top layer (Felder, 2001). The in-situ permeability was assessed, using rising head, falling head, and constant head tests. The interpreted results indicated an average value, valid for the project area, equal to 2.5 m/day. The maximum value was assessed at 3.2 m/day. On basis of the observations done it was concluded that the building pit could be de-watered economically without taking excessive risk. A 'fall-back scenario', however, including possible dividing in compartments of the building pit and (limited) use of under-water concrete was developed in parallel.

Classification of the limestone appeared possible based on a careful examination of fossils present. The Nekum limestone appeared to dominate the project area. Only in the southern part of the building pit, Emael limestone was encountered in the top of the profile, but limited in thickness. In the northern part of the building pit the Emanuel limestone crops out, separated from the Nekum limestone by the well-known marker layer 'horizont of Laumont', which was encountered in a number of boreholes. From this 'horizont of Laumont' it was observed that the stratigraphy dipped slightly North-west with a dip angle between $1^{\circ}15'$ and $1^{\circ}30'$. From a structural point of view, tectonic faults (if any) and joints were expected to be the dominant features. Based on the stratigraphy encountered it was concluded that the probability that a tectonic (water bearing) fault would be present was very small (Felder, 2001). The occurrence of such a fault was excluded in the Tender documents.

Various laboratory tests were carried out on cored sample material (Fig. 6). The tests focussed specifically on the top layer of the limestone encountered. From the detailed descriptions of the different geological formations, it was concluded that the probability of hard-grounds and/or flints being present in the top 2 m of the limestone would be limited. For tender purposes, the volume of flint and their expected size in the limestone of Nekum were limited to $< 1\%$ and $< 0.03\text{ m}^3$ respectively on basis of the observations done. For the limestone of Emael these numbers are 5% and 0.3 m^3 respectively.

The potential of the limestones to de-flocculate the bentonite slurry used during construction was checked; proposed support mud(s) appeared to remain stable if subjected to limestone samples.

Strength and stiffness were determined by unconfined compressive strength (UCS) tests and by pocket penetrometer tests (the latter providing the possibility to assess strength quickly and on irregular lumps). The relation between the pocket penetrometer tests and UCS is studied at the TU-Delft (Verwaal, 2001).

Relevant test results are summarised in Table 2. In order to get insight in the ‘re-moulded strength’ of the soft limestone, should it act as a granular material due to lack of bonding, direct shear box tests were carried out on disintegrated/granular limestone samples as well. All drained friction angles recorded, mobilised at peak strength, exceeded 35° (with a cohesion 0 kPa).



Fig. 6. Sample (core) box showing limestone of Emael. Length core box equals approximately 1 m.

Table 2. Material properties Maastrichtian limestone, grouped per member (Verwaal, 2001).

<i>formation member</i>	ρ -bulk <i>Mg/m³</i>	ρ -dry <i>Mg/m³</i>	w %	UCS <i>MPa</i>	<i>P-index</i> -	<i>E-50</i> <i>GPa</i>
Emael (sample 1)	1.79	1.30	37.6	0.44	2.51	0.05
Emael (sample 2)	1.54	1.27	21.9	2.74	> 8.0	0.73
Emael (sample 3)	1.71	1.31	30.0	0.89	3.55	0.25
Nekum (sample 1)	1.77	1.37	29.6	1.31	5.80	0.41
Nekum (sample 2)	1.68	1.25	34.1	0.88	5.32	0.29
Nekum (sample 3)	1)	1)	26.9	0.98	2.98	0.08
Nekum (sample 4)	1.80	1.34	33.8	1.16	2.88	0.18
Nekum (sample 5)	1.73	1.33	30.0	0.75	4.85	0.10
Nekum (sample 6)	1.72	1.42	21.1	1.40	6.66	0.46

ρ -bulk : bulk density at moment of testing [Mg/m^3]

ρ -dry : dry density [Mg/m^3]

w : water content (by weight) [%]

UCS : unconfined compressive strength [MPa]

P-index : Pocket penetrometer value (average value of 2 to 7 observations) [-]

E(50) : Tangent modulus of elasticity determined at 50 % of peak strength [GPa].

Conclusions

For the design of the cut-and-cover tunnel below the river Meuse, several risks were evaluated. The risks addressed resulted in a site investigation programme, suited for the purpose that succeeded in the quantification of the geotechnical risks addressed for tender purposes. Risks involved were shown clearly in the Tender documents. The reference values for the various geotechnical parameters, as published in the Tender documents, provided a clear contract basis, resulting in transparency with respect to pricing and project costs. The project has been completed successfully in 2003.

Acknowledgement

The authors thank all parties involved for their valuable contributions. Their help was of great importance for the proper assessment of the (geotechnical) risks involved.

References

- Felder W.M. (2001), Rapport betreffende het onderzoek uitgevoerd ten behoeve van het Markt-Maas project te Maastricht, Vijlen.
- Gerritsen R.H., Van der Schrier J.S. (2001), Besteksontwerp, Rapport geotechnische aspecten, Tunnel onder de Maasboulevard, Markt-Maasproject gemeente Maastricht, Haskoning, Nijmegen.
- Gruijters S.H.L.L (2001), Briefrapportage beschrijving grindformatie Maastricht, Nederlands Instituut voor Toegepaste Geowetenschappen TNO, Nuenen.
- Telkamp B. (2001), Grond(water) onderzoek en laboratoriumonderzoek betreffende Markt-Maas project te Maastricht, Fugro.
- Verwaal W. (2001), Bepaling geotechnische eigenschappen boringen Markt-Maasproject, Laboratorium Ingenieursgeologie, Technische Universiteit Delft.

The Geotechnical Baseline Report as Risk Allocation Tool

Martin Th. van Staveren and Johan G. Knoeff

GeoDelft, Stieltjesweg 2, 2628 CK Delft, The Netherlands
{m.th.vanstaveren, j.g.knoeff}@geodelft.nl
Tel 0031 (0)15-2693583
Fax 0031 (0)15-2610821

Abstract. Today, timely and adequate attention for the risky subsoil is more than ever necessary for a healthy European infrastructure industry. A key success factor for effective risk management is the contractual allocation of risks arising from differing subsoil conditions. Since 2000, the Geotechnical Baseline Report (GBR) is applied in a number of Dutch infrastructure projects. The main objective of the GBR is to provide a clear contractual arrangement for the allocation of the risks arising from differing site conditions.

The underlying philosophy of the GBR is a contractual statement, which is part of most United States, UK, Dutch and probably other European building contracts. It states that the owner is ultimately responsible for any soil conditions, which are materially different from the anticipated soil conditions in geotechnical reports. This philosophy raises the question about what soil conditions are materially different. The GBR provides the answer to that question, by serving contractual definitions of the anticipated soil conditions. These soil conditions can be contractually defined by geotechnical subsoil profiles or geotechnical baseline parameters.

This paper describes the process to draw a GBR. A risk analysis results in the definition of appropriate contractual baseline parameters. These baselines are the borderlines between the subsoil responsibilities of owner and contractor. The benefits of the GBR will be illustrated by an example from a recent Dutch infrastructure project.

Keywords: geotechnical monitoring, risk management, geotechnical baseline report.

1 Introduction

The dark and unknown subsoil is still a serious risk factor for many infrastructure projects. The subsoil will literally make or break a project. In the Netherlands only, failure costs in the entire construction industry are assessed at 3.5 billion euro per year. In the infrastructure segment the failure costs are assessed at 800 million euro per year (SBR 2003). Given the prominent role of the subsoil in infrastructure projects, ground-related failure costs will be at least several hundreds of million euro per year, in the Netherlands only. For instance, in the Dutch pile driving industry failure costs are assessed at 100 million euro per year. Extrapolating these figures to a European scale results into ground-related failure costs of at least a few billion euro per year.

Project	Overrun	
	Planning	Costs
Ramspol inflatable dam	+ 80 %	unknown
Tramtunnel The Hague	+100 %	+ 90 %
Stormsurge barrier Nieuwe Waterweg	+ 50 %	+ 40 %
Betuweroote freight railway	unknown	+ 65 %
Splay railway Amsterdam – Utrecht	+ 65 %	+ 25 %

Fig. 1. Planning an cost overruns of a selection of Dutch infrastructure projects.

Figure 1 presents a table with a number of Dutch infrastructure projects and their overrun of planning and costs (Molendijk and Aantjes 2003)

Many infrastructure projects run out of time and/or budget, because of unforeseen behaviour of the subsoil. This situation is not limited to the Netherlands. Numerous case histories examine that for over a century there has been a repetition of common reasons, which have led to failure to anticipate geological conditions. This in turn has led to project failures (Fookes et al 2000). In other words, differing site conditions of geological origin are a main source of construction risk and associated problems in the construction industry.

What are exactly differing site conditions? Many standardised contract models, such as the international FIDIC and the Dutch UAV have a so-called differing site conditions clause. In the Unites States of America two differing site conditions are defined in the Federal Differing Site Conditions Clause of 1984 (Essex 1997):

- subsurface or latent physical conditions, which differ materially from those indicated in the contract
- unknown physical conditions at the site, of an unusual nature, which differ materially from those encountered and generally recognized as inhering in work of the character provided in the contract.

With such a definition contractual arrangements appear to be very clear about which party is responsible for unforeseen ground conditions. But guidelines about *what* ground conditions are to be considered as “materially different” and of a “unusal nature” are often quite vague or even lacking at all. Far too many are the worldwide examples of projects with serious and unfavourable disputes about differings soil conditions (figure 2). The US National Committee on Tunneling technology reported that low level subsurface site investigations led to differing site conditions claims averaging 28 % of the contract price (Smith 1996).

2 The Geotechnical Baseline Report

The presented difficulty with differing site conditions is not new at all. The first Differing Site Conditions Clause was already defined and approved by the President of the United States itself in 1926 (Essex 1997). However, in spite of this clause and its updates over time the effects of disputes about differing site condi-

tions on the construction industry increased to an unacceptable high level. Already thirty years ago, in 1974, was mentioned that this type of claims would be a serious threat to the health of the entire construction industry (Douglas 1974).



Fig. 2. Differing site conditions? Who pays?

In order to stop this unfavourable development the Technical Committee on Geotechnical Reports of the Underground Technology Research Council of the United States developed the concept of the Geotechnical Baseline Report (GBR) in the nineteen nineties. It describes basically what type of site conditions are materially different, by the definition of baselines for the key risk factors in the subsoil. Risks associated with conditions consistent with or less adverse than the baseline are allocated to the contractor. Those risks more adverse than the baselines are accepted by the owner. A GBR should have the status of contract document.

3 The Geotechnical Baseline Report in the Dutch Practice

In 2000 GeoDelft, the Dutch knowledge institute on geotechnics, introduced the concept of the Geotechnical Baseline Report in the Netherlands. Simultaneously, the GBR concept was applied in a number of Dutch infrastructure projects, such as the underground NorthSouth lightrail in the Dutch capital of Amsterdam and the expansion of the sluices of IJmuiden. This approach resulted in an interactive innovation proces on subsoil risk allocation, together with the Dutch construction industry. The experiences with the GBR in these projects are published by Herb-schleb et al (2001) and Van Staveren and Litjens (2001) respectively.

During a workshop in 2001 at GeoDelft in Delft, The Netherlands, more than 40 representatives of owners, engineers, contractors and lawyers concluded jointly that the concept of the GBR fits into the Dutch contracting practice, for both traditional contracts and more innovative contracts, such as Design, Build and Maintenance (CROW 2002).

In spite of this promising first results, the GBR is not yet completely accepted and implemented in the Dutch and international practice. While geotechnical experts as Morgenstern (2000), Clayton (2001) and Knill (2003) advocate the importance of geotechnical risk management and a geotechnical benchmark or baseline approach in particular, others like Hatem (1998) doubt whether the baseline concept is fruitful at all.

Although clear guidelines for preparing a GBR are presented by the American Society of Civil Engineers (Essex 1997), the recent Dutch experiences learn that there is a demand for “know how” about the Geotechnical Baseline Report. For this reason GeoDelft developed a model with number of steps to arrive at a GBR. In this paper this model is presented, together with a case study to demonstrate the effectiveness of the model.

4 The 5 Steps to Write a GBR

In the next section the process to write a GBR is presented by 5 steps:

- Step 1 – Description of the project
- Step 2 – Inventarisation of project risks
- Step 3 – Qualification of project risks
- Step 4 – Allocation of project risks
- Step 5 – Writing a GBR

This 5 steps process is illustrated by an example, the broadening of a highway in the Netherlands. The example is real project, but for this paper simplified and schematised.

4.1 Step 1 – Description of the Project

In the first step all relevant information is collected in order to make a complete inventarisation of the project risks. The objectives of the project in terms of time, money and quality become clear. At the end of the first step it is known for which parts of the project a GBR has to be written. The following information is needed:

- Project objectives;
- Project history;
- Project phases;
- Project organisation;
- Reference projects;
- Geological and geotechnical information from literature and existing field tests.

Example

Rijkswaterstaat, part of the Dutch Ministry of Public Works, is planning to broaden the motorway A2 from 4 to 6 lanes between the junctions Everdingen and Empel. In this section, the highway crosses the Diefdijk, a primary water retaining structure which reduces the inundation damage after a collapse of a main river dike. This structure has to be renewed. Along the highway a traffic noise barrier will be build.

A GBR has to be written in order to handle the risks dealing with the broadening of the highway. The reconstruction of the water retaining structure and construction of the noise barrier is not incorporated in the GBR. The next information was available for the GBR:

- *Project description (inclusive phasing and organisation)*
- *results of 36 CPT's*
- *15 oedometer tests (5 steps,*
- *16 triaxial tests (CU, single stage)*
- *maps with groundwater tables*
- *experience from reference projects*

4.2 Step 2 – Inventarisation of Project Risks

The next step in the GBR proces is the inventarisation of the (main) factors which may influence the project objectives in a positive or negative way. Especially for large projects, these factors are not always clear. An inventarisation can be done using:

- Evaluating experiences;
- A brain storm session;
- A qualitative risk analysis.

Ordinary risks managed with normal quality systems are not inventarised, in order to limit the number of reasonable risks.

4.3 Step 3 – Qualification of Project Risks

In order to determine whether risks are acceptable or not one has to qualify the project risks. This is possible by qualifying the probability of occurrence and consequences after appearance. A simple method is by summarizing and scoring the different 'risk' components of probability of occurrence and consequences (see example in figure 3).

For each project specific criteria for the risk scores can be defined.

Continuation of Example

The geotechnical risks were collected by checklists and evaluating experiences. In a meeting with the client - owner, Rijkswaterstaat, the following items were jointly considered as dominant project risks with a geotechnical cause:

Probability of Risk occurrence	Low risk score	High risk score
Knowledge	Little to none	Much to intermediate
Period	< 3 Months	> 3 Months
Way	With indications	Without indications
Risk consequences		
Time	< 1 Month	> 1 Month
Money (budget)	< 50,000 Euro	> 50,000 Euro
Quality, safety, image	Risk consequences are acceptable	Risk consequences are not acceptable

Fig. 3. Method for qualification of project risks.

1. Large settlements after the road comes into service
2. Problems by driving piles into the ground
3. Instability of the embankment
4. Settlements of the present highway
5. Uncertainty of water pressures
6. Slow long term settlements
7. Influencing existing objects along the highway
8. Unequal settlements

These risks are qualified in the way as described above. The results of the qualification of the project risks are given in figure 4. Relative ‘large’ risks can be found in the upper right corner. ‘Small’ risks are situated in the lower left corner. It is important that the client recognises and agrees on the main (geotechnical) project risks. Therefore a meeting was organised at the end of step 3.

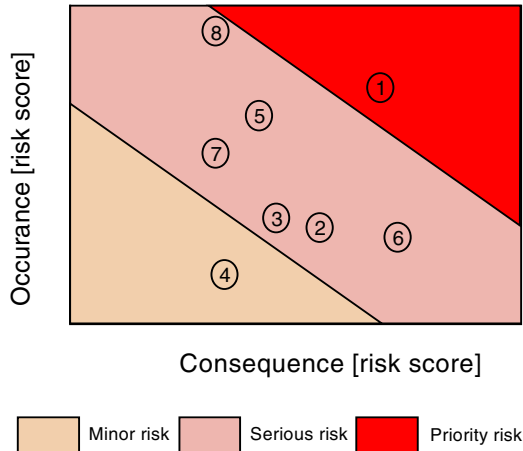


Fig. 4. project risks for the A2 highway.

4.4 Step 4 – Allocation of Project Risks

This step forms the heart of the GBR. Geotechnical mechanisms which determine the project risks are analysed in this step. Key risk drivers and baselines are chosen. A key risk driver is a main and measurable geotechnical aspect or parameter which determines or “drives” the project risk. The baselines are the numerical parameters of the key risk driver to allocate project risks.

The baselines can be determined during a meeting. The client has to make clear which risks he is willing to accept. The geotechnical experts translate this ‘risk’ profile into baselines for the project risks.

Sometimes additional measures have to be taken in order to reduce the risks, for example additional site investigations and monitoring during construction. An example for the baselines of the key risk driver consolidation coefficient, which determines the rate of settlements, is given in figure 5.

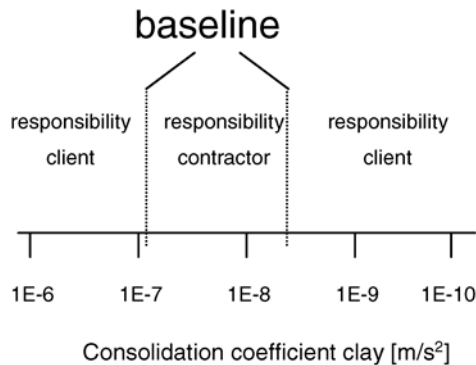


Fig. 5. Key risk driver consolidation coefficient.

Continuation of Example:

The main project risk is unacceptable settlements after the road comes into service (see figure 5). This risk is analysed by considering the subsoil profile and the settlement and consolidation process. Key risk drivers are the thickness of the soft soil layers, the compression parameters and consolidation coefficients of the soft soil layers.

Baselines are derived from the results of the cone penetron tests (CPTs) and oedometer tests. The baselines for the compression parameters (calculated by the method Buisman-Koppejan) are the 5% upper and lower limit of the results of oedometer tests. The baseline for the thickness of the soft soil layers is the layer thickness (+/- 0.5 m), which is established by a geologist from the geological profile. The baselines for the compression parameters and consolidation coefficient are presented in figure 6.

	C_p	C_s	C_p'	C_s'	OCR	c_v
Clay	20.2-34.9	71.1-163	12.1-16.6	37.9-68.1	1.1-1.2	$3.2E^{-8}$ - $1.3E^{-7}$
Peat	13.3-21.6	34.3-85.6	5.4-9.1	13.7-26.9	1.2-1.3	$6.2E^{-8}$ - $1.2E^{-6}$

Fig. 6. Baselines intervals for the large settlements risk after the road comes into service

The GBR principle works as follows in practice. In case unacceptable large settlements occur after the road comes into service, the contractor is responsible for the consequences, if the key risk drivers soft soil layer thickness and the compression parameters and the consolidation coefficient is in between the jointly agreed baselines. If this is not the case, if one of the key risk drivers is outside its baseline interval, the client has to deal with the consequences. In summary, if too large settlements occur due to differing soil conditions, it is now univocal who is responsible and which party has to pay additional costs and measures.

4.5 Step 5: Writing a GBR

The final step in the GBR process is the reporting phase. In this phase, the results of the other steps are written down in a contractual document. With this document it is clear who is responsible for unexpected events dealing with the subsoil. During the construction of the project, the GBR is an effective prevention against time consuming and expensive legal and claim procedures.

5 Conclusions

The GBR is a 'simple' method to allocate geotechnical project risks within a construction contract. With the presented method it is univocal who is responsible and who has to pay for additional costs and measures, in case of unexpected events due to differing soil conditions. Since 2001 the GBR is successfully used in several large and smaller Dutch infrastructure projects. The GBR creates more risk awareness and contractual transparency about the subsoil. Currently, due to market questions, possibilities are investigated to allocate also non-geotechnical risks with the GBR method, such as the presence or traffic intensities or the presence of unknown objects below the surface.

European infrastructure projects are often very large, complex and dealing with a lot of interests. Therefore it is difficult to inventarise and manage the project risks effectively. It is believed that the Geotechnical Baseline Report is a promising tool for effective the allocation of (geotechnical) project risks between owner and contractor. With a well defined GBR the opportunity increases, to realize a high quality project in time and within budget. If the GBR becomes a true document for contract negotiation in the future, reduction of costs might even be possible, due to an increase in effective subsoil risk management. As a consequence, reputation of both, client and contractor, will be established.

Acknowledgements

Special thanks go to the Directie Oost-Nederland of the Dutch Public Works Department Rijkswaterstaat, for the permission to use the case in this article.

References

- Clayton CRI (ed) (2001) *Managing geotechnical risk: Improving productivity in UK building and construction*. The Institution of Civil Engineers, London, 80 p.
- CROW (2002) *Toepassingsmogelijkheden van het Geotechnisch Basis Rapport binnen UAVgc contracten*, CROW report.
- Douglas WS (1974) Role of specifications in foundation construction *Journal of the Construction Division ASCE*, vol 100, CO2: 199-201.
- Essex RJ (ed. (1997) *Geotechnical baseline reports for underground construction*. Technical Committee on Geotechnical Reports of the Underground Technology Research Council, American Society of Civil Engineers, 40 p.
- Fookes PG et al. (2000) Total geological history: A model approach to the anticipation, observation and understanding of site conditions. In *Proceedings EngGeo 2000*, Sydney, Australia.
- Hatem JH (ed) (1998) *Subsurface conditions: risk management for design and construction management professionals*. John Wiley & Sons Inc, New York, 454 p.
- Herbschleb et al. (2001) De Noord/zuidlijn: geotechnische risicoverdeling met het geotechnisch basis rapport. *Geotechniek* 5:83-88.
- Knill J (2003) Core values: The first Hans-Cloos lecture. *Bulletin of Engineering Geology and the Environment*, vol 62, 1:1-34.
- Molendijk WO, Aantjes AT (2003) Risk management of earthworks using GeoQ. In: *Proceedings of Piarc – World Road Congress*, Durban, South Africa.
- Morgenstern NR (2000) Common ground. In: *Proceedings EngGeo 2000*, Sydney, Australia.
- SBR (2003) *Faalkosten genuanceerd*. www.sbr.nl.
- Smith (1996) Allocation of risk – The case for manageability. *The International Construction Law Review*, 4:549-569.
- Staveren MTh van, Litjens PPT (2001) Risico's verdelen met Geotechnisch Basis Rapport. *Land en Water*, vol 41, 1/2:46-47.

Matching Monitoring, Risk Allocation and Geotechnical Baseline Reports

Martin Th. van Staveren and Ton J.M. Peters

GeoDelft, Stieltjesweg 2, 2628 CK Delft, The Netherlands
{m.th.vanstaveren, a.j.m.peters}@geodelft.nl
Tel: + 31 15-2693583
Fax: + 31 15-2610821

Abstract. Monitoring ground and construction behaviour is a well-known risk mitigation tool during the construction of many European infrastructure projects. This paper explains the relationship between geotechnical monitoring, geotechnical risk allocation and the Geotechnical Baseline Report.

The main objective of this paper is to present a rational framework, which can be used to define effective monitoring programmes from a risk management perspective. The framework is supported with a recent case study of the Betuweroute, which is a very complicated railway project in the Netherlands.

Keywords: geotechnical monitoring, risk management, geotechnical baseline report.

1 Introduction

Construction in, at and with the subsoil is still a serious risk factor for many European infrastructure projects. The subsoil literally will make, deform or even break an infrastructure project. Many small and large projects run out of time or budget, because of unforeseen behaviour of the subsoil.

In the Netherlands only, failure costs in the infrastructure construction industry are assessed at 800 million euro per year (SBR 2003). Given the prominent role of the subsoil in infrastructure projects, ground-related failure costs will be at least several hundreds of million euro per year, in the Netherlands only. Extrapolating these figures to a European scale results into ground-related failure costs of at least a few billion euro per year.

Risk management can be considered as an effective tool to reduce these enormous failure costs (Smith 1996). However, risk can be monitored and controlled effectively only, if it is clear who is responsible for which risks. To be effective, risk allocation should be made explicit and measurable. The Geotechnical Baseline Report will be presented as a concept that can be applied for geotechnical risk allocation.

2 Monitoring and Risk

The relationship between monitoring and risk management is presented in the Simplified Risk Management Model in Figure 1.

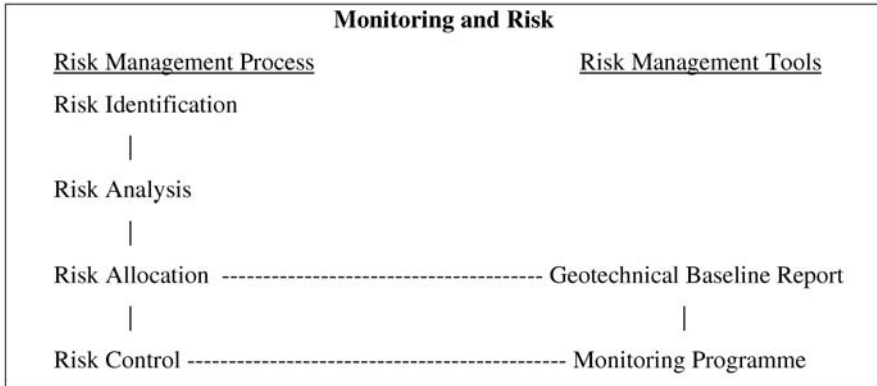


Fig. 1. Simplified Risk Management Model.

The left-hand side of Figure 1 presents the steps of the conventional risk management process: risk identification, risk analysis, risk allocation and risk control. The right-hand side of Figure 1 shows two particular tools: the Geotechnical Baseline Report as a tool for geotechnical risk allocation and the Monitoring Programme as a tool for risk control. There are, of course, also tools for risk identification and analysis, but these are beyond the scope of this paper.

Figure 1 is intended to demonstrate that the purpose of a monitoring programme is risk control, and that a Geotechnical Baseline Report can define a monitoring programme by its risk allocation. Any monitoring programme should be driven by risk control. The required accuracy, reliability, frequency and usability of the monitoring programme, given the expected soil conditions, should be balanced with budget and time constraints.

3 Why Risk Allocation?

The general definition of the term risk is the product of the likelihood of occurrence of an event and the consequences of that event. Normally these events are hazards, with the potential to have negative effects. In this paper risk is considered by definition as potentially harmful. Risk management can be defined as the overall application of policies, processes and practices dealing with risk (Clayton 2001). Allocation of risk means that an identified risk becomes the explicit responsibility of a party or will be shared explicitly between parties as a joint responsibility (Smith 1996).

If a certain identified risk is not explicitly allocated, none of the parties involved in a project will have the drive to take responsibility for that particular risk. This means probably that the risk will not be managed adequately. If that risk occurs, a dispute will start about which party will bear the consequences and should take action to minimise the effects of the risk.

4 Risk Allocation by a GBR

The Geotechnical Baseline Report (GBR) is developed in the United States of America in the nineteen nineties, because disputes about differing soil conditions in civil engineering projects were rising to an unacceptable level for all parties involved. Guidelines for preparing a GBR are presented by the American Society of Civil Engineers (Essex 1997). The steps to arrive at an GBR, as experienced in the Netherlands, are described by Van Staveren and Knoeff (2004).

The essential underlying philosophy of the GBR is a specific contractual statement. It states that the owner is ultimately responsible for any soil conditions which are materially different from the anticipated soil conditions in geotechnical reports. Even if the owner contractually states that the contractor is responsible for all soil conditions, jurisdiction demonstrates that the owner is ultimately responsible, simply because the owner initiates the project.

This philosophy raises the question about *when* soil conditions are materially different. The GBR provides the answer to that question, by contractual definitions of the anticipated soil conditions. The soil conditions can be contractually defined by geotechnical subsoil profiles or geotechnical baseline parameters. The Geotechnical Baseline Report allows the owner to allocate geotechnical risk by definition of geotechnical baselines. The main benefit for the owner is to be able to create an optimum balance between perceived risk and cost of the project. The main benefit for the contractor is clearness about which geotechnical risks are his responsibility and which are the owner's responsibility.

5 How to Allocate Monitoring-Related Risk?

Regarding the allocation of monitoring related risk, two types of risk can be distinguished:

1. Geotechnical risks (strategic) – drives *what* to monitor
2. Competence risks (tactical or operational) – drives *how* to monitor

The geotechnical risks should be controlled by the monitoring system. Occurrence of these risks have to be identified by the monitoring results. Monitoring might, for instance, indicate lower settlement rates than expected of a railway embankment. These results imply a risk of delay or additional costs, because additional measures such as more pre-loading might be necessary to meet the settlement requirements at the end of the construction phase of the project.

Geotechnical risks can obviously not be allocated to a contractor operating solely the monitoring system. That party is only responsible for the competence

risks. Geotechnical risks are the responsibility of either the owner or the main contractor, depending on the risk allocation presented in the Geotechnical Baseline Report.

The design of the geotechnical monitoring system should be driven by the anticipated and allocated geotechnical risks. The major geotechnical risks to be monitored should be derived from the risk identification and analysis steps in the risk management process (see Figure 1). Geotechnical risks should therefore be anticipated and allocated before the actual monitoring system is selected, installed and operated.

Competence risks include all risks which are associated with selecting, installing and operating the monitoring system, given the expected soil conditions as presented in the Geotechnical Baseline Report. Failure of equipment during or after installation, the influence of the instrument on the soil parameters (conformance), the measurement frequency, the measurement range and the accuracy of the instruments are typical examples of competence risk. Adequate control of these risks should be achieved by choosing a competent party, the monitoring contractor, to select, install and operate the monitoring system. The entire set of competence risks should therefore be allocated to the monitoring contractor, as he is able to control the monitoring competence risk.

6 The Betuwe Route Risk Driven Monitoring Case

6.1 Project Description

The Betuweroute is a double-track freight railway linking the Port of Rotterdam directly to the European hinterland. The Betuweroute is being constructed at a cost of 4.3 billion euro (price level of 1999). In the year 2010, the Betuweroute is expected to carry 75 percent of Dutch railway freight transport.

The Sliedrecht-Gorinchem traverse is 22 km in length and consists of 10-12 m of very soft clay and peat layers with a high groundwater table. Under the soft layers lies Pleistocene sand, with a water pressure level rising above ground level. In this paper one major strategic risk and the resulting operational monitoring aspects are highlighted briefly. Additional technical and contractual information is presented by Molendijk and Peters (2003), Molendijk and Van den Berg (2003), Molendijk and Aantjes (2003) and Molendijk et al (2003). The following case is collected from these references.

6.2 A Major Strategic Geotechnical Risk

The railway embankment varies between 1.5 m and 8 m height and is constructed on very soft subsoil, using the hydraulic fill method. Geotextile is used to reinforce the embankment. The sand will be deposited in several stages. It is a fast, cost-effective method with long-term construction and environmental effects, due to the slow consolidation process of the underlying soft soils. As the construction planning and the post construction settlement are of critical importance, a slower



Fig. 2. The Slidrecht – Gorinchem part of the Betuwe Route

consolidation process than anticipated is a major geotechnical risk in this project. This paper will focus on the monitoring of this particular consolidation risk.

6.3 Dealing with Operational Monitoring Risks

In order to construct at lowest cost, construction and protective measures such as extra drainage, overheight and sheet piling will be kept to a minimum. These types of expensive measures were postponed as long as possible, by relatively fast filling of the embankment with smaller safety margins for stability. As construction progresses, the actual soil behaviour was monitored and evaluated, the so-called observational method.

The acceptance of smaller safety margins introduced tactical or operational monitoring risks, which were controlled by systematic risk assessment, based on the available Geotechnical Baseline Report, a tailored monitoring program with a structured data management system and the availability of fall back scenario's and control measures.

Advantages of the resulting risk driven monitoring programme were transparency in the actual risk profile (less time-consuming discussions with owners of objects and infrastructure near the railway track), less safety measures on the adjacent existing railway track and motorway and structured data transfer at the end of the project, (allowing data use during the maintenance period, to minimise maintenance costs in the future).

6.4 The Role of the Geotechnical Baseline Report

Starting point for the design of the monitoring programme was the risk analysis in the Geotechnical Baseline Report. Key risk drivers were defined. Examples are the thickness of soft layers and their consolidation coefficients. For each key risk driver, a prediction of the expected (best-guess) values was made. Next the threshold value or baseline for unacceptable values was determined and the action to be taken was defined, in case of reaching the baseline. For every key risk driver, a suitable monitoring instrument and the required frequency of data acquisition and processing was selected.

Monitoring of soil behaviour was a good indicator to compare design assumptions on consolidation time with the true behaviour, as measured on site. The advantage of these type of measurements is the early warning for unwanted behaviour, allowing remedial actions to be taken in time, before unacceptable damage occurs.

The Geotechnical Baseline Report proved to be a valuable document, in order to define the optimum monitoring programme to control the consolidation risk. The risk driven monitoring programme for the Betuwe Route, based on the Geotechnical Baseline Report, contributed importantly to the completion within planning and to 10 % costs savings as well.

7 Conclusions

The following general conclusions are supported by the very complicated and successfully completed Sliedrecht – Gorinchem section of the Betuwe Route.

A risk driven approach helps owners and contractors to define monitoring programmes with the best possible benefit-to-cost ratios.

Distinguishing geotechnical and competence monitoring risks appears to be useful. It clarifies which party is responsible for what risk. The relatively new concept of the Geotechnical Baseline Report serves as a useful document to identify and allocate responsibilities for differing soil conditions and associated risks. The Geotechnical Baseline Report may therefore serve as basis for more effective and efficiently operated monitoring programmes.

References

- Clayton CRI (ed) (2001) *Managing geotechnical risk: Improving productivity in UK building and construction*. The Institution of Civil Engineers, London, 80 p.
- Essex RJ (ed. (1997) *Geotechnical baseline reports for underground construction*. Technical Committee on Geotechnical Reports of the Underground Technology Research Council, American Society of Civil Engineers, 40 p.
- Molendijk WO, Aantjes AT (2003) Risk management of earthworks using GeoQ. In: *Proceedings of Piarc – World Road Congress, Durban, South Africa*.
- Molendijk WO, Berg F.P.W. van den (2003) Well-founded risk management for the Betuweroute freight railway by the observational method. In: *Proceedings of XIIIth European Conference on Soil Mechanics and Geotechnical Engineering, Praag*.
- Molendijk WO, Peters AJM (2003) Online monitoring for the construction of embankments for Betuwe Route. In: *Proceedings of Piarc – World Road Congress, Durban, South Africa*.
- Molendijk WO et al (2003). Improved reliability of (rest) settlement predictions of embankments on soft soils. In: *Proceedings of Piarc – World Road Congress, Durban, South Africa*.
- SBR (2003) Faalkosten genuanceerd. www.sbr.nl.
- Smith (1996) Allocation of risk – The case for manageability. *The International Construction Law Review*, 4:549-569.
- Staveren MTh van, Knoeff JG (2004). The Geotechnical Baseline Report as risk allocation tool. In: *Proceedings of EurEnGeo, Liege*.

Smart Site Investigations Save Money!

Martin Th. van Staveren¹ and Adriaan J. van Seters²

¹ GeoDelft, Stieltjesweg 2, 2628 CK Delft, The Netherlands
m.th.vanstaveren@geodelft.nl

² Fugro Ingenieursbureau BV, Postbus 63, 2260 AB Leidschendam, The Netherlands
a.vseters@fugro.nl
Tel: +31 15 2693583
Fax: +31 15 2610821

Abstract. More appropriate and well-timed site investigations have a major positive impact in order to reduce the risk of failure. Design and construction of any infrastructure project can be optimised within the project specifications by smart site investigations, in order to save money and time. In this paper this statement is supported by three recent Dutch infrastructure projects, in which smart site investigations resulted in major cost and or time savings. A number of generic key success factors are derived from the presented case histories. These success factors are a risk driven approach of the project, challenging existing codes of practice by state of the art techniques, true consideration of the impact of geological heterogeneity on the project and last but not least, application of hard and soft experience data. These aspects can be defined as the characteristics of smart site investigations. They flourish in particular when applied in combination. In conclusion, more attention towards the strategy and quality of site investigations pays off. It is therefore considered as the responsibility of the European engineering geological and geotechnical communities to send this message with clear examples to the owners, designers and constructors of infrastructure projects. Finally all stake holders of these projects, owners, contractors, engineers, insurance parties and the European societies as a whole, will benefit from the strength of smart site investigations.

Keywords: site investigation, costs, degree of risk, cone pressuremeter, liquefaction risk control.

1 Introduction

The strategy and quality of site investigations for infrastructural projects needs much more attention in the day-to-day practice. In the Netherlands, and probably also in most other European countries, there is unfavourable tendency to buy site investigations on the cheapest price criterion only. The owner provides a “shopping list” with a number of in-situ and laboratory tests, often with minor or even no context of the project requirements. The bidder with the lowest price wins the contract, and apparently, everybody is happy...

As figure 1 from Molendijk and Aantjes (2003) demonstrates, the failure costs in the Dutch infrastructure construction industry are high. In each of the projects presented in table 1 the subsoil played a major role. Often the lowest cost only site investigations, without a well-defined strategy and degree of quality, are not the cheapest solution for all parties involved, at the end of the project.

Table 1. Planning an cost overruns of a selection of Dutch infrastructre projects.

Project	Overrun Planning	Costs
Ramspol inflatable dam	+ 80 %	Unknown
Tramtunnel The Hague	+100 %	+ 90 %
Stormsurge barrier Nieuwe Waterweg	+ 50 %	+ 40 %
Betuweroute freight railway	unknown	+ 65 %
Splay railway Amsterdam – Utrecht	+ 65 %	+ 25 %

2 Why Site Investigations at All?

Anyone involved in design and/or construction of infrastructural projects will understand that any form of site investigation is required, in order to arrive at an effective design and construction. Nothing new so far. Probably less well-known is the fact that about 85 % of all ground related problems are directly related to the extend and quality of site investigations. Clayton (2001) demonstrates a number of types of ground-related problems, such as ground geometry not as anticipated and inadequate planning or execution of the site investigation. The majority of these problems can at least be reduced by adequate site investigations. Typically costs of site investigations are less than 1 % of the construction costs (Smith 1996). Site investigation costs of 0.2 to 0.5 % are typically considered as adequate in the construction industry (Knill 2003). Groundrelated problems can easily add 5 % to the cost of construction, while figures as high as 30-50 % are not unheard of. If real severe unforeseen ground conditions are encountered during construction, additional costs as high as 100 % of the entire project price may be incurred (Clayton 2001). It can be even worse. A study by Hoek and Palmieri (1998), involving the study of 71 World Bank hydroelectric projects indicated not only that costs and schedules were in general 25 % higher than originally estimated, but als that projects have been stopped and abandoned entirely. For these projects cost and schedules escalated to several times the original estimates, due to unforeseen geological conditions. As summarised by Fookes (2000), many similar publications demonstrate that unforeseen ground conditions are one of the largest drivers of technical and financial risk in civil engineering projects. The combination of these figures create an enormous potential to demonstrate the added value of adequate site investigations. What would you decide, if for instance 5 times more site investigation activities (2.5 % instead of the conventional 0.5 % of the total construction costs) would reduce a 25 % cost overrun by a factor 5 to 5 % cost overrun only? Depending on the size of the project, the absolute cost – benefit ratio can easily be 1 : 10 or higher. This nice cost – benefit ratio is demonstrated in this paper by a number of recent cases in the Dutch construction industry. However, firstly the smart site investigation concept needs an introduction.

3 The Smart Site Investigation Concept

The smart part of the smart site investigation concept is its simplicity. Smart site investigations are very project and site specific and risk driven. It is a matter of an open mind and creative holistic thinking. The smart site investigation concept means basically that there is no one receipt for site investigation, as well as there are no general valid rules, guidelines and standards. Every infrastructural project is unique, therefore every project needs its own specific approach. Sometimes a limited site investigation with just some CPTs will be sufficient, other times very sophisticated and multi-phased site investigations are required, to meet an acceptable level of certainty about the ground conditions. Basically, the type and extent of a smart site investigation depends on three main factors:

1. the expected geological heterogeneity of the subsoil
2. the boundary conditions of the construction
3. the degree of risk the responsible party accepts to bear

The last factor, the risk factor, should be the main driver in the definition of the site investigation programme, as the first two factors depend largely on risk acceptance. A main and common pitfall is the mindset that a risk driven approach is inherently difficult and complex, as for instance mentioned by Smith (1996) and Ho (2000). Risk management does not automatically involve very difficult probabilistic calculations and a jungle of cause and effects diagrammes. Risk management starts with common sense and well-structured thinking about the main project goals to achieve, the probability of unfavourable events with might obstruct those goals and the effects of those events on the goals. Based on this type of analysis, which can be very brief for small projects and extensive for large complicated projects, effective risk remediation measures can be taken. These measures will almost automatically define the required site investigations and the smart site investigation concept has been applied! Next the application of this smart site investigation concept, together with its benefits will be demonstrated by three studies.

4 Smart Site Investigation Case Studies

4.1 Observational Method Avoids Sheet Pile Wall

The Betuweroute is a 160 km double-track freight railway. It should ensure that cargo arriving at the port of Rotterdam is transported quickly and safely to the European hinterland. The section between the cities of Sliedrecht and Gorinchem is the most difficult part of the new railway track. It runs parallel to sensitive existing infrastructure, available construction time is short and critical for the total project and last but not least, local soil conditions are very poor. The alliance of the owner and a consortium of contractors was challenged to go beyond traditional design standards, because covering all soft soil uncertainties with a traditional type of design would cost many millions of euro extra in advance. One example is the 9

km of embankment section, where Betuweroute runs parallel to the existing railway Dordrecht-Geldermalsen and the Motorway A 15. Originally, to minimise disturbance of the existing rail track, a sheet pile wall was planned in between the two embankments of the existing and new rail tracks. However, a risk analysis at the start of the alliance provided interesting new insights. The combination of the observational method, supported by a smart site investigation, proved to be a much better cost-effective remediation measure for the deformation risks (Molendijk and Aantjes 2003). The site investigation involved on-line monitoring during the construction by open standpipes and vertical inclinometers every 500 m. Settlement plates were installed every 50 m. At geologically relevant cross sections, where heterogeneity was expected, vibration wire piezometers were used. A specific aspect of the site characterisation by monitoring is the “on-line” availability of the monitoring results. All monitoring data was sent immediately to a database, which was accessible via internet for all authorised parties (Molendijk and van den Berg 2003). The presented observational method, supported by a smart site characterisation, avoided the requirement of 9 km of sheetpile, which saved the alliance about 4 million euro. The additional monitoring costs were about 0.2 million euro, which gives a cost – benefit ratio of 1 : 20.

4.2 Smart Liquefaction Risk Control

One of the most densely populated parts of the Netherlands is underlain by the worst soft soil conditions of the Netherlands. In this Rotterdam – The Hague area a light-rail link will be constructed, RandstadRail. Part of this link will be realised in a bored tunnel, which will cross the existing and very busy railway Rotterdam - Utrecht at 14 m depth. During the risk analysis in the design phase, with input of experience data and historical data, it became clear that the existing Rotterdam – Utrecht railway was constructed on 14 m of very loose anthropogene sand, which pushed away the originally very soft peat layers. Figure 1 demonstrates a cross section with soil profile, the proposed tunnel, and the CPT result.

The risk of large soil settlements above the proposed tunnel, affecting the existing Rotterdam – Utrecht railway, was classified as very high. A temporary bridge, supporting the tracks of the existing railway was proposed as risk mitigation measure. However, during the risk evaluation it became clear that this measure was not only very expensive, it would be needed to take the existing railway out of duty for a couple of weekends as well. In addition, an additional settlement risk during installation of the temporary bridge was identified. Therefore, another settlement risk mitigation measure was highly required. In this stage, the benefits of a smart soil characterisation became clear. The CPT shows cone resistances of about 3 MPa until a depth of more than 10 m. But how loose would that sand layer really be? To answer this question a detailed and non-routine additional smart site investigation was performed. The test programme included 3 in-situ electrical density measurements, 3 CPTs and a boring. All tests were performed by CPT equipment and pushed by an angle of inclination of 30 to 45 degrees below the existing railtrack. Figure 2 demonstrates the performance of the electrical density test in the field.

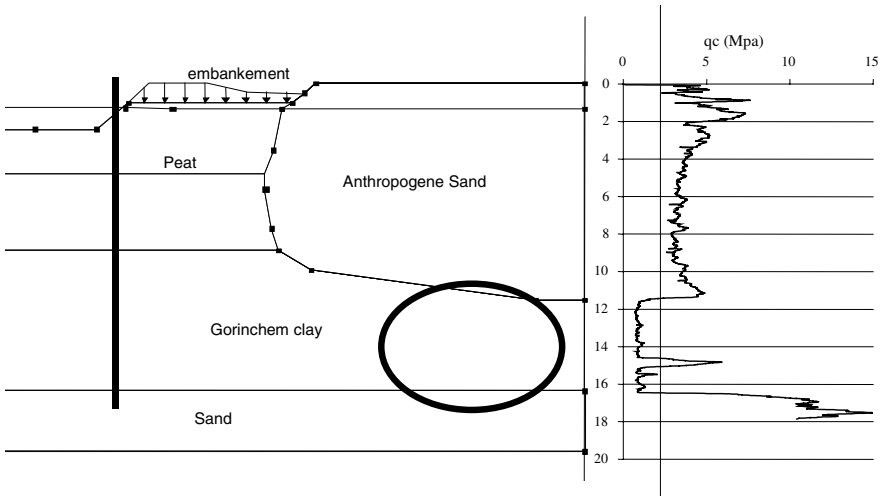


Fig. 1. Cross section with soil profile and CPT



Fig. 2. Electrical density test below railway.

With special cones the electrical density method measures in-situ and continuously the electrical conductivity of the soil and the groundwater. The results are calibrated by laboratory tests. The results of the additional site characterisation demonstrated quite better soil conditions, than could be concluded based on CPTs

only. The temporary bridge support was not needed anymore. Adding extra weight adjacent to the railway, in combination with a limited lowering of the groundwater table, was selected as an effective risk mitigation measure (Korff 2003). The risk-driven and non-routine site investigation saved a significant amount of money on risk remediation measures, by avoidance of the temporary bridge. The costs of the additional additional site investigation, including the laboratory tests was much lower than the savings. The cost-benefit ratio of the smart site investigation for this case is 1:20.

4.3 Essential Soil Stiffness Investigation for the Hubertus Tunnel

In The Hague plans are developed for the execution of a bored tunnel as part of the “Noordelijke Randweg”. The tunnel consists of two 8,65 m inside diameter tunnels with a bored length of 1600 m each. At both ends a shaft and a cut-and-cover section are foreseen. The location of the tunnel is near the North Sea coast, therefore the subsoil conditions consist mainly of sands. The surface level varies around NAP + 7 m, with at the western side the large (artificially constructed) Hubertusdune with top at NAP + 23 m. A 1 m thick peat layer is present over almost the entire tunnel area at NAP 0 m level. The groundwater level is around NAP 0,0 m. The tunnel itself will be constructed horizontally between NAP – 5 m (top) and NAP – 15 m (bottom). At the tunnel entrances the road level will be at NAP 0 m. The stiffness of the soil is of great importance for dimensioning of the tunnel lining and therefore largely determines the tunnel cost. This case will focus on a smart determination of soil stiffness, which was a major topic in the third phase of the soil investigation in 2003. In this phase the soil investigation consisted of 36 CPT's, 13 boreholes and 31 Cone Pressiometer tests at 7 locations. In the first two phases already 45 CPT's and a limited number of borings were performed. In the design of the tunnel lining the (un)loading stiffness of the sand is a key parameter, as the forces in the lining depend highly upon the soil stiffness. In the first phase of the design, these stiffness values were estimated based upon literature. In order to maximise the reliability of this crucial parameter during the third phase of the soils investigation, two methods of determination were applied: CD-triaxial tests with unloading loop on reconstituted samples and in situ determination by Cone Pressuremeter testing. In total 23 CD Triaxial tests with unloading phase (triaxial extension test) and 31 Cone Pressuremeter tests were performed. The triaxial tests were multistage consolidated drained tests on isotropically consolidated samples. The samples were prepared on the in situ density, using the results of minimum/maximum density determinations and correlations with the cone resistance q_c from literature. As the unloading stiffness proved to be essential in the design, a direct determination of the parameter was included to minimise the uncertainty in the value. Thus, an unloading stage was added after each loading phase, as shown on figure 3. An example of the load/unload curve of a Cone Pressuremeter test is given on figure 4.

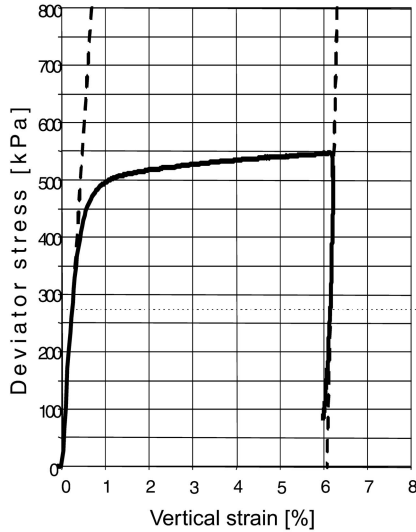


Fig. 3. Triaxial test result.

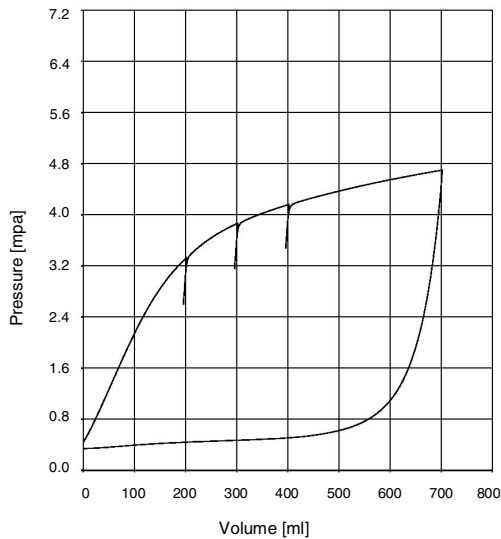


Fig. 4. Cone Pressuremeter test result.

From both tests stiffness parameters E_{50} and E_{ur} were derived for all sand layers. Caution must be taken in the interpretation of the tests. The triaxial tests during loading were performed at lower strain levels than the CPM tests, whereas the unloading occurs at lower strains for the CPM tests than for the triaxial tests. Based on these differences in strain level, it was found that both test methods were

consistent. Finally mean, low characteristic and high characteristic values for the loading stiffness E_{50} and unloading stiffness E_{ur} were derived statistically, as shown on figure 5.

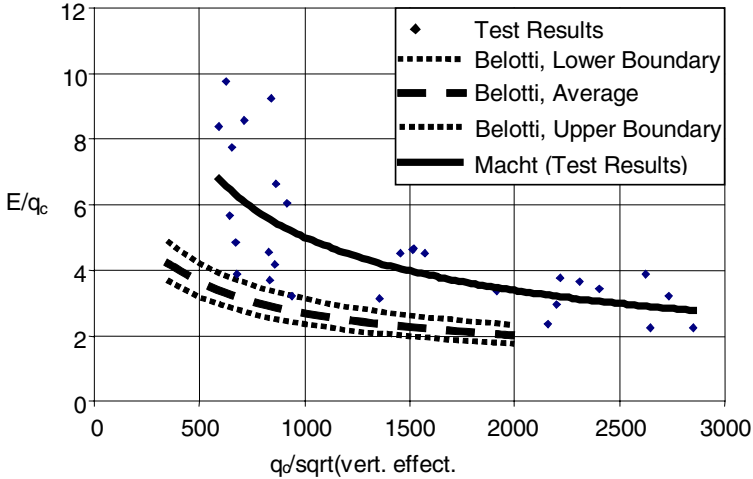


Fig. 5. Statistically derived loading stiffness E_{50} and unloading stiffness E_{ur} .

As can be observed from figure 5, the stiffness values derived from the tests are approximately a factor 2 larger than the well used relation by Bellotti et al. (1989). This proved very favourable in the design. The mean values were found to be as follows related to the average cone resistance and the vertical effective stress in the layer:

$$\frac{E_{50}}{q_c} = 189 \left(\frac{q_c}{\sqrt{\sigma'_v}} \right)^{-0.53} \quad \text{and:} \quad E_{ur} = 4 * E_{50} \quad (1)$$

where: E_{50} = Youngs modulus at 50 % deviator stress in triaxial test; E_{ur} = Youngs modulus at unloading/reloading conditions; q_c = average cone resistance in the layer; σ'_v = vertical effective stress. By the presented correlation statistically based stiffness parameters, based on two types of tests, can be derived at every CPT location for the tunnel. This smart soils investigation was characterised by a step by step approach, which gradually per phase zoomed into more detail on one of the most crucial design parameters, i.e. the soils stiffness of the sand layers. The stiffness was derived from two independent test methods, laboratory and in situ testing. A large number of tests was carried out, to enable statistical evaluation of the data, which resulted in a factor two larger stiffness than would be expected from literature correlation only. The investment in state of the art testing resulted therefore clearly in a more economic lining design.

5 Conclusions

In total four generic key success factors for the smart site investigations concept are derived from the briefly presented individual case histories. These success factors are: 1) a risk driven approach of the project, 2) challenging existing codes of practice by state of the art approaches and techniques, 3) true consideration of the impact of geological heterogeneity on the project, and 4) application of hard and soft experience data. These aspects can be defined as characteristics of smart site investigations. They flourish in particular when applied in combination and result in cost : benefit factors of 1 : 20 in the presented cases. In conclusion, more attention towards the strategy and quality of site investigations pays off. It is therefore considered as the responsibility of the European engineering geological and geotechnical communities, to send this message with clear examples to the owners, designers and constructors of infrastructure projects. Because finally all stakeholders of these projects, owners, contractors, engineers, insurance parties and the European societies as a whole, will benefit from the strength of smart site investigations.

References

- Bellotti R, Ghiona V, Jamiolkowski M, Robertson PK (1989) Shear strength of sands from CPT. In: Proceedings 12th International Conference on Soil Mechanics and Foundation Engineering, Rio de Janeiro.
- Clayton CRI (ed) (2001) Managing geotechnical risk: Improving productivity in UK building and construction. The Institution of Civil Engineers, London, 80 p.
- Fookes PG (2000) Total geological history: A model approach to the anticipation, observation and understanding of site conditions. In Proceedings EngGeo 2000, Sydney, Australia.
- Ho (2000) Quantitative Risk Assessment: application, myths and future direction. In: Proceedings EngGeo 2000, Sydney, Australia.
- Hoek E, Palmieri A (1998) Geotechnical Risks on large civil engineering projects. In: Proceedings 8th Congress IAEG 1:79-88.
- Knill J (2003) Core values: The first Hans-Cloos lecture. Bulletin of Engineering Geology and the Environment, vol 62, 1:1-34.
- Korff M (2003) Crossing of bored tunnel with existing railway. In Proceedings of 2nd International Young Geotechnical Engineering Conference, Bucharest, Romania.
- Molendijk WO, Aantjes AT (2003) Risk management of earthworks using GeoQ. In: Proceedings of Piarc – XXII World Road Congress, Committee C12, Durban, South Africa.
- Molendijk WO, Berg F.P.W. van den (2003) Well-founded risk management for the Betuweroute freight railway by the observational method. In: Proceedings of XIIIth European Conference on Soil Mechanics and Geotechnical Engineering, Prague, Czechoslovakia.
- Smith (1996) Allocation of risk – The case for manageability. The International Construction Law Review, 4:549-569.

Author Index

- Abreu, Rui 31
Aggitalis, Georgios 527
Åkesson, Urban 94
Areias, Lou 110
Aroglou, Harry 393
Auriol, Jean-Claude 275
Azzam, Rafiq 117
- Bachmann, Gregor 9
Baliak, Frantisek 694
Bauch, Enrico 244
Bekendam, Roland F. 657
Bell, Fred 719
Ben-David, Ram 708
Benissi, Maria 393
Berkelaar, Robert 422
Bock, Helmut 1
Bosch, Melinda van den 422
Bouhenni, Saâd 485
Boukpeti, Nathalie 255
Bourdeau, Céline 671
Broch, E. 1
Brouwer, Jan 368
- Camelbeeck, Thierry 614
Cevik, Engin 265
Charlier, Robert 236, 255
Chartres, R. 1
Conde, Patrick 285
Cornelles, Josep 153
Corominas, Jordi 405
Cotthem, Alain Van 475
Couchard, Iwan 475
Coudyzer, Christophe 604
Cruchaudet, Martin 341
Culshaw, Martin 565, 719
- Dachy, Marie 624
Dagrain, Fabrice 359
Dassargues, Alain 624
David, Jean-Pierre 275
Debecker, Bjorn 211
Delay, Jacques 219, 341, 377
- Deloge, K. Pierre-Alexandre 604
Delouvrier, Jacques 377
Deschamps, Benoît 359, 604
Dethy, Bernard 485
Distinguin, Marc 219
Donnelly, Laurance 565, 719
- Eder, Stefan 39, 435, 504
Eitner, Volker 74, 101
Estévez, Hugo 727
- Faure, René-Michel 59
Feller, Vincent 285
Ferber, Valéry 275
Ferrer, Mercedes 727
Fleurisson, Jean-Alain 671
Floris, Mario 738, 745
Fornaro, Mauro 574
Freitas, Michael H. de 54
Fripiat, Christophe 285
- Gambin, M. 1
Garbarino, Elena 685
García, J. Carlos 727
Gareau, Laurent F. 327
Gerritsen, Rijk H. 767
Giere, Johannes 513
Gokceoglu, Candan 203, 466
Golser, Johann 593
González de Vallejo, Luis 727
Gori, Umberto 444, 745
Grandjean, Gilles 226, 671
Greco, Otello Del 685
Grégoire, Colette 385
Grgec, Damir 549
- Hack, Robert 179
Hammer, Helmut 39
Hanisch, Jörg 754
Havenith, Hans-Balder 671
Heitfeld, Michael 86
Herbschleb, Jurgen 294, 631
Hick, Servais 475
Hoegaerden, Vincent van 368

- Holeyman, Alain 285
Hueckel, Tomasz 255
- Impe, William Van 110
Ivanova, Nadezhda 172
- Joesten, Peter K. 385
- Katzenbach, Rolf 9, 513
Kazilis, Nikolaos 527
Khayat, Navid 316
Knoeff, Johan G. 777
Kohl, Bernhard 435
Koyuncu, N. Pınar 125
Kruse, Britta 304
Kühne, Manfred 521
Kühnel, Markus 585
Klukanová, Alena 650
Kuznetsova, Irina 172
- Lambarki, Mouad 117
Lambert, Nicolas 641
Lane, Jr., John W. 385
Legrain, Hughes 359
Lehmann, Bodo 521
Lempp, Christof 244
Le Nickel-SLN 144
Liscak, Pavel 650
Liu, Zejia 255
Loew, Simon 347
Lovera, Enrico 574
López, Carlos 153
Łuczak-Wilamowska, Beata 308
- Maertens, J. 1
Maertens, L. 1
Mainz, Mark 86
Malgot, Jozef 694
Mari, Milena 745
Marinos, Paul 393
Marinos, Vassilios P. 527
Marinos, Vassilis 393
Martinez-Bofill, Joan 405
Mattle, Bruno 39
Maurenbrecher, P. Michiel 133
McCann, David 565
Merrien-Soukatchoff, Véronique 144
Mlinar, Željko 549
- Mortier, Hans 455
Moser, Michael 701
Moya, José 414
Muñoz, Pere 153
- Ngan-Tillard, Dominique 133
Nieuwenhuis, Jan Dirk 538
Norbury, David 1, 15
Novack, Mark 393
Novosel, Tomislav 549
- Oggeri, Claudio 685
Oliveira, Ricardo 31
Omraci, Kamel 144
- Paassen, Leon A. van 327
Pakbaz, Mohammad C. 316
Pesendorfer, Marc 347
Peters, Ton J.M. 786
Pinto, P. 1
Pittino, Gerhard 593
Plana, Didac 153
Polidori, Ennio 444
Pollak, Davor 162
Poscher, Gerhard 435, 504
Pöttler, Rudolf 521
- Quinif, Yves 614
- Radinger, Alexander 521
Ramirez, Julio A. 321
Ragozin, Alexei 760
Richter, Roland 69
Rijkers, Richard 368
Rivkin, Felix 172
Rodríguez, Angel 727
Romeo, Roberto W. 745
Ruymbeke, Michel Van 614
- Sage, Sandrine 226, 624
Schetelig, Kurt 86
Schmitz, Robrecht M. 236
Schokking, Floris 555
Schouenborg, Björn 94
Schrier, Joost S. van der 767
Schroeder, Christian 236
Schubert, W. 1
Schwarz, Ludwig 39
Sedlacek, Christoph 504

- Seip, Matthias 513
Seters, Adriaan J. van 792
Slob, Siefko 179
Smith-Pardo, J. Paul 321
Soler, Albert 405
Sonmez, Harun 203
Soos, Paul von 86
Sozen, Mete A. 321
Staveren, Martin Th. Van 777, 786, 792
Stille, H. 1
Stocker, Manfred 86
Stölben, Ferdinand 74, 101
Suhodolsky, Sergey 172
- Talbaoui, Mohammed 285
Thimus, Jean-François 59
Thorez, Jacques 236
Tonelli, Gianluigi 444
Tonoz, M. Celal 466
Topal, Tamer 265
Treve, Christian 47
Tshibangu, Jean-Pierre 359, 604, 614
- Tuunter, Léon L.T.C. 455
- Ulusay, Resat 125, 466
- Vandycke, Sara 614
Veneri, Francesco 444, 738
Verly, Jacques 226
Verruijt, Arnold 538
Verstraelen, Jan 211
Vervoort, André 211
Vlasblom, Willem J. 190
- Wassing, Brecht B.T. 631
Wauters, Benoît 285
Weerts, Henk J.T. 631
Weidner, Stefan 701
Westerhoff, Rogier 368
Wevers, Martine 211
- Yolkin, Vladimir 760
- Zaczek, Yannick 641
Zorlu, Kivanc 203